ZOOLOGICAL SCIENCE

An International Journal

VOLUME 11
1994

published by

The Zoological Society of Japan

CONTENTS OF VOLUME 11

NUMBER 1, FEBRUARY 1994

REVIEWS

Hanke, W., W. Kloas: Hormonal regulation of osmo-mineral content in amphibia 5

Nässel, D. R., E. Bayraktaroglu, H. Dircksen: Neuropeptides in neurosecretory and efferent neural systems of insect thoracic and abdominal ganglia 15

ORIGINAL PAPERS

Phisiology

Takahashi, T., O. Matsushima, F. Morishita, M. Fujimoto, T. Ikeda, H. Minakata, K. Nomoto: A myomodulin-CARP-related peptide isolated from a polychaete annelid *Perinereis vancaurica* 33

Sugimoto, M., T. Kawamura, R. Fujii: Changes in the responsiveness of melanophores to electrical nervous stimulation after prolonged background adaptation in the medaka, *Oryzias latipes* 39

Wilder, M. N., T. Okumura, Y. Suzuki, N. Fusetani, K. Aida: Vitellogenin production induced by eyestalk ablaton in juvenile giant freshwater prawn *Macrobrachium rosenbergii* and trial methyl farnesoate administration 45

Cell and Molecular Biology

Meyer-Rochow V. B., Y. Ishihara, J. R. Ingram: Cytochemical and Histological details of muscle fibers in the southern smelt *Retropinna retropinna* (Pisces; Galaxioidei) 55

Genetics

Patil, J. G., V. Wong, H. W. Khoo: Assessment of pMTL construct for detection in vivo of luciferase expression and fate of the transgene in the zebrafish, *Brachydanio rerio* 63

Developmental Biology

Furukawa, T., Y. Maeda: K252a, a potent inhibitor of protein kinases, promotes the transition of *Dictyostelium* cells from growth to differentiation 69

Iwamatsu, T., S. Nakashima, K. Onitake, A. Matsuhisa, Y. Nagahama: Regional differences in granulosa cells of preovulatory medaka follicles 77

Kanno, Y., S. Koike, T. Noumura: Immunohistochemical localizations of epidermal growth factor in the developing rat gonads 83

Satoh, Y., T. Shimizu, Y. Sendai, H. Kinoh, N. Suzuki: Nucleotide sequence of the proton ATPase beta-subunit homologue of the sea urchin *Hemicentrotus pulcherrimus* (RAPID COMMUNICATION) 153

Kanbayashi, H., Y. Fujita, K. Yamasu, T. Suyemitsu. K. Ishihara: Local change of an exogastrula-inducing peptide (EGIP) in the pluteus larva of the sea urchin *Anthocidaris crassispina* (RAPID COMMUNICATION) 157

Reproductive Biology

Hosokawa, K., Y. D. Noda: The acrosome reaction and fertilization in the bivalve, *Laternula limicola*, in refernce to sperm penetration from the posterior region of the mid-piece 89

Endocrinology

Iga, C., I. Koshimizu, S. Takahashi, Y. Kobayashi: Experimental manipulation of pituitary hemorrhage induced by intraperitoneal injection of a hypertonic solution in mice 101

Yamashita, K., S. Kikuyama: Immunohistochemical study of ontogeny of pituitary prolactin and growth hormone cells in *Xenopus laevis* (RAPID COMMUNICATION) 149

Asahina, M., H. Fugo, S. Takeda: Ecdysteroid synthesis in dissociated cells of the prothoracic gland of the silkworm, *Bombyx mori* 107

Behavior Biology

Naruse, M., T. Oishi: Effects of light and food as zeitgebers on locomotor activity rhythms in the loach, *Misgurnus anguillicaudatus* 113

Suzuki, H., T. Sekiguchi, A. Yamada, A. Mizukami: Sensory preconditioning in the terrestrial mollusk, *Limax flavus* 121

Environmental Biology and Ecology

Ohdachi, S.: Growth, metamorphosis and gape-limited cannibalism and predation on tadpoles in larvae of salamanders *Hynobius retardatus* 127

Lawrence J. M., M. Bryne: Allocation of resources to body components in *Heliocidaris erythrogramma* and *Heliocidaris tuberculata* (Echinodermata: Echinoidea) 133

Systematics and Taxonomy

Ishikawa, K.: Two new species of the genus *Holaspulus* (Acarina: Gamasida: Parholaspidae) from the Ryukyu Islands, Japan 139

Experimental Animal

Kiguchi, K., M. Shimoda: The sweet potato hornworm, *Agrius convolvuli*, as a new experimental insect: Continuous rearing using artificial diets 143

Announcements 161
Instructions to Authors 163

NUMBER 2, APRIL 1994

REVIEWS

Ward, A., P. Bierke, E. Pettersson, W. Engström: Insulin-like growth factors: Growth, transgenes and imprinting 167

Mizunami, M: Processing of contrast signals in the insect ocellar system 175

ORIGINAL PAPERS

Physiology

Aonuma, H., T. Nagayama, M. Hisada: Output effect of identified interneurons upon the abdominal postural system in the crayfish *Procambarus clarkii* (Girard) 191

Immunology

Hirose, E., T. Ishii, Y. Saito, Y. Taneda: Phagocytic activity of tunic cells in the colonial ascidian *Aplidum yamazii* (Polyclinidae, Aplousobranchia) 203

Biochemistry

Harumi, T., K. Hoshino, N. Suzuki: In vitro autophosphorylation and cyclic nucleotide-dependent dephosphorylation of sea urchin sperm histone kinase 209

Mukaí, M., T. Kondo, K. Yoshizato: Rapid and quantitative detection of aspartic proteinase in animal tissues by radio-labeled pepstatin A 221

Furukohri, T., S.Okamoto, T. Suzuki: Evolution of phosphagen kinase (III). Amino acid sequence of arginine kinase from the shrimp *Penaeus japonicus* 229

Developmental Biology

Furuya, H., K. Tsuneki, Y. Koshida: The development of the vermiform embryos of two mesozoans, *Dicyema acuticephalum* and *Dicyema japonicum* 235

Kimura, K., K. Usui, T. Tanimura: Female myoblasts can participate in the formation of a male-specific muscle in *Drosophila* 247

Yazaki, I., H. Harashima: Induction of metamorphosis in the sea urchin, *Pseudocentrotus depressus*, using L-glutamine 253

Ohya, Y., K. Watanabe: Control of growth and differentiation of chondrogenic fibroblasts in soft-agar culture: Role of basic fibroblast growth factor and transforming growth factor-β 261

Reproductive Biology

Okia, N. O.: Membrane-bound inclusions in the leydig cell cytoplasm of the broad-headed skink, *Eumeces laticeps* (Lacertilia: Scincidae) 269

Yoshizaki, N.: Identification and localization of a ligand molecule of *Xenopus* cortical granule lectins 275

Nakamura, M., T. Yamanobe, M. Takase: Localization and purification of serum albumin in the testis of *Xenopus laevis* 285

Endocrinology

Ohta, N., T. Mori, S. Kawashima, S. Sakamoto, H. Kobayashi: Spatio-temporal pattern of DNA synthesis detected by bromodeoxyuridine labeling in the mouse endometrial stroma during decidualization .. 291

Tsai, P. I., S. S. Madsen, S. D. McCormick, H. A. Bern: Endocrine control of cartilage growth in coho salmon: GH influence *in vivo* on the response to IGF-I *in vitro* 299

Environmental Biology

Takaku, G., H. Katakura, N. Yoshida: Mesostigmatic mites (Acari) associated with ground, burying, roving carrion and dung beetles (Coleoptera) in Sapporo and Tomakomai, Hokkaido, northern Japan 305

Systematics and Taxonomy

Amemiya, S., Y. Mizuno, S. Ohta: First fossil record of the family Phormosomatidae (Echinothurioida: Echinoidea) from the Early Miocene Morozaki Group, central Japan 313

Grismer, L. L., H. Ota, S. Tanaka: Phylogeny, classification, and biogeography of *Goniurosaurus kuroiwae* (Squamata: Eublepharidae) from the Ryukyu Archipelago, Japan, with description of a new subspecies 319

Ohtani, H.: Polymorphism of lampbrush chromosomes in Japanese populations of *Rana nigromaculata* 337

Matsuoka, N., K.Fukuda, K. Yoshida, M. Sugawara, M. Inamori: Biochemical systematics of five asteroids of the family Asteriidae based on allozyme variation 343

NUMBER 3, JUNE 1994

REVIEWS

Tsutsui, K., S. Kawashima: Regulation of gonadotropin receptors and its physiological significance in higher vertebrates 351

Rastogi, R. K., L. Iela: Gonadotropin-releasing hormone: present concepts, future directions 363

ORIGINAL PAPERS

Physiology

Nakamura, M., M. Tani, T. Kuramoto: Effects of rapid cooling on heart rate of the Japanese lobster *in vivo* 375

Naitoh, T., M. Matuura, R. J. Wassersug: Effectiveness of metoclopramide, domperidone and ondansetron as

antiemetics in the amphibian, *Xenopus laevis* 381
Sata, O., T. Sato: Electrical responses of non-taste cells in frog tongue and palate to chemical stimuli 385

Cell Biology

Arikawa K., A. Matsushita: Immunogold colocalization of opsin and actin in *Drosophila* photoreceptors that undergo active rhabdomere morphogenesis 391
Ricci, N., F. Verni: Experimental perturbations of the *Litonotus-Euplotes* predator-prey system 399

Biochemistry

Ohtsuka, Y., H. Nakae, H. Abe, T. Obinata: Immunochemical studies of an actin-binding protein in ascidian body wall smooth muscle 407
Takikawa, S., M. Nakagoshi: Developmental changes in pteridine biosynthesis in the toad, *Bufo vulgaris* 413

Developmental Biology

Hou, L., T. Takeuchi: Neural crest development in reptilian embryos, studied with monoclonal antibody, HNK-1 423
Suzuki, H., A. Kondo: The second maturation division and fertilization in the spider *Achaearanea japonica* (Bös. et Str.) 433
Nishiyama, I., T. Oota, M. Ogiso: Neuron-like morphology expressed by perinatal rat C-cells *in vitro* 441

Endocrinology

Uesaka, T., K. Yano, M. Yamasaki, M. Ando: Glutamate substitution for glutamine at position 5 or 6 reduces somatostatin action in the eel intestine (RAPID COMMUNICATION) 491
Takahashi, S., S. Oomizu, Y. Kobayashi: Proliferation of pituitary cells in streptozotocin-induced diabetic mice: effect of insulin and estrogen 445
Takano, M., Y. Sasayama, Y. Takei: Molecular evolution of shark C-type natriuretic peptides 451

Systematics and Taxonomy

Aizawa, T., M. Hatsumi, K. Wakahama: Systematic study on the *Chaenogobius* species (family Gobiidae) by analysis of allozyme polymorphisms 455
Ohtani, H.: Speciation of Japanese pond frogs deduced from lampbrush chromosomes of their diploid and triploid hybrids 465
Ono, T., Y. Obara: Karyotypes and Ag-NOR variations in Japanese Vespertilionid bats (Mammalia: Chiroptera) 473
Matsui, M., G. Wu: Acoustic characteristics of treefrogs from Sichuan, China, with comments on systematic relationship of *Polypedates* and *Rhacophorus* (Anura, Rhacophoridae) 485

NUMBER 4, AUGUST 1994

REVIEWS

Larriva-sahd, J., A. Matsumoto: The vomeronasal system and its connections with sexually dimorphic neural structures 495
Hosoya, H.: Cell-cycle-dependent regulation of myosin light chain kinase 507

ORIGINAL PAPERS

Physiology

Shibayama, R., T. Kobayashi, H. Wada, H. Ushitani, J. Inoue, T. Kawakami, H. Sugi: Stiffness changes of holothurian dermis induced by mechanical vibration 511

Cell and Molecular Biology

Kosaka, T.: Life cycle of *Paramecium bursaria* syngen 1 in a natural pond 517
Goda, M., J. Toyohara, M. A. Visconti, N. Oshima, R. Fujii: The blue coloration of the common surgeonfish, *Paracanthurus hepatus*—I. Morphological features of chromatophores 527
Harigaya, T., S. Tsunoda, M. Mizuno, H. Nagasawa: Different gene expression of mouse transforming growth factor α between pregnant mammary glands and mammary tumors in C3H/He mice (RAPID COMMUNICATION) 625

Biochemistry

Miura, K., M. Nakagawa, Y. Chinzei, T. Shinoda, E. Nagao, H. Numata: Structural and functional studies on biliverdin-associated cyanoprotein from the bean bug, *Riptortus clavatus* 537

Developmental Biology

Matsuda, M., H. Keino: An open cephalic neural tube reproducibly induced by cytochalasin D in rat embryos *in vitro* 547

Endocrinology

Shinobu, N., Y. Mugiya: Effects of hypophysectomy and replacement therapy with bovine growth hormone and triiodothyronine on the *in vitro* uptake of calcium and methionine by scales in the goldfish, *Carassius aurautus* 555
Sawada, K., T. Noumura: Characterization of androgen receptors for testosterone and 5α-dihydrotestosterone in the mouse submandibular gland 563
Takagi, K., S. Kawashima: Effects of sex steroids on

dopamine neurons in cultured hypothalamus and preoptic area cells derived from neonatal rats 571
Itoh, M. T., A. Hattori, Y. Sumi, T. Suzuki: Identification of melatonin in different organs of the cricket, *Gryllus bimaculatus* 577
Wakahara, M., N. Miyashita, A. Sakamoto, T. Arai: Several biochemical alterations from larval to adult types are independent on morphological metamorphosis in a salamander, *Hynobius retardatus* 583

Ecology

Nishi, E., M. Nishihara: Colony formation via sexual and asexual reproduction in *Salmacina dysteri* (Huxley) Polychaeta, Serpulidae 589

Phylogeny

Masuda, R., M. C. Yoshida, F. Shinyashiki, G. Bando: Molecular phylogenetic status of the Iriomote cat *Felis iriomotensis*, inferred from mitochondrial DNA sequence analysis 597
Masuda, R., M. C. Yoshida: A molecular phylogeny of the family Mustelidae (Mammalia, Carnivora), based on comparison of mitochondrial cytochrome b nucleotide sequences 605
Fukatsu, T., S. Aoki, U. Kurosu, H. Ishikawa: Phylogeny of Cerataphidini aphids revealed by their symbiotic microorganisms and basic structure of their galls: implications for host-symbiont coevolution and evolution of sterile soldier castes 613
Errata 629

NUMBER 5, OCTOBER 1994

REVIEWS

O'Brien, M. A., P. H. Taghert: The genetic analysis of neuropeptide signaling systems 633
Morisawa, M.: Cell signaling mechanisms for sperm motility 647

ORIGINAL PAPERS

Physiology

Kobayashi, M., K. Kitayama, G. Satoh, K. Ishigaki, K. Imai: Relationships between the slope of the oxygen equilibrium curve and the cooperativity of hemoglobin as analyzed using a normalized oxygen pressure scale 663
Karakisawa, H., S. Tamotsu, A. Terakita, K. Ohtsu: Identification of putative photoreceptor cells in the siphon of a clam, *Ruditapes philippinarum* 667
Nakagawa, T., E. Eguchi: Differences in flicker fusion frequencies of the five spectral photoreceptor types in the swallowtail butterfly's compound eye (RAPID COMMUNICATION) 759

Cell Biology

Yoshikawa, T., Y. Yashiro, T. Oishi, K. Kokame, Y. Fukada: Immunoreactivities to rhodopsin and rod/cone transducin antisera in the retina, pineal complex and deep brain of the bullfrog, *Rana catesbeiana* 675

Genetics

Nakamura, M., M. Sumida, T. Yamanobe, M. Nishioka: Identification of protein C in sera of the frogs, *Rana nigromaculata* and *Rana brevipoda* (RAPID COMMUNICATION) 763

Immunology

Ohtake, S., T. Abe, F. Shishikura, K. Tanaka: The phagocytes in hemolymph of *Halocynthia roretzi* and their phagocytic activity 681

Developmental Biology

Suzuki, H., A. Kondo: Changes at the egg surface during the first maturation division in the spider *Achaearanea japonica* (Bös. et Str.) 693

Reproductive Biology

Mita, M., A. Oguchi, S. Kikuyama, R. de Santis, M. Nakamura: Ultrastructural study of endogenous energy substrates in spermatozoa of the sea urchins *Arbacia lixula* and *Paracentrotus lividus* 701

Endocrinology

Cvijić, G., R. Radojičić, Z. Matijašević, V. Davidović: The effect of glucocorticoids on the activity of monoamine oxidase and superoxide dismutase in the rat interscapular brown adipose tissue 707
Suzuki, N., Y. Nosé Y. Kasé Y. Sasayama, Y. Takei, H. Nagasawa, T. X. Watanabe, K. Nakajima, S. Sakakibara: Amino acid sequence of sardine calcitonin and its hypocalcemic activity in rats 713
Ge, W., R. E. Peter: Evidence for non-steroidal gonadal regulator(s) of gonadotropin release in the goldfish, *Carassius auratus* 717

Behavior Biology

Nakagawa, A., A. Iwama, A. Mizukami: Age-dependent changes related to reproductive development in the odor preference of blowflies, *Phormia regina*, and fleshflies, *Boetteherisca peregrina* 725
Hongoh, Y., H. Ishikawa: Changes of mycetocyte symbiosis in response to flying behavior of alatiform aphid (*Acyrthosiphon pisum*) 731

Morphology

Hirose, E., T. Ishii, Y. Saito, Y. Taneda: Seven types of tunic cells in the colonial ascidian *Aplidium yamazii* (Polyclinidae, Aplousobranchia): morphology, classification, and possible functions 737

Ando, K., N. Okura: Aminergic and acetylcholinesterase-positive innervation in the cerebral arterial system and choroid plexus of the newt *Triturus pyrrhogaster*, with special reference to the plexus innervation 745

Taxonomy

Tanaka, T., M. Matsui, O. Takenaka: Estimation of phylogenetic relationships among Japanese brown frogs from mitochondrial cytochrome b gene (Amphibia: Anura) 753

NUMBER 6, DECEMBER 1994

REVIEWS

Sato, T., T. Miyamoto, Y. Okada: Comparison of gustatory transduction mechanisms in vertebrate taste cells 767

Baguñà, J., E. Saló R. Romero, J. Garcia-Fernàndez, D. Bueno, A. M. Muñoz-Marmol, J. R. Bayascas-Ramirez, A. Casali: Regeneration and pattern formation in planarians. Cells, molecules and genes 781

ORIGINAL PAPERS

Genetics

Miura, I.: Sex chromosome differentiation in the Japanese brown frog, *Rana japonica*. I. Sex-related heteromorphism in the distribution pattern of constitutive hetero-chromatin in chromosome No.4 of the Wakuya population 797

Miura, I.: Sex chromosome differentiation in the Japanese brown frog, *Rana japonica*. II. Sex-linkage analyses of the nucleolar organizer regions in chromosome No. 4 of the Hiroshima and Saeki populations 807

Immunology

Sawada, T., S. Ohtake: Mixed-incubation of allogeneic hemocytes in tunicate *Halocynthia roretzi* 817

Biochemistry

Maki, S., S. Kimura, K. Maruyama: Localization of connectin-like proteins in the giant sarcomeres of barnacle muscle 821

Developmental Biology

Iwamatsu, T.: Stages of normal development in the medaka *Oryzias latipes* 825

Harigaya, T., S. Tsunoda, H. Yokoyama, K. Yamamoto, H. Nagasawa: Mouse TGFα gene expression in normal and neoplastic mammary glands and uteri of four strains of mice with different potentials for mammary gland growth and uterine adenomyosis 841

Murakami, R., K. Miyake, I. Yamaoka: Androgen-induced differentiation of the fibrocartilage of os penis cultured *in vitro* 847

Reproductive Biology

Harada, T.: Adult diapause induced by the loss of water surface in the water strider, *Aquarius paludum* (Fabricius) 855

Asahina, K., J. G. D. Lambert, H. J. Th. Goos: Bioconversion of 17α-hydroxyprogesterone into 17α, 20α-dihydroxy-4-pregnen-3-one and 17α, 20β-dihydroxy-4-pregnen-3-one by flounder (*Platichthys flesus*) spermatozoa 859

Endocrinology

Horiuchi, T., M. Isobe, M. Suzuki, Y. Kobayashi: Calcitonin induces hypertrophy and proliferation of pars intermedia cells of the rat pituitary gland 865

Environmental Biology and Ecology

Prevot, S., J. Senaud, J. Bohatier, G. Prensier: Variation in the composition of the ruminal bacterial microflora during the adaptation phase in an artificial fermentor (RUSITEC) 871

Peng, K. W., Y. K. Ip,: Is the coelomic plasma of *Phascolosoma arcuatum* (Sipuncula) hyperosmotic and hypoionic in chloride to the external environment? 879

Saulich, A. H., T. A. Volkovich, H. Numata: Control of seasonal development by photoperiod and temperature in the linden bug, *Pyrrhocoris apterus* in Belgorod, Russia 883

Systematics and Taxonomy

Katakura, H., S. Saitoh, K. Nakamura, I. Abbas: Multivariate analyses of elytral spot patterns in the phytophagous ladybird beetle *Epilachna vigintioctopunctata* (Coleoptera, Coccinellidae) in the province of Sumatera Barat, Indonesia 889

Author index 895

Acknowledgment 899

Contents of ZOOLOGICAL SCIENCE, Vol. 11, Nos. 1–6 i

Development
Growth & Differentiation

Published Bimonthly by the Japanese Society of Developmental Biologists
Distributed by Business Center for Academic Societies Japan, Academic Press, Inc.

Papers in Vol. 36, No. 6. (December 1994)

55. T. Yagi: Src Family Kinases Control Neural Development and Function
56. S. H. Keller and V. D. Vacquier: N-Linked Oligosaccharides of Sea Urchin Egg Jelly Induce the Sperm Acrosome Reaction
57. S. K. Satoh, M. T. Oka and Y. Hamaguchi: Asymmetry in the Mitotic Spindle Induced by the Attachment to the Cell Surface during Maturation in the Starfish Oocyte
58. P. Hardman, E. Landels, A. S. Woolf, and B. S. Spooner: TGF-β1 Inhibits Growth and Branching Morphogenesis in Embryonic Mouse Submandibular and Sublingual Glands *in Vitro*
59. A. Obinata, Y. Akimoto, T. Kawamata, and H. Hirano: Induction of Mucous Metaplasia in Chick Embryonic Skin by Retinol-Pretreated Embryonic Chick or Quail Dermal Fibroblasts through Cell-Cell Interaction: Correlation of a Transient Increase in Retinoic Acid Receptor β mRNA in Retinol-Treated Dermal Fibroblasts with Their Competence to Induce Epidermal Mucous Metaplasia
60. M. Yoshida, K. Inaba, K. Ishida and M. Morisawa: Calcium and Cyclic AMP Mediate Sperm Activation, but Ca^{2+} Alone Contributes Sperm Chemotaxis in the Ascidian, *Ciona savignyi*
61. T. A. Ferguson, J. Vozenilek and C. M. West: The Differentiation of a Cell Sorting Mutant of *Dictyostelium discoideum*
62. M. Asaoka, M. Myohara and M. Okada: Digitonin Activates Different Sets of Puff Loci Depending on Developmental Stages in *Drosophila melanogaster* Salivary Glands
63. T. A. Quill and J. L. Hedrick: Oviductal Localization of the Cortical Granule Lectin Ligand Involved in the Block to Polyspermy of *Xenopus Laevis*
64. V. Gangji, E. Bastianelli, M. Rooze, and R. Pochet: Transient Calretinin Expression during Intervertebral Disc Formation of the Chick Embryo
65. S. Kobayashi, H. Saito and M. Okada: A Simplified and Efficient Method for *in situ* Hybridization to Whole *Drosophila* Embryos, Using Electrophoresis for Removing Non-hybridized Probes
66. K. Akasaka, N. Sakamoto, T. Yamamoto, J. Morokuma, N. Fujikawa, K. Takata, S. Eguchi and H. Shimada: Corrected Structure of the 5′ Flanking Region of Arylsulfatase Gene of the Sea Urchin, *Hemicentrotus pulcherrimus*

Development, Growth and Differentiation (ISSN 0012–1592) is published bimonthly by The Japanese Society of Developmental Biologists. Annual subscription for Vol. 35 1993 U. S. $ 191,00, U. S. and Canada; U. S. $ 211,00, all other countries except Japan. All prices include postage, handling and air speed delivery except Japan. Second class postage paid at Jamaica, N.Y. 11431, U. S. A.

Outside Japan: Send subscription orders and notices of change of address to Academic Press, Inc., Journal Subscription Fulfillment Department, 6277, Sea Harbor Drive, Orlando, FL 32887–4900, U. S. A. Send notices of change of address at least 6–8 weeks in advance. Please include both old and new addresses. U. S. A. POSTMASTER: Send changes of address to *Development, Growth and Differentiation,* Academic Press. Inc., Journal Subscription Fulfillment Department, 6277, Sea Harbor Drive, Orlando, FL 32887–4900, U. S. A.

In Japan: Send nonmember subscription orders and notices of change of address to Business Center for Academic Societies Japan, 16–9, Honkomagome 5-chome, Bunkyo-ku, Tokyo 113, Japan. Send inquiries about membership to Business Center for Academic Societies Japan, 16–9, Honkomagome 5-chome, Bunkyo-ku, Tokyo 113, Japan.

Air freight and mailing in the U. S. A. by Publications Expediting, Inc., 200 Meacham Avenue, Elmont, NY 11003, U. S. A.

ISSN 0289-0003

An International Journal

ZOOLOGICAL SCIENCE

Vol. 11 No.1

February 1994

PHYSIOLOGY
CELL and MOLECULAR BIOLOGY
GENETICS
IMMUNOLOGY
BIOCHEMISTRY
DEVELOPMENTAL BIOLOGY
REPRODUCTIVE BIOLOGY
ENDOCRINOLOGY
BEHAVIOR BIOLOGY
ENVIRONMENTAL BIOLOGY and ECOLOGY
SYSTEMATICS and TAXONOMY

published by Zoological Society of Japan
distributed by Business Center for Academic Societies Japan
VSP, Zeist, The Netherlands

ZOOLOGICAL SCIENCE

The Official Journal of the Zoological Society of Japan

The Zoological Society of Japan:
Toshin-building, Hongo 2–27–2, Bunkyo-ku,
Tokyo 113, Japan. Phone 03-3814–5461
Fax 03-3814-5352

ZOOLOGICAL SCIENCE is devoted to publication of original articles, reviews and rapid communications in the broad field of Zoology. The journal was founded in 1984 as a result of unification of Zoological Magazine (1988–1983) and Annotationes Zoologicae Jasponenses (1897–1983), the former official journals of the Zoological Soceity of Japan. An annual volume consists of six regular numbers and one supplement (abstracts of papers presented at the annual meeting of the Zoological Society of Japan) of more than 850 pages. The regular numbers appear bimonthly.

MANUSCRIPTS OFFERED FOR CONSIDERATION AND CORRESPONDENCE CONCERNING EDITORIAL MATTERS should be sent to:

Dr. Tsuneo Yamaguchi, Managing Editor, Zoological Science, Department of Biology, Faculty of Science, Okayama University, Okayama 700, Japan, in accordance with the instructions to authors which appear in the first issue of each volume. Copies of instructions to authors will be sent upon request.

SUBSCRIPTIONS. ZOOLOGICAL SCIENCE is distributed free of charge to the members, both domestic and foreign, of the Zoological Society of Japan.To non-member subscribers within Japan, it is distributed by Business Center for Academic Societies Japan, 5–16–9 Honkomagome, Bunkyo-ku, Tokyo 113. Subscriptions outside Japan should be ordered from the sole agent, VSP, Godfried van Seystlaan 47, 3703 BR Zeist (postal address: P. O. Box 346, 3700 AH Zeist), The Netherlands. Subscription rates will be provided on request to these agents. New subscriptions and renewals begin with the first issue of the current volume.

[Publication of Zoological Science has been supported in part by a Grant-in-Aid for Publication of Scientific Research Results from the Ministry of Education, Science and Culture, Japan.]

ZOOLOGICAL SCIENCE 11: 1–3 (1994)

OBITUARY

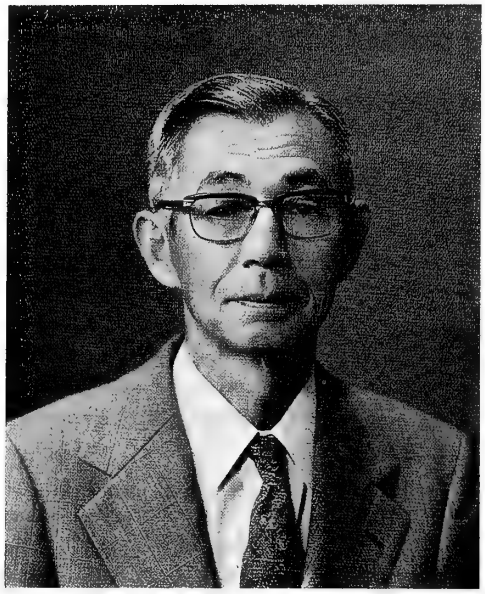

Masao Sugiyama (1908–1993)

It is very sad for us to have to announce that Masao Sugiyama, Professor Emeritas of Nagoya University, passed away at the age of 84 on the 14th of September 1993, following nearly 5 years of illness. His death has deeply grieved both those who knew him and those who worked with him. His death is a great loss to the field of biological science both in Japan and abroad.

Masao Sugiyama was born on the 11th of November 1908 in Nagoya City in central Honshu. As a junior high school student, he first encountered a sea urchin shell on the sea shore near Nagoya and was deeply impressed by its beautiful, elaborately carved patterns. At that moment, although he did not suspect it, his long-life connection with the sea urchin might be said to have begun. In 1925, he entered the Eighth High School, Science Course, in Nagoya. Inspired by his high school biology teachers, the late Professors Usaburo Kohno and Noboru Takamine, Sugiyama took an interest in Zoology and was determined to become a Zoologist. After graduating in 1928, he entered the Zoological Institute of the Faculty of Science, the Imperial University of Tokyo (now the University of Tokyo). He became a student of the late Professor Naohide Yatsu and studied the spermatogenesis of *Asellus nipponensis,* a kind of isopod, crustacean, for his graduation thesis. In 1931, he was enrolled in the Graduate School of the Imperial University of Tokyo and proceeded with studies on the behavior of the sex chromosomes in the spermatogenesis of Japanese earwig *Anisolabis marginalis*. Thus, during the early period of his post-graduate course, he wrote the two papers concerned with spermatogenesis mentioned above. Soon after, however, he became aware of the importance of Experimental Cytology and began to study the effects of mitogenetic rays on cell division, under the direction of the late Professor Tokusuke Gôda. At that time, whether or not mitogenetic rays could induce cell division was an exciting problem which was paid much attention by many scientists with several hundred papers published on the subject. Despite his efforts, Sugiyama could not obtain positive results on induction of cell division, using yeast, root-tip cells and sea urchin eggs. He thus reached the conclusion that mitogenetic rays are not emitted from dividing cells. In 1938, he published three papers denying the presence of such rays. Since the 1940's, the number of studies concerned with mitogenetic rays has rapidly decreased, with even the term "mitogenetic rays" completely disappearing from recent text-books on Cytology. This means that his conclusion was certainly correct. Then, following a suggestion by Professor Gôda, he started to investigate the effects of heparin and hirudine, anticoagulants, on cleavage in sea urchin eggs and found the very interesting fact that nuclear divisions occur without cytoplasmic segmentations, so that multi-nucleated eggs are induced. In 1936, he finished his post-graduate course and for these excellent studies he was awarded the degree of Dr. Sc. from Imperial University of

Tokyo in 1938.

On the other hand, he took an interest in the behavior of the cell surface during cleavage in sea urchin eggs. Professor Katsuma Dan (former President of Tokyo Metropolitan University) had the same idea. Therefore, Sugiyama cooperated with Professor Dan and Professor Tomosuke Yanagita in such studies. In 1938, they attained their objective using a very simple but very skilfull technique, namely the measurement of the distance between two kaoline particles attached to the egg surface. As a result of such series of experiments, Prof. Dan proposed his famous hypothesis on cell division in sea urchin eggs in 1943. In 1938, too, he wrote two papers concerned with the fertilization and formation of fertilization membrane in sea urchin eggs. His full-fledged research on fertilization or artificial activation seems to have begun around this period and marks the start of his successful scientific career. It should be noted here that he published a book "Physiological Fertilization" in 1940.

In 1939, he became a staff member of the Nagoya Medical College and was then appointed associate professor at Nagoya Imperial University. In those days, there was no Marine Biological Station in central Honshu. Therefore, he planned and made great effort to found a Marine Biological Station available to all for research as well as education in marine biology. In 1942, a new building for such a Station was completed on Sugashima, a small island near Toba City, Mie-Prefecture, a place very rich in fauna. He was nominated Director of the Sugashima Marine Biological Station in 1943 and subsequently served as Director for nearly 30 years. During this period, he devoted his efforts to fitting out the station for modern scientific research and he succeeded in the introduction of both transmission and scanning electron microscopes and facilities for radio-isotopes. In 1962, he was promoted to full professor at the same university and retired in 1972. He successively served as professor of biology at Sugiyama-jogakuen University until 1984.

The following is an abbreviated resume of Prof. Sugiyama's most significant accomplishments since moving to Nagoya University in 1939.

Once sea urchin eggs are fertilized by a single spermatozoon, they do not accept other spermatozoa if insemination is repeated. This is the case even when fertilization membrane, formed at the time of the first insemination, is mechanically removed. This fact means that some changes blocking extra sperm-entrance into eggs occur at the time of fertilization; in other words, re-fertilization does not take place. In 1952, however, Sugiyama found that when eggs are washed in Ca-, Mg-free sea water just after insemination and the fertilization membrane is removed, those eggs can accept re-inseminated spermatozoa. This finding clearly demonstrated that a sperm-block mechanism is destroyed under such Ca-, Mg-free circumstances.

On the other hand, since 1947, he had done a series of experiments on artificial activation in sea urchin eggs. And, by introducing a very simple but skilfull method, he succeeded in analyzing a mechanism of egg activation following formation of fertilization membrane. From the results obtained by such experiments, he divided cortical changes, provoked by insemination and various activating reagents, in nature into two groups; that is, a propagating and non-propagating one. He called the former propagating cortical change a fertilization wave, according to the definition of activation in Medaka eggs reported by the late Professor Tokio Yamamoto (Nagoya University). Thus, Sugiyama proposed a working hypothesis, the so called "Fertilization Wave Hypothesis". He supposed that, in the process of fertilization or activation, a chain reaction on the cell surface is involved in which a spermatozoon or an activating reagent triggers stimulation of the egg surface and this stimulation in turn induces the propagating cortical change, fertilization wave, with this wave provoking the formation of fertilization membrane via the breakdown of cortical granules. Later, in 1969, this scheme was improved by the addition of new findings such as insufficient activation without breakdown of cortical granules, published by himself and his co-workers in 1967 and 1969. In 1974 and 1975, Mazia and his collaborators reported that ammonia can induce activation without cortical granule breakdown in sea urchin eggs. It should be noted here that as mentioned above, Sugiyama and his group had already published papers on such phenomena "insufficient activation" nearly 5 years before. In recognition of his pioneering work, he was invited to participate in the "International Symposium of Fertilization in the Sea Urchin Eggs" held at Palermo in Italy in 1955. At the symposium, he played a very important role as chairman as well as a speaker. He read a paper on his "Fertilization Wave Hypothesis" that made a very strong impression on fellow delegates. For this contribution, he was awarded the Zoological Society of Japan Prize in 1957.

In 1973, he and his co-worker, the late Mr. Yoshiteru Takahashi, clearly demonstrated the importance of acrosome reaction at the time of fertilization in sea urchin eggs. They found that spermatozoa in which the acrosome reaction has once been induced are fertilizable even in Ca-free sea water. This means that Ca ions are not indispensable for membrane fusion between egg and spermatozoon but only for induction of the acrosome reaction. In his later years following retirement from Nagoya University in 1974, his interests extended to grasping the process of fertilization as one of the processes of cell membrane fusion and spent much time on such studies. In this manner, he continued his efforts as an investigator until the end of his active life.

Sugiyama contributed much to the Zoological Society of Japan as an active member of the Board from 1963 to 1972 and from 1975 to 1979. He was also on the Board of the Japan Society for Cell Biology from 1965 to 1974. He was

President of the Japanese Society of Developmental Biologists from 1973 to 1976 and, further, he served as Editor-in-Chief of Development, Growth and Differentiation from 1968 to 1973. In 1978, he was elected as a member of the Science Council of Japan and was an active participant until 1984. In addition, he was also on the Board of the National Institute of Basic Biology in Okazaki City. He also served as chairman of the Council of Japanese National Marine and Inland Biological Stations for many years and made a great effort to improve mutual communication and cooperation between stations and to expand their facilities. Thus, Sugiyama's contributions to the academic world went far indeed.

He was warm, gentle, quite and always generously prepared to listen to his students. We never heard him raise his voice. He was not a narrow-minded scientist. He loved literature, art and music. He was especially fond of works by Beethoven. He was an accomplished pianist. Occasionally, he kindly played a part of the first movement of Piano Sonata No.14 op. 27–2 (the so called Moon Light) for us. He also loved taking photographs and 16 mm motion pictures. For some time, his poetic feeling led him to write Japanese verse with thirty one-syllables (Tanka). Here is one of them which was composed by him on the occasion of his retirement.

Fumikoeshi yamano kanatani miyuru mine
Sarani noboramu chikarano kagiri
"A new peak appears
beyond the mountain I have just climbed
However, I'll try to conquer this peak too
as best as I can"

This verse vividly highlights Sugiyama's continuous devotion to, and passion for, scientific research which never ceased even after his official retirement.

Manabu K. Kojima

Department of Environmental
Biology and Chemistry
Faculty of Science
Toyama University

ZOOLOGICAL SCIENCE 11: 5–14 (1994)

REVIEW

Hormonal Regulation of Osmomineral Content in Amphibia

WILFRIED HANKE and WERNER KLOAS

Department of Zoology, University of Karlsruhe, Kaiserstr. 12, D-76128 Karlsruhe, Germany

INTRODUCTION

Osmomineral regulation is among the most important physiological functions in Amphibia. These animals live in fresh water or depend strongly on water in the environment to prevent desiccation. Only one species, *Rana cancrivora,* is found in sea water where the frogs capture food and are able to survive for a longer time. The larval stages of Amphibia live generally in fresh water and develop during metamorphosis the capability to survive in air except those like the clawed toad, *Xenopus laevis,* which stay in fresh water for the whole life.

Different types of adaptation are found. Most of the Ampibia living in fresh water, larvae or adults, are stenohaline animals. They are hyperregulators, but the osmotic concentration is mostly low compared with other vertebrates. It is equivalent to saline of 0.6% which is approximately 180 mOsm. These fresh water animals can be acclimated to 1.2% salt concentration which is mostly the limit for the hyperregulatory capacity, because the animals must adjust the internal osmolality about 10% above the external value to survive. Another type of adaptation is represented by euryhaline toads and *Rana cancrivora.* These animals can survive in higher external NaCl concentration or under extreme dry conditions. They adjust the internal osmolality by increasing the urea concentration. Internal osmotic values of 800–1000 mOsm can be reached. Using this mechanisms, toads living under arid conditions avoid desiccation.

The regulation of the processes which enable the animals to survive under osmotic stress is exerted by several hormones. Generally, all hormonal systems take part in osmoregulation, but several hormones are especially important. These are the hormones of the hypophysial-adrenocortical axis, the nonapeptides of the eurohypophysis, tissue derived peptide hormones like angiotensin II or natriuretic peptides, catecholamines from the adrenal medulla, and regulators of energy metabolism, like thyroid hormones, insulin, glucagon, or of Ca^{++} metabolism, e.g. prolactin, calcitriol (Table 1).

In the same way, several organs are involved in osmoregulatory processes. Not only those which directly take up or release water and electrolytes, like skin, bladder, and kidney, but also organs for general physiological functions, e.g. liver, circulatory organs, muscles, intestine etc. These organs are important because of supply with metabolites and oxygen, for transport processes etc. (Table 2).

This review mainly focusses on the mechanisms working in two representative of *Anura* and *Urodela,* the clawed toad and the axolotl. Both represent specific types of adaptation. Larvae and adults of *Xenopus laevis* live in water. The adults can survive on air only for about half a day. Axolotls are neotenic animals which means that they also stay in water for the whole life. This implies that these species may be especially adapted to the life in water and are not typical for *Anura* or *Urodela.* In this review special attention is given to two main questions. Firstly, the cooperation between the different hormones and the target organs is described. Secondly, the regulation of the release of corticosteroids from the interrenal tissue by osmoregulatory hormones is most extensively discussed.

1. Effects and significance of hormonal systems

1.1. Role of the hypothalamo-hypophysial system in osmoregulation

The hormones of the hypothalamo-hypophysial system involved in osmoregulation have two different origins. They derive from the pars nervosa or the adenohypophysis. In both cases the role of the hypothalamus is to regulate the release of the hypophysial hormones and to transmit information about the environment and the internal milieu to the gland-like structures. This results in changing the titre of the hormones which act on peripheral organs.

It is well known for a long time that the nonapeptides of the pars nervosa control the water economy of the Amphibia. They stimulate water uptake by the skin or the bladder (Brunn effect). It is interesting that the effectiveness of these hormones depends on the adaptational type. Amphibia living in water do not respond as strong to nonapeptides as those living on land and are subject to changes of water supply or desiccation. On the other hand, it has been reported that those animals living in extremely dehydrating situations, e.g. *Rana cancrivora* or *Scaphiopus couchii,* while staying in the holes for aestivation do not respond to nonapeptides at this time. The effects of nonapeptides on

Received July 14, 1993

TABLE 1. Hormones effective in osmoregulation of Amphibia

Gland	Hormone	Target	Function
Neurohypophysis	Nonapeptides, Hydrins	Skin, Bladder	Water uptake
		Interrenals	Steroid secretion
		Liver cells	Glycogenolysis
Adenohypophysis	ACTH	Interrenals	Steroid secretion
	PRL	Skin	Ca-uptake
Interrenal gland	Corticosteroids	Skin	Na-uptake
	(Corticosterone, Aldosterone)	Liver cells	Gluconeogenesis
Chromaffin (adrenal) tissue	Catecholamines	Liver cells	Glycogenolysis
	(Adrenaline, Noradrenaline)		
Heart etc.	ANF	Kidney	Natriuresis
Liver, Kidney etc.	Angiotensins	Kidney	Water retention
		Interrenals	Steroid secretion
	Calcitriol	Skin etc.	Ca-uptake
Thyroid gland	T4, T3	different organs	Metabolism

TABLE 2. Mechanisms of osmotic adaptation in Amphibia

Effectors	Function
Interrenal gland	Na-uptake by the skin
Corticosterone	Glucose-production by the liver
Aldosterone	Electrolyte shift between organs and blood
Chromaffin tissue	Glycogenolysis
Adrenaline	Changes of circulation
Noradrenaline	
Skin	Water-uptake
	Na-uptake
	Ca-uptake
Liver	Glucose production
	Urea production
Circulation	Blood supply for skin, intestine etc.
Bladder and kidney	Water and electrolyte homeostasis

the regulation of water content have been recently reviewed [2].

The water balance of Amphibia is also affected by special neuropeptides called hydrins [36] which are isolated from *Xenopus* and *Rana* neurointermediate lobes. The peptides derive from the pro-vasotocin-neurophysin precursor. It has been suggested that these peptides are specific regulators of water and electrolyte content of amphibians.

The water retardation stimulated by neurohypophysial hormones (Brunn effect) is quite clear. The permeability of the skin or bladder epithelium increases which allows water to penetrate rapidly into the animal. It is the type of permeability called the osmotic permeability which is influenced. The effect still depends on an osmotic gradient between the internal milieu and the environment. Water molecule aggregates follow the gradient. Besides, the short circuit current is also influenced by nonapeptides which means that not only water, but also sodium uptake increase. This is recently reported for *Xenopus laevis* [17].

The direct actions of hypophysial hormones important for osmoregulation are not limited to skin and bladder. Receptor binding of nonapeptides is also found at the glomeruli of the kidney [21] which is congruent with the observation that AVT reduces the glomerular filtration rate [12]. A vasoconstrictor effect of AVT on glomerular blood vessels is quite common in Amphibia [4, 32]. Receptor binding of AVP was also found at the glomeruli of axolotls (Kloas and Hanke, unpublished).

Very interesting effects of the nonapeptides were found at the interrenal tissue and at the liver. At least, these effects support the osmoregulatory processes by providing metabolites.

There is a quite strong stimulatory effect of AVT on the corticosteroid release from the interrenal tissue of the clawed toad *in vitro* (Fig. 5). The stimulation already occurs with very low amounts of AVT added to the medium. 0.2 nM given for 5 min (=1 ml, total 0.2 pM) were already effective. This dose is in the same range as the effective dose of ACTH in molar units. The receptors which are involved in the stimulatory action of nonapeptides cannot be described as V_1 or V_2 receptors. V_1 antagonists did not prevent the effect of the nonapeptides and the V_2 agonists could not mimic the effects of AVT. Therefore, it has been postulated that a special type of Amphibian receptor exists in this case [18].

Nonapeptides induce glycogenolysis in liver cells of Amphibia. This effect has been described in several papers for *Xenopus* and axolotl [13–16] and also for lungfish tissue [10].

In a recent study, isolated hepatocytes (primary cultures) of the clawed toad have been carefully analyzed. Figure 1

demonstrates a dose-effect relation between the dose of arginine-vasotocin (AVT) and glucose release. It is evident that addition of 1 nM AVT to the medium has already quite clear effects. There is also a good correlation between glycogen content after incubation and dose of AVT. The higher the dose the lower the glycogen that is left in the cells (Fig. 2). To analyze the type of nonapeptide receptor which is involved an antagonist to the V_1 receptor, (1-β-mercapto-β, β-cyclo-penta methylene propionic acid)-2-(0-methyl)-tyrosine-arginine vasopressin), was given. The antagonist did not inhibit the response. Furthermore, a V_2-agonist, (1-deamino-8-D-arginine)-vasopressin, was as effective as AVT (Figs. 3 and 4). This demonstrates that a V_2-type receptor which works via cAMP mediates the effect which is in contrast to that known for rat liver [1].

Summarizing the effects of the nonapeptides, three main targets must be pointed out. The hormones stimulate water and Na-uptake through skin and bladder, they induce corticosteroid release by the adrenals with some effect on the catecholamine release, too, and they have a glycogenolytic effect on the liver.

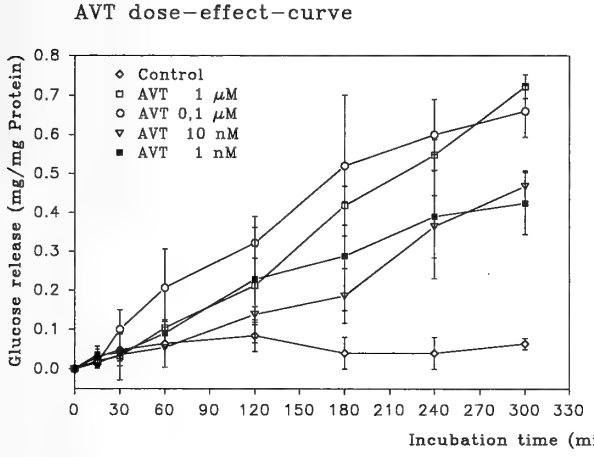

FIG. 1. Changes of glucose release from hepatocytes of the clawed toad after addition of different doses of AVT (according to [1]).

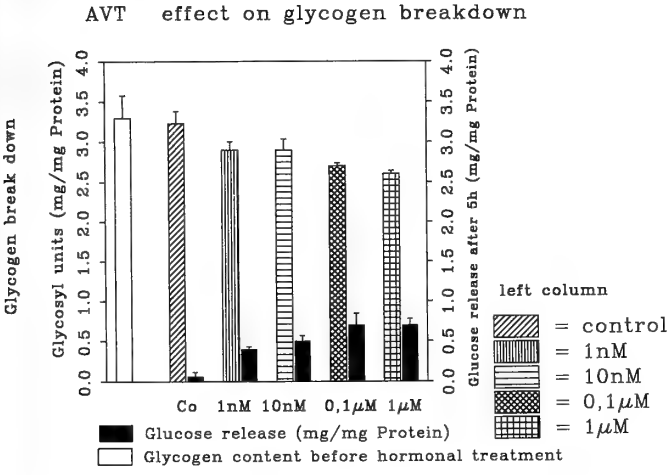

FIG. 2. Changes of glycogen breakdown in hepatocytes of the clawed toad after addition of different doses of AVT (according to [1]).

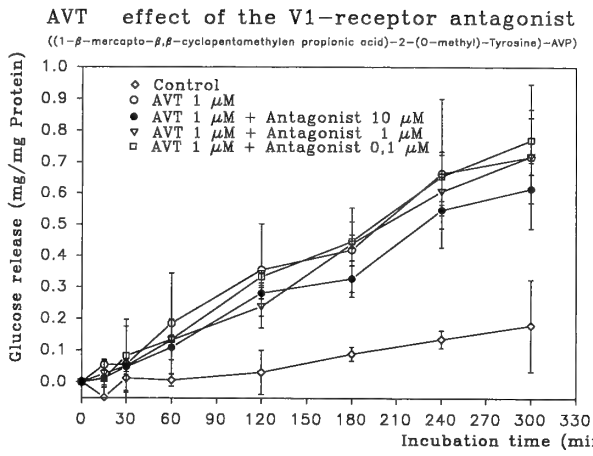

FIG. 3. Effects of the V_1-receptor antagonist, added in different doses to the medium containing 1 μM AVT (according to [1]).

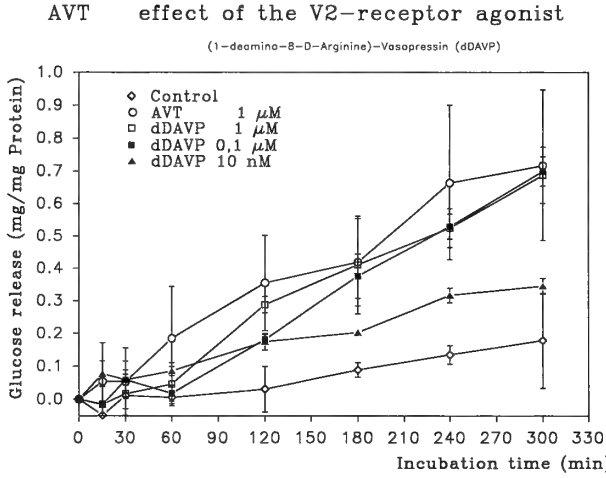

FIG. 4. Effects of the V_2-receptor agonist added in different doses to the medium in comparison to the effect of 1 μM AVT (according to [1]).

1.2. Role of the adrenocortical hormones in osmoregulation

1.2.1. Osmoregulatory function of the corticosteroids

The two main corticosteroids of Amphibia, corticosterone and aldosterone, are both involved in osmoregulation. It is well known that the skin is the main target and Na^+ transport is strongly enhanced by these hormones. In a general view, it has been suggested that aldosterone as well as corticosterone and cortisol (the latter may not be present in Amphibia) increase sodium transport across the toad bladder and skin [3]. This is mainly based on the work of Crabbé [5, 6] who described this effect at the skin of *Bufo marinus* and other toads. With respect to this classic work it must be pointed out that the main problems of this effect are not clearly elaborated, especially not in the clawed toad which may not have a very effective Na^+ transport system. The following questions are not answered. Are both corticosteroids equally effective on a molar basis? Is the transport

system influenced by the acclimation condition, e.g. desiccation, osmotic stress etc., and does the response on corticosteroids depend on these conditions? Much more work must be done.

The importance of corticosteroids for osmoregulation is clearly demonstrated when the clawed toads are acclimated to salt water. During acclimation the titre of both corticosteroids increased (see chapter 1.2.2.3.). In connection with these changes of the corticosteroids blood glucose levels also increase and are adjusted to normal levels during next days. Long term acclimation (for about 4 weeks) in hypertonic solutions, 1.2% salt, 340 mM urea or 340 mM mannitol, resulted in insignificantly elevated levels of aldosterone or corticosterone [17].

The congruence of the changes of corticosterone and aldosterone in response to acclimation conditions clearly points out that the secretion of both hormones is strongly correlated. There is no separate regulation of one hormone. Furthermore, it is evident that glucose levels in the blood are also correlated with the titre of both hormones. The increase of glucose levels is likely to be the most important effect of both corticosteroids.

The action of corticosteroids is involved in stress responses. Since hypertonicity of the environment or desiccation are important stressors in lower vertebrates, it can be suggested that the normal physiological function of osmoregulation is correlated with stress response.

Till now it cannot be clearly decided whether the several functions of corticosteroids are separate direct effects. It could still be possible that some of the target organs are only indirectly influenced via the metabolic effects.

1.2.2. Regulation of the secretion of corticosteroids

1.2.2.1. Effects of telocrine factors

The discussion of the regulation of corticosteroid secretion must begin with the statement that in all interrenal cells of Amphibia one biosynthetic pathway occurs which starts with cholesterol esters and runs via pregnenolone to corticosterone (Table 3). This is then converted to aldosterone. Both the intermediate product corticosterone and the end-product aldosterone are secreted by the cell in definite amounts. The exact amounts of both products cannot be easily determined. The amount present in the blood depends on the turnover rate besides the secretion rate. In the clawed toad, 4–6 ng/ml of corticosterone and 0.8–1.0 ng/ml of aldosterone were found under normal conditions. The C/A ratio in the blood serum is about 5. The release from interrenal preparations depends strongly on the medium composition. The less polar corticosterone needs a protein carrier to be released, while aldosterone is less dependent on it. Interrenals of the clawed toad produce under the defined conditions used in our laboratory 150–250 pg/min corticosterone while about 50–100 pg/min aldosterone is produced. The C/A ratio is mostly less than 3 which may show that the corticosterone secretion is reduced under the more artificial conditions described.

Stimulaltory signals can change the C/A ratio, because there are two main steps where the biosynthesis can be regulated. The first step is at the level of the 3 OH-steroid dehydrogenase converting pregnenolone, the second one is the 18-hydroxylation changing corticosterone to aldosterone. When the first step is influenced, a change of the C/A ratio is unlikely unless a limitation of the rate of the corticosterone

TABLE 3. Regulation of hormone production in the Amphibian interrenal cell

Biosynthesis	Regulatory steps	Effectors
		Stimulation
CHOLESTEROL		<10 nM
|		ACTH
PREGNENOLONE		AVT
| ———	3-OH-Steroiddehydrogenase	UROT. II
PROGESTERONE		
		>10 nM
		UROT. I
		ANG II
		Substance P
CORTICOSTERONE		Inhibition
		ANF
| ———	18-Hydroxylation	
		Modulation
ALDOSTERONE		minus: Met-enkephaline
		plus: Endorphin
		Adrenaline
Release: C/A	plus or const.-stimulation of 3-OH-SDH minus-stimulation of 18-Hydroxylase	

conversion occurs. The stimulation of the second step decreases the C/A ratio by increasing the aldosterone secretion (Table 3).

It is not known whether a change in the C/A ratio has any physiological impact. One assumption may be that aldosterone is less active in inducing glucose release by the liver but this is only supported by results on the specificity of the receptors in the liver and not by the amount of glucose produced.

There are two effective groups of peptides which stimulate the corticosteroid release [9]. The first group stimulates in low doses (less than 10 nM must be added for 5 min, total of 10 pM/ml in 1 ml). ACTH, AVT and urotensin II belong to this group (Figs. 5 and 6). The second group of peptides act only in higher doses (more than 10 nM for 5 min). Urotensin I, substance P and angiotensin II are representative of this group (Table 3). Some of the mentioned peptides may act on a paracrine way and shall be discussed in the

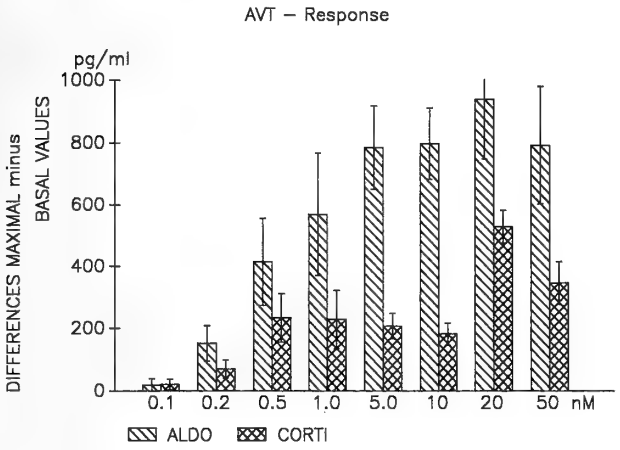

FIG. 5. Changes of corticosteroid release *in vitro* after addition of different doses of AVT. Differences in pg/ml between the highest value (ca. 30 min after addition) and the basal value before AVT. Abscissa nM AVT given for 5 min (=1 ml).

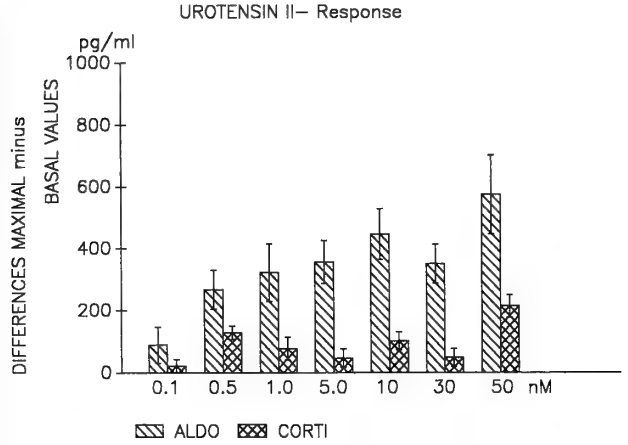

FIG. 6. Changes of corticosteroid release *in vitro* after addition of different doses of urotensin II. Differences in pg/ml between the highest value (ca. 30 min after addition) and the basal value before urotensin II. Abscissa nM urotensin II given for 5 min (=1 ml).

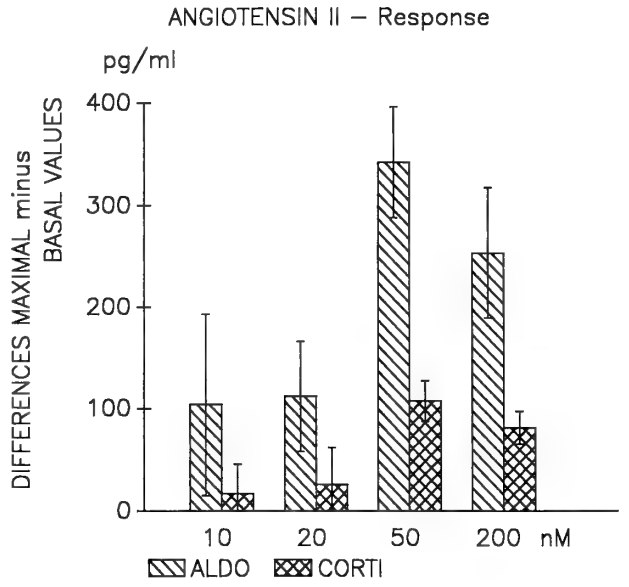

FIG. 7. Changes of corticosteroid release *in vitro* after addition of different doses of angiotensin II. Differences in pg/ml between the highest value (ca. 30 min after addition) and the basal value before angiotensin II. Abscissa nM angiotensin II given for 5 min (=1 ml).

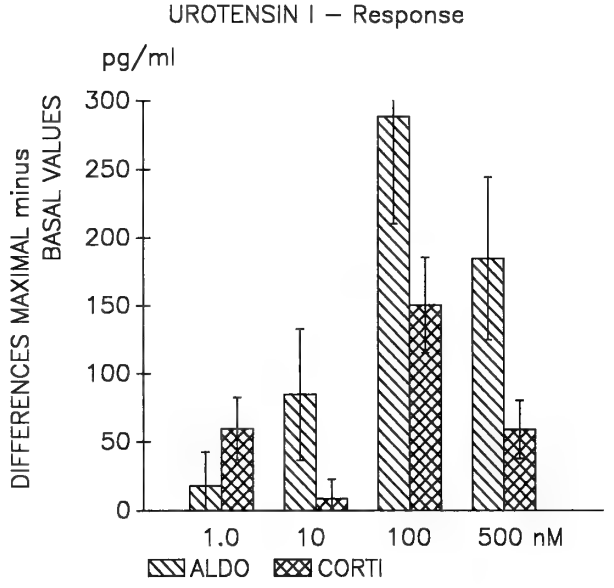

FIG. 8. Changes of corticosteroid release *in vitro* after addition of different doses of urotensin I. Differences in pg/ml between the highest value (ca. 30 min after addition) and the basal value before urotensin I. Abscissa nM urotensin I given for 5 min (= 1 ml).

next chapter (Figs. 7–9). In most of the experiments, the changes of aldosterone were larger than those of corticosterone.

1.2.2.2. Effects of paracrine factors

There is a lot of evidence that the adrenal gland, including the interrenal and the chromaffin tissue, contains a

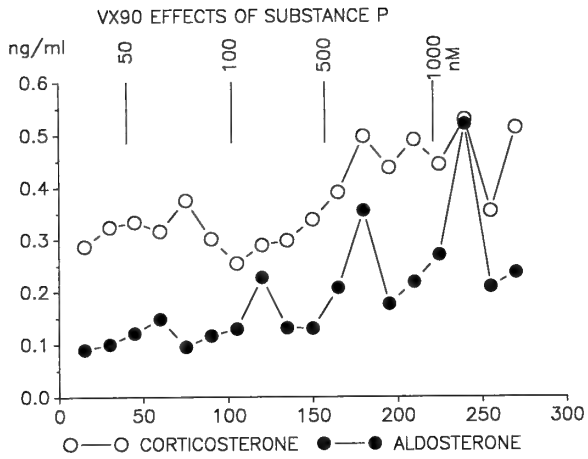

FIG. 9. Changes of corticosteroid release *in vitro* after addition of 4 different doses of substance P. Normal course for 5 hrs. The doses are given in 60 min intervals.

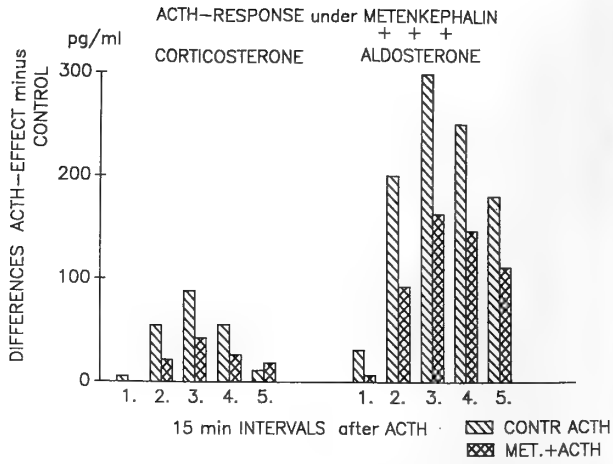

FIG. 10. Influence of 1 μM met-enkephalin on the response to ACTH. Comparison of the response of controls and experimentals with added met-enkephalin. 5 successive 15 min intervals are indicated.

high amount of different factors, peptides as well as catecholamines. Using immunohistochemistry, it has been shown that the gland of several anuran species contain opioid peptide, natriuretic peptides, tachykinines, substance P, angiotensins and others besides catecholamines [27, 28, 34, 35]. The peptide content of the adrenal gland of *Xenopus* has not been determined. Differences between the species certainly exist, because the gland of the water frogs contains Stilling cells which are not present in the gland of grass frogs or the clawed toad. Despite of not knowing which substances are produced in the *Xenopus* adrenal gland, it must be expected that several peptides can act on corticosteroid secretion.

The influence of several peptids and catecholamines has been tested on corticosteroid release from *Xenopus* interrenal preparation *in vitro*. Substance P has already been mentioned as stimulator in quite high doses, which suggests that paracrine application of low doses might be effective. Opioid peptides clearly modulate the steroid release. Met-enkephaline has no clear effects *per se,* but it reduces the response on ACTH. There is a very clear and significant reduction of the amount of aldosterone secreted under the stimulatory influence of ACTH (Fig. 10), when met-enkephalin is present. In the same type of experiment α-endorphin enhances the response on ACTH. Especially, aldosterone secretion is much larger, when α-endorphin is present at the time of stimulation (Fig. 11). In the same way, catecholamines may influence the corticosteroid release. It is difficult to find a direct effect on the secretion rate. For dopamine, inhibiton has been reported [30], but the situation is not yet clear. In the case of adrenaline, we found good evidence in our preparations that the release of corticosterone under the influence of ACTH was reduced. But, the aldosterone secretion rate stimulated by ACTH was higher when adrenaline was present. This effect would explain that adrenaline regulates the biosynthesis in such a way that stimulation of the more potent corticosteroid by ACTH is

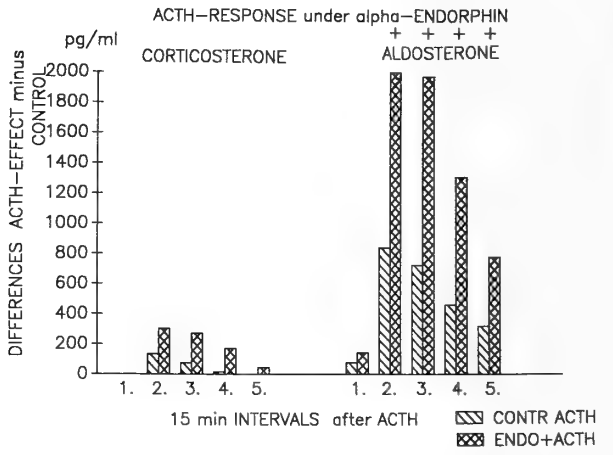

FIG. 11. Influence of 100 nM α-endorphin on the response to ACTH. Comparison of the response of controls and experimentals with added α-endorphin. 5 successive 15 min intervals are indicated.

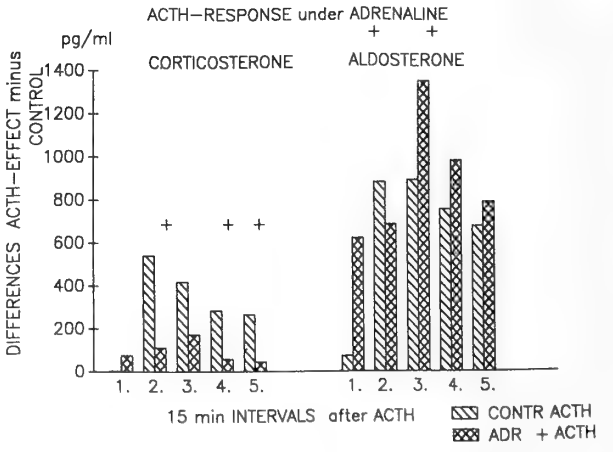

FIG. 12. Influence of 1 μM adrenaline on the response to ACTH. Comparison of the response of controls and experimentals with added adrenaline. 5 successive 15 min intervals are indicated.

more pronounced (Fig. 12) [7].

It is difficult to incorporate all these evidences for paracrine effects of peptides and catecholamines on corticosteroid production and secretion to the current picture for osmomineral regulation. But it can be concluded that all these factors are involved when the *Amphibia* are osmotically stressed.

1.2.2.3. Effects of electrolyte concentrations

Osmotic stress for the amphibians is mostly followed by changes of the osmotic and electroyte concentrations in the blood serum. It is well known, that clawed toads can be acclimated to 1.2% salt solution, to quite high concentrations of 500 mM urea, however only to about 300 mM mannitol. These three osmolytes act differently. Salt solution stimulates an increase of Na^+ concentration. Urea can penetrate into the animal and increase the osmotic value by accumulation of urea. Mannitol acts by desiccation which also increases the electrolyte levels.

It has been shown that after 3 weeks of acclimation a steady state has been reached when the three osmolytes are applied with 340 mOsm [17]. In all three cases the osmolality is increased to 340–380 mOsm instead of 230 mOsm. The Na^+ concentration is elevated from 110 mM to approximately 120–130 mM, and it is a bit higher in salt water acclimated toads. But, the urea content increases to 80 mM in the urea or mannitol treated toads in contrast to 10 mM which is characteristic for the clawed toad in tap water. The urea concentration reaches about 60 mM when the osmotic stress is due to 1.2% NaCl. Together with the level of Na^+ which is about 20 mM higher the same osmotic pressure is adjusted.

It is known from former experiments [37] that acclimation to 1.2% NaCl resulted in a strong increase of Na^+ within the serum till the higher production of urea after about 3 days joins the necessary increase of the osmotic value and allows a reduction of the Na^+ concentration. The electrolyte changes under osmotic stress suggest that there might be a correlation between changes of Na^+ or K^+ concentrations and steroid production. It has been shown that elevation of K^+ in the medium increases the corticosteroid release as well as reduction of Na^+ concentration in *Rana temporaria* [29]. To check the influence of Na^+ and K^+ concentrations in the surrounding medium more carefully in *Xenopus laevis* the following combination of *in vivo* and *in vitro* experiments were designed;

1. *in vivo*; The toads were kept in 1.2% sea salt solution (SW) (approx. 1/3 of sea water) or in 0.5% KCl solution. The electrolyte content and the corticosteroid concentration were followed for 3 days. The changes of glucose concentration were also determined to decide whether a stress like correlation is present.
2. *in vitro*; The interrenals were subjected to media with different Na^+ and K^+ concentrations and the direct influence was measured.

The results of the *in vivo* experiment are demonstrated in Figures 13–17. In 1.2% sea salt, the increase of the serum Na^+ concentration during 3 days is obvious. At the same time the K^+ level decreases but the effect is not statistically significant because of a large variation of the values. Sometimes haemolysis occurs which increases the K^+ concentration. In 0.5% KCl, a trend of increasing K^+ concentration is observed, while the Na^+ level is lowered. The opposite changes of Na^+ and K^+ levels under both acclimation conditions demonstrate that the levels of the both monovalent ions are inversely correlated (Figs. 13 and 14).

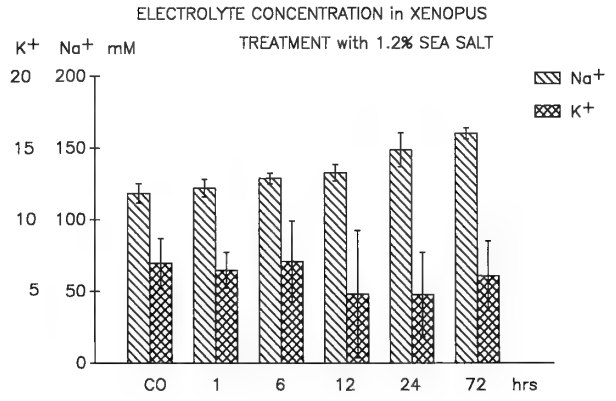

FIG. 13. Changes of serum electrolyte concentrations when the clawed toads are kept in 1.2% salt solution. Increase of Na^+ concentration and trend of decrease of K^+ levels are found.

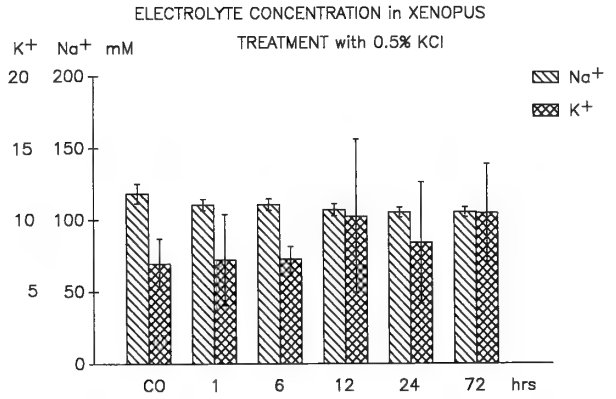

FIG. 14. Changes of serum electrolyte concentrations when the clawed toads are kept in 0.5% KCl solution. Increase of K^+ concentration and trend of Na^+ decrease are found.

At the same time glucose concentration increases reaching maximal levels at 12–24 hrs (Fig. 15). The glucose level is adjusted to normal after 72 hr, which indicates that the acclimation status is approached. The elevation of glucose is stronger in toads acclimated to 1.2% sea salt than those in 0.5% KCl. This may indicate that the higher concentration (1.2%) is more effective than the lower (0.5%). The type of the ions is not so important despite of the toxicity of high K^+ concentration.

The concentration of both corticosteroids is increased.

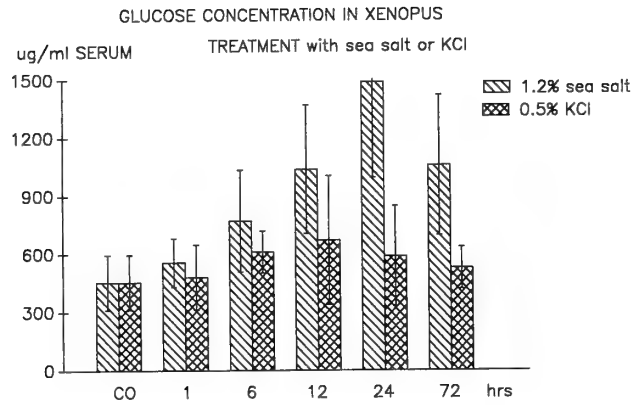

FIG. 15. Changes of the glucose levels in the serum of the clawed toads treated with 1.2% salt solution or 0.5% KCl.

Corticosterone is raised from about 4 mg/ml to 14 mg/ml after 24 hr of acclimation. It decreases afterwards to nearly normal levels after about 7 days (final values not indicated in Fig. 16). Aldosterone increases from less than 1 ng/ml to 2.5 ng/ml after 12 hr and reaches normal values after 3 days. The same trends are seen during acclimation to 0.5% KCl, but again the extent of the increase is smaller (Fig. 17).

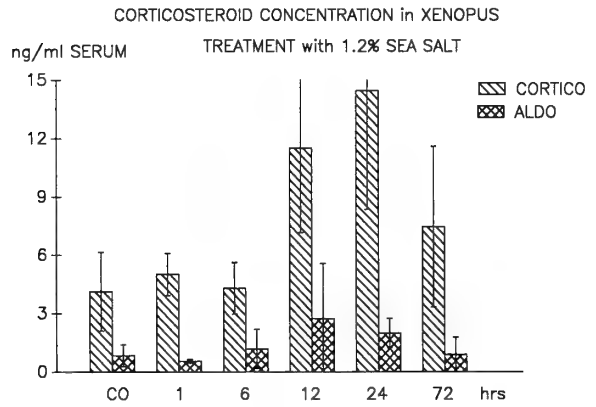

FIG. 16. Changes of the corticosteroid concentration in the serum of the clawed toads treated with 1.2% salt solution.

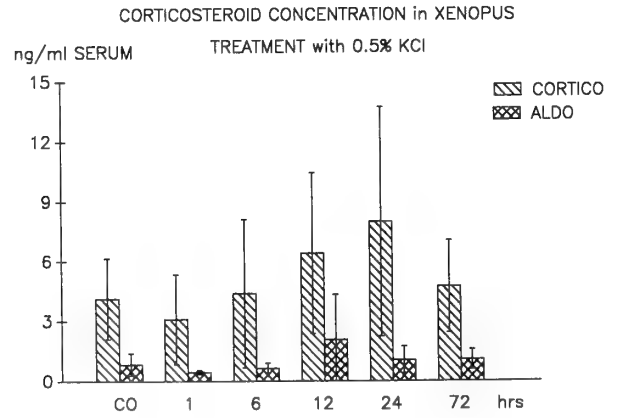

FIG. 17. Changes of the corticosteroid concentration in the serum of the clawed toads treated with 0.5% KCl.

In *in vitro* experiments, the Na^+ and K^+ concentrations of the media were changed. The normal medium contains 100 mM Na^+ and 4 mM K^+. This was changed to Na^+/K^+ 95/15, 90/20, 85/25, 78/35 mM. In all cases, corticosterone was not significantly changed. But the release of aldosterone increased when the Na^+ concentration was lowered and the K^+ level increased. The extent of the release depends on the concentration (Fig. 18).

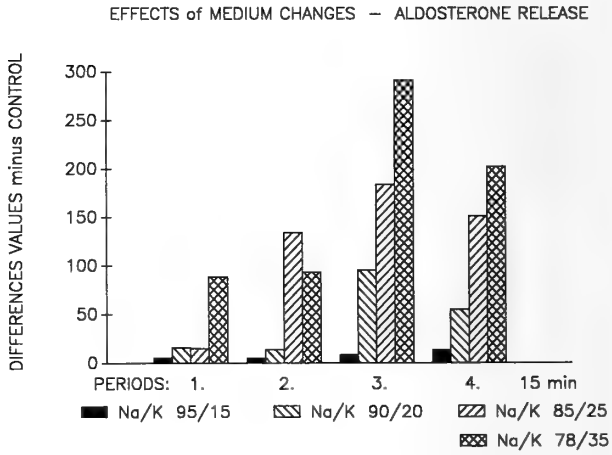

FIG. 18. Changes of aldosterone release from *in vitro* preparations of Xenopus interrenals after changes of the medium. The difference between the value after change minus the basal value is given for 4 periods of 15 min.

1.3. Role of the tissue derived peptides in osmoregulation

A very strong influence on osmoregulation comes from two tissue derived peptides, the effector of the renin-angiotensin system, angiotensin II, and the most important natriuretic factor, the atrial natriuretic peptide (ANF). Both peptides and systems are found in Amphibia and affect mainly the kidney function. Both systems have very often opposite effects and can be regarded as systems balancing excretion by the kidney. Generally, angiotensin II causes vasoconstriction and retention of sodium and water, while ANF promotes sodium secretion and diuresis. They also have opposite effects on the level of corticosteroid production. Angiotensin II stimulates the release of aldosterone. ANF is an inhibitor of aldosterone production. These effects are well known from mammals but there is also good evidence that similar effects occur in *Amphibia*.

1.3.1. Role of the renin-angiotensin system

Angiotensin II reduces primarily the glomerular filtration rate and increases blood pressure. Indirectly the urine production is reduced in Amphibia. The decrease of urine production after AII injection has been shown in *Bufo arenarum* [33]. Stimulatory influence on aldosterone and corticosterone secretion was demonstrated in *Rana ridibunda* [31] and *Rana temporaria* [11]. The situation within the clawed toad, *Xenopus laevis*, is complicated. Quite large

doses of AII are necessary to stimulate the corticosteroid release (Fig. 14). Binding sites for AII are found in the structure of the glomeruli of the kidney and at the adrenal tissue of *Rana temporaria* [25], but are only found at the glomeruli and not at the adrenals in *Xenopus*. This points to the fact that the aquatic living clawed toad does not respond as well to the renin-angiotensin system at the adrenal level [23]. The physiological significance for AII binding at the glomeruli in *Xenopus* can be seen when the animals are acclimated to 1.2% salt water. During acclimation a much higher binding capacity of AII at the glomeruli is found 12 hrs after the start of the experiment. The binding is reduced to normal levels, when the animals are acclimated for 7 days. It can be suggested that the amount of urine is reduced at the beginning of the salt water influence. When the acclimation is completed, the urine production returns back to normal.

1.3.2. Role of the atrial natriuretic peptide

Several natriuretic peptides are meanwhile found, but the atrial one is surely the most important of the Amphibia. In mammals, specific receptors have been found in the kidney and in the adrenal tissue (for reference see [20]). This suggests that ANF antagonizes the effects of AII and vasopressin in the main target organs. Frog cardiac extract has diuretic and natriuretic effects in rats. ANF binding sites in *Xenopus laevis* have been localized in the glomeruli and the adrenal tissue. The binding sites have been characterized with respect to specificity, association and dissociation constants etc. Again acclimation to 1.2% increases the amount of bound ANF in glomerular region. This does not fit into the picture of osmoregulatory influence and, therefore, the physiological significance of this is not clear[20, 24]. *In vitro* experiments measuring corticosteroid and catecholamine release from preparation of adrenal tissue, have shown that ANF clearly inhibits the release of corticosteroids. The secretion rate of catecholamines is not affected [22].

1.4. Role of catecholamines in osmoregulation

Hyperosmotic conditions of the environment are a very important stress situation for Amphibia. An important hormonal response *versus* stress is the increase of circulating catecholamines. In the case of most Amphibia, adrenaline is secreted in higher amounts than noradrenaline. There are several indications that these catecholamines are involved in osmoregulation. Firstly, it has been reported that catecholamines increase the uptake of Na^+ by the skin. But, this effect is not clearly analyzed. Secondly, glycogenolysis is induced by catecholamines. The process of osmoregulation depends on energy, provided by glucose the level of which increases in the blood after gluconeogenesis. Thirdly, there is a connection between catecholamine secretion from the chromaffin tissue and the stimulation of corticosteroid release from the interrenal cell. In this report, the effect of catecholamines on liver tissue and cells should be discussed. There are several papers dealing with the effect of adrenaline on liver pieces of *Xenopus* or axolotol [13, 15, 16]. These glycogenolytic effects of adrenaline in Amphibia are mediated by a β-adrenergic receptor mechanism which involves cAMP as mediator.

The same effects have been clearly elaborated using *Xenopus* hepatocytes. Adrenaline works via receptors which can be blocked by β-antagonist, e.g. propranolol. Noradrenaline is not effective. Forskoline, the stimulator of adenylate cyclase, is as effcetive as adrenaline [1].

The question how catecholamine and corticosteroid secretion affect each other has been often discussed. Influence in both directions, catecholamine stimulation of corticosteroid secretion and *vice versa,* is proposed in the literature. The aldosterone secretion of the interrenals of *Xenopus laevis* is significantly stimulated by adrenaline (Fig. 12) [7]. But, reduction of corticosteroid secretion by catecholamines has been found in *Rana ridibunda* [30]. On the other hand, stimulators of corticosteroid release in *Xenopus laevis,* like ACTH or AVT, induce an increase of catecholamine release [19].

All these findings indicate that catecholamines support the mechanisms of osmoregulation at different levels, the target organs, the metabolic support and effects at the level of the adrenal gland, the mixture of interrenal and chromaffin tissue.

2. Cooperation at the level of peripheral organs

The different hormonal systems discussed in the preceeding chapter act together at different target organs. The cooperation at the level of the hypophysis, the liver, the skin and the kidney shall be discussed briefly. Other targets like intestine and muscle may also be of interest in this respect.

Binding sites for ANF and angiotensin II have been found at the pituitary [26]. This suggests that these hormones cooperate with AVT and adenohypophysial hormones like ACTH. It is possible that ANF inhibits the release of AVT, because both hormones have opposite effects at the renal level. On the other hand, angiotensin II may modulate the release of nonapeptides from the pituitary. Both peptide systems act synergistically at the renal level.

Catecholamines, corticosteroids and nonapeptides act on the liver and stimulate at least the release of glucose. The mechanisms are different. Catecholamines induce gluconeogenesis via β-receptors. The effect of nonapeptides is mediated by cAMP and might be a V_2-receptor mechanism. It is not clear whether besides glycogenolytic also gluconeogenetic pathways are involved. Corticosteroids act on gluconeogenesis to elevate glucose release. In all cases glucose is provided to support the process with energy.

Nonapeptides induce water retardation by the skin and bladder. They also affect the glomerular filtration rate and reduce the urine volume. At the level of the skin, Na uptake is also stimulated by nonapeptides. The mechanism is not clear. These effects are in accordance with those of the corticosteroids on the skin. It has to be investigated if catecholamines support these actions. The mechanisms of these hormones at the the skin, bladder and glomeruli are still

not exactly known. It must be studied whether the mechanisms of the different hormones are similar.

REFERENCES

1 Ade T, Hanke W (1992) Proc Int Symp on Amphibian Endocrinology, Tokyo

2 Barker-Jorgensen C (1993) Comp Biochem Physiol 104A: 1–21

3 Bentley PJ (1971) Endocrines and Osmoregulation, Springer Verlag, Berlin, Heidelberg, New York

4 Boyd SK, Moore FL (190) Gen Comp Endocrinol 78: 344–350

5 Crabbé J (1963) Effects of adrenocortical steroids on active sodium transport by the urinary bladder and ventral skin of amphibia. In "Hormones and the Kidney" Memoirs Soc Endocrinol 13: 75–87

6 Crabbé J (1964) Endocrinology 75: 809–811

7 Gussetti C, Müller R, Hanke W (1993) Exp Clin Endocrinol 101: 111

8 Hanke W (1985) A comparison of endocrine function in osmotic and ionic adaptation in amphibians and teleost fish. In "The endocrine system and the environment" Ed by BK Follett, S Ishii, A Chandola, Springer Verlag, Tokyo, Berlin, pp 33–43

9 Hanke W (1990) Corticosteroid function: evoluionary aspects. In "Progress in Comparative Endocrinolgy" Ed by A Epple, CG Scanes, MM Stetson, Wiley-Liss, Inc., New York, pp 445–452

10 Hanke W, Janssens PA (1983) Gen Comp Enocrinol 51: 364–369

11 Hanke W, Maser C (1985) Regulation of interrenal function in amphibians. In "Current Trends in Comparative Endocrinology" Ed by B Lofts, WN Holmes, Honkong Univ Press, Honkong, pp 447–449

12 Henderson IW, Edwards BR, Garland HO, Chester Jones I (1972) Gen Comp Endocrinol, Suppl 3: 350–359

13 Janssens PA, Caine AG, Dixon JE (1983) Gen Comp Endocrinol 49: 477–483

14 Janssens PA, Grigg JA (1984) Comp Biochem Physiol 77C: 403–408

15 Janssens PA, Maher F (1986) Gen Comp Endocrinol 61: 64–70

16 Janssens PA, Grigg JA (1984) Gen Comp Endocrinol 67: 227–233

17 Katz U, Hanke W (1993) J Comp Physiol B 163: 189–195

18 Kloas W, Hanke W (1990) Gen Comp Endocrinol 80: 321–330

19 Kloas W, Hanke W (1990) Proc Soc Comp Endocrinol, Leuven, p 146

20 Kloas W, Hanke W (1992) Gen Comp Endocrinol 85: 26–35

21 Kloas W, Hanke W (1992) Gen Comp Endocrinol 85: 71–78

22 Kloas W, Hanke W (1992) Gen Comp Endocrinol 85: 269–277

23 Kloas W, Hanke W (1992) Gen Comp Endocrinol 86: 173–183

24 Kloas W, Hanke W (1992) Peptides 13: 297–303

25 Kloas W, Hanke W (1992) Peptides 13: 349–354

26 Kloas W, Hanke W (1992) Cell Tissue Res 267: 365–373

27 Larcher A, Delarue C, Idres S, Lefebvre M, Feuilloley M, Vandesande F, Pelletier G, Vaudry H (1989) Endocrinology 125: 2691–2700

28 Leboulenger F, Leroux P, Delarue C, Tonon MC, Charnay Y, Dubois PH, Coy DH, Vaudry H (1983) Life Sci 32: 375–384

29 Maser C, Janssens PA, Hanke W (1982) Gen Comp Endocrinol 47: 458-466

30 Morra M, Leboulenger F, Vaudry H (1990) Endocrinology 127: 218–226

31 Perroteau I, Netchitailo P, Homo-Delarche F, Delarue C, Lihrmann I, Leboulenger F, Vaudry H (1984) Endocrinology 115: 1765–1773

32 Pang PKT, Galli-Gallardo SM, Collie N, Sawyer WH (1980) Am J Physiol 239: R156–R160

33 Reboreda JC, Segura ET (1989) Comp Biochem Physiol 93A: 505–509

34 Reinecke M, Heym C, Forssmann WG (1992) Cell Tissue Res 268: 247–256

35 Rossier J, Dean MD, Livett BG, Udenfriend S (1981) Life Sci 28: 781–789

36 Rouillè Y, Michel G, Chauvet MT, Chauvet J, Acher R (1989) Proc Natl Acad Sci USA 86: 5272–5275

37 Shröck H, Hanke W (1979) Comp Biochem Physiol 63A, 393–397

ZOOLOGICAL SCIENCE 11: 15–31 (1994)

REVIEW

Neuropeptides in Neurosecretory and Efferent Neural Systems of Insect Thoracic and Abdominal Ganglia

DICK R. NÄSSEL[1], EMINE BAYRAKTAROGLU[2] and HEINRICH DIRCKSEN[3]

[1]*Department of Zoology, Stockholm University, S-10691 Stockholm, Sweden,*
[2]*Department of Biological Sciences, Middle East Technical University, Ankara, Turkey, and* [3]*Department of Zoophysiology, Rheinische Friedrich-Wilhelms-Universität, Bonn, FRG*

INTRODUCTION

Over the last ten years there has been a dramatic increase in the number of identified insect neuropeptides [38, 39, 55, 56, 63, 94]. Many of these peptides have been attributed biological actions in a variety of assays, and it is clear that insect neuropeptides play important roles in different regulatory processes involved in development, reproduction, diapause, metabolism, osmoregulation, muscle activity and behavior [38, 55, 56, 86, 90, 95, 105]. With the development of further bioassays and extensive testing of novel neuropeptides even in heterologous bioassays, it has become increasingly apparent that neuropeptides have more actions that those ascribed to them at the time of isolation [22, 56, 62, 94]. In fact, it may well be that it is a rule rather than an exception that neuropeptides have several functions and thus many names given to neuropeptides may become misleading as novel important functions are revealed.

Classically the isolation of peptides involved ablation of endocrine organs followed by reconstitution of regulatory functions by injections of purified "factors" extracted from these organs. Most insect neuropeptides have, however, been isolated with the aid of *in vitro* assays of actions on peripheral target organs. In either case it is likely that *in vivo* many physiological actions of these peptides are of hormonal nature. Hence, it is not surprising that a large number of insect neuropeptides have been demonstrated by immunocytochemistry in neurosecretory cells and neurohemal release organs [40, 66, 86]. In addition many of the same neuropeptides are present in central neurons and in endocrine cells of the gastro-intestinal tract (reviewed in Refs [18, 66, 94, 110]) indicating that also in insects peptides can act as neuromodulators and local neurohormones [80, 90]. Immunocytochemistry has proved to be a powerful technique for the localization of storage and release sites of both neuropeptides and other neuroactive compounds such as monoamines and amino acid transmitters. By now quite a number of neuropeptides have been mapped in the nervous and neuroendocrine systems of different insects and it is apparent that the complexity in peptidergic signalling is staggering [18, 66, 86, 94]. The number of known insect neuropeptide sequences by far exceed 100 [56, 66, 94]. Only from a single species of insect, *Locusta migratoria,* not less than 32 different neuropeptides have been isolated and sequenced as of mid 1993 and many more are under way [94]. Just a fraction of these have been mapped by immunocytochemistry and almost nothing is known about their receptors and physiological actions in the nervous system and at peripheral targets. For most peptides suspected to be acting as neurohormones it remains to demonstrated that they are actually released into the circulation.

Actions of neuropeptides can be assayed more conveniently at peripheral targets than in the central nervous system. To draw attention to possible peripheral targets for studies of peptide action, the present review focuses on neuropeptides in the neurosecretory and efferent systems of the thoracic and abdominal ganglia of insects, with special emphasis on blowflies. The distribution of neuropeptides in the insect brain [66] and intestine [110] has recently been reviewed.

ORGANIZATION OF INSECT NEUROSECRETORY SYSTEMS

Neurosecretory cells have been classified into a few main groups [86]: (i) neurosecretory cells with cell bodies in central ganglia and axon terminals in peripheral neurohemal organs or release areas, (ii) central neurosecretory cells with peripheral so called neuroeffector junctions (secretory-motorneurons and other efferents with peripheral innervation areas), (iii) central neurosecretory cells with arborizations ("neurosecretory endings") in neuropils of the central nervous system and (iv) peripheral neurosecretory cells with peripheral release sites. Some of this organization is illustrated in Figures 1 and 2.

The first type of neurosecretory cells are found in a few locations of the cephalic ganglia and in the subesophageal, thoracic and abdominal ganglia and send axons to neurohe-

Received August 25, 1993

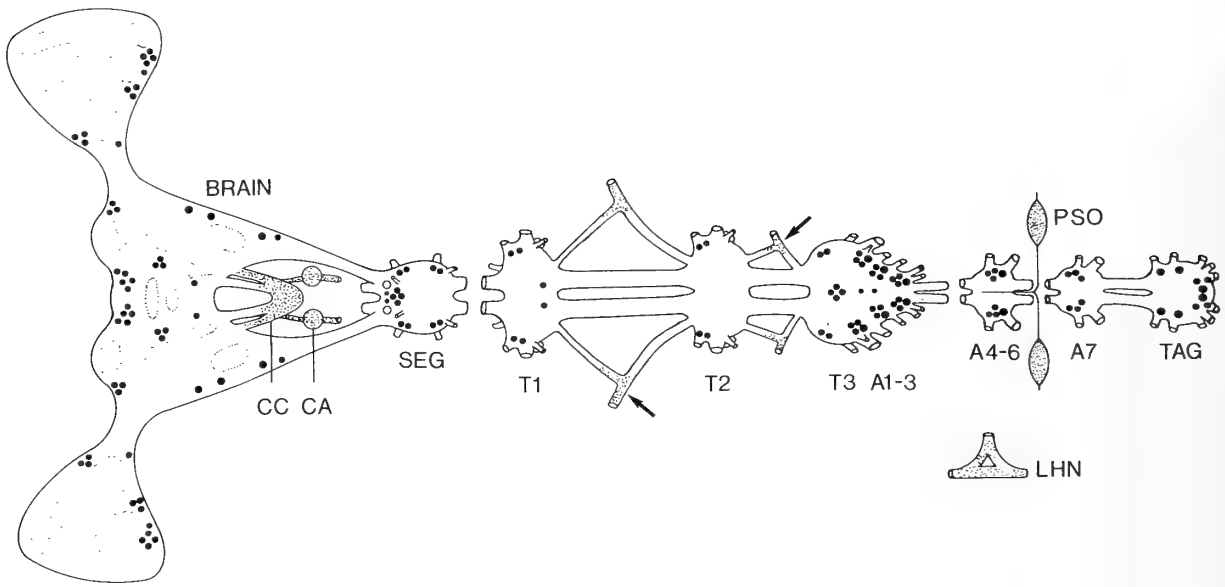

FIG. 1. Distribution of CCAP immunoreactive neurons (black circles) and some neurohemal areas (shaded) in the nervous system of the locust. The neurohemal areas are not drawn for all segments. Arrows point at neurohemal areas in junctions of nerves 1 and 6. Abbreviations: CC=corpora cardiaca, CA=corpora allata, SEG=subesophageal ganglion, T1–T3=thoracic ganglia, A1–A7=abdominal ganglia, TAG=terminal abdominal ganglion, PSO=perisympathetic organ, LHN=lateral heart nerve. From Dircksen *et al.* [19] with permission from Springer Verlag.

mal organs or release areas associated with these ganglia [86]. The cephalic neurosecretory cells supply axons to the neurohemal organs termed corpora cardiaca and corpora allata (Fig. 1) and in some insect species to neurohemal areas in the wall of the anterior aorta (see Fig. 4), in the so called antennal heart and at the surface of certain cranial nerves. The neurosecretory cells of the ventral cord supply segmental neurohemal organs, termed perisympathetic or perivisceral organs, located in the median and/or transverse nerves (Figs. 1–3). Other release sites of ventral cord neurosecretory cells are found in neurohemal areas in the pericardial septum of the abdominal aorta, the lateral cardiac nerve, the dorsal diaphragm and the intestine (Figs. 2, 3).

The "neurosecretory cells" with arborizations in central neuropil and the efferents with targets such as glands and different types of muscle were originally identified with classical neurosecretory staining methods (see Ref. [86]). Some of these cells have later been identified by immunocytochemistry as peptidergic and/or monoaminergic neurons. An example of this kind of cells is the pair of vasopressin immunoreactive neurons of the locust subesophageal ganglion with extensive arborizations restricted to the central nervous system and the core of some peripheral nerve roots [89, 100].

Peripheral neurosecretory cells have been found at several locations: in nerves (link nerves, connecting transverse and segmental nerves) of the thoracic and abdominal ganglia and in nerves associated with the heart and alary muscles and the intestinal tract [28, 86]. Neurosecretory cells have also been reported in the frontal and hypocerebral ganglia.

We shall be concerned here with the neurohemal release sites of the body segments only since the cephalic neurohemal organs have been more frequently dealt with in the literature [33, 40, 56, 86]. In the less evolved insects, such as the locust, the distinct segmental neurohemal organs associated with the dorsal median and transverse nerves are easily distinguished in the larval and adult stages [86] (Figs. 1, 2). In blowflies and other higher diptera, however, these neurohemal organs can only be clearly distinguished before metamorphosis in the larval stages [72] (see Fig. 10). In the adult flies the terminals of the neurosecretory cells are located in the dorsal neural sheath of the fused thoracic and abdominal ganglia [31, 68, 72] (Fig. 4). These "centralized" neurohemal structures represent the most evolved type of neurohemal perisympathetic organs associated with the ventral nerve cord of insects. Intermediate types of organs derived from median or transverse nerve types that anastomose with connectives or segmental nerves are found in hymentopterans, some coleopterans and orthopterans [32, 86].

NEUROPEPTIDES DEMONSTRATED IN THE THORACIC AND ABDOMINAL GANGLIA

Most insect neuropeptides known today have been isolated from whole heads, whole insects, dissected brains and corpora cardiaca-corpora allata complexes or from dissected entire nervous systems [39, 55, 63, 94, 97]. Some neuropeptides have, however, specifically been isolated from dissected thoracic-abdominal ganglia as is the case for some blowfly peptides: thirteen different FMRFamide-related peptides (FaRPs) and two callatostatins, peptides structurally closely related to the cockroach allatostatins [22, 24]. As

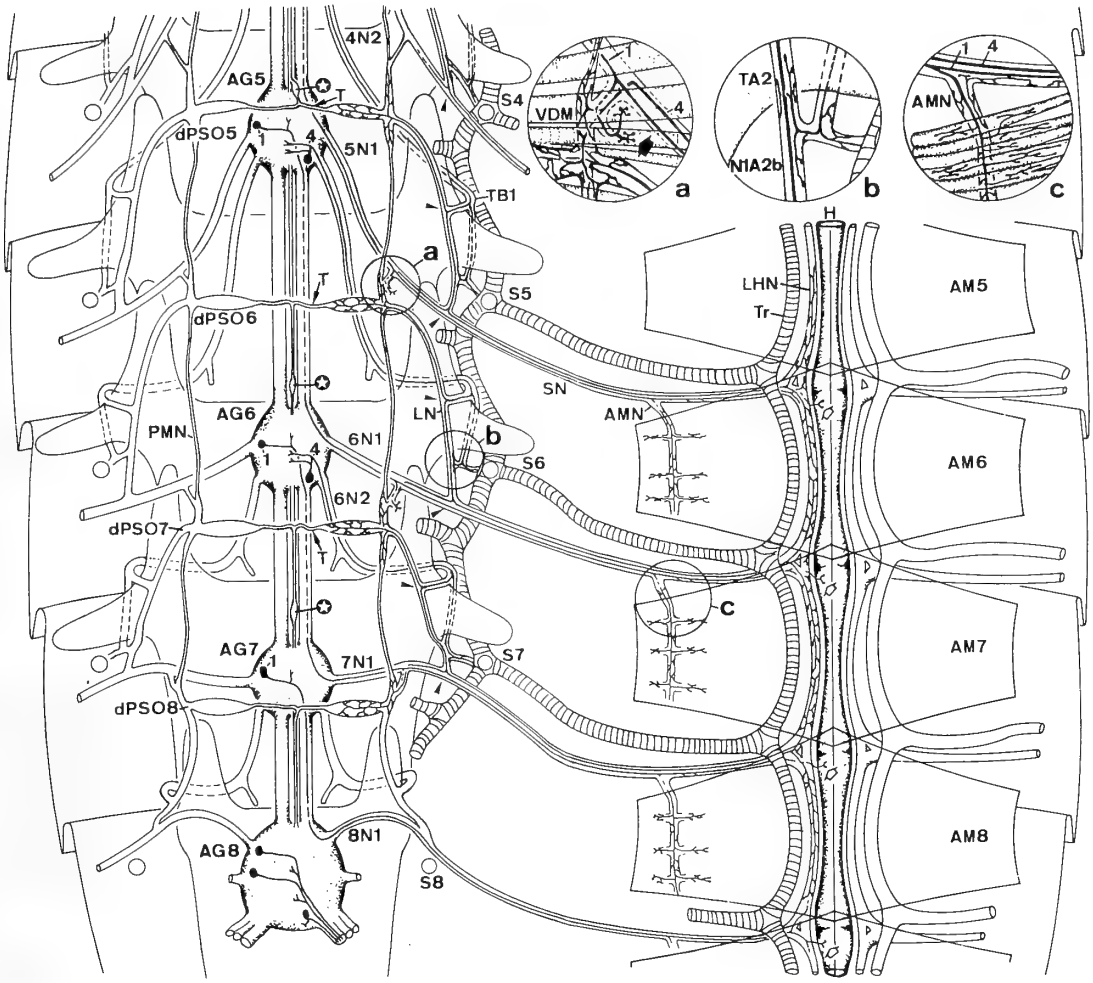

FIG. 2. Semischematic drawing of pathways of CCAP immunoreactive (CCAP-IR) neurons and neurohemal release sites in the locust abdomen. Of interest here are the segmentally repeated neurons 1 and 4 which send axons to segmental nerves 1 and 2 (N1 and N2). From these nerves CCAP-IR supply terminals to neurohemal distal perisympathetic organs (dPSO 5–8), to stigmata of tracheal system (S4–8; *inset circle b*), ventral diaphagm muscles (VDM; *inset circle a*), alary muscles (AM5–8; *inset circle c*) and lateral heart nerve (LHN). No CCAP-IR fibers were seen in median PSOs (asterisks). This drawing is useful as a basis for the organization of primitive and segmental neurohemal structures in insects. Many of these structures are fused in the higher dipteran insects. From Dicksen *et al.* [19] with permission from Springer Verlag.

indicated by immunocytochemistry it appears that most peptides isolated from whole insects, whole heads, whole CNS or dissected brain-corpora cardiaca are present in the ventral cord ganglia. The neuropeptides indicated by immunocytochemistry in the thoracic-abdominal ganglion of blowflies (*Calliphora vomitoria* and *Phormia terraenovae*) are listed in Table 1. In other insect species the presence of some additional native neuropeptides have been indicated in the ventral ganglia by immunocytochemistry. In *Locusta migratoria*: crustacean cardioactive peptide (CCAP) [19], locustamyotropin [94]; male accessory gland myotropin [81], ovary maturating neurohormone [89]. In cockroaches: proctolin [25, 80], leucokinins [70]. In moths: pheromone-biosynthesis-activating neuropeptide (PBAN) in *Helicoverpa zea* [43] and eclosion hormone in *Manduca sexta* larvae [103]. It should be noted that the above mentioned neuropeptides are commonly found not only in neurosecretory cells, but also in different types of interneurons of the thoracic and abdominal ganglia (Table 1). In addition proctolin has been demonstrated in motorneurons [80] and leucokinin in putative sensory neurons (intestinal stretch receptors) [70].

GENERAL ORGANIZATION OF THORACIC-ABDOMINAL NEUROSECRETORY SYSTEMS AND NEUROHEMAL ORGANS AND RELEASE SITES

Before turning to the neurosecretory systems of the fused ventral cord of higher Diptera it may be useful to present the organization of the less evolved neurosecretory system of the locust where the segmental peptidergic neurons and neurohemal structures are clearly discernible. The

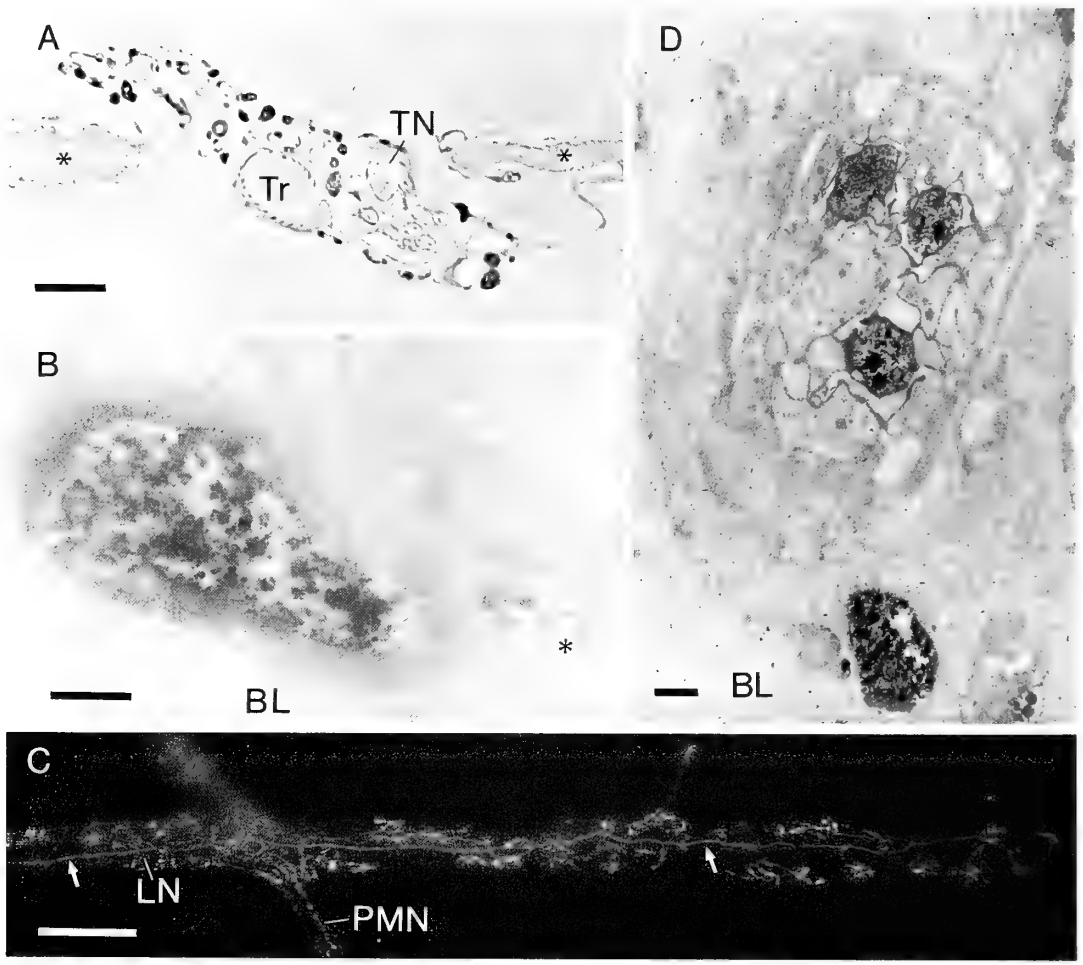

FIG. 3. CCAP immunoreactive structures in sections and whole mount preparations of *Locusta migratoria*. **A.** labeled semithin cross-section through seventh distal perisympathetic organ (dPSO7), showing axon profiles and terminals. Note lack of label in motor axons of the transverse nerve (TN); Ventral diaphragm muscles are labeled by asterisks. Tr= trachea. **B.** Axon terminal in a dPSO7 containing neurosecretory granules (pre-embedding immunocytochemistry; peroxidase labeling). Note unlabeled axon profile (asterisk). BL=basal lamina. **C.** *In situ* whole mount immunofluorescence preparation of a dPSO5 showing and axon originating in the link nerve (LN; arrow) that gives rise to fine terminals at the surface of the dPSO and the paramedian nerve (PMN). **D.** Cross section through the neurohemal lateral heart nerve showing three labeled central axons and axon profiles next to the surface of the nerve. Note the granule contents of almost all profiles. BL=basal lamina. Scales: A=10 μm, B=500 nm, C=100 μm, D=500 nm.

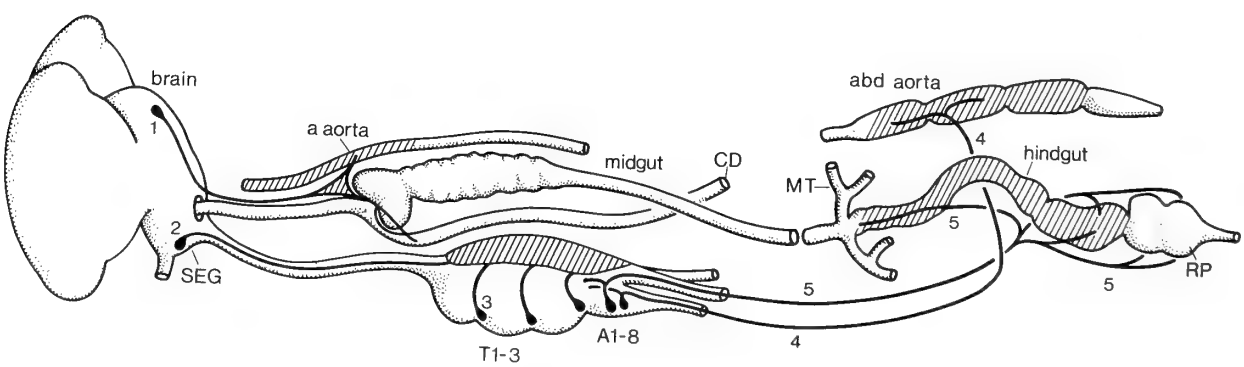

FIG. 4. Schematic dissected view of the nervous system, intestinal tract and aorta of the blowfly. The cross hatched areas are putative release sites of peptidegic neurons. In most cases these areas probably represent neurohemal release sites. Release sites are found in the anterior aorta (a. aorta), corpora cardiaca (triangular cross hatched structure below anterior aorta), dorsal sheath of thoracic-abdominal ganglion (T1–3, A1–8), pericardial septum at posterior aorta (abd aorta) and hindgut. Cell bodies (filled circles; not accurate numbers) of neurons are shown in one hemisphere only. The systems displayed are (1) protocerebral neurosecretory cells with axons to corpora cardiaca, anterior aorta and crop duct (CD); (2) subesophageal system (serotonergic) with axons to thoracic-abdominal dorsal neural sheath and several other targets not shown here; (3) thoracic system with terminals in dorsal neural sheath; (4) Lateral abdominal system with axons to pericardial septum of abdominal aorta; (5) median abdominal system with axons to hindgut and sometimes rectal pouch (RP) and its papillae. MT=Malpighian tubules. SEG=subesophageal ganglion.

TABLE 1. Neuropeptides indicated in the blowfly thoracic-abdominal ganglia[1]

Antisera to	native neuropeptide[2]	distribution
FMRFamide	*CalliFMRFamide 1–13*	IN, NC, EF
pigment-dispersing hormone	PDH-like[3]	IN, EF
proctolin	proctolin[4]	IN, NC, EF, MN
leucokinin I	leucokinin-like	IN, NC
locustatachykinin I	*locustatachykinin-like*[5]	IN
crustacean cardioactive peptide	CCAP-like	EF, IN
corazonin	corazonin-like	IN
allatostatin	*Callatostatins 1–5*	EF[6]
adipokinetic hormone	AKH-like or AKH$^{4-10}$-like[7]	IN, EF, NC?
myomodulin (*Aplysia*)	locustamyotropin-like[7]	NC
galanin (mammalian)	?	IN, NC
galanin message associated peptide	?	IN, NC, EF
enkephalins (mammalian)	?	IN, NC
substance P (mammalian)	? (not locustatachykinin-like)	NC
gastrin/CCK (mammalian)	FaRPs or drosulfakinin-like	IN, NC

Abbreviations: IN=interneurons, NC=neurosecretory cells, EF=efferent neurons, MN=motorneurons

1. Literature references in text. Further neuropeptides have been indicated in ganglia of *Drosophila* (see text)
2. The native peptides in italics have been isolated from *Calliphora*. Others are suggested by analogy with peptides isolated from other insect species.
3. Strong indication for peptide homologous to PDH in *Calliphora* (partial sequence obtained).
4. Proctolin isolated from different arthropods so far is identical (see Ref. [66])
5. Peptides with strong sequence homologies to locustatachykinins have been isolated from *Calliphora* (Lundquist, Holman, Nichols, Nachman, Clottens, Nässel, in press)
6. In *Drosophila* allatostatin immunoreactivity was detected in neurons and neurosecretory cells throughout the CNS.
7. See Schools et al. (Ref. [94])

schematic diagram of Figure 2 highlights the morphology of two types of typical segmental peptidergic neurosecretory cells with terminals in peripheral neurohemal organs. These are the CCAP-immunoreactive (CCAP-LI) type 1 and type 4 neurons of the locust (*L. migratoria*) abdominal ganglia described by Dircksen *et al.* [19]. Terminals of these neurons occur in the distal perisympathetic organs, the lateral heart nerves and the alary muscles associated with the dorsal diaphragm (Figs. 2, 3). Electron microscopy of the CCAP-LI terminals show that they contain large granular vesicles typical of neurosecretory neurons [19] as shown in Figure 3B. The Type 1 and 4 neurons reach the periphery *via* the lateral segmental nerves (N1, N2) of the abdominal ganglia, which is also the case for segmental leucokinin-like immunoreactive neurons [20]. Other putative neurosecretory cells of the locust have axons running dorsally *via* the perisympathetic organs in the median and transverse nerves to the peiphery: locustamyotropin-, FMRFamide- and pancreatic polypeptide-like immunoreactive neurons [27, 60, 94].

In the adult blowfly there are two major neurohemal release sites in the body segments (Fig. 4). One is located in the neural sheath of the dorsal part of the fused thoracic-abdominal ganglion and may correspond to the neurohemal organs of the median and transverse nerves mentioned above. The other is in the pericardial septum or dorsal diaphragm surrounding the abdominal aorta, possibly corresponding to the release sites in the lateral heart nerve and alary muscles of the locust.

NEUROPEPTIDES IN THE NEUROHEMAL AREA IN THE DORSAL NEURAL SHEATH OF THE BLOWFLY THORACIC-ABDOMINAL GANGLION

Although neurohemal areas were known in the neural sheath of thoracic-abdominal ganglia of higher diptera [2, 31], the full extent of the release area in the blowfly neural sheath was first recognized when serotonin immunoreactive (5-HTIR) terminals were revealed in *Calliphora* by immunocytochemistry [68]. The 5-HTIR fibers supply the entire dorsal surface of the thoracic-abdominal ganglion (see Fig. 6D) and also the neural sheath of many of the nerve roots of the ganglion. It was found that these arborizing 5-HTIR fibers are derived from four large neurons in the subesophageal ganglion [68], earlier shown to supply fibers to the neural sheath of ventral nerve roots of the subesophageal ganglion [67]. Later it became apparent that the dorsal neural sheath of the blowfly and fruitfly thoracic-abdominal ganglion also is the termination area of different systems of peptide containing neurons (Figs, 5, 6A, C, Table 2). The first system to be outlined in some detail is formed by six large gastrin/cholecystokinin-like immunoreactive (CCK-LI) ventral neurosecretory cells forming an extensive plexus of fibers in the dorsal sheath of *Calliphora* [65, 72]. This CCK-LI system formed by the ventral thoracic neurosecretory cells

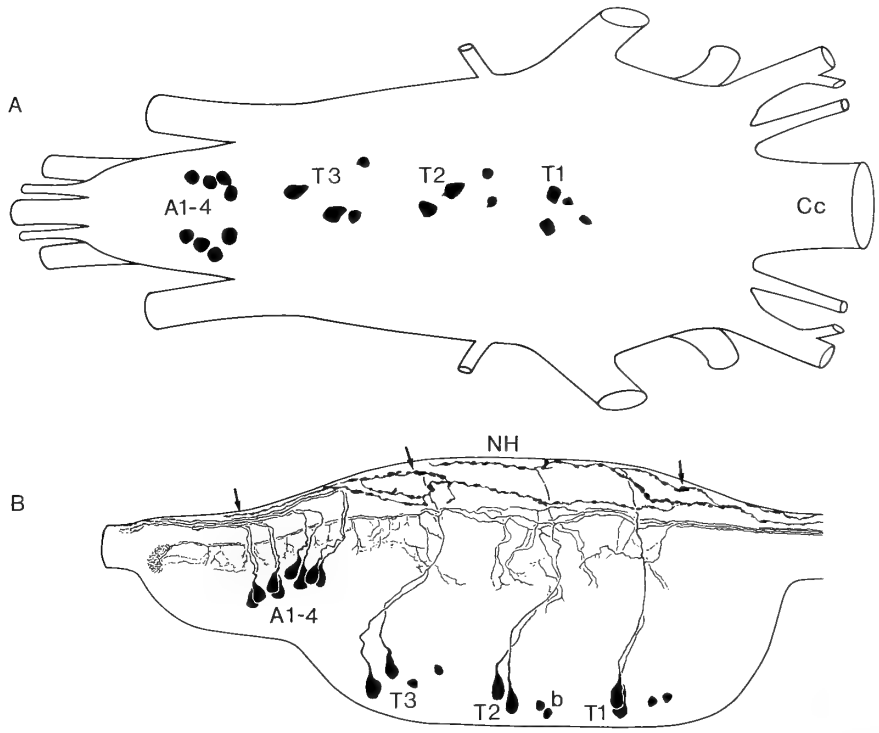

FIG. 5. Myomodulin-like immunoreactive neurons (neurosecretory cells) in the fused thoracic-abdominal ganglion of the adult blowfly. **A.** Ventral view of immunoreactive cell bodies. The six large VTNCs are located in the thoracic neuromeres (T1–3). Four pairs of VANCs are found in the abdominal neuromeres (A1–4). Cc=cervical connective. **B.** Sagittal view of the ganglion displaying the same neurons with their processes. Note terminals in the neurohemal release area dorsally in the neural sheath (NH and arrows). Immunoreactive processes are also found in central neuropil and in axons projecting to the subesophageal ganglion *via* the cervical connective. From Nässel *et al.* [74] with permission.

TABLE 2. Neuropeptides in neurons and neurohemal areas of blowflies

Putative release site	Location of cell bodies Thoracic neuromeres (T1–3)	Abdominal neuromeres
hindgut		proctolin, FaRPs, PDH, CCAP, CavAS
pericardial septum area	GMAP[1]	proctolin, FaRPs, LK, LVP
thoracic neurohemal area	FaRPs, SP, MM, GAL	
abdominal neurohemal area		MM, FaRPs[2]
fibers in thoracic-abdominal nerves	AKH[1], GAL/GMAP[1]	proctolin, FaRPs, LK, LVP

Abbreviations: FaRPs=FMRFaminde related peptides, PDH=pigment dispersing-hormone-like peptide, CCAP=crustacean cardioactive peptide, CavAS=callatostatins, LK=leucokinin-like peptide, GMAP=galanin message associated peptide-like peptide, LVP=lysine vasopressin-like peptide (?), SP=substance P-like peptide, MM=myomodulin-like peptide, GAL=galanin-like peptide, AKH=adipokinetic hormone-like peptide

1. The location of the cell bodies is not clear.
2. The "specific" FMRFamide antisera raised in Guinea pig do not label these cells

(VTNCs) was studied in more detail and turned out to be immunopositive with a number of antisera to non-insect peptides: bovine pancreatic polypeptide, CCK, methionine enkephalin, methionine enkephalin-Arg-Phe [21], FMRFamide, molluscan small cardioactive peptide (SCP_B) (Fig. 6), substance P [50] and the molluscan peptide myomodulin [74] (Fig. 5). It is likely that the VTNCs contain peptides of the CalliFMRFamide series which have been isolated from *Calliphora* thoracic-abdominal ganglia [22] and it is possible that many of the antisera listed above cross react with different epitopes of the CalliFMRFamides. In *Drosophila* the homologs of the VTNCs can also be identified by antisera against FMRFamide [50, 106, 109]. Several FMRFamide-related peptides (FaPRs) have been isolated from *Drosophila* tissue or deduced from isolated cDNAs [64, 75-77, 92] and the FaRPs appear to be the products of three different genes [76]. It was shown by *in situ* hybridization histochemistry that the message encoding one of the FMRFamide precursors is expressed in the *Drosophila* VTNCs [78, 93]. In addition to FaRPs it is possible that the VTNCs contain colocalized

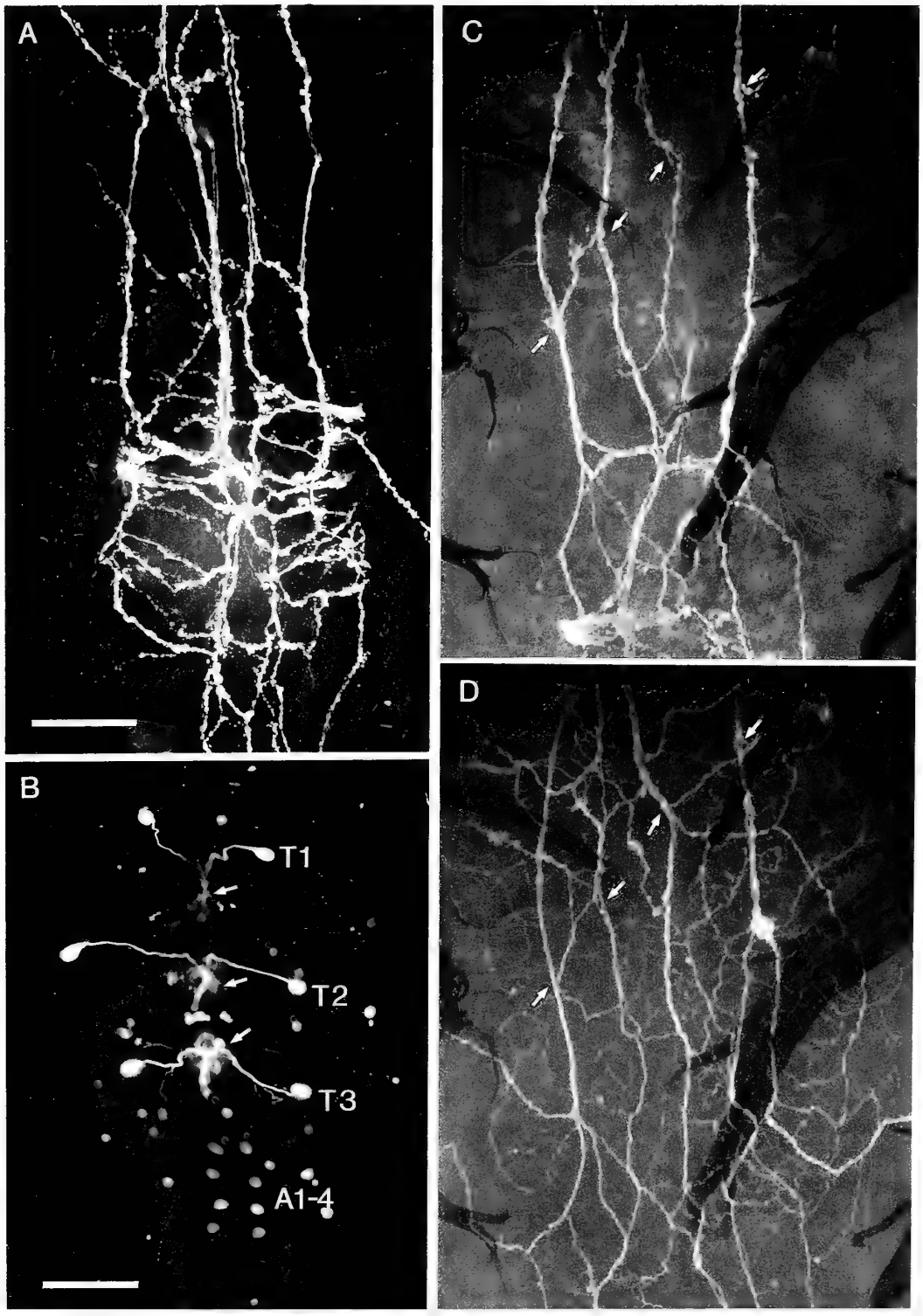

FIG. 6. Fluorescence micrographs of thoracic-abdominal neurons in wholemounts of the blowfly. **A.** The neurohemal plexus in the dorsal neural sheath of the thoracic-abdominal ganglion labeled with monoclonal antibody to SCP_B. **B.** The six cell bodies (T1–3) and segmental neurohemal release sites (arrows) of the VTNCs of a pupal blowfly (48 h pupa). At this stage the segmental organization of the release sites is still apparent. Antiserum to SCP_B. **C and D.** Double labeling of the same wholemount with antisera against FMRFamide (**C**) and serotonin (**D**) viewed with filters for fluorescein (FITC) and Texas red (using biotin-streptavidin detection). The fibers in the FMRFamide immunoreactive plexus are closely adjacent to the serotonergic plexus (see arrows for correlation) along the ganglion midline. Scales A, C, D = 50 μm; B = 100 μm.

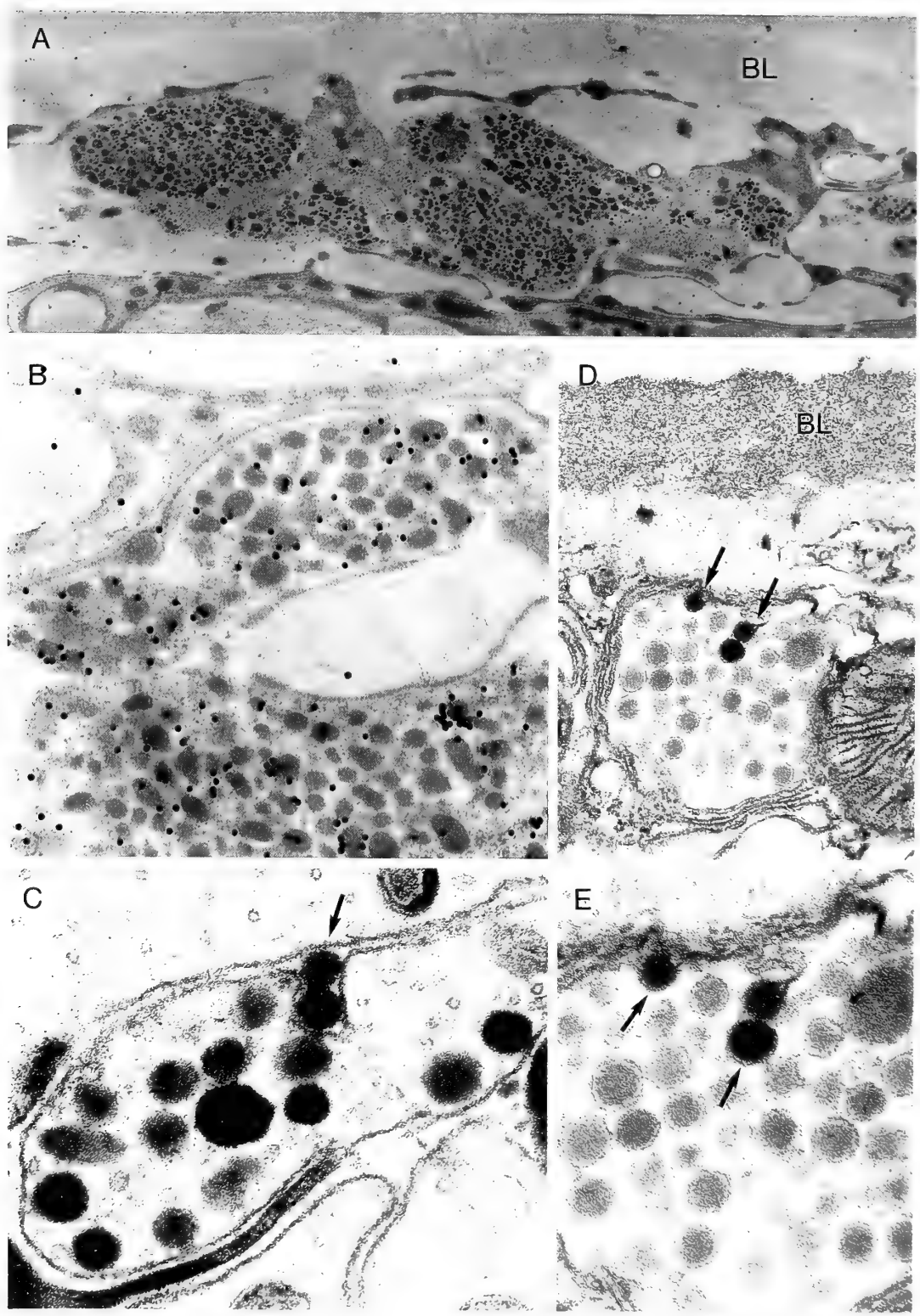

FIG. 7. Electron microscopy of peptidergic terminals in the dorsal neural sheath of the thoracic-abdominal ganglion of *Calliphora*. **A.** Immuno-gold labeling to display cluster of FMRFamide immunoreactive terminals in the sheath just below the acellular basal lamina (BL). **B.** Detail in higher magnification of FMRFamide immunoreactive terminals with large granular vesicles. **C.** Conventional electron microscopy of exocytotic profile (arrow) in one of the peptidergic terminals in the sheath. Two peptidergic vesicles are being released. **D and E.** With the TARI method exocytosis is more easily detected. Here three vesicles (arrows) are being released by a peptidergic terminal. With the TARI method the exocytosing vesicles become osmophilic and hence stand out (arrows in **D**). BL = the acellular basal lamina. E is a higher magnification of terminal in D. Magnifications: A = 14.000×, B = 46.000×, C = 86.000×, D = 36.000×, E = 72.000×.

peptides related to substance P and myomodulin (or locustamyotropins). A recent study of larval and adult *Drosophila* has indicated the presence in the VTNC homologs of peptides reacting with antisera to *Manduca* allatotropin and allatostatin [111]. The same authors showed similar cells with terminals in the dorsal neurohemal area reacting with antisera to *Bombyx* PTTH and *Manduca* diuretic hormone.

The peptidergic neurohemal plexus formed by the VTNCs is not as extensive as the one formed by the 5-HTIR cells. The plexus of the VTNCs is restricted to a median portion of the sheath of the dorsal thoracic-abdominal ganglion, whereas the 5-HTIR plexus covers the entire dorsal surface (Fig. 6C, D). Double labeling experiments with 5-HT- and FMRFamide- or SCP_B antisera revealed that the fibers of the VTNCs and the 5-HTIR fibers are located adjacent to each other in the plexus of the median region of the dorsal neural sheath (Fig. 6C, D).

The VTNCs also arborize extensively within the thoracic neuropils (Fig. 5) and each cell sends an axonal process anteriorly to the subesophageal ganglion [50]. It has not been determined whether any of the arbors represent input regions of the neurons. The possibility exists that the dendritic arbors of the VTNCs were not immunolabeled, by analogy with the vasopressin-like immunoreactive neurons of the locust subesophageal ganglion where the exclusion of such immunostaining was determined by intracellular dye injection [100].

Additional neurosecretory cells forming terminals in the dorsal neural sheath are found in the abdominal ganglion. Most clearly this was seen for ventral abdominal neurosecretory cells (VANCs) labeled with an antiserum to the molluscan neuropeptide myomodulin [74] (Fig. 5). Myomodulin [15] shares the C-terminus -RLamide with the locustamyotropins I-IV [94] and probably the myomodulin antiserum recognizes native blowfly peptide(s) of myotropin type. Therefore it is not surprising that in the locust locustamyotropin antiserum labels abdominal neurosecretory cells with terminals in median nerve perisympathetic organs [94]. In *Calliphora* and *Phormia* double labeling experiments with antisera to myomodulin and FMRFamide (raised in Guinea pig) and SCP_B reveal that the myomodulin immunoreactive VANCs in the abdominal ganglion, do not contain epitopes recognized by the SCP_B and the more specific FMRFamide antiserum. A dense myomodulin-like immunoreactive plexus extends over the entire abdominal portion of the neural sheath, whereas in the same specimens the plexus labeled with SCP_B or FMRFamide antisera is more insignificant in the abdominal portion. Thus it is possible to determine that most of the peptide containing fibers in the most caudal portion of the neurohemal plexus in blowflies are derived from the abdominal neurosecretory cells. A separate plexus of fibers in the thoracic-abdominal sheath derived from cell bodies distinct from the VTNCs was labeled with an antiserum against the mammalian neuropeptide galanin [51].

The only substance that so far has been shown to be released from the thoracic-abdominal ganglion of *Calliphora* by high potassium depolarization is serotonin; the likely role of the released serotonin is to induce secretion in the salivary glands [101]. No experimental evidence for peptide release from thoracic-abdominal neurohemal areas are available for blowflies, but the peptide immunoreactive terminals in the neural sheath are located outside the blood brain barrier [21, 72] (Fig. 7), like the serotonergic terminals [68]. For indirect demonstration of peptide release we applied the tannic acid ringer incubation (TARI) method [7] on living ganglia *in vitro* to augment the detection of exocytosis (diagnostic of release) in peptidergic terminals in the sheath of the thoracic-abdominal ganglion. The dissected ganglia were left in a dish with 0.5% tannic acid in insect saline for 2 hr followed by fixation in glutaraldehyde and osmium [3]. The TARI method renders the core of extruded peptidergic vesicles osmophilic (Figs. 7D, E) which facilitated the detection of numerous exocytosis profiles in peptidergic fibers of the *Calliphora* thoracic-abdominal neurohemal release site (cf. Fig. 7C).

What are the actions of neurohormones released from the neurohemal area in the thoracic-abdominal ganglion? It is presumed that the serotonin released from this area induces fluid secretion in the blowfly salivary gland [10]. It is also known that serotonin can induce diuresis and modulate activity of heart, visceral and oviduct muscles [13, 14, 54, 58]. For the FaRPs some clues have been obtained from *in vitro* studies on *Calliphora* salivary glands: three of the CalliFMRFamides induce fluid secretion in the salivary glands [22]. If this action is physiological it is likely that the peptide(s) reach the salivary glands *via* the circulation like serotonin does. Duve *et al.* [23] have also demonstrated that two of the CalliFMRFamides increase the spontaneous activity of the abdominal heart. Since a direct innervation of the abdominal heart has been demonstrated (see below), it is not clear whether hormonally released peptide is involved in this action. The FaRPs, if released into the circulation, can reach a whole host of peripheral targets all of which need to be tested for their response.

PEPTIDES IN THE NEUROHEMAL AREA IN THE PERICARDIAL SEPTUM OF THE BLOWFLY

The organization of the neurohemal area of the pericardial septum (dorsal diaphragm) was first described in the stable fly by electron microscopy [57]. The first identified neurons innervating this neurohemal area were detected in the blowfly with antiserum against the cockroach myotropic peptide leucokinin I [10]. The leucokinin-like immunoreactive (LK-LI) fibers reach the septum *via* the segmental abdominal nerves and are derived from a set of about 20 cell bodies in the abdominal ganglion (Figs. 4, 8A, 9A, B). These cell bodies also form central processes within the median portion of the abdominal neuropil. It is likely that these central processes represent release sites within the neuropil, but it cannot be excluded that they also receive synaptic inputs in this region. Interestingly the cell bodies

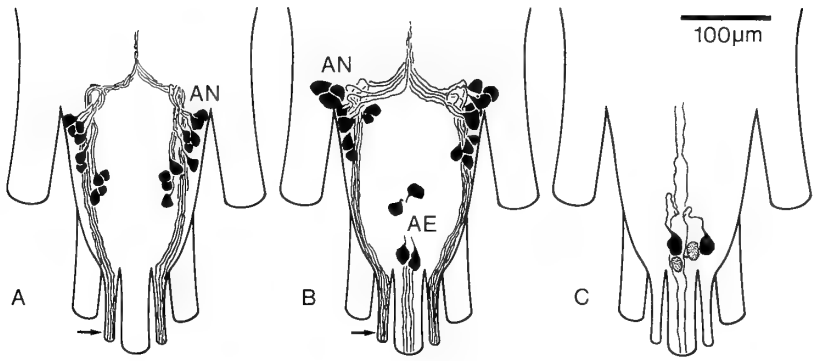

FIG. 8. The abdominal portion of the blowfly thoracic-abdominal ganglion with efferent peptidergic neurons. **A.** Antiserum to leucokinin I labels about 20 neurons (AN) with axons to pericardial septum (altered from [10]). **B.** Antiserum to proctolin labels a similar (but not identical) set of 20 efferents with axons to the pericardial septum and a set of four caudal abdominal efferent neurons (AE) with axons to the hindgut (altered from [69]). **C.** An antiserum to CCAP labels four cells posteriorly in the abdominal neuromeres. At least two of these send axons to the hindgut (Nässel and Dircksen, unpublished).

and fibers of the 20 LK-IR efferents could also be immunolabeled with an antiserum to lysine vasopressin [71]. Similar abdominal LK-LI efferents in the cockroach *Leucophaea maderae* were also found lys-vasopressin immunoreactive [70] (see also Ref. [17]). The native blowfly peptide(s) related to the cockroach leucokinins have not yet been isolated, but radioimmunoassays of blowfly tissue extract indicate the presence of leucokinin-immunoreactive material that eluted in HPLC in two zones, one of which has the same retention time as synthetic leucokinin I [53]. The biological actions of leucokinin-related peptides in blowflies are not known. Although present in fibers in the lateral cardiac nerves of *L. maderae* [70], none of the leucokinins are cardioactive in this cockroach [39]. Possibly these peptides are instead released in into the circulation *via* the pericardial septum in *L. maderae* and blowflies, and have targets elsewhere. Clues to such targets have been obtained from studies of the actions of some of the leucokinins and achetakinins in some other insects by *in vitro* assays. It is clear that apart from myotropic actions of the leucokinins at the cockroach foregut, hindgut and oviduct [39], some of the achetakinins and leucokinins can regulate fluid secretion in the Malpighian tubules of the mosquito *Aedes aegypti* and the cricket *Acheta domesticus* [30, 35]. It is to be expected that the leucokinin-related peptides from different insect species have diverse physiological roles (as neurohormones, as well as modulators within the CNS). A calcium dependent release of leucokinins could be induced *in vitro* from the corpora cardiaca of *L. maderae* by potassium depolarization [59], but was not yet tested for abdominal neurohemal areas. The hemolymph of *L. maderae* was also shown to contain leucokinin immunoreactive material in the nanomolar range [59], indicating that leucokinins may be released as hormones *in vivo*.

FMRFamide-like immunoreactive (F-LI) fibers have been detected in the wall of the abdominal aorta and the pericardial septum of *Calliphora*. The origin of these fibers was not determined, but they are probably originating from cell bodies in the abdominal neuromeres. As noted above, two of the CalliMRFamides increase the spontaneous heart rhythm [23] and it is possible that this effect is by peptide released from the F-LI efferents innervating the heart.

Proctolin-like immunoreactive (P-LI) material has been detected in a relatively large number of neurons in the blowfly thoracic-abdominal ganglion [69]. Two sets of efferent P-LI neurons have cell bodies located in the abdominal neuromeres (Fig. 8B). They send axons *via* the median and lateral abdominal nerves respectively. The approximately 10 P-LI neurons located laterally in each side of the abdominal ganglion send axons *via* the lateral abdominal nerves to the pericardial septum. Proctolin is known to increase the heart beat in a number of insect species [79], but no records of activity in flies exist. In different dipteran insects myogenic actions of proctolin have, however, been noted in hindgut and oviduct, and in larval body wall muscle [79].

Recent experiments reveal that an antiserum to the mammalian peptide galanin message associated peptide (GMAP) labels an extensive plexus of varicose fibers in the pericardial septum of *Calliphora*. So far, no biological action for this peptide has been recorded for any organism (Lundquist *et al.*, 1992), but the action of GMAP on the blowfly heart can be probed quite easily. The cellular origin of the GMAP immunoreactive fibers in the septum has not been determined.

Antisera to three more peptides, crustacean cardioactive peptide (CCAP), corazonin and pigment-dispersing hormone (PDH), were tested on the dorsal abdominal diaphragm and pericardial septum. Although the first two of these are cardioactive in other insects [11, 19, 41, 48, 107], no immunolabeling was obtained with any of the three antisera in the blowfly pericardial septum. Serotonin immunoreactive fibers could, however, be detected in the pericardial septum of *Phormia*. These fibers are likely to be derived from the four large subesophageal cell bodies, *via* the superficial fiber system in the neural sheath emerging also through the sheath of the lateral abdominal nerves. A direct action of serotonin on the heart or alary muscle as indicated in other insects is

possible [58].

In conclusion it is not clear whether the substances indicated by immunocytochemistry in fibers in the blowfly pericardial septum act on the heart muscle (and alary muscles) or if they are released into the circulation for action elsewhere (or both). An exception may be the F-LI fibers since some of the CalliFMRFamides have been shown to be cardiactive in *Calliphora* [23].

VARICOSE AXONS IN THE NEURAL SHEATH OF PERIPHERAL NERVES

In several insect there are plexuses of varicose fibers in the neural sheath of several of the peripheral nerve roots. For instance antisera against FMRFamide, pancreatic polypeptide, glucagon, adipokinetic hormone (AKH) and CCA label plexuses of varicose fibers in the perineurium of segmental and link nerves of crickets and locusts [19, 61, 86, 96, 99] (see also Fig. 2). Some of these fibers are derived from cell bodies in the CNS, others from peripherally located neurosecretory cells. In blowfies there are also systems of varicose fibers in the neural sheath of some of the peripheral nerves. These fibers have in some cases been traced from abdominal cell bodies to the periphery where they form terminals in neurohemal release areas: fibers in sheath of the lateral abdominal nerves, destined for the pericardial septum, react with antisera against antisera against leucokinin [10], proctolin, FMRFamide and lysine vasopressin [9, 69, 61]. In the sheath of the anterior prothoracic-, anterior dorsal mesothoracic- and haltere nerves superficial fibers react with antisera to AKH and the mammalian neuropeptides galanin and galanin message associated peptide (GMAP) [51, 52]. The origin of these fibers has not been determined. Furthermore, 5-HTIR fibers from cell bodies in the subesophageal ganglion were seen in the sheath of most cephalic and thoracic-abdominal nerve roots [67, 68].

NEUROPEPTIDES IN EFFERENT NEURONS TO THE BLOWFLY HINDGUT

The blowfly hindgut is innervated by abdominal neurons *via* the median abdominal nerve (Fig. 4). As will be shown below, several neuropeptides have been indicated in some of these efferent abdominal neurons by immunocytochemistry with antisera to proctolin, FaRPs, PDH, callatostatin and CCAP. It is not clear whether these peptides act on hindgut motility, water and ion balance or are released as neurohormones into the circulation around the intestine (or have several functions).

Proctolin. Proctolin was isolated on basis of its myotropic action on the cockroach hindgut [98], and early on proctolin was detected immunocytochemically in six efferent abdominal neurons with terminals in muscle of the hindgut of *Periplaneta americana* [25]. It has also been shown that proctolin increases the frequency and amplitude of myogenic contractions of the hindgut of a dipteran insect, the stable fly *Stomoxys calcitrans* [37]. In blowflies four abdominal proctolin immunoreactive (P-LI) neurons (Fig. 8B) send axons *via* the median narve to the hindgut where P-LI terminals could be found on the hindgut, rectal valve, rectum and rectal papillae [9]. Some of the P-LI fibers innervate the muscular is of the intestine and in the rectal papillae the fibers invade the medullary region. The P-LI fibers may hence mediate control of muscle activity as well as regulation of water and ion balance.

FMRFamide related peptides. Efferent F-LI nuerons of the abdominal ganglion send axons *via* the median abdominal nerve to the hindgut where they form an innervation pattern very similar to that of the proctolin containing neurons, but with larger number of arborizations [9, 50]. The Fa-LI fibers innervate the hindgut (Fig. 9C), rectal valve, rectum and rectal papillae. Also FaRPs may have myotropic actions on the hindgut and/or be involved in the regulation of water and ion balance.

Pigment dispersing hormone (PDH). Members of the pigment dispersing hormone family of peptides have been isolated from a number of crustacean and insect species [87] and a partial amino acid sequence (12 of 18 amino acids) of a *Calliphora* peptide with strong homologies to β-PDH has been obtained (Lundquist *et al.*, in prep.; see also Ref. [73]). In blowflies there are neurons reacting with PDH antiserum in the brain and thoracic abdominal ganglion [73]. In the abdominal ganglion six PDH-LI neurons send axons to the hindgut where they form varicose terminals in the posterior region of the midgut and anterior portion of the hindgut (Fig. 9D), the rectum and the rectal papillae [73]. The six PDH-LI neurons also have varicose arborizations within abdominal neuropil. An additional release site for PDH-related peptide may be the wall of the anterior aorta where PDH-LI terminals, derived from cephalic neurosecretory neurosn, are found [73].

Crustacean cardioactive peptide (CCAP). The nonapeptide CCAP was first isolated from the crab *Carcinus maenas* and later in identical form from the insects *Locusta migratoria* and *Manduca sexta* [11, 48, 97]. In the locust CCAP immunoreactivity (CCAP-LI) was demonstrated in numerous neurons and neurosecretory cells as seen in Figures 1 and 2 [19]. Some of these supply fibers to segmental distal perisympathetic organs and neurohemal release sites in the dorsal diaphragm including the alary muscles and lateral heart nerve [19]. In adult blowflies there are only four CCAP-LI cells in the entire fused thoracic-abdominal ganglion, two of which are only weakly immunoreactive (Fig. 8C). These cells are located posteriorly in the abdominal portion of the ganglion and send axons to the hindgut via the median abdominal nerve (Fig. 8C). The CCAP-LI fibers supply only the hindgut and rectum, but not the rectal papillae or pouch. Similar CCAP-LI neurons occur in adult *Drosophila* (Dircksen and Breidbach, unpublished).

Allatostatin-related peptides (callatostatins). Five neuropeptides termed callatostatins 1–5 have been isolated from adults of the blowfly *Calliphora vomitoria* [24]. Two of

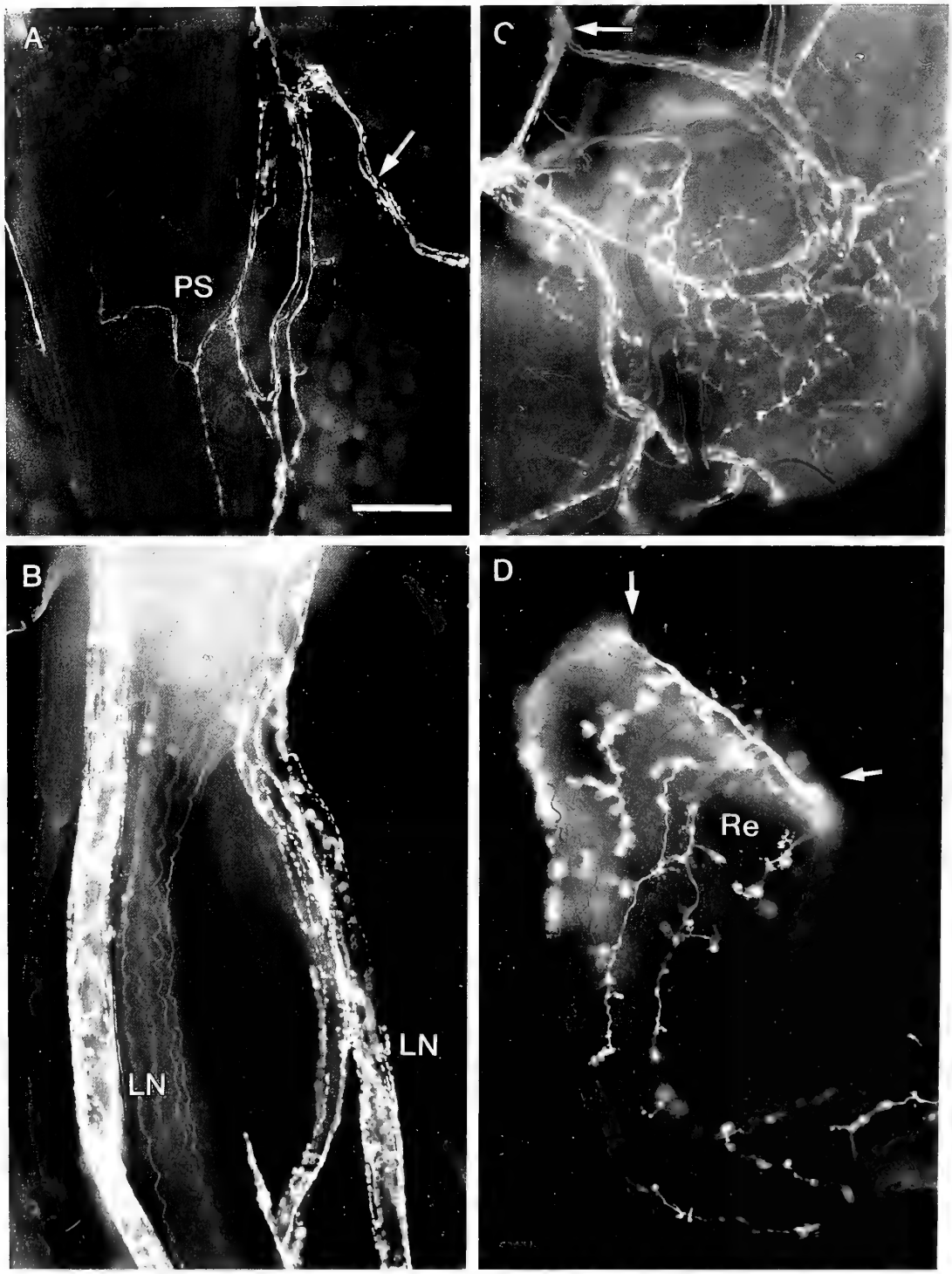

FIG. 9. Fluorescence micrographs of peripheral peptidergic axons in blowfly. **A.** Leucokinin immunoreactive terminals in the pericardial septum (PS). The fibers arrive by the segmental nerves (one indicated by arrow). **B.** Leucokinin immunoreactive varicose fibers at the surface of the lateral abdominal nerves (LN) on route to the pericardial septum. **C.** FMRFamide immunoreactive fibers in the hindgut anterior to rectal valve. The axons arrive from the abdominal nerve at arrow. **D.** PDH immunoreactive fibers in first part of the rectum (Re) of the hindgut (rectal valve at arrows). Scales: A-D = 50 μm. A-D altered from [9, 10, 73].

these were specifically isolated from dissected thoracic-abdominal ganglia. In the cockroach *Diploptera punctata* the cockroach allatostatins as well as the fly callatostatins inhibit juvenile hormone production in the corpora allata *in vitro*, whereas in the adult blowfly these peptides have no action on the production of juvenile hormone in the corpora allata [24]. In accordance with this Duve *et al.* [24] found no callatostatin immunoreactive material in the corpora allata or

any of the neurosecretory cell systems of the blowfly nervous system. Instead, callatostatin immunoreactivity was found in neurons of the abdominal ganglion with axons emerging through the median abdominal nerve to terminals in the hindgut, rectum, rectal papillae and oviduct. These authors therefore suggest that functions other than allatostatic ones may have to be sought for the callatostatins in adult blowflies. In sharp contrast to the findings of Duve *et al.* [24], allatostatin-like immunoreactivity was, however, found in neurons and neurosecretory cells both in the brain and thoracic-abdominal ganglion of *Drosophila* by Zitnan *et al.* [111]. It is not clear whether this discrepancy is caused by species differences or methodological differences.

LARVAL NEUROHEMAL ORGANS AND PERIPHERAL RELEASE SITES IN BLOWFLIES

In the larvae of higher diptera the corpora cardiaca, corpora allata and prothoracic gland form a composite organ, the ring gland or Weissman's ring [108]. In *Calliphora* serotonin and gastrin/CCK immunoreactive cell bodies and fibers were detected in the ring gland [8]. Additionally cephalic neurosecretory cells reacting with antisera against gastrin/CCK [8], FMRFamide, PDH (Nässel, unpublished) and corazonin (Cantera, Veenstra, Nässel, in prep.) form plexuses of varicose axons in the wall of the anterior portion of the aorta.

The presence of neurohemal release sites in the larval thoracic-abdominal nervous system of *Drosophlia* and *Calliphora* was first indicated by immunocytochemistry with antisera against FMRFamide and gastrin/CCK [65, 72, 101, 109]. In these flies each of the three thoracic segments have a dorsal unpaired median nerve which contributes to an extended bulb-like neurohemal organ [65, 72] (Fig. 10). In some specimens there is one neurohemal organ on each dorsal unpaired nerve, in others these fuse to one or two organs. FMRFamide-, myomodulin- and CCK-like immunoreactive fibers invade these thoracic neurohemal structures *via* the dorsal unpaired nerves (Fig. 11A) and peptidergic terminals could be revealed in the neural sheath outside the blood brain barrier [72]. The immunoreactive fibers are derived from two large cell bodies ventrally in each thoracic segment (Fig. 11A). By analysis of the postembryonic development of these immunoreactive cells it could be demonstrated that they persist throughout metamorphosis (see Fig. 6B) and form the six VTNCs of the adult blowfly and fruitfly [72, 101]. Interestingly, it can thus be concluded that the segmentally organized larval thoracic neurohemal organs transform into a large fused neurohemal area. There are also varicose myomodulin immunoreactive fibers emerging through the first four dorsal unpaired nerves (A1-4) of the abdominal ganglion in larvae of *Calliphora* (Fig. 11A) and *Phormia* (Nässel, unpublished). These nerves bifurcate laterally and the immunoreactive fibers continue along the length of the branches. The fibers entering the first four abdominal dorsal median nerves are derived from five pairs of ventral myomodulin immunoreactive cell bodies in abdominal neuromeres A1-5 (Fig. 11A). Four of these probably correspond to the myomodulin immunoreactive VANCs seen in the adults. As mentioned earlier the larval VTNCs of *Drosophila* were shown to contain peptide reacting with antisera to allatostatin and allatotropin [111].

Peptide containing cells with abdominal cell bodies and peripheral axonal projections can also be detected in the larval blowflies. Some of them have been followed through metamorphosis. The neurons of interest react with antisera

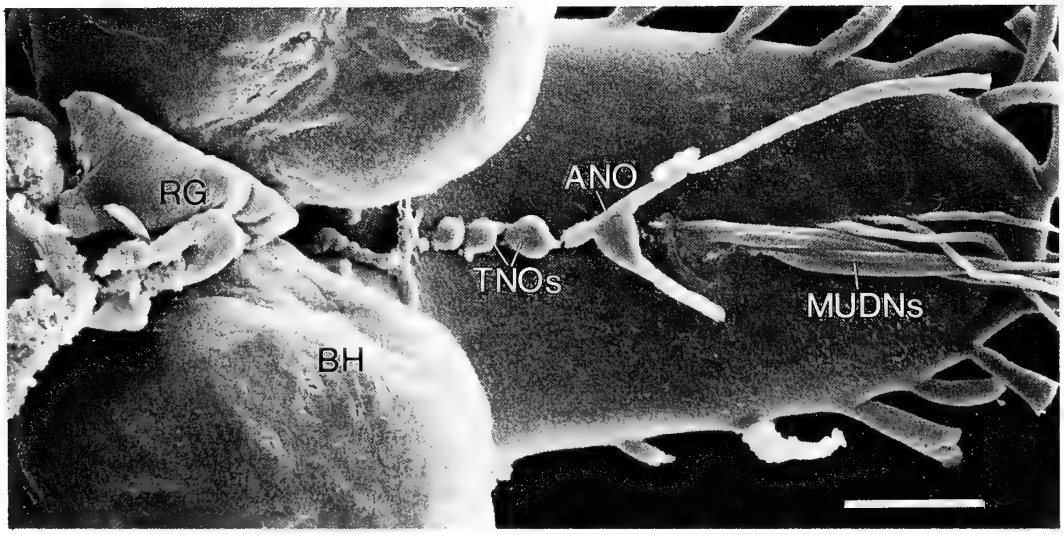

FIG. 10. The larval nervous system of *Calliphora*. Scanning electron micrograph of the larval nervous system in dorsal view. The three thoracic neurohemal organs (TNOs) are seen as spherical structures. A neurohemal organ (ANO) is also formed by the first abdominal dorsal unpaired nerve. The remaining abdominal median unpaired dorsal nerves (MUDNs) also contain some varicose fibers from neurosecretory cells (myomodulin immunoreactive). Altered from [72]. BH=brain hemishere. RG=portion of the ring gland. Scale=100 μm.

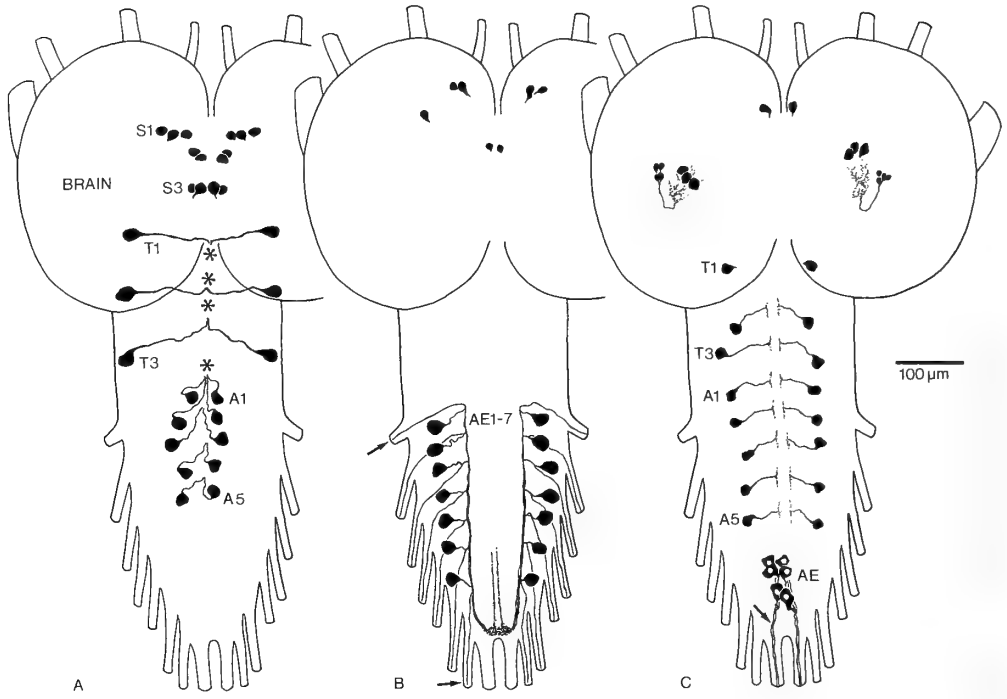

FIG. 11. Peptidergic neurons in the larval blowfly nervous system. **A.** Myomodulin immunoreactive neurons located ventrally (some dorsal cells in the brain are not shown). Neurons are found in two of the three subesophageal segments (S1 and S3). The three VTNCs are seen in segments T1–T3. These cells send their axons to the three median neurohemal organs of the thoracic neuromeres (location indicated by asterisks). Five pairs of ventral abdominal neurosecretory cells (A1–5) send their axons into the dorsal unpaired median nerves (location of one indicated by asterisk). **B.** Leucokinin immunoreactive neurons in the brain and abdominal neuromeres. The seven pairs of abdominal neurons (AE1–7) send axons through the segmental nerves 1–7 (arrows). The axons terminate on segmental abdominal body wall muscles. **C.** Pigment dispersing-hormone immunoreactive neurons in brain and thoracic-abdominal ganglia. The 8 pairs of thoracic and abdominal neurons (T1–3 and A1–5) appear to be interneurons, whereas three pairs of posterior abdominal neurons (AE) are efferents probably destined for the hindgut. A-C (Nässel, unpublished).

against proctolin, lysinevasopressin [71], leucokinin [10] and PDH (Nässel, unpublished).

The leucokinin (and lysine vasopressin) immunoreactive cells of the larva are segmentally distributed laterally in the abdominal neuromeres A1-7 (one pair of cells per neuromere, except in A8; Fig. 11B). These cells form efferent axons projecting to segmental muscle of the abdominal body wall of the larva [10]. The abdominal LK-LI and vasopressin immunoreactive cells survive metamorphosis and their peripheral axons innervate the pericardial septum as described above [10, 71].

A proctolin antiserum labels four cells with axons in the median abdominal nerves (A8) and seven pairs of lateral neurons with axons emerging through the lateral nerves (A1-7) in the blowfly and fruitfly larvae [1, 71]. In *Drosophila* the lateral cells send axons to body wall musculature and in both insects the median one innervate the intestine [1, 71]. Both sets of abdominal P-LI cells survive metamorphosis and in adults supply the pericardial septum and hindgut respectively.

In the blowfly larva six efferent PDH-LI neurons can be seen in the caudal portion of the abdominal ganglion (Fig. 11C). It has not yet been determined whether these cells survive metamorphosis and transform into the six cells of the adults that innervate the hindgut [73].

In summary, it can be proposed that many of the neurosecretory and efferent cell systems of the blowfly are present already in the larva. The cells survive metamorphosis, attain slightly altered morphologies and form novel release sites. It is not known whether the functions of the larval neurosecretory systems and the peptides they release are retained into the adult organism or if they obtain new actions.

CONCLUSIONS

Insects possess an impressive set of multiple specialized neurohemal release sites in different portions of the head and body compartments. Raabe [86] suggested that the multiple release sites are necessary due to the poorly developed circulatory system of insects. Thus it is not unusual to detect putative release sites for the same neuropeptide in the corpora cardiaca, the thoracic and abdominal perisympathetic organs and in the abdominal heart region (pericardial septum and alary muscles) [19, 49]. In this account we have shown that also in flies such as *Calliphora, Phormia* and *Drosophilla* there are several neurohemal release sites in addition to the corpora cardiaca. In fact, in these flies the

neurohemal part of the corpora cardiaca is insignificant in size compared to the neurohemal release sites in the neural sheath of the thoracic-abdominal ganglion and the pericardium. Thus the release of peptides from corpora cardiaca and the attending neurohemal plexus in the anterior aorta may be small in comparison with that of neurohemal release sites in structures derived from the body segments.

Many of the neurosecretory cells in addition to peripheral release sites have putative release sites within neuropils of the central nervous system. An interesting example is provided by the eclosion hormone containing neurons of larval moths (*Manduca sexta*). These neurons have varicose axons running through the entire length of the cephalic and thoracic-abdominal ganglia before they reach their neurohemal release sites on the hindgut [103]. Another example are the blowfly and *Drosophila* VTNCs which have extensive central arborizations in the subesophageal and thoracic neromeres as well as terminals in a substantial neurohemal release site [50]. Release of peptides or monoamines by the same neurons at different peripheral neurohemal release sites in addition to central neuropil regions would ensure synchronous action on (regulation of) peripheral targets and central circuits and thus enable orchestration of behavioral routines or other physiological functions [5, 45, 104, 105].

Some peptidergic neurons, that were originally classified as neurosecretory cells have all their known processes within the central nervous system [88, 100]. Are they still to be considered as neurosecretory cells? With the data available today on the distribution of a large number of different neuropeptides in many types of interneurons it may be called for to be cautious about terminology. Scharrer [90] noted that neurons employing chemical messenger substances have secretory capacity and may, in case of interneurons, release their regulatory substances in certain distinct neuropils without forming typical synaptic contacts. However, with the emergence of the concept of colocalized neuropeptides and classical transmitters [49] the classification into neurosecretory cells and neurons may be obsolete. Neuropeptides in central neurons may have a host of actions as neurotransmitters, cotransmitters, neuromodulators or even as trophic factors [36] and in insects we are only just starting to learn about central functions. Neuropeptide release often is episodic [36, 90, 104, 105] and many neuropeptides act in pacemaker circuits [34] indicating that central roles of neuropeptides are in regulation of rhythmic events or triggering of innate behaviors.

A large number of neuropeptides have been isolated from crustaceans and insects [38, 42, 55, 56, 94], and probably most of them have some actions at peripheral targets. Why are so many peptides needed in a "simple" organism like an insect? It is likely that many regulatory processes are finely tuned and that this requires several chemical messengers. Studies on diuresis in insects have for example provided evidence that more than one peptide may be involved only at the level of the Malpighian tubules [4, 30]. In the cricket A. *domesticus* fluid secretion can be induced by two different types of neuropeptides, achetakinin I and the 46 amino acid diuretic peptide [30]. The two peptides act *via* different receptors and second messenger systems in the Malpighian tubules, achetakinin by an unknown pathway and diuretic peptide *via* cAMP. Additionally serotonin acts on cricket Malpighian tubules [12] indicating that diuresis is a finely tuned proces in insects, notwithstanding further medhanisms involved in water reabsorption in the hindgud (See Ref. [4]). We also know that a variety of neuropeptides in addition to monoamines act on skeletal, visceral and heart muscle in insects [16, 82, 94]. For instance the spontaneous contractions of locust oviduct muscle appear regulated by a number of neuropeptides as well as by octopamine [46, 47, 82, 94] and a very large number of neuropeptides and serotonin act on the *Leucophaea* hindgut [39, 94]. The role of insect hormonal neuropeptides in regulation and initiation of behaviors has been explored for eclosion hormone and cardioactive peptides during development of the moth *Manduca* [104, 105]. It is to be expected that for instance feeding behavior is under peptide hormone control since salivary glands, intestinal muscle and skeletal muscle are regulated by different peptides and central circuits associated with feeding are innervated by peptidergic neurons [16, 22, 66, 80, 94]. Peptides originating from cells outside the nervous system have also been implicated in behavior regulation. As an example the *Drosophila* 36 amino acid sex peptide of the male accessory glands is transferred to females during copulation and elicit rejection of further males as well as an ovulation and oviposition response [91].

Characterization of receptors mediating the action of different neuropeptides and studies of the structure of the active cores of neuropeptides have been initiated [30, 44, 56, 62, 85], but much is to be learned about interactions of different peptides at the receptor and second messenger level. We also need to know more about the degradation of peptides at their target organs such as Malpighian tubules, hindgut and ovaries [83, 84] or within the hemolymph [29]. These studies are necessary to be able to determine whether peptides released from neurohemal organs will be available in physiological concentrations for actions at their targets (at threshold concentrations indicated in *in vitro* assays) or if they are likely to act by direct release from neuronal terminals supplying the targets. It is also critical to employ sensitive assays such as radioimmunoassay or ELISA to determine the content of peptides in the hemolymph in *in vivo* experiments to corroborate claimed hormonal actions.

Analysis of neuroendocrine systems at the molecular and genetic level will no doubt be helpful in filling many gaps in the understanding of hormonal control of development, behaviour and homeostasis [6, 95]. It is to be expected that some of the diversity in neuropeptides and peptides in non-neural cells will be explained by a certain redundancy of mediators in regulatory systems which is partly caused by a need for subtle control mechanisms. It is also likely that peptides are involved in processes other than classical neurotransmission, hormonal actions or neuromodulatory roles,

such as being cytokines or factors in development and maintenance of the nervous system.

ACKNOWLEDGMENTS

Our colleagues in Bonn and Stockholm are thanked for their contributions to much of the original research presented. The technical assistance of Anne Karlsson, Ylwa Lilliemarck and Bibbi Meyrhofer is gratefully acknowledged. Financial support by the Swedish Natural Science Research Council is also acknowledged.

REFERENCES

1 Anderson MDS, Halpern ME, Keshishian H (1987) J Neurosci 8: 283–294
2 Baudry-Partiaoglu N (1975) CR Acad Sci Paris 281: 921–924
3 Bayrahtaroglu E, Golding DW, Whittle AC (1989) Acta Zool (Stockholm) 70: 87–94
4 Beyenback KW (Ed.) (1993) "Structure and function of primary messengers in invertebrates: insect diuretic and antidiuretic peptides". Mol Comp Physiol, Vol. 12, Karger, Basel
5 Bicker G, Menzel R (1989) Nature 337. 33–39
6 Buchner E (1991) J Neurogenet 7: 153–192
7 Buma P, Roubos EW, Buijs RM (1984) Histochemistry 80: 247–257
8 Cantera R (1988) Cell Tissue Res 253: 425–433
9 Cantera R, Nässel DR (1991) Comp Biochem Physiol 99C: 517–525
10 Cantera R, Nässel DR (1992) Cell Tissue Res 269: 459–471
11 Cheung CC, Loi PK, Sylwester AW, Lee TD, Tublitz NJ (1992) FEBS Lett 313: 165–168
12 Coast G (1989) Physiol Entomol 14: 21–20
13 Cook BJ, Holman GM (1979) J Gen Physiol 74: A5–A6
14 Cook BJ, Meola S (1978) Physiol Entomol 3: 273–280
15 Cropper EC, Tenenbaum R, Kolks MAG, Kupferman I, Weiss KR (1987) Proc Natl Acad Sci USA 84: 5483–5486
16 Cuthbert BA, Evans PD (1989) J Exp Biol 144: 395–415
17 Davis NT, Hildebrand JG (1992) J Comp Neurol 320: 381–393
18 De Loof A (1987) Entomol Exp Appl 45: 105–113
19 Dircksen H, Müller A, Keller R (1991) Cell Tissue Res 263: 439–457
20 Dircksen H, Nässel DR (1993) In "Gene -Brain- Behaviour" Ed by N Elsner, M Heisenberg, Thieme, Stuttgart, p 519
21 Duve H, Thorpe A, Nässel DR (1988) Cell Tissue Res 253: 583–595
22 Duve H, Johnsen AH, Sewell JC, Scott AG, Orchard, I, Rehfeld JF, Thorpe A (1992) Proc Natl Acad Sci USA 89: 2326–2330
23 Duve H, Elia AJ, Orchard I, Johnsen AH, Thorpe A (1993) J Insect Physiol 39: 31–40
24 Duve H, Johnsen AH, Scott AG, Yu CG, Yagi KJ, Tobe SS, Thorpe A (1993) Proc Natl Acad Sci USA 90: 2456–2460
25 Eckert M, Agricola H, Penzlin H (1981) Cell Tissue Res 217: 633–645
26 Elia AJ, Tebrugge VA, Orchard I (1993) J Insect Physiol 39: 459–469
27 Ferber M, Pflüger HJ (1992) Cell Tissue Res 267: 85–98
28 Finlayson LH, Osborne (1968) J Insect Physiol 14: 1793–1801
29 Fox AM, Reynolds SE (1991) Peptides 12: 937–944
30 Goldsworthy G, Coast G, Wheeler C, Cusinato O, Kay I, Khambay B (1992) In "Insect molecular science" Ed. by JM Crampton, P Eggleston, Academic Press, London, pp 205–225
31 Grillot JP (1977) Int J Insect Morphol Embryol 6: 303–343
32 Grillot JP (1983) In "Neurohemal organs of arthropods" Ed. by AP Gupta, CC Thomas, Spring-field, Illinois, pp 481–512
33 Gupta AP (Ed.) (1983) "Neurohemal organs of arthropods". CC Tomas, Spring-field, Illinois
34 Harris-Warrick R, Marder E (1991) Annue Rev Neurosci 14: 39–57
35 Hayes TK, Pannabecker TL, Hinckley DJ, Holman GM, Nachman RJ (1989) Life Sci. 44: 1259–1266
36 Hökfelt T (1991) Neuron 7: 867–879
37 Holman GM, Cook BJ (1979) Comp Biochem Physiol 62C: 231–235
38 Holman GM, Nachman RJ, Wright MS (1990b) Annu Rev Entomol 35: 201–217
39 Holman GM, Nachman RJ, Schoofs L, Hayes TK, Wright MS, De Loof A (1991) Insect Biochem 21: 107–112
40 Homberg U, Davis NT, Hildebrand JG (1991) J Comp Neurol 303: 35–52
41 Jahn G, Käuser G, Koolman J (1991) Gen Comp endocrinol 82: 287
42 Keller R (1992) Experientia 48: 439–448
43 Kingan TG, Blackburn MB, Raina AK (1992) Cell Tissue Res 270: 229–240
44 Konopinska D, Rosinski G, Sobótka W (1992) Int J Pept Protein Res 39: 1–11
45 Kravitz EA (1988) Science 241: 1775–1781
46 Lange AB, Orchard I, Adams ME (1986) J Comp Neurol 254: 279–286
47 Lange AB, Orchard I, Te Brugge V (1991) J Comp Physiol A 168: 383–391
48 Lehman HK, Murgiuc CM, Miller TA, Lee TD, Hildebrand JG (1993) Peptides 14: 735–741
49 Lundberg JM, Hökfelt T (1983) Trends Neurosci 6: 325–333
50 Lundquist CT, Nässel DR (1990) J Comp Neurol 294: 161–178
51 Lundquist CT, Rökaeus Å, Nässel DR (1991) J Comp Neurol 312: 77–96.
52 Lundquist CT, Rökaeus Å, Nässel DR (1992) J Neuroendocrinol 4: 605–616
53 Lundquist CT, Brodin E, Muren JE, Nässel R (1993) Peptides 14: 651–663
54 Maddrell S, Herman WS, Mooney RL, Overton JA (1991) J Exp Biol 156: 557–566
55 Masler EP, Kelly TJ, Menn JJ (1993) Arch Insect Biochem Physiol 22: 87–111
56 Menn JJ, Kelly TJ, Masler EP (Eds.) (1991) Insect Neuropeptides: Chemistry, Biology and Actions, ACS Symposium Series 453. American Chemical Society, Washington
57 Meola S, Cook BJ (1986) Int J Insect Morphol Embryol 15: 269–281
58 Miller TA (1979) Am Zool 19: 77–86
59 Muren JE, Lundquist CT, Nässel DR (1993) J Exp Biol 179: 289–300
60 Myers CM, Evans PD (1985) J Comp Neurol 234: 1–16
61 Myers CM, Evans PD (1988) J Morphol 195: 45–58
62 Nachman RJ, Holman GM, Haddon WF (1993) Arch Insect Biochem Physiol 22: 181–197
63 Nagasawa H (1992) Experientia 48: 425–430
64 Nambu JR, Murphy-Erdosh C, Andrews PC, Feistner GJ, Scheller RH (1988) Neuron 1: 55–61
65 Nässel DR (1987) In "Nervous systems of Invertebrates" Ed. by MA Ali, Plenum Press, New York, pp 171–212
66 Nässel DR (1993) Cell Tissue Res 273: 1–29
67 Nässel DR, Elekes K (1984) Neurosci Lett 48: 203–210

68 Nässel DR, Elekes K (1985) Neurosci 15: 293–307
69 Nässel DR, O'Shea M (1987) J Comp Neurol 265: 437–454
70 Nässel DR, Cantera R, Karlsson A (1992) J Comp Neurol 322: 45–67
71 Nässel DR, Holmqvist BI, Movérus BJA (1989) J Comp Neurol 283: 450–463
72 Nässel DR, Ohlsson LG, Cantera R (1988) J Comp Neurol 267: 343–356
73 Nässel DR, Shiga S, Mohrherr CJ, Rao KR (1993) J Comp Neurol 331: 183–198
74 Nässel DR, Cantera R, Johard HAD, Lundquist CT, Muren JE, Shiga S (1992) In "Nervous systems: principles of design and function". Ed. by RN Singh, Wiley Eastern, New Dehli, pp 189–212
75 Nichols R (1992a) Molec Cell Neurosci 3: 342–347
76 Nichols R (1992b) J Mol Neurosci 3: 213–218
77 Nichols R, Schneuwly SA, Dixon JE (1988) J Biol Chem 263: 12167–12170
78 O'Brien MA, Schneider LE, Taghert PH (1991) J Comp Neurol 304: 623–638
79 Orchard I, Belanger JH, Lange AB (1989) J Neurobiol 20: 470–496
80 O'Shea M, Schaffer M (1985) Ann Rev Neurosci 8: 171–198
81 Paemen L, Schoofs L, De Loof A (1992) Cell Tissue Res 268: 91–97
82 Peeff NM, Orchard I, Lange AB (1993) J Insect Physiol 39: 207–215
83 Picquot M, Proux J (1980) Regul Pept 31: 139–156
84 Puiroux J, Loughton BG (1992) Arch Insect Biochem Physiol 19: 193–202
85 Puiroux J, Pedelaborde A, Loughton BG (1992) Insect Biochem 22: 547–551
86 Raabe M (1989) Recent developments in insect neurohormones. Plenum, New York
87 Rao KR, Riehm JP (1989) Biol Bull 177: 225–229
88 Remy C, Girardie J (1980) Gen Comp Endocrinol 40: 27–35
89 Richard O, Girardie J (1992) Cell Tissue Res 270: 587–596
90 Scharrer B (1987) Ann Rev Neurosci 10: 1–17
91 Schmidt T, Choffat Y, Klauser S, Kubli E (1993) J Insect Physiol 39: 361–368
92 Schneider LE, Taghert PH (1988) Proc Natl Acad Sci USA 85: 1993–1997
93 Schneider LE, Roberts MS, Taghert PH (1993) Neuron 10: 279–291
94 Schoofs L, Vanden Broeck J, De Loof A (1993) Insect Biochem Molec Biol 23: 859–881
95 Segal D (1993) Arch Insect Biochem Physiol 22: 199–231
96 Spörhase-Eichman U, Dircksen H, Hect T, Helle J, Schürmann FW (1991) In "Synapse—Transmision—Modulation" Ed. by N Elsner, H Penzlin, Thieme, Stuttgart, p 339
97 Stangier J, Hilbich C, Keller R (1989) J Comp Physiol B 159: 5–11
98 Starrat AN, Brown BE (1975) Life Sci 17: 1253–1256
99 Taghert PH, Carr JN, Wall JB (1988) Adv Insect Physiol 20: 87–117
100 Thompson KSJ, Tyrer NM, May ST, Bacon JP (1991) J Comp Physiol A 168: 605–617
101 Trimmer BA (1985) J Exp Biol 114: 307–328
102 Truman JW (1990) J Neurobiol 21: 1072–1084
103 Truman JW, Copenhaver PF (1989) J Exp Biol 147: 457–470
104 Tublitz NJ, Copenhauer PF, Taghert PH, Truman JW (1986) Trends Neurosci 9: 359–363
105 Tublitz N, Brink D, Broadie KS, Loi P, Sylwester AW (1991) Trends Neurosci 14: 254–259
106 Veenstra JA (1987) Neurosci. Lett. 73: 33–37
107 Veenstra JA (1989) FEBS Lett 250: 231–234
108 Vogt M (1943) Biol Zentralbl 63. 56–71
109 White K, Hurteau T, Punsal P (1986) J Comp Neurol 247: 430–438
110 Zitnan D, Sauman I, Sehnal F (1993) Arch Insect Biochem Physiol 22: 113–132
111 Zitnan D, Sehnal F, Bryant PJ (1993) Dev Biol 156: 117–135

ZOOLOGICAL SCIENCE 11: 33–38 (1994)

A Myomodulin-CARP-related Peptide Isolated from a Polychaete Annelid, *Perinereis vancaurica*

Toshio Takahashi[1], Osamu Matsushima[2]*, Fumihiro Morishita[2], Masaaki Fujimoto[2], Tetsuya Ikeda[3], Hiroyuki Minakata[3] and Kyosuke Nomoto[3]

[1]*Faculty of Integrated Arts and Sciences, Hiroshima University, Higashi-Hiroshima 724,* [2]*Department of Biological Science, Faculty of Science, Hiroshima University, Higashi-Hiroshima 724, and* [3]*Suntory Institute for Bioorganic Research, Osaka 618, Japan*

ABSTRACT—Myomodulin-CARP-family peptides have been isolated only from molluscs. In the present study, a heptapeptide, Ala-Met-Gly-Met-Leu-Arg-Met-NH_2, termed Pev-myomodulin, was isolated from a polychaete annelid, *Perinereis vancaurica* using the esophagus of the animal as the bioassay system. The sequence of the annelid peptide is highly homologous with those of the myomodulin-CARP-family peptides found in molluscs. The annelid peptide is regarded as a member of the myomodulin-CARP family, though all the molluscan peptides have a Leu-NH_2 at their C-termini. The annelid peptide showed a potnet contractile action on the esophagus of the annelid. The peptide may be an excitatory neuromediator involved in the regulation of the esophagus. Among various myomodulin-CARP-family peptides and their analogues, the annelid peptide showed the most potent contractile action on the esophagus. Replacement of the C-terminal Met-NH_2 of the annelid peptide with a Leu-NH_2 decreased its contractile potency, while replacement of the C-terminal Leu-NH_2 of myomodulin and CARP with a Met-NH_2 increased their potency. The C-terminal Met-NH_2 of the annelid peptide seems to be important, but not essential, for exhibiting its contractile activity on the esophagus. On the anterior byssus retractor muscle of the bivalve mollusc *Mytilus edulis*, the annelid peptide showed catch-relaxing and contraction-modulating effects qualitatively similar to those of the authentic peptide CARP, though the annelid peptide was less potent than CARP.

INTRODUCTION

Over the past two decades, a large number of bioactive peptides have been isolated from invertebrates, especially from arthropods and molluscs [5, 9, 12, 18, 20. 21]. As to annelids, however, only several FMRFamide-related peptides have been identified using radioimmunoassay for detection of the peptides. Krajniak and Price [13] found FMRFamide in the polychaete *Nereis virens*. Baratte *et al.* [1] isolated FMRFamide and its analogue from *Nereis diversicolor*. Evans *et al.* [4] identified FMRFamide and four analogues in the medicinal leech *Hirudo medicinalis*.

In the previous study, we isolated two S-Iamide-family peptides, AKSGFVRIamide and VSSFVRIamide, from the polychaete annelid, *Perinereis vancaurica* [16]. The peptides show a potent contractile effect on the esophagus of the annelid [16], while FMRFamide shows an inhibitory effect [14]. This was the first finding of annelid peptides which were not considered to be FMRFamide-family peptides. Since this finding, we have continued to search for bioactive peptides in the annelid *P. vancaurica* using its esophagus as the bioassay system. In the present study, we found a novel heptapeptide, Ala-Met-Gly-Met-Leu-Arg-Met-NH_2, that showed a potent excitatory action on the esophagus. The sequence of the peptide is highly homologous to myomodulin, catch-relaxing peptide (CARP) and their related peptides, all of which have been isolated from molluscs ([2, 3, 8, 10, 11], See also Table 1). That is, the annelid peptide is regarded as a member of myomodulin-CARP family. Here, we report purification, structure determination and pharmacological characterization of the annelid myomodulin-CARP-family peptide.

MATERIALS AND METHODS

Animals

The marine polychaete annelid worms, *Perinereis vancaurica,* were purchased from a fishing-bait store and the sea mussels, *Mytilus edulis,* were collected in the Hiroshima Bay. These animals were kept in laboratory tanks filled with aerated seawater at 15°C.

Extraction and purification

Extraction procedures for bioactive peptides in *P. vancaurica* were essentially the same as those reported previously [16]. Briefly, 0.5 kg of the animals were boiled for 10 min at 100°C in 2 l of water containing 4% acetic acid and homogenized with a Waring blender and then with a Polytron homogenizer. The homogenate was centrifuged at 15,000×*g* for 40 min at 4°C. The supernatant was concentrated with a rotary evaporator, and 1/10 volume of 1 N HCl was added to the concentrated solution with constant agitation. The concentrated solution was centrifuged again. The supernatant was applied to two C-18 cartridges (Mega Bond Elut, Varian) in series. After the cartridges were washed with 0.1% trifluoroacetic acid (TFA), the retained material was eluted with 50% methanol. The

Accepted October 27, 1993
Received October 4, 1993
* To whom correspondence should be addressed.

eluate was applied to four steps of reversed-phase and cation-exchange high performance liquid chromatography (HPLC). The eluting substances were monitored with an UV detector at 220 nm. Each of the fractions obtained at each HPLC step was bioassayed using the isolated esophagus of *P. vancaurica*.

At the first HPLC-purification step, the eluate from the C-18 cartridges was applied to a Capcell-Pak C-18 reversed-phase column (Shiseido, 10×250 mm). The column was eluted with a 120-min linear gradient of 0–60% acetonitrile (ACN) in 0.1% TFA (pH 2.2). The flow rate was 1 ml/min. An aliquot (1/250) of each 2-ml fraction was evaporated to dryness, dissolved in artificial seawater (ASW) and subjected to bioassay. A bioactive peak eluted at around 20% ACN was then subjected to the second step of HPLC purification. At this step, another C-18 reversed-phase column (ODS-80TM, Tosoh, 4.6×150 mm) was used. The column was eluted with a 50-min linear gradient of 15–25% ACN in 0.1% TFA. A bioactive peak was observed at around 16% ACN. At the third step, the bioactive substance was applied to a cation-exchange column (SP-5PW, Tosoh, 7.5×75 mm), and the column was eluted with a 70-min linear gradient of 0–0.7 M NaCl in 10 mM phosphate buffer (pH 7.1) at a flow rate of 0.5 ml/min. The bioactive substance was eluted at around 0.22 M NaCl. At the fourth step (final step), the bioactive substance was applied to the reversed-phase column (ODS-80TM), and the column was eluted with a 25-min linear gradient of 15–25% ACN in 0.1% TFA at a flow rate of 0.5 ml/min. The substance was eluted at around 20% ACN as a single absorbance peak (Fig. 1).

The purified bioactive substance was subjected to peptide sequence analysis (Shimadzu PSQ-1 Protein Sequencer) and fast atom bombardment mass spectrometric (FAB-MS) analysis (JEOL JMS-HX 110/110A). These analyses suggested that the substance is a pentapeptide with an amidated C-terminus. The peptide having the suggested structure was then synthesized by a solid-phase peptide synthesizer (Applied Biosystems 430A) and purified by HPLC. The structure of the synthesized peptide was confirmed by amino acid sequence analysis and FAB-MS analysis. The synthetic peptide was compared with the native one in the behavior on HPLC.

Bioassay

The anterior half of the body was cut open ventrally and the esophagus (about 15 mm long) was excised. Both ends of the isolated esophagus were ligated with cotton threads. One of the thread was tied to a fixed support of a trough (2 ml) filled with aerated ASW, and the other was connected to a force-displacement transducer attached to a manipulator. Changes in the esophagus tension in response to bioactive substances were recorded on a chart recorder through an amplifier.

Aliquots (1/250–1/100) of the fractions obtained at each HPLC purification step were evaporated to dryness, dissolved in 0.1 ml ASW and injected into the aerated trough in which the isolated esophagus was mounted. After each recording of the effects of the fractions, the esophagus was washed with ASW. The next test was started 10 min after the recording.

Pharmacology

The contractile actions of 10 myomodulin-CARP-family peptides including the annelid peptide isolated in the present study and nine synthetic analogues were examined on the isolated esophagus of *P. vancaurica*. It has been shown that CARP powerfully relaxes catch tension in the anterior byssus retractor muscle (ABRM) of *M. edulis* and that the peptide potentiates phasic contraction of the ABRM in response to repetitive electrical stimulation at lower concentrations and inhibits the contraction at higher concentrations [6, 7, 18]. Therefore, the actions of the annelid peptide on catch tension and phasic contraction of the ABRM were also examined to compare them with those of CARP. Catch contraction was produced by applying 10^{-4} M acetylcholine (ACh) to the ABRM for 2 min at 20 min intervals and phasic contractions was elicited by stimulating the muscle with repetitive electrical pulses (15 V, 3 msec, 10 Hz, 50 pulses) at 10 min intervals. This procedure was basically the same as that of Muneoka and Twarog [19].

Saline

The saline used for the esophagus of *P. vancaurica* and the ABRM of *M. edulis* was ASW of the following composition: 445 mM NaCl, 10 mM KCl, 10 mM $CaCl_2$, 55 mM $MgCl_2$ and 10 mM Tris-HCl (pH 7.6).

RESULTS

After the three steps of HPLC purification, the final purification was performed with the reversed-phase column (Fig. 1). The single absorbance peak obtained was found to coincide with an active peak. At the first step of HPLC purification on a Capcell-Pak C-18 reversed-phase column, the active substance was recovered in the same fraction (No. 34) as a previously reported S-Iamide peptide, VSSFVRIamide [16]. At the second step of HPLC using another C-18 reversed-phase column (ODS-80TM), these two substances were separated from each other: VSSFVRIamide was recovered in fractions 7, 8, and 9, while the present substance was in fractions 12 and 13.

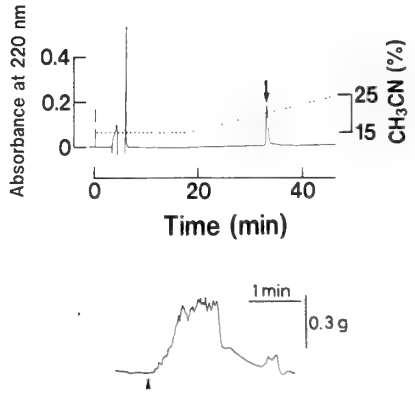

FIG. 1. HPLC profile at the final step of purification of the bioactive substance on the C-18 ODS-80TM column (upper) and the activity of the purified substance on the esophagus of *P. vancaurica* (lower). The elution was performed with a linear gradient of 15–25% ACN (0.1% TFA) at a flow rate of 0.5 ml/min. The absorbance was monitored at 220 nm. The broken line shows the concentration of ACN. An aliquot (1/100) of the purified substance was applied at the time indicated by an arrow head.

The determined sequence and detected amount (picomoles) of each amino acid in the amino acid sequence analysis of the purified substance were as follows: Ala (820.6)-Met

(892.2)-Gly (508.6)-Met (808.2)-Leu (729.2)-Arg (114.3)-Met (293.1). In the FAB-MS spectrum of the purified substance, a molecular ion peak was observed at 810.1 m/z $(M+H)^+$. The results of these analyses suggested that the purified substance is an amidated heptapeptide having the following primary structure: Ala-Met-Gly-Met-Leu-Arg-Met-NH_2. The yield of this peptide from 500 g of the worms was roughly estimated to be 3 nmoles using the data on amino acid sequence analysis. The value was comparable to the yield of an S-Iamide peptide, AKSGFVRIamide, and larger than the yield of another S-Iamide peptide, VSSFVRIamide [16].

A mixture of the synthetic peptide with the suggested structure and the native peptide (purified substance) showed a single absorbance peak when applied to a C-18 reversed-phase column and a cation-exchange column (Fig. 2). We were not able to compare the bioactivity between the synthetic and native peptides, because the quantity of the native peptide obtained was not enough for the comparison. However, we confirmed contraction-eliciting activity of the synthetic peptide at concentrations of 10^{-8} M or higher (Fig. 3).

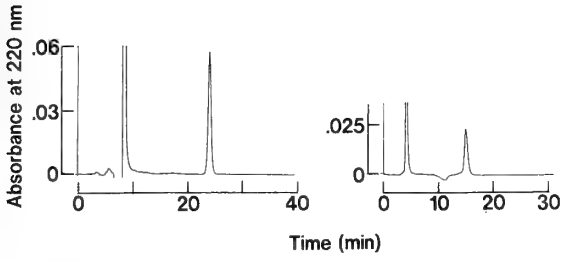

FIG. 2. HPLC profiles of mixtures of the native and synthetic peptides on a C-18 ODS-80TM column with an isocratic elution of 21% ACN (0.1% TFA) at a flow rate of 0.3 ml/min (left) and on the cation-exchange SP-5PW column with an isocratic elution of 0.2 M NaCl (10 mM phosphate buffer, pH 7.1) at a flow rate of 0.5 ml/min (right).

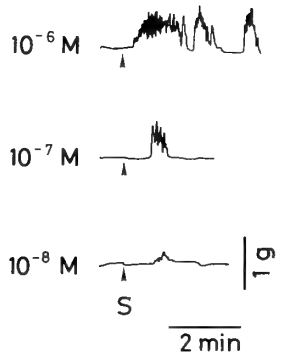

FIG. 3. Actions of the synthetic peptide on the isolated esophagus at different concentrations. The peptide was applied at the times indicated by arrow heads.

The sequence of the annelid peptide is highly homologous to those of myomodulin-CARP-family peptides found in several molluscs (Table 1). We examined the effects of these molluscan peptides and several synthetic analogues on the esophagus of *P. vancaurica,* and compared the effects with those of the annelid peptide which we designated Pev-myomodulin (Table 2).

Pev-myomodulin showed the most potent contractile effect on the esophagus, and was approximately 10 times more potent than myomodulin and CARP. In Figure 4, the effects of 10^{-6} M Pev-myomodulin and 10^{-6} M CARP on a preparation of the esophagus are shown. Met^7-CARP and Met^7-myomodulin were also more potent than the respective authentic molluscan peptides, though they were slightly less potent than Pev-myomodulin. Phe^7-CARP and Phe^7-myomodulin were far less potent than Pev-myomodulin. Leu^7-Pev-myomodulin was also far less potent than the authentic annelid peptide. C-terminal-free CARP did not show any effect even at 10^{-5} M. Met-Leu-Arg-Leu-NH_2, a common C-terminal fragment of the most molluscan myomodulin-CARP-family peptides, showed a considerable effect,

TABLE 1. Myomodulin-CARP-family peptides

Phyla	Animals	Structures	References
Annelida	*Perinereis*	AMGMLRMamide	this study
Mollusca	*Mytilus*	AMPMLRLamide	Hirata *et al.* (1987)
	Aplysia	PMSMLRLamide	Cropper *et al.* (1987)
		GSYRMMRLamide	Cropper *et al.* (1991)
	Fusinus	PMSMLRLamide	Kanda *et al.* (1990)
		PMNMLRLamide	Kanda *et al.* (1990)
	Helix	PMSMLRLamide	Ikeda *et al.* (1993)
		SLGMLRLamide	Ikeda *et al.* (1993)
		GLNMLRLamide	Ikeda *et al.* (1993)
		pQLSMLRLamide	Ikeda *et al.* (1993)
		pQLPMLRLamide	Ikeda *et al.* (1993)
	Achatina	SLGMLRLamide	Ikeda *et al.* (unpublished)
		GLHMLRLamide	Ikeda *et al.* (unpublished)

pQ, pyroglutamic acid.

TABLE 2. Contractile effects of myomodulin-CARP-family peptides and synthetic analogues on the isolated esophagus of *Perinereis vancaurica*

Peptides	Concentrations (M) 10^{-8}	10^{-7}	10^{-6}	10^{-5}
Myomodulin-CARP-family peptides				
AMGMLRMamide	+	++	+++	NT
AMPMLRLamide	NT	−	++	+++
PMSMLRLamide	−	+	+++	NT
GSYRMMRLamide	−	+	++	+++
PMNMLRLamide	NT	−	++	+++
SLGMLRLamide	−	+	++	+++
GLNMLRLamide	−	+	++	+++
pQLSMLRLamide	−	+	++	+++
pQLPMLRLamide	−	−	−	+++
GLHMLRLamide	−	+	++	+++
Analogue peptides				
AMPMLRMamide	−	++	+++	NT
PMSMLRMamide	−	++	+++	NT
AMGMLRLamide	NT	−	−	++
AMPMLRFamide	NT	NT	−	+
PMSMLRFamide	−	−	+	++
AMPMLRL	NT	NT	NT	−
MLRLamide	NT	+	++	+++
WLRLamide	NT	−	−	+++
LRLamide	NT	−	−	−

+++, strong effect. ++, moderate effect. +, weak effect. −, no effect. NT, not tested. pQ, pyroglutamic acid.

but Leu-Arg-Leu-NH_2 did not show any effect at 10^{-5} M or lower. Replacement of the Met residue of Met-Leu-Arg-Leu-NH_2 with a more hydrophobic residue Trp decreased the contractile potency.

The effects of Pev-myomodulin on catch tension and phasic contraction of the ABRM were also examined, and compared with those of CARP. The effects of 10^{-6} M of these peptides on a preparation of the ABRM are shown in Figure 5. The actions of CARP and Pev-myomodulin (10^{-6} M) on the phasic contractions were apparently opposite. However, those actions were found to be dose-dependent (Fig. 6), indicating that actions of these peptides on the phasic contractions were not qualitatively different. Dose-response relationships of these peptides showed that CARP was much more potent than Pev-myomodulin in exerting both modulatory effects on the phasic contraction and relaxing effects on the catch tension (Fig. 6).

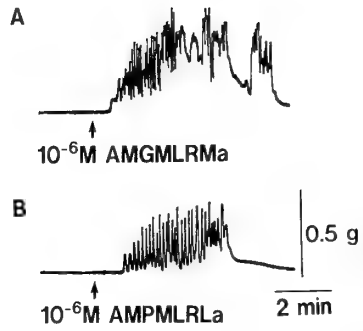

FIG. 4. Actions of 10^{-6} M AMGMLRMamide (Pev-myomodulin) and 10^{-6} M AMPMLRLamide (CARP) on the isolated esophagus of *P. vancaurica*. A, Pev-myomodulin. B, CARP.

DISCUSSION

The novel heptapeptide Pev-myomodulin isolated from the annelid, *P. vancaurica*, in the current study is apparently a member of myomodulin-CARP family. The members of the myomodulin-CARP family have so far been identified only in molluscs (Table 1). Thus, this is the first report on

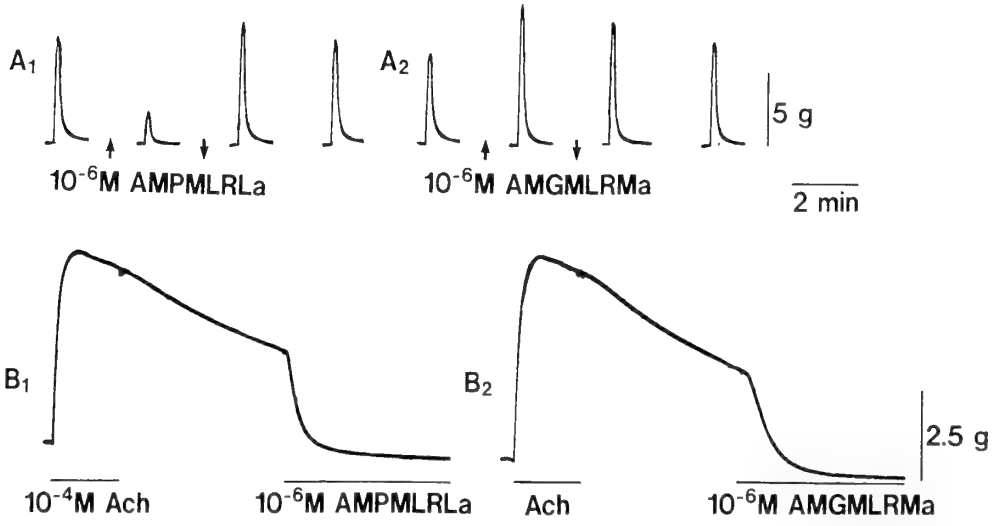

FIG. 5. Effects of AMPMLRLamide (CARP) and AMGMLRMamide (Pev-myomodulin) on phasic contractions (A_1, A_2) in response to repetitive electrical stimulation (15 V, 3 msec, 10 Hz, 50 pulses) and on catch contractions (B_1, B_2) induced by 10^{-4} M ACh.

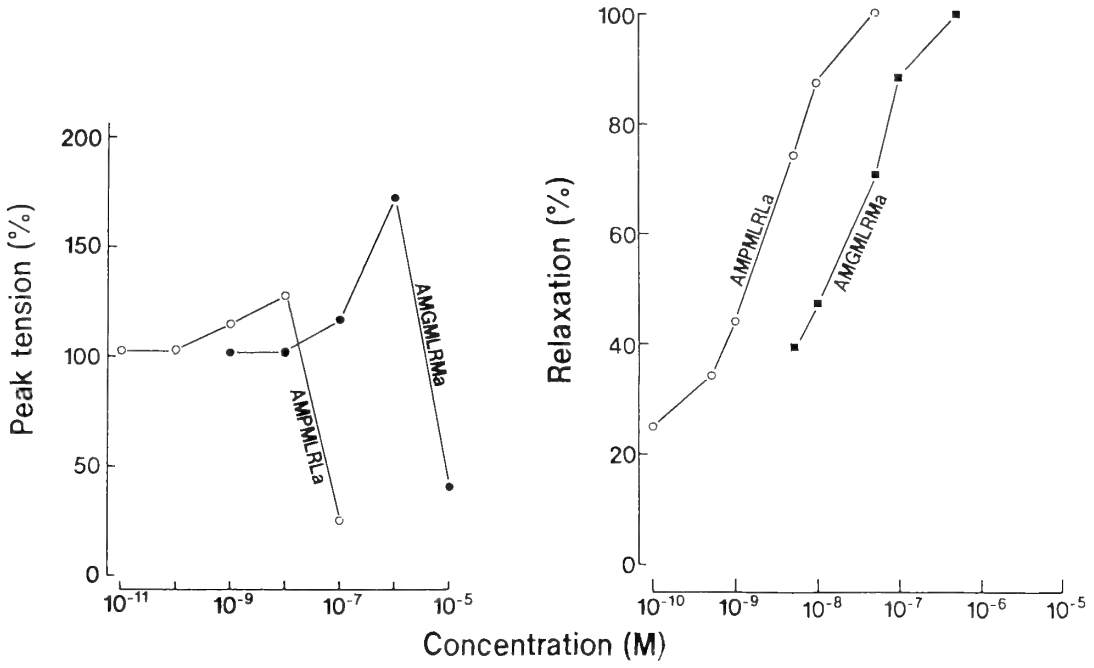

FIG. 6. Dose-response relationships of AMPMLRLamide (CARP) and AMGMLRMamide (Pev-myomodulin) for modulating actions on the phasic contractions (left) and for relaxing actions on the catch contractions (right) of the *Mytilus* ABRM.

the occurrence of a member of the family in the Annelida. Since Pev-myomodulin showed a potent contractile effect on the esophagus of *P. vancaurica,* this peptide may be involved in the regulation of the esophagus of the animal. We have isolated previously two S-Iamide peptides from *P. vancaurica,* both of which elicit spontaneous contraction of the esophagus of the same animal as did Pev-myomodulin [16]. It is probable that some other peptides, which affect gut motility, may be found in *P. vancaurica,* and in other annelids as well, in future.

A conspicuous difference in structure between the annelid peptide and the molluscan peptides is at their C-termini. The annelid peptide has a Met-NH_2 at its C-terminus, while all the molluscan peptides have a Leu-NH_2. Among the myomodulin-CARP-family peptides including Pev-myomodulin, the annelid peptide shows the most potent contractile effect on the esophagus of *P. vancaurica.* The C-terminal Met-NH_2 of the peptide seems to be important in eliciting the potent effect. This notion is supported by the facts that Leu^7-Pev-myomodulin is far less potent than Pev-myomodulin and that Met^7-CARP and Met^7-myomodulin are more potent than CARP and myomodulin, respectively.

The synthetic analogues Phe^7-CARP and Phe^7-myomodulin show less potent effects than CARP and myomodulin, respectively. This may be partly due to FMRFamide-like actions of the analogue peptides, because it has been known that FMRFamide has an inhibitory action on the esophagus of a polychaete annelid, *N. virens* [14]. FMRFamide has been shown to be present in some annelids [1, 4, 13].

C-terminus-free CARP, Ala-Met-Pro-Met-Leu-Arg-Leu-OH, does not show any contractile effect on the esophagus, suggesting that the C-terminal amide is essential for exertion of the contractile effects of the myomodulin-CARP-family peptides. It has been reported that the C-terminal amide is essential for catch-relaxing action of CARP on the ABRM of *M. edulis* [6]. Another example for essentiality of C-terminal amide for bioactivity is the RPCH-related peptide, APGWamide, which has been isolated from ganglia of the gastropod mollusc *Fusinus ferrugineus* [15]. On electrically-elicited phasic contractions of the *Mytilus* ABRM, the C-terminal dipeptide fragment of APGWamide, GWamide, shows a comparable activity to the native tetrapeptide, while C-terminal-free dipeptide, GW, does not show any activity [17]. Therefore, the C-terminal amide of small bioactive peptides having amidated C-termini may be generally essential for exertion of their bioactivity.

The tetrapeptide fragment, Met-Leu-Arg-Leu-NH_2, shows a considerable effect on the esophagus, but the tripeptide fragment, Leu-Arg-Leu-NH_2, does not show any effect. These facts suggest that the C-terminal tetrapeptide sequence is the minimum structure required for expression of the contractile effect of the myomodulin-CARP-family peptides on the esophagus, though the Met residue can be substituted at least with Trp.

It has been shown that CARP potentiates phasic contraction of the ABRM of *M. edulis* in response to repetitive electrical stimulation at lower doses and inhibits at higher doses [7, 18]. The annelid peptide Pev-myomodulin also shows a potentiating effect at lower doses and an inhibitory effect at higher doses on phasic contraction of the ABRM. However, CARP exerts these effects at about 100 times lower

concentrations than Pev-myomodulin. As shown in Figure 5A, therefore, 10^{-6} M CARP inhibits the phasic contraction while 10^{-6} M Pev-myomodulin potentiates it. The reason why the myomodulin-CARP-family peptides show such dual actions is obscure at present. The annelid peptide, as well as CARP, relaxes catch tension of the ABRM. However, the annelid peptide is approximately 10 times less potent than CARP. In the ABRM, therefore, the authentic peptide CARP is more potent than the foreigh peptide Pev-myomodulin.

In conclusion, we isolated a novel member of myomodulin-CARP family from the marine polychaete, *P. vancaurica*. It has been shown that S-Iamide-family peptides [16] and FMRFamide-family peptides [1, 4, 13] are present not only in molluscs but also in annelids. Annelids seem to have many neuropeptides closely related to molluscan neuropeptides.

ACKNOWLEDGMENTS

The authors wish to express their sincere thanks to Professor Y. Muneoka, Hiroshima University, for his valuable comments throughout the present study and critical review of the manuscript.

REFERENCES

1 Baratt B, Gras-Masse H, Ricart G, Bulet P, Dhainaut-Courtois N (1991) Isolation and characterization of authentic Phe-Met-Arg-Phe-NH_2 and the novel Phe-Thr-Arg-Phe-NH_2 peptide from *Nereis diversicolor*. Eur J Biochem 198: 627–633

2 Cropper EC, Tenenbaum R, Kolks MAG, Kupfermann I, Weiss KR (1987) Myomodulin: a bioactive neuropeptide present in an identified cholinergic buccal motor neuron of *Aplysia*. Proc Natl Acad Sci USA 84: 5483–5486

3 Cropper EC, Vilim FS, Alevizos A, Tenenbaum R, Kolks MAG, Rosen S, Kupfermann I, Weiss KR (1991) Structure, bioactivity, and cellular localization of myomodulin B: a novel *Aplysia* peptide. Peptides 12: 683–690

4 Evans BD, Pohl J, Kartsonis NA, Calabrese RL (1991) Identification of RFamide neuropeptides in the medicinal leech. Peptides 12: 897–908

5 Greenberg MJ, Price DA (1992) Relationships among the FMRFamide-like peptides. In "Progress in Brain Research Vol 92" Ed by J Joose, RM Buijis, FJH Tilders, Elsevier Science Publishers BV, pp 25–37

6 Hirata T, Kubota I, Imada M, Muneoka Y (1989) Pharmacology of relaxing response of *Mytilus* smooth muscle to the catch-relaxing peptide. Comp Biochem Physiol 92C: 289–295

7 Hirata T, Kubota I, Imada M, Muneoka Y, Kobayashi M (1989) Effects of the catch-relaxing peptide on molluscan muscles. Comp Biochem Physiol 92C: 283–288

8 Hirata T, Kubota I, Takabatake I, Kawahara A, Shimamoto N, Muneoka Y (1987) Catch-relaxing peptide isolated from *Mytilus* pedal ganglia. Brain Res 422: 374–376

9 Holman GR, Nachman RJ, Wright MS, Schoofs L, Hayes TK, DeLoof A (1991) Insect myotropic peptides. Isolation, structural characterization, and biological activities. In "Insect Neuropeptides. Chemistry, Biology and Action" Ed by JJ Menn, TJ Kelly, EP Masler, American Chemical Society, Washington, DC. pp 40–50

10 Ikeda T, Minakata H, Fujita T, Muneoka Y, Kiss T, Hiripi L, Nomoto K (1993) Neuropeptides isolated from *Helix pomatia*. I. Peptides related to MIP, buccalin, myomodulin-CARP and SCP. In "Peptide Chemistry 1992" Ed by N Yanaihara, ESCOM Science Publishers BV, pp 576–578

11 Kanda T, Kuroki Y, Kubota I, Muneoka Y, Kobayashi M (1990) Neuropeptides isolated from the ganglia of a prosobranch mollusc, *Fusinus ferrugineus*. In "Peptide Chemistry 1989" Ed by N Yanaihara, Protein Research Foundation, Osaka, pp 39–44

12 Keller R (1992) Crustacean neuropeptides: structure, function and comparative aspects. Experientia 48: 439–448

13 Krajniak KG, Price DA (1990) Authentic FMRFamide is present in the polychaete *Nereis virens*. Peptides 11: 75–77

14 Krajniak KG, Greenberg MJ (1992) The localization of FMRFamide in the nervous and somatic tissues of *Nereis virens* and its effects upon the isolated esophagus. Comp Biochem Physiol 101C: 93–100

15 Kuroki Y, Kanda T, Kubota I, Fujisawa Y, Ikeda T, Miura A, Minamitake Y, Muneoka Y (1990) A molluscan neuropeptide related to the crustacean hormone, RPCH. Biochem Biophys Res Commun 167: 273–279

16 Matsushima O, Takahashi T, Morishita F, Fujimoto M, Ikeda T, Kubota I, Nose T, Miki W (1993) Two S-Iamide peptides, AKSGFVRIamide and VSSFVRIamide, isolated from an annelid, *Perinereis vancaurica*. Biol Bull 184: 216–222

17 Minakata H, Kuroki Y, Ikeda T, Fujisawa Y, Nomoto K, Kubota I, Muneoka Y (1991) Effects of the neuropeptide APGWamide and related compounds on molluscan muscles —GWamide shows potent modulatory effects. Comp Biochem Physiol 100C: 565–571

18 Muneoka Y, Kobayashi M (1992) Comparative aspects of structure and action of molluscan neuropeptides. Experientia 48: 448–456

19 Muneoka Y, Twarog BM (1977) Lanthanum block of contraction and of relaxation in response to serotonin and dopamine in molluscan catch muscle. J Pharmac Exp Ther 202: 601–609

20 Penzlin H (1989) Neuropeptides—occurrence and function in insects. Naturwissenschaften 76: 243–252

21 Walker RJ (1992) Neuroactive peptides with an RFamide or Famide carboxyl terminal. Comp Biochem Physiol 102C: 213–222

ZOOLOGICAL SCIENCE 11: 39–44 (1994)

Changes in the Responsiveness of Melanophores to Electrical Nervous Stimulation after Prolonged Background Adaptation in the Medaka, *Oryzias latipes*

Masazumi Sugimoto, Takayuki, Kawamura, Ryozo Fujii and Noriko Oshima

Department of Biomolecular Science, Faculty of Science, Toho University, Miyama, Funabashi, Chiba 274, Japan

ABSTRACT—The effects of prolonged background adaptation on the responses of melanophores were studied using electrical nervous stimulation. Electrical stimulation at various intensities and frequencies and for various periods of time was applied to scales isolated from *B* and *W* fish and the responses of melanophores in the scales were recorded photoelectrically. When electrical stimulation at enough intensity to induce maximal melanosome-aggregation response ("maximal stimulus") was applied, there was no significant difference, in terms of the relationship between the magnitude of the aggregation response and the frequency or period of stimulation, between melanophores of *B* and *W* fish. However, the minimum effective voltage necessary to provoke the discernible aggregation of melanosomes in *B* fish was lower than that in *W* fish. With application of stimulation at intensities less than intensity of maximal stimulus, the response of melanophores in *B* fish was greater than that in *W* fish. These results suggest that prolonged background adaptation may induce changes in the excitability or in the density of distribution of chromatic nerve fibers, with a resultant change in the concentration of released norepinephrine, upon electrical stimulation.

INTRODUCTION

Color changes in teleost fish are under both neural and hormonal control, and melanophores in the skin play an important role in such changes. Bidirectional movements of melanosomes within melanophores, which are responsible for the physiological color change, are known to be regulated mainly by neural control. Norepinephrine, the neurotransmitter liberated from sympathetic postganglionic fibers, causes the aggregation of melanosomes via stimulation of α-adrenoceptors on the melanophore membrane [7, 10, 11]. In addition, various hormonal principles, such as melatonin, alpha melanophore-stimulating hormone (α-MSH) and melanin-concentrating hormone (MCH), have the ability to cause translocation of melanosomes [4, 5, 9, 15, 16]. Changes in the number and in the size of melanophores, which give rise to the morphological color change, are considered to be controlled by hormones. Several investigators have reported that the pituitary hormones, namely, α-MSH and MCH, are responsible for the morphological color change [2, 3, 22]. The two types of color change may be interrelated, but the interrelationship is not well understood.

Background adaptation is considered to be composed of two phases; an initial physiological color change and a subsequent morphological change [1, 24]. Therefore, an analysis of background adaptation may contribute to clarification of the relationship between the two types of color change. Recently, using chemically denervated medaka, Sugimoto [19] found that innervation also influenced the density of melanophores during background adaptation. Moreover, a change in the responsiveness of melanophores to exogenous norepinephrine occurred after prolonged background adaptation [19]. In the present study, therefore, we used electrical stimulation of chromatic nerves to examine, at the tissue level, whether a change in the responsiveness of melanophore to endogenous neurotransmitter liberated from sympathetic nerve fibers could be recognized after prolonged background adaptation. On the basis of our results, we discuss the effects of prolonged background adaptation on the nerves that control the aggregation of pigment in melanophores.

Accepted October 29, 1993
Received September 2, 1993

MATERIALS AND METHODS

Wild-type medaka, *Oryzias latipes,* of both sexes, 25–35 mm in total length, were purchased from local commercial sources.

For background adaptation, fish were maintained for 10 days in a black- or a white-background aquarium under continuous illumination at 2000 lx at the surface of the water. In the present paper, these fish are referred to as *B* fish and *W* fish, respectively. Scales isolated from the dorsal trunk of *B* or *W* fish were immersed for 10 min at 4°C in Ca^{2+}- and Mg^{2+}-free physiological saline solution (CMF-PSS) of the following composition: NaCl, 129.8 mM; KCl, 2.7 mM; D-glucose, 5.6 mM; EDTA, 1 mM; Tris-HCl buffer (pH 7.4), 5.0 mM. The epidermal layer of the scales was then ripped off with forceps, and the epidermis-free scales were kept in physiological saline solution (PSS) of the following composition: NaCl, 125.3 mM; KCl, 2.7 mM; $CaCl_2$, 1.8 mM; $MgCl_2$, 1.8 mM; D-glucose, 5.6 mM; Tris-HCl buffer (pH 7.4), 5.0 mM. These scales were used for electrophysiological studies within 3 hr of their isolation from fish.

The system employed for the perfusion of experimental solutions and the electrical stimulation of chromatic nerves was similar to that

described by Fujii & Novales [6] and Fujii & Miyashita [8]. A platinum wire of 300 μm in diameter was fully insulated, except at its tips, and used as the stimulating electrode. The electrode was placed vertically on the central part of a scale in order to stimulate melanosome-aggregating nerves. As an indifferent electrode, another platinum wire was dipped in the solution in the perfusion chamber at a distance of 5 mm from the stimulating electrode. Electrical stimulation at various intensities and frequencies and for various periods of time was delivered as a volley of negative pulses of 1-msec duration by means of an electric stimulator, SEN-2101 (Nihon Kohden, Tokyo). A synchroscope, SS-5116 (Iwatsu, Tokyo) was used to monitor the stimulating pulses.

Response of each single melanophore, located at a distance of 100–200 μm from the stimulating electrode, was recorded photoelectrically. The method used for recording the motile response of a melanophore was identical to that described by Oshima and Fujii [17]. Since there are many xanthophores in the scales of the wild-type medaka, a red filter (R-60; Toshiba, Tokyo), which blocked light with wavelengths below 600 nm, was placed across the light path in the optical part of the recording system to eliminate any influence from the motile activity of these cells. In each series of measurements, the extent of the response of a melanophore was expressed as a percentage of the complete aggregation of melanosomes produced by norepinephrine hydrochloride at 10 μM (NE; Sankyo, Tokyo).

All measurements were performed at a room temperature, which fluctuated between 18° and 26°C.

RESULTS

After background adaptation for 10 days, which was taken as "prolonged background adaptation", remarkable differences in terms of the number and the size of melanophores were apparent between the scales of *B* and *W* fish. In both fish, electrical nervous stimulation at 5 V to central portions of isolated scales brought about the rapid aggregation of melanosomes within the melanophores (Fig. 1). For as much as 3 hr after the isolation of scales, melanophores responded repeatedly to electrical nervous stimulation with similar aggregation of pigment. Therefore, one and the same melanophore was observed in a series of experiments in which electrical stimulation with various parameters was applied to the scale. The melanosomes redispersed within 4 min after cessation of electrical stimulation, and the next stimulus was applied after complete redispersion.

Effects of changes in stimulus intensity on the responses of melanophores

Figure 2 is a typical recording of melanosome-aggregating responses to electrical nervous stimulation at various intensities in a melanophore from a *B* fish and that from a *W* fish. In these experiments, the frequency and duration were kept constant at 1 Hz and 1 msec, respectively. Stimulation was applied for 30 sec since the medaka really adapted to a white background within 30 sec. In both *B* and *W* fish, melanin-aggregating responses started 5–10 sec after the initiation of the stimulus, and redispersion began immediately after cessation of the stimulation. The relationship between the intensity of the stimulus and the magnitude of the response of melanophores is summarized in

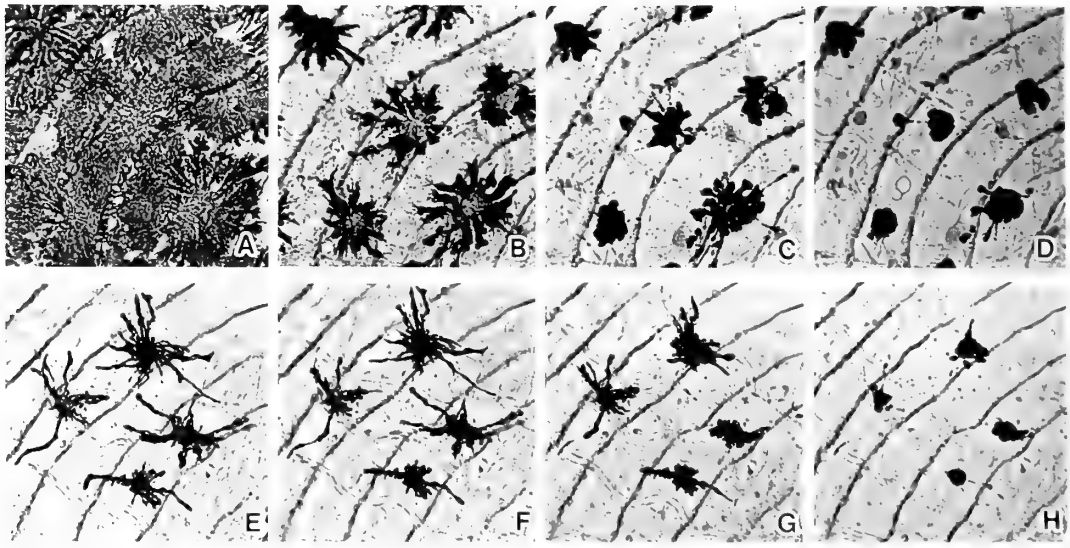

FIG. 1. Photomicrographs showing the melanosome-aggregating responses of melanophores in scales to electrical nervous stimulation. The upper series (A-D) shows the responses in a scale from a B fish and the lower series (E-H) shows those in a scale from a *W* fish. In each series, photographs were taken with transmission optics of the same part of a given scale from the dorsal trunk. A and E: equilibrated in PSS. Melanosomes in melanophores are fully dispersed. Note that larger melanophores are present at higher density in the *B* fish. B and F: 15 sec after the application of stimulating pulses at an intensity of 5 V, at a frequency of 1 Hz and with a duration of 1 msec. Melanosomes are in the process of aggregating. C and G: 1 min after the start of electrical stimulation. The melanosome-aggregating responses have reached the maximal level. D and H: 4 min after treatment with 10 μNE, which was applied at the end of the electrical stimulation. Melanosomes are completely aggregated. Note that the extent of melanosome aggregation caused by NE is greater than that induced by the electrical stimulation ($\times$160).

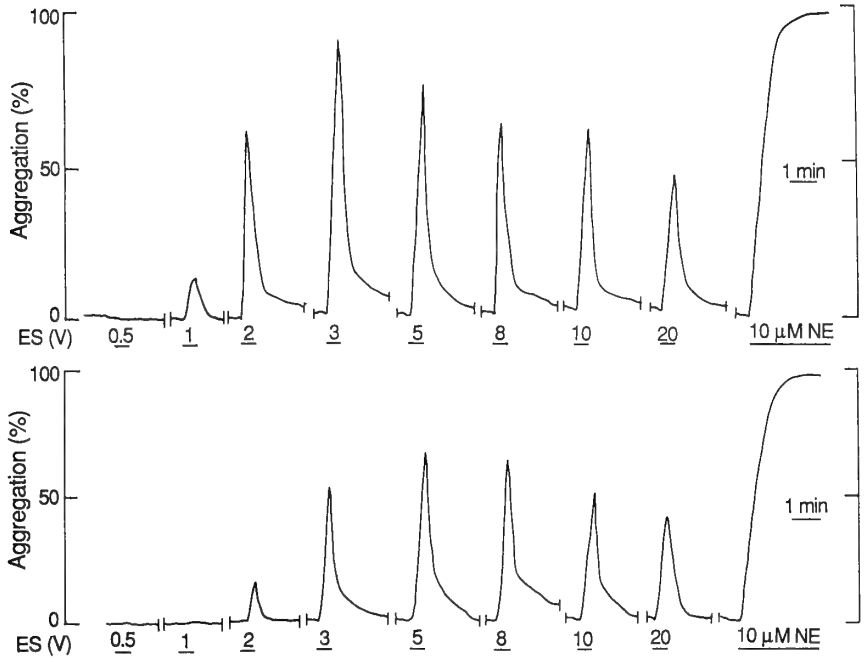

FIG. 2. Typical recordings of the responses of melanophores to electrical stimulation at various intensities. The upper and lower recordings show the responses of a melanophore from a *B* fish and those of a melanophore from a *W* fish, respectively. The frequency and period of stimulation were 1 Hz and 30 sec, respectively. After the cessation of electrical stimulation, 10 μM NE was applied for 4 min to bring about complete (100%) aggregation of melanosomes. Although there was a difference in the threshold intensity between melanophores from *B* and *W* fish, the magnitude of the response increased depending on the intensity of the stimulus in both cases. ES, electrical stimulation.

Figure 3. In *B* fish, melanosomes in melanophores slightly aggregated in response to 1-V pulses and considerably in response to the intensities above 2 V. In melanophores of *W* fish, however, no distinct aggregation response was seen at intensities of 2 V and lower. Thus, the response of melanophores to 2-V pulses in *B* fish was significantly greater than that in *W* fish ($P<0.001$). In melanophores of both fish, stimulation at 5 V induced the maximal response, which was about 70% of the full response caused by 10 μM NE, and a further increase in the intensity of the stimulus caused a gradual decrease in the magnitude of the response.

Effects of changes in the period of stimulation on responses of melanophores

Electrical stimulation was applied for various periods of time at an intensity of 5 V, a frequency of 1 Hz and a duration of 1 msec. The relationship between the period of stimulation and the response of melanophores is shown in Figure 4. Five-sec stimulation, namely, five pulses of 1-msec duration over the course of 5 sec, induced discernible aggregation of melanosomes in both *B* and *W* fish. Until the responses of melanophores reached a plateau at about 30-sec stimulation, increases in the period of stimulation were accompanied by gradual increases in the magnitude of the response. As indicated in Figure 4, the curves for *B* and *W* fish were similar, and the response in both cases did not exceed 80% of the full response caused by NE at 10 μM.

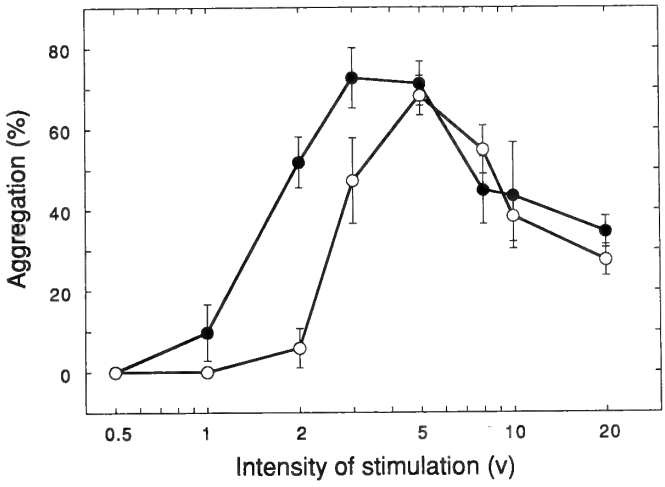

FIG. 3. Relationship between the intensity of the stimulus and the magnitude of the melanosome-aggregating response in a single melanophore. The curves drawn through solid and open circles indicate the relationships in *B* and *W* fish. respectively. Stimulation was applied at a frequency of 1 Hz (1-msec duration) for 30 sec. Complete (100%) aggregation of pigment was caused by treatment with 10 μM NE for 4 min. Each point represents the mean of measurements on scales from five different fish. Vertical lines indicate standard errors.

Effects of changes in the frequency of the stimulus on responses of melanophores

The frequency of pulses also affected the responses of

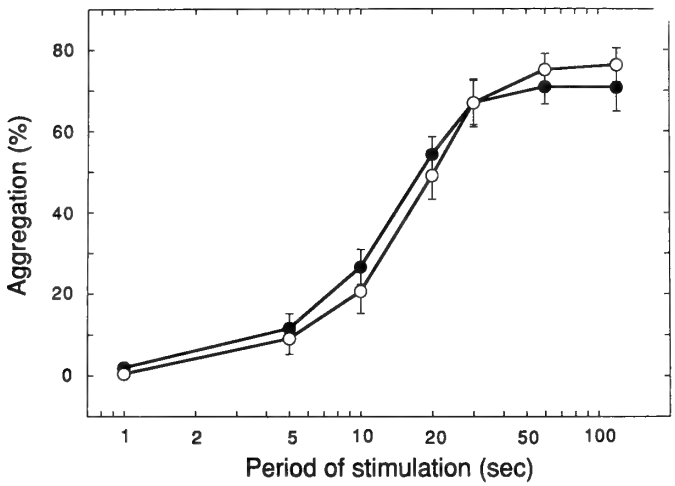

FIG. 4. Relationship between the period of stimulation and the magnitude of the melanosome-aggregating response in a single melanophore. The curves through solid and open circles indicate the relationships in *B* and *W* fish, respectively. Stimulation at 5 V and 1 Hz was applied for various periods of time. Complete (100%) aggregation of pigment was caused by the treatment with 10 μM NE for 4 min. Each point represents the mean of measurements on scales from five different fish. Vertical lines indicate standard errors.

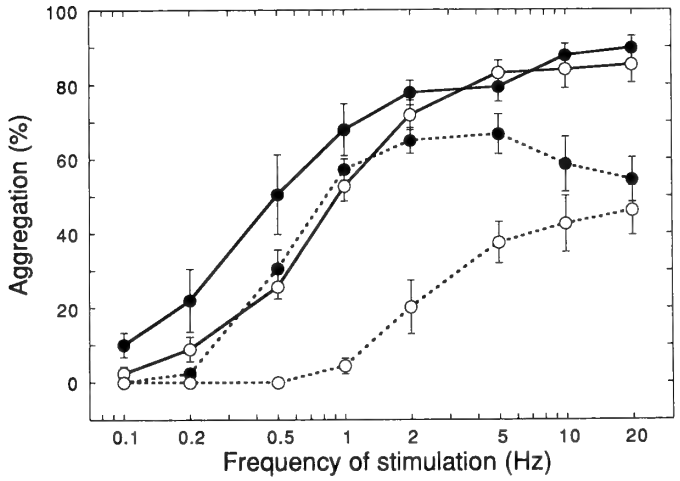

FIG. 5. Relationship between the frequency of the stimulus and the magnitude of the melanosome-aggregating reaction in a single melanophore. The curves through solid and open circles indicate the relationships in *B* and *W* fish, respectively. Stimulation was applied at an intensity of 2 V (dashed line) or 5 V (uninterrupted line) for 30 sec. Complete (100%) aggregation of pigment was caused by treatment with 10 μM NE for 4 min. Each point represents the mean of measurements on scales from five different fish. Vertical lines indicate standard errors.

melanophores. Figure 5 shows the frequency-response curves. The frequency was changed from 0.1 Hz to 20 Hz and other parameters were kept constant (5 V, 1-msec duration, 30-sec stimulation). As the frequency of the stimulation was increased from 0.1 to 5 Hz, the magnitude of the response increased by degrees. The response reached a plateau at more than 5 Hz, and the maximal responses were about 90% of the full response to 10 μM NE in both *B* and *W* fish. There was no significant difference between the curves for *B* and *W* fish. However, frequencies below 1 Hz had a tendency to provoke a greater response in *B* fish than in *W* fish. Next, the frequency of stimulation was reduced successively without a cessation of stimulus for 4 min among measurements at each frequency, unlike the experiments mentioned above. The magnitude of the response also decreased, reaching a stable value at each frequency (Fig. 6). The effective frequencies of the stimulation for the induction of 50% aggregation of melanosomes [EF_{50} (95% confidence limits)] in *B* and *W* fish, that were estimated by experimental results shown in Figure 5, were 0.66 Hz (0.22–2.00 Hz) and 1.29 Hz (0.56–2.97 Hz), respectively.

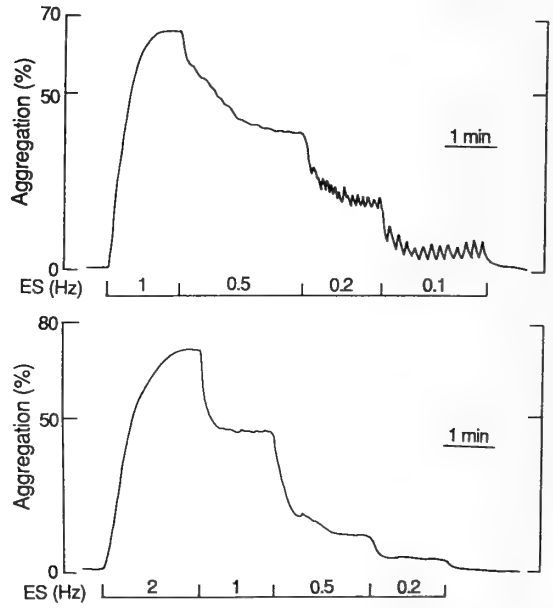

FIG. 6. Typical recordings showing the changes in the magnitude of the melanophore response with changes in the frequency. The upper panel shows a recording from a *B* fish melanophore at frequencies of 1, 0.5, 0.2 and 0.1 Hz, in turn. The lower panel shows a recording from a *W* fish melanophore at frequencies of 2, 1, 0.5 and 0.2 Hz, in turn. The intensity of the stimulus was 5 V and the duration was 1 msec. Complete (100%) aggregation of pigment was caused by treatment with 10 μM NE for 4 min. ES, electrical stimulation.

When a volley of pulses at 2 V was applied, which induced only a small response at 1 Hz in *W* fish (see Fig. 3), the threshold frequency for the induction of the response in *B* fish was lower than that in *W* fish (dashed line in Fig. 5). Within the range from 0.5 to 5 Hz, the magnitude of the response in *B* fish was significantly different from that in *W* fish ($P<0.01$) and EF_{50} (95% confidence limits) was 1.23 Hz (0.36–4.22 Hz) and 17.67 Hz (4.5–68.18 Hz), respectively. The response of melanophores in *B* fish reached a plateau value at 5 Hz, whereas that in *W* fish gradually increased with increases in the frequency. The maximal responses caused by 2-V pulses were 74% and 51% of the maximal aggregation

at 5 V in *B* and *W* fish, respectively.

DISCUSSION

Since the melanophore itself is a nonexcitable type of cell [5], neural control of its motility has been effectively studied by electrical nervous stimulation [6, 7, 8, 11, 18, 21]. Fujii and Novales [6], using split tail-fin preparations of *Fundulus,* showed that even a single stimulating pulse to chromatic nerves causes moderate aggregation of melanosomes in a melanophore. They also suggested that multiple chromatic nerve fibers might control the motility of a single melanophore since the melanosome-aggregation response increased with increases in the intensity of electrical stimulation. In the present study, we used melanophores in scales isolated from the medaka and obtained similar results for the relationship between the extent of the response and the intensity of the stimulus (see Fig. 3). More than two nerve fibers seem to be present in the scale, as well as in the tail fin. Our results are also consistent with morphological observations on the innervation of teleost melanophores reported by Yamada *et al.* [25] and Miyata & Yamada [14], who found networks of adrenergic varicose fibers labeled with [^{3}H]-NE in the scale and the tail fin, respectively.

In general, an indication of the excitability of nerve fibers is proved by the extent of effector responses caused by stimulation at various intensities [23]. We compared responses of melanophore from *B* fish to electrical stimulation at various intensities with those of *W* fish. At 5 V, all chromatic fibers in the scales of *W* fish seemed to participate in the response because stimulation at this intensity elicited the maximal response. In *B* fish, by contrast, the maximal response was induced at 3 V, and 5-V stimulation did not further augment the magnitude of the response, which was not the full response, being only 70% of the complete aggregation of pigment caused by 10 μM NE. These findings suggest a change in the excitability of chromatic nerve fibers in response to the electrical stimulation. These data may also suggest that the density of distribution of chromatic nerve fibers in the scales of *B* fish might be higher than that in the scales of *W* fish. It is unclear why the magnitude of the response was reduced at intensities above 8 V in both fish but polarization of stimulating electrode might be involved in this phenomenon, at least to some extent.

The magnitude of the response also depended on the period of stimulation (see Fig. 4). In both *B* and *W* fish, however, the period of stimulation required for the maximal response was the same. Melanophores in scales from *B* fish possessed many thick dendritic processes, and dendrites of *W* fish melanophores were thin and small in number (see Fig. 1). Therefore, the area occupied by each melanophore of *B* fish was larger than that of *W* fish [19]. However, melanophores of *W* fish seemed to be roughly equal to these of *B* fish in the total length of a cell: the distance between the tips of two dendrites which project in an opposite direction each other with the cell body between. Thus, the distances that melanosomes would migrate within melanophores of both *B* and *W* fish might be almost the same. About 30 sec were required to induce the maximal response by stimulation at 5 V and 1 Hz.

In order to investigate the effect of prolonged background adaptation on the mechanism of release of the neurotransmitter, melanophore responses of *B* and *W* fish to various frequencies of stimulation were examined. Stimulation at 5 V was applied for 30 sec to activate all chromatic fibers and to achieve the maximal response at a given frequency. It is generally known that, when electrical stimulation at an intensity that activates all fibers is used to stimulate the peripheral neuroeffector system, the amount of NE released per stimulating pulse is constant. An increase in frequency increases the concentration of the released neurotransmitter that diffuses in the synaptic cleft [23]. Thus, the frequency-response curves in the present study indicate the relationships between the amount of NE released and the extent of the melanosome-aggregating response (see Fig. 5). Since there was no significant difference between the curves for *B* and *W* fish at an intensity of 5 V, no difference in the sensitivity of melanophores to the endogenous neurotransmitter was demonstrated. However, Sugimoto [20] reported that, as judged from the EC_{50}, the responsiveness of melanophores to exogenous NE in *B* fish was about 16 times higher than that in *W* fish. Such disagreement with the present result implies that the action of neurotransmitter released *in situ* from chromatic nerves differs from that of exogenous NE *in vitro*. In the former case, released NE is rapidly inactivated by neuronal re-uptake and metabolizing enzymes [13]. Moreover, Kumazawa and Fujii [12] demonstrated the concomitant release of ATP together with the true transmitter, NE, and they suggested that ATP is successively dephosphorylated to adenosine and functions as a cotransmitter to promote the effective redispersion of pigment. An increase in levels of released NE by high-frequency stimulation is also accompanied by increased release of ATP, with resultant prompt recovery from the effects of NE. In fact, as shown in the Figure 6, the extent of melanosome aggregation decreased quickly upon reduction of the frequency of stimulation, whereas a decrease in the concentration of exogenous NE did not rapidly reduce the extent of the responses of melanophores in the reaction chamber (data not shown). Thus, the change in the sensitivity of melanophores to NE, which was observed by Sugimoto [20] of the addition of exogenous NE, was not clear in the present experiments at the tissue level.

When electrical stimulation at 2 V was applied, the EF_{50} in *B* fish was about 14 times lower than that in *W* fish, suggesting the enhanced excitability of the chromatic fibers of *B* fish at various frequencies of electrical stimulation. The response in *B* fish reached a plateau at a frequency of 5 Hz, but the aggregation of pigment was far from complete. Probably, increases in frequency above 5 Hz failed to increase the concentration of liberated transmitter.

From the present results, we conclude that the prolonged

background adaptation affects the responses of melanophores to electrical nervous stimulation *in situ*, as a result of the changes in the excitability of nerves to stimulation and/or in the density of distribution of nerve fibers. In addition, a change in the sensitivity to exogenous NE of melanophores themselves has also been pointed out [20]. It seems likely that the change in the responsiveness of melanophores contributes to adaptation to a new background color after prolonged background adaptation. As an illustration, when fish that have fully adapted to a dark background are transferred to a new background that is brighter than the previous one, the increased excitability of chromatic nerve fibers and the increased sensitivity of melanophores to melanosome-aggregating agents may be advantageous since the fish can adapt to the new background rapidly. By contrast, decreased excitability and sensitivity may be of advantage to fish that are fully adapted to a bright background. In our next report, patterns of innervation of melanophores in *B* and *W* fish will be described.

REFERENCES

1 Bagnara JT, Hadley ME (1973) Chromatophores and Color Change. Prentice-Hall, Englewood Cliffs, New Jersey

2 Baker BI, Wilson JF, Bowley TJ (1984) Changes in pituitary and plasma levels of α-MSH in teleost during physiological color change. Gen Comp Endocrinol 55: 142–149

3 Baker BI, Bird DJ (1992) The biosynthesis of melanin-concentrating hormone in trout kept under different conditions of background colour and stress, as determined by an in vitro method. J Neuroendocrinol 4: 673–679

4 Fain WB, Hadley ME (1966) In vitro response of melanophores of *Fundulus heteroclitus* to melatonin, adrenaline and noradrenaline. Am Zool 6: 596

5 Fujii R (1961) Demonstration of the adrenergic nature of transmission at the junction between melanophore-concentrating nerve and melanophore in bony fish. J Fac Sci Univ Tokyo, IV, 9: 171–196

6 Fujii R, Novales RR (1969) The nervous mechanism controlling pigment aggregation in *Fundulus* melanophores. Comp Biochem Physiol 29: 109–124

7 Fujii R, Miyashita Y (1975) Receptor mechanisms in fish chromatophores—I. Alpha nature of adrenoceptors mediating melanosome aggregation in guppy melanophores. Comp Biochem Physiol 51C: 171–178

8 Fujii R, Miyashita Y (1976) Receptor mechanisms in fish chromatophores—III. Neurally controlled melanosome aggregation in a siluroid (*Parasilurus asotus*) is strangely mediated by cholinoceptors. Comp Biochem Physiol 55C: 43–49

9 Fujii R, Miyashita Y (1978) Receptor mechanisms in fish chromatophores—IV. Effects of melatonin and related substances on dermal and epidermal melanophores of the siluroid, *Parasilurus asotus*. Comp Biochem Physiol 59C: 59–63

10 Fujii R, Oshima N (1986) Control of chromatophore movements in teleost fishes. Zool Sci 3: 13–47

11 Iwata KS, Fukuda H (1973) Central control of color changes in fish. In "Responses of Fish to Environmental Changes" Ed by W Chavin, Springfield, Illinois, pp 316–341

12 Kumazawa T, Fujii R (1984) Concurrent release of norepinephrine and purines by potassium from adrenergic melanosome-aggregating nerve in tilapia. Comp Biochem Physiol 78C: 263–266

13 Langer SZ (1981) Presynaptic regulation of the release of catecholamines. Pharmacol Rev 32: 337–362

14 Miyata S, Yamada K (1987) Innervation pattern and responsiveness of melanophores in tail fins of teleosts. J Exp Zool 241: 31–39

15 Nagai M, Oshima N, Fujii R (1986) A comparative study of melanin-concentrating hormone (MCH) action on teleost melanophores. Biol Bull 171: 360–370

16 Negishi S, Obika M (1980) The effects of melanophore-stimulating hormone and cyclic nucleotides on teleost fish chromatophores. Gen Comp Endocrinol 42: 471–476

17 Oshima N, Fujii R (1984) A precision photoelectric method for recording chromatophore responses in vitro. Zool Sci 1: 545–552

18 Parker GH (1948) Animal color change and their neurohumours. Cambridge Univ Press, London

19 Sugimoto M (1993) Morphological color changes in the medaka, *Oryzias latipes*, after prolonged background adaptation—I. Changes in the population and morphology of melanophores. Comp Biochem Physiol 104A: 513–518

20 Sugimoto M (1993) Morphological color changes in the medaka, *Oryzias latipes*, after prolonged background adaptation—II. Changes in the responsiveness of melanophores. Comp Biochem Physiol 104A: 519–523

21 Ueda K (1955) Stimulation experiment on fish melanophores. Annot Zool Jap 28: 194–205

22 van Eys GJJM, Peters PTW (1981) Evidence for a direct role on α-MSH in morphological background adaptation of the skin in *Sarotherodon mossambicus*. Cell Tissue Res 217: 361–372

23 von Euler US (1959) Autonomic neuroeffector transmission. In "Neurophysiology". Ed by Am Physiol Soc, Washington, D.C., pp 215–237

24 Waring H (1963) Color Change Mechanisms of Cold-blooded Vertebrates. Academic Press, New York London

25 Yamada K, Miyata S, Katayama H (1984) Autoradiographic demonstration of adrenergic innervation to scale melanophores of a teleost fish, *Oryzias latipes*. J Exp Zool 229: 73–80

ZOOLOGICAL SCIENCE 11: 45–53 (1994)

Vitellogenin Production Induced by Eyestalk Ablation in Juvenile Giant Freshwater Prawn *Macrobrachium rosenbergii* and Trial Methyl Farnesoate Administration

MARCY N. WILDER, TAKUJI OKUMURA[1], YUZURU SUZUKI, NOBUHIRO FUSETANI and KATSUMI AIDA

Department of Fisheries, Faculty of Agriculture, The University of Tokyo, 1-1-1 Yayoi, Bunkyo-ku, Tokyo 113, Japan

ABSTRACT—Juvenile *Macrobrachium rosenbergii* were bilaterally eyestalk-ablated and hemolymph-sampled at 3 to 6 day-intervals for three weeks. In males, vitellogenin appeared several days after ablation, increased slightly for 1–2 weeks, and then decreased. Quantification by enzyme immunoassay indicated peak vitellogenin levels ranging from 0.1 to 0.8 mg/ml. Females showed a similar profile, but peak levels ranged from 0.5 to 3.0 mg/ml; one individual was however exceptional with titers reaching nearly 30 mg/ml. Vitellogenin was not detectable in non-ablated animals. Juvenile male and female vitellogenin was shown by SDS-PAGE/Western blotting to consist of a single polypeptide component of 199K; however, in the exceptional female only, vitellogenin was composed of three polypeptides of 199, 102 and 90K as in adult female vitellogenin. Nevertheless, all ablated juvenile females exhibited increased gonadosomatic index and vitellogenic oocytes, as demonstrated by immunocytochemical techniques. Subsequently, juvenile males were employed to examine the effects of methyl farnesoate (MF) administration on vitellogenin production. In ablated animals, no significant differences in vitellogenin production were observed between the MF-injected and saline-injected groups. MF administration could not induce vitellogenin production in non-ablated animals. The physiological significance of the appearance of vitellogenin in juveniles of both sexes in context of the above results is discussed.

INTRODUCTION

In decapod crustaceans, the processes of molting and reproduction are inextricably linked; these are under the negative control of the peptide hormones, vitellogenesis-inhibiting hormone (VIH) and molt-inhibiting hormone (MIH). MIH and VIH originate in the X-organ/sinus gland complex of the eyestalk and have been extensively characterized in several species [5, 9, 29, 35]. Stimulatory factors also exist but their identities are not fully known; the thoracic ganglia have been demonstrated by several investigators [15, 33, 39] to be a source of a vitellogenesis-stimulating hormone (VSH) or gonad-stimulating hormone (GSH), and the ovary to be the putative site of vitellogenesis-stimulating ovarian hormone (VSOH) and factors considered to induce secondary sexual characteristics [20, 22, 32]. Also of much interest regarding crustacean reproduction, is the role of methyl farnesoate (MF), which in insects is the unepoxidated precursor of juvenile hormone (JH) III. MF, a product of the mandibular organs, has been detected in the hemolymph of adult *Macrobrachium rosenbergii* [27, 37] and has been demonstrated to be at high levels during active vitellogenesis in crabs [19].

It has been observed that eyestalk ablation results in the production of vitellogenin and the acceleration of ovarian maturation and spawning in adult female *Macrobrachium rosenbergii* [23], and in mature female Crustacea in general. However, little information has been available concerning the likelihood that juvenile crustaceans can synthesize vitellogenin and whether such factors as MIH and VIH are present at the juvenile stage. Therefore, the main aim of this investigation was to examine the effects of eyestalk ablation on vitellogenin production in juvenile *M. rosenbergii* of both sexes and to gain more understanding of what factors may be involved in the control of its production. The appearance of vitellogenin after eyestalk removal was followed, and the nature of juvenile vitellogenin was examined immunologically and electrophoretically.

Given the current implications that MF may be involved in vitellogenin synthesis in Crustacea as JH is in insects [21, 38], it was considered here that juvenile males could be used as a system for testing the effects of methyl farnesoate administration in *M. rosenbergii*. For trial purposes, MF was prepared from farnesoic acid and injected intramuscularly.

MATERIALS AND METHODS

Sampling: Vitellogenin production in ablated and non-ablated juveniles

Thirty juveniles (body weight, BW=2–5 g) were divided into two groups to be hemolymph-sampled for three weeks at intervals of several days irrespective of sex. In the first group (eyestalkless), bilateral ablation was carried out by simply holding the animal half-submerged in water, and snipping both eyestalks using scissors rinsed in crustacean saline. After allowing hemolymph flow to stop,

Accepted December 27, 1993
Received November 5, 1993
[1] Present address: Japan Sea National Fisheries Research Institute 5939-22, Suido-cho 1-chome Niigata City, Niigata 951, Japan

the animal was fully returned to its tank. In the second group (intact) no treatment was employed. Hemolymph samples (less than 20 μl for each occasion) were taken by 25G needle and syringe, quick frozen at -80°C and stored at -30°C until analysis by enzyme immunoassay (EIA) and sodium dodecyl sulfate-polyacrylamide gel electrophoresis (SDS-PAGE). At the end of the sampling period, animals were dissected for sex determination.

Enzyme immunoassay (EIA)

Antiserum raised against purified vitellin from *Macrobrachium nipponense* [14, 24] shown to be specific for vitellin in *M. rosenbergii* [23] was employed in EIA in this investigation. The details of the development and validation of this EIA have been reported previously [23]; this system utilizes *M. rosenbergii* vitellin for expression of the standard curve and *M. rosenbergii* hemolymph in the preparation of m-CB (0.01% male hemolymph-containing carbonate buffer used in the dilution of standards and samples). Otherwise, procedures are identical to those of the *M. nipponense* EIA [24] in which standards or samples are adsorbed onto wells, blocked, and subsequently incubated with vitellin antiserum followed by goat anti-rabbit IgG alkaline phosphatase conjugate.

In this investigation, after adding substrate (nitrophenylphosphate disodium salt) to wells, absorbance was measured at 405 nm; sample concentrations were calculated from the standard curve and expressed in terms of milligram equivalents of vitellin per milliliter hemolymph. The lower limit of detection was 0.03 mg/ml.

Sodium dodecyl sulfate-polyacrylamide gel electrophoresis (SDS-PAGE) and immunoblotting

SDS-PAGE was carried out on 7.5% polyacrylamide separating gels with 3% polyacrylamide stacking gels. Sample preparation was done by mixing sample dilution buffer (20 mM Tris-HCl pH 6.8, containing 4% SDS, 40% glycerol, 2% mercaptoethanol, and 0.005% bromophenol blue) and hemolymph diluted 10-fold with distilled water at a 1 : 1 ratio. These were heat-treated at 100°C for 5 min. For purposes of comparison, vitellin (Vn) purified by gel filtration and ion exchange chromatography from *M. rosenbergii* ovary [14] and female hemloymph from adult female *M. rosenbergii* with mature ovaries (reproductive molt) were also run concurrently. For molecular weight determination, high molecular weight (200, 116, 97, 66, 45K) markers (Bio-Rad molecular weight marker kit) were employed.

For subsequent immunoblotting procedures, proteins were firstly transferred electrophoretically from gels to Immunobilon PVDF Transfer Membranes (Millipore). Membranes were soaked in 10% Block Ace (Yukijirushi Nyugyou K.K.)/TBS (Tris-HCl pH 8.0 containing 0.9M NaCl), washed with TBS-Tween (TBS containing Tween 20) and transferred to a dilution of protein A purified and biotinylated anti-Vn IgG (approx. 3 μg/ml) in TBS-Tween. Membranes were stained using the Vectastain Avidin-Biotin Complex kit (Vector Laboratories) and 3,3′-diaminobenzidine (25 mg DAB, 4 μl 31% H_2O_2, 20 ml TBS-Tween). After saturating the membranes in DAB solution, staining was enhanced with the addition of 40 μl each 200 mM $CoCl_2$ and $NiCl_2$. Reference gels were stained with Coomassie brilliant blue.

Histology

Histological studies were employed to confirm the extent of vitellogenesis in ovaries of eyestalk-ablated juvenile females. Ovarian tissue was fixed for 24–48 hrs in Bouin's solution and dehydrated through an alcohol gradient as described previously [36]. Tissues embedded in paraffin were sectioned to 5–7 μm and stained with hematoxylin-eosin to examine ovarian stages.

Additionally, immunocytochemical techniques were undertaken to confirm the presence in oocytes of vitellin-immunoreactive material. Sections were treated with 3% hydrogen peroxide to block endogenous peroxidase activity, and incubated in anti-Vn IgG (Protein A purified) diluted to 1.3 μg/ml in 0.1 M phosphate-buffered saline (0.9% NaCl, pH 7.5) overnight at 4°C. Immunocytochemical procedures were done using the Histofine immunostaining kit (Nichirei): biotinylated goat anti-rabbit IgG was firstly applied to sections, followed by the application of peroxidase-conjugated streptavidin. Final staining was done using 3,3′-diaminobenzidine (12.5 mg DAB in 50 ml 0.1 M phosphate buffer, pH 7.4, containing 750 μl 0.3% H_2O_2). As a control, the same anti-Vn IgG dilution (1 ml) was preincubated overnight with 2 μg purified vitellin.

Methyl farnesoate (MF) injection experimental protocol

Forty juvenile males already showing development of male gonopores and petasma were chosen. These were divided into four groups to be subjected to the following protocol: 1) eyestalk ablation, MF injection; 2) eyestalk ablation, saline injection; 3) no ablation, MF injection; 4) no ablation, saline injection. MF was prepared from farnesoic acid (gift of Kuraray Co., Ltd.) by methylation with diazomethane; confirmation of identity was done via gas chromatography-mass spectrometry (GC-MS) as in Laufer *et al.* [19]. Stock solutions in ethanol at 4 mg/ml were made up and MF for injection was prepared as a suspension of 5% ethanol in crustacean saline. This gave 200 μg MF per ml and injections were carried out intramuscularly (at the base of the fifth pleiopod) using 25 μl, or 5 μg MF. In MF-injected animals, injections were carried out every day after ablation for 5 days, and then blood-sampled. In control animals, injection was done with 5% ethanol in saline. At the end of the experiment, experimental animals were dissected to confirm the presence of testes; hemolymph samples were taken and quick-frozen at -80°C and stored at -30°C until use in EIA and SDS-PAGE. Initial samples were taken in some cases to confirm non-detectable (ND) values at the outset. The Student's *t*-test was employed to examine final vitellogenin levels.

RESULTS

1. *Vitellogenin production and molt frequency in juveniles*

A. Enzyme immunoassay (EIA) and molting

In the first phase of this investigation, 20 individuals were ablated, and 10 were left intact and followed for a three-week period. Eyestalk ablation led to increased molting and rapid development of the gonads. Of 20 eyestalk-ablated individuals, 5 females and 6 males survived for the duration of the experiment. In addition, 2 females showing developed ovaries apparent through the carapace and 1 male showing gonopores survived into the second week. Other individuals did not survive after ablation. Of 10 intact individuals, 8 survived the three-week duration; animals were dissected, but sex could not be determined. Ovaries of eyestalk-ablated females were additionally examined histologically (see below).

Vitellogenin titers of individuals followed for the three week duration are shown for males M1–6 (Fig. 1), females F1–5 (Fig. 2a, b) and intact animals, L1–8 (Fig. 3). In males

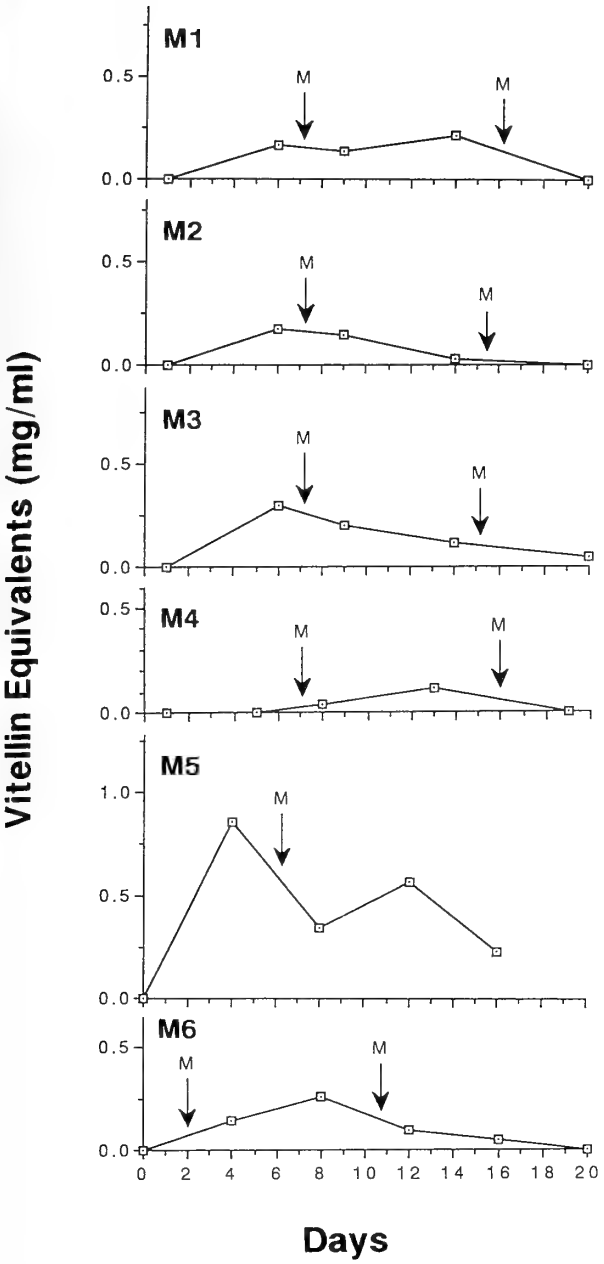

FIG. 1. Vitellogenin titers in ablated juvenile males M1–6 as quantified by enzyme immunoassay (expressed in vitellin equivalents). Peak levels ranged from 0.1 to 0.8 mg/ml. Vitellogenin appeared several days after ablation, increased slightly for 1–2 weeks, and then decreased. Eyestalk removal was performed on Day 0, and the first hemolymph sample was taken several hours later or within 24 hr of this. Individuals were then followed for the days indicated. Arrows marked by "M" indicate occurrence of molting.

(body weight, BW=4.02±0.45 g), no immunoreactive material was detectable at initial sampling occasions, performed within 24 hr of ablation. Vitellogenin generally appeared several days after ablation, increased slightly for 1–2 weeks, and then decreased. Molts are indicated by arrows; all but one male individual molted twice during the twenty-day period. Maximum titers were between 0.1 and 0.8 mg/ml.

Females (BW=3.80±0.29 g) also molted twice during the 3-week duration, but peak levels were greater than those of males, ranging between 0.5 to 3.0 mg/ml. F5 was however exceptional, with levels reaching almost 30 mg/ml. It should be noted that in this species, normally maturing adult females exhibit peak Vg levels around 10 mg/ml [23]. Intact animals (BW=3.10±0.18 g) were non-detectable (ND) throughout the experiment and molted 0–1 times.

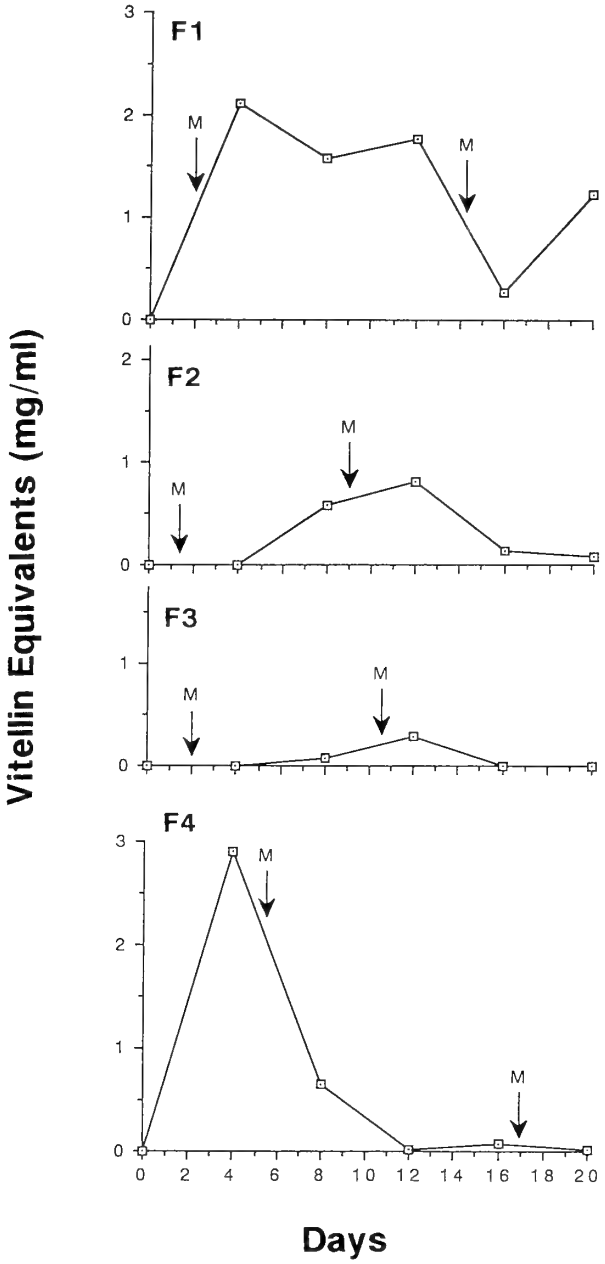

FIG. 2a. Vitellogenin titers in ablated juvenile females F1–F4 as quantified by enzyme immunoassay (expressed in vitellin equivalents). Peak levels ranged from 0.5 to 3 mg/ml. Vitellogenin appeared several days after ablation, increased slightly for 1–2 weeks, and then decreased. Eyestalk removal was performed on Day 0, and the first hemolymph sample was taken several hours later. Individuals were then followed for the days indicated. Gonadosomatic index ranged from 0.54 to 1.02%. Arrows marked by "M" indicate occurrence of molting.

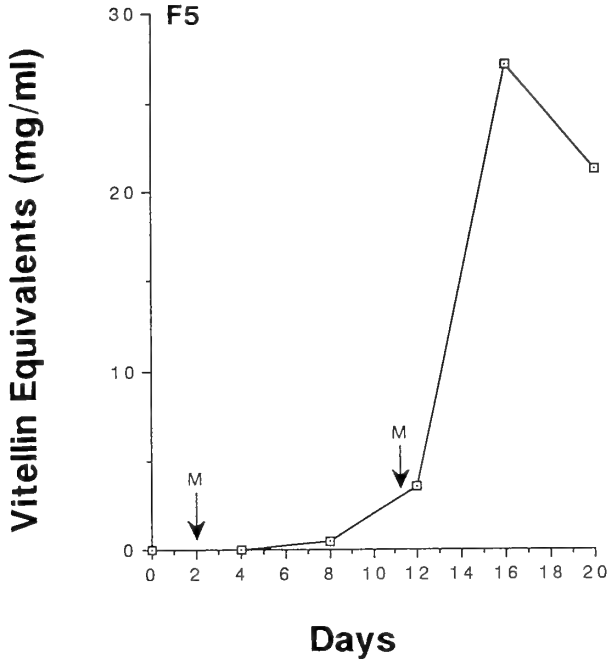

FIG. 2b. Vitellogenin titers in ablated female F5 as quantified by enzyme immunoassay (expressed in vitellin equivalents). Vitellogenin concentrations initially reached levels of about 3 mg/ml; thereafter, titers increased exceptionally to nearly 30 mg/ml. Eyestalk removal was performed on Day 0. Final gonadosomatic index was 4.10%. Arrows marked by "M" indicate occurrence of molting.

B. SDS-PAGE and Western blotting

Representative Western blots are shown for ablated males and females using M3 (Fig. 4a) and F1 (Fig. 4b) representatively. Exception F5 (Fig. 4c) is also shown. Numbers 1–5 or 1–6 correspond to sampling occasions done at 3–6 day intervals (Days 0, 3, 8, 13, 19 for M3 and Days 0, 4, 8, 12, 16, 20 for F1 and F5). Vitellin purified from eggs of *M. rosenbergii* eggs (102, 90K) and adult female vitellogenin (199, 102, 90K) are shown for reference in lanes A and B, respectively. Individuals M3 and F1 which are representative of all males and females except F5, show only the 199K band. Its appearance and apparent quantity at each sampling occasion reflect vitellogenin titers as determined by EIA. In F5, after only the 199K band appeared on Day 12, the full three-band pattern was observed on Days 16 and 20.

C. Ovarian development in females

Females F1, F2, F3, and F4 exhibited gonadosomatic indices (GSI) of 1.02, 0.54, 0.60, and 0.65%. These values are higher than those corresponding to immature ovaries which average about 0.4% during the common molt cycle of the adult female, but are low compared to GSI values that

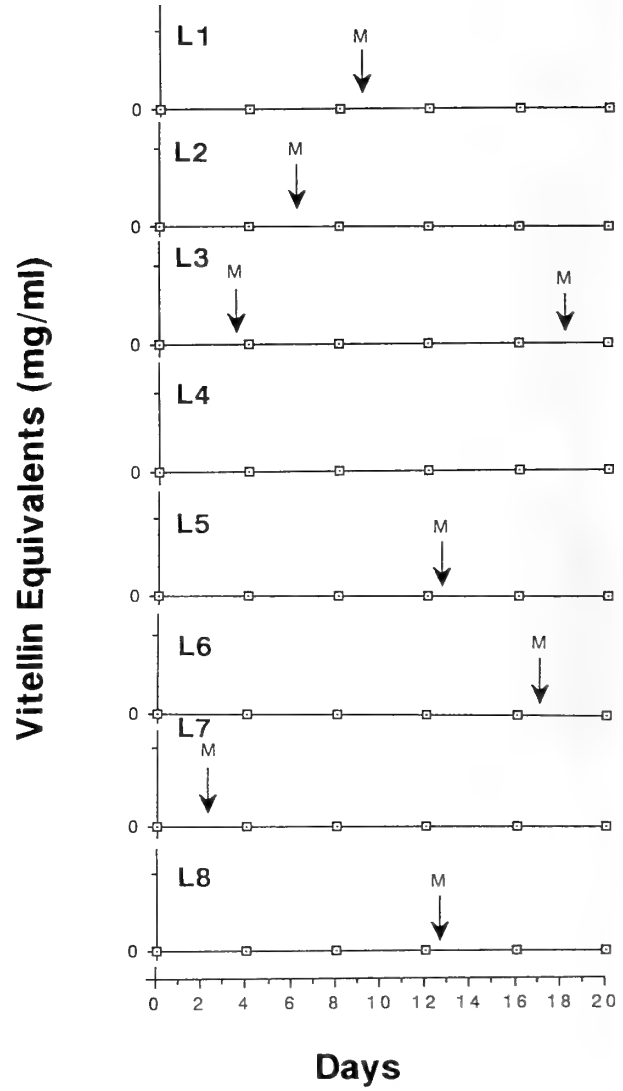

FIG. 3. Vitellogenin titers in intact individuals L1–8 as determined by enzyme immunoassay (expressed in vitellin equivalents). Non-ablated individuals were followed as in Figs. 1 and 2a-b for a three-week duration. No immunoreactive material was detected throughout the observation period. Occurrence of molting is indicated by arrows marked by "M".

reach above 9 percent in fully mature ovaries [36]. F5 with exceptionally high vitellogenin levels also had a much greater GSI, of 4.10%. In histological examination using hematoxylin-eosin, it was observed that ovaries in females F1–F4 were in secondary vitellogenesis, exhibiting oocytes partially filled with yolk globules. In these oocytes, the nucleoli were clearly visible within the nucleus, which was not condensed in appearance (Fig. 5a). Ovaries in female F5 were quite

FIG. 5. Extent of oocyte development in ablated juvenile females. (a) F1 was typical of the degree of ovarian maturity in females F1–F4. Oocytes are enlarged, contain yolk globules, and can be considered to be in secondary vitellogenesis. The nucleoli are clearly visible within the nucleus. Germinal vesicle breakdown (GVBD) has not yet begun, as the nucleus is not condensed in appearance. Gonadosomatic index (GSI) ranged from 0.54 to 1.02%. (b) F5, exhibiting extremely high titers of full vitellogenin, possessed oocytes which appeared to have undergone GVBD as the nucleus is no longer observable. However, F5 did not undergo spawning. GSI was above 4%. Scale bar: 50 μm.

different in appearance (Fig. 5b). Oocytes were extremely enlarged in size in comparison to those of the other individuals. The nucleus was not present, and oocytes gave the appearance of having undergone germinal vesicle breakdown (GVBD) [36]. However, this individual did not spawn eggs within the duration of the experiment.

Employing immunocytochemical techniques, we were able to confirm the accumulation of vitellin-immunoreactive material in oocytes in the latter stages of secondary vitellogenesis. Figure 6 shows histology for female F1. Maturing oocytes partially filled with yolk globules indicate an immunocytochemical reaction (a), but immature oocytes from the center of the ovary exhibit no reaction (b). In the control version of the same individual, mature oocytes in sections which were incubated with pre-absorbed antibodies did not exhibit a reaction (c). Likewise, immature oocytes also showed no indication of staining (d).

Methyl farnesoate (*MF*) administration in males

Male juveniles were divided into four groups of ten individuals each and received combinations of ablation/non-ablation and MF injection/saline injection. Results are shown in Table 1, along with average body weights for each

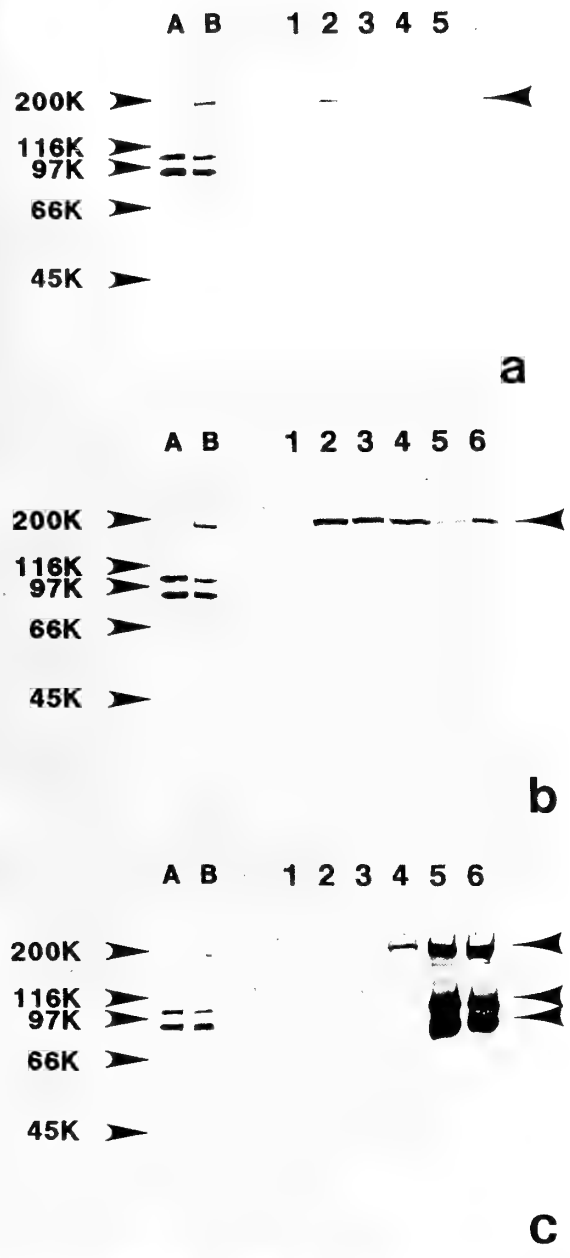

FIG. 4. Examination of juvenile vitellogenin by SDS-PAGE and Western blotting. (a) Vitellogenin was shown to consist of a single polypeptide component of 199K in juvenile males (M1–M6) (ex. M3; lanes 1–5 correspond to Days 0, 5, 8, 13, 19). In comparison, adult female vitellogenin (lane B) was composed of three polypeptides of 199, 102, and 90K, and purified vitellin (lane A) of 102 and 90K. Western blotting results were in agreement with enzyme immunoassay results. (b) Vitellogenin consisted of a single polypeptide component of 199K also in juvenile females (F1–F4) (ex. F1; lanes 1–6 correspond to Days 0, 4, 8, 12, 16, 20). Lanes A and B are as in (a). (c) Juvenile female F5, however, was exceptional. Vitellogenin first became detectable by enzyme immunoassay (lane 4–Day 12), showing only the 199K component, but thereafter, full vitellogenin became very abundant, and all three peptide components, e.g. 199, 102 and 90K, were observed (lanes 5, 6–Days 16, 20), as in adult female vitellogenin. Lanes A and B are as in (a).

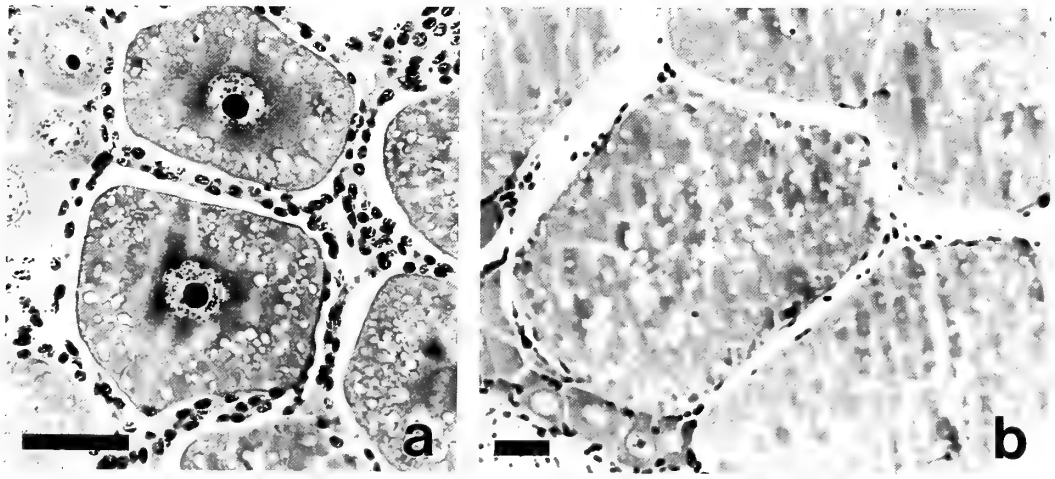

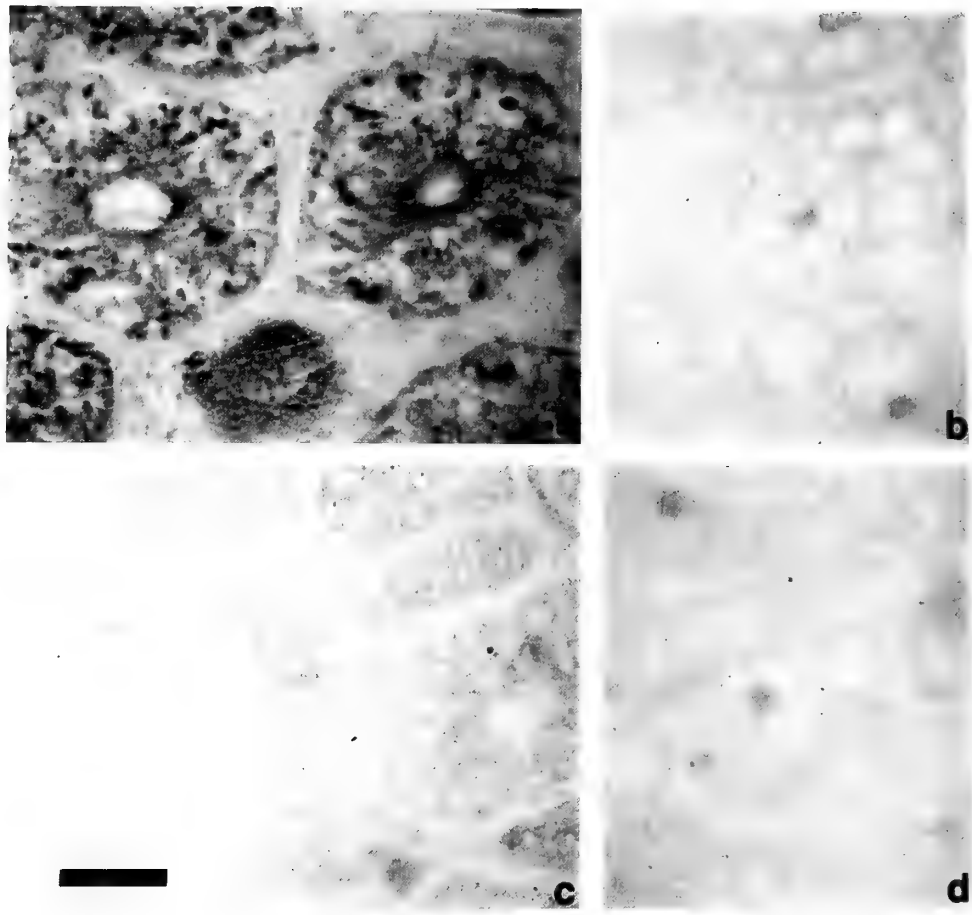

FIG. 6. Immunohistology, and examination of uptake of vitellin-immunoreactive material in oocytes (ex. F1). (a) Mature oocytes, occurrence of immunocytochemical reaction. (b) Immature oocytes from core of ovary; absence of immunocytochemical reaction. (c) and (d) Same oocytes as in (a) and (b) respectively, incubated with pre-absorbed antiserum as a control; absence of immunocytochemical reaction. Scale bar: 50 μm.

TABLE 1. Experimental protocol for methyl farnesoate (MF) administration in eyestalk-ablated (ES) and non-ablated (intact) juvenile males. Data for final vitellogenin levels, average body weight, and average number of molts pare shown

Treatment	No. ind.	Schedule (Days)							BW(g)	No. molts	Vg (mg/ml)
		0	1	2	3	4	5	6			
MF inj. + ES	N=10	a	*	*	*	*	*	h	3.24±0.38	0.6±0.2	0.15±0.04[1]
Saline + ES	N=10	a	o	o	o	o	o	h	3.82±0.11	1.0±0.0	0.14±0.04[1]
MF inj. + Intact	N=10		*	*	*	*	*	h	3.21±0.21	0.3±0.2	ND
Saline + Intact	N=10		o	o	o	o	o	h	2.37±0.24	0.3±0.2	ND

[1] Difference not significant.
* 5 μg MF injected as suspension in 25 μl 5% ethanol/saline.
o Blank injection as 25 μl ethanol saline.
a Eyestalk ablation performed.
h Hemolymph samples taken.

group. For ablated animals, number of molts was 0.6 ± 0.2 and 1.0 ± 0.0 for MF-injected, and saline-injected groups, respectively, but was 0.3 ± 0.2 for both groups of intact individuals. At the end of the experiment, only 3 individuals in the MF-injected, and 2 individuals in the saline-injected ablated groups exhibited non-detectable (ND) values. There was no significant difference in average value between MF-injected animals (0.15 ± 0.04 mg/ml) and saline-injected animals (0.14 ± 0.04 mg/ml). Some of the ablated animals were examined by SDS-PAGE; these showed only the 199K banding pattern (data not shown). In non-ablated groups, all final EIA values were ND, irrespective of whether animals were injected with MF or with saline.

DISCUSSION

In this investigation, it was revealed that eyestalk removal in juvenile male and female *M. rosenbergii* results in the production of a vitellin-immunoreactive substance which consists of a 199K peptide component. Adult female vitellogenin has been shown by Okumura [23] to be comprised of the 199K component as well as of lighter molecular weight components of 102K and 90K. In eyestalk-ablated juveniles of both sexes, 199K vitellogenin was seen to increase for 1–2 weeks and then decrease; in general, females reached higher overall levels (0.5–3 mg/ml) than did males (0.1–0.8 mg/ml). One female individual was exceptional; initially only 199K vitellogenin appeared, but thereafter, full three-component vitellogenin was manifested with levels in the hemolymph reaching nearly 30 mg/ml.

The advancement of ovarian development in eyestalk-ablated juvenile females was confirmed for all individuals. In females F1–F4 expressing only the 199K component, gonadosomatic indices (GSI) ranged from 0.54 to 1.02%. In comparison to the state of the immature ovary in the adult female, ovaries in these females were enlarged in appearance and bright orange in color, and thus similar to normally maturing ovaries in the adult female. Histological examination revealed that oocytes were in secondary vitellogenesis, with the nucleus uncondensed in appearance. In the exceptional female F5, GSI was 4.10% and oocytes appeared to have already undergone germinal vesicle breakdown (GVBD). These results suggested a correlation between the extent of ovarian development and the ability to produce full vitellogenin; whether this is related to an ovarian factor such as vitellogenesis-stimulating ovarian hormone (VSOH), is as of yet unclear.

The accumulation of yolk proteins in oocytes of females expressing only the 199K band was further confirmed using immunocytochemical techniques. In females F1–F4, maturing oocytes in secondary vitellogenesis stained via immunocytochemical reaction, and immature oocytes in the core of the ovary exhibited no reaction. This indicated that although juvenile vitellogenin lacked the 102 and 90K components of adult vitellogenin, increases in the hemolymph of the 199K peptide were correlated with oocyte development, providing further support that juveniles, not only females, but also males have the ability to produce vitellogenin to a certain extent. The small size of the ovaries of the above individuals did not permit analysis on SDS-PAGE in parallel to the above histological studies; this will be investigated subsequently.

While little information is available concerning vitellogenin in juveniles, vitellogenin and vitellin structure have been examined in a number of adult crustacean species [8, 25, 26, 34]. Adult *M. rosenbergii* seems similar to many of these; for example, in *Penaeus monodon,* vitellogenin and vitellin are comprised of subunits of 74, 83, 104 and 168K [26]. Less is known however, concerning how crustacean vitellogenins and vitellins are processed while becoming sequestered in eggs. In the terrestrial isopod, *Armadillidium vulgare* [30], four forms of vitellin are initially accumulated in oocytes, but the higher molecular weight ones undergo proteolytic processing, leaving only the lightest component. Komatsu and Ando [18] have reported a low density lipoprotein (LDL) present in the egg yolk of the sand crayfish, *Ibacus ciliatus,* which degrades vitellogenin and may be involved in vitellogenin processing in this species.

The native form of vitellin in *M. nipponense* has been estimated by gel filtration as 350K [14], and preliminary work indicates that this is similar in *M. rosenbergii* (Okumura, unpublished data). In *M. rosenbergii,* as vitellin yields the 102K and 90K components on SDS-PAGE, it seems plausible that the 199K protein is initially synthesized as a precursor vitellogenin and undergoes further processing in the mature female in relation to a factor perhaps produced by the ovary. Vitellin in its final form may be a multimer association of the 102K and 90K proteins subunits, thus the 199K protein would not appear in eggs, but occurs in the hemolymph. Of note, in Derelle *et al.* [12], *M. rosenbergii* female vitellogenin and vitellin examined on SDS-PAGE was comprised of subunits of 84 and 92.2K. Regarding vitellin, these results are similar to those obtained in our investigation. However, these authors did not observe a higher molecular weight component in hemolymph vitellogenin, such as the 199K component obtained here. Discrepancies in results between their investigation and this study could be due to differences in methods of antisera preparation.

This is the first report to our knowledge concerning vitellogenin production in male decapods, but in isopods, this can occur as a result of loss of androgenic gland function due to natural or artificial circumstances [28, 31], In *A. vulgare* andrectomized males, vitellogenin levels are in fact higher than those of normal females; male vitellogenin does not differ electrophoretically from that of females [31], although the ovary is suggested to be necessary to maintain vitellogenin titers during the molt cycle. In *Porcellio dilatatus,* fat bodies from surgically-untreated males synthesize vitellogenin *in vitro* [13]. In *M. rosenbergii,* vitellogenin production can be induced by simply removing the eyestalks. As some sinus gland peptides are thought to be involved in the maintenance of the male reproductive system and the control of the

androgenic gland in other decapod species [3, 10], in this investigation, whether the appearance of vitellogenin in *M. rosenbergii* is due to the absence of a putative VIH or is more related to the removal of other eyestalk factors, is at present unclear. However, vitellogenin levels in males do not reach those of juvenile females, suggesting that there may be additional factors of female origin involved in further stimulation of early vitellogenin production. On the other hand, in adult males, eyestalk ablation results in the appearance of vitellogenin in only occasional individuals (Yang *et al.*, unpublished data); this suggests some involvement of the androgenic gland in that it is expected to be less developed and therefore less inhibitory in juveniles than in adults.

In male insects, several authors have studied by immunological and electrophoretic methods the induction of vitellogenin synthesis by juvenile hormone and/or ecdysone treatment [2, 16, 21]. The actions of juvenoids and ecdysteroids vary with species. Agui *et al.* [4] have examined production of vitellogenin mRNA in male and female housefly *Musca domestica,* revealing that in males, 20-hydroxyecdysone, but not juvenile hormone can stimulate transcription of the vitellogenin genes; this has indicated the necessity of the ovary. In *Diploptera punctata,* vitellogenin synthesis is directly inducible by application of juvenile hormone analogue [21]. Induced male vitellogenin levels are often lower than levels in normal females (similar to *M. rosenbergii*).

Along these lines, it was postulated that methyl farnesoate (MF) may be necessary for further stimulation and processing of vitellogenin in *M. rosenbergii.* MF being highly insoluble in water, was firstly dissolved in stock solutions of ethanol, which were adjusted in crustacean saline. This formed a cloudy suspension. However, as discussed in the results, MF injection did not produce significantly higher levels of vitellogenin (0.15 ± 0.04 mg/ml) above those of ablated animals injected with saline (0.14 ± 0.04 mg/ml). MF injection also did not induce vitellogenin synthesis in non-ablated animals. In preliminary work, other methods of injection were attempted, for example, cardiac injection with either MF (and farnesoic acid) in saline or in purified sesame oil, or similar intramuscular injections using oil instead, but these were also ineffective in stimulating vitellogenin production in either sex. Thus, eyestalk removal was observed to be a prerequisite for induction of vitellogenin production in males, but MF administration seemed to have no influence.

From these results, it was not possible to obtain positive evidence that MF has any connection to vitellogenin production in *M. rosenbergii,* but it also can not be conclusively stated that MF has no physiological role whatsoever. MF has been shown to activate Na/K-ATPase in *Artemia,* indicating its potential role in osmoregulation and molting [6, 7]. MF has been detected in both sexes in *M. rosenbergii* by Sagi *et al.* [27]; we have additionally determined that MF is present in females during both the reproductive molt and common molt cycles, and seems highest during the early premolt stages [37]. Additionally, it is not ruled out that MF has no involvement in the process of vitellogenin uptake. In insects, juvenoids affect increased membrane Na/K-ATPase activity in the ovarian follicles, causing cell volume to shrink, and creating spaces through which vitellogenin can pass through to access the oocytes [1, 11, 17]. This is known as "patency".

The results of this study have suggested that vitellogenesis- and molt-inhibiting eyestalk factors are present in juveniles as well, but this is not sufficient to explain the means by which precursor vitellogenin is processed into the full vitellogenin observed in the adult female and how vitellogenin production is possible in males. In subsequent studies, it will be important to investigate the involvement of ovarian factors in concert with MF and the relationship between androgenic gland functioning and male vitellogenin production.

ACKNOWLEDGMENTS

We thank Kuraray Co., Ltd. for the farnesoic acid sample used to prepare methyl farnesoate (MF), and S. Okada, The University of Tokyo, for GC-MS of sample MF. This study was supported in part by Grants-in-Aid for Scientific Research from the Ministry of Education, Science, and Culture of Japan. Additionally, M.N. Wilder acknowledges the support of a Japan Society for the Promotion of Science Postdoctoral Fellowship.

REFERENCES

1 Abu-Hakima R, Davey KG (1977) The action of juvenile hormone on the follicle cells of *Rhodnius prolixus*: The importance of volume changes. J Exp Biol 69: 33–44

2 Adams TS, Filipi PA, Kelly TJ (1989) Effect of 20-hydroxyecdysone and a juvenile hormone analogue on vitellogenin production in male houseflies, *Musca domestica.* J Insect Physiol 35: 765–773

3 Adiyodi R (1984) Seasonal changes and the role of eyestalks in the activity of the androgenic gland of the crab, *Paratelphusa hydrodromous* (Herbst). Comp Physiol Ecol 9: 427–431

4 Agui N, Shimada T, Izumi S, Tomino S (1991) Hormonal control of vitellogenin mRNA levels in the male and female housefly, *Musca domestica.* J Insect Physiol 37: 383–390

5 Aguilar MB, Quackenbush LS, Hunt DT, Shabanowitz J, Huberman A (1992) Identification, purification and initial characterization of the vitellogenesis-inhibiting hormone from the Mexican crayfish *Procambarus bouvieri* (Ortmann). Comp Biochem Physiol 102B: 491–498

6 Ahl JSB, Brown JJ (1990) Salt-dependent effects of juvenile hormone and related compounds in larvae of the brine shrimp, *Artemia.* Comp Biochem Physiol 95A: 491–496

7 Ahl JSB, Brown JJ (1991) The effect of juvenile hormone III, methyl farnesoate, and methoprene on Na/K-ATPase activity in larvae of the brine shrimp, *Artemia.* Comp Biochem Physiol 100A: 155–158

8 Andrieux N, de Frescheville J (1992) Caractérisation de la vitelline chez le Crustacé Brachyoure *Carcinus maenus.* CR Acad Sci t314, ser III: 227–230

9 Chang ES, Prestwich GD, Bruce MJ (1990) Amino acid sequence of a peptide with both molt-inhibiting and hyperglycemic activites in the lobster, *Homarus americanus.* Biochem Biophys Res Commun 171: 818–826

10 Charniaux-Cotton H, Payen GG (1988) Crustacean reproduc-

tion. In "Endocrinology of Selected Invertebrate Types" Ed by H Laufer and RGH Downer, Alan R. Liss, Inc. pp 279–303.

11 Davey KG, Huebner E (1974) The response of the follicle cells of *Rhodnius prolixus* to juvenile hormone and antigonadotropin *in vitro*. Can J Zool 52: 1407–1412

12 Derelle E, Grosclaude J, Meusy J-J, Junéra H, Martin M (1986) ELISA titration of vitellogenin and vitellin in the freshwater prawn, *Macrobrachium rosenbergii,* with monoclonal antibody. Comp Biochem Physiol 85B: 1–4

13 Gohar M, Souty C (1983) Mise en évidence in vitro d'une synthèse et d'une libération de vitellogénine dans le tissu adipeux mâle de *Porcellio dilatatus* Brandt (Crustacé Isopode terrestre). CR Acad Sci Paris, t297: 145–148

14 Han C-H (1988) Physiological and reproductive studies on a freshwater prawn, *Macrobrachium nipponense* (De Haan). Ph. D. Dissertation, The University of Tokyo, Japan.

15 Hinsch GW, Bennett DC (1979) Vitellogenesis stimulated by thoracic ganglion implants into destalked immature spider crabs, *Libinia emarginata.* Tissue Cell 11: 345–351.

16 Huybrechts R, De Loof A (1977) Induction of vitellogenin synthesis in male *Sarcophaga bullata* by ecdysterone. J Insect Physiol 23: 1359–1362

17 Ilenchuk TT, Davey KG (1987) The development of responsiveness to juvenile hormone in the follicle cells of *Rhodnius prolixus.* Insect Biochem 17: 525–529

18 Komatsu M, Ando S (1992) A novel low-density lipoprotein with large amounts of phospholipid found in the egg yolk of crustacea sand crayfish *Ibacus ciliatus*: Its function as vitellogenin-degrading proteinase. Biochem Biophys Res Commun 186: 498–502

19 Laufer H, Borst D, Baker FC, Carrasco C, Sinkus M, Reuter CC, Tsai LW, Schooley DA (1987) Identification of a juvenile hormone-like compound in a crustacean. Science 235: 202–205

20 Meusy J-J, Payen GG (1988) Female reproduction in malacostracan Crustacea. Zool Sci 5: 217–265

21 Mundall EC, Szibbo CM, Tobe SS (1983) Vitellogenin induced in adult male *Diplotera punctata* by juvenile hormone and juvenile hormone analogue: Identification and quantitative aspects. J Insect Physiol 29: 201–207

22 Nagamine C, Knight AW (1987) Induction of female breeding characteristics by ovarian tissue implants in androgenic gland ablated male freshwater prawns *Macrobrachium rosenbergii* (de Man) (Decapoda, Palaemonidae). Int J Invertebr Reprod Dev 11: 225–234

23 Okumura T (1992) Physiological studies on molting and gonadal maturation in prawns. Ph.D. Dissertation, The University of Tokyo, Japan

24 Okumura T, Han C-H, Suzuki Y, Aida K, Hanyu I (1992) Changes in hemolymph vitellogenin and ecdysteroid levels during the reproductive and non-reproductive molt cycles in the freshwater prawn, *Macrobrachium nipponense.* Zool Sci 9: 37–45

25 Quinitio ET, Hara A, Yamauchi K, Mizushima T, Fuji A (1989) Identification and characterization of vitellin in a hermaphrodite shrimp, *Pandalus kessleri.* Comp Biochem Physiol 94B: 445–451

26 Quinitio ET, Hara A, Yamauchi K, Fuji A (1990) Isolation and characterization of vitellin from the ovary of *Penaeus monodon.* Invertebr Reprod Dev 17: 221–227

27 Sagi A, Homola E, Laufer H (1991) Methyl farnesoate in the prawn *Macrobrachium rosenbergii*: Synthesis by the mandibular organ *in vitro,* and titers in the hemolymph. Comp Biochem Physiol 99B: 879–882

28 Souty-Grosset C, Juchault P (1987) Etude de la synthèse de la vitellogénine chez les mâles intersexués d'*Armadillidium vulgare* Latreille (Crustacé Isopode Oniscoïde): Comparison avec les mâles et les femelles intactes ou ovariectomisées. Gen Comp Endocrinol 66: 163–170

29 Soyez D, Le Caer JP, Noel PY, Rossier J (1991) Primary structure of two isoforms of the vitellogenesis inhibiting hormone from the lobster *Homarus americanus.* Neuropeptides 20: 25–32

30 Suzuki S (1987) Vitellins and vitellogenins of the terrestrial isopod, *Armadillidium vulgare.* Biol Bull 173: 345–354

31 Suzuki S, Yamasaki K, Katakura Y (1990) Vitellogenin synthesis in andrectomized males of the terrestrial isopod, *Armadillidium vulgare* (Malacostracan Crustacea). Gen Comp Endocrinol 77: 283–291

32 Suzuki S, Yamasaki K (1991) Ovarian control of oostegite formation in the terrestrial isopod, *Armadillidium vulgare* (Malacostraca, Crustacea). Gen Comp Endocrinol 84: 381–388

33 Takayanagi H, Yamamoto Y, Takeda N (1986) An ovary-stimulating factor in the shrimp, *Paratya compressa.* J Exp Zool 240: 203–209

34 Tirumalai R, Subramoniam T (1992) Purification and characterization of vitellogenin and lipovitellins of the sand crab *Emerita asiatica*: Molecular aspects of crab yolk proteins. Mol Reprod Dev 33: 16–26

35 Webster SG, Keller R (1986) Purification, characterisation and amino acid composition of the putative moult-inhibiting hormone (MIH) of *Carcinus maenas* (Crustacea, Decapoda). J Comp Physiol B 156: 617–624

36 Wilder MN, Okumura T, Aida K (1991) Accumulation of ovarian ecdysteroids in synchronization with gonadal development in the giant freshwater prawn, *Macrobrachium rosenbergii.* Zool Science, 8: 919–927

37 Wilder MN (1993) Physiochemical studies on ecdysteroids and juvenoids in relation to molting, reproduction and embryogenesis in the giant freshwater prawn, *Macrobrachium rosenbergii.* Ph. D. Dissertation, The University of Tokyo, Japan.

38 Wyatt GR (1988) Vitellogenin synthesis and the analysis of juvenile hormone action in locust fat body. Can J Zool 66: 2600–2610

39 Yano I (1992) Effect of thoracic ganglion on vitellogenin secretion in kuruma prawn, *Penaeus japonicus.* Bull Natl Res Inst Aqacult 0: 9–14

ZOOLOGICAL SCIENCE 11: 55–62 (1994)

Cytochemical and Histological Details of Muscle Fibers in the Southern Smelt *Retropinna retropinna* (Pisces; Galaxioidei)

VICTOR B. MEYER-ROCHOW[1], YOSHIMI ISHIHARA[2] and JOHN R. INGRAM[3]

[1]*Experimental Zoology and Electron Microscopy Lab., University of the West Indies, Mona Campus, Kingston 7, Jamaica, W. I.,* [2]*Department of Molecular Life Science, School of Medical, Tokai University, Bohseidai, Isehara-shi, Kanagawa 259-11, Japan, and* [3]*Animal Behavior and Welfare Center, Ruakura Agriculture Center, Hamilton, New Zealand*

ABSTRACT—Cytochemical and histological details are presented on the localization of actomyosin adenosine triphosphatase (am-ATPase), succinic dehydrogenase, lipid, and glycogen in the body musculature of the Southern smelt *Retropinna retropinna*. The results clearly show that in addition to the red and white muscle fibers a variety of pink fibers are present, which can be further classified according to fiber diameter, staining characteristics, and location. Using acid and alkaline preincubation with myofibrillar am-ATPase stain, both large and small diameter pink fibers were distinguishable from red as well as white fibers. It is suggested that a transition between aerobic and anaerobic metabolisms exists in intermediate zone fibers of which those with small diameters are likely to possess aerobic and those of large diameters a more anaerobic capacity. The difference in metabolism could be related to fiber diameter and the associated constraints of large diffusion distances on oxygen availability.

INTRODUCTION

Early histochemical studies on the localization and activities of oxydative enzymes in vertebrate muscles [19] have shown that muscle fibers can be classified into three types. These three types are traditionally referred to as red, white, and pink in fishes. However, the development of the technique for the demonstration of myofibrillar adenosine triphosphatase (ATPase) for mammalian muscle [8] and its modification for fish muscle [12] has allowed the employment of an alternative classification based on myofibrillar ATPase activity. According to Johnston *et al.* [13] and numerous other investigators [3, 6, 9, 14, 18, 22, 24, 25] fiber types within the intermediate (=pink) group can be further subdivided.

They display a variety of staining activities, but are characterized by their relatively small diameter and a gradation in staining intensity for ATPase after acid and alkaline preincubation [6, 25]. As part of a study on red/white muscle distribution and fiber growth dynamics in different populations of the Southern smelt *Retropinna retropinna,* we decided to commence with a histochemical survey of fiber types present in sections of the fish corresponding to 70% fork length, i.e. the region located near the point of maximum flexure [17].

MATERIALS AND METHODS

Specimens of the Southern smelt, *Retropinna retropinna,* were caught during the day and late evenings at two locations along the Waikato River (New Zealand) or in Lake Rotomanuka located 10 km to the south of Hamilton (New Zealand). The fish were kept in a large aquarium in a 15°C constant temperature room.

Accepted October 29, 1993
Received January 22, 1993

All histological studies were carried out using frozen material. The smelt were killed by either decapitation or pithing and their fork length, total weight, and sex were recorded. To be able to compare results, a consistent sampling regime was adopted, which involved sampling from a point corresponding to 70% of the fork length.

Blocks of fish myotomal muscle were immersed in isopentane cooled to near its freezing point by liquid nitrogen, as soon as possible after death. They were then mounted on cryostat chucks that had been cooled in liquid nitrogen using O.C.T.-compound, an embedding medium for frozen tissue specimens. The samples were then placed in a cryostat set at −20°C to equilibrate for 1 hr. The specimen blocks were sectioned at a thickness of 10–20 μm and the sections were mounted on glass slides and allowed to dry for 30 min.

Sections were stained for glycogen using the periodic acid Schiff's method [7] and for lipid using Sudan Black B. Sections were stained for succinic dehydrogenase activity using the nitro-blue tetrazolium method of Dubowitz and Brooke [7] or the method of Pearse [21]. The myofibrillar adenosine triphosphatase (ATPase) activity was demonstrated by using the method of Guth and Samaha [8] as modified by Johnston *et al.* [12]. Sections were preincubated, without prior fixation in the alkaline (pH 10.4) solution at room temperature (21°C). The time of preincubation was adjusted until a differential pattern of staining was obtained without total inactivation of all fibers (30–300 sec). Some sections were also preincubated in the acidic (pH 4.35, 30–90 sec) preincubation solution at room temperature (21°C) for comparative purposes [18]. The preincubated sections were then incubated for 20 min at 37°C.

As a control, some sections were incubated with 3.5 mM sodium azide in the incubation solution to inhibit Ca^{2+}-activated mitochondrial ATPase [13]. Freshly frozen muscle tissue was used as muscle tissue stored in liquid nitrogen for prolonged periods before sectioning and incubation, was found to have a radically changed pattern of ATPase activity. White muscle ATPase activity decreased and red muscle ATPase increased, which is similar to that found by Korneliussen *et al.* [14]. Control sections in the PAS-technique for glycogen were treated in a 0.5% alpha-amylase solution for 10–15 min before staining [15].

In the Sudan Black B technique for the presence of lipid, counterstaining in filtered haematoxylin was omitted as good results were obtained without it. Some sections were immersed in acetone for 30 min prior to staining to act as a control [18]. To demonstrate the activity of the mitochondrial enzyme succinic dehydrogenase, the technique of Dubowitz and Brooke [7] was used. The results from this staining technique were then confirmed using the method of Pearse [21]. As a control the nitro-blue tetrazolium salt was omitted in some incubations.

RESULTS

The results obtained from the histological localization of actomyosin adenosine triphosphatase (am-ATPase), succinic dehydrogenase (SDH), lipid, and glycogen are presented in Tables 1, 2, and 3. The results clearly show that in addition to the red and white fibers, a variety of pink muscle fibers are present.

TABLE 1. Staining intensities of different fiber types in the myotomal musculature of the Southern smelt *Retropinna retropinna*

Fibre types	Staining techinique for:		
	Lipid	Glycogen	SDH
White	0	0	0
Ping large	0	+	+
Pink small	0	+, ++	++
Red	++	+++, 0#	+++
S.D.F.	+, 0	+, 0	+, 0

# red fibers of Seitenlinie and the elongate red fibers adjacent to the perimysium.
0 =Background stain
\+ =Lightly stained
++ =Moderately stained
+++=Heavily stained
S.D.F =Small Diameter Fiber

TABLE 3. Effect of different preincubation times on the myofibrillar ATPase in the Southern smelt *Retropinna retropinna*

Fibre type	Preincubation time at pH 10.4		
	0 sec	30 sec	5 min
White	+++	++	0
Pink large	+++	+++	0
Pink small	+++	++++, +++, 0	+
Red	+++	+#	+#
S.D.F.	++, +	+	0

=Staining probably due to mitochondrial ATPase activity

The comparatively small diameter red muscle fibers were located in a superficial wedge-shaped region at the periphery of the horizontal septum adjacent to the lateral line, but they were also present in a superficial sheet 1–2 fibers thick, located between the dermis and the main mass of white fibers. The fibers of the *musculus lateralis superficiales* displayed similar staining characteristics, except for a monolayer of elongate fibers adjacent to the perimysium, which appeared to form a continuum of the "Seitenlinie" red fibers. The latter displayed staining activities that differed from the red fibers of the *lateralis superficiales* in respect to glycogen and acid-stable myofibrillar ATPase.

TABLE 2. Staining activities of myofibrillar ATPase under different preincubation conditions

Fiber types	Myofibrillar ATPase preincubation			
	none	Alkaline pH 10.4	Acid pH 4.35	Na Azide
White	+++	++	0	++
Pink large	+++	+++	+	++
Pink small	+++	++++, +++, 0	++	+++
Red	+++	+#	++++*, +++	0
S.D.F.	++, +	+	++	0?

? =Unable to fully determine
=Staining probably due to mitochondrial ATPase activity
* =Elongated red fibers located next to the perimysium and red fibers of the seitenlinie

FIG. 1. Distribution of lipid in the lateral musculature of the smelt using Sudan Black B stain for lipid. Note intense staining in the red fibers (R) and the more intensely stained Seitenlinie fibers. Also shown is the variety of staining intensities displayed by the small diameter fibers (SDH) and the limited background staining displayed by the pink fibers (P). Magnification: 400×.

FIG. 2. Localization of glycogen within the lateral musculature of the smelt using the PAS-stain. Note gradation in staining from intense in the red fibers (R) through intermediate levels in the pink fibers (P) to no staining in the white fibers (W). Also note the lack of staining in the Seitenlinie fibers (arrow). Magnification: 125×.

FIG. 3. Distribution of mitochondrial enzyme succinic dehydrogenase in myotomal musculature of the smelt using nitro-blue tetrazolium stain for SDH. Note the gradation of staining intensities with red fibers (R), staining most small pink fibers (arrow) and large pink fibers (P) displaying intermediate staining and white fibers (W) no activity at all. Also note the small diameter fibers (SDH) show very little activity. Magnification: 125×.

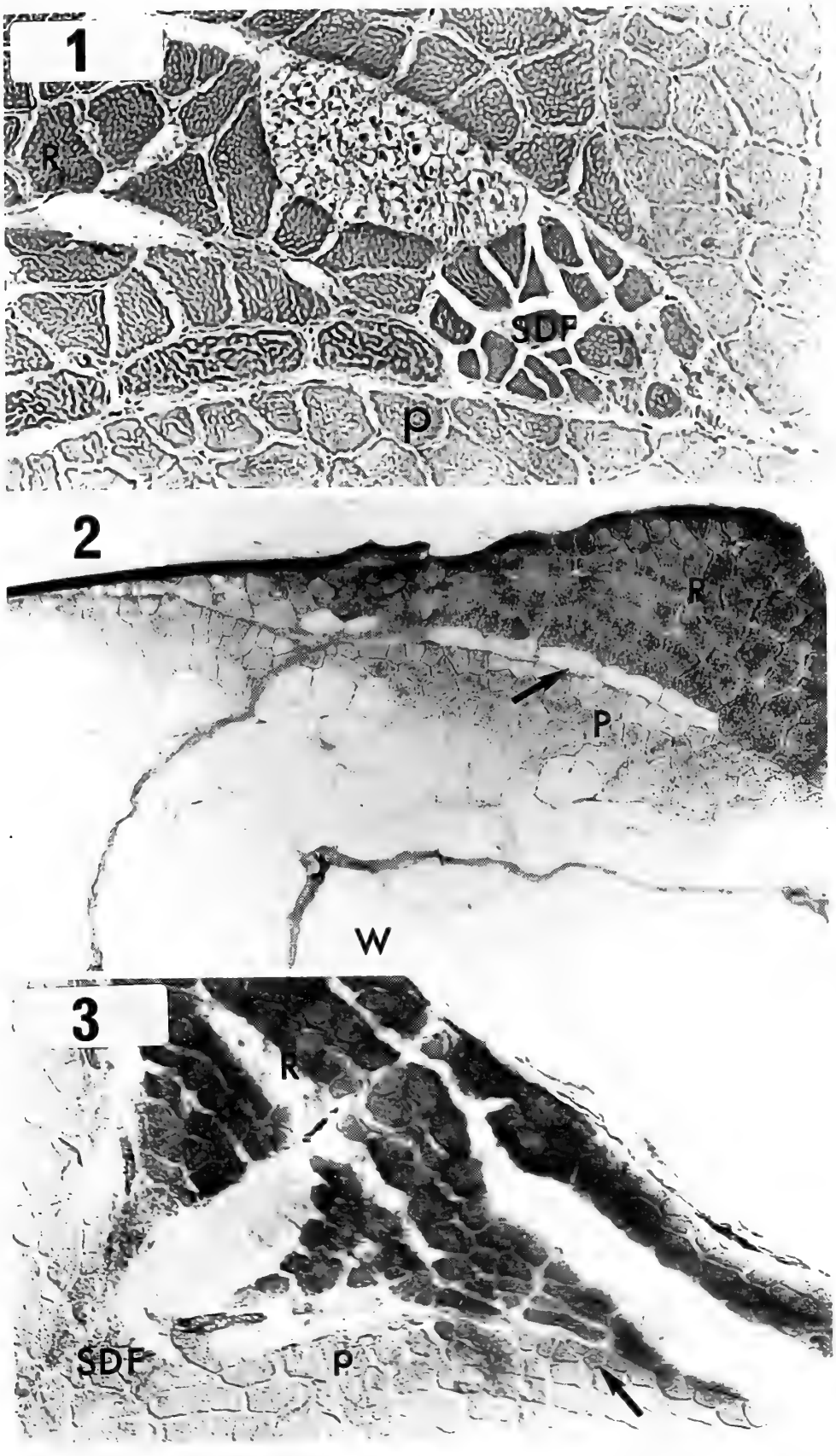
1
R
SDF
P
2
R
P
W
3
R
SDF
P

The *musculus lateralis profundus,* which is composed entirely of white muscle fibers, comprises the bulk of the musculature present in the myotome. These fibers which possessed a large mean diameter, displayed a homogeneous, non-mosaic appearance with respect to staining intensities as reported for other teleosts [18, 25]. The intermediate pink fibers were categorized as small diameter pink fibers. The former were situated adjacent to the perimysium in a layer one to three fibers thick and were of a smaller mean diameter than the red fibers, displaying a variety of staining intensities for SDH and myofibrillar ATPase. The other form of intermediate muscle fibers were located between the small diameter pink fibers and the white fibers. They were classified as large diameter pink fibers according to Patterson *et al.* [20] and were distinguished by (a) their homogeneous staining intensities for all staining techniques used, and (b) an intermediate range of fiber diameters between that of red and white fiber types.

One other fiber type was sometimes observed to be located near the junction of the perimysium and additional myosepta at the point of the wedge-shaped *musculus lateralis superficialis.* When not replaced by connective tissue, these fibers were differentiated from the red muscle fibers by their extremely small mean diameter and their low staining intensities. These fibers were classified as small diameter fibers as they displayed similar properties to the small diameter fibers described by Johnston [10] and Davison [5].

Sudan Black B Technique for lipid

The staining of red muscle fibers for lipid using the Sudan Black B was relatively intense and could be used to distinguish them from white and intermediate pink fibers (Fig. 1). The white and pink fibers developed no significant staining for lipid, except for their cellular boundaries. This was probably due to lipoprotein complexes of the cell membranes or extracellular lipid. Within the intermediate fiber types no differentiation was observed between the small diameter and large diameter pink fibers. The small diameter fibers, when present, also developed no significant staining activity.

PAS stain for glycogen (Fig. 2)

Red fibers displayed intense staining activity for glycogen. A heterogeneous effect was observed in most preparations with a small number of fibers, consisting of elongate fibres adjacent to the perimysium, displaying little or no staining activity for glycogen. The red fibres of the *Seitenlinie* displayed a variety of staining intensities, from moderate to no staining at all. The variety of staining patterns apparent in the red fibers was dependent on the immediate past activity of the fish and may possibly display some hierarchy of recruitment or function resulting in glycogen depletion [23].

Succinic dehydrogenase stain

The staining pattern for SDH was similar to glycogen, that is the red fibers staining intensely and the white fibers showing no staining activity at all. The two categories of intermediate fibers exhibited differential staining using this technique with the large diameter pink fibers displaying moderate staining activity localized primarily at the cell boundary. The small diameter pink fibers developed a moderate staining intensity which lay between that of the red fibers and that of the large diameter pink fibers (Fig. 3). The small diameter fibers again displayed little or no staining activity (Fig. 3).

Myofibrillar adenosine triphosphatase

The pattern of staining for myofibrillar ATPase was found to be dependent on both the pH and duration of preincubation (Tables 2 and 3). All the muscle fiber types present in the myotome stained heavily when incubated for myofibrillar ATPase without preincubation. A differential pattern of staining was obtained by preincubating sections at pH 10.4 for a period of 30 sec at 21°C (Figs. 4, 5, and 7). Longer periods of preincubation were found to cause inactivation of the ATPase in all fiber types, though some staining of pink fibers was still evident.

The reportedly high alkali-stable myofibrillar ATPase activity present in white fibers displayed a variable intensity of staining for different alkaline pH values, and was completely inactivated in a relatively short period of time (Table 3). These fibers displayed no activity when incubated for acid-stable ATPase using acidic preincubation (Fig. 6).

The staining pattern of white fibers was also altered if the specimens were stored in liquid nitrogen for more than several days, resulting in inactivation of the enzyme (Fig. 8).

The alkali-labile ATPase present in the red fibers of the *musculus lateralis superficiales* also demonstrated a variation in staining over the whole range of pH values tested. Alkaline preincubation, which is generally considered to inactivate red myofibrillar ATPase actually resulted in staining of these fibers. A staining pattern was, thus, produced showing alkali-stable ATPase activity in white, red, and intermediate

FIG. 4. Demonstration of alkali-stable myofibrillar ATPase in the myotomal musculature. Note the low staining intensity of the red fibers (R), moderate staining of white fibers (W), the more intense staining of the large diameter pink fibers (P), and the variety of staining patterns exhibited by the small diameter pink fibers (arrow). Magnification: 125×.

FIG. 5. Localization of alkali-stable myofibrilla ATPase in the myotomal musculature. Note the staining of the red fibers (R) due to Ca^{2+}-activated mitochondrial ATPase, which results in a granular appearance. Also of importance is the variety of staining intensities exhibited by the small diameter pink fibers (P) and small diameter fibers (SDH). Magnification: 400×.

FIG. 6. Demonstration of acid-stable myofibrillar ATPase in the myotomal musculature. Note that the red (R) and some pink small diameter fibers were the only fibers that stained. White (W) and large pink fibers show no staining activity. An important point to note is the intense staining of the Seitenlinie fibers (arrow). Magnification: 80×.

pink fibers. The alkali-stable staining activity of the fibers was determined to be due to Ca^{2+}-activated mitochondrial ATPase, as this was the only staining artefact abolished (other fibers stayed the same), if sections were incubated in the presence of 3.5 mM sodium azide, a known inhibitor of mitochondrial activity. Acid-stable myofibrillar ATPase activity developed relatively intensely in the red fibers with the Seitenlinie and elongated red fibers adjacent to the

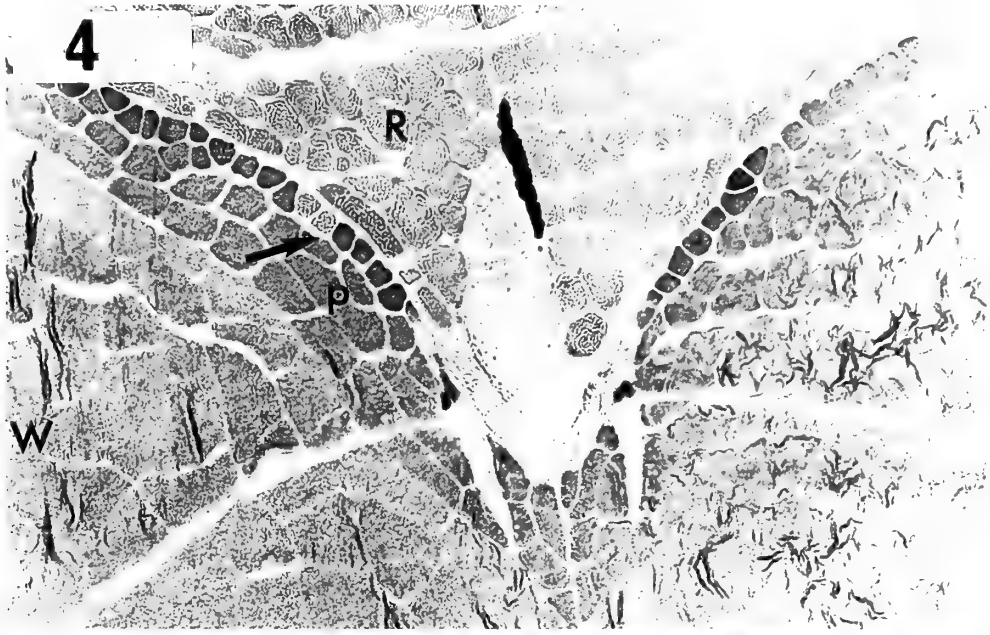

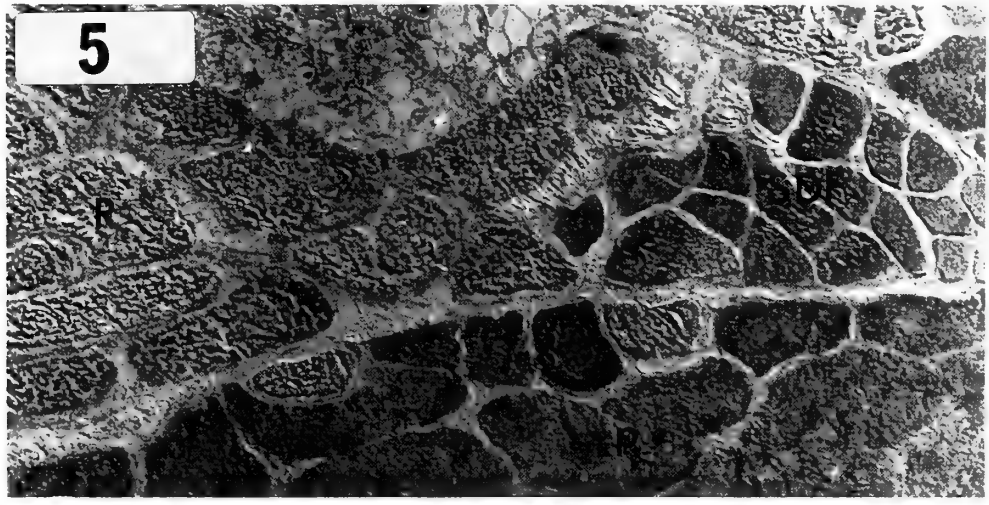

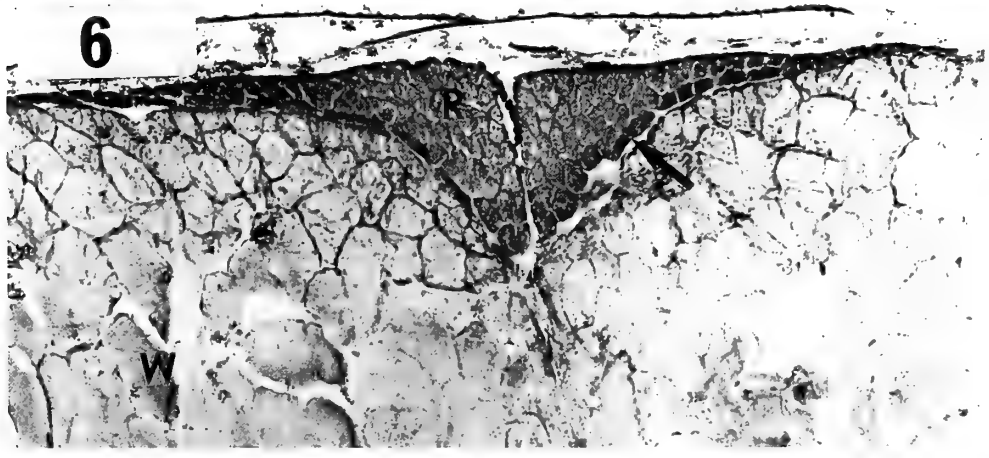

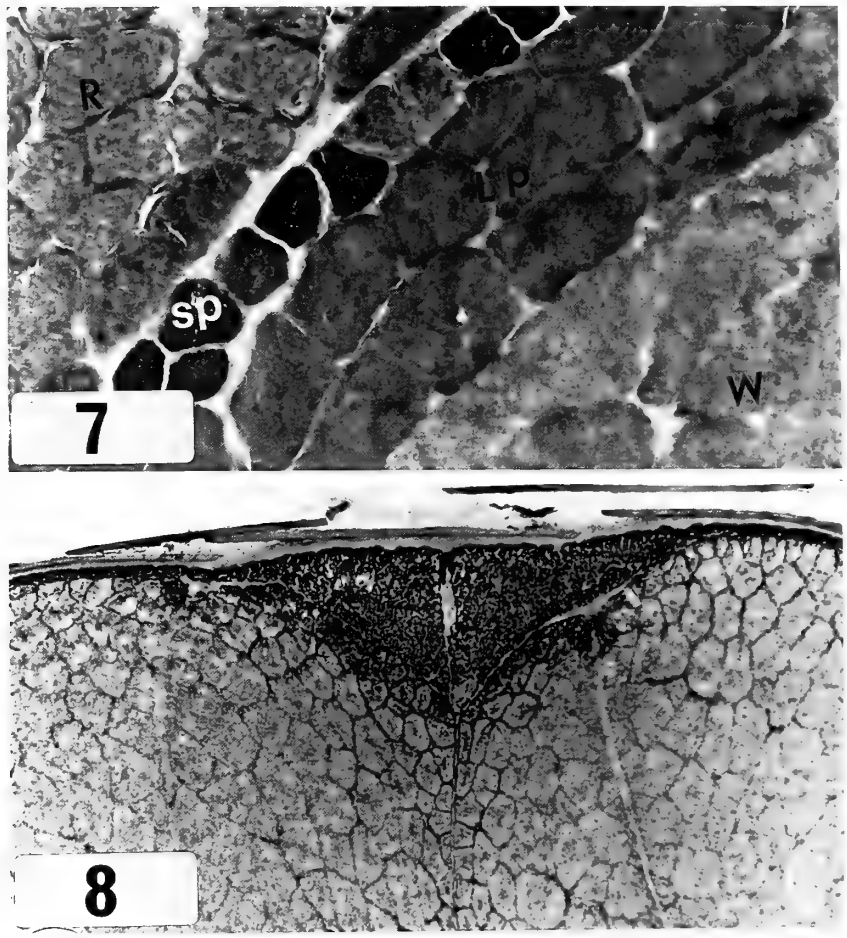

FIG. 7. Localization of alkali-stable myofibrillar ATPase in the myotomal musculature. Note differential staining of the intermediate fibers with small diameter pink fiber (SP) exhibiting a variety of staining intensities while the large pink fibers (LP) are relatively homogeneous. Also of importance is the intensity of staining shown by intermediate fibers, which is more intense than either that of the white (W) or the red (R) fibers. Magnification: 400×.

FIG. 8. Consequence of storage in liquid nitrogen for one week on alkali-stable myofibrillar ATPase activity. Note that the staining activity is greatly reduced in the white muscle with red and some pink fibers showing the only staining activity of any greater degree. Magnification: 80×.

perimysium displaying more activity (Fig. 6).

Both the large and small diameter pink fibers were distinguishable from red and white fibers using alkaline and acid preincubation (Figs. 4–7). In the histochemical demonstration of the alkali-stable ATPase, the large diameter pink fibers stained differently from the small diameter pink fibers (Figs. 4 and 7). A homogeneous staining pattern was produced in the large diameter fibers which displayed higher alkali-stable ATPase activity than the white and red fiber types (Fig. 7). The small diameter pink fibers showed a variety of staining intensities ranging from the darkest of all the fiber types to others displaying an intensity similar to that of red fibers.

In acidic preincubation, both types of pink fibers exhibited a moderate staining activity, with the small diameter fibers having stained slightly darker (Fig. 6). The staining patterns in both fibers, when viewed under high magnification, appeared granular in appearance with most of the stain localized along the periphery and in granules throughout the cell. These locations probably correspond to the positions of subsarcolemmal staining for myofibrillar ATPase with no preincubation and slight staining for alkalistable ATPase. The activity for acid-stable ATPase was marginally more intense.

DISCUSSION

In muscle, metabolic differentiation of fiber types is related to the enzymatic organization of the systems supplying energy [2]. Lipid is an important fuel particularly in species that migrate. It also seems likely that oxidation of fats as fuels is much more important in red than in white muscle as reflected by strong staining for lipid in red fibers [16]. The red fibers of the *Seitenlinie* and those elongate fibers next to the perimysium displayed similar lipid and SDH-activities to the other red fibers, but glycogen levels were not as high. Two possible explanations are that oxidation of lipids is the main source of energy for these fibers or

that during the preparation for this technique these fibers were recruited, resulting in total depletion of their glycogen stores.

The staining pattern of white muscle fibers when stained for SDH, lipid, and glycogen suggests that these fibers have only small concentrations of lipid and glycogen and low densities of mitochondria. From these results it can be concluded that white muscle fibers posses a predominantly anaerobic metabolism and lack the ability to oxidize lipids as an energy source for ATP. Therefore, utilization of glycogen in glycolysis and lactate fermentation appears to be the probable source of ATP for white fiber metabolism. Johnston and Goldspink [11], who were studying glycogen utilization in the myotomal musculature of the Crucian carp, concluded that the low levels of glycogen found in the white muscle fibers were still significant in determining the metabolism of that muscle type. They found that glycogen was utilized at levels two to three times higher in red than in white but since red muscle comprises such a small amount of the musculature, it accounts for only 15–20% of the total glycogen utilized.

The intermediate fibers displayed a differential pattern of staining from red and white fiber types. Patterson *et al.* [20] subdivided the pink fibers on the basis of size and histochemical profiles into large and small categories, which resembled the white and red fibers, respectively, except in staining for SDH where both categories stained equally lightly. In this study the two categories stained differentially for SDH, with the small diameter pink fibers staining more intensely than the large ones. Mosse and Hudson [18] reported a similar staining pattern and suggested that graded staining patterns (obtained when stained for SDH, glycogen) implied that both the large and small diameter pink fibers represented a transition zone between the red and white muscle mass. It is, therefore likely that not only an anatomical, but a functional transition between aerobic and anaerobic metabolism exists in this intermediate zone with the small diameter fibers possessing an aerobic and the large fibers having a more anaerobic capacity. This could possibly relate to fiber diameter and the constraints of large diffusion distances on oxygen availability. The source of energy for the metabolism for these fibers is one factor that contradicts the hypothesis of a gradual transition zone between red and white fibers.

No staining for lipid was evident in any of the intermediate pink fibers, but the presence of glycogen was obvious in all of them. Previous histological studies on a number of fish species [1, 6, 12, 18, 22, 24] have demonstrated that small diameter fibers are characterized by poor staining characteristics compared to other fiber types, possessing low lipid content and low SDH-activity, but differing in respect to the pH stability of their myofibrillar ATPase. The small diameter fibers present in the smelt displayed similar staining characteristics to those cited in previous studies. This pattern of staining implies a fiber with very low metabolic activity, which would correlate well with its function as a tonic fiber used in postural support as in the fishes [4].

ACKNOWLEDGMENTS

The authors wish to thank Dr. Owen Young of the Meat Industry Research Institute of New Zealand for his much appreciated advice upon matters histochemical and our laboratory technician Mrs. Lee Laboyrie, who was always a pleasure to work with.

REFERENCES

1 Akster HA, Osse JWM (1978) Muscle fiber types in head muscles of the perch *Perca fluviatilis* L., Teleostei: A histochemical and electromyographical study. Neth J Zool 28: 94–110

2 Bass A, Brdiczka D, Eyer P, Hofer S, Pette D (1969) Metabolic differentiation of distinct muscle types at the level of enzymatic organization. Europ J Biochem 10: 198–206

3 Carpene E, Veggetti A, Mascarello F (1982) Histochemical fiber types in the lateral muscle of fishes in fresh, brackish, and salt water. J Fish Biol 20: 379–396

4 Davison W (1983) The lateral musculature of the common bully, *Gobiomorphus cotidianus,* a freshwater fish from New Zealand. J Fish Biol 23: 143–151

5 Davison W (1985) Swimming against the tide: adaption of three species of fish for life in the intertidal zone. Mauri Ora 12: 95–104

6 Davison W, Macdonald JA (1985) A histochemical study of the swimming musculature of Antarctic fish. N Z J Zool 12: 473–483

7 Dubowitz V, Brooke MH (1973) Muscle biopsy: a modern approach. W. B. Saunders & Co. London-Philadelphia-Toronto

8 Guth L, Samaha FJ (1970) Procedure for the histochemical demonstration of actomyosin ATPase. Exp Neurol 28: 365–367

9 Hulbert WC, Moon TW (1978) A histochemical light and electron microscopic examination of eel *Anguilla rostrata* red and white muscle. J Fish Biol 13: 527–533

10 Johnston IA (1981) Structure and function of fish muscle. In "Vertebrate locomotion: Symposia of the Zool. Soc. of London" Ed by MH Day, Academic Press, London-New York, pp 71–113

11 Johnston IA, Goldspink G (1973) A study of glycogen and lactate in the myotomal muscles and liver of the coalfish *Gadus virens* during sustained swimming. J Mar Biol Assoc U K 52: 17–26

12 Johnston IA, Patterson S, Ward P, Goldspink G (1974) The histochemical demonstration of myofibrillar ATPase activity in fish muscle. Can J Zool 53: 871–877

13 Johnston IA, Ward P, Goldspink G (1975) Studies on the swimming musculature of the rainbow trout: fiber types. J Fish Biol 7: 451–458

14 Korneliussen H, Dahl HA, Paulsen JE (1978) Histochemical definition of muscle fiber types in the trunk musculature of a teleost fish (cod: *Gadus morhua* L.). Histochem 55: 1–16

15 Kryvi H, Totland GK (1978) Fiber types in locomotory muscles of cartilaginous fish *Chimaera monstrosa.* J Fish Biol 12: 257–265

16 Meyer-Rochow VB, Devine C (1986) Ultrastructual observations and pH-measurements on red and white muscle from two Antarctic fish. Polar Biol 6: 241–246.

17 Meyer-Rochow VB, Ingram JR (1992) Red/white muscle distribution and fiber growth dynamics: a comparison between lacustrine and riverine populations of the Southern smelt *Retro-*

pinna retropinna Richardson. Proc Roy Soc London B in press

18 Mosse PRL, Hudson RCL (1977) The functional roles of different muscle fiber types identified in the myotomes of marine teleosts: a behavioral, anatomical and histochemical study. J Fish Biol 11: 417–430

19 Ogata T, Mori M (1964) Histochemical study of oxydative enzymes in fish muscle. J Histochem Cytochem. 12: 171–182

20 Patterson S, Johnston IA, Goldspink G (1975) A histochemical study of the lateral muscles of five teleost species. J Fish Biol 7: 159–166

21 Pearse AGE (1972) Histochemistry: theoretical and applied. Churchill Livingstone, Edinburgh-London

22 Pool CW, Raamsdonk W van, Diegenbach PC, Mijzen P, Schenkken EJ, Stelt A van der (1976) Muscle fiber typing with sera against myosin and actin: a comparison between enzyme and immunohistochemical classification. Acta Histochem 57: 20–23

23 Proctor C, Mosse PRL, Hudson RCL (1980) A histochemical and ultrastructural study of the development of the propulsive musculature of the brown trout *Salmo trutta* L. in relation to its swimming behaviour. J Fish Biol 16: 309–329

24 Raamsdonk W van, TeKronnie G, Pool CW, Laarse W van de (1980) An immune-histochemical and enzyme characterization of the muscle fibers in myotomal muscle of the teleost *Brachydanio rerio* Hamilton-Buchanan. Acta Histochem 67: 200–216

25 TeKronnie G, Tatarczuch L, Raamsdonk KW van, Kilarski W, (1983) Muscle fiber types in the myotome of the stickleback *Gasterosteus aculeatus* L.: a histochemical, immunohistochemical, and ultrastructural study. J Fish Biol 22: 303–316

ZOOLOGICAL SCIENCE 11: 63–68 (1994)

Assesment of pMTL Construct for Detection *in vivo* of Luciferase Expression and Fate of the Transgene in the Zebrafish, *Brachydanio rerio*

JAWAHAR G. PATIL, VERONICA WONG and HONG WOO KHOO

Fisheries Biology Laboratory, Department of Zoology, National University of Singapore, 10, Kent Ridge Crescent, Singapore-0511

ABSTRACT—Early embryos of the zebrafish *Brachydanio rerio* were cytoplasmically microinjected with pMTL plasmid containing firefly luciferase gene, in both linearized- and supercoiled-plasmid forms, to evaluate *in vivo* expression, pattern of integration and germ-line transmission of the transgene in the host fish. It was possible to detect luciferase expression *in vivo*, and the pattern of time-course expression was similar in both linearized- and supercoiled-plasmid injected groups. Strong luciferase activity was detected 15–20 hours after injection, coinciding with early somitogenesis. Expression was detectable in a few 1 week-old individuals but was not detectable in all adults and in F_1 progeny. *In vivo* screening for expression of the transgene in the developing embryo using luciferase assay as a method for detecting the presence of the transgenic fish compares favourably, with PCR and Southern blot analysis (SBA). No integration of the introduced DNA into the genome of treated fish and their progeny, was detected, instead it remained in extrachromosomal form. Most of the first generation founders were mosaic. Germline transmission was observed in one individual only. A probable reason for the absence of integration in this study when compared to the varying frequencies of integration reported earlier in the same fish is discussed.

INTRODUCTION

Considerable research and progress has been made in the production of transgenic fish in recent years [for review see 7]. To demonstrate the occurrence of transgenic animals, tedious methods such as PCR and Southern blot analysis (SBA) have been used, followed by genetic crossing to isolate the required phenotype. The PCR and SBA techniques often require sacrifice of the animals to extract the DNA. Such invasive procedures preclude subsequent breeding experiments on germ-line transmission. Alternatively, treated individuals are grown to large size and part of the animal such as fin sample were used for assay. Raising fish to the adult stage is, however, time consuming and expensive. A more expeditious method for detecting transgenes is therefore required.

This study investigates the use of firefly luciferase as a reporter gene for convenient detection of the presence of the transgene in zebrafish *in vivo*. The sensitivity, rapidity, non-invasiveness and use of this non-radioactive technique for positive indication of presence, when compared to other commonly used reporter genes such as CAT, make this luciferase assay a more efficient one. A few reports on the use of firefly luciferase gene as reporter in fish are available [1, 6, 19]. Sato *et al.* [14] have shown the expression of luciferase in medaka, using tissue lysate. This study investigates the efficiency of luciferase expression *in vivo* as well as the fate and outcome of the introduced pMTL reporter with regard to its integration into the fish genome and its germ-line transmission.

Accepted October 26, 1993
Received July 27, 1993

MATERIALS AND METHODS

We have used the zebrafish in this study. The zebrafish stock was bought from local suppliers and fish were raised in aquarium tanks. The pMTL plasmid used in this study was earlier used by Sato *et al.* [14] in medaka. It contains Chinese hamster metallothionein I (MT-I) promoter, the cDNA for luciferase from the firefly (*Photinus pyralis*), the SV40 polyA tail and the vector sequence of pBR322. The construct was a gift from Dr. T. Ishikawa, Dept. of Experimental Pathology, Tokyo University.

The method of microinjection described by Khoo *et al.* [8] was followed, with slight modifications. About 1–2 nl of a solution of Hind III-linearized or supercoiled-plasmid DNA (100 μg/ml DNA in 0.1 M Tris-HCl, pH 7.2, containing 0.25%, w/v, phenol red) were injected into embryos at the one or two-cell stage (about 1.4×10^7 copies/embryo), with a sharpened glass needle (3–5 μm in diameter). Injection volume was controlled with an automatic microinjector (Model IM-1, Narishige, Tokyo).

To monitor the expression of luciferase, embryos were immersed in 100 μl of luciferase assay reagent (LAR; Promega, Madison, USA.) and luminescence was detected with a liquid scintillation counter (model LS 5801; Beckman.) in the single-photon monitor mode. For subsequent screening of expression in individual live embryos, the counting was performed in 60 μl of LAR+40 μl of distilled water, at about 15 hr after microinjection. For adult fish fin samples were washed twice in PBS (Ca^{2+} and Mg^{2+} free); a quarter of the fin was assayed intact by immersion of the tissue in 100 μl LAR and another quarter was homogenised in 100 μl of 1X lysis buffer (supplied by the manufacturer; Promega.) and then assayed with 100 μl of LAR. Remaining half of the fin sample was used for DNA extraction.

To extract genomic DNA, each fry or fin was rinsed in embryonic solution containing 10 μg/ml of DNAse I for a period of 1 hr and washed 4× in PBS and once in Tris-EDTA (10 mM Tris; 1 mM EDTA). The fry was digested in 25 μl of polymerase chain

reaction (PCR) buffer supplemented with nonionic detergent and proteinase K (50 mM KCl, 10 mM Tris-HCl, pH 8.3, 2.5 mM $MgCl_2$, 0.025 mg gelatin, 0.45% NP 40, 0.45% Triton X-100 and 60 μg/ml proteinase K) at 55°C for 90 min and heat inactivated at 95°C for 10 min. The digested mixture was then cleared by centrifugation (3000 g for 3 min). An aliquot of 2 μl was used for PCR. The remaining 23 μl was purified by phenol: chloroform: isoamyl alcohol extraction. DNA from adult fish was extracted as described elsewhere [9].

Two oligonucleotide primers 5′-CGGCGGCGGGAAGTTCA-CCGGCG-3′ and 5′-CCGGGCGCGGTCGGTAAAG-3′ were used for detection of the firefly gene for luciferase. PCR was carried out following the method of Saiki [13] with slight modification. The crude genomic extract (2 μl) was placed in 0.5 ml microfuge tube containing PCR mixture (1X PCR buffer containing 50 μM each of dATP, dCTP, dGTP, dTTP, 0.25 μM each of primer and 0.25 unit of Taq DNA polymerase). The entire reaction mixture was overlaid with mineral oil and amplified in a Techne PHC-2 thermal cycler (Princeton, USA) for 30 cycles. Amplification was performed with initial denaturation at 94°C for 5 min, with subsequent incubations at 95°C, 55°C and 72°C for 1, 1.3, and 1 min, respectively. Then 8 μl of the amplified mixture were mixed with 2 μl of loading buffer and subjected to electrophoresis on a 1.5% agarose gel, stained with ethidium bromide and photographed under UV light.

The remaining 23 μl of the genomic DNA extract were digested by Hind III (New England Biolabs, Beverly), subjected to electrophoresis on a 0.8% agarose gel and transferred to a Hybond-N (Amersham, UK.) nylon membrane by vacuum blotting using a trans-Vac TE 80 system (Hoefer Scientific Instruments, San Francisco). Membranes were probed with Hind III linearized plasmid that had been labelled with [^{32}P]-dCTP (Amersham, UK.) by random priming. Hybridization was performed at 65°C overnight. Filters were then washed and autoradiographed using Kodak (X-OMAT) diagnostic film. In case of adult fishes where there was sufficient genomic DNA extract, 5 μg was HindIII digested and another 5 μg undigested for SBA.

Three experiments were conducted. The first was an *in vivo*-time course expression assay of zebrafish embryo treated with pMTL plasmid. Microinjected embryos in duplicates of 5 were monitored for expression in each treatment groups. Embryos injected with injection buffer only and those not injected served as injected and non-injected controls, respectively.

In the second experiment we tested whether the presence of the transgne could be detected by PCR and Southern blot in all the embryos expressing the transgene *in vivo*. About 400 embryos were microinjected with supercoiled- and linear-plasmid separately. Embryos which gave more than 1.5 times the background counts at 10–15 hr after injection were considered as positive for expression. Three days after hatching, 200 each hatchlings from the treated groups were sampled for PCR and Southern blot analysis.

The third experiment was to conduct a germ-line transmission study. Embryos microinjected with supercoiled- and linear-plasmid, were screened for luciferase expression and expression positive individuals were reared to maturity. All the individuals whose fin samples were positive for both PCR and SBA (henceforth referred to as fin-positives) were then bred with untreated fish to produce F_1. The F_1 progeny were first tested by luciferase expression assay and subsequently the same samples were tested by PCR and SBA. Similarly, some individuals whose fin samples tested negative by PCR and SBA (fin-negatives) were also bred with untreated fish and their progeny assayed as above.

RESULTS

Experiment I

The time-course expression of luciferase in the developing embryos is presented in Figure 1. Scintillation counts recorded from the sample blank and the control groups were not significantly different ($P<0.05$) from one another. Both injected groups (supercoiled and linear) gave significantly higher scintillation counts ($P<0.05$) than the controls and the blanks. The results indicate that the luciferase expression in injected embryos increased rapidly to a maximum at 15 hr after injection coinciding with early somitogenesis. The first evidence of expression was obtained 10 hr post-injection and this coincided with the late gastrula stage. Subsequently, the counts declined gradually but still was detectable 48 hr post-injection. The decline in expression was more rapid in supercoiled-plasmid injected group than in the linear-plasmid injected group. Some fry (3 days old) gave scintillation counts similar to those observed at 48 hr, but no values higher than those at 15–25 hr after injection. Expression in such fry persisted for up to 8 days. Since, in preliminary experiments, we neither detected endogenous luciferase activity nor any evidence of inhibitory factors, the observed pattern of luciferase activity must represent luciferase expression by the introduced gene.

Experiment II

Forty nine of the 200 (24.5%) inidividuals in the supercoiled-plasmid injected group were found to be positive for expression (Table 1). Similarly, 37 individuals out of 200 (18.5%) in the linear-plasmid injected group were positive for expression (Table 2). All individuals that expressed the transgene were also positive by PCR and Southern blot, in both treatment groups. The remaining 75.5% and 81.5% in the supercoiled- and linear-plasmid treated groups, respectively, did not express the inserted gene. These non-expressing embryos were also PCR and Southern blot-negative except for a few individuals i.e. 4% in supercoiled-plasmid and 3% in linear-plasmid injected groups were PCR-positive, whereas 2% in the supercoiled-plasmid and none in linear-plasmid treated groups were Southern blot-positive. Typical examples of PCR results for the supercoiled group are shown in Figure 2.

All the 26.5% and 18.5% SBA positive individuals in the supercoiled- and linearized-plasmid injected groups respectively were invariably PCR-positive. However, the inverse was not true as 2% and 3% of the individuals in supercoiled and linear-plasmid injected groups respectively were PCR-positive but Southern blot-negative. Southern blot profile (Fig. 3) of 11 fry from the supercoiled-plasmid injected group that were PCR-positive showed only one band (lanes 2–11) at the size of linearized-plasmid (6.65 kb) suggesting that, there was no genomic integration of the introduced gene. SBA of fry from linear-plasmid injected group gave similar results (Data not shown).

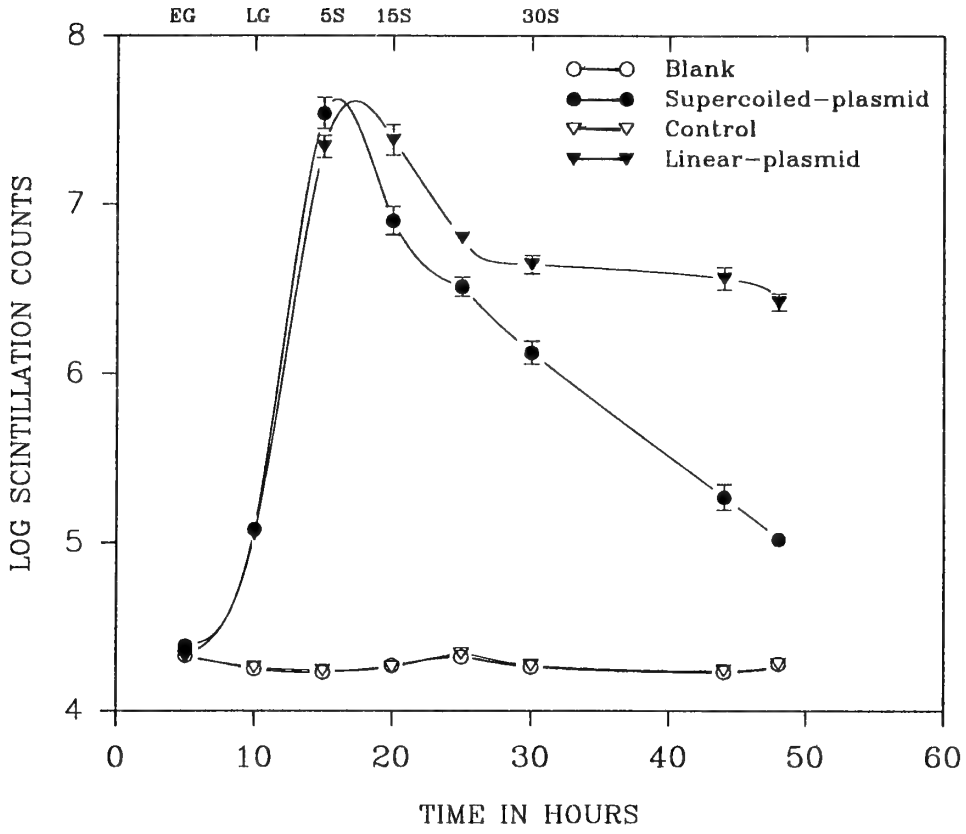

FIG. 1. Time course of expression of the luciferase gene after microinjection into zebrafish embryos as measured with a scintillation counter (in the single-photon counting mode). Hours after microinjection are indicated on the abscissa. Above the figure several events in the development of the fish are indicated. (EG, early gastrula; LG, late gastrula; 5s, 15s and 30s, correspond to 5-, 15- and 30-somite stages respectively.) Scintillation counts are expressed logarithmically ($\log_{10}$).

TABLE 1. Frequency of the transgene in the supercoiled-plasmid microinjected group

		PCR	
		% Positive	% Negative
Expression	% Positive	24.5* (49)	0
	% Negative	4 (8)	71.5 (143)
Southern blot	% Positive	26.5 (53)	0
	% Negative	2 (4)	71.5 (143)

* Southern blot positive as well.
Figures in parenthesis indicate number of individuals out of the 200 assayed.

TABLE 2. Frequency of the transgene in the linear-plasmid microinjected group

		PCR	
		% Positive	% Negative
Expression	% Positive	18.5* (37)	0
	% Negative	3 (6)	78.5 (157)
Southern blot	% Positive	18.5 (37)	0
	% Negative	3 (6)	78.5 (157)

* Southern blot positive as well.
Figures in parenthesis indicate number of individuals out of the 200 assayed.

Experiment III

Of the 36 individuals in the supercoiled- and 29 in the linear-plasmid injected groups which grew to maturity, eight and five individuals, respectively, were both PCR and SBA positive (Table 3). None showed expression of the luciferase gene. The SBA profile obtained from fin samples of 8 SBA positive individuals of supercoiled-plasmid treated group are shown in Figure 4. In all eight individuals only one band about the size of the linearized plasmid (6.65 kb) was detected (lanes 2–9). This suggests that the injected

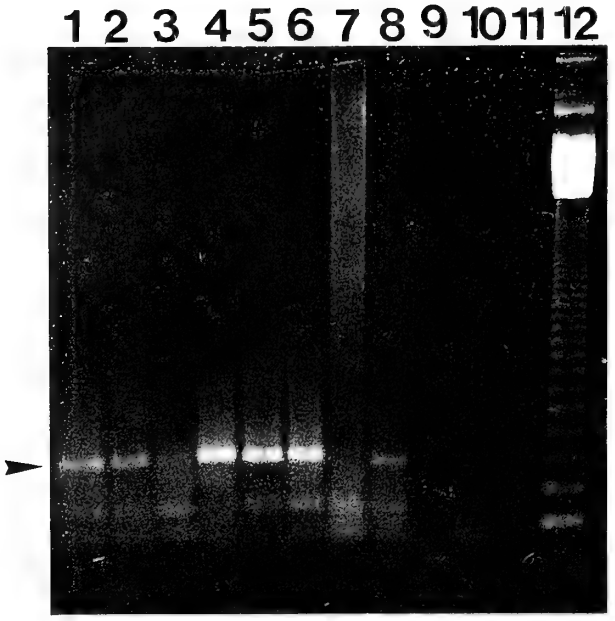

FIG. 2. Detection by PCR analysis of foreign DNA in transgenic zebrafish that had been injected with supercoiled plasmid. 8 μl of DNA from the total reaction mixture after PCR were fractionated on a 1.5% agarose gel. The gel was stained with ethidium bromide and photographed under ultraviolet light. Lanes 1–3 and 7–9, amplified genomic DNA from expression-negative individuals; lanes 4–6, amplified genomic DNA from expression-positive individuals; lane 10, amplified genomic DNA from an untreated control fish; lane 11, reagent blank and lane 12, ladder. Arrowhead indicate the expected, amplified 376-bp bands.

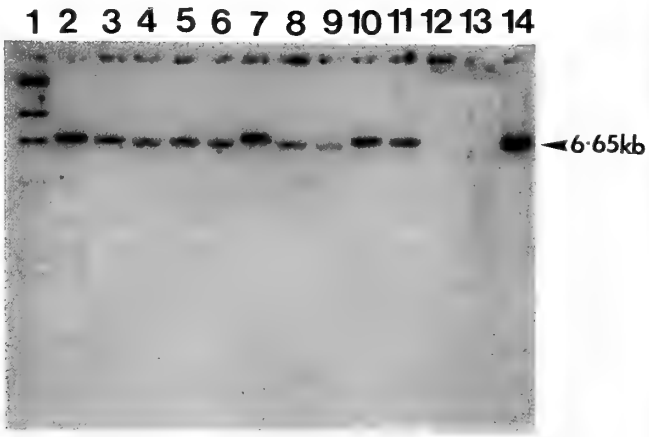

FIG. 3. Southern blot analysis of supercoiled-plasmid injected group. Genomic DNA of individuals that had been assayed for expression and by PCR were digested with Hind III (single restriction site) then the entire aliquot was subjected to electrophoresis on a 0.8% agarose gel, transferred to a Hybond-N membrane and probed with [^{32}P]-rediolabelled pMTL (Hind III-linearized). Lane 1, λ DNA/HindIII size markers; lanes 2–12, genomic DNA of the individuals that were PCR positive; lane 13 genomic DNA of control fish; lane 14 genomic DNA of control fish spiked with pMTL (positive control). Arrowhead indicate to the size of the linearized plasmid.

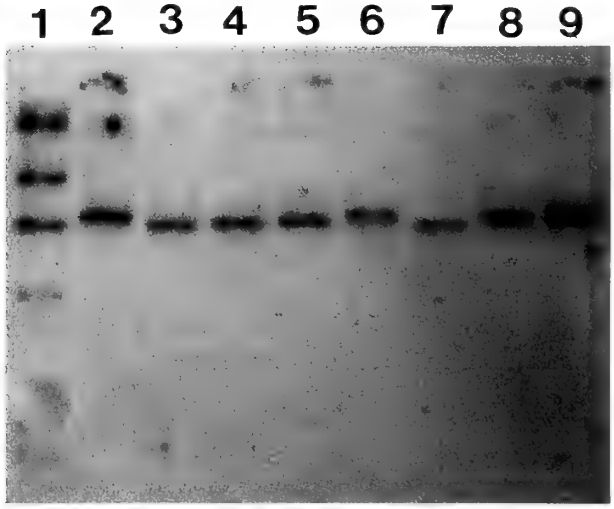

FIG. 4. Detection of transgene in F_0 of supercoiled-plasmid injected group. Genomic DNA (about 5 μg) extracted from fin clip of adult fish (that were PCR positive) were Hind III digested and analyzed by Southern blot as in legend to Fig. 3. Lane 1 λ Hind III marker; lane 2–9 genomic DNA from 8 different adult F_0 fish that were earlier found PCR positive.

reporter gene remained unintegrated with the fish genome. None of these fin-positive individuals transmitted the transgene to their offspring (F_1), as their offspring were neither expression-, PCR- nor Southern blot-positive (Data not shown).

One of the fin-negative individuals in the supercoiled-plasmid injected group, transmitted the foreign DNA to its offspring. The transmission was evident from SBA profiles of 4 F_1 fish (1 month old), resulting from a mating between the SBA negative founder and a control fish (Fig. 5). All the four F_1 fish tested had similar Southern blot signal patterns that hybridized with the plasmid probe. The inherited gene was about 2.48 kb in size following digestion with Hind III (lanes 1, 3, 5 and 7). The undigested genomic

TABLE 3. Transgenic adult fish after injection of supercioled- and linear-pMTL DNA

		Supercoiled plasmid injected group		Linear plasmid injected group	
		Southern blot		Southern blot	
		No. Positive	No. Negative	No. Positive	No. Negative
PCR	No. Positive	8	0	5	0
	No. Negative	0	28	0	24

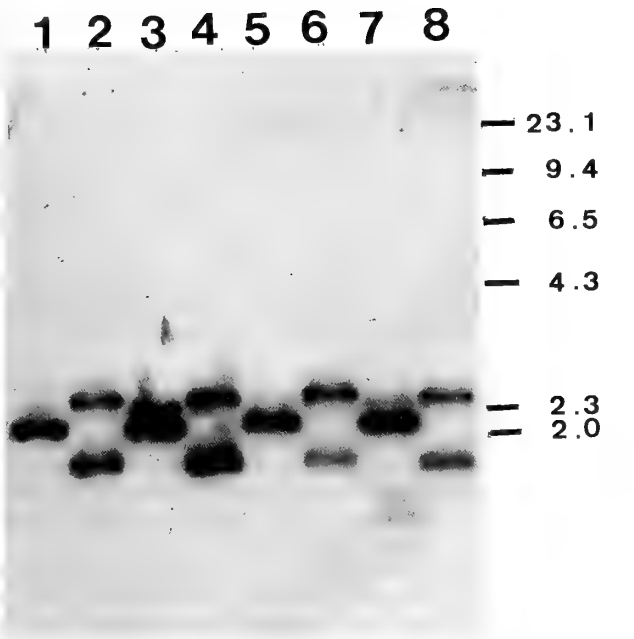

FIG. 5. Southern blot analysis of F_1. Genomic DNA (about 7 μg) from whole fish of four individuals from the progeny of a founder crossed to control fish was either Hind III digested or undigested and probed (please see legend to Fig. 3.). Fin clip assay of the founder was negative for both PCR and Southern blot. Lanes 1, 3, 5 and 7, Hind III digested samples; lanes 2, 4, 6 and 8, undigested samples.

DNA showed two bands of about 2.4 kb and 1.9 kb (lanes 2, 4, 6 and 8). This pattern suggests that a portion of the introduced plasmid had been excised out. PCR gave negative results for the four samples (F_1 fish), supporting the hypothesis that the deletion included a portion of the luciferase fragment in the introduced plasmid. Higher intensities of the Hind III linearized band in all four analyzed samples when compared to band 1 in undigested samples suggest that the transgene remained extrachromosomal in two different forms.

DISCUSSION

We have demonstrated that it is possible to detect the *in vivo* expression of firefly luciferase in zebrafish embryos nondestructively. The LAR penetrates easily into the embryos and larvae and does not seem to harm the developing embryos. This not only facilitates monitoring of the reporter gene activity during development but also the detection of foreign DNA from the same embryo. Papp *et al.* also detected *in vivo* expression of the luciferase gene in zebrafish embryos injected with another plasmid, pCMV1 containing the luciferase gene (unpublished data). The expression of the luciferase gene was transient with the onset of expression coinciding with the late gastrula stage. This onset differs from that observed by Chong and Vielkind [4], who found in the medaka, that the onset of CAT (pUSVCAT) expression occurred prior to gastrulation, at the flat-blastula stage. However, they reported that onset of expression was 10 hr post-injection, similar to the time of first detection in the present study. The difference in stage dependent expression could be due to species differences. For both the supercoiled- and linear-plasmid DNA forms, the luciferase time-course expression patterns were very similar, though not identical. These results indicate that the physical conformation of the administered DNA does not appear to affect its expression.

PCR seemed slightly more sensitive than detection of luciferase expression as a method for detection of the transgene. Nevertheless, the ability to detect the expression in embryos without destroying them (non-destructive) and the rapidity of the assay favour the latter method, aiding both in the rapidity of screening and in limiting the rearing of founders to maturity.

Our Southern analysis of the genomic DNA of several transgenic fish microinjected with supercoiled-plasmid indicated no integration of the foreign DNA. Rather the introduced DNA remained extrachromosomal. Extrachromosomal occurrence and inheritance of transgenes in *Caenorhabditis elegans* [11, 15], mice [12, 18] and zebrafish [2, 9] have been previously reported. Integration of the introduced foreign genes in zebrafish have been earlier reported [2, 5, 16, 17].

The inability of the fin positive parents to transmit the transgene to their offspring suggests that germ cells of these tested individuals did not contain the transgene. Whilst the ability of one of the fin-negative individual to transmit suggests that the majority of the founders are mosaics. Mosaicism is consistent with the earlier observations made in this fish [2, 5, 16, 17].

Occurrence of the inherited transgene in smaller fragments than the plasmid in the F_1 of the fin-negative founder suggests that a part of the transgene was excised. Furthermore, inability of PCR to detect the inherited gene implies that the deletion encompassed the luciferase gene. Deletion of integrated transgenes in mice have been observed by Komori *et al.* [10] and Bluthmann *et al.* [3].

The discrepancy between the low frequency of germ-line transmission and absence of integration observed in the present study, and that of 4–5% [16, 17] and 17% [5] reported previously in this species require further clarification; however these differences may be attributable to the nature of the plasmid constructs. In the studies of Stuart *et al.* [16, 17] and Culp *et al.* [5], the plasmid constructs (pUSVCAT and pRSV-βGal, respectively) contained RSV-LTR enhancer/promoter sequences. In contrast the pMTL construct used in this study had MT-I promoter and SV40 poly A tail, which for unknown reasons seems to have lower tendency to integrate or no integration at all in this fish. This argument is further supported by the fact that following injection of the plasmid construct SV40-*lacz* (pCH110; that lacked RSV-LTR fragments), containing the same reporter as in pRSV-βGal, Culp *et al.* [5] also did not detect any germ-line transgenic fish.

ACKNOWLEDGMENTS

We thank Dr. T. Ishikawa of the Department of Experimental Pathology, Tokyo University, for plasmid gift and Prof. S. S. Tobe, University of Toronto for critical reading and suggestions in preparation of the manuscript. Thanks to Mr. H. K Yip for the photographs. JGP sincerely acknowledges the Research scholarship awarded by the National University of Singapore (NUS). The work was supported by a grant from the NUS (RP 332/87).

REFERENCES

1 Alestrom P, Klunguand H, Kiser G, Andersen O (1991) Fish GnRH gene and molecular control of sexual maturation. 2_{nd} International Marine Biotechnology Conference Baltimore, MD. Abstracts, p. 65

2 Bayer TA, Compos-ortega JA (1992) A transgene containing *lacz* is expressed in primary sensory neurons in zebrafish. Development 115: 421–426

3 Bluthmann H, Kisielow P, Uemasatu Y, Malissen M, Kimpenfort P, Berns A, von Boehmer H, Steinmetz M (1988) T-cell specific deletion of T-cell receptor transgenes allows functional rearrangement of endogenous α- and β-genes. Nature 334: 156–159

4 Chong SSC, Vielkind JR (1989) Expression and fate of CAT reporter gene microinjected into fertilized medaka (*Oryzias latipes*) eggs in the form of plasmid DNA, recombinant phage particles and its DNA. Theor Appl Genet 78: 369–380

5 Culp P, Volhard CN, Hopkins N (1991) High-frequency germline transmission of plasmid DNA sequences injected into fertilized zebrafish eggs. Proc Natl Acad Sci USA 88: 7953–7957

6 Gibbs PDL, Peek A, Thorgaard GH (1991) An *in vivo* screening for transgenic fish utilizing the luciferase reporter gene. 2_{nd} International Marine Biotechnology Conference Baltimore, MD. Abstracts, p. 79

7 Houdebine LM, Chourrout D (1991) Transgenesis in fish. Experientia 47: 891–897

8 Khoo HW, Ang LH, Lim HB (1993) Gene transfer by microinjection in the zebrafish *Brachydanio rerio*. In "Methods in Molecular Biology: Transgenesis techniques-Principles and Protocols Vol 18" Ed by D Murphy, DA Carter, Humana Press, Totowa, New Jersey, pp 87–94

9 Khoo HW, Ang LH, Lim HB, Wong KY (1992) Sperm cells as vectors for introducing foreign DNA into zebrafish. Aquaculture 107: 1–19.

10 Komori S, Katsumata M, Greene MI, Yui K (1993) Frequent Deletion of the Transgene in T-Cell Receptor Beta Chain Transgenic Mice. Int Immunol 5: 161–167

11 Mello CC, Kramer JM, Stinchcomb D, Ambros V (1991) Efficient gene transfer in *C. elegans*: extrachromosomal maintenance and integration of transforming sequences. EMBO J 12: 3959–3971

12 Rassoulzadegen M, Leopold P, Vailly J, Cuzin F (1986) Germline transmission of autonomous genetic elements in transgenic mouse strains. Cell 46: 513–519

13 Saiki RK (1990) Amplification of genomic DNA. In "PCR protocols: A guide to methods and applications" Ed by MA Innis, DH Gelfand, JJ Sninsky, TJ White, Academic Press, New York pp 13–20

14 Sato A, Komura J, Masahito, Matsukuma S, Aoki K, Ishikawa T (1992) Firefly luciferase gene transmission and expression in transgenic medaka (*Oryzias latipes*). Mol Marine Biol Biotech 1: 318–325

15 Stinchcom DT, Shaw JE, Carr SH, Hirsh D (1985) Extrachromosomal DNA transformation of *Caenorhabditis elegans*. Mol Cell Biol 5: 3484–3496

16 Stuart GW, McMurry JV, Westerfield M (1988) Replication, integration and stable germ-line transmission of foreign sequences injected into early zebrafish embryos. Development 103: 403–412

17 Stuart GW, Vielkind JR, McMurry JV, Westerfiled M (1990) Stable lines of transgenic zebrafish exhibit reproducible patterns of transgene expression. Development 109: 577–584

18 Sudo K, Ogata M, Sato Y, Iguchi-Ariga SMM, Ariga H (1990) Cloned origin of DNA replication in c-myc gene can function and be transmitted in transgenic mice in episomal state. Nucl Acids Res 18: 5425–5432

19 Tamiya E, Sugiyama T, Masaki K, Hirose A, Okashi T, Karube I (1990) Spatial imaging of luciferase gene expression in transgenic fish. Nucl Acids Res 18: 1072

ZOOLOGICAL SCIENCE 11: 69–76 (1994)

K252a, a Potent Inhibitor of Protein Kinases, Promotes the Transition of *Dictyostelium* Cells from Growth to Differentiation

TAKESHI FURUKAWA and YASUO MAEDA[1]

Biological Institute, Faculty of Science, Tohoku University, Aoba, Sendai 980, Japan

ABSTRACT—Cell differentiation and proliferation are mutually exclusive processes in many cases. The transition of starving *Dictyostelium* cells from growth to differentiation phase has been shown to occur at a particular position (putative shift point; PS-point) in the cell cycle of *D. discoideum* Ax-2. The significance of phosphorylation states of proteins such as 101 kDa, 90 kDa, and 32 kDa phosphoproteins has been argued, particularly around the PS-point. In this study we examined effects of the protein kinase inhibitors and activators on the transition of Ax-2 cells from growth to differentiation. K252a, a potent inhibitor of protein kinases, inhibited growth possibly through the blockage of pinocytotic activity of cells, and promoted the progress of development after starvation when applied to Ax-2 cells at the growth phase. Such a K252a-effect was most pronouncedly exhibited on the cells located near the PS-point. Unexpectedly, however, the development of starved cells was found to be considerably delayed by staurosporine bearing a structural and functional resemblance to K252a when it was applied during the growth phase. Pulse-labelings of growing Ax-2 cells with inorganic ^{32}P (^{32}Pi) showed that K252a induces the disappearance of a 48 kDa phosphoprotein and the appearance of a 50 kDa phosphoprotein, specifically in the cells located around the PS-point. Phosphorylation of 32 kDa and 24 kDa proteins was also inhibited by K252a, but this inhibition was not necessarily specific to the K252a-treatment and occurred independently of the cell-cycle phases. The possible significance of these results is discussed in relation to a breakaway of cells from proliferation to differentiation at the PS-point.

INTRODUCTION

Cellular differentiation generally goes against growth, and the relationship between the two is a critical issue to be solved in developmental biology. In the life cycle of the cellular slime mold *Dictyostelium discoideum* axenic strain Ax-2, amoeboid cells grow and multiply by binary fission during the growth phase, as long as sufficient nutrients are supplied. This is followed by initiation of differentiation in response to nutritional deprivation to form multicellular structures that eventually develop to sorocarps consisting of a sorus (a mass of spores) and a supporting cellular stalk. Since the growth and differentiation phases are temporarily separated from each other and easily controlled by nutritional conditions, this organism is an excellent experimental system to analyze the mechanism of the transition from cell proliferation to differentiation at the cellular and molecular levels.

Ax-2 cells grow axenically with a doubling time of about 7.5 hr and have little or no G_1 phase [12, 21]. Commitment of Ax-2 cells to differentiation has been shown to occur depending upon the cell's position in the cell cycle at the onset of starvation [2, 6, 14, 16, 18, 22]. We have previously demonstrated using synchronized Ax-2 cells that cells progress through the cell cycle to a particular point (a putative shift point; PS-point) of mid-late G_2 phase, irrespective of the presence or absence of nutrients, and enter the differentiation phase from this point in response to nutritinal deprivation [14]. Thus the nutrient-responsive events occurring around the PS-point are of particularly importance for understanding the regulatory mechanisms of cell proliferation and differentiation. Recently, McPherson and Singleton [15] have reported a gene (V4) required for the transition from growth to differentiation in *D. discoideum* strain KAx-3; The V4 gene is expressed only during the growth phase, and the transformant into which the anti-sense RNA of the V4 gene was introduced shows normal growth but fails to express some differentiation-specific genes.

In general, it has been emphasized that phosphorylation and dephosphorylation of proteins play important roles in cell-cycle regulation and oncogenesis. For example, p105RB, the product of the retinoblastoma (RB) tumor suppressor gene, is maximally phosphorylated at the S phase of the cell cycle, while the RB protein is dephosphorylated at the G_0 and G_1 phases (reviewed in [4]). Dephosphorylation of the RB protein also occurs in cooperation with the induction of differentiation in several cell lines by phorbol ester- or retinoic acid-treatment [5]. Recently, we have proposed that in addition to dephosphorylation of a 32 kDa protein low phosphorylation levels of 101 kDa and 90 kDa proteins may be required for the transition of Ax-2 cells from growth to differentiation [1]. The experiments using the protein phosphatase inhibitors showed that the 101 kDa and 90 kDa proteins fail to be phosphorylated at the PS-point under the conditions of starvation [1]. On the other hand, Simon *et al.* [19] have found that intracellular 3′,5′-cyclic adenosine monophosphate (cAMP) facilitates early develop-

Accepted October 28, 1993
Received September 13, 1993
[1] To whom correspondence should be addressed.

ment of Ax-2 cells, probably by activating the cAMP-dependent protein kinase (PKA). In the light of these findings, we paid attention to the involvements of protein kinases in the transition process of growing Ax-2 cells to the differentiation phase. For this, we examined pharmacologically how growth and differentiation are controlled by protein kinases, using a variety of inhibitors and activators of kinase activities. The results obtained showed that K252a, a potent inhibitor of protein kinases, inhibits growth and facilitates development when applied to Ax-2 cells growing around the PS-point. The autoradiographical analysis of ^{32}P-labeled proteins also demonstrated that a 48 kDa (or 50 kDa) phosphoprotein is affected specifically by K252a. The possible significance of our findings is discussed, with special emphasis on the mechanism of choice between growth and differentiation.

MATERIALS AND METHODS

Chemicals

K252a, staurosporine, and herbimycin A were purchased from Kyowa Medex (Tokyo, Japan) and dissolved in dimethyl sulfone oxid (DMSO) at 1.0 mg/ml as the stock solutions. KT5720 and calphostin C purchased from Kyowa Medex were dissolved in DMSO at 4.0 mg/ml. 50 mM BAPTA/AM (Dojin Chem.) dissolved in DMSO was used as the stock solution. The stock solutions (200–720 mM) of W7 (N-(6-aminohexyl-5-chloro-1-naphthalene-sulfonamide; Sigma), 8-bromo 3′,5′-cyclic adenosine monophosphate (8Br-cAMP), and 8-bromo 3′,5′-cyclic guanosine monophosphate (8Br-cGMP) were prepared by dissolving them in ultra-pure water.

Growth conditions and synchronization of cell-cycle phase

Dictyostelium discoideum Ax-2 (clone 8A) was used in this study. Vegetative cells were grown axenically in HL-5 medium (Bacteriological peptone (Oxoid) 1.4 g, yeast extract (Oxoid) 0.7 g, $Na_2HPO_4 \cdot 12H_2O$ 0.13 g, KH_2PO_4 0.05 g in 100 ml of utra-pure water) supplimented with 1.5% glucose [20]. Usually 10 ml of the cell suspension was shaken at 22°C at 150 rpm in a 200 ml-Erlenmeyer flask coated with Sigmacote (Sigma) on a gyratory shaker. Good synchrony was attained by a slight modification of the temperature shift method [12]: Ax-2 cells ($1–2\times10^6$ cells/ml) growing exponentially at 22.0°C were shifted to 9.7°C, shaken for 14.0 hr at 150 rpm, and then shifted again to 22.0°C. Under this condition, cell doubling occurred over about a 2-hr period after a lag phase of about a 1 hr; the PS-point being located near 7 hr after the shift-up from 9.7°C to 22.0°C.

Application of protein kinase inhibitors and activators to growing and starving cells

Non-synchronized or synchronized Ax-2 cells growing in HL-5 medium were treated with various concentrations of the drugs described in *Chemicals*, followed by monitor of change in the cell number. In another experiment, non-synchronized or synchronized Ax-2 cells were harvested, washed once by centrifugation (2,500 rpm, 75 sec) in 20 mM Na/K-phosphate buffer, pH 6.2 (PB) and resuspended in 1.0–1.5 ml of PB containing various concentrations of the drugs at a density of 1×10^7 cells/ml. The cell suspension was shaken at 22°C at 150 rpm in a 20 ml-Erlenmeyer flask coated with Sigmacote. After various periods of shaking, the cells were collected by centrifugation, washed once in PB, and plated as droplets (10 μl) on non-nutrient agar (1.5% Agar Bacteriological, Oxoid) at 1×10^6 cells/cm^2. The preparations were incubated for various times at 22°C to allow development.

Pulse-labeling of cellular proteins with inorganic ^{32}P (^{32}Pi)

Non-synchronized or synchronized cell populations from various phases of the cell cycle (referred to as Tt cells), after the shift-up from 9.7°C to 22.0°C, were washed once in modified HL-5 (no addition of phosphate salts). The washed cells were suspended in 2 ml of modified HL-5 containing 0.3 mCi/ml of [^{32}P] ortho-phosphate (ICN, HCl-free) at a density of 2×10^6 cells/ml, and shaken for 3 hr at 22°C in a 20 ml-Erlenmeyer flask coated with Sigmacote.

SDS-PAGE and autoradiography

The ^{32}P-labeled cells (3.5×10^6 cells) were washed twice in ice-cold BSS (Bonner's standard salt solution; [3]) and dissolved in 90 μl of 10 mM Tris-HCl (pH 6.8) containing 2% SDS, 10 mM DTT, and 10% (V/V) glycerol, followed by heating in a boiling water-bath for 1 min. After cooling, 30 μl of the stock solution (0.5 M Tris-HCl, pH 7.0, 50 mM $MgCl_2$, 1 mg/ml DNase I (Sigma), 0.5 mg/ml RNase A (Sigma)) was added to the sample, as described previously [1]. The samples (10–15 μl) were loaded on SDS-polyacrylamide gel (10%) and electrophoresed according to Laemmli [10]. Electrophoresis was carried out at 25 mA constant current until the dye (BPB) reached the bottom of the gel. Proteins in the gels were visualized by staining with silver [17]. For autoradiography, the electrophoregrams were fixed, dried, and exposed to a X-ray film (Amersham Hyperfilm-MP) with an intensifying screen (Kodak) for about 24 hr at −80°C.

Assay for pinocytosis

FITC-dextran FD-70S (Sigma) was used as a fluid-phase marker, as described previously [13]. Two ml of cell suspension ($2–3\times10^6$ cells/ml) growing exponentially in HL-5 was shaken in a 20 ml-Erlenmeyer flask for 1 hr at 22°C with and without either K252a (10 μg/ml in 1% DMSO) or staurosporine (3 μg/ml in 0.3% DMSO), followed by the addition of FITC-dextran at a final concentration of 3 mg/ml. After 1 hr of shaking at 22°C, pinocytosis was stopped by diluting a 2 ml-sample with 8 ml of ice-cold 20 mM PIPES buffer, pH 6.8. Cells were collected by centrifugation for 2 min at 1,500 rpm, washed, and resuspended in 2 ml of buffer. After centrifugation through 10% (W/W) sucrose for 3 min at 2,500 rpm, the cell pellet was resuspended in 3 ml of 50 mM Na_2HPO_4. Cells were counted with a hematocytometer. Subsequently, cells were lysed by adding Triton X-100 (0.2% final concentration). The fluorescence intensity of the solution was measured with a fluorimeter (excitation wavelength, 470 nm; emission wavelength, 520 nm), and the amount pinocytosed was determined by comparison with a standard curve.

RESULTS

Effects of K252a and staurosporine on growth and pinocytotic activity

When K252a was applied to exponentially growing Ax-2 cells in HL-5, their growth was inhibited in a concentration-dependent manner, as shown in Fig. 1. In the presence of 5–15 μg/ml K252a, growth of Ax-2 cells was completely inhibited at least during the first 5 hr of shake culture after the addition of K252a. Growth was also inhibited by 1 μg/ml of

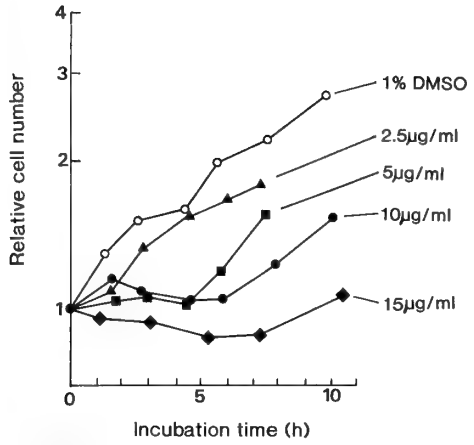

FIG. 1. Effect of K252a on growth of Ax-2 cells in axenic medium. Non-synchronized Ax-2 cells at the exponential growth phase were shaken in axenic growth medium (HL-5) containing the designated concentrations of K252a. Since 1% DMSO is contained in the test solution of 10 μg/ml K252a, 1% DMSO (final conc.) was added to HL-5 as a control. In the presence of 15 μg/ml K252a, cell proliferation is completely inhibited. A representative pattern of growth inhibition by K252a from one in three experiments is shown.

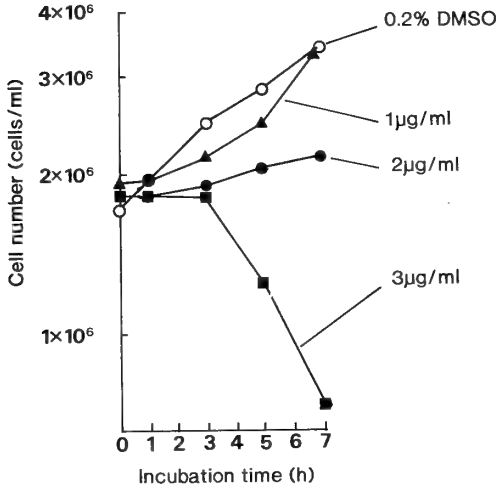

FIG. 2. Effect of staurosporine on growth of Ax-2 cells in axenic medium. Non-synchronized Ax-2 cells were shaken in HL-5 containing the designated concentrations of staurosporine. Since 0.2% DMSO is contained in the test solution of 2 μg/ml staurosporine, 0.2% DMSO (final conc.) was added to HL-5 as a control. Cell proliferation is almost completely inhibited by 1–3 μg/ml staurosporine at least during the first 3 hr after the drug application. A representative pattern of growth inhibition by staurosporine from one in three experiments is shown.

staurosporine during the first 3 hr of shake culture after its application, and almost completely in the presence of 2 μg/ml (Fig. 2). A higher concentration (3 μg/ml) of staurosporine was toxic to the cells, thus resulting in a drastic decrease in cell number after 3 hr of shake culture. As shown in Fig. 1 and 2, growth of non-synchronized Ax-2 cells stopped immediately after the addition of K252a (5–15 μg/ml) or staurosporine (1–3 μg/ml). This seems to indicate that the progression of cell-cycle phases is blocked by these drugs at the time-point of application.

Cellular drinking behavior (pinocytosis) is believed to be a characteristic property of many cells constituting a mechanism of nutrient uptake, and the pinocytotic activity of Ax-2 cells is high during the growth phase [11]. To light on the reason why K252a and staurosporine inhibited growth of Ax-2 cells, we examined their effects on pinocytotic activity using FITC-dextran as a fluid-phase marker. The results showed that pinocytotic activity is reduced by K252a or staurosporine in a concentration-dependent manner and is almost completely inhibited by 5–10 μg/ml K252a or 1–3 μg/ml staurosporine (Fig. 3). Thus it is most likely that growth inhibition by these drugs might be due to the failure of Ax-2 cells to pinocytose extracellular nutrients. Interestingly, however, the protein phosphatase inhibitors such as okadaic acid and calyculin A, which are known to inhibit completely growth of Ax-2 cells [1], scarcely inhibited the pinocytotic activity (data not shown).

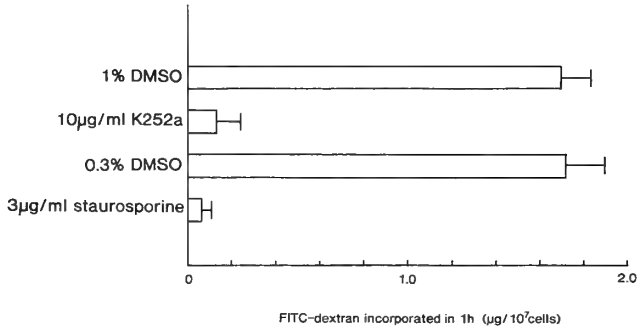

FIG. 3. Inhibition of the pinocytotic activity of Ax-2 cells by K252a or staurosporine. Pinocytotic activities were measured as described in Materials and Methods. 1% DMSO and 0.3% DMSO were used as controls of 10 μg/ml K252a- and 3 μg/ml staurosporine-treatments, respectively. Error bars represent standard deviations of three independent experiments.

Opposing effects of K252a and staurosporine on development

When Ax-2 cells at the growth phase were treated with 5 μg/ml of K252a containing 0.5% DMSO for 3 hr, during which their growth was completely inhibited, washed free of the drug by repeated centrifugations in PB, and then allowed to develop on non-nutrient agar, the starved cells exhibited about 2–3 hr faster development as compared with a control containing 0.5% DMSO but not K252a (Fig. 4). In contrast to K252a, staurosporine (1.5 μg/ml) containing 0.15% DMSO caused delayed development of starved Ax-2 cells as compared with a control containing 0.15% DMSO but not staurosporine, when it was beforehand applied to growth-phase cells (Fig. 5). Although DMSO-treatment of Ax-2 cells at the growth phase caused somewhat delayed development by about 30 min as compared with another control without DMSO, 5 μg/ml K252a (or 1.5 μg/ml staurosporine) always elicited faster (or slower) development as compared with the control when the treated cells were starved.

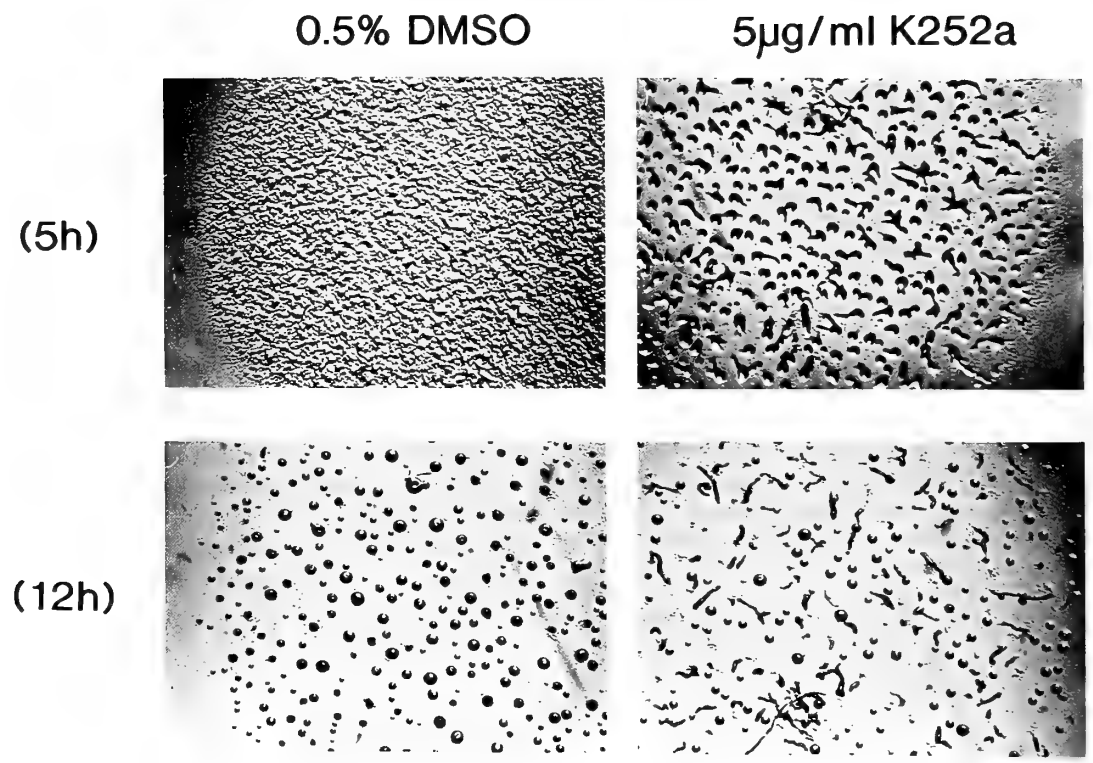

FIG. 4. K252a promotes the development of starved Ax-2 cells, if it was beforehand applied to growth-phase cells. Ax-2 cells at the exponential growth phase were treated with 5 μg/ml K252a for 3 hr, washed, and then were allowed to develop on agar for the designated periods after starvation. As a control, cells were treated with 0.5% DMSO. The process of development including cell aggregation advances more rapidly in K252a-treated cells than in non-treated ones. A representative result from one in three experiments is shown.

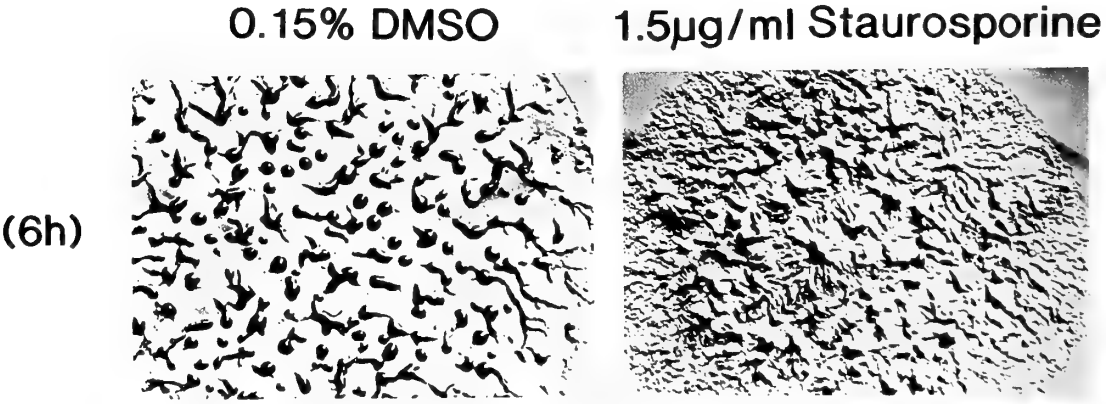

FIG. 5. Staurosporine inhibits the development of starved Ax-2 cells, if it was beforehand applied to growth-phase cells. Ax-2 cells at the exponential growth phase were treated with 1.5 μg/ml staurosporine for 3 hr, washed, and then were allowed to develop on agar for 6 hr. The cells treated with 0.15% DMSO were used as a control. Development is considerably delayed by the staurosporine-treatment. A representative result from one in three experiments is shown.

The opposing effects of K252a and staurosporine on growing Ax-2 cells were found to be completely reversed if the drugs were applied to starving Ax-2 cells; t_0 cells (cells just after starvation) treated with 10 μg/ml of K252a for 3 hr exhibited delayed development by about 1.5 hr as compared with a control. Meanwhile, $t_{0.5-3.0}$ cells (cells 0.5–3.0 hr after starvation) treated with 0.6 μg/ml of staurosporine exhibited faster development (Fig. 6). Incidentally, the application of staurosporine to t_0 cells had an inhibitory effect on their development, as the case for K252a (data not shown). Taken in conjunction, the effects of K252a and staurosporine on growing or starving Ax-2 cells are schematically shown in Fig. 7.

Cell-cycle dependency of K252a-effect

To examine whether or not the development-promotive

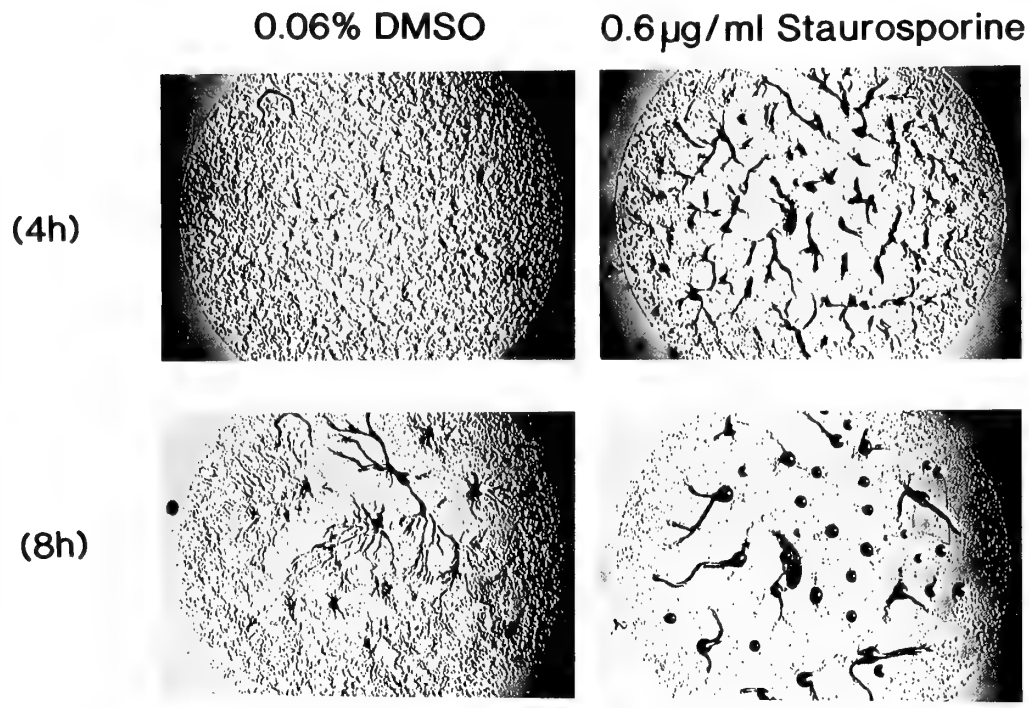

FIG. 6. Promotive effect of staurosporine on the development of starving cells. Ax-2 cells ($t_{2.5}$-cells) 2.5 hr after starvation were treated with 0.6 μg/ml staurosporine or 0.06% DMSO (as a control) for 2.5 hr, followed by washing and incubating on agar for the designated periods at 22.0°C. Cellular development is considerably promoted by the staurosporine-treatment. A representative result from one in three experiments is shown.

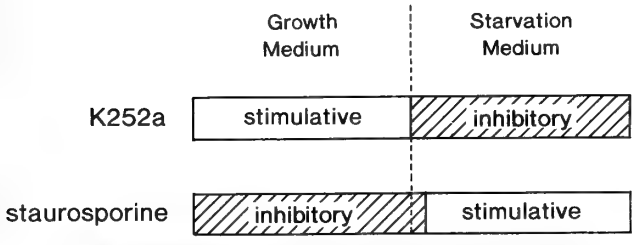

FIG. 7. A schematic diagram showing the opposing effects of K252a and staurosporine on growing and starving Ax-2 cells. Applications of K252a and staurosporine to cells either in growth medium or in starvation medium gave the contrasted effects on the development of starved cells, as indicated. See the text for details.

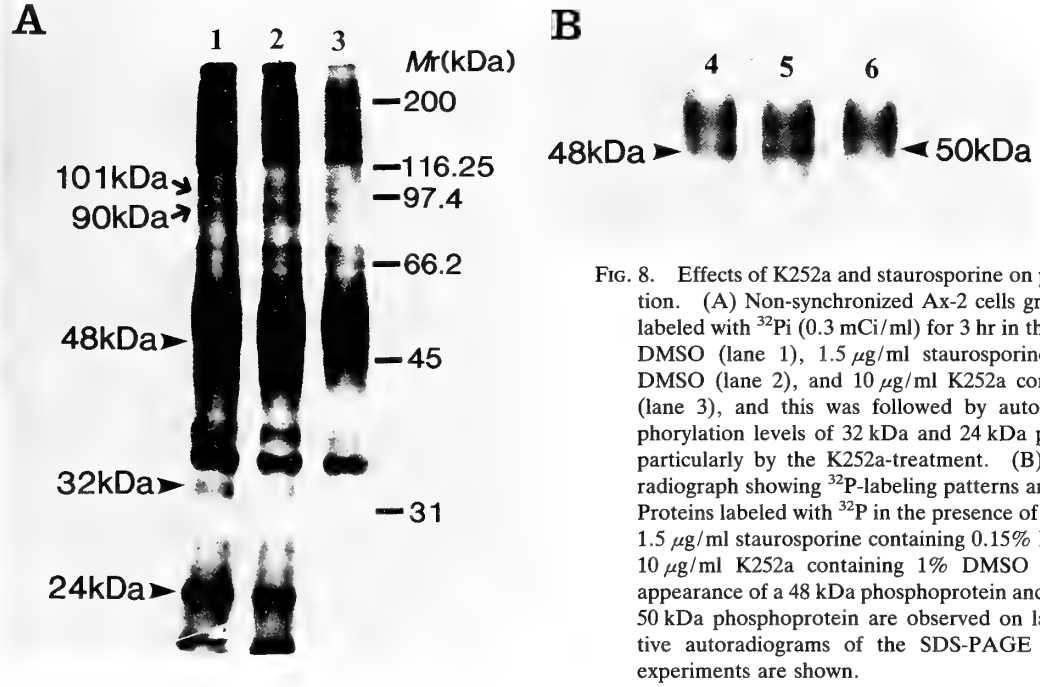

FIG. 8. Effects of K252a and staurosporine on protein phosphorylation. (A) Non-synchronized Ax-2 cells growing in HL-5 were labeled with ^{32}Pi (0.3 mCi/ml) for 3 hr in the presence of 0.15% DMSO (lane 1), 1.5 μg/ml staurosporine containing 0.15% DMSO (lane 2), and 10 μg/ml K252a containing 1% DMSO (lane 3), and this was followed by autoradiography. Phosphorylation levels of 32 kDa and 24 kDa proteins are reduced particularly by the K252a-treatment. (B) An enlarged autoradiograph showing ^{32}P-labeling patterns around Mr of 50 kDa. Proteins labeled with ^{32}P in the presence of 1% DMSO (lane 4), 1.5 μg/ml staurosporine containing 0.15% DMSO (lane 5), and 10 μg/ml K252a containing 1% DMSO (lane 6). The disappearance of a 48 kDa phosphoprotein and the appearance of a 50 kDa phosphoprotein are observed on lane 6. Representative autoradiograms of the SDS-PAGE from one in three experiments are shown.

effect of K252a on growth-phase cells is manifested in a cell-cycle dependent manner, K252a was applied to synchronized cells from various phases of the cell cycle (referred to as Tt cells), after the temperature shift from 9.7°C to 22.0°C. K252a promoted markedly cellular development, particularly when applied to the cells at T6.5 (just before the PS-point). Application of K252a to T0.5-cells (just after the PS-point) caused less promotion of subsequent development after starvation. Therefore, it seems likely that the K252a-sensitive phase of the cell cycle may be located just before the PS-point.

Analysis of signal transducers affected by K252a

It is of interest to know which pathways of signal transduction are inhibited by K252a in growth-phase cells. For this, we applied specific inhibitors or activators as presented in Table 1 to Ax-2 cells growing in HL-5, followed by monitoring their effects on development as well as on growth. As summarized in Table 1, W7, the calmodulin inhibitor, blocked completely growth at a concentration of 30 μM, but the W7-treated cells exhibited normal development when they were starved by washings and allowed to develop on agar. Although 8Br-cAMP and 8Br-cGMP also inhibited growth at a extremely high concentration (40 mM), the development of the drug-treated cells after starvation was normal, as the case for W7-treatment. Other inhibitors including KT5720 (the specific inhibitor of PKA) had no effects on growth and development, when separately applied within a range of concentrations indicated in Table 1.

Phosphoproteins affected specifically by K252a

To find out proteins whose phosphorylation is inhibited specifically by K252a, non-synchronized Ax-2 cells were labeled with $^{32}P_i$ for 3 hr of shake culture in HL-5 with or without 10 μg/ml K252a, followed by autoradiography. As a reference, another ^{32}P-labeling experiment was carried out in the presence of 1.5 μg/ml staurosporine, because it delayed the progression of development in contrast to K252a when applied to growth-phase cells, as previously described. From comparison of the ^{32}P-labeling patterns, K252a was found to induce the disappearance of a 48 kDa phosphoprotein and the appearance of a 50 kDa phosphoprotein. K252a also inhibited markedly phosphorylation of 32 kDa and 24 kDa proteins, though it reduced the total amount of ^{32}P-labeled proteins (Fig. 8). Phosphorylation of 32 kDa and 24 kDa proteins, however, was found to be moderately inhibited by staurosporine, thus indicating that the inhibition is not necessarily specific to K252a. In contrast, the change of a 48 kDa (or 50 kDa) phosphoprotein seemed to be a specific event induced by K252a (Fig. 8B). Considering from our previous findings [1], we expected that phosphorylation of 101 kDa and 90 kDa proteins would be reduced by K252a, but such reduction was not detected. Based on the development-promoting effect of K252a particularly on Ax-2

Table 1. Effects of various inhibitors and activators of protein kinases on growth and development of *Dictyostelium discoideum* cells

Drugs	Possible functions	Effects on	
		Growth	Development
K252a	inhibitor of protein kinases	I (5 μg/ml)	A (5 μg/ml)
Staurosporine	inhibitor of protein kinases	I (1.5 μg/ml)	I (0.75 ag/ml)
KT5720	specific inhibitor of PKA	N (5–17.5 μg/ml)	N (5–17.5 μg/ml)
Calphostin C	specific inhibitor of PKC	N (1–40 μg/ml)	N (1–10 μg/ml)
Herbimycin A	specific inhibitor of tyrosine kinase	N (1–40 μg/ml)	N (1–10 μg/ml)
W7	inhibitor of calmodulin	I (30 μM)	N (40–70 μM)
BAPTA/AM	Ca^{2+}-chelator	N (10–500 μM)	
8Br-cAMP	membrane-permeable cAMP analogue	I (40 mM)	N (10–50 mM)
8Br-cGMP	membrane-permeable cGMP analogue	I (40 mM)	N (10–40 mM)

Non-synchronized Ax-2 cells growing in HL-5 were treated with the indicated drugs for 3–5 hr at 22.0°C, washed for starvation, and allowed to develop on non-nutrient agar. Effects of the drugs used are summarized as follows: A, promotion; I, inhibition; N, no effect. The value in the parenthesis indicates the optimum concentration of the drug for the case of A or I. In the case of N, the concentration-range examined is shown.

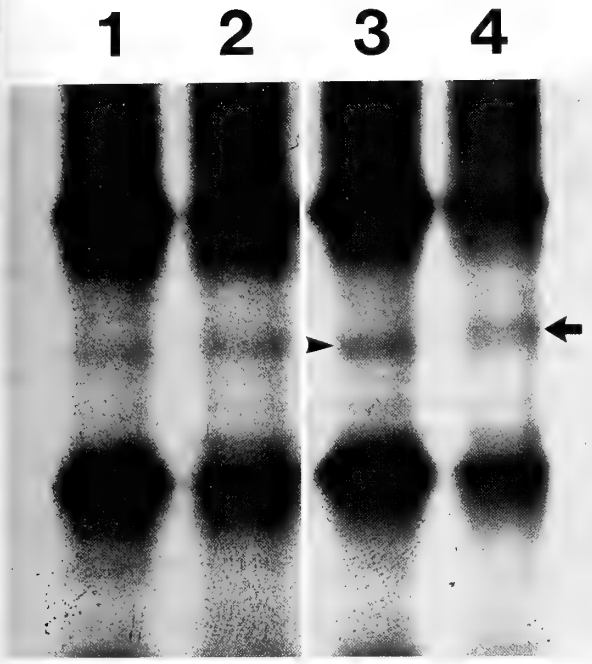

FIG. 9. Induction of the disappearance of a 48 kDa phosphoprotein and the appearance of a 50 kDa phosphoprotein by K252a in a cell-cycle dependent manner. Synchronized T0.5- and T6.5-cells were labeled with ^{32}Pi (0.3 mCi/ml) for 3 hr in the presence of 1% DMSO (lane 1, T0.5-cells; lane 3, T6.5-cells) or 10 ug/ml K252a containing 1% DMSO (lane 2, T0.5-cells; lane 4, T6.5-cells), and this was followed by autoradiography. The change of a 48 kDa (arrowhead) or a 50 kDa (arrow) phosphoprotein seems to occur only in the K252a-treated T6.5-cells (lane 4). A representative autoradiogram of the SDS-PAGE from one in three experiments is shown.

cells growing around the PS-point, we examined effects of K252a on the phosphorylation patterns of proteins in synchronized cells. As a result, the disappearance of a 48 kDa phosphoprotein and the appearance of a 50 kDa phosphoprotein were found to occur in K252a-treated cells (T6.5-cells) just before the PS-point, but not in cells (T0.5-cells) just after the PS-point (Fig. 9). Incidentally, phosphorylation of the 32 kDa and 24 kDa proteins was inhibited by K252a, independently of the cell-cycle phases.

DISCUSSION

The present work was undertaken to examine the involvement of protein kinases in the transition of *D. discoideum* Ax-2 cells from growth to differentiation, using several inhibitors and activators of protein kinases. K252a, a potent inhibitor of protein kinases, promoted the progression of development, particularly when it was beforehand applied to Ax-2 cells growing just before the PS-point of the cell cycle. Unexpectedly, however, staurosporine that is believed to be similar in structure and function to K252a was found to delay the development of starved cells, thus being in striking contrast to K252a. In this connection, it is of interest to note that the sexual process (zygote formation) of *D. mucoroides-7* cells is promoted by K252a and inhibited by staurosporine [9]. Since K252a (or staurosporine) exerts an opposing effect on cellular development when applied under either the growth or starvation condition (Fig. 7), it is most likely that some of protein kinases are working differently depending upon the nutritional status of cells.

To specify the nature of kinase activities inhibited by K252a, we applied several specific inhibitors and activators of protein kinases, Ca^{2+}-chelater (BAPTA/AM), or calmodulin inhibitor (W7) to Ax-2 cells growing in HL-5, and this was followed by monitoring their subsequent development after starvation. Neither of them, however, had effects on the development of starved cells when they were separately applied to growth-phase cells (Table 1). Here, it is of interest to note that a combined application of KT5720 (a specific inhibitor of PKA) and W7 promotes the sexual development of *D. mucoroides-7* cells, as K252a does it, thus suggesting the involvements of PKA and calmodulin in zygote formation [9].

As presented here, phosphorylation of the 32 kDa and 24 kDa proteins was greatly inhibited by K252a. The 32 kDa protein has been previously shown to be perfectly dephosphorylated by serine/threonine-specific protein phosphatases in response to nutritional deprivation [1]. The low phosphorylation level of the 32 kDa protein in the presence of K252a might relate to the fact that K252a-treatment inhibits almost completely nutrient uptakes by pinocytosis, thus having Ax-2 cells starved. Dephosphorylation of the 24 kDa protein, however, was not induced by starvation in normal development. Recently, Hinze *et al.* [7] have shown by immunological analysis that a *Dictyostelium* protein of 32 kDa (p32) is equivalent to the cdc2 and/or cdk2 products of *Schizosaccharomyces pombe,* which contain the EGVP-STAIREISLLKE (PST) domain and bind $p13^{suc1}$-agarose beads, a characteristic property of cdc2/cdk2-encoded protein kinases. It is of interest to know if the p32 is the same as the 32 kDa phosphoprotein reported by us.

We expected that phosphorylation of the 101 kDa and 90 kDa proteins would be inhibited by K252a, since their low phosphorylation levels might be associated with the entry of Ax-2 cells into differentiation from the PS-point. However, the phosphorylation level was not affected by K252a in the presence of rich nutrients around cells, suggesting that the 101 kDa and 90 kDa proteins might fail to be phosphorylated only after cells were starved around the PS-point. Interestingly, the disappearance of the 48 kDa phosphoprotein and the appearance of the 50 kDa phosphoprotein seemed to be specifically induced by K252a that promoted the progression of development, particularly around the PS-point. With respect to this phenomenon, one can imagine two possibilities; 1) a 48 kDa phosphoprotein exerts a phase-shift to 50 kDa, or 2) the disappearance of a 48 kDa phosphoprotein coincides with the appearance of another phosphoprotein of 50 kDa. Although it is presently unknown which is the case and remains to be elucidated, the observed change might be favorable to the transition of cells from growth to differentia-

tion at the PS-point. Hinze *et al.* [7] have reported that a *Dictyostelium* protein of 49 kDa (p49) is recognized by one of the PST antibodies, but not absorbed by $p13^{suc1}$-agarose, suggesting its partial resembrance to $p34^{cdc2}$ in the PST domain. Based on the M_r and character, the p49 could be the same as the 48 kDa (or 50 kDa) phosphoprotein. We are now planning to isolate the gene encoding the 48 kDa or 50 kDa phosphoprotein to determine the chemical structure and also to analyze its function in cellular development.

ACKNOWLEDGMENTS

We wish to thank Dr. T. Takagi for his technical help with the phosphoamino acid analysis, Mr. S. Sato for assistance with the measurement of pinocytotic activity, and Mr. N. Iijima for his help with the autoradiographical analysis. This work was supported by a Grant-in-Aid (no. 04454018) from the Ministry of Education, Science and Culture of Japan.

REFERENCES

1 Akiyama M, Maeda Y (1992) Possible involvements of 101 kDa, 90 kDa, and 32 kDa phosphoproteins in the phase-shift of *Dictyostelium* cells from growth to differentiation. Differentiation 51: 79–90

2 Araki T, Nakao H, Takeuchi I, Maeda Y (1994) Cell-cycle dependent sorting in the development of *Dictyostelium* cells. Dev Biol 162 (in press)

3 Bonner JT (1947) Evidence for the formation of cell aggregates by chemotaxis in the development of the cellular slime mold *Dictyostelium discoideum*. J Exp Zool 106: 1–26

4 Buchkovich K, Duffy LA, Harlow ED (1989) The retinoblastoma protein is phosphorylated during specific phases of the cell cycle. Cell 58: 1097–1105

5 Chen P-L, Scully P, Shew J-Y, Wang JYJ, Lee W-H (1989) Phosphorylation of the retinoblastoma gene product is modulated during the cell cycle and cellular differentiation. Cell 58: 1193–1198

6 Gomer RH, Firtel RA (1987) Cell-autonomous determination of cell-type choice in *Dictyostelium* development by cell-cycle phase. Science 237: 758–762

7 Hinze E, Michaelis C, Daya-Makin M, Pelech S, Weeks G (1992) Immunological characterization of cdc2 and wee1 proteins during the growth and differentiation of *Dictyostelium discoideum*. Develop Growth & Differ 34: 363–369

8 Hunter T, Sefton BM (1980) Transforming gene product of Rous sarcoma virus phosphorylates tyrosine. Proc Natl Acad Sci USA 77: 1311–1315

9 Kawai S, Maeda Y, Amagai A (1993) Promotion of zygote formation by protein kinase inhibitors during the sexual development of *Dictyostelium mucoroides*. Devel Growth & Differ 35: 601–607

10 Laemmli UK (1970) Cleavage of structural proteins during the assembly of the head of bacteriophage T4. Nature 227: 680–685

11 Maeda Y (1983) Axenic growth of *Dictyostelium discoideum* wild-type NC-4 cells and its relation to endocytotic ability. J Gen Microbiol 129: 2467–2473

12 Maeda Y (1986) A new method for inducing synchronous growth of *Dictyostelium discoideum* cells using temperature shifts. J Gen Microbiol 132: 1189–1196

13 Maeda Y, Kawamoto T (1986) Pinocytosis in *Dictyostelium discoideum* cells: A possible implication of cytoskeletal actin for pinocytotic activity. Exp Cell Res 164: 516–526

14 Maeda Y, Ohmori T, Abe T, Abe F, Amagai A (1989) Transition of starving *Dictyostelium* cells to differentiation phase at a particular position of the cell cycle. Differentiation 41: 169–175

15 McPherson CE, Singleton CK (1992) V4, a gene required for the transition from growth to differentiation in *Dictyostelium discoideum*. Development 150: 231–242

16 Ohmori T, Maeda Y (1987) The developmental fate of *Dictyostelium discoideum* cells depends greatly on the cell-cycle position at the onset of starvation. Cell Differentiation 22: 11–18

17 Poehling H-M, Neuhoff V (1981) Visualization of proteins with a silver "stain": a critical analysis. Electrophoresis 2: 11–18

18 Sharpe PT, Watts DJ (1985) The role of the cell cycle in differentiation of the cellular slime mould *Dictyostelium discoideum*. Mol Cell Biochem 67: 3–9

19 Simon M-N, Driscoll D, Mutzel R, Part D, Williams J, Veron M (1989) Overproduction of the regulatory subunit of the cAMP-dependent protein kinase blocks the differentiation of *Dictyostelium discoideum*. EMBO J 8: 2039–2043

20 Watts DJ, Ashworth JM (1970) Growth of myxamoebae of the cellular slime mold *Dictyostelium discoideum* in axenic culture. Biochem J 119: 171–174

21 Weijer CJ, Duschl G, David CN (1984a) A revision of the *Dictyostelium discoideum* cell cycle. J Cell Sci 70: 111–131

22 Weijer CJ, Duschl G, David CN (1984b) Dependence of cell type proportioning and sorting on cell cycle phase in *Dictyostelium discoideum*. J Cell Sci 70: 133–145

ZOOLOGICAL SCIENCE 11: 77–82 (1994)

Regional Differences in Granulosa Cells of Preovulatory Medaka Follicles

TAKASHI IWAMATSU[1]*, SEIKO NAKASHIMA[1], KAZUO ONITAKE[2], ARITO MATSUHISA[1] and YOSHITAKA NAGAHAMA[3]

[1]*Department of Biology, Aichi University of Education, Kariya 448,* [2]*Department of Biology, Faculty of Science, Yamagata University, Yamagata 990, and Reproductive Laboratory, National Institute for Basic Biology, Okazaki 444, Japan*

ABSTRACT—The regional differences in morphology and steroid production of granulosa cells of the animal and vegetal hemispheres of the preovulatory medaka (*Oryzias latipes*) follicles were investigated. Granulosa cells in the animal pole region were distinguishable from those in the vegetal pole region in their shape and distribution. The distribution of tall granulosa cells was more compact in the vegetal pole area than in the remaining areas. The gonadotropin-induced production of 17α,20β-dihydroxy-4-pregnen-3-one by granulosa cells alone was at a level sufficient to induce *in vitro* maturation of the oocyte. Production was significantly greater in the vegetal hemisphere than in the animal hemisphere. These results indicate that medaka follicles have morphological and physiological differences in granulosa cells corresponding to regional differences along the animal-vegetal axis of the oocyte.

INTRODUCTION

Eggs of oviparous fishes generally have distinct polarity. The polarity reflects the functional organization of the cellular constituents necessary for development. It must be determined by the interaction of the oocyte with follicle cells, especially the granulosa cells that are in contact with the oocyte during oogenesis. Accessory structures such as attaching filaments, which are located at the animal or the vegetal pole side of the egg membrane (chorion) have been found in a great number of teleost fishes (cf. [14]). In medaka oocytes, the difference in the distribution of accessory filaments on the chorion is detectable in the early stages of oogenesis [5]. The differences in their morphology and distribution seem to be established by the interaction with granulosa cells.

In some teleosts, one of the maturation-inducing steroids (MIS: [11, 16]), 17α,20β-dihydroxy-4-pregnen-3-one (17α, 20β-diOHp: cf. [13]) is produced and secreted by follicle cells in the presence of gonadotropin. The maturation of medaka oocytes *in vitro* is also induced by the same steroid, which is produced by granulosa cells [6, 8–10, 15]. It is generally believed that whole surface of the oocyte is simultaneously evenly stimulated by MIS from the granulosa cells. However, there is no evidence that this is true.

In the medaka MIS is produced by granulosa cells with probably little or no participation of the thecal cells. Therefore, the spatial and functional differences in granulosa cells may be very important for the establishment of oocyte polarity and oocyte maturation in this fish. For this season, we are interested in the regional differences in steroidogenesis, particularly MIS production, and cytological characteristics of granulosa cells surrounding the oocyte before maturation. At present there is little information on the differences in the distribution between the animal and vegetal hemispheres and the structure of granulosa cells surrounding fully-grown oocytes.

We investigated the local differences in the structure and function of granulosa cells of the medaka follicle. The results indicated that granulosa cells had regional differences in morphology and steroid production along the animal-vegetal axis of the fully-grown oocyte.

MATERIALS AND METHODS

Follicle preparation

Preovulatory medaka follicles were isolated from the ovaries of mature females which had spawned every day under the light- and temperature-conditions controlled to induce reproduction. The follicles were removed from the ovaries by using fine forceps under a binocular dissecting microscope (×20). The follicles were handled in saline [3]. Fine watchmaker's forceps were then used to peel the thecal cell layer and the basement membrane off from follicles starting at the vegetal pole area (VPA) identified by the long attaching filaments [4]. These oocytes surrounded by a granulosa cell layer alone were cut precisely with small scissors into two halves, the animal and the vegetal hemispheres. The ooplasm was removed from the hemispherical chorion within the granulosa cell layer by washing the specimens in saline with a small pipette. Thus, preparations consisted of granulosa cell layers on the chorion hemispheres.

Follicle incubation

Ten of the animal or vegetal hemispheres prepared above were placed separately in 1 ml of culture medium (Earle's Medium 199, Dainippon-seiyaku, Osaka) in each well of a 24-well culture dish (Cell Wells: Corning, N.Y.) and incubated for 24 hr at 27°C.

Observations by fluorescence and electron microscopy

Immediately after removal of the thecal cell layer and the basement membrane, oocytes surrounded by a granulosa cell layer

Accepted December 14, 1993
Received October 20, 1993
* To whom reprint requests should be addressed.

alone were pre-fixed in 4% glutaraldehyde, rinsed in 0.1 M phosphate buffer (pH 7.4) and post-fixed in osmium tetroxide at 4°C for 2 hr. These samples were washed in 0.01 M phosphate buffer (pH 7.4), dehydrated in a graded series of acetone, dried according to the critical point method with CO_2 and coated with gold. They were observed with a JEOL scanning electron microscope (SEM).

For transmission electron microscopy (TEM), the similarly fixed samples were dehydrated in ethanol followed by propylene oxide and embedded in Epon 812. Ultrathin-sections were observed after staining with lead citrate and uranyl acetate.

Measurement of steroids

Animal and vegetal hemispheres prepared above were incubated in the presence of 100 IU pregnant mare serum gonadotropin (PMSG) or 100 ng/ml progesterone for 24 hr at 27°C. One milliliter of culture medium from each well was then collected and assayed to compare the production of 17α,20β-diOHp and estradiol-17β (E_2) by granulosa cells of the two hemispheres. 17α,20β-DiOHp and E_2 were measured in the samples of culture medium using radioimmunoassay (RIA) as described in a previous report [9, 10]. The sensitivity of each assay was 30 pg/ml.

All experiments were performed in triplicate and the data were analysed by statistical comparison (the Student's *t*-test) with control values.

RESULTS

1 Morphology of granulosa cells

As shown in the TEM images (Figs. 1 and 2), granulosa cells on the chorion of preovulatory oocytes differed in shape and number between the animal and vegetal hemispheres. Short cylindrical granulosa cells (diameter ca. 8 μm, height 13 μm) were aligned in a monolayer on the chorion (Fig. 1), except in the vegetal pole area(Fig. 2) (VPA, diameter ca. 430 μm, [5]). The nucleus was located centrally in these short cylindrical cells. The cells contained well developed

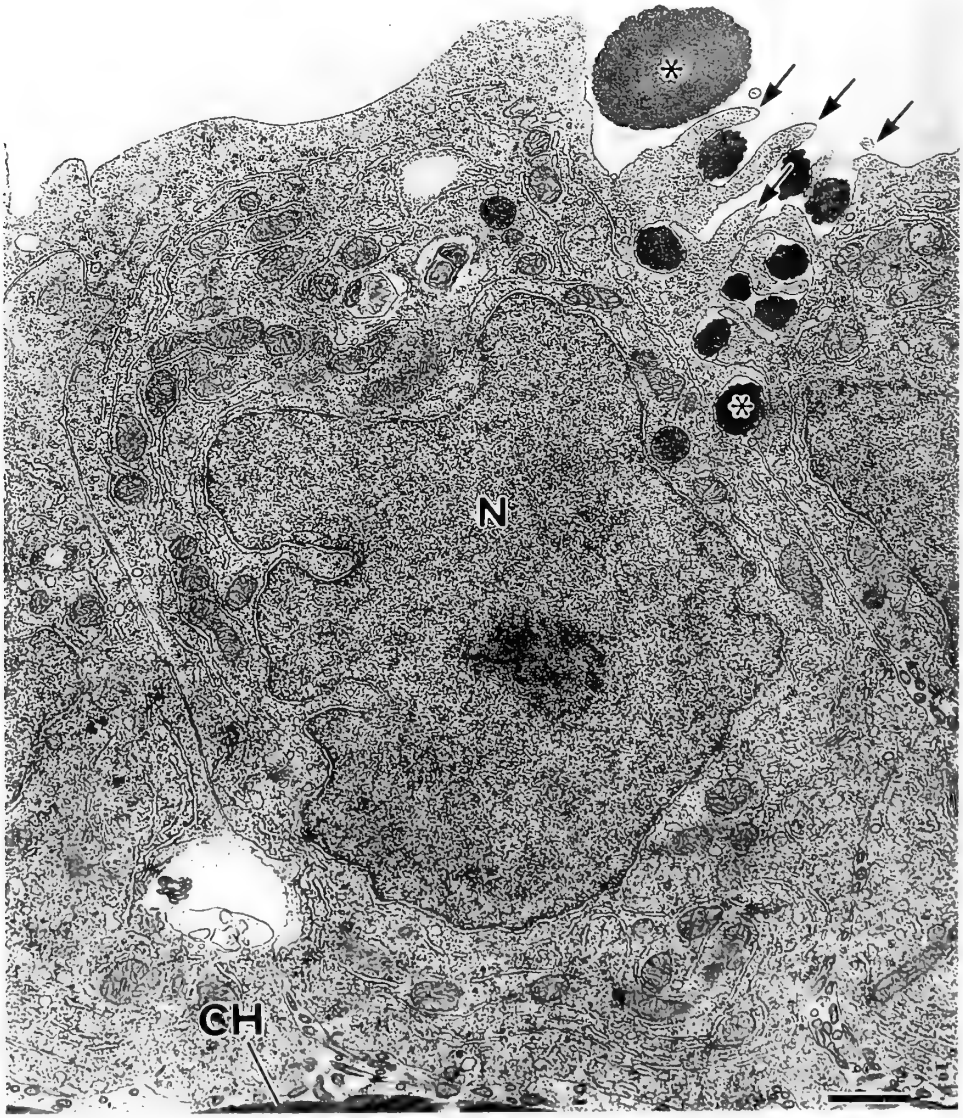

FIG. 1. Granulosa cells in the animal hemisphere of the preovulatory medaka follicle. The granulosa cell contains many mitochondria, rough endoplasmic reticula and Golgi apparatus in the cytoplasm. Note microvilli (arrows) without these organelles at the apical surface of the cell. Asterisks, non-attaching filaments; CH, chorion; N, nucleus. (bar 1 μm)

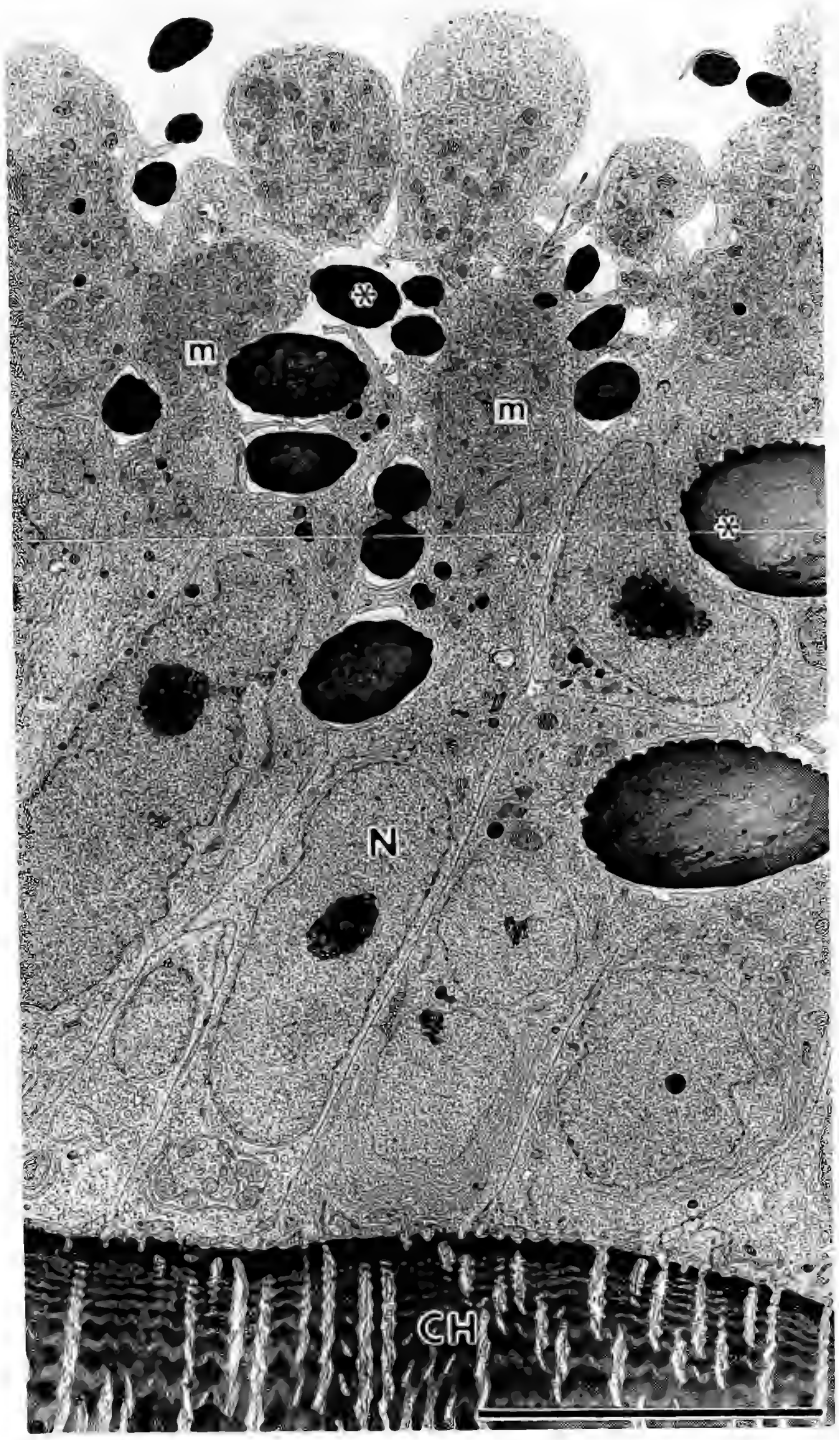

FIG. 2. Granulosa cells in the vegetal pole area of the preovulatory medaka follicle. Tall granulosa cells contain a mitochondrial mass (m), dilated endoplasmic reticula (vesicles), and developed Golgi lammellae in the apical region of the cell. Note the breb-like apices of the granulosa cells which contain many cytoplasmic inclusions. Asterisks, attaching filaments; CH, chorion; N, nucleus. (bar 10 μm)

rough endoplasmic reticula (ER), some of which were dilated, mitochondria with an electrondense matrix, Golgi complexes with very small vesicles, and large lysosomal vesicles. The granulosa cells in the VPA were slimmer and taller (diameter ca. 5 μm, height ca. 37 μm) than those in the animal hemisphere. The nucleus was basally located near the chorion, and the conspicuously crowded mitochondria were in the apical region. Other cell organelles in these tall cells were similar to those contained in the short cylindrical cells.

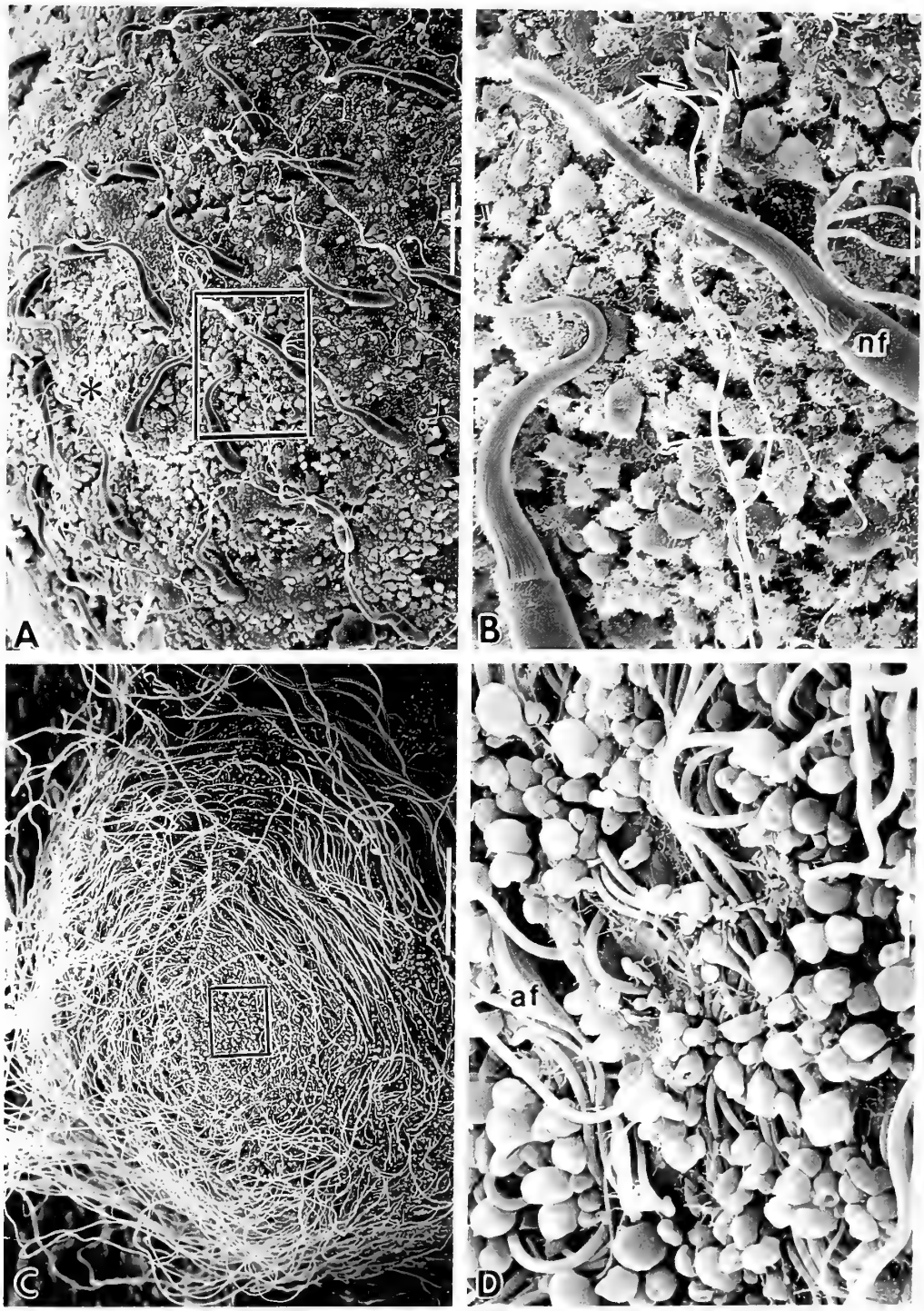

FIG. 3. Scanning electron micrographs of the surface of the granulosa cell layer in the animal and vegetal hemispheres. A, B: In the animal pole region (asterisk)(A; bar 50 μm), granulosa cells interact with each other by thread-like microvilli (B; bar 10 μm). nf, Non-attaching filaments; arrows, flat granulosa cells. C, D: In the vegetal pole region (asterisk) (C; bar 100 μm), which is encircled by the long distal portions of attaching filaments (af), the breb-like tips of the granulosa cells exhibit smooth surfaces (D; bar 10 μm) except for a few special cells with long microvilli.

The animal pole of the oocyte could be easily recognized by its position opposite the location of the attaching filaments on the chorion and by the bending direction of the non-attaching filaments (Fig. 3A). Granulosa cells at the animal pole region had many microvilli on the cell surface (Figs. 1 and 3B). The apical surface of these irregular-shaped granulosa cells was flat and smooth, as previously reported for the intact follicle [6, 7]. These flat granulosa cells were adherent to each other. The surface of the granulosa cells in the VPA is shown in Figs. 3C and D. In the VPA, tall granulosa cells

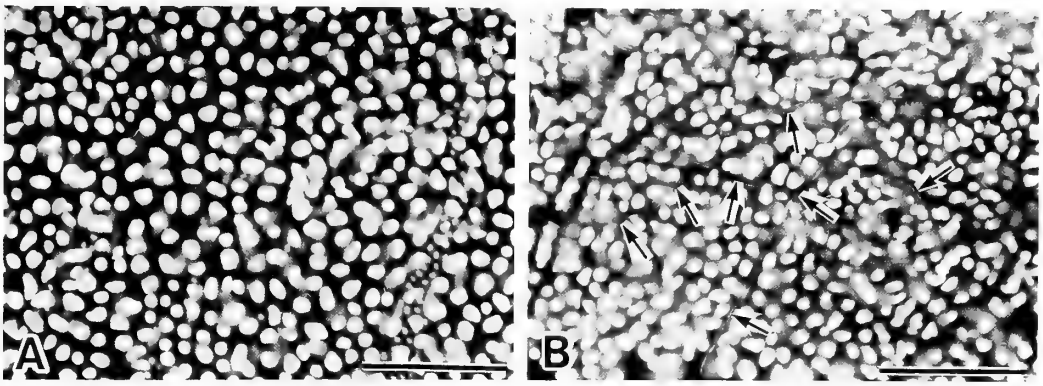

FIG. 4. Distribution of the nuclei of granulosa cells in the preovulataory follicle. After fixation with glutaraldehyde, the follicle was stained with 10 μg/ml Hoechst for 30 min (bar 100 μm). A: The animal hemisphere showing the nuclei of granulosa cells. B: The vegetal pole region showing the nuclei of granulosa cells and attaching filaments (arrows). Bars, 100 μm.

TABLE 1. Difference in steroid production by the animal and the vegetal hemispheres of medaka follicles

Group	Estradiol-17β (pg/ml)		17α,20β-Dihydroxyprogesterone (pg/ml)	
	AH	VH	AH	VH
PMSG (100IU/ml)	666±57	745±70	405±54	615±29*
Progesterone (100ng/ml)	723±52	868±112	667±32	720±110
Control (no hormone)	200±28	300±49	6±4	31±29

* Significant difference ($P<0.05$) between the animal (AH) and vegetal (VH) hemispheres. In each group, values represent mean±S.E. of three incubations.

were compactly distributed, although it was difficult to precisely determine their size and shape by SEM.

The apical portions of the tall granulosa cells were lobular in shape (Figs. 2 and 3D). Many proximal portions of attaching filaments were observed in the VPA. The nuclei of the granulosa cells when observed by Hoechst staining appeared to avoid the areas of non-attaching filaments on the chorion (Fig. 4), because the nuclei existed out of focus. Calculated by the number of nuclei, the mean number of granulosa cells was about 1.5×10^4 in the animal hemisphere. This coincided with the value determined by calculation from the cell size (assuming the diameter as ca. 8 μm). The mean number of cells in the vegetal hemisphere including the VPA with its tall cells (mean diameter ca. 5 μm) was 1.7×10^4 as determined by the calculation from the cell size.

2 Production of steroids by granulosa cells

E_2 and 17α,20β-diOHp produced by cultured granulosa cells were measured and the values for the animal and vegetal hemispheres were compared. The production of E_2 was stimulated by the presence of 100 IU/ml PMSG and 100 ng/ml progesterone (Table 1). No significant difference ($P>0.05$) in E_2 production was measured between the animal and the vegetal hemispheres. The production of 17α,20β-diOHp by granulosa cells was also stimulated by the presence of PMSG or progesterone. The concentrations (more than 0.4 pg/ml; [9]) of 17α,20β-diOHp were sufficient to induce oocyte maturation, and significantly greater in the vegetal hemisphere than in the animal hemisphere in the presence of PMSG.

DISCUSSION

The granulosa cells are in contact with the oocyte via cytoplasmic processes that pass through the pore canals in the chorion in the medaka [2] and the pipefish [1]. The present observations revealed morphological differences in granulosa cells localized at special regions (VPA) surrounding the oocyte. These differences seem to reflect the different interactions of the granulosa cells with the oocyte, the polarity of which is established during oogenesis. In the early stage of oogenesis, the VPA is determined by the position of the Balbiani body in the ooplasm, and the granulosa cells aligned compactly on the VPA (Iwamatsu, unpublished data). The attaching filaments differentiate and elongate on a restricted region of the chorion in the VPA, and then spirally wind around the VPA probably due to rotation of the oocyte and granulosa cells [6].

We recently found that growing oocytes with granulosa cells may rotate within the basement membrane [5]. The granulosa cells in the animal pole region possess many microvilli on their apical surfaces, but those in the remaining area do not. The difference in the distribution of the

granulosa cells with microvilli may be related to a difference in the interactions with the basement membrane, or movement of granulosa cells beneath the basement membrane. Whether the morphological differences in the granulosa cells depend on regional differences in the chorion regions with which they are in contact is not clear from the present study, but it was suggested that the patterns of spiral structures on the chorion are due to the movement of follicular cells during oogenesis [6].

The steroidogenic response to exogenous hormones of granulosa cells from the animal pole hemisphere differed from that of cells from the vegetal hemisphere. The production of 17α,20β-diOHp by granulosa cells that were stimulated by gonadotropin was greater in the vegetal hemisphere than in the animal hemisphere. A similar tendency was also observed in the steroid production by progesterone-stimulated follicles, although it was not significant statistically. The difference may be due to the difference in cell number, since there are more cells in the vegetal hemisphere than in the animal hemisphere. On the other hand, another cause of the difference may relate to the high ability of the tall granulosa cells with crowded mitochondria to produce steroids in the vegetal pole area. The cells that produce steroids are generally filled with mitochondria with well-developed tubular cristae and tubular or dilated ER (see [12]). However, no difference in E_2 production was recognized between the two hemispheres, in spite of the difference in cell number. This may indicate that the E_2 production by each granulosa cell in the vegetal hemisphere is not different from that in the animal hemisphere during the maturation period. Therefore, the granulosa cells with gonadotropin receptors seem to differ physiologically or distributively along the animal-vegetal axis of the oocyte.

ACKNOWLEDGMENTS

The authors thank Dr. Cherrie A. Brown, California Regional Primate Research Center, University of California, Davis, for critical reading of the manuscript.

REFERENCES

1 Begovac PC, Wallace RA (1989) Major vitelline envelope proteins in pipefish oocytes originate within the follicle and are associated with the Z3 layer. J Exp Zool 251: 56–73

2 Hirose K (1972) The ultrastructure of the ovarian follicle of medaka, *Oryzias latipes*. Z Zellforsch 123: 316–329

3 Iwamatsu T (1975) Medaka as a teaching material. II. Maturation and fertilization of oocytes. Bull. Aichi Univ. Educ., 24 (Nat. Sci.): 113–144 (in Japanese)

4 Iwamatsu T (1980) Studies on oocyte maturation of the medaka, *Oryzias latipes*. VIII. Role of follicle cells in gonadotropin- and steroid-induced maturation of oocytes *in vitro*. J Exp Zool 206: 355–364

5 Iwamatsu T (1992) Morphology of filaments on the chorion of oocytes and eggs in the medaka. Zool Sci 9: 589–599

6 Iwamatsu T, Nakashima S, Onitake K (1993) Spiral patterns in the micropylar wall and filaments on the chorion in eggs of the medaka, *Oryzias latipes*. J Exp Zool 267: 225–232

7 Iwamatsu T, Ohta T (1981) On a relationship between oocyte and follicle cells around the time of ovulation in the medaka, *Oryzias latipes*. Annot Zool Japon 54: 17–29

8 Iwamatsu T, Ohta T, Oshima E, Sakai N (1988) Oogenesis in the medaka *Oryzias latipes*. —Stages of oocyte development. Zool Sci 5: 353–373

9 Iwamatsu T, Takahashi SY, Sakai N, Asai K (1987) Inductive and inhibitory actions of a low molecular weight serum factor on *in vitro* maturation of oocytes of the medaka. Biomed Res 8: 313–322

10 Iwamatsu T, Takahashi SY, Sakai N, Onitake K (1987) Induction and inhibition of *in vitro* oocyte maturation and production of steroids in fish follicles by forskolin. J Exp Zool 241: 101–111

11 Masui Y, Clarke HJ (1979) Oocyte maturation. Intern Rev Cytol 57: 185–282

12 Nagahama Y (1983) Functional morphology of teleost gonads. In "Fish Physiology", vol. IXA (WS Hoar, AJ Randall and E M Donaldson, eds), pp. 223–275, Academic Press, New York

13 Nagahama Y, Adachi S (1985) Identification of maturation-inducing steroid in a teleost, the amago salmon (*Oncorhynchus rhodurus*). Develop Biol 109: 428–435

14 Riehl R, Appelbaum S (1991) A unique adhesion apparatus on the eggs of the catfish *Clarias gariepinus* (Teleostei, Clariidae). Jap J Ichthyol 38: 191–197

15 Sakai N, Iwamatsu T, Yamauchi K, Suzuki N, Nagahama Y (1988) Influence of follicular development on steroid production of the medaka (*Oryzias latipes*) ovarian follicle in response to exogenous substances. Gen Comp Endocrinol 71: 516–523

16 Schuetz AW (1967) Action of hormoness on germinal vesicle breakdown in frog (*Rana pipiens*) oocytes. J Exp Zool 166: 347–354

ZOOLOGICAL SCIENCE 11: 83–87 (1994)

Immunohistochemical Localization of Epidermal Growth Factor in the Developing Rat Gonads

YASUHIKO KANNO, SATOSHI KOIKE[1] and TETSUO NOUMURA[2]

Department of Regulation Biology, Faculty of Science, Saitama University, Urawa, Saitama 338, and [1]Upjohn Pharmaceuticals Limited, Wadai, Tsukuba, Ibaraki 300-42, Japan

ABSTRACT—Epidermal growth factor (EGF) is known to have various endocrine, paracrine and autocrine roles in adult mammalian tissues. In order to clarify the participation of EGF in rat gonadal differentiation, immunohistochemical localization of EGF as chronologically studied in perinatal rat gonads. Sprague-Dawley rat gonads from gestational day (GD) 13 to postnatal day (PD) 21 were fixed in acetic acid-free Bouin's solution and stained with a polyclonal antibody against mouse EGF by using avidin-biotin complex technique. Immunohistochemical reactivity was positive in almost all cell types in the prenatal male gonads. Male germ and Leydig/interstitial cells showed a positive reactivity from GD 15 to 21. Slight and moderate staining were seen in the Sertoli/supporting cells from GD 13 to 21. After birth, positive expression was not seen in any types of cells in male gonads except for germ cells on PD 21. On the other hand, in prenatal female gonads positive signs were found in the interstitial cells from GD 14 to 21 and in the granulosa cells on GD 21. During the postnatal period from PD 5 to 21, the granulosa and theca cells were slightly positive and the interstitial cells moderately positive. Wolffian ducts in males and Müllerian ducts in females were stained during the prenatal period. These results indicate that EGF shows stage-specific patterns of expression in the developing rat gonadal cells and may be involved in the rat gonadal development and diffferentiation.

INTRODUCTION

Epidermal growth factor (EGF), a single-chain polypeptide of 53 amino acid residues, was first isolated from the submandibular gland of male mice [8]. This peptide is a potent mitogen for a wide variety of cell types *in vivo* and *in vitro* and distributes in various tissues and fluids in mammals [7]. EGF is mainly synthesized in the submandibular gland of mice [5] and rats [22], and its synthesis is under the control of androgens [6] and thyroid hormones [9].

EGF is involved in many physiological functions in the adult gonads [24]. EGF reduced follicle-stimulating hormone (FSH)-stimulated testosterone production in rat Leydig cells *in vitro* [15], which was due to a regulation in 17β-hydroxylase activity [25]. EGF also attenuated FSH-stimulated aromatase activity in the Sertoli cells [2] and the granulosa cells [15], but stimulated Sertoli cell proliferation [16]. FSH-stimulated inhibin production in the Sertoli cells [20] and plasminogen activator production in the granulosa cells were increased by EGF [10]. Although basic properties and functions of EGF have been reported in adults, little is known about its contribution to the fetal gonadal development and diffferentiation.

In order to clarify the participation of EGF in developing rat gonads, immunohistochemical expression of EGF was chronologically studied in the fetal and prepubertal rat gonads from gestational day (GD) 13 to postnatal day (PD) 21.

Accepted December 17, 1993
Received October 21, 1993
[2] To whom reprint requests should be addressed.

MATERIALS AND METHODS

Aminals

Crj: CD (Sprague-Dawley) rats from 13 to 20 weeks of age were housed in constant temperature (23±1°C), relative humidity (55±10%) and light-dark cycle (light on 7:00–19:00). Animals were given a commercial diet (CRF-1, Charles River Japan Co.) and tap water *ad libitum*. Cohabitation was done in the evening of vaginal proestrus in the 1:1 basis of male: female. In the next morning, copulation was checked by the presence of sperm in the vaginal smear. The day when sperm-positive smear was found was designated as GD 0, and the day when litter was found was designated as PD 0.

Preparation of tissues for immunostaining

Dams were sacrificed from GD 13 to 21 and neonates on PDs 5, 11 and 21 by diethyl ether anesthesia. The gonads and genital ducts dissected from more than three fetuses and pups in different litters were fixed in acetic acid-free Bouin's solution for a few hours at 4°C. The sexes of fetuses were determined as described by Agelopoulou et al. [1]. Then the tissues were dehydrated through a series of graded concentrations of ethanol and xylene, embedded in paraffin and sectioned in 5 μm thickness. The male rat submandibular glands on PD 35 were also dissected and fixed in the same fixative, for checking the specificity of the antibody used.

Immunohistochemistry

Sections were deparaffinized with xylene and hydrated in decreasing concentrations of ethanol. The sections were incubated with 0.5% periodic acid (Sigma Chemical Co.) in 50 mM Tris-buffered saline (TBS, pH 7.6, Wako Pure Chemical Industries, Ltd.) at room temperature for 30 min to block endogenous peroxidase. Sections were subsequently rinsed with 50 mM TBS for 20 min, blocked non-specific staining with 1.5% normal goat serum in 50 mM

TBS for 20 min. Then, sections incubated overnight at 4°C with the polyclonal antibody against mouse EGF raised in the rabbit (Collaborative Research Inc.) at 0.02 mg/ml in 10 mM PBS. Dose response study indicated that this concentration of the antibody gave optimal labelling results. Follwing this incubation the sections were rinsed with TBS and then treated with 0.5% biotinylated goat anti-rabbit secondary antibody (Vector Lab, Inc. ABC kit Elite) diluted in 50 mM TBS for 30 min at room temperature. Sections were again washed in TBS and subsequently incubated with 2% avidin-biotin complex (Vector Lab, Inc, ABC kit Elite) in 50 mM TBS for 40 min at room temperature. Avidin and biotin were prepared at least 30 min before applied to the sections to allow the complex to form. The sections were again washed in TBS, and the bound antibody was visualized with 0.05% 3,3′-diaminobenzidine tetrachloride (Dojindo Laboratories) in 50 mM TBS (pH 7.2) and 0.02% hydrogen peroxide for 5 min. These sections were counterstained with hematoxylin.

Controls included (a) replacing the primary antibody with normal rabbit serum, (b) using the primary antibody that had been pre-incubated overnight at 4°C with 0.04 mg/ml mouse EGF (Chemicon International, Inc.) before this mixture was applied to the section to check specificity of the primary antibody, and (c) omitting the primary antibody to check the specificity of the secondary antibody.

RESULTS

Specificity of antibody

Preparations which were stained with the antibody to EGF, and with the immunoneutralized antibody by pre-incubated with the antigen were shown in Fig. 1. EGF antibody stained the granular convoluted tubule cells of submandibular gland in male rats on PD 35, but the neutralized antibody did not stain any cells. Therefore, these results showed that this polyclonal antibody specifically stained EGF-containing cells, because the rat submandibular gland was confirmed to contain EGF-positive cells [22].

Immunohistochemical localization

Immunohistochemical expression of EGF in the developing rat gonads was summarized in Table 1. In male gonads, many germ cells were moderately stained from GD 15 to 21 and PD 21 (Fig. 2.A-C). A few Sertoli/supporting cells and almost all Leydig/interstitial cells showed positive reactivity; the staining intensity was moderate or slight in Sertoli/supporting cells from GD 13, the time when the supporting cells were firstly recognized by histological examination, to GD 21 and marked in Leydig/interstitial cells from GD 15 to 21 (Fig. 2.A-C). On the other hand, in female gonads, a few interstitial cells expressed slight reactivity from GD 14 to 21 and moderate from GD 21 to PD 21 (Fig. 2.E-G). A few theca cells slightly stained from PD 5 to 21 and a few granulosa cells slightly stained from GD 21 to PD 21 (Fig. 2.E-G). But the germ cells in females were not shown any positive reactivity during the experimental period (Fig. 2.E-G).

The epithelial cells of the genital ducts were stained in sex-specific manner during the prenatal period: the Wolffian ducts in males were moderately or markedly stained from GD 16 to 21 (Fig. 2.D) and the Müllelrian ducts in females were slightly or moderately stained from GD 16 to PD 21 (Fig. 2.H).

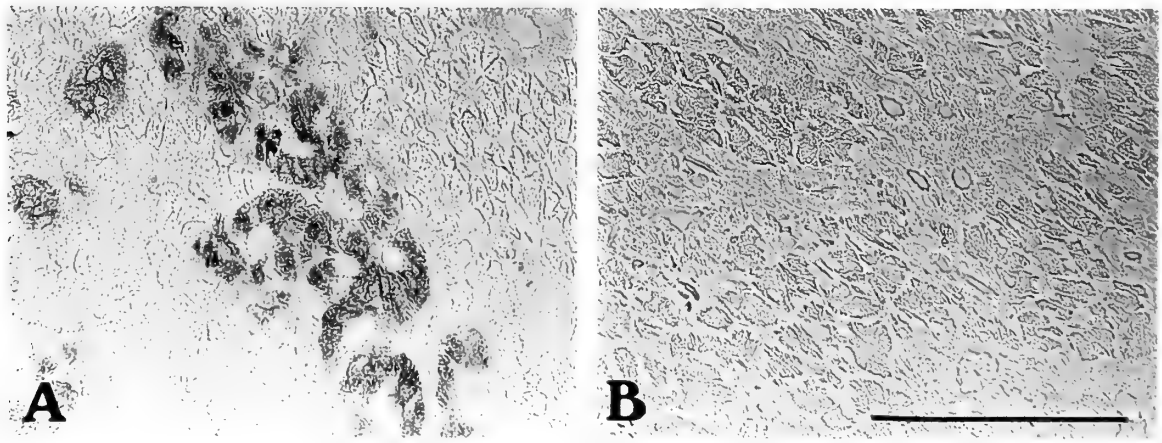

FIG. 1. Demonstration of staining specificity. Male rat submandibular glands on PD 35 incubated with the EGF antibody (A), or with the neutralized antibody (B). Staining is seen in the granular convoluted tubule cells of A, but those of B. Bar: 50 μm.

FIG. 2. Immunohistochemical localization of EGF in the gonad of perinatal rats. (A) Male gonad on GD 14. The Sertoli/supporting cells (arrow) show slight staining. (B) Male gonad on GD 17. In the Leydig/interstitial cells (arrow head), and the moderate stainings in the germ (thick arrow) and the Sertoli/supporting cells (arrow) express marked staining. (C) Male gonad on PD 5. Gonadal cells do not express any positive sign. (D) Male Wolffian duct and on GD 17. The epithelial cells (arrow) show marked staining. (E) and (F) Female gonads on GDs 14 and 17. The interstitial cells (arrow) express slight staining. (G) Female gonad on PD 5. The interstitial cells (arrow head) are stained moderately and the granulosa (arrow) and theca (thich arrow) cells slightly. (H) Female Müllerian duct on GD 17. The epithelial cells (arrow) are moderately stained. All sections are shown in the same magnification. Bar: 50 μm.

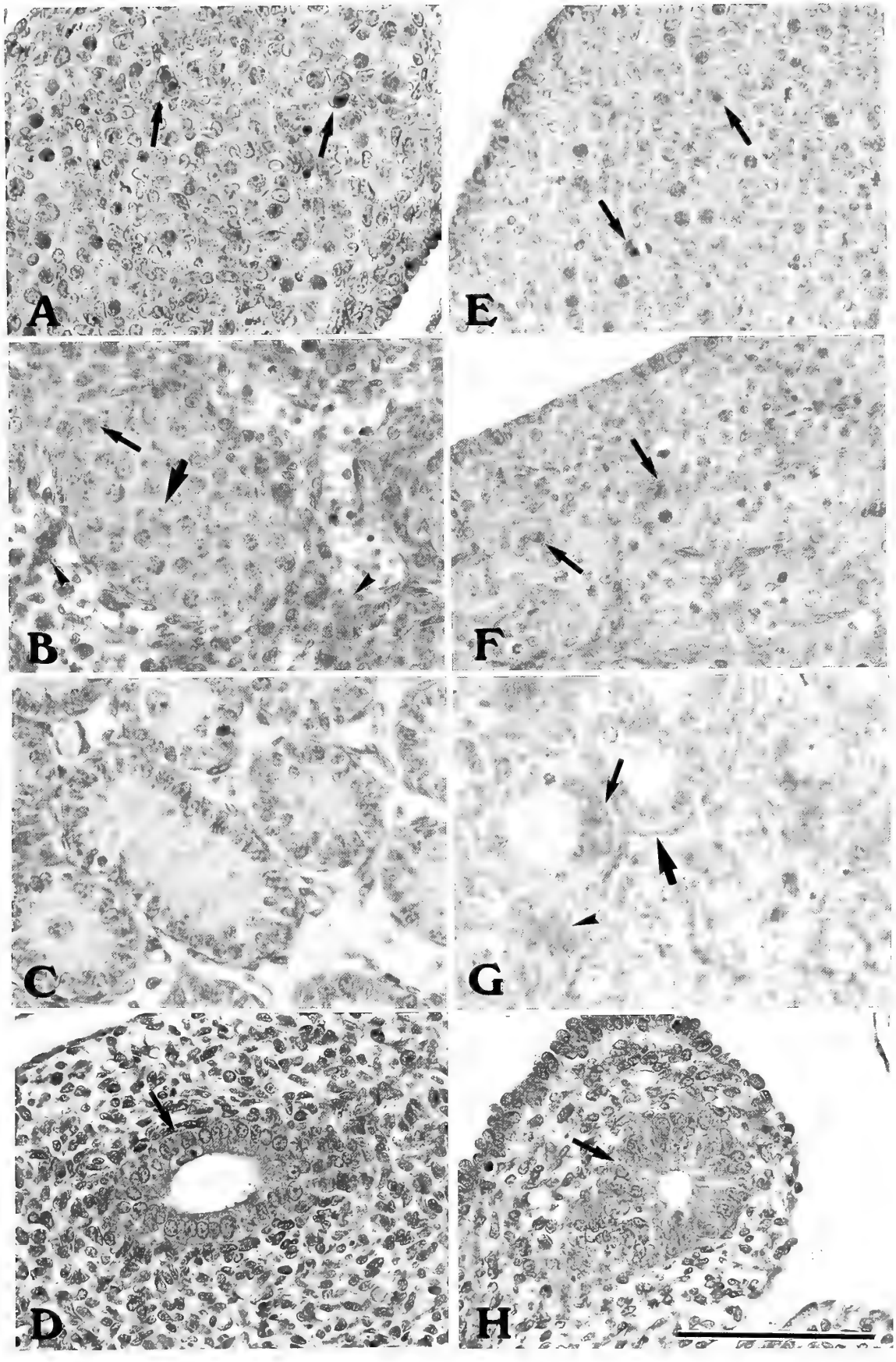
A
B
C
D
E
F
G
H

TABLE 1. Immunohistochemical localization of EGF in the developing rat gonad

		Male						Female					
		Gonad				Duct		Gonad				Duct	
		G	S	P	L	W	M	G	Gr	T	I	W	M
GD	13	−	+/−	*	*	−	*	−	*	*	*	−	*
	14	−	+/−	*	*	−	−	−	−	*	+/−	−	−
	15	++	+/−	*	+++	−	−	−	−	*	+/−	−	−
	16	++	+/−	*	+++	++	−	−	−	*	+	−	++
	17	++	++/−	*	+++	+++	*	−	−	*	+	−	++
	18	++	++/−	−	+++	++	*	−	−	*	+	−	+
	19	++	++/−	−	+++	++	*	−	−	*	+	*	+
	20	++	++/−	−	+++	++	*	−	−	*	+	*	+
	21	++	+/−	−	+++	++	*	−	+/−	*	++	*	++
PD	5	−	−	−	−	−	*	−	+/−	+/−	++/−	*	++
	11	−	−	−	−	−	*	−	+/−	+/−	++	*	+
	21	++	+/−	−	−	−	*	−	+/−	+/−	++	*	+

GD: Gestational day, PD: Postnatal day, G: Germ cell, S: Sertoli/Supporting cell, P: Peritubular cell, L: Leydig cell, W: Wolffian duct, M: Müllerian duct, Gr: Granulosa/Supporting cell, T: Theca cell, I: Interstitial/Stromal cell, Grade, −: Not detectable, +: Slight but above background levels, ++: Moderate, +++: Marked staining, *: The cells or tissues were not found in that day.

DISCUSSION

Differentiation and development of gonads are complex events which involve various cell-cell interactions. EGF is a potent mitogen [12, 13] and affects to gonadal steroid and peptide syntheses [15, 26]. Male germ cells showed a positive reactivity from GD 15. Germ cells in males are encompassed by the somatic cells from GD 14 ([11] and this experiment) and thereafter undergo mitotic division. Therefore, positive expression from GD 15 indicates that EGF may have a function in the germ cell proliferation during the fetal period.

The positive reactivity to anti-EGF antiserum was shown from GD 13 in the somatic cells of the developing gonads. The supporting and interstitial cells in the gonads proliferate rapidly during the fetal period [19]. Therefore, the expression in the Sertoli/supporting and Leydig/interstitial cells may indicate that EGF stimulates the proliferation of these gonadal somatic cells as well as the germ cells. EGF decreased FSH-stimulated testosterone production by regulating 17β-hydroxylase activity in Leydig cells *in vitro* [15, 25]. Fetal rat testes have steroidogenic activity during the prenatal period *in vitro* [21]. So positive reactivity in the Leydig/interstitial cells indicates that EGF may contribute to the fetal Leydig cell steroidogenesis. But the marked staining of the Leydig/interstitial cells during the prenatal period was lost after birth. This may be due to a regression of fetal Leydig cells which begin shortly before birth and replace to adult-type Leydig cells after birth in the rat [11].

The interstitial cells in female gonads have not been known to participate in physiological roles on the ovary, at least, during the prenatal and early postnatal period. The positive staining in these cells suggests that EGF is likely to mediate the ovarian functions in autocrine and/or paracrine fashions. EGF stimulates or inhibits the immature rat granulosa cell proliferation depending on the presence or absence of FSH [3]. In addition, the theca cells produce an EGF-like substance, which may regulate the granulosa cell functions [23]. Together with these results, positive staining in the granulosa and theca cells during the perinatal period suggests that EGF contributes to the follicle formation through the granulosa and theca cell poliferation.

The immuno-reactivity was seen in the Wolffian ducts in males and Müllerian ducts in females. EGF plays important roles in the male and female reproductive-tract development during the perinatal or critical period [4, 14]. Therefore, the immuno-positive expression in the gonoducts in this stage supports the previous findings that EGF has been reported to be concerning with the development and differentiation in the gonoducts.

Other growth factors have also been reported to participate in the gonadal development in rat fetuses. Transforming growth factor-β (TGF-β) localized in many types of cells in developing fetal gonads [18], like EGF. However, inhibin-α, a member of TGF-β superfamily, localized in Sertoli cells at the time of seminiferous tubule formation and in the Leydig cells during the late gestational period [17]. Together with these results, growth factors could play an important role in the gonadal development during the perinatal period. The mechanisms and roles of these growth

factors on gonadal development are under investigation.

REFERENCES

1 Agelopoulou R, Magre S, Patsavoudi E, Jost A (1984) Initial phases of the rat testis differentiation *in vitro*. J Embryol Exp Morph 83: 15–31

2 Ascoli M, Euffa J, Segaloff DL (1986) Epidermal growth factor activates steroid biosynthesis in cultured Leydig tumor cells without affecting the levels of cAMP and potentiates the activation of steroid biosynthesis by choriogonadotropin and cAMP. J Biol Chem 262: 9196–9203

3 Bendell JJ, Dorrington JH (1990) Epidermal growth factor influences growth and differentiation of rat granulosa cells. Endocrinology 127: 533–540

4 Bossert NL, Nelson KG, Ross KA, Takahashi T, MacLachlan JA (1990) Epidermal growth factor binding and receptor distribution in the mouse reproductive tract during development. Dev Biol 142: 75–85

5 Byyny RL, Orth DN, Cohen S (1972) Radioimmunoassay of epidermal growth factor. Endocrinology 90: 1261–1266

6 Byyny RL, Orth DN, Cohen S, Doyne ES (1974) Epidermal growth factor: effects of androgens and adrenergic agents. Endocrinology 95: 776–782

7 Carpenter G, Wahl MI (1991) The epidermal growth factor family. In "Peptide Growth Factors and Their Receptors II" Ed by MB Sporn and AB Roberts, Springer-Verlag, New York, pp 70–171

8 Cohen S (1962) Isolation of mouse submaxillarly gland protein accelerating incisor eruption and eyelid opening in the newborn animal. J Biol Chem 237: 1555–1562

9 Fisher DA (1990) Hormone epidermal growth factor interactions in development. Hormone Research 33: 69–75

10 Galway AB, Oikawa M, Tor NY, Hasueh AJW (1989) Epidermal growth factor stimulates tissue plasminogen activator activity and messenger ribonucleic acid levels in cultured rat granulosa cells: mediation by pathways independent of protein kinases-A and -C. Endocrinology 125: 126–135

11 Gondos B (1977) Testicular development. In "The Testis" Vol. 4, Ed by AD Johnson, WR Gomes, Academic Press, New York, pp 1–37

12 Gospodarowicz D. Ill CR, Birdwell CR (1977) Effects of fibroblast and epidermal growth factors on ovarian cell prolifration *in vitro*. I. Characterization of the response of granulosa cells to FGF and EGF. II. Proliferative response of luteal cells to FGF but not EGF. Endocrinology 100: 1108–1120; 1121–1128

13 Gospodarowicz D, Bialecki H (1979) Fibroblast and epidermal growth factors are mitogenic agents for cultured granulosa cells of rodent, porcine, and human origin. Endocrinology 104: 757–764

14 Gupta C, Siegel S, Ellis D (1991) The role in testosterone-induced reproductive tract differentiation. Dev Biol 146: 106–116

15 Hsueh AJW, Welsh TH, Jones PJC (1981) Inhibition of ovarian and testicular steroidogenesis by epidermal growth factor. Endocrinology 108: 2002–2004

16 Jaillard, C, Chatelain PG, Saez JM (1987) *In vitro* regulation of pig Sertoli cell growth and function: effects of fibroblast growth factor and somatomedin-C. Biol Reprod 37: 665–674

17 Koike S, Noumura T (1993a) Immunohistochemical expression of inhibin-α subunit in the developing rat gonads. Zool Sci 10: 449–454

18 Koike S, Noumura T (1993b) Immunohistochemical localizations of TGF-β in the developing rat gonads. Zool Sci 10: 671–677

19 Loading DW, de Kretser DM (1972) Comparative ultrastructural and histochemical studies of the interstitial cells of the rat testis during fetal and postnatal development. J Reprod Fertil 29: 216–269

20 Morris PL, Vale WW, Cappel S, Bardin CW (1988) Inhibin production by primary Sertoli cell-enriched cultures: regulation by follicle-stimulating hormone, androgens, and epidermal growth factor. Endocrinology 122: 717–725

21 Noumura T, Weisz J, Lloyd GW (1966) *In vitro* conversion of 7-^{3}H-progesterone to androgens in the rat testis during the second half of fetal life. Endocrinology 78: 245–253

22 Poulsen SS, Nexo E, Olsen PS, Hess J, Kirkegaard P (1986) Immunohistochemical localization of epidermal growth factor in rat and man. Histochemistry 85: 389–394

23 Skinner MK, Lobb D, Dorrington JH (1987) Ovarian thecal/interstitial cells produce an epidermal growth factor-like substance. Endocrinology 121: 1892–1899

24 Tsutsumi O, Kurachi H, Oka T (1986) A physiological role of epidermal growth factor in male reproductive function. Science 233: 975–977

25 Welsh THJr, Hsueh AJW (1982) Mechanism of the inhibitory action of epidermal growth factor on testicular androgen biosynthesis *in vitro*. Endocrinology 110: 1498–1506

26 Zhiwen, Z, Carson RS, Herington AC, Lee VWK, Burger HG (1987) Follicle-stimulating hormone and somatomedin-C stimulate inhibin production by granulosa cells *in vitro*. Endocrinology 120: 1633–1638

ZOOLOGICAL SCIENCE 11: 89–100 (1994)

The Acrosome Reaction and Fertilization in the Bivalve, *Laternula limicola*, in Reference to Sperm Penetration from the Posterior Region of the Mid-piece

KAZUKO HOSOKAWA[1] and YOSHIO D. NODA[2]

[1]*Laboratory of Biology, Tokyo Dental College, Masago, Mihama-ku, Chiba 261, and* [2]*Biological Institute, Faculty of Science, Ehime University, Matsuyama, Ehime 790, Japan*

ABSTRACT—The processes of acrosome reaction and sperm penetration in the bivalve *Laternula limicola* were observed using light and electron microscopy. The spermatozoon of *Laternula limicola* is unique with respect to the position of the acrosome. The acrosome of the mature spermatozoon is situated posterior to the mitochondria in the sperm mid-piece. The acrosome consists of a bipartite structure, the acrosomal vesicle and the subacrosomal region. In the first stage of the acrosome reaction, a pit forms at the posterior tip of the acrosomal vesicle. In the second stage, the outer membrane of the acrosomal vesicle and the sperm plasma membranes fuse at the lateral part of the acrosome and open. In the third stage, the plasma membrane continually degrades and the inner acrosomal membrane is exposed. In the fourth stage, the exposed inner acrosomal membrane contacts the apex of an egg microvillus. At the site of contact, a fertilization cone is rapidly formed. Sperm incorporation in this species first begins at the posterior lateral region of the sperm mid-piece, not at the anterior region of the sperm head in the manner of many other species, because the acrosome lies at the most posterior end of the mid-piece. Sperm incorporation from the mid-piece has not been previously described. The present report on normal fertilization is the first description of the morphological changes in the acrosome of *Laternula limicola* spermatozoa and sperm incorporation beginning at the posterior region of the sperm mid-piece.

INTRODUCTION

The mature spermatozoon in most animals is fundamentally composed of three distinct parts, the head, mid-piece and tail. Reports on the morphology of spermatozoa have so far described the nucleus occupying the main portion of sperm head and the acrosome as situated at the apex of the head [38], except in species such as the Ostheichthyes [3, 43, 48, 53], Thaliacea [17], Crustacea [42], Kinorhyncha [24, 39], Nematodea [5, 22, 34], Cestoidea [32] and Anthozoan [13], in which lack an acrosome. The actual structure of the intact acrosome varies morphologically from one species to another.

Since Dan [9] first stated that the acrosome reaction plays an important role in fertilization, many subsequent experiments have confirmed that the acrosome reaction is essential for the success of sperm entry in species in which the spermatozoa possess an acrosome. During the normal course of fertilization in many species, including those lacking acrosome, spermatozoa initially contact the egg or the oocyte in the region of the sperm head and enter the ooplasm starting at the head [1, 15, 21, 31, 35, 44, 45, 49, 50, 56].

The fine structure of spermatozoa of the bivalve, *Laternula limicola,* was first observed by Kubo in 1977 [25]. Kubo reported that mature spermatozoa of this species do not have a "typical acrosome" situated at the anterior area of the head, but have an acrosome-like structure that is uniquely located at the sperm mid-piece and assigned it the new name of "temporary acrosome". However, the role of the posterior temporary acrosome in fertilization was not defined in this report.

For this reason, the authors studied the process of fertilization in the bivalve, *Laternula limicola,* with particular attention to whether or not any morphological changes occur in the posterior temporary acrosoma structure and to what region of the sperm first touches and fuses with the egg plasma membrane.

MATERIALS AND METHODS

Specimens of the bivalve *Laternula limicola* (REEVE) were collected from a tideland in the vicinity of the Imakiri River mouth in Tokushima prefecture Japan during August and September from 1986 to 1989. The shells of this species are frail, light gray in color, and elliptical in shape, measuring about 35 mm along the major axis and 15 mm along the minor axis. Since this species is a hermaphrodite, the ovotestis concurrently matures during the breeding season.

After the shells were removed, the bodies of mature adult specimens were placed in a Petri dish filled with 80% sea water containing 0.1 M acetylcholine. This treatment induced spawning of mature spermatozoa and prophase I oocytes from the parallel openings of the oviduct and spermiduct. The spermatozoa and the oocytes were separately collected by a pipette before the spermatozoa could disperse. The spermatozoa were quickly placed in a Petri dish separate from the oocytes. The oocytes were inseminated in 80% sea water.

To examine the interaction between the spermatozoon and the oocyte, the fertilization process in specimens was observed using a light microscope within 8 min after insemination. To induce the acrosome reaction, the spermatozoa were exposed to Ionophore

Accepted November 3, 1993
Received March 11, 1993

A23187. Ionophore A23187 was dissolved in dimethyl sulfoxide and diluted as a 40 μg/ml solution in sea water. An equal volume of Ionophore solution was added to the sperm suspension. These specimens were used for electron microscopic observations.

The specimens were fixed at room temperature for 2 hr in 2.5% glutaraldehyde buffered to pH 7.2 with 0.1 M cacodylate. They were then post-fixed for 1 hr in 1% osmium tetroxide. After they were dehydrated through a graded acetone series, the specimens were embedded in an Epoxy 812 resin mixture. Ultra-thin sections were stained with uranyl acetate and lead citrate and observed with a Hitachi H-600 transmission electron microscope operated at 100 KV. For scanning electron microscopic observations, fixed specimens were dried with a critical point drying apparatus, coated with gold by ion sputtering and observed with a Hitachi 450 DX scanning electron microscope operated at 15 KV. Light microscopic observations of living materials were conducted with Nomarski differential interference-contrast optics.

OBSERVATIONS

1 Spermatozoon and oocyte

The mature spermatozoon of *L. limicola* is composed of three parts; a tapering head about 5 μm in length and 1 μm in width, a large mid-piece about the same length as the head and a long flagellated tail about 60 μm in length (Figs. 1a, b). The mid-piece contains five mitochondria accompanied by the acrosome, which lies posterior to the mitochondria and a pair of centrioles, the proximal and distal centrioes (Fig. 2a). This spermatozoon has a clearly discernible dorsoventral asymmetry due to the dorsal location of the distal centriole, from which the axonemal complex arises, and the ventral location of the proximal centriole. The distal centriole is not surrounded by the five mitochondria. The sperm flagellum is separated dorsally from the mid-piece and extends parallel to the mid-piece. The basal body which is elongated from the distal centriole at the base of the axonemal filament is about 4 μm in length.

The acrosome is situated posterior to the five mitochondria and is comprised of a bipartite structure, the acrosomal vesicle and the subacrosomal region. The acrosomal vesicle is an elongated bell-shaped structure enclosed by a limiting membrane in longitudinal section. The subacrosomal region is contained within a 3 μm deep invagination of the acrosomal vesicle (Fig. 2b). The homogeneous materials enclosed within the acrosomal vesicle are more electron dense than the materials of the subacrosomal region.

During the breeding season, *L. limicola* spawn primary

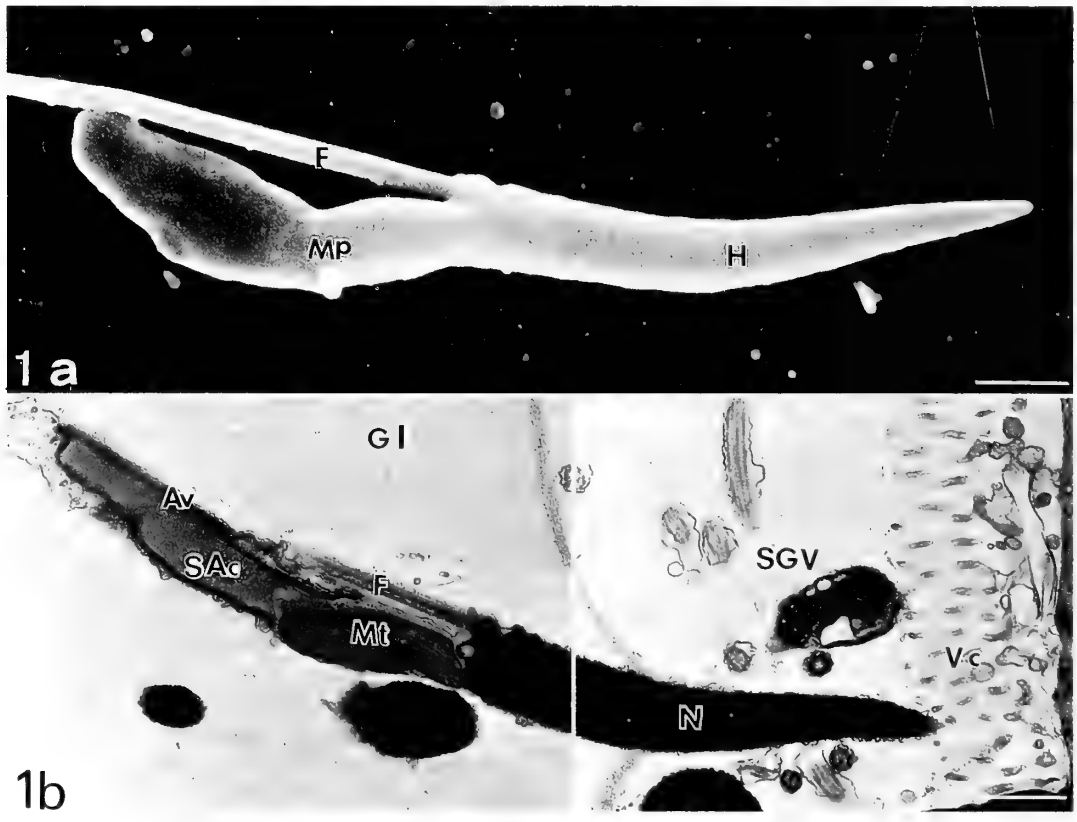

FIG. 1. Electron micrographs of whole views of mature spermatozoa of *Laternula limicola*.
a: Scanning electron micrograph (SEM) of the spermatozoon. The flagellum (F) is separated dorsally from the mid-piece (Mp). Bar: 1 μm. b: Transmission electron micrograph (TEM) of a spermatozoon travelling from the granular layer (Gl) of the egg investments to the SGV. It has a large acrosome posterior to the mitochondrial mid-piece and ventral to the flagellum. The acrosome is comprised of the acrosome vesicle (Av) and the subacrosomal region (SAc). The acrosome reaction has not yet begun. Bar: 1 μm.
H: Head, Mt: Sperm mitochondria, N: Nucleus, SGV: Space between granular layer and vitelline coat, Vc: Vitelline coat

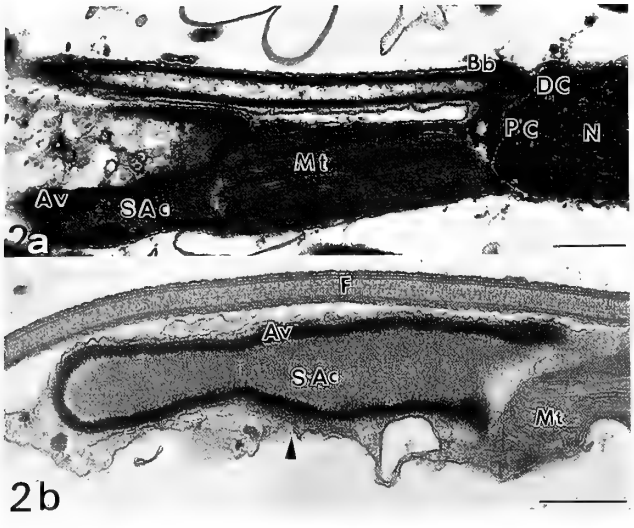

FIG. 2. Micrographs (TEM) of longitudinal sections through the acrosomal structure posterior to the mitochondrial mid-piece.
a: A pair of centrioles with the distal centriole (DC) dorsal and the proximal centriole (PC) ventral. The basal body (Bb) elongated from the distal centriole. Bar: 0.5 μm.
b: An intact acrosomal vesicle (Av) forming a slender bell-shaped sheath around the subacrosomal region (SAc). The acrosomal vesicle is more electron dense than the subacrosomal region. An arrowhead indicates the ventral lateral part of the acrosome. Bar: 0.5 μm.
F: Flagellum, Mt: Sperm mitochondria, N: Nucleus

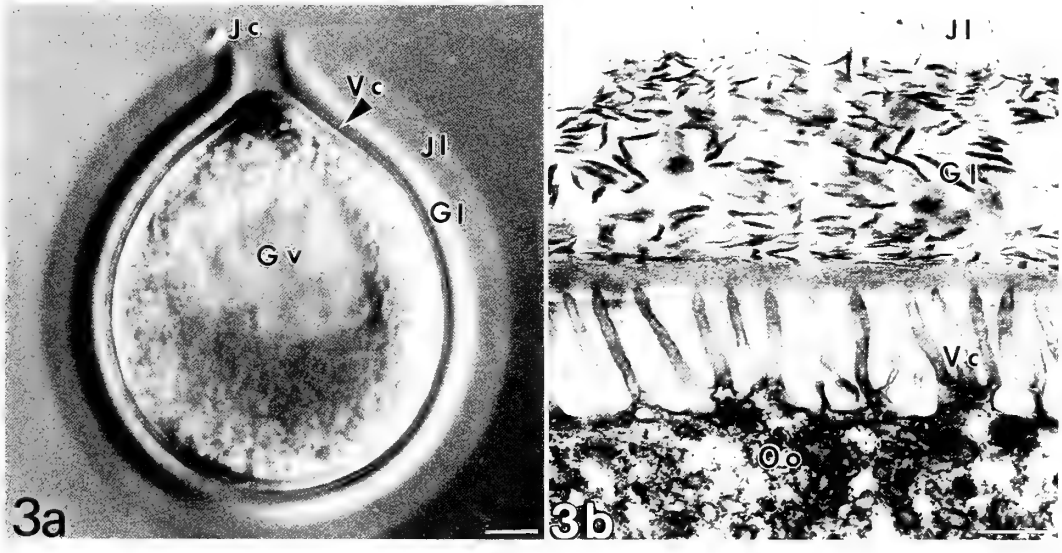

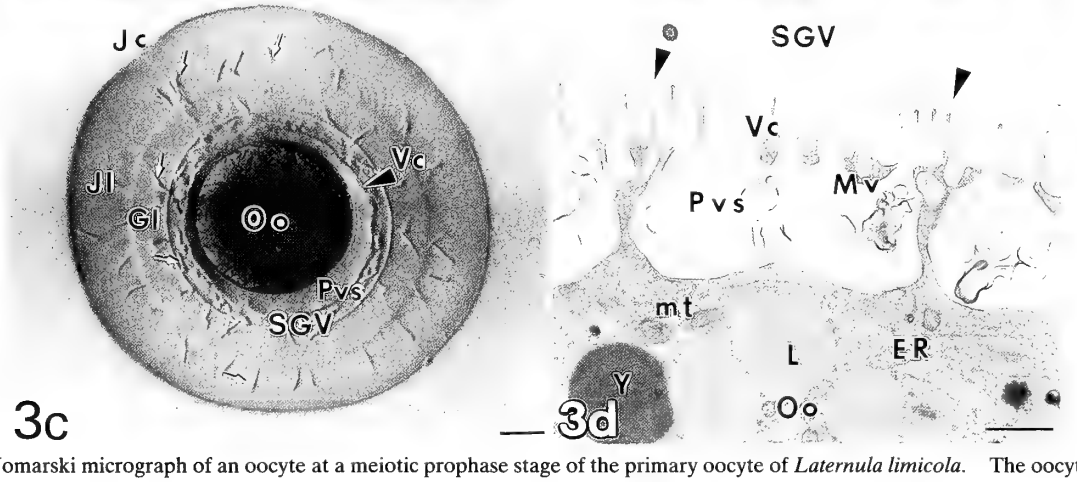

FIG. 3. a: Nomarski micrograph of an oocyte at a meiotic prophase stage of the primary oocyte of *Laternula limicola*. The oocyte is enveloped by the egg investments: jelly layer (Jl), granular layer (Gl) and vitelline coat (arrowhead Vc). The jelly canal (Jc) lacks the jelly and granular layers. Bar: 5 μm.
b: Micrograph (TEM) of the jelly layer (Jl), granular layer (Gl) and vitelline coat (Vc). Bar: 0.5 μm.
c: Nomarski micrograph of an oocyte within 1 min after insemination. The two spaces: SGV and perivitelline space (Pvs), are formed in the egg investments. Many spermatozoa (arrows) entering through the jelly canal and the jell and granular layers into the SGV. Bar: 10 μm.
d: The vitelline coat (Vc) has lifted from the oocyte surface and caused elongation of the oocyte microvilli (Mv). Arrowheads indicate the tips of microvilli remaining in association with the oocyte surface. Bar: 1 μm.
ER: Endoplasmic reticulum, Gv: Germinal vesicle, L: Lipid granule, Oo: Oocyte, mt: Oocyte mitochondria, Y: Yolk granule.

oocytes that are at prophase of meiosis. In longitudinal profile, the primary oocyte is droplet shaped and a jelly canal is visible at the point where the oocyte was attached to the ovarian wall during the process of maturation (Fig. 3a). This jelly canal is similar to that of the sea urchin egg [33]. The primary oocyte is enveloped by multiple layers of egg investments consisting of a jelly layer, a granular layer and a vitelline coat from the outside to the inside. The vitelline coat consists of fine fibrous material associated with the microvilli that are ooplasmic protrusions (Fig. 3b) [37]. When the oocyte is emitted into sea water, the granular layer transforms into a fibrillar structure indistinguishable from the jelly layer in electron micrographs [18]. When all the egg investments swell rapidly due to absorption of sea water, two spaces are newly formed in the egg investments. One space (SGV) develops between the granular layer and the vitelline coat. The other space is the perivitelline space (Pvs) between the vitelline coat and the egg plasma membrane (Figs. 3c, d) [20].

During fertilization, the spermatozoa reach the SGV

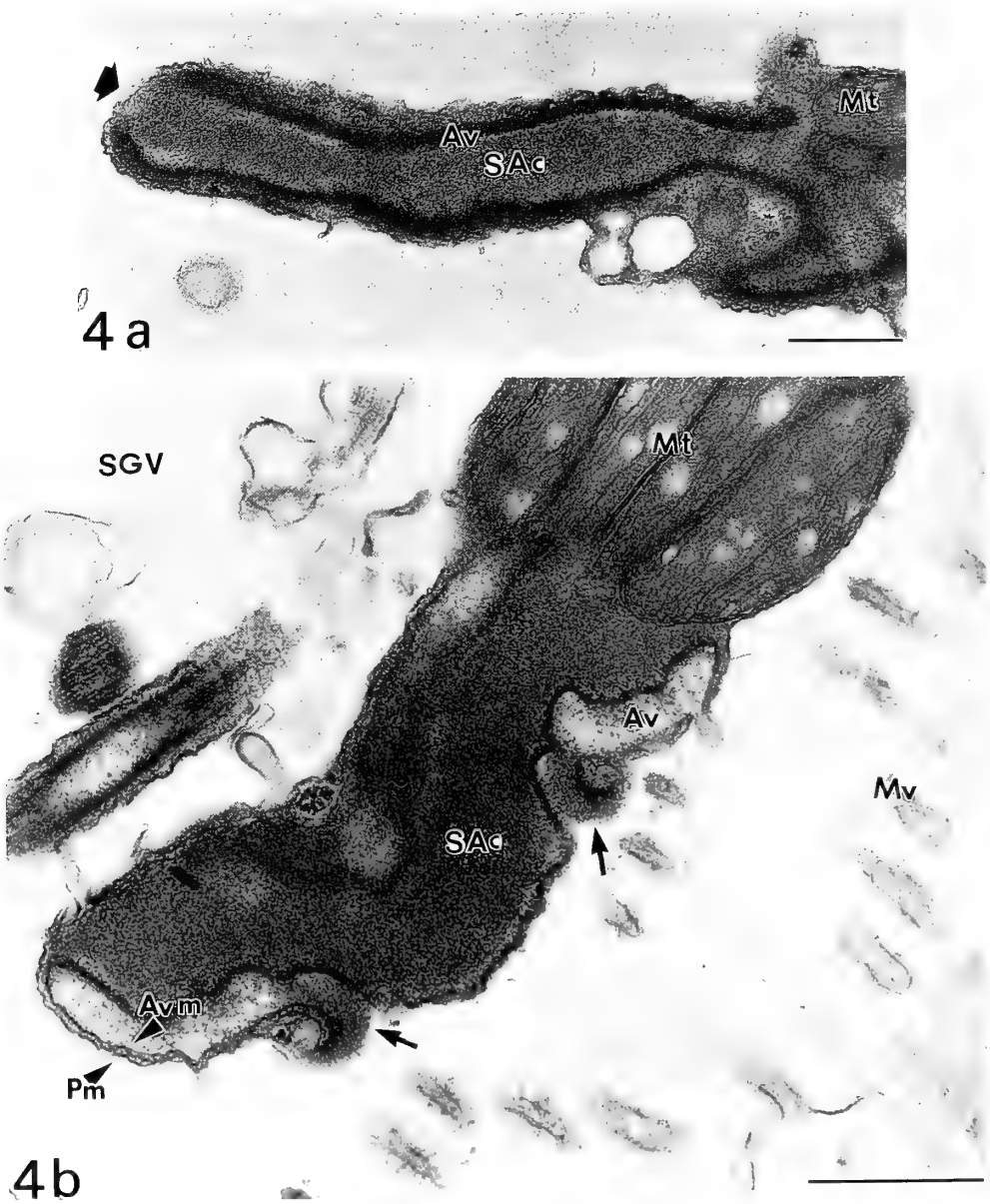

FIG. 4. a: The initial stage of the acrosome reaction. A pit (arrow) is observed at the most posterior point of the acrosomal vesicle (Av). This feature can also be seen in specimens treated with Ionophore A23187. Bar: 0.5 μm.
b: The second stage of the acrosome reaction. The acrosomal vesicle (Av) has swollen. The sperm plasma membrane (arrowhead Pm) and the exterior membrane of the acrosomal vesicle (arrowhead Avm) have fused to each other at the lateral region of the acrosome and opened the acrosome. Some of the acrosomal vesicle material has spread out around the opening. Arrows indicate the extruded materials. The membrane of the subacrosomal region (SAc) has been exposed by this process. Oocyte microvilli (Mv) in diagonal section are visible at the lower right corner of the micrograph. Bar: 0.5 μm.
Mt: Sperm mitochondria, SGV: Space between granular layer and vitelline coat.

sooner by passing through the jelly canal than by way of the jelly layer. The spermatozoa remain in the SGV for a few minutes while beating their tails vigorously. As they pass through the jelly canal, the active movement of the live spermatozoa can be seen clearly with Nomarski optics (Fig. 3c). Many of the spermatozoa in the SGV have a curved head. In electron microscopic observations, the spermatozoa remaining in the SGV appear to have undergone morphological changes in their acrosomes. However, the spermatozoa passing through the jelly and granular layers of the egg investments show no such changes.

2 *Acrosome reaction*

The morphological changes in the acrosome are divided into the following four stages. In the first stage, a pit forms at the posterior apical part of the acrosomal vesicle (Fig. 4a). In a longitudinal section through this pit, the acrosomal vesicle appears to be divided into two parts. Nearly all the micrographs of spermatozoa treated with Ionophore A23187 also reveal this feature. The entire acrosomal vesicle than swells becoming somewhat rounded and slightly less electron dense than the subacrosomal region. The arrow in Figure 4a shows the discontinuity at the posterior apical tip of the acrosomal vesicle. In the second stage, a morphological change takes place in the ventral lateral part of the acrosomal vesicle. The sperm plasma membrane and the outer membrane of the acrosomal vesicle open and fuse with one another in this ventral lateral region (Fig. 4b). The

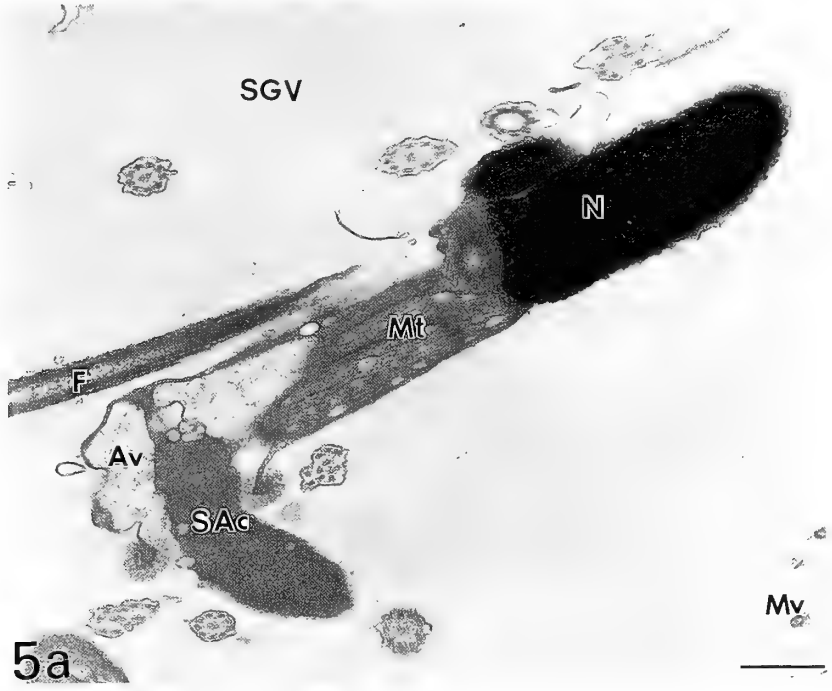

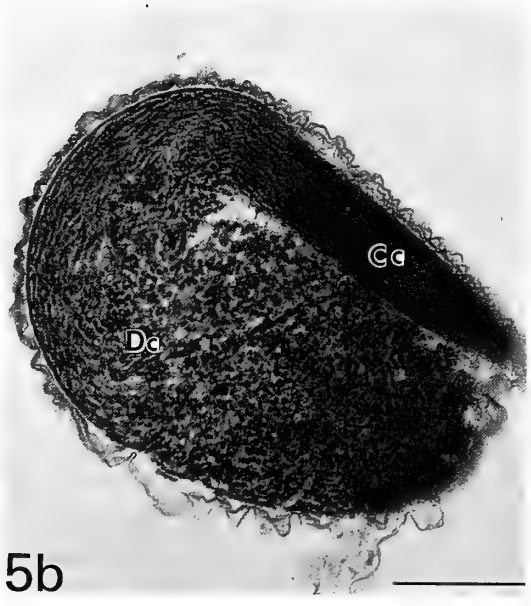

FIG. 5. a: The third stage of the acrosome reaction. A longitudinal section of a reacted spermatozoon in the SGV. The subacrosomal region (SAc) is forced out to the side of the vitelline coat. Note that no extension of an axial rod can be seen in the reacted acrosome. Bar: 0.5 m.

b: Sperm nucleus undergoing the chromatin decondensation. The decondensation of chromatin coincides with the acrosome reaction. The anterior half of nucleus still contains condensed chromatin (Cc). The latter half of the nucleus contains the decondensed chromatin (Dc). Bar: 0.5 μm.

a, b: Note that the sperm head has become round due to folding of the nucleus.

F: Flagellum, Mt: Sperm mitochondria, Mv: Microvilli, N: Nucleus, SGV: Space between granular layer and vitelline coat.

homogeneous electron dense material contained within the acrosomal vesicle exudes from the openings and accumulates at the outer surface of the membrane around the opening (Fig. 4b, arrows). The effusion of materials is accompanied by a regression of the membrane causing the material to spread out along the outer surface. In the third stage, the membrane of the subacrosomal region, the inner acrosomal membrane, is exposed to the SGV. The exposed membrane has the capacity to fuse with the egg plasma membrane. An axial rod cannot be observed as a notable extension from the subacrosomal region, but the subacrosomal region is forced out into the SGV toward the vitelline coat as shown the Figure 5a. In the fourth stage, the exposed and slightly protruding inner acrosomal membrane comes into contact with the tip of one of the intact microvilli that passes through the vitelline coat from the egg plasma membrane. At the point of contact the two membranes rapidly fuse with one another (Fig. 6). A fertilization cone is then formed in the SGV as illustrated in Figures 7a, b. The formation of the fertilization cone is observed within 5 min after insemination.

FIG. 6. The final stage of the acrosome reaction. The subacrosomal membrane of the spermatozoon has contacted a microvillus passing through the vitelline coat (Vc). This spermatozoon cannot immediately penetrate into the oocyte. But, if the microvillus which contacts the reacted subacrosomal region (SAc) is in continuous contact with the egg plasma membrane, the spermatozoon can probably be incorporated into the oocyte. An arrowhead indicates the point of membrane fusion between the microvillus and subacrosomal membranes. Bar: 0.5 μm.
Av: Acrosome vesicle, Mt: Sperm mitochondria, Mv: Microvilli, Oo: Oocyte, SGV: Space between granular layer and vitelline coat.

At the same time, the sperm head undergoes unique structural change also. The nucleus folds in half toward the dorsal side of the head, and then the sperm head become round (Fig. 5a, b). The condensed sperm chromatin begins to decondense beginning at the basal region of the nucleus bordering the mid-piece mitochondria. The zone of decondensed chromatin expands gradually until nearly one half of the nucleus is decondensed (Fig. 5b). The chromatin decondensation occurs at the same time as the acrosome reaction.

3 Sperm penetration

It is very difficult to find the fertilizing spermatozoon in electron microscopic thin sections. The steps in the process of sperm penetration are shown in Figures 7a, b and Figure 8. In *L. limicola,* sperm incorporation begins at the posterior region of the spermatozoon. The sperm organelles are incorporated into the ooplasm in the following order: the microfilaments of the subacrosomal region are incorporated first and are immediately followed by the five sperm mitochondria, the pair of centrioles and the axial filament. The sperm nucleus with partially decondensed chromatin is the last to enter the ooplasm closely following the other organelles (Fig. 8). After penetration, the nucleus moves away from the mitochondria at the base of the fertilization cone, migrates into the ooplasm and developes into the sperm pronucleus.

Within a few seconds after insemination, before the SGV and Pvs have completely formed in the egg investments, the spermatozoa which have reached the oocyte surface by directly passing through the egg investments or by way of the jelly canal enter the ooplasm polyspermically beginning at their heads. This form of sperm entry bears a resemblance to phagocytosis. The acrosomes of these spermatozoa remain unchanged. Since these spermatozoa cannot fuse with the egg plasma membrane due to their abnormal entry, they are ejected from the oocyte surface into the SGV as rapid

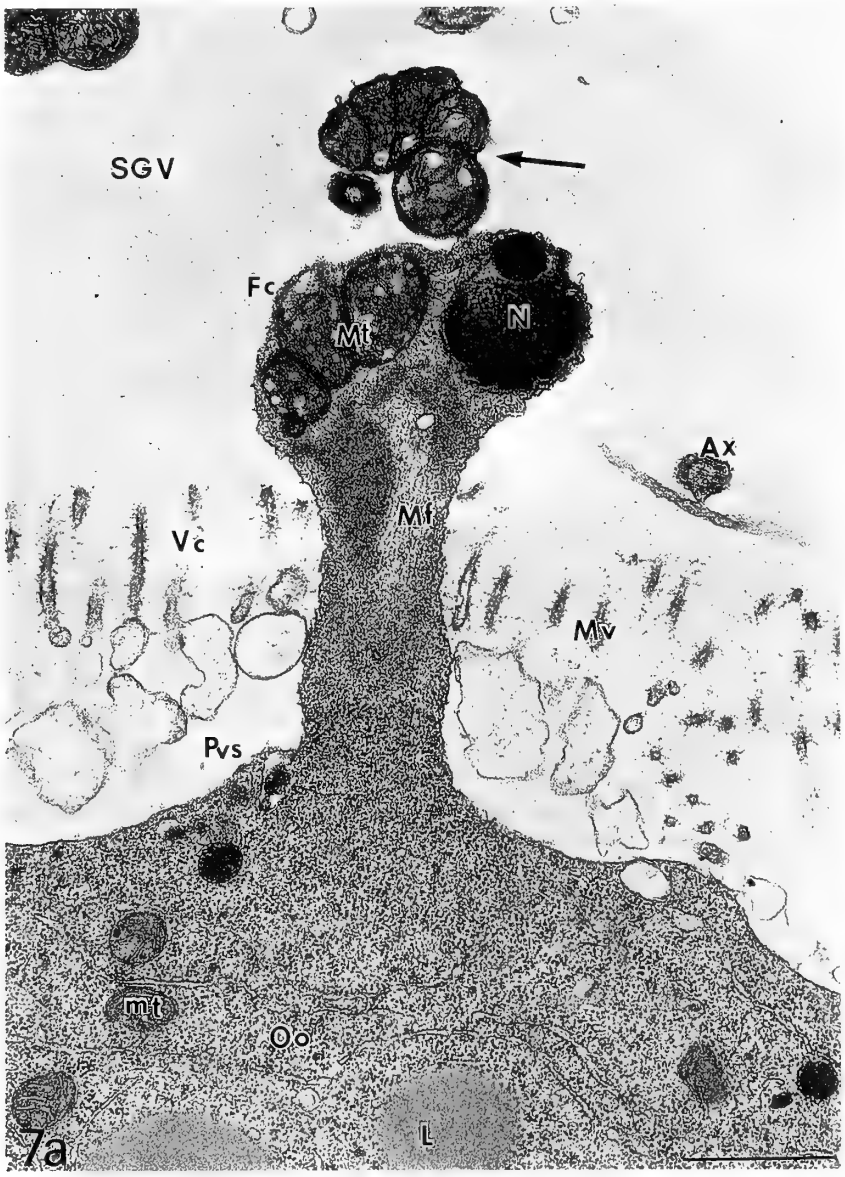

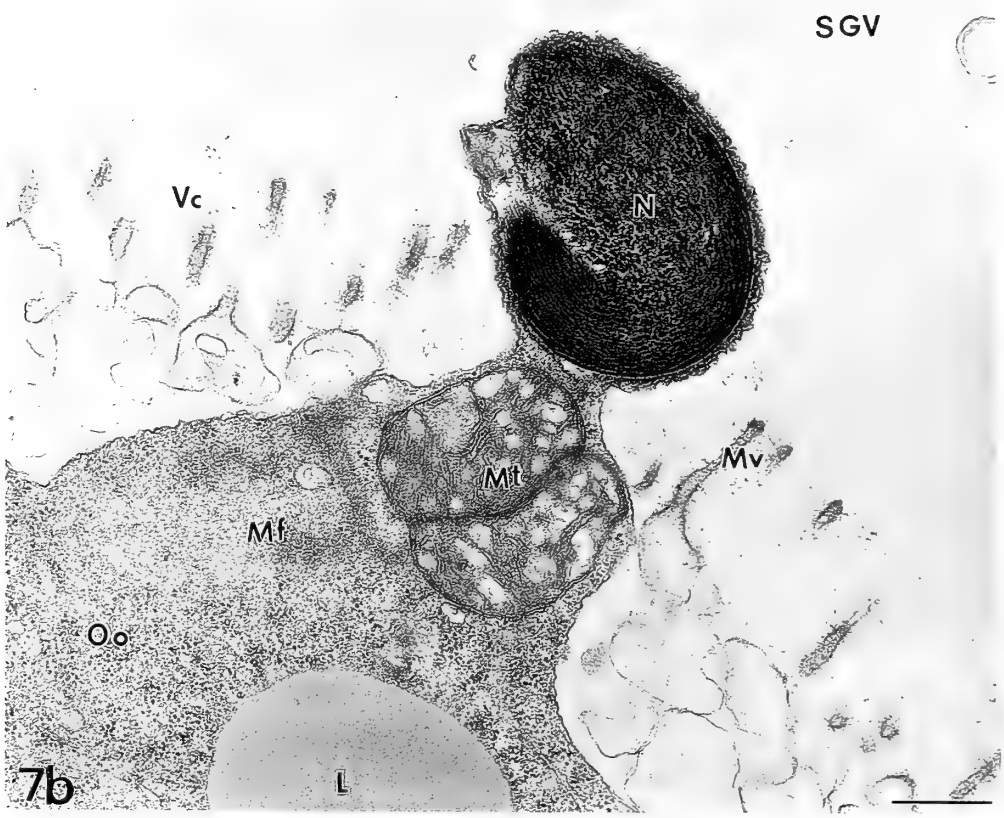

FIG. 7. Fertilization cone (Fc) formed by a spermatozoon fused with a microvillus (Mv).
a: The fertilization cone has formed through and beyond the vitelline coat (Vc). The subacrosomal microfilaments (Mf) precede the mitochondria and nucleus in the fertilization cone. An arrow indicates the mitochondria (Mt) of another spermatozoon. Bar: 1 μm.
b: A spermatozoon of which the mitochondrial mid-piece has traversed the vitelline coat (Vc). The nucleus (N) follows behind the mitochondria (Mt), but it is still outside the vitelline coat. Note the disposition of the microfilaments (Mf), mitochondria (Mt) and nucleus in the fertilization cone. The fertilization cone is gradually shrinking in extent until at last the nucleus enters into the oocyte (Oo). Bar: 0.5 μm.
Ax: Axial filament, L: Lipid granule, mt: Oocyte mitochondria, Pvs: Perivitelline space, SGV: Space between granular layer and vitelline coat.

changes in the egg investments occur.

The main findings of this study are outlined diagrammatically in Figure 9.

DISCUSSION

In this study, the processes of acrosome reaction, the contact and fusion of the sperm plasma membrane with the egg plasma membrane, and sperm penetration into the oocyte were observed at the ultrastructural level in the bivalve *Laternula limicola*.

According to Kubo [25], the mature spermatozoon does not have a typical acrosome situated anterior to the nucleus. However, in the spermatid, a structure similar to an acrosome and derived from the Golgi complex is temporarily located anterior to the nucleus. In late spermiogenesis, this acrosome-like structure finally moves to the posterior region of the mitochondrial mid-piece along the lateral side of the nucleus. Its formation is almost identical to that of a typical acrosome. Due to this structural shift to the posterior mid-piece, Kubo assigned it the new name of "temporary acrosome" and then suggested that the temporary acrosome is a kind of degressive acrosome.

Our observations of the ultrastructural features of mature spermatozoa are nearly consistent with Kubo's description [25]. The authors found that during fertilization the temporary acrosome changed in structure. Moreover, our electron microscopic observations revealed that sperm penetration occurs through this temporary acrosome. The morphological changes in this acrosome correspond closely to the general concept of the acrosome reaction as described by Dan [9, 10] and Colwin and Colwin [7, 8], but the structure of the reacted acrosome lacks the extension of an axial rod as seen in other invertebrate species such as the mussel [36], the sea urchin [12], the asteroid [47] and the abalone [46, 54]. The microfilaments that appear in the fertilization cone may be reorganized from invisible fibrillar elements included in the subacrosomal region. These are presumably similar to

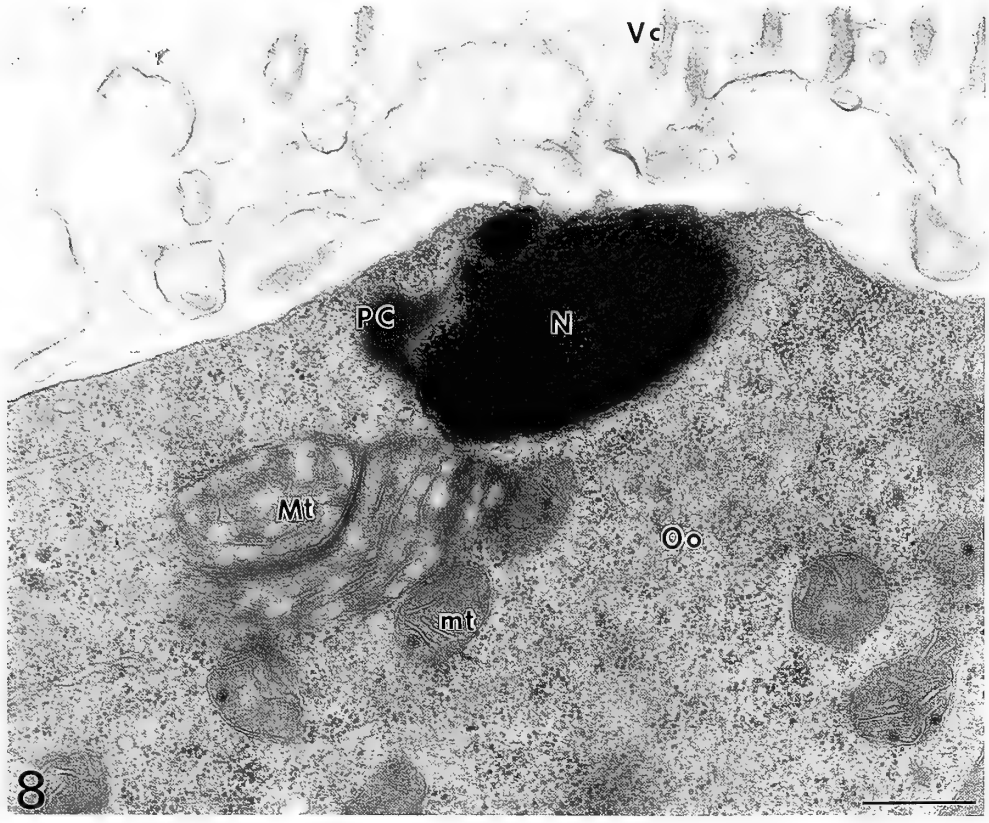

FIG. 8. The incorporated spermatozoon. The sperm mitochondria (Mt) are larger than the oocyte mitochondria (mt). Bar: 0.5 μm.
N: Nucleus, Oo: Oocyte, Pc: Proximal centriole, Vc: Vitelline coat.

the acrosomal actin filament of the axial rod extending from the reacted acrosome as reported previously by Tilney [51, 52] and Shiroya [46].

Further observation is necessary to elucidate the triggers [11] for this acrosome reaction and to obtain detailed information on the significance of the pit formed in the first stage of the acrosome reaction.

It is a matter of common knowledge that the spermatozoa of a number of invertebrate species enter the egg or the oocyte from the apex of the nucleus [1, 6, 14, 15, 35, 44, 45, 50] or in mammals from the lateral side of the nucleus [56]. This pattern has been observed in almost all studies on fertilization including those of species in which the spermatozoa lack an acrosome [4, 21, 23, 28, 40].

The mature spermatozoon of *L. limicola* not only possesses an acrosome at the posterior end of the mid-piece, in contrast to its ordinary position, but also fuses with the egg plasma membrane at the ventral lateral region of the reacted acrosome during fertilization of mature egg. The spermatozoon enters the oocyte through a fertilization cone formed by fusion betwkeen the inner acrosomal membrane and the plasma membrane of an oocyte microvillus. The sperm organelles enter the oocyte in reverse order to that observed in other species; that is, the nucleus follows the mid-piece mitochondria. This mode of sperm penetration has not been previously reported. This is the first report of this unusual mode of fertilization. The fertilized eggs used in this study continued to develop through the D-shaped veligier larvae phase as previously reported by the authors [19]. Thus, participation of the posterior acrosome in fertilization is normal for this species. The authors suggest that the acrosome of *L. limicola* spermatozoa ought to be referred to as a "typical acrosome" rather than the term "temporary acrosome" coined by Kubo [25].

In 1979, Kubo *et al.* have reported their ultrastrutural studies on sperm-egg interaction at the time of fertilization from a viewpoint that the mature spermatozoon in *L. limicola* has an atypical acrosome [27]. Their observations were as follows. The temporary acrosome does not change morohollogically. The sperm penetrates into the egg leaving the mid-piece with its mitochondria and temporary acrosome on the outside of the egg. The sperm head is engulfed by the egg surface, but the sperm plasma membrane and egg plasma membrane do not fuse. Thus, the temporary acrosome has no function in sperm-egg interaction.

In the present studies, the authors found that the posterior acrosome undergoes the acrosome reaction and enters the egg along with the mitochondria, nucleus and tail. Our observations of the fertilization process in *L. limicola* did not coincide with the description presented by Kubo *et al.* [27].

The role of the posterior acrosome in the process of fertilization is one of the more intriguing questions regarding

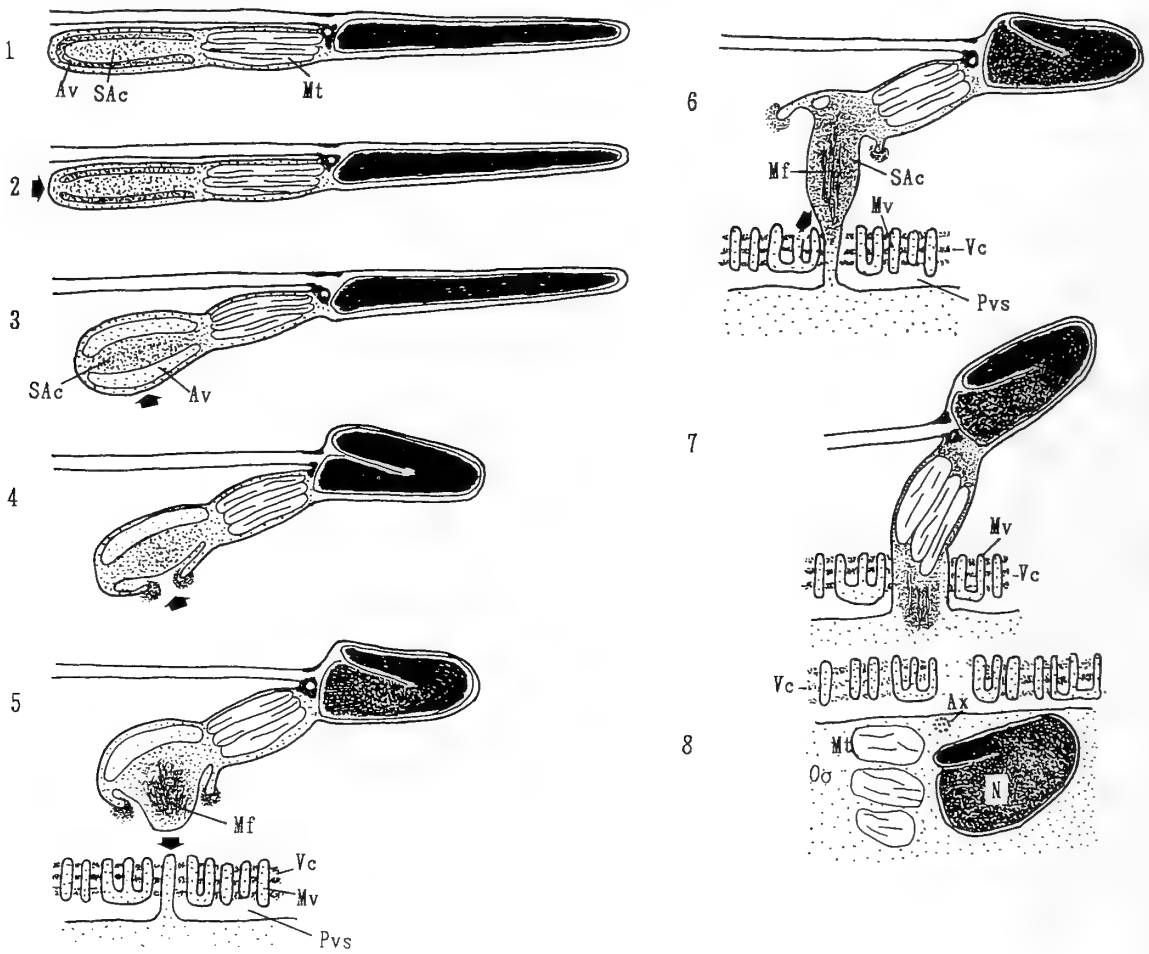

FIG. 9. Diagrammatic illustration of the spermatozoon and successive steps of sperm pentration into the oocyte.
1: Intact spermatozoon.
2: A spermatozoon at the beginning of the acrosome reaction. An arrow indicates the pit formed at the posterior apical part of the acrosoma vesicle.
3: An arrow indicates the ventral lateral part of the acrosome.
4: An arrow indicates the opening at the lateral part of the acrosome and the acrosomal vesicle contents that have been extruded from the opening.
5: The spermatozoon approaching the vitelline coat. An arrow indicates the point where the subacrosomal region will be able to contact the microvilli.
6: An arrow indicates the membrane fusion between the subacrosomal region and the tip of a microvillus in continuous contact with the egg plasma membrane.
7: The formation of the fertilization cone.
8: The incorporated spermatozoon.
Av: Acrosomal vesicle, Ax: Axial filament, Mf: Microfilament, Mt: Sperm mitochondria, Mv: Miocrovilli, N: Nucleus, Oo: Oocyte, Pvs: Perivitelline space, SAc: Subacrosomal region, Vc: Vitelline coat.

the mode of sperm penetration, but as yet relatively little is known about acrosomes situated at the posterior region of the sperm mid-piece as reported by Kubo in the bivalve, *Laternula limicola* [25], Kubo and Ishikawa in the bivalve, *Lyonsia ventricosa* [26], Reger in the tick *Amblyomma dissimili* [41] and Bawa in the fire-brat insect, *Thermobla domestica* [2]. The significance of the posterior relocation of the acrosome during late spermiogenesis with regard to sperm penetration has not been defined for other species. Further studies in species with spermatozoa similar to those of *L. limicola* would be necessary for consideration of any phylogenetic comparative significance.

One notable observation is that the sperm nucleus folds in half dorsaly and begins decondensation of its chromatin while the acrosome reaction is progressing. According to Longo [29] and Longo and Anderson [30], the condensed chromatin generally undergoes decondensation after the sperm nucleus has been incorporated into the ooplasm. However, this phenomenon in *L. limicola* is different from the ordinary form of chromatin decondensation. In this study, it was not possible to determine why the nucleus folded in half and why the condensed chromatin started to decondense before sperm incorporation. It may be interesting to determine whether or not the acrosome reaction is directly

related to chromatin decondensation, although these two events are quite distinctive from each other.

Schatten and Mazia [45] have described a phenomenon in fertilization of the sea urchin egg in which the incorporated spermatozoon rotates to position its centriole end to face inward. In the case of the *L. limicola* spermatozoon, it does not seem necessary to rotate 180°, because the sperm enters with the mid-piece facing the oocyte. A full-process of male pronuclear development has not described in this study.

The SGV, which is newly created in the egg investments just before fertilization, provides the place where the acrosome undergoes morphological change. The reacted acrosome contacts and fuses with the egg plasma membrane and the fertilization cone forms in the SGV. It appears that the oocyte must secrete into the SGV some materials which induce the sperm to activate. The creation of the Pvs in the egg investments has a restraining effect on polyspermic penetration, since the Pvs interrupts the connections between most microvilli and the egg plasma membrane. In consequence, the success of fertilization depends on whether or not the reacted acrosomal region touches a microvillus which is still in continuous contact with the egg plasma membrane.

This report has not made mention of the role of the material contained in the acrosomal vesicle. However, there is no doubt that it participates in the fertilization of this species as a sperm agent (lysin? [10], bindin? [55]) acting on the oocyte. The spermatozoon does not need to disperse this material within the jelly and granular layers of the egg investments, because the spermatozoa can pass through these layers without undergoing the acrosome reaction. The authors tried to immunocytochemically test using an antibody (provided by Haino-Fukushima [16]) against the 15.5K vitelline coat lysin extracted by Haino-Fukushima from spermatozoa of the abalone, *Haliotis discus,* to determine whether it would cross-react immunocytochemically with any antigen in a thin section of a *L. limicola* acrosomal vesicle. The protein A-Gold technique was used [16]. The gold label was not found in the region of the *L. limicola* acrosomal vesicle. The chemical characterization and role of the acrosomal vesicle contents in *L. limicola* spermatozoa are subjects of intense and continuing interest.

ACKNOWLEDGMENTS

The authors wish to thank Dr. Cherrie A. Brown, Calif. Regional Primate Research Ctr. Univ. of California, for reading of the manuscript, and Dr. Haino Fukushima, Department of Biology, Metropol. Univ., Tokyo, who kindly provided an antibody against the 15.5K Vc. Lysin of the abalone.

REFERENCES

1 Anderson WA and Eckberg WR (1983) A cytological analysis of fertilization in *Chaetopterus pergamentaceus.* Biol Bull 165: 110–118

2 Bawa SR (1961) Electron microscope study of spermiogenesis in a fire-brat insect, *Thermobia domestica* pack. 1. Mature spermatozoon. J Cell Biol 23: 431–446

3 Billard R (1983) Ultrastructure of trout spermatozoa: Changes after dilution and deep-freezing. Cell Tiss Res 228: 205–218

4 Brummett AR, Dumont JN, Richter CS (1985) Later stages of sperm penetration and second polar body and blastodisc formation in the egg of *Fundulus heteroclitus.* J Exp Zool 234: 423–439

5 Burghardt RC, Foor WE (1978) Membrane fusion during spermiogenesis in ascaris. J Ultrastr Res 62: 190–202

6 Colwin AL, Colwin LH (1961) Changes in the spermatozoon during fertilization in *Hydroides hexagonus* (ANNELIDA). II. Incorporation with the egg. J Biophys Biochem Cytol 10: 255–274

7 Colwin AL, Colwin LH (1963) Role of the gamete membranes in fertilization in *Saccoglossus kowalevskii* (ENTEROPNEUSTA). I. The acrosomal region and its changes. J Cell Biol 19: 477–500

8 Colwin LH, Colwin AL (1961) Changes in the spermatozoon during fertilization in *Hydroides hexagonus* (ANNELIDA). 1. Passage of the acrosomal region through the vitelline membrane. J Biophys Biochem Cytol 10: 231–254

9 Dan JC (1956) The acrosome reaction. Intern Rev Cytol 5: 365–393

10 Dan JC (1967) Acrosome reaction and lysins. In "Fertilizatioin. Vol 1" Ed by CB Metz and A Monroy, Academic Press, New York, 237–293

11 Dan JC, Kakizawa Y, Kushida H, Fujita K (1972) Acrosomal triggers. Exp Cell Res 72: 60–68

12 Dan JC, Ohori Y, Kushida H (1964) Studies on the acrosome. VII. Formation of the acrosome process in sea urchin spermatozoa. J Ultrastr Res 11: 508–524

13 Dewel WC, Clark WH (1972) An ultrastrutural investigation of spermiogenesis and the mature sperm in the anthozoan *Bunodosoma cavernata* (Cnidaria), J Ultrastr Res 40: 417–431

14 Dube LD, Picheral B, Guerrier P (1983) An ultrastructural analysis of *Dentalium vulgare* (Mollusca, Scaphopoda) gametes with special reference to early events at fertilization. J Ultrastr Res 83: 242–257

15 Franklin LE (1965) Morphology of gamete membrane fusion and of sperm entry into oocytes of the sea urchin. J Cell Biol 25: 81–100

16 Haino-Fukushima K, Usui N (1986) Purification and immunocytochemical localization of the vitelline coat lysin of abalone spermatozoa. Develop Biol 115: 27–34

17 Holland LZ (1988) Spermatogenesis in the salps *Thalia democratica* and *Cyclosalpa affinis* (Tunicata: Thaliarea): An electron microscopic study. J Morphol 198: 189–204

18 Hosokawa K, Noda YD (1986) Electron microscopic observation of egg investments in the bivalve, *Laternula limicola.* Zool Sci 3: 1039 (abstract)

19 Hosokawa K, Noda YD (1991) Oogenesis and development in the bivalve, *Laternula limicola.* Mem Lib Sci Tokyo Dent Coll 7: 1–33 (in Japanese)

20 Hosokawa K, Noda YD (1991) The elevation of the vitelline coat in the bivalve, *Laternula limicola.* Zool Sci 8: 1093 (abstract)

21 Iwamatsu T, Ohta T (1978) Electron microscopic observation on sperm penetration and pronuclear formation in the fish egg. J Exp Zool 205: 157–179

22 Jamuar MP (1966) Studies of spermiogenesis in a nematode, *Nippostrongylus Brasiliensis.* J Cell Biol 31: 381–396

23 Kobayashi W, Yamamoto TS (1987) Light and electron microscopic observations of sperm entry in the chum salmon egg. J Exp Zool 243: 311–322

24 Koehler LD (1979) Unique case of cytodifferentiation: Spermiogenesis of the prawn, *Palaemonetes paludosus.* J Ultrastr

Res 69: 109–120

25 Kubo M (1977) The formation of a temporary-acrosome in the spermatozoon of *Leternula limicola* (Bivalvia, Mollusca). J Ultrastr Res 61: 140–148

26 Kubo M, Ishikawa M (1978) Organizing process of the temporary-acrosome in spermatogenesis of the bivalve *Lyonsia ventricosa*. J Submicr Cytol 10: 411–421

27 Kubo M, Ishikawa M, Numakunai T (1979) Ultrastructural studies on early events in fertilization of the bivalve *Leternula limicola*. Protoplasma 100: 73–83

28 Kudo S (1980) Sperm penetration and the formation of a fertilization cone in the common carp egg. Develop Growth & Differ 22: 403–414

29 Longo FJ (1973) Fertilization: A comparative ultrastructural review. Biol Reprod 9: 149–215

30 Longo FJ, Anderson E (1970b) An ultrastructural analysis of fertilization in the surf clam, *Spisula solidissima*. II Development of the male pronucleus and the association of the maternally and paternally derived chromosomes. J Ultrastr Res 33: 515–527

31 Longo F, Clark WH, Hinsch GW (1988) Gamete interactions and sperm incorporation in the nemertean, *Cerebratulus lacteus*. Zool Sci 5: 573–584

32 Mackinnon BM, Burt MBD (1984) The comparative ultrastructure of spermatozoa from *Bothrimonus sturionis Duv. 1842* (Pseudophyllidea), *Pseudanthobothrium hansei Beer 1956* (Tetraphllidea), and *Menoecocestus americanus Stiles, 1895* (Cyclophyllidea). Can J Zool 62: 1059–1066

33 Maruyama YK, Nakaseko Y, Yagi S (1985) Localization of cytoplasmic determinations responsible for primary mesenchyme formation and gastrulation in the unfertilized egg of the sea urchin, *Hemicentrotus pulcherrimus*. J Exp Zool 236: 155–163

34 Nelson GA, Ward S (1981) Amoeboid motility and actin in *Ascaris lumbricoides* sperm. Exp Cell Res 131: 149–160

35 Nicks JB, Koss R, Chia F-S (1988) Fertilization in a chiton: Acrosome-mediated sperm-egg fusion. Gamete Res 21: 199–212

36 Niijima L, Dan JC (1965) The acrosome reaction in *Mytilus edulis*. I. II. J Cell Biol 25: 243–259

37 Noda YD (1966) Structural changes of the oocyte surface during oogenesis in *Laternula limicola*. Jap J Exp Morphol 20: 137 (in Japanese)

38 Noda YD (1992) Fundermental structure of spermatozoon. In "Spermatology" Ed by H Mohri, M Morisawa and M Hoshi Univ. Tokyo Press, Japan, pp24-41 (in Japanese)

39 Nyholm K-G, Nyholm P-G (1982) Spermatozoa and spermatogenesis in *Homalorhagha kinorhyncha*. J Ultrastr Res 78: 1–12

40 Ohta Y (1985) Electron microscopic observation on sperm entry into eggs of the bitterling during cross-fertilization. J Exp Zool 233: 291–300

41 Reger JF (1963) Spermiogenesis in the tick, *Amblycomma dissimili*, as revealed by electron microscopy. J Ultrastr Res 8: 607–621

42 Reger JF (1964) The fine structure of spermatozoa from the isopod *Asellus militaris* (Hay). J Ultrastr Res 11: 181–192

43 Sakai YT (1976) Spermiogenesis of the teleost, *Oryzias latipes*, with special reference to the formation of flagellar membrane. Develop Growth & Differ 18: 1–13

44 Sato M, Osanai K (1983) Sperm reception by an egg microvillus in the polychaete, *Tylorrhynchus heterochaetus*. J Exp Zool 227: 459–469

45 Schatten G, Mazia D (1976) The penetration of the sjpermatozoon through the sea urchin egg surface at fertilization. Exp Cell Res 98: 325–337

46 Shiroya Y, Hosoya H, Mabuchi I, Sakai YT (1986) Actin filament bundle in the acrosome of abalone spermatozoa. J Exp Zool 239: 105–115

47 Sousa M, Azevedo C (1985) Acrosomal reaction and early events at fertilization in *marthasterias glacialis* (Echinodermata: Asteroidea). Gamete Res 11: 157–167

48 Stanley HP (1969) An electron microscope study of spermiogenesis in the teleost fish *Oligocottus maculosus*. J Ultrastr Res 27: 230–243

49 Summers RG, Hylander BL, Colwin LH, Colwin AL (1975) The functional anatomy of the echinoderm spermatozoon and its interaction with the egg at fertilization. Amer Zool 15: 523–551

50 Takashima R, Takashima Y (1960) Electron microscopical observations on the fertilization phenomenon of sea urchin with special reference to the acrosome filament. Tokushima J Exp Medicine 6: 334–340

51 Tilney LG (1975) Actin filaments in the acrosomal reaction of *Limulus sperm*. J Cell Biol 64: 289–310

52 Tilney LG (1978) Polymerization of actin. V. A new organelle, the actomere, that initiates the assembly of actin filaments in *Thyone* sperm. J Cell Biol 77: 551–564

53 Todd PR (1976) Ultrastructure of the spermatozoa and spermiogenesis in New Zealand fresh water eels (Anguillidae). Cell Tiss Res 171: 221–232

54 Usui N (1987) Formation of the cylindrical structure during the acrosome reaction of abalone spermatozoa. Gamete Res 16: 37–45

55 Vacquier VD, Moy GW (1977) Isolation of bindin: The protein responsible for adhesion of sperm to sea urchin eggs. Proc Nat'l Acad Sci USA, 74: 2456–2460

56 Yanagimachi R, Noda YD (1970) Ultrastructural changes in the hamster sperm head during fertilization. J Ultrastr Res 31: 465–485

ZOOLOGICAL SCIENCE 11: 101–106 (1994)

Experimental Manipulation of Pituitary Hemorrhage Induced by Intraperitoneal Injection of a Hypertonic Solution in Mice

CHIE IGA, ICHIRO KOSHIMIZU, SUMIO TAKAHASHI and YASUO KOBAYASHI*

Department of Biology, Faculty of Science, Okayama University, Okayama 700, Japan

ABSTRACT—Acute and intense hemorrhage into the anterior pituitary in mice can be induced by the intraperitoneal injection of a 35% glucose solution at a dose of 0.03 ml/g bw. Experimental manipulations that stimulate or inhibit this pituitary hemorrhage were investigated. A rise in plasma osmolality paralleled a rise in the incidence of pituitary bleeding. Water deprivation facilitated the incidence of pituitary hemorrhage at a low dose of a 35% glucose solution (0.015 ml/g bw) that was without effect in control mice. In contrast, the incidence of the pituitary hemorrhage reduced in nursing dams. Enhancement of the pituitary hemorrhage was obtained by the pretreatment with agents including norepinephrine, epinephrine, bromocriptine and thiamazole despite a low dose of a glucose solution applied. On the other hand, pituitary hemorrhage was evidently suppressed by treatment with agents including haloperidol, sulpiride, metoclopramide, pentobarbital and ether inhalation prior to the injection of a high dose of the glucose solution. These results suggested a stimulative effect of dopamine on induction of the pituitary hemorrhage.

INTRODUCTION

Our previous study has revealed that intraperitoneal injection of either 9% NaCl, 8% $NaHCO_3$, 3 M glucose or 3 M sucrose caused acute and intense hemorrhage into the anterior pituitary in mice [13]. Ultrastructural evidence at the initial stage of this pituitary hemorrhage was "diapedesis" by which red blood cells migrate through the wall of capillaries without structural destruction of endothelial cells [12]. Intense hemorrhage eventually resulted in profound necrosis of the anterior pituitary followed by some restoration in volume afterwards [15].

No causal analysis has been available, at present, on this pituitary hemorrhage. Then, the present study was designed to explore some experimental conditions and pharmacological agents that act as either stimulative or inhibitory ones on the experimental pituitary hemorrhage.

MATERIALS AND METHODS

Animals

Young and old male mice, and lactating dams of the Jcl/ICR strain were used. Animals were injected intraperitoneally (ip) with a 35% glucose solution at a dose indicated below, and they were killed by decapitation 30 min after the injection. Pituitary hemorrhage was inspected with the naked eyes by dark red color and edematous appearance of the anterior pituitary.

Physiological studies

Animals were divided into 5 groups. In Group 1, mice were used to test the effective dose of a 35% glucose solution. Animals were injected ip with the solution at a dose of either 0.015 ml/g bw, 0.02ml/g bw or 0.03 ml/g bw, respectively. Group 2 consisted of young and old mice at 5, 20 and 30 weeks of age, and they received the ip injection of 35% glucose at a low dose of 0.02 ml/g bw. In Group 3, mice were subjected to water deprivation for 1 or 3 days, and they were given a 35% glucose solution at a low dose of 0.015 ml/g bw. In Group 4, nursing dams of postpartum day 17 were used, and they received a 35% glucose solution at a dose of 0.03 ml/g bw. Day-matched lactating dams were served as the control and their pups were separated for 24 hr prior to the ip injection of a 35% glucose solution. In Group 5, the hematocrit (%) was determined and the plasma osmolality (mOsm/kg) was measured with a Shimadzu OSM-1 Osmometer in mice injected ip with a 35% glucose solution at either a low dose of 0.02 ml/g bw or a high dose of 0.03 ml/g bw.

Pharmacological analysis

The following agents were administered subcutaneously (sc) at the back skin of the neck either alone or in combination 30 min prior to the ip injection of a 35% glucose solution. Animals were divided into 2 groups; Group 1 was applied for an excitatory experiment and Group 2 for a suppressive one.

Animals in Group 1 were given an insufficient low dose of a 35% glucose solution (0.02 ml/g bw). Test agents used and each dose were as follows; phenylephrine-HCl 1 μg/g bw, an α-adrenaline receptor agonist; isoproterenol-HCl 1 μg/g bw, a β-adrenaline receptor agonist; phenoxybenzamine-HCl 20 μg/g bw, an α-adrenaline receptor antagonist; dl-propranolol-HCl 1 μg/g bw, a β-adrenaline receptor antagonist; adrenocorticotropic hormone (ACTH) 40 mU/g bw; vasopressin 5 mU/g bw; 5-hydroxytryptophan (5-HTP) 25 μg/g bw for 3 days; 5-hydroxytryptamine (5-HT) 2 μg/g bw; norepinephrine 3 μg/g bw, epinephrine 2 μg/g bw; bromocriptine methylate 5 μg/g bw, a D-2 dopamine receptor agonist; thiamazol 100 μg/g bw, an anti-thyroid agent.

In Group 2, suppression of this pituitary hemorrhage was tested in mice pretreated with following agents either alone or in combination; d-chlorpheniramine maleate 50 μg/g bw, a histamine receptor antagonist; dl-p-chlorophenylalanine either 100 μg/g bw or 100 μg/g bw for 3 consecutive days, a serotonin synthesis inhibitor; haloperidol

Accepted October 26, 1993
Received August 18, 1993
* To whom requests for reprints should be addressed.

either 5 μg/g bw or 5 μg/g bw for consecutive 3 days, a dopamine receptor antagonist metochlopropamide-HCl 30 μg/g bw, a D-2 dopamine receptor antagonist; sulpiride 150 μg/g bw, a D-2 dopamine receptor antagonist; ether vapor inhalation for 20 min; pentobarbital sodium 50 μg/g bw; and adrenaline receptor agonists and antagonist with the same doses used in Group 1. Statistical significance was assessed by Student's t-test for the mean of hematocrit and osmolality and by χ^2-test for the incidence of pituitary hemorrhage.

RESULTS

Histology

Intense hemorrhage into the anterior pituitary occurred after the ip injection of a 35% glucose solution at a dose of 0.03 ml/g bw. The anterior pituitary was somewhat edematous with the blood cells and plasma migrated out of the capillaries, and the distended hypophysial lumen contained a large mass of blood cells (Fig. 1).

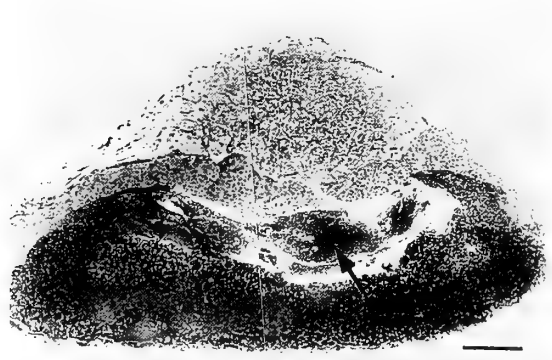

FIG. 1. A parasagittal section of the mouse pituitary gland after intraperitoneal injection of a 35% glucose solution. Erythrocytes migrated from sinusoidal capillaries are darkly stained in the anterior pituitary. The hypophysial lumen is distended and filled with a large mass of blood cells (arrow). Bar indicates 0.2 mm.

Physiological analysis

Intraperitoneal injection of a 35% glucose solution at a dose of 0.03 ml/g bw resulted in pituitary hemorrhage in all 55 young mice tested (100%), but a low dose of either 0.02 ml/g bw or 0.015 ml/g bw was not efficacious (Table 1).

Aging increased an incidence of this pituitary hemorrhage in 8 out of 13 mice (61.5%) at 20 weeks of age and in 9 out of 11 mice (81.8%) at 30 weeks of age despite the low dose (0.02 ml/g bw) of a glucose solution administered (Table 2).

TABLE 1. Effect of intraperitoneal injections of 35% glucose on the incidence of pituitary hemorrhage in 5-week-old male mice

Dose of 35% glucose (ml/g bw)	No. of mice hemorrhaged /no. of animals tested (%)
0.015	0/12 (0%)
0.02	0/27 (0%)
0.03	55/55 (100%)

Animals were sacrificed 30 min after the injection.

TABLE 2. Age-related incidence of anterior pituitary hemorrhage in mice given the intraperitoneal injection of 35% glucose at a low dose of 0.02 ml/g bw

Age (weeks)	No. of mice hemorrhaged /no. of mice tested (%)
5	0/27 (0)
20	8/13 (61.5)*
30	9/11 (81.8)*

* $p<0.01$ vs 5 weeks.
No significant difference between those of 20 and 30 weeks.

TABLE 3. Effect of water deprivation on the incidence of anterior pituitary hemorrhage in mice given the intraperitoneal injection of 35% glucose solution at a low dose of 0.015 ml/g bw

Water deprivation (day)	No. of mice hemorrhaged /no. of mice tested (%)
0	0/12 (0%)
1	6/12 (50%)*
3	12/12 (100%)*+

*, $p<0.01$ vs day 0; +, $p<0.01$ vs day 1.

Water deprivation for 1 and 3 days increased an incidence of this pituitary hemorrhage in 6 out of 12 mice (50%) and in 12 of 12 mice (100%), respectively, despite the lowest dose (0.015 ml/g bw) of a glucose solution administered (Table 3).

In contrast, in nursing dams of day 17 postpartum an injection of a high dose (0.03 ml/g bw) of 35% glucose resulted in the bleeding only 4 out of 10 (40%), whereas in day-matched control dams, whose pups were separated for 24 hr prior to the glucose treatment, the injection of 35% glucose resulted in pituitary bleeding in 6 of 6 dams (100%) (Table 4).

TABLE 4. Effect of lactation on the incidence of pituitary hemorrhage and the hematocrit values (HCT) in suckling mice on day 17 postpartum

	No. of hemorrhage /no. of mice tested (%)	HCT (%)
Control	6/6 (100)	54.4±1.4
Suckling	4/10 (40)*	55.2±0.4 NS

In the control, pups were removed their mother for 24 hr before the ip injection of 35% glucose at a dose of 0.03 ml/g. *, $p<0.05$ vs control; NS, non-significant.

High levels of hematocrit values were observed after a 35% glucose treatment, but no significant difference was obtained between two groups of a non-bleeding low dose (0.02 ml/g bw) and a heavy-bleeding high dose (0.03 ml/g bw) (Table 5). Serum osmolality in a low dose and high dose groups was significantly higher than that in the normal control ($p<0.01$, in both comparison, Table 5).

TABLE 5. Hematocrit (%) and osmolality (mOsm/kg) of mice 30 min after the intraperitoneal injection of a 35% glucose solution at either a low dose of 0.02 ml/g bw or a high dose of 0.03 ml/g bw

	Dose of a 35% glucose solution		
	Control	0.02 ml/g bw	0.03 ml/g bw
Hematocrit	47.3±1.0 (8)	57.1±0.6 (9)[1)]	58.0±0.8 (9)[2)]
Osmolality	301.8±2.0 (8)	360.9±3.6 (9)[3)]	397.1±3.7 (9)[4)]

Number of animals is in parentheses. 1), 2), 3) and 4) are different from each control value ($p<0.01$). No significant difference between 1 and 2, and significant difference between 3 and 4 ($p<0.01$).

Enhancement of pituitary hemorrhage

Pituitary hemorrhage was induced by a low dose of 0.02 ml/g bw (a sub-threshold dose) of a 35% glucose solution in combination with pretreatment of following drugs. The results indicated that bleeding occurred in 8 out of 10 mice (80%) with norepinephrine, in 5 out of 7 mice (71.4%) with epinephrine, and in 16 out of 20 mice (80%) with bromocriptine, and in 9 out of 10 mice (90%) with thiamazole, respectively (Table 6). No effects were observed with injections of adrenocorticotropin, vasopressin, serotonin and serotonin precursor.

TABLE 6. Enhancement of pituitary hemorrhage by agents given subcutaneously prior to the intraperitoneal injection of 35% glucose at a low dose of 0.02 ml/g bw

Agents	Dose (μg/g)	No. of mice hemorrhaged /no. of mice tested (%)
Control	—	0/27 (0)
Phenylephrine	1	0/8 (0)
Isoproterenol	1	0/6 (0)
Phenoxybenzamine	20	0/8 (0)
Propranolol	1	0/6 (0)
Adrenocorticotropin	40 mU	1/10 (10)
Vasopressin	5 mU	0/10 (0)
5-Hydroxytryptophan	25×3 days	0/7 (0)
5-Hydroxytrypatamine	2	1/10 (10)
Norepinephrine	3	8/10 (80)*
Epinephrine	2	5/7 (71.4)*
Bromocriptine	5	16/20 (80)*
Thiamazole	100	9/10 (90)*

* $p<0.01$ vs control

Suppression of pituitary hemorrhage

Pituitary hemorrhage was suppressed by the sc treatment of following drugs prior to the ip injection of a 35% glucose solution at a high dose of 0.03 ml/g bw. In this experiment, the rate of suppression was 0 out of 55 mice in the control (0%) (Table 7). Then, pituitary hemorrhage was suppressed in 8 out of 17 mice (47.1%) with ether inhalation, in 16 out of 20 mice (80%) with pentobarbital, in 3 out of 14 mice (21.4%) with haloperidol, in 5 out of 23 mice (21.7%) with sulpiride, in 4 out of 21 mice (19.0%) with a single dose of metoclopramide and, further, in 10 out of 16 mice (62.5%) with metoclopramide for consecutive 3 days (Table 7).

TABLE 7. Suppression of pituitary hemorrhage by agents given subcutaneously prior to the intraperitoneal injection of 35% glucose at a high dose of 0.03 ml/g bw

Agents	Dose (μg/g bw)	No. of mice suppressed /no. of mice tested (%)
Control	—	0/55 (0)[1)]
Phenylephrine	1	0/6 (0)
Isoproterenol	1	0/6 (0)
Phenoxybenzamine	20	0/6 (0)
Propranolol	1	0/8 (0)
Chlorpheniramine maleate	50	0/8 (0)
p-Chlorophenylalanine	100	0/6 (0)
p-Chlorophenylalanine	100×3 days	0/6 (0)
Haloperidol	5×3 days	3/14 (21.4)*
Sulpiride	150	5/23 (21.7)*
Ether vapor	20 min	8/17 (47.1)*
Pentobarbital	50	16/20 (80.0)*
Metoclopramide	30	0/13 (0)
Metoclopramide	60	4/21 (19.0)*
Metoclopramide	30×3 days	10/16 (62.5)*
Ether vapor +Metoclopramide	(20 min) 30×3 days	16/20 (80.0)*
Pentobarbital +Metoclopramide	50 30×3 days	39/39 (100)[2)]*
Pentobarbital +Metoclopramide	50 60	11/11 (100)*

*, $p<0.01$ vs control. Hematocrit of 1) and 2) was 51.7±0.5 and 50.5±0.5, respectively.

Further, metoclopramide (30 μg/g bw) for 3 days in combination with a single exposure of ether vapor was highly suppressive in 16 of 20 mice (80%). Again, three consecutive metoclopramide (30 μg/g bw) in combination with a single injection of pentobarbital (50 μg/g bw) completely inhibited the pituitary bleeding in 39 out of 39 mice (100%). The combined pretreatment of a single high dose of metoclopramide (60 μg/g bw) and pentobarbital (50 μg/g bw) also resulted in the complete suppression of pituitary hemorrhage in 11 out of 11 mice (100%) (Table 7). Both a histamine receptor antagonist and a serotonin synthesis inhibitor had no effects on the bleeding.

Neither stimulative nor inhibitory effects on pituitary hemorrhage were observed in agents of all adrenergic receptor agonists except for norepinephrine and epinephrine, and antagonists (Tables 6 and 7).

DISCUSSION

The present study demonstrated new data concerning experimental manipulations and pharmacological agents

which stimulated or suppressed the occurrence of pituitary hemorrhage induced by the ip injection of a 35% glucose solution in mice.

Physiological study

An efficacious dose of a 35% glucose solution to induce pituitary bleeding is in a narrow range of a sublethal dose, and it depends on age of animals. In our previous studies, a 9% NaCl solution was given to induce pituitary hemorrhage in mice and a sufficient dose for the induction was 0.03 ml/g bw [13]. When a 8.5% NaCl solution of the same dose was used, no pituitary bleeding had been observed in ddY mice [22, 23]. In the present study, a dose of 0.02 ml/g bw of a 35% glucose solution was ineffective to induce pituitary bleeding in young male mice. In old mice, however, a low dose (0.02 ml/g bw) of a 35% glucose solution was sufficient to produce pituitary hemorrhage. This is probably due to either age-associated attenuation in the physiological tolerance to acute dehydration caused by the ip injection of a hypertonic solution or an absolute increase in the volume of the glucose solution injected in old mice (ca. 40–45 g). Therefore, male mice at 5–6 weeks of age and weighing about 30–35 g were used in the present experiments.

Water deprivation for 3 days significantly elicited the occurrence of this pituitary hemorrhage. Gradual dehydration by water deprivation and a subsequent acute dehydration by the ip injection of a hypertonic solution (a sub-threshold dose) could exert their effects on the pituitary bleeding additively in mice. Under this pretreatment of water deprivation, the pituitary seemed to be highly susceptible to subsequent changes in plasma osmolality. Water deprivation-associated rise in osmolality [1], a large increase in the anterior pituitary dopamine content [6] and also an increase in dopamine receptors of human pituitary adenomas [14] are assumed to be involved in the possible mechanism of this pituitary hemorrhage.

In contrast, the decline in the incidence of pituitary hemorrhage in nursing dams may relate to attenuation of inhibitory control by dopamine over prolactin secretion during nursing behavior [6, 17]. Thus, it is likely that a reduced dopamine activity could arrest this pituitary bleeding in mice. Hematocrit values were not different between the control dams and nursing dams each other, so alterations in the condition of body fluid might be ruled out in this case.

An acute rise in osmolality seems to be one of factors necessary to produce pituitary hemorrhage, because pituitary hemorrhage occurred after the injection of a 35% glucose solution in the present study. A gradual increase in osmolality (mOsm/l) by water deprivation did not induce pituitary bleeding [1]. The ip injection of hypertonic saline is assumed to increase serum viscosity by rapid transport of water from the blood into the peritoneal cavity, resulting in high osmotic pressure of the blood [23]. Heavy congestion of hypertonic solution revealed by electron microscopy [13] might reflect the increased serum viscosity.

Pharmacological study

Enhancement of pituitary hemorrhage was obtained by the pretreatment of norepinephrine, epinephrine, bromocriptine and thiamazole in mice given an insufficient low dose (0.02 ml/g bw) of a 35% glucose solution. At present, it is hard to deduce a common action of these agents to explain a possible mechanism of this pituitary bleeding. However, vascular excitatory action of these agents may be partly involved in the pituitary hemorrhage. Epinephrine and norepinephrine are potent vasopressor drugs [10, 24], and epinephrine has long been known to accelerate blood coagulation in animals and man [9]. Both α- and β-adrenoreceptor agonists and antagonists had neither stimulative nor inhibitory effects on pituitary hemorrhage, although epinephrine and norepinephrine enhanced a hypertonic solution-induced-hemorrhage. Association of bundles of unmyelinated nerve fibers with blood vessels in the anterior pituitary was often observed, and these nerve fibers are assumed to be not vasomotor nerves in rats [16]. Epinephrine and norepinephrine may act at vascular systems other than the pituitary portal one.

Furthermore, bromocriptine is a potent dopaminergic agonist at D_2 receptors [18]. Bromocriptine is well known to regress the bulk of tumors such as prolactin- and growth hormone- secreting adenomas. Pituitary apoplexy occurring in the course of chronic bromocriptine therapy has been reported in man [25], suggesting that bromocriptine suppression of the growth of pituitary adenomas resulted from a necrosis of the tumor tissue followed by hemorrhage into adenomas. Although pituitary apoplexy has not been described as a complication of bromocriptine therapy in man, the pretreatment of bromocriptine has induced significant enhancement of the pituitary hemorrhage in mice. Bromocriptine must have acted as a dopaminergic agonist at the pituitary level.

The use of thiamazole, an anti-thyroid gland drug, was based on the previous observation that thyroidectomy in rats usually resulted in apparent congestion of the anterior pituitary (unpublished data). These actions of thiamazole may be indirect ones, because TRH raised blood pressure in hypothyroidal animals [11]. A significant increase in portal plasma flow (140%) in hypothyroid rats rendered by propylthiouracil has been demonstrated [7]. Although it is uncertain that responses of TRH secretion and of blood flow could occur immediately after the administration of thiamazole, either direct or indirect actions of thiamazole might be involved in the mechanism of this pituitary bleeding.

Pituitary apoplexy has been documented in patients given a triple bolus test of TRH, LRH and insulin [5]. Thus, various hormones and agents are known to cause incidental pituitary apoplexy in man. In the present study, catecholamines, dopamine agonists and anti-thyroidal drugs were shown to enhance the incidence of experimental pituitary hemorrhage through an unestablished mechanism(s) in mice.

On the contrary, agents that arrested pituitary hemorrhage were haloperidol, metoclopramide, ether vapor and

pentobarbital. Haloperidol, metoclopramide and sulpiride were used as dopaminergic blockers [8, 19]. There is a good contrasting relation between effects of dopamine receptor agonists as an enhancer of the pituitary hemorrhage in mice and those of dopamine receptor antagonists as a suppressor. The rates of suppression of pituitary hemorrhage with haloperidol, sulpride and metoclopramide were, however, rather low (20%), although pharmacologically over-doses were used. In this connection, the present study indicated that the combined pretreatment of dopamine antagonists and anesthetics resulted in complete suppression of the pituitary hemorrhage in some cases.

Anesthetics such as pentobarbital and ether vapor alone showed a highly suppressive effect on the bleeding by 80.0% and 47.1%, respectively. In our previous experiments, neither intestinal peristalsis nor pituitary bleeding occurred although a rather excess volume of a hypertonic solution was infused into the opened peritoneal cavity of mice after laparotomy under ether anesthesia (unpublished data). Thus, inhibition of pituitary bleeding by anesthetics may be related to deterioration of the intestinal peristalsis, but at least to the reported action of brain ischemia by barbital [20, 21]. When peristalsis was enfeebled by anesthetics, the intestines could not respond normally to hypertonic solutions and the incidence of pituitary hemorrhage would be lowered.

If the site of action of dopamine antagonists and anesthetics is different, combined treatment with dopamine antagonists and anesthetics would give additive or synergistic effects on pituitary hemorrhage. As speculated, combination of pentobarbital (50 μg/g bw) and metoclopramide (60 μg/g bw) resulted in complete suppression of this pituitary bleeding. However, ED_{50} should be matched between two agents of pentobarbital and metoclopramide. The present study is the first report on experimental manipulations as to stimulation and inhibition of the hypertonic solution-induced pituitary hemorrhage in mice. The exact mechanism of this bleeding remains to be disclosed.

As to the organ specificity of this pituitary hemorrhage, the specific vascular architecture of the anterior pituitary may be concerned. The capacity of the venous connections draining the adenohypophysis to the cavernous sinus appeared small when compared to that of the long portal vessels supplying the adenohypophysis [3, 4]. Thus, it is supposed that venous hyperemia would easily take place in the anterior pituitary when the inflow of the blood into the gland is larger than the outflow in mice given the ip injection of a hypertonic solution.

No enhancement of the pituitary bleeding was observed by the pretreatment of vasopressin, adrenocorticotropin, 5-hydroxytryptophan and 5-hydroxytryptamine, respectively, probably due to lack of interaction of these agents to the sinusoidal capillaries of the anterior pituitary in mice.

REFERENCES

1 Aguilera G, Lightman SI, Kiss A (1993) Regulation of the hypothalamic-pituitary-adrenal axis during water deprivation. Endocrinology 132: 241–248

2 Alper RH, Demarest KT, Moore KE (1980) Dehydration selectively increases dopamine synthesis in tuberohypophyseal dopaminergic neurons. Neuroendocrinology 31: 112–115

3 Bergland RM, Page RB (1978) Can the pituitary secrete directly to the brain? (Affirmative anatomical evidence). Endocrinology 102: 1325–1338

4 Bergland RM, Page RB (1979) Pituitary-brain vascular relations: A new paradigm. Science 204: 18–24

5 Bernstein M, Hegele RA, Gentili F, Brothers M, Horgate R, Sturtridge WC, Deck J (1984) Pituitary apoplexy associated with a triple bolus test. Case report. J Neurosurg 61: 586–590

6 Demarest KE, Riegle GD, Moore KE (1984) Adenohypophysis dopamine content during physiological changes in prolactin secretion. Endocrinology 115: 2091–2097

7 Eckland DJA, Lightman SL (1987) Hypothalamo-hypophyseal blood flow: A novel control mechanism in pituitary function? J Endocrinol 113: R1–2

8 Fielding S, Lal H (1978) Behavioral actions of neuroleptics. In "Handbook of Psychopharmacology Vol 10" Ed by LL Iversin, SD Iversien, SH Snyder, Plenum Press, New York, pp 91–128

9 Forwell GD, Ingram GIC (1957) The effect of adrenaline infusion on human blood coagulation. J Physiol Lond 135: 371–383

10 Goldengerg M, Aranow H Jr, Smith AA, Faber M (1950) Pheochromocytoma and essential hypertensive vascular disease. Arch Intern Med 86: 823–836

11 Horita A, Carino MA, Lai H (1987) Pharmacology of thyrotropin-releasing hormone. Annu Rev Pharmacol Toxicol 26: 311–332

12 Kobayashi Y, Iga C (1989) Erythrocyte diapedesis in anterior pituitary hemorrhage after intraperitoneal injection of hypertonic solution in mice. Zool Sci 6: 359–365

13 Kobayashi Y, Masuda A, Kumazawa T (1982) Hypertonic solutions induce hemorrhage in the anterior pituitary in mice. Endocrinol Japon 29: 647–652

14 Koga M, Nakano H, Arai M, Sato B, Noma M, Morimoto Y, Kishimoto S, Mori S, Uozumi T (1987) Demonstration of specific dopamine receptors on human pituitary adenomas. Acta Endocrinol 114: 595–602

15 Koshimizu I, Awamura N, Takeuchi S, Kobayashi Y (1992) Structural changes and morphometrical analysis of the pituitary gland after hemorrhage induced by intraperitoneal injection of hypertonic solution in mice. Biomed Res 13: 253–258

16 Kurosumi K, Kobayashi Y (1980) Nerve fibers and terminals in the rat anterior pituitary gland as revealed by electron microscopy. Arch Histol Jpn 43: 141–155

17 Leong DA, Frawley LS, Neill JD (1983) Neuroendocrine control of prolactin secretion. Annu Rev Physiol 45: 109–127

18 Markstein R (1981) Neurochemical effects of some ergot derivatives: A basis for their antiparkinson actions. J Neural Trans 51: 49–59

19 McCallum RW, Albibi R (1983) Metoclopramide: Pharmacology and clinical application. Ann Intern Med 98: 86–95

20 Shapiro HM (1985) Barbiturates in brain ischemia. Br J Anaesth 57: 82–95

21 Steer CR (1982) Barbiturate therapy in the management of cerebral ischemia. Dev Med Child Neurol 24: 219–231

22 Takeshita M, Doi k, Mitsuoka T (1988) Brain lesions induced by hypertonic saline in mice: Dose and injection route and

incidence of lesions. Exp Anim 37: 191–194

23 Takeshita M, Doi K, Imaizumi Mitsuoka T (1989) Initial Lesions in the mouse brain induced by intraperitoneal injection of hypertonic saline. Exp Anim 38: 31–39

24 Whelan RF, De La Lande IS (1936) Action of adrenalin on limb blood vessels. Br Med Bull 19: 125–131

25 Yamaji T, Ishibashi M, Kosaka K, Fukushima T, Hori T, Manaka S, Sano K (1981) Pituitary apoplexy in acromegaly during bromocriptine therapy. Acta Endocrinol 98: 171–177

ZOOLOGICAL SCIENCE 11: 107–111 (1994)

Ecdysteroid Synthesis in Dissociated Cells of the Prothoracic Gland of the Silkworm, *Bombyx mori*

MASAKO ASAHINA[1], HAJIME FUGO[1]* and SATOSHI TAKEDA[2]

[1]*Department of Environmental Science and Resources, Faculty of Agriculture, Tokyo University of Agriculture and Technology, Fuchu-shi, Tokyo 183 and*
[2]*National Institute of Sericultural and Entomological Science, Tsukuba, Ibaraki 305, Japan*

ABSTRACT—A method for the preparation of viable cells of prothoracic glands of *Bombyx mori* was developed. Dissected prothoracic glands (PGs) from larvae at the spinning stage were incubated in the Grace's insect culture medium containing dispase (6,000 PU/ml of medium at pH 6.5) at 37°C for 15 min. After centrifugation for 2 min at 250 rpm, resultant cells were incubated with Grace's insect medium for designated times. After this treatment 87±7% of the cells remained viable as judged by exclusion of trypan blue. The amounts of ecdysteroid secreted into medium by these cells were approximately 70 to 80% of the amounts secreted by intact PGs. The rates of ecdysteroid secretion over 6 hr in organ culture and in cell culture were quite similar, although the amounts of ecdysteroid detected in the latter medium were somewhat lower.

INTRODUCTION

The synthesis of radioactive ecdysone made possible the development of the radioimmunoassay (RIA) which provided an extremely sensitive, simple and cheap method of detecting ecdysteroid [2, 5, 17]. By using these techinques, it is now well established that ecdysone is the product of the PGs and that its production and release is controlled by the prothoracicotropic hormone (PTTH) [1, 3, 8, 13, 18].

In *Bombyx* the studies on the mode of action of PTTH on the PGs and biochemical processes on the regulation of ecdysteroid synthesis by PTTH are quite few, although identification and isolation of PTTH have been developed [6, 7, 9]. In the present study, we demonstrate an improved method for preparing the dispersed cells of PG for the investigation of mode of action of PTTH.

MATERIALS AND METHODS

Insects

Larvae of the silkworm, *Bombyx mori* (J122×C115), were reared with mulberry leaves or artificial diet (Nihon Nosan Kogyo, Yokohama) in a rearing room of our laboratory at 25±1°C in a 16 hr light: 8 hr dark photoperiod. Larvae were staged on the day of 4th ecdysis, and this day was designed as Day 0 of 5th instar. Only female animals were used throughout the experiments.

Preparation of larval prothoracic gland

After immersing the larvae into 75% of ethanol for 2 to 3 min, the prothoracic glands (PGs) of the staged larvae were removed. The PGs were rinsed with physiological saline (0.85% NaCl) for *Bombyx* and then with Grace's medium (GIBCO, USA) two to three times to avoid contamination by haemolymph. Thereafter, PGs were incubated in Grace's medium or were treated with a medium containing dispase as described below.

Preparation of incubation medium containing dispase

To dissociate the cells of the PG, we used a proteolytic enzyme, dispase, (Godo Shusei, Tokyo). The optimal pH for this enzyme is between 7.5 and 8.0 and the optimal temperature is 25 to 37°C. The pH of the silkworm haemolymph is about 6.5. Accordingly, the pH of the medium was adjusted with 1 N NaOH to either pH 6.5 or pH 8.0 before use. The dispase was then dissolved in this medium. Activity of this enzyme was represented as protease units per ml of medium. Incubation temperature was 25 or 37°C.

Incubation of prothoracic gland or its cells

PGs were dissected from the staged animals and incubated immediately. A pair of glands was incubated in 300 μl of Grace's medium at 25°C. Thirty microliter aliquots of the medium were taken for RIA at various times and were replaced by 30 μl of fresh medium.

In the case of dissociated cells, larval PGs were incubated in various concentrations of dispase in Grace's medium for 15–60 min at either 25 or 37°C. After several rinses with Grace's medium, one pair glands equivalent of dissociated cells was incubated in 300 μl of medium. During the incubation, the reaction mixture was shaken gently with a micromixer (TAITEC: EM 33, Japan) and cells were dissociated by drawing the tissue in and out of a siliconized Pasteur pipette about 80 times at 15 min intervals for up to 1 hr.

Viability of the dissociated cells of prothoracic gland

After dispase treatment, the viability of the dissociated cells was checked using 0.1% trypan blue. Viable cells excluded this dye, whereas dead cells became blue.

Estimation of ecdysteroids in haemolymph and in culture medium

Haemolymph (10 μl) or medium (30 μl) was subjected to an ecdysteroid radioimmunoassay (RIA) [15]. Ecdysteroids were extracted with 300 μl of absolute methanol, then aliquots of the

Accepted December 20, 1993
Received October 7, 1993

* To whom all correspondence should be addressed.

supernatant were assayed for ecdysteroid by RIA. Since 20-hydroxyecdysone was used as a standard, the average values of the amount of ecdysteroids are expressed as ng of 20-hydroxy-ecdysone equivalents ± standard deviation. The tritiated ligand[23, 24-^{3}H(N)] ecdysone (82.8 Ci/mmol) was purchased from New England Nuclear.

RESULTS

Dissociation of prothoracic gland cells by a proteolytic enzyme, dispase

For studies of ecdysteroid synthesis in dissociated cells of the PG *in vitro,* the following prerequisites must be fulfilled by the experimental procedure: low variability among replicate samples, rapid and easy methods for handling of large numbers of cells, homogeneity among the dispersed cells, and maintenance of viability for at least 6 to 8 hr during the incubation.

The PG cells in *Bombyx* are compact and surrounded by a thick basal lamina (Fig. 1 [16]). Therefore, we tried various enzymes to obtain viable preparations of single PG cells. Preliminary incubations with either trypsin or collagenase were not satisfactory since most cells were not viable (data not shown). By contrast, with dispase treatment, PG cells partially dissociated and remained viable. In order to obtain viable cells of PG consistently, we sought to establish procedures for preparing single cells of PG.

Firstly, PGs from day 9, 5th instar *Bombyx* larvae, were incubated for various times in Grace's medium containing several concentrations of dispase at different pHs and temperatures. Five pairs of PG were removed and rinsed first with physiological saline for *Bombyx*, then with Grace's medium. These organs were incubated in a disposable plastic dish (Corning, 35×10 mm) with 2 ml of dispase solution (0 to 1,500 PU/ml Grace's medium).

At 25°C the cells of PG showed little dissociation even at the highest enzyme concentration used (1,500 PU/ml for 60 min) irrespective of pH (Table 1). Under these conditions, the cells were dispersed gradually with time and concentration of enzyme but some clusters of cells remained, and the dissociated cells were significantly damaged. Accordingly, these conditions were not sufficient for preparation of viable cells from PG. On the other hand, when the PGs were incubated with dispase at 37°C, quantities of dispersed cells could be obtained both at pH 6.5 (Fig. 2) and pH 8.0 (Table 1). However some precipitates of cellular debris were observed at higher enzyme concentrations at pH 8.0. Thus, it seemed that the treatment with dispase at pH 8.0 was unsatisfactory for preparing viable cells of PG.

Secondly, the effects of dispase concentration on the dissociation of PG cells were investigated. A pair of PG from a larva in the spinning stage (day-9) was treated with various concentration of dispase in Grace's medium (pH 6.5) at 37°C. As shown in Figure 3, there was no correlation between the enzyme concentration and the percentage of viable cells. The yield of viable cells was 86.8±7.2% for all concentrations from 1.5 to 10×10^3 PU/ml.

Lastly, we separated a pair of PGs and treated each individual PG with dispase (pH 6.5, 6000 PU/ml, 15 min, 37°C) to determine the cell number in the PG. There was no difference between the cell number in the right and the left PG throughout development in the 5th instar with the average number of cells between 160 to 230 in both right and left PG (data not shown).

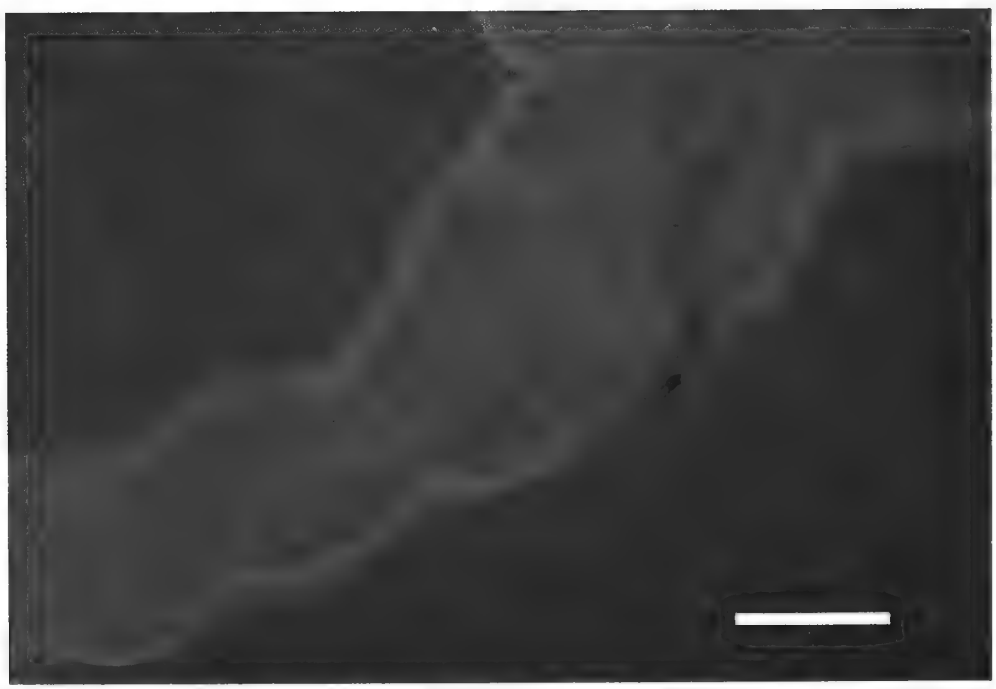

FIG. 1. Prothoracic gland in *Bombyx mori.* Bar, 100 μm.

TABLE 1. Dissociation of prothoracic glands by dispase under different conditions

Concentration of dispase (PU/ml)	Incubation time (min) 15	30	45	60	Incubation time (min) 15	30	45	60
	[pH 6.5 at 25°C]				[pH 6.5 at 37°C]			
0	−	−	−	−	−	−	−	−
500	−	−	±	±	±	+	++	+
1,000	±	±	±	++	±	+	++	++
1,500	±	+	+	++	++	+++	+++	+++
	[pH 8.0 at 25°C]				[pH 8.0 at 37°C]			
0	ND	ND	ND	ND	−	−	−	−
500	ND	ND	ND	ND	ND	ND	+	+
1,000	ND	ND	ND	ND	+	+	++	++
1,500	ND	ND	+	++	+	+++	++	+++

The grades of the dissociation of prothoracic glands were as follows; −: not dissociated, ±: basal lamina was removed but cells were not dissociated. +: some clusters of prothoracic gland cells seen, ++: partial dissociation of prothoracic glands with a mixture of single cells and groups of 2 to 5 cells, +++: complete dissociation of the prothoracic gland yielding dispersed cells as shown in Fig. 2. ND: not determined.

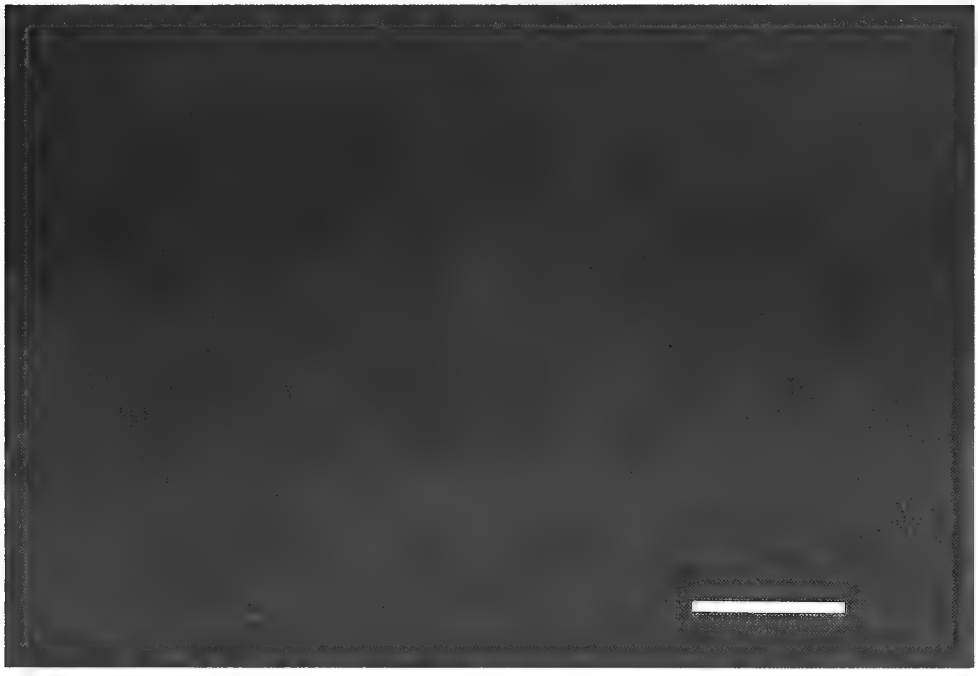

FIG. 2. Dissociated cells of prothoracic glands. The prothoracic glands were treated with 1,500 PU of dispase/ml Grace's medium (pH 6.5) at 37°C for 30 min. Bar, 350 μm.

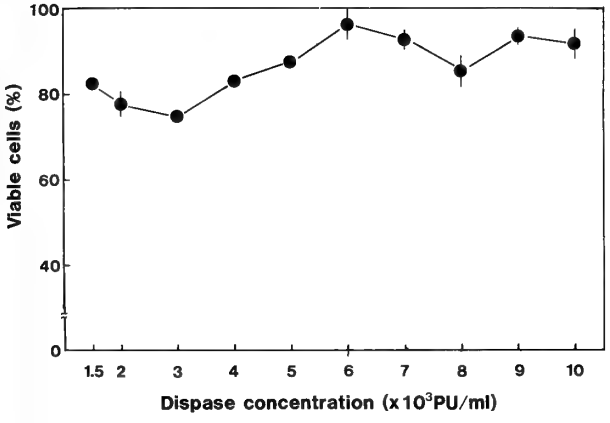

FIG. 3. Relationship between the concentration of dispase in Grace's medium (pH 6.5) and the percentage of viable cells as judged by exclusion of the trypan blue dye.

Secretory activity of ecdysteroid by intact PGs and dissociated PG cells

Intact PGs from larvae in the spinning stage (day-8 to day-10 of 5th instar) were incubated in Grace's medium for 6 hr to determine their secretory ability in comparison to those of dispersed cells. As shown in Figure 4, the secretory activity of PGs on day 8 (1 day after the onset of spinning) was relatively low (10.9±1.8 ng per 6 hr). By day 9, secretory activity increased about 3-fold to 28.6±4.1 ng per 6 hr

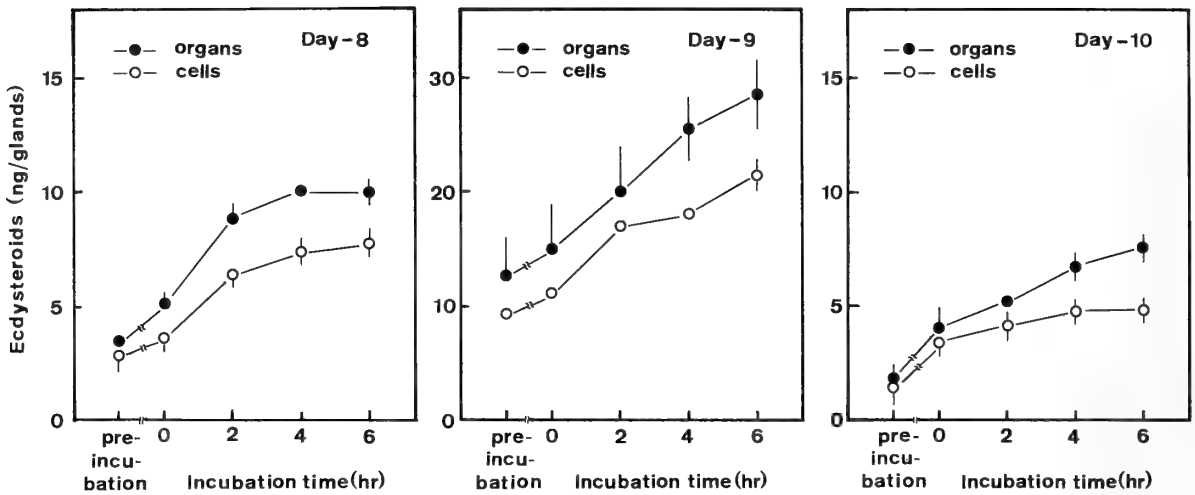

FIG. 4. Ecdysteroid synthesis following incubation of the dissociated cells and intact prothoracic glands of *Bombyx mori* on different days of the final instar. The cells of the prothoracic gland were dispersed with dispase (6,000 PU/ml of Grace's medium, pH 6.5) at 37°C for 15 min. The enzyme was removed by centrifugation at 250 rpm for 2 min. The amount of ecdysteroids in this enzyme solution was estimated by RIA, and was plotted as "pre-incubation" on each abscissa. The resultant cells of prothoracic glands were immediately rinsed with 300 μl Grace's medium. After centrifugation (250 rpm for 2 min), the cells were resuspended in 300 μl of medium at time "0" of incubation. A pair of intact prothoracic glands or a pair of one gland's equivalent of dissociated cells was used. The stage of prothoracic gland is indicated in the upper right side of each figure. The day of 4th ecdysis was designated as "day 0" of 5th instar.

incubation. Ecdysteroid produced by the glands decreased significantly by day 10 (pharate pupal stage).

To measure the amount of ecdysteroid produced by the dispersed PG cells, we used a centrifugation tube with filter (Ultrafree, C3SV, 5 μm Millipore Co. Ltd) to reduce the handling time necessary for the dissociation of PG. Cells from PGs of day 8 to day 10 larvae secreted ecdysteroids into the medium (Fig. 4). However, the amounts of ecdysteroids were about 30 to 35% lower than those produced by the intact PGs. The rate of ecdysteroid production in the dissociated cells was similar to that of intact PG (Fig. 4). Since the mortality of cells by the dispase treatment as described above ranged between about 14 to 25%, the reduced amounts of ecdysteroid in the dissociated cells may be due to the loss of viable cells during the treatment of the glands.

DISCUSSION

The PG cells in *Bombyx* are surrounded by a thick basal lamina (Fig. 1), while the cells in *Hyalophora cecropia* are connected only by a thin strand [4] and the morphology of the glands of *Manduca sexta* is intermediate between these two extremes [3, 11]. *Manduca* PG cells have been successfully dissociated by either 0.4% trypsin/chymotrypsin/elastase [14] or 0.4% elastase [12]. In these experiments, the yield of viable cells was $\geqq$95% and the cells remained viable for at least 4 hr [12, 14]. In the present experiment, a technique was developed whereby the intact PG of *Bombyx* could be dispersed into viable cells by using dispase in Grace's medium. The yield of viable cells ranged between 80 to 94% and these cells remained viable at least 6 hr.

To minimize the handling of the dissociated cells, we used an Ultrafree centrifugation tube. Thus, after incubation the supernatant could be readily removed and assayed for ecdysteroids. With this technique we showed that the dissociated cells were similar to intact glands in their linear production of ecdysteroids over a 2–6 hr period *in vitro*. Previous studies by Okuda *et al.* [10] have shown that *Bombyx* PGs show different rates of ecdysteroids synthesis around the time of gut purge and spinning. Our studies show a similar increase on day 9 for both the intact glands and the dissociated cells. Thus, although the dissociated cells produced less ecdysteroid than the intact gland, their rate of production is similar to that of the intact gland at a particular time.

Dissociated PG cells from *Manduca* lacking the basal lamina respond to PTTH *in vitro* by an increase in ecdysteroid production [12, 14]. Now that PTTH in *Bombyx* has been purified and sequenced [6, 7, 9], studies of its mode of action on the PG are needed. Our dispersed PG cell preparation should be ideal for such a study.

ACKNOWLEDGMENTS

We would like to thank Prof. L. M. Riddiford, University of Washington, for her critical reading and valuable comments on this manuscript. We also thank Mr. Skarlatos Dedos for his help on a preparing the draft of this manuscript.

REFERENCES

1 Bollenbacher WE, Granger NA (1985) Endocrinology of the prothoracicotropic hormone. In "Comprehensive Insect Physiology, Biochemistry and Pharmacology Vol 7" Ed by GA Kerkut, LI Gilbert, Pergamon Press, Oxford, pp 109–152

2 Borst DW, O'Connor JD (1972) Arthopod molting hormone: radioimmune assay. Science 178: 418–419

3 Gilbert LI, Combest WL, Smith WA, Meller VH, Rountree DB (1988) Neuropeptides, second messengers and insect molting. Bio Essays 8: 153–157

4 Herman WS, Gilbert LI (1966) The neuroendocrine system of *Hyalophora cecropia* (L) (Lepidoptera: Saturniidae), I: anatomy and histology of the ecdysial glands. Gen Comp Endocrinol 7: 275–291

5 Horn DHS (1989) Historical Introduction. In "Ecdysone" Ed by J Koolman, Thieme Verlag, Stuttgart, pp 8–19

6 Kataoka H, Nagasawa H, Isogai A, Tamura S, Mizoguchi A, Fujiwara Y, Suzuki C, Ishizaki H, Suzuki A (1987) Isolation and partial characterization of a prothoracicotropic hormone of the silkworm, *Bombyx mori.* Agric Biol Chem 51: 1067–1076

7 Kawakami A, Kataoka H, Oka T, Mizoguchi A, Kawakami KM, Adachi T, Iwami M, Nagasawa H, Suzuki A, Ishizaki H (1990) Molecular cloning of the *Bombyx mori* prothoracicotropic hormone. Science 247: 1333–1335

8 Koolman J (1989) Ecdysone. Thieme Verlag, Stuttgart, pp 482

9 Matsuo N, Aizono Y, Funatsu G, Funatsu M, Kobayashi M (1985) Purification and some propeties of prothoracicotropic hormone in the silkworm, *Bombyx mori.* Insect Biochem 15: 189–195

10 Okuda M, Sakurai S, Ohtaki T (1985) Activity of the prothoracic gland and its sensitivity to prothoracicotropic hormone in the penultimate and last larval instar of *Bombyx mori.* J Insect Physiol 31: 455–461

11 Sakurai S, Warren JT, Gilbert LI (1989) Mediation of ecdysone synthesis in *Manduca sexta* by a hemolymph enzyme. Arch Insect Biochem Physiol 10: 179–197

12 Sakurai S, Gilbert LI (1990) Biosynthesis and Secretion of Ecdysteroids by the Prothoracic glands. In "Molting and Metamorphosis" Ed by E Ohnishi, H Ishizaki, Japan Sci Soc Press, Tokyo, Springer-Verlag, Berlin, pp 83–106

13 Smith SL (1985) Regulation of ecdysteroid titer: synthesis. In "Comprehensive Insect Physiology, Biochemistry and Pharmacology Vol 7" Ed by GA Kerkut, LI Gilbert, Pergamon Press, Oxford, pp 295–341

14 Smith, WA, Rountree DB, Bollenbacher WE, Gilbert LI (1986) Dissociation of the prothoracic glands of *Manduca sexta* into hormone-responsive cells. In "Insect Neurochemistry and Neurophysiology" Ed by AB Borkovec, DB Gelman, pp 319–322

15 Takeda S, Kiuchi M, Ueda S (1986) Preparation of anti-20-hydroxyecdysone serum and its application for radioimmunoassay of ecdysteroids in silkworm hemolymph. Bull Seric Sci Stn 30: 361–374

16 Toyama K (1902) Contributions to the study of silk-worm, I. on the embryology of the silkworm. Bull Coll Agric Tokyo Imp Univ 5: 73–117

17 Warren JT, Gilbert LI (1988) Ecdysteroids. In "Immunological Techniques in Insect Biology" Ed by LI Gilbert, TA Miller, Springer-Verlag, New York, pp 181–214

18 Watson RD, Spaziani E, Bollenbacher WE (1989) Regulation of ecdysone biosynthesis in insects and crustaceans: a comarison. In "Ecdysone" Ed by J Koolman, Thieme Verlag, Stuttgart, pp 188–210

ZOOLOGICAL SCIENCE 11: 113–119 (1994)

Effects of Light and Food as Zeitgebers on Locomotor Activity Rhythms in the Loach, *Misgurnus anguillicaudatus*

MAYUMI NARUSE[1]* and TADASHI OISHI[2]

[1]*Division of Human Life and Environmental Science, Graduate School of Human Culture, and* [2]*Department of Biology, Faculty of Science, Nara Women's University, Nara 630, Japan*

ABSTRACT—Four experiments were performed to examine the synchronizing effects of light and food on the locomotor activity rhythm in the loach (*Misgurnus anguillicaudatus*). In Exp. 1, food was given once a day at the scheduled time in the middle of light (L) or dark (D) phase under LD 12:12. When the fish were fed in the L phase, they showed three types of activity pattern (light-active, dark-active and light-dark-active). On the other hand, most of the fish became dark-active when they were fed in the D phase. In both conditions, the fish were entrained well to the scheduled feeding. In Exp. 2, the scheduled feeding cycle was removed from the previous Exp. 1. Under these conditions, the loach remained to show the same pattern as that in Exp. 1 or tended to become dark-active. The feeding-anticipatory activity peak gradually disappeared during these experiments. In Exp. 3, the fish were exposed to the scheduled feeding and constant darkness (DD). Since almost all fish were entrained to the scheduled feeding, scheduled feeding as well as LD cycles is effective as a zeitgeber for the locomotor activity rhythm in the loach. Under constant conditions (Fig. 4), free-running rhythms were observed, although the duration of the rhythm was short and the ratio of the individuals that showed free-running rhythms was low (7–50%). Therefore, the locomotor activity rhythm in the loach is an endogenous rhythm but the coupling between the oscillator and the locomotor activity seems to be weak and different depending on individuals.

INTRODUCTION

One of the characteristics of the circadian rhythms in fishes is variability of the rhythms compared with those in higher vertebrates [15]. The appearance of the circadian rhythms varies inter- [24] and intra-specifically [5, 7, 27], and even intra-individually [12]. Activity patterns showed diurnal, nocturnal, crepuscular and intermediate types depending on fishes [24]. In the perch (*Perca fluviatilis*), juvenile fish showed a nocturnal activity pattern but adult fish changed the activity pattern to diurnal [7]. Several activity patterns appeared simultaneously such as diurnal and nocturnal in the juvenile pink salmon (*Oncorhynchus gorbuscha*) [5] and diurnal, nocturnal, light-change-active and arrhythmic in the medaka (*Oryzias latipes*) [27]. Locomotor activity changes seasonally in the minnow (*Phoxinus phoxinus*), the sculpin (*Cottus poecilopus*) and the burbot (*Lota lota*) [12], and the medaka [31]. These reports suggest that a plastic reactivity to various zeitgebers may induce the variability of the rhythm. In order to clarify this probability, we selected two environmental factors, light and food. Light is a major environmental factor as a zeitgeber in fishes as well as in other organisms. Food has been reported to act as a zeitgeber in some fishes, such as the goldfish (*Carassius auratus*) [14] and the medaka [29].

Accepted October 15, 1993
Received July 27, 1993
* Present address: Department of Hygiene, Akita University School of Medicine, Akita 010, Japan
[2] To whom reprint requests should be addressed.

The loach (*Misgurnus anguillicaudatus*) is one of the common freshwater fishes in Japan and inhabits paddy fields and small streams. Although there are several studies concerning the spawning behavior and season in the loach [19, 23], there is only one report by Yanagishima and Mori [30] on the locomotor activity rhythm of the loach. They reported that the fish showed the exogenously controlled nocturnal activity rhythm because the rhythmicity immediately disappeared under a constant condition. In this paper, we investigated (1) effects of single environmental factor, light (LD cycle) or food (scheduled feeding cycle), on the locomotor activity rhythm, (2) effects of the phase relationship between two environmental factors, light and food, on the rhythm, and (3) whether the locomotor activity rhythm of the loach is an endogenous circadian rhythm or not.

MATERIALS AND METHODS

Adult loaches (*Misgurnus anguillicaudatus*) including males and females of about 9–16 cm in total length were used. We caught them at a small stream along the paddy fields in Kyoto Prefecture in May, 1988, or obtained cultured fish in the Shikoku districts from a fish shop in April to October, 1987.

The fish were kept individually in a plastic water tank (31.5×17×21H cm) with sand at the bottom and placed in a bioclimatic chamber at 25±1°C at least one month before experiments. Fluorescent lamps (40 W) were used as the light source. Light intensities at the water surface were measured by a radiometer (UDT161, United Detector Technology Inc., California) and adjusted at 460–600 lux (0.26–0.39 mW/cm^2) or 5 lux (0.002 mW/cm^2) in the light (L) phase and 0 lux in the dark (D) phase. We fed about 0.5–1.0 g wet weight of live tubifexes as food by hand or an auto

feeding instrument (SP-10A, Nippon Denshi Kagaku, Kyoto) during scheduled feeding experiments. Tubifexes with water were put in a small plastic tube and thrown into a water tank by overturning this tube at the feeding time. As a control, we gave only water using the tube for 3 days just after the scheduled feeding experiment, but none of the fish reacted to this sham-feeding regimen. Water was always aerated and filtered. The locomotor activity of the loach was measured by a pair of infrared photocells (JU-33P, -33R or PL3-E, -FL, Hokuyo Denki, Osaka) at both sides of the water tank. The light source and receiver of photocells were set at about 1 cm above the sand, since the loach is a benthic fish. Main activity including searching and feeding behavior and most swimming behavior was observed at the bottom layer (see the results of Exp. 3). When the fish interrupted the beam, it was recorded by an actograph (Fuji Denki, Tokyo) and the number of interruptions were counted by a digital data recorder (DDR3010, Sanyo Denki, Osaka). Data from the actograph were used for visual examination, and total counts per one hour from the digital data recorder were used for the statistical analyses such as χ^2-test and periodogram analysis. In these analyses, the significance level we adopted was 95% confidence limit.

In the present study, we selected four experimental conditions to examine the synchronizing effects of light-dark (LD) cycles and scheduled feeding in the locomotor activity rhythm of the loach and compared the results individually by using the same members of fish throughout these experiments. Before each experiment, loaches were subjected to constant darkness (DD) without food for at least 10 days to eliminate the after-effect of the previous condition.

Experiment 1 Locomotor activity rhythms under LD cycles and scheduled feeding.

(A) Food was given at the scheduled time (12:00) in the middle of the L phase under LD 12:12 (L: 06:00–18:00, D: 18:00–06:00; L= 460–600 lux, D=0 lux) for 10 (n=6) or 15 (n=14) days.

(B) Food was given at the scheduled time (12:00) in the middle of the D phase under reversed LD 12:12 (L: 18:00–06:00, D: 06:00–18:00) for 12 (n=6) or 15 (n=14) days.

Experiment 2 Effects of LD cycles on the locomotor activity rhythms without food after Exp. 1.

(A) Fish (n=6) were placed under LD 12:12 without food after Exp. 1-A for 10 days.

(B) Fish (n=6) were placed under LD 12:12 without food after Exp. 1-B for 10 days.

Experiment 3 Effects of scheduled feeding on the locomotor activity rhythms under constant darkness (DD).

Fish (n=6) were fed once a day at the scheduled time (12:00) under DD (D=0 lux) for 11 days. In order to analyze the behavior of the loach under the scheduled feeding and constant dim light (dim LL, L =5 lux), we recorded the behavior of a female by VTR (TV camera; WV-1550, Matsushita Tsushin, Osaka, Time Lapse VTR; NV-720, Matsushita Denki, Osaka).

Experiment 4 Free-running rhythms under constant conditions after Exp. 1 and 3.

(A) Fourteen fish were subjected to DD without food after Exp. 1-A for 15 days.

(B) Fourteen fish were placed under DD without food after Exp. 1-B for 15 days.

(C) Six fish were placed under DD without food after Exp. 3 for 14 days.

All experiments were performed during November, 1987 to September, 1988.

RESULTS

Experiment 1 Locomotor activity rhythms under LD cycles and scheduled feeding.

(A) Food was given at the scheduled time (12:00) in the middle of the L phase under LD 12:12.

The locomotor activity of the loach was classified into four patterns in relation to LD cycle, i.e., dark-active (nocturnal) (ex. Fig. 1A-a, B), light-dark-active (ex. Fig. 1A-b, c and Fig. 2a), light-active (diurnal) (ex. Fig. 1A-d) and arrhythmic. The term "light-dark-active" denotes that there are peaks of activity in both L and D phases. Among 20 fish used in this experiment, one fish was dark-active, 12 were light-dark-active and seven were light-active, and the difference was statistically significant ($P<0.05$, χ^2-test for one sample) (Table 1a). It took at least 3–5 days for the loaches to establish the stable locomotor activity pattern (see Fig. 2a). Four out of six light-active fish tended to change their activity patterns from dark- to light-active during this experiment. All fish excluding one dark-active fish (Fig. 1A-a) were entrained to scheduled feeding ($P<0.01$, χ^2-test for one sample), and the activity was classified into two types as follows. Type 1 (E_1): the peak of activity lasted several hours before the feeding time, which probably reflects the anticipation for food (n=11), and among these 11 fish, eight remained inactive for several hours after feeding (ex. Fig. 1A-b) and three continued to be active for several hours after feeding (ex. Fig. 1A-d). Type 2 (E_2): the activity peak lasted several hours after the feeding time without the anticipatory peak (n=8) (ex. Fig. 1A-c). When Exp. 1-A regimen was repeated after Exp. 2-A using the same individuals, a similar tendency of activity patterns was observed for both LD cycle and scheduled feeding.

(B) Food was given at the scheduled time (12:00) in the middle of the D phase under LD 12:12.

In this experiment, all fish except one light-dark-active fish showed a dark-active pattern (ex. Fig. 1B and Fig. 2b) ($P<0.01$, χ^2-test for one sample) (Table 1a). A tendency toward the change of activity pattern from light- to dark-active was observed in four dark-active fish during this experiment. All of the 19 dark-active fish were synchronous to the scheduled feeding ($P<0.01$, χ^2-test for one sample) (Table 1a). The two types of entrainment to scheduled feeding as the previous experiment were also observed in this experiment. The number of fish for type 1 and 2 was 18 (ex. Fig. 1B) and 1, respectively.

When Exp. 1-A was compared with 1-B, various activity patterns appeared under the scheduled feeding in the L phase, while the loach became exclusively dark-active under the scheduled feeding in the D phase, and the difference was highly significant ($P<0.01$, χ^2-test for multiple samples) (Table 1a). When the activity patterns were compared individually between these two conditions, three types were detected in the entrainment to LD cycles; (1) fish strongly affected by the scheduled feeding, as they tended to be light-active when they were fed in the L phase and dark-active

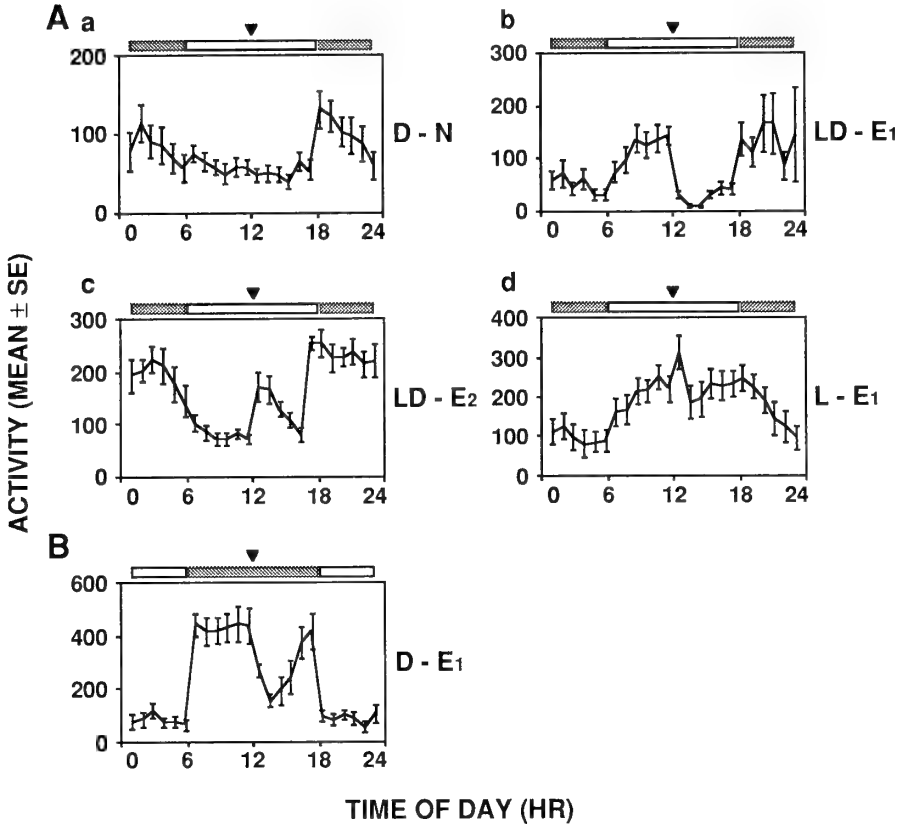

FIG. 1. Examples of locomotor activity rhythms of the loach in Experiment 1. (A) Exp. 1-A (LD 12:12, Food in L). (B) Exp. 1-B (LD 12:12, Food in D). Activity patterns were represented as D, LD and L for the entrainment in relation to LD cycles, and E_1, E_2 and N for the entrainment to scheduled feeding. D: dark-active. LD: light-dark-active. L: light-active. E_1: entrained with the anticipatory activity peak (type 1, see text). E_2: entrained without the anticipatory peak (type 2, see text). N: not entrained. Horizontal bar: light condition (LD 12:12, white bar: L, dotted bar: D). Triangle: feeding time. Data were shown as mean ± standard error (SE) for 10 or 12 days.

TABLE 1. The number of individual fish for each activity pattern

(a)

Experiments	LD cycle					Scheduled feeding		
	Dark-active	Light-dark-active	Light-active	Arrhythmic		Entrained	Not entrained	
1-A (LD 12:12, Food in L)	1	12	7	0	* ††	19	1	**
1-B (LD 12:12, Food in D)	19	1	0	0	** ††	19	1	**
2-A (LD 12:12, Food removed in L)	4	0	2	0		—	—	
2-B (LD 12:12, Food removed in D)	6	0	0	0		—	—	
3 (DD, Food at 12:00)	—	—	—	—		5	1	

(b)

Experiments	Constant condition	
	Free-run	Not free-run
4-A (after LD 12:12, Food in L)	1	13
4-B (after LD 12:12, Food in D)	4	10
4-C (after DD, Food at 12:00)	3	3

*: $P<0.05$, χ^2-test for one sample **: $P<0.01$, χ^2-test for one sample
††: $P<0.01$, χ^2-test for multiple samples

when they were fed in the D phase (n=7), (2) fish affected only by LD cycles, as they were always dark-active irrelevant to the phase of feeding (n=1), and (3) the intermediate type between types (1) and (2) (n=12). In the case of entrainment to scheduled feeding, there were also three types, (1) fish entrained with an anticipatory activity peak (type 1) irrelevant to the phase of feeding (n=11), (2) fish changed their activity patterns to type 1 when they were fed in the D phase (n=7), and (3) fish did not show the anticipatory activity peak (n=2).

Experiment 2 Effects of LD cycles on the locomotor activity rhythms without food after Exp. 1.

(A) Fish were placed under LD 12:12 without food after Exp. 1-A.

In six fish observed, four were dark-active (ex. Fig. 2a) and two were light-active (Table 1a). Under LD 12:12 and the scheduled feeding at the L phase in Exp. 1-A, all of the four dark-active fish showed light-dark-active pattern, while two light-active fish were light-dark- or light-active. A significant reduction in the amount of activity was observed in the two light-active fish (ex. Fig. 2a) and one dark-active fish in a few days after the beginning of this experiment probably because of starvation. The anticipatory activity peak observed before the feeding time disappeared within a few days.

(B) Fish were placed under LD 12:12 without food after Exp. 1-B.

In this experiment, all six fish were dark-active (ex. Fig. 2b) (Table 1a). They were dark-active in the previous Exp. 1-B. Three of them decreased the amount of activity in a few days.

When the results of Exp. 2 was compared with that of Exp. 1, in five fish that were light-dark-active under the scheduled feeding in the L phase (Exp. 1-A), four fish changed their activity patterns to dark-active, and only one fish changed to light-active. One fish that were light-active in Exp. 1-A kept the same pattern. The difference between Exp. 1-A and 2-A was highly significant ($P<0.01$, χ^2-test for multiple samples) (Table 1a). On the other hand, the dark-active pattern in all of the six fish under the scheduled feeding in the D phase (Exp. 1-B) was maintained in the condition without food. Therefore, the loach is mainly a nocturnal species and the activity peak in the L phase seems to depend on the scheduled feeding in the L phase.

Experiment 3 Effects of scheduled feeding on the locomotor activity rhythms under constant darkness (DD).

Five out of six fish were considered to be entrained by the scheduled feeding (Table 1a). They showed a peak of anticipatory activity prior to the feeding time (type 1) (Fig. 3). The amount of activity reduced just after the feeding time and increased gradually until the next feeding time.

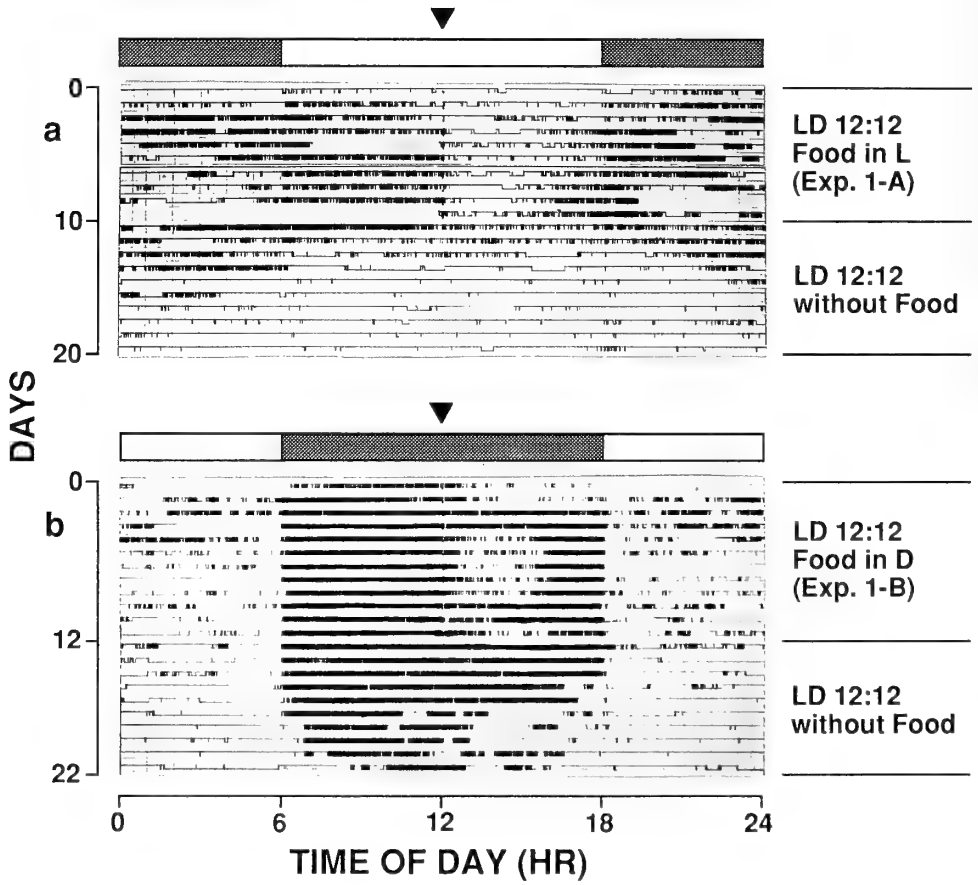

FIG. 2. Examples of locomotor activity rhythms of the loach in Experiment 2 (LD 12:12, without Food). (a) Exp. 2-A was performed after Exp. 1-A (LD 12:12, Food in L). (b) Exp. 2-B was performed after Exp. 1-B (LD 12:12, Food in D). Horizontal bar: light condition (LD 12:12).

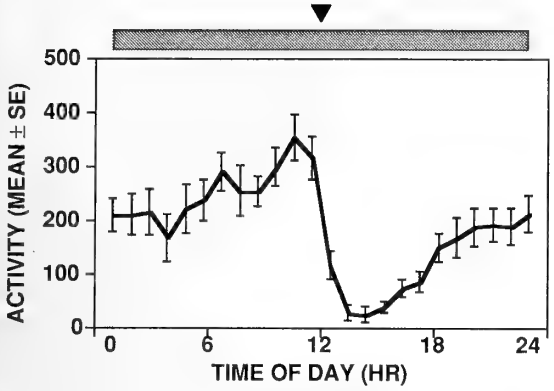

FIG. 3. An example of locomotor activity rhythms of the loach in Experiment 3 (DD, Food at 12:00). Horizontal bar: light condition (DD). Triangle: feeding time. Data were shown as mean ± SE for 11 days.

We recorded and analyzed the behavior of feeding-entrained activity pattern of a female loach under dim LL by a VTR. This female loach showed the type 1 in the feeding-entrained activity pattern. We divided the behavior of the loach into searching and feeding behavior, and other swimming behaviors. Feeding crawl specified as crawling exploration with plowing, plowing ahead and gulping (including dig and twist) was regarded as searching and feeding behavior [28]. From the results observed every one hour, only swimming behavior at the upper and/or the bottom layer was observed till 16:00 (two hours before the scheduled feeding time). Searching behavior and rest were added to swimming at 16:00–17:00. Swimming at the upper layer decreased and searching behavior relatively increased, and swimming near the place where the fish was always fed was frequently

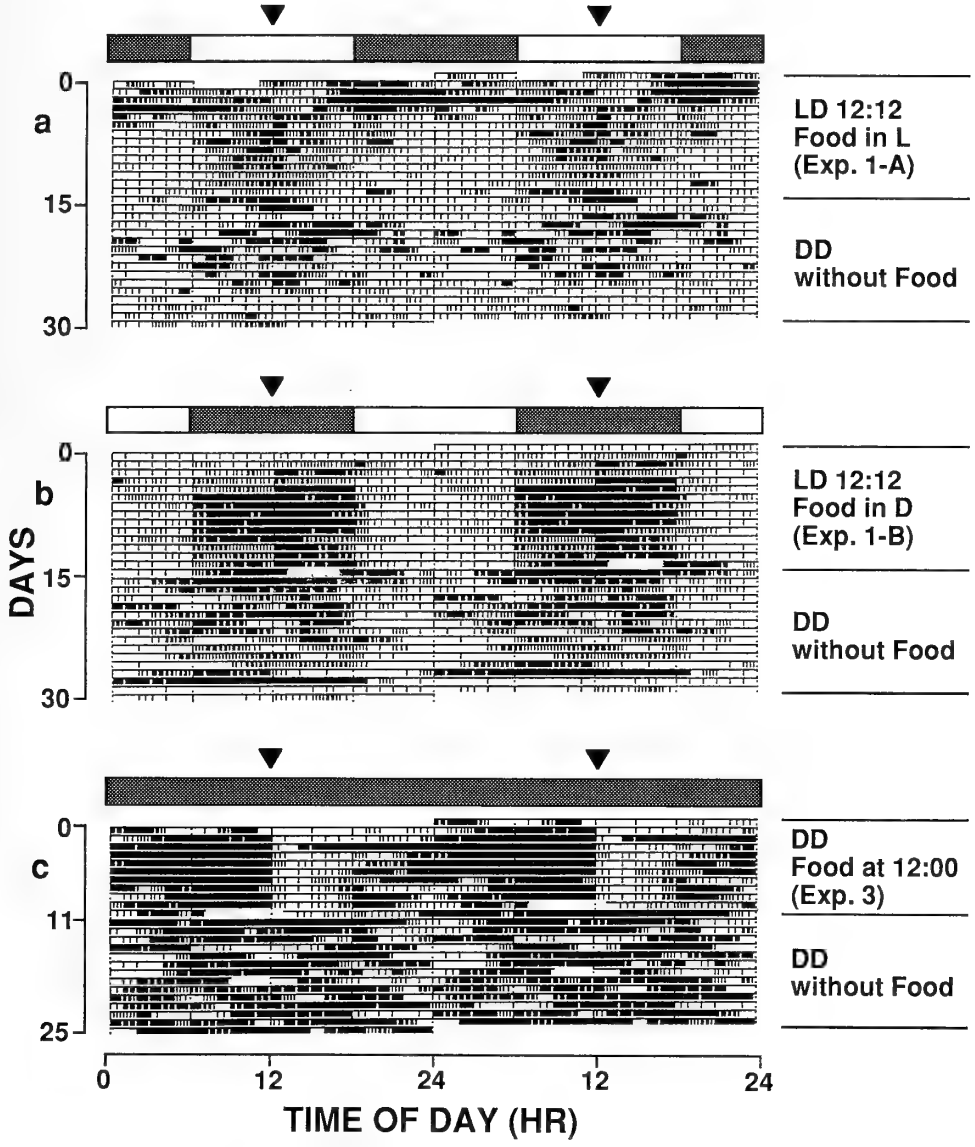

FIG. 4. Free-running locomotor activity rhythms of the loach in Experiment 4 (DD, without Food). (a) Exp. 4-A was performed after Exp. 1-A (LD 12:12, Food in L). Free-running period (τ) = 23.5 hr. (b) Exp. 4-B was performed after Exp. 1-B (LD 12:12, Food in D). τ = 24.1 hr. (c) Exp. 4-C was performed after Exp. 3 (DD, Food at 12:00). τ = 24.7 hr. Data were double-plotted.

observed at 17:00–18:00. When the food was given at 18:00, the fish fed it within a few minutes and gradually became inactive. Whenever the fish was active, it was usually at the bottom layer. There were swimming and rest at the bottom from 19:00 to 22:00. Swimming at the upper layer appeared at 22:00–23:00 and it was increased at 23:00–0:00. This series of behavior corresponded to the feeding-entrained activity pattern of the female loach recorded by the actograph. In this experiment, it was shown that the scheduled feeding could induce the locomotor activity rhythm of the loach.

Experiment 4 Free-running rhythms under constant conditions after Exp. 1 and 3.

(A) Fish were subjected to DD without food after Exp. 1-A.

Only one of the 14 fish showed free-running rhythms for about 15 days (τ=23.5 hr) (Fig. 4a, Table 1b). This fish was light-active and entrained to scheduled feeding as type 1 in the Exp. 1-A.

(B) Fish were placed under DD without food after Exp. 1-B.

Four of the 14 fish showed free-running rhythms for about 7–13 days. One of them showed shorter free-running period than 24.0 hr (τ=22.0 hr) and three fish showed longer free-running periods than 24.0 hr (τ=24.1, 24.1 and 25.6 hr) (Fig. 4b, Table 1b). All of these fish were dark-active and entrained to scheduled feeding as type 1 in the previous Exp. 1-B.

(C) Fish were placed under DD without food after Exp. 3.

Three of the six fish showed free-running rhythms for about 5–9 days. One fish showed the free-running period of 22.1–23.7 hr and two fish showed free-running periods of 24.7 (Fig. 4c) and 28.2 hr (Table 1b). The fish with τ=28.2 hr showed free-running rhythms throughout Exp. 4-A to C. The free-running period in Exp. 4-A and B was 23.5 and 22.0 hr, respectively. Two fish with longer free-running period than 24 hr were entrained to scheduled feeding as type 1 in the previous Exp. 3 and one fish with shorter free-running period than 24 hr was not entrained to scheduled feeding.

Since free-running rhythms were observed after entrainment to the scheduled feeding, feeding can be considered as a zeitgeber in the loach.

DISCUSSION

Reports on the effect of scheduled feeding cycles on the locomotor activity rhythm have been increasing. In the goldfish (*Carassius auratus*), the scheduled feeding with LD cycle affected the locomotor activity rhythm, growth rate, and serum-cortisol and -thyroxine concentrations [14, 21]. In the medaka (*Oryzias latipes*), scheduled feeding cycles had different influences on the different types of behavior, that is, the agonistic behavior was entrained to the feeding cycle, but the egg laying and courtship behavior were entrained rather to LD cycles than to feeding cycles [29]. In the mudskipper (*Periophthalmus cantonensis*), the locomotor activity rhythm could be entrained to the 12-hour feeding cycle [13]. The channel catfish (*Ictalurus punctatus*) showed subjective feeding time under ad-lib feeding regimen [17]. In contrast, the scheduled feeding did not affect the locomotor activity rhythm in the blenny (*Blennius pholis*) [4].

Feeding both in the L phase and in the D phase could entrain the activity rhythm of the loach (Exp. 1). The activity pattern varied widely when the fish were fed in the L phase, but they were consistently dark-active when they were fed in the D phase. In Exp. 2, the activity patterns tended to change to dark-active under the regimen without food. Therefore, fundamentally the loach seems to be a nocturnal species. Benthic fishes, such as the eel, catfish and loach, have been considered as nocturnal or light-dark-active species because benthic fish approach to their food horizontally and rely on not only vision but also other senses to find food [20]. However, since cone cells and cone visual pigments (iodopsin-like substances) existed in the retina of the loach [11], they seem to have an ability to be active during daytime. In the field, probably the availability of food for the loach do not change diurnally because the loach is an omnivorous detritus feeder. In the present study, however, loaches were entrained to the daily feeding cycle, although food (tubifexes) was not taken away, and thus, the fish could feed these tubifexes alive in the bottom sand whenever they want, and this was supposed to provide a weaker influence on the entrainment than the food-removed regimen. Thus, the importance of feeding in the circadian structure of the loach should not be neglected.

Davis and Bardach [3] indicated the importance of the anticipatory activity peak that appeared prior to the scheduled feeding time. This activity peak was also mentioned by Aschoff [1], in which it was suggested to appear under both LD cycles and constant conditions. In the present study, the loach showed the anticipatory activity peak in both LD cycle and constant darkness (DD).

The loach showed conspicuous resting periods of several hours after the feeding time. There were no reports about this type of resting period in the study of the feeding-entrained rhythm. Thus, this resting period may be unique to the locomotor activity rhythm of the loach entrained to the feeding time. The reason why the loach needs this period may be due to the fact that they are benthic fish and they have to spend many hours to digest food [26].

It has been suggested in fishes that free-running rhythms are labile and do not last for a long time [15, 18], and the ratio of individuals with free-running rhythms is lower than those of higher vertebrates, although there are some exceptions such as the lake chub (*Couesius plumbeus*) [9], the goldfish [10], two species of the hagfish (*Eptatretus burgeri, Paramyxine atami*) [8, 16] and the catfish (*Silurus asotus*) [25]. In the loach, free-running rhythms lasted for 5–15 days and thus, the locomotor activity rhythm of the loach is an endogenous circadian rhythm. However, the ratio of individuals which showed free-running rhythms was low and varied from 7 to

50% depending on experiments, and the rhythm persisted only for short periods. This indicates that the extent of coupling between the oscillator and the locomotor activity seems to be weak and might differ depending on individuals.

Since the periodic feeding in the rat caused to uncouple the feeding-anticipatory peak from the component of free-running rhythm [2, 6, 22], it is suggested that the feeding-entrained oscillator is different from the LD cycle-entrained oscillator. The SCN-lesioned animal that showed arrhythmic locomotor activity also showed the anticipatory activity prior to feeding [2, 22]. Different oscillator systems for feeding and LD cycles might also exist in the loach, because the uncoupled anticipatory peak was observed and gradually disappeared in Exp. 1-A and 2-A.

ACKNOWLEDGMENTS

We are grateful to Prof. Yoshihiko Chiba, Dr. Kenji Tomioka, Department of Biology, Yamaguchi University, and Mr. Sou Miyake, Department of Electrical Engineering, Kyoto University, for providing us actographs and the program of the actogram.

REFERENCES

1 Aschoff J (1987) Effects of periodic availability of food on circadian rhythms. In "Comparative Aspects of Circadian Clocks" Ed by T Hiroshige, K Honma, Hokkaido Univ Press, Sapporo, pp 19–41

2 Boulos Z, Rosenwasser AM, Terman M (1980) Feeding schedules and the circadian organization of behavior in the rat. Behav Brain Res 1: 39–65

3 Davis RE, Bardach JE (1965) Time-co-ordinated prefeeding activity in fish. Anim Behav 13: 154-162

4 Gibson RN (1971) Factors affecting the rhythmic activity of *Blennius pholis* L. (Teleostei). Anim behav 19: 336–343

5 Godin J-GJ (1981) Circadian rhythm of swimming activity in juvenile pink salmon (*Oncorhynchus gorbuscha*). Mar Biol 64: 341–349

6 Honma K, von Goetz Ch, Aschoff J (1983) Effects of restricted daily feeding on freerunning circadian rhythms in rats. Z vergl Physiol 62: 93–110

7 Johnson T, Müller K (1978) Different phase position of activity in juvenile and adult perch. Naturwissenschaften 65: 392–393

8 Kabasawa H, Ooka-Souda S (1991) Circadian rhythms of locomotor activity in the hagfish and the effect of reversal of the light-dark cycle. Bull Japan Soc Sci Fish 57: 1845–1849

9 Kavaliers M (1978) Seasonal changes in the circadian period of the lake chub, *Couesius plumbeus*. Can J Zool 56: 2591–2596

10 Kavaliers M (1981) Period lengthening and disruption of socially facilitated activity rhythms of goldfish by lithium. Physiol Behav 27: 625–628

11 Kawata A, Oishi T, Fukada Y, Shichida Y, Yoshizawa T (1992) Photoreceptor cell types in the retina of various vertebrate species : Immunocytochemistry with antibodies against rhodopsin and iodopsin. Photochem Photobiol 56: 1157–1166

12 Müller K (1978) Locomotor activity of fish and environmental oscillations. In "Rhythmic Activity of Fishes" Ed by JE Thorpe, Academic Press, London, pp 1–19

13 Nishikawa M, Ishibashi T (1975) Entrainment of the activity rhythm by the cycle of feeding in the mud-skipper, *Periophthalmus cantonensis* (Osbeck). Zool Mag 84: 184–189

14 Noeske TA, Spieler RE (1984) Circadian feeding time affects growth of fish. Trans Am Fish Soc 113: 540–544

15 Oishi T (1991) Fishes. In "Handbook of Chronobiology (In Japanese)" Ed by Y Chiba, K Takahashi, Asakura Shoten, Tokyo, pp 69–78

16 Ooka-Souda S, Kabasawa H, Kinoshita S (1985) Circadian rhythms in locomotor activity in the hagfish, *Eptatretus burgeri*, and the effect of reversal of light-dark cycle. Zool Sci 2: 749–754

17 Randolph KN, Clemens HP (1976) Some factors influencing the feeding behavior of channel catfish in culture ponds. Trans Am Fish Soc 105: 718–724

18 Richardson NE, McCleave JD (1974) Locomotor activity rhythms of juvenile Atlantic salmon (*Salmo salar*) in various light conditions. Biol Bull 147: 422–432

19 Saitou K, Katano O, Koizumi A (1988) Movement and spawning of several freshwater fishes in temporary waters around paddy field. Jpn J Ecol 38: 35–47

20 Sawara Y (1989) The ecology of rhythmic activity in fishes (I). Biol Sci 41: 57–67

21 Spieler RE, Noeske TA (1984) Effects of photoperiod and feeding schedule on diel variations of locomotor activity, cortisol, and thyroxine in goldfish. Trans Am Fish Soc 113: 528–539

22 Stephan FK (1981) Limits of entrainment to periodic feeding in rats with suprachiasmatic lesions. J Comp Physiol A 143: 401–410

23 Suzuki R (1983) Multiple spawning of the cyprinid loach, *Misgurnus anguillicaudatus*. Aquaculture 31: 233–243

24 Tabata M (1988) 6. Diel and circadian locomotor activity in fishes. In "Daily Rhythmic Activities in Aquatic Animals (In Japanese)" Ed by I Hanyu, M Tabata, Koseikaku Koseisha, Tokyo, pp 79–100

25 Tabata M, Minh-Nyo M, Niwa H, Oguri M (1989) Circadian rhythm of locomotor activity in a teleost, *Silurus asotus*. Zool Sci 6: 367–375

26 Tanaka K (1955) Observation on the length of the digestive time of feed by the mud loach, *Misgurnus anguillicaudatus*. Japan J Ichthyol 4: 34–39

27 Ueda M, Oishi T (1982) Circadian oviposition rhythm and locomotor activity in the Medaka, *Oryzias latipes*. J interdiscipl Cycle Res 13: 97–104

28 Watanabe K, Hidaka T (1983) Feeding behaviour of the Japanese loach, *Misgurnus anguillicaudatus* (Cobitididae). J Ethol 1: 86–90

29 Wever DN, Spieler RE (1987) Effects of the light-dark cycle and scheduled feeding on behavioral and reproductive rhythms of the cyprinodont fish, Medaka, *Oryzias latipes*. Experientia 43: 621–624

30 Yanagishima S, Mori S (1951) Relation between activity and glycogen contents of the Japanese loach. Mem Coll Sci Univ Kyoto, Ser B 20, 1–6

31 Yokota T, Oishi T (1992) Seasonal change in the locomotor activity rhythm of the medaka, *Oryzias latipes*. Int J Biometeorol 36: 39–44

ZOOLOGICAL SCIENCE 11: 121–125 (1994)

Sensory Preconditioning in the Terrestrial Mollusk, *Limax flavus*

HARUHIKO SUZUKI, TATSUHIKO SEKIGUCHI, ATSUSHI YAMADA and ATSUO MIZUKAMI

SANYO Electric Co. Ltd., Tsukuba Research Center 2-1 Koyadai, Tsukuba, Ibaraki 305, Japan

ABSTRACT—Sensory preconditioning (SPC) in the terrestrial slug, *Limax flavus*, was studied with carrot odor and cucumber odor as the conditioned stimuli (CSs) and quinidine sulfate solution as the unconditioned stimulus (US). When slugs experienced CS1-CS2 and CS2-US training pairs, their odor preference for CS1 was reduced as well as that for CS2. The reduction in CS1 odor preference was observable only when slugs experienced both training pairs. In the second experiment, in order to study the stimulus-stimulus associations after SPC, the conditioned slugs were cooled immediately after presentation of CS1 or CS2. As a result, both odor preferences increased after both CS1+cooling and CS2+cooling treatments, which suggested that CS1-CS2 and CS2-US associations were formed after SPC. From these results, it is concluded that *Limax* shows sensory preconditioning and that its stimulus-stimulus associations are similar to those of mammals.

INTRODUCTION

Mollusks are being intensively studied in order to clarify the cellular and molecular mechanisms of associative learning because of the relative simplicity of their nervous systems [2, 3]. Against the background of the excitement generated by these studies, the question of whether one can generalize the emerging principles to vertebrates arises. Comparative studies at the behavioral level might provide an insight into the relationship between vertebrate and invertebrate learning processes and partly answer this question. Gelperin and his colleagues demonstrated that the terrestrial slug, *Limax maximus*, showed some logical operations similar to those known in vertebrates, such as first- and second-order conditioning and blocking [4, 13]. They also showed that stimulus-stimulus associations formed during two types of second-order conditioning in the slug were parallel to those in vertebrates [14]. However, there have been no reports that show sensory preconditioning in mollusks.

Sensory preconditioning (SPC) is a kind of classical conditioning where two conditioned stimuli (CSs) are associated without an unconditioned stimulus (US). The SPC procedure consists of two phases. In phase 1, conditioned stimulus 1 (CS1) is associated with conditioned stimulus 2 (CS2), and in phase 2, CS2 is associated with US. As a result of SPC, CS1, which is not associated directly with US, becomes able to evoke the conditioned response (CR). Sensory preconditioning was first studied by Brogden [1], but has sometimes been dismissed on the grounds that the level of conditioning observed to CS1 is too slight to warrant serious theoretical attention [17]. Later the phenomenon was proved to be a real one [6], and several well-controlled experiments have shown reliable levels of response to CS1 in such diverse situations as conditioned suppression in rats [9, 12], heart-rate conditioning in rabbits [9], and flavor-aversion conditioning in rats [5, 11].

Rizley and Rescorla [12] studied stimulus-stimulus associations after sensory preconditioning using a "postconditioning treatment strategy", in which, after conditioning, the ability of CS2 to evoke CR was reduced by repeated presentation of CS2 to extinguish the CS2-US association. As a result, not only the ability of CS2 to evoke CR but also that of CS1 was dismissed, which indicates that CS1-CS2 and CS2-US associations were formed during sensory preconditioning. Thus, sensory preconditioning is one piece of evidence against strict stimulus-response or S-R theory [7], and is a good example of the ability of animals to integrate several associations into one [8].

In the present study, we demonstrated that the terrestrial slug, *Limax flavus*, showed sensory preconditioning. In addition, the stimulus-stimulus associations formed after the conditioning were studied using cooling-induced retrograde amnesia [15]. It was shown that the associations in *Limax* were parallel to those in vertebrates.

MATERIALS AND METHODS

Animals

Specimens of *Limax flavus* were maintained in laboratory culture on frog chow (Oriental Yeast Co. Ltd.) with a 14 hr/10 hr light-dark cycle at 19°C. Two or three days before the start of training, 3 to 6 month old animals (1.5–2.0 g) were placed into individual plastic containers (113×105×28 mm) lined with moistened filter paper and then starved until the start of the experiments.

Materials used for stimulation

Carrot juice was made in the laboratory. Several carrots were ground in a blender and centrifuged for 30 min at 7,000×*g*. The supernatant was used as carrot juice, which was kept at −20°C until use. Cucumber juice was made in exactly the same way. During

Accepted December 13, 1993
Received October 25, 1993

training, the carrot (Ca) or cucumber juice (Cu) was applied to filter paper and used as the conditioned stimulus (CS). A saturated solution of quinidine sulfate (Q: 1 g/90 ml pure water) was applied to filter paper and used as a bitter-taste unconditioned stimulus (US).

Sensory preconditioning (SPC)

The conditioning procedure consisted of two phases. The slugs were divided into three groups, PP [Paired (phase 1)-Paired (phase 2)], PU (Paired-Unpaired) and UP (Unpaired-Paired). During phase 1 of training, slugs in groups PP and PU were transferred with tweezers to a plastic container lined with filter paper moistened with CS1. After 2 min exposure, the slugs were directly transferred to another plastic container lined with filter paper moistened with CS2, and after 2 min exposure were returned to their individual containers. This paired presentation of CS1 and CS2 was repeated three times with a 2 hr intertrial interval (ITI). Slugs in group UP received the same number of CS1 and CS2 presentations as those in groups PP and PU, but the CS1-CS2 interstimulus interval (ISI) was 30 min. On the next day, in phase 2, slugs in groups PP and UP were exposed to CS2 for 2 min in the same way as in phase 1 training, then transferred to another plastic container lined with filter paper immersed with quinidine sulfate solution. After 1 min exposure, they were rinsed with saline for 5 sec and returned to their individual containers. The paired CS2-US treatment was repeated three times with a 2 hr ITI. Slugs in group PU received three unpaired (ISI=30 min) presentations of CS2 and US with a 2 hr ITI. On the third day, odor preferences for Ca and Cu were tested.

As was described previously [18], although the slugs were able to sense both the odor and taste of the CSs, they did not show taste-taste conditioning by the conditioning procedure. Thus, the taste of the CSs has no influence on the conditioning.

Cooling-induced retrograde amnesia

According to Sekiguchi *et al.* [15], cooling-induced retrograde amnesia reflects Pavlovian conditioning associations. Thus, amnesia was induced to study the associations of sensory preconditioning. The conditioned slugs were tested for their odor preferences and divided into two groups, CS1F and CS2F ("F" represented cooling treatment). They were then exposed to CS1 (group CS1F) or CS2 (group CS2F) for 2 min, transferred to their individual containers, and placed in the freezer compartment of a refrigerator for 5 min. Within 3 min, the body temperature fell to about 1°C as determined by a thermocouple. On the next day, the slugs were again tested for their odor preferences.

Testing and the measure of conditioning

The testing apparatus has been described previously [16]. Briefly, it consisted of three chambers, two of which were for carrot/cucumber juice and frog chow as odor sources. These odor sources were placed on the floor of each side-chamber. The slug was placed in the center chamber, the wall of which was perforated. A line divided the center chamber into a "carrot/cucumber" and a "chow" side.

The testing procedure was exactly the same as that also described previously [16]. For each test, a slug was placed in the center chamber with its body aligned along the center line and observed until it crossed the center line. During the next 120 sec, the time spent by the slug's head on the carrot/cucumber side was recorded. Each slug underwent three trials of carrot odor versus frog chow odor and another three trials of cucumber odor versus frog chow odor, with a 2-hr interval. The observer did not know which treatments had been experienced by the slug being tested.

The measure of conditioning used, "odor preference", was the percentage of the total time the slug spent on the carrot/cucumber side in the carrot/cucumber odor versus frog chow odor trials. This was obtained by dividing the total time each slug's head spent on the carrot/ cucumber side by the total measured time (120 sec×3 trials=360 sec). It has been confirmed that the testing procedure itself does not influence the odor preference [16].

Statistical analysis

Analysis of variance (ANOVA) was used to compare the odor choices of the groups. Newman-Keuls post hoc tests were used for further analysis of the data when the F ratio reached significance. We also used the paired *t*-test when analyzing the pre- and post-amnesia differences for individual slugs.

RESULTS

Sensory preconditioning in Limax flavus

Forty-one slugs were divided into three groups, PP (n=17), PU (n=12) and UP (n=12). In the first experiment, cucumber juice (Cu) and carrot juice (Ca) were used as CS1 and CS2, respectively. Thus, slugs in groups PP and PU were treated with three CuCa conditioning pairs on the first day of training, and slugs in groups PP and UP were treated with three CaQ conditioning pairs on the second day.

The result is shown in Fig. 1a. It is evident that the PP and UP slugs showed much less Ca odor preference than the PU slugs (solid columns). Analysis of variance (ANOVA) showed differences among the groups, $F(2,38)=16.51$, $P<0.001$. Post hoc individual comparisons (Newman-Keuls test) indicated that group PU was significantly different from groups PP and UP ($P<0.05$). On the other hand, the PP slugs showed much less Cu odor preference than PU and UP slugs (clear columns). ANOVA again showed differences among the groups, $F(2,38)=12.93$, $P<0.001$. Individual comparisons revealed that group PP was significantly different from groups PU and UP ($P<0.05$). These results suggest that the reduced preference for Cu odor in group PP slugs is due to SPC.

In the next experiment, to examine the possibility that the observed changes in odor preferences were odor-specific, the CSs were exchanged (CS1: carrot, CS2: cucumber). Twenty-four further slugs were divided into three groups, PP (n=8), PU (n=8) and UP (n=8). Slugs in groups PP and PU experienced three CaCu training pairs, and slugs in groups PP and UP experienced three CuQ training pairs. As shown in Fig. 1b, the results were parallel to those of the previous experiment. ANOVA showed differences among the groups in both Cu and Ca odors (cucumber, $F(2,21)=4.64$, $P<0.025$; carrot, $F(2,21)=17.98$, $P<0.001$). Individual comparison revealed that group PU was significantly different from groups PP and UP in Cu odor preference ($P<0.05$) and that group PP was significantly different from groups PU and UP in Ca odor preference ($P<0.05$). Figure 1c represents combined data from Fig. 1a and 1b, in which the Cu odor preferences from Fig. 1a and the Ca odor

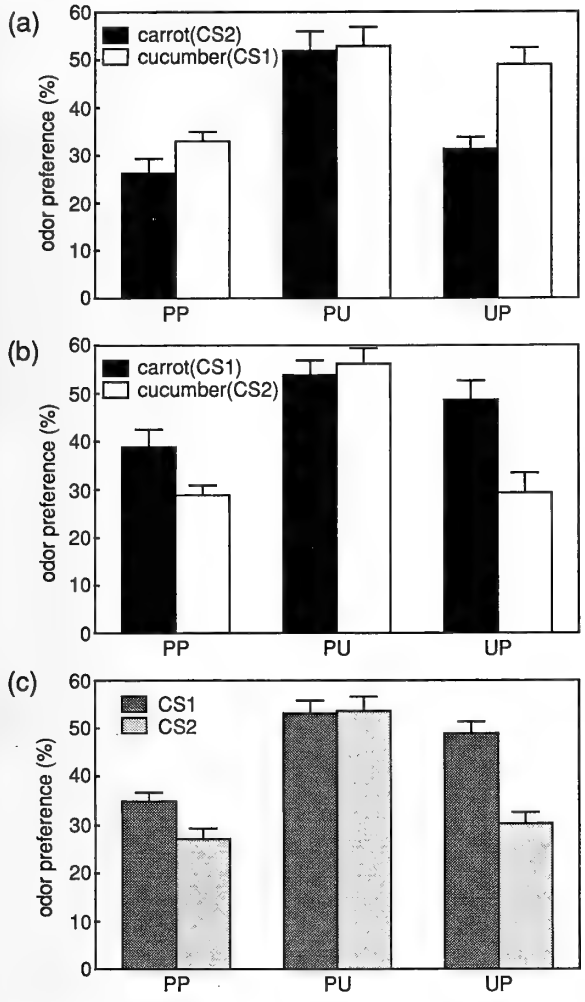

FIG. 1. Odor preferences of slugs that experienced both CS1-CS2 and CS2-US pairs (PP), only CS1-CS2 pairs (PU) and only CS2-US pairs (UP). (a) CS1: cucumber, CS2: carrot. (b) CS1: carrot, CS2: cucumber. (c) combined (a) and (b) data. US is quinidine sulfate solution. Odor preferences for carrot and cucumber are represented by solid and clear columns, respectively. Bars: standard errors of means.

preferences from Fig. 1b are combined to show CS1 odor preferences, and the Ca odor preferences from Fig. 1a and the Cu odor preferences from Fig. 1b are combined to show CS2 odor preferences. These combined results indicate that the slugs showed SPC.

Cooling-induced retrograde amnesia in the conditioned slugs

When slugs conditioned to avoid food odor were cooled immediately after presentation of the conditioned odor, retrograde amnesia was induced. Yamada *et al.* [18] reported that in *Limax flavus* CS presentation reactivates the memory involved with the conditioning and memory reactivation prior to cooling is necessary for amnesia induction. In addition, Sekiguchi *et al.* [15] indicated that cooling-induced retrograde amnesia reflects stimulus-stimulus associations formed after a variety of associative conditionings. Thus, the association after SPC was studied using amnesia.

Nineteen slugs were divided into two groups, CuF (n=9) and CaF (n=10). Slugs in groups CuF and CaF were conditioned to avoid Ca and Cu odors in the same way as those in group PP of Fig. 1a, in which Cu and Ca were used as CS1 and CS2 respectively. On the third day, after testing odor preferences, slugs in groups CuF and CaF were exposed to Cu and Ca respectively, immediately followed by cooling.

As shown in Fig. 2a, when conditioned slugs were treated with CuF (group CuF), both Ca and Cu odor preferences increased [cucumber, $t(8)=3.039$, $P<0.02$; carrot, $t(8)=2.695$, $P<0.05$, paired t-test]. A similar increase in both odor preferences was observed in the slugs treated with CaF [cucumber, $t(9)=3.197$, $P<0.02$; carrot, $t(9)=4.482$, $P<0.002$, paired t-test]. Thus, both CuF and CaF treatments resulted in an increase in both odor preferences.

In order to counterbalance the two CSs, twenty slugs were conditioned identically except that CS1 and CS2 were Ca and Cu respectively (Fig. 2b). They were treated with CaF (CS1+cooling, n=10) or CuF (CS2+cooling, n=10). After CaF treatment, both Ca (CS1) and Cu (CS2) odor preferences increased [carrot, $t(9)=5.708$, $P<0.001$; cucumber, $t(9)=5.820$, $P<0.001$], and similar results were

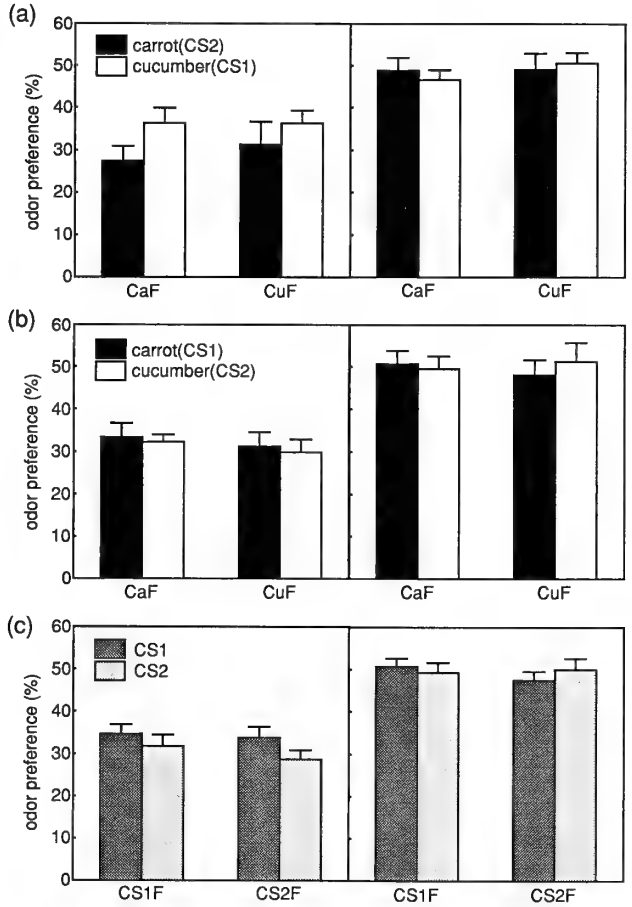

FIG. 2. Odor preferences of conditioned slugs before (left) and after (right) CaF or CuF treatment. (a) CS1: cucumber, CS2: carrot. (b) CS1: carrot, CS2: cucumber. (c) combined (a) and (b) data. Columns are the same as those in Fig. 1. Bars: standard errors of means.

observed after CuF treatment [carrot, $t(9)=3.812$, $P<0.005$; cucumber, $t(9)=3.732$, $P<0.005$]. Fig. 2c represents combined data from Fig. 2a and 2b, in which the CuF group data from Fig. 2a and the CaF data from Fig. 2b are combined to show the CS1F group results and the CaF group data from Fig. 2a and the CuF group data from Fig. 2b are combined to show the CS2F group results. These combined results indicate that in slugs conditioned by SPC, both CS1F and CS2F treatments resulted in amnesia with respect to both CS1 and CS2.

DISCUSSION

Sensory preconditioning in the terrestrial mollusk, *Limax flavus,* was studied. The first experiment indicated that the slug shows sensory preconditioning. In the second experiment, in order to study the stimulus-stimulus associations after SPC, retrograde amnesia was induced by cooling the conditioned slugs. As a result, an increase in both odor preferences was observed in response to CaF and CuF treatments.

Sensory preconditioning in Limax flavus

Although stimulus-stimulus (S-S) association was predictable from the fact that the slug shows two types of second-order conditioning [15–17], *Limax* has not been reported to show SPC. Our results clearly indicated that the slug does show SPC. This result is important because it means that even mollusks like *Limax* can associate one stimulus with others without a reinforcer.

Rescorla [10] reported in a rat that SPC was also successful even when two CSs were presented simultaneously in phase 1 of training and that simultaneous SPC resulted in a stronger conditioned response than sequential SPC. According to our preliminary experiment, simultaneous SPC was also possible in *Limax*. That is, both carrot and cucumber odor preferences were reduced by the presentation of a 1:1 mixture of Ca and Cu in phase 1. However, the preferences were not significantly different from those of sequentially conditioned slugs.

Association of sensory preconditioning

Sekiguchi *et al.* [15] demonstrated that, in cases of high-order Pavlovian conditioning, the stimulus associations are predictable from the conditioning procedure used and induced amnesia patterns.

From the conditioning procedure, it was suggested that CS1-CS2 and CS2-US associations could be formed after SPC. On examining the associations, CS2 could evoke conditioned response (CR) via a CS2-US association, and CS1 via CS1-CS2 and CS2-US associations. The results of the amnesia experiment were fully compatible with these associations; that is, CS2 presentation reactivated the CS2-US association and then the cooling resulted in amnesia of the association. As a result, CS1 as well as CS2 did not evoke CR. On the other hand, CS1 treatment first reactivated the CS1-CS2 association which in turn indirectly activated CS2-US and then cooling resulted in amnesia of both associations. Rizley and Rescorla [12] studied the association after SPC in rats. They conditioned rats by light (CS1)-tone (CS2) pairings and tone (CS2)-shock (US) pairings. After conditioning, the CS2-US association was extinguished by repeated presentation of CS2. Their observeation that this prevented not only the ability of CS2 to evoke CR but that of CS1 as well agreed with ours. Thus, we concluded that CS1-CS2 and CS2-US associations were formed during SPC.

In conclusion, associative learning in *Limax* shares common mechanisms with that in mammals, as described by Sahley *et al.* [14] and *Limax* could be a valuable model system for studies of the cellular or molecular mechanisms of various associative learning.

REFERENCES

1 Brogden WJ (1939) Sensory pre-conditioning. J Exp Psychol 25: 323–332

2 Byrne JH (1987) Cellular analysis of associative learning. Physiol Rev 67: 329–439

3 Carew TJ, Sahley CL (1986) Invertebrate learning and memory: from behavior to molecules. Annu Rev Neurosci 9: 435–487

4 Gelperin A, Hopfield JJ, Tank DW (1985) The logic of *Limax* learning. In "Model Neural Networks and Behavior" Ed by AI Selverston, Plenum Press, New York, pp. 237–262

5 Lavin MJ (1976) The establishment of flavor-flavor associations using sensory preconditioning training procedure. Learn Motivat 7: 173–183

6 Mackintosh NJ (1974) The psychology of animal learning. Academic Press, London.

7 Mackintosh NJ (1983) Conditioning and associative learning. Oxford Univ. Press, Oxford.

8 Pearce JM (1987) Introduction to animal cognition. Lawrence Erlbaum Associates Ltd., East Sussex.

9 Pfautz PL, Donegan NH, Wagner AR (1978) Sensory preconditioning versus protection from habituation. J Exp Psychol Anim Behav Process 4: 286–295

10 Rescorla RA (1980) Simultaneous and successive associations in sensory preconditioning. J Exp Psychol Anim Behav Process 6: 207–216

11 Rescorla RA, Cunningham CL (1978) Within-compound flavor associations. J Exp Psychol Anim Behav Process 4: 267–275

12 Rizley RC, Rescorla RA (1972) Associations in second-order conditioning and sensory preconditioning. J Comp Physiol Psychol 1: 1–11

13 Sahley CL, Rudy JW, Gelperin A (1981) Analysis of associative learning in a terrestrial mullusc. I. High-order conditioning, blocking and a US pre-exposure effect. J Comp Physiol A 144: 1–8

14 Sahley CL, Rudy JW, Gelperin A (1984) Associative learning in mollusk: a comparative analysis. In "Primary Neural Substrates of Learning and Behavioral change" Ed by DL Alkon and J Farely, Cambridge Univ Press, Cambridge, pp 243–258

15 Sekiguchi T, Suzuki H, Yamada A, Mizukami A (1994) Cooling-induced retrograde amnesia reflexes associations of Pavlovian conditioning in *Limax flavus.* Neurosci Res (in press)

16 Sekiguchi T, Yamada A, Suzuki H, Mizukami A (1991) Temporal analysis of the retention of a food-aversive conditioning in

Limax flavus. Zool Sci 8: 103–111

17 Spence KW (1951) Theoretical interpretation of learning. In "Handbook of Experimental Psychology". Ed by SS Stevens, Wiley, New York, pp 690–729

18 Yamada A, Sekiguchi T, Suzuki H, Mizukami A (1992) Behavioral analysis of internal memory states using cooling-induced retrograde amnesia in *Limax flavus*. J Neurosci 12: 729–735

ZOOLOGICAL SCIENCE 11: 127–131 (1994)

Growth, Metamorphosis, and Gape-limited Cannibalism and Predation on Tadpoles in Larvae of Salamanders *Hynobius retardatus*

SATOSHI OHDACHI[1]

Institute of Applied Zoology, Faculty of Agriculture, Hokkaido University, 060 Sapporo, Japan

ABSTRACT—Growth, metamorphosis, and gape-limited cannibalism and predation on tadpoles (*Rana pirica*) in larvae of salamanders (*Hynobius retardatus*) were investigated in laboratory. Larval period and the size at metamorphosis were correlated positively to one another in the salamanders. When embryos were exposed to low temperature, larval period were prolonged and the size at metamorphosis increased in the salamanders while larval period were extended and the size at metamorphosis decreased in the frogs. Salamander larvae reared in group had shorter larval period and smaller size at metamorphosis than those reared individually. Small salamander larvae were more vulnerable to cannibalism and mutilation than large ones. Tadpoles incurred high probability of predation and mutilation by salamander larvae even when the head widths of tadpoles attained the maximum sizes.

INTRODUCTION

Populations and communities of amphibian larvae are regarded as "size-structured" and their intra- and interspecific relationships change with body size rather than age [15–18]. Therefore, growth and metamorphosis (larval period, size, etc.) are essential keys to understand their intra- and interspecific interactions.

Two amphibian species, salamander *Hynobius retardatus* and frog *Rana pirica,* are common and wide-spread in Hokkaido, northern Japan. They spawn at the same sites such as small transient ponds and their larvae co-exist during their larval periods [7, 8]. The salamander larvae eat conspecific larvae and tadpoles of the frog [9], and cannibalism and predation seem to be important intra- and interspecific interactions for them.

Since the success of cannibalism and predation in salamander larvae depends on both of their own gape size and prey's body size [18], larvae of *H. retardatus* and *R. pirica* might regulate growth rates and the timing of metamorphosis to avoid or facilitate cannibalism and predation. On the other hand, growth and metamorphosis of most amphibians are negatively affected by low temperature [1]. The two amphibian species in Hokkaido initiate oviposition in early spring immediately after snow begins to melt [7, 10]. Thus, their eggs or embryos may experience low temperature, and it is desirable to examine the effects of low temperature during embryonic stages on larval growth and metamorphosis in order to investigate intra- and interspecific interactions of these amphibians.

Few studies of larval growth and metamorphosis in ecological context have been conducted for *H. retardatus* and *R. pirica* (but see [5], [6]). The aim of this paper is to obtain basic information about the relationships between growth and cannibalism/predation in the salamander larvae.

Herein, I investigated (1) the relationship between larval period and the size at metamorphosis in *H. retardatus,* (2) the effect of low temperature during embryonic stages on larval growth and metamorphosis in *H. retardatus* and *R. pirica,* (3) the effect of the presence of conspecific larvae on larval growth and metamorphosis in *H. retardatus,* and (4) the effect of gape size of *H. retardatus* larvae on the success of cannibalism and predation on *R. pirica* tadpoles.

MATERIALS AND METHODS

Egg sacs of the salamander (*H. retardatus*) and egg masses of the frog (*R. pirica*) were collected on 2–4 May, 1991 at Teshio Experimental Forest of Hokkaido University in northern Hokkaido. The egg sacs and masses were brought to laboratory at Sapporo campus of Hokkaido University, and experiments were conducted from May to September, 1991.

Three clutches of salamanders were used to examine the relationship between larval period and the size at metamorphosis. The three clutches consisted of 32, 41, and 26 larvae, for each. Larvae were reared with their siblings in polyethylene containers (26×18×8 cm, 3600 ml water contained) under uncontrolled room condition (19–23°C in spring and 22–26°C in summer, natural day light).

Three experiments were designed for growth studies of the salamander larvae. *Experiment 1* (*moderate temperature treatment, individually reared*). After most larvae in a clutch had hatched in a room condition (19–23°C, natural day light), 16 larvae chosen randomly from the clutch were kept separately in glass vials (5-cm diameter and 10-cm height, 180 ml water) under 20°C and 16L8D (16 hr light and 8 hr dark period cycle) condition. *Experiment 2* (*low temperature treatment, individually reared*). After introduced into laboratory, a pair of egg sacs (=a full clutch) was kept in a refrigerator (4–7°C, all dark period) for 20 days. Most embryos in the egg sacs were in the tail-bud stage at the beginning of the

Accepted October 12, 1993
Received September 9, 1993

[1] Present and correspondence address: Zoological Section, Institute of Low Temperature Science, Hokkaido University, 060 Sapporo, Japan

treatment. Then, the egg sacs were brought into the room condition. Some larvae began to hatch within one day. After most larvae had hatched, 16 larvae randomly chosen were separately kept in the glass vials under 20°C and 16L8D condition. *Experiment 3* (*low temperature treatment, reared in group*). Descriptions were the same as in Experiment 2 except that 20 larvae were reared together in a polyethylene container (3600 ml water). In the container, some pieces of plastic net were put so that larvae could rest on them and escape from severe antagonistic interactions by other larvae. Individuals were not identified in this experiment. Larvae examined in Experiments 2 and 3 were from the same clutch, and mean total length and head width were not different significantly between the two groups at the beginning of the experiments (Mann-Whitney's $U=142$, $P=0.567$). Artificial feeds for salmon fry were given for larvae in early stages and dried *Tubifex* for developed ones. Foods were given every 1–2 day, and a given amount of food per capita was the same for all experimental designs. Water was replaced every 2 days.

Two experiments were designed for growth studies of the tadpoles. *Experiment 1* (*moderate temperature treatment, individually reared*). After most tadpoles had hatched, 16 tadpoles were chosen randomly and kept separately in glass vials (180 ml water). *Experiment 2* (*low temperature treatment, individually reared*). After introduced into laboratory, a part of egg mass was kept in a refrigerator (4–7°C, all dark period) for 17 days, and then brought into a room condition (19–23°C, natural day light). The embryos in the egg mass were in the late tail-bud stage at the beginning of the treatment, and some embryos began to hatch one day before the introduction to the room condition. After most tadpoles had hatched, 16 tadpoles were kept separately in the glass vials under 20°C and 16L8D condition. Both in Experiments 1 and 2, kinship among tadpoles was unknown. Artificial feeds for salmon fry were given ad libitum every day. Water was replaced every 1–2 days.

For the experiments of cannibalism and predation on tadpoles in salamander larvae, salamander and frog larvae in various sizes were prepared by controlling water temperature. Experimental procedures were as follows. Larvae were introduced separately in glass vials under 20°C and 16L8D condition, and no foods were provided for two days. After body size (head width and total length) was measured, two individuals (salamander-salamander or salamander-tadpole combination) were introduced into a glass vial (180 ml water). Three types of interactions, predation/cannibalism, mutilation (including killing but not eating a whole body), and non-antagonism, were recorded 24 hours later. Kinship among salamander and frog larvae was unknown.

Definitions of body measures are as follows. Total length, length from the anterior point of head to the posterior point of tail; head width, the maximum width of head without gills. Total length and head width were measured by digital vernier calipers to the nearest 0.1 mm, and wet weight by a micro-electrobalance to the nearest 1 mg. In this paper, 'metamorphosed' refers to the condition that gills became degenerated and skins began to be melanised for salamander larvae and that total length attained the maximum size for tadpoles. Larval period was defined as the period from the day when larvae began to hatch in a clutch to the day when an individual larva metamorphosed.

RESULTS

Growth and metamorphosis of salamanders

Mean time lag between the first and last hatching dates was 4.7 days (N=11, SD=1.10, Range=2–6). In a clutch, hatching began on May 27 and continued until May 31. The majority of larvae hatched on the first and second days; 25 larvae on May 27, 31 on May 28, and 5 on May 29–31. The hatchlings which emerged on earlier days had significantly smaller total length and head width than those hatched on later days (Table 1; Mann-Whitney's *U*-test, $P<0.003$).

TABLE 1. Total length and head width (mm) of hatchlings in a clutch of salamander *Hynobius retardatus* on different dates. The egg sac was kept in uncontrolled room condition. Hatchlings were removed from water tank immediately after they hatched and then fixed in 10% formalin.

Date	Total length	Head width
	Mean±SD (N)	Mean±SD (N)
May 27	15.8±0.7 (25)	2.6±0.3 (23)
May 28	16.5±0.8 (31)	3.2±0.3 (30)
May 29–31	18.7±1.4 (5)	4.0±0.4 (5)

Head width continued to increase until metamorphosis in some larvae, but other larvae showed abrupt decline of head width just before metamorphosis (Fig. 1). The power function curves showed good fit to the growth trajectories of head width. The power function curve is defined as follows; $Y=aX^b$, where X is period (day) from the first hatch day of a clutch, Y the head width for X, a and b constants. The constants were calculated by the least square method. I also applied the exponential curve ($Y=ae^{bX}$; a and b, constants), which was often used as a growth model of amphibian larvae (e.g., [17], [19]), but it fitted worse than the power function curve.

Larval period and the size at metamorphosis (total length, head width, wet weight) were correlated positively with each other, and all the regression lines were significant (ANOVA, $P<0.001$). However, correlation was rather weak in head width ($R=0.41$) than in total length ($R=0.67$) and wet weight ($R=0.65$). Furthermore, the third ordered regression curves fitted better (ANOVA, $P<0.0001$) and had higher R^2 values than the linear and second ordered regressions in all the body size dimensions. The two-way plot for larval period and the wet weight at metamorphosis was shown as a representative in Figure 2.

The body size at metamorphosis (total length, head width, wet weight) tended to be larger for the low temperature treatment than for the moderate temperature treatment (Table 2, Exp. 1 *vs.* 2), and wet weight showed significant difference between them ($U=34.0$, $P<0.02$). Larval period was longer significantly for the low temperature treatment than for the moderate temperature treatment (Table 2; $U=12.5$, $P<0.004$).

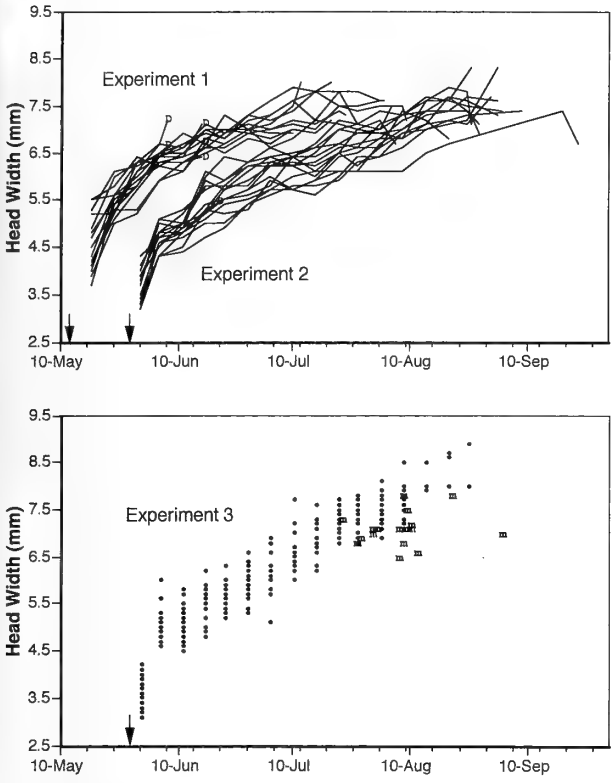

FIG. 1. Head width until metamorphosis for individual larvae of salamanders *Hynobius retardatus* in three experiments. Experiment 1, separately reared and moderate temperature treatment during embryonic stages; Experiment 2, separately reared and low temperature treatment; Experiment 3, reared in group and low temperature treatment. Individuals were not identified in Experiment 3. All larvae were reared under 20°C and 16L8D condition. Larvae within each experiment were from the same clutches, and larvae of an identical clutch were used in Experiments 2 and 3. Arrows indicate the first hatch days. Marks "D" and "m" denote death before metamorphosis and metamorphosis, respectively.

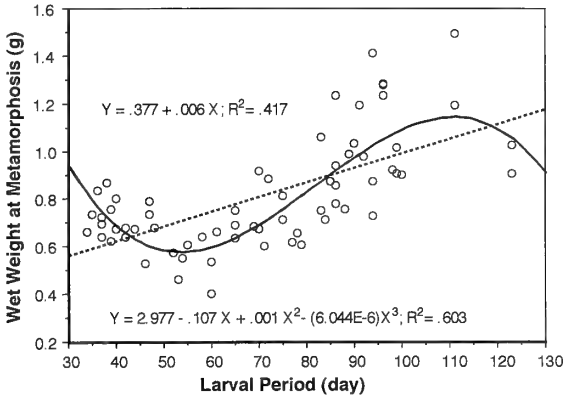

FIG. 2. Two-way plot of larval period and the wet weight at metamorphosis in salamanders *Hynobius retardatus*. Larvae were reared with their siblings under uncontrolled room conditions. Both the regression line and the third-order regression curve were significant ($P<0.001$).

The larvae reared in group had significantly shorter larval period and smaller wet weight and head width at metamorphosis than those reared individually (Table 2, Exp. 2 *vs.* 3; $U=25.5$ for period, 22.0 for wet weight, and 73.5 for head width, $P<0.05$), but total length demonstrated no significant difference between the larvae reared in group and individually ($U=80.0$, $P<0.054$). No larvae were eaten by conspecifics during Experiment 3, but one larva died before metamorphosis.

Growth and metamorphosis of tadpoles

Growth trajectories for head width until metamorphosis were fitted well to the power function curves, $Y=aX^b$ (ANOVA, $P=0.01$). I also applied the exponential curve but they fitted worse than the power function curve.

Mean larval period was significantly longer for the low temperature treatment than for the moderate temperature

TABLE 2. Larval period and the size at metamorphosis in salamanders *Hynobius retardatus* in three experiments. Experiment 1, separately reared and moderate temperature treatment during embryonic stages; Experiment 2, separately reared and low temperature treatment; Experiment 3, reared in group and low temperature treatment

Experiment	N	Period (day)	Total length (mm)	Head width (mm)	Wet weight (g)
		Mean±SD	Mean±SD	Mean±SD	Mean±SD
1	11	73.9±10.0	48.8±2.4	7.4±0.4	0.733±0.124
2	14	96.0±11.1	49.1±3.0	7.4±0.5	0.895±0.161
3	19	71.4± 9.3	47.1±2.8	7.1±0.3	0.623±0.101

TABLE 3. Larval period and the size at metamorphosis in frogs *Rana pirica* in two experiments. Experiment 1, separately reared and moderate temperature treatment during embryonic stages; Experiment 2, separately reared and low temperature treatment

Experiment	N	Period (day)	Body length (mm)	Head width (mm)
		Mean±SD	Mean±SD	Mean±SD
1	15	37.3±3.0	42.5±2.3	8.6±0.7
2	10	40.0±2.1	34.7±1.4	7.9±0.3

treatment ($U=22.5$, $P=0.0036$), while mean size at metamorphosis was significantly smaller for the former than for the latter ($U=0.0$ for total length and 26.0 for head width, $P<0.01$) (Table 3).

Gape-limited cannibalism and predation

No cannibalism occurred in salamander larvae when both larvae had similar head width, but mutilation occurred even when opponents were much larger (Fig. 3). Small larvae were more vulnerable to cannibalism than large ones.

When salamander larvae were small, tadpoles were not eaten by them even if head widths of tadpoles were smaller than those of salamanders (Fig. 4). A number of tadpoles were eaten or mutilated by the salamander larvae whose head widths were larger than approximately 4.5 mm, even if head widths of tadpoles were larger than those of salamanders. No tadpoles could escape from predation nor mutilation by the salamanders larger than approximately 7.5 mm.

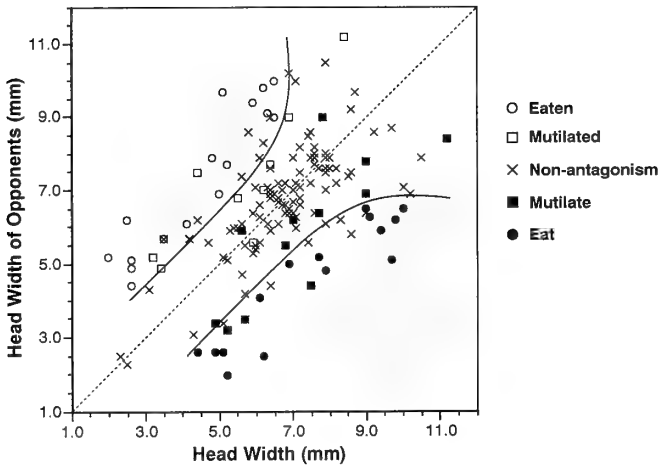

FIG. 3. Head width and cannibalism in larvae of salamanders *Hynobius retardatus*. Shaded areas indicate the regions of high probability of cannibalism (curves were drawn by hand). Broken line is an isoline.

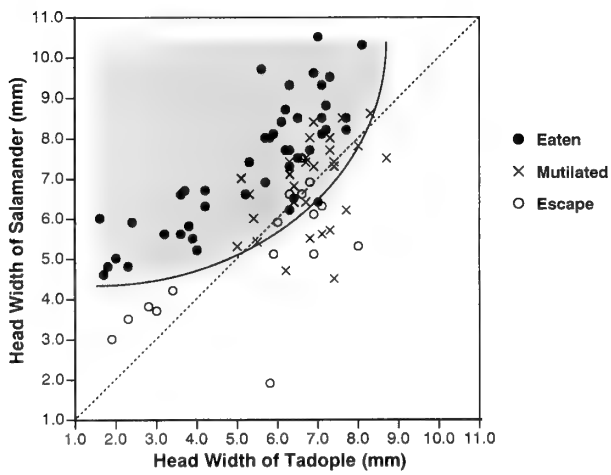

FIG. 4. Head width and predation in larvae of frogs *Rana pirica* and salamanders *Hynobius retardatus*. Shaded area indicates the region of high probability of predation (a curve was drawn by hand). Broken line is an isoline.

DISCUSSION

Relationship between larval period and size

Larval period and the size at metamorphosis were correlated positively with each other in *H. retardatus* (Fig. 2). A similar relationship has been reported in many amphibian species [1, 3, 5]. The third ordered regression curve was more explainable for the scattering of the data than the linear regression line (Fig. 2). I interpreted the formation of the third ordered function curves as follows. First, the larvae with higher growth rates begin to metamorphose. Subsequently, those with lower growth rates begin to metamorphose until the minimum point of the curve. The larvae that could not metamorphose by the minimum point decide to prolong their larval periods and grow more. The minimum point might be the compromise point between negative effects of long larval period, such as risk of pond desiccation and higher probability of predation [4, 15, 17, 18], and positive effects of large body size, such as high resistance against starvation and desiccation or high fertility in adults [13]. In contrast, the meaning of the maximum point of the curve is vague. In natural conditions, some larvae of *H. retardatus* over-winter in natural pond [9]. Thus, the larvae with extremely low growth rates will not metamorphose in the year of birth.

Effect of conspecifics on metamorphosis and cannibalism

It has been reported that the presence of other conspecific individuals caused long larval period and low growth rate owing to interference competition in salamander *Ambystoma opacum* [12] and anurans [2, 11, 14]. In contrast, *H. retardatus* demonstrated short larval period when they were reared in group (Table 2). The shortened larval period might be a tactics to avoid cannibalism as Wilbur [18] insisted; small larvae are more vulnerable to cannibalism than larger ones (Fig. 3), and short larval period seems to be a solution for the avoidance of cannibalism. In addition, it could be also regarded as the avoidance of cannibalism among siblings that small larvae hatched earlier than large ones (Table 1).

Low temperature effects on metamorphosis

It has been known that metamorphosis postponed when larvae were reared in low temperature in many species of amphibians [1] including *Hynobius* spp. and *R. pirica* [3, 5, 6]. In the present study, it was found that low temperature exposure during embryonic stages also prolonged larval periods in the amphibians even when larvae were reared in moderate temperature (Tables 2 and 3). The prolongation of larval period was accompanied by large body size at metamorphosis in *H. retardatus* (Table 2), while it occurred with small body size in *R. pirica* (Table 3). Therefore, low temperature in early spring seems to be more malignant for *R. pirica* than *H. retardatus*, since the latter could deny the negative effects of long larval period by the positive effects of large metamorph size while the former could not.

Predation on tadpoles by salamanders

Even large tadpoles of *R. pirica* have high probability of predation and mutilation by the salamander larvae unless salamander larvae are in early stages (Fig. 4). Tadpoles can lessen the risk of predation or mutilation by hatching earlier and/or leaving ponds earlier than the salamanders. Certainly, many *R. pirica* oviposit earlier than *H. retardatus* in Tokachi region [10], although oviposition in early spring may be in danger of low temperature exposure during embryonic stages, which has unfavorable effects (long larval period and small metamorph size) at metamorphosis for them (Table 3). Period for hatching is shorter in *R. pirica* than *H. retardatus* at 10 and 20°C [5], and growth rate until metamorphosis of *R. pirica* was much higher than that of *H. retardatus* (Fig. 1 and Table 3). Therefore, most of *R. pirica* appear to leave ponds earlier than *H. retardatus*.

ACKNOWLEDGMENTS

Takanori Sato, Takayuki Ohgushi, and Shigeru Nakano reviewed earlier versions of this paper. Members of Hokkaido University Brown Bear Research Group and Masatoshi Toyama assisted me for this work. I deeply express my gratitude to them.

REFERENCES

1 Dellman WE, Trueb L (1986) "Biology of Amphibians" McGraw-Hill, New York, pp 670

2 Griffiths RA, Edgar PW, Wong AL (1991) Interspecific competition in tadpoles: growth inhibition and retrieval in natterjack toads, *Bufo calamita*. J Anim Ecol 60: 1065–1076

3 Kusano T (1981) Growth and survival rate of the larvae of *Hynobius nebulosus tokyoensis* Tago (Amphibia, Hynobiidae). Res Popul Ecol 23: 360–378

4 Morin PJ (1981) Predatory salamanders reverse the outcome of competition among three species of anuran tadpoles. Science 212: 1284–1286

5 Moriya T (1979) Effect of temperature on embryonic and post embryonic development of salamander, *Hynobius retardatus*. Low Temp Sci, Ser B 37: 113–115

6 Moriya T (1983) The effect of Temperature on the action of thyroid hormone and prolactin in larvae of the salamander *Hynobius retardatus*. Gen Comp Endocrinol 49: 1–7

7 Sato T (1989) Breeding environment and spawning of a salamander, *Hynobius retardatus*, at the foot of Hidaka mountains, Hokkaido, Japan. In "Current Herpetology in East Asia" Ed by M Matsui, T Hikida, and RC Goris, Herpetological Society of Japan, Kyoto, pp 292–304

8 Sato T (1990) Breeding sites of a salamander, *Hynobius retardatus*. (In Japanese with English abstract). Bull Obihiro Centennial City Mus 8: 1–10

9 Sato T (1990) Temperature and velocity of water at breeding sites of *Hynobius retardatus*. Jpn J Herpetol 13: 131–135

10 Sato T (1993) "Kushiro Shitsugen Nature Guid" Japanese Society of Preservation of Birds, Kushiro Onnenai, Tsurui Vill., Akangun, Hokkaido, p 23

11 Semlitsch RD, Caldwell JP (1982) Effects of density on growth, metamorphosis, and survivorship in tadpoles of *Scaphiopus holbrooki*. Ecology 63: 905–911

12 Smith CK (1990) Effects of variation in body size on intraspecific competition among larval salamanders. Ecology 71: 1777–1788

13 Smith DC (1987) Adult recruitment in chorus frogs: effects of size and date at metamorphosis. Ecology 68: 344–350

14 Smith DC (1990) Population structure and competition among kin in the chorus frog (*Pseudacris triseriata*). Evolution 44: 1529–1541

15 Werner EE (1986) Amphibian metamorphosis: growth rate, predation risk, and the optimal size at transformation. Amer Natur 128: 319–341

16 Wilbur HM (1980) Complex life cycles. Ann Rev Ecol Sys 11: 67–93

17 Wilbur HM (1984) Complex life cycles and community organization in amphibians. In "A New Ecology. Novel Approaches to Interactive Systems" Ed by PW Price, CN Slobodchikoff, and WS Gaud, John Wiley & Sons, New York, pp 195–224

18 Wilbur HM (1988) Interactions between growing predators and growing prey. In "Size-structured Populations" Ed by B Ebenman and L Persson, Springer-Verlag, Berlin, pp 157–172

19 Wilbur HM, Collins JP (1973) Ecological aspects of amphibian metamorphosis. Science 182: 1305–1314

ZOOLOGICAL SCIENCE 11: 133–137 (1994)

Allocation of Resources to Body Components in *Heliocidaris erythrogramma* and *Heliocidaris tuberculata* (Echinodermata: Echinoidea)

JOHN M. LAWRENCE[1] and MARIA BYRNE[2]

[1]*Department of Biology, University of South Florida, Tampa, Florida 33620, U.S.A.*
and [2]*Department of Histology and Embryology, University of Sydney, Sydney, N.S.W. 2006, Australia*

ABSTRACT—Adult *Heliocidaris erythrogramma* (*He*) (50 g wet body weight) and *H. tuberculata* (*Ht*) (200 g wet body weight) are compared. The relative sizes of the test and spines are the same for both species, but that of the Aristotle's lantern is 2-fold larger in *He*. The gonad index shows no sexual differences and is similar for both species (*He*: 10, *Ht*: 12). The proximate composition of the gut, Aristotle's lantern, test, and spines of both species are similar. The percent organic material in the ovaries of *He* is greater than in the testes and in the ovaries and testes of *Ht*. Lipid is 50% of the dry weight of the ovaries of *He*, twice that in the ovaries and testes of *Ht*. DNA is 6% of the dry weight of the testes of *He*, half that in the testes of *Ht*. The direct development in *He* and indirect development in *Ht* is correlated with differences in body size and proximate composition of the gonads.

INTRODUCTION

Grime [11] pointed out the desirability of dtudying both the established and regenerative phases in the life-history of an organism in considering adaptive strategies, as they may be subject to different forms of natural selection or respond differently to the same selecltive force. Grime stated these phases are uncoupled, noting the radical differences between larval and adult phases of invertebrates. He suggested a particular regenerative strategy may be modified by two important variables: the strategy adopted during the established phase and the breeding system. A case in point is the genus *Heliocidaris*.

Clark [3] stated the genus *Heliocidaris* A. Agassiz and Desor 1846 contains only two species that differ obviously in general appearance but not in specifics. He separated the species on the basis of number of pore-pairs, a characteristics not expected to cause major functional differences. Among the gross differences is the smaller size of *H. erythrogramma* Valenciennes 1846 (to 86 mm horizontal diameter) compared to *H. tuberculata* Lamarck 1816 (to 106 mm horizontal diameter). The two species differ in habitat. *In general, Heliocidaris erythrogramma* is a rock-burrowing species at low-tide level and *H. tuberculata* is subtidal on the Australian coast and on the reef flat on Lowe Howe Island [3, 4]. The two species probably have different levels of resource availability as well as exposure.

Considerable interest in the two species has resulted from the differences in their development noted by Mortensen [19, 20] and documented by Williams and Anderson [30]. *H. erythrogramma* has direct development in contrast to *H. tuberculata*. Their divergent ontogenies have provided a model for studying the evolution of development [22]. Studies of the established adult phase have not accompanied these studies.

The ways resorces are allocated to structures and functions are important lief-history characteristics [2]. Amont the most important is the trade-off associated with increased age and size involving a transition to increased allocation to reproduction and decreased allocation to growth. Strathmann & Strathmann [27] noted the association of brooding with small adult-size in marine invertebrates, and pointed out the smaller of co-occurring species are the brooders. None of the hypotheses considered (allometry of egg protection and brood care, longevity with iteroparity, variable recruitment, dispersal) involved the allometry of acquisition and allocation of resources.

Being aware of the difference in size of the established phase of the two species and the trade-off models involving growth and reproduction, we hypothesized allocation of resources to body components in *Heliocidaris erythrogramma* and *H. tuberculata* would differ and that the difference could be correlated with their biology and ecology and with the differences in their regenerative phases. We believe an understanding of the characterisitics of the established phase can assist in understanding those of the regenerative phase.

MATERIALS AND METHODS

Heliocidaris erythrogramma were collected at Little Bay on 21 November 1991 and *H. tuberculata* were collected at Shelley Beach, New South Wales, Australia on 7 June and 2 August 1992. These dates are at the maximal gonad indexes of the species' broad reproductive cycles [13]. Individuals were dissected into body compartments that were lyophilized and weighed. The components were homogenized in a Wiley mill for proximate analysis. Ovaries and testes were analyzed separately, but no sexual distinction was made for the somatic compartments as evidence indicates no sexual

Accepted January 4, 1994
Received October 7, 1993

differences in echinoids [18]. Lanterns were treated with hydrogen peroxide to obtain the demi-pyramids and rotules by the method of Ebert [5]. Pigmented growth lines in the lantern were counted by the method of Jensen [12] of three specimens of each species. Proximate analysis and calculation of energy equivalents was done by the methods used by Lawrence [14] and Watts and Lawrence [29]. Significant differences were tested by ANOVA except for concentration of DNA, which was compared by Student's *t*-test ($P<0.05$). Data were transformed as necessary to satisfy conditions of normality and equal variances.

RESULTS

The sized of the individuals and weights of the body compartments are given in Table 1. Neigher *Heliocidaris erythrogramma* or *H. tuberculata* showed sexual dimorphism in size. *Heliocidaris erythrogramma* was smaller than *H. tuberculata,,* the difference in weight (4-fold less) being greater than the difference in diameter (1.4-fold less). The weights of the body compartments were correspondingly smaller in *H. erythrogramma* than in *H. tuberculata.* The relative sizes, indexes based on dry weight, did not differ significantly except for the Aristotle's lantern, which was 2-fold greater in *H. erythrogramma* (Table 2). The demi-pyramids of specimens of both species had 4 to 6 pigmented lines, indicating equivalent age and faster growth in *H. tuberculata.*

The proximate composition of the body compartments of the two species (Table 3) are similar except for the gonads.

TABLE 1. *Heliocidaris erythrogramma* and *Heliocidaris tuberculata*: Horizontal diameter (mm); wet body weight and compartment dry weights (g)

	Sex	*Heliocidaris erythrogramma*	*Heliocidaris tuberculata*
Horizontal diameter		67 (1)	94 (1)
		[23]	[30]
Wet body weight		53 (2)	201 (6)
		[23]	[30]
Gonads dry weight	M	1.00 (0.32)	6.56 (0.61)
		[9]	[14]
	F	1.22 (0.15)	5.59 (1.76)
		[14]	[9]
Test dry weight		14 (1)	57 (3)
		[23]	[19]
Spines dry weight		16 (1)	63 (3)
		[23]	[20]
Lantern dry weight		1.6 (0.01)	3.2 (0.01)
		[23]	[19]
Rotule dry weight		0.027 (0.001)	0.063 (0.003)
		[19]	[18]
Demi-pyramid dry weight		0.096 (0.004)	0.182 (0.007)
		[19]	[18]

Sexes are combined except for gonads. Means, standard error (in parenthesis), and n (in brackets) are given. All values for the two species are significantly different ($P<0.05$).

TABLE 2. *Heliocidaris erythrogramma* and *Heliocidaris tuberculata*: Gonad index (% wet body weight); test, spine, and lantern indexes (% dry weight of somatic compartments).

	Sex	*Heliocidaris erythrogramma*		*Heliocidaris tuberculata*	
Gonad index		9.9 (1.5)		13.3 (0.6)	
		[9]		[10]	
	F	9.1 (0.7)		11.1 (0.8)	
		[14]		[8]	
Test index		45 (1)		47 (1)	
		[23]		[16]	
Spines index		50 (1)		50 (1)	
		[23]		[16]	
Lantern index		5.3 (0.1)	A	2.7 (0.1)	B
		[23]		[16]	

Sexes are combined except for gonads. Means, standard error (in parenthesis), and n (in brackets) are given. The indexes are not significantly different ($P>0.05$) except for the lantern index.

TABLE 3. *Heliocidaris erythrogramma* and *Heliocidaris tuberculata*: Proximate composition (% dry weight)

	Sex	*Heliocidaris erythrogramma*		*Heliocidaris tuberculata*	
Gonads					
% organic material	M	91 (1)	A	91 (1)	A
		[9]		[14]	
	F	96 (0)	B	92 (1)	A
		[13]		[8]	
% carbohydrate	M	11 (1)	A	11 (1)	A
		[8]		[14]	
	F	8 (1)	B	12	A
		[14]		[8]	
% lipid	M	26 (2)	A	22 (1)	A
		[9]		[13]	
	F	50 (2)	B	27 (1)	A
		[14]		[9]	
% soluble protein	M	37 (3)	AB	42 (2)	BC
		[9]		[13]	
	F	29 (2)	A	45 (3)	B
		[14]		[9]	
% insoluble protein	M	11		2	
	F	9		9	
% DNA	M	5.5 (1.9)	A	14.1 (1.2)	B
		[4]		[5]	
Test					
% organic material		18 (1)		22 (2)	
		[20]		[18]	
% carbohydrate		3.21 (0.18)		3.68 (0.35)	
		[9]		[9]	
% lipid		1.28 (0.04)		1.38 (0.08)	
		[12]		[10]	
% soluble protein		4.85 (0.28)		4.97 (0.30)	
		[12]		[10]	
% insoluble protein		9		12	

Spines		
% organic material	16 (1) [27]	17 (1) [18]
% carbohydrate	0.36 (0.10) [10]	0.27 (0.02) [10]
% lipid	1.14 (0.10) [12]	0.02 (0.07) [10]
% soluble protein	3.98 (0.30) [12]	2.51 (0.13) [10]
% insoluble protein	11	14
Lantern		
% organic material	20 (1) [20]	24 (2) [19]
% carbohydrate	4.09 (0.32) A	0.78 (0.15) B
% lipid	1.55 (0.10) [12]	1.38 (0.23) [10]
% soluble protein	5.95 (0.68) [12]	1.38 (0.23) [10]
% insoluble protein	9	15

Means, standard error (in parentheses), and n (in brackets) are given. Insoluble protein values were calculated from means. Values with the same letter or no letter are not significantly different.

The ovaries of *H. erythrogramma* had a slight but significantly higher concentration of organic material than those of *H. tuberculata*. This was due to a 2-fold greater concentration of lipid in the ovaries compared to the testes of *H. erythrogramma* and both the ovaries and testes of *H. tuberculata*. The concentrations of the other proximate components in the ovaries of *H. erythrogramma* were correspondingly reduced. The concentration of DNA in the testes of *H. erythrogramma* was one-third that in the testes of *H. tuberculata*.

Most energy in the body compartments was in the form of protein, even in the gonads, except in the ovaries of *Heliocidaris erythrogramma* where most was lipid (Table 4). Most energy in the somatic compartments was in the form of insoluble protein. The ratios of the weights of the wet body and dry somatic components of *Heliocidaris erythrogramma* to *H. tuberculata* were similar, indicating isometry. Likewise the somatic component indexes were similar but the gonad indexes were ca. 2-fold greater in energy units than in gravimetric units for both species.

Five to six growth lines were present on the demi-pyramids of three specimens of each species.

DISCUSSION

The established, mature phases of *Heliocidaris erythrogramma* and *H. tuberculata* differ in three major ways: the dimensions and weights of the body and body compartments are smaller in *H. erythrogramma*; the concentration of lipid in the ovaries is greater in H. erythrogramma and the concentration of DNA in the testes is less in *H. erythrogramma*; the relative sizes of the body compartments are similar except the Aristotle's lantern index is greater in *H. erythrogramma*.

TABLE 4. *Heliocidaris erythrogramma* and *Heliocidaris tuberculata*: Kilojoules in body compartments of females

	Heliocidaris erythrogramma	*Heliocidaris tuberculata*
Ovaries		
Carbohydrate	1.17	10.63
Soluble protein	8.03	54.56
Insoluble protein	3.54	19.37
Lipid	23.30	54.91
Sum	36.41	139.47
Test		
Carbohydrate	1.37	7.88
Soluble protein	2.83	14.64
Insoluble protein	53.61	266.64
Lipid	1.19	6.72
Sum	59.00	295.88
Spines		
Carbohydrate	0.17	0.51
Soluble protein	2.36	6.38
Insoluble protein	56.92	245.38
Lipid	0.19	<0.01
Sum	60.64	252.27
Lantern		
Carbohydrate	0.17	0.17
Soluble protein	0.47	1.18
Insoluble protein	6.61	16.30
Lipid	<0.01	0.40
Sum	7.25	18.05
Sum all somatic tissues	126.89	566.20
Sum all somatic tissues and ovaries	163.30	705.67
Ovaries/total somatic tissue and ovaries	22	20

The high concentration of lipid in the ovaries of *Heliocidaris erythrogramma* is at the upper limit reported for the ovaries and eggs of other direct developing echinoderms [8, 15]. Wray & Raff [in 24] reported the eggs of *H. erythrogramma* were ca. 50% lipid by volume. Energy investment per egg would be greater in *H. erythrogramma* than in *H. tuberculata* as a result of the higher concentration of lipid and the larger egg-size.

This is the first report of the concentration of DNA in echinoderm testes. As the sperm-head length of *Heliocidaris erythrogramma* is ca. two-fold greater than that of *H. tuberculata* while the DNA content of the sperm is only ca. 1.3-fold [13, 23], the difference in concentration seems to result from a packing phenomenon. The difference in sperm size affects both energy investment per sperm and sperm number per individual. *Heliocidaris erythrogramma* invests more energy per sperm, and produces fewer sperm per individual as a results of its larger sperm and smaller body size.

Allometry is the general rule with increase in body size [21]. consequently, the isometry of the test, spine, and particularly the gonad indexes of the asymptotic sized of *Heliocidaris erythrogramma* and *H. tuberculata* was not expected. Allometry of the gonads has been reported in several strongylocentrotid species up to a body size at which isometry occurs [9, 10, 28]. The continued increase in relative gonadal production in *Strongylocentrotus franciscanus* beyond the body size at which it ceases to increase in *S. intermedius* and *S. purpuratus* is correlated with lantern size and allometric coefficient (Lawrence et al., unpub.). Consumption is the largest term in the energy budget and sets the upper limit for all other variables [21]. Assuming the relative size of the lantern is indicative of feeding capacity [5], *H. erythrogramma* should have a greater relative capacity for resource acquisition than *H. tuberculata* at asymptotic body sized. The lantern sizes of similarly-sized (horizontal diameter=60–70 mm) *H. tuberculata* and *H. erythrogramma* are similar (ca. 1.5 g dry weight, Lawrence and Byrne, unpub.).

It seems the conclusion of Strathmann & Strathmann [27] that the species of related co-occurring marine invertebrates that broods has the smaller adults can be extended to species with direct development. This generalization does not address the question of absolute size. *Heliocidaris erythrogramma* is no smaller than the strongylocentrotid species that have indirect development. If stressful conditions (decreased potential for production) tend to result in the evolution of species that invest more energy per propagule [16, 17], *H. erythrogramma* may have less capacity for production so that it ceases somatic growth at a smaller size, and makes up for decreased fecundity by direct development. These considerations fit Ebert's [6] conclusion that *H. erythrogramma* is a very long-lived species. The longevity of *H. tuberculata* is not known. The similar number of growth lines but different body sizes indicates *H. tuberculata* grows more rapidly than *H. erythrogramma.* Overall, the differences in asymptotic body size, growth rates, and fecundity between the two species seem related to their potential for production.

Growth has both genetic and environmental controls [25]. *Although* echinoids fit the indeterminate growth pattern (plastic asymptotic, growth), in which the growth trajectory and adult size are determined by energy intake and costs, a genetic component exists as seen here with the two species of *Heliocidaris.* We assume the differenc in growth rates and asymptotic sizes of *Heliocidaris erythrogramma* and *H. tuberculata* involved the evolution of genetic control of growth patterns. The difference in developmental pattern in *H. erythrogramma* involved the evolution of genetic control of developmental processes [22]. Did the evolution of both the regenerative and established phase occur simultaneously or sequentially? If indirect development is lost more frequently than gained evolutionarily [7, 8, 26], the direction of evolution was from *H. tuberculata* to *H. erythrogramma.*

ACKNOWLEDGMENTS

We thank Daniel Bishop and Steven Beddingfield (University of Alabama at Birmingham) for analyzing the DNA in the testes and growth lines in the lantern, and Carolyn Yates (USF) for proximate analysis.

REFERENCES

1 Brody S (1945) Bioenergetics and Growth. Hafner Publishing Company, New York, pp 1023

2 Calow P (1984) Economics of ontogeny—adaptational aspects. In "Evolutionary Ecology" Ed by B Shorrocks, Blackwell Scientific Publications, Oxford, pp 81-104

3 Clark HL (1946) The echinoderm fauna of Australia: its composition and origin. Carnegie Inst Wash Pub 566, pp 567

4 Dakin WJ (1952) Australian Seashores. Angus and Robertson, Sydney, p 372

5 Ebert TA (1980) Relative growth of sea urichin jaws: an example of plastic resource allocation. Bull Mar Sci 30: 467–474

6 Ebert TA (1982) Longevity, life history, and relative body wall size in sea urchins. Ecol Monogr 52: 353–394

7 Emlet RB (1990) World patterns of developmental mode in echinoid echinoderms. Adv Invert Reprod 5: 329–335

8 Emlet RB, McEdward LR, Strathmann RR (1987) Echinoderm larval ecology viewed from the egg. Echinoderm Studies 2: 55–136

9 Fuji A (1967) Ecological studies on the growth and food consumption of Japanese common littoral sea urchin, (*Strongylocentrotus intermedius*) (A. Agassiz). Mem Fac Fish Hokkaido Univ 15: 83–160

10 Gonor JJ (1972) Gonad growth in the sea urchin (*Strongylocentrotus purpuratus*) (Stimpson) (Echinodermata: Echinoidea) and the assumptions of the gonad index methods. J Exp Mar Biol Ecol 10: 89–103

11 Grime JP (1979) Plant strategies and vegetation. John Wiley & Sons, Chichester

12 Jensen M (1969) Age determination of echinoids. Sarsia 37: 41–44

13 Laegdsgaard P, Byrne M, Anderson DT (1991) Reproduction of sympatric populations of *Heliocidaris erythrogramma* and *H. tuberculata* (Echinoidea) in New South Wales. Mar Biol 110: 359–374

14 Lawrence JM (1973) Level, content, and caloric equivalents of the lipid, carbohydrate, and protein in the body components of *Luidia clathrata* (Echinodermata: Asteroidea: Platyasterida) in Tampa Bay. J Exp Mar Biol Ecol 11: 263–274

15 Lawrence JM (1987) A Functional Biology of Echinoderms. Crooms-Helm, London, p 340

16 Lawrence JM (1990) The effect of stress and disturbance on echinoderms. Zool Sci 7: 17–28

17 Lawrence JM (1991) Analysis of characteristics of echinoderms associated with stress. In "Bioology of Echinodermata" Ed by T Yanagisawa, I Yasumasu, C Oguro, N Suzuki, T Motokawa, Balkema, Rotterdam, pp 11–26

18 Lawrence JM, Lane JM (1982) The utilization of nutrients by postmetamorphic echinoderms. In "Echinoderm Nutrition" Ed by M Jangoux, JM Lawrence, Balkema, Rotterdam, pp 331–371

19 Mortensen TH (1915) Preliminary note on the remarkable, shortened development of an Australian sea-urchin, *Toxocidaris rtythrogramma.* Proc Linn Soc N S Wales 40: 203–206

20 Mortensen TH (1921) Studies of the development and larval

forms of echinoderms. IV. K Danske Vidensk Selsk (Naturvid Math Afd Ser 9) 7(3): 1–59

21 Peters RH (1983) The Ecological Implications of Body Size. Cambridge Univ. Press, Cambridge

22 Raff RA (1992) Direct-developing sea urchins and the evolutionary reorganization of early development. Bio Essays 14: 211–218

23 Raff RA, Herlands L, Morris VB, Healy J (1990) Evolutionary modification of echinoid sperm correlates with developmental mode. Dev Growth Diff 32: 283–291

24 Scott LB, Lennarz WJ, Raff RA, Wray GA (1990) The "lecithotrophic" sea urchin *Heliocidaris erythrogramma* lacks typical yolk platelets and yolk glycoproteins. Develop Biol 138, 188–193

25 Sebens KP (1987) The ecology of indeterminate growth in animals. Ann Rev Ecol Syst 18: 371–407

26 Strathmann RR (1987) The evolution and loss of larval feeding stages of marine invertebrates. Evolution 32: 894–906

27 Strathmann RR, Strathmann MF (1982) The relationship between adult size and brooding in marine invertebrates. Am Nat 119: 91–101

28 Tegner MJ, Levin LA (1983) Spiny lobsters and sea urchins: analysis of a predator-prey interaction. J Exp Mar Biol Ecol 73: 125–150

29 Watts SA, Lawrence JM (1985) The effect of feeding and starvation on the level and content of nucleic acids in the pyloric caeca of *Luidia clathrata* (Say). In "Echinodermata" Ed by BF Keegan & BDS O'Connor, Balkema, Rotterdam, pp 571–576

30 Williams DHC, Anderson DT (1975) The reproductive system, embryonic development, larval development and metamorphosis of the sea urchin *Heliocidaris erythorogramma*. Aust J Zool 23: 371–403

ZOOLOGICAL SCIENCE 11: 139–141 (1994)

Two New Species of the Genus *Holaspulus* (Acarina: Gamasida: Parholaspidae) from the Ryukyu Islands, Japan

KAZUO ISHIKAWA

Laboratory of Biology, Matsuyama Shinonome College, Matsuyama 790, Japan

ABSTRACT—Two new mite species of the genus *Holaspulus* belonging to the gamasid family Parholaspidae are described from litter or soil layer of the Ryukyu Islands: *H. reticulatus* and *H. ishigakiensis*.

The genus *Holaspulus* was proposed by Berlese in 1904 for *Holostaspis* (*Holaspulus*) *tenuipes* from Italy [1], and was later dealt with by Evans [2], Krantz [5] and Ishikawa [3, 4].

The Ryukyu Archiperago consists of a chain of many islands and harbours various animals of zoogeographic interest. From the acarological viewpoint, it is worth noting that a plesiomorphic species with claws on the tarsus I was found by this study. In the present paper, the author is going to describe two new species, *Holaspulus reticulatus* sp. nov. and *H. ishigakiensis* sp. nov. The holotype, allotype and a part of paratypes of the new species are deposited in the collection of the Department of Zoology, National Science Museum (Nat. Hist.), Tokyo. The remaining paratypes are retained in the collection of the Laboratory of Biology, Matsuyama Shinonome College, Matsuyama.

MATERIALS AND METHODS

Litter or soil samples were brought back to the author's laboratory in the cotton bags, and the mites were extracted from the samples by using modified Tullgren apparatus. The specimens were preserved in 70% ethanol, cleared in lactophenol, and mounted in Hoyer's medium. The holotype or allotype were used in measuring the length of dorsal setae, gnathosoma and legs.

DESCRIPTION

Holaspulus reticulatus sp. nov.
[Japanese name: Iriomote-heragehokodani]
(Fig. 1 A-G)

Female. Length of idiosoma ca. 590 μm; width of idiosoma ca. 390 μm; length of dorsal shield with a range of 553–592 μm, av.569 μm; width of dorsal shield at the level of coxae IV with a range of 290–332 μm, av. 313 μm; light brown in colour.

Dorsum. Dorsal shield sclerotized and ornamented with punctations and reticulations, especially in the posterior portion. Dorsal shield bearing thirty pairs of setae, which are spatulate distally except for simple and minute setae *z1*, and with twenty-two pairs of pores. Extra-marginal setae spatulate distally and lying on striated lateral interscutal membrane. Length of setae (the length of dorsal shield of holotype 560 μm): verticals *z1* 41 μm, *j2* 38 μm, *j3* 34 μm, *j4* 33 μm, *j5* 30 μm, *j6* 33 μm, *J1* 35 μm, *J2* 26 μm, *J6* 43 μm, *z1* 3 μm, *z2* 40 μm and humerals *r2* 50 μm. The distribution of setae and pores are as shown in Figure 1A.

Venter. Tritosternum well developed, a pair of pilose laciniae more than twice longer than tritosternal base. Presternal shields composed of a pair of narrow platelets. Sternal shield ornamented with a network of ridges and punctations, and fused with endopodal shields. Sternal setae I longer than setae II and III, setae III lying well inside the bases of setae II. Metasternal shields narrow, located behind the posterior angles of sternal shield, and with a pair of simple setae and pores. Epigynial shield coalesced posteriorly with ventri-anal shield, and with a pair of genital setae. Ventri-anal shield fused with epigynial, podal-peritrematal shields, and with four pairs of preanal setae in addition to three perianal ones. Expulsory vesicles of ventri-anal shield absent. Interscutal membrane between dorsal and ventral shields bearing fourteen pairs of setae, seven of which are conspicuously spatulate. Metapodal shields present. Stigmata situated at a position antero-lateral to coxae IV. Peritremes extending to coxae I.

Gnathosoma. Epistome consisting of elongated median and lateral extensions, and with denticulated anterior margin. Palpal apotele bearing three tines, two of which are spatulate distally. Fixed digit of chelicera tridentate and with a pilus dentilis; the movable digit (150 μm) is bidentate and longer than corniculus (116 μm). Length of anterior hypostomatic seta 53 μm, external posterior hypostomatic seta 25 μm, internal posterior hypostomatic seta 25 μm and deutosternal seta 22 μm.

Legs. Tarsus I with neither claws nor pulvilli; tarsus I (168 μm) much longer than tibia I (77 μm). Tarsi II to IV each with well developed claws and pulvilli. Length of legs: I (excl. sensory setae) 578 μm, II 460 μm, III 385 μm and IV 501 μm.

Male. Length of idiosoma ca. 513 μm; width of idiosoma ca. 325 μm; length of dorsal shield with a range of 480–518 μm, av. 503 μm; width of dorsal shield at the level of

Accepted November 11, 1993
Received November 30, 1993

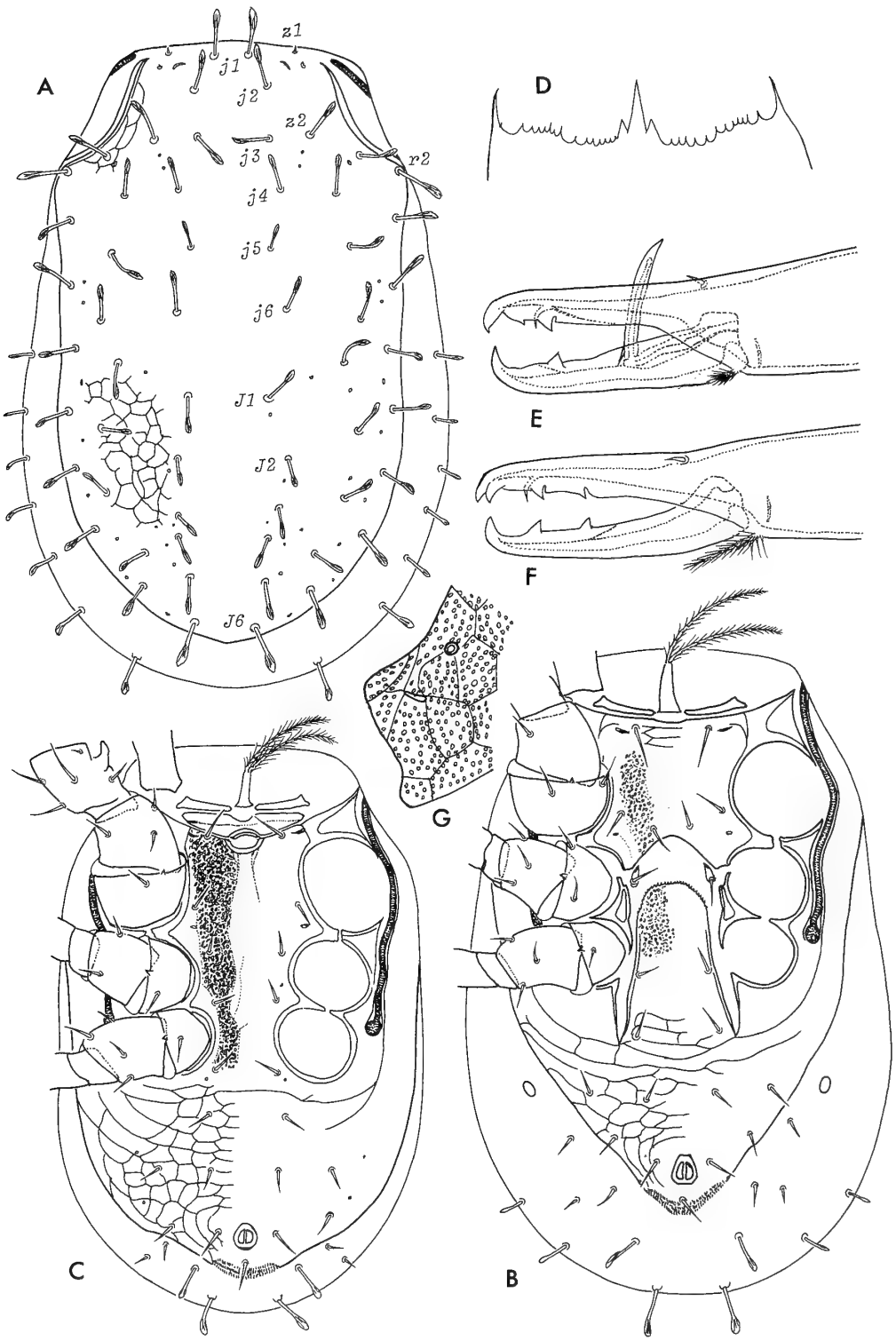

FIG. 1. *Holaspulus reticulatus* sp. nov. (A-B, D, F-G, female; C, E, male). A, Dorsum; B-C, venter; D, epistome; E-F, chelicera; G, ornamentation of sternal shield.

coxae IV with a range of 290–328 μm, av. 311 μm.

Dorsal chaetotaxy and ornamentation similar to those of female. Sterniti-genital portion ornamented with network and punctations, and with five pairs of simple setae. Ventri-anal portion reticulated and with four pairs of simple setae and three perianal setae. Fixed digit of chelicera bidentate; movable digit (127 μm) unidentate and approximately twice the length of spermatodactyl (63 μm). Tarsus I without claws and pulvilli. Femur II with a large thumb-like spur, and genu, tibia and tarsus II each with a small spur. Length

of legs: I (excl. sensory setae) 562 μm, II 450 μm, III 378 μm and IV 493 μm.

Type series. Holotype ♀ (NSMT-Ac 10429) and allotype ♂ (NSMT-Ac 10430), Kanbira-no-taki, Iriomote Is., Ryukyus, 3-X-1978, K. Ishikawa. Paratypes: 6♀♀, 8♂♂, same data as the holotype; 5♀♀, 3♂♂, Ohtomi, Iriomote Is., Ryukyus, 4-X-1978, K. Ishikawa.

Remarks. No close relatives of this new species have been known up to now. However, this species may be remotely related to *Holaspulus ishigakiensis* sp. nov., from

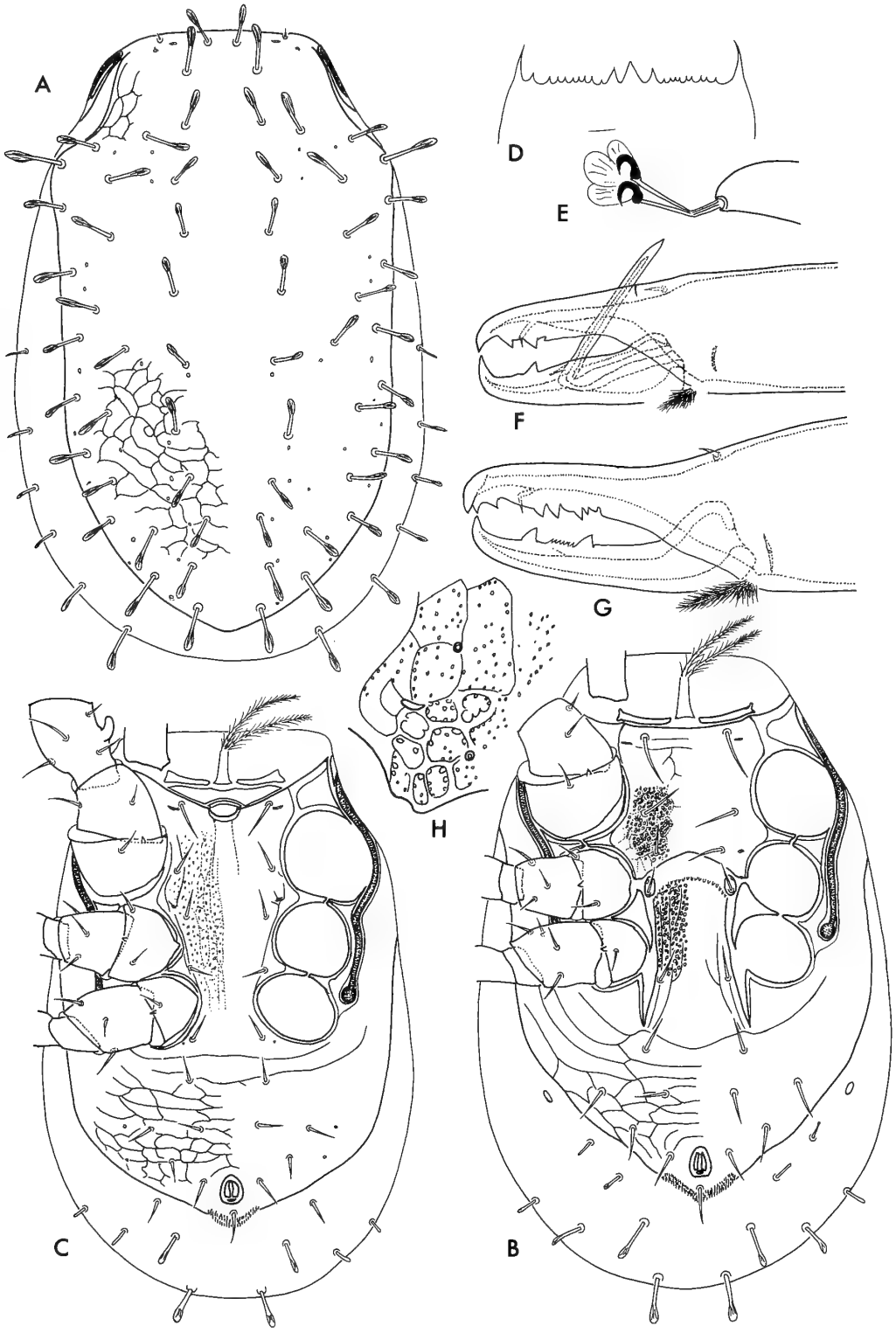

FIG. 2. *Holaspulus ishigakiensis* sp. nov. (A-B, D, G-H, female; C, E-F, male). A, Dorsum, B-C, venter, D, epistome; E, claws of tarsus I; F-G, chelicera; H. ornamentation of sternal shield.

Ishigaki Is., because of the following characteristic features: movable digit of chelicera of female with two large teeth, instead of bearing two large and several small teeth; tarsus I of male without claws and pulvilli, instead of the presence of claws and pulvilli.

Holaspulus ishigakiensis sp. nov.
[Japanese name: Ishigaki-heragehokodani]
(Fig. 2 A-H)

Female. Length of idiosoma ca. 570 μm; width of idiosoma ca. 380 μm; length of dorsal shield with a range of 523–565 μm, av. 546 μm; width of dorsal shield at the level of coxae IV with a range of 290–347 μm, av. 312 μm.

Dorsum. Dorsal shield sclerotized and ornamented with punctations and reticulations, particularly in the posterior portion. Dorsal shield provided with thirty pairs of setae and twenty-two pairs of pores; its setae spatulate distally with the exception of simple minute setae *z1*. Extramarginal setae spatulate distally and increasing in length from anterior to posterior. Length of setae (the length of dorsal shield of holotype 550 μm): verticals 40 μm, *j2* 38 μm, *j3* 37 μm, *j4* 34 μm, *j5* 32 μm, *j6* 36 μm, *J1* 29 μm, *J2* 33 μm, *J6* 41 μm, *z1* 2 μm, *z2* 41 μm and humerals 55 μm. The distribution of setae and pores are as shown in Figure 2A.

Venter. Tritosternum well developed, a pair of pilose laciniae more than twice as long as tritosternal base. Presternal shields consisting of a pair of narrow platelets. Sternal shield ornamented with network and closely set punctations; three pairs of simple setae present, setae III lying well inside the bases of setae II. Metasternal shields free, and with a pair of simple setae and pores. Epigynial shield fused posteriorly with ventri-anal shield, and with a pair of simple setae. Ventri-anal shield fused with epigynial, podal-peritrematal shields, and with four pairs of preanal setae and three perianal setae. Expulsory vesicle of ventri-anal shield absent. Interscutal membrane between dorsal and ventral shields bearing twelve pairs of setae, six pairs of which are conspicuously spatulate. Metapodal shields present. Stigmata located at a position antero-lateral to coxae IV. Peritremes extending to coxae I.

Gnathosoma. Epistome with spinose median projection, and with several short spines on either side and a pair of elongate lateral extensions. Palpal apotele provided with three tines, two of which are spatulate distally. Fixed digit of chelicera with six teeth and a pilus dentilis; the movable digit (123 μm) is bidentate in addition to several small teeth, and longer than corniculus (108 μm). Salivary stylus (95 μm) well developed. Length of anterior hypostomatic seta 67 μm, external posterior hypostomatic seta 32 μm, internal posterior hypostomatic seta 36 μm and deutosternal seta 30 μm.

Legs. Tarsus I (192 μm) much longer than tibia I (87 μm), without claws and pulvilli. Tarsi II to IV each with well developed claws and pulvilli. Length of legs: I (excl. sensory setae) 578 μm, II 440 μm, III 380 μm and IV 478 μm.

Male. Length of idiosoma ca. 500 μm; width of idiosoma ca. 320 μm; length of dorsal shield with a range of 475–527 μm, av. 493 μm; width of dorsal shield at the level of coxae IV with a range of 280–305 μm, av. 292 μm.

The chaetotaxy and ornamentation of dorsal shield are essentially the same as in the female. Sterniti-genital portion ornamented with network and punctations. Ventri-anal portion reticulated and provided with four pairs of simple setae and three perianal ones. Fixed digit of chelicera bidentate; movable digit (95 μm) unidentate and longer than spermatodactyl (74 μm). Each tarsus provided with claws and pulvilli. Femur II with a large thumb-like spur, and genu, tibia and tarsus II each with a small spur. Length of legs: I (excl. sensory setae) 561 μm, II 458 μm, III 370 μm and IV 443 μm.

Type series. Holotype ♀ (NSMT-Ac 10431) and allotype ♂ (NSMT-Ac 10432), Kabira, Ishigaki Is., Ryukyus, 10-VII-1987, K. Ishikawa. Paratypes: 7♀♀, 4♂♂, same data as the holotype; 2♀♀, 3♂♂, Yoon, Ishigaki Is., 6-XII-1972, J. Aoki; 5♀♀, 3♂♂, Mt. Yonahadake, Okinawa Is., 6-X-1978, K. Ishikawa; 6♀♀, 5♂♂, Yonehara, Ishigaki Is., 2-X-1978, K. Ishiakawa.

Remarks. The present species differs from the previously known members of the genus *Holapulus* in the movable digit of the female chelicera provided with two large and several small teeth, instead of only two large teeth. On the other hand, this species seems closely related to *H. reticulatus* sp. nov., from Iriomote Is., but is distinguished from that species by the following points: tarsus I of male provided with claws and pulvilli, instead of lacking them; the length of spermatodactyl is 0.8 times that of movable digit, instead of 0.5.

ACKNOWLEDGMENTS

The author wishes to express his hearty thanks to Dr. Shun-Ichi Uéno of the Department of Zoology, National Science Museum (Nat. Hist.), Tokyo, for his advice and criticism. Deep gratitude is also due to Dr. Kuniyasu Morikawa, President of Matsuyama Shinonome Junior College, for giving him valuable suggestions. Sincere thanks are also due to Prof. J.-I. Aoki of the Institute of Environmental Science and Technology, Yokohama National University, who kindly offered valuable materials. He is also indebted to Miss Yumiko Nishino for her help in the course of this study.

REFERENCES

1 Berlese A (1904) Acari nuovi Manipulus I. Redia 1: 258–280
2 Evans GO (1956) On the classification of the family Macrochelidae with particular reference to the subfamily Parholaspinae (Acarina-Mesostigmata). Proc zool Soc London 127: 345–377
3 Ishikawa K (1969) Taxonomic investigations on free-living mites in the subalpine forest on Shiga Heights IBP Area I.Mesostigmata (Part 1). Bull natn Sci Mus Tokyo 12: 39–64
4 Ishikawa K (1979) Taxonomic and ecological studies in the family Parholaspidae (Acari, Mesostigmata) from Japan (Part1). Bull natn Sci Mus Tokyo (A) 5: 249–269
5 Krantz GW (1960) A re-evaluation of the Parholaspinae Evans(1956) (Acarina: Mesostigmata: Macrochelidae). Acarologia 2: 393–433

ZOOLOGICAL SCIENCE 11: 143–147 (1994)

The Sweet Potato Hornworm, *Agrius convolvuli*, as a New Experimental Insect: Continuous Rearing Using Artificial Diets

KENJI KIGUCHI and MASAMI SHIMODA

Laboratory of Developmental Biology, Department of Insect Genetics and Breeding, National Institute of Sericultural and Entomological Science, Ohwashi 1-2, Tsukuba, Ibaraki 305, Japan

ABSTRACT—We developed a continuous rearing system for the sweet potato hornworm, *Agrius convolvuli*, for use as a new experimental insect for studies on insect biology. This species is closely related to the tobacco hornworm, *Manduca sexta,* which has occupied an important position as an experimental animal. By modifying the artificial diet for the silkworm, *Bombyx mori,* diets suitable for *Agrius convolvuli* were developed. The diets contained various amounts of sweet potato leaf powder as a substitute for mulberry leaf powder. Among the five different diets prepared, SPLP-25 and SPLP-20 (ca. 17–22% leaf powder) were suitable for the first four instar larvae, while SPLP-10 and SPLP-5 (ca. 4–9% leaf powder) for the final 5th instar. Although most of the 5th instar larvae fed and grew on a diet designated as SPLP-0 lacking leaf powder, larval life was prolonged and the resultant pupae were smaller. Year-round egg collection and rearing system were developed after a slight modification of the system devised for *Manduca sexta*. The sweet potato hornworm was successfully reared on the artificial diet for over 20 generations during the past 3 years under this system.

The insect is considered to be a good experimental animal suitable for comparative studies with other large lepidopteran insects, such as *Manduca sexta* and *Bombyx mori.*

INTRODUCTION

Insects offer considerable advantages as experimental animals for studies on various biological phenomena. For example, studies involving more than 3,200 different insects were cited in the book series edited by G. A. Kerkut and L. I. Gilbert in 1985, which covered insect physiology, biochemistry and pharmacology[8]. Insects most frequently cited were the fruit fly, *Drosophila melanogaster*, the American cockroach, *Periplaneta americana*, the desert locust, *Locusta migratoria*, the tobacco hornworm, *Manduca sexta* and the silkworm, *Bombyx mori*.

Bombyx is obviously the most extensively studied lepidopteran insect. The wealth of information on *Bombyx* accumulated for the sericultural industry made it an ideal organism for research on genetics, embryology, physiology and biochemistry, etc., and innumerable contributions have been made with this insect by many researchers in different disciplines [14]. Yet it is important to conduct comparative studies on other lepidopterans as well.

The tobacco hornworm, *Manduca sexta,* is another well studied lepidopteran. It is a rather new experimental animal adopted in the 1970's after the development of a rearing system on artificial diet [5, 18]. Yet *Manduca* is now the most popular lepidopteran model, especially in the field of insect endocrinology and neurobiology (see reviews [10, 11, 15, 16]). Since *Bombyx* and *Manduca* are both large lepidopterans, each characterized by a different scientific background, it would be useful to carry out comparative studies between the two insects. However, as *Manduca* does not occur in Japan, our focus was directed to another related sphingid moth, *Agrius convolvuli*. The size and morphology are almost similar to those of *Manduca* (Fig. 1).

Agrius convolvuli is a cosmopolitan species widely distributed in the tropical,subtropical and temperate zones including Japan. Although it is one of the major defoliators of sweet potato crops, there are few descriptions on its life cycle and physiology [9, 12, 13, 19], and no information on its nutrition or suitable artificial diet. However, we observed that this species could be reared on a diet very similar to the artificial diet for the silkworm, *Bombyx mori*. Here we report the outline of the rearing system of the sweet potato hornworm, *Agrius convolvuli*, using artificial diets, which made it possible to rear the insect throughout the year for conducting research. The procedure has provided a continuous supply of the hornworm for the past 3 years.

MATERIALS AND METHODS

Field collection of Agrius pupae

The initial colony of the sweet potato hornworm, *Agrius convolvuli*, was reared in early September 1989. More than 300 pupae were first collected from the sweet potato field of the National Agriculture Research Center (Yawara farm) located at Tsukuba-gun, Ibaraki, Japan. The collected pupae were kept under a long day photoperiod (16L:8D) at 25±1°C and 70–80% RH. However, about 80% of the pupae died due to heavy infestation with parasitic flies (species undetermined). Most of the remainder developed without entering the diapause. The healthy pharate adults were transferred to a net cage (1.8×1.8×1.8 m) placed on the sweet

Accepted October 28, 1993
Received September 7, 1993

potato field to collect eggs. A potted chrysanthemum and three plastic cups filled with a 25% sucrose solution were located at one corner of the cage to provide food sources. Hatched larvae from the obtained eggs were reared on the host plant leaves in a 20×28×6 cm plastic cage (14–20 larvae/cage during the first to fourth instar; 2–3 larvae/cage during the final fifth instar) under a long day photoperiod (16L : 8D) at 25±1°C. The pupae obtained were used to develop an indoor egg collection method which was essential to devize a continuous rearing system. No wild individuals were introduced into the colony maintained thereafter.

Indoor egg collection

Like *Manduca, Agrius* moths are nocturnal, and mate and lay eggs only at night. It was observed that a sufficient number of eggs could be obtained even during the winter season by modifying the procedure for *Manduca* described by Yamamoto [17] and Bell and Joachim [4]. Pharate adults were placed in a tray on the floor of a wooden cage (73×85×115 cm) one day before adult emergence. The inside-surface of the cage was covered with black paper to prevent extra light reflection. The moths were kept under a photoperiod of 17L : 7D at 26±1°C. During the dark period a low level of illumination (about 2–5 lux) was applied using a rheostat-controlled 6-watt incandescent bulb, since no fertilized eggs could be obtained under complete darkness. As food source, a 25% sucrose solution was placed in a plastic cup. A potted sweet potato plant was placed near the cup as an oviposition site. High humidity, over 70% RH, was usually maintained by using a wide water bath under the mesh floor. Sometimes during the winter season, additional moisture was supplied by a timer-controlled humidifier. Eggs were collected from the plant every morning, and incubated at 25±1°C and about 80% RH until hatching.

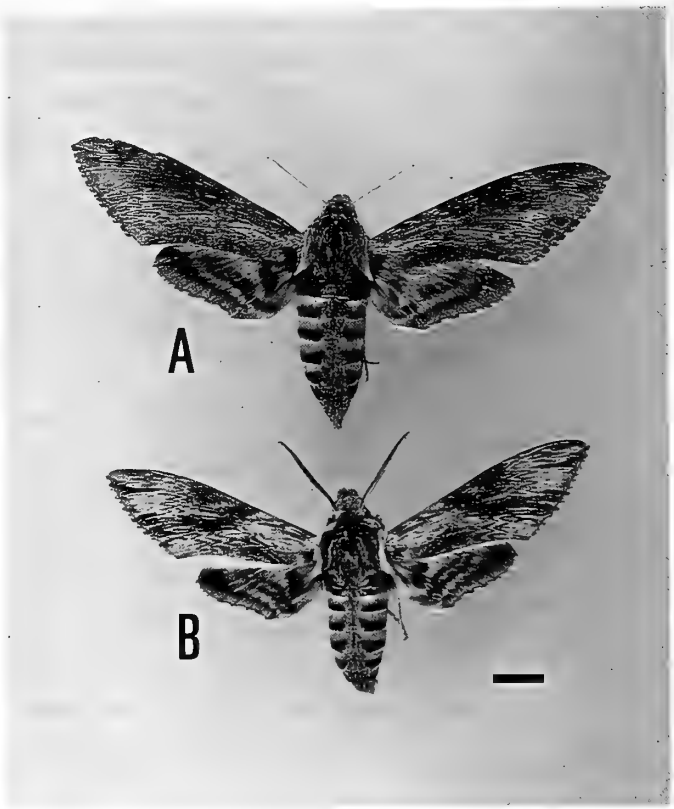

FIG. 1. Adult moths of the sweet potato hornworm, *Agrius convolvuli*. A,female; B,male. Bar=1 cm.

TABLE 1. Composition of artificial diets for the sweet potato hornworm, *Agrius convolvuli*

Ingredient (dry matter)	Diet-A[1] (g)	SPLP-25 (g)	SPLP-20 (g)	SPLP-10 (g)	SPLP-5 (g)	SPLP-0 (g)
Mulberry leaf powder	25.0	—	—	—	—	—
Sweet potato leaf powder	—	25.0	20.0	10.0	5.0	—
Soybean meal	36.0 [2]	20.0 [3]	25.0 [3]	26.0 [3]	28.0 [3]	30.0 [3]
Agar	7.5	10.0	10.0	10.0	10.0	10.0
Potato starch	7.5	10.0	10.0	12.0	13.5	15.0
Sucrose	8.0	10.0	10.0	12.0	13.5	15.0
Cellulose powder	20.8	29.6	29.6	34.6	34.6	34.6
Soybean oil,not refined	1.5	2.0	2.0	2.0	2.0	2.0
β-Sitosterol	0.2	0.2	0.2	0.2	0.2	0.2
Sorbic acid	0.2	0.2	0.2	0.2	0.2	0.2
Ascorbic acid	2.0	2.0	2.0	2.0	2.0	2.0
Citric acid	4.0	4.0	4.0	4.0	4.0	4.0
Wesson's salt mixture	3.0	3.0	3.0	3.0	3.0	3.0
Total	115.7	116.0	116.0	116.0	116.0	116.0
Vitamin B mixture[4]	Added	Added	Added	Added	Added	Added
Antiseptics[5]	Added	Added	Added	Added	Added	Added
Distilled water(ml/g dry diet)						
for 1–4th instar diet	3.0	4.0	4.0	4.0	4.0	4.0
for 5th instar diet	2.2	3.0	3.0	3.0	3.0	3.0

1) Diet A: Standard diet for *Bombyx mori* developed by Horie *et al.* [7]; 2) Crude soybean meal, defatted; 3)Soybean meal, high nitrogen content (Solpea 600); 4)See Horie *et al.* [6]; 5)Antiseptics consisted of 0.015% (dry matter) of chloramphenicol and 0.75% (dry matter) of propionic acid.

Preparation of artificial diets

Artificial diets were developed after slight modifications of the diet for the silkworm, *Bombyx mori*, described by Horie *et al.* [7]. The diet composition is shown in Table 1. The main change was the substitution of sweet potato leaf powder for mulberry leaf powder. Five different diets designated as SPLP-0, SPLP-5, SPLP-10, SPLP-20 and SPLP-25 were prepared, each of which contained different amounts of sweet potato leaf powder. Mixed ingredients were stored in a refrigerator at 5°C. For the preparation of the diets, 300–400 ml of distilled water was added to 100 g of the mixed dry powder. The diet with a high water content (400 ml) was supplied to the first four larval instars, and that with a low content (300 ml) to the final 5th instar. After blending in the prescribed amount of water, the mixture was steamed for about 50 minutes at 100°C, then the diet was cooled down to room temperature. Each wet diet was covered with a wrapping film (Krewrap) and stored at 5°C until use.

Rearing method on artificial diets

A rearing system was developed after slight modifications of the system for *Manduca* adopted by L. M. Riddiford and J. W. Truman, University of Washington, Seattle. Namely, each newly hatched larva was individually confined in a plastic cup (50 ml) with a small piece of food (ca. 6 g). The diet was changed to a fresh one 7 days after feeding. When larvae molted into the 5th instar, each larva was transferred to a larger plastic cup (200 ml) with a lid on which several small circular holes were made to provide adequate aeration for the growing larva, and given a larger amount of food (ca. 25 g). Wandering larvae were transferred to another cup of the same size only with a piece of tissue paper, where they pupated. Throughout this experiment, eggs, larvae and pupae were kept in an environmental room maintained at 25±1°C, 50–60% RH, and under a long day photoperiod (16L : 8D).

RESULTS

Rearing on fresh host plant leaves

Mean pupal weights of the field-collected *Agrius convolvuli* were 5.13±0.83 g for males (n=53) and 5.47±1.01 g for females (n=50). Hatched larvae from the obtained eggs were reared on fresh harvested leaves of sweet potato without difficulty (Table 2). Percentage of survival to the adult stage exceeded 90%. However this method required much space, large quantities of fresh sweet potato leaves, and time to handle the hornworms. The life cycle from egg to egg was

TABLE 2. Growth and development of *Agrius* larvae on the fresh sweet potato leaves

No. of eggs collected		255
No. of hatched larvae		207 (82%)
No. of larvae placed on diets		207
No. of larvae that molted into 5th instar		196 (95%)
No. of 5th instar larvae reared		163
No. of individuals that became pupae		152 (93%)
No. of individuals that became adults		148 (91%)
Days from hatching to 4th larval ecdysis		12.5±0.8 (92)*
Days from 4th larval ecdysis to wandering		5.8±0.8 (65)
Days from wandering to pupation		4.2±0.5 (64)
Days from pupation to adult emergence		17.0±0.8 (60)
Pupal weight (g)	Male	3.51±0.51 (89)
	Female	4.01±0.72 (63)

The rearing experiment was conducted in October 1989.
* Values are mean±S.D., and number of insects observed is indicated in parentheses.

TABLE 3. Growth and development of *Agrius* larvae on various artificial diets

Diets used		No. of larvae tested*	Pupation (%)	Duration of 5th instar (day) (Mean±S.D.)	Pupal weight (g) (Sex, Mean±S.D.)
1–4th instar	5th instar				
Early generation (July, 1990)					
SPLP-25	SPLP-25	36	97.2	5.7±0.8	M 4.70±0.34 (20)**
					F 5.26±0.45 (18)
SPLP-25	SPLP-20	36	94.4	5.7±0.8	M 4.72±0.41 (16)
					F 5.18±0.45 (15)
SPLP-25	SPLP-10	36	100.0	5.8±0.7	M 4.77±0.46 (19)
					F 5.23±0.49 (17)
SPLP-25	SPLP- 5	35	91.4	5.8±0.6	M 4.62±0.56 (10)
					F 5.18±0.62 (22)
SPLP-25	SPLP- 0	36	91.7	6.9±1.2	M 4.46±0.53 (18)
					F 4.79±0.93 (15)
Advanced generation (July, 1993)					
SPLP-25	SPLP-25	59	100.0	5.2±0.4	M 4.54±0.40 (34)
					F 5.11±0.30 (25)
SPLP-20	SPLP- 5	52	100.0	5.0±0.5	M 4.55±0.34 (23)
					F 4.96±0.55 (29)

* Larvae were selected on day 0 of the 5th instar (see text for detail).
** Number of insects observed is indicated in parentheses.

about 42 days at 25±1°C and 65–75% RH (roughly, egg: 4, larva: 18, pupa: 18, preoviposition: 2 days). Mean pupal weights were 3.51 g for males and 4.01 g for females, which were significantly smaller than those of the field-collected individuals.

Rearing on artificial diets

We prepared five different diets (Table 1) after slight modifications of an artificial diet for *Bombyx* larvae (Diet-A in Table 1). Preliminary experiments revealed that newly hatched larvae showed a high feeding activity on the SPLP-25 and SPLP-20 diets. Moreover, we could successfully rear the hornworm on the SPLP-25 diet throughout the larval stage and obtained two further generations of larvae. Also, we observed that the 5th instar larvae fed and grew well, even on the diets containing smaller amounts of host plant leaf powder. To determine the optimum regimen for the least expense, we carried out combination experiments of two different diets.

In July 1990, a total of 300 larvae were reared on the SPLP-25 diet until the molt to the 5th instar, then the 5th instar larvae were divided into several groups which were given different diets. As shown in Table 3, insects reared on the SPLP-25 diet throughout the larval stage showed a considerably higher performance in three developmental parameters examined than the individuals reared on fresh host plant leaves (Table 2). For example, the values for the mean pupal weights of the former were significantly larger than those of the latter in both sexes, although they were slightly smaller than those of the wild population. When 5th instar larvae were reared on the SPLP-0 diet, larval duration was prolonged by 1 to 2 days, and the resultant pupae were smaller. By contrast, the other groups reared on the SPLP-5, SPLP-10 and SPLP-20 diets did not show significant differences in the duration of larval life and in pupal weights when compared with those of the insects reared on the SPLP-25 diet.

Although the initial colony consisted of less than 50 pupae at the start, and no wild individuals were introduced thereafter, we have not yet observed any serious inbreeding depression. For example, the hatchability in the first generation which was 81% (Table 2) remained at the level of 70–90% after 20 generations. Also, the pupal weights were nearly the same in the early and the recent generations as shown in Table 3. Thus, viability has remained stable.

DISCUSSION

We initially intended to identify an experimental insect suitable for comparative studies with the silkworm, *Bombyx mori*, which has been an important research target in our institute. Our attention was first directed to the tobacco hornworm, *Manduca sexta*, which has played an important role as an experimental insect. Since *Manduca* does not occur in Japan, we selected the sweet potato hornworm, *Agrius convolvuli*, a species closely related to *Manduca sexta*. As the morphology and life cycle of *Agrius* are similar to those of *Manduca*, the information accumulated on *Manduca* has been extremely useful in our attempt to develop an egg collection and rearing system. Actually, the system adopted for *Agrius* is basically the same as that for *Manduca*. Yet the composition of the artificial diet is very different from that developed for *Manduca*. We simply modified the diet for the commercial silkworm, *Bombyx mori*, by substituting sweet potato leaf powder for mulberry leaf powder. Our diets are satisfactory in nutritional requirements since we were able to rear the hornworm on the diet for over 20 generations during the past 3 years. During this time the hatchability of the eggs and survival rates did not change significantly, indicating that the diet is satisfactory for continuous rearing procedures.

However, there are a few problems which required further attention. First, it is preferable to develop a diet without host plant leaf powder. *Manduca* diets do not contain any leaf powder [1–3, 5, 18], while leaf powder is necessary for the current *Agrius* diet. At present we use SPLP-20 or SPLP-25 (ca. 17–22% leaf powder)for the 1st to 4th instar larvae, and SPLP-5 or SPLP-10 (ca. 4–9% leaf powder) for the last 5th instar. Yet it is noteworthy that most of the 5th instar *Agrius* larvae fed on the SPLP-0 diet lacking leaf powder survived, although their larval development was prolonged and the resultant pupae were smaller (Table 3). Therefore, we consider that an artificial diet without leaf powder could be developed through changes in the diet composition compatible with feeding activity. The second problem concerns the number of changes of diet necessary. In the *Manduca* rearing system, the diet is usually changed only once after a feeding larva reaches the 5th instar. By contrast, food must be changed twice in the *Agrius* rearing system to maintain an adequate larval development: first on the 7th day after hatching and second on the day when the larva molts to the 5th instar. To eliminate the first diet change, further improvement of the diets is required.

Needless to say, research on insects can be greatly facilitated by the development of a year-round rearing system. However, this system provides only one of the necessary conditions for a suitable experimental insect, and it is also important to accumulate fundamental information on the physiology and behavior of the insect. Unfortunately the sweet potato hornworm, *Agrius convolvuli*, had not been studied thoroughly until now. Yet the insect could be a suitable experimental insect as it is closely related to *Manduca sexta*. Presumably, the information accumulated on *Manduca* for the past 25 years will be useful for studies on the sweet potato hornworm. Studies on *Agrius* may also contribute to gain further insights into *Manduca* physiology and development.

Although both *Bombyx* and *Agrius* are large lepidopterans that are similar in many characteristics, they are also very different in various aspects. For example, the silkworm uses ingested nitrogen both for growth and synthesis of the silk

proteins, and its diapause occurs at the embryonic stage. By contrast, the hornworm does not make silk, only builds a pupal chamber in soil, and enters diapause at the pupal stage. A comparative study of these developmental and behavioral differences would be most significant. We hope that such comparative studies among *Bombyx, Agrius* and *Manduca* will mutually contribute to a better understanding of the insect bio-mechanisms and functions.

ACKNOWLEDGMENTS

The authors would like to express their sincere thanks to Professor L. M. Riddiford, University of Washington, Seattle, for her advice and critical reading and comments on this paper. We thank Dr. I. Tarumoto and Mr. H. Ishikawa, Sweet Potato Breeding Laboratory, National Agriculture Research Center,Japan, for their assistance in the field collection of *Agrius* and suggestions on the insect. We also thank Dr. S. Kimura, National Institute of Sericultural and Entomological Science, for his encouragement throughout this work. Deep thanks are due to Mrs. F. Karube and Mrs. Y. Yagihashi for their cooperation in rearing the insect.

REFERENCES

1 Ahmad IM, Waldbauer GP, Friedman S (1989) A defined artificial diet for the larvae of *Manduca sexta*. Entomol exp appl 53: 189–191

2 Baumhover AH (1985) *Manduca sexta*. In "Handbook of Insect Rearing Vol II" Ed by P Singh, RF Moore, Elsevier, Amsterdam, pp 387–400

3 Baumhover AH, Cantelo WW, Hobgod Jr JM, Knott CM, Lam Jr JJ (1977) An improved method for mass rearing the tobacco hornworm. U S Dep Agric, ARS-S-167, pp 1–13

4 Bell RA, Joachim FG (1976) Techniques for rearing laboratory colonies of tobacco hornworm and pink bollworms. Ann entomol Soc Amer 69: 365–373

5 Hoffman JD, Lawson FR, Yamamoto RT (1966) Tobacco hornworms. In "Insect Colonization and Mass Production" Ed by CN Smith, Academic Press, New York, pp 479–486

6 Horie Y, Watanabe K, Ito T (1966) Nutrition of the silkworm, *Bombyx mori* XIV Further studies on the requirements for B vitamines. Bull Sericul Exp Sta 20: 393–409

7 Horie Y, Inokuchi T, Watanabe K, Nakasone S, Yanagawa H (1973) Food efficiency and the composition of artificial diets for the silkworm, *Bombyx mori*. Tech Bull Sericul Exp Sta No. 96, 41–55 (In Japanese)

8 Kerkut GA, Gilbert LI Ed (1985) Comprehensive Insect Physiology, Biochemistry and Pharmacology, Vol. 1–13, Pergamon Press, Oxford

9 Nakagawa K, Setokuchi O, Kobayashi M, Oashi K (1986) Ecological studies on the defoliators of sweet potato. II. Seasonal occurrence of adults of four major pests, *Aedia leucomelas* Linne, *Agrius convolvuli* Linne, *Brachmia triannulella* (Herrich-Schaffer) and *Spodoptera litura* Fabricius. Proc Assoc Pl Prot Kyushu 32: 136–139

10 Riddiford LM (1985) Hormone action at the cellular level. In "Comprehensive Insect Physiology, Biochemistry and Pharmacology Vol 8" Ed by GA Kerkut, LI Gilbert, Pergamon Press, Oxford, pp 37–84

11 Riddiford LM, Hiruma K (1990) Hormonal control of sequential gene expression in lepidopteran epidermis. In "Molting and Metamorphosis" Ed by E Ohnishi, H Ishizaki, Japan Scientific Societies Press, Tokyo and Springer-Verlag, Berlin, pp 207–222

12 Setokuchi O, Nakagawa K, Kobayashi M (1985) Ecological studies on the defoliators of sweet potato. I. Development process in the larval stage of three major pests, *Aedia leucomelas* Linne, *Agrius convolvuli* Linne and *Brachmia trian nulella* (Herrich-Schaffer). Proc Assoc Pl Prot Kyushu 31: 143–147

13 Setokuchi O, Nakagawa K, Kobayashi M (1986) Food consumption of three major sweet potato defoliators, *Aedia leucomelas* Linne, *Agrius convolvuli* Linne and *Brachmia triannulella* (Herrich-Schaffer). Jpn J Appl Ent Zool 30: 93–98

14 Tazima Y (1978) Preface. In "The Silkworm: An Important Laboratory Tool" Ed by Y Tazima, Kodansha LTD, Tokyo, pp vii–viii

15 Truman JW (1992) Developmental neuroethology of insect metamorphosis. J Neurobiol 23: 1404–1422

16 Truman JW, Riddiford LM (1989) Development of the insect neuroendocrine system. In "Development, Maturation, and Senescence of the Neuroendocrine system: A Comparative Approach" Ed by MP Schreibman, CG Scanes, Academic Press, New York, pp 9–22

17 Yamamoto RT (1968) Mass rearing of the tobacco hornworm. I. Egg production. J Econ Entomol 61: 170–174

18 Yamamoto RT (1969) Mass rearing of the tobacco hornworm. II. Larval rearing and pupation. J Econ Entomol 62: 1427–1431

19 Zhai Y-J (1977) Preliminary studies on *Herse convolvuli* Linnaeus. Acta Ent Sin 20: 352–354

ZOOLOGICAL SCIENCE 11: 149–152 (1994)

[RAPID COMMUNICATION]

Immunohistochemical Study of Ontogeny of Pituitary Prolactin and Growth Hormone Cells in *Xenopus laevis*

KAORU YAMASHITA and SAKAE KIKUYAMA[1]

Department of Biology, School of Eduction, Waseda University, Nishiwaseda 1-6-1, Tokyo 169-50, Japan

ABSTRACT—The ontogeny of prolactin (PRL) and growth hormone (GH) cells in the pars distalis of *Xenopus laevis* was examined immunohistochemically using anti-bullfrog PRL serum and anti-bullfrog GH serum. Immunoreactive PRL and GH cells first appeared simultaneously at Nieuwkoop and Faber (NF) stage 42, in the anterodorsal region and in the central region of the pars distalis, respectively. Immunoreactive PRL cells increased moderately as metamorphosis progressed. They were distributed mainly in the anterior portion of the pars distalis. Immunoreactive GH cells showed a marked increase in number at NF stages 50–52 and NF stages 62–64 and a slight decrease at the end of metamorphosis. Throughout late premetamorphosis, prometamorphosis and climax, the GH cell number always exceeded the prolactin cell number. GH cells were situated in the posterior portion of the pars distalis. Examination of consecutive sections stained alternately with anti-PRL and anti-GH did not reveal colocalization of PRL and GH at any stage of development.

INTRODUCTION

Prolactin (PRL) and growth hormone (GH) belong to a family of hormones that are functionally and structurally related [8]. In amphibians, PRL stimulates growth of larval organs such as gills and tail and GH stimulates somatic growth [10]. Amino acid sequences of bullfrog PRL and GH have been determined by direct protein sequencing [12, 24] or deduced from their cDNAs [20, 21]. The two proteins exhibit a considerable sequence homology. Recently, co-localization of PRL and GH in the pituitary of bullfrog larvae at early developmental stages has been reported [9, 13]. Ontogenic differentiation of pituitary GH and/or PRL cells in several species of amphibians has been studied immunohistochemically using antisera against GH and/or PRL of mammalian origin [3, 4, 7, 14, 18, 29]. Recently, however, antisera against PRL [25] and GH [11] of amphibian origin have also become available. The antiserum against bullfrog PRL stained PRL cells in adult *Rana ridibunda, Pleurodeles waltlii, Ambystoma mexicanum, Xenopus laevis, Bufo vulgaris* and *Triturus cristatus* [1, 2, 16]. The antiserum against bullfrog GH has been applied to *Rana ridibunda* [28], *Bufo vulgaris, Bufo japonicus* and *Xenopus laevis* [17]. However, ontogenic studies of amphibian PRL and GH cells using these antisera have been limited to only two species, namely, *Rana catesbeiana* [13] and *Rana dalmatina* [5]. The present study was carried out to study the development of GH and PRL cells in *Xenopus* larvae, paying particular attention to coexistence of PRL and GH within the same cell.

MATERIALS AND METHODS

Animals Fertilized eggs of *Xenopus laevis* were obtained by

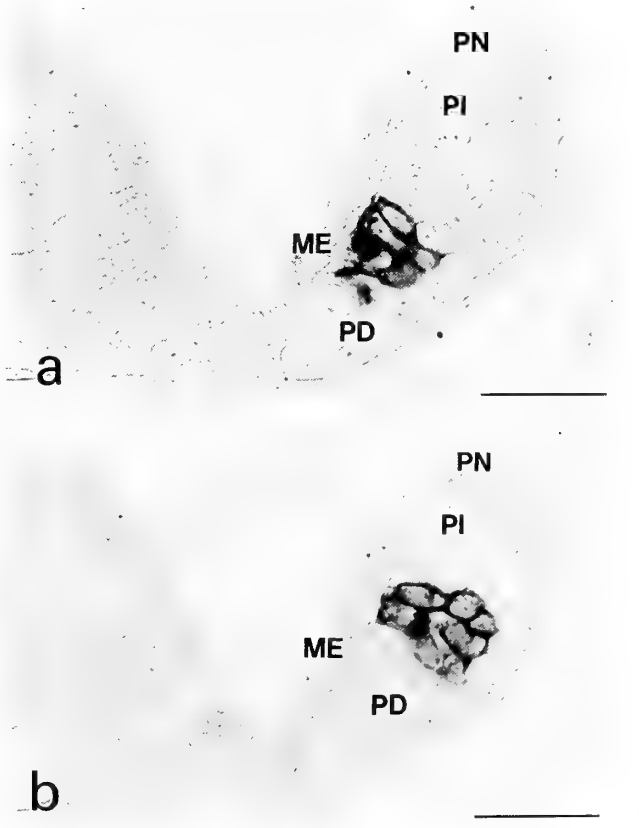

FIG. 1. The consecutive mid-sagittal sections of the pituitary gland of larval *Xenopus* (NF stages 42) stained with anti-bullfrog RPL serum (a) and anti-bullfrog GH serum (b). ME, median eminence; PD, pars distalis; PI, pars intermedia; PN, pars nervosa. Bar, 20 μm.

Accepted November 4, 1993
Received October 14, 1993
[1] To whom requests for reprints should be addressed.

injection of 200–400 IU human chorionic gonadotropin (Teikokuzoki Co, Tokyo) into mature male and female animals. The hatched embryos were reared under laboratory conditions until use. The larvae were staged according to Nieuwkoop and Faber (NF) [15]. In addition to larvae, several juvenile animlas (one month after metamorphosis) were used.

Immunohistochemistry The whole brains were fixed for 24 hr in Bouin's solution. After dehydration and embedding in paraplast, serial sagittal sections (5 μm) were cut and mounted on gelatin-coated slides. The deparaffinized sections were incubated in a solution of 0.3% H_2O_2 in methanol for 30 min. After rinsing 3 times with phosphate-buffered saline (PBS) (pH 7.2), the slides were treated with normal swine serum (1:20) for 1 hr. After washing with PBS, the sections were immunostained by the peroxidase anti-peroxidase (PAP) method [19]. Sections were incubated sequentially with the following: rabbit anti-bullfrog PRL serum (1:2000) [25] or anti-bullfrog GH serum (1:2000) [12], swine anti-rabbit IgG (1:20) (Dako Japan, Kyoto) for 2 hr and rabbit PAP complex (1:50) (Dako Japan, Kyoto) for 1.5 hr. The section were stained with 10 mg of 3,3′-diaminobenzidine tetrahydrochloride and 0.005% H_2O_2 in 100 ml of Tris-HCl buffer (pH 7.6), rinsed with distiled water, stained with 1% methyl green, dehydrated in 100% isopropanol and xylol and mounted in Bioleit. The number of

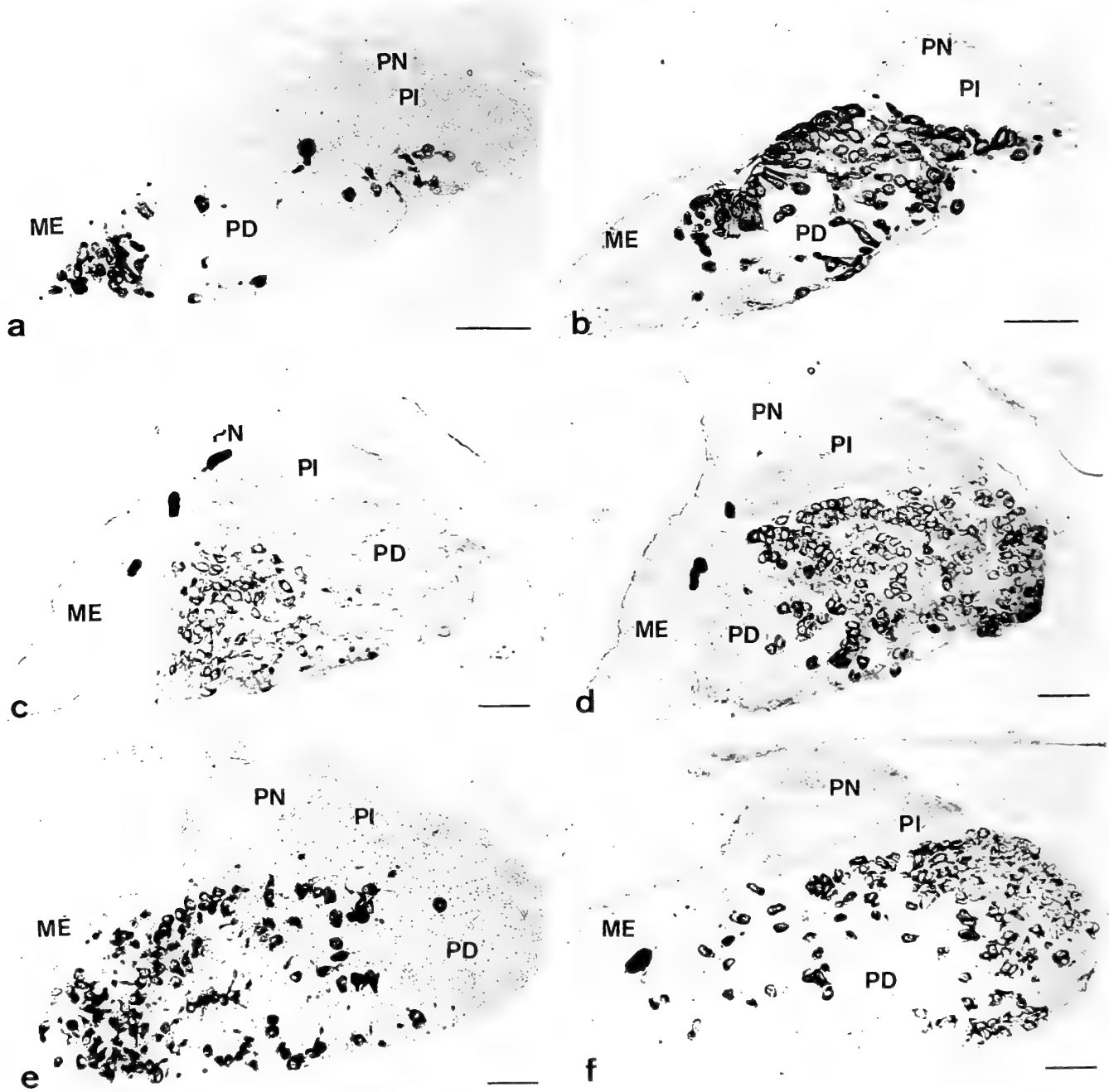

FIG. 2. Mid-sagittal sections of pituitary gland showing localization of immunoreactive PRL (a, c and e) and GH (b, d and f) cells in NF stages 55 (a and b), NF stages 62 (c and d) and juvenile (e and f) *Xenopus laevis*. ME, median eminence; PD, pars distalis; PI, pars intermedia; PN, pars nervosa. Bar, 50 μm.

immunoreactive cells with a visible nucleus in mid-sagittal section was counted to use as an index of the cell population [24]. The values from five specimens of each group were expressed as mean ± standard error of the mean (SEM). Student's *t* test was used for statistical analysis. Control sections were incubated with normal rabbit serum or antisera preadsorbed with an excess of the corresponding antigen instead of the specific antiserum.

RESULTS

The intensity of the immunoreaction was considerable with the antisera against bullfrog PRL and bullfrog GH. No reaction was observed when sections were incubated with normal rabbit serum instead of the antiserm against bullfrog PRL or bullfrog GH. Immunostaining was completely abolished when sections were incubated with the primary antisera preadsorbed with corresponding antigens (data not shown).

At NF stage 42 (embryonic nonfeeding stage), immunoreactive PRL cells first appeared in the anterodorsal region of the pars distalis (Fig. 1a). Almost simultaneously, GH-immunoreactive cells appeared more caudally than PRL cells (Fig. 1b). There was an apparent segregation of PRL and GH groups. Comparison of two consecutive sections stained with anti-bullfrog PRL and anti-bullfrog GH, respectively, did not show colocalization of PRL and GH (Fig. 1, a and b).

At the subsequent premetamorphic stages (NF stages 43-54), the increase in PRL cell population was not so marked (Fig. 3). During prometamorphosis (NF stages 55–61) and climax (NF stages 62-64), PRL cells increased in number moderately. They were located mainly in the anterior portion of the pars distalis (Fig. 2, a and c). On the other hand, a marked increase of GH cell number was observed during the late premetamorphic period (NF stages 50–52). Thereafter, the population of GH cells became 2–3 times larger than that of PRL cells. Again, the increase of GH cell number occurred during early climax (NF stages 62–64). At the end of metamorphosis, a slight but significant decrease of the number of GH cells was observed (Fig. 3). Immunoreactive GH cells were abundant in the caudal portion of the pars distalis (Fig. 2, b and d). In juveniles, localization of PRL and GH cells was fundamentally the same as that in larvae. PRL cells were situated mainly in the rostral portion and GH cells were in the caudal portion of the pituitary gland (Fig. 2, c and e). The presence of PRL cells with occasional long processes was noted. No apparent coexistence of PRL and GH was observed in the pituitary gland of larvae at advanced metamorphic stages or of juveniles.

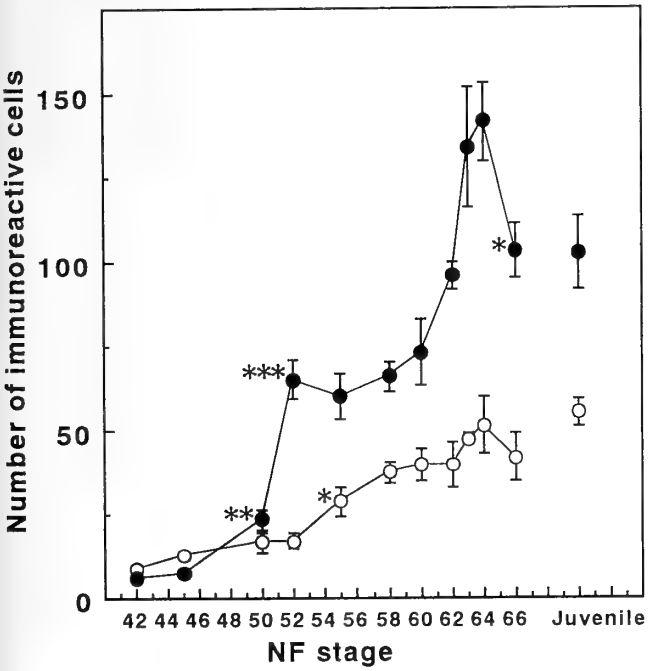

FIG. 3. Population of PRL (clear circles) and GH (solid circles) cells detected in mid-sagittal sections of *Xenopus* larvae at various developmental stages and of juveniles. The values are expressed as mean of 5 determinations ± S.E.M. Significant differences at $^{*}P<0.05$, $^{**}P<0.01$ or $^{***}P<0.001$ versus preceding stage (Student's *t* test).

DISCUSSION

Moriceau-Hay *et al.* [14] have studied the development of PRL and GH cells in *Xenopus* tadpoles using antisera against bovine PRL and GH. According to them, PRL cells first appeared at stage 42. This is consistent with the present result. However, they were able to first recognize immunoreactive GH cells only at stage 44, whereas we detected them at stage 42. This discrepancy may be due to the difference in sensitivity of the antisera used in these two experiments. Moriceau-Hay *et al.* [14] stated that the cross-reactivity of the anti-bovine GH serum they used was quite low. This is often the case when antisera against GH of mammalian origin are used for the detection of GH cells in amphibian hypophyses [5].

In this study, we observed that PRL cells were less abundant than GH cells throughout prometamorphosis and climax. This persisted even one month after metamorphosis. However, with the same antisera as those used in this study, we have confirmed that the population of PRL cells exceeds that of GH cells when the toads become adult [17]. It has been reported that, in *Rana esculenta,* an anti-ovine GH serum stains both PRL and GH cells [23]. Immunological studies by Hayashida [6] also demonstrated cross-reactivity between frog PRL and antiserum against primate GH. In the present study, we used antisera against RPL and GH of amphibian origin. The specificity of these antisera has been confirmed by radioimmunoassay [1, 11, 25] and immunoblotting [13, 17, 28]. Using these anti-PRL and anti-GH sera, coexistence of PRL and GH in secretory granules within the same cells in the pituitary gland of embryonic bullfrogs has been demonstrated [9, 13]. In this study, however, colocalization of PRL and GH in *Xenopus* pituitary cells was not observed. Failure to demonstrate the

coexistence of PRL and GH within the same cell of *Rana dalmatia* pituitaries has also been reported by Guastalla *et al.* [5].

Recently, we have isolated two molecular forms of both PRL and GH [26, 27] from the *Xenopus* pituitary gland. These two forms of PRL and GH showed considerable cross-reactivity with the anti-bullfrog PRL and anti-bullfrog GH, respectively. Production of specific antiserum against each hormonal molecule is under way. If these specific antisera become available and are applied to immunohistochemistry and radioimmunoassay, more precise information about PRL and GH cell function in *Xenopus* larvae could be obtained.

ACKNOWLEDGMENTS

This work was supported by a grant from Waseda University and Grants-in-Aid from the Japanese Ministry of Education to S. K. The authors express their appliciation to Dr. K. Yamamoto, Dr. K. Kawamura and Dr. T. Kobayashi for their help and advice during the course of the experiment.

REFERENCES

1 Andersen AC, Kawamura K, Pelletier G, Kikuyama S, Vaudry H (1989) Gen Comp Endocrinol 72: 299–307
2 Campantico E, Guastalla A (1992) Gen Comp Endocrinol 86: 197–202
3 Eagleson GW, McKeown BA (1978) Cell Tissue Res 189: 53–66
4 Garcia-Navarro S, Maria MM, Gracia-Navarro F (1988) Gen Comp Endocrinol 69: 188–196
5 Guastalla A, Campantico E, Yamamoto K, Kobayashi T, Kikuyama S (1993) Gen Comp Endocrinol 89: 364–377
6 Hayashida T (1970) Gen Comp Endocrinol 15: 432–452
7 Kar S, Naik DR (1986) Anat Embryol 175: 137–146
8 Kawauchi H, Yasuda A (1988) In "Prolactin Gene Family and Its Receptors" Ed by K Hoshino, Elsevier, Amsterdam, pp 61–70
9 Kikuyama S (1994) Can J Zool, in press
10 Kikuyama S, Kawamura K, Tanaka S, Yamamoto K (1993) Int Rev Cytol 145: 105–148
11 Kobayashi T, Kikuyama S (1991) Gen Comp Endocrinol 82: 14–22
12 Kobayashi T, Yasuda A, Yamaguchi K, Kawauchi H, Kikuyama S (1991) Biochim Biophys Acta 1078: 383–387
13 Kobayashi T, Tanaka S, Matsuda K, Yamamoto K, Kikuyama S (1992) Proc Int Symp Amphibian Endocrinol, Tokyo, pp 45
14 Moriceau-Hay D, Doerr-Schott J, Dubois MP (1979) Gen Comp Endocrinol 39: 322–326
15 Nieuwkoop PD, Faber J (1956) Normal Table of *Xenopus larvis* Daudin, North Holland Publ, Amsterdam
16 Olivereau M, Olivereau JM, Kikuyama S, Yamamoto K (1990) Fortschr Zool 38: 371–383
17 Olivereau M, Olivereau JM, Yamashita K, Matsuda K, Kikuyama S (1993) Cell Tissue Res, 274: 627–630
18 Remy C, Dubois MP (1973) C R Soc Biol 167: 1581–1584
19 Sternberger LA (1979) Immunocytochemistry, Wiley, New York, 2nd ed
20 Takahashi N, Yoshihama K, Kikuyama S, Yamamoto K, Wakabayashi K, Kato Y (1990) J Mol Endocrinol 5: 281–287
21 Takahashi N, Kikuyama S, Gen K, Maruyama O, Kato Y (1992) J Mol Endocrinol 9: 283–289
22 Thanaka S, Sakai M, Park MK, Kurosumi K (1991) Gen Comp Endocrinol 84: 318–327
23 Van Kemenade JAM (1974) Fortschr Zool 22: 228
24 Yasuda A, Yamaguchi K, Kobayashi T, Yamamoto K, Kikuyama S, Kawauchi H (1991) Gen Comp Endocrinol 83: 218–226
25 Yamamoto K, Kikuyama S (1982) Endocrinol Japon 29: 159-167
26 Yamashita K, Matsuda K, Hayashi H, Hanaoka Y, Tanaka S, Yamamoto K, Kikuyama S (1993) Gen Comp Endocrinol 91: 307–317
27 Yamashita K, Yamamoto K, Hayashi H, Kikuyama S (1993) Zool Sci 10 (Suppl): p 132
28 Yon L, Feuilloley M, Kobayashi T, Pelletier G, Kikuyama S, Vaudry H (1991) Gen Comp Endocrinol 83: 142–151
29 Zuber M, Dubois M (1975) C R Acad Sci 280 D: 1595–1598

ZOOLOGICAL SCIENCE 11: 153–156 (1994)

[RAPID COMMUNICATION]

Nucleotide Sequence of the Proton ATPase Beta-Subunit Homologue of the Sea Urchin *Hemicentrotus pulcherrimus*[1]

YU-ICHI SATOH, TAKESHI SHIMIZU, YUTAKA SENDAI, HIROAKI KINOH and NORIO SUZUKI[2]

Noto Marine Laboratory, Kanazawa University, Ogi, Uchiura, Ishikawa 927-05, Japan

ABSTRACT—A cDNA with 2.3 kb encoding F_1-F_0 ATP synthase (proton ATPase) beta-subunit homologue was isolated from a testis cDNA library of the sea urchin, *Hemicentrotus pulcherrimus*. The deduced amino acid sequence consisted of 523 residues which contained a 19-residue amino-terminal signal peptide and a 8-residue glycine-rich consensus sequences. Analysis of poly(A)$^+$RNA and/or total RNA from *H. pulcherrimus* testis, ovary, unfertilized eggs, and embryos by Northern blot revealed a 2.4 kb RNA.

INTRODUCTION

A sperm-activating peptide (SAP-I: GLy-Phe-Asp-Leu-Asn-Gly-Gly-Gly-Val-Gly), isolated from the egg jelly of sea urchins, *Hemicentrotus pulcherrimus* [13] and *Strongylocentrotus purpuratus* [3], increases sea urchin sperm respiration rate and motility. It induces a Na^+-dependent net proton efflux and raises the intracellular pH [10]. As the result SAP-I stimulates sperm energy metabolism which depends on the oxidation of endogenous phosphatidylcholine [8]. ATP synthesis by oxidative phosphorylation is a multistep membrane-located process that occurs in the inner membranes of mitochondria. F_0-F_1 ATP synthase (proton ATPase) in membranes of mitochondria synthesizes ATP coupled with an electrochemical gradient of protons generated by the electron transfer chain. The enzyme from many different sources have been studied extensively at the molecular biological level [2]. However, no molecular biological study has been made on the enzyme from spermatozoa of any kind of animals.

In this study, we screened a *H. pulcherrimus* testis cDNA library with oligonucleotide probes synthesized based on the amino acid sequence of peptide obtained from the protease V8 digest of wheat germ agglutinin (WGA)-binding protein of *H. pulcherrimus* spermatozoa and isolated a cDNA encoding the beta-subunit homologue of mitochondrial F_1-F_0 ATP synthase. Here, we report that the cDNA is 2259 bp long and an open reading frame predicts a protein 523 amino acids.

Accepted December 28, 1993
Received December, 1, 1993

[1] The nucleotide sequence data reported in this paper will appear in the DDBJ, GenBank and EMBL Nucleotide Sequence Databases with the following accession number D17361.

[2] To whom correspondence should be addressed.

MATERIALS AND METHODS

Cloning and sequencing of cDNA

A cDNA library (4.9×10^5 pfu) from poly(A)$^+$RNA isolated from growing testes of the sea urchin *H. pulcherrimus* was constructed in λ gt10 using the cDNA Synthesis System and the cDNA Cloning System λ gt10 (Amersham International plc., Amersham, UK). A 220 kDa WGA-binding protein was purified from *H. pulcherrimus* spermatozoa by affinity chromatography on a WGA-Sepharose 4B column as described previously [12], and digested by protease V8. The partial amino acid sequence of a peptide purified from the digest by preparative SDS-gel electrophoresis was determined to be V-S-S-*I-D-N-I-F-R*-V. The sequence indicated by italics was the same as the conserved sequence found in F_1-F_0 ATP synthase beta-subunit from various sources. Based on the sequence of the decapeptide, the mixed oligonucleotides (5′-GACACGGAAGATGTTGTCGATGCTGCTGAC-3′/5′-GACACGGAAGATGTTGTCGATAGAGGAGAC-3′) were synthesized and used to screen. Forty-six positive hybridizing clones were isolated from approximately 6×10^4 recombinants. Restriction endonuclease mapping of the inserts indicated that five different types of clones had been isolated. The insert of 2.3 kb from one member of the largest group in which fifteen clones belong was subcloned into the plasmid vector Bluescript II KS(+) (Stratagene, La Jolla, CA, USA) for further analysis. Serial deletion mutants of subclones were made according to Yanisch-Perron *et al* [16]. Nucleotide sequences were determined by the dideoxy chain termination method [11] using the Sequenase Kit (United States Biochemical Co., Cleaveland, OH, USA) and the 7-DEAZA Sequencing Kit (Takara Shuzo Co., Kyoto, Japan) analyzed on DANASIS software (Hitachi Software Engineering Co., Yokohama, Japan).

Northern blot analysis

Total RNA was prepared from testes, ovaryies, unfertilized eggs, and embryos of *H. pulcherrimus* by the LiCl method of Cathala *et al* [1]. Poly(A)$^+$RNA was prep ared by two passage of the total RNA over a column of oligo(dT)-cellulose (Pharmacia LKB Biotechnology, Uppsala, Sweden). Northern blot analysis was carried out as follows: 2–5 μg of poly(A)$^+$RNA or total RNA was denatured

```
5'CGTGACCCCTGGAAGAATTTCACATCGCCATGTTTAGCAGGGTTGCAAAGACGAGTTTTTCGGCCGTAAGGGCTGCAAAATCACAATTT   89
    *                                M F S R V A K T S F S A V R A A K S Q F   20

TCACACTCATTATCACAACAGACGAGTAAAACATGGGTACCAGCAGCAACTTGTAGCAAAAGATCATATGCTGCTGAGGCAAAGACGTCG  179
 S H S L S Q Q T S K T W V P A A T C S K R S Y A A E A K T S   50

GCAGCCCCAGTTTCGGGTCAGATCGTAGCTGTCATTGGAGCTGTCGTCGACGTTCAGTTCGAGGATGACCTCCCACCCATTCTCAATGCC  269
 A A P V S G Q I V A V I G A V V D V Q F E D D L P P I L N A   80

TTGGAGGTTCAGGGAAGGACATCCAGGCTGGTGTTGGAAGTTGCACAGCATCTTGGTGAGAACACAGTCAGGACAATTGCCATGGACGGT  359
 L E V Q G R T S R L V L E V A Q H L G E N T V R T I A M D G   110

ACAGAAGGTCTGATCCGAGGCCAGAAGTGCGTTGACACTGGCTCCCCCATCAGCATCCCCGTCGGCCCCGAGACGCTGGGACGCATCATC  449
 T E G L I R G Q K C V D T G S P I S I P V G P E T L G R I I   140

AATGTCATTGGTGAACCCATTGACGAGAGAGGACCAATTGGAACAGACAGGAGATCAGCAATCCATGCAGAAGCTCCAGAGTTTGTAGAG  539
 N V I G E P I D E R G P I G T D R R S A I H A E A P E F V E   170

ATGAGTGTAAACCAGGAAATCCTTGTTACTGGAATCAAGGTTGTAGATCTACTCGCCCCATACGCCAAGGGAGGAAAGATTGGTCTGTTT  629
 M S V N Q E I L V T G I K V V D L L A P Y A K G G K I G L F   200

GGCGGTGCTGGTGTAGGAAAGACTGTACTCATCATGGAGCTGATTAACAACGTAGCCAAGGCCCACGGAGGTTACTCTGTGTTTGCCGGT  719
 G G A G V G K T V L I M E L I N N V A K A H G G Y S V F A G   230

GTAGGAGAGAGGACCCGTGAGGGTAACGATCTTTACCATGAGATGATTGAAGGAGGTGTCATCTCCCTCAAGGATGACACATCAAAGGTA  809
 V G E R T R E G N D L Y H E M I E G G V I S L K D D T S K V   260

GCGTTGGTGTACGGACAGATGAACGAGCCTCCCGGCGCCCGTGCCCGTGTCGCCTTGACCGGACTGACCGTTGCCGAATACTTCCGTGAC  899
 A L V Y G Q M N E P P G A R A R V A L T G L T V A E Y F R D   290

CAAGAGGGACAGGATGTGCTGCTCTTCATTGACAACATCTTCCGCTTCACACAGGCTGGATCAGAGGTATCTGCTCTGCTGGGACGTATC  989
 Q E G Q D V L L F I D N I F R F T Q A G S E V S A L L G R I   320

CCATCTGCCGTAGGATACCAGCCAACCCTGGCCACTGACATGGGTACTATGCAGGAGCGTATTACCACCACCAAGAAGGGATCCATCACT 1079
 P S A V G Y Q P T L A T D M G T M Q E R I T T T K K G S I T   350

TCCGTACAGGCCATCTACGTGCCTGCTGACGATCTCACTGACCCTGCCCCTGCCACCACCTTCGCCCATTTGGACGCCACCACTGTGCTG 1169
 S V Q A I Y V P A D D L T D P A P A T T F A H L D A T T V L   380

TCCCGTGGTATCGCTGAGCTGGGTATCTACCCTGCTGTGGATCCTCTGGATTCCTCCTCCCGTATCATGGACCCCAACGTCGTCGGAGAG 1259
 S R G I A E L G I Y P A V D P L D S S S R I M D P N V V G E   410

CGTCACTACAGCATCGCTCGTGGAGTACAGAAAATCCTTCAGGACAACAAGACCCTGCAGGACATCATCGCCATCTTGGGTATGGACGAG 1349
 R H Y S I A R G V Q K I L Q D N K T L Q D I I A I L G M D E   440

TTGTCTGAGGACGACAAACTGACCGTGTCCCGAGCCAGGAAGATCCAGAGGTTCTTGTCCCAACCCTTCCAGGTTGCCGAGGTCTTCACC 1439
 L S E D D K L T V S R A R K I Q R F L S Q P F Q V A E V F T   470

GGCAGTCCAGGCAAGCTCGTCTCAATGGCGGAGACCATCGATGGATTCGAGTCCATTATCAAGGGCGAGTGCGACCATCTACCAGAGATT 1529
 G S P G K L V S M A E T I D G F E S I I K G E C D H L P E I   500

GCTTTCTACATGGTAGGCAACATTCAAGATGTCAAGGATAAGGCCGACAGGCTCGCAGAAGAACTATCATAAATTATCCCCCCTCTCCCA 1619
 A F Y M V G N I Q D V K D K A D R L A E E L S *               523

AACAATGAAGTTTAGAGCTGGCATGGCTACGGGTCAGAGACACCCCTCTTGATTGTTGTTATTCAGGGCTAGTTGTCTAACACTACCCGT 1709
GCCTGGGCCCAAAGAATTTATGTTCAGAGTTATAACTTATATCAAGATTGTTTTCTAAATTGTAATTGTGAAAAATTGAGAGCAAGGGAA 1799
TTCCAACCTAGCGTACTTTTGTCATATGAATCTGTCGTTTTCCTTCTTTTTTTTGCTTGTTATCCACCATAGATTGTAAATGCACAAACA 1889
GCTTGGCAAAGTTTGTAAATTTGATCATAACCAATTATCCCAATTTAAGGCAGTACCTTTAGCACATTGGTGTGTCACCGATGCCTGATT 1979
TCATGTTTATTGTCTGATCTGATCTTACAAGAAATTGGCCGATGTCCAAACATTTCCAATGTAGATATAGACATATATCTTCACTTGATT 2069
TCTGTGTAGAGCCGTTCACGTATGACAGATGATTGGCATTTATTTTGAATGGATGTTTTAGAGCTTTACTGAACCCAGTTGCGATTGTGA 2159
TTTCCTTGTGTGAACAGAATCGCAACTGGCCTTGAAAAAGAAAAACAAGTGTATTAAAAATTATTGGAAGGTTCAAGAACCAAAAAAAAA 2249
AAAAAAAAA 3'                                                                                  2259
```

FIG. 1. Nucleotide sequence and deduced amino acid sequence of the 2.3 kb insert. The shadowed box indicates predicted signal peptide sequence and the open box denotes glycine-rich consensus sequence. The amino acid sequence deisgnated by an underline is the same as partial sequence of the decapeptide used for synthesis of oligonucleotide probes. * denotes start or stop codon.

with 2.1 M formaldehyde, electrophoresed on a 1% agarose gel in the presence of 2.2 M formaldehyde, and transferred onto a Hybond-N-membrane. The RNA on the membrane was hybridized to the random-primed ECL labelled (Amersham International plc., Amersham, UK) or random-primed [α-^{32}P]dCTP-labelled 2.3 kb cDNA insert at 65°C for 18 hr. The membrane was washed with 0.5×SSC and 0.1% SDS at 65°C for 30 min. The size of the RNA was estimated using a 0.24–9.5 kb RNA Ladder (GIBCO BRL, Baithersburg, MD, USA) as a marker.

RESULTS AND DISCUSSION

The 2.3 kb insert contained DNA sequences encoding an open reading frame of 523 amino acids including I-D-N-I-F-R which is the same as the partial sequence of the peptide used for synthesis of oligonucleotide probes (Fig. 1). The deduced amino acid sequence suggests that the protein contains a 19-residue amito terminal signal peptide which has the potential to form amphipathic helix being characteristic of mitochondrial signal peptide sequence [5] and a 8-residue (residues 201-208) glycine-rich consensus sequence (G-X-X-X-G-K-T/S) found in the F_1-F_0 ATP synthase beta-subunit, adenylate kinase, p21 *ras* protein, and other nucleotide-binding proteins [14]. The deduced amino acid sequence has 68% homology with those of chloroplast F_1-F_0 ATP synthase beta-subunits and 85% with those of mitochondrial F_1-F_0 ATP synthase beta-subunits from various

```
                                10        20        30        40        50        60
Spermatozoa (sea urchin)   MFSRVAKTSFSAVRAAKSQFSHSLSQQTSKTWVPAATCSKRSYAAEAKTSA--APVSGQIVAVIGAVVDV
Mitochondria (human)    MLGFVG...AAPA.GALRRLTPSASLPPA.LLLRAA.T.VHPV.D...QTSP.PKAGAAT.R..........
Mitochondria (rat)      MLSLVG...SA.A.GALRGLNPLAALPQAHLLLRTA..GVHPA.D...QSSAAPKAGTAT............
Chloroplast (potato)                                          MRINPTTSGS.VS.VE--KKNL.R..KI..P.L..
Chloroplast (spinach)                                         MRINPTTSDPGVS.LE--KKNL.R.AQI..P.LN.

      70        80                90        100       110       120       130       140       150
QF-EDDLPPILNALEVQGR----TS---RLVLEVAQHLGENTVRTIAMDGTEGLIRGQKCVDTGSPISIPVGPETLGRIINVIGEPIDER
..-DEG.............----ET---.............S.............V....VL.S.A..K...........M..........
..-DEG.............----E.---.............S.............V....VL.S.A..K...........M..........
A.PPGKM.N.Y...V....----GNEQTNVTC..Q.L..N.R..AV..SD.D..M..MEVI...A...V...GS.....F..L.Q.V.NL
A.PPGKM.N.Y...I.K..DTAGQPM--NVTC..Q.L..N.R..AV..SA.D..T..MEVI...A.L.V...GP.....F..L...V.NL

      160       170       180       190       200       210       220       230       240
GPIGTDRRSAIHAEAPEFVEMSVNQEILVTGIKVVDLLAPYAKGGKIGLFGGAGVGKTVLIMELINNVAKAHGGYSVFAGVGERTREGND
...K.KQFAP........M....E.....................................................................
...K.KQFAP........I....E.....................................................................
..VD.NTT.P..RS..A.IQLDTKLS.FE.............RR.......................I......V...G...........
R.VD.RTT.P..RS..A.TQLDTKLS.FE......N.....RR.......................I......V...G...........

      250       260       270       280       290       300       310       320       330
LYHEMIEGGVISLKD-DTSKVALVYGQMNEPPGARARVALTGLTVAEYFRDQEGQDVLLFIDNIFRFTQAGSEVSALLGRIPSAVGYQPT
.......S...N...-A...........................................................................
.......S...N...-A...........................................................................
..L..K.S...NEENIPE.........-.......M..G..A..M......VNE.............V............M..........
..M..K.S...NEQNIAE..................M..G..A..M......VNE.............V............M..........

       340       350       360       370       380       390       400       410       420
LATDMGTMQERITTTKKGSITSVQAIYVPADDLTDPAPATTFAHLDATTVLSRGIAELGIYPAVDPLDSSSRIMDPNVVGERHYSIARGV
.....................................................A.............T.......I..SE..DV....
.....................................................A.............T.......I..SE..DV....
.S.E..YL.....S..E.....I..V.............................L.AK...........T.TMLQ.RI...E..ET....
.S.E..SL.....S..E.....I..V.............................L.AK...........T.TMLQ.RI...E..E..QR.

       430       440       450       460       470       480       490       500       510
QKILQDNKTLQDIIAILGMDELSEDDKLTVSRARKIQRFLSQPFQVAEVFTGSPGKLVSMAETIDGFESIIKGECDHLPEIAFYMVGNIQ
......Y.S..............E.........................HM....PLK...K..QQ.LA..Y.....Q......P.E
......Y.S..............E.........................HM....PLK...K..QQ.LA.DY....Q......P.E
KQT..RY.E.........L.....E.R...A.....E.......F...........Y.GL....R..QL.LS..L.G...Q...L....D
KET..RY.E.........L.....E.R...A.....E.......F...........Y.GL....R..QL.LS..L.S...Q...L....D

       520                Homology
DVKDKADRLAEELS              100%
EAVA...K....H.S              85%
EAVA...K....HGS              85%
EATA..MN.KT                  68%
EATA..MN.EM.SKLKK            68%
```

FIG. 2. Comparison of deduced amino acid sequence of the sea urchin homologue and mitochondrial (human [9], rat [4]) and chloroplast (potato [7], spinach [17]) F_1-F_0 ATP synthase beta-subunits. Dots indicate the same amino acid residues as sea urchin homologue and positions where gap have been introduced for maximum homology are indicated by a dash.

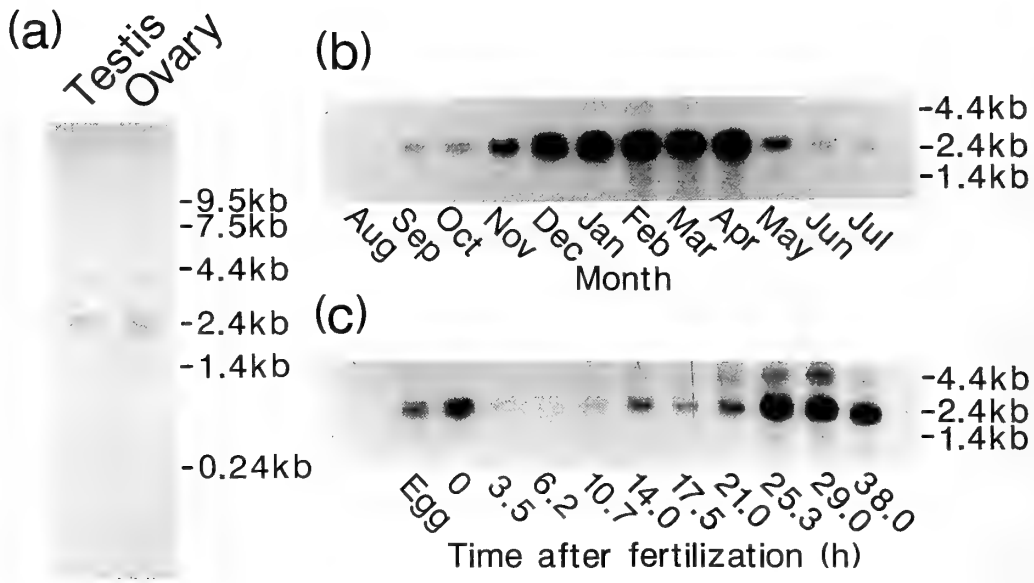

FIG. 3. Analysis of RNA prepared from *H. pulcherrimus* ovaies, testis, unfertilized eggs and embryos by Northern blot hybridization. (a): poly(A)$^+$RNA (2 μg) prepared from ovaries and testis samples collected in March, detected by ECL; (b): total RNA (5 μg) from the testis samples collected throughout the year, detected by autoradiography; (c); total RNA (5 μg) from unfertilized eggs and embryos cultured at 20°C, detected by autoradiography.

sources (Fig. 2) [4, 7, 9, 17]. This suggests that the cDNA clone isolated from the *H. pulcherrimus* testis cDNA library codes for the beta-subunit of mitochondrial F_1-F_0 ATP synthase and the primary strucutres of the beta-subunits are highly conserved in very different species.

Norhtern blot analysis using the 2.3 kb insert as a probe indicated that the mRNA of 2.4 kb presents both in the ovary and testis of the sea urchin (Fig. 3a). In previous study, we demonstrated that *H. pulcherrimus* spermatozoa contained a large amount of membrane-bound guanylate cyclase and creatine kinase and the activities of both enzymes increased during the testis development [6]. As shown in Figure 3b, the mRNA encoding F_1-F_0 ATP synthase beta-subunit began to the accumulated in the testis collected in November when spermatogenic cells appeared along the wall of testicular lobes, suggesting that F_1-F_0 ATP synthase is also synthesized in the testis with formation of mature spermatozoa. The mRNA was also identified in unfertilized eggs and developing embryos, while the signal of hybridizing RNA from the unfertillized eggs was weaker than that from the developing embryos (Fig. 3c). This may be due to imcomplete polyadenylation of the stored mRNA in unfertilized eggs [15]. Additional polyadenylation reaction appears to begin rapidly upon fertilization (Fig. 3c). The mRNA was not appreciably detected in the embryos during early cleavage stage and became detectable in the embryos of the gastrula stage (Fig. 3c).

ACKNOWLEDGMENTS

This work was supported in part of by a "Grant-in-Aid-for Scientific Research (A)", No. 02404006 from the Ministry of Education, Science and Culture of Japan.

REFERENCES

1 Cathala G, Savouret J-F, Mendez B, West BL, Karin M, Martial JA, Baxter JD (1983) DNA 2: 329–335
2 Futai M, Noumi T, Maeda M (1989) Am Rev Biochem 58: 111–136
3 Garbers DL, Watkins HD, Hansbrough JR, Smith AC, Misono KS (1982) J Biol Chem 257: 2734–2737
4 Garboczi DN, Fox AH, Gerring SL, Pedersen PL (1988) Biochemistry 27: 553–560
5 Hawlistschek G, Schneider H, Schmidt B, Tropschung M, Hartl F-U, Neupert W (1988) Cell 53: 795–806
6 Harumi T, Kurita M, Suzuki N (1992) Develop Growth Differ 34: 151–162
7 Kobayashi K, Nakamura K, Asahi T (1987) Nucleic Acids Res 15: 7177–7177
8 Mita M, Ueta N, Harumi T, Suzuki N (1990) Biochim Biophys Acta 1035: 175–181
9 Ohta S, Tomura H, Matsuda K, Kagawa Y (1988) J Biol Chem 263: 11257–11262
10 Repaske DR, Garbers DL (1983) J Biol Chem 258: 6025–6029
11 Sanger R, Nicklen S, Coulson AR (1977) Proc Natl Acad Sci USA 74: 5463–5467
12 Sendai Y, Aketa K (1991) Dev Growth Differ 33: 101–109
13 Suzuki N, Nomura K, Ohtake H, Isaka S (1981) Biochem Biophis Res Commun 99: 1238–1244
14 Walker JE, Saraste M, Runswick MJ, Gay NJ (1982) EMBO J 1: 945–951
15 Wilt FH (1973) Proc Natl Acad Sci USA 70: 2345–2349
16 Yanisch-Perron C, Vieira J, Messing J (1985) Gene 33: 103–119
17 Zurawski G, Bottomley W, Whitfeld PR (1982) Proc Natl Acad Sci USA 79: 6260–6264

ZOOLOGICAL SCIENCE 11: 157–160 (1994)

[RAPID COMMUNICATION]

Local Change of an Exogastrula-Inducing Peptide (EGIP) in the Pluteus Larva of the Sea Urchin *Anthocidaris crassispina*

Hiroaki Kanbayashi, Yoshiaki Fujita, Kyo Yamasu, Takashi Suyemitsu and Katsutoshi Ishihara

Department of Regulation Biology, Faculty of Science, Saitama University, Urawa, Saitama 338, Japan

ABSTRACT—Immunofluorescence staining of cryosections of pluteus larvae of the sea urchin *Anthocidaris crassispina* was performed with an antiserum raised in rabbit against exogastrula-inducing peptide D (EGIP-D). The apical side of the ectoderm and gut of pluteus larvae that had been cultured for 36 hr was stained. However, the gut of pluteus larvae that had been cultured for 38 hr was only partially stained and the gut of larvae that had been culltured for 40 hr was not stained at all. By contrast, the ectoderm of the 38-hr and 40-hr pluteus larvae remained stainable. These results suggest that EGIP-D is present in the gut of pluteus larvae 36 hr after fertilization, but it begins to disappear from the gut at 38 hr and is lost at all from the gut at 40 hr. The significance of the disappearance of EGIP-D from the gut of the pluteus larva is discussed in relation to the differentiation of the gut.

INTRODUCTION

Exogastrula-inducing peptides (EGIPs) are intrinsic factors that are present in mesenchyme blastulae of the sea urchin *Anthocidaris crassispina*. When added exogenously to embryos, they induce the extrusion of the archenteron toward the outside of the embryo, which leads to exogastrulation [2, 6].

In previous studies [6–8], four EGIPs, designated EGIPs A-D, were purified from mesenchyme blastulae of the sea urchin, and the amino acid sequences of all four peptides and the positions of the disulfide bonds in EGIP-D were determined [5]. The results suggest that EGIPs are homologous to epidermal growth factor (EGF), as indicated by the similarities between EGIPs and EGF in terms of the amino acid sequences and the positions of the disulfide bonds [1].

Recently, we reported the presence and quantitative changes in levels of maternal EGIPs during early development [3] and suggested that EGIP-D is present in acidic vesicles [4]. However, during early development, every type of blastomere in embryos of the sea urchin *A. crassispina* contains EGIP-vesicles, which are identical to acidic vesicles [4]. The biological role of EGIPs during the normal development of sea urchin embryos is not clear.

In the present report, we describe the disappearance of EGIP-D from the gut of the pluteus larva of the sea urchin and we discuss the significance of the local change of EGIP-D in relation to the differentiation of this organ.

MATERIALS AND METHODS

The eggs of *Anthocidaris crassispina* were obtained by introducing 0.5 M KCl into the coelom and they were then cultured after fertilization at 24°C for 36–40 hr in normal seawater, at a concentration of 3×10^6 embryos per liter, with gentle agitation. The pluteus larvae of the sea urchin were fixed for 24 hr in seawater that contained 3.7% formaldehyde at room temperature.

After fixation, larvae were embedded in O.T.C. compound (Miles Inc., Elkhardt, IN, USA) and sectioned on a Cryocut microtome (Reichert-Jung, Nussloch, F.R.G.), ad described previously [4]. The cryosections were treated with an antiserm raised in rabbit against EGIP-D and fluorescein isothiocyanate-conjugated antibodies raised in goat against rabbit IgG (Cappel, Malvern, PA, USA). Specimens were observed under UV illumination, as described previously [4].

RESULTS AND DISCUSSION

Immunofluorescence staining of cryosections of pluteus larvae of the sea urchin *Anthocidaris crassispina,* using a polyclonal antiserum raised in rabbit against EGIP-D, was performed here as described in Materials and Methods. Figure 1 shows the results of immunofluorescence staining of cryosections of pluteus larvae that had been cultured at 24°C for 36 hr after fertilization. The apical side of the ectoderm and the gut of 36-hr pluteus larvae was strongly stained, as shown in Figures 1C and E.

The immunofluorescence staining of cryosections was also carried out using larvae that had been cultured for 38 hr after fertilization (Fig. 2). The gut of the 38-hr pluteus larvae was only barely stained, as shown in Figure 2C, or it was partially stained, as shown in Figure 2E. The apical side of the ectoderm of the 38-hr pluteus larvae remained strongly

Accepted January 4, 1994
Received November 8, 1993

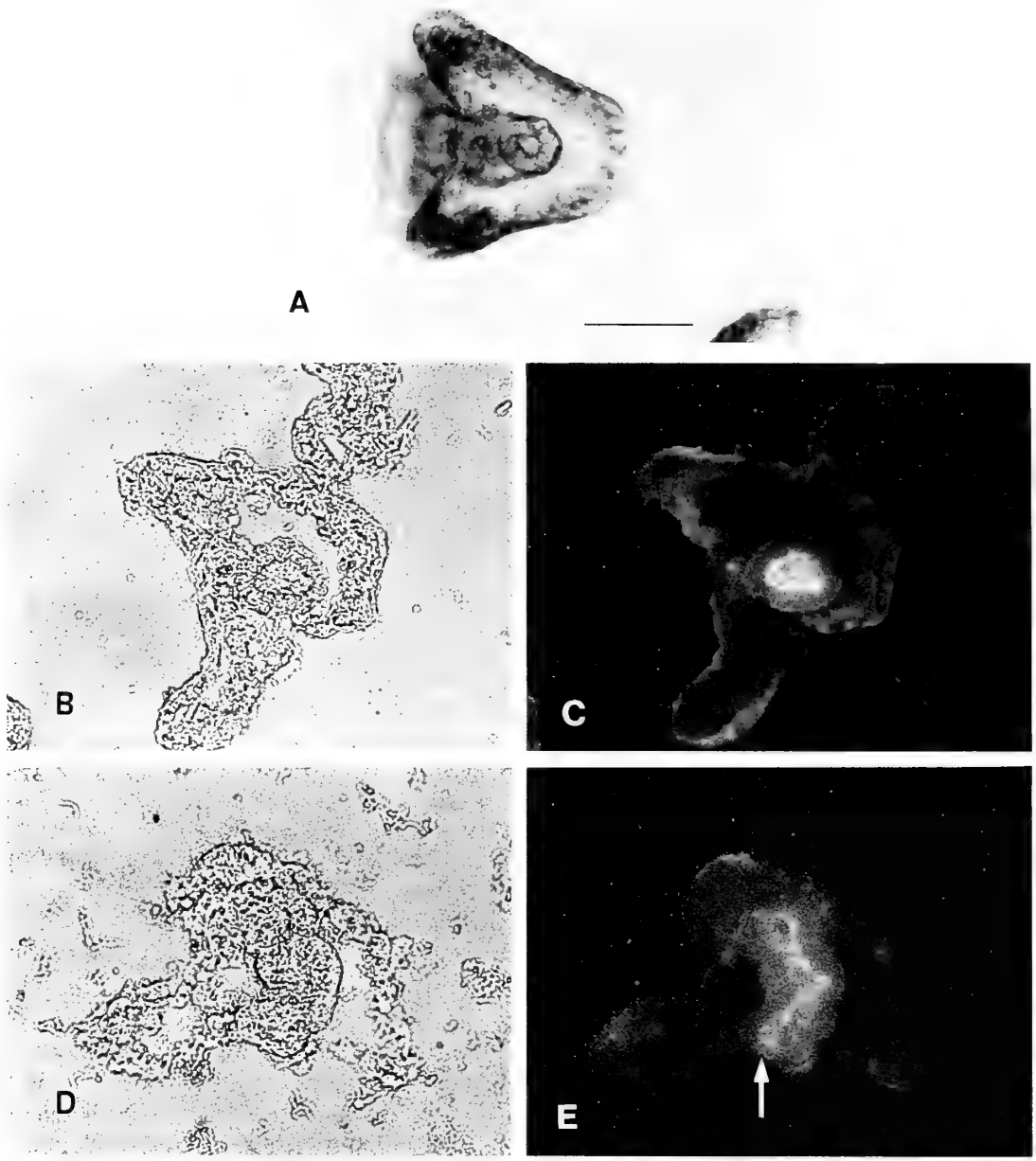

FIG. 1. Localization of EGIP-D in pluteus larvae that had been cultured at 24°C for 36 hr after fertilization. Cryosections of larvae were stained for indirect immunofluorescence with polyclonal antiserum against EGIP-D. (A) Light micrograph of an intact larva. (B, C) A matched pair of a light micrograph and an epifluorescence micrograph of a horizontal section of a larva. (D, E) A matched pair of a light micrograph and an epifluorescence micrograph of a longitudinal section of a larva. The arrow shows the position of the larval anus. Bar, 50 μm.

stainable.

Figure 3 shows immunofluorescence staining of cryosections of pluteus larvae that had been cultured for 40 hr after fertilization. The gut of the 40-hr pluteus larvae was not stained at all, while the apical side of the ectoderm of the 40-hr pluteus larvae was still stained, as shown in Figures 3C and E.

The results described above indicate that EGIP-D is present in the gut of the 36-hr pluteus larvae, begins to disappear from the gut of the 38-hr pluteus larvae and is lost at all from the gut of the 40-hr pluteus larvae. By contrast, EGIP-D remains in the ectoderm of the 40-hr pluteus larvae. The beginning of the desappearance of EGIP-D from the gut of the 38-hr pluteus larvae may be related to the differentiation of the gut of the larva, because the 38-hr pluteus larvae has a distinct oesophagus, stomach and intestine, as compared with the 36-hr pluteus larvae as shown in Figures 1 and 2. However, it remains to be determined whether the gut of

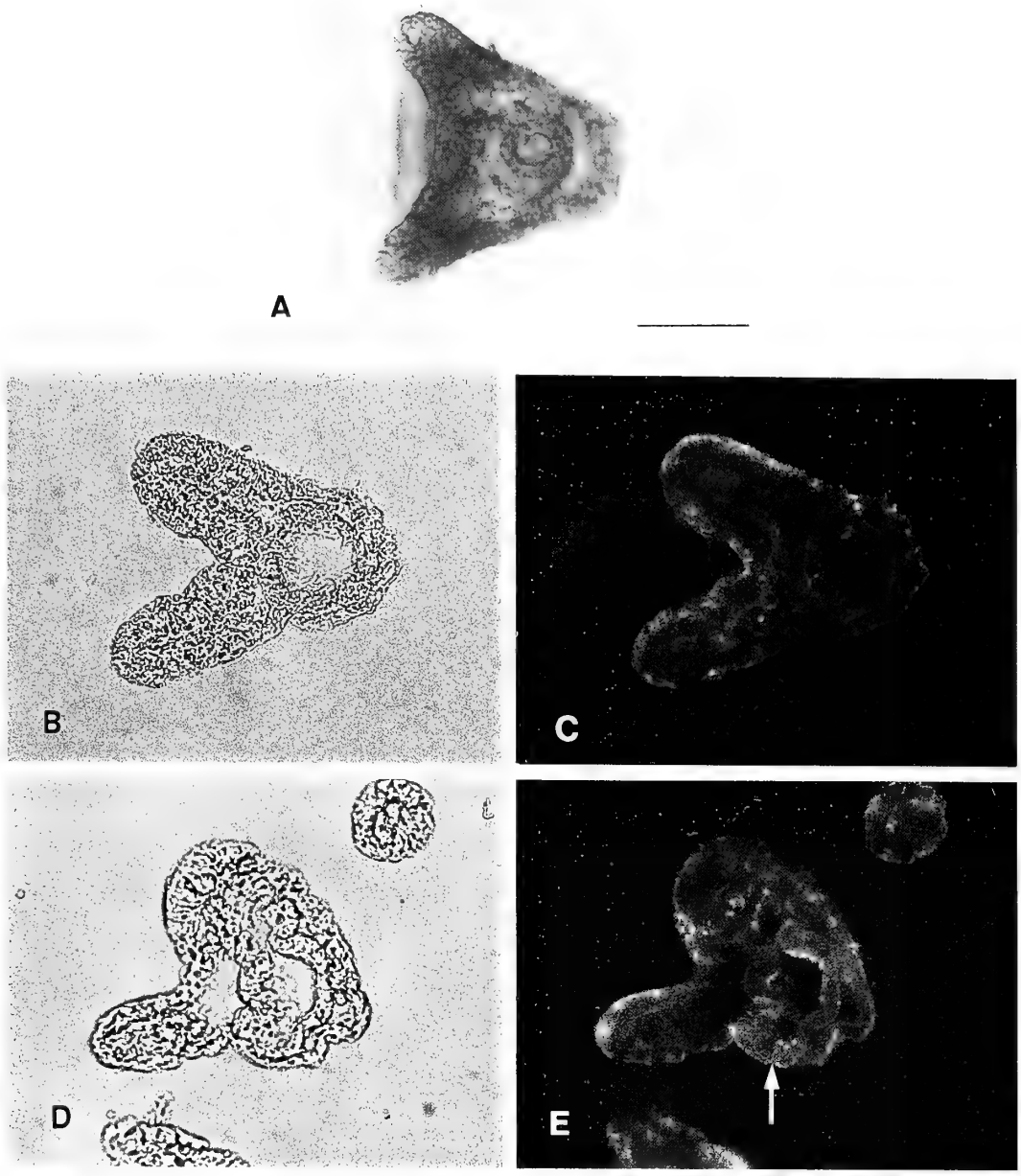

FIG. 2. Localization of EGIP-D in pluteus larvae that had been cultured at 24°C for 38 hr after fertilization. Cryosections of larvae were stained for indirect immunofluorescence in the same way as those in Figure 1. (A) Light micrograph of an intact larva. (B, C) A matched pair of a light micrograph and an epifluorescence micrograph of a horizontal section of a larva. (D, E) A matched pair of a light micrograph and an epifluorescence micrograph of a longitudinal section of a larva. The arrow shows the position of the larval anus. Bar, 50 μm.

the pluteus larva requires the degradation of EGIP-D for further differentiation or whether the differentiated gut of the pluteus larva no longer requires and secretes it.

In exogastrulated larvae of plutei under the influence of EGIPs, EGIP-D was also lost from the extruded gut after differentiation. These changes will be reported later in detail with electron microscopic studies.

Recently, we suggested that EGIP-D is contained in acidic vesicles [4]. Therefore, we are now examining whether acidic vesicles disappear during later development from the gut of the pluteus larvae simultaneously with the disappearance of EGIP-D from the gut.

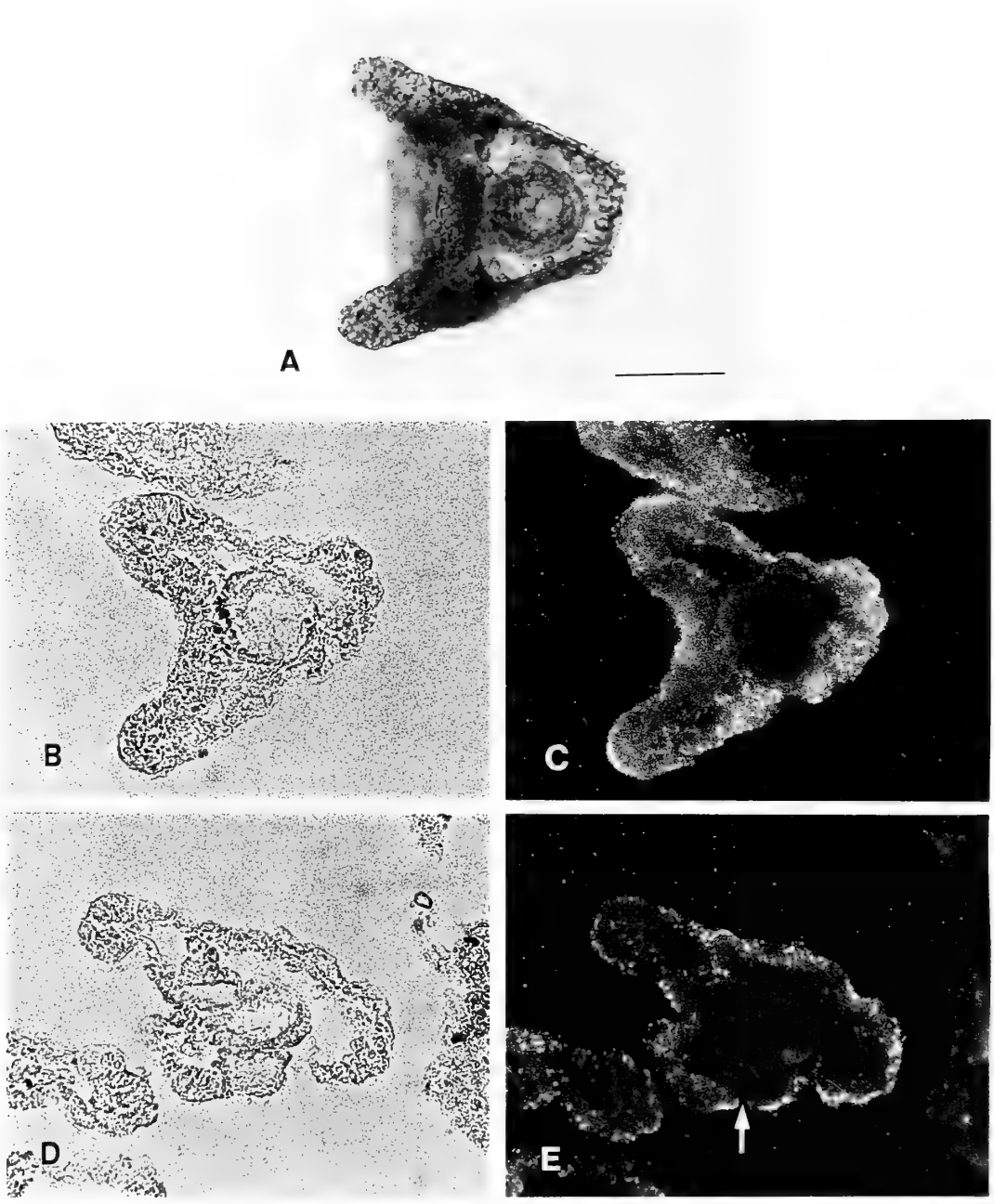

FIG. 3. Localization of EGIP-D in pluteus larvae that had been cultured at 24°C for 40 hr after fertilization. Cryosections of larvae were stained for indirect immunofluorescence in the same way as those in Figure 1. (A) light micrograph of an intact larva. (B, C) A matched pair of a light micrograph and an epifluorescence micrograph of a horizontal section of a larva. (D, E) A matched pair of a light micrograph and an epifluorescence micrograph of a longitudinal section of a larva. The arrow shows the position of the larval anus. Bar, 50 μm.

REFERENCES

1 Carpenter G, Cohen S (1979) Ann Rev Biochem 48: 193–216
2 Ishihara K, Tonegawa Y, Suyemitsu T, Kubo H (1982) J Exp Zool 220: 227–233
3 Kinoshita K, Fujii Y, Fujita Y, Yamasu K, Suyemitsu T, Ishihara K (1992) Develop Growth Differ 34: 661–668
4 Mizuno N, Uemura, I, Yamasu K, Suyemitsu T, Ishihara K (1993) Develop Growth Differ 35: 539–549
5 Suyemitsu T (1991) Zool Sci 8: 505–509
6 Suyemitsu T, Asami-Yoshizumi T, Noguchi S, Tonegawa Y. Ishihara K (1989) Cell Differ Develop 26: 53–66
7 Suyemitsu T, Tonegawa Y, Ishihara K (1989) Biochim Biophys Acta 999: 24–28
8 Suyemitsu T, Tonegawa Y, Ishihara K (1990) Zool Sci 7: 831–839

ANNOUNCEMENTS

The following three papers were not presented at the Sixty-Fourth Annual Meeting of the Zoological Society of Japan.

1) N. Takahashi N. and S. Kikuyama: Molecular cloning and nucleotide sequence analysis of cDNA for β-subunit of thyrotropin of the bullfrog (*Rana catesbeiana*).

2) N. Seo, and N. Makino: Distribution and changes of serotonin-like immunoreactivity in the central nervous system of the slug, *Limax marginatus*

3) M. Komatsu and M. Tamura: Microstructure of the barrel shaped larva of *Astropecten latespinosus* Meissner, with special reference to sensory neurons.

Therefore, the abstracts in the supplement (Volume 10, 1993; p133, p 152, p 153) should be canceled.

INSTRUCTIONS TO AUTHORS

ZOOLOGICAL SCIENCE publishes contributions, written in English, in the form of (1) **Reviews**, (2) **Articles**, and (3) **Rapid Communications** for short reports of timely and unusual interest. A *Review* is usually invited by the Editors. Those who submit reviews should consult with the Editors-in-Chief in advance. *Articles* of less than 5 printed pages and *Rapid Communications* less than 2 printed pages will be published free of charge. Charges will be made for extra pages (13,000 yen/page). A *Rapid Communication* cannot exceed 3 printed pages. No charge will be imposed for invited reviews up to 10 printed pages. No free reprints of Articles and Rapid Communications are available. To the author(s) of an invited review 50 reprints are provided gratis. Submission of papers from nonmembers of the Society is welcome. However, page charges (13,000 yen/page) will be made to nonmembers.

A. SUBMISSION OF MANUSCRIPT

The manuscript should be submitted in triplicate, one original and two copies, each including all illustrations. Rough copies of line drawings and graphs may accompany the manuscript copies, but the two copies of continuous-tone prints (photomicrographs, etc.) should be as informative as the original. The manuscript should be sent to:

Dr. Tsuneo Yamaguchi, Editor-in-Chief, Zoological Science, Department of Biology, Faculty of Science, Okayama University, Okayama 700, Japan.

B. CONDITIONS

All manuscripts are subjected to editorial review. A manuscript which has been published or of which a substantial portion has been published elsewhere will not be accepted. It is the author's responsibility to obtain permission to reproduce illustrations, tables, etc. from other publications. Accepted papers become the permanent property of ZOOLOGICAL SCIENCE and may not be reproduced by any means, in whole or in part, without the written consent of both the Zoological Society and the author(s) of the article in question.

C. ORGANIZATION OF MANUSCRIPT

The desirable style of the organization of an original paper is as follows: (1) Title, Author(s) and Affiliation (2) Abstract (3) Introduction (4) Materials and Methods (5) Results (6) Discussion (7) Acknowledgments (8) References (9) Tables (10) Illustrations and Legends. The author is not obliged to adhere rigidly to this organization. He or she may modify the style when such modification makes the presentation clearer and more effective. In a Rapid Communication, combination of some of these sections is recommended. There is no restriction on the style of review articles.

D. FORM OF MANUSCRIPT

Manuscripts should be typewritten and double spaced throughout on one side of white typewriting paper with 2.5 cm margins on all sides. Abstract not exceeding 250 words, tables, figure legends and footnotes should be typed on separate sheets. All manuscript sheets must be numbered successively. The use of footnotes to the text is not recommended.

1. Title page

The first page of manuscript should contain title, authors' names and addresses of university or institution, abbreviated form of title (40 characters or less, including spaces), the name and address for correspondence, and any footnotes. Authors with different affiliations should be identified by the use of the same superscript on name and affiliation. If one or more of the authors has changed his or her address since the work was carried out, the present address(es) to be published should be indicated in a footnote. In addition, a sub-field of submitted papers to be used as heading of an issue may be indicated in the first page. Authors are encouraged to choose one of the following: physiology, cell biology, molecular biology, genetics, immunology, biochemistry, developmental biology, reproductive biology, endocrinology, morphology, behavior biology, ecology, phylogeny, taxonomy, or others (specify). However, the Editors are responsible for the choice and arrangement of headings.

2. Introduction

This section should clearly describe the objectives of the study, and provide enough background information to make it clear why the study was undertaken. Lengthy reviews of past literature are discouraged.

3. Materials and Methods

This section should provide the reader with all the information that will make it possible to repeat the work. For modification of published methodology, only the modification needs to be described with reference to the source of the method.

4. Results

Results should be presented referring to tables and figures, without discussion.

5. Discussion

The Discussion should include a concise statement of the principal findings, a discussion of the validity of the observations, a discussion of the findings in the light of other published works dealing with the same subject, and a discussion of the significance of the work. Redundant repetition of material in Introduction and Results, and extensive discussion of the literature are discouraged.

6. Statistical analysis

Statistical analysis of the data using appropriate methods is mandatory and the method(s) used must be cited.

7. References

References should be cited in the text at the appropriate places by numbers in square parentheses. All references cited in the text should be listed at the end of the paper on a separate page, arranged in alphabetical order and numbered consecutively. For example:

1 Campbell RC (1974) Statistics for Biologists. Cambridge Univ. Press, London, 2nd ed, pp 59–61
2 Shima A, Ikenaga M, Nikaido O, Takabe H, Egami N (1981) Photoreactivation of ultraviolet light-induced damage in cultured fish cells as revealed by increased colony forming ability and decreased content of pyrimidine dimers. Photochem Photobiol 33: 313–316
3 Takewaki K (1931) Oestrous cycle of female rat in parabiotic union with male. J Fac Sci Imp Univ Tokyo, Sec IV, 2: 353–356
4 Wiersma CAG (1961) Reflexes and the central nervous system. In "The Physiology of Crustacea Vol 2" Ed by TH Waterman, Academic Press, New York, pp 241–279

Titles of cited papers should be omitted in Rapid Communications. The source of reference should be given following the commonly accepted abbreviations for journal titles (e.g., refer to 'International List of Periodical Title Abbreviations'). The use of "in preparation", "submitted for publication" or"personal communication" is not allowed in the reference list. "Unpublished data" and "Personal communication" should appear parenthetically following the name(s) in the text. Text citations to references with three or more authors should be styled as, e.g., Everett *et al.*. [7].

E. ABBREVIATIONS

Abbreviations of measurement units, quantity units, chemical names and other technical terms in the body of the paper should be used after they are defined clearly in the place they first appear in the text. However, abbreviations that would be recognized by scientists outside the author's field may be used without definition, such as *P*, SD, SE, DNA, RNA, ATP, ADP, AMP, EDTA, UV, and CoA. The metric system should be used for all measurements, and metric abbreviations (Table) should, in general, be expressed in lower case without periods.

Table. Abbreviations for units of measure which may be used without definition

Length:	km, m, cm, mm, μm, nm, pm, etc.
Area:	km^2, m^2, cm^2, mm^2 μm^2, nm^2, pm^2, etc.
Volume:	km^3, m^3, cm^3, mm^3, μm^3, nm^3, pm^3, kl, liter (always spellout), ml, μl, nl, etc.
Weight:	kg, g, mg, μg, ng, pg, etc.
Concentration:	M, mM, μM, nM, %, g/l, mg/l, μg/l, etc.
Time:	hr, min, sec, msec, μsec, etc.
Other units:	A, W, C, atm, cal, kcal, R, Ci, cpm, dB, v, Hz, lx, $\times g$, rpm, S, J, IU, etc.

F. PREPARATION OF TABLES

Tables should only include essential data needed to show important points in the text. Each table should be typed on a separate sheet of paper and must have an explanatory title and sufficient explanatory material. All tables should be referred to in the text, and their approximate position indicated in the margin of manuscript.

G. PREPARATION OF ILLUSTRATIONS

All figures should be appropriately lettered and labeled with letters and numbers that will be at least 1.5 mm high in the final reproduction. Note the conventions for abbreviations used in the journals so that usage in illustrations and text is consistent. All figures should be referred to in the text and numbered consequently (Fig. 1, Fig. 2, etc.). The figures must be identified on the reverse side with the author's name, the figure number and the orientation of the figure (top and bottom). The preferred location of the figures should be indicated in the margin of the manuscript. Illustrations that are substandard will be returned, delaying publication. Illustrations in color may be published at the author's expense.

1. Line drawings and graphs

Original artwork of high quality, glossy prints mounted on appropriate mounting card (**less than 25×38 cm**) should be submitted for reproduction. Author(s) may indicate size preference by making on the back of figures, such as "Do not reduce", "Two-column width" (**no wider than 16.5 cm**), or "One-column width" (**no wider than 8 cm**). Lines must be dark and sharply drawn. Solid black white, or bold designs should be used for histograms. Xerox or any other copying mean may be used for the two review copies.

2. Continuous-tone prints

Three sets of continuous-tone prints (photomicrographs, etc.) must be submitted. One set for reproduction should be mounted on appropriate mounting card, and the other two for reviewers may be unmounted prints. Xerox or similar copies of photomicrographs are not acceptable for review purposes. The continuous-tone prints should be submitted preferably at the exact magnification which is to be used in the published papers and trimmed to conform to the page size (**in no case should it exceed 16.5×22.5 cm**). Press-on numbers should be applied to the lower right corner of individual prints. Letters (a, b, c, etc.) should be used for multiple parts of a single figure. If important structures will be covered by use of the lower right corner, identification may be applied in the lower left corner.

Reproduction of color photographs will have to be approved by the Editors. The extra costs of color reproduction will be charged to the author(s).

3. Figure legends

Each figure should be accompanied by a title and an explanatory legend. The legends for several figures may be typed on the same sheet of paper. Sufficient detail should be given in the legend to make it intelligible without reference to

the text.

H. PROOF AND REPRINTS

A galley proof and reprint order will be sent to the submitting author. The first proofreading is the author's responsibility, and the proof should be returned within 72 hours from the date of receipt (by air mail from outside Japan). The minimum quantity for a reprint order is fifty. Manuscript, tables and illustrations will be discarded after the editorial use unless their return is requested when the manuscript is accepted for publication.

I. WORD-PROCESSOR DISKS

The Zoological Science can use your word-processor disks(5 1/4 or 3 1/2 inch). If available, **please send a copy of the disk with your final revised manuscript (two copies of the printout)**. This gives us a substantial decrease in typesetting time and assures you that there are no re-keying errors in the article. Moreover, using word-processor disks helps us to shorten publication times. If you would be willing to lend us the disk, please obey the following instructions.

1. Label the disk with the author's name; the word processor/computer used (e.g., NEC 9801, IBM-PC, Macintosh); the name of program (e.g., WordPerfect, WordStar, MS-Word, MacWrite). If you have an editor's manuscript number, include it on the label.
2. Send the manuscript as three files; if possible **keep the text, figure legends, and tables in separate files**. File names must clearly indicate the content of each file.
3. Send separate disks if you submit more than one article at a time.
4. A hard copy printout of the manuscript that exactly matches the disk files must be supplied. Special characters and symbols which are not included in the printer used, should be left as blank spaces in the files and these should be correctly written in the printout **in red**.
5. Do not use footnote.
6. Do not justify the right-hand margin.
7. For further information on preparing the disk, please contact the publisher (Daigaku Letterpress Co., Ltd., 809-5, Asakita-ku Kamifukawacho, Hiroshima 739-17, Japan; telephone: (082) 844-7500; fax:(082) 844-7800).

Development
Growth & Differentiation

Published Bimonthly by the Japanese Society of Developmental Biologists
Distributed by Business Center for Academic Societies Japan, Academic Press, Inc.

Papers in Vol. 36, No. 1. (February 1994)

1. **REVIEW**: T. Muramatsu: The Midkine Family of Growth/Differentiation Factors
2. H. Yasuo and N. Satoh: An Ascidian Homolog of the Mouse *Brachyury* (*T*) Gene is Expressed Excusively in Notochord Cells at the Fate Restricted Stage
3. I. Nagata and N. Nakatsuji: Migration Behavior of Granule Cell Neurons in Cerebellar Cultures. I. A PKH26 Labeling Study in Microexplant and Organotypic Cultures
4. K. Ono, N. Nakatsuji and I. Nagata: Migration Behavior or Granule Cell Neurons in Cerebellar Cultures. II. An Electron Microscopic Study
5. T. Miya, K. W. Makabe and N. Satoh: Expression of a Gene for Major Mitochondrial Protein, ADP/ATP Translocase, during Embryogenesis in the Ascidian *Halocynthia roretzi*
6. U. A. O. Heinlein, S. Wallat, A, Senftleben and L. Lemaire: Male Germ Cell-Expressed Mouse Gene *TAZ83* Encodes a Putative, Cysteine-Rich Transmembrane Protein (Cyritestin) Sharing Homologies with Snake Toxins and Sperm-Egg Fusion Proteins
7. A. Nagafuchi and S. Tsukita: The Loss of the Expression of α Catenin, the 102 kD Cadherin-Associated Protein, in Central Nervous Tissues during Development
8. E. M. del Pino, I. Alcocer and H. Grunz: Urea is Necessary for the Culture of Embryos of the Marsupial Frog *Gastrotheca riobambae*, and is Tolerated by Embryos of the Aquatic Frog *Xenopus laevis*
9. S. Fukada, N. Sakai, S. Adachi and Y. Nagahama: Steroidogenesis in the Ovarian Follicle of Medaka (*Oryzias latipes*, a Daily Spawner) during Oocyte Maturation
10. A. H. Wikramanayake and W. H. Clark, Jr.: Two Extracellular Matrices from Oocytes of the Marine Shrimp *Sicyonia ingentis* That Idenpendently Mediate Only Primary or Secondary Sperm Binding
11. S. Furuya, Y. Kamata and I. Yasumasu: ADP-Ribosylation of Histones in Nuclei Isolated from Embryos of the Sea Urchin, *Hemicentrotus pulcherrimus*
12. C. Cirotto, L. Barberini and I. Arangi: The Wavy Erythropoiesis of Developing Chick Embryos. Isolation of Each Wave by a Differential Lysis and Identification of the Constituent Erythroid Types

Development, Growth and Differentiation (ISSN 0012–1592) is published bimonthly by The Japanese Society of Developmental Biologists. Annual subscription for Vol. 35 1993 U. S. $ 191,00, U. S. and Canada; U. S. $ 211,00, all other countries except Japan. All prices include postage, handling and air speed delivery except Japan. Second class postage paid at Jamaica, N.Y. 11431, U. S. A.

Outside Japan: Send subscription orders and notices of change of address to Academic Press, Inc., Journal Subscription Fulfillment Department, 6277, Sea Harbor Drive, Orlando, FL 32887–4900, U. S. A. Send notices of change of address at least 6–8 weeks in advance. Please include both old and new addresses. U. S. A. POSTMASTER: Send changes of address to *Development, Growth and Differentiation,* Academic Press. Inc., Journal Subscription Fulfillment Department, 6277, Sea Harbor Drive, Orlando, FL 32887–4900, U. S. A.

In Japan: Send nonmember subscription orders and notices of change of address to Business Center for Academic Societies Japan, 16–9, Honkomagome 5-chome, Bunkyo-ku, Tokyo 113, Japan. Send inquiries about membership to Business Center for Academic Societies Japan, 16–9, Honkomagome 5-chome, Bunkyo-ku, Tokyo 113, Japan.

Air freight and mailing in the U. S. A. by Publications Expediting, Inc., 200 Meacham Avenue, Elmont, NY 11003, U. S. A.

BRANCHES NOW OPEN IN USA AND EUROPE

Narishige.
The complete range for micromanipulation

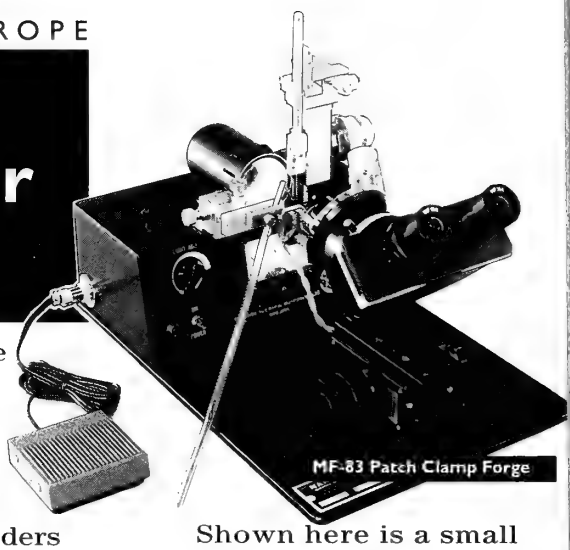
MF-83 Patch Clamp Forge

For over 30 years Narishige have been developing their extensive range of precision instruments for Physiology, Pharmacology, Zoology and Psychology research.

This large range includes micromanipulators, microelectrode pullers and microforges, microinjectors, microgrinders and stereotaxic instruments.

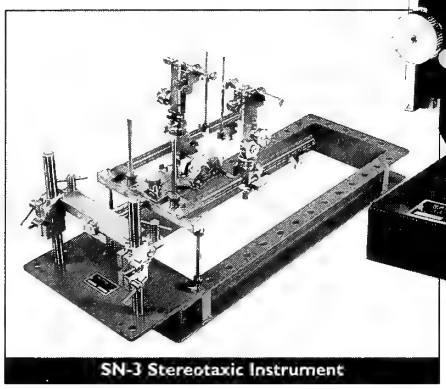
SN-3 Stereotaxic Instrument


MM-31 Miniature Micromanipulator

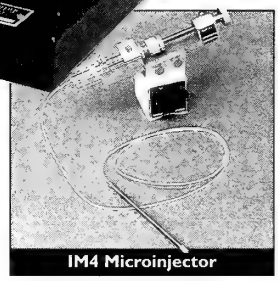
IM4 Microinjector


US-1 Miniature Stand

Shown here is a small selection of instruments from the extensive Narishige range.


Remote Control Hydraulic Micromanipulator

Narishige are pleased to announce that repair facilities have been opened in Europe and the USA.

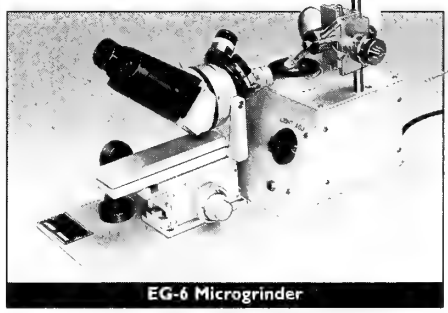
EG-6 Microgrinder

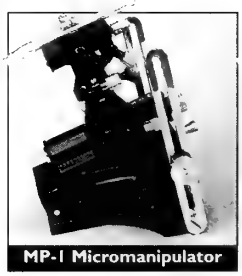
MP-1 Micromanipulator

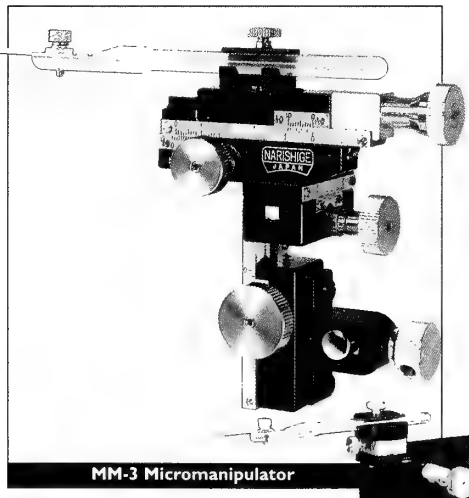
MM-3 Micromanipulator

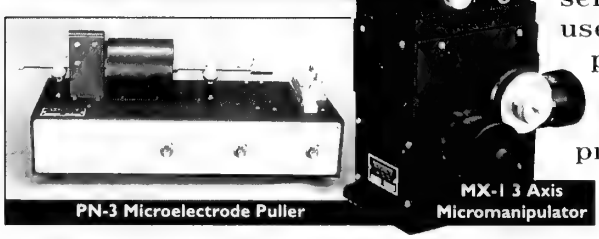
PN-3 Microelectrode Puller

MX-1 3 Axis Micromanipulator

This enables us to provide an improved service to the many users of our quality products throughout the world, including the upgrading of previous types of water filled hydraulic micromanipulators.

PE-2 Microelectrode Puller

Please contact us for more information.

REPAIRS, AFTER SALES SERVICE AND TECHNICAL SUPPORT

JAPAN Narishige Scientific Instrument Laboratory
9-28 Kasuya 4-Chrome, Setagaya-Ku, Tokyo 157, Japan. Tel: +81 (0) 3 3308 8233 Fax: +81 (0) 3 3308 2005

EUROPE Narishige International London Branch
Unit 7 Willow Business Park, Willow Way, London SE26 4QP U.K. Tel: +44 (0) 81 699 9696 Fax: +44 (0) 81 291 9678

U.S.A. U.S. Narishige International Inc
404 Glen Cove Avenue, Sea Cliff, New York 11579 U.S.A. Tel: +1 (516) 759 6167 Fax: +1 (516) 759 6138

NARISHIGE JAPAN

(*Contents continued from back cover*)

Experimental Animal

Kiguchi, K., M. Shimoda: The sweet potato hornworm, *Agrius convolvuli*, as a new experimental insect: Continuous rearing using artificial diets 143

Announcements 161

Instructions to Authors 163

ZOOLOGICAL SCIENCE

VOLUME 11 NUMBER 1 FEBRUARY 1994

CONTENTS

Obituary 1

REVIEWS

Hanke, W., W. Kloas: Hormonal regulation of osmo-mineral content in amphibia 5

Nässel, D. R., E. Bayraktaroglu, H. Dircksen: Neuropeptides in neurosecretory and efferent neural systems of insect thoracic and abdominal ganglia 15

ORIGINAL PAPERS

Physiology

Takahashi, T., O. Matsushima, F. Morishita, M. Fujimoto, T. Ikeda, H. Minakata, K. Nomoto: A Myomodulin-CARP-related peptide isolated from a polychaete annelid *Perinereis vancaurica* 33

Sugimoto, M., T. Kawamura, R. Fujii: Changes in the responsiveness of melanophores to electrical nervous stimulation after prolonged background adaptation in the medaka, *Oryzias latipes* 39

Wilder, M. N., T. Okumura, Y. Suzuki, N. Fusetani, K. Aida: Vitellogenin production induced by eyestalk ablaton in juvenile giant freshwater prawn *Macrobrachium rosenbergii* and trial methyl farnesoate administration 45

Cell and Molecular Biology

Meyer-Rochow V. B., Y. Ishihara, J. R. Ingram: Cytochemical and Histological details of muscle fibers in the southern smelt *Retropinna retropinna* (Pisces; Galaxioidei) 55

Genetics

Patil, J. G., V. Wong, H. W. Khoo: Assessment of pMTL construct for detection *in vivo* of luciferase expression and fate of the transgene in the zebrafish, *Brachydanio rerio* 63

Developmental Biology

Furukawa, T., Y. Maeda: K252a, a potent inhibitor of protein kinases, promotes the transition of *Dictyostelium* cells from growth to differentiation 69

Iwamatsu, T., S. Nakashima, K. Onitake, A. Matsuhisa, Y. Nagahama: Regional differences in granulosa cells of prevulatory medaka follicles 77

Kanno, Y., S. Koike, T. Noumura: Immunohistochemical localizations of epidermal growth factor in the developing rat gonads 83

Satoh, Y., T. Shimizu, Y. Sendai, H. Kinoh, N. Suzuki: Nucleotide sequence of the proton ATPase beta-subunit homologue of the sea urchin *Hemicentrotus pulcherrimus* (RAPID COMMUNICATION) 153

Kanbayashi, H., Y. Fujita, K. Yamasu, T. Suyemitsu, K. Ishihara: Local change of an exogastrula-inducing peptide (EGIP) in the pluteus larva of the sea urchin *Anthocidaris crassispina* (RAPID COMMUNICATION) 157

Reproductive Biology

Hosokawa, K., Y. D. Noda: The acrosome reaction and fertilization in the bivalve, *Laternula limicola*, in reference to sperm penetration from the posterior region of the mid-piece 89

Endocrinology

Iga, C., I. Koshimizu, S. Takahashi, Y. Kobayashi: Experimental manipulation of pituitary hemorrhage induced by intraperitoneal injection of a hypertonic solution in mice 101

Yamashita, K., S. Kikuyama: Immunohistochemical study of ontogeny of pituitary prolactin and growth hormone cells in *Xenopus laevis* (RAPID COMMUNICATION) 149

Asahina, M., H. Fugo, S. Takeda: Ecdysteroid synthesis in dissociated cells of the prothoracic gland of the silkworm, *Bombyx mori* 107

Behavior Biology

Naruse, M., T. Oishi: Effects of light and food as zeitgebers on locomotor activity rhythms in the loach, *Misgurnus anguillicaudatus* 113

Suzuki, H., T. Sekiguchi, A.. Yamada, A. Mizukami: Sensory preconditioning in the terrestrial mollusk, *Limax flavus* 121

Environmental Biology and Ecology

Ohdachi, S.: Growth, metamorphosis and gape-limited cannibalism and predation on tadpoles in larvae of salamanders *Hynobius retardatus* 127

Lawrence J. M., M. Bryne: Allocation of resources to body components in *Heliocidaris erythrogramma* and *Heliocidaris tuberculata* (Echinodermata: Echinoidea) 133

Systematics and Taxonomy

Ishikawa, K.: Two new species of the genus *Holaspulus* (Acarina: Gamasida: Parholaspidae) from the Ryukyu Islands, Japan 139

(*Contents continued on inside back cover*)

INDEXED IN:
Current Contents/LS and AB & ES,
Science Citation Index,
ISI Online Database,
CABS Database, INFOBIB

Issued on February 15
Front cover designed by Saori Yasutomi
Printed by Daigaku Letterpress Co., Ltd.,
Hiroshima, Japan

ISSN 0289-0003

An International Journal

ZOOLOGICAL SCIENCE

Vol. 11 No.2

April 1994

PHYSIOLOGY
CELL and MOLECULAR BIOLOGY
GENETICS
IMMUNOLOGY
BIOCHEMISTRY
DEVELOPMENTAL BIOLOGY
REPRODUCTIVE BIOLOGY
ENDOCRINOLOGY
BEHAVIOR BIOLOGY
ENVIRONMENTAL BIOLOGY and ECOLOGY
SYSTEMATICS and TAXONOMY

published by Zoological Society of Japan
distributed by Business Center for Academic Societies Japan
VSP, Zeist, The Netherlands

ZOOLOGICAL SCIENCE

The Official Journal of the Zoological Society of Japan

The Zoological Society of Japan:
Toshin-building, Hongo 2–27–2, Bunkyo-ku,
Tokyo 113, Japan. Phone 03-3814–5461
Fax 03-3814-5352
Officers:
President: Hideo Mohri (Chiba)
Secretary: Takao Mori (Tokyo)
Treasurer: Makoto Okuno (Tokyo)
Librarian: Masatsune Takeda (Tokyo)
Auditors: Hideshi Kobayashi (Tokyo)
Hiromichi Morita (Fukuoka)

ZOOLOGICAL SCIENCE is devoted to publication of original articles, reviews and rapid communications in the broad field of Zoology. The journal was founded in 1984 as a result of unification of Zoological Magazine (1888–1983) and Annotationes Zoologicae Jasponenses (1897–1983), the former official journals of the Zoological Soceity of Japan. An annual volume consists of six regular numbers and one supplement (abstracts of papers presented at the annual meeting of the Zoological Society of Japan) of more than 850 pages. The regular numbers appear bimonthly.

MANUSCRIPTS OFFERED FOR CONSIDERATION AND CORRESPONDENCE CONCERNING EDITORIAL MATTERS should be sent to:

Dr. Tsuneo Yamaguchi, Editor-in-Chief, Zoological Science, Department of Biology, Faculty of Science, Okayama University, Okayama 700, Japan, in accordance with the instructions to authors which appear in the first issue of each volume. Copies of instructions to authors will be sent upon request.

SUBSCRIPTIONS. ZOOLOGICAL SCIENCE is distributed free of charge to the members, both domestic and foreign, of the Zoological Society of Japan.To non-member subscribers within Japan, it is distributed by Business Center for Academic Societies Japan, 5–16–9 Honkomagome, Bunkyo-ku, Tokyo 113. Subscriptions outside Japan should be ordered from the sole agent, VSP, Godfried van Seystlaan 47, 3703 BR Zeist (postal address: P. O. Box 346, 3700 AH Zeist), The Netherlands. Subscription rates will be provided on request to these agents. New subscriptions and renewals begin with the first issue of the current volume.

[Publication of Zoological Science has been supported in part by a Grant-in-Aid for Publication of Scientific Research Results from the Ministry of Education, Science and Culture, Japan.]

ZOOLOGICAL SCIENCE 11: 167–174 (1994)

REVIEW

Insulin-like Growth Factors: Growth, Transgenes and Imprinting

ANDREW WARD[1], PÄR BIERKE[2,3], EVA PETTERSSON[2], WILHELM ENGSTRÖM[2]*

[1]*Cancer Research Campaign Growth Factors, Department of Zoology, University of Oxford, South Parks Road, Oxford OX13PS, UK and* [2]*Department of Pathology Faculty of Veterinary Medicine Swedish University of Agricultural Sciences S-750 07 Uppsala, Sweden* [3]*National Defenee Research Institute, S-90182 Umeå Sweden*

I BACKGROUND

The idea of integrating stable gene mutations into the germ line has long fascinated developmental biologists. Experimental gene modifications that influence subsequent developmental patterns have therefore been at the top of the list of priorities. The field of experimental embryology took off in the early 1960s when Krystof Tarkowski [86] and Beatrice Mintz [59] succeeded in fusing genetically distinct 8-cell embryos into stable chimaeras. In 1968 Richard Gardner [28] was able to show that by moving the inner cell mass from one embryo to another a chimaera could be formed. But it was not until 1974 when Jaenisch and Mintz [41] could report the first deliberate genetic modification of the mouse embryo. By infecting embryos at the blastocyst stage with SV40-virus they were able to demonstrate a stable integration of viral DNA in the live born progeny. This breakthrough was rapidly followed by Moloney murine leukemia virus mediated germ line transfer of foreign nucleic acid sequences [42]. Since that time the field has exploded, it appears pertinent to briefly discuss some key experimental landmarks during the last 20-year period.

It was in 1980 [30] that the pronuclear microinjection technique was devised and used to demonstrate the possibility of inserting foreign DNA from almost any source into the murine embryo. This technique can be applied to almost any animal species. The next important step forward was the demonstration that integrated foreign DNA can also be expressed. In 1981 Palmiter *et al.* [64] were able to ligate the 5′ regulatory sequence of the murine metallothionein (MT1) gene with the core sequence of the herpes virus thymidine kinase gene. This transgene was injected into pronuclei and properly integrated. In the adult progeny, the herpes thymidine kinase gene was expressed in a pattern as expected from the MT1 gene with abundant expression in kidney and liver. Furthermore, it was concluded from this and subsequent studies that the actual integration site plays an inferior role in determining the level of expression. It is rather the cis-acting regulatory sequences in and adjacent to genes that determine spatial and temporal transcription patterns [32, 63]. There are however important exceptions to this rule. In the case of the beta globin gene the absence of key enhancer elements makes it relatively more dependent on the integration site for adequate expression [13].

This implies that the interplay between structural regulatory elements is imperative in determining stage- and tissue-specific expression. If an isolated promoter sequence is fused with a heterologous coding region and integrated in the germ line, the expression pattern will in many cases differ from that of an integrated genomic clone containing the regulatory and structural elements in intact order. There are also transacting factors that affect expression of integrated foreign genes. The presence or absence of such transactivators indeed differ between species. When a human gene is integrated into transgenic mice, the transgene may therefore be expressed in organs that do normally not express the murine counterpart, but which are sites of expression in man.

Foreign genes normally integrate as head to tail concatamers into one unique site in the mouse genome. However at this single site a considerable number (from one to 50 copies) of transgenes can be integrated. There is ample evidence that this large scale integration is not always a straight forward process. It predisposes delays and recombinations leading to mosaic patterns. It can also lead to strange structural alterations of the mouse host genome including deletions, duplications, translocations and interspersion of islands of genomic DNA within the transgene sequences. The disruption of endogenous gene function upon transgene integration is also an alarmingly frequent event [58]

II METHODOLOGY

1. Pronuclear injection

Broadly, two approaches are currently employed in generating transgenic mice, leading to either over-expression or targeted alteration of the gene of interest. In the first approach, exogenous copies of the gene are incorporated into

Received February 10, 1994
* Reprint requests should be addressed to Dr. W. Engström.

the genome with the aim of elevating its level of expression *in vivo*. This is usually achieved by injecting fertilised eggs, collected approximately 12 hr after mating has taken place, with linear cloned DNA fragments [39]. The injected embryos are then introduced into the uterus of receptive, pseudopregnant females, so that normal development can proceed. Liveborn mice are tested for the presence of the transgene by assaying biopsy material using DNA (Southern) blotting or polymerase chain reaction (PCR) techniques. Although the proportion of transgenic offspring which result is very much dependant on the nature of the injected DNA construct, frequencies of transgenesis over 20% can be achieved, representing one major advantage of this approach. This is offset against the principle disadvantage of this scheme, in that incorporation of the transgene into the genome occurs at essentially randomly determined positions. Since expression of the transgene can be influenced by sequences surrouding the integration site (so called position effects) and since transgene insertion can disrupt the function of a resident gene, the phenotype associated with any given DNA construct must be qualified by studying lines of transgenic mice representing at least two independent integration events.

2. Embryonic stem cells

In the second approach to producing transgenic mice, more recently developed technology allows the targeted alteration of specific endogenous genes by homologous recombination in embryonic stem (ES) cells. ES cells are derived from blastocyst embryos and can be maintained in culture for many generations before being microinjected into host blastocysts and returned to pseudopregnant females. Subsequently, they can colonise all tissues of the resulting animals, which develop to form chimeric mice. Chimeric animals in which the ES cells have given rise to germ cells can be bred to produce transgenic offspring which are entirely ES cell derived [40, 43]. Compared with the one cell embryos used for pronuclear microinjection, ES cells represent a more abundant source of starting material which can be manipulated *in vitro* over a much longer time period, greatly increasing the scope for the manipulation of the genome. This is essential to the success of the gene targeting scheme. Gene targeting requires a construct comprising sequences of the target gene, bearing a mutation which will alter or ablate its function, together with at least one selectable marker gene (such as neo^r, which confers resistance to the drug G418). Often the neo^r gene is positioned within the construct such that it disrupts or replaces part of the coding region of the target gene. This construct can be introduced rapidly into many thousands of ES cells by electroporation. These cells are subsequently grown in the presence of G418 to identify resistant colonies which represent those cells in which the targeting construct was stably incorporated into the genome. The sequences of the target gene which flank the neo^r gene provide regions of homology which allows recombination to take place such that the cloned DNA can replace the target gene following its introduction into embryonic stem cells. However, since homologous recombination events are usually much less frequent than random integration events, the G418 resistant ES cell colonies must be screened to establish which should be used to generate chimeras. This screening process is one of the rate limiting steps of this transgenic route since the homologous recombination events typically represent less than 0.1% of all stable transformants. However, this figure is constantly being improved with the development of methods to enrich for homologous recombination over random integration. These improvements include the use of a second selectable marker which must be lost from the targeting vector during homologous recombination to allow cell survival [53] and the use of DNA within the targeting construct which derives from the same mouse strain as the host ES cells [87, 88].

3. Strategies for increased expression

Perhaps the crudest overexpression strategy relies upon the use of an entire genomic sequence which contains the full coding sequence with cognate upstream regulatory elements as the transgene. This approach has had a practical advantage in compensating for defects in mutant animals lacking a specific gene. A classical experiment succeeded in restoring fertility in hypogonadal mice by introducing the gonadotropin releasing factor gene [55]. In addition to its simplicity, this method can be advantageous where it is important to reproduce the expression patterns of the gene of interest. For instance following cloning of the sex-determining gene Sry, its own regulatory sequences were relied upon to create transgenic mice which were XX males [46]. In this case accumulated molecular and genetic evidence indicated that the testis determining gene was normally expressed transiently in specific cells in the developing gonad [47].

A more widely appreciated approach is based upon the fusion of a coding sequence with a well characterized promoter sequence that operates in a multitude of tissues. Commonly used promoters that induce widespread expression are the actin, H2 and SV40 promoters. Other promoter sequences induce expression in a more limited spectrum of cells and tissues. The mouse Mammary Tumour Virus Long Terminal Repeat (MMTV-LTR) operates mainly in secretory epithelial cells, and as a result transgenes containing this promoter sequence are expressed specifically in this cell type. When the MMTV-LTR was fused with the Granulocyte Macrophage Colony Stimulating Factor gene a strange subset of phenotypes were observed amongst the offspring [48]. Other promoters that allow cell specific expression include the Immunoglobulin promoter. When this sequence was fused with the interleukin-6 (IL-6) gene, mice harbouring this transgene developed plasmocytosis, with IL-6 expressing B-cells circulating throughout the body giving rise to high circulating levels of IL-6 protein [82].

The options can be further narrowed by using tissue specific promoters. The first of its kind to be utilized for this purpose was the rat insulin promoter (RIP) which is only

active in pancreatic beta cells. By fusing RIP with a nerve growth factor (NGF) coding sequence a unique pattern of hyperinnervation of the islets of Langerhans was achieved [20]. The great advantage of this approach is that the phenotypic effects on a single organ is enabled. Now a plethora of organ specific promoters are used for the purpose of site directed expression of transgenes. The bovine keratin 10 promoter directs the expression of transgenes to the supra basal layer of the skin and to the forestomach [2]. Gene expression can be directed to the mammary gland by using either the Whey Acidic Protein (WAP) promoter [35] or the beta lactoglobulin promoter [91]. The latter promoter limits expression to the secretory epithelium of the mammary gland. Moreover, induction of beta lactoglobulin expression coincides with that of beta casein in the tissue, indicating that the pattern of expression is determined by the differentiated state of the mammary cells [35, 91]. Using this promoter, protein products of the transgene can be secreted into milk and form up to 10% of the total milk protein or 30% of whey protein [1]. To achieve kidney specific expression, much attention has been devoted to the three murine renin genes Ren-IC, Ren-1d and Ren-2. However, the three renin genes exhibit distinct expression profiles at a number of extra renal sites [27, 75, 76].

III TRANGENIC STUDIES INVOLVING INSULIN AND THE INSULIN-LIKE GROWTH FACTORS

Insulin and the insulin-like growth factors (IGF-I and IGF-II) are structurally related and share affinities for the same set of trans-membrane receptors (reviewed in [72]). Each factor exhibits a preference for the appropriately named receptor (insulin, IGF type 1 and IGF type 2) but can interact with the others. This family of growth factors and receptors represent probably the most intensively studied using mouse transgenesis; insulin, IGF-I and IGF-II have all been analysed using overexpression strategies and IGF-I, IGF-II and the IGF type 1 receptor have each been the subject of gene targeting experiments to disrupt their function in mice. These experiments have revealed much about the *in vivo* functions of these factors and collectively they amply demonstrate the effectiveness of applying transgenic techniques to the analysis of mammalian growth factors.

1. Insulin

In several reports a common strategy has been adopted to elevate insulin expression at the natural sites of synthesis [11, 26, 54, 74]. By introducing copies of the human insulin gene into mice it was possible to distinguish mRNA and protein of transgene and endogenous origin while harnessing the cognate promoter to ensure expression was obtained in the pancreatic islets. The efficacy of this approach is clear since in all cases transgene expression was restricted to the pancreas and in one case, by comparing various lengths of promoter sequence, it was established that as little as 168 bp upstream of the transcript initiation site are sufficient to ensure correct tissue-specificity of expression from the insulin gene promoter [26]. In mice with detectable levels of human insulin, but no significant increase in total serum insulin levels, appropriate regulation of the human insulin transgene was established by challenging mice with glucose, amino acids or the hypoglycemic drug tolbutamide [11, 74]. In these cases normal pancreatic histology was reported and there were no obvious effects on growth. More recently it was shown that higher than normal serum insulin levels can result from similar transgenic experiments, consequently these mice are hyperglycemic in response to a glucose challenge and their normal fasting glucose levels suggest some insulin tolerance [54]. To date, however, transgenic experiments have not suggested any direct effects on growth *in vivo*, although insulin can promote growth *in vitro* [79] and is a routine addition in culture media. While it may be that insulin has no significant effect on growth *in vivo* further experiments, perhaps involving the targeted mutation of the insulin gene or its overexpression at ectopic sites and during earlier developmental stages, might be more revealing in this context.

2. IGF-I

A key role of IGF-I, in mediating the effects of growth hormone (GH) on postnatal growth, was proposed over ten years ago when adminstration of purified IGF-I was shown to stimulate growth in hypophysectomised rats [70]. This relationship was subsequently bome-out by experiments in which GH or IGF-I over-expression was achieved in transgenic mice. When rat or human GH genes were placed under the control of the mouse metallothionein I (mTM-I) gene promoter serum GH levels could be raised several hundred-fold, typically resulting in a 1.5-fold increase in adult body weight [64, 65]. Growth enhancement was detectable from about 3 weeks of age and was associated with elevated levels of circulating IGF-I. The rise in serum IGF-I was shown to preceed the acceleration in growth by about one week [56]. Although these data are consistent with the proposed role for IGF-I, the findings of Stewart *et al.* [80] suggest the increased circulating IGF-I might not be necessary to mediate GH action. These workers expressed human GH in mice using a mammary tumour virus LTR and these transgenic mice displayed supernormal growth kinetics similar to those described previously but did not always have high serum IGF-I levels. They suggest the extra growth results from direct GH action through the somatogenic and PRL receptors. Alternatively, stimulation of IGF-I production local to its sites of action might be the important factor as this could occur independently of changes in serum levels. In fact a combination fo direct and IGF-I mediated mechanisms of GH action remains likely and is consistent with the results of IGF-I over-expression in transgenic mice [55]. Although only one of two lines of mice established using an mMT-I/hIGF-I construct were found to express the introduced gene these mice were 1.3 fold larger than controls, which is within the range of the effect obtained with mMT-I/GH constructs.

However, the phenotype of the IGF-I transgenic mice differed from that of GH trangenics, notably in the range of organs which were enlarged or exhibited histopathological changes, and that the onset of the effect on live weights was delayed until at least six weeks after birth [7, 16, 57, 66].

Mice lacking a functional IGF-I gene have recently been created by gene targeting [3, 52]. The homozygous mutants were approximately 60% normal size at birth and their survival into adulthood varied with genetic background. Postnatally, the surviving animals continued to grow slowly, eventually attaning only about 30% the weight of normal littermates. These experiments confirm unequivocally that IGF-I has a significant effect on growth during embryogenesis, before any effects of GH are manifest.

3. IGF-II

In contrast with studies involving IGF-I, attempts to produce mice over-expressing IGF-II using promoters with relatively broad fields of activity have been largely unsuccessful. At least three groups of researchers found that, at best, only low levels of transgene expression were obtained when using promoters from the mMT-I (expression reported in 2/17 transgenic lines (63)), rat IGF-II (0/4; (49)) and human H-2k (0/8; (21)) genes. In all of these cases no significant effects on growth were reported. This can be attributed to an embryonic lethal effect which is thought likely to result from the presence of excess IGF-II, perhaps at critical sites and/or periods during development. Recent genetic evidence supports this theory as mice lacking the type 2 IGF receptor (T^{hp} mutant mice) usually die at mid-gestation, but this phenotype is rescued when they also lack a functional *Igf-2* gene [25]. The principle role for the type 2 receptor seems to be one of targeting its ligands (IGF-II and mannose-6-phosphate) for lysosomal degradation, and not mitogenic signalling. Thus, the lethality observed in T^{hp} mice is seen as an absence of this important regulator of IGF-II action.

Very recently the problems associated with producing IGF-II transgenic mice were circumvented by using a keratin gene promoter which had previously provided tissue restricted expression of a *h-ras* transgene [2]. IGF-II transgene expression was seen in all of the transgenic lines established using this promotor (Ward *et al.*, unpublished). These mice exhibited dramatic local effects on growth, consistent both with the paracrine/autocrine mode of action suggested for IGF-II by *in situ* expression studies (reviewed in [90]) and with proposed roles for IGF-II in growth related diseases, including Beckwith-Wiedemann syndrome and certain cancers [51, 73, 89]. These over-expression experiments complement studies of mice in which the IGF-II gene was disrupted by gene targeting.

Growth of IGF-II null mice was compromised during development, but not postnatally as recorded for mice without an intact IGF-I gene, and their size at birth was about 60% that of their normal littermates. Further differences between IGF-I and IGF-II null mice demonstrated that IGF-II acts at least two embryonic days earlier than IGF-I and that only IGF-II has an effect on placental growth [3, 73, 89]. The type 1 receptor was also mutated as part of this spectacular series of experiments and IGF-I-R null mice were more severely dwarfed at birth than either of those lacking individual functioning IGF genes. The availability of these three types of gene targeted mice, together with T^{hp} mutants, allowed the breeding of various double mutants [3, 25, 52]; some of their characteristics are summarized in Table 1. Comparison of all the resulting single and double mutants yeilded several important conclusions, including that IGF-I acts solely through the type 1 receptor (since the phenotypes of mice null for either *Igf-1r* or *Igf-1* and *Igf-1r* were indistinguishable) while IGF-II acts through both the type 1 receptor and at least one other (since similar phenotypes were

Table 1. Gross effects on growth of mice null for IGF and/or IGF receptor functions

Nullitype	Birth weight (% normal)	Placenta	Onset	Notes
Igf-1	60%	100%	E13.5	Survival to adulthood varies with genetic background. Some distortion in proportionality of features. Delays in ossification.
Igf-2	60%	75%	E11	Proportionally dwarfed. Delays in ossification.
Igf1r or Igf-1/Igf1r	45%	100%	E11	Neonatal death (respiratory failure). Marked hypoplasia in muscle and skin. Extended delays in ossification.
Igf1r/Igf-2 Igf-1/Igfr-2	30%	75%	E11	Neonatal death (respiratory failure). Marked hypoplasia in muscle and skin. Extended delays in ossification.
Igf2r	—	—	—	Mid-gestational lethality.
Igf-2/Igf2r	60%	75%	—	Neonatal lethality.

These results are implicit and all quantities are approximate. Data from (3, 14, 15, 25, 52). Note that Igf-2 results were obtained with heterozygous mutations, following paternal transmission of the null allele and the intact maternal allele is known to be expressed in some tissues.

displayed by mice null for either *Igf-1* and *Igf-2* or *Igf-1r* and *Igf-2* and in both cases these phenotypes were more severe than that of *Igf-1r* mutants). The identity of the second IGF-II receptor remains ambiguous, although it could be the insulin receptor, and this receptor was deemed the sole mediator of IGF-II action on placental growth.

IV TRANSCRIPTION FACTORS

One alternative approach to studying growth factor production *in vivo*, involves manipulation of relevant transcription factor genes and introducing them into transgenic animals. It has been suggested that many growth factor defects arise as a consequence of a defect in transcriptional regulation rather than mutations in the growth factor gene itself. This is particularly important in embryogenesis, and it was recently shown that deregulation of the pax-2 gene had a dramatic impact on kidney development [19]. This gene belongs to a family of transcription factors that display organ and stage specific activity. *pax-2* is expressed in the embryonic kidney after mesenchymal induction, in the ureter epithelium and early epithelial structures [17]. Furthermore, its expression is repressed upon terminal differentiation but persists at increased levels in Wilms tumours [18]. In this respect it mirrors the transcriptional activity of the IGF II gene which makes studies of persistent *pax-2* gene expression in transgenic animals particularly interesting. Deregulated *pax-2* expression in transgenic mice gave rise to histologically abnormal and dysfunctional renal epithelium reminiscent of the congenital nephrotic syndrome. The interrelationship between *pax-2* and IGF II and their combined detrimental impact on development however remains to be further clarified.

It has been shown that both the IGF-I and IGF-II genes contain AP-1 binding sites [12, 45]. Therefore studies which aim at altering the availability of Fos and Jun proteins ought to influence the expression of the IGF genes and would be of particular interest from a developmental point of view. When both copies of *c-jun* were inactivated by homologous recombination, perfectly viable ES-cells were obtained [37]. When these were integrated into the germ line it was found that heterozygous mutant mice were normal, but embryos lacking *c-jun*, died at mid or late gestation, and displayed impaired hepatogenesis, altered fetal liver erythropoesis and generalized oedema. Moreover, it was found that *c-jun* -/- ES cells were capable of participation in development of all somatic cells in chimaeras except liver cells [38]. An example of the opposite approach, namely an overexpression of the AP-1 component fos yielded an unexpected series of results. Expression of *c-fos* has for more than a decade been considered an early step in the chain of events between growth stimulation and onset of DNA-synthesis. However, embryonic development is a fine balance between proliferation, differentiation and programmed cell death. By studying *fos*-lacZ transgenic mice it was possible to demonstrate that continuous *fos* expression begins hours or days before the morphological demise of a condemned cell. Expression, therefore appears to be a hall mark of terminal differentiation and a harbinger of death [77]. These examples show that alteration of transcription factors expression lead to dramatic biological effects in transgenic animals. Therefore they should be taken into account when growth factors are to be considered as prime candidates for developmental processes in transgenic animals.

V GROWTH FACTORS, TRANSGENESIS AND GENOMIC IMPRINTING

One surprising outcome of the IGF-II gene knock-out experiments was the finding that the growth deficient phenotype occurred in heterozygous mutant mice when the mutation was inherited from a male but not from a female [15]. This led to the discovery that IGF-II is subject to genomic imprinting, with only the allele inherited from the male being expressed in most tissues [14]. The phenomenon of genomic imprinting was known before this, since nuclear transplantation experiments had demonstrated the nonequivalence of the male and female genetic contribution in mammalian development [84, 85], but *Igf-2* was the first gene known to be influenced by this peculiar form of regulation. Soon afterwards the *Igf-2r* gene was also shown to be imprinted after it was mapped within deletions of chromosome 17 harboured by the T^{hp} and T^{lub2} mutants [4]. In this case, in accord with the lethality associated with female but not male transmission of the T^{hp} and T^{lub2} mutations, the maternal allele was found to be active.

Opposite imprinting of the *Igf-2* and *Igf-2r* genes immediately brought to life an hypothesis of parent-offspring conflict predicted in plant and animal species in which the growth of progeny is dependent on a maternal nutient supply (e.g. the mammalian placenta) and in which multiple paternity is likely among offspring of individual females [45]. Under these circumstances, and given that larger offspring are the most well equipped to survive, the interest of the father is best served if each of his progeny are as large and strong as possible. As there is a chance that he may be usurped the father makes the most of each opportunity to reproduce although this might involve an increased burden on the mother. Obviously, she is guaranteed to be equally related to each of her offspring, irrespective of any changes in mate choice and it follows that it is in the mothers interest to distribute resources evenly among her unborn young whether within a litter or in conserving the capacity to produce later litters. Since this parental conflict of interest requires that a "choice" is made regarding growth during embryonic life, Haig and Westoby [34] suggested that this would be reflected at the molecular level. That *Igf-2* and the *Igf-2r* can be viewed as molecular weapons in this conflict is entirely in keeping with their antagonistic effects on growth and, of course, that it is respectively the paternally- and maternally-derived copies of each that are expressed [33].

Genomic imprinting of human IGF-II was recently con-

firmed [29] and is implicated in the ontogeny of the fetal overgrowth disease Beckwith Wiedemann syndrome [36]. Furthermore, it has been suggested that mis-regulation of imprinted genes might be important in a range of neoplastic diseases since, for instance, as only one allele is normally expressed then a single mutation would effectively result in a nullisomy. Conversely, activation of the normally silent allele would result in the gene product being overrepresented [23, 44]. Indeed relaxation of imprinting was recently demonstrated for IGF-II in a proportion of Wilms' tumours [60, 67].

There is one further intriguing link between IGF-II and imprinting in that the *H19* gene, located only about 80 kb from IGF-II [92], is also imprinted with the maternally derived copy being active in mouse and man [6, 93]. This gene has no ascribed function *in vivo* and might exert its effect as an RNA product since it does not encode an open reading frame [8]. However, the influence of *H19* on development is evidenced by transgenic experiments in which overexpression of intact H19 genes resulted in mid-gestational lethality [10]. It has been suggested that the regulation of IGF-II and H19 might be linked in some fashion since these two oppositely imprinted genes are such near neighbours [5, 83, 92]. The perceived importance of genomic imprinting in both normal development and growth related disease has fuelled an intense interest in achieving an understanding of the mechanism which underlies this phenomenon. An epigenetic signal which can be appropriately modified during passage of genes through either the male or female germline is required to establish and maintain allele specific expression of imprinted genes. Studies of the *Igf-2* [69], *Igf-2r* [81] and H19 [5, 24] genes indicate that DNA methylation might be involved in this process, and this was recently confirmed through the discovery that all three loci were lost in mice with a methyltransferase gene deficiency [50]. However, the race towards a full understanding is far from over. Early evidence suggests that not all of the signals required for properly imprinted expression have yet been discovered as only a minor proportion of *Igf-2* [49] and *H19* [5] transgenes behave in accord with their parent of origin, but it is without doubt that transgenesis will play a key role in unravelling this biological conundrum.

ACKNOWLEDGMENTS

The authors have been generously supported by the Cancer Research Campaign of Great Britain as well as by Cancerfonden and Barncancerfonden, Sweden.

REFERENCES

1 Archibald AL, McClenaghan M, Hornsey V, Simons JP, Clark AJ (1990) High levels of expression of biologically active human alpha1-antitrypsin in the milk of transgenic mice. Proc Natl Acad Sci USA 87: 5178–5182

2 Baillcul B, Surani MA, White S, Barton SC, Brown K, Blessing M, Jorcano J, Balmain A (1990) Skin hyperkeratosis and papilloma formationin transgenic mice expressing a ras oncogene from a suprabasal keratin promoter. Cell 62: 697–728

3 Baker J, Liu J, Robertson LJ, Efstriatiadis A (1993) Role of insulin-like growth factor type 2 receptor in embryonic and postnatal growth. Cell 75: 73–82

4 Barlow DP, Stoger R, Herrmann BG, Saito K, Schweifer N (1991) The mouse insulin-like growth factor type-2 receptor is imprinted and closely linked to the Tme locus. Nature 349: 84–87

5 Bartolomei MS, Webber AL, Brunkow ME, Tilghman SM (1993) Epigenetic mechanisms underlying the imprinting of the mouse H19 gene. Genes Dev 7: 166–167

6 Bartolomei MS, Zemel S, Tilghman SM (1991) Parental imprinting of the mouse H19 gene. Nature 351: 153–155

7 Behringer RR, Lewin TM, Quaife CJ, Palmiter RD, Brinster RL, d'ErcoLe AJ (1990) Expression of insulin-like growth factor I stimulates normal somatic growth in growth hormone-deficient transgenic mice. Endocrinology 127: 1033–1040

8 Brannan CI, Dees EC, Ingram RS, Tilghman SM (1990) The product of the H19 gene may function as an RNA. Mol Cell Biol 10: 28–36

9 Brinster RL, Chen HY, Trumbauer ME, Senear AW, Warren R, Palmiter RD (1981) Somatic expression of herpes thymidine kinase in mice following injection of a fusion gene into eggs. Cell 27: 223–231

10 Brunkow ME, Tilghman SM (1991) Ectopic expression of the H19 gene in mice causes prenatal lethality. Genes Dev 5: 1092–1101

11 Bucchini D, Ripoche M-A, Stinnakre M-G, Desbois P, Lores P, Monthioux E, Absil J, Lepesant J-A, Picter R, Jami J (1986) Pancreatic expression of human insulin gene in transgenic mice. Proc Natl Acad Sci USA 83: 2511–2515

12 Caricasole A, Ward A (1993) Transactivation of mouse IGF II gene promoters by the AP-1 complex Nucl Acids Res 21: 1873–1879

13 Chada K, Magram J, Raphael K, Radice G, Lacy E, Constantini F (1985) Specific expression of foreign beta globin gene in erythroid cells of transgenic animals. Nature 314: 377–380

14 deChiara TM, Efstratiadis A, Robertson EJ (1991) Parental imprinting of the mouse insulin-like growth factor gene. Cell 64: 849–859

15 deChiara TM, Robertson EJ, Efstratiadis A (1990) A growth deficiency phenotype in heterozygous mice carrying an insulin-like growth factor II gene disrupted by targetting. Nature 345: 78–80

16 Doi T, Striker LJ, Gibson CC, Agodoa LY, Brinster RL, Striker GE (1990) Glomerular lesions in mice transgenic for growth hormone and insulin like factor-I. Am J Path 137: 541–552

17 Dressler GR, Deutsch U, Chowdbury K, Nornes HO Gruss P (1990) Pax-2, a new murine paired box containing gene and its expression in the developing secretory system. Development 109: 787–795

18 Dressler GK, Douglas EC (1992) Pax-2 is a ANA-binding protein expressed in embryonic kidney and Wilms tumour. Proc Natl Acad Sci USA 89: 1179–1183

19 Dressler GR, Wilkinsson JE, Rothenpieler UW, Patterson LT, Williams L, Westphal H (1993) Deregulation of pax-2 expression in transgenic mice generates severe kidney abnormalities. Nature 362: 65–67

20 Edwards RH, Rutter WJ, Hanahan D (1989) Directed expression of NGF to pancreatic beta cells in transgenic mice leads to selective hyperinnervation of the islets. Cell 58: 161–170

21 Ellis C (1990) Studies of the roles of IGF-II during mouse development. DPhil Thesis Oxford University

22 Engström W, Lindham S, Schofield PN, Wiedemann Beckwith Syndrome. Eur J Pediatr 147: 450–457

23 Feinberg AP (1993) Genomic imprinting and gwnw activation in cancer. Nature Genet 4: 110–113

24 Ferguson-Smith AC, Sasaki H, Cattanach BM, Surani MA (1993) Parental-origin-specific epigenetic modification of the mouse H19 gene. Nature 362: 751–755

25 Fitson A, Louvi A, Efstradiatis A, Robertson EJ (1993) Rescue of the T-associated maternal effect in mice carrying null mutations in IGF-2 and IGF-2-r, two reciprocally imprinted genes. Development 118: 731–736

26 Fromont-Racine M, Bucchini D, Madsen O, Desbois D, Linde S, Nielsen J, Saulnir C, Ripoche M-A, Jami J, Picet R (1990) Effect of 5'-flanking sequence deletions on expression of the human insulin gene in transgenic mice. Mol Endocrinol 4: 669–677

27 Fukamizu A, Seo MS, Hatae T, Yokohama M, Nomura T, Katsuki K and Murakami K (1990) Tissue specific expression of the human renin gene in transgenic mice. Biochem Biophys Comm 165: 826–832

28 Gardner RL (1968) Mouse chimaeras obtained by the injection of cells into the blastocyst. Nature 220: 596–597

29 Giannourakis N, Deal C, Paquette J, Goodyear CG, Polychronakas C (1993). Parental genomic. imprinting of the human IGF2 gene. Nature Genet 4: 98–101

30 Gordon JW, Scangos GA, Plotkin DJ, Barbariosa JA, Ruddle FH (1980) Genetic transformation of mouse embryos by microinjection of foreign DNA. Proc Natl Acad Sci USA 77: 7380–7384

31 Gordon JW, Ruddle FH (1981) Intergration and stable germ line transmission of genes injected into mouse pronuclei. Science 214: 1244–1246

32 Gordon JW (1989) Transgenic Animals. Int Rev Cytol 115: 171–229

33 Haig D, Graham C (1991) Genomic imprinting and the strange case of the insulin-like growth factor II receptor. Cell 64: 1045–1046

34 Haig D, Westoby M (1989) Parent-specific gene expression and the triploid endosperm. Am. Nat 134: 147–155

35 Harris S, McClenaghan JP, Simons JP, Ali S, Clark AJ (1990) Gene expression in the mammary gland. J Reprod Fert 88: 707–715

36 Henry B-PC, Chenbensse V, Beldjord C, Schwartz C, Utermann G, Junien C (1991) Uniparental patenal disomy in a genetic cancer disposing syndrome. Nature 351: 665–667

37 Hilberg F, Wagner EF (1992) Embryonic stem cells lacking functional c-jun. Consequences for growth and differentiation, AP-1 activity and tumorigenicity. Oncogene 7: 2371–2380

38 Hiberg F, Aguzzi A, Howells N, Wagner EF (1993) C-jun is essential for normal mouse development and hepatogenesis. Nature 365: 179–181

39 Hogan B, Constantini F, Lacy E (1986) Manipulating the mose embryo a laboratory manual. Cold Spring Harbor Press, Cold Spring Harbor, New York

40 Hooper ML (1992) Embryonal stem cells: introducing planned chances into the animal germ line. In "Modern Genetics" Harwood Academic Publishers, Switzerland

41 Jaenisch R, Mintz B (1974) Simian virus 40 DNA sequences in DNA of healthy adult mice derived from preimplantation blastocysts injected with viral DNA. Proc Natl Acad Sci USA 71: 1250–1255

42 Jaenisch R (1976) Germ line integration and mendelian transmission of the exogenous Moloney leukemia virus. Proc Natl Acad Sci USA 73: 1260–1264

43 Joyner AL (1993) Gene targeting: a practical approach. Oxford University Press, Oxford

44 Junien C (1992) Beckwith-Wiedemann syndrome, tumourigenesis and imprinting. Curr Opin Gen Dev 2: 431–438

45 Kajimoto Y, Kawamori R, Umayahara Y, Iwama N, Imano E, Morishima T, Yamasaki Y, Kamada T (1993) An AP-1 enhancer mediates TPA-induced transcriptional activation of the chicken insulin-like growth factor I gene. Biochem Biophys Res Comm 190: 767–773

46 Koopman P, Gubbay J, Collignon J, Lovell-Badge R (1989) Zfy gene expression patterns are not compatible with a primary role in mouse sex determination. Nature 342: 940–942

47 Koopman P, Gubbay J, Vivian N, Goodfellow P, Lovell-Badge R (1991) Male development of chromosomally female mice transgenic for Sry. Nature 351: 117–121

48 Lang RA, Metcalf D, Cuthbertson RA, Lyons I, Stanley E, Kelso A, Kannourakis G, Williamsson DJ, Klintworth GK, Gonda TJ, Dunn A (1987) Transgenic animals expressing a hematopoetic growth factor gene develop accumulation of macrophages, blindness and a fatal syndrome of tissue damage. Cell 51: 675–686

49 Lee JE, Tantravahi U, Boyle AL, Efstratiadis A (1993) Parental impriting of an IGF-2 transgene. Mol Rep Dev 35: 382–390

50 Li JE, Beard C, Jaenish R (1993) Role for DNA methylation in genomic impriting. Nature 366: 362–365

51 Little M, van Heyningen, Hastie N (1991) Dads and disomy and disease. Nature 351: 609–610

52 Liu J, Baker J, Perkins AS, Robertson LJ, Efstratiadis A (1993) Mice carrying null mutations of the genes encoding insulin like growth factor I and type 1 IGF receptor. Cell 75: 59–72

53 Mansour SL, Thomas KR, Capecchi M (1988) Disruption of the proto-oncogene int-2 in mouse embryo-derived stem cells: a general strategy for targeting mutations to non-selectable genes. Nature 336: 348–353

54 Marban SL, DeLoia JA, Gearhart JD (1988) Hyperinsulinemia in transgenic mice carrying multiple copies of the human insulin gene Dev Gene 10: 356–364

55 Mason AJ, Pitts SL, Nikolics K, Szonyi E, Wilcox JN, Seeberg PH, Stewart TA (1986) The hypogonadal mouse. Reproductive functions restored by gene therapy. Science 234: 1372–1378

56 Mathews LS, Hammer RE, Behringer R, d'Ercole AJ, Bell CI, Brinstcr R, Palmiter RD (1988) Growth enhancement of transgenic mice expressing human insulin-like growth factor I. Endocrinology 123: 2827–2833

57 Mathews LS, Hammer RE, Brinster RL Palmiter RD (1988) Expression of insulin-like growth factor I in transgenic mice with elevated levels of growth hormone is correlated with growth. Endocrinology 123: 433–437

58 Meisler M (1992) Insertional mutations of classical and novel genes in transgenic mice. Trends Genet 8: 341–344

59 Mintz B (1962) Formation of genotypically mosaic mouse embryos. Am Zool 2: 432 (Abstract)

60 Ogawa O, Eccles J, Szeto J, McNoe LA, Dun K, Maw MA, Smith PJ, Reeve AE (1993) Relaxation of insulin like growth factor II gene imprinting implicated in Wilms' tumour. Nature 366: 749–751

61 Ohlsson R, Nyström A, Pfeifer-Ohlsson S, Tohonen V, Hedberg F, Schofield PN, Flarn F, Ekström T (1993) *IGF2* is parentally imprinted during human embryogenesis and in the Beckwith-Wiedemann syndrome. Nature Genet 4: 95–97

62 Palmiter RD, Brinster RL (1985) Transgenic mice. Cell 41: 343–345

63 Palmiter RD, Brinster R (1986) Germ line transformation of mice. Ann Rev Genet 29: 233–236

64 Palmiter RD, Brinster RL, Hammer RE, Trumbauer MG,

Rosenfeld MG, Birnberg NC, Evans RM (1982) Dramatic growth of mice that develop from eggs microinjected with metallothionein-growth hormone fusion genes. Nature 300: 611–615

65 Palmiter RD, Norstedt G, Gelinas RE, Hammer RE, Brinster RL (1983) Meallothionein-human GH fusion genes stimulate growth of mice. Science 222: 809–814

66 Quaife CJ, Mathwes LS, Pinkel C, Hammer RE, Brinster RL, Palmiter RD (1989) Histopathology associated with elevated levels of growth hormone and insulin like growth factor I in transgenic mice. Endocrinology 124: 40–48

67 Rainier S, Johnson LA, Dobry CJ, Ping AJ, Grundy PE, and Feinberg AP (1993) Relaxation of imprinted genes in human cancer. Nature 362: 747–749

68 Robertson EJ (1991) Using embryonic stem cells to introduce mutations into the mouse germ line. Biol Reprod 44: 238–245

69 Sasaki H, Jones PA, Chaillet JR, Ferguson-Smith AC, Barton SC, Reik W, Surani MA (1992) Parental imprinting; potentially active chromatin of the repressed maternal allele of the mouse insulin-like growth factor II gene. Genes Dev 6: 1843–1856

70 Schoenle E, Zapf J, Humbel R, Froesch E (1982) IGF-I stimulates growth in hypophysectomized rats. Nature 296: 252–253

71 Schofield PN, Lindham S, Engström W (1989) Analysis of gene dosage on chromosome 11 in children suffering from Beckwith Wiedemann Syndrome. Eur J Pediatr 148: 320–324

72 Schofield PN (1992) The insulin-like growth factors structure and biological functions. Oxford University Press, Oxford

73 Schofield PN, Engström W (1992) Insulin like growth factors in human cancer. In "The insulin-like growth factors structure and biological functions" Oxford University Press, Oxford pp. 240–257

74 Selden RF, Skoskicwicz MZ, Burke Howie K, Russell PS, Goodman HM (1986) Regulation of human insulin gene expression in transgenic mice. Nature 321: 525–528

75 Sigmund CD, Jones CA, Mullins JJ, Kim U, Gross K (1990) Expression of murine cutaneous renin genes in subcutaneous connective tissue. Proc Natl Acad Sci USA 87: 7993–7997

76 Sigmund CD, Jones CA, Fabian JR, Mullins JJ, Gross KW (1990) Tissue and cell specific expression of a renin promoter reporter gene construct in transgenic mice. Biochem Biophys Comm 170: 344–350

77 Smeyne RJ, Vendrell M, Hayward M, Baker SJ, Miao GG, Schilling K, Robertson LM, Curran T, Morgan JI (1993) Continuous c-fos expression precedes programmed cell death in vivo. Nature 363: 166–169

78 Sola C, Tronik D, Dreyfus M, Babinet C, Rougeon F (1989) Renin promoter SV40 Large T antigen transgenes induce tumors irrespective of normal cellular expression of renin genes. Oncogene Res 5: 149–153

79 Spaventi R, Antica M, Pavclic K (1990) Insulin and insulin-like growth factor I (IGF-I) in early mouse embryogenesis. Development 108: 491–495

80 Stewart TA, Clift S, Pitts-Meek S, Martin L, Terrell G, Liggitt D, Oakley H (1992) An evaluation of the functions of the 22-kilodalton (kDa) the 20-kDa, and the N-terminal polypeptide forms of human growth hormone using transgenic mice. Endocrinology 130: 405–414

81 Stoger R, Kubicka P, Liu C-G, Kafri T, Razin A, Cedar H, Barlow DP (1993) Maternal-specific methylation of the imprinted mouse locus identifies the expressed locus as carrying the imprinted signal. Cell 73: 61–71

82 Suematsu S, Matsuda T, Aozasa K, Akira S, Nakano N, Ohno S, Yamamura J, Hirnao T, Kishimoto T (1989) IgG plasmocytosis in IL-6 transgenic mice. Proc Natl Acad Sci USA 86: 7547–7551

83 Surani MA (1993) Silence of the genes. Nature 366: 302–303

84 Surani MA, Kothary R, Allen ND, Singh P, Fundele R, Ferguson-Smith AC, Barton SC (1990) Genomic imprinting and development in the mouse. Development (suppl) 89–98

85 Surani MA, Reik W, Norris MI, Barton SC (1986) Influence of germline modifications of homologous chromosomes on mouse development. J Embryol Exp Morphol 97 (suppl) 123–126

86 Tarkowski K (1961) Mosue chimaeras developed from fused eggs. Nature 190: 857–860

87 te Riele H, Maandag ER, Berns M (1992) Highly efficient gene targeting in embryonic stem cells through homologous recombination. Proc Natl Acad Sci USA 89: 5128–5132

88 Van Deursen J, Wieringa B (1992) Targeting of creatin kinase M gene in embryonic stem cells uisng isogenic and nonisogenic vectors. Nucleic Acids Res 20: 3815–3820

89 Van Heyningen V, Hastie ND (1992) Wilms' tumour: reconciling genetics and biology. Trends Genet 8: 16–21

90 Ward A, Ellis CJ (1992) The insulin like growth factor genes. In "Insulin like growth factors - Structure and function" Oxford University Prees

91 Wilde CJ, Clark AJ, Kerr MA, Knight CH, McCleanaghan M, Simons P (1992) Mammary development and milk secretion in transgenic mice expressing the sheep beta lactoglobulin gene. Biochem J 284: 717–720

92 Zemel S, Bartolomei MS, Tilghman SM (1992) Physical linkage of two mammallan imprinted genes, H19 and insulin-like growth factor 2. Nature Genet 2: 61–65

93 Zhang Y, Tycko B (1992) Monoallelic expression of the human H19 gene. Nature Genet 1: 40–44

ZOOLOGICAL SCIENCE 11: 175–190 (1994)

REVIEW

Processing of Contrast Signals in the Insect Ocellar System

MAKOTO MIZUNAMI

Laboratory of Neuro-Cybernetics, Research Institute for Electronic Science, Hokkaido University, Sapporo 060, Japan

INTRODUCTION

Most visual systems are designed to analyze space, and each array of their photoreceptors encodes light intensity at its narrow receptive field directed at different parts of the surrounding environment. The intensity signals are then converted into temporal and spatial contrast signals, i.e., the ratio of changes in light intensity in time and space, as a necessary pre-processing for detection of visual images. Indeed, all biologically significant visual information, such as movement, shape, and color of objects can be extracted from temporal and spatial contrasts but not directly from absolute light intensities. Although neural mechanisms for detecting spatial contrast are well examined, as reviewed by Laughlin [41], neural mechanisms for detecting temporal contrast are not well understood. This is mainly because the mechanisms for detecting temporal contrast signals are incorporated into complicated neural mechanisms for detecting more specific visual features such as spatial and color contrasts and movement, thus, it is almost impossible to separate neural circuits for detecting temporal contrast signals from those subserving advanced visual functions.

Insect ocelli are simple photoreceptive organs incapable of detecting shape, motion or color of small objects; they detect only intensity changes averaged over their large visual field. The ocelli, therefore, provide excellent material for studying neural mechanisms underlying the processing of temporal contrast signals. In this review I will summarize our present knowledge of the mechanisms underlying the processing of contrast signals in insect ocellar systems. This will include a discussion of spatial, temporal, and spectral properties of insect ocellar systems with special reference to their behavioral roles, as well as a review of neural organization of the insect ocellar system. I will examine the mechanisms to detect and process temporal contrast signals and summarize some neural principles underlying information processing in insect ocellar systems. I will then show that simple modifications and duplications of neural circuits for detecting temporal contrast signals are sufficient to explain neural circuits for detecting more elaborate visual features, such as the direction of motion. Finally, I will discuss possible evolutionary pathways by which advanced neural networks subserving advanced visual functions have emerged from simpler neural networks subserving simpler visual functions.

Received February 25, 1994

FUNCTIONAL PROPERTIES OF INSECT OCELLI

Most adult insects possess two or three ocelli in addition to a pair of compound eyes. Three ocelli is the usual number but some insects like cockroaches and moths have two ocelli. The compound eyes are sophisticated visual organs responsible for functions that require good spatial resolution, such as the perception of movement, fixation of objects and pattern recognition. In contrast, the ocelli are simple photoreceptive systems with very poor spatial resolution [21]. Why then do insects need simple photoreceptors, i.e., ocelli, even though they are equipped with sophisticated compound eyes? Although this question has not been fully resolved, some answers have emerged recently from extensive anatomical, physiological and behavioral studies [51].

Insect ocelli possess high-aperture dioptrics which exhibit wide visual fields [9, 21, 82]. Measurements of the focal length of the ocellar lens show that the image plane lies well behind the retinal receptory layer. Due to underfocussing, an object entering the ocellar visual field results in a change in the light intensity impinging on the photoreceptor layers rather than the formation of an image. The output of a large number of photoreceptor cells converges upon a small number of large second-order neurons, called L-neurons [21]. Such a system is best suited for the detection of small changes in light intensity integrated over its wide visual field [111]. Thus, the ocelli are specialized for the effective capture of photons, at the cost of spatial resolution.

The spectral properties of ocellar L-neurons are characterized by broad spectral tuning with sensitivity to both ultraviolet (UV) and visible light. Ocellar spectral sensitivity curves have a marked UV peak with an additional peak in either the blue (in flies [31, 34]) or green (in dragonflies [6], locusts [111], moths [14, 69], and honeybees [19]). The combined UV-blue or UV-green sensitivity in the ocelli appears to be an adaptation for increased sensitivity.

Although the ocelli of most insects have sensitivity to both UV and visible light, a few insects living in extreme light

environments have ocelli with only UV or green sensitivity. Mote and Wehner [59] found that the ocelli of desert ants, which live under bright and UV-rich sunlight, have only a UV peak and are not sensitive at wavelengths longer than 445 nm. The ocelli of some nocturnal insects which rarely encounter UV-rich sunlight such as field crickets, *Gryllus firmus* [40] and cockroaches, *Periplaneta americana* [19] have only single receptor systems maximally sensitive to green and not sensitive to UV. These examples nicely fit the theory that visual pigments have evolved in accordance with environmental light conditions.

Measurement of the absolute sensitivity of large second-order ocellar neurons, called L-neurons, of the locust suggests that the sensitivity of ocelli is at least several times as high as that in compound eyes. Wilson [111] concluded that L-neurons of locust ocelli are 5 times more sensitive to a point source than lamina monopolar cells, a major class of second-order neurons of compound eyes. Wilson [111] also concluded that L-neurons of locusts are 5000 times more sensitive to extended sources than the lamina monopolar cells, although pooling of signals from monopolar cells could improve the sensitivity of higher visual neurons.

What are the advantages of having high sensitivity? Light intensity is defined as the average number of photons per unit time, and the fewer the photons, the larger is the uncertainty about the true average. The absolute sensitivity, i.e., the effectiveness in catching a photon and converting it to a voltage signal, is an essential limiting factor for visual systems. In any arbitrary visual system, increased absolute sensitivity can be used to see at lower intensities, to see faster events, or to detect objects of less contrast.

There is evidence to show that ocelli contribute to low light intensity perception. Schricker [81], for example, examined phototactic runs of honeybees where bees could choose between two lights. He noted that a significantly greater number of them chose the brighter light. Below 1 Lux, only a two-fold difference of intensity was needed for this to occur. Bees with one ocellus blinded needed a four-fold difference, bees with two ocelli blinded needed a six-fold difference and bees with all their ocelli blinded needed an eight-fold difference before a significantly greater number of the bees chose the brighter of the two lights.

Initiation and cessation of diurnal activities of insects often depend on light intensity levels [12, 81]. Under natural environmental conditions where the light-dark cycle consists of dawn and dusk ramps, it would be advantageous for insects to be sensitive to minute changes in illumination. There is evidence to show that signals from ocelli are utilized to determine the threshold light intensity for diurnal activities in bees [23, 81], moths [15, 92] and crickets [74]. In the bee, the first and last of its daily flights is dependent upon the intensity level [81]. If the ocelli are occluded, foraging bees behave normally in most respects [81]. Occlusion of the ocelli, however, does interfere with the timing of the first and last foraging flights. Bees with one, two or three ocelli occluded start to collect food later in the morning and cease collecting earlier in the evening than normal workers. The light intensity required for the first and last collecting flight is increased by a factor of two if one ocellus is covered, 3.3 if two ocelli are covered and 4.5 if all the ocelli are covered. Further evidence of an ocellar contribution to low light intensity perception is reviewed by Mizunami [51].

Another notable advantage of ocelli over compound eyes is the higher speed of signal transmission. In bees, the latency of ocellar and compound eye pathways were measured in descending multimodal neurons which receive inputs from both the compound eyes and ocelli [25]. The descending neurons received ocellar input before the arrival of the delayed compound eye input. The latency of ocellar pathways was 9 msec, while that of the compound eye pathway was 25–35 msec.

For fast-flying insects, the ability to perform rapid visual steering is essential for survival. There is evidence to show that insect ocelli contribute to rapid visual steering in flight. Taylor [101] measured the delay of the head motion response of a tethered locust after the motion of an artificial horizon. Both the ocelli and compound eyes were involved in this response. The delay was 45.4 ± 4 msec when all eyes were intact. The delay was almost unchanged when the compound eyes were ablated (47.4 ± 12 msec) but significantly increased when the ocelli were cauterized (103.4 ± 7 msec), thereby demonstrating that the high speed of signal transmission by the ocelli contributes to shortening the latency of the locust's response to motion of horizon.

The perfect suitability of insect ocelli for detecting movement of the horizon, i.e., the contrast between the earth and sky, and for stability control in flight have been discussed in detail [29, 111]. Wilson [111] argued that locust ocelli have a large receptive field directed horizontally, providing the animal with heavily blurred neural images of the skyline, where unwanted information about structural details are eliminated. Ocellar sensitivity to UV facilitates horizon detection since the contrast between bright sky and dark ground is highest in UV. The high speed of signal detection and transmission in the ocellar system is ideal for rapid course control. Pitch and roll deviation of the flight course are independently detectable by the combination of signals from three ocelli. A roll (turning around the long axis of the body) will cause no change in signal from the median ocellus but will tend to cause a decrease of illumination in one lateral ocellus and an increase in the other lateral ocellus. Detection of pitch can be achieved through measurement of the output of the median ocellus. This hypothesis was confirmed by behavioral studies in dragonflies [93, 94] and locusts [20, 100, 101]. The neural mechanisms underlying the ocellar contribution to the flight steering are well established in locusts [24, 73, 75, 85].

In conclusion, although the ocelli can detect only intensity changes averaged over its large receptive field, they are superior to the co-existing compound eyes in sensitivity and speed. Thus, the ocelli play a major role in insects where functions such as stability control in flight and low light

intensity perception require for high speed or high sensitivity. Insects have successfully extended the range of visual stimuli to which they can respond by having two fundamentally different visual systems, i.e., compound eyes and ocelli, the former designed to attain a high spatial resolution and the latter to attain a fast signal transmission and a high absolute sensitivity. The specific functional design of insect ocelli makes them a suitable model system for examining the neural basis of the processing of temporal contrast signals.

NEURAL ORGANIZATION OF THE COCKROACH OCELLAR SYSTEM

The neural circuits of the insect ocellar system have been studied in a number of species including locusts [22, 44, 90] and bees [25, 68]. Here I will briefly discuss the neural organization of the cockroach ocellar system, as a representative example. Comparative aspects of the neural circuits of insect ocellar systems have been discussed (Mizunami, submitted). Cockroaches have two ocelli, each of which contains about 10,000 photoreceptor cells [108], which converge synaptically upon four large second-order neurons in the ocellar plexus [10, 55, 104]. The large second-order neurons, called L-neurons, exit the ocellus and project into the ocellar tract neuropil of the protocerebrum, through the ocellar nerve (Fig. 1) [52, 55]. Electron microscopic studies show that the ocellar nerve and the ocellar tract are a continuous neuropil area where second-order neurons make synaptic interactions with third-order and efferent neurons [102; 104]. The morphology and physiology of neurons involved in the cockroach ocellar system have been successfully identified by combining extracellular and intracellular staining techniques [52, 55, 63, 64, 65, 105]. Recently, the number and gross morphologies of interneurons in the ocellar tract neuropils were estimated by injecting cobalt ions into the ocellar tract neuropil via microelectrodes. Cobalt ions were taken up and transported by neurons in the ocellar tract; thus, the morphologies of these neurons could be revealed by subsequent histological treatment. By comparing the morphologies of neurons in more than 50 cobalt-filled preparations, it was concluded that each ocellar tract neuropil contains at least 25 interneurons. Twenty-two out of 25 neurons have been characterized anatomically and physiologically by intracellular recordings and stainings [52, 55, 64, 65; Mizunami, submitted], which are: (1) four large second-order neurons projecting into the ocellar tract [55], (2) 16 third-order neurons [52, 55; Mizunami, submitted] which receive monosynaptic inputs from second-order neurons in the ocellar nerve and the ocellar tract [54, 102, 104] and project into various neuropil areas of the brain, (3) two possible efferent neurons modulating the activity of large second-order neurons [64]. Morphology of some of the third-order neurons are shown in Fig. 2. The remaining three neurons still to be characterized. The projection areas of the third-order ocellar neurons include: (1) visual, olfactory and mechanosensory centers, (2) the mushroom body (a higher associative center) [58], (3) premotor centers, including the posterior slope, from which descending brain neurons originate [97, 98] and (4) the thoracic motor systems. The abundance of target neuropil areas in the cockroach ocellar system suggests a multiplicity of ocellar functions: (1) to modulate the activity of visual, olfactory and mechanosensory systems, (2) to influence the activity of higher associative centers, (3) to modulate the activity of descending brain neurons and (4) to produce direct behavioral actions. The projection areas of ocellar neurons of the cockroach are more or less similar to those reported for other insects including locusts [22], bees [68], and crickets [39]. In conclusion, the neural organization of the cockroach ocellar system is summarized as follows: (1) the large number of photoreceptors converge onto only a very small number (four) of second-order neurons in the ocellar plexus and (2) in the ocellar tract neuropil, second-order neurons synapse onto a large number of third-order neurons which project into a number of target neuropils.

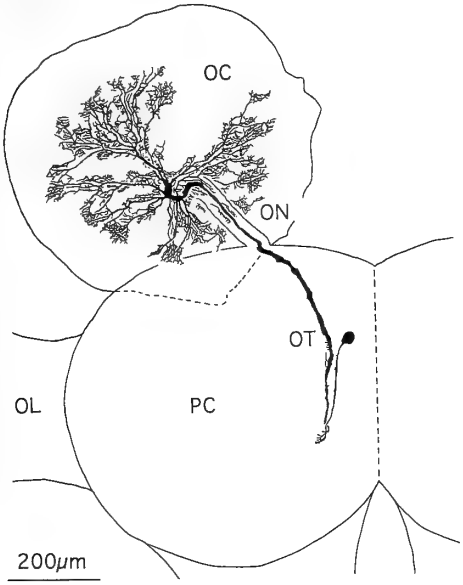

FIG. 1. Morphology of an large second-order neuron (L-neuron) of the cockroach ocellus. The L-neuron extends their dendritic branches into the ocellar plexus, and its axon projects into the ocellar tract neuropil of the protocerebrum, through the ocellar nerve. OC, ocellus; ON, ocellar nerve; PC, protocerebrum; OT, ocellar tract neuropil; OL, optic lobe. Viewed posterodorsally. Modified from Mizunami *et al.* [56].

LINEAR PERIPHERAL MECHANISMS FOR THE DETECTION OF CONTRAST SIGNALS

An effective approach for understanding information processing in the ocellar system is to analyze the dynamics and sensitivity of the responses of its interneurons to changes in light intensity around a mean level, because this system is characterized by a high sensitivity for detecting changes in intensity and high speed for transmitting them to various target neuropils including thoracic motor centers. Analysis

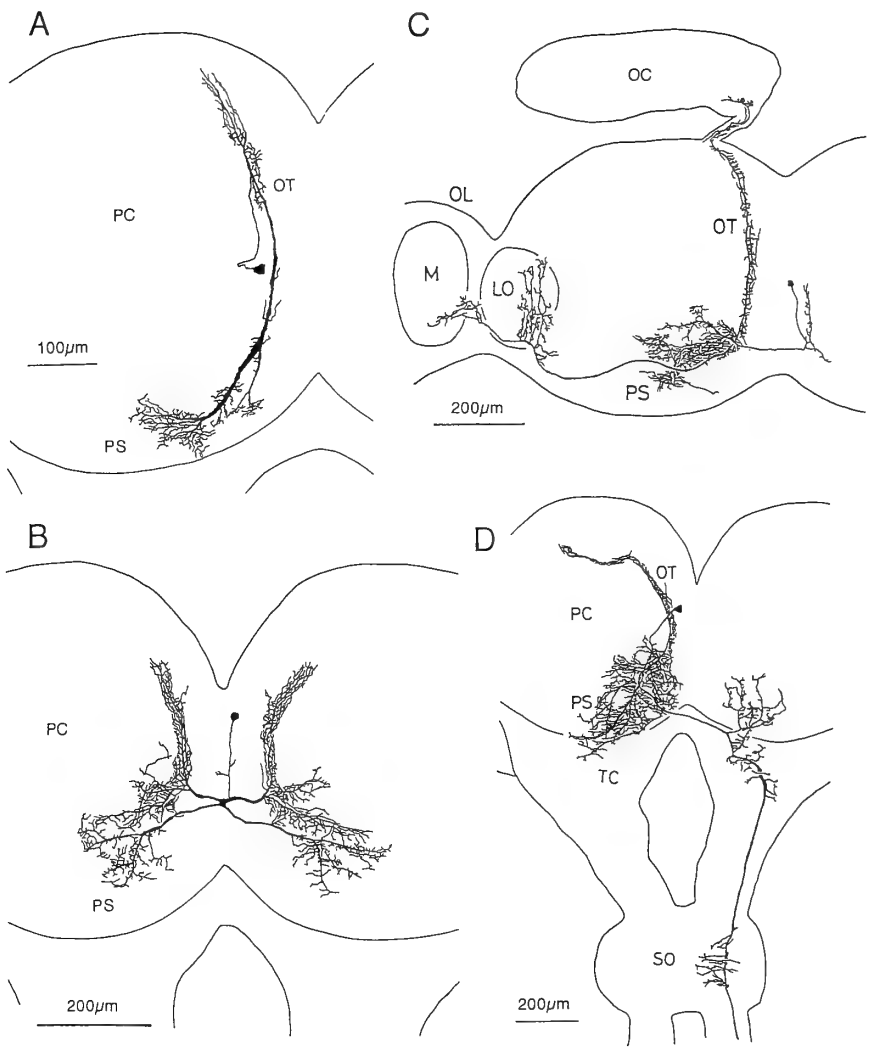

FIG. 2. Examples of third-order ocellar neurons of the cockroach ocellar system. Viewed postero-dorsally. (A) A PS-I neuron which arborizes in an ocellar tract and projects into the ipsilateral posterior slope. (B). A PS-III neuron which arborizes in bilateral ocellar tracts and projects into bilateral posterior slopes. (C) A OL-I neuron which projects into the lobula and medulla of the optic lobe. (D) A D-I neuron which arborizes in the ocellar tract, posterior slope and tritocerebrum. Its axon descends contralaterally toward the thoracic ganglia. There is evidence to show that these neurons receive monosynaptic inputs from L-neurons [54]. OC, ocellus; PC, protocerebrum; OT, ocellar tract neuropil; PS, posterior slope; OL, optic lobe; M, medulla; LO, lobula; TC, tritocerebrum; SO, suboesophageal ganglion. Modified from Mizunami and Tateda [52].

of intracellularly-recorded responses of ocellar neurons to changes in light intensity was pioneered by Chappell and Dowing [7] who studied the responses of photoreceptors and the second-order neurons of dragonfly ocelli, and discussed signal processing at synapses between them, which I refer to as first synapses. Subsequently, Mizunami and his colleagues [49, 53, 54, 56] have analyzed response properties of second- and third-order neurons of cockroach ocelli and examined information processing at synapses between second and third-order ocellar neurons, which I refer to as second synapses, by using white-noise and sinusoidally modulated light. This section deals with information processing by photoreceptors and second-order neurons. Further processing of contrast signals by higher-order neurons will be discussed in the next section.

Signal processing at first synapses

Insect ocelli contain a large number of photoreceptors which make synapses with a small number of large second-order neurons, called L-neurons. Both the photoreceptors and L-neurons generate graded, slow potential responses to light stimuli. Photoreceptors exhibit a depolarizing response to a step of light given in the dark, whereas L-neurons exhibit a hyperpolarizing response (Fig. 3A, B) [7, 35, 70, 88]. The hyperpolarizing response of L-neurons is due to an increase in membrane permeability to ions whose equilibrium potential is negative to the membrane potential in the dark [111].

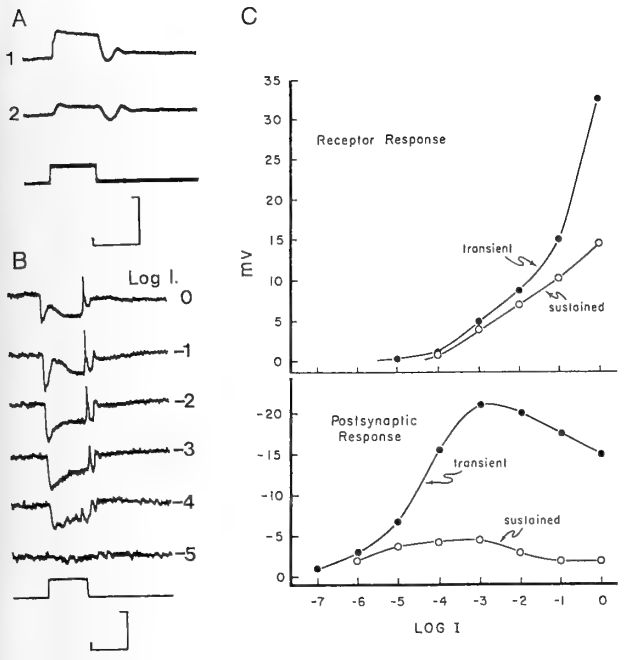

FIG. 3. Responses of a photoreceptor and a large second-order neuron of the median ocellus of the dragonfly, *Aeschna*. Intracellularly recorded responses of a photoreceptor (A) and a large second-order cell (B) to illumination of the median ocellus with pulses of white light at different intensities Log I, $\log_{10}$ relative intensity of illumination. Scales: 200 ms; 20 mV. (C) Intensity-response relationships for receptor and postsynaptic units. The amplitude of the peak of the transient wave and the sustained component of the receptor response and the postsynaptic response are plotted as a function of intensity. The sustained component of the receptor response was measured 3 sec after the start of illumination. A and B are from Patterson and Chappell [70]; C is from Chappell and Dowling [7].

Chappell and Dowling [7] have compared responses of photoreceptors and L-neurons of dragonfly ocelli to a step of light given in the dark, and have noted two important differences between the responses of photoreceptors and L-neurons. First, the sensitivity of L-neurons is larger than that of photoreceptors by 1–2 log units (Fig. 3A, B). This is explained by a high ratio of convergence of photoreceptors onto L-neurons [11]. Second, the waveform of the response of L-neurons is much more transient (Fig. 3A, B), and the sustained component of the response of L-neurons is much less prominent (Fig. 3C) than that of photoreceptors.

The functional significance of the enhancement of transience was clarified by further examinating the responses of photoreceptors and second-order neurons to changes in light intensity around a mean level [7, 56]. The photic inputs that visual systems receive naturally is a modulation of light intensity around a mean illuminance. The mean illuminance changes slowly but covers a large range in the course of one day. The depth of fluctuation around the mean is moderate and remains roughly constant. The photoreceptor response to changes in intensity consists of two components, a steady mean potential and a time-varying component, which signal mean illuminance levels and intensity changes, respectively. The steady response component of L-neurons, however, is highly compressed (in dragonflies [7, 56, 88]) or completely eliminated (in bees [3]), indicating that L-neurons signal relative intensity changes rather than absolute light intensity level. It is concluded that, at the first synapses, the photoreceptor responses signaling absolute intensity level is high-pass filtered to produce a postsynaptic response signaling about relative intensity change. The enhancement of the response to intensity changes by temporal highpass filtering have been noted at first synapses of most visual systems studied so far, including barnacle ocelli [28, 95, 99], insect compound eyes [42, 84, 109], *Limulus* lateral eyes [72] and vertebrate retinas [4, 60, 62, 110]. This apparent common principle among visual systems reflects the fact that visual systems are designed to detect the contrast between objects and background in the presence of background illumination, rather than the light intensity itself.

Dowling and Chappell [11] performed an electron microscopic study of the dragonfly ocellar plexus and found that L-neurons make observed feedback synapses onto photoreceptors. They [11] proposed that these feedback synapses play major roles in the temporal highpass filtering. Klingman and Chappell [35] have studied the effects of various drugs on the response of L-neurons in dragonflies and suggested that the receptor synapses are inhibitory (sign-inverting) and curare-sensitive, whereas there are excitatory (sign-conserving) GABAergic feedback synapses from L-neurons which facilitate photoreceptor transmitter release. Stone and Chappell [96] have suggested that hyperpolarizing oscillation at the off-set of illumination in dragonfly photoreceptors reflects GABAergic feedback synapses onto photoreceptor terminals. Subsequent studies, however, have failed to confirm the feedback hypothesis for the enhancement of response transience. Simmons [87] made simultaneous intracellular recordings from a photoreceptor and an L-neuron of a dragonfly ocellar retina; no response was evoked in the photoreceptors when depolarizing or hyperpolarizing currents were injected into L-neurons, although L-neurons produced responses when current was injected into photoreceptors. In addition, no immunoreactivity to GABA was observed from L-neurons, at least in locusts [2] and bees [80]. Unfortunately, GABA-immunocytochemical studies have not been performed on dragonfly L-neurons. The response of bee L-neurons is very phasic [25], although no feedback synapses have been observed between L-neurons and receptors in the bee [103]. There should be a mechanism to enhance the transience other than the feedback from L-neurons, at least in the bee. Simmons [87] proposed that the intrinsic membrane properties of the photoreceptor terminals and L-neurons, and excitatory synapses made by small second-order neurons on L-neurons are included in the mechanisms to enhance the response transience of dragonfly L-neurons. Ammermüler and Weiler [85] discussed the possible contribution of GABAergic small second-order neurons in a feedback system of the locust. In summary, neural mechanisms underlying the enhancement of response

transience at first synapses of insect ocelli still to be established.

Dynamics of slow potential responses of second-order neurons

The most extensive analysis of responses of ocellar L-neurons have been made in the cockroach by using white-noise modulated light with various mean illuminances (Fig. 4) [56]. The kernels, obtained by cross-correlating the white-noise input against the resulting response, provided a measure of incremental sensitivity as well as of response dynamics (Fig. 5). The first-order kernels, the product of first-order cross-correlation, represent the linear component of the cell's response, and second- and higher-order kernels, products of second- and higher-order cross-correlation, represent the nonlinear components of the response.

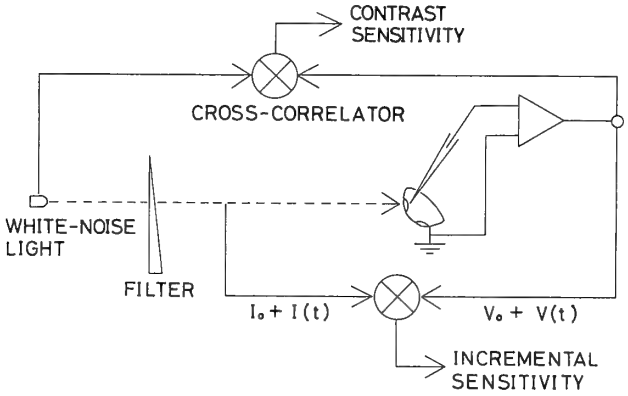

FIG. 4. Schematic drawing of experimental procedure to study incremental response of cockroach ocellar L-neurons. A series of ND filters were interposed between the light source and the preparation to attenuate both the mean illuminance and white-noise modulation by the same proportion, so that the "contrast" of the stimulus was kept unchanged. The light signal was monitored before it was attenuated by filters and a correlation was made between the unattenuated light signal and the cellular response. The correlation produces kernels on a contrast sensitivity scale. Kernels were converted to an incremental sensitivity scale by multiplying the kernel's amplitude by the attenuation factor. From Mizunami *et al.* [56].

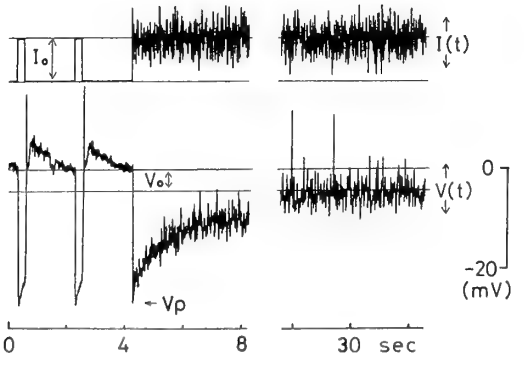

FIG. 5. Responses from a cockroach ocellar L-neuron evoked either by steps of light given in the dark or by white-noise-modulated light. The relationship between I_o and V_p or V_o is the cell's DC (static) sensitivity and the relationship between I(t) and V(t) is incremental sensitivity. Spike potentials are seen at the offset of step stimulation as well as during white-noise stimulation. From Mizunami *et al.* [56].

A brief step of light given in the dark produced step-like hyperpolarization in L-neurons. At the off-set of light stimulation, L-neurons generate solitary spikes. Here I will concentrate on the slow potential response of L-neurons; their spike response will be discussed in the next section. With continued white-noise stimulation, the membrane potential reaches a steady level within 30 sec (Fig. 5). At this dynamic steady state, the actual responses of L-neurons to white-noise stimulus can be predicted by a linear model (Fig. 6) with mean-square-errors of about 11%. This indicates that the response is practically linear, i.e., the magnitude of the response is proportional to the depth of modulation. The linear nature of the response to intensity changes has been reported from peripheral visual neurons in a variety of visual systems including the photoreceptors of the *Limulus* compound eye [18], vertebrate retina [5, 61] and insect compound eye [71], as well as the second-order neurons of vertebrate retina [8, 60, 107], the *Limulus* compound eye [38] and insect compound eye [17]. Linear coding of photic signals thus appear to be a general principle of peripheral visual systems.

In Fig. 7, first-order kernels which represent the linear

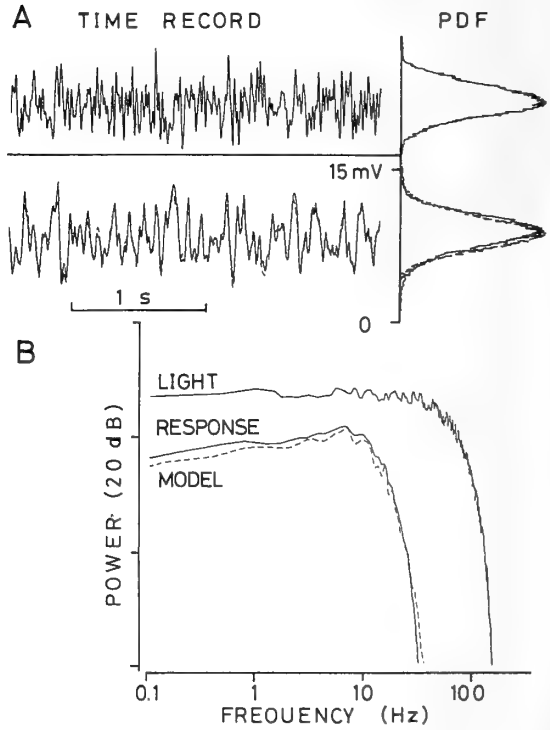

FIG. 6. Responses of a cockroach ocellar L-neuron to a white-noise modulated light. (A) Time records of part of a white-noise stimulus and the resulting response of a cockroach L-neuron (continuous line). Superimposed on the response trace is the linear model (broken line). Probability distribution function (PDF) for the light stimulus and the recorded response are also shown. The light PDF is also superimposed on the response PDF. (B) Power spectra of the light stimulus, response (continuous line), and linear model (broken line). The mean illuminance of the stimulus is 20 $\mu W/cm^2$. From Mizunami *et al.* [56].

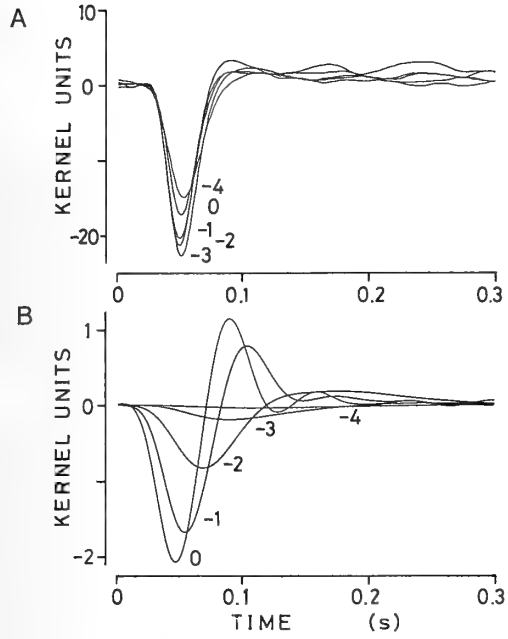

FIG. 7. Comparison of first-order kernels of second-order neurons of cockroach ocelli and vertebrate retinas. (A) First-order kernels from a cockroach ocellar L-neuron, plotted on a contrast sensitivity scale, obtained at five mean illuminance levels. The first-order kernels were calculated by cross-correlating the white-noise light stimuli with the recorded responses. Kernels are labeled 0 through −4 to indicate the log density of the filters interposed. Note that the amplitudes of the kernels did not differ by more than 30% and the peak response times were constant at 50 msec for all kernels, although the mean levels covered a range of 1 : 10,000. Stimuli dimmer than −4 log units did not produce any reliable results. (*B*) First-order kernels from a turtle retinal horizontal cell, plotted as in *A*. The peak response times, waveforms, and amplitudes differed at various levels of mean illuminance. Kernel units are in millivolts per microwatt per square centimeter per second. The larger incremental sensitivity for ocellar kernels was due to a dimmer mean illuminance ($20\mu W/cm^2$ at 0 log) of the white-noise stimulus than in the turtle experiment ($50\mu W/cm^2$ at 0 log). From Mizunami *et al.* [56].

component of the response obtained at four log ranges of mean luminance levels have been plotted on a contrast sensitivity scale. The waveforms are almost identical, with constant peak response times of about 50 msec, while the amplitudes differ only by 30%. The results show that the response is an exact Weber function, i.e., contrast sensitivity remains unchanged over at least a four log range of mean illuminance levels and that the response dynamics remains unchanged at the same range of mean illuminance levels. For comparison, an example of kernels from a horizontal cell of turtle retina obtained under comparable conditions is shown in Fig. 7, where the amplitude of kernels differs at different levels of mean illuminance, the peak response times shorten from 100 to 50 msec, and the waveforms become more biphasic (differentiating) with an increase in mean luminance. These studies show that (1) the cockroach L-neurons are ideal contrast detectors since their response amplitude is exactly proportional to the contrast of intensity change for at least 4 log ranges of mean illuminance levels and (2) signal processing in the cockroach ocellus differs from other visual systems, including *Limulus* lateral eyes [18], insect compound eyes [13, 71], vertebrate retinas [5, 60], and the human visual system [33], in that the system's dynamics change depending on the levels of mean illuminance. Frequency-response characteristics of L-neurons have also been studied using sinusoidally-modulated light [49, 54]. The response of L-neurons is bandpass with an optimal frequency of 1–3 Hz, a lower cut-off frequency (−3 dB) of 0.05–0.1 Hz and a higher cut-off frequency of 12–15 Hz, indicating that this neuron can respond to slowly occurring events.

Interestingly, there are marked differences in incremental responses of light-adapted L-neurons among different insects. Contrast sensitivity of bee L-neurons [3] is much lower than that of the cockroach [56], i.e., they can not respond to stimuli of small contrast. However, some L-neurons of the bee exhibit a higher cut-off frequency of about 30 Hz [3], and thus can respond to stimuli of much higher frequency than can cockroach L-neurons. These findings are consistent with the hypothesis proposed by Mizunami (in preparation) that the ocellar system of the bee is more concerned with speed than sensitivity, while that of the cockroach is more concerned with sensitivity than speed. In addition, the waveform of the response of bee L-neurons to sinusoidally-modulated light highly deviates from sinusoid [3], indicating that the response contains a high degree of nonlinearity. The bee L-neurons are not suited to faithfully monitoring the stimulus contrast, and are perhaps more related to the initiation of direct behavioral reactions. Furthermore, Simmons [89] has recently measured frequency response characteristics of locust L-neurons using sinusoidally modulated light, and has noted that the optimal frequency, where the contrast sensitivity is highest, changes from 2 Hz to 10 Hz with an increase in mean illuminance levels. Since such changes have not been observed in the responses of cockroach L-neurons [56], ocellar systems of locusts and cockroaches must adopt different strategies to adjust their response dynamics to environmental light intensity levels. Such differences may imply that there are fundamental differences between the behavioral roles of locust and cockroach ocelli, a possibility which should be examined further.

NONLINEAR CENTRAL MECHANISMS FOR THE PROCESSING OF CONTRAST SIGNALS

The signals about temporal contrast encoded in the graded responses of ocellar L-neurons are further processed to detect specific visual features. In the following section, I will first discuss signal conversion at the spike initiation process in L-neurons, and then discuss signal processing at synapses from second- to third-order neurons (second synapses) of cockroach ocellar system.

Dynamics of the spike initiation process in L-neurons

L-neurons of most insects respond to light stimuli with regenerative spikes, in addition to graded slow potentials (cockroaches [55, 57]; bees [45, 46]; locusts [88, 112]). The relationship between the slow potential and spikes of L-neurons have been analyzed in the cockroach using a sinusoidally modulated light with various mean illuminances [53]. L-neurons generated a solitary spike at the depolarizing phase of the modulation response (Fig. 8). The relationship between the peak-to-peak amplitude of the slow potential response and the rate of spike generation was sigmoidal, with a linear part covering the spike rate ranging from 10 to 90% (Fig. 9A). In Fig. 9B, the spike rate has been plotted against the amplitude of the slow potential response at five different frequencies. The results at a spike rate of between 10 to 90% are shown. The extrapolated regression lines for each frequency cross the vertical axis at almost the same point, suggesting that the nonlinear threshold is frequency independent. In contrast, the slope of the lines changes with frequency, which indicates that the spike initiation process contains dynamic linearity. Subsequent studies have shown that the spike threshold at optimal frequency (0.5–5 Hz) remains unchanged over a mean illuminance range of 3.6 log units, whereas the spike threshold at frequencies of <0.5 Hz was lower at a dimmer mean illuminance (Fig. 10A), where the L-neurons exhibited a larger voltage noise and their mean membrane potential levels were more positive (Fig. 10B). Steady or noise current injection during sinusoidal light stimulation showed that (1) the decrease in the spike threshold at a dimmer mean illuminance was due to an increase in the noise variance, i.e., the noise had a facilitatory effect on the spike initiation and (2) the change in the mean potential level had little effect on the spike threshold (Fig. 11). In summary, the spike response of L-neurons is repre-

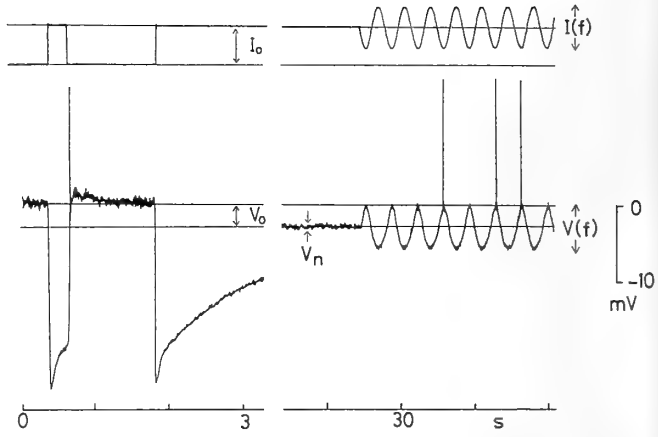

FIG. 8. Responses of a cockroach ocellar L-neuron evoked either by a step light stimulus given in the dark or by a sinusoidally modulated light stimulus. The L-neuron responded to the sinusoidal stimulation with a sinusoidal voltage modulation, $V(f)$, around a mean voltage, V_o. A spontaneous voltage fluctuation (voltage noise), V_n, was superimposed on the modulation response. Spikes were seen at the offset of step stimulation and at the peak of the voltage modulation. The mean illuminance of the stimulus, I_o, was 20 μW·cm^{-2}; the modulation frequency, f, was 2 Hz; the depth of modulation of the stimulus, $I(f)$, was 60%. From Mizunami and Tateda [53].

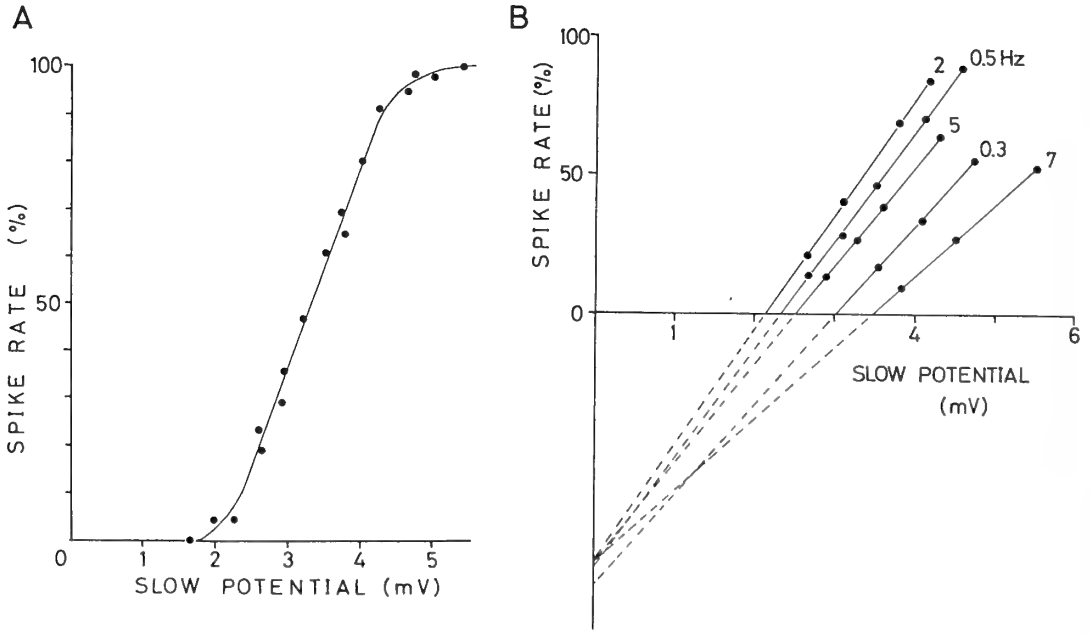

FIG. 9. Dynamics of the spike initiation process in a cockroach ocellar L-neuron. (A) The rate of spike generation plotted against the peak-to-peak amplitude of the slow potential response of a cockroach L-neuron, obtained at a frequency of 1 Hz. The form of the curve was sigmoidal, with the linear part covering the range of spike rate from ~10–90%. (B) The spike rate plotted against the amplitude of the slow response of a cockroach L-neuron, obtained at five different frequencies. The extrapolated broken lines are the regression lines for each frequency. These lines cross the vertical axis at almost the same point. The stimulus had a mean illuminance of 2 μW·m^{-2}. From Mizunami and Tateda [53].

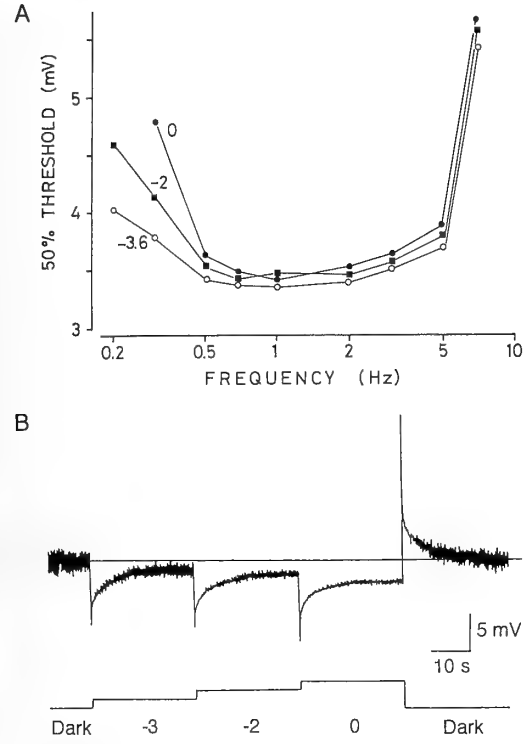

FIG. 10. Effects of mean illuminance changes on the dynamics of the spike initiation process in a cockroach L-neuron. (A) 50% threshold of spike response, defined as the peak-to-peak amplitude of the potential modulation at a spike rate of 50%, plotted against the modulation frequency. The plots are from the responses of a cockroach L-neuron to sinusoidal lights with a mean illuminance of 0.005 (−3.6 log), 0.2 (−2 log), and 20 $\mu W \cdot cm^{-2}$ (0 log). (B) Responses of a cockroach ocellar L-neuron to prolonged illuminations. The light intensities are indicated as $\log_{10}$ attenuation (0 log units = 20 $\mu W \cdot cm^{-2}$). From Mizunami and Tateda [53].

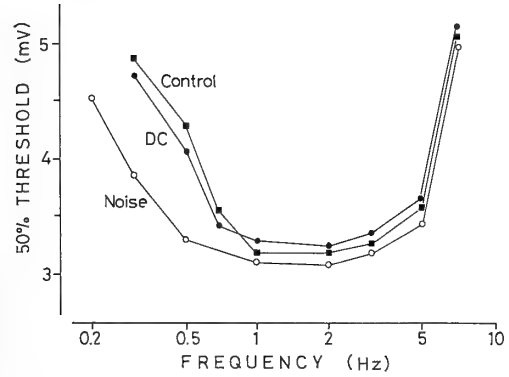

FIG. 11. Effects of noise current and steady current injection on the 50% threshold of a cockroach L-neuron. A noise current having a peak-to-peak amplitude of ~4 nA or a steady depolarizing current of 4 nA was injected during sinusoidal light stimulation. The light stimulus had a mean illuminance of 20 $\mu W \cdot cm^{-2}$. The estimated potential change produced by the injection of a 4 nA current was ~3 mV (the estimated input resistance at that mean illuminance was ~0.8 MΩ). The 50% threshold at a low-frequency range decreased when the noise current was injected. The steady depolarizing current had little effect on the 50% threshold. From Mizunami and Tateda [53].

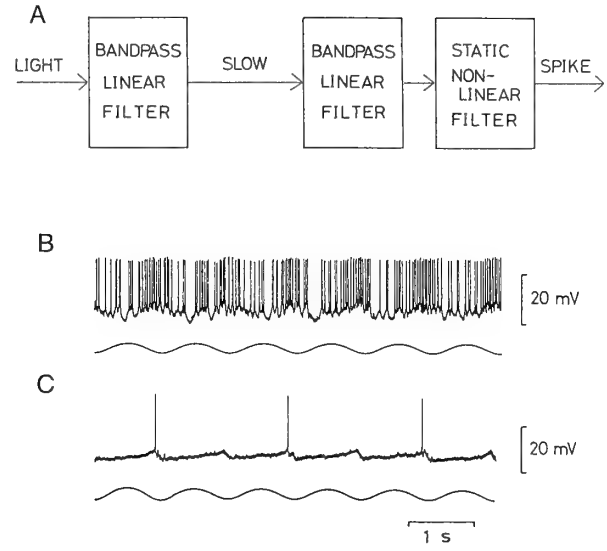

FIG. 12. (A) A model for the spike response of cockroach ocellar L-neurons. Light signals are passed through a bandpass linear filter, producing a slow potential response in L-neurons. The slow potential contains a noise which reflects that contained in the synaptic potential from photoreceptors. The slow potential is further passed through a linear/nonlinear cascade and produces a spike discharge. The linear filter is bandpass, and the nonlinear filter is a static threshold. (B, C) Typical responses of two types of third-order ocellar neurons of the cockroach to sinusoidal light stimulation. One type of third-order neuron, the OL-I neuron (type 1 neuron projecting into the optic lobe), showed sinusoidal modulation of spike frequency (B), whereas the other type, the D-I neuron (type 1 neuron descending to the thoracic ganglia), generated solitary spikes at the decremental phase of light modulation (C). The lower traces indicate the stimulus light, monitored by a photodiode. The stimulus had a modulation frequency of 1 Hz and a modulation depth of 50%. The mean illuminance was 2 $\mu W \cdot cm^{-2}$. From Mizunami and Tateda [53].

sented by a simple cascade model (Fig. 12A). A light stimulus is passed through a bandpass linear filter and produces a slow potential response in L-neurons. The slow potential is passed through a cascade of a linear filter followed by a nonlinear filter and produces a spike discharge in L-neurons. The linear filter is bandpass containing both a differentiating and an integrative nature. The nonlinear filter is a static threshold with a sigmoidal (probablistic) input/output relationship. It is concluded that fundamental signal modifications occur during spike initiation in cockroach L-neurons, a finding which differs from the spike initiation process in other visual systems, including the *Limulus* compound eye [36, 37] and catfish retina [78], in that it is presumed that little signal modification occurs at the analog-to-digital conversion process. It would be interesting to see if the slow potential or the spike signals of L-neurons, or both, are encoded in the response of third-order neurons. Figs. 12B and C show typical examples of responses of third-order ocellar neurons to sinusoidally modulated light. A type of third-order neuron, OL-I neuron (type I neuron projecting into the optic lobe), had spontaneous spike activity and exhibited a modula-

tion of the spike frequency around a mean (Fig. 12B). The pattern of the response was similar to the slow potential response of L-neurons. The other type, the D-I neuron (type I neuron descending to the thoracic ganglia), had no spontaneous spike activity and exhibited single spikes at the decremental phase of light modulation (Fig. 12C). The pattern of the response was similar to that of the spike response of L-neurons. Thus, it is concluded that both graded and spike signals of L-neurons are encoded in the spike responses of third-order neurons [48, 53]. The graded response of L-neurons appears to continuously monitor the contrast of intensity changes, whereas the spike response possibly signals an urgent event which requires rapid behavioral reactions.

Nonlinear signal processing at second synapses

Analysis of the signal transmission at synapses between second- and third-order neurons (second synapses) of the insect ocellar system was initiated by Simmons [86] who examined the operations of synapses which L-neurons make with a pair of large descending third-order ocellar neurons, DNI (an ipsilaterally descending neuron), of the locust. Both L-neurons and DNI neurons hyperpolarize when their ocellus is illuminated. L-neurons and DNI neurons produce sharply rising regenerative responses when a bright light is switched off. L-neurons make excitatory (sign-conserving) chemical synapses with the DNI neurons. Under steady daylight illumination, L-neurons continually release transmitters onto the DNI neurons. The hyperpolarizing responses of DNI neurons to an increase in illumination are due to a decrease in the rate of release of transmitter from the L-neurons.

Further detailed analyses of transfer characteristics of the second synapses of ocellar systems have been made in the cockroach. Mizunami and Tateda [52] identified nine types of interneurons in the cockroach with arborizations in the ocellar tract neuropil. When recordings were made in the ocellar tract, all types of neurons exhibited a similar response to step stimulus given in the dark, i.e., a tonic hyperpolarization during illumination and one or a few transient depolarizations at the end of illumination. These neurons can be classified into several physiological types from responses recorded in their axons or terminal regions. Some neurons exhibited spontaneous spike discharge, some neurons had no spontaneous discharge and others generated no spikes to either ocellar illuminations or extrinsic current injections into the neurons [52, Mizunami, personal observation]. Mizunami and Tateda [54] made simultaneous intracellular recordings from these neurons and L-neurons and found that these neurons receive monosynaptic inputs from L-neurons. The synapses made from L-neurons to these neurons had similar properties to those reported for the synapses made from L-neurons to DNI neurons of locusts. Excitatory (sign-conserving) synaptic transmission was tonically maintained under normal resting potentials, so that hyperpolarizing responses of L-neurons produced hyperpolarizations in third-order neurons.

Mizunami [49] further studied the transfer characteristics of synapses made from L-neurons to third-order neurons of the cockroach ocellar system using simultaneous microelectrode penetrations and the application of tetrodotoxin. The stimulus used was a sinusoidally- modulated light around a mean illuminance or an extrinsic current applied to the L-neurons. The waveform of the response of L-neurons to sinusoidally-modulated light is almost sinusoidal, which indicates that the response is linear, but the waveform of the response of third-order neurons deviates from sinusoid and exhibits a half-wave rectification, i.e., the depolarizing response to light decrement is much larger than the hyperpolarizing response to light increment (Fig. 13). Analysis of the synaptic transfer curve relating pre- and postsynaptic voltages showed that the synapses made from L-neurons to third-order neurons operate at an exponentially rising part of the overall sigmoidal transfer curve (Fig. 14). Due to the nonlinear characteristics of the synaptic transfer, the linear responses of presynaptic neurons are converted into half-wave rectified responses of postsynaptic neurons (Fig. 15A).

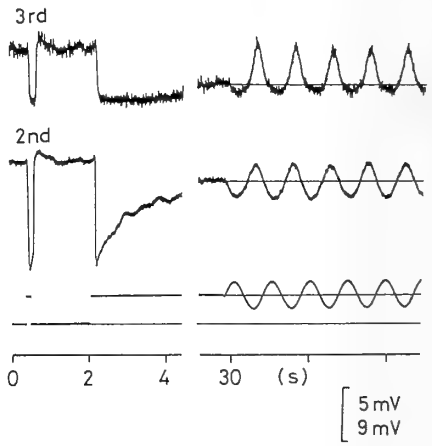

FIG. 13. Responses of a second- and a third-order ocellar neuron of the cockroach evoked either by step-stimuli given in the dark or by a sinusoidally modulated stimulus around a mean illuminance. The sinusoidal stimulus has a modulation depth of 0.7 and a modulation frequency of 2 Hz. Horizontal lines in the records are the steady (DC) potential levels maintained during steady illumination. The lowest trace indicates the stimulus light, monitored by a photodiode. Calibration: 5 mV for the third-order neuron; 9 mV for the second-order ocellar neuron. From Mizunami [49].

The properties of the second synapses of cockroach ocelli were compared to those reported for first synapses of other visual systems. In most visual systems studied thus far, both photoreceptors and second-order neurons exhibit linear responses to changes in intensity, thereby suggesting the linear nature of signal transmission at first synapses. Indeed, studies of first synapses in turtle retina [62], barnacle ocelli [28], dragonfly ocelli [87] and fly compound eyes [43] show that signal transmission occurs at the mid-region of the sigmoidal transfer curve where the transmission is linear. It is concluded, therefore, that operation ranges over the synaptic

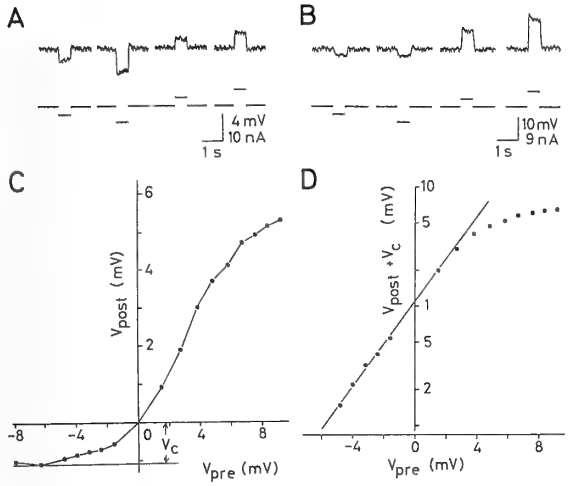

FIG. 14. Measurements of transfer characteristics of second synapses in the cockroach ocellar system. (A) Typical records of a current/voltage relationship of a second-order ocellar neuron (L-neuron) measured by impaling the neuron with two electrodes. (B) Responses of a third-order ocellar neuron evoked by current stimuli applied to an L-neuron. Averaged current-voltage relationships from six L-neurons were used to estimate presynaptic potential changes during current stimuli for the experiments in C. Actual input resistance of L-neurons deviates slightly from cell to cell ($\sim \pm 13\%$), thus, the estimated synaptic transfer curve may have slight errors. Lower traces in A and B indicate the magnitude of the stimulus current. (C) Input/output voltage relationship of the synaptic transmission. Measurements were made at the steady-state value for 0.5 sec current pulses. V_c is the synaptic potential maintained in the dark. V_{pre} and V_{post} are the potentials of the second- and third-order neuron, respectively. The potentials were measured from the dark level, thus, $V_{post}+V_c$ is the actual postsynaptic potential. (D) Semilogarithmic plot of the input/output voltage relationship of the synaptic transmission. From Mizunami [49].

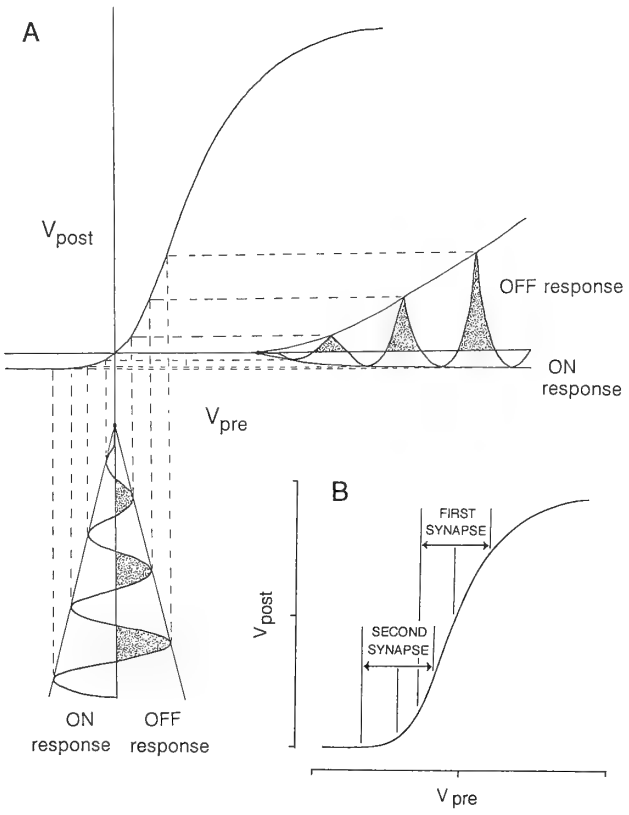

FIG. 15. Nonlinear signal transmission at second synapses. (A) Signal rectification by nonlinear synaptic transmission from second- to third-order ocellar neurons of the cockroach. Synaptic transmission occurs using an exponentially-rising part of the over-all sigmoidal transfer curve, thus, the depolarizing response to light decrement of presynaptic neurons is amplified, while the hyperpolarizing response to light increment is compressed. From Mizunami ([51]). (B) Linear and nonlinear signal transmission at graded synapses. The synapse between second- and third-order neurons (second synapse) of cockroach ocelli operates at an initially rising part of the S-shaped input/output relationship; thus, the transmission is nonlinear and rectifying. The synapse between photoreceptors and second-order neurons (first synapse) of visual systems presumably operates at a mid-region of the S-curve, where the transmission is essentially linear. From Mizunami [49].

transfer curve differ between first synapses and second synapses (Fig. 15B), thus resulting in fundamental differences in signal transmission, i.e., transmission is nonlinear and half-wave rectifying at second synapses whereas it is linear at first synapses.

Rectified responses have been noted in some third-order neurons of a variety of visual systems including ganglion cells of goldfish retina [91] and cat retina [16, 30], third-order neurons of locust compound eyes [32, 66, 67], locust ocelli [86], and barnacle ocelli [99]. The rectified responses seen in third-order neurons of these visual systems can be explained if their second synapses have a nonlinear rectifying nature, as do second synapses of the cockroach ocellar system.

The response of cockroach ocellar third-order neurons to brightening is much smaller than that to dimming. In barnacle ocelli, Stuart and Oertel [99] noted that the response to dimming is enhanced as signals are passed from second- to third-order neurons. Because the major function of barnacle ocelli is to detect dimming to facilitate a shadow-induced withdrawal of the animal into the shell [26], it is reasonable to use a large part of the dynamic range to code signal about dimming. In insect ocelli, Stange [93] studied the role of ocelli in visual steering behavior of dragonflies in flight and concluded that a decrease in illuminance of the ocelli has a strong effect on inducing steering behavior to avoid nose-diving toward the ground, whereas an increase in illumination is less effective. It appears that in these simple visual systems, the detection of dimming is more important than that of brightening, and thus dimming-specific responses are formed by removing redundant signals.

NEURAL PRINCIPLES FOR THE DETECTION AND PROCESSING OF CONTRAST SIGNALS

In this section, I will briefly summarize information

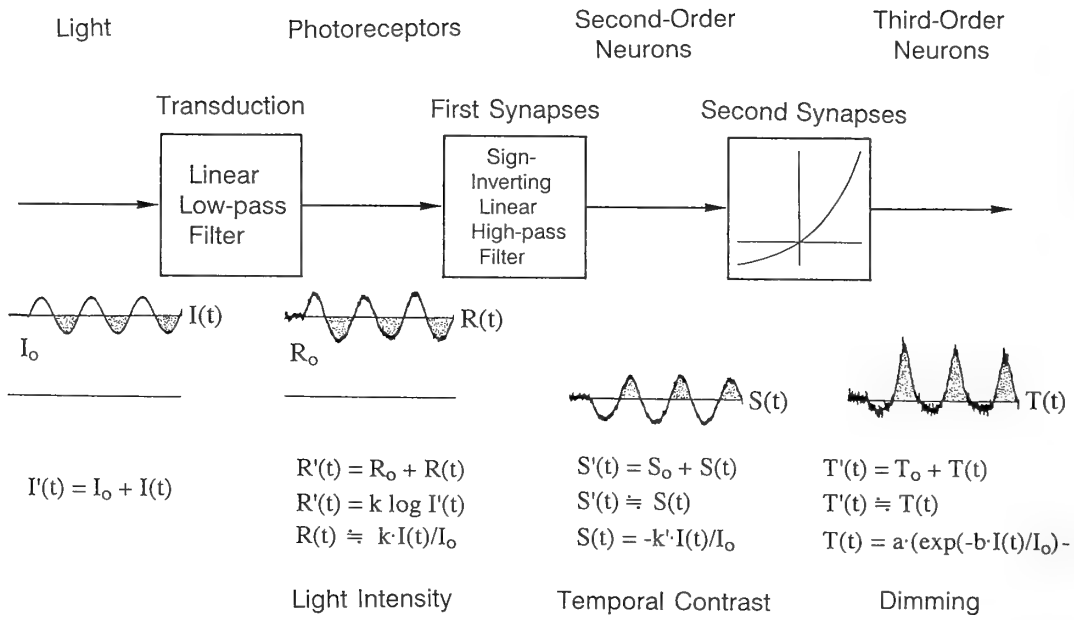

FIG. 16. Summary diagram of signal processing in the cockroach ocellar system. The light-to-voltage transduction process in photoreceptors has a linear lowpass filtering property. The photoreceptor responses encode absolute light intensity and feed into first synapses, which have a sign-inverting, linear lowpass filtering property. The response of second-order neurons, which encodes contrast of intensity changes, feeds into second synapses. The second synapse is static (frequency-independent) and has an exponential input/output relationship. The response of third-order neurons encodes dimming. From Mizunami [51].

processing in the cockroach ocellar system (Fig. 16). The light inputs which enter the ocellar photoreceptors, I'(t), consist of two components, a time-varying component, I(t), and a steady mean, I_o. The light-to-voltage transduction process in ocellar photoreceptors is linear and has a lowpass filtering property. Its output, i.e., photoreceptor response R'(t), consists of two components, a time-varying component R(t), and a steady component R_o. R(t) is related to I(t), and R_o is related to I_o. The photoreceptor response then feeds into first synapses, i.e., synapses between receptors and second-order neurons. The first synapses are linear, sign-inverting, and have a highpass filtering property. The output, i.e., the response of second-order neurons S'(t), can be divided into two components, a time-varying part S(t), and a steady mean S_o. S(t) is linearly related to the stimulus contrast $I(t)/I_o$. Because of the highpass nature of first synapses, the S_o is small. Thus, S'(t) can be written as:

$$S'(t) \fallingdotseq S(t) = -k' \, I(t)/I_o, \qquad (1)$$

where $k'(f) > 0$. To simplify the discussion, the spike response of L-neurons is not considered here. The response of second-order neurons S'(t), feeds into second synapses. The second synapses are static (frequency-independent) and have an exponential input/output relationship. The response of third-order neurons T'(t), can be written as:

$$T'(t) \fallingdotseq T(t) = a(\exp(S'(t)/k'') - 1)$$
$$= a(\exp(-b \, I(t)/I_o) - 1), \qquad (2)$$

where T(t) is a time-varying component of the response of third-order neurons; $k''(f) > 0$; $a > 0$; $b(f) > 0$. Because the exponential filter enhances the response to dimming and compresses the response to brightening, the response of third-order neurons mainly codes for dimming.

This model suggests that dimming detection in the insect ocellar system is performed by a cascade of a few processing steps. Each step extracts an aspect of visual signals by removing redundant signals, so that the system can finally detect specific, biologically significant features. It can be argued that this cascade organization may reflect the pathways by which insect ocellar systems have evolved. The ocellar systems may have originated from simple photoreceptors whose functions were to detect the distribution of light intensity around the animal, and then first-order interneurons followed, enabling detection of temporal contrast signals representing the movement of self or large objects. Finally, second-order interneurons followed to specifically code for dimming, enabling the evaluation of an approach of large objects to perform an appropriate avoidance behavior. In short, the present neural circuits of the cockroach ocellar system may involve ancestral neural circuits from which the ocellar system has evolved.

DETECTION OF TEMPORAL CONTRAST AS A BASIS OF HIGHER VISUAL FUNCTIONS

Detection of temporal contrast is a basic pre-processing necessary for the extraction of biologically significant visual

information such as color, motion, and shape of objects. Knowledge of the neural mechanisms for the detection of contrast signals obtained in the cockroach ocellar system, therefore, provides a basis for understanding neural mechanisms subserving advanced visual functions. Mizunami [49, 50] discussed two examples in which neural mechanisms of higher visual function can be explained by simple duplications and modifications of dimming detection circuits which represent the cockroach ocellar system. One is the neural circuit for segregating contrast signals into ON, OFF and ON-OFF channels [49], and the other is the neural circuit for detecting the direction of motion [50], both of which are major components of visual processing in advanced visual systems including insect compound eyes and vertebrate visual systems.

Formation of ON and OFF channels

Some classes of third-order neurons of vertebrates (retinal ganglion cells [76–78, 91]) and insect compound eyes [66] exhibit half-wave rectified, ON-depolarizing or OFF-depolarizing responses. These neurons form separate ON and OFF channels which specifically code for light increments and decrements, respectively. Some third-order neurons of vertebrate retinas [76, 77] and insect compound eyes [32, 66, 67] also show full-wave rectified, ON- and OFF-depolarizing responses, which form flicker-sensitive, ON-OFF channels. The reasons that signals for intensity changes are not transmitted by linear contrast detectors but by separate ON and OFF channels have been discussed by Shiller et al. [83], who pointed out that by having both ON and OFF channels, signals for both dimming and brightening can be transmitted without maintaining a high rate of spike discharges which require a high rate of metabolic activity. This allows for an economical coding of contrast. Mizunami [50] pointed out that the segregation of contrast signals into ON, OFF and ON-OFF channels can be explained if the synapses from second- to third-order neurons (second synapses) of these visual systems have a rectifying nature, as do those of cockroach ocelli (Fig. 17). Indeed, Toyoda [106] and Miller [47] proposed that the full-wave rectified response of ON-OFF amacrine cells of vertebrate retina can be explained if the cells receive half-wave rectified synaptic input from both ON and OFF bipolar cells. It is concluded that simple modification of dimming detection circuits is sufficient to explain the mechanisms to form ON and OFF channels.

Directionally-selective motion detection

Advanced visual systems such as insect compound eyes

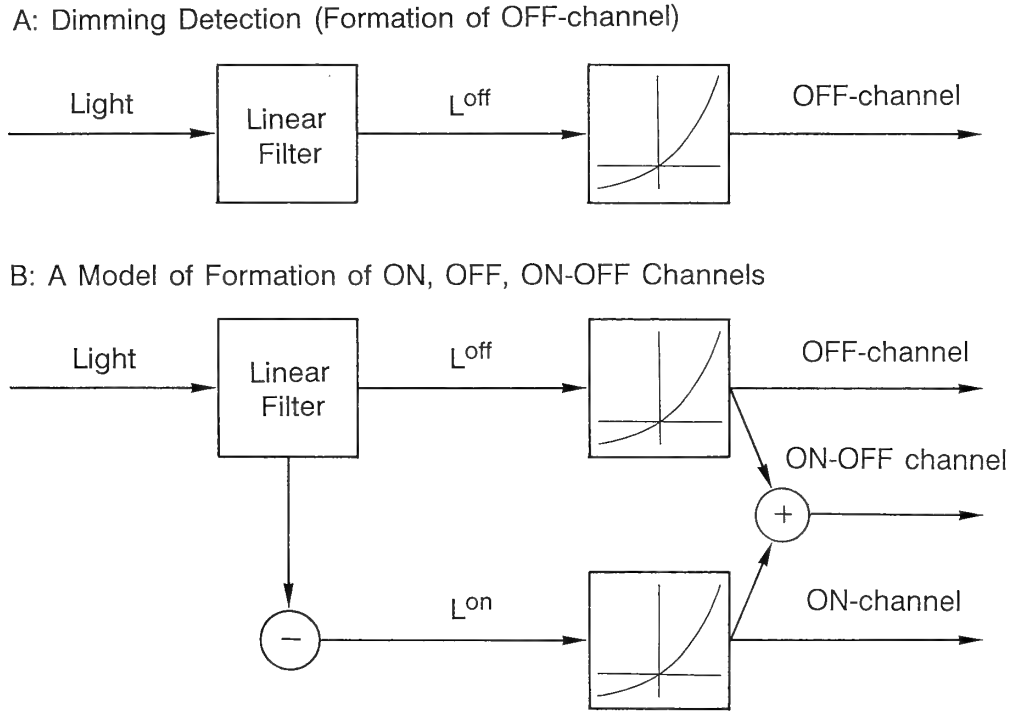

FIG. 17. Neural circuits for dimming detection and for formation of ON and OFF channels. (A) A circuitry model of dimming detection in the cockroach ocellar system, consisting of a sign-inverting bandpass linear filter followed by a synaptic rectifier with an exponential input-output relationship. The output of the linear filter, L^{off}, and that of the rectifier, OFF-channel, represents the response of second- and third-order ocellar neurons, respectively. (B) A model of a contrast detector which comprises the main structure of the movement detection circuit of Fig. 18A. L^{on} and L^{off} are on- and off-depolarizing linear responses, respectively. The outputs of the circuitry consist of three classes: on-, off-, and on-off depolarizing rectified responses. These specifically encode light increment, light decrement and flicker, respectively, and are indicated as ON, OFF and ON-OFF channels. Modified from Mizunami [50].

and vertebrate visual systems have movement detectors which code visual motion in a directionally selective manner. Behavioral and psychophysical studies show that movement detection by insects and humans can be represented by a mathematical algorithm referred to as a correlation model (Fig. 18C) [1, 27, 79]. The neural mechanism of this motion computation, however, has not been established as yet. Mizunami [50] described a model mathematically equivalent to the correlation-type movement detector (Fig. 18A). The main structure of the model is comprised of contrast detectors in Fig. 17B which consist of bandpass linear filters followed by synaptic rectifiers. Linear, one-directional, lateral interactions are assumed among the contrast detectors. Thus, the basic assumption of this model is that synapses between second- and third-order neurons of movement detection systems are nonlinear and rectifying, as are those of cockroach ocellar systems. Mizunami [50] showed that synaptic rectifiers convert linear spatial interactions into a multiplication-like (quadratic) interaction, which is the core of the correlation-type movement detector. One of the neural models, which contains both excitatory (additive) and inhibitory (subtractive) lateral interactions among contrast detectors (Fig. 18B), well approximates the correlation model (Fig. 18C, D) in both time-averaged and dynamic (instantaneous) responses. Some of the basic features of the model agree with those of actual movement detector neurons of insects [50].

Evolutionary perspective

I have shown that: (1) step-by-step modifications of simple photoreceptors are sufficient to explain the evolution of dimming-detection circuits of cockroach ocelli; (2) simple modifications and duplications of dimming-detection circuits are sufficient to explain contrast coding circuits with separate ON and OFF channels; and (3) simple modifications and duplications of contrast coding circuits with separate ON and OFF channels are sufficient to explain neural circuits for motion detection. These findings imply that complex neural circuits subserving advanced visual functions have evolved through step-by-step modifications of simper neural circuits subserving simpler visual functions, and that the present complex neural circuits contain, at least in part, simple neural circuits from which the present neural circuits have evolved. I conclude that careful comparison of neural circuits of

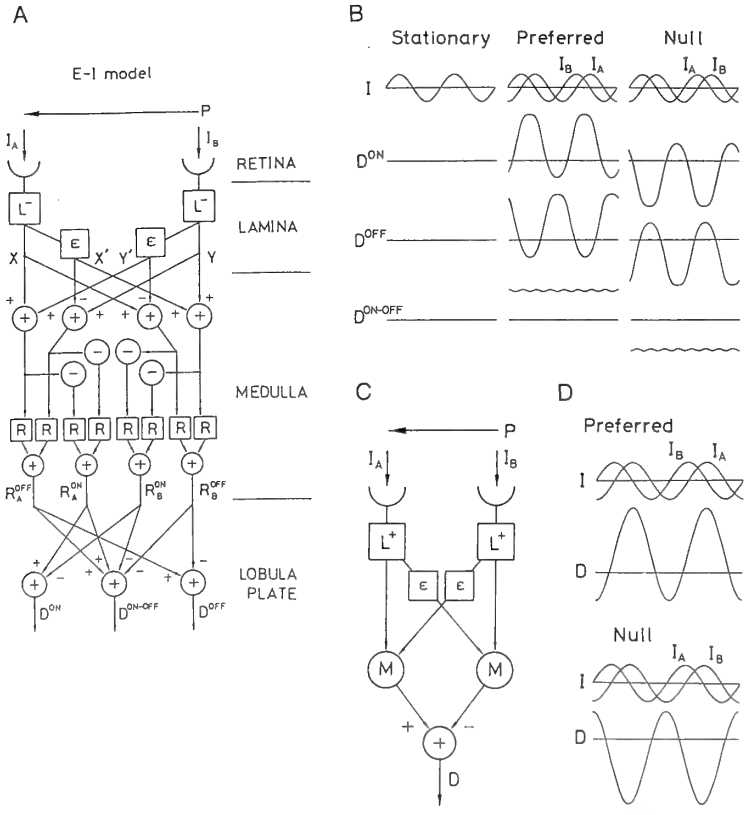

FIG. 18. Computational and neural models for motion detection. (A) A model of neural circuits for directional-selective motion detection. Possible location of each process in a fly's compound eye is illustrated (*right*). The model (E-I model) consists of one-directional linear interactions among contrast-detection circuits of Fig. 17B. The model involves both excitatory and inhibitory lateral interactions. I_A and I_B are inputs to left and right detectors. L^- is a sign-inverting bandpass linear filter, the output of which approximates the response of lamina monopolar cells. ε is a sign-conserving lowpass linear filter. R is a synaptic rectifier with an exponential input/output relationship. Lateral interaction and rectification may take place in the medulla neuropil. On- and off-depolarizing linear responses feed into rectifiers, producing on- and off-depolarizing rectified responses, R^{on} and R^{off}. R^{on} and R^{off} are assumed to represent responses of ON- and OFF-EMDs (elementary movement detectors). The final outputs of the models consist of three classes, D^{on}, D^{off} and $D^{on\text{-}off}$. The model outputs may represent responses of motion-sensitive neurons of the lobula plate. P is the preferred direction of motion. (B) Responses of the E-I model to a stationary flickering light and to a sinusoidal grating moving in the preferred and null directions. The ON-OFF motion detector ($D^{on\text{-}off}$ in A) exhibits a steady response to motion, whereas responses of ON and OFF motion detectors (D^{on} and D^{off}) oscillate, depending on the spatial phase of the stimulus pattern. The stimulus parameters are: 1) for response to motion in the preferred direction, the phase lag due to the spatial separation of left and right input channels, ϕ_s, is $\pi/2$ and the phase lag due to the delay in lateral interaction, ϕ_t, is $\pi/2$; 2) for response to motion in the null direction, $\phi_s=\pi/2$ and $\phi_t=-\pi/2$; and 3) for response to a stationary flickering light, $\phi_s=0$ and $\phi_t=\pi/2$. (C) The correlation model proposed by Hassenstein and Reichardt [27]. L^+ and ε are sign-conserving, lowpass linear filters. M is a multiplier. D is the final output. (D) Responses of the correlation model to a sinusoidal grating moving in the preferred and null directions. The stimulus parameters are the same as for (B). From Mizunami [50].

different animals is an effective approach to understanding possible evolutionary pathways by which complicated neural circuits of animal brains have formed.

ACKNOWLEDGMENTS

I thank Ms. Janet Kramer for helpful comments. My work is supported in part by the Uehara Memorial Foundation, the Naitoh Science Foundation and by grants from the Ministry of Education of Japan.

REFERENCES

1 Adelson EH, Bergen JR (1985) J Opt Soc Am A2: 284–299
2 Ammermüler J, Weiler R (1985) J Comp Physiol 157: 779–788
3 Baader A (1989) J Neurobiol 20: 519–529
4 Baylor DA, Fuortes MGF, O'Bryan PM (1971) J Physiol 214: 256–294
5 Baylor DA, Hodgkin AL (1974) J Physiol 242: 729–758
6 Chappell RL, DeVoe RD (1975) J Gen Physiol 65: 399–419
7 Chappell RL, Dowling JE (1972) J Gen Physiol 60: 121–147
8 Chappell RL, Naka K -I, Sakuranaga M (1985) J Gen Physiol 86: 423–453
9 Cornwell PB (1955) J Exp Biol 32: 217–237
10 Cooter RJ (1975) Int J Insect Morphol Embryol 4: 273–288
11 Dowling JE, Chappell RL (1972) J Gen Physiol 60: 148–165
12 Dreisig H (1980) Physiol Entomol 5: 327–342
13 Dubs A (1981) J Comp Physiol 144: 53–59
14 Eaton JL (1976) J Comp Physiol 109: 17–24
15 Eaton JL, Tignor KR, Holtzman GI (1983) Physiol Entomol 8: 371–375
16 Enroth-Cugell C, Freeman AW (1987) J Physiol 384: 49–79
17 French AS, Järvilehto M (1978) J Comp Physiol 126: 87–96
18 Fuortes MGF, Hodgkin AL (1964) J Physiol 172: 239–263
19 Goldsmith TH, Ruck PR (1958) J Gen Physiol 41: 1171–1185
20 Goodman LJ (1965) J Exp Biol 42: 385–407
21 Goodman LJ (1981) In "Handbook of sensory physiology". vol VII 6C. Eds by H Autrum, Springer-Verlag, Berlin, Heidelberg, New York, pp 201–286
22 Goodman CS, Williams JLD (1976) Cell tissue Res 175: 203–226
23 Gould JL (1975) Science 189: 685–693
24 Griss C, Rowell CHF (1986) J Comp Physiol 158: 765–774
25 Guy RG, Goodman LJ, Mobbs PG (1979) J Comp Physiol 134: 253–264
26 Gwilliam GF, Stuart AE (1990) J Exp Biol 151: 83–107
27 Hassenstein B, Reichardt W (1956) Z Naturforsch 11b: 513–524
28 Hayashi JH, Moore JW, Stuart AE (1985) J Physiol 368: 175–195
29 Hesse R (1908) Das Sehen der neideren Tiere. G Fischer, Jena
30 Hochstein S, Shapley RM (1976) J Physiol 262: 265–284
31 Hu KG, Reichert H, Stark WS (1978) J Comp Physiol 126: 15–24
32 Jansonius NM, Hateren JH van (1993) J Comp Physiol 172: 467–471
33 Kelly DH (1971) J Optical Soc Am 61: 537–546
34 Kirschfeld K, Lutz B (1977) Z Naturforsch 32c: 439–441
35 Klingman A, Chappell RL (1978) J Gen Physiol 71: 157–175
36 Knight BW (1972a) J Gen Physiol 59: 734–766
37 Knight BW (1972b) J Gen Physiol 59: 767–778
38 Knight BW, Toyoda J -I, Dodge FA (1970) J Gen Physiol 56: 421–437
39 Koontz MA, Edwards JS (1984) Cell Tissue Res 236: 133–146
40 Lall AB, Trouth CO (1989) J Insect Physiol 35: 805–808
41 Laughlin SB (1981) In "Handbook of sensory physiology", vol. VII/6B. Ed by H Autrum, Springer-Verlag, Berlin, Heidelberg, New York, pp 135–280
42 Laughlin SB, Hardie RC (1978) J Comp Physiol 128: 319–340
43 Laughlin SB, Howard J, Blakeslee B (1987) Proc R Soc Lond B 231: 437–467
44 Littlewood PMH, Simmons PJ (1992) J Comp Neurol 325: 493–513
45 Milde JJ (1981) J Comp Physiol 143: 427–434
46 Milde JJ (1984) J Comp Physiol 154: 683–693
47 Miller RF (1979) In "The Neuroscience: Fourth Study Program". Eds by FC Schmitt, FG Worden, The MIT press, Cambridge, pp 227–245
48 Mizunami M (1989) In "Neurobiology of Sensory Systems" Eds by NR Singh, NJ Strausfeld, Plenum Press, New York, pp 71–84
49 Mizunami M (1990a) J Gen Physiol 95: 297–317
50 Mizunami M (1990b) Biol Cybern 64: 1–6
51 Mizunami M Adv Insect Physiol (in press)
52 Mizunami M, Tateda H (1986) J Exp Biol 125: 57–70
53 Mizunami M, Tateda H (1988a) J Gen Physiol 91: 703–723
54 Mizunami M, Tateda H (1988b) J Exp Biol 140: 557–561
55 Mizunami M, Yamashita S, Tateda H (1982) J Comp Physiol 149: 215–219
56 Mizunami M, Tateda H, Naka K -I (1986) J Gen Physiol 88: 275–292
57 Mizunami M, Yamashita S, Tateda H (1987) J Exp Biol, 130: 259–274
58 Mizunami M, Weibrecht JM, Strausfeld NJ (1993) In "Biological neural networks in invertebrate neuroethology and robotics" Eds by RD Beer, R Ritzmann, T McKenna, Academic Press, San Diego, pp 199–225
59 Mote MI, Wehner R (1980) J Comp Physiol 137: 63–71
60 Naka K -I, Chan RY, Yasui S (1979) J Neurophysiol 42: 441–454
61 Naka K -I, Itoh M -A, Chappell RL (1987) J Gen Physiol 89: 321–337
62 Normann RA, Perlman I (1979) J Physiol 286: 509–524
63 Ohyama T, Toh Y (1986) J Exp Biol 125: 405–409
64 Ohyama T, Toh Y (1990a) J Comp Neurol 301: 501–510
65 Ohyama T, Toh Y (1990b) J Comp Neurol 301: 511–519
66 Osorio D (1987) J Comp Physiol 161: 431–440
67 Osorio D (1991) Visual Neurosci 7: 345–355
68 Pan KC, Goodman LJ (1977) Cell Tissue Res 176: 505–577
69 Pappas LG, Eaton JL (1977) J Insect Physiol 23: 1355–1358
70 Patterson JA, Chappell RL (1980) J Comp Physiol 139: 25–39
71 Pinter RB (1972) J Comp Physiol 77: 383–397
72 Purple RL, Dodge FA (1965) Cold Spr Harb Sym. Quant Biol 30: 529–537
73 Reichert H, Rowell CHF, Griss C (1985) Nature 315: 142–144
74 Rence BG, Lisy MT, Garves BR, Quinlan BJ (1988) Physiol Entomol 13: 201–212
75 Rowell CHF, Reichert H (1986) J Comp Physiol 158: 775–794
76 Sakai H, Naka K -I (1987a) J Neurophysiol 58: 1307–1328
77 Sakai H, Naka K -I (1987b) J Neurophysiol 58: 1329–1350
78 Sakuranaga M, Ando Y -I, Naka K -I (1987) J Gen Physiol 90: 229–259

79 Santen DPH van, Sperling G (1985) J Opt Soc Am A2: 300–321
80 Schäfer S, Bicker G (1986) J Comp Neurol 246: 287–300
81 Schricker B (1965) Z Vergl Physiol 49: 420–458
82 Schuppe H, Hengstenberg R (1993) J Comp Physiol 173: 143–149
83 Shiller PH, Sandell JH, Maunsell JHR (1986) Nature 322: 824–825
84 Shaw SR (1979) In "The Neurosciences: Fourth study program". Eds by FO Schmitt, FG Worden, MIT press, Cambridge, pp 275–295
85 Simmons PJ (1980) J Exp Biol 85: 281–294
86 Simmons PJ (1981) J Comp Physiol 145: 265–276
87 Simmons PJ (1982a) J Comp Physiol 147: 401–414
88 Simmons PJ (1982b) J Comp Physiol 149: 389–398
89 Simmons PJ J Comp Physiol (1993) 173: 635–648
90 Simmons PJ, Littlewood PMH (1989) J Comp Neurol 283: 129–142
91 Spekreijse H (1969) Vision Res 9: 1461–1472
92 Sprint MM, Eaton JL (1987) Ann Entomol Soc Am 80: 468–471
93 Stange G (1981) J Comp Physiol 141: 335–347
94 Stange G, Howard, J (1979) J Exp Biol 83: 351–355
95 Stockbridge N, Ross WN (1984) Nature 309: 266–268
96 Stone SL, Chappell RL (1981) Brain Res 221: 374–381
97 Strausfeld NJ (1976) Atlas of an insect brain. Springer-Verlag, Berlin Heidelberg New York
98 Strausfeld NJ, Bassemir UK (1985) Cell Tissue Res 240: 617–640
99 Stuart AE, Oertel D (1978) Nature 275: 287–290
100 Taylor CP (1981a) J Exp Biol 93: 1–18
101 Taylor CP (1981b) J Exp Biol, 93: 19–31
102 Toh Y, Hara S (1984) J Ultrastruct Res 86: 135–148
103 Toh Y, Kuwabara M (1975) J Neurocytol 4: 271–287
104 Toh Y, Sagara H (1984) J Ultrastruct Res 86: 119–134
105 Toh Y, Tateda H (1991) Zool Sci 8: 395–413
106 Toyada J -I (1974) J Gen Physiol 63: 214–234
107 Tranchina D, Gordon J, Shapley R (1983) J Gen Physiol 82: 573–598
108 Weber G, Renner M (1976) Cell Tissue Res 168: 209–222
109 Weckström M, Juusola M, Laughlin SB (1992) Proc R Soc Lond B 250: 83–89
110 Werblin FS (1972) Ann NY Acad Sci 193: 75–85
111 Wilson M (1978a) J Comp Physiol 124: 297–316
112 Wilson M (1978b) J Comp Physiol 124: 317–331

ZOOLOGICAL SCIENCE 11: 191–202 (1994)

Output Effect of Identified Ascending Interneurons upon the Abdominal Postural System in the Crayfish *Procambarus Clarkii* (Girard)

HITOSHI AONUMA[1], TOSHIKI NAGAYAMA[1] and MITUHIKO HISADA[2]

[1]*Animal Behaviour and Intelligence, Division of Biological Sciences, Graduate School of Science, Hokkaido University, Sapporo, 060 and,* [2]*Faculty of Industrial Science and Technology, Science University of Tokyo, Oshamanbe, Hokkaido, 049-35, Japan*

ABSTRACT—The output effects of 16 identified ascending interneurons originating in the terminal abdominal ganglion were examined with intracellular recording and stimulating techniques in isolated nerve cord composed of 6 abdominal ganglia (from the 1st to 6th ganglion). The activity of the uropod closer and opener motor neurons was recorded extracellularly with pin electrodes from the terminal abdominal (A6) ganglion and that of the abdominal extensor and flexor motor neurons was recorded from the 1st to 5th abdominal (A1-A5) ganglion. This technique allowed us to monitor the activity of the motor neurons innervating different muscles of more than 10 simultaneously in the same preparation. Majority of ascending interneurons had output effects upon not only the uropod motor neurons but also the abdominal postural motor neurons. The premotor effects of the ascending interneurons were the same in all of abdominal ganglia (A1-A5). Some ascending interneurons also affected the abdominal postural motor neurons on both sides of each ganglion with a similar fashion. Neurobiotin staining revealed that the ascending axons spreaded their branches in each abdominal ganglion. Their branches were extended within the side ipsilateral to their axons. The possible function of ascending interneurons as multi-functional units in the sensory-motor system of crayfish was discussed. Since they received sensory inputs from the tailfan and affected the activity of both uropod and abdominal postural motor neurons simultaneously, they would coordinate the behavioural sequence controlling both the uropod motor system and abdominal postural system.

INTRODUCTION

The central nervous system (CNS) of arthropod animals, like insects and crustacean, consists of a series of segmental ganglion chained by a pair of connectives [e.g. 1]. Each ganglion is bilaterally symmetrical and contains most of motor neurons for its relevant segment. A segmental movement is basically controlled by local circuit within its relevant ganglion [2], then a series of movement and postural changes must be coordinated by intra- and intersegmental activation of different muscles [16, 31, 32].

For example, crayfish avoidance reaction consists of serially ordered behavioural acts [26]. Unilateral mechanical stimulation of the tailfan elicited a rapid closing movement of uropods followed by the completion of locomotor acts with a change in abdominal posture and pattern generation of walking legs. This assembly of elementary acts must be activated sequentially at the level of central neurons, since few afferents projected anteriorly through the abdominal nerve cord [11]. Neural elements controlling uropod motor system and abdominal postural system have been so far analyzed respectively. Motor neurons in each system have been identified [24, 36 in uropod motor neurons; 8, 17, 40 in abdominal postural motor neurons]. A vast number of premotor interneurons which affected the activity of motor neurons has been also characterized both physiologically and morphologically [20–22, 25 in uropod system; 13,18, 19, 37 in abdominal postural system]. Many of earlier behavioural and physiological works have expected that certain interneurons would contribute to the segmental linking between uropod and abdominal movement, though no attempt has been carried out to clarify this point.

About 65 pairs of ascending interneurons originating in the terminal abdominal ganglion of the crayfish [10, 33] have ascending axons through the anterior abdominal connective and receive sensory inputs directly from the tailfan [23, 34]. Twenty-four ascending interneurons are identified as unique individuals, and many of them affect the activity of the antagonistic sets of uropod motor neurons [21]. These identified ascending interneurons should be, therefore, the most possible candidate to mediate intersegmental coordination between uropod and abdominal movement. The present study examined this hypothesis to characterize their output effects upon the abdominal postural motor neurons.

Our results show the majority of ascending interneurons have premotor effects upon the abdominal postural motor neurons from the 1st to 5th abdominal ganglion as well as upon the uropod motor neurons. The homologous postural motor neurons throughout the anterior abdominal ganglia are affected in a similar fashion by ascending interneurons.

Accepted March 25, 1994
Received Feburary 3, 1994

MATERIALS AND METHODS

Animals and preparations

Adult male and female crayfish, *Procambarus clarkii* (Girard) (5–9 cm body length from rostrum to telson) were used in all experiments. They were obtained commercially and maintained in laboratory tanks before use.

Abdominal nerve chain including all abdominal (A1-A6) ganglia with relevant nerve roots was isolated from the abdomen. This preparation was pinned, ventral side up, to the floor of a Sylgard-lined Petri dish and perfused continuously with cooled physiological saline [38].

Extracellular recording and stimulation

The activity of motor neurons innervating closer and opener muscles of exopodite was recorded extracellularly by using pin electrodes from the 2nd and 3rd motor root in the terminal (6th) abdominal ganglion respectively [25]. In the anterior abdominal ganglia (from the 1st to 5th ganglion), the activity of tonic extensor motor neurons was recorded from the 2nd root and the activity of tonic flexor motor neurons was recorded from the superficial 3rd root of each ganglion. The pin electrodes were placed contact with each nerve root and insulated with petroleum jelly (Vaseline : liquid paraffin=3 : 1 in the volume) to perform multi-recording from a single preparation (Fig. 1).

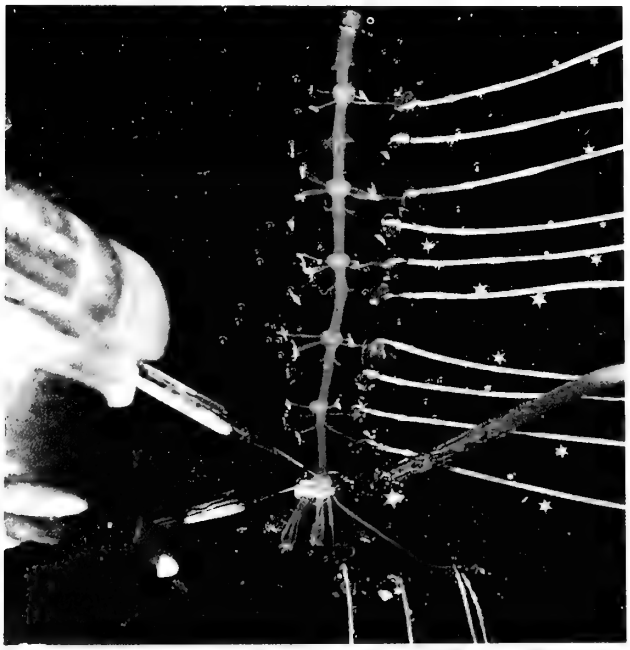

Fig. 1. The picture of experimental arrangement with extracellular and intracellular electrodes. The abdominal nerve cord was dissected out from the 1st to terminal abdominal (A6) ganglion. The motor activities of the uropod and abdominal postural system were monitored from relevant motor nerve root with pin electrodes. Electrical stimulation was delivered to the 2nd root afferents of the terminal abdominal ganglion by the bipolar electrode. The intracellular recording and stimulation was made from the terminal abdominal ganglion.

Each motor neuron of the tonic abdominal postural system was identified by its spike amplitude and firing pattern of the extracellular recordings [4, 7, 8, 40]. Six tonic extensor motor neurons (EX) and 6 tonic flexor motor neurons (FL) were numbered in order of increasing spike size (i. e. No. 1 is the smallest and No. 6 is the largest). The second largest spike in each extensor or flexor motor neuron was the peripheral inhibitor, No. 5. In *in vitro* preparation, the peripheral inhibitor of the extensor motor neurons (No. 5) showed tonic discharge, although the largest unit of the extensor excitors (No. 6) did not fire spontaneously [37]. On both of the extensor and flexor excitor units, No. 3 and 4 and No. 1 and 2 were similar in amplitude within each grouping and thus were distinguishable as single unit, i. e., there were two No. 3/4 and two No. 1/2 spikes [15]. The premotor effect of ascending interneurons upon the abdominal postural motor neurons was judged to be excitatory if depolarizing current injected into the interneuron elicited or increased tonic spikes of excitors (No. 1/2, No. 3/4, and No. 6) and/or decreased tonic spikes of the inhibitor (No. 5). Inhibitory interaction was identified by the decrease in tonic spikes of excitors and/or the increase in tonic spikes of inhibitor. When the current injection caused no change in activity of motor neurons, the ascending interneuron was judged to have no obvious output effect.

The mechanosensory afferents (2nd root) innervating the right exopodite [3] were stimulated electrically by the bipolar stimulating pin electrode. Square pulses of 0.1 ms duration at 20 Hz were delivered to the stimulating electrode. Stimulus intensity was determined to be appeared that spikes of closer motor neuron increased and spikes of opener motor neurons decreased.

Intracellular recording and staining

Intracellular recordings were made with glass microelectrodes filled either with a 3% solution of Lucifer yellow CH [35] with 0.1 M lithium chloride (100 to 150 MΩ resistance) or a 3% solution of neurobiotin [9] with 1 M potassium chloride (40 to 80 MΩ resistance). Interneurons were always impaled in the right half of the neuropiler processes or axons in the terminal abdominal ganglion. A constant polarizing current could be injected into interneurons through the recording electrode by a bridge circuit to characterize their premotor effects upon both the uropod and abdominal postural motor neurons. In most records, the monitor of membrane potential of ascending interneurons during current injection, especially that of depolarization, was difficult because of extremely high resistance, so only the monitor of current was displayed.

After physiological examination, Lucifer yellow was injected into the interneuron with hyperpolarizing current pulses of 10 nA of 500 msec in duration at 1 Hz for 20 min. The ganglion was then fixed in a 10% formalin for 20 min, dehydrated with an alcohol series and cleared with methyl salicylate. Ascending interneurons were observed using a fluorescence microscope in whole mount, and photographed for subsequent reconstruction.

Neurobiotin was injected into the interneuron with depolarizing current pulse of 10 nA of 500 msec duration at 1 Hz for 3 hr. The preparations were then diffused for 10 hr at room temperature and fixed in a 10% formalin over 1 hr. They were dehydrated and immersed in methyl salicylate for 30 min to increase staining intensity and reduce background staining. They were rehydrated with an alcohol down series, rinsed with detergent A: 0.01% Triton X-100 and 0.01% Tween 20 in 0.15 M sodium phosphate buffer solution (pH 7.4) (PBS), and immersed in detergent B (2% Triton X-100 and 2% Tween 20 in PBS) for 90 min. After rinsed with detergent A 3 times for 5 min each, they were incubated in HRP conjugated streptavidin for 30 min. They were rinsed with detergent A 3 times for 15 min each, immersed in 0.025% diaminobenzidine (DAB) in PBS for 20 min and reacted with DAB and H_2O_2 (0.003%) in PBS.

After rinsed with DW several times, they were dehydrated and cleared. Ventral up views of the dye-filled cells were drawn with the aid of a camera lucid.

Each ascending interneuron in this study was identified as the criteria described previously [21]. According to their gross morphology (including soma position, number of main branches and axonal projection in the connective) and physiological properties (input from sensory afferents and output to uropod, closer and opener motor neurons), 24 ascending interneurons were divided into 6 classes; co-activating (CA), co-inhibiting (CI), reciprocally closing (RC), reciprocally opening (RO), no effective (NE) and variably effective (VE) interneurons. In total, 103 crayfish were studied in this paper and 78 ascending interneurons were identified and analyzed their output effect upon abdominal postural motor neurons. Other types of ascending interneurons were encountered only once and were not described here.

All the recordings were stored on a digital tape recorder (Biologic DTR-1801) and displayed using a chart recorder (Gould TA240S).

RESULTS

Serially ordered motor pattern elicited by stimulation of the uropod

Mechanical stimulation of the exopodite in small crayfish (less than 8 cm in length from rostrum to telson) frequently produced avoidance "dart" response ($P<0.0001$ with Chi square test) (Fig. 2A). The animals showed bilateral closing of uropods and forward walking with abdominal extension.

Repetitive electrical stimulation of the 2nd root afferents which innervated hairs on the surface of the exopodite increased the spike frequency of the closer motor neurons and decreased that of the opener motor neurons on the

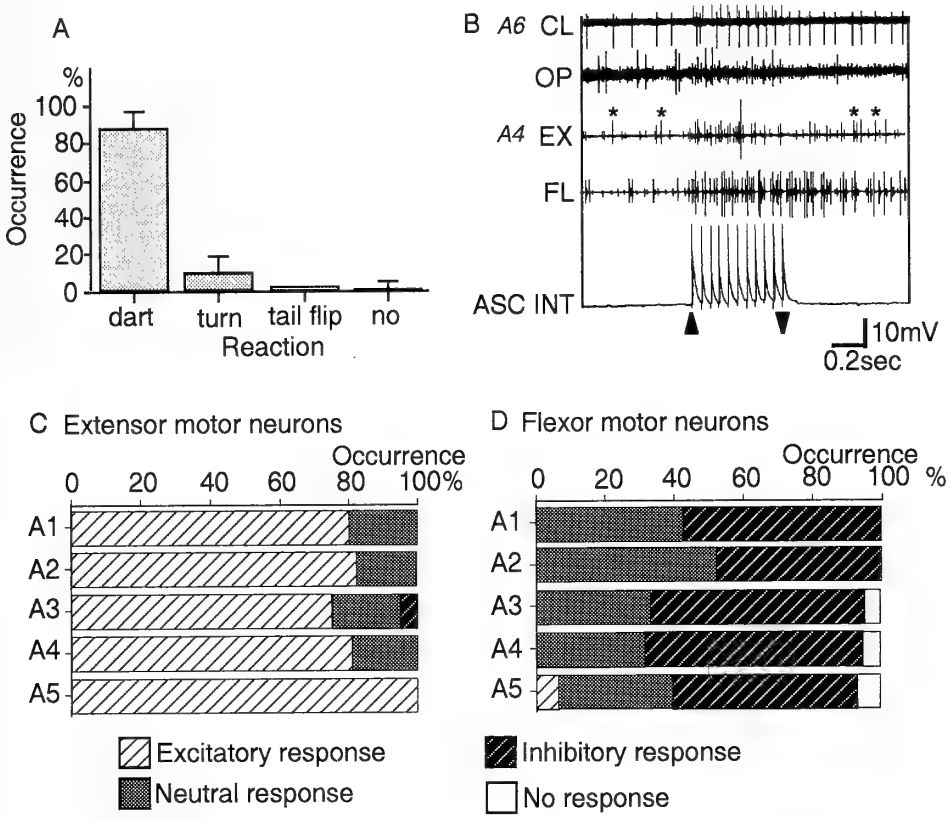

FIG. 2. Effect of sensory inputs upon the abdominal postural motor neurons. A. Patterns of crayfish reactions in response to unilateral mechanical stimulation of the exopodite. Twenty-five animals were used in the test and 20 trials were made in each. Observed reactions of the animals were categorized as one of four types: dart, turn, tailflip and no response [26]. B. Typical pattern of spike activity of motor and interneurons in response to the repetitive electrical stimulation (20 Hz) of the 2nd root afferent innervating the exopodite (indicated by arrowheads). The 1st and 2nd traces were extracellular recordings from the uropod, closer and opener motor neurons in the terminal abdominal ganglion. The 3rd and 4th traces were from the extensor and flexor motor neurons in the 4th abdominal ganglion. The spike unit indicated by asterisks in the 3rd trace was tonic extensor inhibitor (No. 5). The 5th trace was intracellular recording of the ascending interneuron (ASC INT) from the terminal ganglion. C and D. Pattern of the activity of the abdominal postural motor neurons (C: tonic extensor motor neurons, D: tonic flexor motor neurons) from the 1st to 5th abdominal ganglion (A1-A5) in response to electrical stimulation of the 2nd root afferents. The results were based on 21 preparations. The pattern of motor response was judged to be excitatory if stimulation of the afferents elicited or increased the spikes of excitors and/or decreased the spikes of the inhibitor. Inhibitory response was identified by the decrease in the spikes of excitors and/or the increase in the spikes of inhibitor. Neutral response was defined as when both the excitatory and inhibitory motor neurons were excited simultaneously.

TABLE 1. Summary of output effects of the identified ascending interneurons upon the abdominal postual motor neurons and uropod motor neurons

ASC INT	n	A1		A2		A3		A4		A5		A6		INPUT
		EX	FL	EX	FL	EX	FL	EX	FL	EX	FL	CL	OP	
CA-1	3	E	E	E	E	E	E	E	E	?	?	E	E	EPSP
CI-1	3	E	E	E	E	E	E	E	E	E	E	I	I	EPSP
RC-2	6	E	I	E	I	E	I	E	I	E	I	E	I	EPSP
RC-3	3	E	E	E	E	E	E	E	E	E	E	E	I	EPSP
RC-4	3	I	E	I	E	I	E	I	E	I	E	E	I	EPSP
RC-6	6	E	E	E	E	E	E	E	E	E	E	E	I	EPSP
RC-7	2	E	I	E	I	E	I	E	I	E	I	E	I	EPSP
RC-8	7	E	E	E	E	E	E	E	E	E	E	E	I	EPSP
RO-2	2	I	E	I	E	I	E	I	E	I	E	I	E	EPSP*
RO-3	2	I	E	I	E	I	E	I	E	I	E	I	E	EPSP*
RO-4	5	I	E	I	E	I	E	I	E	I	E	I	E	IPSP
RO-5	2	E	E	E	E	E	E	E	E	E	E	I	E	EPSP
RO-6	5	E	I	E	I	E	I	E	I	E	I	I	E	EPSP
VE-1	19	E	I	E	I	E	I	E	I	E	I	V	V	EPSP
NE-1	7	E	E	E	E	E	E	E	E	E	E	N	N	EPSP
NE-2	3	N	N	N	N	N	N	N	N	N	N	N	N	EPSP

n: Sampling number of ascending interneurons E: Excitatory effect; output effect upon the abdominal postural motor neurons was judged to be excitatory if current injection elicited or increased the spikes of excitors and/or decreased the spikes of inhibitor. I: Inhibitory effect; inhibitory effect was identified by the decrease in the spikes of excitors and/or the increase in the spikes of inhibitor. V: Variable effect; when the current injection caused inconstant change in the activity of motor neurons, the ascending interneuron was judged to be variable effect. N: No effect; when the current injection caused no change in the activity of motor neurons, the ascending interneuron was judged to be no effect. ?: No record *: Interneurons showed antifacilitation when repetitive electrical stimulation (20 Hz) was applied.
Input of each interneuron was characterized by the electrical stimulation of the 2nd root afferents of terminal abdominal ganglion on the side ipsilateral to axons of interneurons.

stimulating side (Fig. 2B). At the same time, the activity of the abdominal postural motoneurons was also changed by the electrical stimulation. On the extensor motor neurons from the 1st to 5th abdominal ganglion, inhibitory motor neuron (No. 5) decreased the spike frequency and excitatory motor neurons increased the spike frequency ($P<0.0001$ with Chi square test) (Fig. 2C). The response of the flexor motor neurons was somewhat variable, but the spike frequency of the flexor inhibitor (No. 5) was usually increased (Fig. 2D). Thus, mechanosensory stimulation elicited abdominal extension-like motor pattern in the anterior abdominal ganglia as well as closing pattern of the uropod in the terminal abdominal ganglion.

Output effects of ascending interneurons upon abdominal postural motor neurons

Since the majority of branches in the sensory afferents ended in the terminal abdominal (A6) ganglion [11], the change in the activity of the abdominal postural motor neurons induced by sensory stimulation (Fig. 2C and D) was mediated by certain interneurons with intersegmental projection. Ascending interneurons originating in the terminal abdominal ganglion had intersegmental ascending axon and received sensory inputs directly from the afferents [21]. In this study, 16 identified ascending interneurons were characterized by their premotor effects upon both the extensor and flexor motor neurons from the 1st to 5th abdominal (A1-A5) ganglion (Table 1).

Of 16 identified ascending interneurons, 15 interneurons had output effect upon the abdominal postural motor neurons. Seven interneurons excited both the extensor and flexor motor neurons co-actively. Four interneurons had excitatory effects upon the extensor motor neurons and inhibitory effects upon the antagonistic flexor motor neurons. Another four interneurons had excitatory effects upon the flexor motor neurons and inhibitory effects upon the extensor motor neurons. One identified interneuron (NE-2) had no obvious effect upon the abdominal postural motor neurons.

Interneurons with co-activating effect

Ascending interneurons identified as CA-1, CI-1, RC-3, RC-6, RC-8, RO-5 and NE-1 [21] activated both the extensor and flexor motor neurons (Table 1).

For example, CA-1 was identified by its soma location of rostralateral region and two main neurites projected laterally (Fig. 3A). Physiologically, this interneuron excited both the closer and opener motor neurons (not shown). In the 1st abdominal ganglion, tonic spikes of extensor inhibitor (No. 5) were inhibited by the passage of depolarizing current (top in Fig. 3B). At the same time, this interneuron increased the

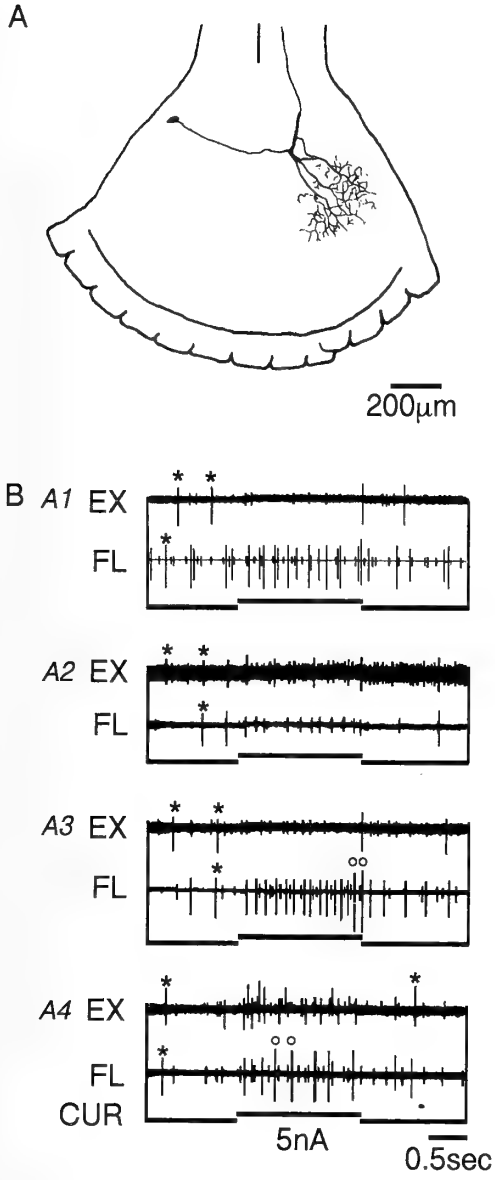

FIG. 3. Output effect of CA-1. A. Morphology of CA-1 in the terminal ganglion. Interneuron was drawn within the outline of the ganglion to show its relative position in the ganglion. B. Output effect of CA-1 upon both the extensor (EX) and flexor (FL) motor neurons in the abdominal (A1-A4) ganglia. In this paper, the spike unit indicated by asterisks was tonic extensor or flexor inhibitor (No. 5) and circles was the largest spike unit of excitor (No. 6).

spike frequency of the flexor excitors (No. 1/2 and 3/4). In the 2nd abdominal ganglion, this interneuron increased the spike frequency of the extensor excitors (No. 3/4). At the same time, the flexor excitors spiked and tonic spikes of the flexor inhibitor were suppressed during current injection. In the 3rd abdominal ganglion, tonic spikes of extensor inhibitor (No. 5) were inhibited while those of flexor excitors (No. 1/2 and 3/4) were increased. In the 4th abdominal ganglion, this interneuron increased tonic spikes of excitors of both the extensor and flexor motor neurons. Thus, CA-1 excited the excitors of both the extensor and flexor motor neurons and inhibited the extensor inhibitors of from the 1st to 4th abdominal ganglion, though we could not test the effect of the interneuron upon the 5th abdominal ganglion (Fig. 3B).

NE-1 was characterized by its thick axon and the limited extent of main branches (Fig. 4A). Neurobiotin staining showed that the ascending axon ran through, at least, the 4th abdominal ganglion. In the 5th abdominal ganglion, several small branches projected mainly medially from the axon. No axonal branches, however, crossed the midline. Physiologically, NE-1 had no obvious output to the uropod motor neurons. The spike frequency of either closer or opener motor neurons did not change significantly even if depolarizing current of high intensity was injected into the interneuron (12 nA in Fig. 4B). This interneuron, however, affected the abdominal postural motor neurons in the anterior abdominal ganglia. In each abdominal ganglion (A1-A5), the passage of depolarizing current increased the spike activity of both the extensor and flexor excitors (Fig. 4C). Thus, NE-1 had output effect upon the abdominal postural motor neurons, though it had no effect upon the uropod motor neurons. NE-2 (not shown) was another identifiable ascending interneuron which had no output effect upon the uropod motor neurons [21]. In this study, NE-2 was obtained three times but no output effect upon the abdominal postural motor neurons was recognized.

The other interneurons, CI-2, RC-3, RC-6, RC-8 and RO-5 had similar co-activating effect upon the antagonistic extensor and flexor motor neurons, though their effects upon the uropod motor neurons were variable (Table 1).

Interneurons with extension effect

Four identified interneurons, RC-2, RC-7, RO-6, and VE-1 [21], elicited abdominal extension-like motor pattern. For example, RC-2 was characterized by its looped primary neurite from the soma (A6 in Fig. 5A) and the output effect of reciprocally closing pattern upon the uropod motor neurons (Fig. 5B). This interneuron could produce closing movement of exopodite. Neurobiotin staining revealed the morphology of ascending axon through the 3rd abdominal ganglion (Fig. 5A). Many small branches extended both medially and laterally within the axon side of the interneuron in each anterior ganglion. When the depolarizing current was injected into RC-2, this interneuron increased the spike frequency of the flexor inhibitor (No. 5) in all anterior abdominal ganglia (A1-A5) with the inhibition of the spikes in the flexor excitors (Fig. 5C). At the same time, this interneuron significantly increased the spike frequency of the extensor excitors, especially those in the posterior ganglia (A4 and A5). In the 1st abdominal ganglion, this interneuron decreased the frequency of small extracellular spikes (No. 1/2) in the extensor excitors but increased that of intermediate spikes (No. 3/4) (top in Fig. 5C). RC-7 had similar output effect to RC-2 upon both the uropod and abdominal postural motor neurons, while RO-6 had reversed effect upon the uropod motor neurons (Table 1).

VE-1 was identified by its characteristic shape of the

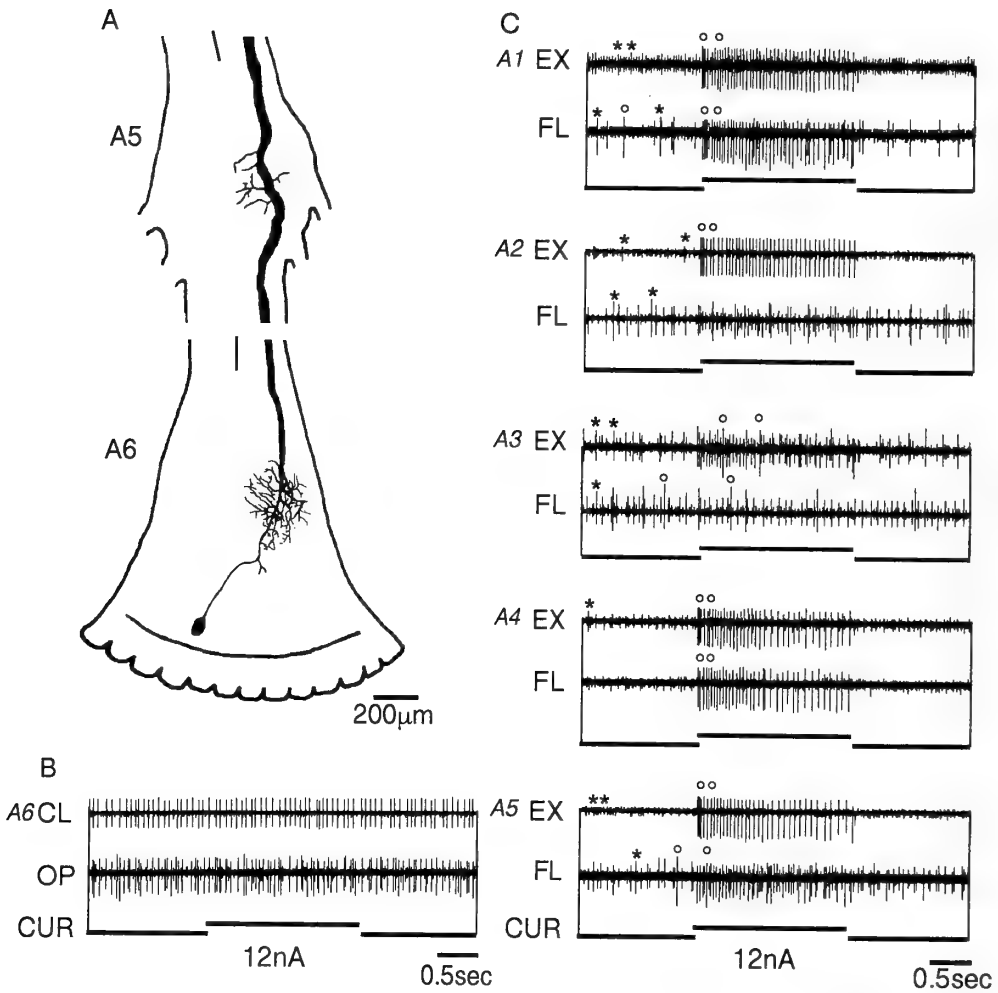

FIG. 4. Output effect of NE-1. A. Morphology of NE-1 in the 5th and terminal (A6) abdominal ganglion. The projection of the axonal branches (A5) was in the ipsilateral neuropil only. B. Output effect of NE-1 upon both the closer (1st trace) and opener (2nd trace) motor neurons. C. Output effect of NE-1 upon both the extensor and flexor motor neurons in the abdominal (A1-A5) ganglia.

most posterior secondary neurite crossing the midline (A6 in Fig. 6). Neurobiotin staining revealed that the ascending axon of VE-1 projected into at least the 2nd to 3rd abdominal connective. In each anterior abdominal ganglion (A5, 4 or 3), several small branches extended from the axon within the unilateral half of the neuropil (Fig. 6A). The extent and number of axonal branches in each ganglion were similar. The anterior, medial and posterior branches projected both medially and laterally. These axonal branches were usually extended within the ventral half of the neuropil (Fig. 6B, C). One of the physiological characteristics of VE-1 was variable output effect upon the uropod motor neurons [21]. In this study, VE-1 was impaled 19 times but their effects upon the uropod motor neurons were inconsistent: 3 interneurons activated both the closer and opener motor neurons while 13 interneurons activated the closer motor neurons and inhibited the antagonistic opener motor neurons. The remaining 3 interneurons had no effect upon the uropod motoneurons. The output effect upon the abdominal postural motor neurons was, by contrast, consistent in almost all preparations. On 17 occasions, this interneuron decreased spike frequency of the extensor inhibitor with the increase in the activity of the extensor excitors (No. 3/4) in all the anterior ganglia (Fig. 7A). At the same time, tonic spikes of the flexor excitors (No. 3/4) in all the anterior ganglia were inhibited with the increase in the spikes of the flexor inhibitor. Another 2 VE-1 had no effect upon the postural motor neurons in any anterior ganglia. In many cases, VE-1 also affected the postural motor neurons on the contralateral side. The output effect was the same as that upon the ipsilateral postural motor neurons and elicited reciprocal extension-like pattern from the 1st to 5th abdominal ganglion (Fig. 7B).

Interneurons with flexion effect

Four identified ascending interneurons, RC-4, RO-2, RO-3 and RO-4 [21], elicited abdominal flexion-like motor pattern. For example, figure 8A showed the morphology of RO-2 in the terminal abdominal ganglion. Physiologically, RO-2 showed antifacilitation in responses to repetitive electrical stimulation of the afferents. Spikes followed only the

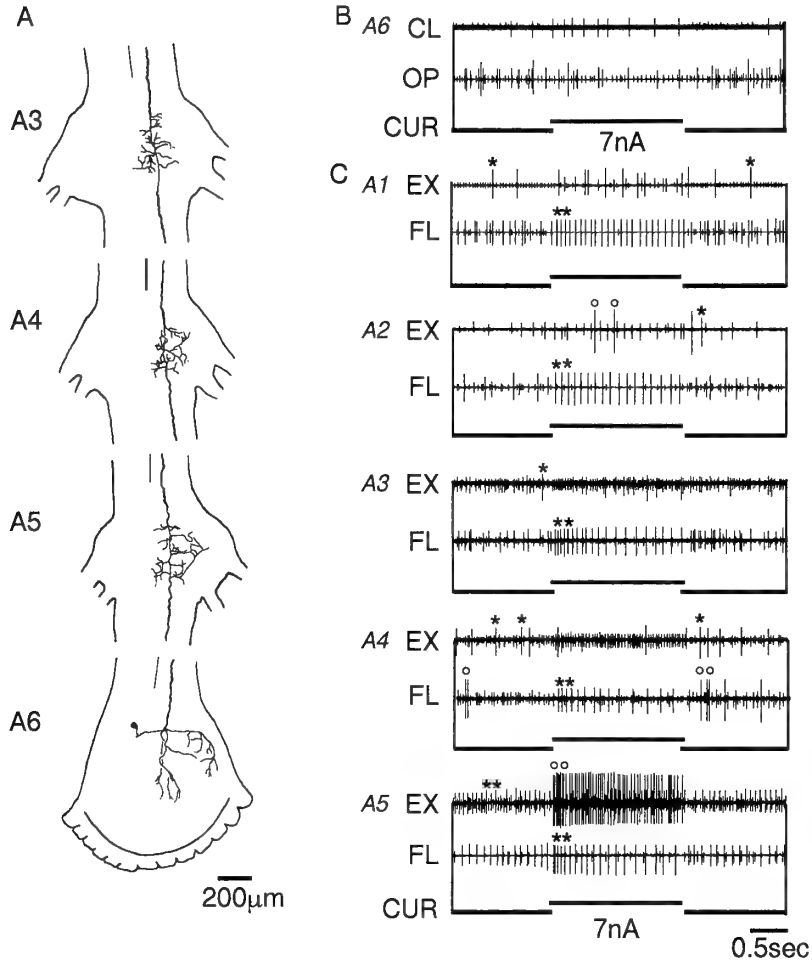

FIG. 5. Output effect of RC-2. A. Morphology of RC-2 from the 3th to terminal (A3-A6) abdominal ganglion. The projection of the axonal branches in each abdominal ganglion (A1-A5) was in the ipsilateral neuropil only. B. Output effect of RC-2 upon both the closer and opener motor neurons. C. Output effect of RC-2 upon both the extensor and flexor motor neurons in the anterior abdominal (A1-A5) ganglia.

1st stimulus and then continuously depressed after the 2nd stimulus (Fig. 8B). When the depolarizing current was injected into RO-2, tonic spikes of the opener motor neurons increased while those of the closer motor neurons decreased (not shown). At the same time, this interneuron increased the spike frequency of extensor inhibitor (No. 5) and also activated that of the flexor excitors (No. 3/4 and 6) in all the anterior abdominal ganglia (Fig. 8C). Another 3 interneurons, i.e., RC-4, RO-3, RO-4, had similar output effects upon the abdominal postural motor neurons, though the effect of RC-4 upon the uropod motor neurons was opposite from other interneurons (Table 1).

DISCUSSION

Output effect of ascending interneurons upon abdominal postural system

This study has demonstrated that many identified ascending interneurons originating in the terminal abdominal ganglion of the crayfish [21] have premotor effects upon the abdominal postural motor neurons in the anterior abdominal ganglia. Each interneuron controlled the homologous postural motor neurons from the 1st to 5th abdominal ganglia simultaneously in the same way (Table 1). For example, if the extensor excitors in the 5th abdominal ganglion were excited by a particular interneuron, the activity of extensor excitors in the remaining abdominal ganglia (A1-A4) were also increased. These physiological results suggested that the axons of ascending interneurons ran through the abdominal connective and projected into thoracic or more anterior ganglia. Neurobiotin staining could reveal the intersegmental structure of ascending interneurons, since this dye spreaded rapidly for a long distance (about 3 cm). The ascending interneurons extended several axonal branches with similar projection in each anterior ganglion (e.g. Fig. 6), though we could not trace the whole structure of interneurons.

The patterns of output effects of ascending interneurons upon the abdominal postural motor neurons were divided into three types. About half of interneurons encountered in this study (7 out of 16 interneurons) co-actively excited both

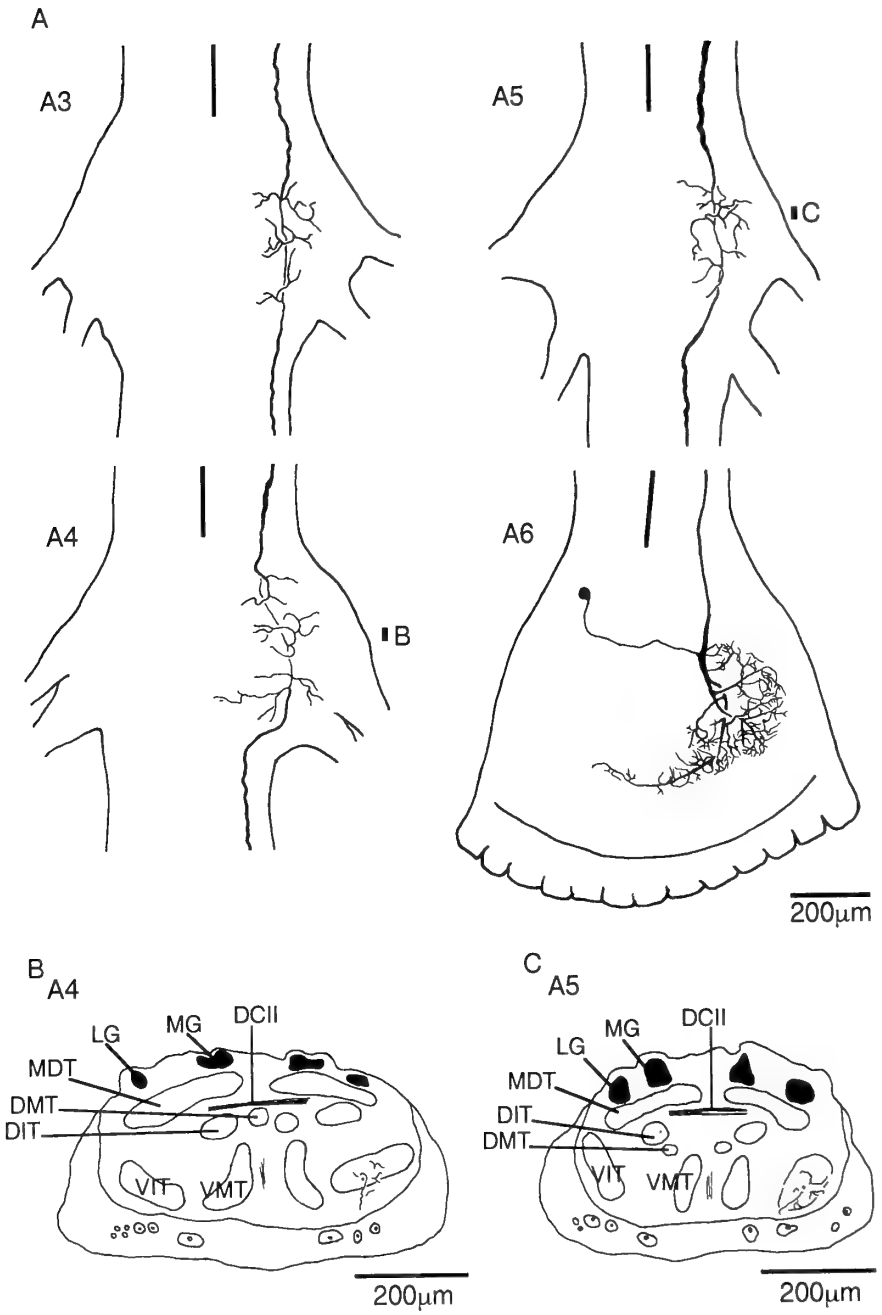

FIG. 6. Morphology of VE-1. A. Morphology of ascending interneuron VE-1 in the 3rd (A3), 4th (A4), 5th (A5), and terminal (A6) ganglion. The projections of the axonal branches in the anterior abdominal ganglia (A3-A5) were in the ipsilateral neuropil only. B, C. Drawing of sections (20 μm) of the 4th and 5th abdominal ganglion. Transverse sections arranged from the homologous part of each ganglion. The axon of VE-1 in each ganglion ran through ventral intermediate tract and project axonal branches both medially and laterally. DC II,dorsal commissure II; DIT, dorsal intermediate tract; DMT, dorsal medial tract; LG, lateral giant; MDT, medial dorsal tract; MG, medial giant; VIT, ventral intermediate tract; VMT, ventral medial tract.

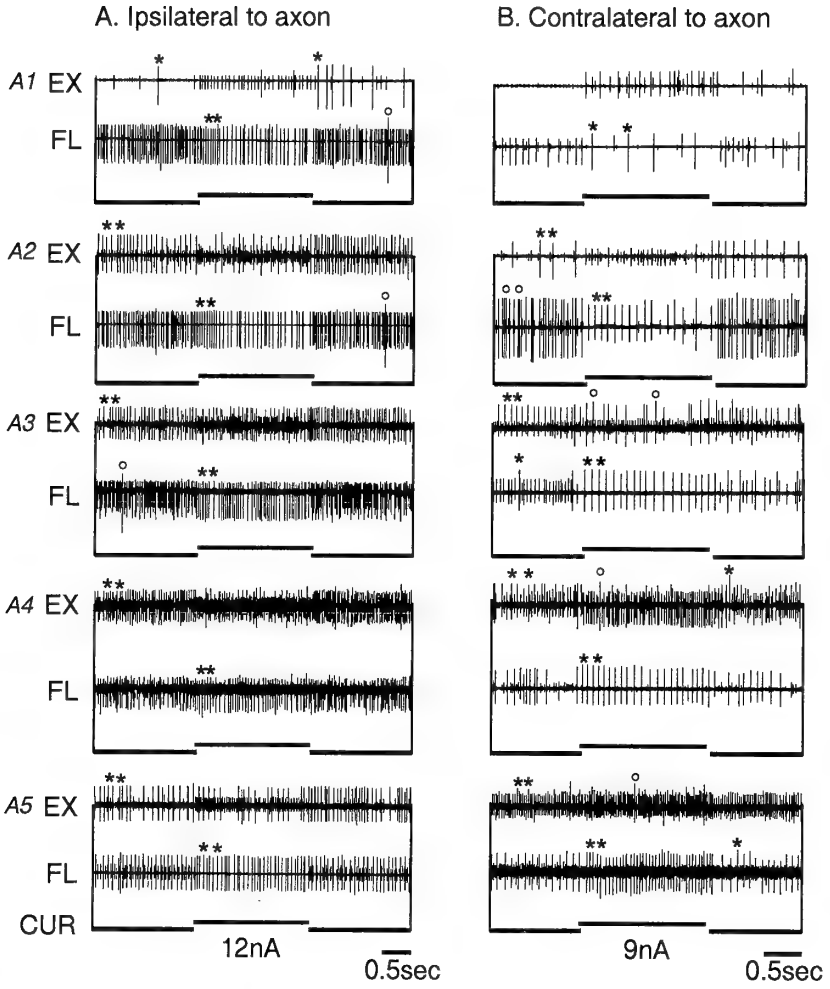

FIG. 7. Output effect of VE-1 upon abdominal postural motor neurons. A. Activity change of extensor (1st trace in each ganglion) and flexor (2nd trace in each ganglion) motor neurons on the side ipsilateral to the axonal branches of VE-1. The response of motor neurons from the 1st to 5th abdominal ganglion was drawn succeedingly. B. The response of postural motor neurons on the opposite side. On the flexor motor neurons in the 3rd abdominal ganglion (2nd trace in A3), the largest tonic flexor excitor (No. 6) spiked spontaneously and the current injection decreased the spike (No. 6) and increased the flexor inhibitor (No. 5).

the extensor and flexor excitors. Four interneurons elicited reciprocally extension-like motor pattern while another 4 interneurons elicited reversed flexion-like motor pattern. In both the crayfish and lobster, abdominal positioning interneurons have been known to produce abdominal movement [5, 6, 13, 14]. Many of them had somata in the anterior abdominal ganglia (A2-A5) and had ascending and/or descending axons through the abdominal connective. Parts of them were originated from the terminal abdominal ganglion and some of them might be similar to the interneurons described in this study [5]. In the previous works, abdominal positioning interneurons were categorized as one of either FPIs (flexion producing interneurons), EPIs (extension producing interneurons) or inhibitory interneurons [e.g. 6]. By contrast, no interneurons in this study inhibited both the extensor and flexor excitors, but many interneurons coactively excited both the antagonistic motor neurons.

Multiple function of ascending interneurons

Ascending interneurons in the terminal ganglion received excitatory input directly from the mechanosensory afferents innervating hairs on the surface of the tailfan [23] and/or from the proprioceptive afferents innervating the chordotonal organ of the uropod [28]. They, in turn, propagated encoded sensory signals into anterior segments and affected abdominal postural motor neurons in all the anterior (A1-A5) abdominal ganglia [this study]. At the same time, many interneurons also affected the uropod motor neurons in a various fashion [21]. Some interneurons further recruited the unidentified motor neurons of swimmerets (1st root) that were homologous appendages with uropods, though rhythmic period of power- and return-stroke was not affected [Aonuma, unpublished data]. The ascending interneurons, therefore, acted as multifunctional units that controlled the different motor systems simultaneously.

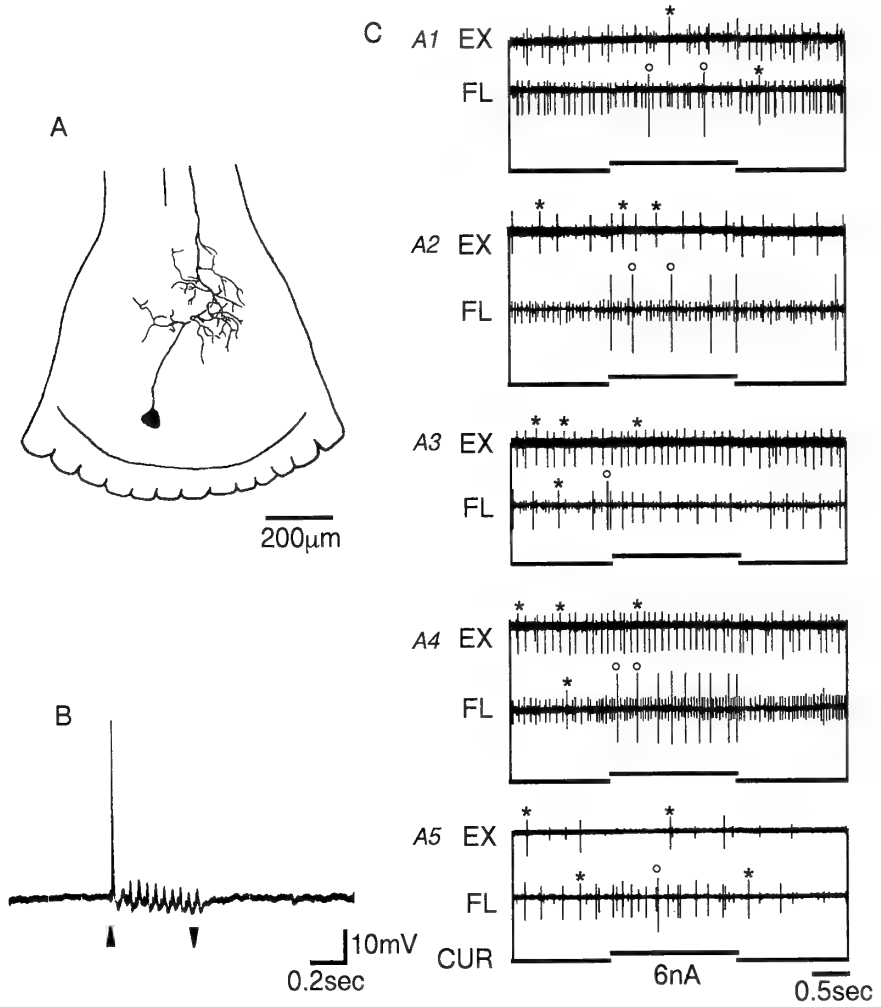

FIG. 8. Output effect of RO-2. A. Morphology of RO-2. B. Repetitive electrical stimulation (indicated by arrowheads) of the 2nd root afferent (20 Hz) elicited antifacilitation in RO-2. C. Output effect of RO-2 upon both the extensor and flexor motor neurons in the abdominal (A1-A5) ganglia.

There was, however, no close correlation between the output effect upon the uropod motor neurons and that upon the abdominal postural motor neurons (Table 1). Interneurons that elicited reciprocally closing pattern of the uropod produced either extension-like or flexion-like motor pattern of the abdomen. Furthermore, interneurons that activated both the extensor and flexor excitors had different effect upon the uropod motor neurons. CA-1 excited both the closer and opener motor neurons while CI-1 inhibited both motor neurons. Interneurons of RC group (RC-3, -6, -8) produced closing pattern of the uropod, while RO-5 produced reversed opening pattern. Only interneurons with flexion effect tended to elicit the reciprocally opening pattern of the uropod (3 out of 4 interneurons). This variety of combination of output to uropod and abdominal postural system in ascending interneurons would partly be derived from the complexity of movement of the abdominal segments. During equilibrium reactions [41], leg reflexes [27], avoidance reaction [26], escape swimming [39], backward walking [12] and defensive reaction [29], coordinated movement with a various pattern between abdomen and uropod was performed. The intersegmental coordination between uropod and abdomen was also essential for posture and locomotion of animals. For example, the flexion producing interneurons (e.g. RO-2, -3 and -4) would be related to the LG mediated tail-flip that was initiated by the rapid flexion of the abdomen [39]. On the other hand, RC-2 and RC-7 had potential to mediate avoidance "dart" response that consisted of immediate closing of uropods followed by the forward walking with abdominal extension [26]. These interneurons produced a train of spikes in response to the repetitive sensory stimulation, elicited the closing pattern of the uropod and produced the abdominal extension (Fig. 5). The physiological result that interneurons with flexion effect failed to respond spikes continuously by the repetitive sensory stimulation of the tailfan as a result of antifacilitation (Table 1) might be consistent with the behavioural observation that the mechanical stimulation of the tailfan preferably elicited the "dart" response (Fig. 2A). Furthermore, slow postural movement of the abdomen was usually accompanied with the activation of both the extensor and flexor muscles [30]. The interneurons such as CA-1, RC-3 and RC-6 would contribute

to increase the tonus of the postural muscles, since they co-actively excited both the extensor and flexor excitors and/or inhibited the inhibitors. Thus, each ascending interneuron will contribute to one or more specific behavioural act(s) and the coordinated sequence of movement between uropod and abdominal posture will be completed by the activation of these ascending interneurons as multisegmental integrators. A particular behavioural act might be triggered through selective activation and certain central interaction between these ascending interneurons.

ACKNOWLEDGMENTS

T. N. was supported by a Grants (04740394) from the Ministry of Education, Science and Culture. M. H. was supported by a Grant of Human Frontiers Science Program.

REFERENCES

1 Bullock TH, Horridge GA (1965) Structure and function in the nervous systems of invertebrate. W H Freeman San Francisco

2 Burrows M (1992) Local circuits for the control of leg movements in an insect. TINS 15. 6: 226–227

3 Calabres R (1976) Crayfish mechanoreceptive interneurons; I. The nature of ipsilateral excitatory inputs. J Comp Physiol 105: 83–102

4 Fields HL, Evoy WH, Kennedy D (1967) Reflex role played by efferent control of an invertebrate and vertebrate stretch receptor. J Neurophysiol 30: 859–874

5 Jellies J, Larimer JL (1986) Activity of crayfish abdominal-positioning interneurons during spontaneous and sensory-evoked movements. J Exp Biol 120: 173–188

6 Jones KA, Page CH (1986) Postural interneurons in the abdominal nervous system of lobster. III. Pathways mediating intersegmental spread of excitation. J Comp Physiol A 158: 281–290

7 Kennedy D, Evoy WH, Fields HL (1966) The unit basis of some crustacean reflexes. Symp Soc Exp Biol 20: 75–109

8 Kennedy D, Takeda K (1965) Reflex control of abdominal flexor muscles in the crayfish. II. The tonic system. J Exp Biol 43: 229–246

9 Kita H, Armstrong W (1991) A biotin-containing compound N-(2-aminoethyl) biotinamide for intercellular labeling and neuronal tracing studies: comparison with biocytin. J Neuro Meth 37: 141–150

10 Kondoh Y, Hisada M (1986) Neuroanatomy of the terminal (sixth abdominal) ganglion of the crayfish, *Procambarus clarkii* (Girard). Cell Tissue Res 243: 273–288

11 Kondoh Y, Hisada M (1987) The topological organization of primary afferents in the terminal ganglion of crayfish, *Procambarus clarkii*. Cell Tissue Res 247: 17–24

12 Kovac M (1974) Abdominal movements during backward walking in crayfish. I. Properties of the motor program. J Comp Physiol 95: 61–78

13 Larimer JL, Jellie J (1983) The organization of flexion-evoking interneurons in the abdominal nerve cord of the crayfish, *Procambarus clarkii*. J Exp Zool 226: 341–351

14 Larimer JL, Moore D (1984) Abdominal positioning interneurons in crayfish: projections to and synaptic activation by higher CNS centers. J Exp Zool 230: 1–10

15 Ma PM, Beltz BS, Kravitz EA (1992) Serotonin-containing neurons in lobsters: their role as gain-setters in postural control mechanisms. J Neurophysol 68: 36–54

16 Macmillan DL, Altman JS, Kein J (1983) Intersegmental coordination in the crayfish swimmeret system reconsidered. J Exp Zool 228: 157–162

17 Miall RC, Larimer JL (1982a) Central organization of crustacean abdominal posture motoneurons: connectivity and command fiber inputs. J Exp Zool 224: 45–56

18 Miall RC, Larimer JL (1982b) Interneurons involved in abdominal posture in crayfish: structure, function and command fiber responses. J Comp Physiol 148: 159–173

19 Murchison D, Larimer JL (1990) Dual motor output interneurons in the abdominal ganglia of the crayfish *Procambarus Clarkii*: synaptic activation of motor outputs in both the swimmeret and abdominal positioning systems by single interneurons. J Exp Biol 150: 269–293

20 Nagayama T, Hisada M (1987) Opposing parallel connections through crayfish local nonspiking interneurons. J Comp Neurol 257: 347–358

21 Nagayama T, Iosogai Y, Sato M, Hisada M (1993) Intersegmental ascending interneurones controlling uropod movements of the crayfish *Procambarus clarkii*. J Comp Neurol 332: 155–174

22 Nagayama T, Isogai Y, Namba H (1993) Physiology and morphology of spiking local interneurons in the terminal abdominal ganglion of the crayfish. J Comp Neurol 337: 584–599

23 Nagayama T, Sato M (1993) The organization of exteroceptive information from the uropod to ascending interneurons of the crayfish. J Comp Physiol 172: 281–294

24 Nagayama T, Takahata M, Hisada M (1983) Local spikless interaction of motoneurons dendrites in the crayfish *Procambarus clarkii*. J Comp Physiol 152: 335–345

25 Nagayama T, Takahata M, Hisada M (1984) Functional characteristics of local non-spiking interneurons as the premotor elements in crayfish. J Comp Physiol 154: 499–510

26 Nagayama T, Takahata M, Hisada M (1986) Behavioral transition of crayfish avoidance reaction in response to uropod stimulation. J Exp Biol 46: 75–82

27 Newland PL (1989) The uropod righting reaction of the crayfish *Procambarus clarkii* (Girard): an equilibrium response driven by two largely independent reflex pathways. J Comp Physiol A 164: 685–696

28 Newland PL, Nagayama T (1993) Parallel processing of proprioceptive information in the terminal abdominal ganglion of the crayfish. J Comp Physiol A 172: 389–400

29 Notvest RR, Page CH (1982) Role of the hemigiant neurons in the crayfish defense response. Brain Research 292: 57–62

30 Page CH (1975) Command fiber control of crayfish abdominal movement. II. Generic differences in the extension reflexes of *Orconectes* and *Procambarus*. J Comp Physiol 102: 77–84

31 Pearson KG, Iles JF (1973) Nervous mechanisms underlying intersegmental co-ordination of leg movements during walking in the cockroach. J Exp Biol 58: 725–744

32 Reichert H, Wine JJ (1982) Neural mechanisms for serial order in a stereotyped behaviour sequence. Nature 296: 86–87

33 Reichert H, Plummer MR, Hagiwara G, Roth RL, Wine JJ (1982) Local interneurons in the terminal abdominal ganglion of the crayfish. J Comp Physiol 149: 145–162

34 Sigvardt KA, Hagiwara G, Wine JJ (1982) Mechanosensory integration in the crayfish abdominal nervous system: structural and physiological differences between interneurons with single and multiple spike initiating sites. J Comp Physiol 148: 143–157

35 Stewart W (1978) Functional connections between cells as revealed by dye-coupling with the highly fluorescent naphthalimide tracer. Cell 14: 741–759

36 Takahata M, Yoshino M, Hisada M (1985) Neuronal mechanisms underlying crayfish steering behaviour as an equilibrium response. J Exp Biol 114: 599–617

37 Toga T, Takahata M, Hisada M (1990) An identified set of local nonspiking interneurons which control the activity of abdominal postural motoneurons in crayfish. J Exp Biol 148: 477–482

38 van Harreveld A (1936) A physiological solution for freshwater crustaceans. Proc Soc Exp Biol 34: 428–432

39 Wine JJ, Krasne FB (1972) The organization of escape behaviour in the crayfish. J Exp Biol 56: 1–18

40 Wine JJ, Mittenthal JE, Kennedy D (1974) The structure of tonic flexor motoneurons in crayfish abdominal ganglia. J Comp Physiol 93: 315–335

41 Yoshino M, Takahata M, Hisada M (1980) Statocyst control of the uropod movement in response to body rolling in crayfish. J Comp Physiol 139: 243–250

ZOOLOGICAL SCIENCE 11: 203–208 (1994)

Phagocytic Activity of Tunic Cells in the Colonial Ascidian *Aplidium yamazii* (Polyclinidae, Aplousobranchia)

EUICHI HIROSE[1], TERUHISA ISHII[2], YASUNORI SAITO[2] and YASUHO TANEDA[3]

[1]*Biological Laboratory, College of Agriculture and Veterinary Medicine, Nihon University, Fujisawa, Kanagawa 252,* [2]*Shimoda Marine Research Center, University of Tsukuba, Shimoda, Shizuoka 415, and* [3]*Department of Biology, Faculty of Education, Yokohama National University, Yokohama, Kanagawa 240, Japan*

ABSTRACT—The phagocytic activity of tunic cells of the colonial ascidian *Aplidium yamazii* was assessed by incubation of thin tunic slices including these cells with fluorescent microparticles. Only one type of tunic cell engulfed the microparticles. These phagocytic tunic cells are irregularly shaped, motile, and often contain phagosomes. Many of them also contain vesicles laden with round granules. Occasionally, they engulf another tunic cell. Because this type of tunic cell is always found in the tunic of histological sections prepared from whole (unsliced) colony specimens, these cells are probably distributed in the tunic under normal conditions. Peroxidase activity was demonstrated exclusively within granule-containing vesicles of some phagocytic tunic cells. This finding indicated that the phagocytic tunic cells might possess an oxygen-dependent microbicidal system. It is presumed that the phagocytic tunic cells migrate throughout the tunic matrix, engulf extraneous substances (including bacteria) and also function as scavengers to keep the tunic free of discarded tunic cells and other debris, such as from wounds.

INTRODUCTION

The tunic is an integumentary tissue in urochordates, such as ascidians; it is a gelatinous or leathery matrix covering the outer surface of epidermis. The tunic is a unique tissue in animals because of its cellulosic component [1,12]. The main function of the tunic is protection of the body, although little is known about this defense system. The tunic is an attractive material for studying defense systems from the viewpoint of comparative immunology because of its peculiarity and the phylogenetic position of ascidians, whose ancestors may be the same as those of the vertebrates.

Ascidians have two types of free cells: hemocytes and tunic cells. Hemocytes circulate in the blood vessels and in the mesenchymal space, and tunic cells are distributed in the tunic; both cell types are presumed to have immunological activity. The phagocytic activity of these free cells was mainly studied by injection or insertion of foreign substances (reviewed in [13]). These studies could not determine whether one or both of these cell types was involved in phagocytosis, because hemocytes seem to infiltrate the tunic that is responding to the experimental operations. Recent studies have demonstrated that particular types of hemocytes have phagocytic activity *in vitro* [9, 10, 14]. As for tunic cells, De Leo *et al.* [2] described the "phagocyte" that is characterized by one or two "heterolysosomic vacuoles" as a type of tunic cell in the solitary ascidian *Ciona intestinalis*. Parrinello *et al.* [5, 6, 7] reported on the phagocytic activity and inflammatory reaction in the tunic by introducing foreign substances into tunic. However, dealing with tunic cells has following difficulties: It is almost impossible to isolate the tunic cells from tunic matrix, and the specimens are usually contaminated by leakage or infiltration of hemocytes.

Aplidium yamazii, a colonial ascidian belonging to the family Polyclinidae and the suborder Aplousobranchia, forms a white, sheet-like colony, and its elongated zooids are separately embedded in a transparent, gelatinous tunic. When a live colony is cut into slices of about 0.5 mm thick, the tunic cells in the slices are observable under a light microscope and remain alive for several hours to a few days. Using these live colony slices, the present study experimentally demonstrated phagocytosis of fluorescent microparticles in the tunic. In this study, the possibility of hemocyte contamination was almost eliminated, because this polyclinid species has no blood vessels in the tunic. We also performed cytochemical determinations for peroxidase, which may be involved in microbicidal activity.

MATERIALS AND METHODS

Animals

Colonies of *Aplidium yamazii* were collected in Nabeta Bay, Shimoda (Shizuoka Pref., Japan). They were attached to glass slides with cotton thread and were reared in culture boxes immersed in Nabeta Bay. The sheet-like colonies grew and spread on the glass slides (Fig. 1A).

Assay for phagocytic activity

A growing part of a live colony was cross-sectioned into slices about 0.5 mm thick using a razor blade (Fig. 1B). Each colony slice consisted of the gelatinous, transparent tunic, the tunic cells, and some fragments of zooids. A solution of fluorescent microparticles (fluoresbrite carboxylate microspheres, 0.5 μm in diameter, 2.5%

Accepted January 7, 1994
Received November 1, 1993
[1] To whom all correspondences should be addressed.

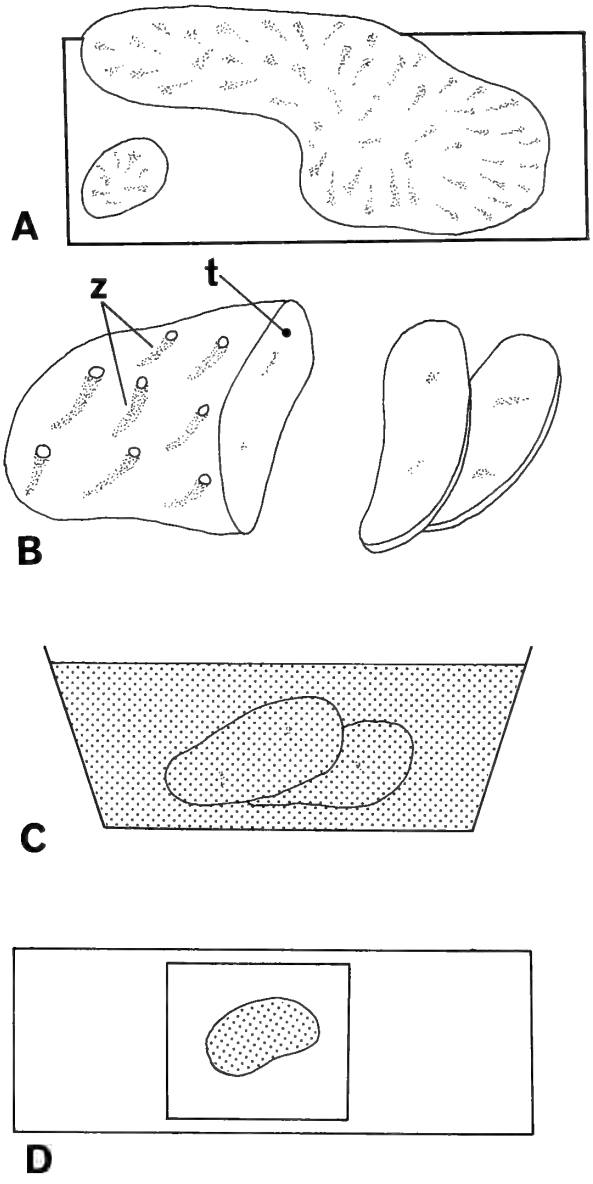

Fig. 1. The procedures of the assay for phagocytic activity. t, tunic; z, zooids. A: Colonies of *A. yamazii* growing on a glass slide. B: Sectioning of a live colony. C: Incubation of colony slices in filtered seawater containing fluorescent microparticles. D: Mounting a colony slice on a glass slide.

solid latex; Polyscience) was diluted in 1:5 with filtered seawater (FSW). The colony slices were incubated in this solution for 30 min at room temperature, allowing the microparticles to permeate the tunic (Fig. 1C). After extensive washing with FSW, the slices were incubated in FSW or FSW containing penicillin (100 IU/ml) and streptomycin (1 mg/ml) for 1–2 hr, 24 hr, or 48 hr at room temperature. Because the specimens that were incubated for 24 hr or 48 hr markedly shrank, they were sliced again for microscopic observation. Each slice was observed under a light microscope equipped with epifluorescence and Nomarski differential interference contrast (DIC) optics (Fig. 1D).

For electron microscopy, some colony slices incubated with microparticles were fixed in 2.5% glutaraldehyde-0.1M sodium cacodylate-0.45 M sucrose (pH 7.4) for 2 hr on ice. They were rinsed in 0.1 M sodium cacodylate-0.45 M sucrose (pH 7.4), and postfixed in 1% osmium tetroxide-0.1 M sodium cacodylate (pH 7.4) for 1–1.5 hr on ice. They were dehydrated through a graded ethanol series, cleared with *n*-butyl glycidyl ether, and embedded in low viscosity epoxy resin. Thin sections were stained with uranyl acetate and lead citrate and examined using a Hitachi HS-9 transmission electron microscope at 75 kV.

We also fixed colony pieces of about 5 mm × 10 mm (containing more than 30 zooids) and processed them for electron microscopy as described above. We wanted to determine whether the phagocytic cells observed in the above experiment were always distributed in the tunic or were contaminating hemocytes from the slicing process.

Cytochemistry for peroxidase activity

The colony pieces were fixed in 2.5% glutaraldehyde-2% NaCl-0.1 M Millonig's phosphate buffer (pH 7.4) on ice for 15 min, and the fixed pieces were cut into slices with a razor blade. After washing in the same buffer, they were pre-incubated in 0.1% diaminobenzidine (DAB; Sigma)-0.1 M phosphate buffer (pH 6.8) for 30 min at room temperature and then incubated in 0.1% DAB-0.3% H_2O_2-0.1 M phosphate buffer for 15 min. The specimens were washed with 0.1 M phosphate buffer and postfixed with 1% osmium tetroxide. They were dehydrated and embedded in epoxy resin as described above for electron microscopy. Thick sections were stained with toluidine blue. In negative controls, we omitted H_2O_2 from the incubation medium or added 50 mM 3-amino-1,2,4-triazole (Sigma) in the pre-incubation and incubation media as an inhibitor.

RESULTS

In the tunic of colony slices of *Aplidium yamazii*, there were tunic cells of various types; some types have protruding filopodia, some types have an elongated cell shape, some contain many granules, and some form multicellular vesicles. Particular types of tunic cells showed phagocytic activity (Fig. 2). Although these phagocytic cells were found throughout the tunic matrix, they did not appear to be evenly distributed. This was caused by the uneven distribution of microparticles within the tunic slices; that is, there were more microparticles per unit area at the surface of the slices than at the core region. For this reason, we could not make a quantitative description of the distribution of phagocytic tunic cells in this study. The tunic cells phagocytizing microparticles were essentially irregularly shaped cells with extending filopodia. There was, however, some variation in their appearance. For instance, Figure 3 shows three tunic cells, all of which engulfed the microparticles. Cell "a" was a thin, flattened cell with numerous filopodia; cell "b" was almost round; and cell "c" was elliptical. Cells "b" and "c" had thicker cell bodies and fewer filopodia than cell "a". Because many tunic cells that exhibit phagocytosis showed intermediate appearances among these three, we classified them as a single cell type, namely, phagocytic tunic cells. These cells occasionally engulfed another tunic cell, and thus might be considered scavengers. A tunic cell engulfing a relatively large cell did not have prominent filopodia, and its cell body became a thin sheet that wrapped around the engulfed cell. With respect to the characteristics of phagocytic cells (i.e. cell

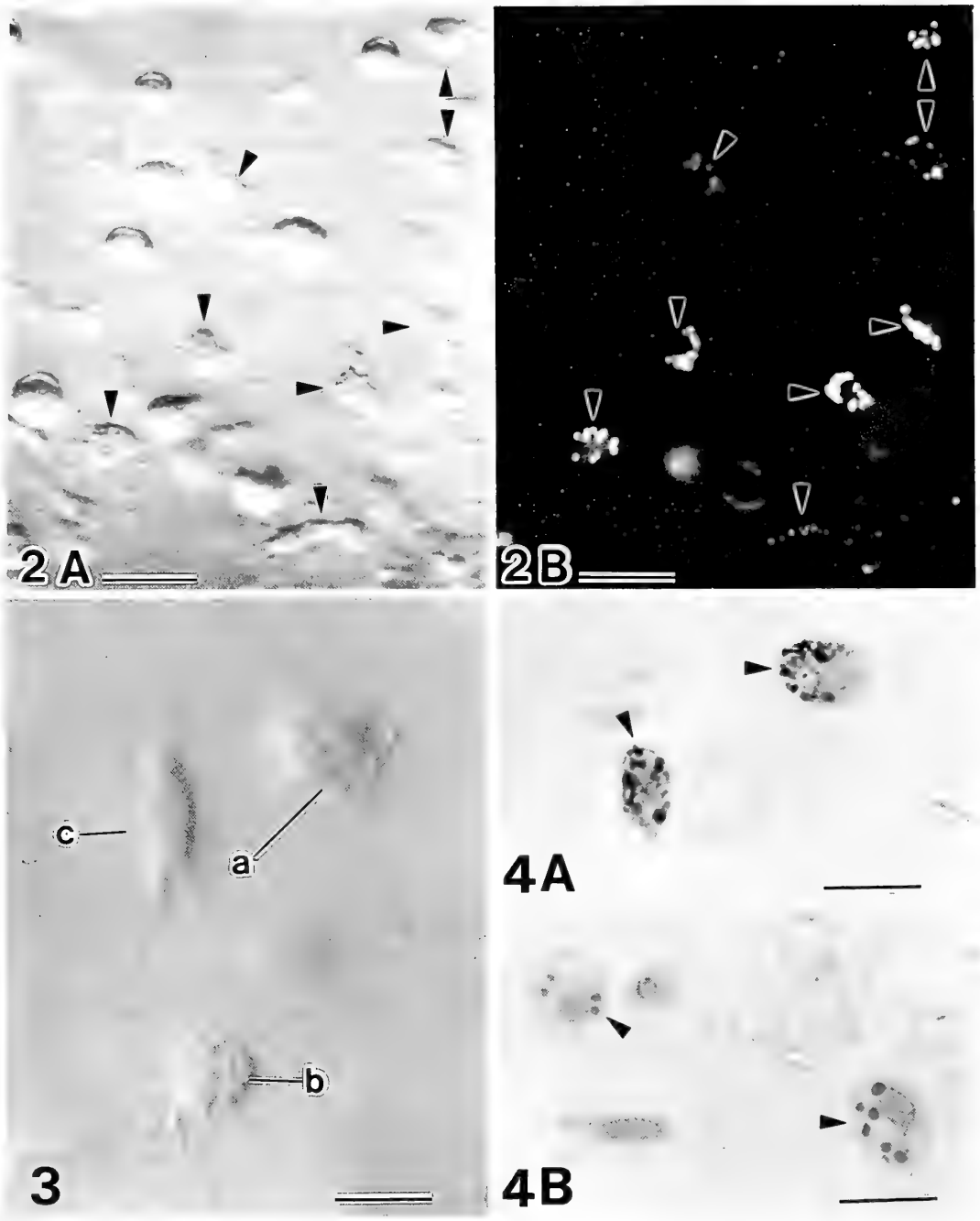

FIG. 2. Paired images of a live colony slice incubated for 2 hr in FSW. A: Nomarski DIC. B: Epifluorescence. Arrowheads indicate tunic cells phagocytizing fluorescent microparticles. Note round granular cells and some thin filopodial cells do not contain the microparticles. (Scale bar = 25 μm)

FIG. 3. Light micrograph (Nomarski DIC) of three phagocytic tunic cells (a, b, c) in live colony slice incubated for 2 hr in FSW. Each cell has a different appearance from the others with respect to cell shape, thickness of cell body, and number of filopodia. (Scale bar = 10 μm)

FIG. 4. Cytochemistry for peroxidase in the tunic. A) Dark reaction product indicates peroxidase activity in phagocytic tunic cells (arrowheads). B) A negative control in which peroxidase inhibitor (3-amino-1,2,4-triazole) was added. The reaction product is not found in any tunic cells. The granular inclusions are only stained with toluidine blue (arrowheads). (Scale bar = 10 μm)

shape, granular inclusions, and distribution of engulfed microparticles within the cells), prominent differences were not found among the specimens incubated for 2 hr, 24 hr, and 48 hr. In preliminary observations using time-lapse video recording, these phagocytic tunic cells actively migrated within the tunic matrix and some non-phagocytic ones did not. The ability to migrate may be indispensable for phagocytic activities.

In the cytochemical study, only some of the phagocytic tunic cells showed peroxidase activity. In thick sections for light microscopy, the dark product indicating peroxidase activity is uniquely localized within the phagolysosome-like vesicles and/or vesicles carrying round granules (Fig. 4A). No specific activity is demonstrated in the other cell compartments or in the other types of tunic cells. For example, a phagocytic cell engulfing another cell has peroxidase activity in its vesicles that contain round granules, but not in the large phagosome that engulfs the cell. No peroxidase activity was demonstrated in the negative controls (Fig. 4B).

In electron microscopic observations, the microparticles were recognized as electron-lucent rounds or ellipsoids whose margins were moderately electron dense. Some microparticles adhered to exposed surface of the tunic matrix, and some permeated the tunic slices. In phagocytic tunic cells engulfing the microparticles, the latter were found within the vesicles, and these cells also had some vesicles laden with round, electron-dense granules (Figs. 5 and 6). The largest of these granules were about 1.5 μm in diameter, with some

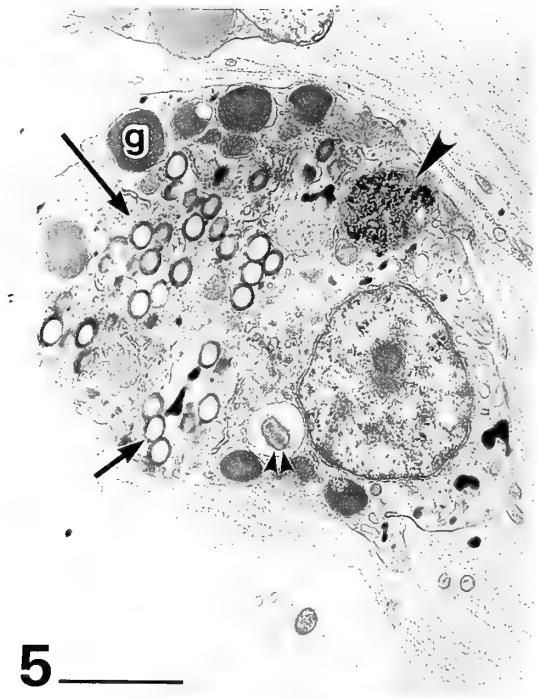

FIG. 5. A phagocytic tunic cell in the colony slice incubated for 2 hr in FSW. The cell contains granules (g), the engulfed microparticles (arrows) and a phagolysosome-like vesicle (arrowhead). This cell also carries a vesicle containing a bacteria-like structure (double arrowheads). (Scale bar=2 μm)

FIG. 6. A phagocytic tunic cell in the colony slice incubated for 24 hr in FSW. The cell engulfs microparticles (arrow) and another tunic cell (c). (Scale bar=2 μm)

FIG. 7. A phagocytic tunic cell in a specimen fixed as a whole colony piece. The cell contains electron-dense granules (arrowheads) and phagolysosome-like vesicles (p). (Scale bar=2 μm)

being discernible under the light microscope. Some of the phagocytic tunic cells also had phagolysosome-like vacuoles containing disorganized structures that appeared to be disintegrating cellular components. In addition, a bacteria-like structure was occasionally found in a vesicle (double arrowheads in Fig. 5). In Figure 6, the phagocytic tunic cell carrying microparticles has engulfed another tunic cell. Tunic cells with the same characteristics described above were also found in specimens fixed as whole colony pieces (Fig. 7).

DISCUSSION

When colony slices of *Aplidium yamazii* are incubated with microparticles, particular tunic cells show phagocytic activity. These phagocytic cells usually have protruding filopodia, often contain some round granules, and occasionally engulf another cell. It is presumed that phagocytic tunic cells migrate throughout the tunic matrix, engulf extraneous substances including bacteria, and also function as scavengers, thereby keeping the tunic free of discarded tunic cells and wound debris.

Cellular defense reactions in the tunic involve two groups of free cells: infiltrating hemocytes that respond to infections or trauma, and tunic cells that always "stand by" in the tunic. In the allogeneic rejection reaction of botryllid ascidians (colonial species belonging to the family Botryllidae, the suborder Stolidobranchiata), many hemocytes infiltrate the tunic from the blood vessels and participate in the necrotic reactions [3, 11]. In *Ciona intestinalis* (a solitary species), when particulate or soluble agents are injected in the tunic, a capsule and/or tissue injury is produced, depending on the dose of the irritant [5, 6, 7]. In this tunic reaction of *C. intestinalis*, the hemocyte infiltration may also occur, induced by the irritant injection, because some of the cells appear around the wound are different from tunic cells [6]. In *Aplidium yamazii*, the phagocytic cells observed here are tunic cells that are always present in the tunic, because they are usually observed in the tunic part of the specimens fixed as whole colony pieces that were not sliced before fixation.

In *C. intestinalis*, De Leo *et al.* [2] studied the fine structure of the tunic and described the "phagocyte" as one type of tunic cell. The characteristics of the "phagocyte" in *C. intestinalis* are very similar to those of phagocytic tunic cells in *A. yamazii*: protruding thin cytoplasmic extensions, phagolysosome-like vesicles, and occasional engulfment of other cells. These phagocytic cells of *C. intestinalis* and *A. yamazii* probably belong to a homologous cell type. In botryllid ascidians, although we have already found amoeboid tunic cells containing bacteria in their vesicles [4], we have not found cells that engulf other cells. The phagocytic tunic cells in *A. yamazii* have some morphological variations in their cell shape and in the number of filopodia (see Fig. 3). These variations are probably caused by different states of phagocytosis, migration, and/or cell differentiation in the same cell type. It is noteworthy that Sawada *et al.* [10] described two types of phagocytes among the hemocytes of the solitary ascidian, *Halocynthia roretzi*: one type (p1-cell) spreads as thin, flat sheets, and the other type (p2-cell) is thicker than the former. P2-cells in *H. roretzi* are similar in morphology to some of phagocytic tunic cells, such as cell "c" in Figure 3, in *A. yamazii*.

In the phagocytic tunic cells, peroxidase activity was demonstrated within the phagolysosomes and/or the vesicles carrying the round granules. Peroxidase is known to inactivate peroxide ions generated in the oxygen-dependent microbicidal pathway. This suggests the following two possibilities: The phagocytic tunic cells may have this microbicidal activity, and the granules in the phagocytic tunic cells are possibly the engulfed materials processed in the phagolysosomes. In contrast to our findings, a cytochemical study using *C. intestinalis* showed that all of the amoebocytes among the hemocytes are peroxidase-negative [8], though the cytochemical methods were different from those of the present study. It is possible that oxygen-dependent microbi cidal activities are not ubiquitous in ascidian tissues or ascidian species.

Based on our observations, we propose a hypothesis on the differentiation of phagocytic tunic cells: 1) The cells with a thin cell body and numerous protruding filopodia are at a young stage. 2) Phagolysosomes are formed after phagocytosis, and their contents subsequently become round granules. The oxygen-dependent microbicidal activity may be carried out during this process. 3) An increase in the number of granules makes the cell body thicker and roundish.

It is thought that almost all tunic cells originate from hemocytes passing through the epidermis. If phagocytic tunic cells originate from hemocytes, the question arises as to whether phagocytic hemocytes migrate into the tunic or hemoblasts differentiate into phagocytic tunic cells within the tunic. For further understanding of the immunological activity and differentiation of tunic cells, a precise description and classification of the tunic cells in *A. yamazii* is required.

ACKNOWLEDGMENTS

This study was supported by a Grant-in-Aid for General Scientific Research (no. 03455008) to Y. S. from the Ministry of Education, Science and Culture of Japan. This is contribution no. 564 from the Shimoda Marine Research Center, University of Tsukuba.

REFERENCES

1 De Leo G, Patricolo E and D'Ancona Lunetta G (1977) Studies on the fibrous components of the test of *Ciona intestinalis* Linnaeus. I. Cellulose-like polysaccharide. Acta Zool 58: 135–141

2 De Leo G, Patricolo E , Frittita G (1981) Fine structure of the tunic of *Ciona intestinalis* L. II. Tunic morphology, cell distribution and their functional importance. Acta Zool 62: 259–271

3 Hirose E, Saito Y, Watanabe H (1990) Allogeneic rejection induced by cut surface contact in the compound ascidian, *Botrylloides simodensis*. Invert. Reprod Dev 17: 159–164

4 Hirose E, Saito Y, Watanabe H (1991) Tunic cell morphology and classification in botryllid ascidians. Zool Sci 8: 951–958

5 Parrinello N, Patricolo E (1984) Inflammatory-like reaction in the tunic of *Ciona intestinalis* (Tunicata). II. Capsule component. Biol Bull 167: 238–250

6 Parrinello N, Patricolo E, Canicatti C (1977) Tunicate immunobiology. I. Tunic reaction of *Ciona intestinalis* L. to erythrocyte injection. Boll Zool 44: 373–381

7 Parrinello N, Patricolo E, Canicatti C (1984) Inflammatory-like reaction in the tunic of *Ciona intestinalis* (Tunicata). I. Encapsulation and tissue injury. Biol Bull 167: 229–237

8 Rowley AF (1982) Ultrastructural and cytochemical studies on the blood cells of the sea squirt, *Ciona intestinalis*. I. Stem cells and amoebocytes. Cell Tissue Res 223: 403–414

9 Rowley AF (1983) Preliminary investigations on the possible antimicrobial properties of tunicate blood cell vanadium. J Exp Zool 227: 319–322

10 Sawada T, Fujikura Y, Tomonaga S, Fukumoto T (1991) Classification and characterization of ten hemocytes types in the tunicate *Halocynthia roretzi*. Zool Sci 8: 939–950

11 Taneda Y, Watanabe H (1982) Studies on colony specificity in the compound ascidian, *Botryllus primigenus* Oka. I. Initiation of "nonfusion" reaction with special reference to blood cell infiltration. Dev Comp Immunol 6: 43–52

12 Van Daele Y, Revol J-F, Gaill F, Goffinet G (1992) Characterization and supramolecular architecture of the cellulose-protein fibrils in the tunic of the sea peach (*Halocynthia papillosa*, Ascidiacea, Urochordata). Biol Cell 76: 87–96

13 Wright RK, Cooper EL (1975) Immunological maturation in the tunicate *Ciona intestinalis*. Amer Zool 15: 21–27

14 Zhan H, Sawada T, Cooper EL, Tomonaga, S (1992) Electron microscopic analysis of tunicate (*Halocynthia roretzi*) hemocytes. Zool Sci 9: 551–562

ZOOLOGICAL SCIENCE 11: 209–219 (1994)

In vitro Autophosphorylation and Cyclic Nucleotide-Dependent Dephosphorylation of Sea Urchin Sperm Histone Kinase

TATSUO HARUMI, KATSUAKI HOSHINO AND NORIO SUZUKI[1]

Noto Marine Laboratory, Kanazawa University,
Ogi, Uchiura, Ishikawa 927-05, Japan

ABSTRACT—We identified two phosphorylatable proteins (33 kDa and 48 kDa) in crude extractes of spermatozoa from the sea urchin, *Hemicentrotus pulcherrimus*. While the 33 kDa protein was phosphorylated in 100 mM Mg^{2+}-containing medium with cAMP or cGMP, phosphorylation of the 48 kDa protein occurred irrespective of the Mg^{2+}-concentration if it was more than 10 mM. Physiological concentration if it was more than 10 mM. Physiological concentrations of cAMP or cGMP triggered dephosphorylation of the [^{32}P]-phosphorylated 48 kDa protein in a concentration dependent manner. The dephosphorylation of 48 kDa protein was inhibited with calyculin A or okadaic acid. The 48 kDa protein was associated with a 39 kDa protein to form a larger oligomer with about 400 kDa. The purified 400 kDa protein showed cyclic nucleotide-dependent histone kinase activity. The histone kinase activity shifted from 400 kDa to 39 kDa on a Superose 6 HR in the presence of 5×10^{-6} M cAMP. Phosphorylation of the 48 kDa protein in the purified 400 kDa protein required only Mg[^{32}P]ATP. A photoaffinity cAMP analogue, 8-N_3-[^{32}P]cAMP, was incorporated into the 48 kDa protein. These results suggest that the 48 kDa protein which is a reguratory subunit of the histone kinase is autophosphorylated, and binding of cAMP to the phosphorylated 48 kDa subunit of the kinase results in dissociation of the 48 kDa subunit(s) from the 39 kDa subunit(s) to allow the 48 kDa subunit accessible to a protein phosphatase.

INTRODUCTION

In sea urchin fertilization, before contacting an egg surface a spermatozoon must pass through the jelly coat which surrounds the egg. The jelly coat contains two high molecular weight glycoconjugates and sperm-activating peptides (SAPs). A fucose sulfate glycoconjugate (FSG), one of the glycoconjugates in the jelly coat has been reported to be a major substance responsible for induction of the acrosome reaction [33–34]. FSG has profound effects on sea urchin spermatozoa such as increases in adenylate cyclase activity [45], cAMP concentrations [9], cAMP-dependent protein kinase (A-kinase) acitivty [10], and induction of phosphorylation of sperm histone H1 [27–28]. Sea urchin spermatozoa contain high A-kinase activity [10, 15, 20-21]. SAPs, which were originally identified as factors which activate sperm respiration and motility [11, 37], also increase sperm cAMP concentrations [9]. In addition, SAPs activate membrane-bound guanylate cyclase [2] and increase cGMP concentrations in sea urchin spermatozoa [11]. These observations show that cyclic nucleotides accumulate in response to FSG and SAPs, which implies an important function in spermatozoa at fertilization.

Cyclic nucleotide-dependent protein phosphorylation is one of the major signal transduction pathways in cells. cAMP-dependent protein phosphorylation in sea urchin spermatozoa was reported by Porter *et al.* [28]. They showed cAMP-dependent histone H1 phosphorylation in *Strongylocentrotus purpuratus*. The mature sea urchin sperm nucleus contains two sperm-specific histone variants, H1 and H2B, which are larger than their somatic counterparts. Within 10 min after the sperm nucleus enters the egg these histones are lost from the sperm chromatin, being replaced by cleavage stage histones contributed by the egg [12]. These histones are characterized by reversibly phosphorylated N-terminal regions consisting largely of multiple clustered "SPKK" tetrapeptides. The SPKK domains bind the extraodinarily long linker DNA in sea urchin sperm chromatin to help stabilize the highly condensed DNA and phosphorylation of these domains appears to weaken the DNA binding [13, 26]. In the present study, we show that cyclic nucleotides induce not only histone H1 phosphorylation but also dephosphorylation of a 48 kDa protein in the *Hemicentrotus pulcherrimus* sperm homogenate. We also demonstrate that the purified 48 kDa protein-associated protein phosphorylates histone, particularily H1 and H2B, in the presence of cyclic nucleotides.

MATERIALS AND METHODS

Materials

Sea urchins (*H. pulcherrimus*) were collected along the coast of Toyama Bay near Noto Marine Laboraotry. Spermatozoa were obtained by intracoelomic injection of 0.5 M KCl, and collected as "dry sperm" at room temperature and stored on ice until use. Just before use, the dry sperm were washed with Ca^{2+}- and Mg^{2+}-free artificial sea water (CaMgFASW: 454 mM NaCl, 9.7 mM KCl, 34.5 mM $(CH_3)_3NClCH_2CH_2OH$, 27.1 mM Na_2SO_4, 4.4 mM $NaHCO_3$ and 10 mM Tris-HCl, pH 7.5).

Reagents

[γ-^{32}P]ATP (111 TBq/mmol) was purchased from New England Nuclear (Boston, MA). 8-N_3-[^{32}P]cAMP (2.22 TBq/mmol) and

Accepted March 1, 1994
Received january 14, 1993
[1] To whom correspondence showed be addressed.

8-N_3-[^{32}P]cGMP (370 GBq/mmol) were products of ICN Radiochemicals (Irvine, CA). Phosphoserine (P-Ser), phosphothreonine (P-Thr), phosphotyrosine (P-Tyr), cAMP, cGMP, calf thymus total histone, histones H1, H2A, H2B, H3 and H4, histone-agarose, catalytic subunit of bovine heart A-kinase, a synthetic protein kinase inhibitor (PKI, rabbit sequence) and DEAE-Sephacel were obtained from Sigma (St. Louis, MO). Calyculin A was from LC Services (Woburn, MA). Okadaic acid was a generous gift from Professor T. Yasumoto (Tohoku University). All other reagents and solvent used were of analytical grade.

Phosphorylation and dephosphorylation of sperm proteins

Dry sperm (0.5 ml) were suspended in 5 ml CaMgFASW and centrifuged at 10,000×g for 10 min at 4°C. The resulting sperm pellet was suspended in 5 ml of a solution containing 0.5 M NaCl, 10 mM $(CH_3COO)_2Mg$, 1 mM 3-isobutyl-methylxanthine (IBMX), 1 mM dithiothreitol (DTT), 1% 3-[(3-cholamidopropyl) dimethylammonio]-1-propanesulfate (CHAPS) and 10 mM Tris-HCl (pH 7.5) and homogenized by ten strokes of a Teflon-glass homogenizer on ice, followed by sonication with a Branson sonifier model 200 for 30 sec on ice. The homogenate was centrifuged at 200×g for 5 min at 0°C. The resulting supernatant fluid (Sup. A) was used for the following experiments. Since Takai *et al.* [41] reported that 100 mM Mg^{2+} concentration was needed for maximal stimulation of cGMP-dependent protein kinase, we also used a solution containing 100 mM $(CH_3COO)_2Mg$ in some experiments.

Sup. A (100μl) was incubated at 20°C with 0.83 pmol of [γ-^{32}P]ATP (92.5 KBq) for 5 min and then 2μl of distilled water (DW) or various agents was added to the sample. At the indicated time, the reaction was terminated by addition of 20μl of 60% (w/v) trichloroacetic acid (TCA). In experiments using protein phosphatase inhibitors, inhibitors were added to Sup. A containing known concentrations of cAMP or cGMP. After addition of 20μl of 60% (w/v) TCA, the resulting precipitate was rinsed with ice-cold acetone and dried under reduced pressure. The residue was dissolved in 100μl of 4% sodium dodecyl sulfate (SDS) and then subjected to SDS-polyacrylamid gel electrophoresis (SDS-PAGE) [19]. The gel was silver-stained according to the method of Morrissey [24]. Radiolabeled protein bands were detected by exposing the gel to a Kodak X-Omat film at −70°C using Kodak intensifying screens. To purify the 48 kDa phosphorylatable protein, fractions (50 or 100μl) obtained from each chromatography were incubated with 0.83 pmol of [γ-^{32}P]ATP (92.5 KBq) in the presence of 10 mM $(CH_3COO)_2Mg$ for 10 min at 20°C, and the reaction was stopped by addition of final 10% TCA, followed by SDS-PAGE and autoradiography as described above.

Identification of phosphoamino acids in the [^{32}P]-labeled sperm protein

A sperm protein phosphorylated with 1 pmol of [γ-^{32}P]ATP (111 KBq) was separated by SDS-PAGE. The gel was stained with Coomassie brilliant blue [46]. The radioactive protein band (monitored by autoradiography) was cut out of the gel and homogenized. Then, the protein was retrieved with a Max-Yield Protein Concentrator (ATTO, Tokyo), dialysed against DW, and lyophilized. The residue was dissolved in 200μl of DW (7.1 mg protein/ml). A sample of 420μg protein was mixed with authentic P-Ser (20μmol), P-Thr (10μmol) and P-Tyr (0.1μmol) and lyophilized. The residue was hydrolysed in 400μl of 5.7 N HCl for 1 or 4 hr at 110°C according to Yang *et al.* (44) The hydrolysate was lyophilized and the residue was dissolved in 100μl of a solution containing 12.5% methanol in 10 mM potassium phosphate (pH 3.0). The sample (10μl) was analyzed by a shimadzu LC-6A HPLC system equipped with a Whatman Partisil-10 SAX anion exchange column (26×250 mm;particle size 10μm). The colum was equilibrated with the sample-dissolving solution and eluted with the same solution at a flow rate of 1 ml/min at 40°C. The absorbance at 210 nm of the colum effluent was monitored. Fractions of 1 ml were collected and the radioactivity in the fractions was measured with an Aloka LSC-1000 liquid scintilation counter.

Gel filtration of sperm proteins

Sup. A was centrifuged at 30,000×g for 30 min at 4°C. The resulting supernatant solution (Sup. B, 120μl) was incubated with 1 pmol of [γ-^{32}P] (111 KBq) for 10 min at 20°C and filtered with a Millipore Ultrafree-C3HV filter. The filtrate was applied to a TSK/GEL G3000SW column equipped to a Hitachi L-6200 HPLC system. The colum was equilibrated with a solution containing 0.1% CHAPS and 0.1 M sodium phosphate (pH 6.8) and eluted with the same solution at a flow rate of 0.5 ml/min at room temperature. The absorbance at 280 nm of the column effluent was monitored, and fractions of 0.5 ml were collected. For determination of the dephosphorylation activity in these fractions, Sup. B was subjected to chromatography on a TSK-GEL G3000SW without incubation of 1 pmol of [γ-^{32}P] (111 KBq).

To prepare the substrate for determining the cyclic nucleotide-dependent protein dephosphorylating activity, Sup. B incubated with 1 pmol of [γ-^{32}P]ATP (111 KBq) was subjected to chromatography on the TSK column, and the fraction (No. 13) which contained the [^{32}P]-phosphorylated 48 kDa protein was saved and purified further by chromatography on the same column. Fractions (No. 13 and No. 14) containing radioactivity were pooled and dialysed against 10 mM Tris (pH 7.5) containing 0.1% CHAPS at 4°C. The [^{32}P]-labeled protein in the dialysate was used as the substrate for determining the dephosphorylating activity of the fractions obtained from the TSK-GEl G3000SW column chromatography of Sup. B. The substrate (100μl) was incubated with 100μl of each fraction obtained from a TSK-GEl G3000SW column for 5 min at 20°C and then 2μl of 10 mM cAMP or cGMP were added to the reaction mixture. At 5 min after addition of cAMP or cGMP, the reaction was terminated by addition of 40μl of 60% TCA (w/v). The sample was processed for SDS-PAGE as described above, and analyzed by SDS-PAGE and then autoradiography. As control experiments incubation without cyclic nucleotides was performed.

Determination of protein phosphatase activity

Protein phosphatase (PPase) activity was determined with [^{32}P]-phosphohistones as substrate by methods described by Meisler and Langan [23], Swarup and Garbers [39], and Shacter [35] with slight modifications. The reaction mixture in a total volume of 50μl consisted of 50 mM Tris (pH 7.5), 1 mM DTT, 100 mM NaCl, [^{32}P]-phosphohistones containing 60μM [^{32}P]-serine and 5μl of sample solution. The reaction was initiated by addition of the sample solution, incubated for 10 min at 30°C, and terminated by addition of 100μl of 10 mM silicotungstic acid in 0.01 N H_2SO_4. The mixture was centrifuged at 10,000×g for 5 min. To the resulting deproteinized supernatant fluid (100μl), a 25μl of 5% (w/v) ammonium molybdate in 4 N H_2SO_4 was added. The resulting phosphomolybdate complex was extracted with 200μl of isobutyl alcohol/toluene (1/1, v/v). After centrifugation of the mixture at 1,000×g for 5 min to separate the organic and aqueous phases, a 160μl aliquot of the organic phase was measured for radioactivity with the liquid scintilla-

tion counter.

Preparation of [^{32}P]-phosphorylated histones

Phosphorylation of histones was carried out using the catalytc subunit of bovine haert A-kinase as described by Meisler and Langan [23] and Swarup *et al.* [40] with slight modifications. The reaction mixture in a total volume of 4.0 ml contained 40 mg of calf thymus total histones, 400μM [γ-^{32}P]ATP (37 MBq), 1 mM DTT, 25 mM $MgCl_2$, 50 mM Tris-HCl (pH 7.5) and 250 units of the catalytic subunit. After incubation at 30°C for 12 hrs, phosphorylated histones were precipitated with 25% (w/v) TCA, collected by centrifugation, dissolved in DW, and re-precipitated with 25% (w/v) TCA. The resulting precipitate was washed twice with ethanol/ether (1/4, v/v) and twice with 0.1 N HCl in ethanol/ether (1/4, v/v), and lyophilized. The residue was dissolved in DW to give a final concentration of 100 nmol of incorporated Pi/ml and stored at −20°C until use.

Purification of the [^{32}P]-phosphorylatable 48 kDa protein

All experiments were carried out at 4°C unless otherwise mentioned. CaMgFASW-washed dry sperm (50 ml) were suspended in 500 ml of ice-cold Buffer A [10 mA $(CH_3COO)_2Mg$, 1 mM DTT, 10 mM benzamidine-HCl, 5 mM 6-amino-n-caproic acid, 1 mM phenylmethylsulfonyl fluoride and 20 mM Tris-HCl, pH 7.5] containing 1% CHAPS, homogenized with a Teflon-glass homogenizer, and sonicated with a Branson sonifier model 200. The homogenate was centrifuged at 30,000×g for 30 min. The resulting supernatant fluid was applied to a DEAE-Sephacel column (2.5×18 cm) equilibrated with Bffer A containing 0.1% CHAPS, and eluted with a linear gradient of NaCl from 0 M to 0.5 M in Buffer A containing 0.1% CHAPS at a flow rate of 50 ml/hr. Fractions containing the [^{32}P]-phosphorylatable 48 kDa protein were pooled and applied to a Toyopearl HW-55 column (1.6×58 cm) equilibrated with Buffer B [10 mM $(CH_3COO)_2Mg$, 1 mM DTT, 0.1% CHAPS and 10 mM Tris-HCl, pH 7.5] containing 0.1 M NaCl and 10 mM benzamindine-HCl, and eluted with Buffer B containing 0.1 M NaCl at a flow rate of 17.5 ml/hr. Fractions containing the [^{32}P]-phosphorylatable 48 kDa protein were pooled and concentrated with an Amicon Diaflo Cell. The resulting sample was mixed with an equal volume of Buffer B, applied to a Mono Q HR5/5 column (Pharmacia) equilibrated with Buffer B, and eluted with a linear gradient of NaCl from 0 M to 0.5 M in Buffer B at a flow rate of 1 ml/min. Fractions containing the [^{32}P]-phosphorylatable 48 kDa protein were pooled and mixed with an equal volume of Buffer B. The sample was applied to a histone-agarose column (0.9×2.4 cm) equilibrated with Buffer B, and eluted with a linear gradient of NaCl from 0 M to 1 M in Buffer B at a flow rate of 10 ml/hr. Fractions containing the [^{32}P]-phosphorylatable 48 kDa protein were pooled and concentrated with an Amicon Diaflo Cell. Then, the sample was applied to a Superose 6 HR10/30 column (Pharmacia) equilibrated with Buffer B containing 0.1 M NaCl, and eluted with the solution at a flow rate of 0.4 ml/min. Fractions containing the [^{32}P]-phosphorylatable 48 kDa protein were pooled and used for the following experiments.

Photoaffinity incorporation of 8-N_3-[^{32}P]cAMP and 8-N_3-[^{32}P]cGMP into the 48 kDa protein

A fifty microliter of Sup. B or the fractions obtained from a TSK-GEl G3000SW column was incubated with 3.3 pmol of 8-N_3-[^{32}P]cAMP (7.4 KBq) or 20 pmol of 8-N_3-[^{32}P]cGMP (7.4 KBq) in the presence of 4 mM IBMX for 10 min at 20°C, and then irradiated at 0.3 J/cm^2 at 254 nm with a Funa-UV-linker (Funakoshi Chemical Co., Tokyo). Thereafter, the sample was mixed with 12.5μl of a SDS-PAGE sample buffer (50% glycerol, 25% 2-mercaptoethanol, 5 mM EDTA, 0.5% bromophenol blue and 0.31 M Tris-HCl, pH 6.8), heated at 90°C for 30 sec and subjected to SDS-PAGE, followed by autoradiography.

Assay of protein kinase

Protein kinase was assayed as described by Roskoski [30] with slight modifications. The reaction mixture (100μl) contained 50 mM MES (pH 6.5), 10 mM magnesium acetate, 1 mg/ml calf-thymus or sea urchin sperm histone, 200μM [γ-^{32}P]ATP, 2μM cAMP, and varying amounts of kinase. After incubation at 30°C for 10 min, a 25μl-aliquot was withdrawn and spotted onto a 1×2 cm piece of Whatman P81 cellulose, and dropped into a beaker containing 75 mM phosphoric acid. The paper was subjected to four washes of 75 mM phosphoric acid for 2 min each and then air-dried, followed by measuring the radioactivity in the liquid scintillation counter.

Isolation of sea urchin sperm histones

Sperm heads were obtained from *H. pulcherrimus* spermatozoa as described previously [38]. Total histones were extracted from the sperm heads with 0.2 N H_2SO_4, precipitated with final 20% (w/v) TCA, and washed with acetone, as described by Green *et al.* [13]. Total sperm histones were dissolved in 10 mM Tris-HCl, pH 8.0 and perchloric acid (PCA) was added to final 5%, followed by incubation on ice for 1 hr. The precipitate containing core histones was removed by centrifugation at 10,000×g for 10 min, and sperm H1 histones were precipitated from the clear supernatant by the addition of final 20% (w/v) TCA and incubation on ice for 1 hr. Sperm histone H1, which migrated at 33 kDa in SDS-PAGE, were collected by centrifugation at 10,000×g for 10 min, washed three times with acetone, and dried in air.

Other methods

Intensity of darkness of the band on the autoradiogram was measured quantitatively by a Shimadzu CS-9000 dual wavelength flying spot scanner at an absorbance of 600 nm. Protein concentration was determined by the method of Lowry *et al.* [22] modified by Schacterle and Pollack [32].

RESULTS

Phosphorylation and dephosphorylation of sperm proteins

When CHAPS-solubilized sperm proteins were incubated with [γ-^{32}P]ATP in 10 mM Mg^{2+} medium, a 48 kDa protein was phosphorylated within 1 min and no other proteins appeared to be phosphorylated even after incubation for up to 10 min (Fig. 1). Addition of cAMP or cGMP to the reaction mixture resulted in a rapid dephosphorylation of the protein (Fig. 1). The half-maximal effective concentrations of cAMP and cGMP to trigger dephosphorylation of the protein were 0.3μM and 4μM, respectively (Fig. 2). When Mg^{2+} in the incubation mixture was replaced by Mn^{2+}, the 48 kDa protein was less phosphorylated (data not shown). PKI (9μM) which is known to be a potent inhibitor for A-kinase [5] did not inhibit phosphorylation of the 48 kDa protein (Fig. 3). On the other hand, when CHAPS-solubilized sperm proteins were incubated with [γ-^{32}P]ATP in 100 mM Mg^{2+}-medium, addition of cAMP or cGMP to the reaction mixture

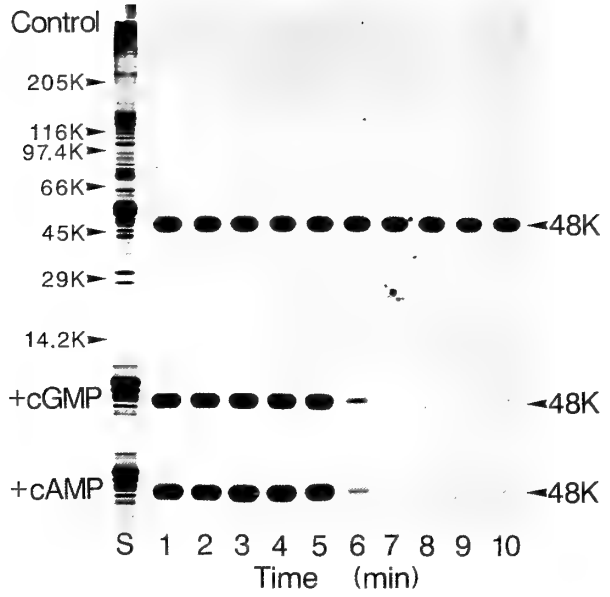

FIG. 1. Time course of phosphphorylation and cyclic nucleotide-dependent dephosphorylation of a sperm protein. Sup. A was incubated with [γ-^{32}P]ATP as described in MATERIALS AND METHODS. At 5 min of the incubation, cAMP or cGMP was added to the reaction mixture to give a final 100μM. Then, TCA (final 10%, w/v) was added at 6 through 10 min of the incubation to stop the reaction. About a 30μg of protein sample was applied per a lane of the SDS-gel. The gel, after being dried, was exposed to a Kodak X-Omat film. S; silver-stained gel. 1–10; autoradiograms.

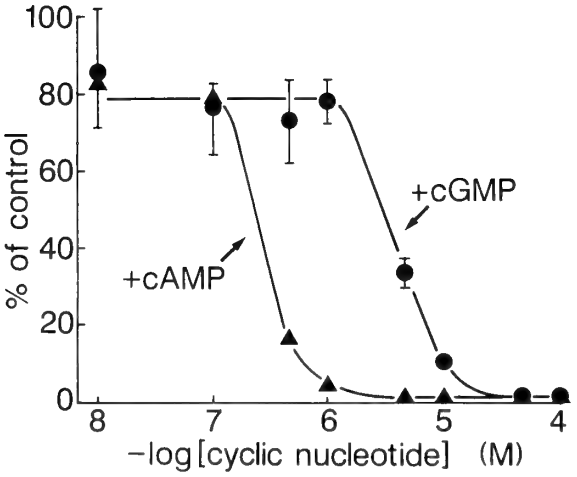

FIG. 2. Concentration-dependent effects of cAMP and cGMP on the dephosphorylation of the [^{32}P]-phosphorylated 48 kDa protein. At 5 min of the incubation of Sup. A (100μl) with [γ-^{32}P]ATP (0.83 pmol), cAMP or cGMP at the indicated concentration was added to the reaction mixture and the incubation was continued for another 5 min. The reaction was terminated by addition of TCA (final 10%, w/v) and the resulting protein precipitate, after being rinsed with ice-cold acetone, was analyzed by SDS-PAGE and then autoradiography. Intensity of darkness of the band on the autoradiogram was determined by scanning densitometry and expressed as the ratio to the darkenss of the band obtained in the absence of cyclic nucleotides.

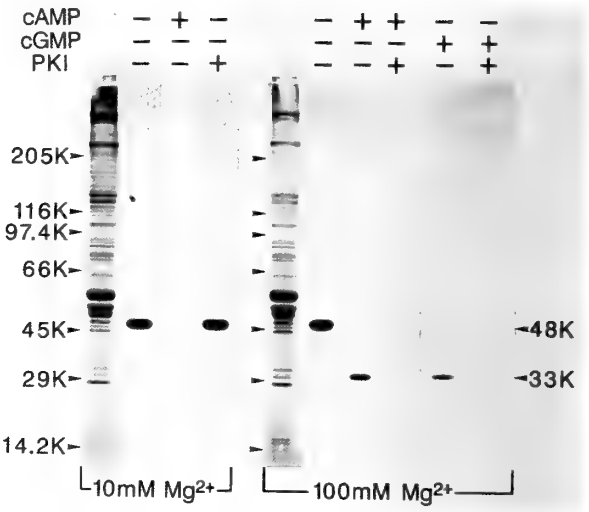

FIG. 3. Effects of cAMP, cGMP, and PKI on protein phosphorylation in sea urchin spermatozoa. CHAPS-solubilized sperm proteins (100μl) in 10 mM or 100 mM Mg^{2+}-containing medium were incubated with 0.83 pmol of [γ-^{32}P]ATP (92.5 KBq) in the presence or absence of PKI at 20°C. At 5 min of the incubation 2μl of 5 mM cAMP or cGMP were added to the reaction mixture and the incubation was continued for another 5 min. The reaction was stopped by the addition of 20μl of 60% (w/v) TCA, and the resulting protein precipitate, after being rinsed with ice-cold acetone, was subjected to SDS-PAGE and autoradiography.

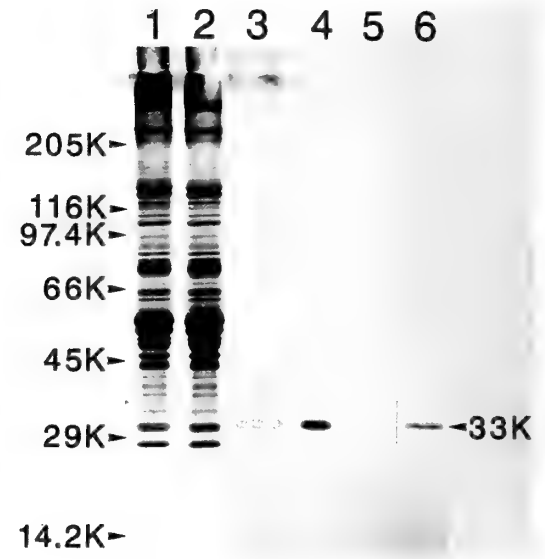

FIG. 4. Phosphorylation of a 33 kDa protein in *H. pulcherrimus* spermatozoa. CHAPS-solubilized sperm proteins in 100μl of 100 mM Mg^{2+}-containing medium was incubated with 0.83 pmol of [γ-^{32}P]ATP (92.5 KBq) at 20°C for 5 min, and then 2μl of 5 mM cAMP were added to the reaction mixture. At 5 min after addition, the reaction was stopped by addition of final 10% (w/v) TCA or 5% (v/v) PCA. The PCA-soluble protein was pelleted by the addition of final 20% (w/v) TCA. Protein samples were analyzed by SDS-PAGE and autoradiography. 1, 2 and 3, siver-stained gels. 4, 5 and 6, its autoradiogram. 1 and 2, 10% TCA-insoluble proteins; 2 and 5, 5% PCA-insoluble proteins; 3 and 6, 5% PCA-soluble and 20% TCA-insoluble proteins.

resulted in dephosphorylation of the 48 kDa protein and phosphorylation of a 33 kDa protein, and this phosphorylation of the 33 kDa protein was blocked by 9μM of PKI (Fig. 3). The [^{32}P]-phosphorylatable 33 kDa protein was soluble in 5% (w/v) PCA but insoluble in 20% (w/v) TCA (Fig. 4).

Identification of the [^{32}P]-phosphoamino acid in the 48 kDa protein

To identify [^{32}P]-phosphoamino acid in the 48 kDa protein, the [^{32}P]-phosphorylated 48 kDa protein band was excised from the gel and hydrolysed in 5.7 N HCl. Since it has been reported that a long term hydrolysis resulted in degradation of P-Tyr [29], the [^{32}P]-phosphorylated 48 kDa protein was hydrolyzed for 1 hr or 4 hrs at 110°C and the hydrolysate was analysed by HPLC on an anion exchange column (Whatman Partisil 10 SAX). Two radioactive peaks were obtained in the sample from 1 hr hydrolysis: one peak (Peak 1) prior to P-Tyr and another peak (Peak 2) corresponding to P-Ser. The peak corresponding to P-Thr did not have radioactivity.

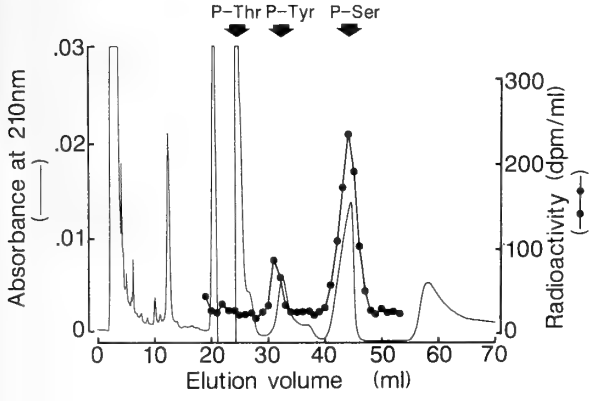

FIG. 5. HPLC profile of the hydrolysate of the [^{32}P]-phosphorylated 48 kDa protein with P-Thr, P-Tyr and P-Ser on a Whatman Partisil 10 SAX column. The [^{32}P]-phosphorylated 48 kDa protein excised from the SDS-gel and authentic P-Ser, P-Thr and P-Tyr were hydrolysed in constant-boiling HCl for 4 hrs. The hydrolysate was applied to the column as decribed in MATERIALS AND METHODS.

As hydrolysis was continued for 4 hrs, Peak 1 became smaller while Peak 2 became larger. Fig. 5 shows the chromatogram of 4 hrs hydrolyzed sample. Since Peak 1 did not overlap with the peak of P-Tyr in both samples from 1 hr and 4 hrs hydrolysis, we concluded that serine residues in the 48 kDa protein were phosphorylated by [γ-^{32}P]ATP.

Effects of PPase inhibitors on cyclic nucleotide-dependent dephosphorylation of the [^{32}P]-phosphorylated 48 kDa protein

Fluoride, zinc and vanadate inhibit PPase activity. Table 1 shows the effects of other agents including these on cyclic nucleotide-dependent dephosphorylation of the [^{32}P]-phosphorylated 48 kDa protein. In the experiments without cyclic nucleotides, addition of 20 mM molybdate or vanadate resulted in dephosphorylation of the [^{32}P]-phosphorylated 48

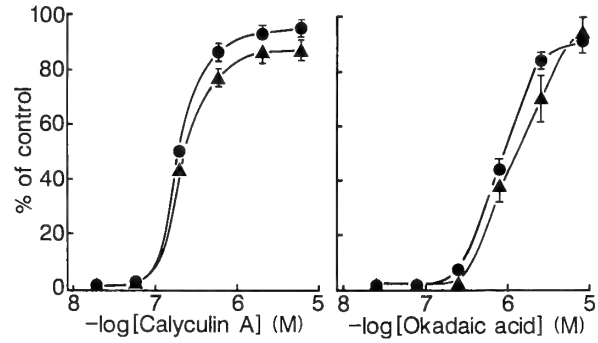

FIG. 6. Dose-dependent effects of calyculin A and okadaic acid on the cyclic nucleotide-dependent dephosphorylation of [^{32}P]-phosphorylated 48 kDa protein. After 5 min incubation of Sup. A (100μl) with [γ-^{32}P]ATP, various concentrations of calyculin A (left panel) with final 100μM of cAMP (●) or cGMP (▲), or okadaic acid (right panel) with final 100μM of cAMP (●) or cGMP (▲) were added to the reaction mixture and the incubation was continued for another 5 min. The reaction was stopped by the addition of final 10% (w/v) TCA. The proteins in the precipitate was analyzed by SDS-PAGE and autoradiography. Intensity of darkness of the band on the autoradiogram was quantitatively measured by scanning densitometry, and expressed as the ratio to the value for the band obtained in the absebce of cyclic nucleotides and inhibitors.

TABLE 1. Effect of various inhibitors on cyclic nucleotide-dependent dephosphorylation of the [^{32}P]-phosphorylated 48 kDa protein[1)]

		Control	+cAMP	+cGMP
None		100%	0%	1%
$(CH_3COO)_2Zn$	20 mM	79	78	49
	2	56	11	6
	0.2	68	0	0
Na_2MoO_4	20	50	0	0
Na_3VO_4	20	52	18	6
NaF	100	80	5	21
	50	69	1	2
	20	74	0	0
β-glycero-phosphate	50	89	0	5

1) Values are expressed as the ratio to the remaining [^{32}P]-radioactivity in the 48 kDa protein as 100%.

kDa protein up to about 50% of no addition. EDTA also induced dephosphorylation of the protein up to 15% of control. In the experiments with cyclic nucleotides, zinc inhibited cAMP-dependent dephosphoryration of the [^{32}P]-phosphorylated 48 kDa protein completely and cGMP-dependent dephosphorylation of the protein partially (49% of control). High concentration (100 mM) of fluoride or vanadate (20 mM) slightly inhibited both cAMP- and cGMP-dependent dephosphorylation of the [^{32}P]-phosphorylated 48 kDa protein. β-Glycerophosphate (50 mM) exhibited no significant inhibitory effect on the dephosphorylation.

Calyculin A and okadaic acid obtained from sea sponges are potent and specific inhibitors for many PPases [3, 7, 16]. Fig. 6 shows the effects of varying concentrations of calyculin A and okadaic acid on cyclic nucleotide-dependent dephosphorylation of the [^{32}P]-phosphorylated 48 kDa protein. Calyculin A inhibited both cAMP- and cGMP-dependent dephosphorylations at the same concentration (IC_{50}= 0.2μM). Okadaic acid also inhibited both cAMP- and cGMP-dependent dephosphorylations, but the apparent IC_{50}

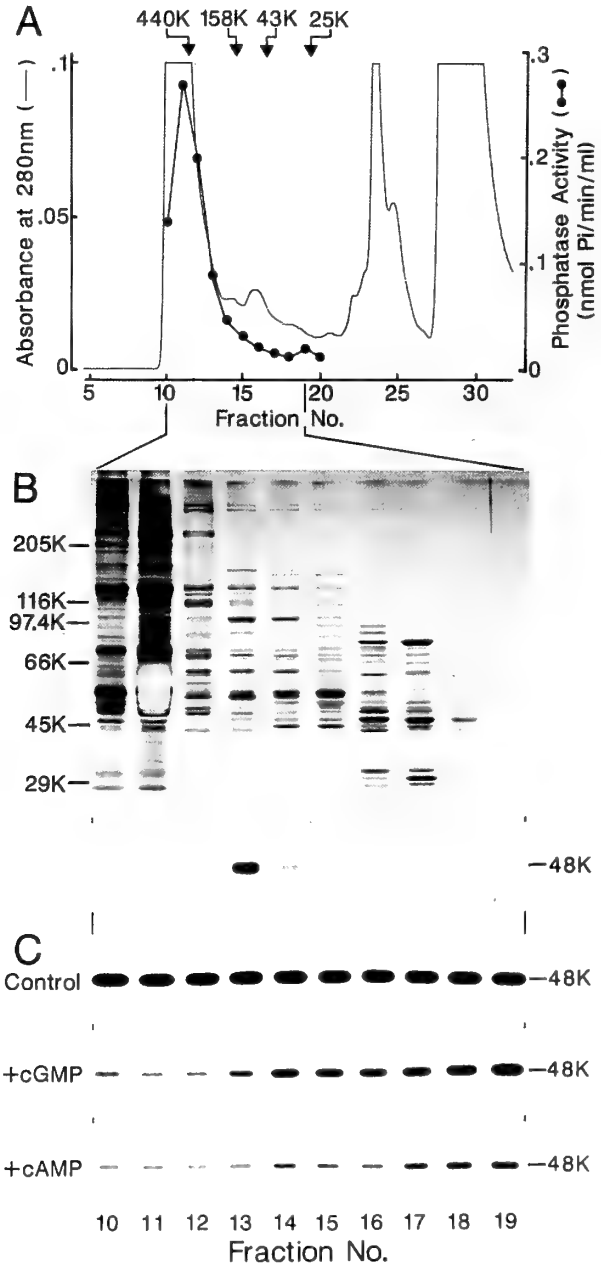

FIG. 7. HPLC profile of Sup. B on a TSK-GEL G3000SW column and the SDS-PAGE pattern. Fractions obtained from the column were determined for PPase activity (A), 48 kDa protein-phosphorylating activity (B), and cyclic nucleotide-dependent dephosphorylation activity for the [^{32}P]-phosphorylated 48 kDa protein (C) as described in MATERIALS AND METHODS.

of okadaic acid was 4-6 fold higher (0.8–1.2μM) than that of calycylin A.

Purification of the [^{32}P]-phosphorytable 48 kDa protein

In preliminary experiments, we estimated the molecular mass of the [^{32}P]-phosphorylatable 48 kDa protein by gel filtration. Sup. B was incubated with [γ-^{32}P]ATP and then subjected to TSK-GEL G3000SW gel chromatography. As shown in Fig. 7A and 7B, most of the [^{32}P]-phosphorylated 48 kDa protein was recovered in the fraction (No. 13) in which proteins with molecular masses from 250 kDa to 400 kDa were eluted. PPase activity was recovered in the fraction (No. 10) in which proteins with molecular masses of over 400 kDa were eluted. In different experiments, dephosphorylating activity for the [^{32}P]-phosphorylated 48 kDa protein in all the fractions obtained from the TSK-GEL G3000SW column was examined with the fraction (No. 13) as the substrate (Fig. 7C). In the absence of cyclic nucleotides, none of the fractions tested showed dephosphorylating activity for the [^{32}P]-phosphorylated 48 kDa protein. However, addition of cGMP or cAMP to the fractions which contained proteins with the molecular masses of over 400 kDa induced dephosphorylation of the [^{32}P]-phosphorylated 48 kDa protein.

To purify the [^{32}P]-phosphorylatable 48 kDa protein, CHAPS-solubilized sperm protein prepared from 50 ml of dry sperm was centrifuged at 30,000×g and the resulting supernatant fluid was applied to a DEAE-Sephacel column. The [^{32}P]-phosphorylatable 48 kDa protein was eluted at 150–240 mM NaCl. PPase activity was also eluted at the same concentration of NaCl. Fractions containing the 48 kDa protein also contained PPase activity. Further purification of the protein was carried out by ion exchange chromatography on a Mono Q HR5/5 column. The 48 kDa protein was eluted at 280–330 mM NaCl, in which a major PPase activity was also eluted. To remove the PPase activity, the fractions containing the 48 kDa protein were subjected to chromatography on a histone-agarose column. In this chromatography, the 48 kDa protein was obtained mainly in the fractions eluted at 320–440 mM NaCl. However, these fractions still contained PPase activity, although a major PPase activity was eluted after the 48 kDa protein. The 48 kDa protein and PPase activity were separated by chromatography on a Superose 6 HR10/30 column (Fig. 8). In this chroma-

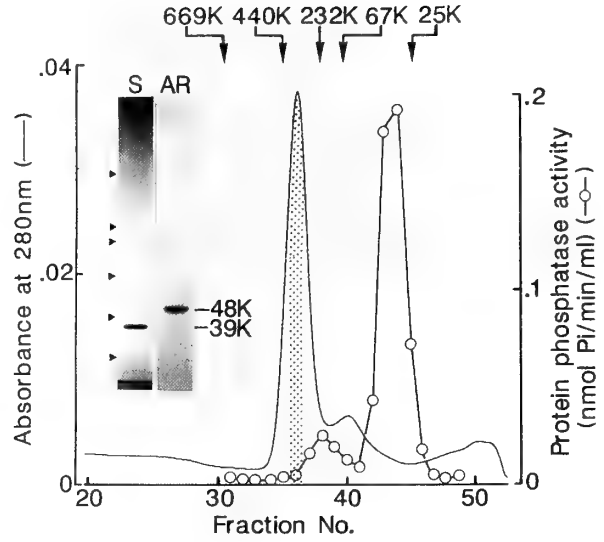

FIG. 8. HPLC profile of the 48 kDa protein-containing fraction on a Superose 6 HR10/30 column. Fractions obtained from the column were assayed for phosphorylating activity of the 48 kDa protein. Dotted area indicates the fractions which contained practically pure 400 kDa protein consisting of the 48 kDa and 39 kDa proteins. The 400 kDa protein was phosphorylated with [γ-^{32}P]ATP and then analyzed by SDS-PAGE, followed by autoradiography. Silver-stained gel (S) and its autoradiogram (AR) of the [^{32}P]-phosphorylated 48 kDa protein are shown in *insert* in the figure. Triangle points on the left side of the gel in *insert* indicate standard proteins as the same as in Fig. 3. Molecular weight standards used for the gel chromatography were thyroglobulin (669 kDa), ferritin (440 kDa), catalase (232 kDa), bovine serum albumin (67 kDa), and chymotrypsinogen A (25 kDa).

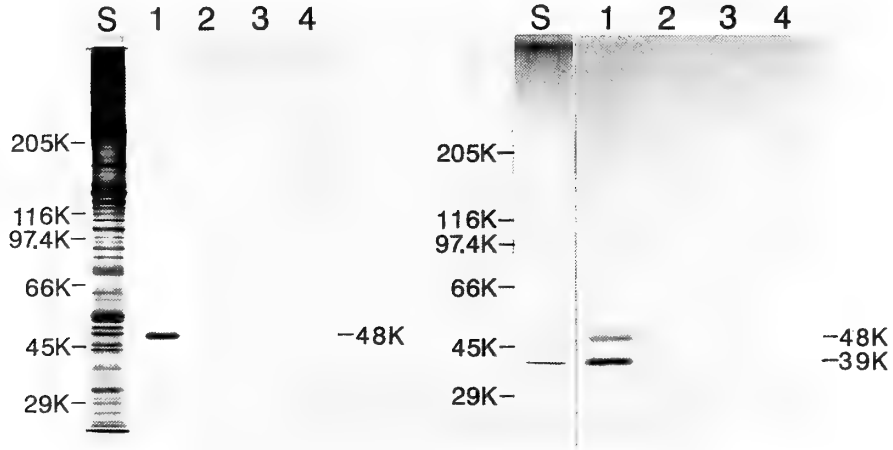

FIG. 9. SDS-PAGE and its autoradiogram of 8-N^3-[^{32}P]cAMP or 8-N$_3$-[^{32}P]cGMP-treated CHAPS-solubilized sperm proteins (left panel) or the purified 400 kDa protein (right panel). Protein samples were incubated with 1: 66 nM 8-N$_3$-[^{32}P]cAMP, 2: 66 nM 8-N$_3$-[^{32}P]cAMP and 20μM cAMP, 3: 0.4μM 8-N$_3$-[^{32}P]cGMP, 4: 0.4μM 8-N$_3$-[^{32}P]cGMP and 20μM cGMP. S; silver stained gel.

tography, the 48 kDa protein was eluted as a single protein peak at molecular mass of approximately 400 kDa. The protein with the molecular mass of 400 kDa was separated to 48 kDa and 39 kDa proteins by SDS-PAGE. Incubation of the 400 kDa protein with [γ-^{32}P]ATP resulted in phosphorylation of only the 48 kDa protein.

Incorporation of 8-N_3-[^{32}P]cAMP and -[^{32}P]cGMP into sperm proteins

When Sup. B or the purified 400 kDa protein was incubated with a photoaffinity cAMP analogue 8-N_3-[^{32}P]cAMP or cGMP analogue 8-N_3-[^{32}P]cGMP, cAMP analogue was incorporated into the 48 kDa protein (Fig. 9, left panel). When the purified 400 kDa protein was incubated with the cyclic nucleotide analogues, both of the 48 kDa and the 39 kDa proteins were labeled (Fig. 9, right panel). The binding of 8-N_3[^{32}P]cAMP to these proteins was mostly blocked in the presence of 20μM cAMP.

Properties of the autophosphorylatable sperm protein

The purified 400 kDa protein which consisted of the [^{32}P]-phosphorylatable 48 kDa protein and the 39 kDa protein showed histone kinase activity. Table 2 shows the ability of the histone kinase to phosphorylate various histone types. The lysine rich histones (H1 and H2B) were the best substrates, while the arginine rich histones (H2A and H3) were poor substrates. The kinase did not phosphorylate histone H4. Total histones, core histones and histone H1 isolated from sea urchin sperm heads were also tested for substrates. The sea urchin sperm-derived histones were also good substrates for the kinase (Table 2). Phosphorylation of these histones by the kinase in the presence of cAMP was blocked by 9μM of PKI. The kinase was activated by cGMP as well as cAMP in a concentration-dependent manner, but cGMP was less potent than cAMP. Maximal response of the kinase to cGMP was seen at 10μM (Fig. 10). cAMP- or

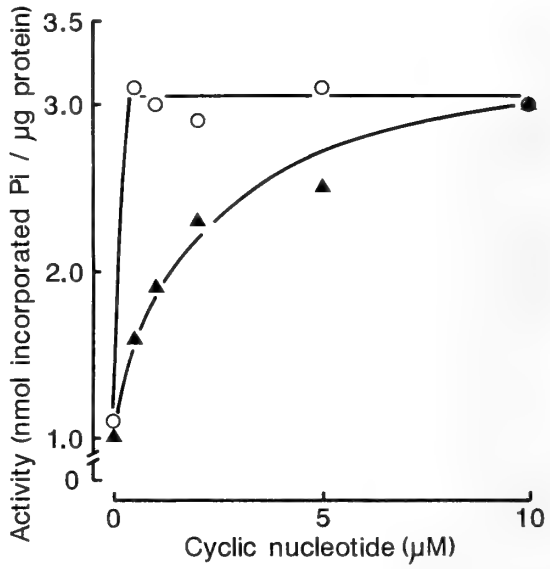

FIG. 10. Concentration-dependent effects of cAMP and cGMP on activation of sea urchin sperm histone kinase to phosphorylate *H. pulcherrimus* sperm histone H1. Reaction was started by addition of 41.9 ng of purified sperm histone kinase to 18.5μl of reaction mixture containing 1 mg/ml sea urchin sperm histone H1, 10 mM $(CH_3COO)_2Mg$, 0.2 mM [γ-^{32}P]ATP, indicated concentration of cAMP/cGMP and 50 mM MES, pH 6.5). After incubation at 30°C for 10 min, the reaction was terminated by heating at 100°C for 5 min. A 10μl-aliquot was withdrawn, spotted onto a 1×2 cm strip of Whatman p 81 phsophocellulose and then immersed in 75 mM phosphoric acid. The strip was subjected to four washes of 75 mM phosphoric acid and then air-dried, followed by measuring the radioactivity by the liquid scintillation counter. cAMP (○), cGMP (●).

TABLE 2. Substrate specificity of cAMP-dependent histon kinase

		Calf thymus histones					
		Total histone	H1	H2A	H2B	H3	H4
cAMP	inhibitor	nmol Pi incorporated/μg protein					
+	−	20.6	17.2	5.5	25.7	1.4	0.0
+	+	0.1	0.1	0.1	0.1	0.0	0.0
−	−	0.9	0.6	0.2	0.9	0.0	0.0
−	+	0.0	0.0	0.1	0.0	0.0	0.0
		Sea urchin sperm histones					
		Total histone	Core histone		H1		
cAMP	inhibitor	nmol Pi incorporated/μg protein					
−	−	6.8	4.5		7.1		
+	−	34.0	37.5		53.7		
+	+	1.1	1.7		0.6		

Purified enzyme (56 ng in 5μl) was added to 95μl of reaction mixture containing 1 mg/ml calf thymus or sea urchin sperm histones, 0.2 mM ATP (74 kBq [γ-^{32}P]ATP), 10 mM $(CH_3COO)_2Mg$ and 50 mM MES (pH 6.5) in the presence or absence of 2μM cAMP and/or 9μM protein kinase inhibitor (TTYADFIASGRTGRRNAIHD), and incubated at 30°C for 10 min. The reaction was stopped by heating at 100°C for 5 min. An aliquot of the reaction mixture (25μl) was transferred onto a Whatman P81 phosphocellulose filter paper. The filter was washed with 75 mM phosphoric acid five times, dried in air, and the radioactivity was measured.

cGMP-dependent histone kinase activity required Mg^{2+} more than 5 mM. The histone kinase was incubated for 2 min on ice in the presence of 1μM cAMP or cGMP, and the reaction mixture was then subjected to gel chromatography on a Superose 6 HR10/30 column equilibrated with Buffer B containing 5μM cAMP. Chromatography with 5μM cAMP gave a peak histone kinase activity at molecular mass of about 39 kDa which was active even in the presence of cAMP less than 0.25μM (Fig. 11). However, treatment of the kinase with 10μM cGMP did not result in shift of kinase activity from 400 kDa to 49 kDa.

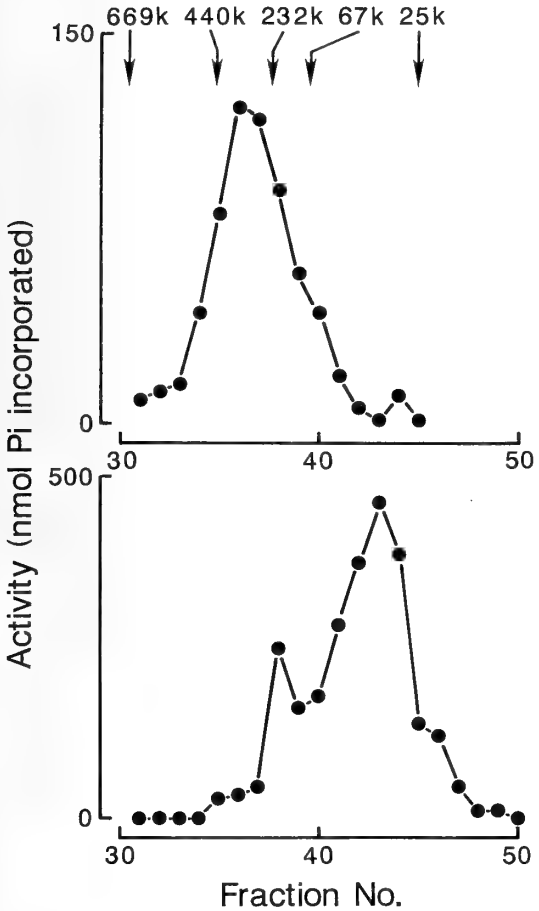

FIG. 11. Gel filtration profiles of sea urchin histone kinase on a Superose 6 HR10/30 column in the presence or absence of cAMP. Autophosphorylatable 48 kDa protein-containing fractions obtained from chromatography on a histone-agarose column were pooled and concentrated, and then subjected to a Superose 6 HR10/30 column equilibrated with Buffer B (upper panel). Purified sea urchin histone kinase was incubated in Buffer B containing 1μM cAMP at 0°C for 20 min and then subjected to chromatography on the Superose column equilibrated with Buffer B containing 5μM cAMP (lower panel). An aliquot of each fraction was assayed for histone kinase activity using sea urchin sperm histone H1 as substrate in the presence of 2μM cAMP (upper panel) or 0.25μM cAMP (lower panel). Molecular weight standards used for the gel chromatography were thyroglobulin (669 kDa), ferritin (440 kDa), catalase (232 kDa), bovine serum albumin (67 kDa) and chymotrpsinogen A (25 kDa).

DISCUSSION

When detergent-solubilized sea urchin sperm proteins are incubated with [γ-^{32}P]ATP, a 42 kDa protein and histone H1 in *S. purpuratus* [27–28] and a 45 kDa protein in *Arbacia punctulata* [43] were phosphorylated. Furthermore, phosphorylation of histone H1 in *S. purpuratus* has been reported to be cAMP-dependent [27–28]. Here, we demonstrated that in *H. pulcherrimus* spermatozoa a 48 kDa protein and a 33 kDa protein were phosphorylated but phosphorylation of the latter protein by an endogenous kinase was observed only in 100 mM Mg^{2+}-containing medium while phosphorylation of the 48 kDa protein occurred irrespective of the concentration of Mg^{2+}. The 33 kDa protein could be histone H1 based on the following properties: 1) it is PCA-soluble and TCA-incoluble, 2) it is cAMP-dependently phosphoryltable, and 3) it has correct apparent molecular size [17, 25, 27, this study]. Unlike the phosphorylation of the 33 kDa protein, which was PKI-inhibitable, phosphorylation of the 48 kDa protein which was not inhibited by PKI, occurred only in the absence of cyclic nucleotides. Even after the 400 kDa protein was purified, 48 kDa protein was phosphorylated by incubation with [γ-^{32}P]ATP. Therefore, the phosphorylation of the 48 kDa protein may be autophosphorylation. Addition of cAMP or cGMP triggered dephosphorylation of the [^{32}P]-phosphorylated 48 kDa protein in a concentration-dependent manner. Since calyculin A and okadaic acid, which are potent inhibitors specific for serine/threonine PPases, inhibited the cyclic nucleotide-dependent dephosphorylation of the [^{32}P]-phosphorylated 48 kDa protein, such a type of PPase may be involved in dephosphorylation of the protein.

Gel filtration of the [^{32}P]-phosphorylatable 48 kDa protein demonstrated that it was associated with a 39 kDa protein to form a 400 kDa protein molecule. After SDS-PAGE of the 400 kDa protein, the 48 kDa and 39 kDa protein bands were stained by Coomassie brilliant blue to almost the same darkness on the gel, suggesting that the 400 kDa oligomer consists of an equal number of the 48 kDa and 39 kDa subunits. However, the 48 kDa protein was stained less intensively with silver than the 39 kDa protein, so careful quantitative analysis will be required to confirm this idea.

Incorporation of a photoaffinity cGMP analogue 8-N_3-[^{32}P]cGMP to sperm protein was not detected probably because of low specific radioactivity of the analogue. However, a photoaffinity cAMP analogue 8-N_3-[^{32}P]cAMP was incorporated into the same molecular mass protein as the protein phosphorylated with [γ-^{32}P]ATP. Similarly, 8-N_3-[^{32}P]cAMP was incorporated into the 48 kDa protein in the purified 400 kDa protein. These results indicate that cAMP binds to the 48 kDa protein. In this regard, it should be mentioned that several enzymes and certain mambrane receptor proteins have been known to be regulated by substrate-directedly [1, 4, 8, 18]. Thomas *et al.* [42] proposed that in the case of phosphorylation of bovine lung cGMP-binding cGMP-specific phosphodiesterase (cG-BPDE), the

binding of cGMP to cG-BPDE induces a conformational change in cG-BPDE to expose the phosphorylation site for the protein kinases. In the present study, we demonstrated that the protein consisting of [^{32}P]-phosphorylatable 48 kDa protein(s) and 39 kDa protein(s) phosphorylates calf thymus histones and also sea urchin sperm histones in cyclic nucleotide-dependent manner. In this regard, it should be mentioned that certain A-kinase activity is regulated by cAMP-dependent dephosphorylation of autophosphorylated enzyme [6, 31]. Type II A-kinase consists of an autophosphorylatable regulatory (R) dimer and two catalytic (C) subunits. Binding of cAMP to R subunit triggers the dissociation of R, and C results in the elevation of protein kinase activity. Considering these results, our results presented here may be explained by the idea that the binding of cAMP to the 48 kDa subunit(s) in the 400 kDa kinase results in dissociation of the 48 kDa regulatory subunit(s) and 39 kDa catalytic subunit(s), which allows the autophosphorylated 48 kDa subunit(s) accessible to a protein phosphatase which is abundant in the detergent-solublized sperm fraction. An alternative explanation may be possible: sea urchin spermatozoa may contain a novel cyclic nucleotide-dependent protein phosphatase. When we first obtained the results to show cyclic nucleotide-dependent dephosphorylation of the [^{32}P]-phosphorylated 48 kDa protein we thought that it might be explained by the latter intriguing idea. However, so far we only obtained three different protein phosphatases and none of phosphatases could be activated by cyclic nucleotides (unpublished observation). Therefore, at this moment we prefer the former idea.

Sperm histone kinase isolated in this study was activated by both cAMP and cGMP, and phosphorylated sea urchin sperm histone H1 as well as calf thymus histones (H1 and H2B). It has been reported that the egg jelly of *H. pulcherrimus* contains sperm-activating peptide I (SAP-I:GFDLNGGGVG) and FSG which elevate sperm cGMP and/or cAMP upto some μM levels (14, 36-37). Green and Poccia [12] reported that phosphorylation of sperm histones H1 and H2B of *S. purpuratus* precedes sperm chromatin decondensation and histone H1 exchange during pronuclear formation. Therefore, we presume that upon fertilization sperm histone kinase isolated here may be activated in the spermatozoon by SAP-I-elevated cGMP and/or cAMP or FSG-elevated cAMP and phosphorylates these histones before entering sperm nuclei into the egg.

ACKNOWLEDGMENTS

We would like to thank the staff members of the Radioisotope Center, Kanazawa University, for technical supports throughout this work, and Dr. Daniel Hardy (University of Texas Southwestern Medical Center) for critical reading of this manuscript. We also thank Mr. M. Matada for collecting and culturing sea urchins. This work was supported by Grants-in-Aid 02404006 and 02044059 from the Ministry of Education, Science and Culture of Japan.

REFERENCES

1 Benovic JL, Regan JW, Matsui H, Mayor FJr, Cotecchia S, Leeb-Lundberg LMF, Caron MG, Lefkowitz RJ (1987) Agonist-dependent phosphorylation of the α_2-adrenergic receptor by the β-adrenergic receptor kinase. J Biol Chem 262: 17251–17253

2 Bentley JK, Tubb DJ, Garbers DL (1986) Receptor-mediated activation of spermatozoan guanylate cyclase. J Biol Chem 261: 14859–14862

3 Bialojan C, Takai A (1988) Inhibitory effect of a marine-sponge toxin, okadaic acid, on protein phosphatases. Biochem J 256: 283–290

4 Bownds D, Dawes J, Miller J, Stahlman M (1972) Phosphorylation of frog photoreceptor membranes induced by light. Nature 237: 125–127

5 Cheng H-C, Kemp BE, Pearson RB, Smith AJ, Misconi L, Van Patten SM, Walsh DA (1986) A potent synthetic peptide inhibitor of the cAMP-dependent protein kinase. J Biol Chem 261: 989–992

6 Chou C-K, Alfano J, Rosen OM (1977) Purification of phosphoprotein phosphatase from bovine cardiac muscle that catalyzes dephosphorylation of cyclic AMP-binding protein component of protein kinase. J Biol Chem 252: 2855–2859

7 Cohen P (1989) The structure and regulation of protein phosphatases. Annu Rev Biochem 58: 453–508

8 El-Maghrabi MR, Claus TH, Pilks SJ (1983) Substrate-directed regulation of cAMP-dependent phosphorylation. Methdos Enzymol 99: 212–219

9 Garbers DL, Kopf GS (1980) The regulation of spermatozoa by calcium and cyclic nucleotides. Adv Cyclic Nucleotide Res 13: 251–306

10 Garbers DL, Tubb DJ, Kopf GS (1980) Regulation of sea urchin sperm cyclic AMP-dependent protein kinases by an egg associated factor. Biol Reprod 22: 526–532

11 Garbers DL, Watkins HD, Hansbrough JR, Smith A, Misono KS (1982) The amino acid sequence and chemical synthesis of speract and of speract analogues. J Biol Chem 257: 2734–2737

12 Green GR, Poccia DL (1985) Phosphorylation of sea urchin sperm H1 and H2B histones precedes chromatin decondensation and H1 exchange during pronuclear formation. Dev Biol 108: 235–245

13 Green GR, Lee H-J, Poccia DL (1993) Phosphorylation weakens DNA binding by peptides containing multiple "SPKK" sequences. J Biol Chem 268: 11247–11255

14 Harumi T, Hoshino K, Suzuki N (1992) Effects of sperm-activating peptide I on *Hemicentrotus pulcherrimus* spermatozoa in high potassium sea water. Develop Grwth Differ 34: 163–172

15 Ishiguro K, Murofushi H, Sakai H (1982) Evidence that cAMP-dependent protein kinase and a protein factor are involved in reactivation of Triton X-100 models of sea urchin and starfish spermatozoa. J Cell Biol 92: 777–782

16 Ishihara H, Martin BL, Brautigan DL, Karaki H, Ozaki H, Kato Y, Fusetani N, Watabe S, Hashimoto K, Uemura D, Hartshorne DJ (1989) Calyculin A and okadaic acid: inhibitors of protein phosphatase activity. Biochem Biophys Res Commun 159: 871–877

17 Johns EW (1977) The isolation and purification of histones. Methods Cell Biol 16: 183–203

18 Kuhn H, Dreyer WJ (1972) Light dependent phosphorylation of rhodopsin by ATP. FEBS lett 20: 1–6

19 Laemmli UK (1970) Cleavage of structural proteins during the assembly of the head of bacteriophage T4. Nature 227: 680–685.

20 Lee MYW, Iverson RM (1972) Protein kinase in sea urchin gamets and embryos. Exptl Cell Res 75: 300–304

21 Lee MYW, Iverson RM (1976) An adenosine 3′:5′ monophosphate dependent protein kinase from sea urchin spermatozoa. Biochim Biophys Acta 429:123–136

22 Lowry OH, Rosebrough NJ, Farr AL, Randall RJ (1951) Protein measurement with the folin phenol reagent. J Biol Chem 193: 265–275

23 Meisler MH, Langan TA (1969) Characterization of a phosphatase specific for phosphorylated histones and protamine. J Biol Chem 244: 4961–4968

24 Morrissey JH (1981) Silver stain for proteins in polyacrylamide gels: A modified procedure with enhanced uniform sensitivity. Anal Biochem 117: 307–310

25 Ozaki H (1971) Developmental studies of sea urchin chromatin. Chromatin isolated from spermatozoa of the sea urchin *Strongylocentrotus pururatus*. Dev Biol 26: 209–219

26 Poccia DL, Green GR (1992) Packaging and unpackaging the sea urchin sperm genome. TIBS 17: 223–227

27 Porter DC, Vacquier VD (1986) Phosphorylation of sperm histone H1 is induced by the egg jelly layer in the sea urchin *Strongylocentrotus purpuratus*. Dev Biol 116: 203–212

28 Porter DC, Moy GW, Vacquier VD (1988) cAMP-dependent protein kinase of sea urchin sperm phosphorylates sperm histone H1 on a single site. J Biol Chem 263: 2750–2755

29 Robert JC, Soumarmon A, Lewin (1985) Determination of o-phosphothreonine, o-phosphoserine, o-phosphotyrosine and phosphate by high-performance liquid chromatography. J Chromatogr 338: 315–324

30 Roskoski RJr (1983) Assays of protein kinase. Methods Enzymol 99: 3–6

31 Scott CW, Mumby MC (1985) Phosphorylation of type II reguratory subunit of cAMP-dependent protein kinase in intact smooth muscle. J Biol Chem 260: 2274–2280

32 Schacterle GR, Pollack RL (1973) A simplified method for the quantitative assay of small amounts of protein in biologic material. Anal Biochem 51: 654–655

33 SeGall GK, Lennarz WJ (1979) Chemical characterization of the component of the jelly coat from sea urchin eggs responsible for induction of the acrosome reaction. Dev Biol 71: 33–48

34 SeGall GK, Lennarz WJ (1981) Jelly coat and induction of the acrosome reaction in echinoid sperm. Dev Biol 86: 87–93

35 Shacter E (1984) Organic extraction of P_i with isobutanol/toluene. Anal Biochem 138: 416–420

36 Shimizu T, Kinoh H, Yamaguchi M, Suzuki N (1990) Purification and characterization of the egg jelly macromolecules, sialglycoprotein and fucose sulfate glycoconjugate, of the sea urchin *Hemicentrotus pulcherrimus*. Develop Growth Differ 32: 473–487

37 Suzuki N, Nomura K, Ohtake H, Isaka S (1981) Purification and the primary structure of sperm-activating peptides from the jelly coat of sea urchin eggs. Biochem Biophys Res Commun 99: 1238–1244

38 Suzuki N, Kurita M, Yoshino K, Yamaguchi M (1987) Speract binds exclusively to sperm tails and causes and electrophoretic mobility shift in a major sperm tail protein of sea urchins. Zool Sci 4: 641–648

39 Swarup G, Garbers DL (1982) Phosphoprotein phosphatase activity of sea urchin spermatozoa. Biol Reprod 26: 953–960

40 Swarup G, Cohen S, Garbers DL (1981) Selective dephosphorylation of proteins containing phosphotyrosine by alkaline phosphatases. J Biol Chem 256: 8197–8201

41 Takai Y, Nishiyama K, Yamamura H, Nishizuka Y (1975) Guanosine 3′:5′-monophosphate-dependent protein kinase frrom bovine cerebellum. Purification and characterization. J Biol Chem 250: 4690–4695

42 Thomas MK, Francis SH, Corbin JD (1990) Substrate- and kinase-directed regulation of phosphorylation of a cGMP-binding phosphodiesterase by cGMP. J Biol Chem 265: 14971–14978

43 Vacquier VD, Porter DC, Keller SH, Aukerman M (1989) Egg jelly induces the phosphorylation of histone H3 in spermatozoa of the sea urchin *Arbacia punctulata*. Dev Biol 133: 111–118

44 Yang JC, Fujitaki JM, Smith RA (1982) Separation of phosphohydroxyamino acids by high-performance liquid chromatography. Anal Biochem 122: 360–363

45 Watkins HD, Kopf GS, Garbers DL (1978) Activation of sperm adenylate cyclase by factors associated with eggs. Biol Reprod 19: 890–894

46 Weber K, Osborn M (1969) The reliability of molecular weight determination by dodecyl sulfate polyacrylamide gel electrophoresis. J Biol Chem 244: 4406–4412

ZOOLOGICAL SCIENCE 11: 221–227 (1994)

Rapid and Quantitative Detection of Aspartic Proteinase in Animal Tissues by Radio-labeled Pepstatin A

MASANORI MUKAI[1], TOSHIHIKO KONDO[2] and KATSUTOSHI YOSHIZATO[1,3]

[1]*Molecular Cell Science Laboratory, Department of Biological Science, Faculty of Science, Hiroshima University, 1-3-1 Kagamiyama, Higashihiroshima-shi, Hiroshima 724 and* [2]*Department of Physical Biochemistry, Institute of Endocrinology, Gunma University, Maebashi 371, Japan*

ABSTRACT—A new radio-derivative of pepstatin A was developed and was shown to be used as a probe for rapidly and quantitatively detecting aspartic proteinases in animal tissues. The carboxyl group of pepstatin A was activated by the water soluble carbodiimide, 1-ethyl-3-(3-dimethylaminopropyl) carbodiimide hydrochloride and was then coupled with N-hydroxysulfosuccinimide (Sulfo NHS). [^{35}S]-Methionyl-pepstatin with a relatively high specific activity was obtained by coupling the Sulfo NHS-pepstatin with L-[^{35}S]-methionine. Binding specificity of the pepstatin A derivative was characterized using pepsin as a test enzyme. Binding experiments showed that the radio-labeled pepstatin can be used as a probe which binds specifically to aspartic proteinases and detects them. The probe could detect as low as 0.1 nmoles of pepsin. To know whether the radio-labeled probe can be actually used to detect aspartic proteinases in animal tissues, it was applied to the tail tissue of metamorphosing amphibian tadpole which had been known to show high activity of cathepsin D. The assay demonstrated marked increase in aspartic proteinases at the climax stage. It was concluded that the radio-labeled pepstatin derivative developed by the present study is useful for quick and quantitative determination of pepstatin-reactive enzymes in animal tissues.

INTRODUCTION

The aspartic proteinase is a group of proteinases (EC 3.4. group 23) which has an optimum pH at an acidic region. The family contains pepsin, cathepsin D, cathepsin E, renin, chymosin and gastricsin. Amino acid sequences of mammalian aspartic proteinases and the corresponding nucleotide sequences of their cDNA clones revealed that they have the active center, which contains two aspartic residues and are highly conserved among aspartic proteinases [4, 8, 10, 12, 32, 33, 35].

Pepstatin A is produced by actinomyces [37] and is a potent inhibitor of pepsin ($Ki=4.5\times10^{-11}$ M), cathepsin D ($Ki=10^{-10}$ M) and other aspartic proteinases [3, 27]. Pepstatin A binds to the active center of the enzyme in a stoichiometric manner which is surrounded by two aspartic moieties [3, 19, 37].

Radio-labeled pepstatin derivatives have been chemically synthesized. Pepstatin was coupled with [^{3}H]-glycine and used for determining Kd values of a complex of pepstatinyl-[^{3}H]-glycine-cathepsin D [15]. A radio-iodinated derivative of pepstatin was prepared by introducing a tyrosine residue which was then iodinated with ^{125}I. This was utilized for the determination of Kd of pepsin-pepstatin-[^{125}I]-monoiodotyrosine methyl ester complex [41]. However, ^{3}H-labeled compound is chemically unstable because tritium is exchangeable with surrounding hydrogen. ^{125}I-Labeling has disadvantages because of its short half life of radioactivity.

Accepted March 11, 1994
Received January 27, 1994

Chemical modification of pepstatin has been designed to utilize the inhibitor as an experimental probe which tightly binds to the active site of aspartic proteinases and carries reporter groups [16]. Bimane-labeled pepstatin [21] and dinitrophenyl-pepstatin [22] have been synthesized and used for the determination of the subcellular location of cathepsin D in cultured human synovial cells. These methods of modifications require relatively complicated techniques of organic chemistry and contain multiple steps including techniques of column chromatography. Because both pepstatin derivatives described above are detected by fluorescence, these derivatives cannot be used as a probe in cases where samples to be analyzed contain fluorescent materials.

In the present study the authors aimed at developing a much simple radio-labeling procedure of pepstatin to obtain a stable derivative. For this purposes, 1-ethyl-3-(3-dimethylaminopropyl) carbodiimide hydrochloride (EDC) [42] and N-hydroxy-sulfosuccinimide (Sulfo NHS) [2, 34] were selected as activating agents since they are easy to handle because of their hydrophilicity. The activated pepstatin was coupled with L-[^{35}S]-methionine which has longer half life of decay than ^{125}I.

In the amphibian metamorphosis, the larval tail tissue is subject to the histolysis by several proteinases such as collagenase [11, 25] and cathepsin D [18, 29, 38]. This phenomenon was utilized to see validity and usefulness of the radio-labeled pepstatin derivative for detecting proteinases in animal tissues. The present study succeeded in demonstrating that the radio-labeled pepstatin is a useful probe for quick and quantitative detection of aspartic proteinases in animal tissues.

MATERIALS AND METHODS

Materials

Pepstatin A was purchased from Peptide Institute, Inc. (Osaka, Japan). EDC and Sulfo NHS were obtained from Pierce (Rockford, IL). L-[^{35}S]-methionine was from New England Nuclear (Boston, MA). SEP-PAK C_{18} was from Waters (Milford, MASS). Pepsin was a product of Wako Pure Chemicals (Osaka, Japan). All other reagents were of analytical grade. Tadpoles of bullfrog, *Rana catesbeiana*, were purchased from a local animal supplier. They were staged as described by Taylor and Kollros (TK stage) [36].

Coupling reaction

Pepstatin A (0.7 mg, 1 μmoles) was dissolved in 200 μl of dimethyl sulfoxide. Sulfo NHS (10 μmoles) and EDC (100 μmoles) were dissolved in 800 μl of 16 mM sodium phosphate buffer, pH 7.4, containing 20% dimethyl sulfoxide. These were mixed together and were incubated at room temperature (ca. 20°C) for 1 hr. The product of this reaction, Sulfo NHS-pepstatin, was diluted with 4 ml of 20 mM sodium phosphate buffer, pH 7.4, and was applied slowly to a SEP-PAK C_{18} column (1 drop/sec) using a syringe. The column was washed twice with 5 ml of 20 mM sodium phosphate buffer, pH 7.4, for removing excess amounts of activating agents (Sulfo NHS and EDC). Sulfo NHS-pepstatin was eluted from the column twice with 2 ml of dimethyl sulfoxide, mixed with 4 ml of 10 mM sodium phosphate buffer, pH 7.4, containing L-[^{35}S]-methionine (100 pmoles, 4.1 MBq, 1.6×10^8 cpm) and was incubated at room temperature (ca. 20°C) for 2 hr. The reaction mixture in which [^{35}S]-methionyl-pepstatin was produced was diluted with deionized water and loaded on a SEP-PAK C_{18} column in the same way as described above. The column was washed twice with 10 ml of deionized water. This step separated the labeled pepstatin from uncoupled L-[^{35}S]-methionine and other by-products which did not covalently bind to pepstatin A. The eluate containing [^{35}S]-methionyl-pepstatin (0.72 MBq, 2.8×10^7 cpm/4 ml dimethyl sulfoxide) was kept at −20°C before use.

Separation of [^{35}S]-methionyl pepstatin A from free pepstatin A

[^{35}S]-Methionyl pepstatin prepared as described above still contained excess amounts of pepstatin A. Free pepstatin A was removed mainly by HPLC as follows. The preparation was 4-fold diluted with deionized water and loaded on a SEP-PAK C_{18} column which was then eluted with acetonitrile. The eluate containing pepstatin A and its [^{35}S]-methionyl derivative was evaporated to dryness at 40°C *in vacuo* and was dissolved in an appropriate amount of dimethyl sulfoxide. The concentrated radio-labeled pepstatin A was subjected to reversed phase high-performance liquid chromatography (HPLC, Inertsil 300-C_8, 4.6×100 mm, Gasukuro Kogyo Inc. Tokyo, Japan) and eluted at 50°C with a linear gradient of acetonitrile (from 25 to 55%) containing 0.1% trifluoroacetic acid (TFA). The flow rate was 0.4 ml/min. The eluate was monitored by 220 nm for pepstatin A and by the radioactivity for the labeled one. Radioactive fractions were collected and concentrated by evaporation.

Binding assays

Appropriate amounts of pepsin (10–440 μg/20 μl H_2O/membrane) were spotted on nitrocellulose membranes (1.5×1.5 cm^2). Membranes were dried and incubated in 20 mM sodium acetate buffer, pH 5.0, containing 1% bovine serum albumin (BSA) for 10 min on ice for protecting nonspecific binding of pepstatin A to the membranes. Then, the blocking buffer was replaced with 2 ml of 20 mM sodium acetate buffer, pH 5.0, which contained radio-labeled pepstatin A ([^{35}S]-methionyl-pepstatin A, 10^4–10^6 cpm/assay). The membranes were incubated for additional 30 min on ice. Membranes were then washed 4 times on ice with 2 ml of 20 mM sodium acetate buffer, pH 5.0, to remove radio-labeled pepstatin A that had not bound to pepsin, and were dried and placed in 5 ml of a scintillation cocktail (Atomlight, New England Nuclear, Boston, MA) to count radioactivities using a liquid scintillation counter (LSC-3000, Aloka). Nonspecific binding of radio-labeled pepstatin A to the nitrocellulose membrane was estimated through the identical procedure described above with an exception that membranes were washed with neutral buffer (20 mM sodium phosphate buffer, pH 7.4).

Binding of [^{35}S]-methionyl-pepstatin to the tail tissue of bullfrog tadpole

The tail of tadpole of bullfrog, *Rana catesbeiana*, was used as a source of aspartic proteinases for the binding assay of [^{35}S]-methionyl-pepstatin A. Tails were dissected from bullfrog tadpoles at the premetamorphic stage (TK stage XVII) or the climax stage of metamorphosis (TK stage XXIII) and kept at −20°C until use. The frozen tail tissues were defrosted on ice and finely minced to small pieces (about $3\times3\times3$ mm^3) at 0–4°C with scissors in the solution containing 0.1 M NaCl and 20 mM sodium acetate buffer, pH 5.0. Tissue pieces were collected in microfuge tubes (Ca. 100 mg wet weight tissue/tube) and suspended in 1 ml of 20 mM sodium acetate buffer containing 0.1 M NaCl at 0–4°C. The radio-labeled pepstatin A (2.0×10^4 cpm/assay) was added to the tissue suspension and allowed to stand for binding at 0–4°C for 30 min. For removal of unbound pepstatin probe, tubes were then centrifuged at $1{,}700\times g$ for 5 min at 4°C and the supernatants were discarded. The precipitates were washed 3 times with 1 ml of 20 mM sodium acetate buffer containing 0.1 M NaCl, pH 5.0. Then, for recovering radio-labeled pepstatin A bound to tissues, precipitates were lysed in 600 μl of 0.1 N NaOH at 37°C for 2 hr and were centrifuged at $7{,}000\times g$ for 10 min at room temperature. Radioactivity in the supernatant was counted. The protein concentration of lysates was determined by the procedure described by Lowry *et al.* using BSA as a standard [20].

RESULTS

The carboxyl group of pepstatin A was activated by EDC to form o-acylurea which was then coupled with Sulfo NHS. Sulfo NHS-pepstatin thus obtained was more resistant to hydrolysis than o-acylurea and was hydrophobic. Excess amounts of hydrophilic activating reagents were easily removed from the reaction mixture using a reversed phase column of SEP-PAK C_{18}. Coupling of the activated pepstatin A with the amino group of L-[^{35}S]-methionine produced [^{35}S]-methionyl-pepstatin A with specific activity of 0.72 MBq/μmole (2.8×10^7 cpm/μmole).

Specificity of the radio-labeled pepstatin A was characterized by analyzing its binding properties to pepsin that had been immobilized on a nitrocellulose membrane. The radio-labeled pepstatin was bound to the enzyme at pH 5.0, but not at pH 7.4, same as pepstatin A (Fig. 1). The binding of

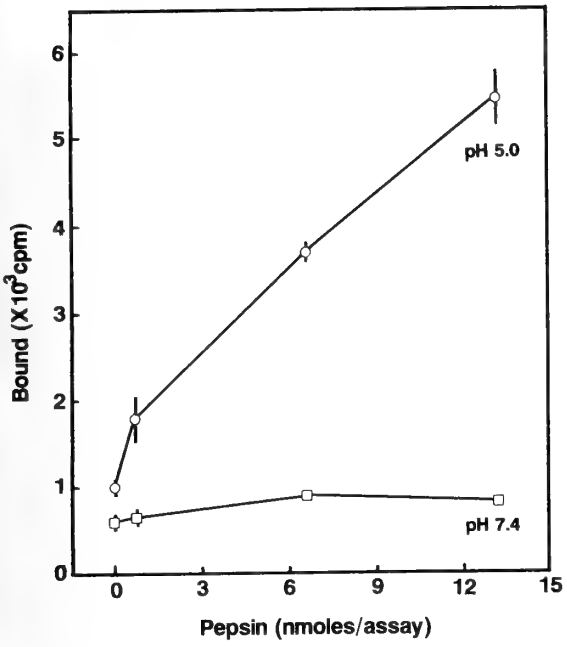

FIG. 1. pH-Dependent binding of [^{35}S]-methionyl-pepstatin A to pepsin. The radio-labeled derivatives (3.6×10^4 cpm/assay) were incubated with various amounts of pepsin (0.7–14.6 nmoles) that had been dotted on nitrocellulose membranes. For removing unbound pepstatin A probes, membranes were washed with 20 mM sodium acetate buffer, pH 5.0, (circle) or with 20 mM sodium phosphate buffer, pH 7.4, (square). Each point represents the mean of triplicate assays and bars indicate standard errors of the mean.

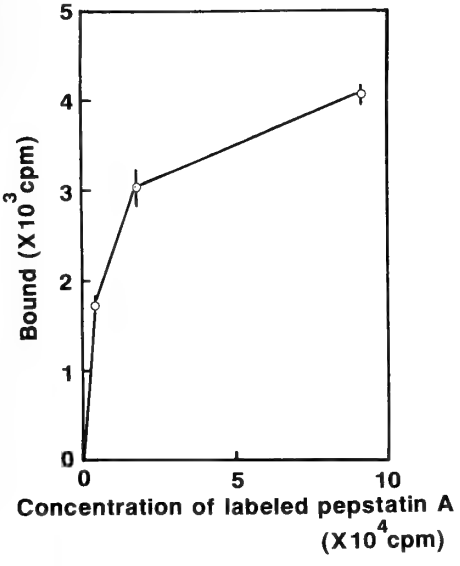

FIG. 2. Binding of [^{35}S]-methionyl-pepstatin A to the fixed amount of pepsin. Pepsin (5.7 nmoles) was immobilized on a nitrocellulose membrane (1.5×1.5 cm^2) and incubated with indicated amounts of labeled pepstatin A (4.4×10^3–8.8×10^4 cpm/assay). Radioactivity bound to membranes was counted as amounts of labeled pepstatin A bound to pepsin. The radioactivity of 10^3 cpm corresponds to 35 pmoles of the pepstatin A probe. Each point represents the mean of triplicate assays. Bars indicate standard errors of the mean.

[^{35}S]-methionyl-pepstatin A to pepsin is proportional to pepsin concentrations in the range of 1–12 nmoles. Radio-labeled pepstatin A bound increasingly to the fixed amount of pepsin as the amount of labeled pepstatin increased up to around the dose of 2×10^4 cpm and then the binding was leveled off (Fig. 2), suggesting that the labeled pepstatin A binds to limited and specific sites of pepsin.

Binding of [^{35}S]-methionyl-pepstatin A to pepsin was competitively suppressed by pepstatin A (Fig. 3), indicating that the radio-labeled derivative shows the same binding specificity as pepstatin A.

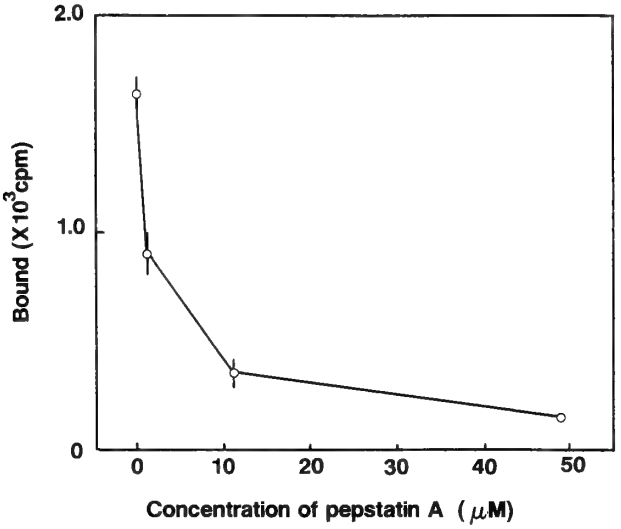

FIG. 3. Suppression of the binding of the radio-labeled pepstatin A to pepsin by pepstatin A. Pepsin (5.7 nmoles/assay) spotted on membranes was incubated with the fixed amount of the pepstatin derivatives (8.8×10^3 cpm/assay) and varied amounts of pepstatin A (0–48 μM) as a competitor. The radioactivity bound to pepsin was counted. Each point represents the mean of triplicate assays with its standard error indicated by a bar.

Figure 1 shows that the [^{35}S]-methionyl-pepstatin A prepared as above can detect pepsin when its amount is more than 1.0 nmoles. To get the probe for aspartic proteinases showing a higher specific radioactivity, the labeled pepstatin A was further purified by subjecting it to reversed phase HPLC (Fig. 4). Pepstatin A was eluted at 38% acetonitrile as a single peak. The radio-labeled pepstatin A was eluted at 44% acetonitrile also as a single peak. The pepstatin derivative thus purified had a specific activity of 3.6 MBq/μmole and could detect as low as 0.1 nmoles of pepsin. Its binding to pepsin was proportional to the concentration of the enzyme in the range of 0.1–0.3 nmoles (Fig. 5).

The radio-labeled pepstatin A was tried to use as a probe to detect aspartic proteinases in the animal tissue. The metamorphosing tadpole tail was quantitated for the pepstatin-reactive enzymes (Fig. 6). The specific binding of the probe to the tail of a metamorphosing tadpole was 18-fold higher than the binding to the tail of a premetamorphic animal. If we postulate that all the bound probe recovered

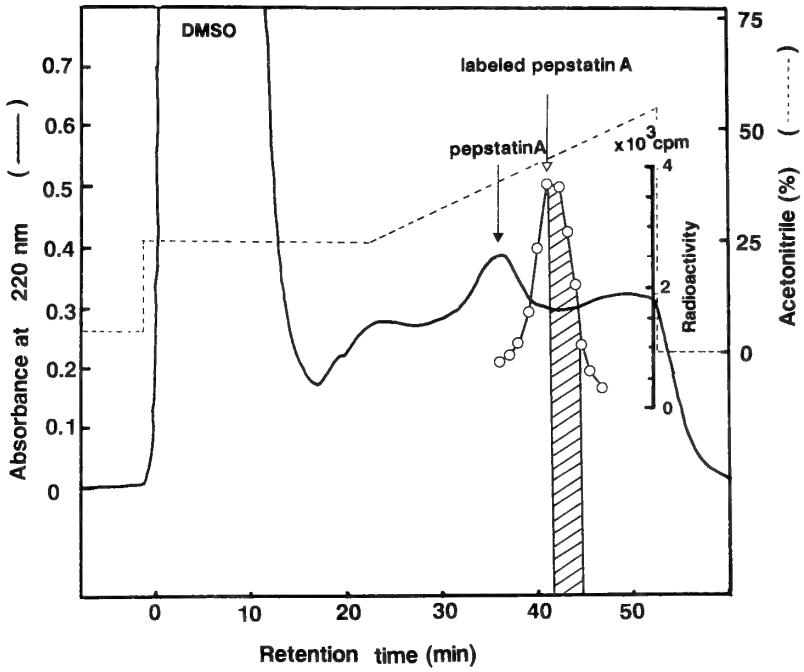

FIG. 4. Separation of [^{35}S]-methionyl-pepstatin A and pepstatin A by reversed phase HPLC. The radio-labeled pepstatin A fraction obtained at the second reaction was applied to a Inertsil 300-C_8 (4.6×100 mm) and eluted at 50°C with a linear gradient of 25–55% of acetonitrile (dotted line) containing 0.1% TFA. The flow rate was 0.4 ml/min. The solid line indicates the absorbance at 220 nm. The radioactivity of each fraction (0.4 ml) was counted (circle). The first peak of 220 nm contains dimethyl sulfoxide which was used as the solvent of pepstatin A. The closed arrow at 38% acetonitrile shows the peak of pepstatin A and the open arrow at 44% acetonitrile the peak of [^{35}S]-methionyl-pepstatin. The shaded fractions were collected as [^{35}S]-methionyl pepstatin and used as a probe for aspartic proteinases (3.6 MBq/μmole).

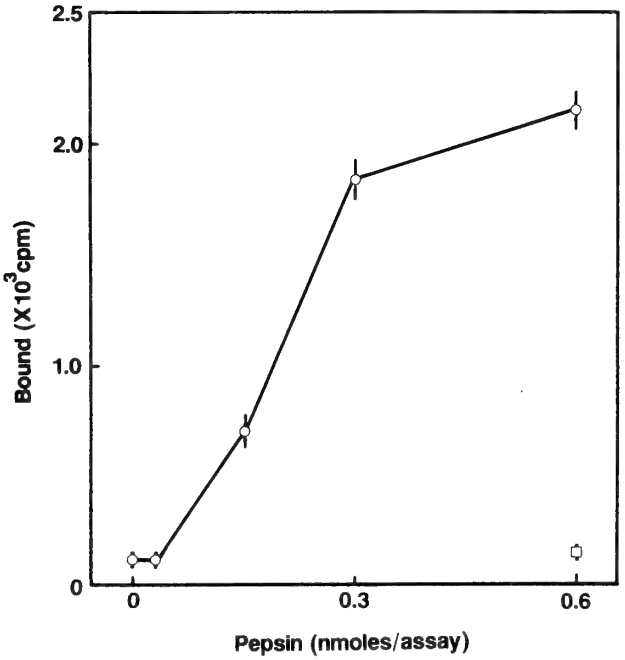

FIG. 5. Binding of the [^{35}S]-methionyl-pepstatin A to pepsin. HPLC-purified radio-labeled pepstatin A (10^4 cpm/assay) was incubated for 30 min at 0–4°C with nitrocellulose membranes containing varied amounts of pepsin. Membranes were washed with acidic buffer and counted for radioactivity (circle). Non-specific binding to nitrocellulose membranes was obtained as the radioactivity remaining on membranes when they were washed with neutral pH (square). The radioactivity of 10^3 cpm is equivalent to 7.1 pmoles of the pepstatin A probe. Each point represents the mean of triplicate assays and bars indicate standard errors of the mean.

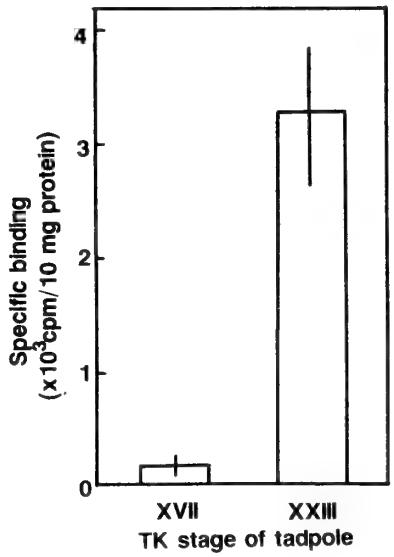

FIG. 6. Detection of aspartic proteinase in the tail of tadpole by the [^{35}S]-methionyl-pepstatin A. The specific binding of the probe was calculated by subtracting the value of radioactivity obtained in the presence of excess amounts of pepstatin A (30 μM) from that without it. Tail tissues of bullfrog tadpole (about 100 mg wet weight/assay) at premetamorphosis (TK stage XVII) or the climax of metamorphosis (TK stage XXIII) were incubated with the radio-labeled pepstatin A (HPLC-purified, 2.0×10^4 cpm/assay) in solution of 20 mM sodium acetate buffer and 0.1 M NaCl, pH 5.0, with or without a competitor, pepstatin A (30 μM). The radioactivity of 10^3 cpm is equivalent to 7.1 pmoles of the pepstatin probe as in Fig. 5. Each value represents the mean of triplicate assays with its standard error indicated by a bar.

from tissues, the tail contained binding sites of 0.7 nmoles/10 mg protein at the climax stage and 0.04 nmoles/10 mg protein at the premetamorphic stage. These values of binding sites are expressed as those for "pepsin equivalent".

DISCUSSION

Pepstatin A is a proteinase inhibitor that is not specific to one species of enzyme but shows the activity toward several species of enzymes grouped as the aspartic proteinase family including pepsin, cathepsin D, cathepsin E, renin, chymosin and gastricsin. Therefore, [^{35}S-]-methionyl-pepstatin A developed in the present study can be applied to animal tissue for the first screening of proteinases which is grouped into this family.

The radio-labeled pepstatin A keeps the same activity as pepstatin A. We used the carboxyl group of pepstatin A as the site of modification, as pepstatin-conjugated resins have been usually prepared by modifying this residue and utilized for purification of aspartic proteinases such as cathepsin D [1]. The present study also confirms that the carboxyl group of pepstatin can be modified as a connecting site for reporter groups without destroying properties which are required for the inhibitor to bind aspartic proteinases. Radioactive methionine can be successfully introduced by this modification into pepstatin A.

Since this additional chain of methionine is neutral in charge, it does not disturb the ionic condition of the binding site of aspartic proteinases. The [^{35}S]-methionyl-pepstatin A we prepared is more hydrophobic than pepstatin A, which may help the derivative to approach more easily for the binding site of the enzymes than pepstatin A because the site is thought as a hydrophobic pocket in pepsin [27].

Pepstatin A binds to aspartic proteinases in a stoichiometric manner. The present study shows that the binding of the radio-labeled pepstatin A to pepsin is proportional to concentrations of pepsin, indicating that it can be used as a sensitive probe for the quantitative analysis of aspartic proteinases. Utilizing this probe, we could detect 0.1 nmoles of pepsin. It seems that other methods such as radio-immuno assay are more sensitive than the method described in the present study. However, the radio-labeled pepstatin A is much useful as compared to the antibody against aspartic proteinases. We have to prepare the specific antibody in each case of the study against the enzyme of target. In contrast, the radio-labeled pepstatin A can be used for detecting the enzyme belonging to the family of aspartic proteinases.

We made some alterations in the assay of binding of the pepstatin A derivative when we tried to detect aspartic proteinases in tadpole tissues. Binding was assayed on nitrocellulose membranes for the test enzyme (pepsin), while the assay for the tissue sample was done in tissue pieces suspended in acid solution. The pepstatin A derivative bound to enzymes in the tissue was then removed by centrifugation in alkaline condition. The reason for this alteration was the relatively low capacity of nitrocellulose membranes to hold tissue proteins. We first tried to assay enzymes in the tissue samples using nitrocellulose membranes as we did for the test enzyme. However, reliable and reproducible values of binding of the radio-labeled pepstatin A could not be obtained in the membrane assay.

This probe is shown to detect pepstatin-sensitive proteinase(s) in the tail of bullfrog tadpole. The amount of specific binding to the tail tissue much increases at the climax stage of metamorphosis (TK stage XXIII) as compared to the premetamorphic one. Several reports demonstrated that cathepsin D like proteinase activity in the tail increases at the climax of metamorphosis [9, 18, 29, 38, 39, 43] and pepstatin sensitive proteinase plays important roles in the regression of tail during metamorphosis [31]. Pepstatin A binding sites at the climax stage of metamorphosis increases 18-fold as compared to those at the premetamorphic stage. The ratio of cathepsin D activity of the tail at the climax stage to that at the premetamorphic stage is 18 in *Rana catesbeiana* [29] and 16 in *Xenopus laevis* [39]. These values are very close to that obtained by our method.

Pepstatin-sensitive proteinases are found also in a wide variety of life including vertebrates such as human [5], bovine [30], porcine [14], rabbit [6], rat [10], chicken [5, 26], frog [23] and fish [7], and invertebrates such as marine mussel [24] and hemipteran insect [13]. Plant [28], bacteria [17] and retrovirus [40] have also been reported to contain pepstatin-sensitive proteinases. Therefore, it is considered that aspartic proteinases might play fundamental roles in metabolic processes of varieties of life. However, the information on the enzyme other than mammalian origin has been poor. There is a possibility that the binding site recognized by pepstatin A is highly conserved in the molecular evolution of aspartic proteinases. The pepstatin derivative reported here is expected to be useful in detecting unknown aspartic proteinases in the wide range of life and studying them from a comparative point of view.

It has been shown that aspartic proteinase of HIV virus can be converted by the gene technology into a mutant enzyme that has no enzymatic activity but can bind to pepstatin A [40]. This indicates that the catalytic site of the enzyme is different from the pepstatin binding site, although both sites are in the active center. The radio-active pepstatin developed in the present study is expected to be useful in detecting enzymes of the aspartic proteinase family that lose their catalytic activity.

We could not develop pepstatin A derivative which shows higher sensivity of detection than the method to directly measure the enzyme activity or conventional immunological detection method using specific antibody. It remains as a future study to develop a method to prepare [^{35}S]-methionyl-pepstatin A with much more higher specific activity.

ACKNOWLEDGMENTS

The authors would like to express their thanks to Drs. S. Yasugi, T. Ohoka and S. Tomino for their kind discussions on this study.

REFERENCES

1 Afting EG, Becker ML (1981) Two-step affinity-chromatographic purification of cathepsin D from pig myometrium with high yield. Biochem J 197: 519–522

2 Anjaneyulu PSR, Staros JV (1987) Reactions of N-hydroxysulfosuccinimido active esters. Int J Pep Pro Res 30: 117–124

3 Aoyagi T, Morishima H, Nishikawa R, Kunimoto S, Takeuchi T, Umezawa H, (1972) Biological activity of pepstatins, pepstanone A and partial peptide on pepsin, cathepsin D and renin. J Antibiot 25: 689–694

4 Azuma T, Liu W, Laan DJV, Bowcock AM, Taggart RT (1992) Human gastric cathepsin E gene. J Biol Chem 267: 1609–1614

5 Barrett AJ (1970) Cathepsin D, purification of isoenzymes from human and chicken liver. Biochem J 117: 601–607

6 Barrett AJ (1971) Purification and properties of cathepsin D from liver of chicken, rabbit and man. In "Tissue proteinases" Ed by Barrett AJ, Dingle JT North-Holland Publishing Co., Amsterdam, pp 109–133

7 Bonete MJ, Manjon A, Llorca F, Iborra JL (1984) Acid proteinase activity in fish II. Purification and characterization of cathepsins B and D from *Mujil auratus* muscle. Comp Biochem Physiol 78B: 207–213

8 Faust PL, Kornfeld S, Chirgwin JM (1985) Cloning and sequence analysis of cDNA for human cathepsin D. Proc Natl Acad Sci USA 82: 4910–4914

9 Fujii Y, Taguchi M, Kobayashi K, Horiuchi S (1991) Immunochemical studies on cathepsin D like enzyme in the tadpole tail of *Rana catesbeiana*. Zool Sci 8: 511–520

10 Fujita H, Tanaka Y, Noguchi Y, Kona A, Himeno M, Kato K (1991) Isolation and sequencing of a cDNA clone encoding rat liver lysosomal cathepsin D and the structure of three forms of mature enzymes. Biochem Biophys Res Commun 179: 190–196

11 Gross J, Lapiere CM (1962) Collagenolytic activity in amphibian tissues : A tissue culture assay. Proc Natl Acad Sci USA 48: 1014–1022

12 Hobart PM, Fogliano M, O'Connor BA, Schaefer IM, Chirgwin JM (1984) Human renin gene : Structure and sequence analysis. Proc Natl Acad Sci USA 81: 5026–5030

13 Houseman JG, Downe AER (1983) Cathepsin D-like activity in the posterior midgut of hemipteran insect. Comp Biochem Physiol 75B: 509–512

14 Huang JS, Huang SS, Tang J (1979) Cathepsin D isozymes from porcine spleens. J Biol Chem 254: 11405–11417

15 Knight CG, Barrett AJ (1976) Interaction of human cathepsin D with the inhibitor pepstatin. Biochem J 155: 117–125

16 Knight CG, Hornebeck W, Matthews ITW, Hembry RM, Dingle JT (1980) Interaction of dinitrophenyl-pepstatins with human cathepsin D and with anti-dinitrophenyl antibody. Biochem J 191: 835–843

17 Kobayashi H, Kusakabe I, Murakami K (1982) Rapid isolation of microbiral milk-clotting enzymes by N-acetyl(or N-isobutyryl)-pepstatin-aminohexyl agarose. Anal Biochem 122: 308–312

18 Kobayashi K, Hara M, Horiuchi S (1985) Isolation of lysosomes from the tail of metamorphosing bullfrog tadpole. Comp Biochem Physiol 81B: 603–607

19 Kunimoto S, Aoyagi T, Nisizawa R, Komai T, Takeuchi T, Umezawa H (1974) Mechanism of inhibition of pepsin by pepstatin II. J Antibiot 27: 413–418

20 Lowry OH, Rosebrough NJ, Farr AL, Randall RJ (1951) Protein measurement with the folin phenol reagent. J Biol Chem 193: 265–275

21 Matthews ITW, Decker RS, Knight C G (1981) Bimane-labelled pepstatin, a fluorescent probe for the subcellular location of cathepsin D. Biochem J 199: 611–617

22 Matthews ITW, Decker RS, Hornebeck W, Knight CG (1983) Dinitrophenyl-pepstatins as active site directed localization reagents for cathepsin D. Biochem J 211: 139–147

23 Nanbu M, Kobayashi K, Horiuchi S (1988) Purification and characterization of cathepsin D-like proteinase from the tadpole tail of bullfrog, *Rana catesbeiana*. Comp Biochem Physiol 89B: 569–575

24 Okada S, Aikawa T (1986) Cathepsin D-like acid proteinase in the mantle of the marine mussel, *Mytilus edulis*. Comp Biochem Physiol 84B: 333–341

25 Oofusa K, Yoshizato K (1991) Biochemical and immunological characterization of collagenase in tissues of metamorphosing bullfrog tadpoles. Develop Growth and Differ 33: 329–339

26 Retzek H, Steyrer E, Sanders EJ, Nimpf J, Schneider WJ (1992) Molecular cloning and functional characterization of chicken cathepsin D, a key enzyme for yolk formation. DNA Cell Biol 11: 661–672

27 Rich DH (1986) Inhibitors of aspartic proteinase. In "Proteinase inhibitors" Ed by Barret AJ, Salvesen G, Elsevier Science Publishers BV., Amsterdam, pp 179–217

28 Runeberg-Roos P, Törmäkangas K, Östman A (1991) Primary structure of a barley-grain aspartic proteinase. Eur J Biochem 202: 1021–1027

29 Sakai J, Horiuchi S (1979) Characterization of cathepsin D in the regressing tadpole tail of bullfrog, *Rana catesbeiana*. Comp Biochem Physiol 62B: 269–273

30 Sapolsky AI, Woessner FJ (1972) Multiple forms of cathepsin D from bovine uterus. J Biol Chem 247: 2069–2076

31 Seshimo H, Ryuzaki M, Yoshizato K (1977) Specific inhibition of triiodothyonine-induced tadpole tail-fin regression by cathepsin D-inhibitor pepstatin. Develop Biol 59: 96–100

32 Shewale JG, Tang J (1984) Amino acid sequence of porcine spleen cathepsin D. Proc Natl Acad Sci USA 81: 3703–3707

33 Sogawa K, Fujii-Kuriyama Y, Mizukami Y, Ichihara Y, Takahashi K (1983) Primary structure of human pepsinogen gene. J Biol Chem 258: 5306–5311

34 Staros JV, Wright RW, Swingle DM (1986) Enhancement by N-hydroxysulfosuccinimido of water soluble carbodiimide-mediated coupling reactions. Anal Biochem 156: 220–222

35 Takahashi T, Tang J (1983) Amino acid sequence of porcine spleen cathepsin D light chain. J Biol Chem 258: 6435–6443

36 Taylor AC, Kollros JJ (1946) Stages in the normal development of *Rana pipiens* larvae. Anal Rec 94: 7–23

37 Umezawa H, Aoyagi T, Morishima H, Matsuzaki M, Hamada M, Takeuchi T (1970) Pepstatin, a new pepsin inhibitor produced by actinomycetes. J Antibiot 23: 259–262

38 Weber R (1967) Biochemical and cellular aspects of tissue involution in development. Exp Biol Med 1: 63–76

39 Weber R (1977) Biochemical characteristics of tail atrophy during anuran metamorphosis. Colloq Int C N R S 226: 137–146

40 Wondrak EM, Louis JM, Mora PT, Oroszlan S (1991) Purification of HIV-1 wild type proteinase and characterization of proteolytically inactive HIV-1 proteinase mutants by pepstatin A affinity Chromatography. FEBS Lett 280: 347–350

41 Workman RJ, Burkitt DW (1979) Pepsin inhibition by a high

specific activity radioiodinated derivative of pepstatin. Arc Biochem Biophys 194: 157–164

42 Yamada H, Imoto T, Fujita K, Motomura M (1981) Selective modification of aspartic acid-101 in lysozyme by carbodiimide reaction. Biochemistry 20: 4836–4842

43 Yoshizato K (1989) Biochemistry and cell biology of amphibian metamorphosis with a special emphasis on the mechanism of removal of larval organs. In "International Review of Cytology" Academic Press, New York, 119: 97–149

ZOOLOGICAL SCIENCE 11: 229–234 (1994)

Evolution of Phosphagen Kinase (III). Amino Acid Sequence of Arginine Kinase from the Shrimp *Penaeus japonicus*

TAKAHIRO FURUKOHRI, SUMITO OKAMOTO and TOMOHIKO SUZUKI*

Department of Biology, Faculty of Science, Kochi University, Kochi 780, Japan

ABSTRACT—The amino acid sequence of arginine kinase (AK) from the shrimp *Penaeus japonicus* has been determined chemically. It consists of 355 amino acid residues, and has a calculated molecular mass of 40,018 Da. The amino acid sequence of *Penaeus* AK showed 91% and 51% identity, respectively, with those of AKs from the lobster *Homarus vulgaris* and the abalone *Nordotis madaka*. It also showed significant homology (39–43%) with vertebrate or invertebrate creatine kinases and annelid glycocyamine kinase, suggesting that these enzymes evolved from a common origin.

INTRODUCTION

Phosphagen kinases (PKs) are the enzymes that catalyze the reversible transfer of the high energy phosphoryl group of ATP to the naturally occurring guanidines, and play a key role to interconnect energy production and utilization in animals [9]. In vertebrates, the only phosphagen kinase is creatine kinase (CK), but in invertebrates, at least five phosphagen kinases, arginine kinase (AK), glycocyamine kinase (GK), taurocyamine kinase (TK), lombricine kinase (LK) and CK, have been identified by partial or complete sequencing [1–3, 15, 18, 20]. Moreover, the presences of hypotaurocyamine kinase (HTK), opheline kinase (OK) and thalassemine kinase (ThalK) are proposed by their enzyme activity [11, 19]. The homologous amino acid sequences of about 15 residues around the putative active site of these enzymes suggest that they have evolved from a common origin [1], and thus provide an excellent model system to elucidate how enzymes developed the recognition site for substrate during evolution.

AK is the phosphagen kinase that is most widely distributed in animals. Very recently, two cDNA-derived amino acid sequences of AKs from the lobster *Homarus vulgaris* [3] and the abalone *Nordotis madaka* [18] have been determined. Here we report the primary structure of AK from the shrimp *Penaeus japonicus*, to be sequenced chemically. A preliminary account of this work has been presented [13].

MATERIALS AND METHODS

AK was isolated from the tail muscle of *Penaeus japonicus* according to our previous method [12].

The protein (50 nmoles) was carboxymethylated and cleaved with CNBr in 70% formic acid. Larger CNBr peptides were digested further with lysyl endopeptidase, chymotrypsin, *S. aureus* V8 protease and pepsin. To obtain overlap peptides, the protein was also digested with lysyl or arginyl endopeptidases. The digestion conditions are the same as described previously [16]. The digested products were purified on a reverse-phase column (Cosmosil $5C_{18}$-300, 2.5×150 mm) with a linear gradient of 0–80% acetonitrile in 0.1% trifluoroacetic acid (TFA) at a flow rate of 1 ml/min. Some peptides were purified further by rechromatography. Amino acid analyses and the manual Edman sequencing of the peptides were done with our standard methdos [16]. The N-terminal peptide CN1C1 was digested with acylamino acid releasing enzyme (0.025U, Takara) in 5 mM phosphate buffer (pH 7.2) contianing 1 mM 2-mercaptoethanol at 37°C for 2 hr, before sequencing.

Accepted March 24, 1994
Received Feburary 10, 1994

* To whom all correspondence should be addressed.

RESULTS AND DISCUSSION

Fig. 1 shows the elution profile of CNBr peptides of *Penaeus* AK on reverse-phase chromatography. Most of the CNBr peptides were separated successfully, and the larger peptides were digested further with several enzymes. Two small CNBr peptides, Gln-Met at positions 233–234 and C-terminal Glu-Lys-Glu-Met, were not recovered. The overlap of CNBr peptides was obtained with the peptides derived from lysyl or arginyl endopeptidase digestions of the whole protein. Amino acid compositions of the CNBr peptides and the whole protein are given in Table 1. The strategy to establish the complete amino acid sequence is shown in Fig. 2. The Gly-Arg bond at position 206–207, Arg-Ala at 279–280, Arg-Gly at 308–309 and Lys-Arg at 327–328 were unusually cleaved with *S. aureus* V8 protease. The sequence is supported by at least two amino acids overlap, and the C-terminal half of 129 residues was also confirmed by the cDNA sequencing [17]. *Penaeus* AK begins with the blocked Val, is composed of total 355 amino acid residues and the molecular mass was calculated to be 40,018 Da.

So far, all the amino acid sequences of phosphagen kinases were determined by their cDNA sequencing, and therefore this work is the first example to be sequenced chemically.

Amino acid sequence of *Penaeus* AK was aligned with *Homarus* AK, *Schistosoma* (trematode) PK domain 1, *Neanthes* (annelid) GK, *Nordotis* (mollusc) AK, sea urchin CK domains 2 and 3 and chicken three CK isoforms (muscle, brain and mitochondrial types), with the algorithm of Feng &

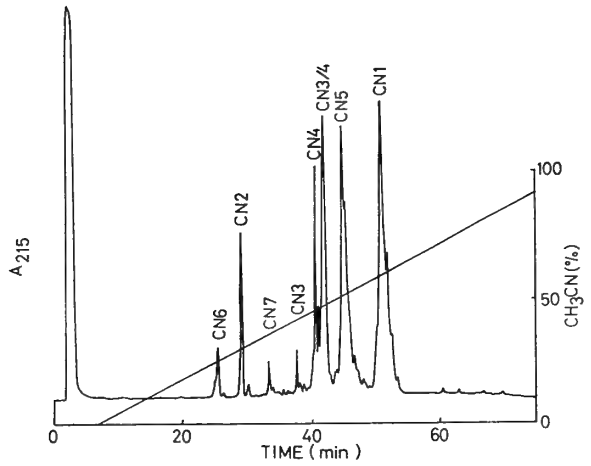

FIG. 1. Elution profile of CNBr peptides of *Penaeus* AK on reverse-phase chromatography. The column (Cosmosil $5C_{18}$-300, 2.5× 150 mm) was eluted with a linear gradient of 0–80% acetonitrile in 0.1% TFA at a flow rate of 1 ml/min.

Doolittle [5], in Fig. 3. It is noted that sea urchin CK has an unusual three-domain structure which may be resulted from a gene triplication [20] and *Schistosoma* PK has a two-domain structure, of which the second domain lacks the C-terminal 50 residues [15]. *Penaeus* AK is aligned with *Homarus* AK without any insertions or deletions. Furthermore, their sequences are characterized by a unique delation at positions 117–118 and an insertion at position 311 in Fig. 3. In the alignment, there are 68 amino acid residues (indicated by asterisks) conserved in all of the phosphagen kinases.

All of the phosphagen kinases can be inactivated partially or completely under the chemical modification with thiol-specific regents [5]. The reactive cysteine, that would be located near or in the center of the putative active site, was identified as Cys-286 (see Fig. 3). Recent site-directed mutagenesis study shows that the active cysteine is necessary to confer conformational changes upon substrate binding, but is not essential for catalysis [6].

The percent identity between the 10 amino acid sequences of phosphagen kinases is shown in Table 2. The sequence of *Penaeus* AK showed 91% and 51% identity, respectively, with those of *Homarus* and *Nordotis* AKs. It also showed significant homology (39–43%) with verebrate or inverebrate CKs and *Neanthes* GK. These sequence homologies would be enough to conclude that CK, GK and AK are derived from a common origin.

A phylogenetic tree was constructed from the sequence alignment in Fig. 3 with the algorithm of Feng & Doolittle [5] (Fig. 4). The same topology was also obtained with the protein parsimonious algorithm using the program **Protpars** in the PHYLIP package ver 3.5c [4]. The tree separated phosphagen kinases into two clusters, a cluster containing vertebrate and invertebrate CKs and invertebrate GK and a cluster containing three AKs and *Schistosoma* PK. The branching pattern clearly shows that CK and GK must have evolved from a common ancestor [18]. The phylogenetic position of *Schistosoma* PK is noted. Our tree placed the PK near the cluster of AKs (Fig. 4). In fact, *Schistosoma* PK has the highest sequence homology (46–52%) with AKs (see Table 2). Moreover, *Schistosoma* PK shares the sequence characteristics with invertebrate AKs: deletions at posi-

TABLE 1. Amino acid compositions of *Penaeus* AK and its CNBr peptides

	whole	CN1	CN2	CN3	CN3/4	CN4	CN5	CN6	CN7
Asx	37.8(36)	15.4(16)	1.0(1)		8.8(9)	8.6(9)	9.3(9)		1.1(1)
Thr	16.9(19)	5.4(6)	1.0(1)	3.0(3)	3.6(4)	1.0(1)	6.2(7)	1.1(1)	
Ser	15.8(19)	7.1(9)		3.4(4)	5.2(6)	1.9(2)	3.4(4)		
Glx	11.0(11)	11.0(11)	4.1(4)	4.5(4)	11.9(11)	7.5(7)	10.2(9)	3.6(3)	2.3(2)
Pro	10.6(12)	4.8(5)	1.9(2)	0.8(1)	1.9(2)	0.9(1)	2.9(3)		
Gly	31.2(29)	9.5(10)	1.0(1)	3.3(3)	6.2(6)	3.3(3)	9.9(10)	1.1(1)	1.1(1)
Ala	22.6(22)	9.7(10)	1.0(1)		4.0(4)	3.9(4)	6.2(6)	1.1(1)	
Cys	5.0(5)	1.5(2)	0.9(1)		0.8(1)	0.9(1)	1.0(1)		
Val	22.6(22)	9.1(11)		1.2(1)	4.1(4)	3.1(3)	6.0(6)	1.3(1)	
Met	9.7(9)	+ (1)	+ (1)	+ (1)	+ (2)	+ (1)	+ (1)	+ (1)	+ (1)
Ile	15.8(17)	3.8(6)			2.7(4)	2.8(4)	4.5(5)		1.6(2)
Leu	37.0(35)	12.5(13)	1.1(1)	4.3(4)	8.9(9)	4.9(5)	9.7(9)	1.3(1)	1.8(2)
Tyr	11.9(12)	4.4.(5)	1.8(2)	0.5(1)	2.4(3)	1.3(2)	2.0(2)		
Phe	18.9(18)	6.4(7)	1.0(1)	1.1(1)	5.1(5)	3.9(4)	4.2(4)	1.3(1)	
Lys	26.8(29)	12.0(13)	1.0(1)	2.0(2)	6.0(6)	4.0(4)	6.0(6)	1.0(1)	1.0(1)
His	10.1(9)	1.7(2)			2.9(3)	2.7(3)	3.8(4)		
Arg	15.6(17)	2.7(3)			3.7(4)	3.6(4)	9.5(10)		
Trp	+ (2)				+ (2)	+ (2)			
Total	(355)	130	17	25	85	70	96	11	10
Position		1–130	131–147	148–172	148–232	173–232	235–330	331–341	342–351
Yield(%)		57.9	42.3	9.0	35.4	15.6	41.0	34.5	46.7

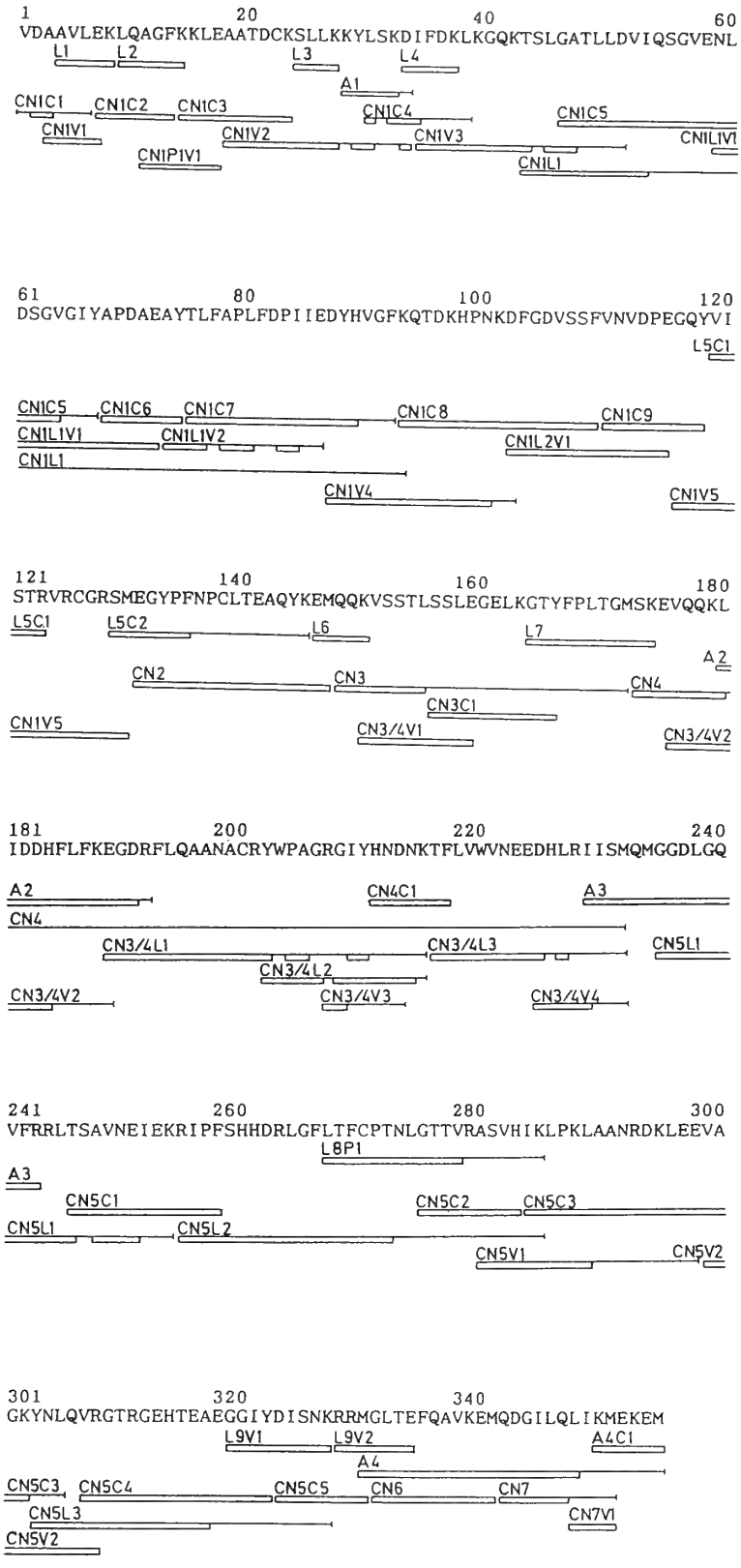

FIG. 2. Summary of data to establish the amino acid sequences of *Penaeus* AK. The sequence was determined by manual Edman degradation (□). Key; CN, CNBr; L, lysyl endopeptidase; C, chymotrypsin; V, *S. aureus* V8 protease; P, pepsin; A, arginyl endopeptidase.

```
                                25                        50
AK  shrimp     VDAAVLEKLQ AGFKKLEAATDCKSLLKKYLSKDIFDKLKGQKTSLGATLLDVIQSGVENLD
AK lobster    MADAATIAKLE EGFKKLEAATDCKSLLKKYLSKDIFDSLKAKKTSLGATLLDVIQSGVENLD
AK abalone       MLAMASVE ELWAKLDGAADCKSLLKNNLTKERYEALKDKKTKFGGTLADCIRSGCLNLD
PK Schis.1        MQVESLQ NLQAKIRNDERNHSLTKKYLTDDIVKKYQATKTSLGGTLAQCVNTNAYNPG
CK-M chick   PFSSTHNKHKLKFSAEEEFPDLSKHNNHMAKVLTPELYKRLRDKETPSGFTLDDVIQTGVDNPGH
CK-B chick   PFSNSHNLLKMKYSVDDEYPDLSVHNNHMAKVLTLDLYKKLRDRQTSSGFTLDDVIQTGVDNPGH
CK sea ur2                     YPDLSKHNNHLAHCLTYDIWKSLKDKKTPSGFTLDGCIQTGVMNPGH
CK sea ur3                     YPDFSLHNNWMSKCMTEEIYNKLCNLKTKGGVTLNDCIQTGIDNPGH
CK-Mt chic      TVHEKRKL FPPSADYPDLRKHNNCMAECLTPAIYAKLRDKLTPNGYSLDQCIQTGVDNPGH
GK ma.worm      MFKDYSREKF AKENFPDLSKHNNVMASHLTYELYEKYWDKVTPNGVTLDKCIQTGVDNPGN
                                                 *  *  *        *

                75                       100                       125
AK  shrimp       SGVGIYAPDAEAYTLFAPLFDPIIEDYHVGFKQTDKHPNKDFGDVSS  FVNVDPEGQYVI
AK lobster       SGVGIYAPDAEAYSLFAPLFDPIIEDYHKGFKQTDKHPAKDFGDVSK  FINVDPEGTFVI
AK abalone       SGVGIYACDPDAYTVFADVLDAVIKEYHKV  PELKHPEPEMGDLDKLNFGDLDPSGEYIV
PK Schis.1       ALLPR SCDLNAYETFRDFFDAVIADYHKVPDGKIQHPKSNFGDLKSLSFTDLNTYGNLVV
CK-M chick   PFI MTVGCVAGDEESYEVFKDLFDPVIQDRHGGYKP TDKHRTDLNHENLKGGDDLDP  KYVL
CK-B chick   PFI MTVGCVAGDEESYEVFKELFDPVIEDRHGGYKP TDEHKTDLNADNLQGGDDLDP  NYVL
CK sea ur2   PHI MTVGMVAGDEESYDVFADIFDPVIDARHGGYPK DAVHVTNINHADLKGGDNLDP  KYVL
CK sea ur3   PYI MTVGLVAGDEECYEVFAPLFDPVISARHGGYAL DAKHPTNLNAAELKGGDDLDP  EFVL
CK-Mt chic   PFI KTVGMVAGDEESYEVFAEIFDPVIKARHNGYDPRTMKHHTDLDASKITHG QFDE  RYVL
GK ma.worm   KFYGKKTGCVFGDEHSYETFKDFFDRVIEEIHH FKPEDVHPATDLDETKLVGG VFDE  KYVK
                      *   *  *    *  *   *

                         150                       175
AK  shrimp   STRVRCGRSMEGYPFNPCLTEAQYKEMQQKVSSTLSSLEGELKGTYFPLTGMSKEVQQKLIDDHF
AK lobster   STRVRCGRSMEGYPFNPCLTEAQYKEMEEKVSSTLSGLEGELKGSYFPLTGMTKEVQQKLIDDHF
AK abalone   STRVRVGRSHDSYGFPPVLTKQERLKMEEDTKAAFEKFSGELAGKYFPLEGMSKEDQKQMTEDHF
PK Schis.1   STRVRLGRTVEGFGFGPTLTKETRIELENKISTALHNLSGEYEGTYYPLTGCQRGQNQTSKRHHF
CK-M chick   SSRVRTGRSIKGYSLPPHCSRGERRAVEKLSVEALNSLEGEFKGRYYPLKAMTEQEQQQLTDDHF
CK-B chick   SSRVRTGRSIRGFCLPPHCSRGERRAIEKLSVEALGSLGGDLKGKYYALRNMTDAEQQQLIDDHF
CK sea ur2   SCRVRTGRSIIGYSLPPHCTVEERAAVETITIGALDKFDGDLQGKYYPLEGMSDETQTQLIDDHF
CK sea ur3   SCRVRTGRCIRGLALPPCCTRAERAEVEKITTEALSTLSGPLKGKYYPLTGMTDEEQEKLIEDHF
CK-Mt chic   SSRVRTGRSIRGLSLPPACSRAERREVENVVVTALAGLKGDLSGKYYSLTNMSERDQQQLIDDHF
GK ma.worm   SCRIRCGRSVRGVCLPPAMSRAERRLVEKVVSNALGGLKEDLAGKYFPLTTMNDKDMEALIEDHF
             * * * **       *                          * *  *                **

               200                       225                       250
AK  shrimp   LF KEGDRFLQAANACRYWPAGRGIYHNDNKTFLVWVNEEDHLRIISMQMGGDLGQVFRRLTSAV
AK lobster   LF KEGDRFLQAANACRYWPAGRGIYHNDNKTFLVWCNEEDHLRIISMQMGGDLGQVYRRLVSAV
AK abalone   LF KDDDRFLRDAGGYNDWCSGRGIFFNTAKNFLVWVNEEDHLRLISMQKGGDLAAVYKRLVVAI
PK Schis.1   LF RNDDNVLRDAGGYIDWPTGRGIFINKQKKFLVWINEEDHIRVISMQKGRDLIAVYKRLADAI
CK-M chick   LFDKPVSPLLLASGMARDWPDARGIWHNDNKTFLVWVNEEDHLRVISMEKGGNMKEVFRRFCVGL
CK-B chick   LFDKPVSPLLLASGMARDWPDARGIWHNDNKTFLVWINEEDHLRVISMQKGGNMKEVFTRFCTGL
CK sea ur2   LFDKPVSPLLTAARMHRDWPQGRGIWHNENKNFLVWVNEEDHIRVISMEKDGNMRAVFKRFCEGL
CK sea ur3   LFDKPVSPLLLCANMARDWPQGRGIWHNDEKNFLVWVNEEDHTRVISMEKSGNMKRVFERFCDGL
CK-Mt chic   LFDKPVSPLLTCAGMARDWPDARGIWHNNDKTFLVWINEEDHTRVISMEKGGNMKRVFERFCRGL
GK ma.worm   LFEKPTGALLTTSGCARDWPDGRGIWHNNGKNFLVWINEEDHIRIISMQKGGDMRAVFSRFGRGL
             **       *          *   ***  *  * **** ***** * ***         *  *

                        275          $          300                       325
AK  shrimp   NEIE     KR IPFSHHDRLGFLTFcPTNLGTTVRASVHIKLPKLAANRDKLEEVAGKYNLQVRG
AK lobster   NDIE     KR VPFSHHDRLGFLTFcPTNLGTTVRASVHIKLPKLAANREKLEEVAAKFSLQVRG
AK abalone   NTMT     ASGLSFAKRDGLGYLTFcPSNLGTALRASVHMKIPNLAASPE FKSFCDNLNIQARG
PK Schis.1   QELS     KS LKFAFNDRLGFITFcPSNLGTTLRASVHAKIPMLASLPN FKEICEKHGIQPRG
CK-M chick   KKIEEIFKKAGHPFMWTEHLGYILTcPSNLGTGLRGGVHVKLPKLSQHPK FEEILHRLRLQKRG
CK-B chick   TQIETLFKSKNYEFMWNPHLGYILTcPSNLGTGLRAGVHIKLPNLGKHEK FGEVLKRLRLQKRG
CK sea ur2   QKFEQMIKKDGKEFMWNKHLGYVLTcPSNLGTGLRAGVHVKLPLLSKYPR FDQILRALRLQKRG
CK sea ur3   KKVEDSIKSKGYQFMWNEHLGYVLTcPSNLGTGLRAGVHVKVPLLSQQKI FDSILDHMRLQKRG
CK-Mt chic   KEVERLIKERGWEFMWNERLGYVLTcPSNLGTGLRAGVHVKLPRLSKDPR FPKILENLRLQKRG
GK ma.worm   TEVERLMKEKGYELMRNERLGYICTcPTNLGTVVRASVHLRLANLEKDKR FDDFLAKLRLGKRG
                           **    ** ****  *  **     *                    **

                                  350                       375
AK  shrimp   TRGEHTEAEGGIYDISNKRRMGLTEFQAVKEMQDGILQLIKMEKEM
AK lobster   TRGEHTEAEGGIYDISNKRRMGLTEFQAVKEMQDGILELIKIEKEM
AK abalone   IHGEHTESVGGVYDLSNKRRLGLTEYQAVEEMRVGVEACLAKEKELAAAKK
PK Schis.1   THGEHTESVGGIYDLSNKRRLGLTELDAVTEMHSGVRALLELEVMLQEYNKGAPEGV
CK-M chick   TGGVDTAAVGAVFDISNADRLGFSEVEQVQMVVDGVKLMVEMEKKLEQNQPIDDMIPAQK
CK-B chick   TGGVDTAAVGGVFDVSNADRLGFSEVELVQMVVDGVKLLIEMEKRLEKGQSIDDLMPAQK
CK sea ur2   TGGVDTASTDGTFDISNLDRLGSSEVQQVQFVVDGVELLVQMEKKLEKGEDIFDILPQQCRPKPP
CK sea ur3   TGGVDTASTDGTFDISNSDRIGFSEVHLVQQLVDGVKLLVNLEKALMKGEDINSLLPEKLREDSS
CK-Mt chic   TGGVDTAAVADVYDISNLDRMGRSEVELVQIVIDGVNYLVDCEKKLEKGQDIKVPPPLPQFGRK
GK ma.worm   TGGESSLAEDSTYDISNLARLGKSERELVQVLVDGVNVLIEADKRLEAGKPIDDLTPRLNSSTGT
               *          * **  * *  *   *     *

                    400
AK  shrimp
AK lobster
AK abalone
PK Schis.1
CK-M chick
```

```
CK-B chick
CK sea ur2  IKPFSYD
CK sea ur3
CK-Mt chic
GK ma.worm  SISATASRHMTL
```

FIG. 3. Alignment of the amino acid sequences of 10 phosphagen kinases. This alignment was obtained with the algorithm of Feng & Doolittle [5]. Invariable residues are indicated by asterisks. The reactive cysteine is shown by $. References; CK-M chick (chicken muscle isoform) [10, 14]; CK-B chick (chicken brain isoform) [7]; CK sea ur2 and 3 (domains 2 and 3 of sea urchin) [20]; CK-Mt chic (chicken mitochondrial isoform) [8]; GK ma.worm (*Neanthes*) [18]; AK shrimp (*Penaeus*) (this work); AK abalone (Nordotis) [18]; AK lobster (*Homarus*) [3]; PK Schis. 1 (domain 1 of *Schistosoma*) [15].

TABLE 2. Percent identity between the sequences of phosphagen kinases

	AK lob	AK aba	PK Sch	CK-M	CK-B	CK ur2	CK ur3	CK-Mt	GK wor
Ak shr	91.0	50.9	46.3	42.5	43.0	42.3	41.7	39.8	38.5
AK lob		52.6	45.7	41.8	41.8	41.7	41.7	39.3	38.8
AK aba			51.8	38.3	36.9	43.3	39.8	37.3	37.1
PK Sch				34.4	35.8	36.8	36.2	35.9	34.6
CK-M					80.3	68.2	65.2	67.2	53.2
CK-B						65.8	65.8	66.7	56.2
CK ur2							68.9	65.5	51.1
CK ur3								64.1	51.0
CK-MT									57.4

Abbreviations: shr, *Peanaeus*; lob, *Homarus*; aba, *Nordotis*; Sch, domain 1 of *Schistosoma*; CK-M, chicken muscle isoform; CK-B, chicken brain isoform; ur2 and ur3, domains 2 and 3 of sea urchi; CK-Mt, chicken mitochondrial isoform; wor, *Neanthes*.

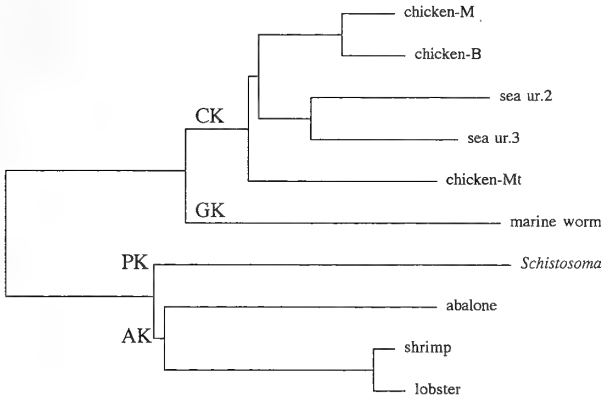

FIG. 4. A phylogenetic tree constructed from 10 sequences of phosphagen kinases aligned in Fig. 2. The tree was obtained with the program of Feng & Doolittle [5].

tions 13, 65–69, 198 and 265–268 in Fig. 3. Stein *et al.* [15] assigned tentatively *Schistosoma* PK as CK, based on the very weak, but reproducible CK activity in the crude extracts. However, since the enzyme activities of CK, GK, AK are strictly specific and those of TK, HTK, LK, OK and ThalK are more or less interspecific [1, 19], it is very likely that *Schistosoma* PK belongs to a member of the latter group. Dumas & Camonis [3] also suggest this possibility, based on the higher % identity between *Schistosoma* PK and lobster AK.

The evolutionary origin of phosphagen kinases is of primary concern. Of the phosphagen kinases, AK is most widely distributed in animals. However the wide distribution does not imply that AK is closer to an ancestral phosphagen kinase. To solve this problem, we are planning to analyze the phosphagen kinases from more primitive animals, such as sea anemones and protozoa.

REFERENCES

1 Brevet A, Zeitoun Y, Pradel LA (1975) Comparative structural studies of the active site of ATP: guanidine phosphotransferases. The essential cysteine tryptic peptide of taurocyamine kinase from *Arenicola marina*. *Biochim Biophys Acta* 393: 1–9

2 Der Terrossian E, Desvages G, Pradel LA, Kassab R, Thoai NV (1971) Comparative structural studies of the active site of ATP: guanidine phosphotransferases. The essential cysteine tryptic peptide of lombricine kinase from *Lumbricus terrestris* muscle. *Eur J Biochem* 22: 585–592

3 Dumas C, Camonis J (1993) Cloning and sequence analysis of the cDNA for arginine kinase of lobster muscle. *J Biol Chem* 268: 21599–21605

4 Felsenstein J (1993) PHYLIP (Phylogeny Inference Package) version 3.5c Distributed by the author. Department of Genetics, University of Washington, Seattle, USA

5 Feng DA, Doolittle RF (1987) Progressive sequence alignment as a prerequisite to correct phylogenetic tree. *J Mol Evol* 25: 351–360

6 Furter R, Furter-Graves EM, Wallimann T (1993) Creatine kinase: The reactive cysteine is required for synergism but is nonessential for catalysis. *Biochemistry* 32: 7022–7029

7 Hossle JP, Rosenberg UB, Schafer B, Eppenberger HM, Perriard JC (1986) The primary structure of chicken B-creatine

kinase and evidence for heterogeneity of its mRNA. *Nucl Acids Res* 14: 1449–1463

8 Hossle JP, Schlegel J, Wegmann G, Wyss M, Bohlen P, Eppenberger HM, Wallimann T, Perriard JC (1988) Distinct tissue specific mitochondrial creatine kinases from chicken brain and striated muscle with a conserve CK framework. *Biochem Biophys Res Commun* 151: 408–416

9 Kenyon GL, Reed GH (1986) Creatine kinase: Structure-activity relationships. *Adv Enzymol* 54: 367–426

10 Kwiatkowski RW, Schweinfest CW, Dottin RP (1984) Molecular cloning and the complete nucleotide sequence of the creatine kinase-M cDNA from chicken. *Nucl Acids Res* 12: 6925–6934

11 Morrison JF (1973) Arginine kinase and other invertebrate guanidino kinases. In *The Enzymes*. vol. VIII (Ed by PC Boyer) Academic Press, New York and London, 457–486

12 Okamoto S (1992) Primary structure of arginine kinase from *Penaeus japonicus* (in Japanese). *M Sci Thesis Kochi Univ*, Kochi, Japan

13 Okamoto S, Iwasaki K, Furukohri T, Suzuki T (1991) Primary structure of arginine kinase from the tail muscle of the prawn *Penaeus japonicus*. *Zool Sci* 8: 1141 (Abstract)

14 Ordahl CP, Evans GL, Cooper TA, Kunz G, Perriard JC (1984) Complete cDNA-derived amino acid sequence of chicken muscle creatine kinase. *J Biol Chem* 259: 15224–15227

15 Stein LD, Harn DA, David JR (1990) A cloned ATP: Guanidino kinase in the trematode *Schistosoma mansoni* has a novel duplicated structure. *J Biol Chem* 265: 6582–6588

16 Suzuki T (1986) Amino acid sequence of myoglobin from the mollusc *Dolabella auricularia*. *J Biol Chem* 261: 3692–3699

17 Suzuki T (1994) Evolution of phosphagen kinase (II). PCR amplification of cDNAs of *Sulculus* and *Penaeus* arginine kinases with a universal phosphagen kinase primer. (in Japanese) *Mem Fac Sci Kochi Univ Ser D* (*Biology*) 15: 1–5

18 Suzuki T, Furukohri T (1994) Evolution of phosphagen kinase. Primary structure of glycocyamine kinase and arginine kinase from invertebrates. *J Mol Biol* in press

19 Watts DC (1968) Variation in enzyme structure and function: The guidelines of evolution. *Adv Comp Physiol Biochem* 3: 1–115

20 Wothe DD, Charbonneau H, Shapiro BM (1990) The phosphocreatine shuttle of sea urchin sperm: Flagellar creatine kinase resulted from gene triplication. *Proc. Natl. Acad. Sci USA* 87: 5203–5207

ZOOLOGICAL SCIENCE 11: 235–246 (1994)

The Development of the Vermiform Embryos of Two Mesozoans, *Dicyema acuticephalum* and *Dicyema japonicum*

HIDETAKA FURUYA, KAZUHIKO TSUNEKI, and YUTAKA KOSHIDA[1]

Department of Biology, College of General Education, Osaka University, Toyonaka 560, and [1]The National Center for University Entrance Examination, Tokyo 153, Japan.

ABSTRACT—The pattern of cell division and the cell lineage of the vermiform embryos of dicyemid mesozoans were studied under the light microscope using fixed and stained specimens of two species, namely, *Dicyema acuticephalum,* which has 16 to 18 peripheral cells, and *Dicyema japonicum,* which has 22 peripheral cells. An agamete first divides into two apparently equivalent daughter cells which remain in contact with one another. One of these cells becomes the mother cell of the head of the embryo. The other cell divides again equally to produce the prospective axial cell and the mother cell of the trunk and the tail of the embryo. The division proceeds spirally in the early stages but becomes bilateral from the fifth cell division onward. The embryo finally exhibits apparently bilateral symmetry. In two lines of cells, namely, those descended from the prospective axial cell and those from the mother cell of the head, extremely unequal divisions occur and the resultant, much smaller cells from each unequal division degenerate and ultimately disappear during embryogenesis. At the thirteen-cell stage, peripheral cells surround the prospective axial cell. At the final stage of embryogenesis, the prospective axial cell divides into two daughter cells. The anterior one is the axial cell itself and the posterior one is incorporated into the axial cell to form an agamete. Differences in numbers of peripheral cells are due to the number of times that divisions of the mother cells occur. The cell lineage of the calotte differs between *D. acuticephalum* and *D. japonicum.*

INTRODUCTION

Dicyemid mesozoans are found in the renal sac of benthic cephalopod molluscs. The bodies of dicyemids consist of only 20 to 40 cells and are organized in a very simple fashion [14, 15]. It has long been debated whether dicyemids are truly primitive multicellular animals [2, 10, 11, 13, 17], or they are actually organisms that have degenerated as a result of parasitism [7, 16, 18].

Two adult forms of dicyemids, namely, nematogens and rhombogens, are found. Asexual reproduction occurs within the axial cells of nematogens and vermiform embryos develop from agametes (axoblasts), while sexual reproduction takes place within the axial cells of rhombogens. A hermaphroditic gonad, which is called an infusorigen, is formed within the axial cell and fertilization occurs around the infusorigen. The zygote undergoes cleavages and develops into an infusoriform embryo within the axial cell. The processes of gametogenesis and cleavage have recently been described in detail [4, 5]. The development of vermiform embryos was described in the early literature [6, 8 cited in 14, 12, 14, 16], but the pattern of cell divisions and the process of cell arrangement during embryogenesis remain to be established. Moreover, cell lineages have not been completely characterized. In this report, we describe details of the development of the vermiform embryo of *Dicyema acuticephalum,* which has from 16 to 18 peripheral cells [16], and of *Dicyema japonicum,* which has 22 peripheral cells [3]. Dicyemids are examples of animals with a fixed cell number and their somatic cells undergo only a limited number of divisions during embryogenesis. The analysis of embryonic cell lineages in dicyemids is important since it provides clues towards an understanding of a simple or basic pattern of cell differentiation in multicellular animals.

Accepted January 11, 1994
Received December 2, 1993

MATERIALS AND METHODS

Forty-seven octopuses, *Octopus vulgaris,* were purchased or collected by the authors in the waters off the western coast of Japan. In this region, four species of dicyemids are found in the kidneys of *Octopus vulgaris* [3]. In this study, only *Dicyema acuticephalum* and *Dicyema japonicum* were examined.

After sacrifice, the renal sacs of each octopus were removed and smeared directly on glass slides. Smeared dicyemids were immediately fixed with Carnoy's fixative or with alcoholic Bouin's solution (a mixture of absolute ethanol saturated with picric acid, formalin and acetic acid, 15:5:1, v/v). Specimens fixed with Carnoy's fixative were stained with Feulgen's stain or by the PAS method and were poststained with Ehrlich's hematoxylin and light green. Specimens fixed with alcoholic Bouin's solution were stained with Ehrlich's hematoxylin and light green only. The embryos in the axial cells of nematogens were observed under a light microscope with an oil-immersion objective at a final magnification of 2,000 diameters. Cells were identified by various criteria, such as the position within the embryo, the size of the nucleus and the cell, and the stainability of the nucleus and the cell. Paying careful attention, we identified each swollen nucleus that was about to divide and each metaphase figure in terms of the cell that was going to divide and the resultant two daughter cells. Each developing embryo with or without dividing cells was sketched at three different optical depths and a three-dimensional diagrams were generated from these

sketches.

The early division of the vermiform embryos is somewhat spiral, but not absolutely so, and it proceeds cell by cell and not by quartets. Therefore, a new terminology was developed to describe the cells. Although the body of a vermiform specimen does not differentiate into a dorsal and a ventral side, or a left and a right side, the embryos are apparently formed bilaterally during embryogenesis. In order to facilitate descriptions, a dorso-ventral axis for the embryo was tentatively defined. The cells of the vermiform were named in accordance with the nomenclature of earlier authors [14, 16].

Terminology for identification of cells

At the two-cell stage, the two cells are designated A and B. Cell A divides and produces two daughter cells. One is designated 2a, the prospective axial cell, while the other is designated as 2A, the mother cell of peripheral cells. The first digit is equal to the cell generation, namely, the number of prior cell divisions. At the four-cell stage, two daughter cells of cell B are situated on the tentatively defined left and right sides of the embryo. The cell on the right side is distinguished from the cell on the left by underlining. Thus, the left and right cells are designated as 2B and $\underline{2B}$, respectively. Cell 2B produces two daughter cells. The anterior cell is designated $3B^1$ and the posterior one is designated $3B^2$. Thus, the anterior and posterior daughter cells of $3B^1$ are designated $3B^{11}$ and $3B^{12}$, respectively.

RESULTS

At the nematogen stage, an agamete divides equally and produces two separate daughter agametes. They increase in number by mitosis, and some of them develop asexually into vermiform embryos within the axial cell of the nematogen (Figs. 1, 2a, and 8a).

Dicyema acuticephalum; the type with 16 peripheral cells (Figs. 2, 3, 4, and 5)

Before the first division, an agamete occasionally undergoes an extremely unequal division (Fig. 3a). The resultant much smaller cell remains attached to the larger one but it ultimately degenerates without contributing to embryogenesis. The first division is meridional and equal, producing two daughter cells, A and B (Fig. 3b). Cell B is the mother cell of the head peripheral cells. The second division involves only cell A. This division is latitudinal and equal, producing two daughter cells, 2A and 2a (Figs. 3c and d). Cell 2A is the mother cell of the peripheral cells of the trunk and tail, while cell 2a is the prospective axial cell. The third division involves cell B. This division is meridional and equal, producing two daughter cells, 2B and $\underline{2B}$ (Fig. 3e). At this four-cell stage, two pairs of cells, 2A-2a and 2B-$\underline{2B}$, are arranged crosswise with respect to one another. The third division furrow coincides with the plane of bilateral symmetry of the embryo. The pattern of division and the cell lineage of descendants of cell 2B are the same as those of cell $\underline{2B}$.

The fourth division involves at cell 2A. This division is also meridional and equal, resulting in the five-cell stage (Figs. 3f-h). The division plane again coincides with the plane of bilateral symmetry and it separates the right cell ($\underline{3A}$) from the left cell (3A). The division pattern and the cell lineage of descendants of cell 3A are the same as those of cell $\underline{3A}$. At around the five-cell stage, cell 2a, the prospective axial cell, undergoes an extremely unequal division and produces two daughter cells that are quite different in size (Figs. 3i and j). The larger cell, 3a, retains the characteristic of the parent cell, while the much smaller cell degenerates and ultimately disappears during embryogenesis. Cell 3a gradually becomes larger prior to the next division.

The pattern of cell division beyond the five-cell stage changes from spiral to bilateral. After the five-cell stage, divisions occur not one by one but in pairs, and they become almost synchronous. Therefore, subsequent developmental stages proceed with odd numbers of cells, yielding, for example, a seven-cell stage, and so on. The fifth division is an equal division and results in the seven-cell embryo (Figs. 3k and l). Thus, cells 2B and $\underline{2B}$ divide and produce two pairs of daughter cells, $3B^1$ and $3B^2$ plus $\underline{3B^1}$ and $\underline{3B^2}$, respectively. The future anterior-posterior axis of the embryo corresponds almost exactly to the $3B^1$–3A axis of the seven-cell embryo. The sixth division is extremely unequal (Fig. 3m). Cells $3B^1$ and $\underline{3B^1}$ divide and together they produce a pair of large cells and a pair of much smaller

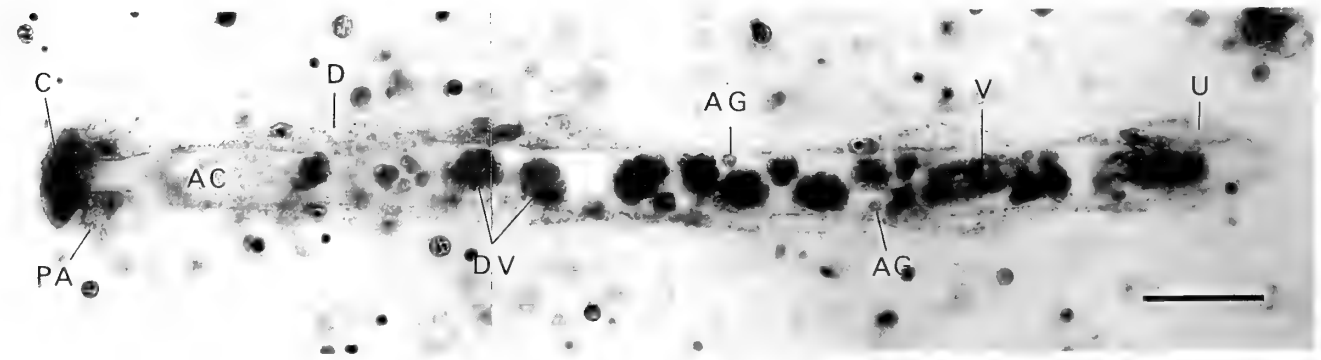

FIG. 1. Light micrograph of a nematogen of *Dicyema japonicum*. Scale bar represents 50μm. Abbreviations for this and subsequent Figures (Figs. 2–4, 6, 8–10): AC, axial cell; AG, agamete; C, calotte; D, diapolar cell; DV, developing vermiforms; M, metapolar cell; N, nucleus of the axial cell of a nematogen; P, propolar cell; PA, parapolar cell; PAC, prospective axial cell; U, uropolar cell; V, fully formed vermiform.

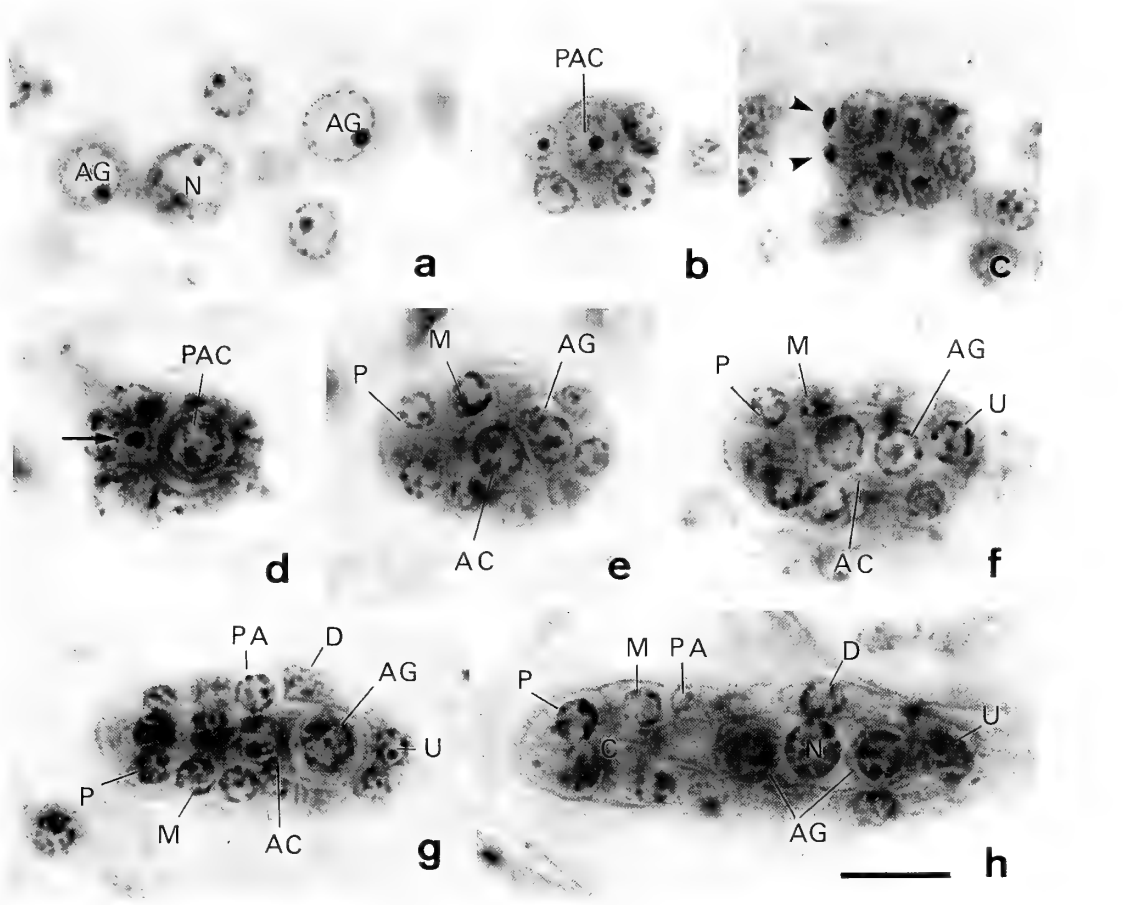

FIG. 2. Light micrographs of developing vermiforms within the axial cells of nematogens of *D. acuticephalum*. Photographs were taken at a magnification of 2,000 diameters under an oil immersion objective. Scale bar represents 10μm. (**a**): Agametes (AG) and the nucleus of an axial cell of a nematogen (N). (**b**): Nine-cell stage (optical section). (**c**): Thirteen-cell stage (surface). The arrowheads indicate degenerating cells produced after extremely unequal divisions of mother cells of peripheral cells. (**d**): Fifteen-cell stage (optical section). The arrow indicates a degenerating cell produced after an extremely unequal division of the prospective axial cell (PAC). (**e**)-(**h**): Vermiform embryos (optical section). In (f), an agamete (AG) is incorporated into the cytoplasm of an axial cell (AC).

daughter cells. Although they remain in place on the developing embryo until later stages, the smaller cells eventually degenerate and disappear. At this stage, cell 3a again divides unequally into a larger daughter cell, 4a, and a much smaller daughter cell which degenerates and ultimately disappears (Figs. 3n and o).

The seventh division is slightly unequal. Cells 3A and 3A divide into two pairs of daughter cells, $4A^1$ and $4A^2$ plus $\underline{4A^1}$ and $\underline{4A^2}$ (Figs. 3o, p). Cells $4A^2$ and $\underline{4A^2}$ are the smallest cells at this stage. They do not divide further but become the diapolar cells. At the nine-cell stage, the $3B^2$ pair undergo extremely unequal divisions, to form the larger cells $4B^2$ and $\underline{4B^2}$ and two much smaller cells (Fig. 3q). The much smaller cells remain around the larger cells until later stages (Fig. 2c) but they degenerate and ultimately disappear, while the larger cells undergo no further divisions and become the parapolar cells. The $4A^1$ pair divide equally and produce two pairs of daughter cells, $5A^{11}$ and $5A^{12}$ plus $\underline{5A^{11}}$ and $5A^{12}$ (Figs. 3r and s). Neither pair divides further and these cells become diapolar cells and uropolar cells. At around the nine-cell stage, cell 4a again undergoes an extremely unequal division (Fig. 3p). The resultant much smaller cell remains between the axial cell and the peripheral cells until later stages, but it finally disappears (Fig. 2d). As peripheral cells are formed, the larger daughter cell, 5a, is gradually enveloped by peripheral cells. Soon, the prospective axial cell, 5a, is completely surrounded by peripheral cells (Fig. 3v). Then cell 5a again divides unequally into a larger daughter cell, 6a, and a much smaller daughter cell. The smaller cell remains for a while between the prospective axial cell and the peripheral cells but it ultimately disappears during embryogenesis.

The thirteen-cell stage is achieved by equal divisions of cells $4B^1$ and $\underline{4B^1}$ (Figs. 3t and u). The resultant cells $5B^{11}$ and $5B^{12}$ divide again into two pairs of daughter cells, $6B^{111}$ and $6B^{112}$ plus $6B^{121}$ and $6B^{122}$, in the anterior part of the embryo (Figs. 4a-e). These cells undergo no further divisions, and the $6B^{111}$ and $6B^{121}$ pair become the propolar cells, while the $6B^{112}$ and $6B^{122}$ pair become the metapolar cells. The lineage of cell $4B^1$ is the same as that of cell $\underline{4B^1}$. At the

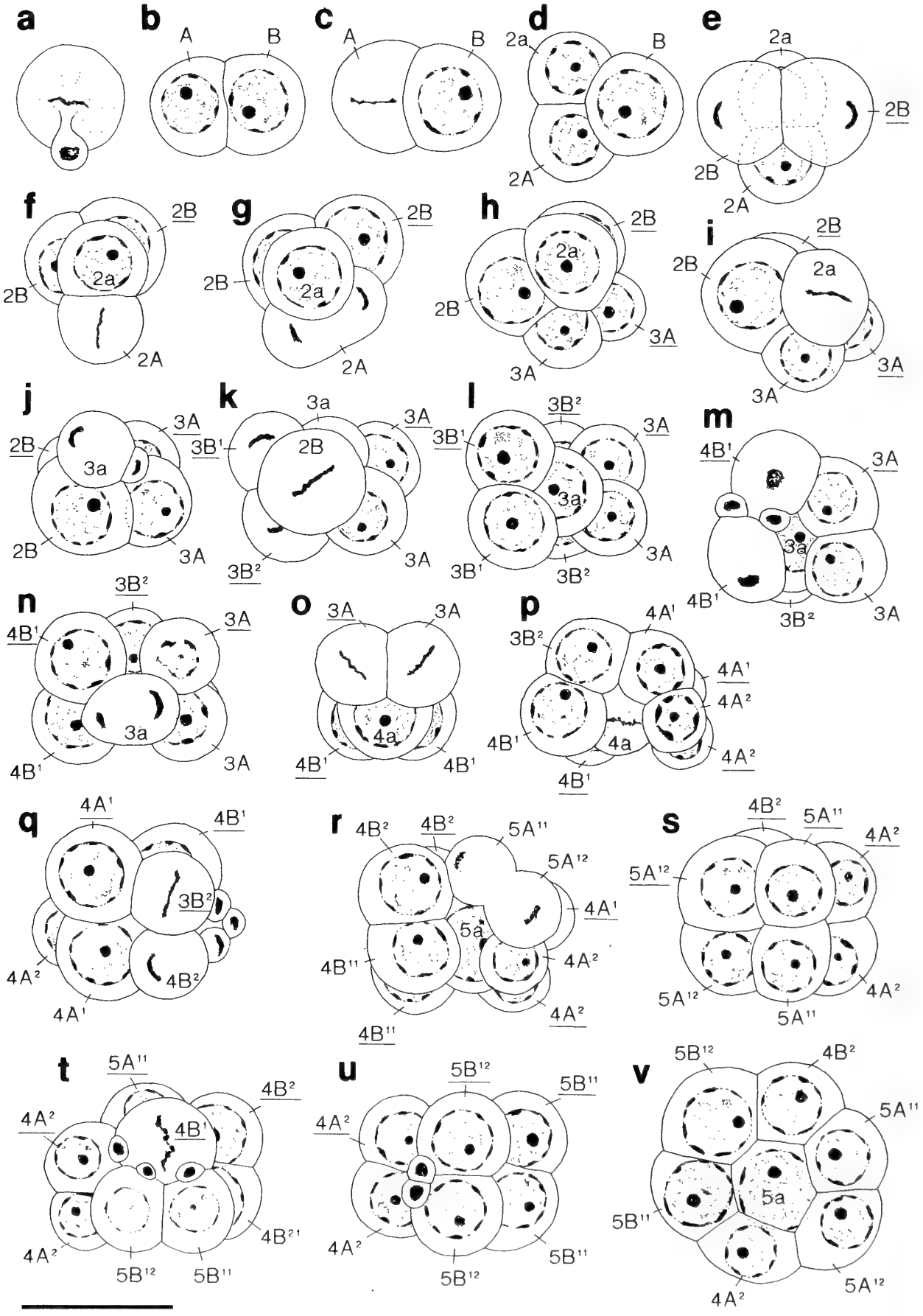
a
b
A
B
c
A
B
d
2a
B
2A
e
2a
2B
2B
2A
f
2B
2a
2B
2A
g
2B
2a
2B
2A
h
2B
2a
2B
3A
3A
i
2B
2B
2a
3A
3A
j
3A
2B
3a
3B¹
2B
3A
k
3a
3A
2B
3B¹
3B²
3A
l
3B²
3A
3B¹
3a
3B¹
3B²
3A
m
4B¹
3A
3a
4B¹
3B²
3A
n
3B²
3A
4B¹
3a
4B¹
3A
o
3A
3A
4a
4B¹
4B¹
p
4A¹
3B²
4A¹
4A²
4B¹
4a
4A²
4B¹
q
4A¹
4B¹
3B²
4A²
4B²
4A¹
r
4B²
4B²
5A¹¹
5A¹²
4A¹
5a
4B¹¹
4A²
4A²
4B¹¹
s
4B²
5A¹¹
4A²
5A¹²
5A¹²
4A²
5A¹¹
t
5A¹¹
4B²
4A²
4B¹
4B²¹
4A²
5B¹²
5B¹¹
u
5B¹²
5B¹¹
4A²
4A²
5B¹²
5B¹¹
v
5B¹²
4B²
5A¹¹
5B¹¹
5a
5A¹²
4A²

same time, the internal cell 6a, namely the prospective axial cell, divides equally into two daughter cells. The anterior cell, $7a^1$, becomes an axial cell and the posterior one, $7a^2$, becomes the first agamete (Figs. 2e and 4b). The agamete is soon incorporated into the axial cell (Figs. 2e and f). A pair of parapolar cells situated in the dorsal region elongate and approach each other in the ventral region (Fig. 4f). Then, the peripheral cells become ciliated. Cilia on the propolar and metapolar cells are more densely distributed than those on the other peripheral cells. The fully formed embryo consists of sixteen peripheral cells and one axial cell, which contains two to four agametes (Figs. 2h and 4f). Further development involves only the enlargement and intracellular differentiation of cells that have already formed (Fig. 2f-h). The body length, excluding cilia, of the fully formed embryo is about 55μm and the body width is about 11μm.

Dicyema acuticephalum; the type with 17 or 18 peripheral cells

(Figs. 6 and 7)

At the thirteen-cell stage of the embryo, which ultimately has 18 peripheral cells, the $4B^2$ pair divide equally to produce two pairs of daughter cells, the $5B^{21}$ and $5B^{22}$ pairs (Figs. 6a and b). The anterior $5B^{21}$ pair become parapolar cells, while the posterior $5B^{22}$ pair become the fourth diapolar cells (Fig. 6c). In the embryo that finally has 17 peripheral cells, terminal division of cell $4B^2$ or cell $\underline{4B^2}$ occurs. Other aspects of embryogenesis are the same as those described above for *D. acuticephalum* with 16 peripheral cells.

Dicyema japonicum

(Figs. 8, 9, 10, and 11)

Up to the nine-cell stage, the pattern of development and the cell lineage in *D. japonicum* are the same as those described for *D. acuticephalum*. In the 2a line, extremely unequal divisions occur at around the five-, seven-, nine-, and seventeen-cell stages (Figs. 8c, d and 11).

At the eleven-cell stage, in *D. japonicum*, the $3B^2$ pair of cells divide equally into $4B^{21}$ and $4B^{22}$ pairs (Figs. 9a-c). Almost simultaneously, the cells of the $3B^1$ pair undergo extremely unequal divisions, generating the larger daughter pair $4B^1$ and $\underline{4B^1}$ and a much smaller pair (Figs. 9d and e). The smaller pair of cells degenerate and finally disappear. At the thirteen-cell stage, the $5A^{11}$ pair divide equally and produce two pairs of daughter cells, $6A^{111}$ and $6A^{112}$ plus $\underline{6A^{111}}$ and $\underline{6A^{112}}$ (Fig. 9f). The plane of this division is parallel to the antero-posterior axis in contrast to the previous division that occurs parallel to the dorso-ventral axis. As the result, cells $6A^{111}$ and $\underline{6A^{111}}$ are situated on the left and right sides of the embryo, respectively.

The $4B^{22}$ pair divide equally and produce two pairs of daughter cells, $5B^{221}$ and $5B^{222}$ plus $\underline{5B^{221}}$ and $\underline{5B^{222}}$ (Fig. 9g). Cells $5B^{221}$ and $\underline{5B^{221}}$ and cells $5B^{222}$ and $\underline{5B^{222}}$ undergo no further divisions and become parapolar cells and diapolar cells, respectively (Figs. 10a and c).

At the seventeen-cell stage, the $5A^{12}$ pair undergo slightly unequal divisions and produce two pairs of daughter cells, $6A^{121}$ and $6A^{122}$ plus $\underline{6A^{121}}$ and $\underline{6A^{122}}$ (Fig. 9h). Neither pair divide further. Cells $6A^{121}$ and $\underline{6A^{121}}$ become uropolar cells, while cells $6A^{122}$ and $\underline{6A^{122}}$ become diapolar cells (Figs. 10a and c).

The $4B^1$ pair divide equally into two pairs of daughter cells, $5B^{11}$ and $5B^{12}$ plus $\underline{5B^{11}}$ and $\underline{5B^{12}}$ (Figs. 9i and j). Soon after these divisions, the $\underline{4B^{21}}$ pair divide equally into two pairs of daughter cells, $5B^{211}$ and $5B^{212}$ plus $\underline{5B^{211}}$ and $\underline{5B^{212}}$ (Figs. 9k and l). $5B^{211}$ and $\underline{5B^{211}}$ become propolar cells, while cells $5B^{212}$ and $\underline{5B^{212}}$ become metapolar cells. At around this stage, the prospective axial cell, 6a, divides unequally (Figs. 8e and f). The anterior large cell, $7a^1$, undergoes no further divisions and becomes an axial cell, while the posterior small cell, $7a^2$, becomes an agamete and is soon incorporated into the axial cell (Figs. 8g, h, and 10b). A pair of parapolar cells, situated in the dorsal region, elongate and approach each other in the ventral region (Figs. 10a and c). The vermiform embryo finally consists of twenty-two peripheral cells and one axial cell, which contains one or two agametes (Fig. 8i). The body length, excluding cilia, of the fully formed embryo is about 65μm and the body width is about 12μm. No variations in cell lineage were found among embryos examined.

FIG. 3. Sketches of early embryos of *Dicyema acuticephalum*. Scale bar represents 10μm. (**a**): An agamete undergoing an extremely unequal division. This division is not always seen. (**b**) and (**c**): Two-cell stage. In (c), a metaphase figure in cell A is depicted. This division produces a prospective axial cell (2a) and a mother cell of peripheral cells (2A). (**d**) and (**e**): Three-cell stage. In (e), a telophase figure in cell B is depicted. This division produces a mother cell of the left head (2B) and of the right head ($\underline{2B}$). (**f**) and (**g**): Four-cell stage. In (f), a metaphase figure in cell 2A is shown. In (g), an anaphase figure in cell 2A is depicted. This division produces a mother cell of the left trunk (3A) and of the right trunk ($\underline{3A}$). (**h**)-(**k**): Five-cell stage. In (i), a metaphase figure in cell 2a is shown. In (j), a telophase figure in cell 2a is depicted. This extremely unequal division produces cell 3a and a much smaller cell which is destined to die. In (k), the left (2B) and right cell ($\underline{2B}$) divide almost synchronously. (**l**)-(**o**): Seven-cell stage. In (m), cells $3B^1$ and $\underline{3B^1}$ undergo an extremely unequal division to produce cells $4B^1$ and $\underline{4B^1}$ and two much smaller cells which are destined to die. In (n), cell 3a undergoes an extremely unequal division. In (o), metaphase figures in cells 3A and $\underline{3A}$ are shown. (**p**)-(**r**) Nine-cell stage. In (p), a metaphase figure (lower center) in cell 4a is depicted. In (q), a metaphase figure in cell $3B^2$ (upper right) and a telophase figure (lower right) in cell $3B^2$ are shown. The cell divisions are extremely unequal. In (r), an anaphase figure (upper right) in cell $4A^1$ is shown. This equal division produces cells $5A^{11}$ and $5A^{12}$. (**s**): Eleven-cell stage. (**t**): Twelve-cell stage. Note a metaphase figure in cell $\underline{4B^1}$ that is dividing equally to produce cells $\underline{5B^{11}}$ and $\underline{5B^{12}}$. (**u**): Thirteen-cell stage (surface view). (**v**): Thirteen-cell stage (sagittal optical section).

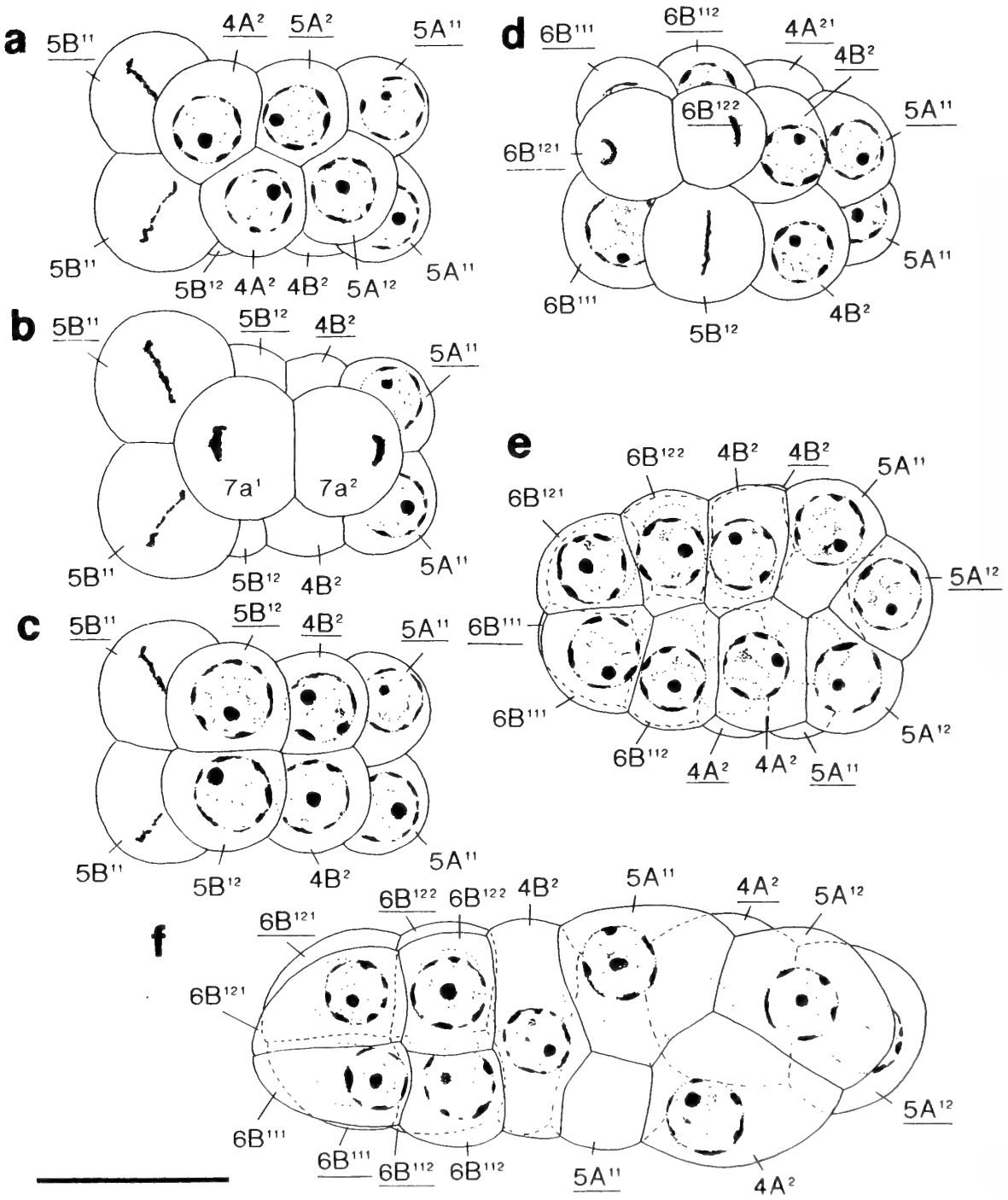

FIG. 4. Sketches of late embryos of *D. acuticephalum*. Scale bar represents 10μm. (**a**): Thirteen-cell stage (ventral view). Note metaphase figures in cells $5B^{11}$ and $\underline{5B}^{11}$ that are dividing equally to produce propolar cells and metapolar cells. (**b**): Thirteen-cell stage (horizontal optical section). Note a telophase figure in cell $6a^1$. This division produces an axial cell ($7a^1$) and the first agamete ($7a^2$). (**c**): Thirteen-cell stage (dorsal view). (**d**): Fifteen-cell stage (dorsal view). Cell $5B^{12}$ divides equally to produce a propolar cell and a metapolar cell. (**e**): Nearly formed embryo (lateral view). (**f**): Fully formed embryo (lateral view). Cilia have been omitted.

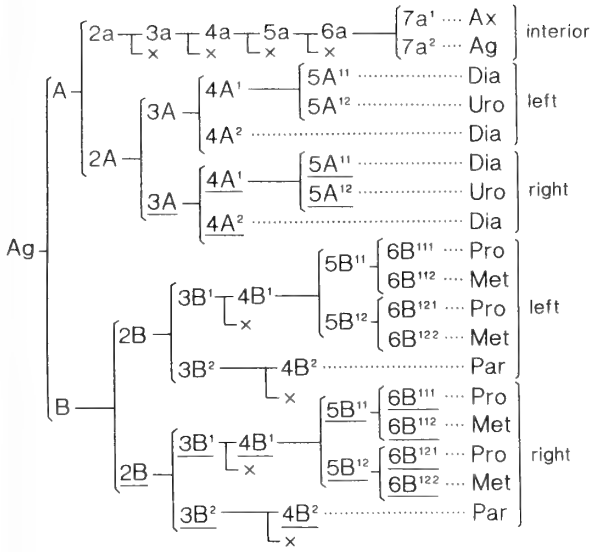

FIG. 5. Cell lineage of the vermiform embryo of *Dicyema acuticephalum* that has sixteen peripheral cells. A cross (x) indicates that a cell, formed as the result of an extremely unequal division, degenerates and does not contribute to the formation of the embryo. Abbreviations in Figs. 5, 7, and 11: Ag, agamete; Ax, axial cell; Dia, diapolar cell; Par, parapolar cell; Pro, propolar cell; Met, metapolar cell; Uro, uropolar cell.

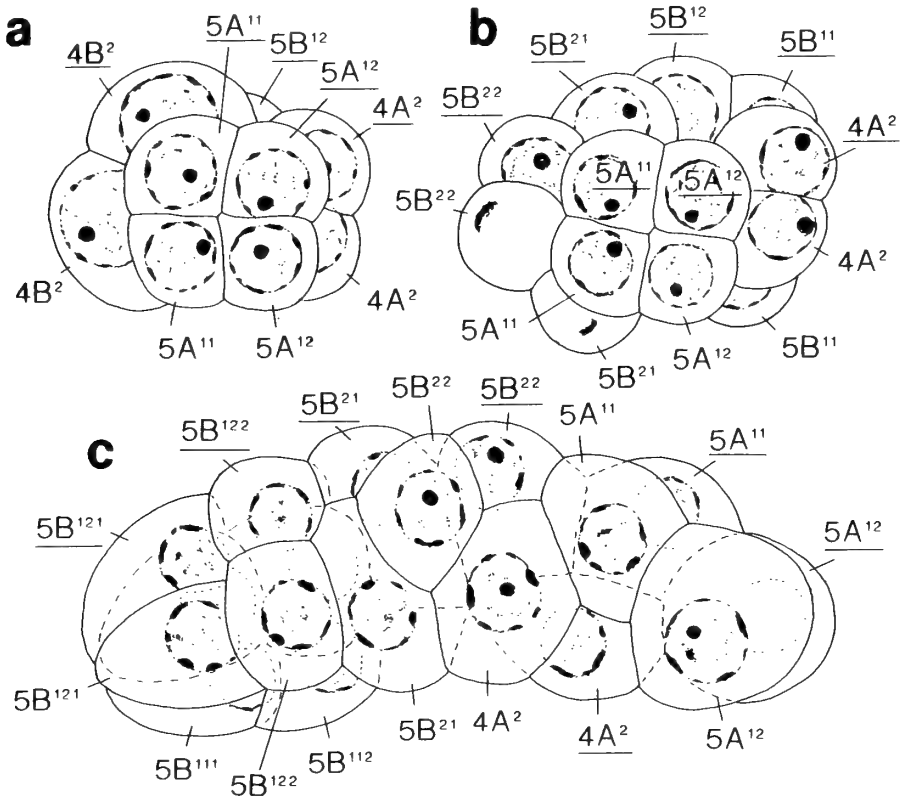

FIG. 6. Sketches of late embryos and a fully formed embryo of *Dicyema acuticephalum* that has eighteen peripheral cells. Scale bar represents 10μm. (**a**): Thirteen-cell stage (from the tail). (**b**): Fourteen-cell stage (from the tail). Note a telophase figure in cell $4B^2$. This division produces a parapolar cell ($5B^{21}$) and a diapolar cell ($5B^{22}$). (**c**): Fully formed embryo. Cilia have been omitted.

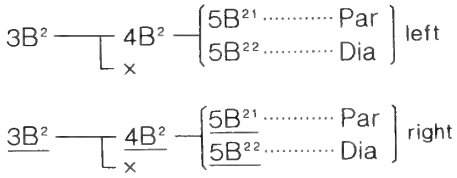

FIG. 7. The lineage of cells $3B^2$ and $\underline{3B^2}$ of the vermiform embryo of *Dicyema acuticephalum* that has eighteen peripheral cells. The other aspects of cell lineage are the same as those of *D. acuticephalum* with sixteen peripheral cells. See the legend to Fig. 5 for abbreviations.

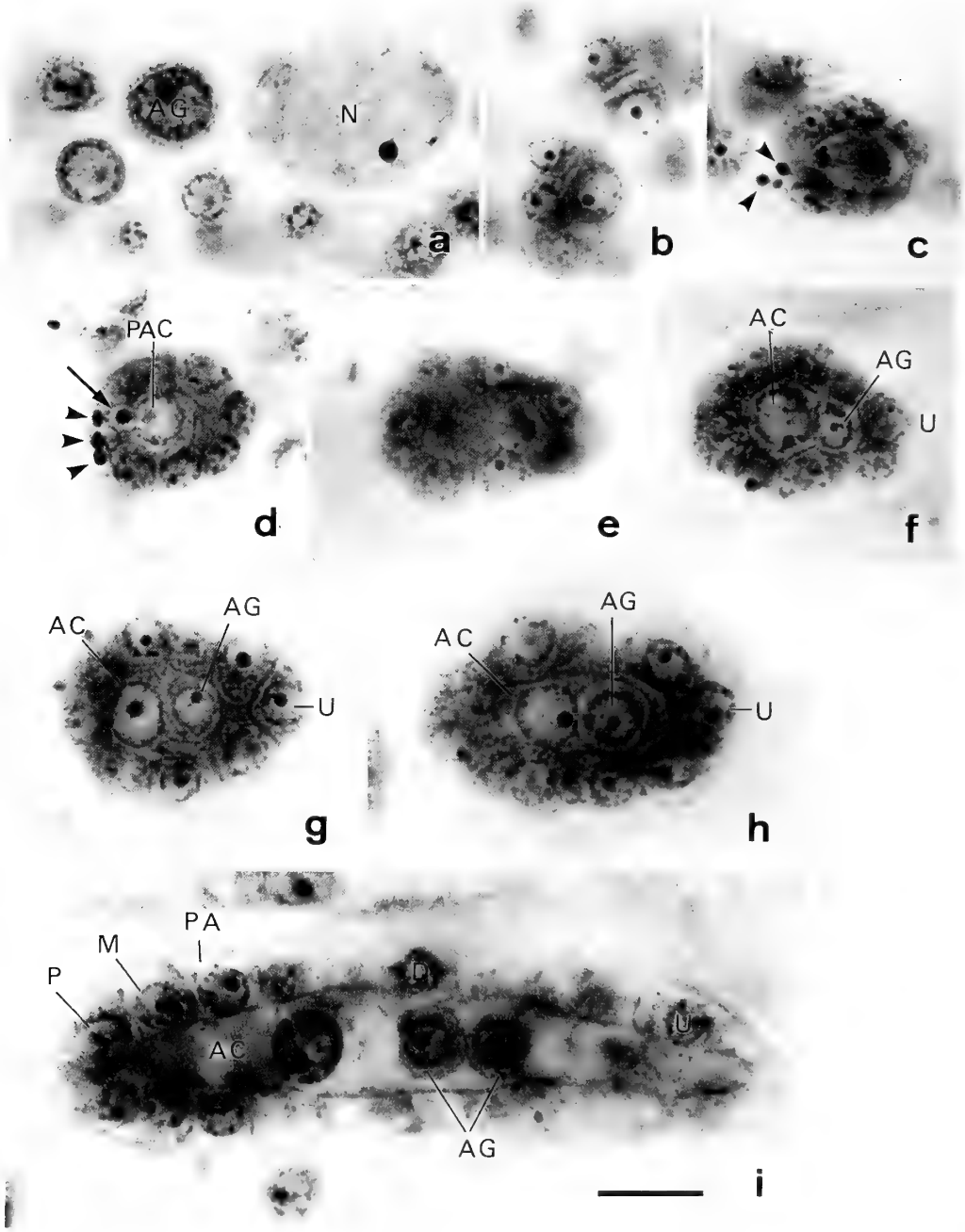

FIG. 8. Light micrographs of developing vermiform embryos within the axial cells of nematogens of *D. japonicum*. Scale bar represents 10μm. (**a**): An agamete (AG) and the nucleus (N) of an axial cell of a nematogen. (**b**): Two-cell stage (upper) and three-cell stage (lower). (**c**): Thirteen-cell stage (optical section). A prospective axial cell (center) is undergoing an extremely unequal division. The arrowheads indicate degenerating cells produced after extremely unequal divisions. (**d**): Fifteen-cell stage (optical section). The arrowheads indicate degenerating cells produced after extremely unequal divisions of peripheral cells, while the arrow indicates a degenerating cell produced after an extremely unequal division of a prospective axial cell (PAC). (**e**): Seventeen-cell stage (optical section). A prospective axial cell (center) is undergoing an unequal division. (**f**) to (**h**): Developing vermiforms (optical section). In (g) and (h), an agamete (AG) is incorporated in the cytoplasm of an axial cell (AC). (**i**): Fully formed embryo (optical section).

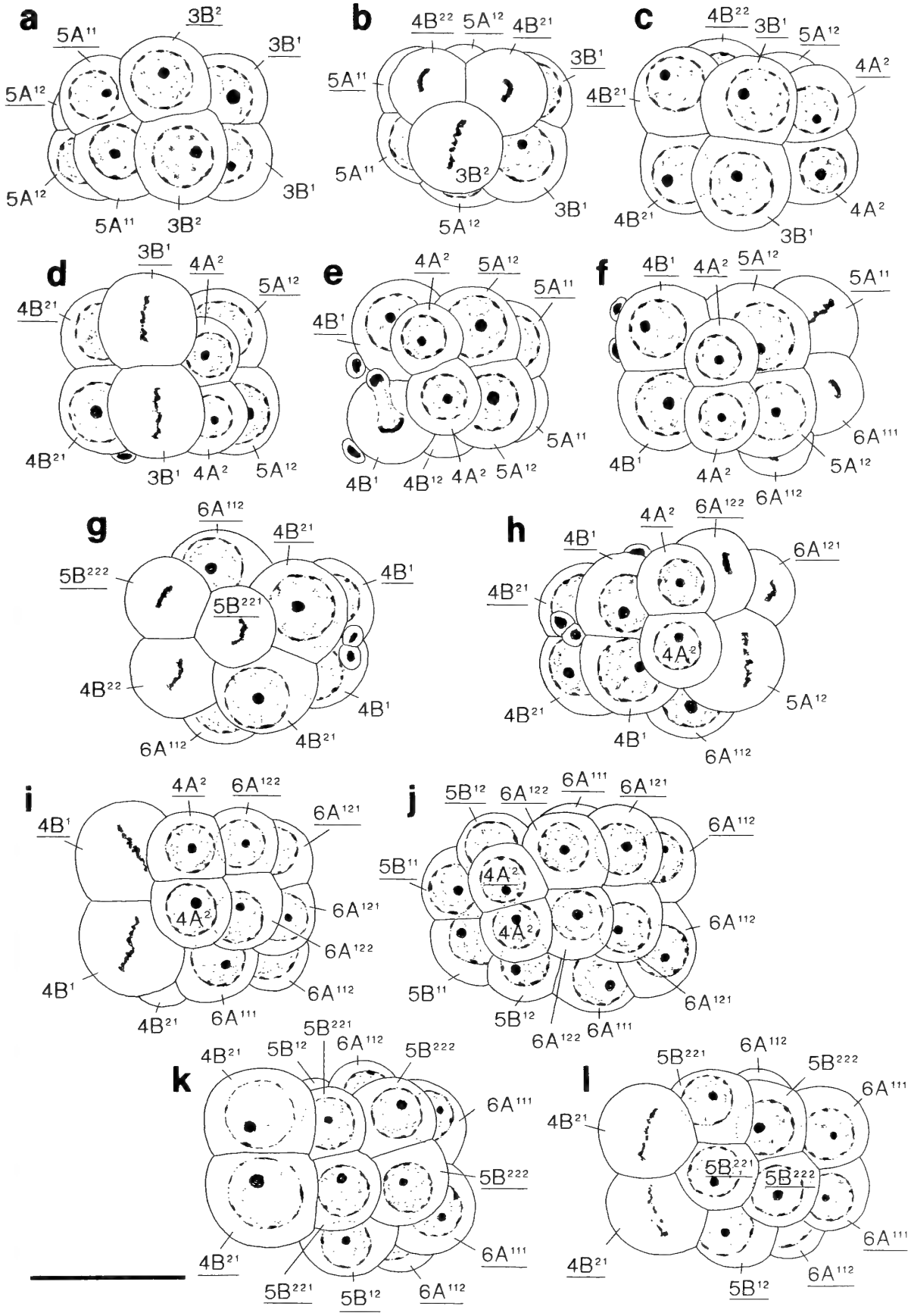
a
5A11
3B2
3B1
5A12
5A12
3B1
5A11
3B2
b
4B22
5A12
4B21
3B1
5A11
3B2
3B1
5A12
c
4B22
3B1
5A12
4A2
4B21
4A2
4B21
3B1
d
3B1
4A2
5A12
4B21
4B21
3B1
4A2
5A12
e
4A2
5A12
5A11
4B1
5A11
4B1
4B12
4A2
5A12
f
4B1
4A2
5A12
5A11
6A111
4B1
4A2
5A12
6A112
g
6A112
4B21
5B222
4B1
5B221
4B22
4B1
6A112
4B21
h
4A2
6A122
6A112
4B1
6A121
4B21
4A2
5A12
4B21
4B1
6A112
i
4A2
6A122
6A121
4B1
4A2
6A121
6A122
4B1
6A112
4B21
6A111
j
5B12
6A122
6A111
6A121
6A112
5B11
4A2
4A2
6A112
5B11
6A121
5B12
6A122
6A111
k
4B21
5B12
5B221
6A112
5B222
6A111
5B222
4B21
6A111
5B221
5B12
6A112
l
5B221
6A112
5B222
6A111
4B21
5B221
5B222
6A111
4B21
6A112
5B12

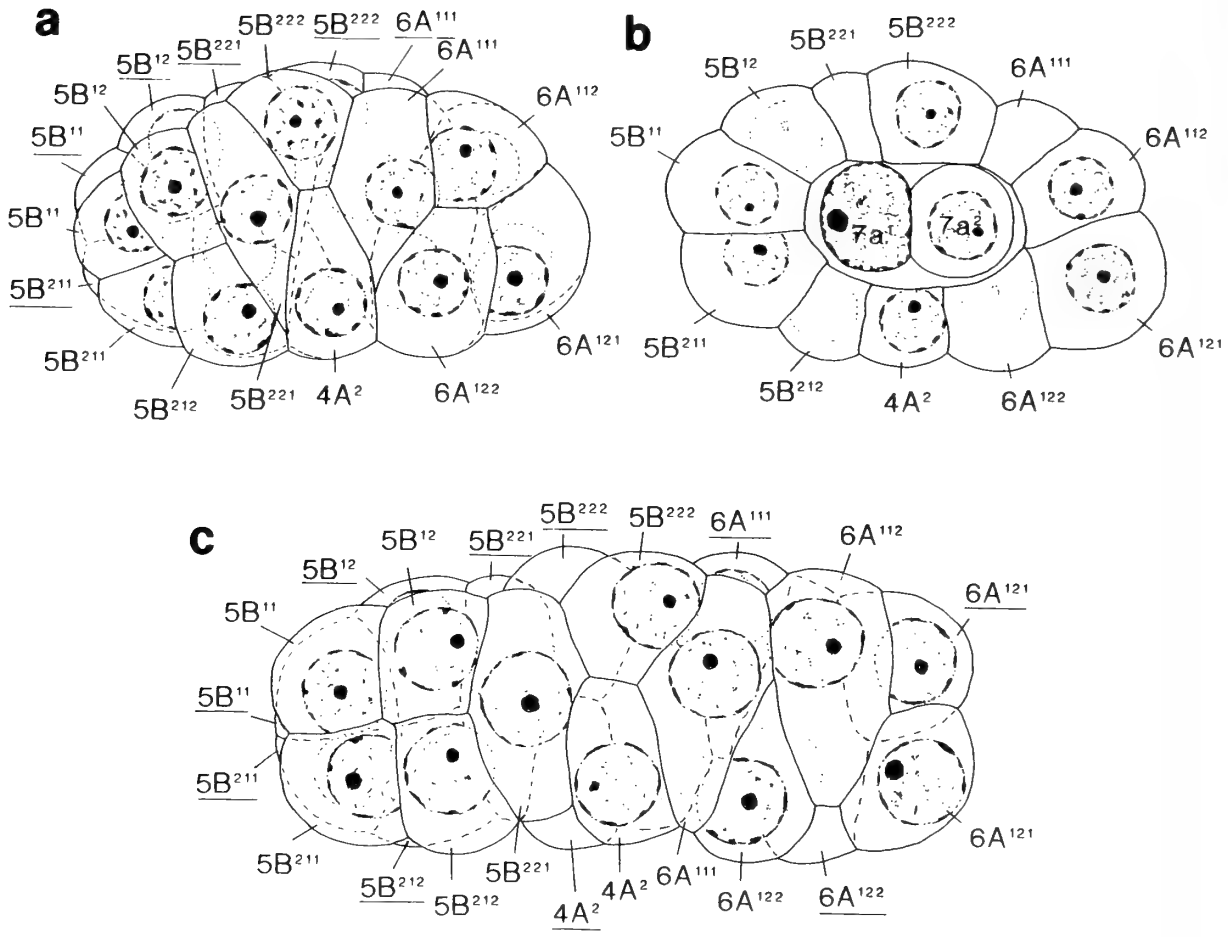

FIG. 10. Sketches of formed embryos of *Dicyema japonicum*. Scale bar represents 10μm. (**a**): Lateral view. (**b**): Sagittal optical section. Note an agamete ($7a^2$) in the cytoplasm of an axial cell ($7a^1$). (**c**): A formed embryo (lateral view).

DISCUSSION

The patterns of development of the vermiform embryos of *Dicyema acuticephalum* and *Dicyema japonicum*, as described in detail, are very similiar. However, these patterns are very different from those described for *Microcyema vespa* and *Pseudicyema truncatum* by Lameere [12], for *Dicyema typus* by Gersch [6], and for *Dicyema balamuthi, Dicyemennea abelis,* and *Dicyemennea californica* by McConnaughey [14].

In both species studied here, the first division is equal and produces two daughter cells of equal size. However, in other dicyemid species, namely, *Microcyema vespa, Pseudicyema truncatum* [12], *Dicyema typus* [6], *Dicyema balamuthi, Dicyemennea abelis* and *Dicyemennea californica* [14], the first division is unequal and the two daughter cells are of different sizes. In this study, we noted that one of the two equal daughter cells enlarges after the division, as observed by Hartmann [8 cited in 14]. There may be at least two patterns that typify the first cell division in the various

FIG. 9. Sketches of embryos of *Dicyema japonicum* from the eleven-cell to the twenty-one-cell stage. Scale bar represents 10μm. (**a**) and (**b**): Eleven-cell stage. In (b), a telophase figure in cell $3B^2$ (upper) and a metaphase figure in cell $3B^2$ (lower) are seen. (**c**)-(**f**): Thirteen-cell stage. In (d), metaphase figures in cells $3B^1$ and $3B^1$ are shown. In (e), a later anaphase figure (lower left) in cell $3B^1$ is depicted. This division is extremely unequal and produces cell $4B^1$ and a much smaller cell. In (f), a metaphase figure in cell $5A^{11}$ (upper right) and a telophase figure in cell $5A^{11}$ (lower right) are shown. (**g**): Sixteen-cell stage. Note a telophase figure of cell $4B^{22}$ (upper left) and a metaphase figure in cell $4B^{22}$ (lower left). (**h**): Seventeen-cell stage. Note a telophase figure of cell $5A^{12}$ (upper right) and a metaphase figure in cell $5A^{12}$ (lower right). (**i**): Nineteen-cell stage (ventral view). Note metaphase figures (left) in the $4B^1$ pair. These divisions produce propolar cells ($5B^{11}$ and $5B^{11}$) and metapolar cells ($5B^{12}$ and $5B^{12}$). (**j**): Twenty-one-cell stage (ventral view). (**k**) and (**l**): Twenty-one-cell stage (dorsal view). In (l), metaphase figures (left) in the $4B^{21}$ pair are shown. These divisions produce propolar cells ($5B^{211}$ and $5B^{211}$) and metapolar cells ($5B^{212}$ and $5B^{212}$).

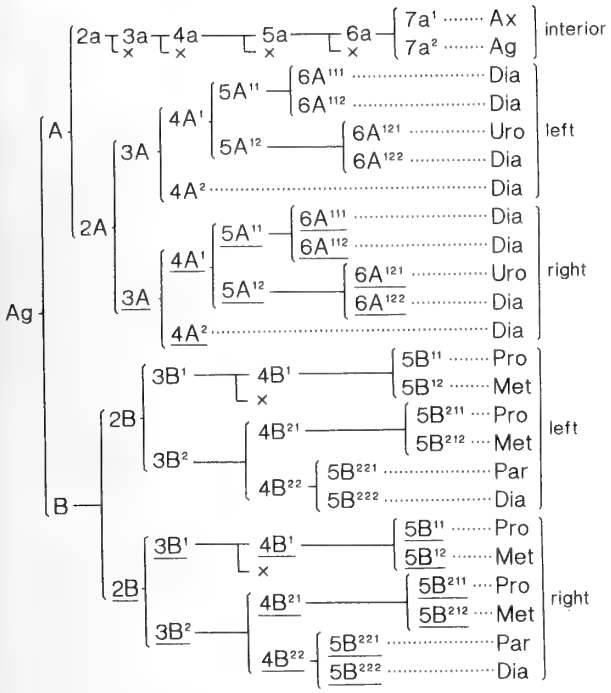

FIG. 11. Cell lineage of the vermiform embryo of *Dicyema japonicum*. See the legend to Fig. 5 for abbreviations.

species of dicyemid. In earlier descriptions [6, 12, 13, 14, 16], one of the daughter cells (usually the larger one) is reported to become a prospective axial cell and the other is regarded as the mother cell of the peripheral cells. However, the prospective axial cell is not generated prior to the four-cell stage in *D. acuticephalum* and *D. japonicum*. This type of species-specific difference during embryogenesis is reminiscent of that observed in the case of the development of infusorigens [5]. In addition, species difference between *D. acuticephalum* and *D. japonicum* was found in the lineage of the cells that form the calotte (Figs. 5 and 11). Research into the cell lineage of vermiforms may be of relevance to the taxonomy of dicyemids.

As shown clearly in Figures 5 and 7, the difference in terms of the peripheral cell number among individual specimens of *D. acuticephalum* is due to the number of divisions of the $4B^2$ pair. In a previous paper [3], we reported that the peripheral cell number of *D. acuticephalum* was consistently 18. In the subsequent study of individuals from a large number of octopuses, we noticed, however, specimens of *D. acuticephalum* with 16 or 17 peripheral cells. In the original description of this species, Nouvel [16] also reported that the peripheral cell number of *D. acuticephalum* is usually 18 but occasionally 16. In other dicyemid species such as *Dicyema bilobum* and *Dicyema benthoctopi*, which have variable numbers of peripheral cells [1, 9], additional terminal divisions may occur towards the end of the establishment of a certain cell lineage, as in the case of the $4B^2$ pair in *D. acuticephalum*. The species-specific difference in the peripheral cell number between *D. acuticephalum* and *D. japonicum* can be attributed to the number of divisions of the $4A^1$ pair (Figs. 5 and 11). Thus, the $4A^1$ pair in *D. japonicum* apparently have a greater ability to divide than the $4A^1$ pair of *D. acuticephalum*. By contrast, the $4A^2$ pair cease divisions early in embryogenesis and soon become the peripheral cells in both species. The number of mother-cell divisions clearly plays a significant role in the morphogenesis of vermiforms. In dicyemids that have relatively large numbers of peripheral cells, mother cells, such as the $4A^1$ pair, may undergo further divisions until the species-specific number of cells has been reached.

The elimination of chromatin during early embryogenesis from the prospective axial cell has been described in some dicyemid species [14]. In *D. acuticephalum* and *D. japonicum* at least, we observed not the elimination of chromatin but extremely unequal cell divisions that resulted in the pycnotic degeneration of the smaller daughter cells. Some earlier workers also reported extremely unequal divisions in the case of the prospective axial cell, but they did not report such divisions do not occur in any of peripheral cell lines [12, 16]. By contrast, McConnaughey described the occurrence of extremely unequal divisions in the peripheral cell line [14, 15]. In *D. acuticephalum* and *D. japonicum*, extremely unequal division occurs not only in the case of the prospective axial cell (2a-line), but also at the one-cell stage (agamete) and in the case of the mother cells of the peripheral cells, namely, cells $3B^1$ and $3B^2$ plus $\underline{3B^1}$ and $\underline{3B^2}$ (in *D. acuticephalum*) or cells $3B^1$ and $\underline{3B^1}$ (in *D. japonicum*). These phenomena may be examples of programmed cell death. The production of these smaller cells, which are destined to die, appears to be a constant feature found in the embryogenesis of vermiforms.

In *D. acuticephalum* and *D. japonicum*, the prospective axial cell (2a-line) divides four times and produces four smaller cells anteriorly until the first agamete is produced posteriorly. In his description of the development of vermiforms of *Microcyema vespa* and *Pseudicyema truncatum*, Lameere [12] noted that one small cell is formed by the unequal division of the prospective axial cell and that this small cell itself divides once or twice to produce two to four smaller cells. However, no divisions of the smaller cell itself could be observed in *D. acuticephalum* and *D. japonicum*.

Hartmann [8 cited in 14] considered that the number of the much smaller cells was consistent with the number of extra axial cells in the stem nematogen. However, the actual number of these smaller cells that we observed was more than he postulated. The number of these smaller cells was larger in our specimens than the number (usually three) of axial cells in the stem nematogen. It is difficult to provide a reasonable interpretation of this phenomenon. McConnaughey [15] maintained that the formation of the smaller cells represents a relict condition of ancestral forms that had more internal cells and that these small cells have no particular function in the present species. If an extremely unequal division of a prospective axial cell represents a phenomenon that is derived secondarily from an equal division during what

has been, most likely, a long history of parasitism, smaller cells that are destined to die might be expected to be formed ultimately. The vermiforms might originally have had some internal cells, as McConnaughey suggested. The prospective axial cell has at least the ability to divide further and produce some internal cells, even though these cells are actually fated to die. It seems possible that these successive, extremely unequal divisions in the 3a-line might contribute to the maintenance of increased amounts of cytoplasm in the resultant larger cell. The larger cell retains most of the cytoplasm of the mother cell and enlarges after each division. The prospective axial cell may require a large amount of cytoplasm to accommodate a prospective agamete.

We must also consider the fact that extremely unequal divisions occur consistently in the cell lineage of the 3B-line and not in 3A-line. The 3B-line gives rise to the head region, which includes the calotte, which has distinctive features among peripheral cells. By contrast, the 2A-line gives rise to the trunk and tail region which are composed of standard peripheral cells. It is likely that extremely unequal divisions in the peripheral cell lineage are somehow associated with the characteristic differentiation of cells. The prospective axial cell also has distinct features and undergoes extremely unequal divisions.

Programmed cell death has also been reported in the development of infusoriforms [4]. Moreover, McConnaughey [14] and Nouvel [16] found that embryos of stem nematogens include a number of degenerating cells. Thus, the formation of much smaller cells that are destined to die during embryogenesis appears to be a constant and general feature of development of dicyemids. In the embryogenesis of infusoriform embryos, a cell line that includes a programme for cell death gives rise to remarkably differentiated cells, such as the capsule cell [4]. Although we can offer no reasonable explanation at present, the programmed cell death might somehow be involved in an accelation of cell differentiation.

In the embryogenesis of vermiforms, cell divisions are determinate and result in an embryo with a definite number and arrangement of cells. The developmental process of the vermiform embryo seems very simple and it seems to be programmed similarly to that of the infusorigen and the infusoriform embryo [4, 5]. There appears to be little plasticity in such development because of the simple body organization of these organisms.

The constant numbers of cells in dicyemids is strongly reminiscent of that of aschelminths. McConnaughey [15] suggested that dicyemids may possibly be related to very early progenitors of aschelminths or to certain of the earliest aschelminths. Programmed cell death has also been noted in the embryogenesis of the nematode *Caenorhabditis elegans* [19]. However, there is apparently no further evidence to support any relationship between dicyemids and aschelminths.

REFERENCES

1 Couch JA, Short RB (1964) *Dicyema bilobum* sp. n. (Mesozoa: Dicyemidae) from the northern Gulf of Mexico. J Parasitol 50: 641–645.

2 Eernisse DJ, Albert JS, Anderson FE (1992) Annelida and Arthropoda are not sister taxa: a phylogenetic analysis of spiralian metazoan morphology. Syst Biol 41: 305–330

3 Furuya H, Tsuneki K, Koshida Y (1992) Two new species of the genus *Dicyema* (Mesozoa) from octopuses of Japan with notes on *D. misakiense* and *D. acuticephalum*. Zool Sci 9: 423–437

4 Furuya H, Tsuneki K, Koshida Y (1992) Development of the infusoriform embryo of *Dicyema japonicum* (Mesozoa: Dicyemidae). Biol Bull 183: 248–257

5 Furuya H, Tsuneki K, Koshida Y (1993) The development of the hermaphroditic gonad in four species of dicyemid mesozoans. Zool Sci 10: 455–466

6 Gersch J (1938) Der Entwicklungszyklus der Dicyemiden. Z wiss Zool 151: 515–605.

7 Ginetsinskaya TA (1988) Trematodes, Their Life Cycles, Biology and Evolution. Amerind Publishing Co. Pvt. Ltd., New Delhi. (Translation of the original Russian edition, 1968)

8 Hartmann M (1906) Untersuchungen über den Generationswechsel der Dicyemiden. Mem Acad R Belg Ser II 1: 1–128

9 Hochberg FG, Short RB (1970) *Dicyemennea littlei* sp. n. and *Dicyema benthoctopi* sp. n.: dicyemid Mesozoa from *Benthoctopus magellanicus*. Trans Amer Micro Soc 89: 216–224

10 Hyman L (1940) The Invertebrates, Vol I, McGraw Hill, New York

11 Hyman L (1959) The Invertebrates, Vol V, McGraw Hill, New York

12 Lameere A (1918) Contributions à la connaissance des dicyémides (3e partie). Bull Biol Fr Belg 53: 234–269

13 Lapan EA, Morowitz HJ (1975) The dicyemid Mesozoa as an integrated system for morphogenetic studies. 1. Description, isolation and maintenance. J Exp Zool 193: 147–160

14 McConnaughey BH (1951) The life cycle of the dicyemid Mesozoa. Univ Calif Publ Zool 55: 295–336

15 McConnaughey BH (1963) The Mesozoa. In "The Lower Metazoa. Comparative Biology and Phylogeny" Ed by EC Dougherty, University of California Press, California, pp 151–165

16 Nouvel H (1947) Les Dicyémides. 2e partie: systématique, générations, vermiformes, infusorigène et sexualité. Arch Biol 58: 59–220

17 Ohama T, Kumazaki T, Hori H, Osawa S (1984) Evolution of multicellular animals as deduced from 5S ribosomal RNA sequences: a possible early emergence of the Mesozoa. Nucleic Acids Res 12: 5101–5108

18 Stunkard H W (1954) The life history and systematic relations of the Mesozoa. Quart Rev Biol 29: 230–244

19 Sulston JE, Schierenberg E, White JG, Thomson JN (1983) The embryonic cell lineage of the nematode *Caenorhabditis elegans*. Dev Biol 100: 64–119

ZOOLOGICAL SCIENCE 11: 247–251 (1994)

Female Myoblasts Can Participate in the Formation of a Male-specific Muscle in *Drosophila*

KEN-ICHI KIMURA[1], KAZUYA USUI[1,3] and TEIICHI TANIMURA[2]

[1]*Laboratory of Biology, Hokkaido University of Education, Iwamizawa Campus, Iwamizawa 068 and* [2]*Biological Laboratory, Kyushu University, Ropponmatsu, Fukuoka 810, JAPAN*

ABSTRACT—In *Drosophila melanogaster*, a pair of dorsal longitudinal muscles in the fifth abdominal segment occurs in males but not in females. This male-specific muscle develops during metamorphosis. We examined how far the sexual identity of myoblast is involved in the formation of the male-specific muscle by transplantation of female myoblasts. A transformant strain which contains a 79B actin promoter fused to *Escherichia coli* β-galactosidase gene was used as a genetic reporter. A part of wing imaginal disc from the male or female donor transformant was transplanted into the abdomen of the male host (wild-type). After the hosts were allowed to develop till pharate adult or adult stage, the male-specific muscle of the host was examined whether it expressed the reporter gene or not. The expression of the reporter gene in the host's male-specific muscle was detected in both cases of donor's sex. The results indicate that myoblasts, independently of their sexual identity, can participate in the formation of the male-specific muscle. Therefore, the information of the sexual identity in the myoblasts itself is not the prerequisite for the formation of the male-specific muscle.

INTRODUCTION

Sexual dimorphism occurs in musculature and nervous system of most organisms, as well as in the external appearance. In *Drosophila melanogaster*, a pair of longitudinal muscles in the fifth abdominal segment occur in male adults but not in female ones [10, 14, 16]. The male-specific muscle, as well as other adult specific muscles, develops during metamorphosis [3, 6, 10]. Myoblasts which form adult abdominal muscles lie on branches of peripheral nerves and proliferate during larval and early pupal stages. They migrate out across the segment along the adult epidermis and fuse to make multinucleate myotubles. Examination of the formation processes of the male-specific muscle during metamorphosis suggested that the male-specific muscle would arise among the same pool of myoblasts to make other adult specific muscles in the 5th dorsal segment [10].

Differentiation of the male-specific muscle in males and the suppression of it in females is controlled by parts of sex-determining genes [19], although it is unknown that the action of the genes is autonomous in the muscle or non-autonomous. From the sex mosaic analyses, Lawrence and Johnston [16, 17] proposed that the formation is dependent on the innervation of the muscle by male-specific motoneurons but neither on a cell autonomous decision by sexual identity of the muscle fibers themselves nor on the sexual identity of the cuticular epidermal cells where the muscle inserts. In the present report, we examined directly the relationship between the sexual identity of myoblasts and the differentiation of the male-specific muscle by myoblast transplantation experiments. We used a transformant strain that contains a 79B actin promoter fused to the *Escherichia coli* β-galactosidase reporter gene, which is an useful differentiation maker of the male-specific muscle, because the 79B actin gene is expressed only in the male-specific muscle in the segment [5]. The transplantation experiments using this transformant showed that even female myoblasts, independently of the sexual identity, can participate in the formation of the male-specific muscle.

MATERIALS AND METHODS

Fly stocks

Flies were reared on cornmeal-yeast medium at 25°C under constant illumination. Males and females from the wild type strain *Canton-Special* (CS) were used for the analysis of normal development. The transformant line 72–3 which contains a 79B actin promoter fused to the *Escherichia coli* β-galactosidase reporter gene (*lacZ*) was used [5]. The resultant β-galactosidase is produced in muscles that activate the 79B actin gene [5]. For the staging of pupa, white pupae were collected and allowed to develop until desired stages at 25°C in a moisture chamber. Ages of these animals are given as hours after puparium formation (APF).

Immunohistochemistry

Mouse monoclonal antibody (Mab) 22C10 which stains the developing myoblasts and myotubles [10, 11] was used to follow the development of muscles during pupa. Immunohistochemical staining was done according to the methods by Usui and Kimura [20].

X-gal staining

X-gal staining for β-galactosidase activity of the reporter gene was performed using the method described by Hiromi *et al.* [12] with slight modifications [20].

Accepted January 31, 1994
Received November 8, 1993

[3] Present address: Laboratory of Neurobiology, Department of Molecular Biology, Universite Libre de Bruxelles, 67, rue des Chevaux, B-1640 Rhode-Saint-Genese, Bilgium

Transplantation experiments

Notum part of the wing disc contains many myoblasts (adepithelial cells) [2, 18]. The wing disc from the donor (72–3) strain at white pupal stage was dissected in phosphate buffered saline. The notum part of the disc was cut and transferred into the abdomen of the host (CS) strain at the same stage using a glass micropipette [7]. The myoblasts can be transplanted with the notum epithelial parts by this method [15]. The hosts are allowed to develop till pharate adult or adult stage. We could find the transplanted disc which had developed into adult tissue secreting cuitcle in the abdomen. The abdomen of the host flies was dissected and stained with X-gal, as described above.

RESULTS AND DISCUSSION

Figure 1 shows a comparison of adult musculature of dorsal abdomen between male and female. There are two types of muscles common to both sexes at least from the first to the 5th segments. One is dorsal oblique muscles of larval origin which persist throughout the metamorphosis. These muscles are temporally used for eclosion behavior and degenerate completely after eclosion [14]. The other is small dorsal longitudinal muscles which are newly formed during metamorphosis and continue to exist after eclosion. The male-specific muscle, a dorsal longitudinal muscle attaching the 5th abdominal tergite, can be distinguished from the others easily by its insertional position and length (Fig. 1).

Immunostaining with Mab22C10 enables us to follow the development of the male-specific muscle during the metamorphosis (Fig. 2). At 24 hr APF, the myoblasts which form adult abdominal muscles have been migrating out across the segment along the developing adult epidermis (Fig. 2A). Then the myoblasts fused to make multinucleate muscle precursors and at 32 hr APF they had aligned on the adult epidermis (Fig. 2B). At this stage, the male-specific muscle could not be recognized. At 36 hr APF, the myotubles had

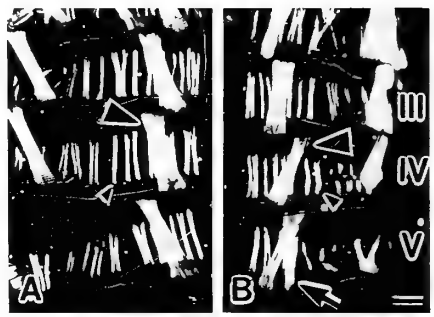

FIG. 1. Polarizing-light micrographs of adult musculature of the dorsal abdomen in female (A, left half) and male (B, right half) just after eclosion (CS strain). Males and females have muscles common to both sexes, larval persisting oblique muscles (large arrowheads) and dorsal longitudinal muscles (small arrowheads). A pair of extra thick longitudinal muscles (arrow) in the fifth abdominal segment occur only in male. The roman numerals in B indicate the abdominal segment. Bar in B, 100μm.

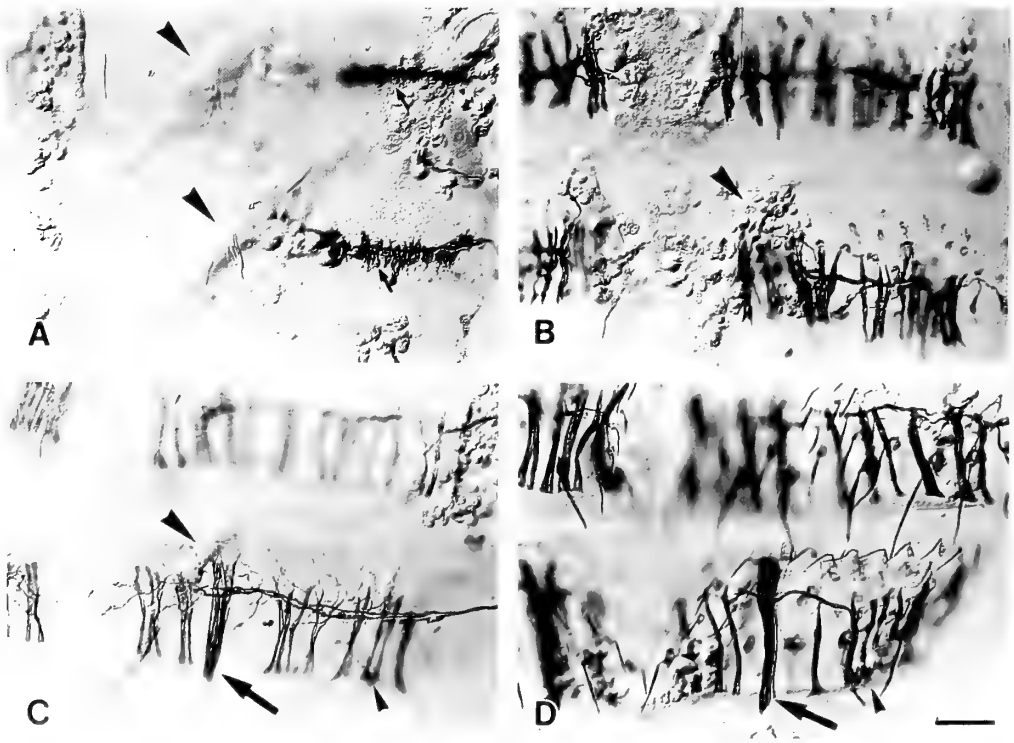

FIG. 2. Micrographs of the right half of the 4th and 5th segment of dorsal abdomen, showing adult muscle development during metamorphosis. Preparations from males of CS strain were stained immunohistochemically with Mab22C10. A, 24 h APF. B, 32 h APF. C, 36 h APF. D, 48 h APF. Large arrowheads, small arrowheads, large arrows and small arrows indicate larval persisting oblique muscles, dorsal longitudinal muscles, the male-specific muscles and myoblasts, respecrtively. Bar in D, 100μm.

formed and the male-specific muscle can be distinguished from the other small dorsal longitudinal muscles by its insertion position (Fig. 2C). At 48 hr, the muscles grow more (Fig. 2D).

The growth of the male-specific muscle was followed by the production of contractile protein, actin. Six actin genes are known in *Drosophila*, which show the tissue-specific and stage-specific expression patterns [9]. In the male-specific muscle, it is ascertained that the 79B actin gene is expressed at adult stage [5]. We examined the termporal pattern of the expression of the 79B actin gene (Fig. 3), using the transformant line 72–3 which contains a 79B actin promoter fused to *Escherichia coli* β-galactosidase reporter gene [5]. Till 50 hr APF, no expression of the reporter gene was observed in the male-specific muscle (Fig. 3A). The expression was observed at 54 hr APF (Fig. 3B) and became stronger as developed (Fig. 3C and D).

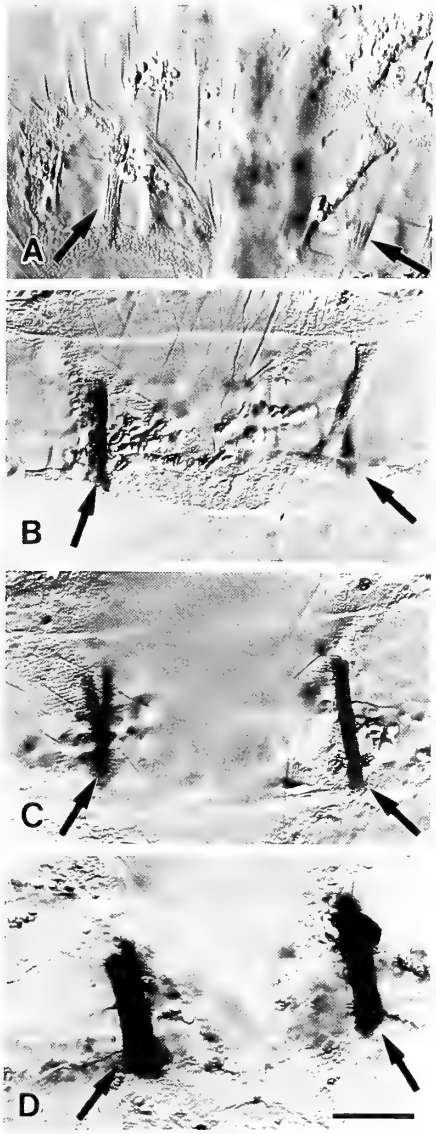

FIG. 3. Specific expression of the 79B actin gene in the male-specific muscle (arrows) during metamorphosis of the transformant pupae. The preparations were stained for β-galactosidase activity with X-gal. At 50 h APF, the reporter gene is not expressed (A). The expression is seen at 54 hr APF (B). Thereafter, the expression became stronger as developed (C, 60 h APF and D, 72 h APF). Bar in D, 100μm.

To understand how far the sexual identity of the myoblasts is involved in the formation of the male-specific muscle, we examined whether female myoblasts can participate in the formation of the male-specific muscle or not (Fig. 4). Firstly, myoblasts in the wing disc were transplanted from the male donor (72–3) into the abdomen of the male host (CS) of the same age. After the hosts were allowed to develop till pharate adult or adult stage, we examined whether the male-specific muscle of the host expressed the reporter gene derived from the male donor nucleus. Out of 9 transplantations, 6 hosts expressed the β-galactosidase in the male-specific muscle (Fig. 4B), indicating that the myoblasts in the wing disc can participate in the formation of the male-specific muscle. However, when myoblast in the wing disc were

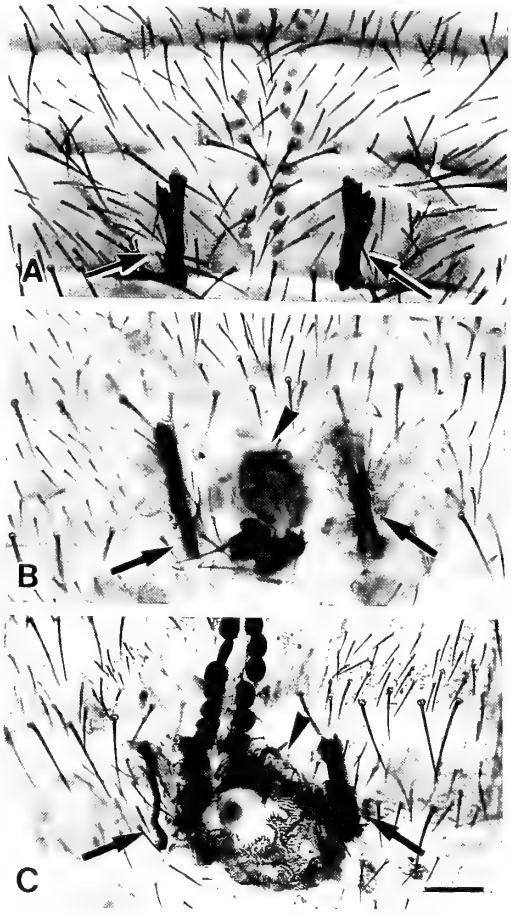

FIG. 4. Expression of the reporter gene transplanted from a transformant donor into a wild type host. The *lacZ* reporter gene expressed in the male-specific muscle of the donor male (A: control). The male-specific muscle of a male host expressed the reporter gene derived from transplanted myoblasts of either male transformant (B) or female one (C). Arrows show the male-specific muscle which expresses the *lacZ* reporter gene. Arrowheads in B and C indicate the transplanted disc which had developed into adult tissue secreting cuticle in the abdomen. Bar in C, 100μm.

transplanted from the male donor (72–3) into the abdomen of the female host (CS), the extra male-specific muscle nor the expression of the reporter gene were not seen in six female transplanted hosts. This indicates that the transplantation surgery does not affect the formation of the male-specific muscle. Next, we transplanted the myoblasts from 72–3 female into the CS male pupa. Out of 5, three hosts showed the expression of the reporter gene from female myoblasts in the male-specific muscle (Fig. 4C). This result indicates that even the female myoblasts can fuse into the developing male-specific muscle and that the expression of the actin gene derived from the female nucleus can be activated. The expression of the reporter gene derived from female myoblasts would be induced by some regulatory factors from host's male nuclei in the syncytium.

In *Drosophila*, determination of developmental fate in sexual dimorphic tissues is regulated through the activity of a cascade of several sex-determining genes [1]. It is shown that the differentiation of the male-specific muscle in males and the suppression of it in females are controlled by parts of sex-determining genes [19]. For examples, female flies mutant for allele of *Sex-lethal* or null alleles of *transformer* or *transformer-2* are converted into phenotypic males that formed the male-specific muscle [19]. Thus, wild-type products of the above genes act to prevent the differentiation of the male-specific muscle in female flies. Our results indicated that the cell autonomous decision of sexual identity in myoblasts themselves is not involved in the fusion process of myoblasts in the formation of the male-specific muscle. From the sex mosaic analyses, Lawrence and Johnston [16, 17] proposed that the formation of the male-specific muscle depends on the innervation of the muscle by male-specific motoneurons but neither on a cell autonomous decision by sexual identity of the muscles themselves nor on the sexual identity of the cuticular epidermal cells at the cuticle where the male-specific muscle inserts. In the embryo of *Drosophila*, the myogenesis occurs before the completion of the innervation by motoneurons [2, 13], indicating that the myogenesis itself occurs without innervation by neurons. Recently, it is shown that the innervation by motoneurons is prerequisite for the later differentiation of the muscles, for example localization of the transmitter receptor [4]. However, in the formation of adult muscles during metamorphosis, it is unknown how the neurons are involved in the processes of development of the muscles.

Our results of transplantation experiments also showed that the myoblasts in the wing disc, which normally form the muscles in the thorax [8], can participate in the formation of unusual muscles at the different position, the male-specific muscle in the abdomen. Similar results were also obtained by Lawrence and Brower [15]. These facts indicated that the specificity of muscles had not been committed in the myoblasts of the wing disc at least by white pupal stage. Commitment of the specificity of muscles may occur fairly late, around the time of innervation by motoneurons.

The male-specific muscle is an excellent material to investigate the relationship of innervating neurons and muscle differentiation. The identification of the male-specific motoneuron would help to reveal the mechanism of determination and differentiation of the sexually dimorphic musculature.

ACKNOWLEDGMENTS

We would like to thank anonymous reviewers, whose comments were very helpful to improve the manuscript. The *Drosophila* stock of the *actin-lacZ* transformant (72–3) was generously provided by Dr. S. L. Tobin. We wish to thank Drs. S. C. Fujita and S. Benzer for providing monoclonal antibody, Mab22C10. This work was supported in part by a Grant-in-Aid for Scientific Research from the Ministry of Education, Science and Culture, Japan.

REFERENCES

1 Baker BS (1989) Sex in flies: the splice of life. Nature 340: 521–524

2 Bate M (1990) The embryonic development of larval muscles in *Drosophila*. Development 110: 791–804

3 Bate M, Rushton E, Currie DA (1991) Cells with persistent *twist* expression are the embryonic precursors of adult muscles in *Drosophila*. Development 113: 79–89

4 Broadie K, Bate M (1993) Innervation directs receptor synthesis and localization in *Drosophila* embryo synaptogenesis. Nature 361: 350–353

5 Courchesne-Smith CL, Tobin SL (1989) Tissue-specific expression of the 79B actin gene during *Drosophila* devleopment. Dev. Biol 133: 313–321

6 Currie DA, Bate M (1991) The development of adult abdominal muscles in *Drosophila*: myoblasts express *twist* and are associated with nerves. Development 113: 91–102

7 Ephrussi B, Beadle GW (1936) A technique of transplantation for *Drosophila*. Am Nat 70: 218–225

8 Fernandes J, Bate M, Vijayraghavan K (1991) Development of the indirect flight muscles of *Drosophila*. Development 113: 67–77

9 Fyrberg EA, Mahaffey JW, Bond BJ, Davidson N (1983) Transcripts of the six *Drosophila* actin genes accumulate in a stage- and tissue-specific manner. Cell 33: 115–123

10 Gailey DA, Taylor BJ, Hall JC (1991) Elements of the *fruitless* locus regulate development of the muscle of Lawrence, a male-specific structure in the abdomen of *Drosophila melanogaster* adults. Development 113: 879–890

11 Hartenstein V, Posakony JW (1989) Development of adult sensilla on the wing and notum of *Drosophila*. Development 107: 389–405

12 Hiromi Y, Kuroiwa A, Gehring W (1985) Control elements of the *Drosophila* segmentation gene *fushi tarazu*. Cell 43: 603–613

13 Johansen J, Halpern ME, Keshishian H (1989) Axonal guidance and the development of muscle fiber-specific innervation in *Drosophila* embryos. J. Neurosci 9: 4318–4332

14 Kimura K-I, Truman JW (1990) Postmetamorphic cell death in the nervous and muscular systems of *Drosophila melanogaster*. J Neurosci 10: 403–411

15 Lawrence PA, Brower DL (1982) Myoblasts from *Drosophila* wing disks can contribute to developing muscles throughout the fly. Nature 295: 55–57

16 Lawrence PA, Johnston P (1984) The genetic specification of pattern in a *Drosophila* muscle. Cell 36: 775–782

17 Lawrence PA, Johnston P (1986) The muscle pattern of a segment of *Drosophila* may be determined by neurons and not by contributing myoblasts. Cell 45: 505–513

18 Poodry CA (1980) Imaginal discs: Morphology and development. In "The genetics and biology of *Drosophila* Vol 2d" Ed by M Ashburner and TRF Wright, Academic Press, New York, pp 407–441

19 Taylor BJ (1992) Differentiation of a male-specific muscle in *Drosophila melanogaster* does not require the sex-determining genes *doublesex* or *intersex*. Genetics 132: 179–191

20 Usui K, Kimura K-I (1992) Sensory mother cells are selected from among mitotically quiescent cluster of cells in the wing disc of *Drosophila*. Development 116: 601–610

ZOOLOGICAL SCIENCE 11: 253–260 (1994)

Induction of Metamorphosis in the Sea Urchin, *Pseudocentrotus depressus*, using L-Glutamine

IKUKO YAZAKI and HIROKI HARASHIMA

Department of Biology, Faculty of Science, Tokyo Metropolitan University
Minamiohsawa 1-1, Hachiohji Tokyo 192-03, Japan

ABSTRACT—Larvae of the sea urchin, *Pseudocentrotus depressus*, were induced to metamorphose using 10^{-6}–10^{-4} M L-glutamine. After being subjected to 6×10^{-5} M glutamine, the larvae ceased swimming, began to retract their arms, extruded primary podia through an opening of the larva at a vestibule of echinus rudiment (ER) and then everted the ER, requiring 1–9 hr, 7–11 hr, 7–38 hr and 12–48 hr (from the time of the recognition of the first larva to the time of the maximum larvae changes), respectively. The effective times needed in the glutamine-treatment were 2 hr for induction of the cessation of larval swimming and the start of arm-retraction, and 4–8 hr to induce the ER-eversion. There was no correlation between the extruding of primary podia and the amount of time needed for the glutamine-treatment. From the difference seen in the effective time of glutamine-treatment, the early changes in metamorphosis; cessation of swimming and start of arm-retraction, are not autonomously linked to the later change; ER-eversion. L-glutamic acid and γ-aminobutyric acid (GABA) did not induce metamorphosis. 10^{-7} M GABA provoked a rapid cramp in the arms and a spreading of spines, and the larva seemed to undergo ER-eversion, but within a few hours they returned to their original larval shape. Thus eversion-like changes induced by GABA may not reach a true ER-eversion due to an absence of process or processes which were induced by the 4–8 hr treatment of glutamine over a long period of time (12–48 hr).

INTRODUCTION

Larvae of marine invertebrates undergo metamorphosis in response to environmental cues [6]. Sands and sediments in the adult habitat cause metamorphosis in larvae of the sand dollar [8] and *Nassarium* [18]. Bacteria and algae substrata are also effective for inducing metamorphosis. In aplysiids and spirorbis (serpulidae), the larvae of each aplysiid or spirorbis species selects a substratum containing their favorite algae in which to settle [7, 20]. In echinoderm, bacterial and algal films, which are prepared by soaking the glass or plastic plates in natural sea water for several days, are effective in inducing metamorphosis of sea star larvae [12, 19] and sea urchin larvae [9, 15, 23]. However, the active factor of these natural cues has been rarely identified. For example, free fatty acid components were extracted from red algae as a chemical inducer of larval settlement and metamorphosis of the sea urchin, *Pseudocentrotus depressus* and *Anthocidaris crassispina* [11], and a pheromonal substance, 980 Da-peptide, was isolated as an active factor in the metamorphosis in the sands in the adult habitat of *Dendraster excentricus* [3].

γ-Aminobutyric acid (GABA), which is known as a neurotransmitter in many species, induced abalone larvae to settle and to undergo metamorphosis [13]. In sea urchins, Burke [2] proposed a neural control of metamorphosis according to his electrical and obsolatory experiments that the larvae of *D. excentricus* were induced to metamorphose by electrical stimulation of their two nerve centers, apical neuropile and oral ganglions, although he noted that GABA was ineffective [2]. In *Strongylocentrotus intermedius* and *S.milabiris*, L-glutamine, which is known as a precursor of glutamic acid and GABA in the central nervous system of mammals, induced metamorphosis in 100% and 50% of the larvae, respectively [16].

In the present study, the effects of L-glutamine on the metamorphosis of *P. depressus* larvae were examined, and the mechanisms of the glutamine-inducing metamorphosis are discussed.

MATERIALS AND METHODS

Larvae which derived from one pair of a male and a female of *Pseudocentrotus depressus* were reared by the method of Noguchi [17] with slight modifications. The cultures in five 3–l beakers were maintained at $19^{\circ}\pm2^{\circ}$C which were stirred with a paddle attached to a 60 rpm motor. At the onset of feeding (3 days after fertilization), there were 25,000 plutei in 2.5 litres of paper-filtered sea water. Two or three ml of *Chaetoceros gracilis* ($3–5\times10^{6}$/ml) were added to each culture every 1 or 2 days [10], and two-thirds of the culture water was changed twice a week. The larval density was initially 10/ml but was diluted to 1/ml at the stage of an 8-armed pluteus. Various developmental stages of larvae were found in culture beakers. Competent larvae to metamorphosis were obtained over a period of one month, beginning from the 40th day after insemination.

Larvae with fully developed ER were selected and transferred into 0.22 μm Millipore-filtered seawater (MFSW) in a 100-ml beaker. To remove microorganisms taken into the larvae as food, the larvae were then kept for 1 day in MFSW. After rinsing twice in MFSW, every 5–10 larvae were randomly apportioned into each well of 12-well plastic plates, which were filled with either 2.5 ml MFSW (control) or with the same volume of various concentrations of L-glutamine- or other substances dissolved in MFSW (adjusted with NaOH at pH 7.8–8.0). Larvae in the wells were retransferred to a well filled with the same medium to avoid diluting the experimental

Accepted February 15, 1994
Received October 29, 1994

medium. Usually, L-glutamine treatment did not exceed 24 hr. If the observations were prolonged, the culture medium (MFSW) was changed every 2 days.

RESULTS

Effective concentrations of L-glutamine needed to induce metamorphosis

Metamorphosis of the echinopluteus occurs after settlement, and includes an eversion of the adult rudiment (echinus rudiment: ER) which develop within the larva, resorption of the larval body into the juvenile, and the subsequent differentiation of the adult form [5]. Larvae used for the present experiments were swimming and had the fully grown adult rudiment whose primary podia were moving within the larva but not extruding out the larval body (Fig. 1A). When the spines and the primary podia of ER were exposed outside the larva by eversion of the ER, the larva was considered to be metamorphosed (Fig. 1B). Larval arms began to retract prior to the eversion of the ER, but had not completely retracted by the time of ER eversion. Parts of the larval arms and epaulets were retained on the newly metamorphosed juvenile (Fig. 1B), and remained for an additional 1 or 2 days after eversion of the ER.

Larvae were treated with various concentrations of L-glutamine solutions from 3×10^{-4} to 6×10^{-6} M for 24 hr, washed with MFSW and then maintained in MFSW (Fig. 2). Out of ten larvae in each concentration, larvae rarely metamorphosed after just 24 hr (the end of glutamine-treatment). Most larvae which were treated with glutamine at concentrations of 3×10^{-4} to 3×10^{-5} M were found to metamorphose after 48 hr. At a concentration of 6×10^{-6} M L-glutamine, no metamorphosis had occurred by 48 hr, and only one larva had metamorphosed at 72 hr (Fig. 2). From these results, 6×10^{-5} M L-glutamine was used as a conventional concentration for induction of metamorphosis of *P. depressus* with the resulting metamorphosis usually observed after 48 hr in the following experiments.

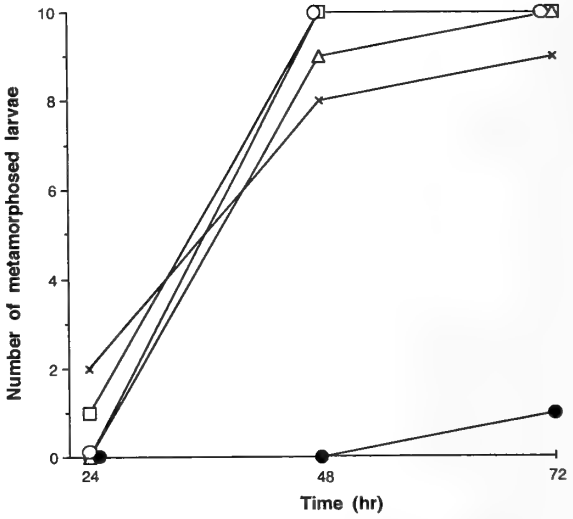

FIG. 2. Effects of L-glutamine at various concentrations. Groups of ten larvae were treated with L-glutamine in MFSW for 24 hr with concentrations of either 6×10^{-6} (●), 3×10^{-5} (△), 6×10^{-5} (×), 1.2×10^{-4} (□) or 3×10^{-4} M (○). At the beginning of the experiments, all larvae had not metamorphosed. $1.2\times$ and 3×10^{-4} M glutamine induced metamorphosis in all ten larvae after 48 hr. $3\times$ and 6×10^{-5} M glutamine induced metamorphosis in 8 and 9 larvae, but 6×10^{-8} M glutamine did not induce any metamorphosis after 48 hr, with only one larva undergoing metamorphosis after 72 hr.

Changes in larvae induced using L-glutamine treatment

To analyse the process of metamorphosis, the behaviour and form of larvae were repeatedly checked from the beginning of the glutamine treatment (Fig. 3). Fifty-one larvae were transferred into five wells filled with 6×10^{-5} M gluta-

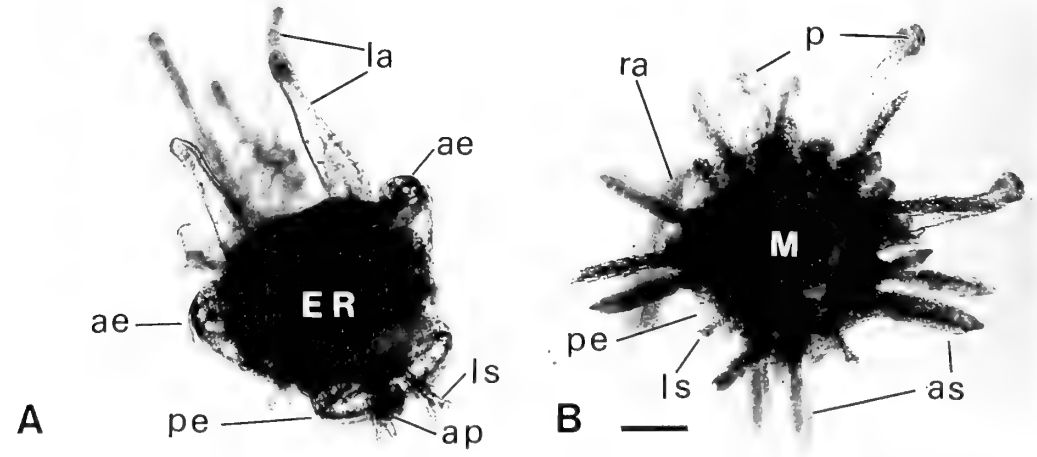

FIG. 1. A competent larva and a juvenile of *P. depressus* which was induced to metamorphose using L-glutamine. A: An 8-armed pluteus larva competent to metamorphose. The larva is swimming around. Neither the spines nor the tube feet (the primary podia) of the echinus rudiment were extruded. B: A juvenile which was metamorphosed after treatment with 6×10^{-5} M L-glutamine for 24 hr, and photographed from beneath with an inverted microscope. la, larval arms; ae, anterior epaulettes; pe, posterior epaulettes; ap, apical pedicellaria; as, adult spine; ls, larval spine; p, primary podia; ra, retracting arm (out of focus); ER, echinus rudiment; M, mouth. Bar = 100 μm.

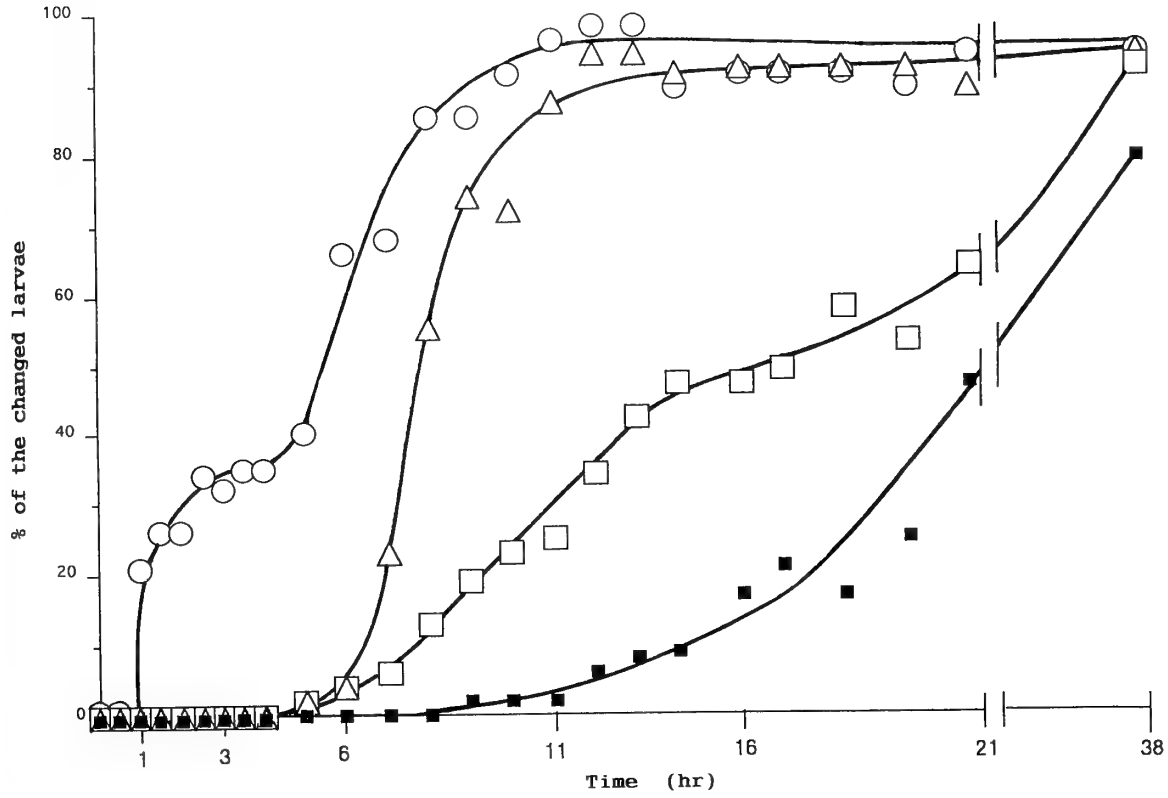

FIG. 3. Time course of larval changes induced by treatment with L-glutamine. Fifty-one competent larvae were kept in 6×10^{-5} M L-glutamine containing MFSW for 21 hr and then tranferred into MFSW. Observations were carried out repeatedly on four changes which occurred in each larvae; 1) cessation of swimming (○), 2) retraction of larval arms (△), 3) extrusion of primary podia through an opening of larva at the vestibule of ER (□), and 4) eversion of ER (■). The echinus rudiments began to evert since each larva ceased swimming and the retraction of arms had occurred. The primary podia seem to be extruded several hours before the ER-eversion.

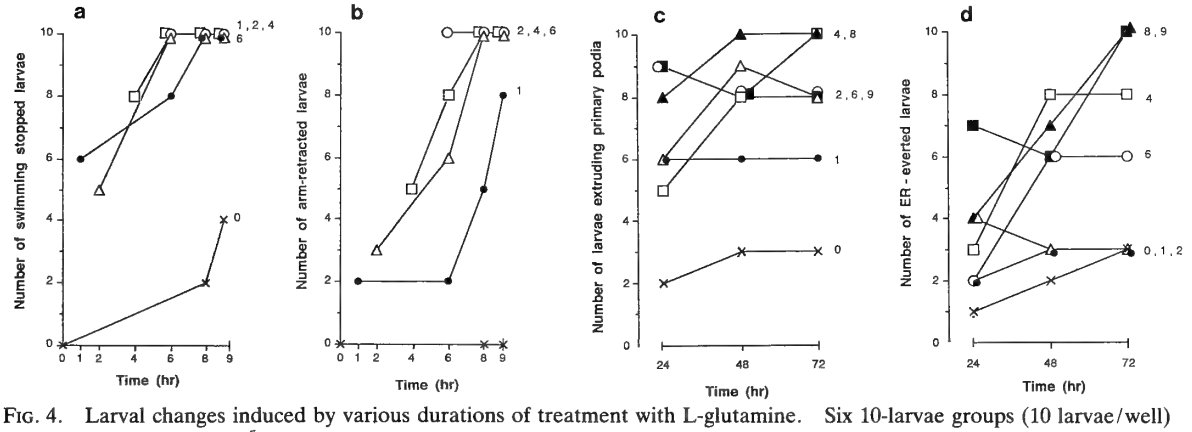

FIG. 4. Larval changes induced by various durations of treatment with L-glutamine. Six 10-larvae groups (10 larvae/well) were treated with 10^{-5} M L-glutamine in MFSW and then transferred into glutamine-free MFSW after 1 hr (●), 2 hr (△), 4 hr (□), 6 hr (○), 8 hr (▲), and 9 hr (■). Control larvae (×) were reared in glutamine-free MFSW. The larval changes of each group were followed for up to 72 hr and are shown in a) cessation of swimming, b) retraction of arms, c) extrusion of primary podia and d) eversion of the echinus rudiment (ER). a) and b) are shown from zero to nine hours, and c) and d) are from 24 to 72 hr. Numerals to the right of figures indicate the elapsed time of treatment with glutamine. Cessation of larval swimming (a) and the start of arm retraction (b) were induced by 2-hr treatment, although arm retraction progressed with longer durations of treatment. Extrusion of the primary podia (c) seemed to be accelerated by treatment with L-glutamine relative to the controls, but does not have any correlation with the treatment time. To evert the ER (d), larvae must be treated with glutamine for 4–8 hr.

mine-MFSW and kept there for 21 hr. All of the larvae examined were swimming around after the first 30 min. After one hour, 20% of the larvae had stopped swimming and almost all larvae became immobile between 9–10 hr after immersion in glutamine-MFSW. The number of larvae which retracted larval arms and extruded the primary podia began to increase after 7 hr. The arm-retractions were observed in all larvae after 11 hr, while the larvae extruding the primary podia slowly increased. Eversions of ER began after 12 hr. By the end of the treatment (21 hr), ER everted in 50% of larvae examined, and after 38 hr (17 hr after the 21 hr-glutamine treatment), the ER had everted in 88% of the larvae.

Times required for induction of metamorphsis using L-glutamine

Seven 10-larvae groups (10 larvae/well) were prepared. Six groups were placed in wells with 6×10^{-5} M glutamine-MFSW while one group was maintained in MFSW alone as a control. Each group of larvae in glutamine-MFSW was transferred into MFSW at an interval of 1 or 2 hr from the beginning up to 9 hours later (Fig. 4). The movement of larval swimming was affected by very short exposure to glutamine. After a 6-hr treatment, all larvae had ceased swimming (Fig. 4a). Only a 2-hr glutamine treatment made all the larvae completely stop swimming after 6 hr. The effect of a 1-hr treatment was a little unstable (Fig. 4a).

Arms had also begun to retract in all larvae examined after a 6-hr treatment. The start of arm-retraction was much more delayed when the duration of glutamine treatment was shorter, and the progression of arm-retraction was proportional to the duration of glutamine treatment (Fig. 4b). One-hour treatment could induce the start of arm-retraction in all larvae after 24 hr (data not shown), and the arms remained a little shortened.

As the extrusion of the primary podia and the ER eversion were not recognized up to 9 hours, the results achieved after 24 hr are given in Figs. 4c and 4d. The extrusion of podia was also accelerated by glutamine treatment. At 24 hr, in each of the experimental groups (even in the larval group given only a 1-hr treatment), more podia were extruded than in the control group (Fig. 4c). However, there seemed to be no close relationship between the number of larvae whose primary podia had extruded and the duration of glutamine treatment (Fig. 4c).

Eversion of ER at a greater rate than controls could not be induced by either a 1- or 2-hr glutamine treatment. At 24 hr, out of 10 larvae which were treated with glutamine for 9 hr, seven had everted ERs, but in the larvae treated for 8 hr or less, the number of ER everted remained low. At 48 hr, larvae treated for more than 4 hr induced ER-eversion in over 60%, and at 72 hr, 100% ER eversion was recorded in larvae given 8 or 9 hr of treatment (Fig. 4d).

Effects of L-glutamic acid and GABA on metamorphosis

L-glutamic acid, which was deaminated from L-glutamine, was examined at the same concentration (6×10^{-5} M) as L-glutamine for 18–22 hr (Fig. 5). In experiments involving four trials, 69 larvae were treated with glutamic acid, 108 with glutamine and 78 with neither (controls). Observations were carried out for 7 days, although on the 6th and 7th days about half the larvae examined were observed as follows. Among the glutamic acid-treated larvae, only one larva was found to have metamorphosed by the 4th day, after which no more larvae underwent metamorphosis. By contrast, most of the 108 larvae treated with glutamine had metamorphosed by the 2nd day (Fig. 5). Seven larvae, which had metamorphosed by the 4th day, had retracted almost all of their arms to look like black balls and all died. Glutamic acid induced the arm-retractions in 80% of larvae within 2 days (Fig. 6b), but their arms were shortened only slightly. Glutamic acid did not interfere with the larval movement of swimming (Fig. 6a) and the extruding of the primary podia (Fig. 6c).

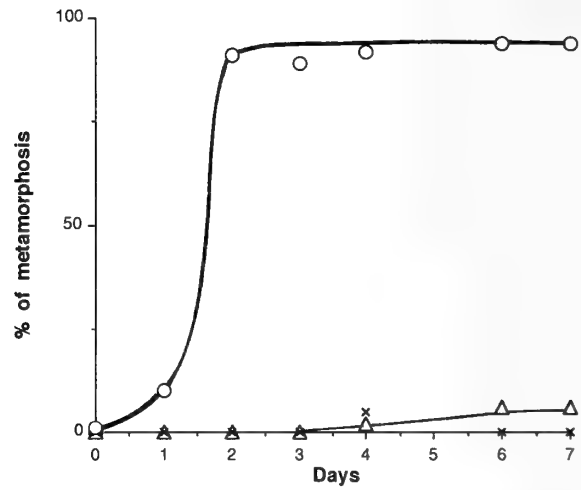

FIG. 5. Effect of L-glutamic acid on metamorphosis compared with that of L-glutamine. Four experiments with different treatment times (18 hr, 20 hr and two experiments with 22-hr treatment) are combined. Observations were continued for 4 days (18-, 20- and 22-hr treatments) and for 7 days (22-hr treatment). The number of experiments totalled 67 for glutamic acid (△), 108 for glutamine (○) and 78 larvae for MFSW (controls) (×). In contrast to the high percentage of metamorphosis-induction using glutamine, glutamic acid induce almost no metamorphosis (there was only one metamorphosed larva among those treated with glutamic acid after 4 days, after which no further metamorphosis occurred).

GABA (γ-aminobutyric acid), a substance which is formed by the decarboxylation of glutamic acid, was applied on each group of 10 competent larvae in concentrations of $5\times$ and 1×10^{-5} M for 24 hr (Exp. 1 in Table 1) or for 8.5 hr (Exp. 2), and at lower concentrations of 1×10^{-6} M or $\times 10^{-7}$ M for 18 hr (Exp. 3) compared with glutamine. When larvae were treated with higher concentrations of GABA for

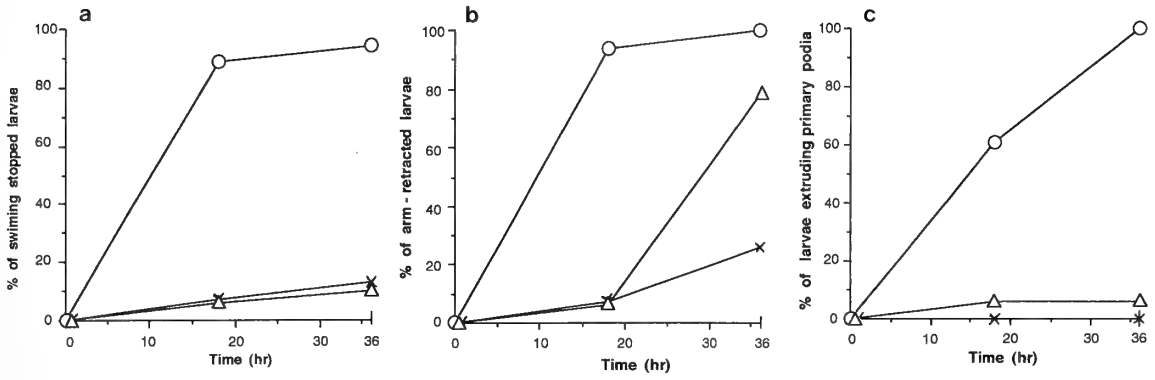

FIG. 6. Changes in larvae treated with L-glutamic acid. Eighteen larvae were treated with 6×10^{-5} M L-glutamic acid (△) for 18 hr. To confirm the larval competency to metamorphose, the same concentration of L-glutamine (○) was applied for the same duration. 16 control larvae (×) were kept in MFSW. L-glutamic acid did not effect cessation of swimming and the extrusion of primary podia, although a slight retraction of arms was observed in 80% of the larvae after 36 hr.

TABLE 1. Effect of various concentration of GABA and various durations of treatment with GABA

Every 10-larvae treated with	Concentrations (M)	Number of metamorphosed larvae		
		at 24 hr	48 hr	72 hr
1) 24-hr treatment				
None	—	0	0	—
L-glutamine	3×10^{-4}	7	8	—
	6×10^{-5}	1	0	—
GABA	5×10^{-5}	5	4*	—
	1×10^{-5}	6	5*	—
2) 8.5-hr treatment				
None	—	0	0	1
L-glutamine	3×10^{-4}	6	10	10
	6×10^{-5}	3	8	9
GABA	5×10^{-5}	0	0	2
	1×10^{-5}	1	1	2
3) 18-hr treatment				
None	—	0	0	0
L-glutamine	6×10^{-6}	1	6	7
GABA	1×10^{-6}	1	3	0
	1×10^{-7}	1	0	0

All larvae had not begun metamorphosis at the start of glutamine- or GABA-treatment. * The echinus rudiments (ER) were exposed but the larvae was dead. In the Exp. 1), the number of metamorphosed larvae (—) were not counted after 72 hr.

24 hr, about half the larvae exposed their spines as the echinus rudiments everted, and they had all died after 48 hr (Exp. 1 in Table 1). As shown in Exp. 2 in Table 1, after reducing the duration of treatment from 24 hr to 8.5 hr, most of the larvae treated with GABA had not exposed their spines at 48 hr, although at 72 hr, 20% had exposed their adult spines at either concentration of GABA. These ER-everted-like larvae seemed to be alive because ciliary movements at the epaulets were observable, but they did not extend any primary podia, and most of their larval arms had not been retracted (Fig. 7). When the concentrations of GABA were reduced to 10^{-6} M or 10^{-7} M, spines of ER spread out and the ER seemed to be everted in 10% (10^{-7} M) at 24 hr and 30% (10^{-6} M) at 48 hr (Exp. 3 in Table 1). However, these spread spines closed again by the next day. In each of the experimental series, a high ratio of glutamine-treated larvae metamorphosed whereas almost none of the larvae cultured in MFSW (non-treated larvae) metamorphosed.

Figure 8 shows the larval changes in the extrusion of the primary podia and the eversion of ER in Exp. 3 presented in Table 1. Fifteen min after being transferred into 10^{-7} M GABA, 80% of the larvae had cramped their larval arms and spread out the spines of the ER. By the end of the next 15

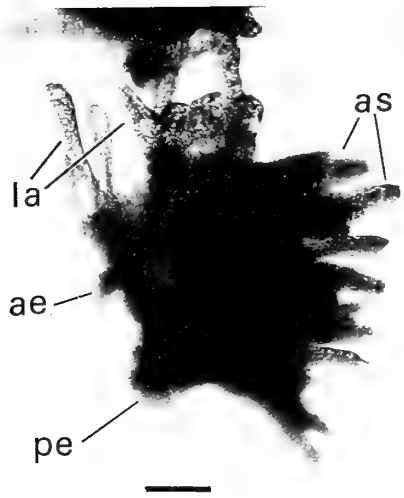

FIG. 7. An ER-exposed larva after treatment with GABA. Competent larvae were treated with 10^{-5} M GABA for 8.5 hr and observed after 48 hr. la, larval arms; ae, anterior epaulet; pe, posterior epaulet; as, adult spines. Spines in ER are exposed but no primary podium is observed. Larval arms remain unretracted. Bar=100 μm.

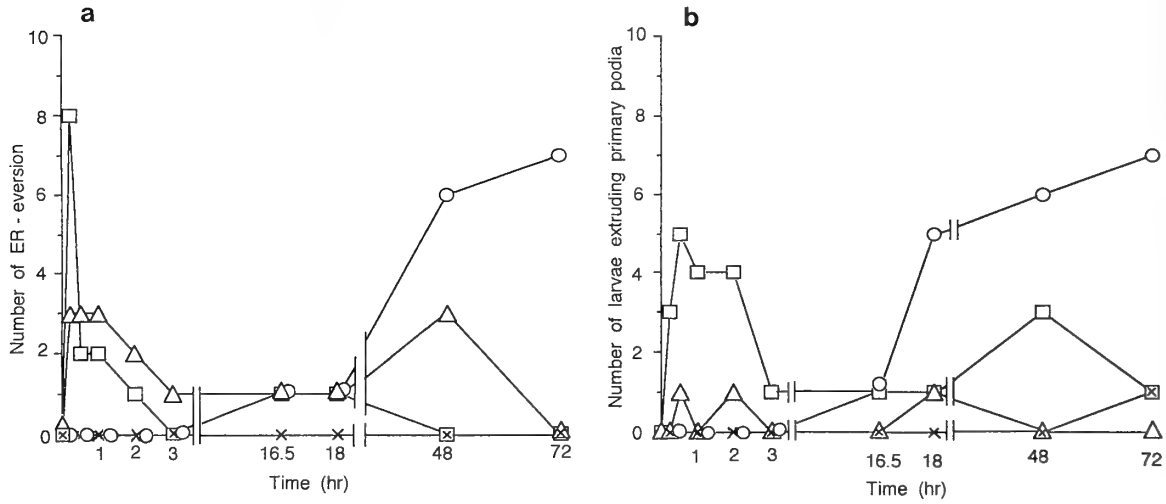

FIG. 8. Effects of GABA on extruding of primary podia and eversion of the echinus rudiment. Each 10-larvae group was treated with 10^{-6} M (△), 10^{-7} M GABA (□) and 6×10^{-7} M L-glutamine (○) for 18 hr. A control group was kept in MFSW alone (×). 15 min from beginning of treatments, GABA-treated larvae everted the echinus rudiments (a) and extruded the primary podia (b), but later returned to their original larval form.

min, however, the number of cramped larvae decreased to two (Fig. 8a). The cramp of larvae occurred instantly after exposure to GABA solution, and then resolved within 1 hour followed by gradual closure of the spine. The primary podia were also retracted later, although initially extended in about half the larvae at the lower concentration (10^{-7} M) of GABA (Fig. 8b). At 10^{-6} M GABA, almost no larvae extended podia (Fig. 8b). The higher concentration of GABA may be toxic. After all, GABA induced rapid changes in the larval arms and spines of ER and did not induce metamorphosis or eversion of the ER, as glutamine did (Figs. 8a, 8b).

DISCUSSION

During the metamorphosis of sea urchin larvae, an eversion of the echinus rudiment (ER), histolysis and resorption of larval body and growth and differentiation of adult tissues occurred. The time courses of these developmental phenomena differ according to each species.

In *Lytechinus pictus* and *D. excentricus*, the echinus rudiment is everted 3–5 min after receiving natural cues; the bacterial film and the sands in the adult habitat, and the larval body subsequently collapses after an additiononal 15–30 min [5, 9]. After these initial phases of metamorphosis, the juvenile undergoes a period of extensive reorganization and differentiation. In other sea urchin species, we do not have detailed information about the time process of metamorphosis after exposure to natural cues. Most larvae of six species of sea urchins (*P. depressus* and others) metamorphosed within 3 days after the addition of bacterial films into culture vessels [23].

In the present study, metamorphosis of *P. depressus*

larvae was induced by L-glutamine. The glutamine-induced metamorphosis began with cessation of larval swimming within 1 hour, followed by the retraction of larval arms at 6–9 hr, and finally, eversion of the echinus rudiment at 12–38 hr (Fig. 3). When larvae of *Hemicentrotus pulcherrimus* were treated with L-glutamine, the time processes were similar to *P. depressus* in the present study (Yazaki, unpublished data). The early changes of metamorphosis; the cessation of swimming and the retraction of arms, seems not to be linked to the eversion of the echinus rudiment, because, while a 2-hr treatment with glutamine was enough to induce the cessation of swimming and the retraction of larval arms (Figs. 4a, 4b), a 4- to 8-hr treatment was necessary to induce ER-eversion (Fig. 4d).

Cameron and Hinegardener [4] and Strathman [19] have suggested that the sucker tips of the primary podia are the location of sensory organs that are responsible for the perception of the substratum-associated cues (rocks and shells from adult habitat) to metamorphose. Sensory cells of primary podia in *D. excentricus* were localized to the podial sucker by Burke [1]. On the basis of the experiments using ablation and electrical stimulation, he further proposed that the apical neuropile and the oral ganglion of competent larvae are nerve centers that both mediate between the perception of natural cues and control the initiation of metamorphosis [2].

In the present experiment, the primary podia extruded in most larvae 6–7 hours after the start of glutamine treatment (Fig. 3), with the podial extrusions being independent of the elapsed treatment time with glutamine. Even if the treatment time was 1 hr, the primary podia were extruded, while a 4- to 8-hr treatment with glutamine was neccessary for inducing ER-eversion (Fig. 4d). Accordingly, it is apparent that glutamine induced the extrusion of primary podia, and that the podia were always extruded when the ER was everted, but the ER did not necessarily evert in larvae whose podia had extruded.

In the central nervous system of mammals, it is known that glutamine is metabolized to glutamic acid by deamination, and then GABA is formed by decarboxylation of glutamic acid. In *P. depressus*, glutamic acid did not induce metamorphosis, and GABA induced a rapid and transient cramp of larval arms and spread out the spines of adult rudiment, but did not go on to induce eversion of the ER of the larvae.

In abalone larvae, GABA induces settlement and complete metamorphosis, but L-glutamine is absolutely inert [13]. At an optimal GABA concentration (10^{-6} M), settlement is rapidly induced, followed by a loss of the ciliated columnar epithelial cells of the velum within 15–20 hr and formation of a new adult shell ca. 40 hr after the addition of GABA. In the induction of the behavioral and developmental metamorphosis of abalone by GABA, cyclic AMP, calcium, and a glycopeptide secretion from the cephalic sensory complex are thought to mediate transduction of the GABA signal in the control of behavioral and morphogenic changes [14]. GABA at high concentrations over 10^{-5} M does not induce the developmental metamorphology (new shell synthesis and de-ciliation), although there is a rapid induction of settling [14]. This is similar to the larvae of *P. depressus* which were treated with 10^{-5} M GABA, i. e., the early changes (cessation of swimming and cramp of arms) were induced, but the later changes (extruding of podia and eversion of ER) were not.

In sea urchins, the apical surface of the larval epithelium is distributed by the egg-originated surface substance (ES-1) [21]. During glutamine-induced metamorphosis, ES-1-containing cells were found to be dispersed in larvae whose arms were retracting, and similar ES-1-containing cells were also found among coelomocytes of adult sea urchins [22]. These ES-1-containing cells may be attributable to the resorption of larval tissues by phagocytosis. In addition, it was found in *H. pulcherrimus* that the competent larvae exhibited high levels of mitotic activity in the epithelial cells of the arms and epaulets. When such larvae were treated with glutamine to induce metamorphosis, the high mitotic activity in epithelial cells decreased, while it did not change when the glutamine treatment was insufficient for ER-eversion (Yazaki, unpublished data). Thus glutamine-sensitive changes in mitotic activity may also be included in sea-urchin metamorphosis induced by glutamine.

ACKNOWLEDGMENTS

The authors would like to thank Dr. K. Kuwasawa for his critical reading of the manuscript, and Drs. H. Shirai and T. Yazawa for their valuable discussions and encouragements. We also express thanks to Dr. K. Inaba and Misaki marine Biological Station for providing the sea urchin, *P. depressus*.

REFERENCES

1 Burke RD (1980) Podial sensory receptors and the induction of metamorphosis in echinoids. J Exp Mar Biol Ecol 47: 223–234

2 Burke RD (1983) Neural control of metamorphosis in *Dendraster excentricus*. Biol Bull 164: 176–188

3 Burke RD (1984) Pheromonal control of metamorphosis in the pacific sand dollar, *Dendraster excentricus*. Science 225: 442–443

4 Cameron RA, Hinegardner RT (1974) Initiation of metamorphosis in laboratory cultured sea urchins. Biol Bull 146: 335–342

5 Chia F-S, Burke RD (1978) Echinoderm metamorphosis: Fate of larval structures. In "Settlement and metamorphosis of marine invertebrate larvae" Eds by F-S Chia, ME Rice, Elsevier, New York, pp 219–234

6 Chia F-S, Rice ME (1978) Settlement and metamorphosis of marine invertebrate larvae, Elsevier, New York, 290 pp.

7 de Silva PHDH (1962) Experiment on the choice of substrate by *Spirorbis* larvae (Serpulidae). J Exp Biol 39: 483–490

8 Highsmith RC (1982) Induced settlement and metamorphosis of sand dollar (*Dendraster excentricus*) larvae in predator free sites: adult sand dollar beds. Ecology 63: 329–337

9 Hinegardner RT (1969) Growth and development of the laboratory cultured sea urchin. Biol Bull 137: 465–475

10 Kakuda N, Nakamura T (1975) Studies on the artificial seeding of the sea urchin II. On the food for larvae of *Pseudocentrotus*

depressus (in Japanese). Aquiculture 22: 56–60

11 Kitamura H, Kitahara S, Koh HB (1993) The induction of larval settlement and metamorphosis of two sea urchins, *Pseudocentrotus depressus* and *Anthocidaris crassispina*, by free fatty acids extracted from the coralline red alga *Corallina pilulifera*. Mar Biol 115: 387–392

12 Kiyomoto M, Shirai H (1993) Reproduction of starfish eggs by electric cell fusion: A new method of detect the cytoplasmic determinant for archenteron formation. Dev Growth Differ 35: 107–114

13 Morse DE, Hooker N, Duncan H, Jensen L (1979) γ-aminobutyric acid, a neurotransmitter, induces planktonic abalone larvae to settle and begin metamorphosis. Science 204: 407–410

14 Morse DE, Duncan H, Hooker N, Baloun A, Young G (1980) GABA induces behavioral and developmental metamorphosis in planktonic molluscan larvae. Fed Proc 39: 3237–3241

15 Naidenko TK (1983) Laboratory cultivation of the sea urchin, *Strongylocentrotus intermedius*. Soviet J Mar Biol 9: 46–51

16 Naidenko TK (1991) Laboratory cultivation of five species of sea urchins from the sea of Japan. In "Biology of echinodermata" Eds by T Yanagisawa et al, AA Balkema, Rotterdam, pp 271

17 Noguchi M (1978) Metamorphosis of the sea urchin. In "Biology of metamorphosis" Ed by The Jap Soc of Develop Biologists, Iwanami-shoten, Tokyo pp 89–115 (in Japanese)

18 Scheltema RS (1961) Metamorphosis of the veliger larvae of *Nassarius obsoletus* (Gastropoda) in response to bottom settlement. Biol Bull 120: 92–109

19 Strathmann RR (1978) Larval settlement in echinoderms. In "Settlement and metamorphosis of marine invertebrate larvae" Eds F-S Chia and ME Rice, Elsevier, New York, pp 235–247

20 S-Dunlap M (1978) Larval biology and metamorphosis of Aplisiid gastropods. In "Settlement and metamorphosis of marine invertebrate larvae" Ed by F-S Chia, ME Rice, Elsevier, New York, pp 197–206

21 Yazaki I (1991) Identification of the egg-surface substance of sea urchin, *Hemicentrotus pulcherrimus*, by monoclonal antibodies. In "Biology of echinodermata" Eds by T Yanagisawa et al, AA Balkema, Rotterdam, pp 433–440

22 Yazaki I (1993) A novel substance localizing on the apical surface of the ectodermal and the esophageal epithelia of sea urchin embryos. Dev Growth Differ 35: 671–682

23 Yoshida M (1986) Manuals for the production of juveniles in labratory cultured sea urchins. In "Report for a Grant in Aid from the Ministry of Education, Science and Culture of Japan, No 58840028" (in Japanese)

ZOOLOGICAL SCIENCE 11: 261–267 (1994)

Control of Growth and Differentiation of Chondrogenic Fibroblasts in Soft-Agar Culture: Role of Basic Fibroblast Growth Factor and Transforming Growth Factor-β

YOSHIE OHYA[1] and KAZUO WATANABE[2]

Cell and Developmental Biology Laboratory, Faculty of Integrated Arts and Sciences, Hiroshima University, Higashi-Hiroshima 724, Japan

ABSTRACT—The sclera of the chick embryo consists of a layer of cartilage cells (scleral chondrocytes) adjacent to a layer of perichondrium (chondrogenic fibroblasts), which can be separated to produce pure populations of each cell type. In soft-agar culture at low concentration of fetal bovine serum (FBS), basic fibroblast growth factor (bFGF) induced clonal growth of many undifferentiated fibroblast-type (F-type) colonies from chondrogenic fibroblasts. Under the same conditions, bFGF induced many differentiated cartilage-type (C-type) colonies from scleral chondrocytes. On the other hand, a high concentration (10%) of FBS induced many C-type colonies from the chondrogenic fibroblasts. These results indicate that bFGF induces the fibroblasts to proliferate without progression of differentiation, while FBS contains an activity which promotes cartilage differentiation of the fibroblasts. The proliferating fibroblasts retained their differentiative capacity for at least 20 days in culture. The bFGF-dependent proliferation of the chondrogenic fibroblasts was inhibited by low concentration of transforming growth factor-β (TGF-β). In contrast, with differentiated chondrocytes, TGF-β did not inhibit the bFGF-dependent proliferation, but promoted it synergistically. Conditioned medium harvested from protein-free monolayer cultures of chondrogenic fibroblasts contained a TGF-β-like molecule. These regulators may play roles in the growth and differentiation of chondrogenic cells *in vivo*.

INTRODUCTION

Locally accumulating growth factors, such as bFGF and TGF-β, have been demonstrated to play morphogenetic roles in chondrogenesis [2, 8, 9, 12]. However, little information is available on the effects of these factors on undifferentiated and differentiated cells of the same cell lineage. Moreover, there has been little work to isolate candidate autocrine regulators directly from the cells involved in differentiative pathways.

To approach this problem, it is necessary to isolate pure cell populations representing different differentiative states, especially the undifferentiated cells. In addition, it is necessary to know the basal *in vitro* conditions for the cells to proliferate with retention of differentiative capacity and to differentiate only when certain signals are applied. Ideally, these cells should also be able to serve as a source of regulatory factors from their conditioned medium.

Recently, we have established an experimental system from the chick sclera [5, 19, 20]. The skeleton of the chick eyeball is composed of the scleral cartilage layer and its perichondrium, the scleral fibroblast layer, both of which are derived from neural crest cells [17]. These two layers are easily separable into two sheets without mutual contamination. The scleral chondrocytes manifest a cartilage phenotype in monolayer culture [20], while the scleral fibroblasts (chondrogenic fibroblasts) are motile, flattened fibroblasts which show no detectable expression of a cartilage phenotype, but proliferate in protein-free medium by producing multiple growth-regulating factors [5, 11, 19]. However, when scleral fibroblasts are cultured in soft agar containing 10% FBS, the cells proliferate and differentiate into rounded chondrocytes [20]. This suggests that the scleral fibroblasts represent a population of undifferentiated chondrogenic fibroblasts, which, although normally fibroblasts, have the capacity to differentiate into chondrocytes when suitable conditions are provided.

In this report, we describe the differential roles of low concentrations of bFGF, TGF-β and serum on chondrogenic fibroblasts or their differentiated progeny, scleral chondrocytes, in serum-deprived soft-agar culture. In addition, we tried to prove the presence of TGF-β-like molecule in conditioned medium harvested from protein-free primary cultures of the same cell type.

MATERIALS AND METHODS

1. Isolation of scleral fibroblasts and scleral chondrocytes: Dissection from embryos and dissociation of cells

Procedures have been published previously [11, 19, 20]. In brief, scleras were isolated from the eyeballs of 12-day chick embryos, and scleral fibroblast layers and scleral cartilage layers were separated under a microsurgery microscope. The isolated tissues were incubated with 0.2% collagenase (*Clostridium histolyticum*, activity 150–300 units/mg, Wako Ltd., Japan) at 37°C, for 40 or 60 min. The softened tissues were pipetted gently two times in culture medium, and the resulting cell suspensions were filtered through 2 sheets of sterile gauze and confirmed to be 99% single cells.

Accepted March 24, 1994
Received March 9, 1994
[1] Present address: Department of Biochemistry, School of Dentistry, Hiroshima University, Hiroshima 734, Japan
[2] To whom correspondence should be addressed.

2. Serum-deprived soft-agar culture and supplementation of test agents

One volume of a 1% aqueous solution of agar (Agar Noble, Difco Laboratories, U.S.A.) was mixed with one volume of 2-fold concentrated Ham's F-12 medium (Nissui Pharmaceutical Co., Japan) at 40–42°C to produce a 0.5%-agar solution in F-12 medium (hard-agar solution). Aliquots of 1 ml of the solution were poured into 35-mm plastic culture dishes (Falcon 3001, Becton Dickinson, U.S.A.) and hardened at room temperature to make a hard-agar layer.

Next, one volume of F-12 medium containing dissociated cells was mixed with two volumes of hard-agar solution at 40–42°C to produce a cell suspension in 0.33%-agar (soft-agar) solution. For each culture, 1 ml of the soft-agar solution containing 2×10^3 cells was quickly poured onto the hard-agar layer. Both of the agar layers were protein-free. After the agar layers hardened, 1 ml of F-12 medium containing the test agents with different concentrations of FBS (GIBCO Laboratories, U.S.A.) was poured onto the soft-agar layer. The cultures were incubated at 38°C in 5% CO_2-moist air, without any supplementation of test agents or serum. Colony-forming effieciency (number of resultant colonies per incubated cell number $\times100$) was calculated after 20 days of culture. The number of F-type colonies [20] was counted; only those F-type colonies larger than 50 μm in diameter were scored. In C-type colonies [20], colonies containing more than 6 cells were counted.

3. Assays for cell differentiation in soft-agar culture: Alcian blue staining and immunohistochemical staining

The culture dishes were dried at 55°C for 60 min and fixed with 10% formalin for 3 hr. Cells were stained with 0.1% Alcian blue dissolved in 0.1 N HCl for 3 hr at room temperature.

Anti-PG-H rabbit serum (provided by Dr. Koji Kimata, Aichi Medical University) was used for detecting cartilage-specific proteoglycan, PG-H [15]. Indirect immunohistochemical staining with biotinylated secondary antibody and β-galactosidase-bound streptavidin was performed as described previously [20].

4. Preparation of conditioned medium from protein-free monolayer culture of the scleral fibroblasts and ELISA of the conditioned medium material for anti-TGF-β immunoreactivity

Methods for preparing protein-free monolayer culture and harvesting conditioned medium were given elsewhere [19]. The harvested conditioned medium was concentrated from 50 ml to 4 ml by centrifugal concentrator (VC-360, Taitec Co., Japan). The concentrate and precipitate were mixed, transferred into membrane tubing (Dialysis Membrane, Size 20; cut off 10 kDa, Waco Ltd.) and dialysed against distilled water for 5 days. After centrifugation at 12,000 rpm for 20 min, the supernatant was further 4-fold concentrated and used as the test sample.

Aliquots of 50 μl of test samples or control TGF-β_1 (serial dilution from 100 ng/ml) were diluted 2-fold with 0.1 M carbonate-bicarbonate buffer (pH 9.5) and immobilized onto a 96-well microplate for ELISA (Japan Intermed Co., Japan) by incubation at 4°C overnight. The plate was washed 3 times with 0.05% Tween-20 (Bio-Rad Lab.) in PBS (TPBS), blocked with 200 μl of 1% gelatin-containing PBS at 37°C for 1 hr, and wahed with TPBS 3 times. A 50-μl aliquot of 150-fold diluted rabbit anti-human TGF-β_1 antibody (IgG; King Brewing Co., Japan) was added to each well. After 30 min, the plate was washed with TPBS 5 times, and peroxidase-labelled goat anti-rabbit IgG (H+L) (Kirkeguard and Perry Lab. Co.) was added to each well. After 1 hr, the plate was again washed with TPBS 5 times and 100 μl of peroxidase substrate solution was added to each well. After 30 min, the reaction was stopped by adding 50 μl of 2 M H_2SO_4. Absorbance at 490 nm was measured with a microplate reader (Bio-Tek, EL-309). As a control for specific antibody, rabbit IgG (Zymed Lab.) was used.

5. Growth factors

Basic FGF (bFGF, purified from bovine brain) was purchased from R & D systems, U.S.A. TGF-β (recombinant human TGF-β_1) was from king Brewing Co., Japan. Insulin (purified from bovine pancreas) was from Sigma Chemical Co., U.S.A. Platelet-derived growth factor (purified from human leucocytes) was from Collaborative Research Inc., U.S.A.

RESULTS

1. Effects of serum deprivation of chondrogenic fibroblasts in soft-agar culture

Chondrogenic fibroblasts in soft-agar culture in 10% FBS gives rise to two types of clonal colonies [20]. The F-type colony is round and consists of mutually adhering flattened fibroblasts (Fig. 1A), and the C-type colony consists of scattered large chondrocytes (Fig. 1B) with a halo of cartilage matrix, which is positive to staining with Alcian blue (Fig. 1C) or anti-PG-H antibody [20]. The colony-forming efficiency decreases by lowering serum concentration (Fig. 1D). Because no colonies were observed in serum-free medium, even in the presence of various growth factors, the analysis of the effects of different factors were performed in medium containing 2% FBS.

2. Basic FGF induces colony formation without promotion of differentiation, and FBS promotes chondrogenic differentiation

As shown in Table 1, 10 ng/ml bFGF induces many large F-type colonies in chondrogenic fibroblasts, which suggests that, relative to TGF-β, PDGF and insulin, bFGF does not promote cartilage differentiation by the proliferating fibroblasts. The number of F-type colonies increases and that of C-type colonies decreases as a function of bFGF concentration (Table 1).

FBS at 10% is effective at promoting C-type colonies, which suggests that FBS contains a strong activity for induction of cartilage differentiation from the fibroblasts (Table 1). The bFGF-induced large F-type colonies can differentiate into C-type colonies (C-type conversion) [20], if the culture medium changed on day 20 to fresh medium containing 2% FBS without bFGF and the cultures are maintained for further 14 days (Fig. 2). This suggests that cells proliferating in the presence of bFGF retain their differentiative capacity for at least 20 days.

With differentiated chondrocytes from the scleral cartilage layer, bFGF also induces rapid proliferation to form many colonies (data not shown). In this case, cell size remains smaller (mean diameter 10 μm) than in the absence of bFGF (mean diameter 30 μm); this suggests that there is no hypertrophic differentiation, which takes place in the

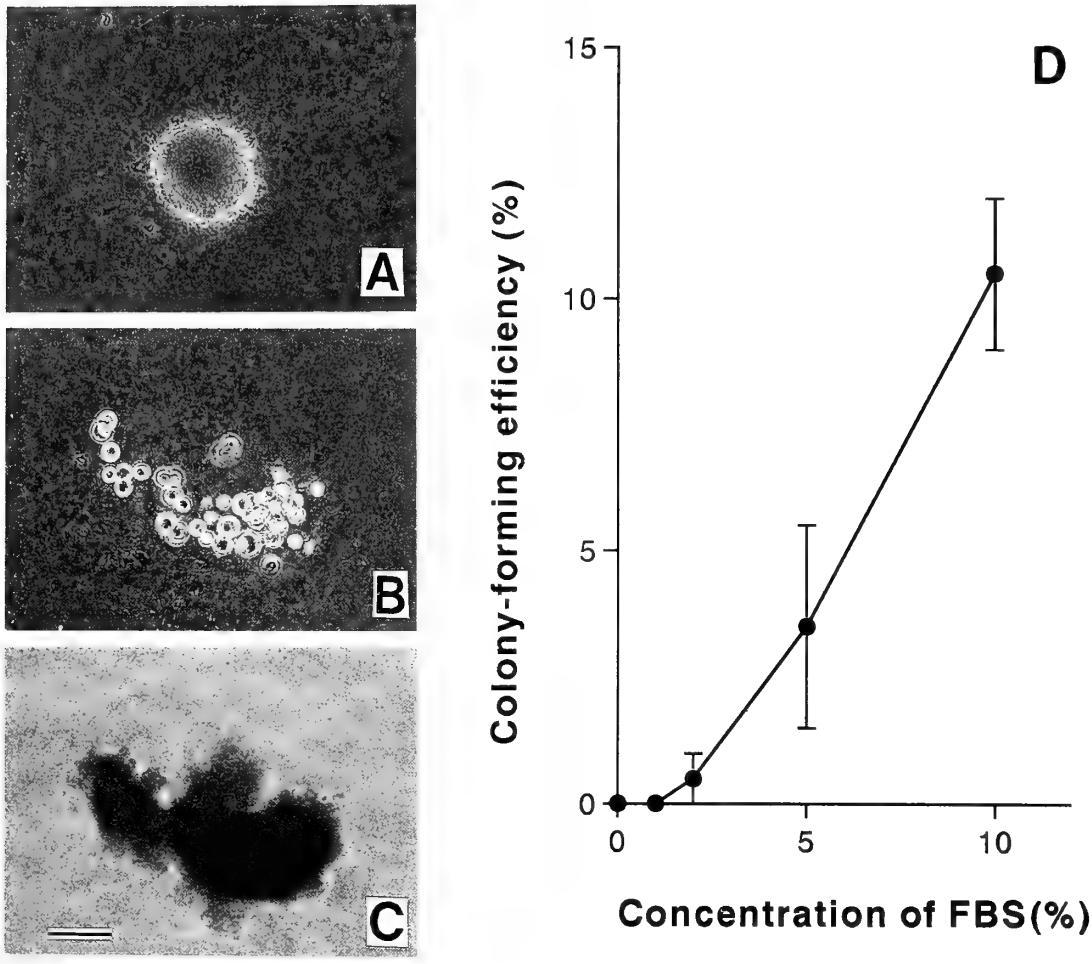

FIG. 1. Colony formation of chondrogenic fibroblasts (scleral fibroblasts) in soft-agar culture and the effects of serum concentration. A: F-type colony. B: C-type colony. Both photographs are the same magnification, suggesting large cell size in C-type colony. A and B were observed on the day 20 of culture by phase-contrast microscope. C: The same colony as B, stained with Alcian blue, showing a halo of cartilage matrix surrounding individual chondrocytes, as described previously [20]. Bar, 100 μm. D: Effects of serum (FBS) concentration on colony formation. Each point represents the average of results from three dishes with standard deviation.

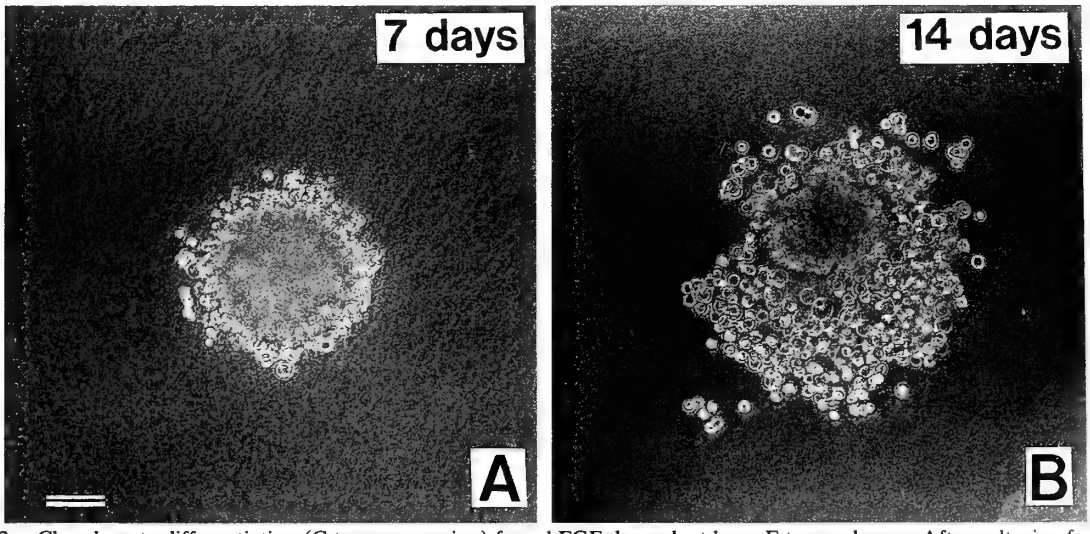

FIG. 2. Chondrocyte differentiation (C-type conversion) from bFGF-dependent large F-type colony. After culturing for 20 days with 10 ng/ml bFGF, the medium was changed to fresh medium containing 2% FBS and no bFGF. The culture was further incubated for 14 days. The same colony was photographed at the 7th day (A) and 14th day (B) after medium change. Rounded cells, which migrate out from the periphery of the F-type colony, are differentiating chondrocytes (C-type conversion, as described previously) [20]. About 5% of the bFGF-dependent F-type colonies manifested the C-type conversion. Bar, 100 μm.

TABLE 1. Effects of various growth-promoting substances on colony formation by chondrogenic fibroblasts in soft-agar culture

	Number of colonies obtained[a]	C-type colony	F-type colony	LF-type colony[b]
(Experiment A)[c]				
None (2% FBS only)	80 (4)	13	67	0
bFGF (10 ng/ml)	780 (39)	0	780	585
TGF-β (1 ng/ml)	140 (7)	10	130	67
PDGF (3 U/ml)	100 (5)	3	97	30
Insulin (10 μg/ml)	140 (7)	36	104	73
10% FBS	420 (21)	311	109	0
10% FBS with bFGF[d]	1960 (98)	510	1450	1058
(Experiment B)				
None (2% FBS only)	60 (3)	30	30	0
bFGF (0.01 ng/ml)	200 (10)	30	170	68
(0.1 ng/ml)	220 (11)	33	187	103
(1 ng/ml)	180 (9)	18	162	97
(10 ng/ml)	280 (14)	0	280	126

a: Dissociated cells were inoculated at 2000 cells per dish. Mean values obtained from three dishes are shown. Parenthesis means colony-forming efficiency.
b: LF-type (large F-type) colony means F-type colonies with diameters more than 81 μm.
c: Experiment A and Experiment B were different sets of cell culture. Growth factors were supplemented together with 2% FBS unless otherwise indicated. The variation in the results between these two experiments is as expected for different sets of cultures.
d: bFGF was added at 10 ng/ml.

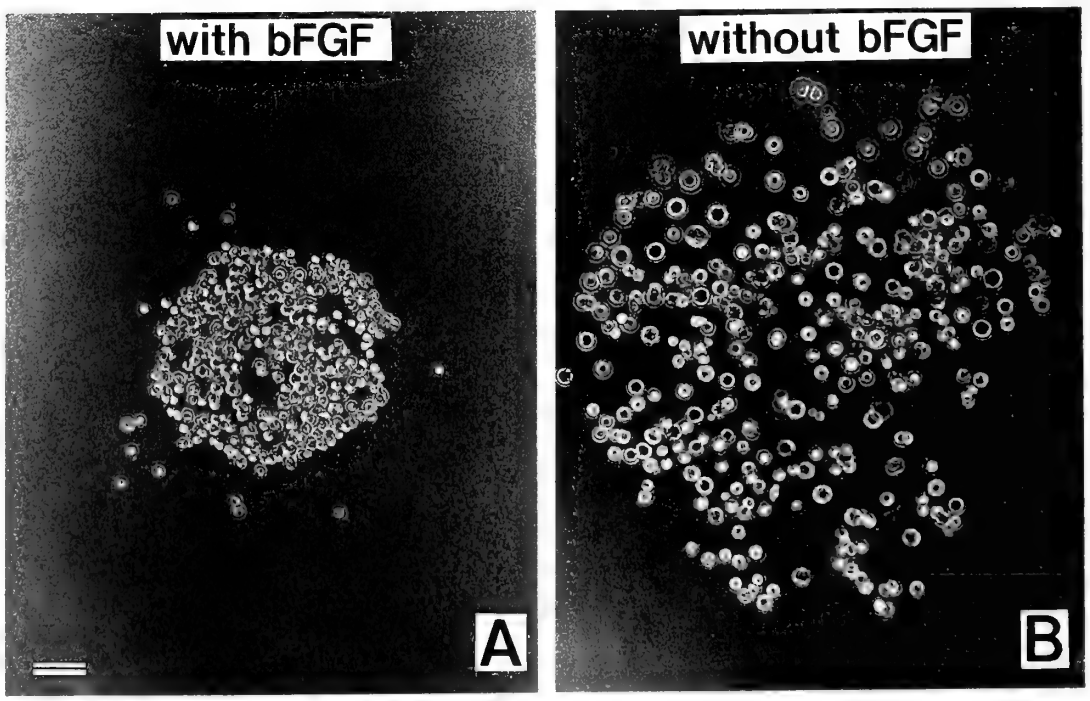

FIG. 3. Two different types of C-type colonies derived from differentiated chondrocytes. A: In the presence of 1 ng/ml bFGF. B: In the absence of bFGF. Both photographs are the same magnification. Both cultures contain 10% FBS. Photographed on day 20 of culture. Bar, 100 μm.

absence of bFGF (Fig. 3) [7].

3. TGF-β modulates the bFGF-dependent proliferation depending on the state of differentiation

Supplementation with bFGF alone raises colony-forming efficiency of both chondrogenic fibroblasts (●; Fig. 4A) and differentiated chondrocytes (●; Fig. 4C). However, supplementation with TGF-β alone does not increase it for either cell type (▲; Fig. 4B, D).

When TGF-β is supplemented with 1 ng/ml bFGF, TGF-β inhibits bFGF-dependent colony formation by chondrogenic fibroblasts in a dose-dependent manner at a range of 0.001–1 ng/ml (△; Fig. 4B). In contrast, in the presence of bFGF, TGF-β increases cloning efficiency by differentiated chondrocyte at the same range of concentrations (△; Fig. 4D). TGF-β at these concentrations does not affect cellular differentiation in soft-agar culture (data not shown).

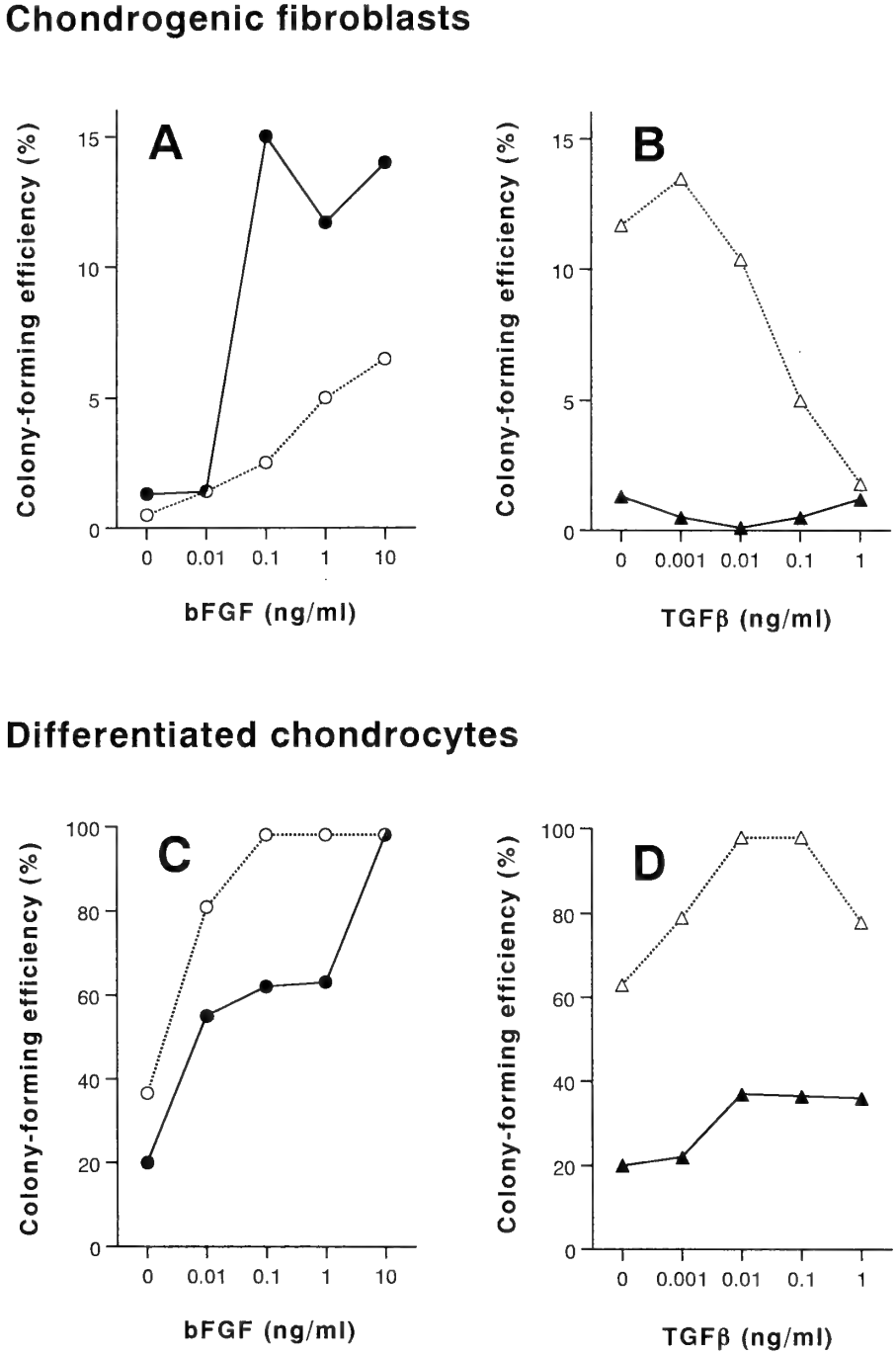

FIG. 4. Effects of bFGF and TGF-β on colony formation. A and B: In the case of chondrogenic fibroblasts. C and D: In the case of differentiated chondrocytes. Solid circles (●): bFGF alone. Open circles (○): bFGF with TGF-β (0.1 ng/ml). Solid triangles (▲): TGF-β alone. Open triangles (△): TGF-β with bFGF (1 ng/ml). Mean values obtained from three dishes are plotted.

4. Presence of anti-TGF-β immunoreactivity as autocrine/paracrine regulators

Assay of concentrated conditioned medium by ELISA with anti-TGF-β_1 antibody indicates that conditioned medium contains a TGF-β-like molecule (Fig. 5). The amount in conditioned medium seems to be higher at the early days of culture.

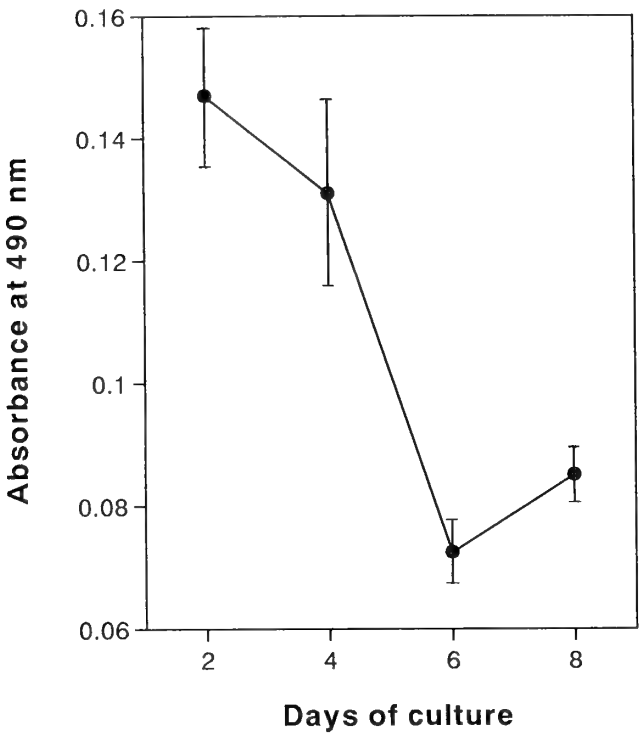

FIG. 5. Detection of TGF-β-like molecule in conditioned medium of chondrogenic fibroblasts in monolayer culture by ELISA with anti-TGF-β_1 antibody. Concentrated conditioned medium was immobilized onto wells (see Materials and Methods). Absorbance of the negative control (non-immune rabbit IgG) was 0.023, and that of the positive control (25 ng/ml TGF-β_1) was 0.127. Data given are the average values from 3 replicate wells with standard deviation.

DISCUSSION

With chondrogenic fibroblasts (scleral fibroblasts), bFGF [6] induced rapid proliferation to produce many large F-type colonies (Table 1). Since many of the chondrogenic fibroblasts possess the capacity to proliferate and differentiate into C-type colonies when 10% FBS is present [20] (Table 1), bFGF was considered to have a capacity to induce these cells to proliferate without promotion of differentiation. The differentiative potentiality of the proliferating cells was maintained even up to 20 days after initial treatment with 10 ng/ml bFGF (Fig. 2).

With differentiated chondrocytes (scleral chondrocytes), bFGF also induced rapid proliferation with suppression of hypertrophic differentiation (Fig. 3), similar to the case for rabbit chondrocytes [7, 8]. The suppression of differentiation by bFGF does not imply inhibition of phenotypic expression. In fact, Kato [8] pointed out that bFGF stabilized phenotypic expression and prevented dedifferentiation of proliferating chondrocytes, and, as a result, promoted proteoglycan synthesis.

Taken together, the function of bFGF is to induce proliferation of both undifferentiated and differentiated chondrogenic cells without promotion of differentiation, i.e., to expand a cell population *as it exists*. We emphasize that an initial treatment with bFGF is sufficient for a persistent effect for at least 20 days. This may suggest the existence of a mechanism to hold a cellular differentiative state steady during persistent proliferation, similar to the auto-induction in steroid-hormonal regulation [18].

As to the differentiation-promoting activity, which at least FBS possessed, bone morphogenetic proteins (BMPs) [14] have been reported to be differentiation factors in limb bud mesoderm of the chick [3, 4]. In fact, recombinant BMP-4 has been found to induce C-type conversion (Watanabe, Hayashibe and Takaoka, unpublished data). It would be of interest to determine, whether FBS contains a member of the BMP family or stimulates autocrine production of one.

As shown in Figure 4, TGF-β [10, 13] displays an inverse effect on the bFGF-dependent proliferation of chondrogenic fibroblasts and differentiated chondrocytes, which are located adjacent to each other *in vivo*. Since our three-dimensional cultures should reflect the *in vivo* function of chondrogenic cells [1, 16], it may be that increased endogenous TGF-β-like molecule gives rise to overall growth of cartilage tissue, together with growth suppression of the adjacent perichondrium, in the presence of endogenous bFGF-like growth-promoting activity [19].

It was found that the chondrogenic fibroblasts secreted TGF-β-like molecule into their conditioned medium (Fig. 5). High activity at the early days in culture might be explained as an induction by primary monolayer cultivation. It is plausible that these factors play regulatory roles in the differential growth and differentiation of chondrogenic cells in *in vivo* scleral chondrogenesis.

ACKNOWLEDGMENTS

We thank Prof. Minoru Amano for his continuous encouragement and Dr. Akira Kawahara for his kind advice. Thanks are also due to Dr. David A. Carrino for reviewing manuscript. This work was supported in part by Grants-in-Aid for Scientific Research (No. 03833023 and No. 03304009) to K. W. from the Ministry of Education, Science and Culture of Japan.

REFERENCES

1 Benya PD, Shaffer JD (1982) Dedifferentiated chondrocytes reexpress the differentiated collagen phenotype when cultured in agarose gels. Cell 30: 215–224

2 Carrington JL, Reddi AH (1990) Temporal changes in the response of chick limb bud mesodermal cells to transforming growth factor β-type 1. Exp Cell Res 186: 368–373

3 Carrington JL, Chen P, Yanagishita M, Reddi AH (1991) Osteogenin (bone morphogenetic protein-3) stimulates cartilage

formation by chick limb bud cells *in vitro*. Develop Biol 146: 406–415

4 Chen P, Carrington JL, Hammonds RG, Reddi AH (1991) Stimulation of chondrogenesis in limb bud mesoderm cells by recombinant human bone morphogenetic protein 2B (BMP-2B) and modulation by transforming growth factor β_1 and β_2. Exp Cell Res 195: 509–515

5 Fujioka M, Shimamoto N, Kawahara A, Amano M, Watanabe K (1989) Purification of an autocrine growth factor in conditioned medium obtained from primary cultures of scleral fibroblasts in the chick embryo. Exp Cell Res 181: 400–408

6 Gospodarowicz D, Neufeld G, Schweigerer L (1986) Molecular and biological characterization of fibroblast growth factor, an angiogenic factor which also controls the proliferation and differentiation of mesoderm and neuroectoderm derived cells. Cell Differ 19: 1–17

7 Kato Y, Iwamoto M (1990) Fibroblast growth factor is an inhibitor of chondrocyte terminal differentiation. J Biol Chem 265: 5903–5909

8 Kato Y (1992) Roles of fibroblast growth factor and transforming growth factor-β families in cartilage formation. In "Biological Regulation of the Chondrocytes" Ed by M Adolphe, CRC Press, Florida, pp 241–279

9 Leonard CM, Fuld HM, Frenz DA, Downie SA, Massague J, Newman SA (1991) Role of transforming growth factor-β in chondrogenic pattern formation in the embryonic limb: Stimulation of mesenchymal condensation and fibronectin gene expression by exogenous TGF-β and evidence for endogenous TGF-β-like activity. Develop Biol 145: 99–109

10 Moses HL, Bramm EB, Proper JA, Robinson RA (1981) Transforming growth factor produced by chemically-transformed cells. Cancer Res 41: 2842–2848

11 Ohya Y, Watanabe K, Shimamoto N, Amano M (1992) Scleral fibroblasts of the chick embryo can proliferate without transferrin in protein-free culture. Zool Sci 9: 749–755

12 Richman JM, Crosby Z (1990) Differential growth of facial primordia in chick embryos: Responses of facial mesenchyme to basic fibroblast growth factor (bFGF) and serum in micromass culture. Development 109: 341–348

13 Roberts AB, Anzano MA, Lamb LC, Smith JM, Sporn MB (1981) New class of transforming growth factors potentiated by epidermal growth factor: Isolation from non-neoplastic tissues. Proc Natl Acad Sci USA 78: 5339–5343

14 Rosen V, Thies RS (1992) The BMP proteins in bone formation and repair. Trends Genet 8: 97–102

15 Shinomura T, Kimata K, Oike Y, Maeda N, Yano S, Suzuki S (1984) Appearance of distinct types of proteoglycan in a well-defined temporal and spatial pattern during early cartilage formation in the chick limb. Develop Biol 103: 211–220

16 Solursh M, Linsenmayer TM, Jensen KL (1982) Chondrogenesis from single limb mesenchymal cells. Develop Biol 94: 259–264

17 Stewart PA, McCallion DJ (1975) Establishment of scleral cartilage in the chick. Develop Biol 46: 383–389

18 Tata JR, Baker BS, McChuca I, Rabelo EML, Yamauchi K (1993) Autoinduction of nuclear receptor genes and its significance. J Steriod Biochem Molec Biol 46: 105–119

19 Watanabe K, Fujioka M, Takeshita T, Tsuda T, Kawahara A, Amano M (1989) Scleral fibroblasts of the chick embryo proliferate by an autocrine mechanism in protein-free primary cultures: Differential secretion of growth factors depending on the growth state. Exp Cell Res 182: 321–329

20 Watanabe K, Yagi K, Ohya Y, Kimata K (1992) Scleral fibroblasts of the chick embryo differentiate into chondrocytes in soft-agar culture. In Vitro Cell Dev Biol 28A: 603–608

ZOOLOGICAL SCIENCE 11: 269–274 (1994)

Membrane-bound Inclusions in the Leydig Cell Cytoplasm of the Broad-headed Skink, *Eumeces laticeps* (Lacertilia: Scincidae)

NATHAN O. OKIA

Department of Biology, Auburn University at Montgomery, 7300 University Drive, Montgomery AL 36117-3596, USA

ABSTRACT—The structure of the Leydig cell was studied in laboratory maintained skinks *Eumeces laticeps* (Schneider). Overall, skink Leydig cell cytology was similar to that of mammalian steroidogenic cells. Under both the light and electron microscope, for example, skink Leydig cells contained large lipid droplets in their cytoplasm. However, skink Leydig cells also contained elongated membrane bound rods and other rounded structures which were also surrounded by tightly packed concentric layers of membranes. The rounded structures were of two types, oval figures with empty interiors and fibrous structures with ribosome-like elements in their interiors. The elongatd, rod-like structures resembled crystalloids found in aging human corpora lutea. The oval structures resembled myelin sheaths and the round but wooly-looking bodies resembled compact whorls of membranes found in mice Leydig cells.

INTRODUCTION

A mammalian Leydig cell is often described as having extensive arrays of smooth endoplasmic reticulum appearing as long connected tubulues [3]. In the cytoplasm may be large lipid inclusions, which in some instances is evidence of cellular regression [1]. In addition, human and other mammalian Leydig cells, contain proteinaceous crystals of Reinke of unknown function or origin [8, 9]. Similarly, active Leydig cells in *Anolis* lizards, have extensive arrays of agranular endoplasmic reticulum, darkly-staining mitochondria and lipid granules without crystalline inclusions [13]. In the current study on the ultrastructure of skink Leydig cells, testes of laboratory maintained skinks *Eumeces laticeps* (Schneider) which were obtained during the periods of testicular recrudescence (January) and breeding (May) in the wild [7] were found to contain membrane-bound inclusions some of which looked crystal-like.

MATERIALS AND METHODS

Four animals captured in late winter around the campus were kept for 6 or more months in glass tanks, provided with water *ad libitum* and fed crickets daily. They were sacrificed either in January or May by decapitation with one stroke of scissors. Small pieces of testes were immersed in Karnovsky's fixative, pH 7.4 for 2 hr, postfixed in 1% OsO_4 in 0.1 M sodium cacodylate buffer at room temperature for 2 hr. After dehydration through alcohols and acetone they were embedded in Spurr's Epoxy mixture. Semi-thin sections were stained with toluidine blue and basic fuchsin (Electron Microscope Science) and ultrathin sections were stained with uranyl acetate and lead citrate and examined with a Philips 200 electron-microscope at an accelerating voltage of 60 kV.

Accepted February 3, 1994
Received November 30, 1993

RESULTS

Under the light microscope, Leydig cells which were close to the basement membrane contained large lipid droplets in their cytoplasm (Fig. 1). Under the electron microscope, some of the Leydig cells similarly showed cytoplasms that were full of lipid granules with few other organelles visible (Fig. 2). The cytoplasm of what were considered Leydig cells was in all cases very granular and in some, contained inclusions consisting of rods which were visible at the level of the light microscope (Fig. 3). At the ultrastructural level, Leydig cell cytoplasm also contained other rounded structures that resembled myelin sheaths (Fig. 4). Between the rod-like structures and lipid granules were several free ribosomes and rough endoplasmic reticulum. Except for the solid dark outlines of the rods, their cores were not stained. The lipid granules on the other hand, had unstained cores and edges which were stained to varying degrees. Confluence between the lipid granules were sometimes observed (Fig. 5). Other than the simple rectangular pattern, some rods showed pointed ends and their darker outlines consisted of multiple layers of membranes (Fig. 6). Some rods contained fiber-like structures inside their cores (Fig. 7). At higher resolution, the dark walls of myelin-like structures and crystalloids consisted of multiple layers of membranes with alternating dark and light bands which resembled unit membranes (Figs. 8 and 9). In some sections, the light inner band between the 2 dark bands was bisected by a longitudinally positioned dark line (Fig. 10). The myelin structures sometimes enclosed portions of cytoplasm (Fig. 8) or empty spaces (Fig. 11). Also found was a wooly structure with whorls of concentric fiber enclosing ribosome-like elements (Fig. 12). All the observed structures were found in testes undergoing spermatogenesis and spermiogenesis and their shape or distribution was invariable in the sections examined.

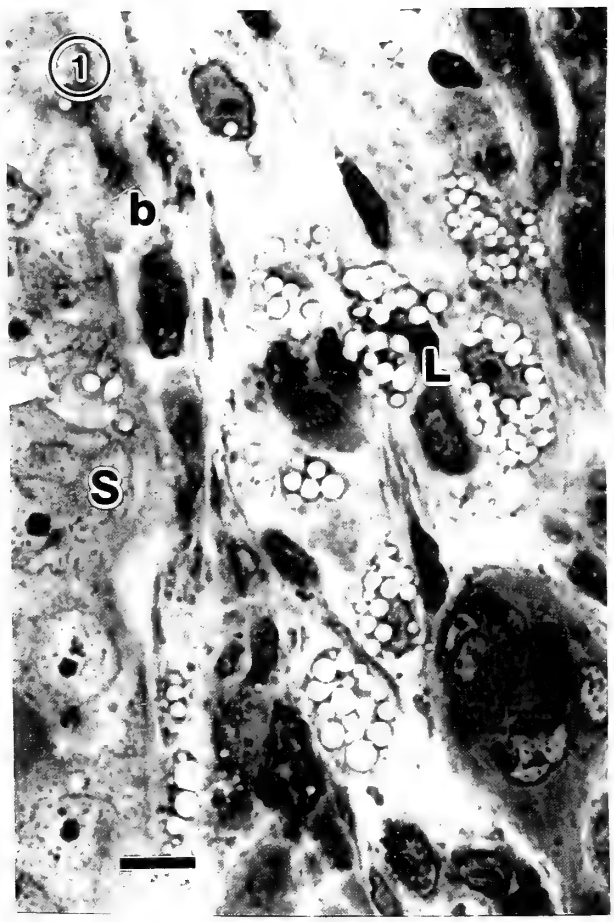
1
b
L
S

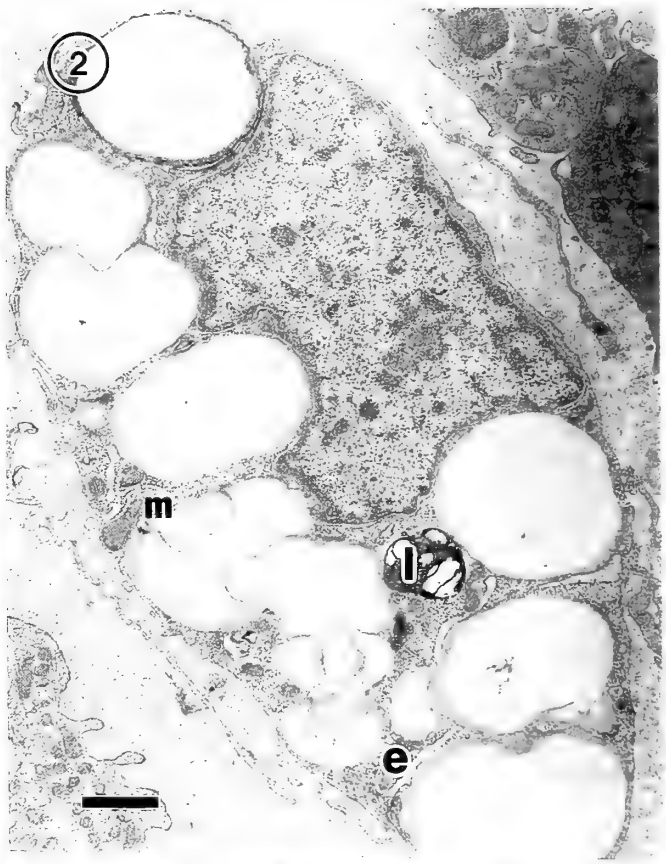
2
m
l
e

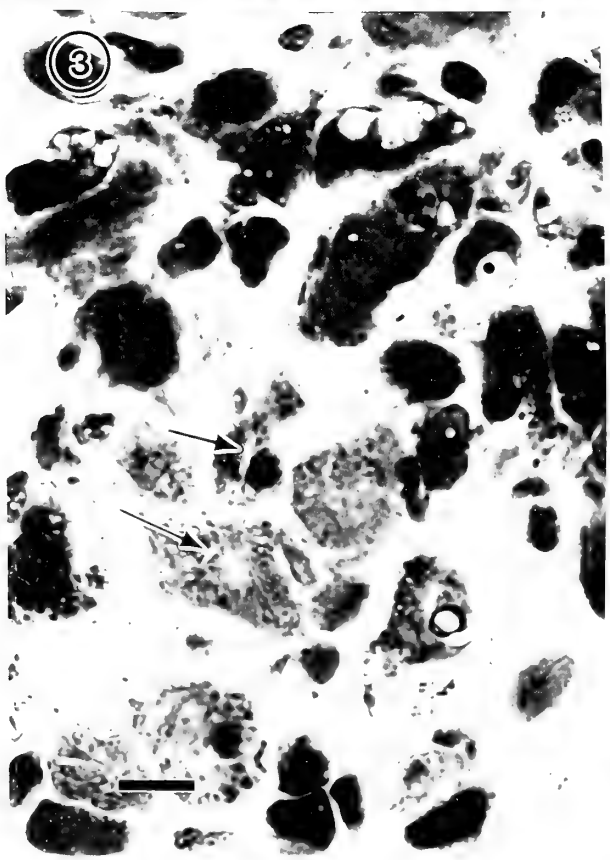
3
O

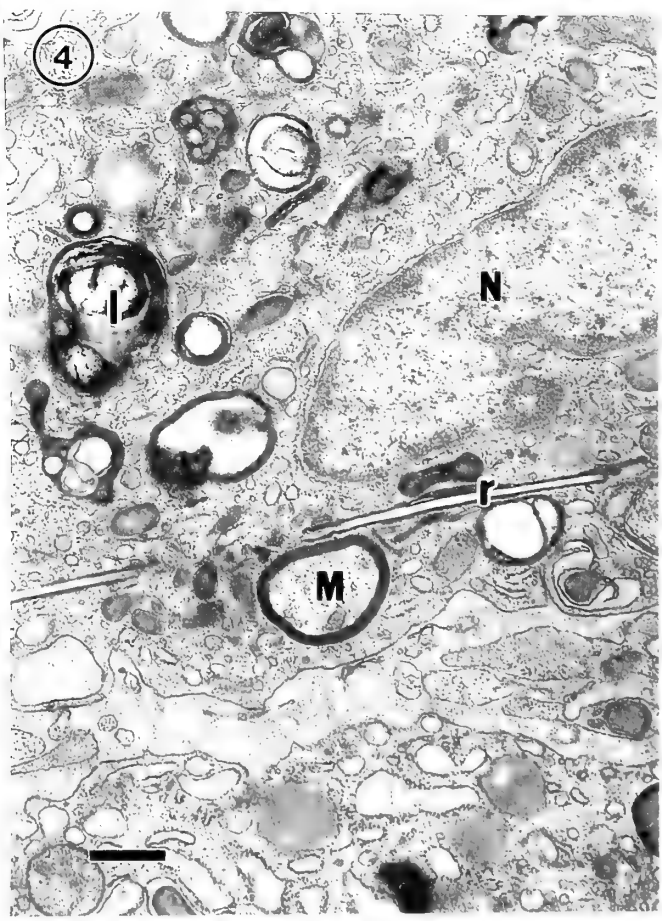
4
l
N
r
M

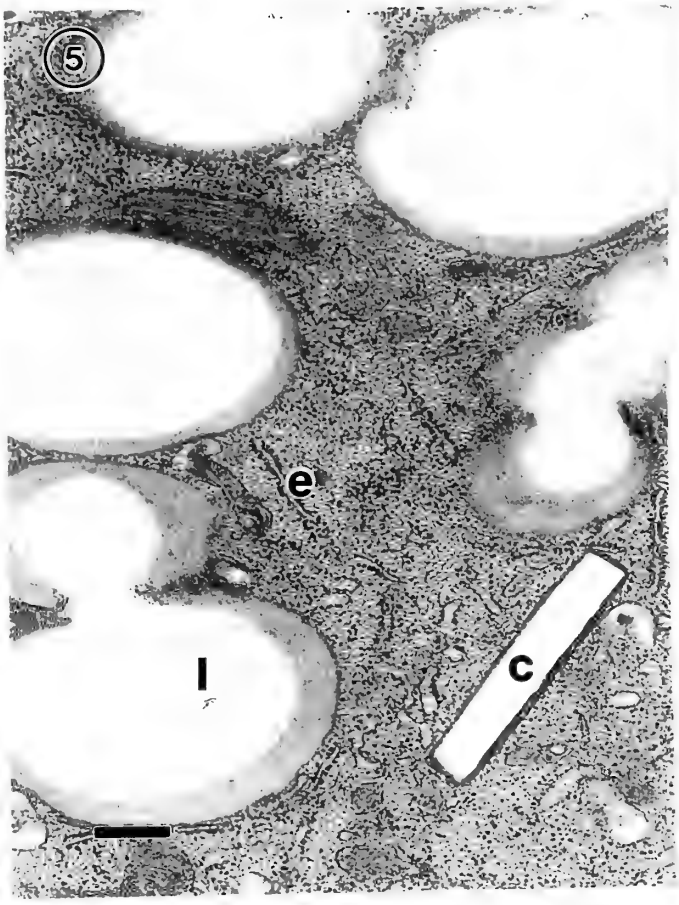
5
e
l
c

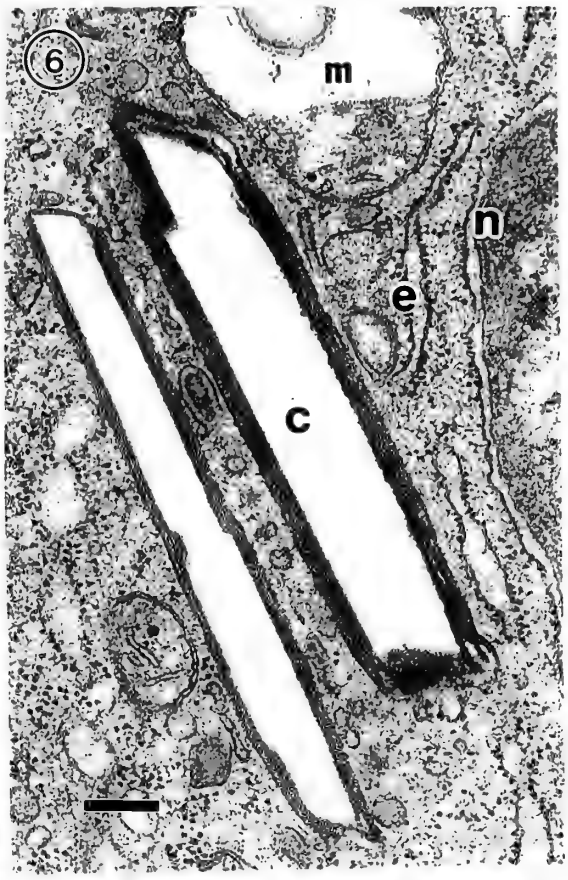
6
m
n
e
c

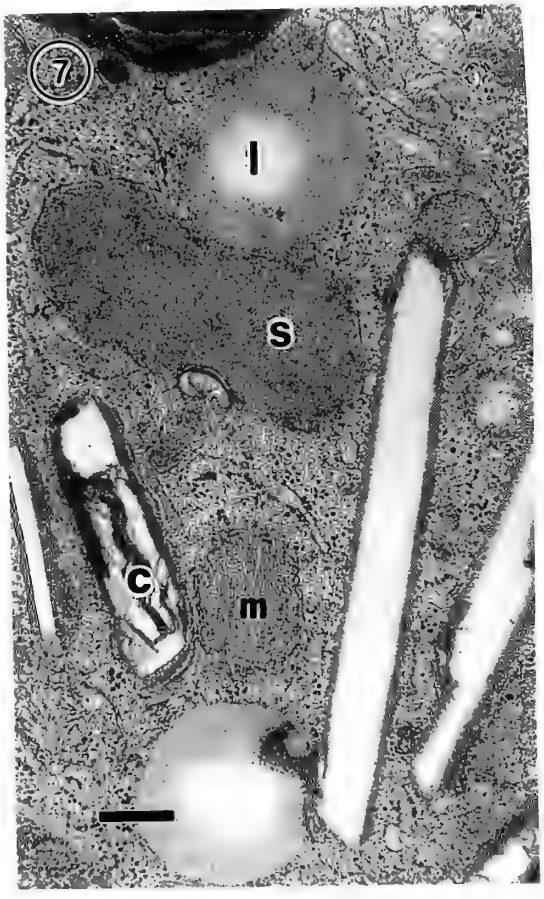
7
l
s
c
m

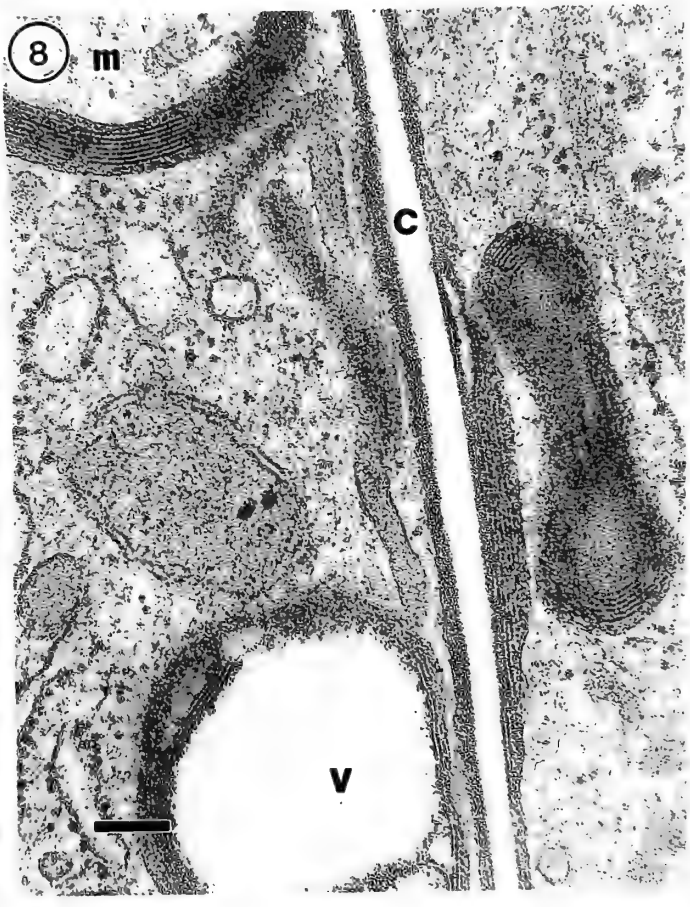
8
m
c
v

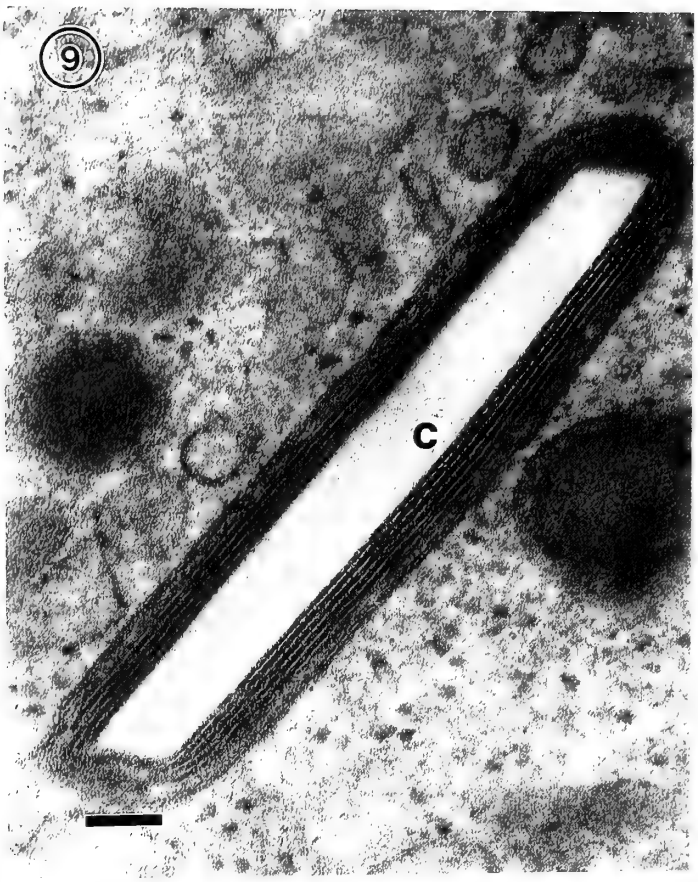
9
C

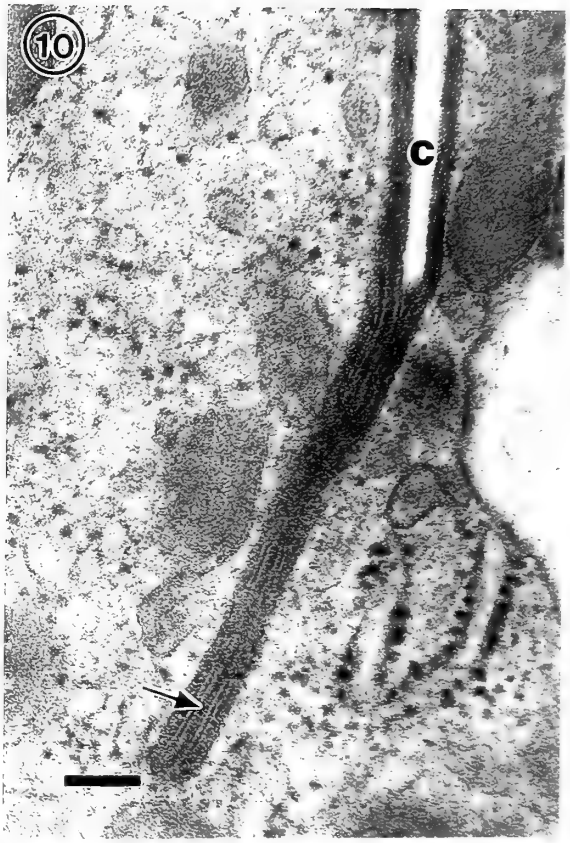
10
C

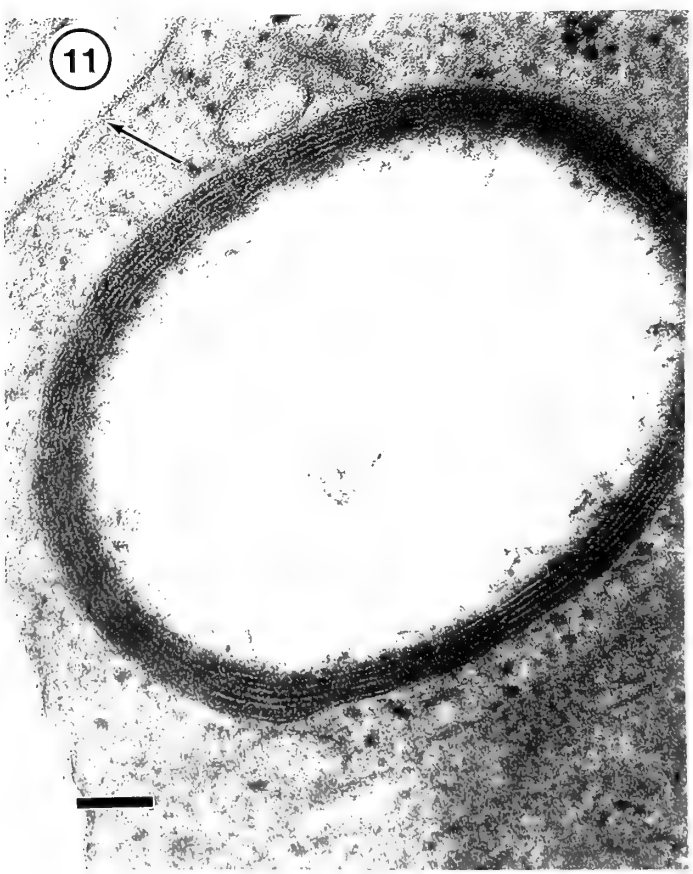
11

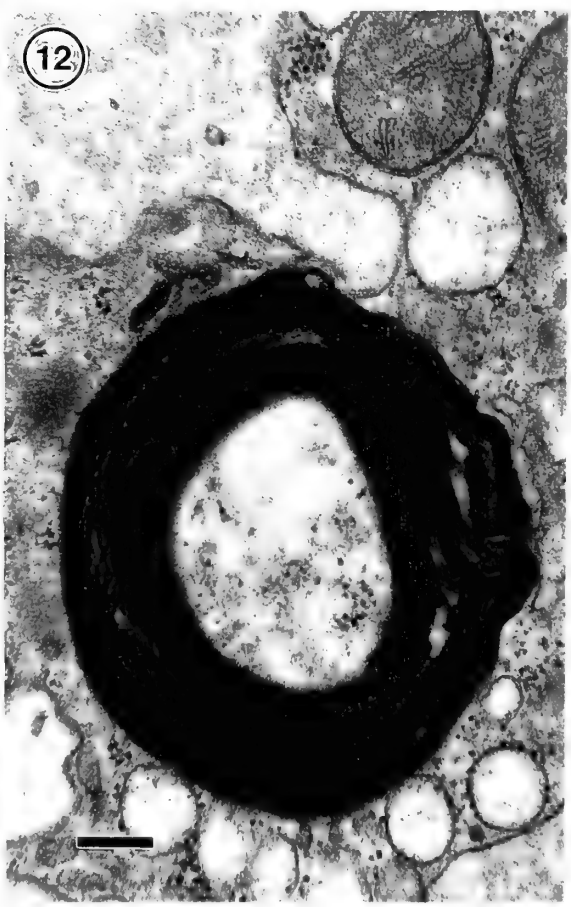
12

DISCUSSION

A steroid producing cell should increase its membrane stores during active steroidogenesis and the increase in smooth endoplasmic reticulum in lipid producing cells is evidence of this. The ordered arrangement of smooth endoplasmic reticulum around liposomes in the armadillo Leydig cell is said to be one means of increasing surface area for cholesterol and steroid production [14]. Based on the appearance of their walls, it is possible that the inclusions found in skink Leydig cell cytoplasm are some special type of smooth endoplasmic reticulum like the kind described as tubular in the opossum Leydig cells [4]. However, only the rod-like inclusions in the skink Leydig cell cytoplasm can be considered tubular. The skink ovoid structures with laminated walls resemble lipid vacuoles found in the armadillo [14] and dog Leydig cells [6], which are surrounded by whorls of smooth endoplasmic reticulum. The skink membranes were however, more tightly packed and uniformly spaced like myelin figures in residual bodies [5]. Similarly, the inclusions with concentric whorls of membranes (Fig. 12) resemble those inclusions that have been described as "compact whorls of membranes" [8, 12] of unknown function rather than smooth endoplasmic reticulum. Therefore, these structures are not specialized smooth endoplasmic reticulum.

Crystals have been found in mammalian but not reptilian Leydig cells and so the data reported here are probably the first indication of crystal-like structures in reptilian Leydig cells. These rod-like structures in the skink Leydig cell cytoplasm resemble rod-like structures in aging human lutein cells [2, 5] described as lipid-soluble and possibly made of cholesterol. The characteristic of having laminated walls links them to cylindrical bodies that were described in rat Leydig cells [11] as having walls composed of a helical array of tubular units possibly derived from the endoplasmic reticulum [11]. But in the skink Leydig cell bodies, there was no connection between the membranes of the laminated walls and the endoplasmic reticulum. Though found in the Leydig cells, these skink rods do not resemble Reinke's crystals which occur in human and other mammalian Leydig cells. These bodies appear to be unique to the skink and their true nature has to await further investigation.

Like crystals, lipid droplets have also been found to increase in regressing Leydig cells [1, 10] and their occurrence in skink Leydig cells could be interpreted as portending their regression, but no evidence of such regression was noted.

ACKNOWLEDGMENTS

I would like to thank Dr. Emilio Mora for use of the electron microscope facility, Dr. William Cooper, for securing and identifying the skinks, and Dr. Tom Denton for financial support from the Department. Partial support for this work was provided by the NSF's Instrumentation & Instrument Development Program Grant # DIR-8907860 for the procurement of the ultramicrotome and the Auburn University at Montgomery Grant-in-Aid Program.

FIG. 1. The skink testis showing a cluster of Leydig cells (L) containing several lipid vesicles in the cytoplasm next to the basement membrane (b) of the seminiferous tubule, which shows four Sertoli cells (S) resting on the basement membrane. Bar=8 μm.

FIG. 2. A Leydig cell with large lipid granules occupying most of the cytoplasm. A few mitochondria (m), lysosome (I), and smooth endoplasmic reticulum (e) are also discernable. Bar=1 μm.

FIG. 3. A segment of the interstitial space showing Leydig cells located further from the basal lamina. The granularity of the cytoplasms and the presence of non-stained rods is evident (arrows). Bar=8 μm.

FIG. 4. This section through a Leydig cell shows a number of cytoplasmic inclusions including a myelin-like body (M), lysosome (I), non-stained rods (r). Also shown is the nucleus (N) with a ring of heterochromatin all along the inside of the nuclear envelope. Bar=0.6 μm.

FIG. 5. A section through a Leydig cell showing lipid granules (I), tubules of rough endoplasmic reticulum (e) and a non-stained rod or cylinder, here called a crystal (c). Bar: 0.3 μm.

FIG. 6. A Leydig cell cytoplasm showing two crystals (c) with their fibrous wall. An enlarged mitochondrion (m) with degenerating cristae is also shown. e, rough endoplasmic reticulum; n, nucleus. Bar=0.2 μm.

FIG. 7. The cytoplasm of a Leydig cell showing 4 crystalloids, one with a fibrous core (c); liposome (l), lysosome (s) and mitochondrion with laminated cristae (m). Bar=0.2 μm.

FIG. 8. A segment of a Leydig cell cytoplasm showing a number of membrane-bound inclusions all of which show evenly spaced parallel or concentric membranes. The figure is an enlargement of (Fig. 4). c, a crystal; m, myelin-like inclusion; v, vacuole. Bar=0.1 μm.

FIG. 9. The cytoplasm of a Leydig cells showing detail of the crystal (c) wall which consists of regularly spaced alternating light and dark bands. Bar=0.1 μm.

FIG. 10. A tangential section through a small crystal (c) in the cytoplasm of a Leydig cell, showing detail of the membranes making up the crystal wall. It shows that the light longitudinal band is bisected by another dark line (arrow). Bar=0.1 μm.

FIG. 11. A section through an oval shaped laminated structure within the cytoplasm of a Leydig cell. The wall of this structure consists of concentrically arranged membranes like those found around the crystalloids. Inside the structure are what appear to be cytoplasmic debris. Arrow points at the cell membrane for comparison with crystal wall membranes. Bar=0.1 μm.

FIG. 12. Another type of membrane-bound structure found in the cytoplasm of Leydig cells which resembles those structures that have been described in literature as "compact whorls of membranes". The wall of this structure encloses what looks like free ribosomes within the cytoplasm. Bar=0.2 μm.

REFERENCES

1 Andersen K (1978) Seasonal change in fine structure and function of Leydig cells in the blue fox, *Alopex lagopus*. Int J Androl 1: 424–439

2 Carsten PM, Merker HJ (1965) Die Darstellung von Cholesterinkristallen im elektronenmikroskopischen. Bild Frankfurt Z Path 74: 539–543

3 Christensen AK (1965) The fine structure of testicular interstitial cells in guinea pigs. J Cell Biol 26: 911–935

4 Christensen AK, Fawcett DW (1961) The normal fine structure of opossum testicular interstitial cells. J Biophys Biochem Cytol 9: 653–670

5 Christensen AK, Gillim SW (1969) The correlation of fine structure and function in steroid-secreting cells, with emphasis on those of the gonads. In "The Gonads" Ed. by KW McKerns, Appleton-Century-Crofts, New York pp. 415–488

6 Connell CJ, Christensen AK (1975) The ultrastructure of the canine interstitial tissue. Biol Reprod 12: 368–382

7 Cooper WE, Vitt LJ (1987) Intraspecific and interspecific aggression in lizards of the scincid genus *Eumeces*: chemical detection of conspecific sexual competitors. Herpertologica 43: 7–14

8 De Kretser DM, Kerr JB (1988) The cytology of the testis. In "The Physiology of Reproduction" Ed. by KE Nejll et al., Raven Press, New York, pp 837–932

9 Fawcett DW, Burgos MH (1960) Studies on the fine structure of the mammalian testis. The human interstitial tissue. Am J Anat 107: 245–269

10 Gustafson AW (1987) Changes in Leydig cell activity during the annual testicular cycle of the bat *Myotis licifugus lucifugus*: Histology and lipid histochemistry. Am J Anat 178: 312–325

11 Murakami M, Kitahara Y (1971) Cylindrical bodies derived from endoplasmic reticulum in Leydig cells of the rat testis. J Electr Microsc 20: 318–323

12 Ohata M (1979) Electron microscope study on the testicular interstitial cells in the mouse. Arch Histol Jap 42: 51–79

13 Pearson AK, Tsui H, Licht P (1976) Effect of temperature on spermatogenesis, on the production and action of androgens and on the ultrastructure of gonadotropic cells in the lizard *Anolis carolensis*. J Exp Zool 195: 291–303

14 Weaker FJ (1977) The fine structure of the interstitial tissue of the testis of the nine-banded armadillo. Anat Rec 187: 11–28

ZOOLOGICAL SCIENCE 11: 275–284 (1994)

Identification and Localization of a Ligand Molecule of *Xenopus* Cortical Granule Lectins

NORIO YOSHIZAKI

Department of Biology, Faculty of General Education, Gifu University, Gifu 501–11, Japan

ABSTRACT—This study aimed to identify the ligand molecule of the cortical granule lectins which participate in the formation of the fertilization (F) layer in *Xenopus laevis*. Comparison of fertilization envelopes (FEs) with and without the F layer by SDS-PAGE showed a 105-kDa glycoprotein (gp 105) only in the former FEs. This glycoprotein was isolated by differential centrifugation and electrophoretical extraction from an F layer extract. Immunoblotting with an antiserum against gp 105 produced staining on the gp 105 in the FEs; the relative amount of gp 105 increased during the hatching period due to the digestion of vitelline envelope components. Staining on westernblots with HRP-conjugated peanut agglutinin suggested that gp 105 contains a small amount of galactosides. With immunoelectron microscopy, gold particles indicating the location of gp 105 were visible on the pre-fertilization (PF) layer of eggs obtained from the pars recta 2 (PR2) and the uterus of the oviduct, but they were few on the F layer of activated eggs. With the PA-CrA-Silver method for detecting carbohydrates, silver particles appeared on the PF layer but not on the main body of the F layer. The binding of gold-conjugated lectins to gp 105 on westernblots showed that gp 105 interacts with the cortical granule lectins. It was concluded from these results that gp 105 is a natural ligand of the lectins, and that it resides in the PF layer and is supplied to eggs at the PR2.

INTRODUCTION

Fertilization in *Xenopus laevis* induces the formation of a fertilization (F) layer in the egg envelopes as well as a hydrolytic event which changes the vitelline envelope (VE) of unfertilized eggs to that (VE*) of fertilized eggs [7, 12, 21]. Subsequently, the fertilization envelope (FE) consists of the VE* and the F layer and it acts as a block to polyspermy [5, 6]. The F layer is formed by the interaction of cortical granule lectins with ligand molecules. The nature of the lectins has been well documented [3, 16, 28, 29] but that of the ligand molecules not. Two sources for the ligand molecules have been proposed, the innermost jelly layer [25] and the pre-fertilization (PF) layer [26, 31].

The jelly layers of *Xenopus* eggs are composed of four morphologically distinct layers [27]. Wyrick *et al.* [25] first demonstrated a precipitation reaction on agar plates between the solubilized jelly of the innermost layer and the lectins. Ligand molecules of the jelly were recently identified immunoelectrophoretically by Birr and Hedrick [2] but have not yet been characterized.

Yoshizaki and Katagiri [31] reported a PF layer lying between the VE and the innermost jelly layer of uterine eggs; it is produced by epithelial cells at the pars recta 2 (PR2) of the oviduct [26]. Its honeycomb structure was shown through quick-freeze, deep-etch electronmicroscopy by Larabell and Chandler [11]. When eggs obtained from the PR2 were activated or treated with lectins, their PF layer became similar to the F layer morphologically and biochemically [31]. Furthermore, the F layer could not be produced in activated eggs when they were deprived of the PF layer [31]. The PF layer, then, seems essential for F layer formation. However, the identity of the ligand molecule in the PF layer was not known. How could this ligand molecule be found? The strategy was to compare FE with and without the F layer electrophoretically and then isolate the molecule from an F layer extract. The result was a 105-kDa glycoprotein (gp 105) which was present in the PF layer and interacted with cortical granule lectins.

Accepted February 16, 1994
Received December 9, 1993

MATERIALS AND METHODS

Collection of eggs

South African clawed frogs, *Xenopus laevis*, were purchased from a dealer in Hamamatsu, Japan and reared at 22–24°C. Ovulation was induced by injection of 1,000 IU gonadotropin (Gonatropin, Teikoku Zoki Co.) and a sufficient number of oviductal eggs were obtained 7–10 hr after hormone injection. Uterine eggs were obtained by squeezing females every hour after the start of oviposition. Artificial insemination was performed by the method of Moriya [14]. Developmental stages were determined according to the normal table of Nieuwkoop and Faber [15].

Procedures for isolating gp 105

Uterine eggs obtained from 3 females were placed in 0.05 De Boer solution (DB: 110 mM NaCl, 1.3 mM KCl, 1.3 mM $CaCl_2$, 10 mM Tris-HCl, pH 7.4), artificially activated with a 100 V AC current for 10 sec, and left for 30 min in the solution. Eggs were then dejellied by brief treatment with 20 mM dithiothreitol (DTT) in Ca-free 0.05 DB (adjusted to pH 9.0 with NaOH) and washed extensively with 0.05 DB. The F layer was extracted from these dejellied eggs by treatment with 5 mM EDTA in Ca-free 0.05 DB for 10 min. The F layer extract (ca. 100 ml) was dialyzed against distilled water overnight and concentrated to 5 ml by ultrafiltration. A precipitate appeared during the procedure of concentration; this was subsequently centrifuged at 7,000×*g* for 30 min at 4°C. The resulting pellet was suspended in a solution of 20 mM DTT and 5 mM

EDTA in Ca-free 0.05 DB (pH 9.0), freeze-thawed and centrifuged at 1,000×*g* for 15 min. The precipitate was subjected to 7.5% SDS-PAGE. Protein bands were visualized by treatment with 4 M sodium acetate [8]. Sections of 3 mm width at Rf=0.3 were sliced out and cut into several pieces. The gp 105 was extracted electrophoretically from the pieces of gel into 2.5 mM Tris-HCl buffer, pH 8.3, in a Max-Yield Protein Concentrator (Atto Co.) at 5 W for 2.5 hr.

Preparation of egg envelopes and cortical granule lectins

A jelly solution was obtained from activated uterine eggs by DTT-treatment and dialyzed against distilled water. It was then lyophilyzed and dissolved in DB when used.

VE*s were isolated by the method of Wolf *et al.* [24] from eggs whose F layer had been removed. The eggs were crushed by passage through a hypodermic syringe with an 18 G-gauge needle and the VE*s were sieved out through a nylon mesh (82 μm). After thorough washing in distilled water, the VE*s were collected by centrifugation. Before being used, they were suspended in DB with an ultrasonic vibrator.

Egg FEs were isolated from dejellied eggs by the same method as mentioned above. Embryonic FEs were prepared as follows. Embryos were dejellied at stages 17–19 and cultured in 0.05 DB. The FEs were isolated from the embryos manually with watchmaker's forceps. Since dejellied embryos would hatch precociously at stage 28, FEs of later embryos were obtained by incubating the FEs and embryos at stage 28 for 15 hr from the time of reaching stage 28 [32].

Cortical granule lectins were obtained from activated coelomic eggs and purified with an affinity column [29]. The lectins were labeled with colloidal gold prepared by the tannic acid procedure of Slot and Geuze [18]. Lectin-gold complexes were made at 4°C by mixing twice the minimal stabilization amount of lectins with the colloidal gold solution. The mixtures were then centrifuged at 100,000×*g* for 30 min and the precipitates suspended at an approximate concentration of 20 μg/ml lectin in DB solution containing 1% BSA.

Electrophoresis

Slab SDS-PAGE in 7.5% gel was carried out as described by Laemmli [10]. The gels were stained with Coomassie blue or PAS. The molecular weights of the protein were estimated from a calibration curve obtained with the standard proteins in the MW-SDS-200 kit (Sigma). Protein was determined by the method of Smith *et al.* [20] using bicinchoninic acid with BSA as a standard.

Detection of carbohydrates on westernblots

Electrophoresed samples were electroblotted to nitrocellulose membranes. Galactosides were detected using the method developed by Kitagaki-Ogawa *et al.* [9]. The membranes were washed with TBS-Tween solution (10 mM Tris-HCl, pH 7.4, 150 mM NaCl, 0.05% Tween 20). Then they were blocked with 0.3% BSA in TBS-Tween for 1 hr and treated with 10 μg/ml horseradish peroxidase-conjugated peanut agglutinin (HRP-PNA) for 1 hr. Control runs were made either by omitting the treatment with HRP-PNA or by treating the membranes with a mixture of HRP-PNA and 2.5 M galactose. The method of Adams [1] was used to detect HRP.

Preparation of antiserum

Antiserum was raised against isolated gp 105 by injection into rabbits. It was absorbed by glutaraldehyde-fixed pars convoluta (PC) tissue from the oviduct.

Immunoblot

Westernblotted membranes were blocked overnight in a phosphate-buffered saline solution (PBS, pH 7.2) containing 10% normal sheep serum and 4% BSA, treated for 1 hr with the antiserum diluted to 1/50 in PBS containing 4% BSA, and immersed for 1 hr with HRP-conjugated sheep antirabbit IgG according to the method of Smith [19]. A control was established by treating the membranes with non-immune rabbit serum in place of the antiserum. HRP was again detected by the Adams method.

Electron microscopy

Eggs were fixed overnight at 4°C in 2.5% glutaraldehyde in 100 mM cacodylate buffer (pH 7.4), rinsed in buffer, and postfixed for 3 hr in similarly buffered 1% OsO_4. The specimens were dehydrated in acetone and embedded in Quetol 812 (Nisshin EM Co.). Ultrathin sections were stained with uranyl acetate and lead citrate and viewed with a JEOL JEM-100SX electron microscope.

Immunoelectron microscopy

Glutaraldehyde-fixed eggs were dehydrated in ethanol and embedded in Lowicryl K4M (Sigma) at −20°C according to the manufacturer's instructions. Thin sections were mounted on collodion-coated nickel grids. The sections were blocked for 10 min with 0.5% BSA in PBS and washed with PBS. They were then incubated for 1 hr at room temperature with a 1/2,000 solution of antiserum. The sections were subsequently washed with PBS and treated for 1 hr with a gold-conjugated goat antiserum against rabbit IgG (E-Y Lab.). Then they were washed with PBS and with distilled water and stained with uranyl acetate and lead citrate. After staining, the sections were dried and coated with carbon vapor. Control sections were treated with a rabbit non-immune serum and then gold-conjugated goat antiserum. There was no significant labeling on the control sections.

Electron microscopic detection of carbohydrates

Ultrastructural localization of carbohydrates was detected by the periodic acid-chromic acid-silver methenamine (PA-CrA-Silver) method according to Rambourg *et al.* [17]. Glutaraldehyde-fixed specimens were dehydrated and embedded in Quetol 812. Thin sections were placed on uncoated stainless-steel grids for staining with PA-CrA-Silver. Control runs were made by treating the sections with silver methenamine without previous oxidation.

Assay of interaction of cortical granule lectins with gp 105

Westernblotted membranes were blocked overnight in DB solution containing 1% BSA and treated for 3 hr with gold-conjugated cortical granule lectins in DB solution containing 1% BSA. Controls were established by treating membranes with the gold-conjugated lectins plus either galactose (1 M) or EDTA (1 mM). The membranes were then processed for silver enhancement with a silver enhancing kit (Bio-Rad).

RESULTS

Isolation of gp 105 from the fertilization layer

The fertilization envelope (FE) consists of a vitelline envelope (VE*) and a fertilization (F) layer in *Xenopus* (Fig. 1A). The F layer was exposed by removal of the jelly with

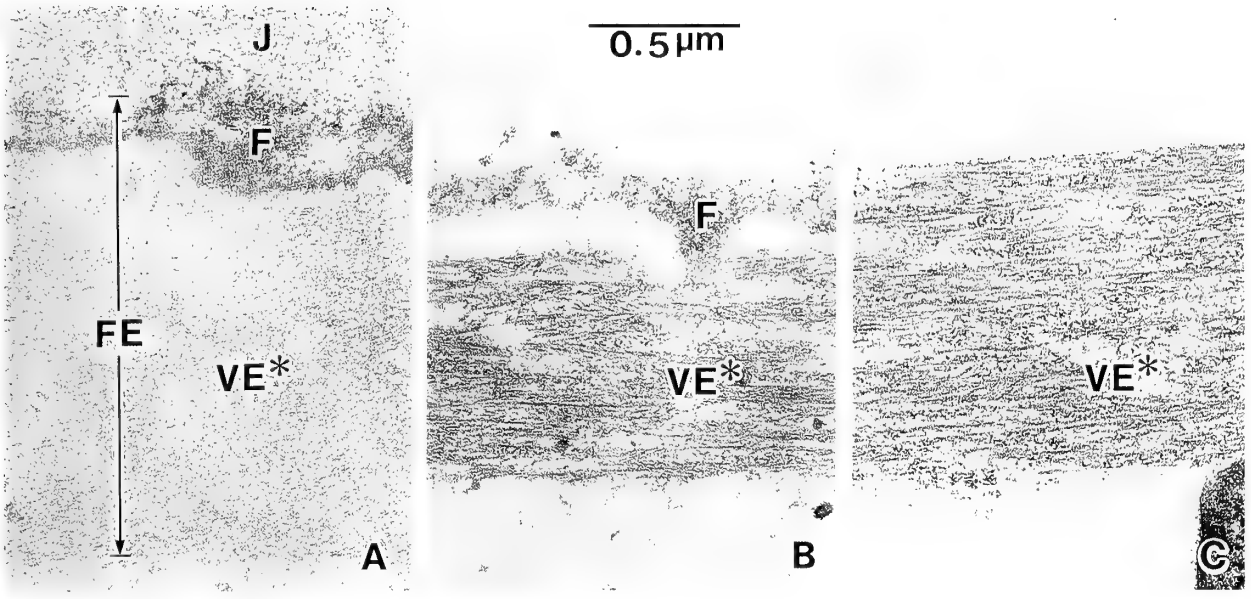

FIG. 1. Electron micrographs showing cross sections of egg envelopes of activated eggs (A), of envelopes whose jelly was removed with 20 mM DTT (B), and of an envelope whose fertilization (F) layer was removed with 5 mM EDTA (C). FE, fertilization envelope; VE*, modified vitelline envelope in the FE.

DTT (Fig. 1B) and was collected after solubilization with EDTA (Fig. 1C). Although DTT may have affected the morphology of the envelopes, as the F layer was loosened from the VE* because of DTT's low salinity, at this stage of investigation, clearer separation of the jelly and the F layer was desirable. The VE* appeared to decrease in width after jelly removal.

Electrophoretic profiles of FEs were compared with those of VE*s to find the constituents of the F layer (Fig. 2). A glycoprotein of 105 kDa (gp 105) appeared with Coomassie blue staining in the profile of the FE but not of the VE* (Fig. 2A), whereas no difference was observed with PAS staining (Fig. 2B). It was also confirmed that gp 105 is not a constituent of the jelly layers (Fig. 2, lane 3). Thus gp 105 is a constituent of the F layer. Although it was expected that 39–46-kDa protein bands of cortical granule lectins [29] would be present in the profiles of FE, the present study failed to show any lectin bands. The amount of the lectins contained in the FE loaded may have been subminimal for detection and/or they may have been hidden by relatively large amounts of gp 41.

Fig. 3 shows SDS-PAGE profiles of preparations at each step of the isolation procedure. Crude F layer extract (lane 1) was centrifuged at 7,000×*g* for 30 min; the pellet (lane 2) was suspended once in a 5 mM EDTA-20 mM DTT solution, freeze-thawed and reprecipitated by centrifugation at 1,000×*g* for 15 min. This 1,000×*g* precipitate (lane 3) contained glycoproteins of 105, 100, 30 and 29 kDa. The 105-kDa band in lane 3 was sliced out and the glycoprotein extracted electrophoretically. The extract (lane 4) gave a single band of gp 105 after reelectrophoresis.

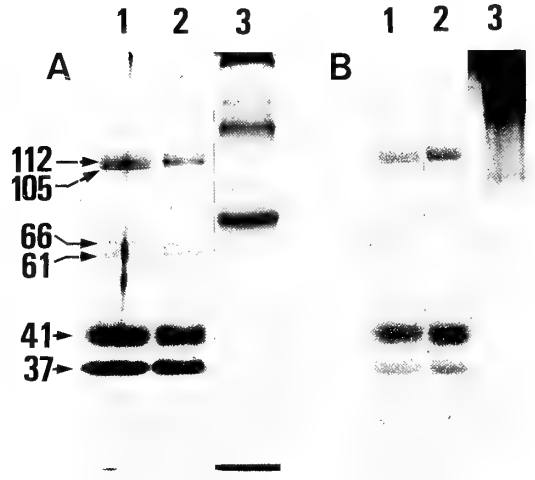

FIG. 2. SDS-PAGE of FE (5 μg, lane 1), VE* (5 μg, lane 2) and jelly (5 μg, lane 3) stained with Coomassie blue (A) or PAS (B). A 105-kDa glycoprotein (gp 105) can be seen only in the FE stained with Coomassie blue. In this and subsequent figures the molecular weights are indicated on the left in kilodaltons.

Immunoblotting demonstration of gp 105 in F layer

Figure 4A shows immunoblots of the 1,000×*g* precipitate (lane 1), FE (lane 2), VE* (lane 3) and jelly (lane 4). The membranes were treated with an antiserum raised against gp 105. There was significant staining on gp 105 and gp 100 in the 1,000×*g* precipitate of the F layer extract and on gp 105 in the FE but no specific staining on the VE* and the jelly. The degree of stainability on gp 37 of the FE and VE* was the same as that on the control (Fig. 4B); thus the staining on gp 37 was not specific.

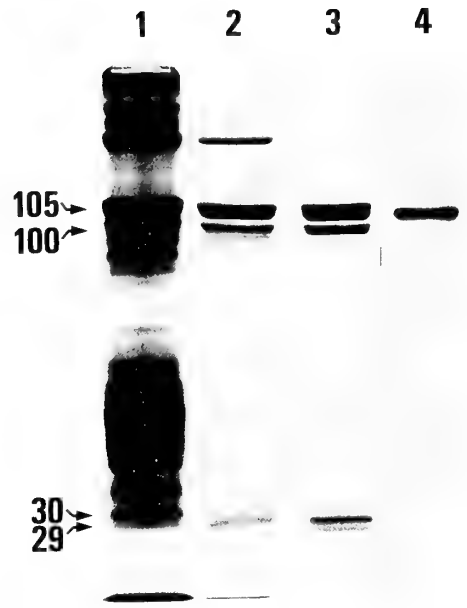

FIG. 3. SDS-PAGE of F layer extract at each step of the isolation procedure. Lane 1, crude extract (20 μg); lane 2, 7,000$\times g$ precipitate (15 μg) of the crude extract; lane 3, 1,000$\times g$ precipitate (15 μg) of the 7,000$\times g$ precipitates after suspension in a 5 mM EDTA-20 mM DTT solution and centrifugation; lane 4, gp 105 (5 μg) extracted from the lane 3 precipitate.

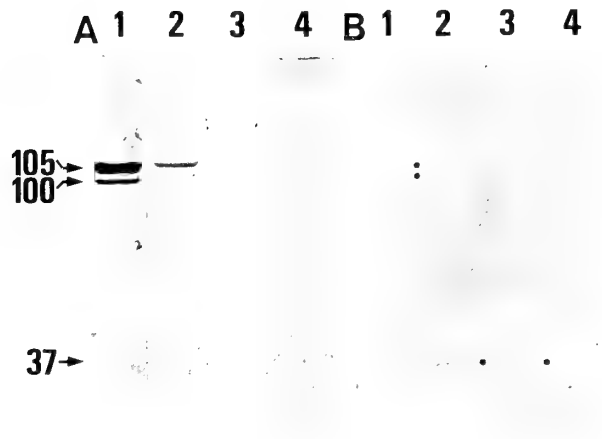

FIG. 4. Immunoblot analysis of a 1,000$\times g$ precipitate of F layer extract (10 μg, lane 1), FE (20 μg, lane 2), VE* (20 μg, lane 3) and jelly (10 μg, lane 4). Membrane A was treated with an antiserum to gp 105. There was staining on gp 105 and gp 100 in the F layer extract and gp 105 in the FE. Membrane B was treated with non-immune serum and shows faint staining on gp 105, gp 100 and gp 37 (to left of dots).

The experiments just discussed showed that gp 105 is a component of the FE but not its location. To localize gp 105 in the FE, the same immunoblotting procedure as above was performed on FEs obtained from embryos at stages 22, 26, 28 and from the 28+15 hr culture. gp 37 staining was used as a control for protein loading. The stainability on gp 105 increased during the hatching period (Fig. 5), which indicates that the relative amount of gp 105 gradually increased in the

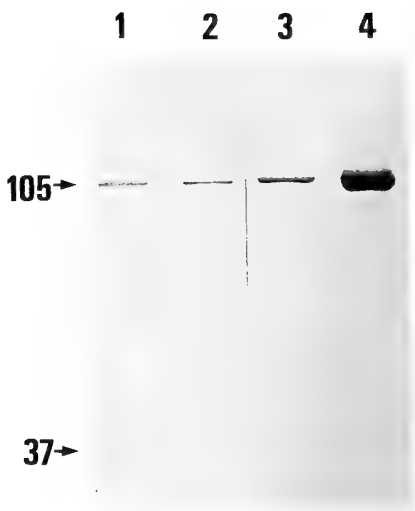

FIG. 5. Immunoblot analysis of FEs from embryos at various stages showing increased amounts of gp 105 as development proceeds. The amounts of FEs loaded in each lane were adjusted such that the amounts of gp 37 appeared approximately the same, in order to provide a control. Lane 1, stage 22; lane 2, stage 26; lane 3, stage 28; lane 4, stage 28+15 hr culture, as described in MATERIALS AND METHODS.

FEs during the hatching process. Since previous ultrastructural observations showed that the F layer remained substantially unaffected even after the VE* portion of the FE was completely digested by the hatching enzyme [32], it seems that gp 105 resides in the F layer.

Immunoelectron microscopical localization of gp 105 in eggs

Sections of eggs obtained from various parts of oviducts were treated with antiserum against gp 105 and then with gold-conjugated goat antiserum, followed by electron microscope observation. Gold particles were absent in eggs obtained from the pars recta 1 (PR1)(Fig. 6A). In PR2 eggs they were present on the layer covering the outer surface of the vitelline envelope (VE), that is, the pre-fertilization (PF) layer (Fig. 6B). A gold-labeled PF layer lay between the VE and the innermost jelly layer in eggs obtained from the pars convoluta 1 (PC1; Fig. 6C), and it occasionally invaginated deeply into the VE in uterine eggs (Fig. 6D). The PF layer appeared to be compressed by the jelly layer. The jelly layer was substantially free of the gold labeling. These observations indicate that gp 105 resides in the PF layer of oviductal eggs which have passed through the PR2.

Figure 7 shows a section of activated eggs treated with the same two antisera as above. The F layer could be divided into two areas, a condensed region immediately adjacent to the outer margin of the VE* and a dispersed region peripheral to the condensed one [5, 23]. The gold particles were limited to the dispersed region.

Biochemical and ultrastructural demonstration of carbohydrates

Since carbohydrate residues are always found with ligand molecules of lectins, they were tested for in the gp 105. PAS

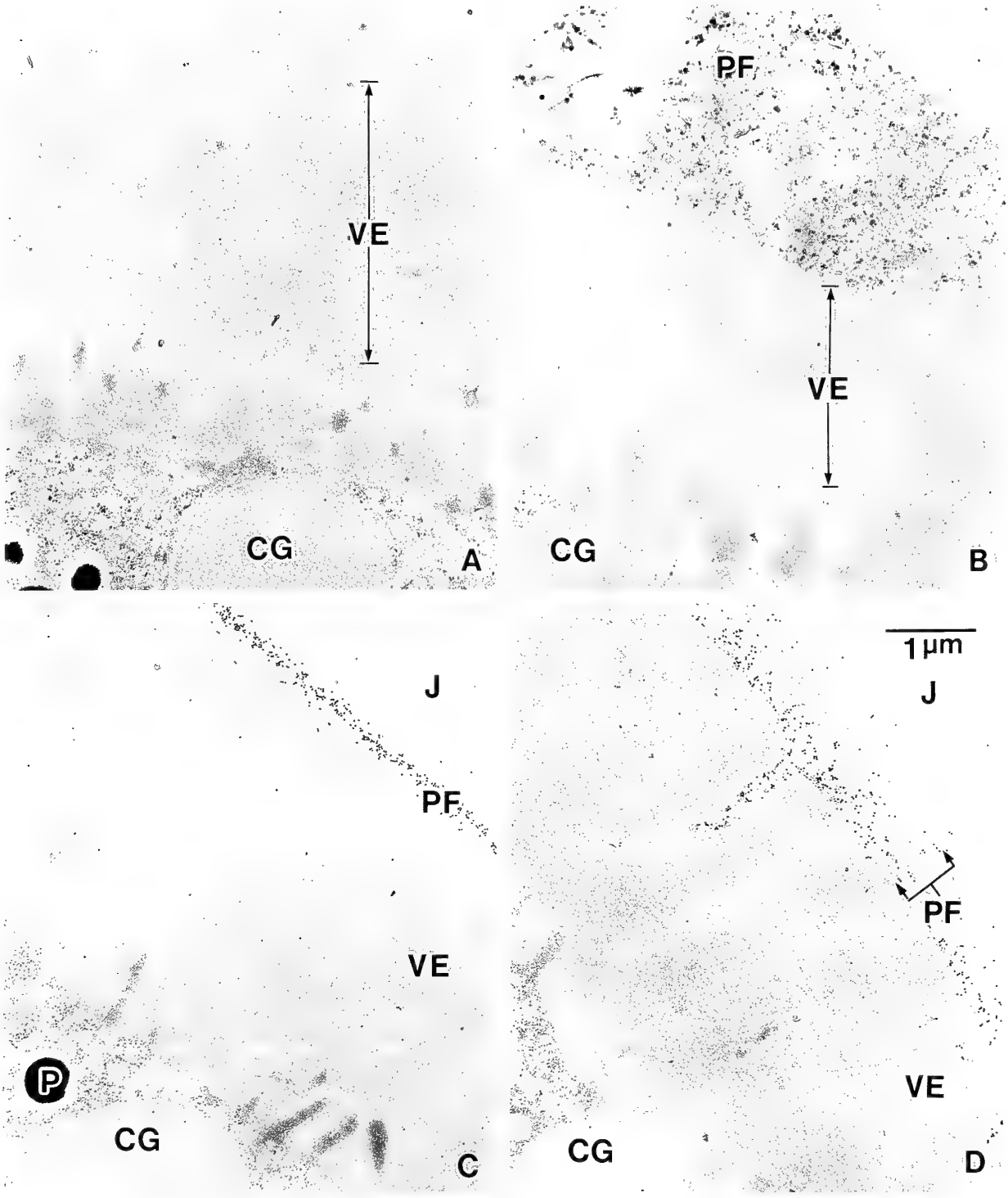

FIG. 6. Immunoelectron micrographs of sections of eggs from the pars recta 1 (A), pars recta 2 (B), pars convoluta 1 (C), and the uterus (D) of the oviduct. Gold particles indicating the location of gp 105 reside in the pre-fertilization (PF) layer adhering to the outer surface of the vitelline envelope (VE) in pars recta 2 eggs and between the VE and the jelly (J) layer in pars convoluta 1 eggs. Occasionally they invaginate into the VE in uterine eggs. CG, cortical granule; P, pigment geranule.

staining on gels of SDS-PAGE did not mark gp 105. (See Fig. 2B again). However, HRP-PNA stained gp 105 and gp 100 in the 1,000×*g* precipitate of F layer extract and gp 105, gp 66/61 and gp 37 in the FE (Fig. 8A, C). Galactose significantly decreased the staining (Fig. 8B). These results suggest that gp 105 possesses, although in very small amounts, carbohydrates of a galactoside nature.

Sections of oviductal or activated eggs were also treated

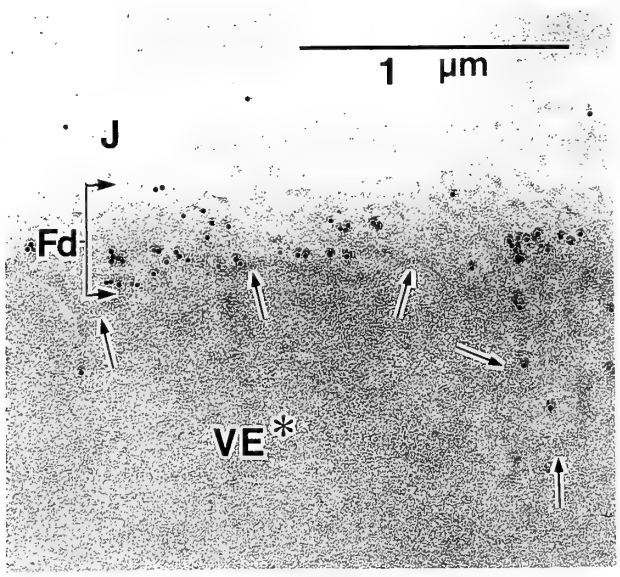

FIG. 7. Immunoelectron micrograph of a section of activated egg. Gold particles are present on the dispersed region of the fertilization (Fd) layer but absent from its condensed regions (arrows). J, jelly layer; VE*, modified vitelline envelope.

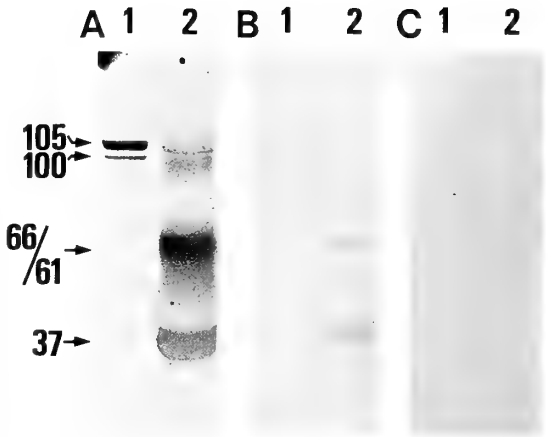

FIG. 8. Detection of galactosides on westernblots of a 1,000×*g* precipitate of the F layer extract (10 μg, lane 1) and of FE (30 μg, lane 2) by treatment with HRP-PNA (A), HRP-PNA plus galactose (B) or no treatment (C). The gp 105 and gp 100 in the F layer extract and the gp 105, gp 66/61 and gp 37 in the FE are stained (A). Galactose significantly decreases the staining (B).

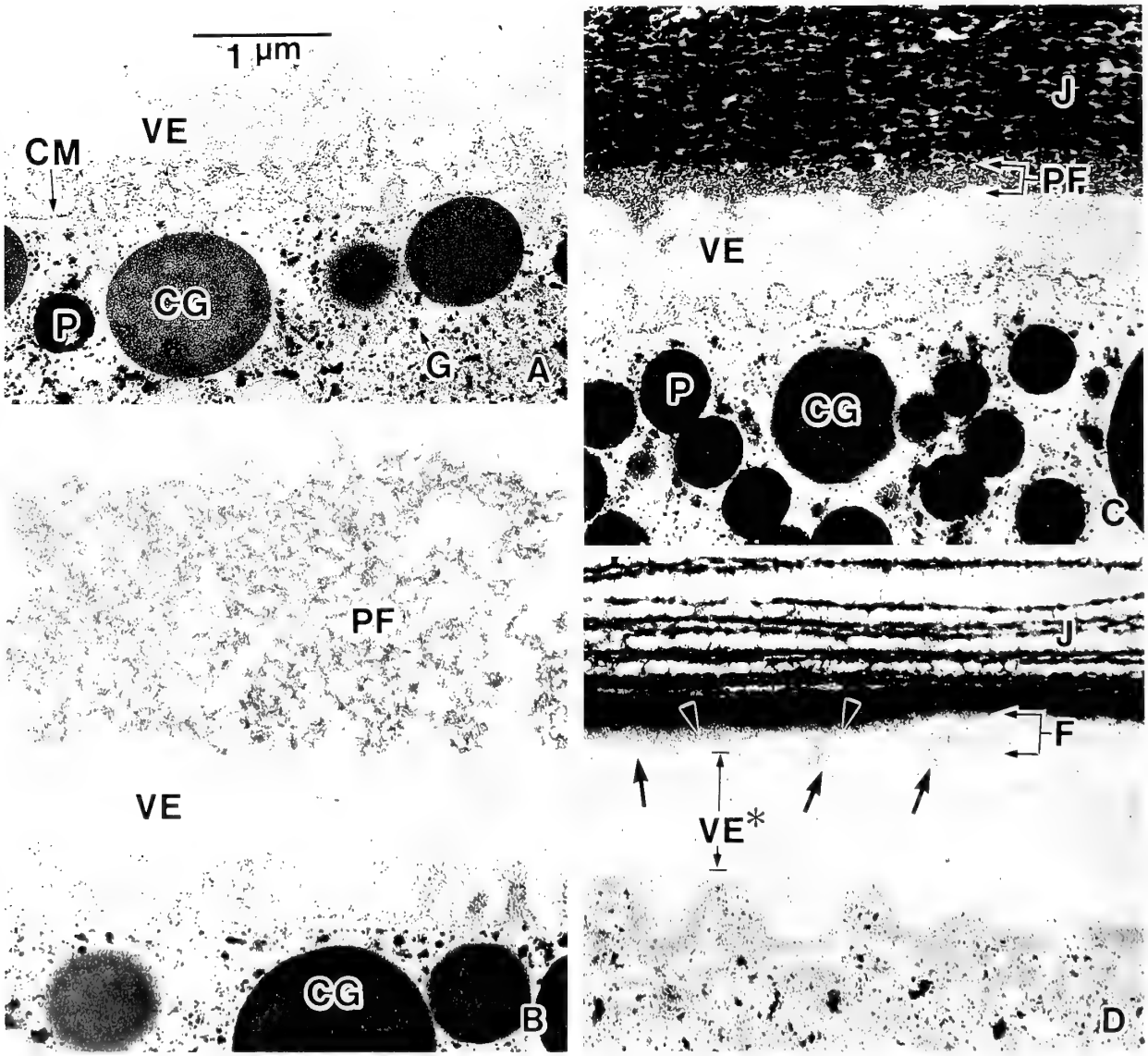

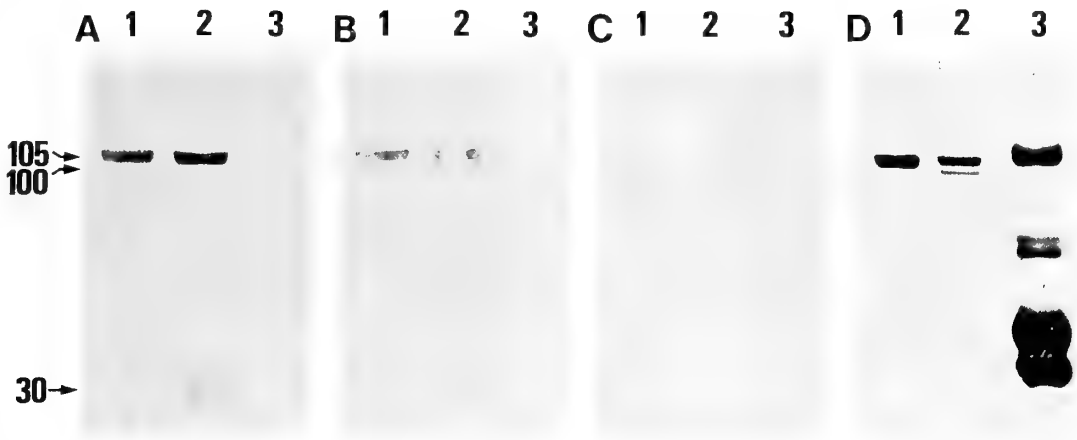

FIG. 10. Interaction of gp 105 with cortical granule lectins. Westernblots of isolated gp 105 (10 μg, lane 1), of a 1,000×g precipitate of the F layer extract (10 μg, lane 2) and FE (30 μg, lane 3) were treated with gold-conjugated lectins alone (approximately 20 μg/ml lectins; A) or with gold-conjugated lectins plus either galactose (1 M; B) or EDTA (1 mM; C). Blotting membranes were further treated with a silver enhancing kit. D, membrane stained with Coomassie blue.

according to the PA-CrA-Silver method for detecting carbohydrates (Fig. 9). In PR1 eggs (Fig. 9A), silver precipitates indicating the location of carbohydrates were present on the cell membrane, cortical granules and glycogen granules. The VEs of these eggs were not stained by the silver, but the PF layer in PR2 eggs (Fig. 9B) and uterine eggs (Fig. 9C) were. The jelly layer in uterine eggs was also stained, but a difference in stainability between the PF layer and the jelly layer is evident, since the silver precipitates on the PF layer are fine whereas those on the jelly layer are coarse and more tightly packed (Fig. 9C). In activated eggs (Fig. 9D), the dispersed region of the F layer was stained by the silver but its condensed region not.

Interaction of gp 105 with cortical granule lectins

Figure 10 shows westernblots of the isolated gp 105, a 1,000×g precipitate of F layer extract and FE. Gold-conjugated cortical granule lectins stained gp 105 in the first two samples (Fig. 10A). The staining on gp 105 in FE was weak, which may be due to a relatively low amount of gp 105 in FE. gp 100 and gp 30 of the 1,000×g precipitate were also stained. Galactose and EDTA, which are inhibitors of lectins [16, 28, 29], decreased the staining (Fig. 10B, C). Such results constitute evidence of the occurrence of a lectin-ligand reaction between gp 105 and the cortical granule lectins, thus indicating gp 105 is a ligand molecule of the lectins.

DISCUSSION

gp 105, a natural ligand to cortical granule lectins

In *Xenopus* the F layer becomes apparent after fertilization as an electron-dense layer between the VE* and the innermost jelly layer [25, 31]. Involvement of cortical granule lectins in the reaction forming the F layer was suggested by Wyrick *et al.* [25] and the localization of the lectins in the F layer was demonstrated by immunoelectron microscopy [30]. However, the identity of the ligand molecule binding to the lectins has been disputed [25, 31].

In the present study gp 105 was isolated from an extract of the F layer. On immunoblot and immunohistochemical test evidence, this glycoprotein is apparently not a component of the jelly. That gp 105 is a constituent of the F layer was suggested by the increase in the relative amount of gp 105 in FEs during the hatching process, an increase which coincides well with the previous ultrastructural finding that the F layer remained substantially unaffected even after the VE* portion of the FE was completely digested [32]. Gold particles indicating the location of gp 105 by immunoelectron microscopy were present on the PF layer of uterine eggs, distributed in the same area as that comprising the F layer of fertilized eggs according to Grey *et al.*[5]. Furthermore, binding of gold-conjugated cortical granule lectins to gp 105 on westernblotted membranes demonstrated that lectin-ligand reactions occur. The PF layer is the first extracellular matrix outside the VE met by cortical granule lectins as they emanate from the egg surface and extrude through the VE

FIG. 9. Ultrastructural localization of carbohydrates by application of the PA-CrA-Silver method to sections of egg from the pars recta 1 (A), pars recta 2 (B), uterus (C) and uterine egg after activation (D). Silver particles appear on both the pre-fertilization (PF) layer (B and C) and the jelly (J) layer (C and D), but those on the PF layer are fine whereas those on the J layer are coarse and more tightly packed. In activated egg (D), the dispersed region of the fertilization (F) layer is stained by the silver (arrowheads) but the condensed region of the F layer (which is visible as a line marked by the arrows) is not. CG, cortical granule; CM, cell membrane; G, glycogen granule; P, pigment granule; VE, vitelline envelope; VE*, VE of activated egg.

[22]. Then the natural ligand of the lectins seems to be the gp 105 in the PF layer.

Resistance to treatment by reducing reagents such as DTT is one of the characteristics of the F layer [23]. The PF layer, however, was dissolved in conjunction with the jelly when treated with mercaptoethanol (see, Wolf *et al.* [24]). A DTT-stable layer could be produced by activating PR2 eggs whose external surface was covered by the PF layer [31] or by treating them with lectins [28]. The present study demonstrated diminution in both the antigenicity of gp 105 and its stainability by the PA-CrA-Silver method at the time of change from PF to F layer. This diminution is understandable if the respective reactive sites on gp 105 are being hidden by added cortical granule lectins, as discussed later. Differential response to DTT between the PF layer and the F layer can be understood along the same lines.

The present study suggested that gp 105 is supplied to eggs at the PR2 of the oviduct. Previous studies have shown that an antiserum against secretory granules of the PR2 stained the PF layer [26, 31], suggesting a PR2 origin for PF layer substances. There are two types of secretory cells in the PR2 and PC1, respectively [27]. An intact antiserum raised against gp 105 in the present study stained not only both types of secretory cells in the PR2 but also one type of secretory cell at the ridge in the PC1 (unpublished). However, when absorbed by the PC1, the antiserum completely lost its ability to stain the cells of either the PC1 or PR2 (unpublished) but retained the ability to stain gp 105. The antiserum may recognize an epitope which is newly produced by an interaction between substances secreted by cells in the PR2.

The gp 100 in F layer extract exhibited the same antigenicity, HRP-PNA stainability and gold-conjugated cortical granule lectin binding as gp 105. It did not appear in the FEs but only in the extract. Since an antiserum raised against gp 105 and absorbed by both the jelly and ovarian homogenates still retained the ability to bind with gp 100 (unpublished), gp 100 is not a contaminant from the jelly, VE, or cellular components of the eggs. gp 100 may be a degraded form of gp 105, since it did not appear when the entire isolation procedure was performed in the presence of the protease inhibitors PMSF (1 mM) and aprotinin (1 μg/ml) (unpublished). Possible agents of degradation are trypsin-like and chymotrypsin-like enzymes [12, 13], both of which are released extracellularly from their binding sites after activation. The gp 30 in the F-layer extract also exhibited gold-conjugated cortical granule lectin binding but did not show HRP-PNA stainability nor antigenicity like gp 105. Thus gp 30 is different from gp 105.

The SDS-PAGE profiles of FE in Figure 2 do not show all of the substances seen in those of Gerton and Hedrick [4]. Proteins of 120 kDa and 57 kDa do not appear in this study. The absence of 120-kDa protein is probably due to the difference in the amount of FE loaded, 5 μg in the present study but 25 μg in Gerton and Hedrick's. gp 105 migrates on SDS-PAGE very close to gp 112 and they fuse with each other when there are large amounts of FE, so that in this study smaller amounts of FE than usual were chosen in order to separate the two glycoproteins. The 57-kDa protein also failed to appear in this study even though 30 μg FEs were loaded, as seen in Figure 10D. The reason for its absence is not clear yet. It is possible that the 57-kDa protein may have been removed from the FEs during the dejellying process in this study. To clearly separate the jelly from the FEs, this study exploited a Ca-free, 0.05 DB solution (a medium containing reducing agents), whereas Gerton and Hedrick adopted a full-strength DB solution. Further studies are needed to explain why the 57-kDa protein did not appear.

Carbohydrates in gp 105

Carbohydrate residues must be demonstrated in order to claim that a particular substance is in fact a ligand. Carbohydrates were detected histochemically in the PF layer and biochemically by the HRP-PNA method in gp 105. The PNA shares carbohydrate-specificity for galactosides with the cortical granule lectins [16, 28, 29]. Apparently, however, there is very little carbohydrate in gp 105, since it was not stained with the PAS method.

There seems to be a discrepancy with respect to histochemical results: PA-CrA-Silver staining, which detects carbohydrates ultrastructurally, stained cortical granules and the PF layer in unfertilized eggs but did not stain the F layer in activated eggs. gp 105 is glycosylated, as mentioned above, and so are cortical granule lectins [16]. With present knowledge, it is difficult to explain the failure in histochemical detection of F-layer carbohydrates, since they are produced by interactions of two biochemically defined glycoproteins. It seems possible that carbohydrate moieties of gp 105 are being bound by lectins in such a way or at such binding sites that the carbohydrate is unavailable for staining in the condensed region of the F layer (see Fig. 9). This region probably corresponds to the area of increased electron density under conventional heavy metal staining [5, 25, 31], which suggests the presence of some additional substance in the F layer, namely, lectins. Taken together, the increase in electron density and the absence of PA-CrA-Silver staining indicates that some reaction has occurred during fertilization; the next studies need to examine exactly how carbohydrate moieties of the cortical granule lectins behave at the time of binding with gp 105.

Ligand molecules in the jelly layer

Since cortical granule lectins can react with the jelly, the jelly layer has been proposed as the site of ligand molecules [25]. Using immunoelectrophoretic analyses, Birr and Hedrick [2] observed three jelly coat ligands bound by cortical granule lectins; two of the three (L-1 and L-2) were sulfated and one (L-3) not. Since L-3 was present in low concentration relative to other components in total jelly solutions and it cross-reacted with anti-envelope sera but not with anti-total jelly sera, they speculated that L-3 is a component of the PF

layer. However, neither association of L-3 with the PF layer nor its molecular weight has been established yet. It has already been shown that in PF layer-depleted eggs, secreted lectins produced an electron-dense layer in the space between the outer surface of the VE* and the inner surface of the jelly layer but were dissolved together with the jelly when treated with DTT [31], suggesting that secreted lectins reacted with the jelly at the innermost surface of its layer but did not penetrate deeply into the jelly layer, and that most of the lectins accumulated in the space. Thus L-1 and L-2 (and perhaps L-3), associated with the innermost jelly coat layer, may be ligands to the cortical granule lectins and seem certain to have a role in natural fertilization. The relationship of these substances to gp 105 might warrant investigation.

The jelly layer may act as a block to outward diffusion of cortical granule lectins. Limited distribution of secreted lectins was demonstrated in activated eggs immunoelectron microscopically [30]: gold particles indicating the locations of the lectins were present in the perivitelline space, on the VE*, and on the F layer, but not on the jelly. Previous observations on morphological and biochemical changes in the FEs suggested that the F layer is resistant to the hatching enzyme secreted by hatching embryos [32]. A thick F layer might be disadvantageous for embryos to break through. As shown in the present study, the PF layer is compressed by externally loaded jelly layers during jelly deposition around the eggs. The jelly layer may minimize the space in which the F layer will be formed but, by blocking dispersing lectins at its innermost surface, guarantee sufficient lectin-gp 105 interactions for production of a polyspermy block.

The present study claims that the F layer is formed by the interaction of gp 105 with cortical granule lectins, but it does not preclude other as yet unrecognized elements of the F layer from candidacy for ligand molecule to the lectins. In particular, immunoelectrophoretically identified ligands of the jelly noted by Birr and Hedrick [2] may also be found in the F layer, for the jelly seems to participate in F layer formation, as discussed above, and the boundary between the jelly layer and F layer is not absolute. That multiple types of secretory cells are involved in producing the extracellular matrix of eggs [27] also suggests the existence of multiple ligand molecules in the F layer. Thus further study is needed to explore other ligand molecules than gp 105 in this layer.

ACKNOWLEDGMENTS

I wish to thank Dr. H. Kubota of Kyoto University for instruction in immunoelectron microscopy and Ms. M. Lynne Roecklein for reading the manuscript.

REFERENCES

1 Adams JC (1981) Heavy metal intensification of DAB-based HRP reaction product. J Histochem Cytochem 29: 775

2 Birr CA, Hedrick JL (1992) Immunoelectophoretic identification of jelly coat ligands bound by the cortical granule lectin from *Xenopus laevis* eggs. Dev Growth Differ 34: 91–98

3 Chamow SM, Hedrick JL (1986) Subunit structure of a cortical granule lectin involved in the block to polyspermy in *Xenopus laevis*. FEBS Letters 206: 353–357

4 Gerton GL, Hedrick JL (1986) The vitelline envelope to fertilization envelope conversion in eggs of *Xenopus laevis*. Dev Biol 116: 1–7

5 Grey RD, Wolf DP, Hedrick JL (1974) Formation and structure of the fertilization envelope in *Xenopus laevis*. Dev Biol 36: 44–61

6 Grey RD, Working PK, Hedrick JL (1976) Evidence that the fertilization envelope blocks sperm entry in eggs of *Xenopus laevis:* Interaction of sperm with isolated envelopes. Dev Biol 54: 52–60

7 Hedrick JL, Nishihara T (1991) Structure and function of the extracellular matrix of anuran eggs. J Electron Microsc Tech 17: 319–335

8 Higgins RC, Dahmus ME (1979) Rapid visualization of protein bands in preparative SDS-polyacrylamide gels. Anal Biochem 93: 257–260

9 Kitagaki-Ogawa H, Matsumoto I, Seno N, Takahashi N, Endo S, Arata Y (1986) Characterization of the carbohydrate moiety of *Clerodendron trichotomum* lectins. Eur J Biochem 161: 779–785

10 Laemmli UK (1970) Cleavage of structural proteins during the assembly of the head of bacteriophage T4. Nature (London) 227: 680–685

11 Larabell C, Chandler DE (1991) Fertilization-induced changes in the vitelline envelope of echinoderm and amphibian eggs: self-assembly of an extracellular matrix. J Electron Microsc Tech 17: 294–318

12 Lindsay LL, Hedrick JL (1989) Proteases released from *Xenopus laevis* eggs at activation and their role in envelope conversion. Dev Biol 135: 202–211

13 Lindsay LL, Larabell CA, Hedrick JL (1992) Localization of a chymotrypsin-like protease to the perivitelline space of *Xenopus laevis* eggs. Dev Biol 154: 433–436

14 Moriya M (1976) Required salt concentration for successful fertilization of *Xenopus laevis*. J Fac Sci Hokkaido Univ Ser VI 20: 272–276

15 Nieuwkoop PD, Faber J (1967) Normal Table of *Xenopus laevis* (Daudin). North-Holland Publ, Amsterdam

16 Nishihara T, Wyrick RE, Working PK, Chen YH, Hedrick JL (1986) Isolation and characterization of a lectin from the cortical granules of *Xenopus laevis* eggs. Biochemistry 25: 6013–6020

17 Rambourg A, Hernandez W, Leblond CD (1969) Detection of complex carbohydrates in the Golgi apparatus of rat cells. J Cell Biol 40: 395–414

18 Slot JW, Geuze HJ (1985) A new method of preparing gold probes for multiple-labeling cytochemistry. Eur J Cell Biol 38: 87–93

19 Smith JC (1987) A mesoderm-inducing factor is produced by a *Xenopus* cell line. Development 99: 3–14

20 Smith PK, Krohn RI, Hermanson GY, Mallia AK, Gartner FH, Provenzano MD, Fujimoto EK, Goeke NM, Olson BJ, Klenk DC (1975) Measurement of protein using bicinchoninic acid. Anal Biochem 150: 76–85

21 Urch UA, Hedrick JL (1981) The hatching enzyme from *Xenopus laevis:* Limited proteolysis of the fertilization envelope. J Supramol Str Cell Biochem 15: 111–117

22 Wolf DP (1974) The cortical granule reaction in living eggs of the toad, *Xenopus laevis*. Dev Biol 36: 62–71

23 Wolf DP (1974) On the contents of the cortical granules from

Xenopus laevis. Dev Biol 38: 14–29

24 Wolf DP, Nishihara T, West DM, Wyrick RE, Hedrick JL (1976) Isolation, physicochemical properties, and the macromolecular composition of the vitelline and fertilization envelope from *Xenopus laevis* eggs. Biochemistry 15: 3671–3678

25 Wyrick RE, Nishihara T, Hedrick JL (1974) Agglutination of jelly coat and cortical granule components and the block to polyspermy in the amphibian *Xenopus laevis*. Proc Natl Acad Sci USA 71: 2067–2071

26 Yoshizaki N (1984) Immunoelectron microscopic demonstration of the pre-fertilization layer in *Xenopus* eggs. Dev Growth Differ 26: 191–195

27 Yoshizaki N (1985) Fine structure of oviducal epithelium of *Xenopus laevis* in relation to its role in secreting egg envelopes. J Morphol 184: 155–169

28 Yoshizaki N (1986) Properties of the cortical granule lectin isolated from *Xenopus* eggs. Dev Growth Differ 28: 275–283

29 Yoshizaki N (1989) Comparison of two lectins isolated from *Xenopus* cortical granules. Zool Sci 6: 507–514

30 Yoshizaki N (1989) Immunoelectron microscopic demonstration of cortical granule lectins in coelomic, unfertilized and fertilized eggs of *Xenopus laevis*. Dev Growth Differ 31: 325–330

31 Yoshizaki N, Katagiri C (1984) Necessity of oviducal pars recta secretions for the formation of the fertilization layer in *Xenopus laevis*. Zool Sci 1: 255–264

32 Yoshizaki N, Yamasaki H (1991) Morphological and biochemical changes in the fertilization coat of *Xenopus laevis* during the hatching process. Zool Sci 8: 303–308

ZOOLOGICAL SCIENCE 11: 285–290 (1994)

Localization and Purification of Serum Albumin in the Testis of *Xenopus laevis*

MASAHISA NAKAMURA[1], TOMOYO YAMANOBE* and MINORU TAKASE

*Laboratory for Amphibian Biology, Faculty of Science, Hiroshima University, 1-3-1 Kagamiyama, Higashi-Hiroshima, Hiroshima 724, and *Central Laboratory of Analytical Biochemistry, School of Medicine, Teikyo University, 2-11-1 Kaga, Itabashi-ku, Tokyo 173, Japan*

ABSTRACT—The distribution of serum albumin is of interest in the *Xenopus (X.) laevis* testis, since albumin is probably a major protein that binds testosterone (T) in the plasma and interstitial fluid. This study was undertaken to determine the localization and purification of serum albumin in the *X. laevis* testis. The interstitial tissue and spermatogonia immunoreacted strongly with a sheep antiserum raised against *X. laevis* albumin. A weak staining was also seen in spermatocytes and early spermatids, but there was no staining in Sertoli cells. In order to clarify whether serum albumin was really localized on the surface of testicular cells in the *X. laevis* testis, a membrane-rich fraction was prepared from testes and extracted with 0.6 M KCl. The KCl extract was then subjected to gel filtration, ammonium sulfate precipitation and high-performance liquid chromatography (HPLC). A protein with Mr=74 kD was obtained by this procedure and its NH_2-terminal amino acid sequence was determined. The sequence of the first 19 amino acids was DTDADXXKXIADVYTALTE, suggesting that this protein was identical to serum albumin (Mr=74 kD). When the membrane fraction of blood cells in this animal was handled in the same manner, no appreciable amount of albumin was detected. These results suggest that the 74 kD serum albumin, possibly associated with bound T, may play an important role in the differentiation of germ cells during spermatogenesis of *X. laevis* testis.

INTRODUCTION

Sperm formation, spermatogenesis, is the result of a complex process of biochemical and morphological differentiation of germ cells. Pituitary gonadotropins and steroid hormones control spermatogenesis [20–22]. As yet, the stage-specificity of hormonal control of spermatogenesis remains unclear. In order to clarify the stage-specificity of steroid hormonal control of this process, immunohistochemical studies have been performed in the mammalian testis using antibodies raised against serum albumin, because this protein has a high capacity to bind T [5] and serves as the major protein transporting T in the plasma and interstitial fluids in adult rats [4]. It is probable that albumin acts on Leydig cells and stimulates steroidogenesis of these cells [5]. In fact, Christensen *et al.* [3] showed under electron-microscopic immunocytochemistry that albumin was localized on the surface of Leydig cells in rat testis, and that immunoreactivity extended between Sertoli cells as well as around spermatogonia and early spermatocytes, but albumin was not present beyond Sertoli cell junctions. In human testis, albumin was observed in Sertoli cells, secondary spermatocytes and early spermatids [6, 15]. The precise localization of albumin within the testis is still controversial.

In amphibians, the regulation of spermatogenesis by steroid hormones is not clear except that T may be required for spermatid formation [17]. This study was undertaken to determine the localization of serum albumin in the *X. laevis* testis, and also to confirm by purifying this protein from the membrane fraction that albumin is really localized on the surface of testicular cells.

Accepted February 26, 1994
Received January 12, 1994
[1] To whom request of reprint should be addressed

MATERIALS AND METHODS

Experimental animals

Adult male *X. laevis* (50–70 gm) were used for all the experiments.

Immunohistochemistry

Testes were fixed in Bouin's solution and further treated according to conventional histological technique. Sections (approximately 5 μm thick) were cut on a microtome (Yamato), placed on alcohol-washed slides, and warmed on a hot plate for 3 hr and then rehydrated in phosphate buffered saline (PBS; pH 7.4) for 10 min. The avidin-biotin-peroxidase complex (ABC) method [8] was used for immunohistochemical stainings using sheep antisera raised against *X. laevis* albumin (a gift of Dr. D. R. Schöenberg) at a 1: 15000 dilution in PBS.

Purification of a 74 kD protein (albumin)

To confirm whether albumin was really localized on the surface of testicular cells, albumin was purified from the membrane-rich fraction of *X. laevis* testes. The membrane-rich fraction of testes was prepared by the method of Millette *et al.* [12]. Testes were removed, wiped with Kimwipes around the tissue, frozen immediately in liquid nitrogen and stored at −80°C until use. Frozen testes were then thawed and homogenized with a glass-Teflon homogenizer in 40 ml of TBS buffer containing 0.16 M NaCl, 3 mM $MgCl_2$, 5 mM KCl in 10 mM Tris-HCl (pH 7.4 at 4°C) [12]. The homogenate was centrifuged at 1000 g for 10 min at 4°C to remove large aggregates and debris. The supernatant was used for preparation of plasma membranes by centrifugation on discontinuous sucrose gradients in TBS. Exactly 2.5 ml of the supernatant was mixed with 2.5 ml of

80% sucrose (w/v) to yield 5 ml of 40% sucrose containing membranes. All the 40% sucrose material (5 ml) was layered on top of 2 ml of 45% sucrose (w/v) in TBS in a cellulose nitrate centrifuge tube (Hitachi RPS 40T). Two ml of 30% sucrose (w/v) in TBS were then layered above the 40% sucrose, followed by 1 ml of TBS to fill the tube. Gradients were centrifuged at 125,000 g for 2 hr at 4°C in a Hitachi SCP 85H2 ultracentrifuge equipped with an RPS 40T rotor. Fractionated material (the interface between 30% and 40% sucrose) was collected, diluted~1: 10 in TBS and pelleted at 125,000 g for 40 min at 4°C. To prepare the membrane-rich fraction of *X. laevis* blood cells the same protocol was used. The membrane-rich fraction of testes or blood cells was suspended in 10 ml of 0.6 M KCl, and stirred for 48 h at 4°C. Then, insoluble materials were removed by centrifugation at 105,000 g for 1 h at 4°C. The resultant KCl extract was fractionated through Sephadex G-200 (Pharmacia) gel filtration. Proteins were eluted with 0.6 M KCl at a flow rate of 10 ml/h. The effluent was collected in 1.8-ml fractions, and the protein content of each fraction was monitored by absorbance at 280 nm. After this, the effluent from the membrane-rich fraction of either testes or blood cells was divided into three fractions. The fraction (designated F2 or F3', respectively) was dialyzed for 12 h at 4°C against 1 liter of saturated ammonium sulfate solution. Precipitates were collected by centrifugation at 105,000 g for 30 min at 4°C and dissolved in 2 ml of 50 mM Tris-HCl (pH 7.4). The sample was applied to a column of Mono Q Sepharose (HR 5/5; Pharmacia) equilibrated with 50 mM Tris-HCl (pH 7.4). Protein concentrations were determined by the method of Peterson [16] using bovine serum albumin as the standard.

SDS-PAGE and immunoblot analysis

Proteins were added to the SDS sample buffer, heat denatured, and electrophoresed on a 12% acrylamide gel [10]. For immunoblot analysis, nitrocellulose membranes were stained after transfer [23] with a sheep anti-*X. laevis* albumin serum at a 15,000 dilution in PBS [13].

NH_2-terminal sequence analysis

An NH_2-terminal amino acid sequence analysis was performed using the 74 kD protein obtained from *X. laevis* testes. An automated protein sequence analysis was performed on an Applied Biosystems Model 470A gas-liquid phase protein sequencer connected on-line to an Applied Biosystems Model 120A HPLC [14].

RESULTS

Immunohistochemical studies for localization of albumin

The immunohistochemical localization of serum albumin was examined by use of a highly diluted specific antiserum. None of cells was stained when non-immune serum was used (Fig. 1a). However, a strong staining was observed in the interstitial tissue and spermatogonia, when the sheep antiserum raised against *X. laevis* albumin was used (Fig. 1b). A weak staining was also seen in spermatocytes and early spermatids, but not in Sertoli cells (Fig. 1b).

Purification of a 74 kD protein (albumin)

The membrane-rich fraction from testes was extracted with 0.6 M KCl and then the 0.6 M KCl extract was applied to a Sephadex G-200 column. The effluent was divided into three fractions (Fig. 2a). The last peak was not saved be-

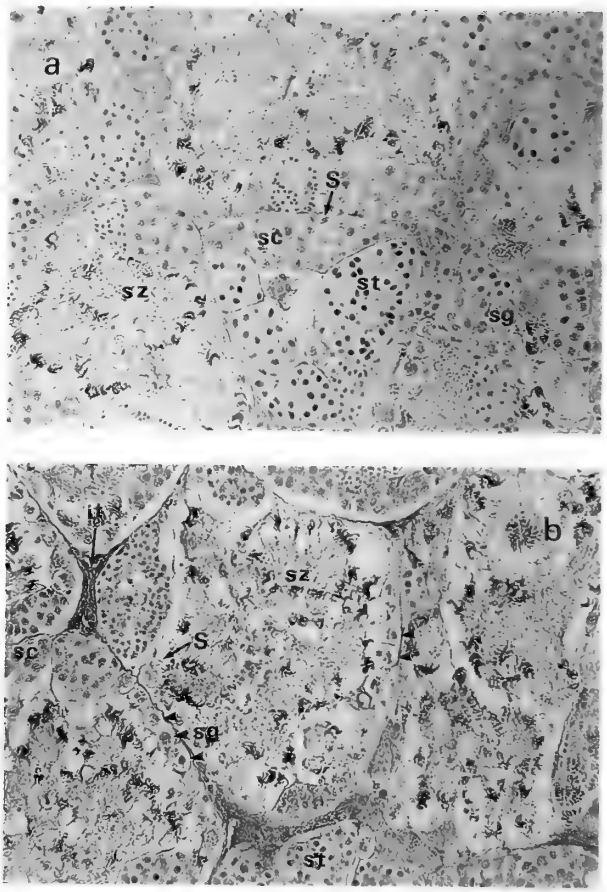

FIG. 1. Localization of albumin in the *X. laevis* testis by indirect ABC analysis with sheep antiserum raised against *X. laevis* albumin.
Immunostaining with sheep non-immune serum (a) and with sheep antiserum raised against *X. laevis* albumin (b). Arrow and arrowheads indicate Sertoli cell and spermatogonia, respectively. Sg, spermatogonia; sc, spermatocytes; st, spermatids; sz, spermatozoa; S, Sertoli cells; it, the interstitial tissue.

cause no detectable amounts of proteins was obtained, although it had an absorbance at 280 nm. This may be due to free amino acids and/or small peptides since all substances in this peak were dialyzable. When the membrane-rich fraction from blood cells was used instead of that from testes, three peaks appeared in the elution profile from the gel filtration (Fig. 2b). The first three fractions were designated F1, F2 and F3 for the testes, or F1', F2' and F3' for the blood cells, respectively (see Figs. 2a and 2b).

The F2 fraction for the testes was dialyzed against a saturated ammonium sulfate solution and then the precipitates were obtained, followed by HPLC. As shown in Figure 3a, a major peak was obtained by the first HPLC. This peak with a dotted area was pooled and dialyzed for 1 hr against 1 liter of 50 mM Tris-HCl (pH 7.4). After dialyzed, the sample was subjected to the second HPLC. When the second HPLC was done, the symmetrical peak with a dotted area containing a 74 kD protein was eluted with 0.25 to 0.35 M NaCl (Fig. 3b). When this peak was analyzed for the

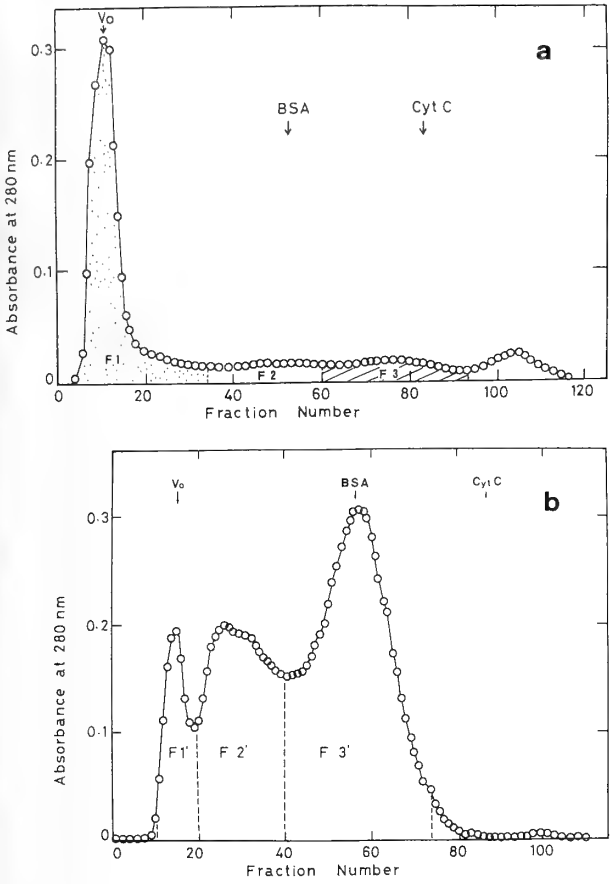

FIG. 2. Gel filtration chromatography on Sephadex G-200 of the 0.6 M KCl extract of *X. laevis* testes (a) and blood cells (b). A column (1.5×120 cm) was calibrated with standard molecular weight proteins [bovine serum albumin (BSA; Sigma, Mr=68 kD)] and cytochrome c (Cyt C; Miles, Mr=14 kD). The void volume (Vo) is indicated with an arrow.

heterogeneity of proteins by SDS-PAGE, a 74 kD protein was not a major protein in the KCl extract (Fig. 4A; lane c). However, the 74 kD protein was a major protein in the precipitate of the fraction F2 obtained by a dialysis against a

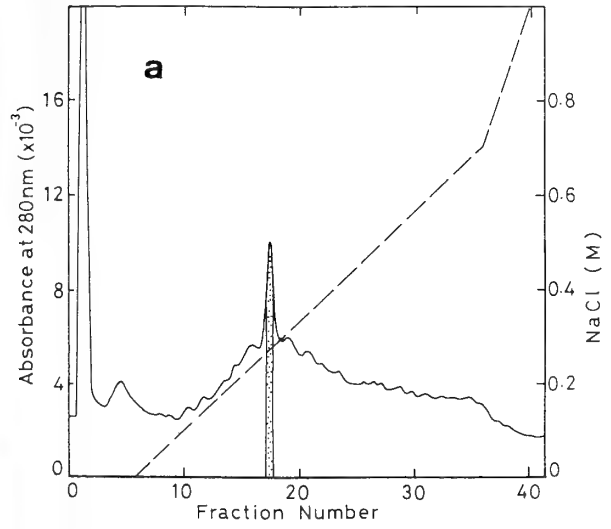

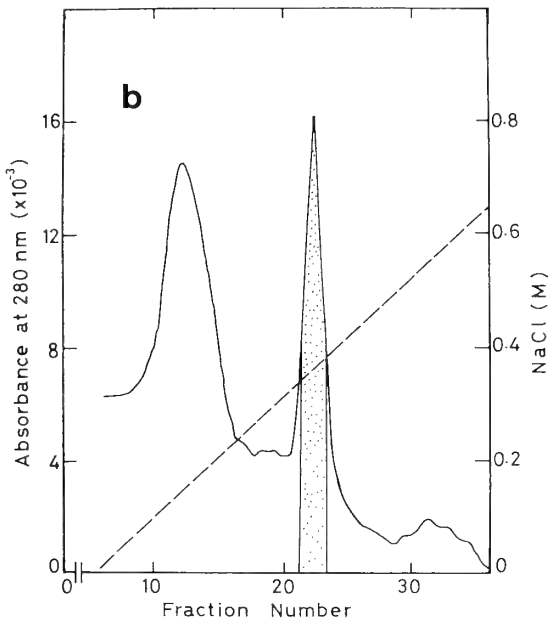

FIG. 3. Elution profiles from the first (a) and second (b) HPLC. Proteins in the F2 fraction obtained from the Sephadex G-200 gel filtration chromatography were eluted with 20 ml of a linear gradient of NaCl (0.0−1.0 M) in 50 mM Tris-HCl (pH 7.4) at a flow rate of 2 ml/min.

saturated ammonium sulfate solution. After the second HPLC, a very strong band with Mr=74 kD and a much weaker band with Mr=68 kD were observed (Fig. 4A; lane g). Based on densitometric tracings of stained gels on SDS-PAGE (Joyce-Loebel Chromatoscan 3), the total amount of the 68 kD protein was <5% of that of the 74 kD protein. In contrast, a 74 kD protein could not be detected

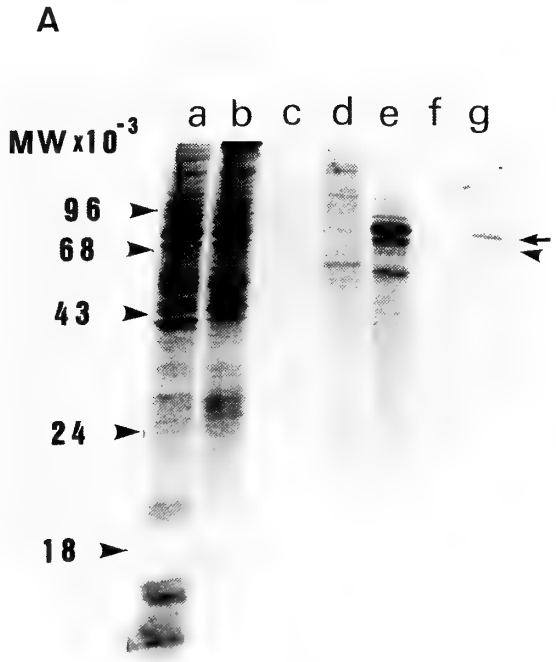

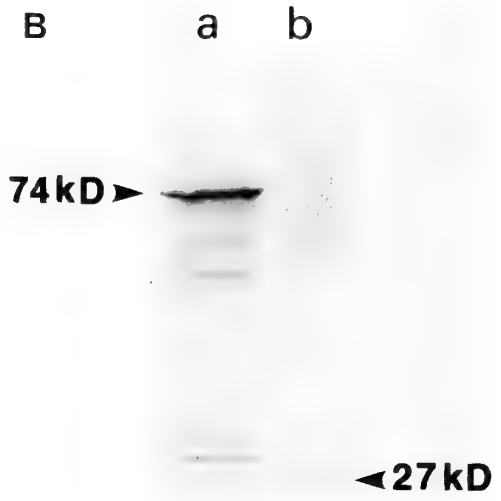

FIG. 4. Profiles of proteins on SDS-PAGE as observed during the purification procedure (A) and the gel filtration (B).
(A): Lane a, the homogenate (50 μg); lane b, the membrane fraction (50 μg); lane c, the KCl extract (5 μg); lanes d-f, the F1 (10 μg), F2 (12 μg), F3 (8 μg) fractions from gel filtration, respectively; lane g, the sample from the second HPLC (2 μg). An arrow and an arrowhead indicate 74 kD and 68 kD proteins, respectively.
(B): Lane a, the precipitate in the F2 fraction from testes after dialysis against a saturated ammonium sulfate solution (10 μg/lane); lane b, the precipitate in the F3' fraction from blood cells after dialysis a saturated ammonium sulfate solution (8 μg/lane).

in the precipitate of the F3' faction from blood cells after dialysis against a saturated ammonium sulfate solution (Fig. 4B; lane b). Yields of each step in the process of purification of the 74 kD protein are summarized in Table 1. The 74 kD protein was obtained to a final yield of 0.1%.

Identification of the 74 kD protein

In order to identify the 74 kD protein, an NH_2-terminal amino acid sequence analysis of this protein was performed. As seen in Fig. 5, the sequence of the first 19 NH_2-terminal amino acids of the 74 kD protein was identical, except for 3 unidentified amino acids, to that of the 74 kD *X. laevis* serum albumin published by Maskaitis et al. [11] and Schorpp *et al.* [18].

DISCUSSION

This study has clearly shown that serum albumin is present in the interstitial tissue of the *X. laevis* testis. According to Christensen *et al.* [3], immunoreactivity of albumin was detected on the surface, but not in the cytoplasm of Leydig cells. It is not clear in this study whether both the cell surface and cytoplasm of cells in the interstitial tissue of the *X. laevis* testis contain albumin. We need further investigation at an ultrastructural immunocytochemical level to answer this question. However, it seems probable that the surface of cells in the interstitial tissue [probably steroid hormone (SH)-secreting cells] is associated with albumin, since albumin was purified from the membrane-rich fraction of *X. laevis* testes, but not from membranes of blood cells. Spermatogonia also had a strong response to the albumin antibody, and spermatocytes and early spermatids had a weak response. A question also arises as to whether albumin is localized on the surface of these germ cells. Presently, we have no direct evidence for this. Immunocytochemical stu-

TABLE 1. Yields of the 74 kD protein from *X. laevis* testes.

	Total protein (mg)			Yield (%)
	exp. 1	exp. 2	exp. 3	
Membrane fraction	23.0	28.0	37.8	100
KCl extract	3.63	4.59	7.23	17.4
Sephadex G-200 gel filtration	0.240	0.320	0.425	1.11
HPLC	0.025	0.024	0.038	0.10

FIG. 5. The N-terminal sequence of the 74 kD protein from the *X. laevis* testis.

	Prepeptide	Propeptide	Mature Protein
74kD Albumin[a]	MKWITLICLLISSSFIES	RILFKR	DTDADHHKHIADVYTALTERTFKG·····
This work			*****XX*X***************

[a]Data from Schorpp *et al.* [18]. The leader peptide of the 74 kD *X. laevis* albumin consists of a hydrophobic sequence of 24 amino acids [11,18].
Note. Regions of identity are noted by an asterisk. X, not determined.

dies will answer this question.

It is of great interest to note that Sertoli cells did not respond to the antibody. Several investigators have localized albumin in Sertoli cells of mammalian testes such as human [6, 15], hamster [9] and rat [3]. It is not clear presently why the immunoreactivity of albumin was not observed in Sertoli cells of *X. laevis* testis. In the seminiferous tubules of mammalian testis, Sertoli cells form a barrier, so-called the blood testis-barrier, to retard or exclude many substances in the blood plasma from entrance into the lumen [19, 25]. Most germ cells, except for spermatogonia, reside within the barrier or the adluminal compartment. In anurans, on the other hand, spermatogenesis takes its course in the cysts of the testes. Germ cells develop within groups of "follicle" cells which are thought to be comparable to the Sertoli cells in the mammalian testis. According to Bergmann *et al.* [1], substances like nutrients and hormones in the blood in this species is probably accessible to most developing germ cells. Taking all these findings into consideration, it is not surprising that Sertoli cells had no response to the antibody of albumin. Perhaps, albumin is not associated with Sertoli cells. T may be transported to germ cells from the interstitial space without going via Sertoli cells.

Finally, the HPLC sample consisted of two proteins, as judged from the result of SDS-PAGE analysis. One with Mr=74 kD was a very strong band and the other with Mr=68 kD was a very faint band (see Fig. 4A; lane g). Both bands immunoreacted with the antibody of albumin (data not shown). This is not unusual. The frog, *X. laevis*, has two albumin genes that code for a 74 kD and a 68 kD serum albumin [11, 18]. In addition, two molecular forms of proteasome [7], calreticulin (a Ca^{2+}-binding protein) [24] and prolactin [26] have also been reported in this animal. Two forms of these proteins may have occurred from a duplication of the entire genome in the genus *Xenopus* [2]. In view of these findings, we must have purified two albumins together, but could not separate one from another by the methods used in this study. One explanation for this may be as follows; albumin exists in two forms that migrate on SDS-PAGE with relative molecular weights of 74 kD and 68 kD, respectively. As the number of amino acids of the two albumins is equivalent (608 residues), the anomalous behaviour on SDS-PAGE may be due to the glycosylation, which is specific for the 74 kD albumin [18]. It might be possible to separate one from another by changing the range of NaCl concentrations on HPLC.

As to which albumins are more closely associated with immunoreacted cells remains unclear at the present time. In the serum of *X. laevis*, the 74 kD albumin exists to a much greater extent than the 68 kD albumin (data not shown). It seems, therefore, very likely that the former is more closely associated with the surface of testicular cells. We do not know yet how spermatogenesis in *X. laevis* is controlled by T. Nevertheless, it is extremely interesting to note that the developing germ cells and the interstitial tissue (probably SH-secreting cells) are associated with albumin. Considering that serum albumin can bind T, spermatogenesis may be influenced under T with the aid of serum albumin in this species as well as in others.

ACKNOWLEDGMENTS

We are indebted to Dr. D. R. Schöenberg, Uniformed Services University of the Health Science, for the generous gift of sheep antisera raised against *X. laevis* serum albumin. We gratefully acknowledge Dr. S. Tanaka, Gunma University, for helpful advice for the identification of specific cell types in the *X. laevis* testis. We wish to thank Dr. E. P. Widmaier, Boston University, for his stimulating discussions and criticisms.

REFERENCES

1 Bergmann M, Schindelmeiser J, Greven H (1984) The blood-testis barrier in vertebrates having different testicular organization. Cell Tiss Res 238: 145–150

2 Bisbee CA, Baker MA, Wilson AC (1977) Albumin Physiology for clawed frogs (*Xenopus*). Science 195: 785–787

3 Christensen AK, Komorowski TE, Wilson B, Ma S-F, Stevens III. RW (1985) The distribution of serum albumin in rat testis, studied by electron microscope immunocytochemistry on ultrathin frozen sections. Endocrinology 116: 1983–1996

4 Corvol P, Bardin CW (1973) Species distribution of testosterone binding globulin. Biol Reprod 8: 277–282

5 Ewing LL, Chubb CE, Robaire BR (1976) Macromolecules, steroid binding and testosterone secretion by rabbit testis. Nature 264: 84–86

6 Forti G, Barni T, Vanelli G, Balboni GC, Orlando C, Serio M (1989) Sertoli cell proteins in the human seminiferous tubule. J Steriod Biochem 32: 135–144

7 Fujii G, Tashiro K, Emori Y, Saigo K, Shiokawa K (1993) Molecular cloning of cDNA for two *Xenopus* proteasome subunits and their expression in adult tissues. Biochim Biophys Acta 1216: 65–72

8 Hsu S-M, Soban E (1982) Color modification of diaminobenzidine (DAB) precipitation by metalic ions and its application for double immunohistochemistry. J Histochem Cytochem 30: 1079–1982

9 Krishna A, Spanel-Borowski K (1990) Albumin localization in the testis of adult golden hamsters by use of immunohistochemistry. Andrologia 22: 122–128

10 Laemmli UK (1970) Cleavage of structural proteins during the assembly of the head of bacteriophage T_4. Nature 227: 680–685

11 Maskaitis JE, Sargent TD, Smith Jr LH, Pastori RL, Schöenberg DR (1989) *Xenopus laevis* serum albumin: sequence of the complementary deoxyribonucleic acids encoding the 68- and 74-kilodalton peptides and the regulation of albumin gene expression by thyroid hormone during development. Mol Endocrinol 3: 464–473

12 Millette CF, O'Brien DA, Moulding CT (1980) Isolation of plasma membranes from purified mouse spermatogenic cells. J Cell Sci 43: 279–299

13 Nakamura M, Michikawa Y, Baba T, Okinaga S, Arai K (1992) Calreticulin is present in the acrosome of spermatids of rat testis. Biochem Biophys Res Commun 186: 668–673

14 Nakamura M, Moriya M, Baba T, Michikawa Y, Yamanobe T, Arai K, Okinaga S, Kobayashi T (1993) An endoplasmic reticulum protein, calreticulin, is transported into the acrosome of rat sperm. Exp Cell Res 205: 101–110

15 Orlando C, Casano R, Forti G, Barni T, Vanelli GB, Balboni

GC, Serio M (1988) Immunologically reactive albumin-like protein in human testis and seminal plasma. J Reprod Fertil 83: 687–692

16 Peterson GL (1977) A simplification of the protein assay method of Lowry et al. which is more generally applicable. Anal Biochem 83: 346–356

17 Rastogi RK, Iela L, Saxena PK, Chieffi G (1976) The control of spermatogenesis in the green frog, *Rana esculenta*. J Exp Zool 196: 151–166

18 Schorpp M, Dobbeling U, Wagner U, Ryffel M (1988) 5'-Flanking and 5'-proximal exon regions of the two *Xenopus* albumin genes. Deletion analysis of constitutive promoter function. J Mol Biol 199: 83–93

19 Setchell BP (1967) The blood testicular barrier in sheep. J Physiol (Lond) 189: 63–65

20 Steinberger E (1971) Hormonal control of mammalian spermatogenesis. Physiol Rev 51: 1–22

21 Steinberger E, Duckett GE (1967) Hormonal control of spermatogenesis. J Reprod Fertil Suppl 2: 75–87

22 Steinberger E, Steinberger A, Ficher M (1970) Study of spermatogenesis and steroid metabolism in cultures of mammalian testes. Rec Prog Hormonal Res 26: 547–588

23 Towbin H, Staehelin T, Gordon J (1979) Electrophoretic transfer of protein from polyacrylamide gels to nitrocellulose sheet: procedure and applications. Proc Natl Acad Sci USA 76: 4350–4354

24 Treves S, Zorzato F, Pozzan T (1992) Identification of calreticulin isoforms in the central nervous system. Biochem J 287: 579–581

25 Waites GMH, Setchell BP (1969) Physiology of the testis, epididymis and scrotum. Adv Reprod Physiol 4: 1–63

26 Yamashita K, Matsuda K, Hayashi H, Hanaoka Y, Tanaka S, Yamamoto K, Kikuyama S (1993) Isolation and characterization of two forms of *Xenopus* prolactin. Gen Comp Endocrinol 9: 307–317

ZOOLOGICAL SCIENCE 11: 291–297 (1994)

Spatio-Temporal Pattern of DNA Synthesis Detected by Bromodeoxyuridine Labeling in the Mouse Endometrial Stroma during Decidualization

NAOSHI OHTA[1,2], TAKAO MORI[1], SEIICHIRO KAWASHIMA[1],
SHINOBU SAKAMOTO[3], HIDESHI KOBAYASHI[2]

[1]*Zoological Institute, School of Science, University of Tokyo, Bunkyo-ku, Tokyo 113,*
[2]*Research Laboratory, Zenyaku Kogyo Co., Ltd. Nerima-ku, Tokyo 178,*
[3]*Department of Endocrinology, Medical Research Institute,*
Tokyo Medical and Dental University, Bunkyo-ku,
Tokyo 113, Japan

ABSTRACT—In order to examine the patterns of proliferation and differentiation of endometrial stromal cells before and during decidualization in pseudopregnant mice, the rate of DNA synthesis was immunocytochemically determined by means of bromodeoxyuridine (BrdU) labeling. On day 4 of pseudopregnancy induced by mating with vasectomized male, both uterine horns were traumatized to induce deciduoma. On day 5 of pseudopregnancy (one day after traumatization), BrdU-labeling index was markedly increased, and the labeled cells were found in almost all parts of endometrial stroma. From day 6 to day 8 of pseudopregnancy (2–4 days after traumatization), the labeling index remained high in the stromal cells of all parts except for the periluminal region. In the endometrial stromal cells in the peripheral region of myometrium, however, the labeling index was maximum on day 8 and decreased remarkably on day 9. In the stromal cells in the periluminal region where deciduomal cells developed, the labeling index was high on day 5 and low on day 6, no labeled cells being found on day 8. There results clearly show that each region of uterine endometrial stroma has a different responsiveness to traumatization, and each region plays a different role in the formation of deciduoma.

INTRODUCTION

Immunohistochemical detection of bromodeoxyuridine (BrdU), which is a uridine analogue and incorporated selectively into the cellular DNA at S-phase of the cell cycle, has been proven useful for the analysis of cell proliferation in place of ^{3}H-thymidine incorporation into replicating cells [5].

Differentiation of the endometrial stromal cells into decidual cells occurs soon after the implantation of blastocysts. In mice and rats, however, decidual reaction can be induced artificially in the uteri without blastocysts by mechanically scratching the luminal surface [17]. Changes in the structure and function of uterine tissue during decidualization are mainly controlled by the ovarian estrogen and progesterone [2, 11, 13, 14]. Decidualization is a highly regulated process characterized by a variety of events including increase in DNA synthesis [1, 8, 15], changes in vascular permeability [7], and polyploidization and hypertrophy of stromal cells [12, 16]. Therefore, formation of deciduoma has been widely applied as a useful experimental model for the study not only of implantation but also of the mechanisms of cell proliferation and differentiation. BrdU labeling patterns of the cells in uterine tissue were reported in normal cycling and prepubertal mice [6].

Because the changes of cell proliferation during decidualization as a function of time have not been reported, the present study was designed to examine the spatial and temporal patterns of DNA synthesis in the mouse uterine stromal cells during decidualization after traumatization.

Accepted February 3, 1994
Received November 11, 1993

MATERIALS AND METHODS

Animals

Female mice of the ICR strain purchased from Japan CLEA Inc. (Tokyo, Japan) were used in the present study. They were housed in plastic cages (3–7 mice per cage) under controlled lighting (12–hr light and 12–hr darkness; lights on at 06:00) and temperature (25 ± 0.5°C), and were provided with a commercial diet (CE-7: Japan CLEA) and tap water *ad libitum*.

Induction of deciduoma

Virgin female mice at 50–60 days of age were mated with vasectomized males to induce pseudopregnancy. The day when a vaginal plug was found was designated as day 1 of pseudopregnancy. On day 4 of pseudopregnancy, the anti-mesometrial luminal surface in both uterine horns was traumatized by a single scratch with a bent needle. The needle was inserted into the uterine lumen from a small incision made with a small scissors at the posterior end of uterine horn, adjacent to the uterine cervix, under light nembutal anesthesia [17]. The pseudopregnant mice were killed by cervical dislocation on various days after traumatization (Fig. 1). In order to check the effect of trauma, some pseudopregnant mice without traumatization were killed as controls between 2 and 10 days after mating with vasectomized males. Immediately after autopsy, the uterine horns were removed and weighed. The uterine weight was used as a parameter of decidual reaction.

In addition, virgin cycling mice at 50–60 days of age were also killed at varius phases of the estrous cycle and the uterine weights were recorded.

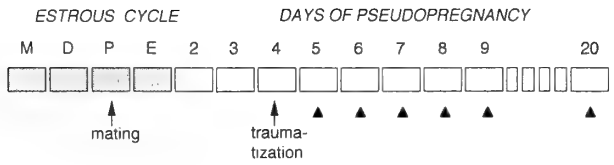

FIG. 1. Experimental schedule. Pseudopregnant mice received a deciduogenic stimulus (traumatization) on day 4 of pseudopregnancy and were given a single injection of BrdU on various days (▲) after traumatization. M: metestrus, D: diestrus, P: proestrus, E: estrus.

BrdU labeling and immunocytochemistry

The pseudopregnant mice received a single intravenous injection of bromodeoxyuridine (BrdU, 30 mg/kg body weight: Amersham, UK) at 24-hr intervals after traumatization. Four hr after BrdU injection, the uteri were fixed in ice cold 10% phosphate-buffered neutral formalin for 5 hr at room temperature. The uteri were dehydrated, embedded in paraffin, and the sections were cut at 4μm thickness.

After deparaffinization, the sections were washed in 0.01M phosphate-buffered saline (PBS, pH 7.4) three times and digested with 0.1% trypsin (Sigma) in 0.1% $CaCl_2$ (pH 7.8) for 20 min at 37°C. After washing in PBS (15 min, 3 times), endogenous peroxidase activity was blocked by immersing the sections in 0.3% H_2O_2 in methanol for 20 min, followed by washing in PBS (15 min, 3 times). Thereafter, the sections were incubated with monoclonal anti-BrdU antibody containing 10 units/ml nuclease (Amersham) for 1 hr at room temperature and then rinsed in PBS (15 min, 3 times). Finally, the sections were incubated with peroxidase-conjugated rabbit anti-mouse IgG for 30 min at room temperature. After washing in PBS (15 min, 3 times), the antibody binding sites were visualized by 0.05% 3, 3′-diaminobenzidine tetrahydrochloride solution. Each incubation was conducted in a moist chamber at room temperature. After immunostaining, the sections were counterstained with 0.1% Kernechtrot in 5% $Al_2(SO_4)_3$, dehydrated through an ethanol series, cleared in xylene, and mounted. The immunocytochemistry was controlled by sections overlaid with PBS instead of anti-BrdU antibody, which showed no immunoreactivity.

Measurement of labeling index

In order to examine the BrdU labeling index, two sections which were separated by at least 40μm apart were randomly chosen from the middle part of the uterine horn or the middle part of deciduoma in each mouse. Cell counting was carried out in the four regions; anti-mesometrial side of the endometrial stroma (AME), periluminal endometrial stroma (PLE), peripheral endometrium adjacent to the myometrium (PPE), and mesometrial side of the endometrial stroma (MME) (Fig. 2). Total number of BrdU labeled cells was counted out of 1,000 cells each in two sections from the four regions by using

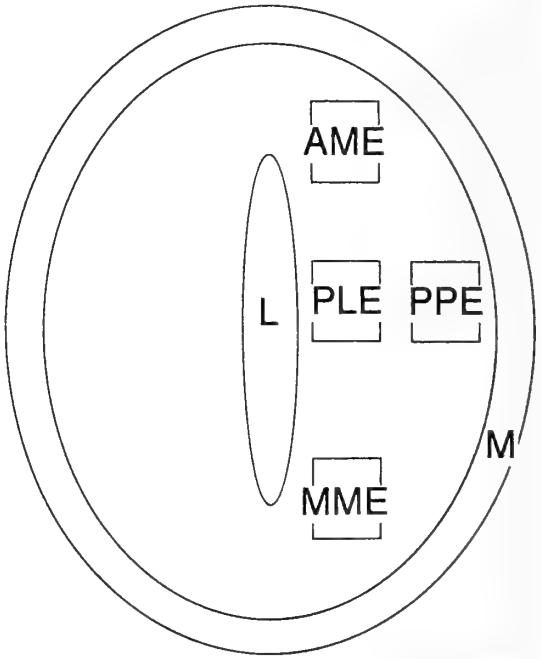

FIG. 2. Four regions of uterus for examining BrdU labeling index. L: lumen, M: myometrium, AME: antimesometrial side of endometrial stroma, PLE: periluminal endometrial stroma, PPE: peripheral endometrial stroma adjacent to myometrium, MME: mesometrial side of endometrial stroma.

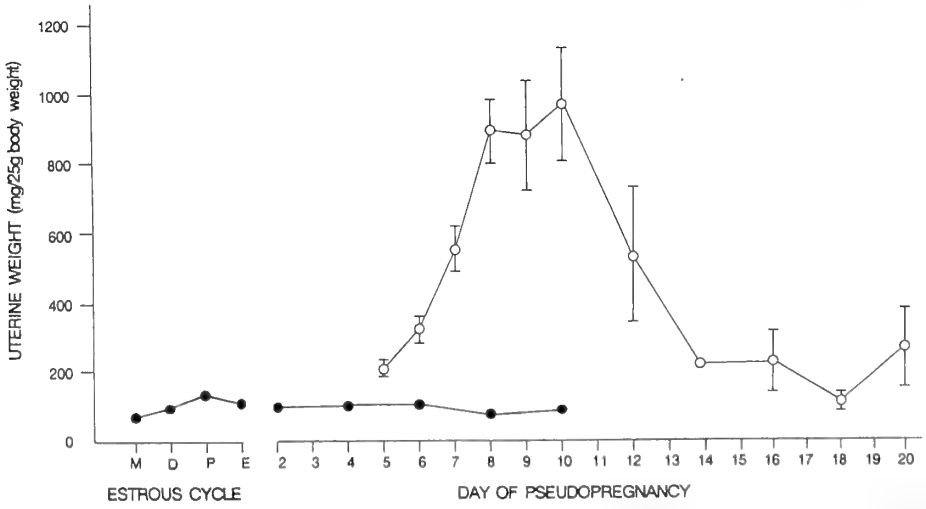

FIG. 3. Changes in uterine weights in mice during estrous cycle and pseudopregnancy with (-○-) or without (-●-) traumatization. Deciduoma were induced on the next day of traumatization given on day 4 of pseudopregnancy. Each point depicts the mean and SEM of 3–5 mice. M: metestrus, D: diestrus, P: proestrus, E: estrus.

an image processor-analyzer (LUZEX; NIRECO Co. Ltd, Tokyo). The labeled indices were expressed as percentages of labeled cells per 1,000 cells.

Statistical analysis

The statistical significance of the difference between groups were evaluated by one-way analysis of variance (ANOVA), followed by Duncan's multiple range test for the uterine weights and labeled indices.

RESULTS

Changes in uterine weight during decidualization

Changes in uterine weights during the estrous cycle and pseudopregnancy before and after traumatization are shown in Figure 3. In normal cycling mice, the uterine weight was lowest at metestrus, followed by an increase during diestrus ($P<0.01$). The weight reached maximum at proestrus, the value being significantly higher than those in the other phases of estrous cycle ($P<0.01$).

The uterine weight of pseudopregnant mice without traumatization between 2 and 10 days after the mating was almost the same as that of diestrous mice. Traumatization of the uteri on day 4 of pseudopregnancy resulted in the development of deciduoma in the next day. The weight increased rapidly after traumatization, reaching maximum on day 8 of pseudopregnancy, and decreased on day 12 and onward. The weights were significantly higher between days 6 and 12 than the other stages of pseudopregnancy with traumatization ($P<0.01$, in all comparisons).

BrdU labeling index

On day 2 of pseudopregnancy before traumatization, BrdU labeled cells were observed in the luminal and glandular epithelia but not in the endometrial stroma. On days 3 and 5 of pseudopregnancy before and one day after traumatization, a large number of labeled cells were observed in the endometiral stroma but very rarely in the luminal epithelium (Fig. 4a). On days 7 and 8 of pseudopregnancy given no traumatization, labeled cells were not found in the stroma and appeared again in the luminal epithelium.

The BrdU-positive cells on day 5 of pseudopregnancy in mice given traumatization (Fig. 4b) were more numerous compared to those on day 3 of pseudopregnancy (Fig. 4a) and on day 5 of pseudopregnancy without traumatization (data not shown, but regardless of the regions, the indices were less than 1% in mice given no traumatization).

Detailed spatio-temporal patterns of BrdU labeling index during decidualization are shown in Figure 5. On day 5 through 8 of pseudopregnancy with traumatization, the indices were significantly higher in the endometrial stroma than

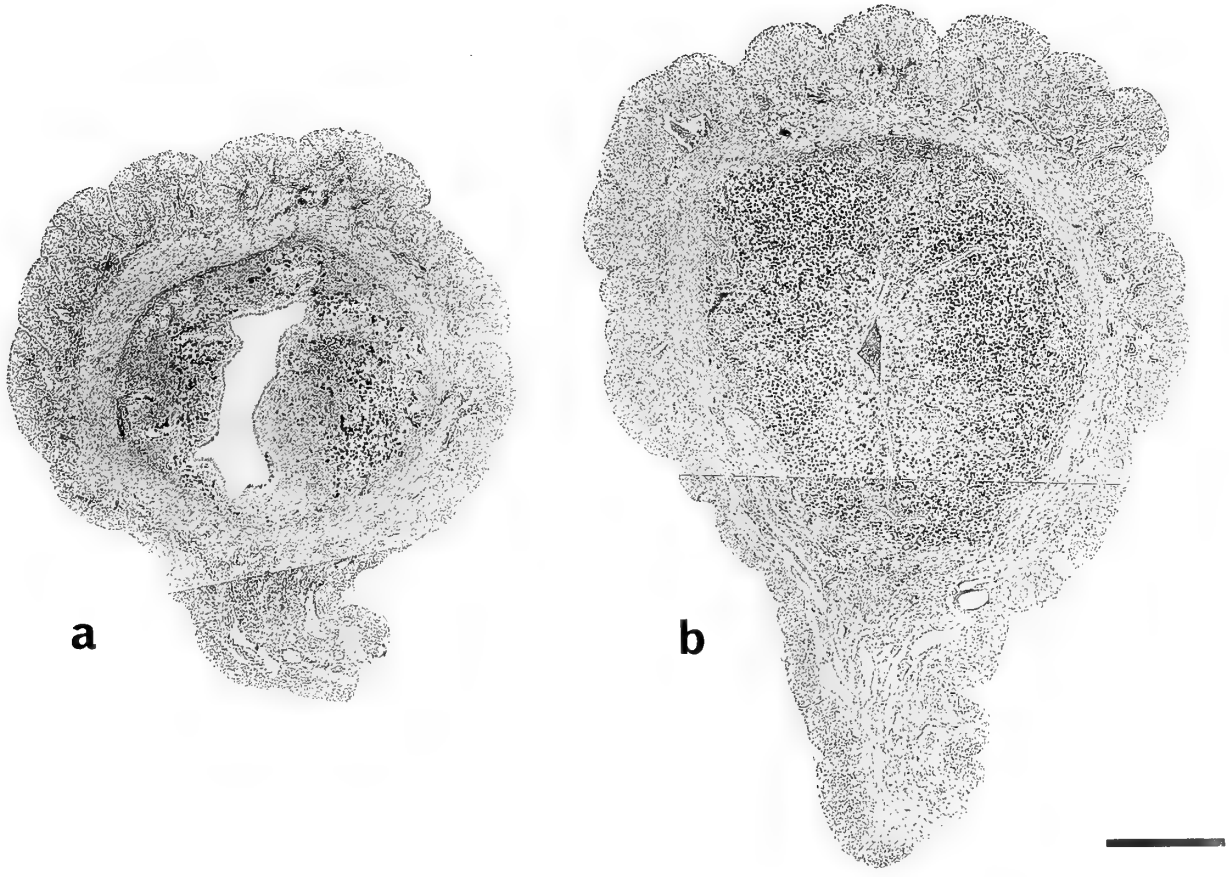

FIG. 4. Uteri of mice on day 3 (a) and day 5 (b) of pseudopregnancy, one day before and after traumatization, respectively. BrdU-labeled cells (black dots) were visible in the endometrial stroma. Bar: 500μm

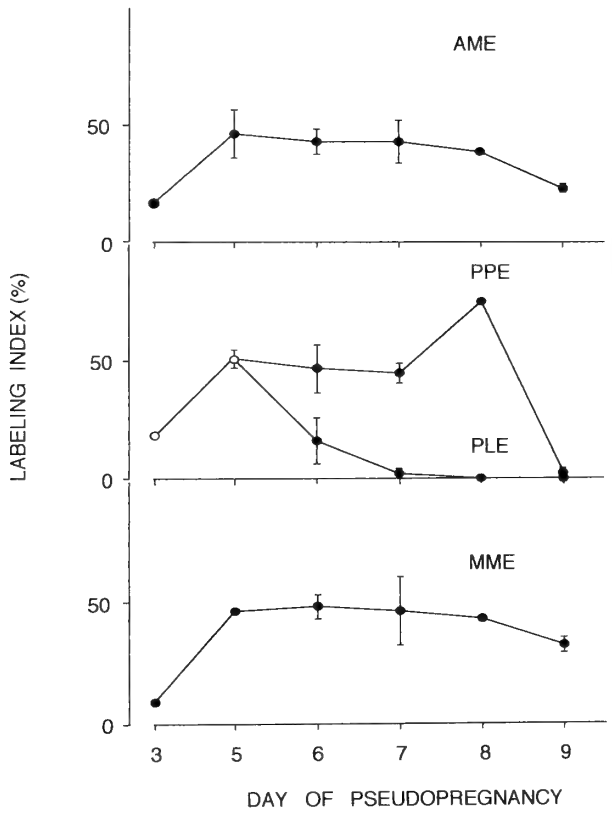

FIG. 5. Changes of BrdU lebeling index in the endometrial stromal cells during decidualization. Each point depicts the mean and SEM of 3–5 mice. AME: antimesometrial side of endometrial stroma, PPE: peripheral endometrial stroma adjacent to myometrium, PLE: periluminal endometrial stroma, MME: mesometrial side of endometrial stroma. On days 3 and 5, as PPE and PLE could not be counted separately, pooled data are shown.

FIG. 6. Uterus of a mouse on day 6 of pseudopregnancy 2 days after traumatization. BrdU-labled cells were present in almost all regions of the endometrial stroma except for PLE. Bar: 500μm

those on day 3 at 0.01 level, except for PLE (Figs. 5–7). On day 6 of pseudopregnancy with traumatization, the plump cells with large nuclei over 25μm in diameter appeared in the PLE and AME (Fig. 8). In PLE, the percentage of labeled stromal cells on day 5 was significantly higher than that in the other stages, respectively ($P<0.01$). The percentage reduced rapidly on day 6 and BrdU labeling was no more detected on day 8 (Fig. 5). On day 8, labeling indices tended to be lower in the regions of the endometrium except for PPE. On day 9, all labeling indices were almost the same as those on day 3 except for MME (Figs. 5 and 9). Many degenerating cells with pyknotic nuclei appeared on days 8 and 9 of psudopregnancy with traumatization.

DISCUSSION

Cell proliferation and differentiation during decidualization in pregnant [3] or pseudopregnant rodents [4, 9, 17] have extensively been studied. It is well known that the differentiation of endometrial stromal cells to decidual cells occurs in response to the implantation of blastocysts or traumatization of artificial stimuli. In mice, the sensitivity of the uterus to a deciduogenic stimulus is known to be the highest on day 4 of pseudopregnancy [2, 10]. In the present study, the uterine weight increased immediately after traumatization on day 4 and reached maximum on day 10 of pseudopregnancy. The weight markedly decreased on day 12 and returned to the normal diestrous level on day 18. These findings accord well with the previous results in rats [17].

In the present study, DNA synthesis was detectable by the presence of BrdU-labeled cells in the luminal epithelial cells on day 2 of pseudopregnancy. On day 3 of pseudopregnancy, some stromal cells in the endometrium began to show DNA synhesis. If deciduogenic stimuli were not given to the uterus, the activity of DNA synthesis in the stromal cells decreased within a few days. These findings may reflect that the stromal cells are ready to respond to deciduogenic stimuli on day 3 of pseudopregnancy. On day 5 of pseudopregnancy with traumatization, the labeled cells were present extensively and evenly in all the four regions of endometrial stroma. Thereafter, BrdU-labeled cells greatly decreased in the PLE on days 6 and 7 of pseudopregnancy. Ledford *et al.* [8] have stated that in mice rapid cell proliferation begins approximately 30 hr after deciduogenic stimulation and continued for 72 hr in the endometrial stroma. After the initiation of decidualization, however, a population of stromal cells

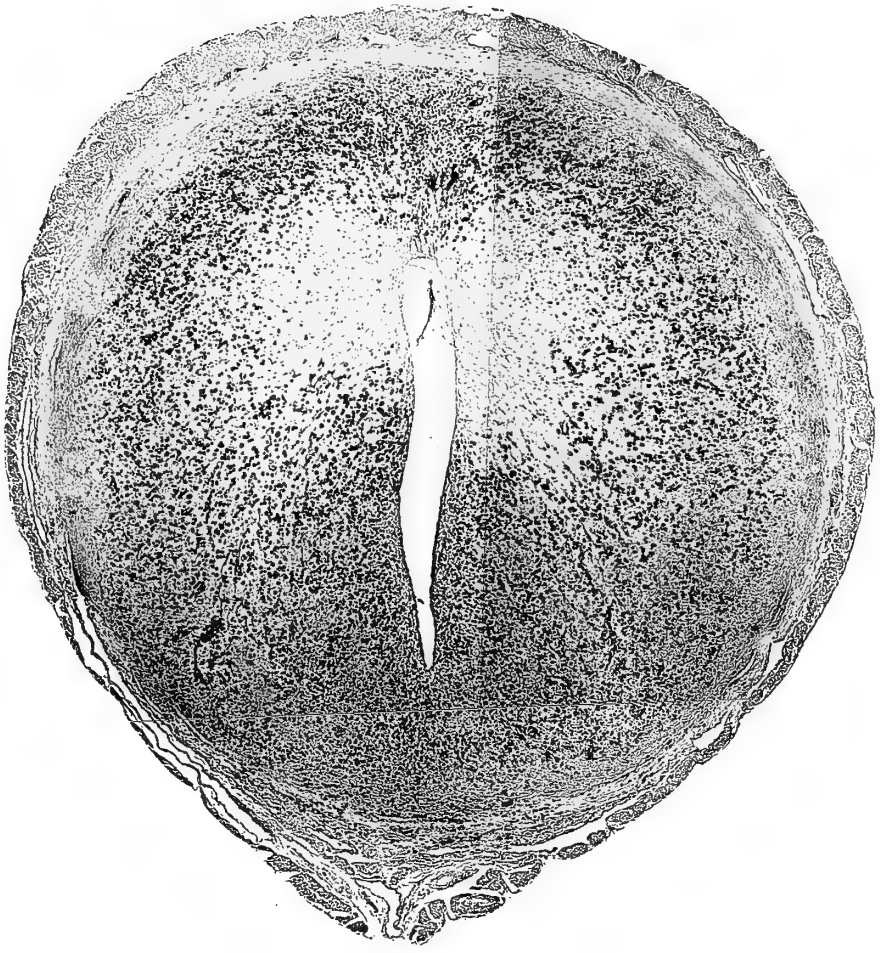

FIG. 7. Uterus of a mouse on day 7 of pseudopregnancy 3 days after traumatization. Only a few BrdU-labeled cells were visible in PLE. Bar: 500μm

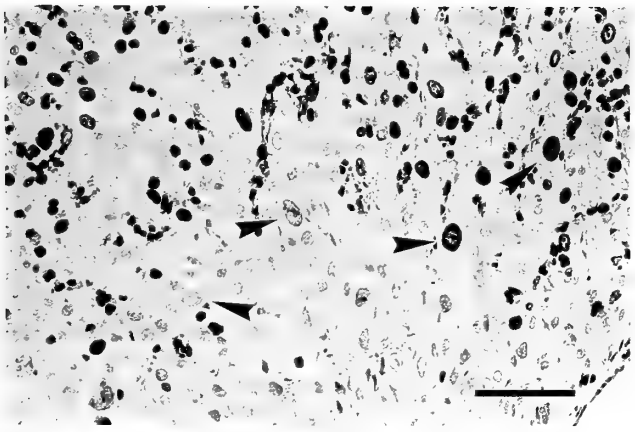

FIG. 8. Antimesometrial side of endometrial stroma in a mouse on day 6 of pseudopregnancy 2 days after traumatization. Plump cells with large nuclei (arrowheads) appeared. Bar: 100μm

is known to synthesize DNA and differentiate into polyploid decidual cells without cell division [1]. Deciduomal cells called plump cells in the present study are distributed exclusively in the periluminal part of endometrial stroma where the implantation normally occurs. Thus, it seems likely that the proliferation of deciduomal cells ceases and differentiation begins on day 6 or 7 of pseudopregnancy (2–3 days after traumatization/implantation).

During decidualization, a remarkable rise of DNA synthesis in peripheral endometrial stroma adjacent to the myometrium (PPE) occurred between day 6 and day 8 of pseudopregnancy. Proliferated stromal cells in this region may contribute to the reconstruction of endometrial tissue after the regression of preformed deciduomal tissue. It is known that the life span of the rat deciduoma is limited and frequent cell death occurs on day 9 of pseudopregnancy [14]. The present findings clearly show that regression of deciduoma begins in most parts of the endometrium from day 8 of pseudopregnancy, because many degenerated cells were encountered on days 8 and 9 of pseudopregnancy.

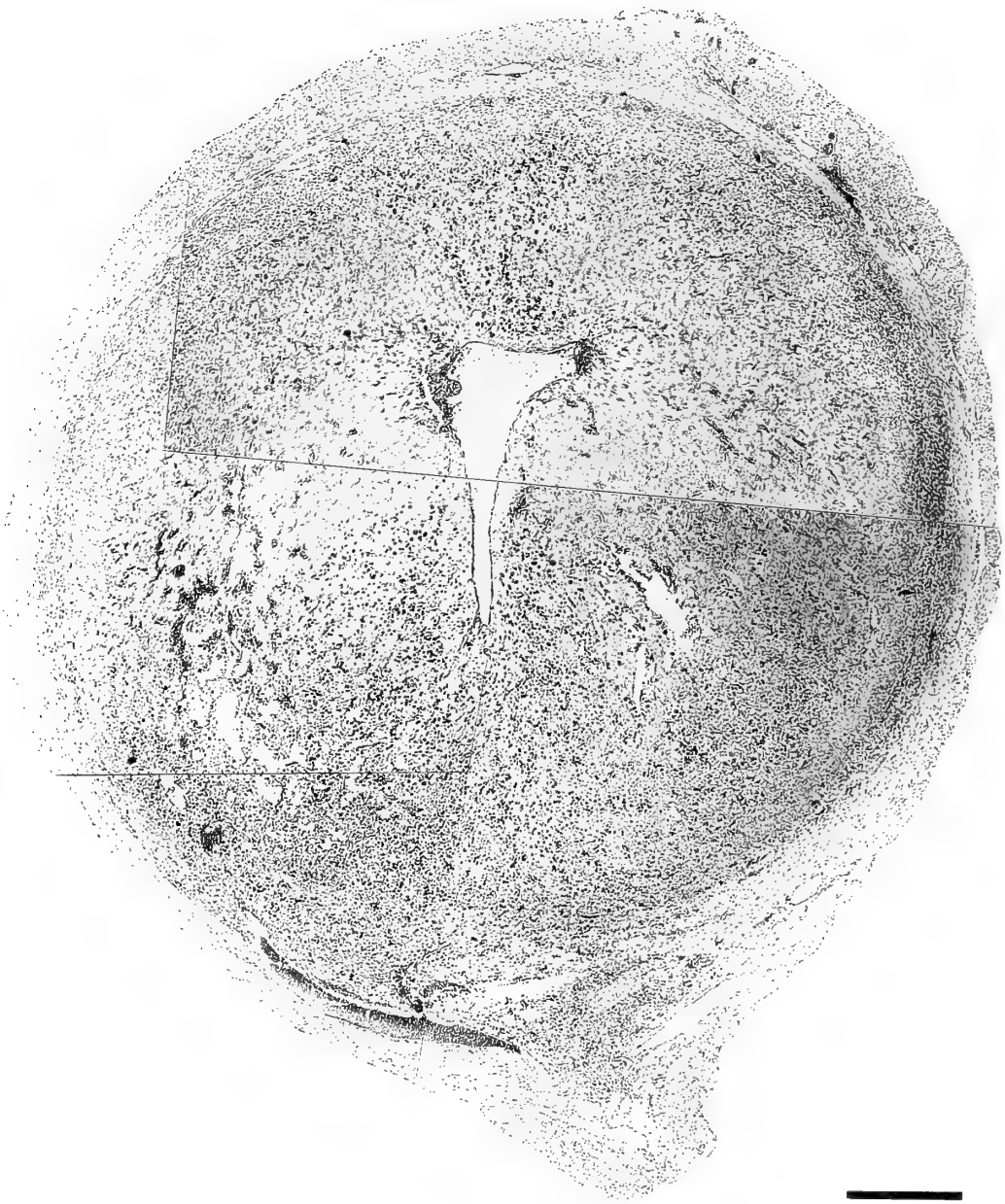

FIG. 9. Uterus of a mouse on day 9 of pseudopregnancy 5 days after traumatization. The number of BrdU-labeled cells became decreased. Bar: 500μm

The present findings demonstrated that activity of DNA synthesis in the endometrium varies during decidualization in several regions of the endometrial stroma. This implies that each region has a different responsiveness to traumatization and that it plays a different role during the development of deciduoma.

ACKNOWLEDGMENTS

The authors would like to express our cordial thanks to Dr. M. K. Park for his advice and encouragement during this study. This study was supported by Grants-in-Aid for Scientific Research from the inistry of Education, Science and Culture, Japan to T. M., S. K. and S. S., respectively and a Research Grant from Zenyaku Kogyo, Ltd. to S. K.

REFERENCES

1 Das RM, Martin L (1978) Uterine DNA synthesis and cell proliferation during early decidualization induced by oil in mice. J Reprod Fert 53: 125–128

2 Finn CA (1966) Endocrine control of endometrial sensitivity during the induction of the decidual cell reaction in the mouse. J Endocr 36: 239–248

3 Finn CA, Martin L (1967) Patterns of cell division in the mouse uterus during early pregnancy. J Endocr 39: 593–597

4 Galassi L (1968) Autoradiographic study of the decidual cell reaction in the rat. Dev Biol 17: 75–84

5 Gratzner HG (1982) Monoclonal antibody to 5-bromo- and

5-iododeoxyuridine: a new reagent for detection of DNA replication. Science 218: 474–475

6 Hanazono M, Yoshiki A, Ota K, Kitoh J, Kusakabe M (1990) DNA replication in uterine cells of adult and prepubertal mice under normal and hormonally stimulated conditions detected by bromodeoxyuridine labeling method. Endocrinol Japon 37: 183–191

7 Kennedy TG (1979) Prostaglandins and increased endometiral vascular permeability resulting from the application of an artificial stimulus to the uterus of the rat sensitized for the decidual cell reaction. Biol Reprod 20: 560–566

8 Ledford BE, Rankin JC, Froble VL, Serra MJ, Markwald RR, Baggett B (1978) The decidual cell reaction in the mouse uterus : DNA synthesis and autoradiographic analysis of responsive cells. Biol Reprod 18: 506–509

9 Marcus GJ (1974) Mitosis in the rat uterus during the estrous cycle, early pregnancy, and early pseudopregnancy. Biol Reprod 10: 447–452

10 Martin L, Finn CA (1968) Hormonal regulation of cell division in epithelial and connective tissues of the mouse uterus. J Endocr 41: 363–371

11 Moulton BC, Blaha GC (1978) Separation of deciduomal cells by velocity sedimentation at unit gravity. Biol Reprod 18: 141–147

12 Moulton BC, Koening BB (1984) Uterine deoxyribonucleic acid synthesis during preimplantation in precursors of stromal cell differentiation during decidualization. Endocrinology 115: 1302–1307

13 Ohta Y (1991) Deciduoma formation in pseudopregnant rats bearing pituitary grafts. Zool Sci 8: 75–80

14 O'shea JD, Kleinfeld RG, Morrow HA (1983) Urtrastructure of decidualization in the pseudopregnant rat. Am J Anat 166: 271–298

15 Tachi C, Tachi S, Lindner HR (1972) Modification by progesterone of oestradiol-induced cell proliferation, RNA synthesis and oestradiol distribution in the rat uterus. J Reprod Fertil 31: 59–76

16 Takewaki K (1969) Formation of deciduomata in immature rats with luteinized ovaries. Annot Zool Japon 42: 126–132

17 Velardo JT, Dawson AB, Olsen AG, Hisaw FL (1953) Sequence of histological changes in the uterus and vagina of the rat during prolongationof pseudopregnancy associated with the presence of deciduomata. Am J Anat 93: 273–305

ZOOLOGICAL SCIENCE 11: 299–303 (1994)

Endocrine Control of Cartilage Growth in Coho Salmon: GH Influence *in Vivo* on the Response to IGF-I *in Vitro*

PETER I. TSAI, STEFFEN S. MADSEN[1], STEPHEN D. MCCORMICK[2] and HOWARD A. BERN[3]

Department of Integrative Biology, Bodega Marine Laboratory and Cancer Research Laboratory, University of California, Berkeley, California 94720, USA

ABSTRACT—Ceratobranchial cartilages from coho salmon (*Oncorhynchus kisutch*) parr, injected with growth hormone (GH) at 4μg/g body weight or with saline, were sampled monthly from February to July. Thymidine and sulfate uptakes by cartilages were determined as measures of DNA and chondroitin sulfate synthesis, respectively. Cartilages were incubated with IGF-I at 0.01, 0.1 and 1μg/ml to examine the *in vitro* response to this hormone. GH injection increased cartilage thymidine and sulfate uptakes at least four-fold in all experiments. IGF-I treatment *in vitro* further increased sulfate but not thymidine uptake in cartilages from GH-injected coho and increased uptake of both in cartilages from saline-treated coho. However, the IGF-stimulated uptakes were still significantly below the uptakes in cartilages from GH-injected coho. The dual effector hypothesis of GH action [12] in mammals is supported at least in part in teleost fishes by the observation that addition of IGF-I *in vitro* was not equivalent to injection of GH *in vivo*.

INTRODUCTION

The endocrine control of cartilage growth has only recently been examined in teleost fish [see 1, 2, 20]. Studies on the Japanese eel, *Anguilla japonica*, by Duan and Inui [8, 9] have shown that the stimulatory action of GH on sulfate uptake by cartilage is indirect. Duan and Hirano [6, 7] later showed that sulfate uptake by eel cartilage is stimulated by mammalian IGF-I and raised the possibility of regulation by a similar principle in teleosts. McCormick *et al.* [14] and Gray and Kelley [10] have subsequently shown that mammalian IGF-I stimulated sulfate incorporation *in vitro* in cartilages from coho salmon (*O. kisutch*) and goby (*Gillichthys mirabilis*), respectively. These observations are consistent with the somatomedin hypothesis [4].

In anadromous salmonids, smoltification is a period during which the fish undergoes various physiological changes, many of which are cued by the endocrine system. Endogenous levels of growth hormone, prolactin, thyroid hormones and cortisol change in a distinctive pattern in coho salmon (*Oncorhynchus kisutch*) undergoing smoltification [19]. In the period when GH levels in the coho are increasing [16, 19], cartilage growth rate would be expected to increase due to increased liver-derived IGF-I in the circulation [3, 18] and to sensitization of the cartilage to IGF-I by GH [12]. Although injection of GH leads to transient down-regulation of liver GH receptors [10, 11, 15, 17] in several teleost species, increased expression of IGF-I mRNA in the liver was observed in coho salmon [5]. Injection of GH, comparable to natural increases in endogenous GH, may thus stimulate cartilage growth.

The purpose of this study is to examine further the effect of GH on cartilage growth and its potential interaction with IGF-I. *In vivo* GH action and *in vitro* IGF-I action on ceratobranchial cartilage in coho salmon were judged by determining thymidine and sulfate incorporation. Experiments were done repeatedly during the period of parr-smolt transformation to detect possible developmental or seasonal changes in response to GH *in vivo* and to IGF-I *in vitro*.

MATERIALS AND METHODS

Animals

Coho salmon (*Oncorhynchus kisutch*) parr (10–20 g) were obtained from Iron Gate Hatchery, California Department of Fish and Game, in December 1991. They were maintained outdoors at Bodega Marine Laboratory at 12–14°C in a 2000-liter concrete raceway supplied with filtered fresh water and were fed twice daily with Oregon Moist Pellets (Moore-Clarke, LaConner, WA) at a ration of 2% body wt/day.

Injections

The fish for each monthly experiment were randomly separated into two groups: GH-injected (NIADDK-oGH-15 at 4μg/g body wt; n=10) and saline-injected (n=10). The oGH was dissolved in 0.01 N NaOH followed by saline solution to yield a final concentration of 2μg/μl solution (with pH less than 9); the same volume of 0.01 N NaOH was added to the saline used for injecting controls. Fish were injected with 2μl solution/g body wt on alternate days (total of 4 injections).

Accepted February 3, 1994
Received October 12, 1993

[1] Present address: Institute of Biology, Odense University, Campusvej 55, DK-5230 Odense M, Denmark
[2] Present address: Anadromous Fish Research Center, National Biological Survey, 1 Migratory Way, P. O. Box 796, Turners Falls, Massachusetts 01376, USA
[3] To whom correspondence should be directed.

Sampling

Cartilage samples were taken monthly from the above groups from February to July. Fish remained unfed for 7 days before sampling in an attempt to increase the sensitivity of their cartilage to IGF-I [13]. Fish were killed by a blow to the head 24 hr after the last injection. Ceratobranchial cartilages were dissected from the bone of the first three pairs of gill arches of each fish under a dissecting microscope and placed in a pre-culture medium: Minimum Essential Medium (MEM) with Hanks' salts, penicillin (100 U/ml) and streptomycin (100μg/ml). Randomly-selected cartilages (with an average dry wt of 53$\pm$15.6μg in February to 101$\pm$27.2μg in July) from each fish were then placed into wells (24-well plate, Falcon 3047) for different treatments (n=7–10 for each treatment): basal (untreated); non-specific (cartilages frozen at -80°C to measure non-specific thymidine and sulfate uptake); recombinant bovine IGF-I (rbIGF-I; a gift from Monsanto, St. Louis, MO, U.S.A.) at 0.01, 0.1 and 1μg/ml. Each well contained 1 ml culture medium: MEM with Earle's salts, bovine serum albumin (BSA; 25μg/ml), penicillin (50 U/ml), streptomycin (50μg/ml), $^{35}SO_4$ (1μCi/ml) and ^{3}H-thymidine (2μCi/ml). The cartilages were then incubated in a chamber filled with 95% O_2/5% CO_2 at 14°C for 48 hr. During this period, the ceratobranchial cartilage incorporated radioactive sulfate into chondroitin sulfate and radioactive thymidine into DNA. The experiment was terminated by freezing at -80°C. Cartilages were then soaked in cold Na_2SO_4 twice and rinsed with distilled water 3 times in order to eliminate residual unincorporated radioactive sulfate and thymidine. The cartilages were dried in an oven at 60°C and weighed to the nearest μg. Each cartilage was then placed in a scintillation vial containing 0.5 ml 99% formic acid which dissolved the cartilage, thereby releasing the radioactivity ($^{35}SO_4$+^{3}H-thymidine) into the acid. Liquid scintillation fluid (4.5 ml) was added to each vial. ^{35}S and ^{3}H radioactivities in dpm were determined by a dual-label (^{3}H and ^{35}S) program in a Beckman 5000 scintillation counter. The dpm count was normalized for each cartilage weight to yield dpm/μg.

Statistical analysis

Two-way analysis of variance (ANOVA) was used to test for significance of GH injection over time. All other statistical comparisons were done by one-way ANOVA followed by Newman-Keuls analysis for post-hoc comparisons of factor means. Regression analyses and ANOVA were conducted using the Crisp statistical program (CRUNCH, Berkeley, CA). All groups comprised 7–10 fish, and $P \leq 0.05$ was considered significant.

RESULTS

Body weight and smoltification

Mean body weight increased linearly (with a slight decrease in June) from 18 g in February to 39 g in July (data not shown). Signs of smoltification (loss of parr marks, silvering of scales, darkening at edge of fins, and increased condition factor) were most evident in May.

Thymidine and sulfate uptakes

Thymidine uptake (Fig. 1) by the cartilages in GH-injected coho was 4 to 16 times higher than in saline-injected coho throughout the study period (two-way ANOVA, $P < 0.0001$). From February to June, levels of thymidine uptake

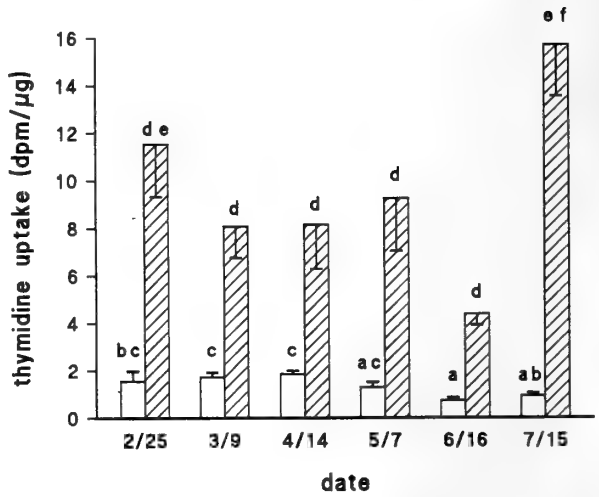

FIG. 1. Basal thymidine uptake (dpm/μg cartilage) by ceratobranchial cartilages from GH- and saline-injected coho salmon (*Oncorhynchus kisutch*) sampled monthly from February to July. Fish were given injections on alternate days (total of 4 injections) and sampled 1 day after the last injection. Hatched and clear boxes represent GH- and saline-injected fish, respectively. Values are mean$\pm$SEM (n=7–10). Values with shared letters are not significantly different ($P > 0.05$).

by cartilage from GH-injected coho showed a decreasing trend without statistical significance, averaging 10 dpm/μg from February to May and dropping to 4.4 dpm/μg in June. Thymidine uptake increased to 15.7 dpm/μg in July ($P < 0.05$ compared to the uptake in March-June). Thymidine uptake in saline-injected coho averaged 1.6 dpm/μg from February to May, and dropped ($P < 0.05$) to 0.8 dpm/μg in June and July.

Sulfate uptake (Fig. 2) by the cartilages in GH-injected

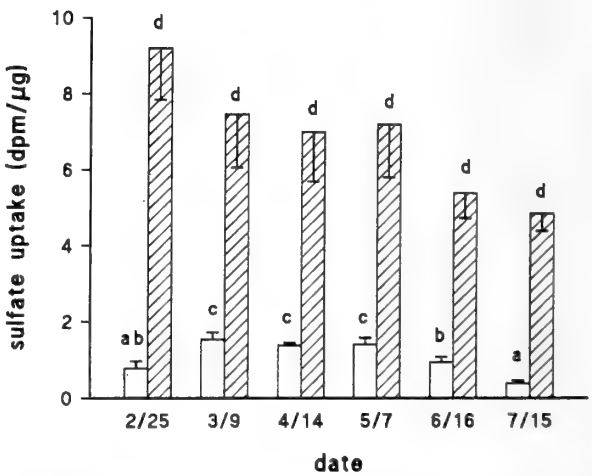

FIG. 2. Basal sulfate uptake (dpm/μg cartilage) by ceratobranchial cartilages from GH- and saline-injected coho salmon (*Oncorhynchus kisutch*) sampled monthly from February to July. Fish were given injections on alternate days (total of 4 injections) and sampled 1 day after the last injection. Hatched and clear boxes represent GH- and saline-injected fish, respectively. Values are mean$\pm$SEM (n=7–10). Values with shared letters are not significantly different ($P > 0.05$).

TABLE 1. Monthly measurements from February-July of thymidine uptake (dpm/μg) by cartilages from GH- and saline-injected (SAL) coho in response to IGF-I *in vitro*

	IGF-I (μg/ml)			
	0	0.01	0.1	1
Feb.				
GH	11.5±2.2 (8)	11.1±1.6 (8)	17.2±2.9 (9)	18.7±2.0 (9)
SAL	1.5±0.4 (8)	2.1±0.4 (9)	2.6±0.3 (9)	3.2±0.4 (10)*
Mar.				
GH	8.1±1.3 (9)	6.7±1.8 (8)	8.5±1.8 (9)	7.3±1.0 (9)
SAL	1.7±0.2 (10)	1.5±0.2 (8)	1.9±0.2 (10)	2.6±0.2 (10)*
Apr.				
GH	8.2±1.9 (9)	6.6±1.1 (8)	11.3±1.8 (9)	11.3±1.8 (9)
SAL	1.8±0.2 (8)	2.1±0.2 (9)	2.9±0.3 (7)*	3.0±0.2 (8)*
May				
GH	9.3±2.2 (9)	11.8±2.2 (10)	22.7±4.7 (10)*	16.9±3.4 (10)
SAL	1.3±0.2 (9)	2.4±0.3 (10)*	3.0±0.2 (10)*	2.9±0.3 (10)*
June				
GH	4.4±0.5 (7)	4.8±0.5 (8)	6.2±0.5 (8)	6.2±0.6 (9)
SAL	0.7±0.1 (8)	1.9±0.3 (8)*	1.9±0.3 (8)*	2.1±0.2 (8)*
July				
GH	15.8±2.2 (7)	21.8±2.8 (7)	21.2±4.3 (7)	18.3±2.3 (7)
SAL	0.9±0.1 (7)	1.9±0.4 (7)*	2.3±0.4 (7)*	2.2±0.3 (7)*

data expressed as ^{3}H-thymidine dpm/μg±SEM (N)
* $P<0.05$ over basal (0) uptake

TABLE 2. Monthly measurements from February-July of sulfate uptake (dpm/μg) by cartilages from GH- and saline-injected (SAL) coho in response to IGF-I *in vitro*

	IGF-I (μg/ml)			
	0	0.01	0.1	1
Feb.				
GH	9.2±1.4 (8)	9.5±0.9 (9)	14.4±1.8 (9)*	14.9±1.0 (9)*
SAL	0.8±0.2 (8)	1.8±0.3 (9)*	2.7±0.3 (9)*	3.1±0.2 (10)*
Mar.				
GH	7.5±1.4 (9)	6.3±1.2 (8)	8.2±1.4 (9)	8.2±1.3 (9)
SAL	1.5±0.2 (10)	1.4±0.2 (10)	1.9±0.2 (10)	2.4±0.3 (10)*
Apr.				
GH	7.0±1.3 (9)	6.3±0.8 (8)	10.8±1.2 (9)*	10.5±1.2 (9)*
SAL	1.4±0.1 (8)	1.5±0.1 (9)	2.7±0.2 (7)*	2.6±0.2 (8)*
May				
GH	7.2±1.4 (9)	11.1±1.6 (10)	17.5±2.8 (10)*	14.1±2.0 (10)*
SAL	1.4±0.2 (9)	2.8±0.3 (10)*	3.4±0.2 (10)*	3.3±0.3 (10)*
June				
GH	5.4±0.7 (7)	6.1±0.5 (8)	7.1±0.5 (8)	7.7±0.9 (9)*
SAL	0.9±0.1 (8)	2.4±0.4 (8)*	2.2±0.3 (8)*	2.2±0.2 (8)*
July				
GH	4.9±0.5 (7)	7.8±0.7 (7)*	6.4±0.8 (7)	6.7±0.7 (7)
SAL	0.4±0.1 (7)	1.0±0.2 (7)*	1.2±0.2 (7)*	1.1±0.2 (7)*

data expressed as $^{35}SO_4$ dpm/μg±SEM (N)
* $P<0.05$ over basal (0) uptake

coho was 5 to 11 times higher than in saline-injected coho throughout the study period (two-way ANOVA, $P<0.0001$). Sulfate uptake by cartilages in GH-injected coho showed a decreasing trend without statistical significance, averaging 8 dpm/μg from February to May and dropping to 5 dpm/μg in June and July. Uptake in saline-injected coho was 0.8 dpm/μg in February, then increased ($P<0.05$) to an average of 1.4 dpm/μg from March to May, and dropped ($P<0.05$) to 0.9 and 0.4 dpm/μg in June and July, respectively. Thymidine and sulfate uptakes were positively correlated in both GH-treated fish ($r=0.65$, $P<0.001$) and in saline-treated fish ($r=0.68$, $P<0.001$).

Cartilage response to IGF-I in vitro

Cartilages from GH- and saline-treated fish in each month were tested for their response to IGF-I *in vitro*; the results are presented in Table 1 (thymidine uptake) and Table 2 (sulfate uptake).

In thymidine uptake (see Table 1), cartilages from GH-treated fish did not respond significantly to further stimulation by IGF-I *in vitro* at 0.01, 0.1 and 1μg/ml; an exception was in May, when cartilage treated with IGF-I *in vitro* at 0.1μg/ml showed an increase over the basal uptake ($P<0.05$). Cartilages from the saline-treated group responded to *in vitro* IGF-I at 1μg/ml in February and March ($P<0.05$), then to both 0.1 and 1μg/ml IGF-I in April ($P<0.05$), and to all IGF-I doses from May to July ($P<0.05$). However, cartilages did not show a dose-dependent response to IGF-I over the doses tested: uptake generally plateaued with increasing doses of IGF-I after the initial or smallest dose that elicited a response.

In sulfate uptake (see Table 2), cartilages from GH-treated fish responded to IGF-I *in vitro* with increases in all months except March. Cartilages sampled in February, April and May responded to IGF-I *in vitro* at 0.1 and 1μg/ml ($P<0.05$). A dose-dependent response to IGF-I was not found, as stimulated sulfate uptake plateaued after 0.1μg/ml. Cartilages in June and July only responded to 1μg/ml and 0.01μg/ml IGF-I, respectively. Cartilages from the saline-treated group responded to *in vitro* IGF-I in all months. Cartilages sampled in February, May, June and July all responded to *in vitro* IGF-I at 0.01, 0.1 and 1μg/ml. Cartilages in March only showed stimulated sulfate uptake at 1μg/ml IGF-I, whereas cartilages in April responded to IGF-I at 0.1 and 1μg/ml. A dose-dependent response to IGF-I again was not found, as stimulated sulfate uptake usually plateaued after the initial or smallest dose that elicited a response.

DISCUSSION

As seen in Figures 1 and 2, GH injection markedly increased thymidine and sulfate uptakes, and the two parameters are strongly correlated ($r=0.65$, $P<0.001$). This indicates that thymidine and sulfate uptakes are generally coupled, even after GH stimulation.

Cartilages from saline-injected fish showed decreased thymidine uptake (Fig. 1) and decreased sulfate uptake (Fig. 2) in June and July. A marked decline in Na^+, K^+-ATPase activity (an indicator of hypoosmoregulatory activity) also occurred in these fish in June and July [13], which may indicate the end of the smoltification period. Cartilages from GH-injected fish also showed a non-significant trend of decreasing thymidine (Fig. 1) and sulfate uptakes (Fig. 2) from February to June and from February to July, respectively. Injected GH might have compensated for the expected decrease in endogenous GH (plasma GH levels were not measured), resulting in a lack of significant decrease in both thymidine and sulfate uptakes. A significant increase in GH-stimulated thymidine uptake ($P<0.05$) was, however, observed in July. This is contrary to the sulfate uptake which stayed low. One explanation may be that the cartilages undergo a new cycle of chondrocyte proliferation at this time. A major increase in thymidine uptake indicating mitotic activity in prechondrocytes/chondrocytes resulted from GH injection in July; this may have led to increased sulfate uptake by maturing chondrocytes at a later date, but this was not examined.

Although GH injection consistently increased thymidine and sulfate uptakes, it did not result in a consistent sensitization to IGF-I *in vitro* as judged by thymidine uptake. The dual effector hypothesis [12] predicts that GH would increase serum levels of IGF-I and increase cartilage sensitivity to IGF-I. Thus, injected GH may have maximally stimulated the mitotic activity of chondrocytes *in vivo* so that further stimulation by IGF-I *in vitro* was not seen. This is in contrast to the findings which showed that priming of gill Na^+, K^+-ATPase resulted from either endogenous or exogenous GH, so that further stimulation by IGF-I *in vitro* was possible [13]. As chondrocytes can also respond to IGF-I by synthesizing chondroitin sulfate, further stimulation of sulfate uptake by IGF-I *in vitro* was still possible. Thus, consistent IGF-I stimulation of sulfate uptake was observed in cartilages from GH-injected coho (March was the only exception).

Although cartilages from the saline-injected group consistently responded to IGF-I *in vitro* with stimulated thymidine and sulfate uptakes, the stimulated uptakes did not approach the basal uptake seen in the GH-injected group (Tables 1 and 2). The observation that GH *in vitro* at 1μg/ml did not increase thymidine or sulfate uptake [14; Tsai, unpublished] suggested that GH has no direct effect on cartilage growth. GH injection may thus act by increasing endogenous IGF-I levels and/or by sensitizing the cartilage cells to hepatic and/or local IGF-I. The dual effector hypothesis of GH action [12] is supported by the observation that no dose of IGF-I alone *in vitro* was able to parallel the effects of GH injection *in vivo*. However, the organ-culture system used did not allow testing of IGF-I *in vitro* in the presence of other serum factors, including IGF-binding proteins. Such factors may modify the responsiveness of cartilage to stimulation by IGF-I. Furthermore, the exposure time of cartilages to IGF-I *in vitro* for 48 hr (maximal sulfate incorporation by eel and salmon cartilage occurs between 24

and 48 hr [8, 9, 14]) was significantly less than the exposure *in vivo* to GH, which was given as 4 injections during a 9-day period (these fish were the same as those used by Madsen and Bern [12]).

As the cartilages seemed to have responded maximally to GH injection and also to IGF-I addition *in vitro*, no significant seasonal change could be discerned. These studies support the relevance of the dual effector theory of GH action [12] to teleost cartilage growth: injection of GH *in vivo* induced consistently higher thymidine and sulfate uptakes by cartilage than were seen in the control cartilages exposed to IGF-I *in vitro*.

ACKNOWLEDGMENTS

P. I. Tsai was a California Sea Grant trainee in 1991–2. S. S. Madsen was a postdoctoral fellow of the Carlsberg Foundation (Denmark). We would like to thank Prof. Charles S. Nicoll for his critical comments on this work, Dr. Richard S. Nishioka for his review of the manuscript, Dr. Elisabeth S. Gray and Richard J. Lin for aid in the statistical analysis, and Kimmakone Siharath, Robert Tsai and Jeanette Endersen for assist in the experiments. This research was funded by a grant from the National Sea Grant College Program, National Oceanic and Atmospheric Administration, U. S. Department of Commerce, under grant number NA89AA-D-SG 138, project R/F-145, through the California Sea Grant College, and in part by the California State Resources Agency. The views expressed herein are those of the authors and do not necessarily reflect the views of NOAA or any of its sub-agencies. The U. S. Government is authorized to reproduce and distribute for governmental purposes. We are grateful to Zenyaku Kogyo Co. of Tokyo for additional support, to NIH and the National Pituitary Program (Baltimore, MD) for the ovine growth hormone and to Monsanto Co. (St. Louis, MO) for the recombinant bovine IGF-I.

REFERENCES

1 Bern HA, McCormick SD, Kelly KM, Gray ES, Nishioka RS, Madsen SS, Tsai PI (1991) Insulin-like growth factors "under water": Role in growth and function of fish and other poikilothermic vertebrates. In "Modern Concepts of Insulin-like Growth Factors" Ed by EM Spencer, Elsevier, New York, pp 85–96

2 Bern HA, Nishioka, RS (1993) Aspects of salmonid endocrinology: the known and the unknown. Bull Fac Fish Hokkaido Univ 44: 55–67

3 Cao O-P, Duguay S, Plisetskaya E, Steiner DF, Chan SJ (1990) Nucleotide sequence and growth hormone-regulated expression of salmon insulin-like growth factor I mRNA. Mol Endocrinol 3: 2005–2010

4 Daughaday WH, Phillips LS, Herington AC (1975) Measurement of somatomedin by cartilage in-vitro. Methods in Enzymology 37: 93–109

5 Duan C, Duguay SJ, Plisetskaya EM (1993) Insulin-like growth factor I (IGF-I) mRNA expression in coho salmon, *Oncorhynchus kisutch*: Tissue distribution and effects of growth hormone/prolactin family proteins. Fish Physiol Biochem 11: 371–379

6 Duan C, Hirano T (1990) Stimulation of ^{35}S-sulfate uptake by mammalian insulin-like growth factor I and II in cultured cartilages of the Japanese eel, *Anguilla japonica*. J Exp Zool 256: 347–350

7 Duan C, Hirano T (1992) Effects of insulin-like growth factor-I and insulin on the in vitro uptake of sulphate by eel branchial cartilage: Evidence for the presence of independent hepatic and pancreatic sulphation factors. J Endocrinol 133: 211–219

8 Duan C, Inui Y (1990) Effects of recombinant eel growth hormone on the uptake of [^{35}S]sulfate by ceratobranchial cartilages of the Japanese eel, *Anguilla japonica*. Gen Comp Endocrinol 79: 320–325

9 Duan C, Inui Y (1990) Evidences for the presence of a somatomedin-like plasma factor(s) in the Japanese eel, *Anguilla japonica*. Gen Comp Endocrinol 79: 326–331

10 Gray E, Kelley KM (1991) Growth regulation in the gobiid teleost, *Gillichthys mirabilis*: Roles of growth hormone, hepatic growth hormone receptors and insulin-like growth factor I. J Endocrinol 130: 57–66

11 Gray E, Kelley KM, Law S, Tsai R, Young G, Bern HA (1992) Regulation of hepatic growth hormone receptors in coho salmon (*Oncorhynchus kisutch*). Gen Comp Endocrinol 88: 243–252

12 Green H, Morikawa M, Nixon T (1985) A dual effector theory of growth hormone action. Differentiation 29: 195–198

13 Madsen SS, Bern HA (1993) In-vitro effects of insulin-like growth factor-I on gill Na^+, K^+-ATPase in coho salmon, *Oncorhynchus kisutch*. J Endocinol 138: 23–30

14 McCormick SD, Tsai PI, Kelley KM, Nishioka RS, Bern HA (1992) Hormonal control of sulfate incorporation by branchial cartilage of coho salmon: role of IGF-I. J Exp Zool 262: 166–172

15 Mori I, Sakamoto T, Hirano T (1992) Growth hormone (GH)-dependent hepatic GH receptors in the Japanese eel, *Anguilla japonica*: effects of hypophysectomy and GH injection. Gen Comp Endocrinol 85: 385–391

16 Prunet P, Boeuf E, Bolton JP, Young G (1989) Smoltification and seawater adaptation in Atlantic salmon (*Salmon salar*): Plasma prolactin, growth hormone, and thyroid hormones. Gen Comp Endocrinol 74: 355–364

17 Sakamoto T, Hirano T (1991) Growth hormone receptors in the liver and osmoregulatory organs of rainbow trout: Characterization and dynamics during adaptation to seawater. J Endocrinol 130: 425–433

18 Sakamoto T, Hirano T (1992) Mode of action of growth hormone in salmonid osmoregulation: Expression of insulin-like growth factor I gene during seawater adaptation. Proc Natl Acad Sci USA 90: 1912–1916

19 Young G, Björnsson BTh, Prunet P, Lin RJ, Bern HA (1989) Smoltification and seawater adaptation in coho salmon (*Oncorhynchus kisutch*): Plasma prolactin, growth hormone, thyroid hormones, and cortisol. Gen Comp Endocrinol 74: 335–345

20 Siharath K, Bern HA (1993) The physiology of insulin-like growth factor (Bengal) (IGF) and its binding proteins in teleost fishes. Proc Zool Soc, Haldane Comm Vol 113–124

ZOOLOGICAL SCIENCE 11: 305–311 (1994)

Mesostigmatic Mites (Acari) Associated with Ground, Burying, Roving Carrion and Dung Beetles (Coleoptera) in Sapporo and Tomakomai, Hokkaido, Northern Japan

GEN TAKAKU[1], HARUO KATAKURA[1] and NOBUYO YOSHIDA[2]

[1]*Division of Biological Sciences, Graduate School of Science, Hokkaido University, Sapporo, Hokkaido 060, and* [2]*Tohoku Agricultural Experiment Station, Morioka, Iwate 020-01, Japan*

ABSTRACT—A total of 19 species belonging to 5 families of mesostigmatic mites were collected in Sapporo and Tomakomai, northern Japan, on four groups of beetles, i.e., ground beetles (Carabinae, Carabidae), burying beetles (Nicrophorini, Silphinae, Silphidae), roving carrion beetles (Silphini, Silphinae, Silphidae) and dung beetles (Scarabaeidae and Geotrupidae), all of which mainly forage on the ground surface. No mite species was found on more than one group of beetles except for *Poecilochirus carabi*, which was found almost exclusively on burying beetles and rarely on ground beetles. Mites also seemed to be specific to particular beetle group(s) at the family level. Thus, the "phoretic" mite faunas were distinctly different between the beetle groups: ground beetles (seven species) were characterized by carrying only one mite species, *Iphidosoma fimetarium*, burying beetles (two species) by two mite species (*Alliphis necrophilus, P. carabi*), roving carrion beetles (three species) by one mite species, Rhodacaridae sp., and dung beetles (11 species) by 15 mite species that included 8 species of *Macrocheles*. Mites associated with dung beetles included specialist species such as *Holostaspella* sp. 1 which was specific to subsocial *Copris ochus*, and generalist species like *Macrocheles* sp. aff. *glaber* that was found on nine dung beetle species.

INTRODUCTION

Various species of mites are found clinging to or moving on the body surface of other organisms, particularly insects. Although such an association between mites and insects sometimes involves complex relationships such as mutualism [37, 41, 42], the association is usually called phoretic on the assumption that the mites use the beetles as vehicles. The majority of larger species of phoretic mites belong to the suborder Mesostigmata [8, 13, 15, 16]. There are a lot of carrier records of these mesostigmatic mites, and carrier specificity of some species has been investigated [5, 9, 10, 12, 27, 28, 30, 34, 40]. Phoretic mesostigmates are also known as an important control agent of house flies [1, 7, 29].

In Japan, too, phoretic mesostigmatic mites are common, and so far 26 species have been recorded on various insect species [21–25]. However, these studies dealt with the mites in the middle and the southern parts of Japan, and no comprehensive study has been undertaken on the mites of the northern part. Furthermore, we know very little on the biology of the Japanese species, except for the carrier records of some species.

Since 1989, we have studied relationships between mesostigmatic mites and various groups of beetles in Hokkaido, northern Japan. As an outcome of this study, we will present below a list of mesostigmatic mites so far confirmed by us on four taxonomically and ecologically different groups of beetles, i.e., ground beetles (Carabidae), burying beetles (Nicrophorini, Silphinae, Silphidae), roving carrion beetles (Silphini, Silphinae, Silphidae), and dung beetles (Geotrupidae and Scarabaeidae). We will also summarize suggested relationships between mesostigmatic mites and carrier beetles.

Accepted January 28, 1994
Received December 24, 1993

MATERIALS AND METHODS

We collected beetles with the aid of pitfall traps set at forest margins and in the forests in the vicinity of Sapporo, and Hokkaido University Tomakomai Experiment Forest, Tomakomai, Hokkaido, northern Japan. The pitfall traps were baited with meat or without any bait. We also collected beetles from cattle dung by hand in pastures of Hokkaido Agricultural Experiment Station in Sapporo. Beetles collected on other occasions were also examined for their phoretic mites. No quantitative sampling of beetles was undertaken. Beetles were anesthetized with chloroform or ethyl-ethel. Mites detached from the anesthetized beetles were fixed in 70% ethanol, softened and cleared in lactophenol and mounted with a gum-chroral medium on a glass slide [27, 36]. Observation and identification of mites were made on these mounted specimens under a phase-contrast microscope.

RESULTS

Beetles examined and those bearing mesostigmatic mites

We examined 33 species of beetles during the course of this study. Mesostigmatic mites were obtained from 23 beetle species, which are asterisked in the following list (scientific names of the beetles followed Hirashima [17], except those of *Aphodius* dung beetles for which we follow Masumoto *et al.* [33]):

Ground beetles (Carabinae, Carabidae, 12 species): *Cychrus morawitzi* Géhin, 1885, *Calosoma maximowiczi*

(Morawitz, 1863), *Cl. inquisitor cyanescens* Motschulsky, 1858, *Campalita chinense* (Kirby, 1818), **Carabus granulatus yezoensis* Bates, 1883, **C. conciliator hokkaidensis* Lapouge, 1924, **C. albrechti albrechti* Morawitz, 1862, **Leptocarabus arboreus arboreus* (Lewis, 1882), **L. opaculus opaculus* (Putzeys, 1875), *Procrustes kolbei aino* (Rost, 1908), **Damaster gehinii gehinii* (Fairmaire, 1876), **D. blaptoides rugipennis* (Motschulsky, 1861).

Burying beetles (Nicrophorini, Silphinae, Silphidae, 5 species): **Nicrophorus maculifrons* Kraatz, 1877, **N. quadripunctatus* Kraatz, 1897, *N. investigator investigator* Zetterstedt, 1824, *N. vespilloides* (Herbst, 1784), *Ptomascopus morio* (Kraatz, 1877).

Roving carrion beetles (Silphini, Silphinae, Silphidae, 4 species): **Silpha perforata venatoria* Harold, 1877, **Eusilpha japonica* (Motschulsky, 1860), **Phosphuga atrata* (Linnaeus, 1758), *Dendroxena sexcarinata* (Motschulsky, 1866).

Dung beetles (Geotrupidae and Scarabaeidae, 12 species): **Geotrupes auratus* Motschulsky, 1857, **G. laevistriatus* Motschulsky, 1857, **Copris ochus* Motschulsky, 1860, **Liatongus phanaeoides* (Westwood, 1840), **Caccobius jessoensis* Harold, 1867, **Onthophagus ater* Waterhouse, 1875, **O. atripennis atripennis* Waterhouse, 1875, **Aphodius elegans* Allibert, 1847, **A. haemorrhoidalis* (Linnaeus, 1758), **A. quadratus* Reiche, 1847, **A. pusillus* (Herbst, 1789), *A. rectus* (Motschulsky, 1866).

List of mesostigmatic mites collected

A total of nineteen species of mites were collected from 23 species of beetles. They are enumerated below with some notes. Full taxonomic accounts of these mites will be published elsewhere by the first author ([38]; in preparation). Mites referred to by the combinations of the generic name and the species code number are undescribed species. Asterisked species are those recorded from Japan for the first time. For each species, a) stages of mites collected; b) carrier beetles confirmed by us; c) attaching site and d) known geographic distribution, are given.

Superfamily Eviphidoidea

Family Eviphididae

1) *Eviphis cultratellus* (Berlese, 1910)*: a) female, male, deutonymph; b) *Copris ochus*; c) ventral surface of body, mainly intersegmental membrane between prothorax and mesothorax; d) Japan (Hokkaido), Java, Egypt, India, South Africa.

This species has been collected on the dung beetles *Onitis* spp. [35], *Copris* sp. [2], and from cattle dung [3].

2) *Eviphis* sp. 1*: a) female; b) *Copris ochus*; c) ventral surface of body, mainly intersegmental membrane between prothorax and mesothorax; d) Japan (Hokkaido).

3) *Alliphis halleri* (G. & R. Canestrini, 1881): a) female, male, deutonymph; b) *Copris ochus, Caccobius jessoensis, Aphodius elegans*; c) mainly around the mouthparts; d) Japan (Hokkaido, Shikoku), Europe, Israel.

This species has so far been collected on the dung beetle *Geotrupes laevistriatus* and on the burying beetle *Nicrophorus quadripunctatus* in southern Japan [21], and on five species of dung beetles (*Copris* [8], *Geotrupes* [6, 18, 26]) in Europe and Israel.

4) *Alliphis necrophilus* Christie, 1983*: a) female, male, deutonymph; b) *Nicrophorus maculifrons, N. quadripunctatus*; c) specifically found on the ventral membranous portion connecting prothorax and mesothorax; d) Japan (Hokkaido), UK.

Unlike *A. halleri*, the present species was exclusively found on burying beetles of the genus *Nicrophorus*. *A. necrophilus* also has been collected on several species of *Nicrophorus* beetles in the UK [6].

5) *Scarabaspis spinosus* Ishikawa, 1968: a) female, male, deutonymph; b) *Geotrupes laevistriatus*; c) ventral surface of body, mainly prothorax; d) Japan (Hokkaido, Shikoku).

This species seems to be specific to the dung beetle *G. laevistriatus* [21, present study].

6) *Pelethiphis hogai* Ishikawa, 1984: a) female, male; b) *Geotrupes auratus*; c) specifically found on the ventral side of the prothorax; d) Japan (Hokkaido, Honshu).

This species is thus far known only on *G. auratus* ([25]; present study).

Family Macrochelidae

7) *Macrocheles insignitus* Berlese, 1918: a) female; b) *Liatongus phanaeoides, Aphodius quadratus*; c) mainly found on the ventral surface of body, in particular the membranous portion between prothorax and mesothorax; d) Japan (Hokkaido, Honshu, Shikoku), Europe, USA.

This species has been found in a variety of habitats including beetles, a rodent, compost, cattle dung, grassland soil, wet mosses, and nests of bumble bees (*Bombus* sp.) [20, 24, 31].

8) *Macrocheles serratus* Ishikawa, 1968: a) female, male, deutonymph; b) *Geotrupes laevistriatus, Aphodius quadratus*; c) mainly found on the ventral surface of body, in particular the membranous portion between prothorax and mesothorax; d) Japan (Hokkaido, Shikoku).

9) *Macrocheles* sp. aff. *glaber* (Müller, 1860)*: a) female; b) *Geotrupes auratus, G. laevistriatus, Copris ochus, Liatongus phanaeoides, Caccobius jessoensis, Aphodius quadratus, A. haemorrhoidalis, A. pusillus, A. elegans*; c) mainly found on the ventral surface of body, in particular the membranous portion between prothorax and mesothorax; d) Japan (Hokkaido); *M. glaber* is nearly cosmopolitan, being distributed in Europe, Mediterranian areas, Russia, USA, Australia and New Zealand.

Although this species can be identified with *M. glaber* we could not obtain deutonymphs which are indispensable for exact identification. *M. glaber* has so far been collected on various groups of coprophagous scarabaeid beetles (*Geotrupes, Typhaeus, Aphodius, Onthophagus, Copris*) in Europe, Australia and Japan. Also collected on burying beetles (*Nicrophorus*), bumble bees (*Bombus*), small mam-

mals and their nests, and in a variety of manure and rotting vegetation habitats [11, 20].

10) *Macrocheles* sp. aff. *monchadskii* Bregetova & Koroleva, 1960*: a) female; b) *Geotrupes laevistriatus, Onthophagus ater*; c) mainly found on the ventral surface of body, in particular the membranous portion between prothorax and mesothorax; d) Japan (Hokkaido); *M. monchadskii* was described from Adzhar (Russia).

Macrocheles monchadskii was recorded from leaf litter [4].

11) *Macrocheles* sp. aff. *hallidayi* Walter & Krantz, 1986*: a) female; b) *Geotrupes auratus, Onthophagus ater, O. atripennis atripennis, Copris ochus, Liatongus phanaeoides, Aphodius quadratus*; c) mainly found on the ventral surface of body, in particular the membranous portion between prothorax and mesothorax; d) Japan (Hokkaido); *M. hallidayi* is widespread in SE Asia, covering India, Thailand, Cambodia, Java and Sarawak.

Macrocheles hallidayi has been found on dung beetles of the genera *Onitis, Heliocopris*, and *Catharsius* [39].

12) *Macrocheles* sp. aff. *moneronicus* Bregetova & Koroleva, 1960*: a) female; b) *Geotrupes laevistriatus, Liatongus phanaeoides*; c) mainly found on the ventral surface of body, in particular the membranous portion between prothorax and mesothorax; d) Japan (Hokkaido); *M. moneronicus* was described from Moneron Island (Russia) [4].

13) *Macrocheles* sp. 1*: a) female; b) *Geotrupes laevistriatus, Onthophagus ater, O. atripennis atripennis*; c) mainly found on the ventral surface of body, in particular the membranous portion between prothorax and mesothorax; d) Japan (Hokkaido).

14) *Macrocheles* sp. 2*: a) female; b) *Copris ochus, Liatongus phanaeoides, Onthophagus ater, Aphodius quadratus, A. elegans*; c) mainly found on the ventral surface of body, in particular the membranous portion between prothorax and mesothorax; d) Japan (Hokkaido).

15) *Holostaspella* sp. 1*: a) female, male, deutonymph, protonymph; b) *Copris ochus*; c) mainly found on the ventral surface of body, in particular the membranous portion between prothorax and mesothorax; d) Japan (Hokkaido).

This species was found exclusively on the subsocial dung beetle *C. ochus*. Not only adults, but also deutonymphs and protonymphs were collected on beetle body surface and from dung balls which were made by the parental beetles as the larval food [38].

Family Pachylaelapidae

16) *Pachylaelaps copris* Ishikawa, 1984: a) female, male; b) *Copris ochus*; c) mainly found on the ventral surface of body, in particular the membranous portion between prothorax and mesothorax; d) Japan (Hokkaido, Kyushu).

Thus far collected only on *C. ochus* ([25]; present study).

Superfamily Parasitoidea
Family Parasitidae

17) *Poecilochirus carabi* G. & R. Canestrini, 1882*: a) deutonymph; b) *Nicrophorus maculifrons, N. quadripunctatus, Carabus albrechti albrechti, Damaster gehinii gehinii*; c) mainly found on the ventral surface of body, in particular the membranous portion between prothorax and mesothorax; d) Japan (Hokkaido), Europe, Russia, China, USA.

P. carabi has been collected on various species of burying beetles (*Nicrophorus*) and carcasses of birds and small mammals, and has been said to be mutualistic with *Nicrophorus* beetles [5, 37, 41, 42]. In the present study, too, this species was mainly collected on *Nicrophorus* beetles. In addition, *P. carabi* has been collected on dung beetles (*Aphodius*) and ground beetles (*Carabus, Pterostichus*) ([19, 34, 37, 40]; present study). The nature of association between *P. carabi* and beetles other than burying beetles is yet unknown.

Superfamily Rhodacaroidea
Family Rhodacaridae

18) *Iphidosoma fimetarium* (Müller, 1859)*: a) female; b) *Carabus granulatus yezoensis, C. conciliator hokkaidensis, C. albrechti albrechti, Leptocarabus arboreus arboreus, L. opaculus opaculus, Damaster gehinii gehinii, D. blaptoides rugipennis*; c) mainly attached to the dorsal side of mesothorax, metathorax and abdomen covered by elytra; d) Japan (Hokkaido), Russia, Europe.

We collected *I. fimetarium* on seven species of carabid beetles. In Russia and Europe, too, this species has been collected on ground beetles of the genera *Carabus, Pterostichus* and *Nebria* [14, 32].

19) Rhodacaridae sp. a) deutonymph; b) *Silpha perforata venatoria, Eusilpha japonica, Phosphuga atrata*; c) mainly attached to the dorsal side of mesothorax, metathorax and abdomen covered by elytra. d) Japan (Hokkaido).

The genus, to which this species belongs, is difficult to determine since only deutonymphs are available.

REMARKS

Summarizing the above findings, we prepared a synoptic list of mesostigmatic mites and carrier beetles (Table 1). Some ecological properties of examined beetles were summarized in Table 2, together with associated mite families. Recent studies have shown that carrier specificity may be different between populations of a single mite species [5, 34, 40]. Furthermore, there may be seasonal difference in mite frequencies on beetles. Since we did not make any quantitative sampling of beetles, our data is not appropriate to analyze such spatio-temporal variation of beetle-mite interaction. However, our results suggest certain noteworthy aspects of mite-beetle associations as shown below.

First, mesostigmatic mites were never collected on the beetles foraging on tree foliage; all the beetles that carried mesostigmatic mites forage on the ground (Table 2), or forage on the foliage of undergrowth plants (*Phosphuga atrata*). Secondly, except for *P. carabi*, which was almost exclusively found on burying beetles but rarely on ground beetles, no mite species were found on more than one beetle

TABLE 1. Synopsis of carrier beetles and associated mesostigmatic mites examined in the present study

Groups and species of carrier beetles	Families and species of mesostigmatic mites																							
	Eviphididae	*Eviphis cultratellus*	*E.* sp. 1	*Alliphis halleri*	*A. necrophilus*	*Scarabaspis spinosus*	*Pelethiphis hogai*	Macrochelidae	*Macrocheles insignitus*	*M. serratus*	*M.* sp. aff. *glaber*	*M.* sp. aff. *monchadskii*	*M.* sp. aff. *hallidayi*	*M.* sp. aff. *moneronicus*	*M.* sp. 1	*M.* sp. 2	*Holostaspella* sp. 1	Pachylaelapidae	*Pachylaelaps copris*	Parasitidae	*Poecilochirus carabi*	Rhodacaridae	*Iphidosoma fimetarium*	Rhodacaridae sp.
Ground beetles																								
Carabus glanulatus yesoensis																							+	
C. conciliator hokkaidensis																							+	
C. albrechti albrechti																					+		+	
Leptocarabus arboreus arboreus																							+	
L. opaculus opaculus																							+	
Damaster gehinii gehinii																					+		+	
D. blaptoides rugipennis																							+	
Burying beetles																								
Nicrophorus maculifrons					+																+			
N. quadripunctaus					+																+			
Roving carrion beetles																								
Silpha perforata venatoria																								+
Eusilpha japonica																								+
Phosphuga atrata																								+
Dung beetles																								
Geotrupes auratus							+				+		+											
G. laevistriatus						+				+	+	+		+	+									
Copris ochus		+	+	+							+		+			+	+		+					
Liatongus phanaeoides									+		+		+	+		+								
Caccobius jessoensis				+							+													
Onthophagus ater												+	+		+	+								
O. atripennis atripennis													+		+									
Aphodius quadratus									+	+	+		+			+								
A. haemorrhoidalis											+													
A. pusillus											+													
A. elegans				+							+					+								

group (Table 1). Such strong associations with particular groups of beetles are also noticed at the family level of mites (Table 2). We briefly examine below these mite-beetle associations for each mite family.

Eviphididae: Five eviphidid species were collected on five species of dung beetles, and one eviphidid species on two species of burying beetles. Since all these beetle species are either presocial or subsocial and bury food under the ground for their larvae, eviphidid mites might be specific to beetles that share this particular behavioral characteristic. Carrier specificity of eviphidid mites seems to be intense. Two closely related *Alliphis* species differ in their carriers, *A. halleri* on dung beetles and *A. necrophilus* on burying beetles (*Nicrophorus*). Furthermore, *Scarabaspis spinosus* and *Pelethiphis hogai* were found to be specific to different species of *Geotrupes* dung beetles, the former to *G. laevistriatus* and the latter to *G. auratus*.

Macrochelidae: About half of the mite species reported in the present paper are macrochelids, and they belong to a single genus *Macrocheles*, except for *Holostaspella* sp. 1. All the species were collected on dung beetles. Some *Macrocheles* species, in particular *M.* sp. aff. *glaber*, are generalists and were found on various species of dung beetles, whereas *Holostaspella* sp. 1 was a specialist and found only on the subsocial *Copris ochus* and in the dung balls prepared by the beetles.

Pachylaelapidae: Only one species, *Pachylaelaps copris*, was collected. Like *Holostaspella* sp. 1, *P. copris* was spe-

TABLE 2. Some ecological properties of beetles examined and associated mite families.

Beetle group and genus	Food type	Foraging at	Flight ability	Sociality	Associated mite family***				
					EV	MA	PC	PR	RD
Ground beetles									
*Cychrus**	Live invertebrates	Ground	−	None					
*Calosoma**	Live invertebrates	Tree foliage	+	None					
*Campalita**	Live invertebrates	Tree foliage	+	None					
Carabus	Live invertebrates	Ground	−	None				(+)	+
Leptocarabus	Live invertebrates	Ground	−	None					+
Procrustes	Live invertebrates	Ground	−	None					
Damaster	Live invertebrates	Ground	−	None				(+)	+
Burying beetles									
Nicrophorus	Small vertebrate carcasses	Ground	+	Subsocial	+			+	
*Ptomascops**	Vertebrate carcasses	Ground	+	None (?)					
Roving carrion beetles									
Silpha	Live and dead organic matter	Ground	−	None					+
Eusilpha	Live and dead organic matter	Ground	−	None					+
Phosphuga	Live invertebrates	Foliage of undergrowth	−	None					+
*Dendroxena**	Live invertedrates	Tree foliage	+	None					
Dung beetles									
Geotrupes auratus	Vertebrate dung	Ground	+	Presocial	+	+			
G. laevistriatus	Vertebrate dung, dead organic matter	Ground	+(?)	Presocial	+	+			
Copris	Vertebrate dung	Ground	+	Subsocial	+	+	+		
Liatongus	Vertebrate dung	Ground	+	Presocial		+			
Caccobius	Vertebrate dung	Ground	+	Presocial	+	+			
Onthophagus	Vertebrate dung	Ground	+	Presocial		+			
Aphodius I**	Vertebrate dung	Ground	+	Presocial	+	+			
Aphodius II**	Vertebrate dung	Ground	+	None		+			

* No mesostigmatic mites were found on these beetles
** *Aphodius* I: *A. quadratus, A. elegans; Aphodius* II: *A. haemorrhoidalis, A. rectus, A. pusillus.*
*** EV, Eviphididae; MA, Macrochelidae; PC, Pachylaelapidae; PR, Parasitidae; RD, Rhodacaridae.

cific to *Copris ochus*.

Parasitidae: Only one species, *Poecilochirus carabi*, was collected. This is the only species that was collected on two different groups of beetles, the ground beetles and burying beetles. In USA and Europe, this species is known to be mutualistic with burying beetles [5, 37, 41, 42], but nothing is known about the association with ground beetles as mentioned before.

Rhodacaridae: Rhodacarid mites in the surveyed habitats may be specific to beetles that forage exclusively on the ground. All the beetle species bearing rhodacarids are either ground beetles or roving carrion beetles that cannot fly, whereas burying beetles and dung beetles, which were rhodacarid-free, can fly well (with the possible exception of *G. laevistriatus* which rarely flies as far as we know). *Iphidosoma fimetarium* was specific to ground beetles but did not show preference to particular species of ground beetles. Likewise, Rhodacaridae sp. was specific to roving carrion beetles but did not show species specificity.

Reflecting these carrier specificities of mesostigmatic mites, the "phoretic mite" faunas of the four beetle groups were distinctly different (Tables 1, 2). Ground beetles (seven species) were characterized by only one mite species (*Iphidosoma fimetarium*), burying beetles (two species) by two species (*Alliphis necrophilus, Poecilochirus carabi*), roving carrion beetles (three species) by one species (Rhodacaridae sp.), and dung beetles (11 species) by 15 species, including 8 species of *Macrocheles*.

Thus, most mite species, or mite families, showed definite preference for a particular group of beetles. The reason is not yet clear. Since the four beetle groups treated in the present study differ phylogenetically and ecologically, both phylogenetic constraints and ecological factors could affect the carrier specificity. Future studies will clarify which factor is most important in shaping the carrier preference of these mites.

ACKNOWLEDGMENTS

We express our thanks to Dr. G. W. Krantz for his review of the manuscript, and two anonymous reviewers for their helpful comments. This study was supported by a Grant in Aid (No. 04264203) from the Ministry of Education, Science and Culture of Japan.

REFERENCES

1 Axtell RC (1964) Phoretic relationship of some common manure-inhabiting Macrochelidae (Acarina: Mesostigmata) to the house fly. Ann Entomol Soc America 57: 584–587

2 Berlese A (1910) Lista di nuove specie e nuovi generi di Acari. Redia 6: 242–271

3 Bhattacharyya SK (1971) The genus *Eviphis* in India (Acarina: Mesostigmata: Eviphididae). Acarologia 13: 266–271

4 Bregetova NG, Koroleva EV (1960) The macrochelid mites (Gamasoidea, Macrochelidae) in the USSR. Parazit Sb 19: 32–154

5 Brown JM, Wilson DS (1994) *Poecilochirus carabi:* Behavioral and life-history adaptations to different hosts and the consequences of geographical shifts in host communities. In "Mites: Ecological and Evolutionary Analyses of Life-History Patterns" Ed by MA Houck, Chapman & Hall, pp 1–22

6 Christie JE (1983) A new species of *Alliphis* (Mesostigmata: Eviphididae) from Britain. Acarologia 24: 231–242

7 Cicolani B (1992) Macrochelid mites (Acari: Mesostigmata) occurring in animal droppings in the pasture ecosystem in central Italy. Agri Ecosys Environ 40: 47–60

8 Costa M (1963) The mesostigmatic mites associated with *Copris hispanus* (L.) (Coleoptera, Scarabaeidae) in Israel. J Linn Soc Zool 45: 25–45

9 Costa M (1967) Notes on macrochelids associated with manure and coprid beetles in Israel. II. Three new species of the *Macrocheles pisentii* complex, with notes on their biology. Acarologia 9: 304–329

10 Costa M (1969) The association between mesostigmatic mites and coprid beetles. Acarologia 11: 411–426

11 Evans GO, Browning E (1956) British mites of the subfamily Macrochelinae Tragardh (Gamasina - Macrochelidae). Bull Br Mus nat Hist (Zool) 4: 1–55.

12 Evans GO, Hyatt KH (1963) Mites of the genus *Macrocheles* Latr (Mesostigmata) associated with coprid beetles in the collections of the British Museum (Natural History). Bull Br Mus nat Hist (Zool) 9: 327–401

13 Evans GO, Sheals JG, Macfarlane D (1961) The Terrestrial Acari of the British Isles. An Introduction to their Morphology, Biology and Classification. 1. Introduction and Biology. British Museum, London

14 Ghilarov MS, Bregetova NG (1977) A Key to the Soil-Inhabiting Mites. Mesostigmata. Zool Inst Akad Sci USSR, Leningrad, 718 pp

15 Halffter G., Matthews GE (1971) The natural history of dung beetles. A supplement on associated biota. Rev lat amer Microbiol 13: 147–164

16 Halliday RB (1986) Mites of the *Macrocheles glaber* group in Australia (Acarina: Macrochelidae). Aust J Zool 34: 733–752

17 Hirashima Y (Ed) (1989) A Check List of Japanese Insects I. xi +540 pp. Published by Entomological Laboratory, Faculty of Agriculture, Kyushu University, Fukuoka.

18 Hyatt KH (1959) Mesostigmatic mites associated with *Geotrupes stercorarius* (L.) (Col., Scarabaeidae). Entomologist's Mon Mag 95: 22–23

19 Hyatt KH (1980) Mites of the subfamily Parasitinae (Mesostigmata: Parasitidae) in the British Isles. Bull Br Mus nat Hist (Zool) 38: 237–378

20 Hyatt KH, Emberson RM (1988) A review of the Macrochelidae (Acari: Mesostigmata) of the British Isles. Bull Br Mus nat Hist (Zool) 54: 63–125

21 Ishikawa K (1968) Studies on the mesostigmatid mites associated with the insects in Japan (I). Rep Res Matsuyama Shinonome Jr Coll 3: 197–218

22 Ishikawa K (1977) On the mesostigmatid mites associated with the cerambycid beetle, *Monochamus alternatus* Hope (I). Annot Zool Japon 50: 99–104

23 Ishikawa K (1977) On the mesostigmatid mites associated with the cerambycid beetle, *Monochamus alternatus* Hope (II). Annot Zool Japon 50: 182–186

24 Ishikawa K (1980) *Macrocheles insignitus*. In "Illustrations of the Mites and Ticks of Japan" Ed by S Ehara, Zenkoku Nôson Kyôiku Kyôkai, Tokyo, pp 90–91 (In Japanese)

25 Ishikawa K (1984) Studies on the mesostigmatid mites associated with the insects in Japan (II). Rep Res Matsuyama Shinonome Jr Coll 15: 89–102

26 Koyumdjieva MI (1981) Gamasid mites (Gamasoidea, Parasitiformes) associated with scarabaeid beetles (Coleoptera, Scarabaeidae) in Bulgaria. Acta Zool Bul 17: 17–26

27 Krantz GW (1978) A Manual of Acarology, Second Edition. Oregon State Univ. Book Stores, Inc., Corvallis, 509 pp

28 Krantz GW (1981) Two new *glaber* group species of *Macrocheles* (Acari: Macrochelidae) from southern Africa. Int J Acarol 7: 3–16

29 Krantz GW (1983) Mites and biological control agents of dung-breeding flies, with special reference to the Macrochelidae. In "Biological Control of Pests by Mites" Ed by MA Hoy, GL Cunningham, L Knutson, University of California, Special Publication 3304, Berkley, pp 91–98

30 Krantz GW, Mellott JL (1972) Studies on phoretic specificity in *Macrocheles mycotrupetes* and *M. peltotrupetes* Krantz and Mellott (Acari: Macrochelidae), associates of geotrupine Scarabaeidae. Acarologia 14: 317–344

31 Krantz GW, Whittaker JO Jr (1988) Mites of the genus *Macrocheles* (Acari: Macrochelidae) associated with small mammals in North America. Acarologia 29: 225–259

32 Lundqvist L (1991) Rearing deutonymphs of *Iphidosoma fimetarium* (J. Müller), a mesostigmatic mite associated with carabid beetles. In "The Acari: Reproduction, Development and Life-history Strategies" Ed by R Schuster, PW Murphy, pp 445–452

33 Masumoto K., Dellacasa G, Kiuchi M (1990) On the *Aphodius* species of Japan. Ent Rev Japan 45: 145–156

34 Müller JK, Schwarz HH (1990) Differences in carrier preference and evidence of reproductive isolation between mites of *Poecilochirus carabi* (Acari, Parasitidae) living phoretically on two sympatric *Necrophorus* species. Zool Jb Syst 117: 23–30

35 Ryke PAJ, Meyer MKP (1957) Eviphidinae Berlese 1913 (Mesostigmata: Acarina) associated with South African beetles. Ann Mag Nat Hist (Ser 12) 10: 593–618

36 Shirasaka A, Ito Y (1980) Technique for the collecting and preparation of mites. In "Illustrations of the Mites and Ticks of Japan" Ed by S Ehara, Zenkoku Nôson Kyôiku Kyôkai, Tokyo, pp 511–520 (In Japanese)

37 Springett BP (1968) Aspects of the relationship between burying beetles, *Necrophorus* spp. and the mite, *Poecilochirus necrophori* Vitz. J Anim Ecol 37: 417–427

38 Takaku G (1994) A new species of the genus *Holostaspella* (Acari; Macrochelidae) from northern Japan. Acarologia 35 (In press)

39 Walter DE, Krantz GW (1986) Description of the *Macrocheles*

kraepelini species complex (Acari: Macrochelidae) with two new species. Can J Zool 64: 212–217

40 Wilson DS (1982) Genetic polymorphism for carrier preference in a phoretic mite. Ann Entomol Soc America 75: 293–296

41 Wilson DS (1983) The effect of population structure on the evolution of mutualism: a field test involving burying beetles and their phoretic mites. Amer Nat 121: 851–870

42 Wilson DS, Knollenberg WG (1987) Adaptive indirect effects: the fitness of burying beetles with and without their phoretic mites. Evol Ecol 1: 139–159

ZOOLOGICAL SCIENCE 11: 313–317 (1994)

First Fossil Record of the Family Phormosomatidae (Echinothurioida: Echinoidea) from the Early Miocene Morozaki Group, Central Japan

SHONAN AMEMIYA[1], YOSHIAKI MIZUNO[2] and SUGURU OHTA[3]

[1]Misaki Marine Biological Station, University of Tokyo, Miura-shi, Kanagawa 238-02, [2]Tokai Fossil Society, 9-21, Sawashita-cho, Atsuta-ku, Nagoya, Aichi 456, [3]Ocean Research Institute, University of Tokyo, 1-15-1, Minamidai, Nakano-ku, Tokyo 164, Japan

ABSTRACT—A fossil echinothurioid echinoid is described from the Early Miocene Morozaki Group in the Chita Peninsula of Aichi Prefecture, central Japan. Based on geological observations, the fossil species is supposed to be the inhabitant of the bathyal zone. The diagnosis of the species is as follows: A small body size for an echinothurioid, large and deep areoles in the oral side, slender teeth with a sharp point, and a large peristome area. From the supposed habitat and the diagnosis, this species is considered to be identical with or a direct ancestor of *Phormosoma bursarium*, a common extant species in the bathyal zone of the Indo-Pacific region including the southern coasts of the Japanese main islands. This is not only the first fossil record in the world of the family Phormosomatidae, but also the third fossil species for the order Echinothurioida.

INTRODUCTION

Fossil echinothurioid echinoids have scarcely been found because the echinothurioids have flexible tests with rich connective tissue and poorly calcified ossicles [19]. Extant echinothurioids are divided into two families, Echinothuriidae and Phormosomatidae [7, 18, 19]. As the firm records, only two fossile species of echinothurioids have been reported [19]. One species is *Echinothuria floris* from the Upper Cretaceous of the British Chalk [20], and another is *Araeosoma thetidis* from the Pliocene of New Zealand [4, 19]. No fossil phormosomatid has been reported so far [19].

The sea along the Pacific coast of the Japanese main island is so extensively exploited that some groups of organisms known elsewhere only from the deep sea seems to occur there in relatively shallower waters. Echinothurioids are one of such groups, and a considerable number of species of the order can be found. The extant species of echinothurioids found on the bottom of or shallower than the upper bathyal zone in the Japanese coast include 5 species of the Echinothuriidae: *Asthenosoma ijimai* from the infralittoral zone, *Araeosoma owstoni* and *Hapalosoma gemmiferum* from the circalittoral (lower sublittoral covering the edge of continental shelf) zone, and *Calveriosoma gracile* and *Hygrosoma hoplacantha* from the upper to middle bathyal zone [1, 2, 8, 10–13, 16, 21], and one species of the Phormosomatidae, that is *Phormosoma bursarium* from the upper bathyal zone [8, 10–13, 16]. However, fossil specimens of echinothurioids have never been reported from Japan.

Miocene deposits known as the Morozaki Group are distributed widely in the southern area of Aichi Prefecture. The Group is characterized by extremely rich marine fossil fauna consisting of bathyal and mesopelagic assemblage [14]. Recently, we obtained a large amount of deep-sea fossils comprising fishes, echinoderms, crustaceans and molluscs, from sandstone and mudstone beds in the Morozaki Group. Among those, some specimens of the Phormosomatidae were found.

In the present paper, a fossil phormosomatid species is described on the basis of seven specimens, and its affinity with *P. bursarium* is discussed.

MATERIALS

The Morozaki Group is distributed in Saku-shima and Himaka-shima Islands in Mikawa Bay, and the southern edge of the Chita Peninsula in Aichi Prefecture situated in central Japan (Fig. 1). The group is subdivided into four formations which are the Himaka, Toyohama, Yamami, and Utsumi Formations in ascending order [14]. The fossil phormosomatid specimens examined were collected with many other echinoderm species (ca. 17 species) from the Toyohama and Yamami Formations (Fig. 1: Locs. 1–3) and were found in the tuffaceous sandstone beds deposited in the bathyal zone between around 500 m to 1,000 m depth or more [5].

The geologic age of the Toyohama and Yamami Formations was estimated to be Middle Miocene, 15.5 Ma to 16.5 Ma [14, 15]. But recent biostratigraphic studies based on planktonic foraminifers [3] and paleomagnetic study [6] showed that the formations are Early Miocene in age. These formations contain various kinds of fossil species including phormosomatid echinoids. They are composed of benthic, nektonic and planktonic organisms such as fishes, crustaceans, molluscs and protozoans having inhabited various depth zones from littoral to bathyal [17]. Echinoids were abundant and accounted for more than a half of the echinoderm specimens collected from the formations.

More than ten specimens of fossil phormosomatids were collected. Six of them (MFM 38057–38060, MI 01, SA 01) are almost intact, and others are fragmental. The fossil specimens examined in this study are deposited in the Mizunami Fossil Museum (MFM

Accepted January 7, 1994
Received April 17, 1992

38057–38060), the Misaki Marine Biological Station (MMBS A1), and in the private collections of Y. Mizuno (MI 01) and F. Sakakura (SA 01).

MFM 38057, 38060, and MI 01 were found in a tuffaceous sandstone bed of the lower part of the Yamami Formation (Fig. 1: Loc. 2), together with crinoids, ophiuroids, crustaceans and molluscs.

MFM 38057 was collected from a sandstone bed of the uppermost part of the Toyohama Formation (Fig. 1: Loc. 1), together with asteroids and ophiuroids.

MFM 38058 and SA 01 was collected from a tuffaceous mudstone bed of the middle part of the Yamami Formation (Fig. 1: Loc. 3), together with asteroids, ophiuroids, crustaceans, molluscs and fishes.

The living specimens of *Phormosoma bursarium* (MMBS P1–P7) for comparison were collected from Suruga Bay at 550 m in depth.

SYSTEMATIC DESCRIPTION

Order Echinothurioida Claus, 1880
Family Phormosomatidae Mortensen, 1934
Subfamily Phormosomatinae Mortensen, 1934
Genus *Phormosoma* Thomson, 1872
Phormosoma sp. cf. *P. bursarium* A. Agassiz, 1881

Diagnosis: 1, a small body size for an echinothurioid; 2, large and deep areoles in the oral side; 3, slender teeth with a sharp point; 4, a large peristome area.

Description: This description is based on six intact (MFM 38057–38060, MI 01, SA 01) and one fragmental (MMBS A1) specimens. The test is circular and rather small in size for an echinothurioid with the diameters ranging from 48 mm to 118 mm (Table 1). The size is comparable to that of *Phormosoma bursarium,* an extant species, but somewhat larger than the other extant species, *P. placenta, P. rigidum,* and *P. verticillatum,* none of which reaches a larger size than 90 mm in diameter [8]. Specimens are squashed along the oral-aboral axis. In most specimens, the oral side is well preserved (Fig. 2), but the aboral side is damaged heavily, or lost. The oral side of the test looks like a honey-comb (Figs. 2, 3), because the areoles of the primary tubercles in the oral side are very large and deep. The five pieces of teeth in the lantern are slender with sharp points (Figs. 2, 4). The areoles in the aboral side, in contrast to the oral side, are small and not so deep (Fig. 4). The peristome area is large (Figs. 2, 4), although not so large as in *P. bursarium* (Table 1). Interambulacra on the oral side are almost 2.5 times as broad as ambulacra, somewhat larger (ca. twice) than in *P. bursarium.* Plates are large, not numerous. An ambulacral plate is composed of a large primary plate and two small demiplates which are situated at the side of the lower edge of the primary plate (Fig. 3). Three pairs of pores are found on these plates. A pair of pores is situated in the margin of the primary plate. Another pair of pores is on each demiplate.

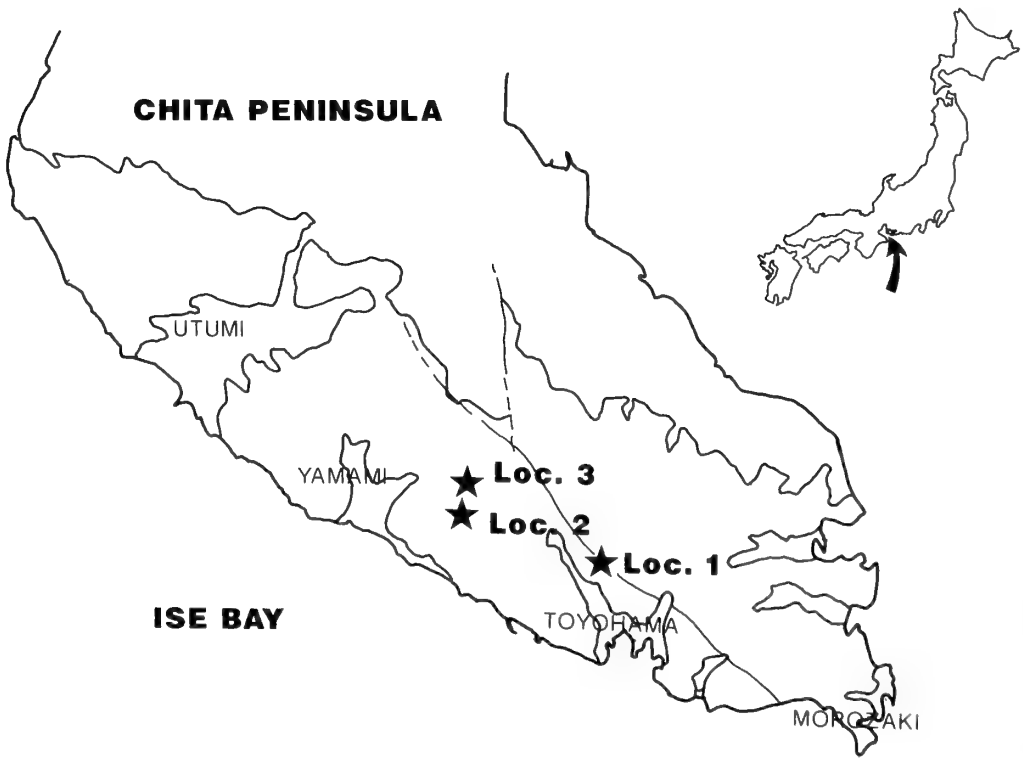

Fig. 1. Map showing the Toyohama and Yamami Formations and Localities 1–3 (Locs. 1–3) in the Morozaki Group in the Chita Peninsula, from where the Miocene phormosomatid specimens were collected. Curved arrow shows the location of the Chita Peninsula in the Japanese main islands.

TABLE 1. Size distribution of tests and peristomes in fossil *Phormosoma* sp. and living *Phormosoma bursarium*

Phormosoma sp.				*P. bursarium*			
Cat. No.	test diameter (A) (mm)	peristome diameter (B) (mm)	B/A	Cat. No.	test diameter (A') (mm)	peristome diameter (B') (mm)	B'/A'
MFM 38060	48	15	0.31	MMBS P1	78	30	0.38
MFM 38058	63	17	0.27	MMBS P2	79	24	0.30
MI 01	74	23	0.31	MMBS P3	79	28	0.35
MFM 38057	82	21	0.26	MMBS P4	89	33	0.37
MFM 38059	100	25	0.25	MMBS P5	92	28	0.30
SA 01	118	31	0.26	MMBS P6	94	36	0.38
				MMBS P7	109	36	0.33
Mean			0.277				0.344
±S.D.			±0.027				±0.035

There are five to six pairs of primary plates in each ambulacrum on the oral surface, and an ambulacral primary tubercle is on each primary plate. The size of the primary tubercles is almost equal except in the ones situated along the peristome which are somewhat smaller than others.

There are four to six interambulacral plates in each column on the oral surface. The number of primary tubercles on an interambulacral plate decreases adapically from 3 (for the outermost 1–2 plates), 2 (for the inner 2 plates) to 1 (for the 1–2 plates adjacent to the peristome). Secondary and miliary tubercles are not preserved. The spines preserved on the marginal fringe of the test of MFM 38058 are short and slender (Fig. 5). The apical system is not preserved well.

Remarks: The specimens from the Morozaki Group have large and deep areoles in the oral side, slender teeth with a sharp point, a large peristome area, and a comparatively small body size. These characteristics clearly indicate that they belong to the genus *Phormosoma* Thomson, 1872. Four extant species belonging to the genus *Phormosoma* have so far been reported [8]. Their distributional ranges are as follows:

P. placenta Thomson, 1872: Northern Atlantic from Iceland and the Davis Strait down to the Azores and the Gulf of Guinea, and to the West Indies, 215–2500 m depths.

P. verticillatum Mortensen, 1904: Indian Ocean, from the Bay of Bengal to the Arabian Sea, 1165–1925 m depths.

P. rigidum A. Agassiz, 1881: Off New Zealand, 1260 m depth.

P. bursarium A. Agassiz, 1881: Indo-Pacific, from the Natal Coast and the Arabian Sea to Australia, New Caledonia, Japan, and the Hawaiian Islands, overall depth range in records 170–2340 m, and dominate between depths of 500–1700 m on the continental slope of the Pacific coast of Japan.

The Morozaki specimens have affinity with *P. bursarium* in some morphological characters such as the test size, or the arrangement of ambulacral plates and pore pairs on the plates, although some differences are also found between them in the peristome area and in the relative width of the ambulacra and interambulacra.

Their habitats seem also to be similar, and a great number of living specimens of *P. bursarium* have been trawled and sometimes gregarious paches of them were photographed on the silty mud bottoms of the bathyal zone along the southeastern coast of Japanese main islands including the area off the Chita Peninsula [12]. The depth range of *Calveriosoma gracile* and *Hygrosoma hoplacantha* overlaps with that of *P. bursarium* in the above locations. However, the usual habitats of them are segregated. The former two species prefer sandy mud bottom on the topographic highs swept by strong bottom currents expecting the occasional drifting sea algae as facultative vegetarians [9, 12], whereas the latter species predominates on the silty mud floor where the regime of bottom water movement is relatively calm. If the habitat of the fossil species is the same as that of the extant species, the taphonomy of the soft-shelled sea urchin in the taffaceous sandstone in a formation of Morozaki Group suggests instantaneous burial beneath turbidity currents. The present *Phormosoma* specimens were collected together with four other echinoid species, 13 species of other echinoderms and with some fishes, crustaceans and molluscs from tuffaceous sandstone beds deposited in the bathyal zone. The four echinoid species are *Temnopleurus* sp. (upper bathyal member), *Brissopsis* sp. (upper to middle bathyal member), a diadematid and a scutellid (littoral members). Their habitats today range from the littoral to bathyal zones, suggesting that some of the fossils have been brought from shallower bottoms into the bathyal zone by turbidity flows and/or episodic disasters involving the littoral, midwater and upper continental slope realms.

The fossil specimens found in the Morozaki Group can be identical with or a direct ancestor of *P. bursarium*, although the information obtained from the present fossil specimens is still insufficient to identify the species exactly. This is the first fossil record in the world of the family Phormosomatidae, and is also the third unequivocal fossil species for the order Echinothurioida [19].

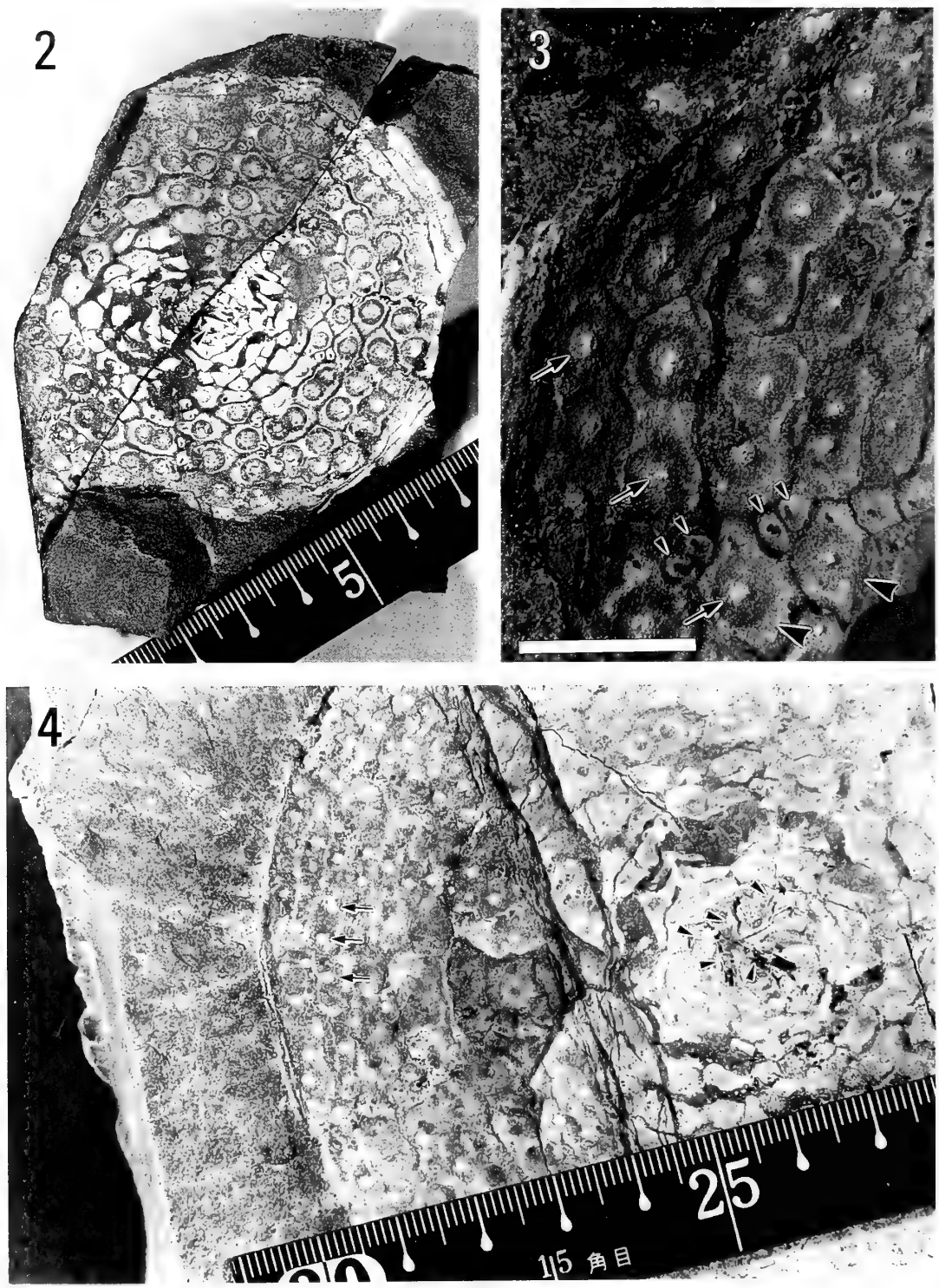

Fig. 2. Oral view of *Phormosoma* sp. (MFM 38057) showing a honey-comb-like structure with large and deep areoles and a large peristome area. A sharp and slender tooth (arrow-head) in the mouth is also seen. The smallest graduation of the measure corresponds to 1 mm.

Fig. 3. Ambulacral and interambulacral plates on the oral-side of *Phormosoma* sp. (MMBS A1) viewed under a higher magnification than in Fig. 2. The areoles (arrows) of the primary tubercles are very large and deep. Large and small arrow-heads show the primary ambulacral plates and the demiplates, respectively. Bar represents 1 cm.

Fig. 4. Oral view of *Phormosoma* sp. (SA 01). Arrow-heads indicate the five slender teeth in the mouth. Part of the test has been removed and the coelom-side of the aboral test is seen in the left-side of the field. The areoles (arrows) on the aboral test are small. The smallest graduation of the measure corresponds to 1 mm.

FIG. 5. The short and slender spines (arrows) on the marginal fringe of the test of *Phormosoma* sp. (MFM 38058). Bar represents 1 cm.

ACKNOWLEDGMENTS

We wish to express our cordial thanks to Mr. K. Hachiya for his technical assistance to take photographs for Figures 2, 4 and 5. Sincere thanks are also due to Drs. T. Sato and T. Oji for their careful reading of the manuscript and advice. We are also indebted to Dr. M. Shigei for his valuable advice.

REFERENCES

1 Amemiya S, Tsuchiya T (1979) Development of the echinothurid sea urchin *Asthenosoma ijimai*. Marine Biol 52: 93–96

2 Amemiya S, Suyemitsu T, Uemura I (1980) Morphological observations on the spermatozoa of echinothurid sea urchins. Develop. Growth Differ 22: 327–335

3 Doi K (1983) On stratigraphy and age of the Miocene Utsumi Formation, Morozaki Group, Southwest Japan. News Osaka Micropaleont. 10: 14–21

4 Fell HB (1966) Diadematacea. In "Treatise on Invertebrate Paleontology Part U, Echinodermata 3, Vol. 1" Ed. by R. C. Moore, The Geological Society of America Inc, New York pp U340–U366

5 Hachiya K, Yamaoka M, Mizuno Y (1988) Deep sea fauna from the Middle Miocene Morozaki Group in the Chita Peninsula, Aichi Prefecture, central Japan. J Growth 27: 119–139

6 Hayashida A (1985) Paleomagnetic study of Miocene strata in the Chita Peninsula, central Japan. Sci Engineer Rev Doshisha Univ 26: 180–185

7 Jensen M (1981) Morphology and classification of Euechinoidea Bronn, 1860 - a cladistic analysis. Vid Meddr Dansk Naturh Foren 143: 7–99

8 Mortensen Th (1935) A Monograph of the Echinoidea II. C.A. Reitzel Publisher, Copenhagen, pp 1–647; pls 1–89

9 Mortensen T (1938) On the vegetarian diet of some deep-sea echinoids. Annot Zool Japan 17: 225–228

10 Nishiyama S (1968) The echinoid fauna from Japan and adjacent regions. In "Part II, Special papers of Palaeontological Society of Japan No. 13" Ed by Palaeontological Society of Japan, University of Tokyo Press, Tokyo p 491

11 Ohta S (1980) Photographic census of the larger-sized epibenthos on the pacific coast of central Japan. In "The Kuroshio IV, Proc 4th CSK Symp Tokyo 1979" pp 602–620

12 Ohta S (1983) Photographic census of large-sized benthic organisms in the bathyal zone of Suruga Bay, central Japan. Bulletin of the Ocean Research Institute, University of Tokyo, No. 15, 1–244

13 Okutani T (1969) Synopsis of bathyal and abyssal megalo-invertebrates from Sagami Bay and the south off Boso Peninsula trawled by the R/V Soyo-Maru. Bull Tokai Reg Fish Res Lab 57: 1–62

14 Shibata H (1977) Miocene mollusks from the southern part of Chita Peninsula, central Honshu. Bull Mizunami Fossil Mus 4: 45–53

15 Shibata H, Ishigaki T (1981) Heteropodous and pteropodous biostratigraphy of Cenozoic strata of Chubu Province, Japan. Ibid 8: 55–70, pls. 12, 13

16 Shigei M (1986) The sea urchins of Sagami Bay, Ed. by Biological Laboratory Imperial Household, Maruzen, Tokyo 204+126 pp

17 Shikama T, Kase T (1976) Molluscan fauna of the Miocene Morozaki Group in the southern part of Chita Peninsula, Aichi Prefecture, Japan. Sci Rep Yokohama Nat Univ Sec 2, 23: 1–25

18 Smith AB (1984) Echinoid Palaeobiology. George Allen & Unwin, London.

19 Smith AB, Wright CW (1990) British Cretaceous Echinoids. The Palaeontographical Society, London. pp 101–198; pls 33–72

20 Woodward SP (1863) On *Echinothuria floris*, a new and anomalous echinoderm from the Chalk of Kent. The Geologist 6: 327–330

21 Yoshiwara S (1897) On two species of *Asthenosoma* from the sea of Sagami. Annot Zool Jap 1: 5–12

ZOOLOGICAL SCIENCE 11: 319–335 (1994)

Phylogeny, Classification, and Biogeography of *Goniurosaurus kuroiwae* (Squamata: Eublepharidae) from the Ryukyu Archipelago, Japan, with Description of a New Subspecies

L. Lee Grismer[1], Hidetoshi Ota[2] and Satoshi Tanaka[3]

[1]*Department of Biology, San Diego State University, San Diego, CA 92182, U.S.A.,*
[2]*Department of Biology, University of the Ryukyus, Nishihara, Okinawa 903–01, and* [3]*Motobu Senior High School, Tokuchi 337 Motobu, Okinawa 905–02, Japan*

ABSTRACT—The phylogenetic relationships of populations of *Goniurosaurus kuroiwae* from the Ryukyu Archipelago, Japan, are resolved using a cladistic analysis and their classification modified accordingly. The resultant phylogeny indicates that five subspecies should be recognized: *G. k. yamashinae* from Kumejima, *G. k. orientalis* from Tonakijima, Tokashikijima, Akajima, and Iejima, *G. k. kuroiwae* from Okinawajima, Sesokojima, and Kourijima, *G. k. toyamai* subsp. nov. from Iheyajima, and *G. k. splendens* from Tokunoshima. *Goniurosaurus k. yamashinae* is the sister taxon of the remainder. *Goniurosaurus k. kuroiwae* and *G. k. orientalis* are sister taxa which collectively form the sister group to the lineage composed of *G. k. toyamai* and *G. k. splendens*. *Goniurosaurus k. yamashinae* and *G. k. orientalis* are designated as metataxa because they are not demonstrably monophyletic or paraphyletic. A discriminant function analysis of the five subspecies shows *G. k. yamashinae* and *G. k. splendens* are separated from each other and from the other subspecies by a wide morphological gap. All these lineages were recognized as subspecies because this increases the phylogenetic content of the classification. The ancestor of the *G. kuroiwae* group may have dispersed into the Ryukyu Archipelago from continental China by way of a late Miocene to early Pliocene landbridge. The paleogeography of the Ryukyu Archipelago suggests that differentiation within *G. kuroiwae* resulted from the formation of the Ryukyu's contemporary configuration caused by rising Pleistocene sea levels.

INTRODUCTION

In a revision of the gecko family Eublepharidae, the genus Goniurosaurus was resurrected to contain the insular populations of eublepharids from the Gulf of Tonkin, China and the Ryukyu Archipelago, Japan [14, 15]. Thus, as it is currently constituted, *Goniurosaurus* contains at least two allopatric insular species; *G. lichtenfelderi* (Mocquard, 1897) [38] from the Island of Hainan and Iles de Norway in the Gulf of Tonkin, China [14] and *G. kuroiwae* (Namiye, 1912) [42] from 10 islands within the Ryukyu Archipelago, Japan [47]. There may also exist an undescribed species of *Goniurosaurus* from the Guizhou province of mainland China [33]. Grismer [15] revised the taxonomy of *G. kuroiwae* and recognized three subspecies; *G. k. yamashinae* (Okada, 1936) [44] of Kumejima Island, *G. k. kuroiwae* of Okinawajima Island and satellite islands to the west, and *G. k. splendens* (Nakamura *et* Uéno, 1959) [40] of Tokunoshima Island. Grismer's [15] classification resulted in the synonymy of *G. k. orientalis* (Maki, 1930) [35] with *G. k. kuroiwae* and placed the Kumejima Island population, considered at the time to be *G. k. orientalis* [41, 51], under the resurrected name of *G. k. yamashinae*. However, Grismer's [15] conclusions were provisional because he was only able to examine small series of specimens from Okinawajima and Tokunoshima Islands and relied on literature descriptions for some of the other insular populations.

In a more recent revision, Ota [47] referred all the insular populations west of Okinawajima Island (including that of Kumejima Island) to *G. k. orientalis*. The Okinawajima, Sesokojima, and Kourijima island populations remained under *G. k. kuroiwae* and the Tokunoshima population remained *G. k. splendens*. Both classifications [15, 47] suffer because they are based on overall similarity rather than derived similarity and not all insular populations were examined. In this paper we readdress the classification of *G. kuroiwae* from a phylogenetic standpoint based on a cladistic analysis of all known insular populations.

MATERIALS AND METHODS

Data were obtained from preserved (Appendix I) and living specimens. Grismer [15] demonstrated that *Goniurosaurus kuroiwae* is monophyletic based on its possession of the derived character states of tuberculate gular scales, unsheathed claws, and the absence of preanal pores. All specimens from the same island were treated as a single operational taxonomic unit and, as such, an *a priori* assumption of insular monophyly was adopted. Character states were polarized [34] based on the relationships suggested by Grismer [14–17] where *Goniurosaurus lichtenfelderi* served as the first outgroup and *Eublepharis, Hemitheconyx,* and *Holodactylus* as the second (Fig. 1).

Maddison *et al.* [34] stressed the importance of two sequentially aligned outgroups to ensure that polarity assignments are maximally parsimonious. It is likely, however, that the *Eublepharis-Hemitheconyx-Holodactylus* clade does not actually comprise the

Accepted January 14, 1994
Received October 28, 1993

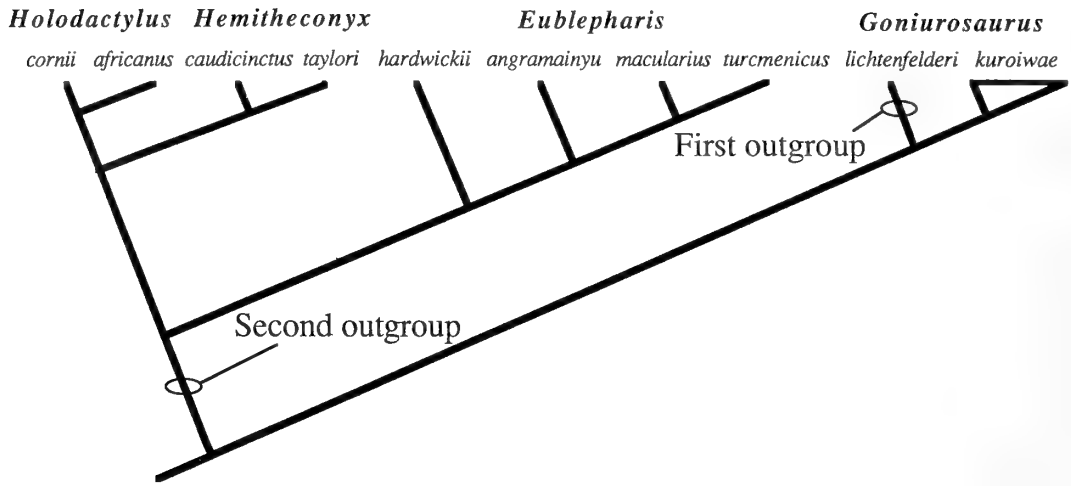

FIG. 1. Outgroup taxa and relationships of the first and second outgroups to *Goniurosaurus kuroiwae* after Grismer [14–17].

immediate second outgroup owing to the possible existence of an undescribed form of *Goniurosaurus* from mainland China [33]. This population is known from only a single specimen which was unavailable to us. Thus, the *Eublepharis-Hemitheconyx-Holodactylus* clade serves, at this point, as the best approximation of an immediate second outgroup. Because of a lack of homoplasy in the data set, computer algorithms were not necessary to aid in tree construction.

Following the cladistic analysis, scale counts from the Kumejima, Tokashikijima, Okinawajima, Iheyajima, and Tokunoshima populations were subjected to a multigroup discriminant function analysis (DA) with the MacIntosh version of BioΣtatII [50], in which each insular population was used as a predefined group. The sample sizes from the remaining islands (Table 1) were too small to yield statistically reliable results. Results from the DA were not used to construct phylogenetic relationships among the populations but only to aid in the morphological characterization and distinction of the terminal taxa suggested by the results of the cladistic analysis.

Terminology follows Grismer [15] and scale counts were taken as follows. *Supralabials*—the series posterior to the rostral and terminating with a scale at least twice the size of the surrounding granular scales. *Infralabials*—the series posterior to the mental and terminating with a scale at least twice the size of the surrounding granular scales. *Postmentals*—all scales except the first infralabials which contact the mental. *Preoculars*—the linear arrangement of granular scales between the anterior corner of the eye and the posterior margin of the external nares. *Eyelid fringe scales*—the lateralmost enlarged triangular scales encircling the eye. *Paravertebral tubercles*—the number of paravertebral tubercles between the limb insertions. *Midbody scales*—number of granular scales surrounding the body midway between limb insertions. *Fourth toe lamellae*—counting from the union of the third and fourth toes and terminating with the distal penultimate scale. *Scales surrounding claw on fourth toe*—all scales contacting the claw. The following counts were not used in the DA because of their incomplete representation in some or all of the populations. *Caudal scales*—the number of granular scales in the transverse caudal whorl of a non-regenerated tail at a point midway between the ankle and the knee when the hindlimb is adpressed against the tail. *Body bands*—number of transverse body bands between the nuchal loop and caudal constriction.

PHYLOGENETIC ANALYSIS OF CHARACTERS

1. *Dorsal tubercles*

In the Tokunoshima population, the dorsal body tubercles between the limb insertions are triangular to elliptical in cross-section and sharply keeled anteriorly. The tubercle keel is most pronounced dorsally, becoming less pronounced towards the base. Also, the degree of tubercle keeling increases posteriorly on the body with those tubercles between hind limb insertions being the most strongly keeled. Keeled tubercles do not occur on the head, nape of the neck, or tail. In the Kumejima population, the dorsal body tubercles are smooth and conical. In all other populations, tubercle-keeling only rarely occurs. When present, it is usually very weak and occurs only in a few tubercles between the hind limb insertions. In *Goniurosaurus lichtenfelderi, Eublepharis,* and *Holodactylus,* the tubercles are smooth and conical. Only in *Hemitheconyx* are the tubercles keeled. Therefore, the condition of sharply keeled tubercles in the Tokunoshima population is considered derived.

2. *Ventral scales*

The ventral scales of eublepharid geckos are usually hexagonal, flat, subimbricate to imbricate, and grade laterally into the granular scales of the dorsum. In the Tokunoshima population, the ventrals are juxtaposed and sharply raised, giving them a pointed or weakly tuberculate appearance. This condition is most evident in the pectoral region and fades posteriorly, grading into flat hexagonal imbricate interfemoral scales. Anteriorly, the pectoral scales grade into even more sharply pointed and raised gular scales. In all other populations of *Goniurosaurus kuroiwae,* as well as *G. lichtenfelderi, Eublepharis* and *Hemitheconyx,* the ventral scales are flat, wide, and subimbricate to imbricate. Anderson and Leviton [1] stated that the ventral scales of *E. angramainyu* are juxtaposed but we find them to be subimbricate. In *Holodactylus,* the ventral scales are juxtaposed but they are

TABLE 1. Meristic differences between the insular populations of *Goniurosaurus kuroiwae*. SL=supralabials; IL=infralabials; PM=postmentals; PO=preoculars; EF=eyelid fringe scales; TU=paravertbral tubercles; BO=midbody scales; 4T=fourth toe lamellae; CL=scales surrounding claw on fourth toe; CA=caudal scales; BB=body bands; I=incomplete; and A=absent.

Character	SL	IL	PM	PO	EF	TU	BO	4T	CL	CA	BB
yamashinae											
Kumejima (n=14)											
$\bar{x}$	8.0	8.4	4.6	21.0	53.6	28.8	148.6	18.4	6.0	47.7	4
range	7–9	7–9	4–5	19–23	44–65	21–33	132–156	17–20	6	43–53	4
SE	±0.2	±0.3	±0.2	±0.6	±2.3	±1.7	±2.7	±0.3	0	±2.9 (n=6)	0
orientalis											
Akajima (n=1)	9	10	5	22	63	35	144	19	6	48	4
Iejima (n=1)	9	8	5	22	63	29	145	20	6	50	4
Tokashikijima (n=50)											
$\bar{x}$	9.4	8.6	3.8	21.5	59.8	35.1	147.2	17.3	6.0	47.5	4 or I
range	8–11	7–11	3–5	17–24	53–66	31–40	135–159	16–19	5–7	42–52	
SE	±0.6	±0.2	±0.1	±0.3	±0.7	±0.5	±1.2	±0.2	±0.1	±1.2 (n=16)	
Tonakijima (n=2)											
$\bar{x}$	9	10	3.5	20.0	52.0	30.5	139.5	20.5	6	A	4
range	9	10	3–4	19–21	48–56	29–32	137–142	20–21	6	A	4
SE	0	0	±0.5	±1.0	±4.0	±1.5	±2.5	±0.5	0	A	0
kuroiwae											
Okinawajima (n=221)											
$\bar{x}$	9.4	8.7	5.0	21.4	60.2	33.4	150.9	17.1	6.0	49.8	A
range	7–11	7–11	4–6	19–23	54–70	29–43	139–162	15–20	6–7	40–57	A
SE	±0.2	±0.2	±0.1	±0.2	±0.7	±0.6	±1.3	±0.2	±0.1	±1.2 (n=124)	A
Kourijima (n=1)	9	9	4	23	51	34	140	15	6	51	A
Sesokojima (n=1)	8	8	5	21	57	31	137	17	6	A	A
toyamai											
Iheyajima (n=14)											
$\bar{x}$	9.3	8.3	4.6	21.4	55.6	37.2	149.8	17.3	5.9	47.5	3.8
range	8–10	7–10	3–5	20–23	53–59	34–42	140–158	16–20	5–6	40–53	3–4
SE	±0.2	±0.3	±0.2	±0.3	±0.5	±0.6	±1.9	±0.3	±0.3	±1.9 (n=6)	±0.1
splendens											
Tokunoshima (n=27)											
$\bar{x}$	9.0	8.6	2.9	20.5	54.1	20.0	132.4	16.2	7.4	50.4	3
range	8–10	7–10	2–4	18–24	46–59	22–29	121–146	15–18	6–9	46–61	3
SE	±0.1	±0.1	±0.1	±0.3	±0.5	±0.4	±1.4	±0.2	±0.2	±1.9 (n=8)	0

flat and not sharply raised. Therefore, juxtaposed and sharply raised ventrals in the Tokunoshima population is considered derived.

3. *Scales at base of digits*

In all *Goniurosaurus kuroiwae* except those from Kumejima Island, there are one to three (usually two) enlarged scales at the base of each digit on the hand and foot. These scales are two to three times the size of the scales of the adjacent palmar and plantar regions. This condition shows a slight indication of ontogenetic variation, being somewhat less pronounced in hatchlings and juveniles. In the Kumejima population, there is a single scale at the base of each digit which is occasionally slightly enlarged but rarely reaching twice the size of the surrounding scales. This is similar to the condition found only in the manus of *G. lichtenfelderi*. Enlarged scales at the base of the digits do not occur in *Eublepharis*, *Hemitheconyx*, and *Holodactylus*. Therefore, this condition in the manus of all populations of *G. kuroiwae*, except that from Kumejima Island, is considered derived.

4. *Lineate middorsal pattern*

Goniurosaurus kuroiwae from Akajima, Tokashikijima, Tonakijima, Iejima, Okinawajima, Kourijima, and Sesoko-

jima Islands have lineate tendencies in their dorsal banding patterns (Figs. 2 and 3). In the Akajima, Tokashikijima, Tonakijima, and Iejima populations, there is a middorsal stripe in the nape which usually extends far enough posteriorly to contact the first transverse body band near the forelimb insertions. Occasionally this stripe will continue far enough to contact the second transverse body band, nearly midway between the forelimb and hindlimb insertions, but rarely any

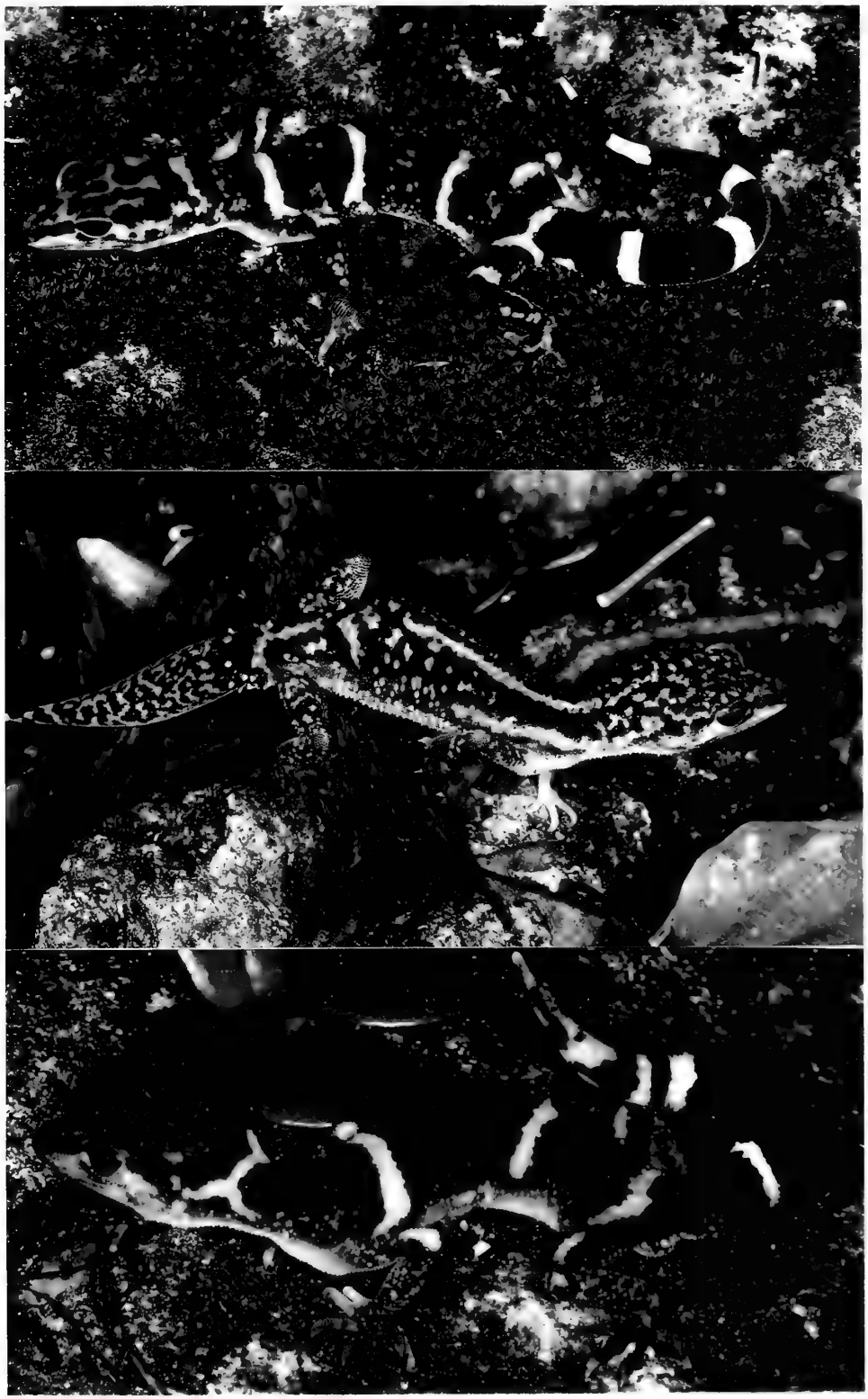

FIG. 2. Photographs of *Goniurosaurus kuroiwae* taken at the site of collection. Upper: juvenile *G. k. yamashinae* from Kumejima Island. Middle: *G. k. kuroiwae* from southern Okinawajima Island. Lower: adult *G. k. splendens* from Tokunoshima Island. Photographs by L. Lee Grismer.

FIG. 3. Photographs of *Goniurosaurus kuroiwae* taken at the site of collection. Upper: adult *G. k. toyamai* from Iheyajima Island. Middle: *G. k. orientalis* from Tokashikijima Island. Lower: juvenile *G. k. orientalis* from Akajima Island. Photographs by Masanao Toyama.

further except in the Okinawajima, Kourijima and Sesokojima populations. The Tonakijima population is known from one adult and one juvenile specimen. The adult (NSMT 02522: holotype of *G. k. orientalis*) has a middorsal stripe extending nearly one-half the way down the body. The juvenile (OPM 489) is banded and shows only weak evidence of striping on the nape of the neck. Middorsal lineation is most pronounced in the Okinawajima, Kourijima,

and Sesokojima populations where a stripe usually extends the entire length of the body and terminates at the caudal constriction (Fig. 2). On Okinawajima Island, there is some variation in that striping in the northernmost populations is not as well defined and a weak, faded banding pattern is sometimes present. Populations from the southern Okinawajima, however, have a bold, well-defined stripe and seldom show evidence of banding. In the remaining populations of *G. kuroiwae,* there is no evidence of middorsal striping (Figs. 2 and 3). In large specimens from Tokunoshima Island, there is occasionally a lack of dark pigmentation in the vertebral region that appears in preserved specimens to be a stripe. However, in living specimens this is merely a lightened area that develops with ontogeny. This region does not contain the same color pigments as the dorsal bands and as such does not constitute a middorsal stripe homologous with that described above. Such pigment loss in the vertebral region is common in large individuals of other eublepharids [18]. Tendencies toward dorsal pattern lineation do not occur in *G. lichtenfelderi*. Lineate tendencies are absent in *Eubelpharis hardwickii* but variable in *E. macularius, E. turcmenicus, E. angramainyu, Hemitheconyx caudicinctus,* and *Holodactylus*. Striping is absent in *Hemitheconyx taylori*. Therefore, the most parsimonious assumption is that lineate tendencies in the dorsal pattern of the Akajima, Tokashikijima, Tonakijima, Iejima, Okinawajima, Kourijima, and Sesokojima populations are derived.

5. *Banding pattern*

In all populations of *Goniurosaurus kuroiwae* except those from Okinawajima, Kourijima, and Sesokojima, there is a prominent dorsal pattern consisting of three to four transverse bands between the nape of the neck and the caudal constriction. Banding is bold and prominent in the Kumejima, Iheyajima, and Tokunoshima populations (Figs. 2 and 3). In the Akajima, Tokashikijima, Tonakijima, and Iejima populations, banding is prominent but the first band in the vicinity of the forelimb insertion may be incomplete (rarely absent). In the Okinawajima, Kourijima, and Sesokojima populations, banding is absent or incomplete. This condition is most obvious in populations from the southern portion of Okinawajima where there is usually no trace of banding (Fig. 2). In populations from northern Okinawajima Island as well as Kourijima and Sesokojima Islands, some specimens may retain some portions of the more posterior body bands. However, the bands are usually very irregular in shape and suffused with dark pigments from the surrounding ground color. This condition shows little or no ontogenetic variation. All outgroup taxa except *Holodactylus cornii* have a prominent banding pattern. Therefore, the incomplete to absent transverse dorsal banding pattern of the Okinawajima, Kourijima, and Sesokojima populations is considered derived.

6. *Hind limb banding*

In the Tokunoshima population, the posteriormost transverse body band extends laterally onto the dorsal surface of the thigh. In many specimens, the band runs parallel to the long axis of the hind limb uninterrupted to the knee. In others, it is interrupted medially and exists as a lineate blotch on the thigh and knee (Fig. 2). In all other populations of *Goniurosaurus kuroiwae,* the posteriormost body band does not extend along the long axis of the hind limbs. There may be light-colored elongate blotches on the dorsomedial surface of thigh of some specimens, but close examination reveals that they are oriented perpendicular rather than parallel to the long axis of the hind limb and in many cases, are discontinuous with the posteriormost transverse body band. In the outgroup taxa, the posteriormost transverse body band does not extend onto the hind limb. Therefore, the condition for the Tokunoshima population is considered derived.

7. *Interspace mottling*

The common condition in eublepharine geckos *sensu* Grismer [15] is for hatchlings to have dark, unicolored interspaces (or ground color) between the body bands, which become increasingly suffused and/or mottled with lighter coloration with age. This is the case in all *Goniurosaurus kuroiwae* except the Iheyajima and Tokunoshima populations where the adults retain unmottled dark interspaces (Figs. 2 and 3). Although the specimen of the Akajima population (OPM 341) is a juvenile, mottling in the interspaces is still observable (Fig. 3) and as with other eublepharines, assumed to be characteristic of adults. In the specimen from Iejima Island (KUZ 9991), the interspaces appear superficially like those in the Iheyajima and Tokunoshima populations. On close examination, however, it is clear that they are considerably lightened and not uniformly dark throughout. Adults of *G. lichtenfelderi* have both mottled and unicolored interspaces. The interspaces of adult *Eublepharis macularius, E. turcmenicus,* and *E. angramainyu* are mottled whereas those of *E. hardwickii* are unicolored. *Holodactylus* and *Hemitheconyx taylori* have mottled interspaces but they are generally unicolored in *Hemitheconyx caudicinctus*. Therefore, dark unicolored interspaces of the adults of the Iheyajima and Tokunoshima populations are considered derived.

8. *Juvenile coloration*

In all populations of *Goniurosaurus kuroiwae* except that of Kumejima Island, the color of the dorsal pattern (striped or banded) overlying the dark-brown ground color is always bright-orange to pink in hatchlings and juveniles. This color intensity usually remains into adulthood but sometimes fades into a cream-yellow hue (Figs. 2 and 3). The juvenile coloration of the dorsal pattern in specimens from the Kumejima population is whitish. The dorsal color pattern in the juveniles of both outgroups consists of yellow to whitish hues and is never bright-orange to pink at any stage of life. Therefore, the latter condition is considered derived for all populations of *G. kuroiwae* except that of Kumejima Island.

9. *Eye color*

The color of the iris in all *Goniurosaurus kuroiwae* except the Kumejima population is blood-red (Figs. 2 and 3). In the Kumejima population, *G. lichtenfelderi,* and *Eublepharis* (*E. hardwickii* and *E. angramainyu* not available for examination), the iris is yellow-brown to gold in color. In *Hemitheconyx caudicinctus* and *Holodactylus africanus,* the iris is usually a very dark brown. Living *Hemitheconyx taylori* and *Holodactylus cornii* were unavailable for examination. Therefore, based on the relationships of the outgroup taxa observed (Fig. 1), a blood-red iris is considered to be derived for the ingroup. If, however, a blood-red iris is present in the outgroup taxa that were not examined, the polarity assignment would be equivocal.

10. *Body stature*

The overall body stature in the Iheyajima population is robust, whereas that in the other populations of *G. kuroiwae,* as well as *G. lichtenfelderi,* more slender (Fig. 4). Thus, although the state of this character is not defined in the members of the second outgroup due to their much divergent body proportion, the robust body stature in the Iheyajima population is considered derived within the genus *Goniurosaurus* by assuming the Kumejima population as a first functional outgroup and *G. lichtenfelderi* as a second outgroup [60] (see below).

RESULTS

There is only one single most parsimonious tree which has a consistency index value of 1.0 (Fig. 5). The distribution of the derived character states (Table 2) suggests that the Kumejima population is the sister taxon of the remaining nine insular populations of *Goniurosaurus kuroiwae* (Fig. 5). Ota [47] placed the Kumejima population (*G. k. yamashinae: sensu* Grismer [15]) in *G. k. orientalis*. However, it is apparent here that such a classification would result in the demonstrative paraphyly of the latter (Fig. 5). Although the Kumejima population is discretely diagnosable from all other *G. kuroiwae*, it lacks character state support for its monophy-

TABLE 2. Distribution of derived (1) and primitive (0) character states among the island populations of *Goniurosaurus kuroiwae* and the outgroup taxa. ?=Character was not examined because live animals were not available to us. —=Character state was not defined due to the great divergence in related body portions.

Characters	1	2	3	4	5	6	7	8	9	10
Taxa										
Ingroup										
G. k. yamashinae										
Kumejima	0	0	0	0	0	0	0	0	0	0
G. k. orientalis										
Akajima	0	0	1	1	0	0	0	1	1	0
Tonakishima	0	0	1	1	0	0	0	1	1	0
Tokashikijima	0	0	1	1	0	0	0	1	1	0
Iejima	0	0	1	1	0	0	0	1	1	0
G. k. kuroiwae										
Okinawajima	0	0	1	1	1	0	0	1	1	0
Kourijima	0	0	1	1	1	0	0	1	1	0
Sesokojima	0	0	1	1	1	0	0	1	1	0
G. k. toyamai										
Iheyajima	0	0	1	0	0	0	1	1	1	1
G. k. splendens										
Tokunoshima	1	1	1	0	0	1	1	1	1	0
Outgroups										
G. lichtenfelderi lichtenfelderi	0	0	0	0	0	0	0,1	0	0	0
G. l. hainanensis	0	0	0	0	0	0	0,1	0	0	0
Eublepharis hardwickii	0	0	0	0	0	0	1	0	?	—
E. angramanyu	0	0	0	0,1	0	0	0	0	?	—
E. turcmenicus	0	0	0	0,1	0	0	0	0	0	—
E. macularius	0	0	0	0,1	0	0	0	0	0	—
Holodactylus africanus	—	0	0	0,1	0	0	0	0	0	—
H. cornii	0	0	0	0,1	0	0	0	0	?	—
Hemitheconyx caudicinctus	1	0	0	0,1	0	0	1	0	0	—
H. taylori	1	0	0	0	1	0	0	0	?	—

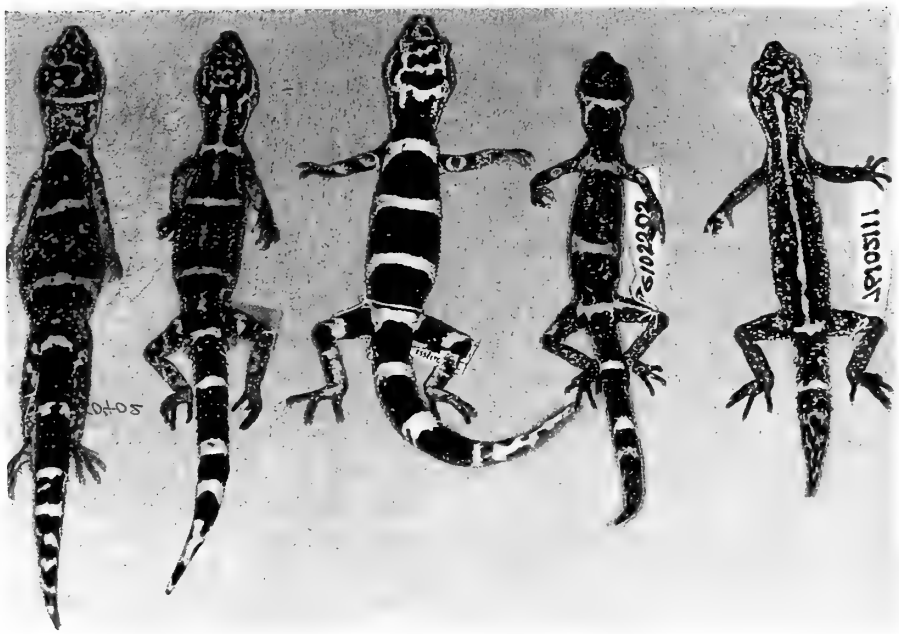

FIG. 4. Body stature of the five subspecies of *Goniurosaurus kuroiwae*. From left to right *G. k. yamashinae*, TPN 78050402 (SVL=87.5) from Kumejima Island; *G. k. orientalis*, TPN 78052101 (SVL=83.8) from Tokashikijima Island; *G. k. toyamai*, KUZ 9983 (SVL=84.6) from Iheyajima Island; *G. k. splendens*, TPN 76102202 (SVL=77.2) from Tokunoshima Island; and *G. k. kuroiwae* TPN 76102111 (SVL=79.9) from Okinawajima Island.

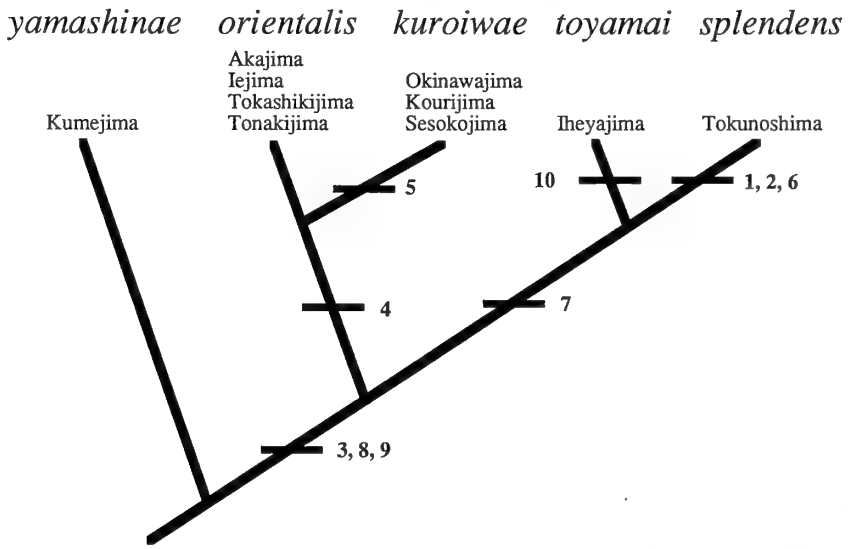

FIG. 5. Cladistic relationships of the insular populations of *Goniurosaurus kuroiwae* and the resultant classification. Numbered horizontal bars represent the presence of the following derived character states: 1=tubercles sharply keeled; 2 =ventrals juxtaposed; 3=enlarged scale(s) at base of digits; 4=lineate tendencies in middorsal pattern; 5=dorsal banding absent; 6=posteriormost body band extending onto hind limb; 7=interspace mottling absent; 8=orange-pink dorsal pattern in juveniles; 9=iris red; 10=body robust.

ly or demonstrable paraphyly, and thus, is given a metataxon designation [12] and recognized here as *G. k. yamashinae* (see [6, 8, 10, 25] for differing viewpoints on usage of this designation). The DA shows that *G. k. yamashinae* is well isolated from all other populations examined along the second axis except for a very slight degree of overlap with that of Okinawajima (Fig. 6). Standardized canonical coefficients for the first two variates presented in Table 3 account for 92.26% of the observed variation.

The remaining nine insular populations form a well-corroborated monophyletic group diagnosed by the derived character states of an enlarged scale at the base of each digit, a blood-red iris, and a bright orange to pink hatchling and juvenile color pattern (Fig. 5). Within this clade, there are two major monophyletic lineages. The first lineage consists of the Okinawajima, Kourijima, Sesokojima, Tonakijima, Tokashikijima, Iejima, and Akajima populations. This group is diagnosed by the derived acquisition of lineate

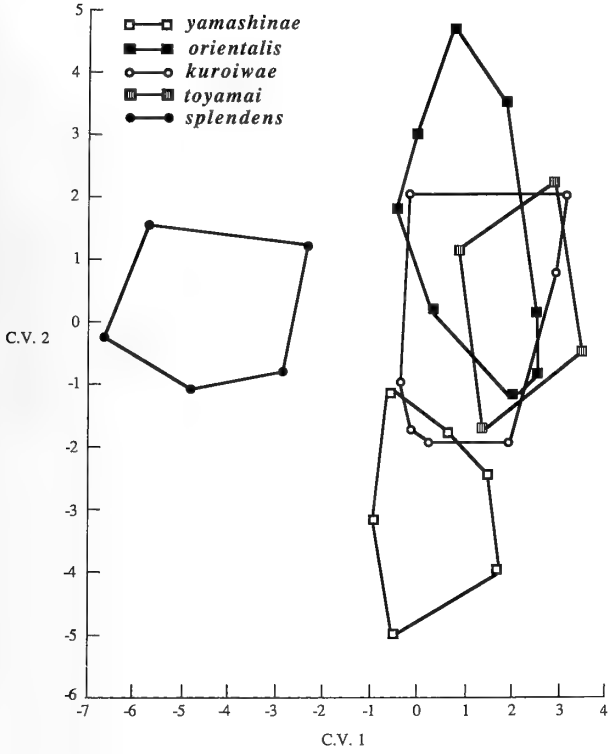

FIG. 6. First two canonical variates of the DA (C.V.1=78.78% and C.V.2=13.48% of the total variation). *Goniurosaurus kuroiwae splendens* from Tokunoshima Island (n=27); *G. k. kuroiwae* from Okinawajima Island (n=221); *G. k. orientalis* from Tokashikijima Island (n=50); *G. k. yamashinae* from Kumejima Island (n=14), *G. k. toyamai* from Iheyajima Island (n=14). Polygons were constructed by connecting the most peripherally located points of each plot.

TABLE 3. Standardized canonical coefficients for the first two variates (C.V.1 and C.V.2) from the multigroup discriminant function analysis (DA) of the nine characters from the Kumejima, Tokashikijima, Okinawajima, Iheyajima, and Tokunoshima populations. Symbols follow those of Table 1.

Character	C.V.1	C.V.2
SL	−0.10	0.70
IL	−0.01	0.05
PM	0.70	−0.78
PO	0.02	0.11
EF	0.05	0.16
TU	0.29	0.15
BO	0.03	−0.02
4T	0.25	−0.38
CL	−0.92	0.31

tendencies in the dorsal pattern (Fig. 5). Within this group there are two recognizable subgroups. The first is a monophyletic lineage containing the Okinawajima, Kourijima, and Sesokojima populations which is diagnosed by the derived acquisition of a dorsal pattern consisting of bands that are incomplete to absent. This group was previously referred to as *Goniurosaurus kuroiwae kuroiwae* [15 (in part), 41, 47] and its monophyly supports its continued recognition. The DA shows that *G. k. kuroiwae* is nearly completely separated from *G. k. yamashinae* along the second axis and completely separated from the Tokunoshima population along the first axis (Fig. 6). However, it greatly overlaps the Tokashikijima and Iheyajima populations along both axes (Fig. 6).

The second subgroup within this lineage is composed of the Tonakijima, Tokashikijima, Iejima, and Akajima (see below) populations (Fig. 5). Although this group is not demonstrably monophyletic or paraphyletic, it is diagnosable from *Goniurosaurus kuroiwae kuroiwae* as well as all the other populations (Fig. 5). Because Tonakijima Island is the type locality of *G. k. orientalis* [35], that name has priority for this group and it is given a metataxon designation (*G. k. orientalis*). The DA shows that *G. k. orientalis* is completely separated from *G. k. yamashinae* along the second axis and from the Tokunoshima population along the first axis but that it greatly overlaps the Okinawajima and Iheyajima populations along both axes (Fig. 6).

The second major monophyletic lineage also comprises two subgroups and is diagnosed by its derived lack of interspace mottling (Fig. 5). The first subgroup is a monophyletic lineage composed of the Tokunoshima population and diagnosed by the derived acquisition of keeled dorsal tubercles, juxtaposed and sharply raised ventral scales, and the posteriormost transverse body hand extending onto the hind limbs. This population was first described as *Eublepharis splendens* by Nakamura and Uéno [40], and has subsequently been recognized as *Goniurosaurus kuroiwae splendens* [15, 41, 47, 51]. The evidence presented here for its monophyly supports its continued recognition. The DA shows that *G. k. splendens* is well separated from *G. k. yamashinae* along the second axis and from all other populations along the first axis (Fig. 6).

The second subgroup of this lineage is composed of the Iheyajima population (Fig. 5). This population was placed within *G. k. orientalis* (*sensu* Ota [47]) based on its overall similarity in color pattern and scale meristics to the populations of Tonakijima, Tokashikijima, Iejima, and Akajima [47, 52, 56]. It is shown here, however, that the Iheyajima population differs from *G. k. orientalis* in that it lacks the derived state of lineate tendencies in the dorsal banding pattern that unite *G. k. orientalis* with *G. k. kuroiwae*. Furthermore, it has the derived state of a lack of interspace mottling which groups it with G. k. *splendens*. Thus, continued placement of this population in *G. k. orientalis* would make the latter demonstrably paraphyletic. Additionally, it is well-separated from *G. k. splendens* by its lacking the derived character states of keeled dorsal tubercles, juxtaposed and sharply raised ventral scales, and posteriormost body band extending onto the hind limbs. The DA shows that it is completely separated from *G. k. yamashinae*, along the second axis and from *G. k. splendens* along the first axis but greatly overlaps *G. k. orientalis* and *G. k. kuroiwae* along

both axes (Fig. 6).

It is clear that the Iheyajima population forms a separate monophyletic lineage differing from *splendens* by its lack of the derived states of characters 1, 2, and 6, and the possession of derived state in character 10. Additionally, its continued recognition as *Goniurosaurus kuroiwae orientalis* would result in the demonstrative paraphyly of the latter. Thus, separate subspecific recognition is warranted and we consider this population to be:

Goniurosaurus kuroiwae toyamai subsp. nov.
(Fig. 7)

Suggested English name: Iheyajima Leopard Gecko
Suggested Japanese name: Iheya-Tokagemodoki
Eublepharis kuroiwae orientalis: Toyama, 1984, p. 270 [56] (part).
Goniurosaurus kuroiwae orientalis: Ota, 1989, p. 230 [47] (part).

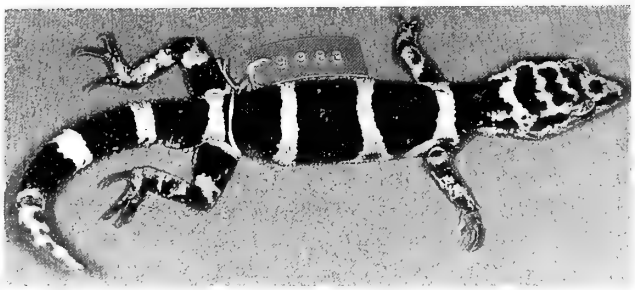

FIG. 7. Holotype of *Goniurosaurus kuroiwae toyamai* KUZ 9983 from Iheyajima Island, Okinawa Prefecture, Japan.

Holotype. KUZ 9983, collected by S. Tanaka on Iheyajima Island, Okinawa Prefecture, Japan, on 4 July 1977.

Paratypes. Thirteen paratypes from the same locality as the holotype: KUZ 9978–9982, 9985–9988; TPN 77032201, 77070301, 7707401–7707402.

Diagnosis. *Goniurosaurus kuroiwae toyamai* differs from all other subspecies of *G. kuroiwae* in its overall robust body stature and greater mean number of paravertebral tubercles (37.2:34–42). It differs further from *G. k. yamashinae, G. k. orientalis,* and *G. k. kuroiwae* in that adults lack interspace mottling; from *G. k. orientalis* and *G. k. kuroiwae* in lacking lineate tendencies in its dorsal pattern and having a lower mean number of eyelid fringe scales (55.6:53–59); from *G. k. orientalis* by having a slightly higher mean number of postmental scales (4.6:3–5); from *G. k. kuroiwae* in having a complete dorsal banding pattern; from *G. k. yamashinae* by having enlarged scales at the base of its digits, orange-pink juvenile color pattern, blood-red iris, a higher mean number of supralabial scales (9.3:8–10), and a lower mean number of fourth toe lamellae (17.3:16–20); and from *G. k. splendens* by lacking sharply keeled dorsal tubercles, juxtaposed and sharply raised ventral scales, the lateral extension of the posteriormost body bar onto the hind limb, and by having a greater mean number of postmental scales (4.6:3–5), midbody scales (149.8:140–158), fourth toe lamellae (17.3:16–20), and a lower mean number of scales surrounding the claw on the fourth toe (5.9:5–6).

Distribution. *Goniurosaurus kuroiwae toyamai* is known only from Iheyajima Island of the Okinawa Group, Ryukyu Archipelago, Japan (Fig. 8).

Description of holotype. Adult male; SVL 83.8 mm; head triangular, wider than neck, covered with uniform granular scales interspersed with enlarged tubercles increasing in size posteriorly; tubercles absent from rostrum, group of enlarged tubercles immediately anterior to orbit; rostral convex and rectangular, twice as wide as high, middorsal portion partially sutured dorsomedially, bordered laterally by first supralabial and prenasal, dorsolaterally by supraprenasal on left and intercalary scale on right, and dorsally by four enlarged granular scales; external nares subelliptical with

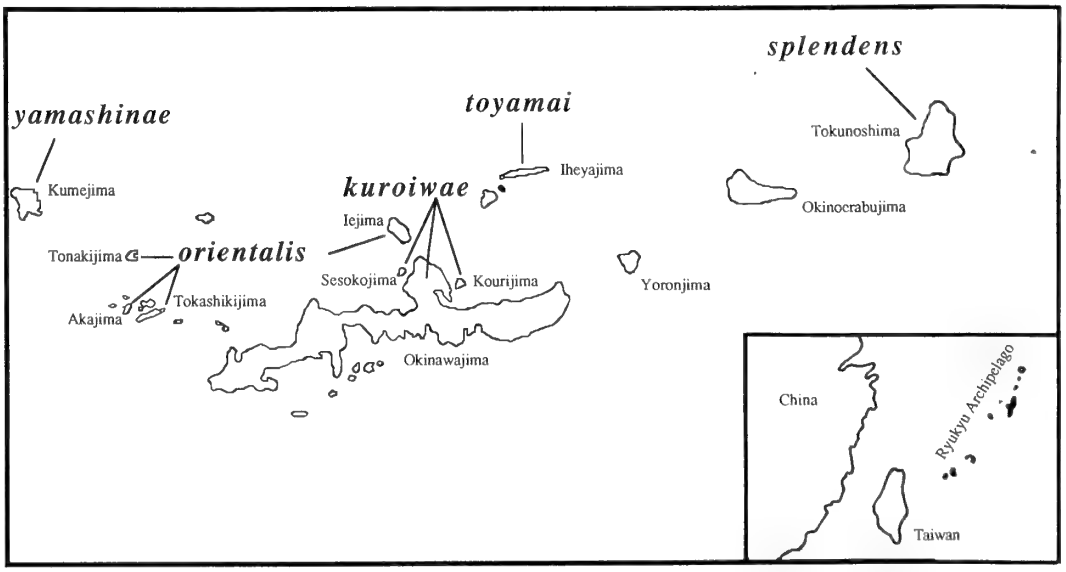

FIG. 8. Distribution of the subspecies of *Goniurosaurus kuroiwae* in the Ryukyu Archipelago, Japan.

long axis sloping forward, bordered anteriorly by prenasal and supraprenasal, dorsally and posteriorly by 8(R)-7(L) granular scales, and ventrally by one (R and L) granular scale and prenasals; prenasals with long recurved ventral portion; supraprenasal square, separated medially by four granular scales; supralabials 9(R)-10(L), first two of series square, the remaining rectangular, decreasing in size posteriorly, grading into granular scales along ventral margin of posterior section of upper jaw, posteriormost raised centrally; rostral granules equal in size; preoculars 21(R)-20(L); eyes relatively large, pupils vertical and with convex slightly serrate margins (visible in life); eyelid fringe scales 59 (R and L), triangular, those of upper eyelid slightly enlarged and conical; outer surface of upper eyelid consisting of small uniform granular scales equal in size to those on top of head, base of upper eyelid bordered by row of enlarged tuberculate scales; 63 scales across top of head between posterior corners of eyes; a fold of skin consisting of granular scales originating in suborbital region extends posteroventrally across angle of jaw; external auditory meatus elliptical with long axis directed dorsoventrally, single elongate tubercle bordering anterior margin; tympanum deeply recessed; mental triangular acutely tapering but rounded at posterior tip, bordered laterally by first infralabials and posteriorly by four slightly enlarged postmentals; 10(R)-9(L) infralabials, anteriormost square grading posteriorly into smaller rectangularly shaped infralabials that grade posteriorly into granular scales bordering dorsal margin of upper jaw; ventral margin of posteriormost infralabials well elevated from surrounding gulars; gular region covered with juxtaposed conical scales interspersed with enlarged tubercles; 56 rows of gulars between postmentals and an imaginary line between posterior margins of auditory meati; gulars grading posteriorly into flat hexagonal subimbricate pectoral scales and larger hexagonal imbricate ventral and interfemoral scales.

Neck narrower than body, covered with uniform granular scales, interspersed with several large sharply pointed conical tubercles on nape; tubercles on body conical and prominent, long axes directed posteriorly; body tubercles numerous, distributed evenly on dorsum and increasing in size posteriorly from nape of neck to caudal constriction, grading into distinct repeating caudal whorls; tubercles at caudal constriction twice the size of those on nape, tubercles surrounded by 9–12 granular scales; 36 paravertebral tubercles between limb insertions, strict vertebral row absent.

Limbs robust, covered with uniform granular scales interspersed with tubercles roughly one-half the size of those on body; granular scales grading distally into slightly flattened, weakly subimbricate scales of dorsal surface of manus and pes; 43(R)-45(L) granular scales around humeral region and 39(R)-38(L) around forearm; hindlimbs roughly twice as thick as forelimbs, covered with uniform granular scales interspersed with enlarged tubercles, those of posterofemoral region equal in size to those on body; 51(R)-53(L) granular scales around femoral region and 47(R)-48(L) around forelegs; pes covered ventrally with juxtaposed scales, those at heel enlarged; 1–2 enlarged scale(s) at base of each digit; subdigital lamellae narrow, nearly equal in size to slightly smaller lateral digital scales; 18(R)-17(L) subdigital lamellae on fourth toe; digits conical, increasing in length from first to fourth, fifth shorter than fourth.

Body robust, covered with granular scales grading ventrally into flattened, subimbricate ventral scales; 141 granular scales around midbody; ventral interfemoral scales large, flat, imbricate, grading posteriorly into small granular scales anterior to vent; region immediately posterior to vent covered with large flat imbricate scales, greatly swollen, with two upward-curving bony spurs arising from lateral margins.

Tail conical, thickest at base, covered with small rectangular imbricate scales arranged in transverse caudal whorls and repeated series of greatly enlarged and sharply pointed tubercles occurring in caudal whorls; caudal tubercles absent ventrally and decreasing in size laterally and posteriorly; ventral caudals larger and more nearly square than dorsal caudals; posterior one-quarter of tail regenerated and covered with slightly raised granular scales.

Coloration in life. Ground color of dorsum (including limbs and tail) uniform dark brown; top of head mottled in dark brown and cream; wide dark brown pre- and postorbital stripes; eyelid fringe scales cream-colored giving slight appearance of eye-ring; labial region light-brown to cream-colored; four wide, immaculate, transverse, cream-colored body bands between nape of neck and caudal constriction; bands blend ventrolaterally into light-colored ventrum; back of head bordered by incomplete nuchal band; forelimbs with large cream-colored symmetrical blotches in brachium, elbow, and antebrachium; hind limbs with large cream-colored symmetrical blotches in groin, knee, and dorsoposterior crus regions; two bands on original portion of tail suffused with reticulate pattern of dark-brown ground color; ventral surface of head, limbs, and body, immaculate light-brown; iris blood-red.

Variation. Paratypes closely approximate the holotype in morphology, meristics, and coloration. The most significant variation occurs in banding pattern and coloration. In three specimens (KUZ 9981–82, 9988), the third transverse body band is incomplete and interrupted medially. Three other (KUZ 9986–87; TPN 77070301) have three instead of four bands between the nuchal band and caudal constriction. All other populations of *Goniurosaurus kuroiwae* have four bands except its sister taxon *G. k. splendens,* which always has three. The coloration of the bands in hatchling and juvenile *G. k. toyamai* is bright orange-pink. This coloration may fade to a yellowish to cream-colored banding pattern in adulthood, although some adults maintain the juvenile coloration to some extent. Regenerated tails lack all aspects of banding observed in original tails. Regenerated tails are mostly dark-brown like the body ground color but become overlain with a reticulum of uneven light-purple uneven blotches.

Etymology. This poulation is named in honor of Mr. Masanao Toyama in recognition of his vast number of

contributions to the herpetology of the Ryukyu Archipelago including the first distributional record of *Goniurosaurus kuroiwae* from Iheyajima Island [56].

DISCUSSION

Phylogeny and similarity

The classification of *Goniurosaurus kuroiwae* presented here does not differ greatly from those of Grismer [15] and Ota [47]. It differs from Grismer [15] only in that it considers the populations of Tonakijima and Tokashikijima Islands to be *G. k. orientalis* rather than *G. k. kuroiwae*. It differs from Ota [47] in that the population from Kumejima Island is considered to be *G. k. yamashinae* rather than *G. k. orientalis,* and that the population from Iheyajima Island is considered to be a distinct subspecies *G. k. toyamai*, rather than *G. k. orientalis*.

Owing to the diagnosability of *Goniurosaurus kuroiwae yamashinae* (Figs. 5 and 6), it is clearly a lineage in the sense of Frost and Hillis [10]; that is, it is a sexual plexus viewed through time. We are less convinced, however, about the lineage status of *G. k. orientalis* primarily because of the inclusion of the Iejima population and the distance of that island from Tonakijima, Tokashikijima, and Akajima Islands (Figs. 8 and 9). The latter three islands are in close geographic proximity and situated within a cluster of islands approximately 35 km west of the southwestern tip of Okinawajima between it and Kumejima Island (Fig. 8). Iejima Island on the other hand, lies only 15 km off the western tip of the Motobu Peninsula of Okinawajima. Populations of *G. kuroiwae* from Kourijima and Sesokojima Islands, which are also geologically associated with the Motobu Peninsula, are not distinguishable from those of Okinawajima and are considered to be *G. k. kuroiwae*. The placement of the Iejima Island population in *G. k. orientalis* is based on the complete dorsal banding pattern of the single known specimen. More specimens from this island would certainly help to clarify its relationships but unfortunately this population may be greatly reduced or extinct due to habitat alteration.

The DA demonstrates the great morphological similarity among *Goniurosaurus kuroiwae orientalis, G. k. kuroiwae*, and *G. k. toyamai*. If we were to construct our classification based on the phenetic relationships of the DA, we would recognize *G. k. yamashinae* and *G. k. splendens* but would consider *G. k. orientalis, G. k. toyamai*, and *G. k. kuroiwae* to all be *G. k. kuroiwae*. However, it is probable that the apparent meristic similarity among the Tokashikijima, Okinawajima, and Iheyajima populations has resulted from independent microevolution in these allopatric populations. Therefore, we prefer to base our classification on the hypothesis of phylogenetic relationships. We believe this results in a more meaningful classification because it is based on common ancestry rather than overall similarity, and thus reflects similarities due to the evolution of shared novelties rather than parallel evolution.

Species vs. subspecies

There recently has been renewed controversy over the use of the subspecies category [2–5, 9–11, 19, 20, 30, 39, 53, 58] as it specifically pertains to herpetology. We believe this issue can be broken down into two general themes. The first concerns the ontology of species and determining wether or not a population represents an individual that should be named and if so, at what taxonomic level. The second is a more general issue concerning the types of information to be retrieved from classifications.

In regard to the second question, phylogenetic systematists want a classification that is consistent with recoverable phylogenetic history [10]. Therefore, they are opposed to classifications that recognize demonstrably paraphyletic taxa including subspecific entities that subjectively divide up various sections of a continuous populational cline. Evolutionary systematists prefer classifications that represent the historical extent of phenetic divergence [36]. Thus, they are willing to recognize demonstrably paraphyletic taxa and consider them one of the consequences of evolution. Therefore, dividing up a continuously breeding population into definable subspecies is acceptable because this may represent the early stages of evolutionary divergence.

Neither system is right or wrong, they are just different. And each is attempting to construct a classification from which different types of information can be extracted. What needs to be decided is which kind of information has more utility to science in general. It is our opinion that a phylogenetic classification has a broader utility because it forms the phylogenetic foundation upon which both systematic and non-systematic evolutionary biologists can formulate hypotheses as to how and why character states and other biological systems have evolved [e.g., 43, 55, 59]. This does not mean that we are advocating abandoning the subspecies concept, however. In fact, at this point in time, we believe that the subspecies categoly may be able in some situations, to provide a classification with additional phylogenetic information. However, the advantages and disadvantages of each situation need to be carefully evaluated on a case by case basis. We do believe that demonstrably paraphyletic taxa should not be used in a classification because they obscure more information than they reveal as well as misrepresent history.

In regard to the first question, the subspecies category was originally intended to be used for populations of geographic variants of continously interbreeding populations [37, 62] and has subsequently enjoyed a broad use of this type of pattern class designation. The problem, however, is that this type of category in a classification, is often inconsistent with the recoverable phylogenetic history. Because these categorical assignments are not lineage (historically) based, they usually do not represent individuals (*sensu* [13, 21, 22]) but classes, and can actually distort history. Additionally, such categories often offer little information because the populations being recognized are usually only weakly diagnosable. It recently has been argued, that if adjacent

populations are interbreeding with one another (e.g. they are not on separate phylogenetic trajectories) they cannot be considered independent evolutionary units [10, 26]. And in such situations, a phylogenetic classification would argue for a single taxon. This criterion is often correct and will go a long way in resolving problems surrounding pattern class taxonomy but it is far too broad. Because of the degrees of differences between varying zones of contact between many diagnosable entities, some of these entities may not be pattern classes or simple geographic variants. They may actually be monophyletic lineages undergoing secondary contact in which case their lineage identity should be retained. Because phylogenetic systematics is a retrodictive discipline and not a predictive discipline, there is no way of knowing from just a slice of time (the present) whether or not these populations will subsume one another. Therefore, it is more conservative to base our decisions on what can be inferred from the past. Before any type of an "all or nothing" criterion can be convincingly argued (or if it can be argued at all) concerning the importance of reproductive compatibility in contact zones, many more case studies will need to be examined. We believe that there may very well be discretely diagnosable widely distributed populations (lineages) that narrowly intergrade on the fringes of their ranges with other such adjacent populations and that this intergradation does not preclude them from being on separate phylogenetic trajectories.

By abandoning the traditional concept of what a subspecies is supposed to represent (geographic variants or pattern classes) and applying the criteria of historical individuality (*sensu* Kluge [26]) to these smallest evolving lineages, the phylogenetic content of classifications may be augmented. This situation is actually less problematic when dealing with allopatric populations and *Goniurosaurus* is a good example with which to work. The evolutionary species concept (*sensu* Frost and Hillis [10]) would recognize all the different taxa of *Goniurosaurus* as distinct species because each is diagnosable and allopatric with respect to one another. This is true, and it clearly indicates that these taxa are on their own separate phylogenetic trajectories. However, this classification would provide less recoverable phylogenetic information (Fig. 10). All that would exist is a list of seven species of *Goniurosaurus* with no indication of how any of them are related. However, if these taxa are considered as subspecies of *G. kuroiwae* and *G. lichtenfelderi*, then more phylogenetic knowledge is imparted into the classification (Fig. 11). In other words, we know that there are at least two monophyletic lineages within *Goniurosaurus* and that within each of those lineages, there has been additional evolution. And if we want our classifications to be information retrieval systems consistent with recoverable phylogenetic history [10], then this system is clearly providing more information.

All the populations of *Goniurosaurus* could be considered as species and the classification indented accordingly [61] which would provide the same amount of information. However, this classification only would be useful when it is at hand for referral. For example, if a paper was written describing various physiological differences between the insular popoulations of *Goniurosaurus* under an indented phylogenetic classification system with no subspecies, we would not know how the taxa were related or the evolutionary implications of the results simply by reading the paper. If, however, the subspecific classification proposed above was used, an evolutionary interpretation of the data becomes more readily apparent because we are able to infer something about relationships from the nomenclature. Now obviously,

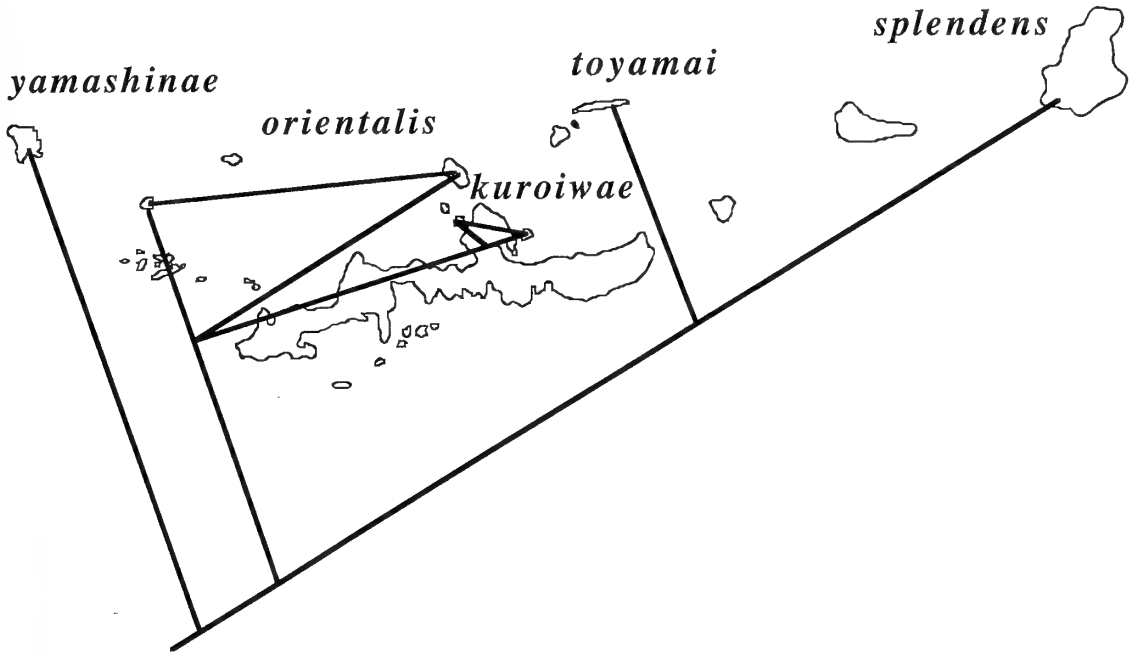

FIG. 9. Area cladogram of the subspecies of *Goniurosaurus kuroiwae*.

Genus *Goniurosaurus*
species *lichtenfelderi*
hainanensis
kuroiwae
yamashinae
orientalis
toyamai
splendens

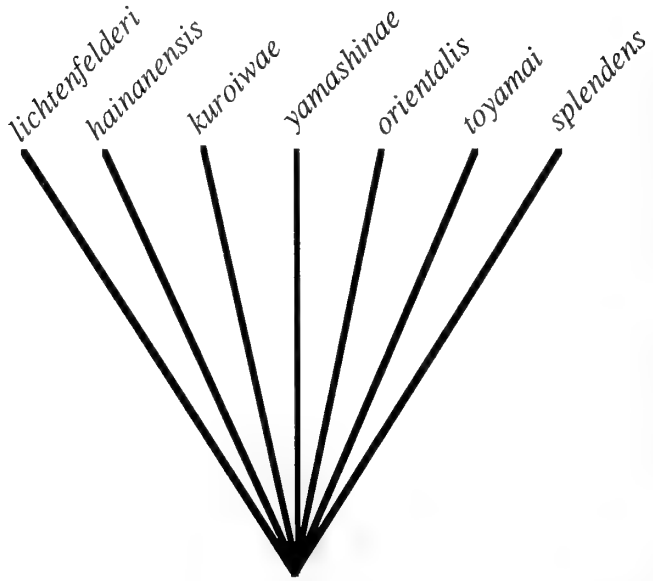

FIG. 10. Classification of *Goniurosaurus* on the left recognizing all populations as species and the amount of recoverable phylogenetic information from that classification on the right.

Genus *Goniurosaurus*
species *lichtenfelderi*
subspecies *lichtenfelderi*
hainanensis
species *kuroiwae*
subspecies *kuroiwae*
yamashinae
orientalis
toyamai
splendens

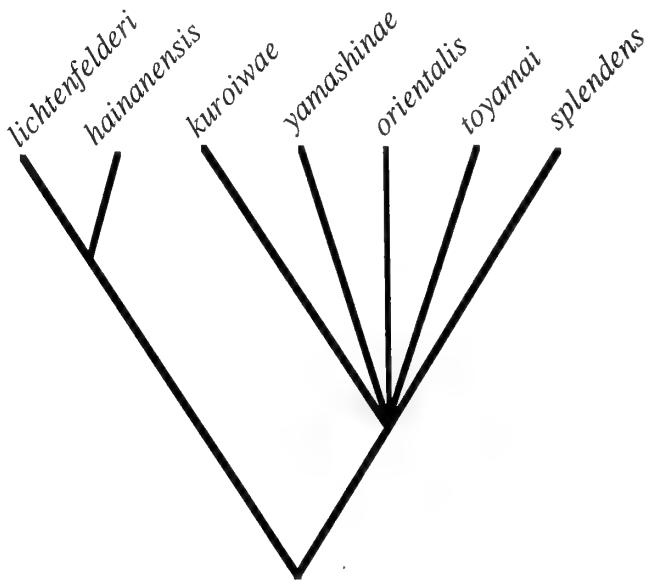

FIG. 11. Classification of *Goniurosaurus* on the left using subspecies and the amount of recoverable phylogenetic information from that classification on the right.

this information could be obtained by reviewing the original phylogeny but unfortunately this is far too often neglected by non-systematic evolutionary biologists (see Dial and Grismer [7]).

The disadvantage in recognizing these taxa as subspecies lies primarily in the original connotation of the subspecies category: that of intergrading geographic variants or pattern classes, which is something these populations are not. In fact, it is the historical inertia of this connotation that is the major disadvantage to considering the name "subspecies" to replace the name Kluge [26] uses for lineage individuality ("species"). However, we believe at this point it is still best to emphasize the phylogeny of this group by way of its nomenclature in light of the disadvantages that the subspecies category carries. It may be that in the future, this disadvantage will be too much to overcome by just a few workers and these populations will best be recognized as different species.

Biogeography

The distribution of *Goniurosaurus kuroiwae* throughout

the Ryukyu Archipelago seems to be rather incomplete. There are large gaps between insular localities within which there are islands with well suited habitat where *G. kuroiwae* is apparently absent (Fig. 8). This absence appears not to be an artifact of collecting because the herpetology of these islands is known quite well [46, 57]. The best example of this is the presence of *G. k. splendens* and *G. k. toyamai* on Tokunoshima and Iheyajima Islands, respectively, and the absence of *G. kuroiwae* from the geographically intermediate Okinoerabujima Island (Fig. 8).

The geological and tectonic history of the Ryukyu Archipelago indicates that the backbone of the Ryukyus was uplifted during the late Miocene as a result of oceanic crust from the Philippine Plate being thrust below the continental crust of Asia [27, 29, 31]. Subsequently, the Ryukyus have had two separate landbridge connections to Taiwan and continental China [23, 24]. The first of these lasted from the late Miocene to the early Pliocene and the second occurred in the early Pleistocene. The majority of the terrestrial reptiles from the Ryukyu Archipelago have their closest relatives occurring in Taiwan and Fukien, the nearest coast on the Chinese continent. Thus, it is assumed here that their ancestors dispersed through the landbridge from the latter regions during the presence of the second landbridge in the early Pleistocene [24, 48, 54]. On the other hand, a few Ryukyu species do not have sister taxa in Taiwan and Fukien and such a relictual distribution pattern is interpreted here as being indicative of a more ancient entry into the Ryukyu Archipelago [23, 24]; perhaps during the first landbridge connection in the late Miocene. The absence of eublepharid geckos from Taiwan and other surrounding regions and the presence of other *Goniurosaurus* from the Gulf of Tonkin (*G. lichtenfelderi*) and southern China (*Goniurosaurus* sp. [14, 15, 33]) may indicate that the ancestral form of *G. kuroiwae* entered the Ryukyus from continental China during the first landbridge formation.

With the submergence of the first landbridge in the middle Pliocene, a large island was formed connecting Kumejima Island of the south to Amamioshima Island of the extreme north [23, 24]. Such a large island would have effectively isolated this ancestral *Goniurosaurus* and presumably promoted the evolution of the ancestor of *G. kuroiwae*. Despite the reunion of this island with Taiwan and continental China during the early Pleistocene, the ancestor of *G. kuroiwae* presumably remained in the Ryukyus probably due to various ecological factors and did not reinvade the continent.

Rising sea levels in the middle Pleistocene resulted in the submergence of the second landbridge. This also began the formation of the contemporary configuration of the Ryukyu Archipelago by creating primary divisions within its central portion. Initially five island groups were formed: Kumejima Island; an island which composed of Tonakijima, Akajima, Tokashikijima, and the other geographically proximate islands; an island composed of Okinawajima, Kourijima, Sesokojima, and Iejima Islands; Iheyajima Island; and Tokunoshima Island [23, 24, 28] (Fig. 8). Unfortunately, there is very little geological data regarding the relative sequence of the isolation of these islands although the biological data presented here (i.e. the phylogenetic relationships) would suggest that it occurred from south to north (Fig. 9).

It is highly probable that all the above islands except Iheyajima and Tokunoshima Islands were re-connected with each other by land bridges during the most recent continental glaciation (ca 15000–18000 yr ago) when the sea level dropped by no less than 120 m [49]. This, however, does not seem to have provided good opportunities for gene flow or range extension for most forest-dwelling reptiles especially on Kumejima Island. The reason is likely due to the very short duration of the connection or the absence of appropriate habitat which would have offered favorable environments on the bridges. Presence of the endemic montane snake, *Opisthotropis kikuzatoi*, on Kumejima [56, 57] and the large genetic divergences between Kumejima, Tokashikijima, and Okinawajima populations of several forest-dwelling species of reptiles revealed by biochemical studies (Ota in prep.), seem to support for this hypothesis. Subsequent rising of the sea level near the end of the Pleistocene would have divided this land mass into the current islands of Kumejima, Tonakijima, Akajima, Tokashikijima, and their surrounding islands, as well as Okinawajima, Sesokojima, Kourijima, and Iejima Islands.

The paleogeographical scenario seems to largely coincide with the evolution of various lineages within *Goniurosaurus kuroiwae* (Fig. 5), although it does not offer any corroborative data as to the chronological sequence in which these lineages evolved. The classification presented above generally reflects the paleogeography of the islands except for the assignment of the Iejima population to *G. k. orientalis*. No evidence suggests that this island was connected to Tonakijima, Akajima, and Tokashikijima Islands to the exclusion of Okinawajima Island [23, 24, 49]. Moreover, similarities in both extant and fossil faunas imply that Iejima Island is historically related to Okinawajima [45]. Thus, it is likely that the apparent similarity of the Iejima population to the Tonakishima, Akajima, and Tokashikijima populations is the result of parallel evolution and not dispersal (*contra* Shimojana [52]).

ACKNOWLEDGMENTS

We wish to express our gratitude to Y. Chigara of the Okinawa Prefectural Museum (OPM), S.-I. Uéno of the National Science Museum (Nat. Hist), Tokyo (NSMT), J. Vindum of the California Academy of Sciences (CAS), C. Myers of the American Museum of Natural History (AMNH), E. N. Arnold of the British Museum (BM), H. Marx of the Field Museum of Natural History (FMNH), J. Wright of the Natural History Museum of Los Angeles County (LACM), I. Darevsky of the Zoological Institute, Academy of Sciences, Leningrad (ZIL), and P. Alberch of the Museum of Comparative Zoology (MCZ) for the loan of specimens. For field assistance we wish to thank H. Hoshikawa, Y. Kane, K. Komemoto, and H. Tomiyama. Special thanks are due to M. Toyama for providing specimens and color photographs of *Goniurosaurus*

kuroiwae from various lacalities, and for the permission to name the subspecies in his honor. For helpful comments on the manuscript we wish to thank R. Etheridge, J. McGuire, B. Hollingsworth, D. Archibald, M. Simpson, and two anonymous reviewers. The work of H. Ota was partially supported by Grants-in-Aid from the Japan Ministry of Education, Science, and Culture (A-63790257, 05740523; to Ota), and the U.S. National Geographic Society Grant (No. 4505–91; to M. Matsui).

Goniurosaurus kuroiwae has been designated as a natural monument of Okinawa Prefecture and the handling of this species is strictly regulated by law. This research was carried out under the permission from the Section of Culture, Okinawa Prefectural Government.

REFERENCES

1 Anderson SC, Leviton AE (1966) A new species of *Eublepharis* from southwestern Iran (Reptilia: Gekkonidae). Occ Pap California Acad Sci 53: 1–5

2 Cole CJ (1990) When is an individual not a species? Herpetologica 46: 104–108

3 Collins JT (1991) Viewpoint: a new taxonomic arrangement for some North American amphibians and reptiles. Herpetol Rev 22: 42–43

4 Collins JT (1992a) Reply to Grobman on variation in *Opheodrys aestivus*. Herpetol Rev 23: 15–16

5 Collins JT (1992b) The evolutionary species concept: a reply to Van Devender et al. and Montanucci. Herpetol Rev 23: 43–46

6 de Queitoz K, Donoghue MJ (1988) Phylogenetic systematics and the species problem. Cladistics 4: 317–338

7 Dial BH, Grismer LL (1992) A phylogenetic analysis of physiological-ecological character evolution in the lizard genus *Coleonyx* and its implications for historical biogeographic reconstruction. Syst Biol 41: 178–195

8 Donoghue MJ (1985) A critique of the biological species concept and recommendations for a phylogenetic alternative. Bryologist 88: 172–181

9 Echelle AA (1990) In defense of the phylogenetic species concept and the ontological status of hybridogenetic taxa. Herpetologica 46: 109–113

10 Frost DR, Hillis DM (1990) Species in concepts and practice: herpetological applications. Herpetologica 46: 87–104

11 Frost DR, Kluge AG, Hillis DM (1992) Species in contemporary herpetology: comments on phylogenetic inference and taxonomy. Herpetol Rev 23: 46–54

12 Gauthier J, Estes R, de Queiroz K (1988) A Phylogenetic analysis of Lepidosauromorpha. In "Phylogenetic Relationships of the Lizard Families" Ed by R Estes, G Pregill, Stanford University Press, Stanford, California, pp 15–98

13 Ghiselin MT (1987) Species concepts, individuality, and objectivity. Biol Phylos 2: 127–143

14 Grismer LL (1987) Evidence for the resurrection of *Goniurosaurus* Barbour (Reptilia: Eublepharidae) with a discussion of geographic variation in *Goniurosaurus lichtenfelderi*. Acta Herpetologica Sinica 6: 43–47

15 Grismer LL (1988) The phylogeny, taxonomy, classification, and biogeography of eublepharid geckos (Reptilia: Squamata). In "Phylogenetic Relationships of the Lizard Families" Ed by R Estes, G Pregill, Stanford University Press, Stanford, California, pp 369–469

16 Grismer LL (1989) *Eublepharis ensafi* Baloutch and Thireau, 1986: A junior synonym of *E. angramainyu* Anderson and Leviton, 1966. J Herpetol 23: 94–95

17 Grismer LL (1991) Cladistic relationships of the lizard *Eublepharis turcmenicus* (Squamata: Eublepharidae). J Herpetol 25: 251–253

18 Grismer LL, Ottley JR (1988) A preliminary analysis of geographic variation in *Coleonyx switaki* (Squamata: Eublepharidae) with a description of an insular subspecies. Herpetologica 44: 143–154

19 Grobman A (1992) On races, clines, and common names in *Opheodrys*. Herpetol Rev 23: 14–15

20 Highton R (1990) Taxonomic treatment of genetically differentiated populations. Herpetologica 46: 114–121

21 Hull DL (1976) Are species really individuals ? Syst Zool 25: 174–191

22 Hull DL (1980) Individuality and selection. Ann Rev Ecol Syst 11: 311–332

23 Kizaki K, Oshiro I (1977) Paleogeography of the Ryukyu Islands. Marine Sciences Monthly 9: 542–549 (in Japanese)

24 Kizaki K, Oshiro I (1980) The origin of the Ryukyu Islands. In "Natural History of the Ryukyus" Ed by K Kizaki, Tsukiji–Shokan, Tokyo, pp 8–37 (in Japanese)

25 Kluge AG (1989) Metacladistics. Cladistics 5: 291–294

26 Kluge AG (1990) Species as historical individuals. Biol Philos 5: 417–431

27 Koba M (1980) Distribution and age of the marine terraces and their deposits in the reef-capped Ryukyu Islands, Japan. Quart Res 18: 189–208 (in Japanese with English abstract)

28 Konishi K (1965) Geotectonic framework of the Ryukyu Islands. J Geol Soc Japan 71: 437–457 (in Jupanese with English abstract)

29 Konishi K, Sudo K (1972) From Ryukyus to Taiwan. Kagaku 42: 221–230 (in Japanese)

30 Lazell J (1992) Taxonomic tyranny and the esoteric. Herpetol Rev 23: 14

31 Lee C, Shor GC, Bibee LD, Lu RS, Hilde TWC (1980) Okinawa trough: origin of a back-arc basin. Marine Geol 35: 219–241

32 Leviton AE, Gibbs RH Jr., Heal E, Dawson CE (1985) Standards in herpetology and ichthyology: Part I. Standard symbolic codes for institutional resource collections in herpetology and ichthyology. Copeia 1985: 802–832

33 Li D, Wang J, Zhao Z (1985) Reptilian survey of karst in Libo, Guizhou. Acta Herpetologica Sinica 4: 140–143 (in Chinese with English abstract)

34 Maddison WP, Donoghue MJ, Maddison DR (1984) Outgroup analysis and parsimony. Syst Zool 33: 83–103

35 Maki M (1930) A new banded gecko, *Eublepharis orientalis*, sp. nov. from Ryu Kyu. Annot Zool Japon 13: 9–11

36 Mayr E (1969) Principles of Systematic Zoology. McGraw Hill, New York

37 Mayr E (1982) Of what use are subspecies ? Auk 99: 593–595

38 Mocquard F (1897) Notes herpetologiques. Bull Mus Hist Nat Paris 5: 211–217

39 Montanucci RR (1992) Commentary on a proposed taxonomic arrangement for some North American amphibians and reptiles. Herpetol Rev 23: 9–10

40 Nakamura K, Uéno S-I (1959) The geckos found in the limestone caves of the Ryu Kyu islands. Mem Coll Sci, Kyoto Univ (ser B) 26: 42–52

41 Nakamura K, Uéno S-I (1963) Japanese reptiles and amphibians in colour. Hoikusha, Osaka (in Japanese)

42 Namiye M (1912) On the gekkonid lizards of Okinawa. Zool Mag (Tokyo) 24: 442–445 (in Japanese)

43 O'Hara RJ (1988) Homage to Clio, or, toward historical philosophy for evolutionary biology. Syst Zool 37: 142–155

44 Okada Y (1936) A new cave gecko, *Gymnodactylus yamashinae* from Kumejima, Okinawa Group. Proc Imp Acad, Japan 6: 71–73

45 Oshiro I, Nohara T (1990) Vertebrate fossils in Okinawa. In "Nature of Okinawa-Geomorphology and Geological Features" Ed by H Ujiie, Hirugi-sha, Naha, pp 213–229 (in Japanese)

46 Ota H (1986) A review of reptiles and amphibians of the Amami Group, Ryukyu Archipelago. Mem Fac Sci, Kyoto Univ (Ser Biol) 11: 57–71

47 Ota H (1989) A review the geckos (Lacertilia: Reptilia) of the Ryukyu Archipelago and Taiwan. In "Current Herpetology in East Asia" Ed by M Matsui, T Hikida RC Goris, Herpetological Society of Japan, Kyoto, pp 222–261

48 Ota H (1991) Systematics and biogeography of terrestrial reptiles of Taiwan. In "Proceedings of the International Symposium of Wildlife Conservation" Ed by Y-S Lin, K-H Chang, Council of Agriculture, Taipei, pp 47–112

49 Ota H, Sakaguchi N, Ikehara S, Hikida T (1993) The herpetofauna of the Senkaku Group, Ryukyu Archipelago. Pacific Sci 47: 248–255

50 Pinmentel RA, Smith JD (1986) BioΣtat II. A multivariate statistical toolbox. Sigma Soft, Placentia, California

51 Sengoku S (1979) Amphibians and Reptiles in Color. Ie no Hikari Kyokai, Tokyo (in Japanese)

52 Shimojana M (1979) Cave animals of Okinawa and adjacent islands. In "Survey Report of the Caves of Okinawa Prefecture II" Ed by Educational Committee of Okinawa Prefecture, Educational Committee of Okinawa Prefecture, Naha, pp 97–153 (in Japanese)

53 Smith HM (1990) The universal species concept. Herpetologica 46: 122–124

54 Takara T (1962) Studies on the terrestrial snakes of the Ryukyu Archipelago. Sci Bull Agr Home Econ Div, Univ Ryukyus 9: 1–202 (in Japanese with English summary)

55 Thope RS (1987) Geographic variation: a synthesis of cause, data, pattern and congruence in relation to subspecies, multivariate analysis and phylogenesis. Boll Zool 54: 3–11

56 Toyama M (1984) Amphibians and reptiles. In "A Guide to Animals of Okinawa, Vol. 1: Terrestrial Vertebrates" Ed by S Ikehara, Y Yonashiro, K Miyagi, M. Toyama, Shinsei-tosho, Naha, pp 209–323 (in Japanese)

57 Toyama M, Ota H (1991) Amphibians and reptiles of the Ryukyu Islands. In "Study of Essential Factors for Preservation of Wildlife in Nansei Islands" Ed by World Wildlife Fund Japan, Japan Agency of Environment (Nature Conservation Department), Tokyo, pp 233–254 (in Japanese)

58 Van Devender TR, Lowe CH, McCrystal H, Lawler H (1992) Viewpoint: reconsider suggested systematic arrangements for some North American amphibians and reptiles. Herpetol Rev 23: 10–14

59 Wantop H-E (1983) Historical constraints in adaptation theory: traits and non-traits. Oikos 41: 157–160

60 Watrous LE, Wheeler QD (1981) The out-group comparison method of character analysis. Syst Zool 30: 1–11

61 Wiley EO (1981) Phylogenetics: the theory and practice of phylogenetic systematics. John Wiley and Sons, New York

62 Wilson EO, Brown WL Jr (1953) The subspecies concept. Syst Zool 2: 97–111

APPENDIX I

Specimens Examined

All abbreviations follow Leviton *et al.* [32] except those as follows: KUZ-Department of Zoology, Faculty of Sciences, Kyoto University, Japan; LLG-L. Lee Grismer, Department of Biology, San Diego State University, San Diego, CA 92182, USA; and TPN-Satoshi Tanaka, Motobu Senior High School, Tokuchi 377, Motobu, Okinawa 905–02, Japan.

Goniurosaurus kuroiwae kuroiwae: JAPAN-RYUKYU ARCHIPELAGO: OKINAWAJIMA ISLAND; Naha (KUZ 10005–06, TPN 76042508, 76042802, 77041005, 7711060–611, 78011101, 78011401, 78020201, 78031801–05, 78041401–09, 78051601–09, 78060502, 78061501–09, 78061801, 78062501, 78063001, 78070301, 78070401, 78071401–10, 78071701, 78071902, 78072001–02, 78072101, 78072201, 78081401–11, 78081601, 78091601, 78091701–07, 78100601, 78091701–07, 78100601, 78102301–09, 79061001, 79070201, 79070301–02, 79072801, 79082601), Seihua (KUZ 7955, 7957–58, 8002, 8004–05, 8051–53, TPN 6091507–13, 76102111–13, 77040802–05, 77040807–42, 78051701–02, 78052202, 78052701–02, 78052901–04, 78062201–02, 78062401, 7806201–03), Chinen (KUZ 10007), Yakena (TPN 77041701), Oyakebaru (TPN 77121001), Yonaha (TPN 76052401, 76052406, 78032701–03), Yona (TPN 77041401, 77050201–04, 77052101, 77060901, 77081804–12, 77081911–12, 77082102–04, 78042302), Hentona (TPN 78042305–08), Haneji (TPN 79081101–03). KOURIJIMA ISLAND; OPM 424. SESOKOJIMA ISLAND; OPM 369. *Goniurosaurus kuroiwae orientalis*: JAPAN-RYUKYU ARCHIPELAGO: AKAJIMA ISLAND; OPM 341. IEJIMA ISLAND; KUZ 9991. TOKASHIKIJIMA ISLAND; KUZ 7976, OPM 325, NSMT 2523–24, TPN 77101501, 77111701, 77120701–05, 78030101–03, 78052001–03, 78052101–09, 78052201, 78060501, 78061101, 78061401, 78061601, 78071101, 78071201, 78071901, 78072003, 78080501–02, 78080508–10, 78080512–15, 78090202–05, 79082602–03. TONAKIJIMA ISLAND; OPM 489, NSMT 02522. *Goniurosaurus kuroiwae splendens*: JAPAN-RYUKYU ARCHIPELAGO: TOKUNOSHIMA ISLAND; Kedoku (KUZ 8408–11, OPM 10, LLG 1180, 1251–52, NSMT 2514–20, 3211–12, TPN 76102201–04, 77041001–04, 77120901). *Goniurosaurus kuroiwae toyamai*: JAPAN-RYUKYU ARCHIPELAGO: IHEYAJIMA ISLAND; KUZ 9978–83, 9985–88, TPN 77032201, 77070301, 77070401–02. *Goniurosaurus kuroiwae yamashinae*: JAPAN-RYUKYU ARCHIPELAGO: KUMEJIMA ISLAND; KUZ 9989, 9998, 13249, OPM 3, 8, 9, TPN 78050401–02, six uncatalogued specimens. *Eublepharis angramainyu*: CAS 86333, 86337, 86361–62, 86366, 86381, 86383, 86385, 86396–98, 86416, 157129. *Eublepharis harwickii*: AMNH 57593, BM 1927.8.9.1, 1962.23, 1962.38. *Eublepharis macularius*: AMNH 57594, CAS 96212, 96245, 101440–41, 104361–63, 133826, FMNH 161142, LACM 109902–03. LLG 1393–94, 131–38. *Eublepharis turcmenicus*: ZIL 10103, 15380, 19414. *Hemitheconyx caudicinctus*: AMNH 104409, CAS 55114, 154299–302, LLG 2119–96. *Hemitheconyx taylori*: BM 1946.8.26.57–59, 1946.8.26.72, 12.5.372–74. *Holodactylus africanus*: CAS 125431, MCZ 21663, 38693, 53593, 77365–67, 77369–70, 96928, 160707. *Holodactylus cornii*: BM 1931.7.20.269.

ZOOLOGICAL SCIENCE 11: 337–342 (1994)

Polymorphism of Lampbrush Chromosomes in Japanese Populations of *Rana nigromaculata*

HIROMI OHTANI

Laboratory for Amphibian Biology, Faculty of Science, Hiroshima University, Higashi-hiroshima 724, Japan

ABSTRACT—The 13 pairs of the lampbrush chromosomes of *R. nigromaculata* are characterized by one to five landmarks situated at specific positions on the axis of each chromosome. In *R. nigromaculata* collected from 28 sites in Japan, eight chromosome pairs did not show any variations, whereas the remaining five pairs consisted of two forms of chromosome which differed in the number or type of the landmarks. The variations in chromosomal polymorphism indicated that Japanese *R. nigromaculata* has genetically differentiated into four groups which were formed by a break in the migration due perhaps to geographic obstacles and the expansion of new genetic materials provided from continental *R. nigromaculata* in the Würm glacial stage. By comparing the distribution of the variations and the lampbrush chromosomes of continental *R. nigromaculata,* the history of the migration of *R. nigromaculata* into Japan is discussed.

INTRODUCTION

Rana nigromaculata is distributed over the north-eastern area of China, the whole of the Korean Peninsula, and Kyushu, Shikoku and Honshu (except the Kanto and Sendai plains) in Japan [5]. This species is supposed to have evolved from an ancestral species population common to *Rana plancyi* in the continent, to adapt to the arid and cold climates [6]. After its own evolution was sufficiently completed, *R. nigromaculata* came to Japan through the Korean Peninsula when Japan was still a part of the continent [6]. Recently, Nishioka *et al.* [12] found that *R. nigromaculata* collected from 45 sites in Japan have differentiated into four groups on the basis of Nei's genetic distances obtained from electrophoretic analyses.

The genetic differentiation was reflected in the characteristics of its lampbrush chromosomes which are composed of 13 pairs of bivalent chromosomes at the diplotene stage of oogenetic meiosis. The lampbrush chromosomes of *R. nigromaculata* are characterized by one to five landmarks, consisting of simple-type giant loops, compound-type giant loops, spheres, and an oval-like structure, at specific positions of each chromosome axis [10], though the landmarks grow conspicuous by accumulating their own gene product around their axes [1]. However, some lampbrush chromosomes showed variations in the landmarks among populations of *R. nigromaculata.* These variations are presumed to relate to the processes of the habitat expansion of *R. nigromaculata* in Japan in the same way as the mitotic chromosomal mutations of *Rattus* species [15–17].

Herein, the geographical distribution and the history of the polymorphism of the lampbrush chromosomes of Japanese *R. nigromaculata* in comparison with those of continental species are described.

Accepted January 19, 1994
Received October 26, 1993

MATERIALS AND METHODS

Lampbrush chromosomes were removed from the ova of 199 female *Rana nigromaculata* Hallowell collected from 28 sites in Japan. Figure 1 shows the collection sites and the number of females. In addition, lampbrush chromosomes were removed from three females from Beijing, China, and six females from Suwon, Korea, which had been bred in the Laboratory for Amphibian Biology, Hiroshima University.

Lampbrush chromosomes were prepared by means of a slight modification of Gall's method [2, 13]. Because the size of the landmarks varies with the stages of oogenesis, ten or more lampbrush chromosome preparations per female were examined under a phase-contrast microscope to avoid misjudgements on the presence or absence of landmarks.

RESULTS

Previously, Nishioka *et al.* [10] described a map of the lampbrush chromosomes of *R. nigromaculata,* which represented the positions and types of landmarks on each chromosomal axis. The map was constructed from the lampbrush chromosomes of three female offspring of a pair collected from Hiroshima. According to that map, 13 lampbrush chromosomes possess one to five landmarks each, or a total of 35 landmarks, and they are all distinguishable by position and type.

In this study, eight of the 13 lampbrush chromosomes of all the populations of Japanese *R. nigromaculata* examined showed the same characteristics (2–5, 8–10, and 12). By contrast, the remaining five, 1, 6, 7, 11, and 13, showed two forms which differed in the number or type of the landmarks they carried. In chromosome 1, one form possessed two simple-type giant loops, one on the short arm and the other on the long arm; the other form possessed one compound-type giant loop on the long arm in addition to these (Fig. 2a). In chromosome 6, one form had one compound-type and one simple-type giant loop on the long arm; the other had another

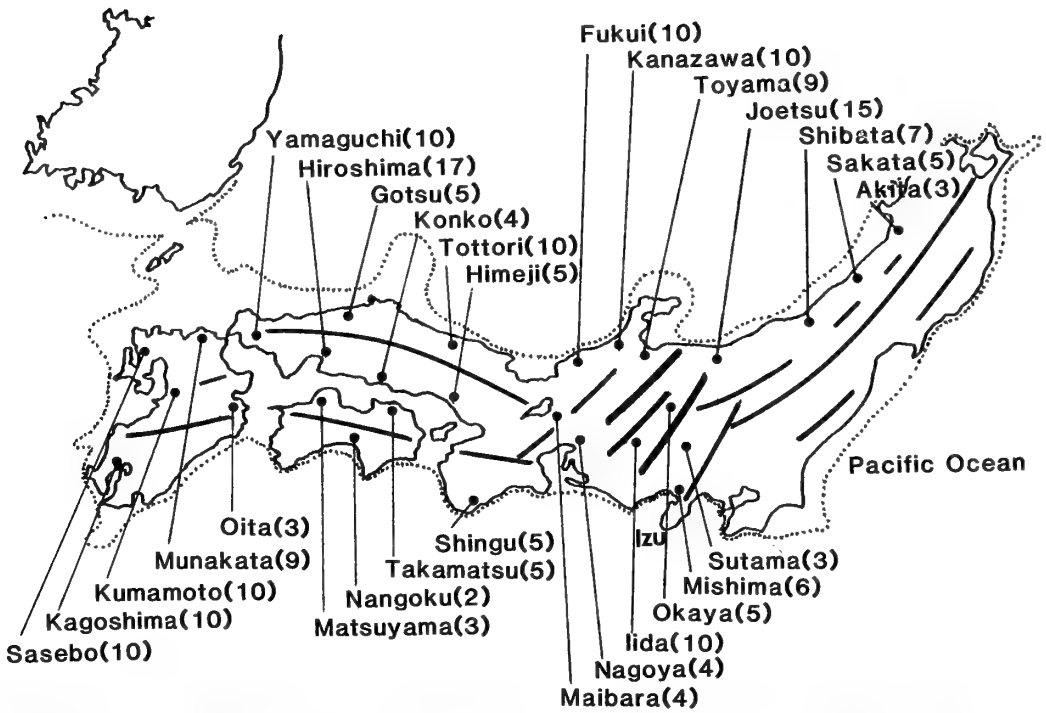

FIG. 1. Map showing the collection sites of *Rana nigromaculata* and the number of females studied. Bold lines mark the mountain ranges and a dotted line marks the location of the presumptive coastline about 2×10^4 years ago [3].

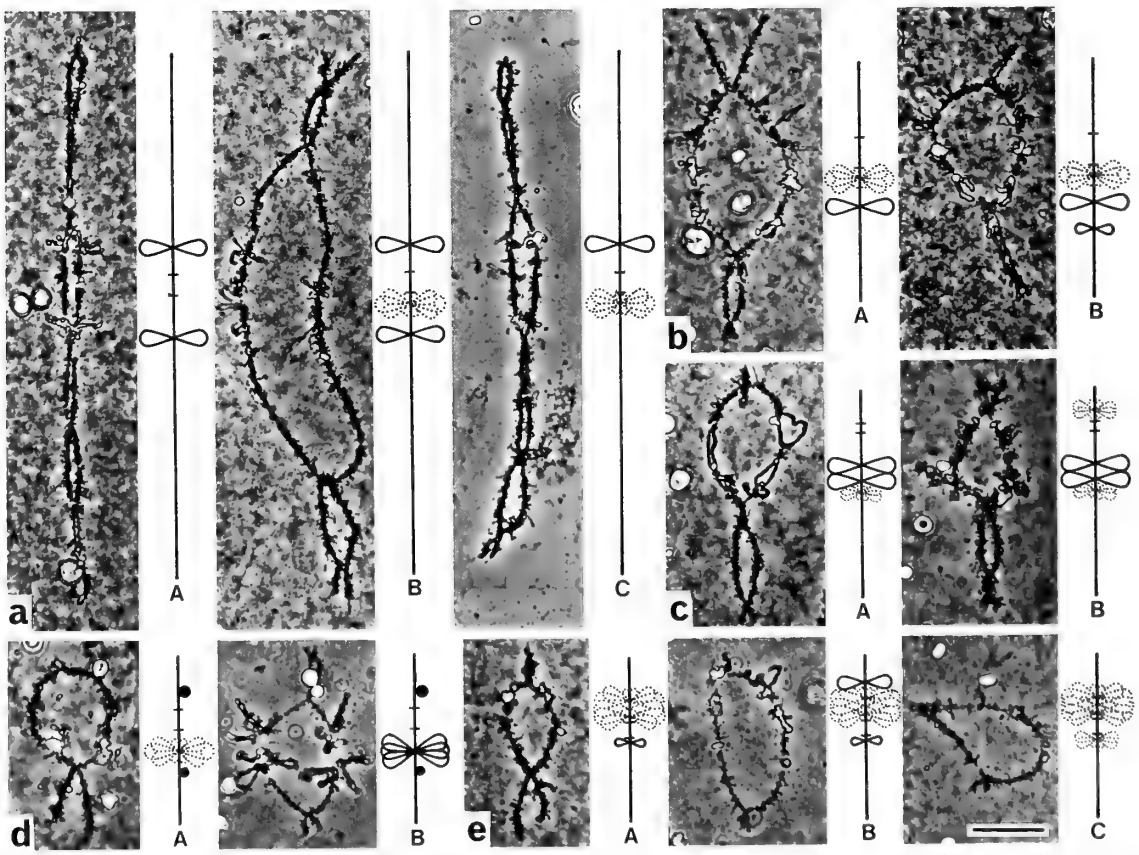

FIG. 2. Variations in lampbrush chromosomes 1(a), 6(b), 7(c), 11(d), and 13(e) of *R. nigromaculata*. In diagrammatic representation, simple- and compound-type giant loops are represented by solid and dotted lines, respectively, and spheres are shown with black circles. A segment between two short parallel lines shows a range consisting of larger normal loops than any other parts and including a centromere. A, B, and C indicate A-, B-, and C-form, respectively. In photographs, simple-type giant loops appear as a stiff loop which becomes thick by covering its axis with a large quantity of matrixes and it has a smooth outline. Compound-type giant loops consist of two or more simple-type giant loops which are more slender than the independent simple-type giant loops and have a notched outline. Scale bar represents 100 μm.

simple-type giant loop on the long arm in addition to these (Fig. 2b). In chromosome 7, one form had two simple-type and one compound-type giant loop on the long arm; the other had another compound-type giant loop on the short arm in addition to these (Fig. 2c). In chromosome 11, one form had one compound-type giant loop on the long arm and two spheres on both the arms; the other had three simple-type giant loops in place of the compound-type giant loop of the former (Fig. 2d). In chromosome 13, one form had one compound-type giant loop on the short arm and one simple-type giant loop on the long arm; the other had another simple-type giant loop on the short arm in addition to these (Fig. 2e). In each of these five chromosomes, the former was named the A-form, and the latter was the B-form.

Based upon the frequencies of the A- and B-forms in each of the 28 collection sites, the *R. nigromaculata* populations were divided into four groups, named the Eastern Honshu, Chubu, Western Honshu-Shikoku, and Kyushu groups, respectively (Fig. 3; Table 1). In chromosome 1, the A-form was predominant in the Chubu group, while the B-form was predominant in the Eastern Honshu and Western Honshu-Shikoku groups. In the Kyushu group, the frequency of the B-form was a little higher than that of the A-form. It was remarkable, however, that nine of the 10 females from Kagoshima had the homologous A-form.

In chromosome 6, the two forms were somewhat similar in distributional pattern to those of chromosome 1. The A-form was found in the Chubu group at a fairly high frequency, not being so predominant as the A-form of chromosome 1. The B-form was predominant in the Eastern Honshu and Western Honshu-Shikoku groups, like chromosome 1. The Kyushu group also involved the B-form at high frequency. It was remarkable, however, that five females from Kagoshima were homozygous for the A-form and four were heterozygous for the A- and B-forms.

In chromosome 7, all the females of the Eastern Honshu, Chubu, and Western Honshu-Shikoku groups had the only A-form. On the other hand, the Kyushu group had the B-form at a nearly equal frequency to that of the A-form. It was remarkable, however, that all females from Kagoshima had the homologous A-form.

In chromosome 11, the B-form was distributed in a similar manner to the A-form of chromosome 7. The B-form was found in all the females of the Eastern Honshu, Chubu, and Western Honshu-Shikoku groups in the homologous condition. The Kyushu group involved both the A- and B-forms at nearly equal frequencies.

In chromosome 13, all the females of the Eastern Honshu and Chubu groups were homologous for the A-form. On the other hand, most of the females of the Western

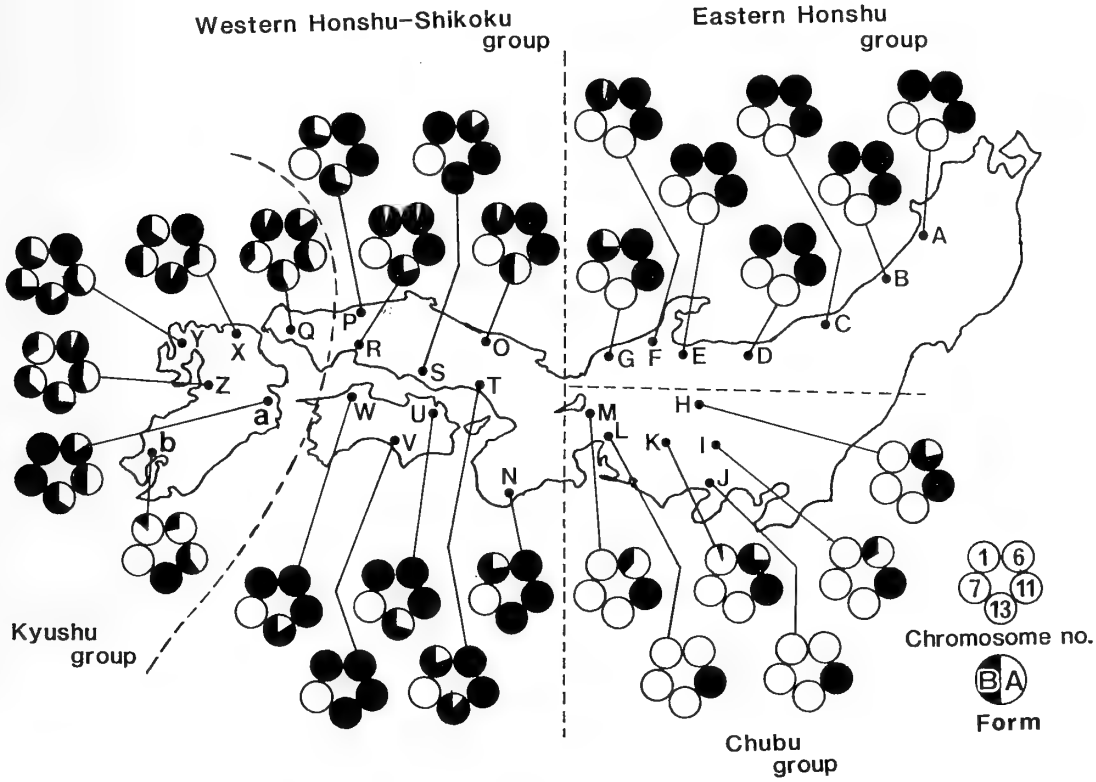

FIG. 3. Frequencies of the A- and B-form of five lampbrush chromosomes, 1, 6, 7, 11, and 13, in each collecting site. Areas partitioned with broken lines represent groups of *R. nigromaculata* females with about the same characteristics in their lampbrush chromosomes. A, Akita. B, Sakata. C, Shibata. D, Joetsu. E, Toyama. F, Kanazawa. G, Fukui. H, Okaya. I, Sutama. J, Mishima. K, Iida. L, Nagoya. M, Maibara. N, Shingu. O, Tottori. P, Gotsu. Q, Yamaguchi. R, Hiroshima. S, Konko. T, Himeji. U, Takamatsu. V, Nangoku. W, Matsuyama. X, Munakata. Y, Sasebo. Z, Kumamoto. a, Oita. b, Kagoshima.

TABLE 1. Frequencies of bivalent chromosomal types in four groups of *R. nigromaculata* Figures in parentheses show expected values based on Hardy-Weinberg hypothesis.

Type	Eastern Honshu	Chubu	Western Honshu Shikoku	Kyushu	Total
Chromosome 1					
AA	0 (0.2)	31 (31.0)	1 (0.4)	19 (9.7)	51
AB	6 (5.7)	1 (1.0)	8 (9.1)	7 (25.5)	22
BB	53 (53.2)	0 (0.0)	47 (46.4)	26 (16.7)	126
Total	59	32	56	52	199
Chromosome 6					
AA	0	12 (10.1)	0 (0.0)	5 (1.7)	17
AB	0	12 (15.8)	2 (2.0)	9 (15.5)	23
BB	59	8 (6.1)	54 (54.0)	38 (34.7)	159
Total	59	32	56	52	199
Chromosome 7					
AA	59	32	56	18 (14.0)	165
AB	0	0	0	18 (26.0)	18
BB	0	0	0	16 (12.0)	16
Total	59	32	56	52	199
Chromosome 11					
AA	0	0	0	17 (11.5)	17
AB	0	0	0	15 (25.9)	15
BB	59	32	56	20 (14.5)	167
Total	59	32	56	52	199
Chromosome 13					
AA	59	32	4 (3.0)	4 (1.9)	99
AB	0	0	18 (20.0)	12 (16.2)	30
BB	0	0	34 (33.0)	36 (33.9)	70
Total	59	32	56	52	199

Honshu-Shikoku and Kyushu groups were homozygous for the B-form.

The lampbrush chromosomes of continental *R. nigromaculata* were identical in characteristics with those of Japanese *R. nigromaculata*, except for chromosome 1. The characteristics of chromosomes 6, 7, 11, and 13, in which Japanese *R. nigromaculata* had variations, were of the A-form. However, of the six females from Suwon, two had the homozygous and heterozygous B-form in chromosome 6 and one was homozygous for the B-form in chromosome 11. Chromosome 1 of all the females from Beijing and Suwon had one simple-type giant loop on the short arm and one compound-type giant loop on the long arm (Fig. 2a). This was named the C-form. Of the two landmarks, the former was also found in the A- and B-forms, and the latter in the B-form. In chromosome 13 of three females from Beijing, there was a variation which was not found in Japanese *R. nigromaculata*. This variation had two compound-type giant loops on the short and long arms and was named the C-form (Fig. 2e). Two females were homologous for the C-form and one was heterologous for the A- and C-forms.

DISCUSSION

Nishioka *et al.* [12] found that *R. nigromaculata* collected from all over Japan can be divided into four groups by a cluster analysis of the genetic distances between local populations. The geographic areas of the four groups are as

follows: 1) the Tohoku area comprising the prefectures of Aomori, Akita, and Niigata; 2) the Chubu area comprising the prefectures of Shizuoka, Aichi, Nagano, and Yamanashi; 3) the Hokuriku, Kinki, Sanyo, Shikoku, and Kagoshima areas comprising the prefectures of Toyama, Ishikawa, Fukui, Shiga, Mie, Wakayama, Osaka, Hyogo, Okayama, Hiroshima, Kagawa, Kochi, Ehime, and Kagoshima; and 4) the San-in and Kyushu areas comprising the prefectures of Tottori, Shimane, Yamaguchi, Fukuoka, Nagasaki, Kumamoto, Oita, and Miyazaki. In this study, it was found that the spread of variations in five lampbrush chromosomes, 1, 6, 7, 11, and 13, is also coincident with this grouping, though there were slight discrepancies in dividing lines. In the four groups based on the chromosomal variations, the geographical area of the Eastern Honshu group comprises the Tohoku and Hokuriku areas, that of the Chubu group comprises the Chubu area, that of the Western Honshu-Shikoku group comprises the Kinki, Sanyo, San-in (except Yamaguchi Prefecture) and Shikoku areas, and that of the Kyushu group comprises the Kyushu area and Yamaguchi and Kagoshima Prefectures.

In each group, the frequencies of the forms of lampbrush chromosomes agreed well with expected values based on the Hardy-Weinberg hypothesis ($P>0.05$), except for chromosomes 1, 6, and 11 of the Kyushu group. This seems to show that three groups other than the Kyushu group are geographically isolated from one another by major mountain ranges. The Kyushu group, however, is not partitioned from the adjoining group by a clear topographical obstacle, since a part of this group encroaches on the western Honshu area. Moreover, this group seems to include a heterogeneous subgroup, because in chromosomes 1 and 6 many *R. nigromaculata* from Kagoshima had the A-forms which were also found in the Chubu group. The Kyushu group may be divided into two subgroups by increasing the sites of examination further.

It seems that the estimation of the period when the ancestral population of *R. nigromaculata* invaded Japan gives an important clue to the process of the formation of the four groups. Japan was a part of the continent up to the end of the Riss glacial stage [4]. It is reasonably certain that the complete separation of Japan occurred in the Riss-Würm interglacial stage (about 0.12 million years ago) [8]. After entering Japan, *R. nigromaculata* is supposed to have moved along the coastal plains without passing over the highly upheaved mountain ranges; the coastal plains which had widened owing to marine regression in the glacial periods were more favorable. The population which had reached the Chubu area, however, could not go further than this area. The reason is that a collision between the central Honshu region and Izu island (presently a peninsula) broke down the coastal plain (about 0.5 million years ago) [7]. The difficulty of migration in this region is evidenced by the cluster analyses of genetic distances in the populations of *Rana rugosa, Rana japonica,* and *Rana brevipoda* [9, 11, 12]. The populations of these species in the Kanto and Sendai plains, which are situated in the Pacific side of eastern Honshu, are divided in the dendrograms from those in the other areas. Consequently, the absence of *R. nigromaculata* in the Kanto and Sendai plains implies that its ancestral population reached Japan through the Korean Peninsula between about 0.5 and 0.12 million years ago. The area of the north end of the eastern Honshu region could not provide another entrance because the mountain ranges virtually reached the shore.

The formation of the Eastern Honshu, Chubu, and Western Honshu-Shikoku groups is attributable to the release of migration due to marine regression during the glacial stage and the geographical isolation due to marine transgression during the interglacial stages. The formation of the Kyushu group is attributed to the introgression of new genetic materials provided from continental *R. nigromaculata* which invaded again during the Würm glacial stage when the Japanese Islands were temporarily reconnected with the Korean Peninsula (between about 20,000 and 18,000 years ago) [14]. This introgression is typified by the presence of the A-form of chromosome 11 which is found in continental *R. nigromaculata.*

In each of the lampbrush chromosomes 6, 7, 11 and 13, it is quite certain that the A-form is older than the B-form, that is, the B-form was derived from the A-form by mutations. The reasons are, firstly, that continental *R. nigromaculata* is of the A-form in these lampbrush chromosomes and the Chubu group, of which the *R. nigromaculata* migrates to the furthest area in Japan, also has the A-form in the lampbrush chromosomes 6, 7, and 13. Secondly, the lampbrush chromosomes 6, 11 and 13 of *R. brevipoda,* which diverged from an ancestral species common to *R. nigromaculata* [6], have the same characteristics as the A-form [10, 13]. In the two forms of lampbrush chromosome 1, an age comparison is difficult because continental *R. nigromaculata* and *R. brevipoda* have forms that differ from these. However, both forms of chromosome 1 somewhat resembled those of chromosome 6 in their distribution pattern. Therefore, the A-form is also probably older than the B-form in chromosome 1.

In view of the probable migration course of *R. nigromaculata* and the distributional extent of the B-forms, the B-form of each lampbrush chromosome is presumed to have occurred in the order of chromosomes 11, 1 and 6, 13, and lastly 7. The B-form of chromosome 7 seems to have occurred toward the Würm glacial stage, because it is very similar in distribution pattern to the A-form of chromosome 11. The B-form of chromosome 13 probably occurred before the Würm glacial stage and spread in this stage, judging from the absence in the Eastern Honshu and Chubu groups. This is because the western Honshu, Shikoku, and Kyushu areas united during the Würm glacial stage, since the Inland Sea dried up owing to marine regression [4]. The B-forms of chromosomes 1 and 6 probably spread during the glacial stages before the Würm glacial stage. The B-form of chromosome 11 spread at the beginning of the migration of *R. nigromaculata.*

REFERENCES

1 Callan HG (1986) Lampbrush Chromosomes. Springer-Verlag, Berlin, pp 50–105

2 Gall JG (1966) Techniques for the study of lampbrush chromosomes. In "Methods in Cell Physiology 2" Ed by DM Prescott, Academic Press, New York, pp 37–60

3 Japan Association for Quaternary Research (1987) Explanatory Text for Quaternary Maps of Japan. (In Japanese) University of Tokyo Press, Tokyo, pp 119

4 Kaizuka S, Naruse Y (1977) Paleogeographic changes. (In Japanese) In "The Quaternary Period: Recent Studies in Japan" Ed by Japan Association for Quaternary Research, University of Tokyo Press, Tokyo, pp 333–351

5 Kawamura T, Nishioka M (1977) Aspects of the reproductive biology of Japanese anurans. In "The Reproductive Biology of Amphibians" Ed by DH Taylor, SI Guttman, Plenum Press, New York, pp 103–139

6 Kawamura T, Nishioka M (1979) Isolating mechanisms among the water frog species distributed in the Palearctic region. Mitt Zool Mus Berlin 55: 171–185

7 Matsuda T (1978) Collision of the Izu-Bonin Arc with central Honshu: Cenozoic Tectonics of the Fossa Magma, Japan. J Phys Earth 26 Suppl: S 409–421

8 Matsuura N (1977) Molluscan fossils from the late Pleistocene marine deposits of Hokuriku region, Japan Sea side of central Japan. Sci Rep Kanazawa Univ 22: 117–162

9 Nishioka M, Kodama Y, Sumida M, Ryuzaki M (1993) Systematic evolution of 40 populations of *Rana rugosa* distributed in Japan elucidated by electrophoresis. Sci Rep Lab Amphibian Biol Hiroshima Univ 12: 83–131

10 Nishioka M, Ohtani H, Sumida M (1980) Detection of chromosomes bearing the loci for seven kinds of proteins in Japanese pond frogs. Sci Rep Lab Amphibian Biol Hiroshima Univ 4: 127–184

11 Nishioka M, Sumida M, Borkin LJ, Wu Z (1992) Genetic differentiation of 30 populations of 12 brown frog species distributed in the Palearctic region elucidated by the electrophoretic method. Sci Rep Lab Amphibian Biol Hiroshima Univ 11: 109–160

12 Nishioka M, Sumida M, Ohtani H (1992) Differentiation of 70 populations in the *Rana nigromaculata* group by the method of electrophoretic analyses. Sci Rep Lab Amphibian Biol Hiroshima Univ 11: 1–70

13 Ohtani H (1990) Lampbrush chromosomes of *Rana nigromaculata, R. brevipoda, R. plancyi chosenica, R. p. fukienensis* and their reciprocal hybrids. Sci Rep Lab Amphibian Biol Hiroshima Univ 10: 165–221

14 Ono Y (1984) Late glacial paleoclimate reconstructed from glacial and periglacial landforms in Japan. Geographical Review of Japan 57: 87–100

15 Yosida TH, Tsuchiya K, Moriwaki K (1971) Frequency of chromosome polymorphism in *Rattus rattus* collected in Japan. Chromosoma 33: 30–40

16 Yosida TH, Tsuchiya K, Moriwaki K (1971) Karyotypic differences of black rats, *Rattus rattus,* collected in various localities of East and Southeast Asia and Oceania. Chromosoma 33: 252–267

17 Yosida TH (1973) Evolution of karyotypes and differentiation in 13 *Rattus* species. Chromosoma 40: 285–297

ZOOLOGICAL SCIENCE 11: 343–349 (1994)

Biochemical Systematics of Five Asteroids of the Family Asteriidae Based on Allozyme Variation

Norimasa Matsuoka[1], Kiyoko Fukuda, Kyoko Yoshida, Miho Sugawara and Megumi Inamori

Department of Biology, Faculty of Science, Hirosaki University, Hirosaki 036, Japan

ABSTRACT—The family Asteriidae of the order Forcipulatida from Japanese waters includes the five common starfish species belonging to the five different genera. They are *Asterias amurensis, Aphelasterias japonica, Distolasterias nipon, Coscinasterias acutispina* and *Plazaster borealis*. The phylogenetic relationship of these five members were investigated by electrophoretic analyses of 15 different enzymes. From the allozyme variation observed in 31 genetic loci, the Nei's genetic distances between species were calculated and the molecular phylogenetic tree for the five species was constructed. The phylogenetic tree indicated the following: (1) The five species are phylogenetically divided into three clusters: (i) *A. amurensis* and *P. borealis*; (ii) *A. japonica* and *D. nipon*; and (iii) *C. acutispina*. (2) *A. amurensis* and *P. borealis* are the most closely related to each other and more recent species which evolved later. (3) *A. japonica* is more closely related to *D. nipon* than to other species. (4) *C. acutispina* is the most distant species of the five members. These electrophoretic results were discussed through the detailed comparison with molecular and non-molecular data, and the differentiation process of five species was speculated.

INTRODUCTION

During the last 10–15 years, the taxonomic, phylogenetic and evolutionary studies have been revitalized by the application of techniques from biochemistry or molecular biology. Protein sequencing, immunological methods, protein electrophoresis, DNA hybridization test and sequence analysis of mitochondrial DNA or ribosomal RNA (DNA) are among the molecular techniques used in evolutionary studies. Of these, enzyme electrophoresis has been most widely used in the field of biochemical systematics [5]. Such molecular studies have made it possible for us to estimate the phylogenetic relationships among taxa and their evolutionary processes quantitatively with common parameters such as enzymes or DNA, and they have been providing much relevant, and in some cases critical, information about phylogenetic relationships in various groups of organisms [10].

One of the present authors (N.M.) has been investigating the phylogeny, taxonomy and evolution within the class Echinoidea (sea-urchins), which is one of the major groups of the phylum Echinodermata, by using the electrophoretic and immunological techniques [13–17, 19, 20]. Another large group of Echinodermata is the class Asteroidea (starfish) and we are also interested in the evolutionary aspect of starfish. The taxonomy and phylogeny of the starfish have been extensively studied by many workers from the morphological and/or paleontological standpoint [1, 2, 4, 9, 28]. However, there are disagreements between asteroid taxonomists, and many unresolved problems concerning the phylogenetic and evolutionary relationships among starfish still remain. For an elucidation of these problems, it would be desirable to actively introduce the molecular approaches which are more analytic and quantitative than the traditional and usual morphological methods into the field of asteroid taxonomy. As already mentioned above, we have been investigating biochemically the phylogenetic relationships among sea-urchins, and found that enzyme electrophoresis is one of the reliable methods in the field of echinoid phylogeny and taxonomy. Therefore, we have an advantage in the biochemical systematic studies of the starfish belonging to echinoderms by enzyme electrophoresis. In the present study, with the background noted above, we have attempted to investigate the phylogeny within the family Asteriidae from the order Forcipulatida by using enzyme electrophoresis.

Five common species were adopted in the present study. They are *Asterias amurensis, Aphelasterias japonica, Distolasterias nipon, Coscinasterias acutispina,* and *Plazaster borealis*. As evident from Figure 1, the former three species have standard five-armed forms, while the latter multi-armed forms. Particularly, *P. borealis* has many arms and shows the clear differentiation between arms and disk. They are common starfish to many zoologists, because *A. amurensis* which is a representative species of the family has been widely used in the embryological, physiological or biochemical study. *C. acutispina* is widely distributed from central Honshu to the Ryukyus, while the other four species are arctic starfish which are commonly found in the seas of northern Japan. Although each of these five species of the family has the characteristic external morphology, it seems to be difficult to establish their phylogenetic relationship and the sequence of the evolutionary divergence by the morphological criteria. Further, there is a little quantitative information available concerning the phylogenetic relationship among these members of the family. In fact, as far as we are aware, there are

Accepted January 3, 1994
Received October 12, 1993
[1] To whom reprint requests should be addressed.

only a few reports: the immunological studies by Kubo [12] and Mochizuki and Hori [22]. Under such situation, further biochemical systematic studies of these species would be desirable and informative.

In this paper, we report on the results of an electrophoretic study designed to clarify the phylogenetic relationship of the five common starfish species of the family Asteriidae from Japanese waters.

MATERIALS AND METHODS

Starfish

The starfish examined in this study were five species from the family Asteriidae of the order Forcipulatida: *Asterias amurensis* Lütken, *Aphelasterias japonica* (Bell), *Distolasterias nipon* (Döderlein), *Coscinasterias acutispina* (Stimpson), and *Plazaster borealis* (Uchida) (Fig. 1). *A. amurensis* and *A. japonica* were collected from the coast near the Asamushi Marine Biological Station, Tohoku University, facing Mutsu Bay, Aomori Pref., by snorkelling. *D. nipon* and *P. borealis* were provided by the Fishermen's Cooperative Association of Yokohama-machi, Kamikita-gun, Aomori Pref. They were collected in the breeding ground of scallops in Mutsu Bay by fishermen. *C. acutispina* was provided by the Misaki Marine Biological Station, University of Tokyo. It was collected from the rocky shore near the Station facing Sagami Bay, Kanagawa Pref. The number of individuals examined was 20 for *A. amurensis*, 39 for *A. japonica*, 20 for *D. nipon*, 21 for *C. acutispina*, and 9 for *P. borealis*. After collection, the pyloric ceaca were cut off from these specimens and stored at −80°C until being analyzed.

Electrophoresis

Electrophoresis was performed on 7.5% polyacrylamide gels by the method of Davis [3] as described previously [14]: About 1 g of pyloric caecum was individually homogenized in 2 vols of 20 mM phosphate buffer, pH 7.0, containing 0.1 M KCl and 1 mM EDTA by using a glass homogenizer of the Potter-Elvehjem type in an ice water bath. After centrifugation at 108,800×*g* for 20 min at 4°C, 0.05–0.10 ml of clear supernatant was used for electrophoretic analyses of enzymes. Electrode buffer was 0.38 M glycine-tris buffer, pH 8.3. After electrophoresis, the gels were stained for the following 15 different enzymes: hexose-6-phosphate dehydrogenase (H6PD), malate dehydrogenase (MDH), malic enzyme (ME), nothing dehydrogenase (NDH), octanol dehydrogenase (ODH), sorbitol dehydrogenase (SDH), xanthine dehydrogenase (XDH), glucose-6-phosphate isomerase (GPI), hexokinase (HK), superoxide dismutase (SOD), aspartate aminotransferase (AAT), alkaline phosphatase (ALK), peroxidase (PO), esterase (EST), and leucine amino peptidase (LAP). Stain recipes for these enzymes have been described previously [21].

RESULTS

From the allozyme variation observed in 15 different enzymes, 31 genetic loci were inferred. Figure 2 shows diagramatically allozyme patterns of four enzymes presenting the typical electrophoretic band patterns, which were chosen from among 15 enzymes analyzed in this study. The major features of variation in these enzymes are summarized as follows: ME exhibited a single band of the same mobility

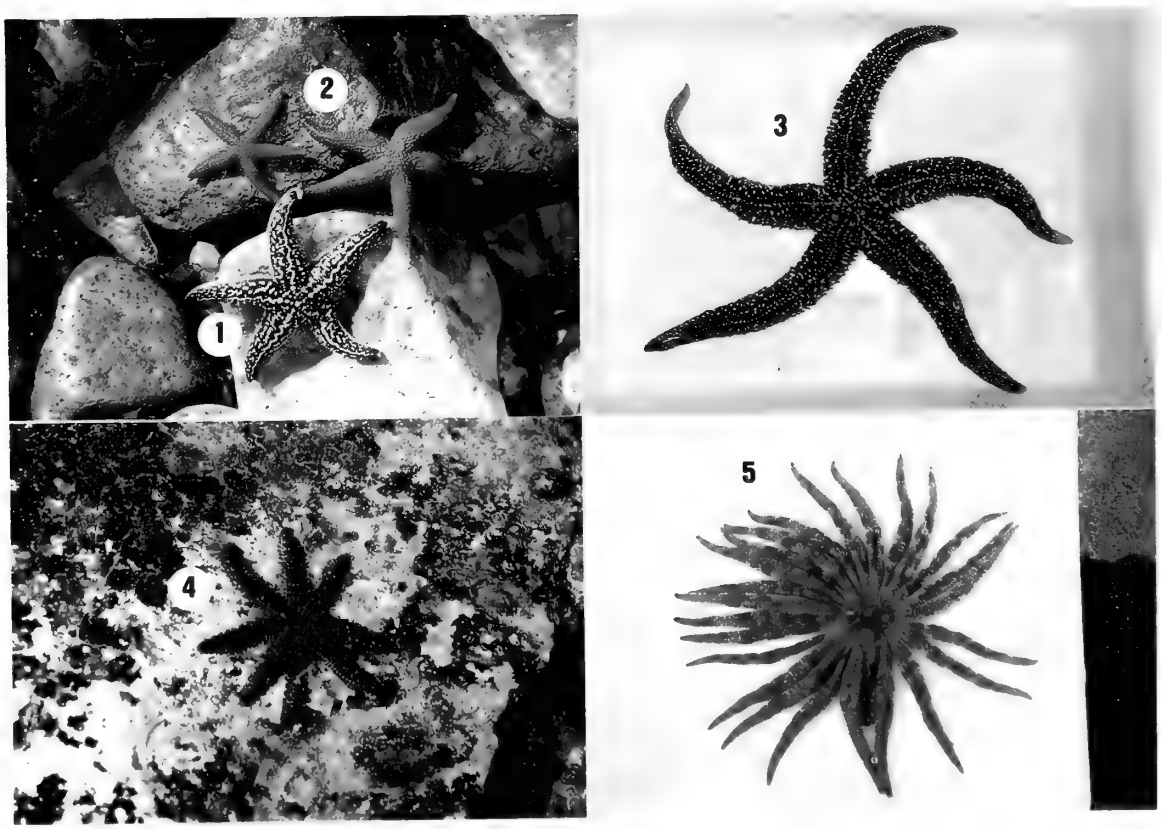

FIG. 1. Five starfish species of the family Asteriidae from Japanese waters. 1=*Asterias amurensis*, 2=*Aphelasterias japonica*, 3=*Distolasterias nipon*, 4=*Coscinasterias acutispina*, 5=*Plazaster borealis*.

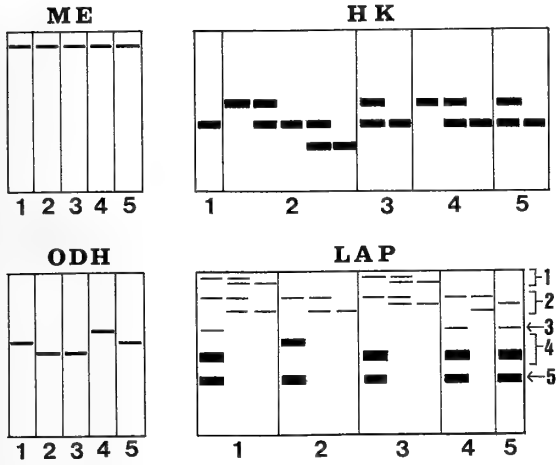

FIG. 2. Electrophoretic band patterns of four typical enzymes in five starfish species of the family Asteriidae. For each enzyme the origin is at the top and the direction of mobility toward the bottom. The number of 1–5 described in the right side of the zymogram of LAP shows the genetic loci of LAP-1 to LAP-5. Genetic loci are numbered downwards from 1, starting with that nearest the origin (i. e., of lowest electrophoretic mobility). The number of 1–5 described in the bottom of each enzyme shows the five starfish species: 1=*Asterias amurensis*, 2=*Aphelasterias japonica*, 3=*Coscinasterias acutispina*, 4=*Distolasterias nipon*, 5=*Plazaster borealis*.

between five species and was monomorphic as well as NDH. ODH also showed a single active band, but varied interspecifically. The similar band pattern was also observed in H6PD and GPI. HK showed extensive polymorphism and exhibited single- and double-banded phenotypes. This variation was interpreted as a diallelic system at a single locus coding for a monomeric protein, with single-banded pattern corresponding to the homozygous state, and double-banded pattern to the heterozygous state. The similar variation was also observed in the following 12 loci: XDH, AAT, MDH-1, PO-2, SOD-3, SOD-4, ALK-1, ALK-4, EST-1, EST-4, LAP-1, and LAP-2. LAP of digestive enzyme was detected as several bands which were grouped into five zones (LAP-1 to LAP-5). LAP-1 and LAP-2 showed single- and double-banded phenotypes as well as HK. The single band of LAP-3 was not scored in two species. Each of LAP-4 and LAP-5 exhibited a single monomorphic band of high enzymatic activity. The multi-banded patterns such as LAP were also observed in EST, ALK and SOD. The LAP activity of the starfish was much stronger than that of various sea-urchin species reported previously at the electrophoretic level [20]. On the other hand, the AMY activity which was scored easily in sea-urchins could not be detected in these starfish species.

The allele frequencies for all loci in the five species are given in Table 1. With respect to the degree of enzyme variation within populations, Table 1 shows that enzymes involved in glucose metabolism (catalysing steps in, or adjacent to, the glycolytic pathway and tricarboxylic acid cycle) were on average less variable than those (e. g., EST or SOD) involved in other reactions, which contain many that are relatively nonspecific with respect to substrate. Table 2 summarizes the extent of genetic variation in five species. The number of alleles per locus was in the range of 1.15–1.38, with a mean of 1.22, the proportion of polymorphic loci (P), in the range of 14.3–38.5%, with a mean of 21.4%, and the expected average heterozygosity per locus (H), in the range of 5.9–16.7%, with a mean of 9.0%. As evident from this table, *D. nipon* showed considerably higher genetic variability than the other four species.

In order to quantify the degree of genetic differentiation among five species, the genetic identity (I) and genetic distance (D) between each species were calculated by the method of Nei [23] from the allele frequencies data in Table 1. Table 3 shows the matrices of I and D values between all pairs of species examined. The highest I value (0.598) was found between *A. amurensis* and *P. borealis*. Figure 3 shows the molecular phylogenetic tree for the five species which was constructed from the Nei's genetic distance matrix of Table 3 by using the unweighted pair-group arithmetic average (UPGMA) clustering method of Sneath and Sokal [27]. The molecular phylogenetic tree indicated the following:

(1) The five species are phylogenetically divided into three large clusters: (i) *A. amurensis* and *P. borealis*; (ii) *A. japonica* and *D. nipon*; and (iii) *C. acutispina*.

(2) Of the five species, *A. amurensis* and *P. borealis* are the most closely related to each other.

(3) *A. japonica* is more closely related to *D. nipon* than to the other three species.

(4) *C. acutispina* is the most distinct species of the five members.

The divergence time (T) of the five species estimated from the genetic distance by the Nei's equation [24] is also given in the phylogenetic tree. The molecular phylogenetic tree with the divergence time provides valuable information with respect to the evolutionary divergence of the five species of the family Asteriidae.

DISCUSSION

Enzyme variation within populations

With respect to the relationship between enzyme function and heterozygosity, Yamazaki [30] showed, using data from various *Drosophila* species, that the substrate-specific enzymes have lower heterozygosity than the nonspecific enzymes. A similar analysis was carried out by Gojobori [7] using data on 20 different proteins (mostly enzymes) from 14 *Drosophila* species, 14 *Anolis* species and 31 other species. As a result, he found that enzymes with various functional constraints tend to have low heterozygosity. These findings are well consistent with our serial electrophoretic studies of echinoderm enzymes. In this study, the glucose metabolizing enzymes (the mean H=6.0%) with functional constraints were less variable than the non-glucose metabolizing enzymes (the mean H=9.9%), and also nonspecific enzymes such as SOD or EST were more highly polymorphic. The similar results have also been obtained in many other echinoderm

TABLE 1. Allele frequencies at various enzyme loci in the five species of the family Asteriidae

Locus	*Aa*	*Aj*	*Ca*	*Dn*	*Pb*
H6PD	b	b	a	b	b
MDH-1	b	b	—	a (0.45)	—
				b (0.55)	
MDH-2	a	c	b	—	a
ME	a	a	a	a	a
NDH	a	a	a	a	a
ODH	b	c	c	a	b
SDH	b	b	b	b	a
XDH	a (0.53)	b	b	c	b
	b (0.47)				
HK	b	a (0.07)	a (0.04)	a (0.47)	a (0.20)
		b (0.76)	b (0.96)	b (0.53)	b (0.80)
		c (0.17)			
PGI	b	b	a	c	—
AAT	b	b	b	a (0.39)	a
				b (0.61)	
SOD-1	a	c	b	—	a
SOD-2	—	a	b	b	a
SOD-3	b	a	—	a (0.73)	—
				c (0.27)	
SOD-4	a	a	c	a (0.75)	a
				b (0.25)	
PO-1	b	a	c	—	b
PO-2	b	a	c	c (0.75)	b
				d (0.25)	
ALK-1	b	c	a (0.50)	c	a (0.25)
			c (0.50)		c (0.75)
ALK-2	a	b	a	b	a
ALK-3	a	—	a	—	a
ALK-4	b	b	b	a (0.35)	b
				b (0.65)	
ALK-5	—	a	b	c	a
EST-1	b (0.70)	a (0.40)	a (0.78)	a (0.42)	b (0.44)
	c (0.30)	b (0.60)	b (0.22)	b (0.58)	c (0.56)
EST-2	b	a	a	b	—
EST-3	a	a	a	a	b
EST-4	a (0.81)	a (0.71)	b (0.38)	a (0.53)	a (0.78)
	c (0.19)	c (0.29)	c (0.62)	b (0.47)	c (0.22)
LAP-1	a (0.37)	—	a (0.40)	—	—
	b (0.63)		b (0.60)		
LAP-2	a (0.50)	a (0.47)	a (0.50)	a (0.83)	b
	c (0.50)	c (0.53)	b (0.50)	c (0.17)	
LAP-3	a	—	—	a	a
LAP-4	b	a	b	b	b
LAP-5	a	a	a	a	a

Alleles are correspondingly lettered from "a". The value in parenthesis represents the frequency of each allele in population.

Aa=*Asterias amurensis*, *Aj*=*Aphelasterias japonica*, *Ca*=*Coscinasterias acutispina*, *Dn*=*Distolasterias nipon*, *Pb*=*Plazaster borealis*.

TABLE 2. Genetic variation in the five species of the family Asteriidae

Parameter	*Aa*	*Aj*	*Ca*	*Dn*	*Pb*
No. of alleles per locus	1.17	1.18	1.21	1.38	1.15
Proportion of polymorphic loci:P(%)	17.2	14.3	21.4	38.5	15.4
Expected average heterozygosity per locus:H(%)	7.6	6.4	8.5	16.7	5.9

Aa=Asterias amurensis, Aj=Aphelasterias japonica, Ca=Coscinasterias acutispina, Dn=Distolasterias nipon, Pb=Plazaster borealis.

TABLE 3. Genetic identities (above diagonal) and genetic distances (below diagonal) between five species of the family Asteriidae

Species	1	2	3	4	5
1. *Asterias amurensis*	—	0.475	0.434	0.484	0.598
2. *Aphelasterias japonica*	0.744	—	0.433	0.506	0.397
3. *Coscinasterias acutispina*	0.835	0.837	—	0.401	0.370
4. *Distolasterias nipon*	0.726	0.681	0.914	—	0.360
5. *Plazaster borealis*	0.514	0.924	0.994	1.022	—

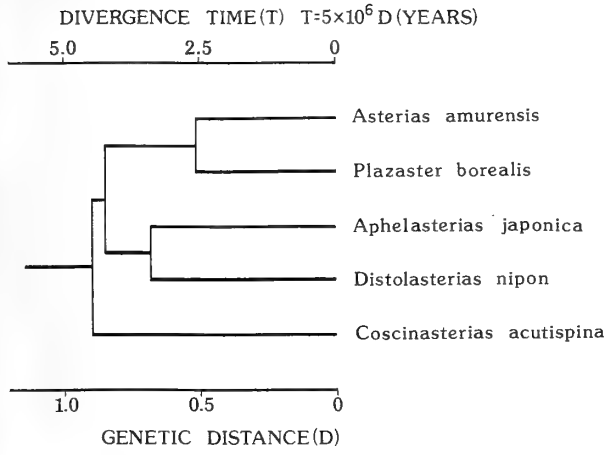

FIG. 3. A molecular phylogenetic tree for the five starfish species of the family Asteriidae. It was constructed from Nei's genetic distances by using the UPGMA clustering method of Sneath and Sokal [27]. The divergence time estimated from the Nei's equation [24] using the genetic distance is given in the phylogenetic tree.

species [14, 15, 19–21]. These results can be explained by the neutral mutation theory of Kimura [11]: The more strictly functional constraint would decrease the neutral regions of the molecules and the probability of a mutation change not being harmful (i.e.,selective neutral) is smaller for the substrate-specific enzymes than for nonspecific enzymes.

I have previously reported on the amount of genetic variation within populations of various echinoderm species [18]. It is interesting to compare the extent of genetic variation (the average heterozygosity per locus: the H value) in the five starfish species studied here with H values observed in other echinoderm populations. *A. amurensis, A. japonica, C. acutispina* and *P. borealis* showed low genetic variabilities (H=7.6, 6.4, 8.5, 5.9%) and these H values were comparable to those (H=0–8.7%) of many other shallow water echinoderms reported previously [18]. On the other hand, *D. nipon* showed much higher genetic variability (H=16.7%) than other shallow water echinoderms and the value was comparable to the H values of deep-sea echinoderms. Nei [25] and Nei and Graur [26] examined the relationship between average heterozygosity and population size for 77 different species. As a result, they found a significant correlation between them. From this evidence, it may be considered that the difference in the extent of genetic variation among five species is related to their population sizes. Namely, it may be expected that *D. nipon* showing the higher genetic variability has larger population size than the other four species. Further extensive population surveys in various marine invertebrates would be required for establishing the validity of this prediction.

Phylogenetic relationship of five species of the family Asteriidae

The molecular phylogenetic tree shown in Figure 3 clearly indicated that the five species of the family Asteriidae are phylogenetically divided into three large clusters: (i) *A. amurensis* and *P. borealis*; (ii) *A. japonica* and *D. nipon*; and (iii) *C. acutispina*. Fisher [6] suggested from the morphological standpoint that the family Asteriidae may be a large and polyphyletic aggregation of genera, and he proposed the subfamily system within the family Asteriidae. The heterogeneity of the family suggested by Fisher seems not contradictory to the present results, excluding the problems what species belongs to each subfamily.

The electrophoretic results showed that *A. amurensis* and *P. borealis* are the most closely related to each other among five species. The genetic distance (D=0.514) be-

tween them was comparable to the D values reported between congeneric species in other animals [29]. The close affinity between them was also suggested by the immunological study of Mochizuki and Hori [22]. They examined the phylogenetic relationships among various starfish species by using the enzyme inhibition method with the specific antibody against purified hexokinase (HK) from the pyloric ceaca of *A. amurensis*. The immunological data indicated that *P. borealis* has the highest immunological similarity to *A. amurensis* among seven species of the family Asteriidae examined. In addition, Fisher [6] stated from the morpholog-ical standpoint that *A. amurensis* and *A. japonica* may be closely related to *P. borealis*. His view is partially consistent with these biochemical results, excepting the phylogenetic position of *A. japonica*.

The allozymic study also showed the close affinity between *A. japonica* and *D. nipon*. The genetic distance (D= 0.681) between them was comparable to the D values observed between congeneric species or closely related confamilial genera in other animals [29]. Interestingly, there are two conflicting views on the systematic position of *A. japonica* from the morphological standpoint: Fisher [6] and Hayashi [8] proposed the close affinity between *A. japonica* and *A. amurensis*, and included these two species into the subfamily Asteriinae. On the other hand, Shigei and Saba (personal communication) suggested that *A. japonica* may be rather closely related to *D. nipon*. The present results are in favor of the view of Shigei and Saba. In contrast, the view of Fisher [6] and Hayashi [8] is inconsistent with not only the present electrophoretic study but also the immunological studies by other workers: Mochizuki and Hori [22] showed by the enzyme inhibition method that *A. japonica* is distantly related to *A. amurensis*. Prior to their study, Kubo [12] examined the phylogenetic relationships among various starfish species by the following immunological method: He prepared rabbit antisera against extracts of tube feet of ambulacral zones taken from several starfish species and measured the cross-reactivity of the antisera to antigens from various species by the quantitative precipitin technique. As a result, he obtained the similar results to those of Mochizuki and Hori [22]. However, there are some differences between the present electrophoretic data and Kubo's immunological results. Namely, Kubo [12] showed that *A. amurensis* was more distantly related to *A. japonica* than to *D. nipon* and *C. acutispina*. On the other hand, the present electrophoretic results (Fig. 3) indicated that *A. amurensis* and *P. borealis* are more closely related to the cluster of *A. japonica* and *D. nipon* than to *C. acutispina*. In spite of such differences, these biochemical studies did not support the close affinity between *A. japonica* and *A. amurensis* which was suggested by the morphological studies [6,8].

The molecular phylogenetic tree (Fig. 3) also indicated that *C. acutispina* is the most distant species of the five members. The result seems to be consistent with the zoogeographical evidence: Of the five species, *C. acutispina* is not commonly found in the cold seas of northern Japan and distributes widely in the more southern regions from central Honsyu to the Ryukyu Islands. On the other hand, the main distributional region of the other four species is the cold seas of northern Japan. From the morphological studies, Fisher [6] and Hayashi [8] proposed the close affinity between *C. acutispina* and *D. nipon*, and included these two species into the subfamily Coscinasterinae. However, their taxonomic system is inconsistent with the present electrophoretic results.

The molecular phylogenetic tree (Fig. 3) shows not only their genetic relationships, but also the sequence of their evolutionary divergence. According to Nei [24], genetic distance (D) corresponds well with the divergence time (T) from the common ancestor, and T of two taxa can be estimated by $T=5\times10^6$ D (years). Application to this equation to the molecular dendrogram constructed from the genetic distances leads to the following speculation of evolutionary process of the five species: Firstly, the common ancestor of the five species diverged into two lineages (one is *Coscinasterias* lineage and the other the common ancestor of the other four genera) 4.5 million years (MY) ago. Then, the latter ancestor diverged into two lineages (one is the *Asterias-Plazaster* lineage and the other the *Aphelasterias-Distolasterias* lineage) after a short time (4.3 MY ago). Finally, these four genera differentiated from one another 2.6–3.4 MY ago. The phylogenetic tree suggests that *Asterias* and *Plazaster* are more recent genera which evolved later.

The biochemical systematic studies of sea-urchins reported previously suggested that the more recent species which evolved later tend to become predominant species [14–17, 20]. Among the five species of the family Asteriidae, *A. amurensis* which evolved later seems to be more predominant species than others. The species is more frequently found in Japanese waters than the other four species and shows the extensive morphological variations between local Japanese populations in some morphological characters such as body color, body size, spine and so on. This may suggest the speciation within *A. amurensis*. At present, we have been investigating the genetic differentiation between local populations of *A. amurensis* by using enzyme electrophoresis and attempting the molecular approach concerning the speciation and evolution of the species.

As evident from Figure 1, *P. borealis* is considerably specialized at the morphological level, and shows the clear differentiation between disk and arm, in contrast with the other four species with standard morphology. The molecular phylogenetic tree (Fig. 3) implies that *P. borealis* of such specialized morphology might have differentiated from the *Asterias*-like starfish with standard morphology, since the cluster consisted of *P. borealis* and *A. amurensis* is also closely related to the cluster of *A. japonica* and *D. nipon* with standard morphology. If it is true, the evolutionary rate at the morphological level in the *Plazaster* lineage might have been much accelerated. In future, further detailed investigation on the close genetic relationship between *P. borealis* and *A. amurensis* which highly differentiated with each other at the morphological level would produce some useful and

valuable information on the morphological evolution in starfish.

ACKNOWLEDGMENTS

We are grateful to the Fishermen's Cooperative Association of Yokohama-machi, Aomori Prefecture, the Misaki Marine Biological Station, University of Tokyo, and the Asamushi Marine Biological Station, Tohoku University, for their kind help in collecting the starfish specimens. We also thank Dr. M. Shigei, Kyoto Institute of Technology, and Dr. M. Saba, Mie Prefectural Ise High School, for their valuable advice. This study was supported by a Grant-in-Aid (Grant No. 05640779) for scientific research from the Ministry of Education, Science and Culture of Japan to Norimasa Matsuoka.

REFERENCES

1 Blake DB (1987) A classification and phylogeny of post-Palaeozoic sea stars (Asteroidea: Echinodermata). J Nat Hist 21: 481–528

2 Clark AC, Downey ME (1992) Starfishes of the Atlantic. Chapman and Hall, London

3 Davis BJ (1964) Disc electrophoresis—II. Method and application to human serum proteins. Ann NY Acad Sci 121: 404–427

4 Downey ME (1973) Starfishes from the Caribbean and the Gulf of Mexico. Smithsonian Contr Zool 126: 1–158

5 Ferguson A (1980) Biochemical Systematics and Evolution. Blackie, Glasgow

6 Fisher WK (1928) Asteroidea of the North Pacific and adjacent waters. Part 2. Forcipulata (part). US Nat Mus Bull 76

7 Gojobori T (1982) Means and variances of heterozygosity and protein function. In "Molecular Evolution, Protein Polymorphism and the Neutral Theory" Ed by M Kimura, Japan Scientific Societies Press Berlin, Springer-Verlag pp 137–148

8 Hayashi R (1943) Contributions to the classification of the sea-stars of Japan. II. Forcipulata, with the note on the relationships between the skeletal structure and respiratory organs of the sea-stars. J Fac Sci Hokkaido Univ Ser VI 8: 133–281

9 Hayashi R (1974) Asteroids. In "Systematic Zoology" Vol. 8b Ed by T Uchida, Nakayama, Tokyo (In Japanese) pp 82–141

10 Hills DM, Moritz C (1990) Molecular Systematics. Sinauer, MA

11 Kimura M (1983) The Neutral Theory of Molecular Evolution. Cambridge University Press, Cambridge

12 Kubo K (1961) Studies on the systematic serology of sea-stars. V. Jpn J Zool 13: 15–37

13 Matsuoka N (1980) Immunological relatedness of sea-urchin glucose-6-phosphate dehydrogenases: Phylogenetic implication. Comp Biochem Physiol 66B: 605–607

14 Matsuoka N (1985) Biochemical phylogeny of the sea-urchins of the family Toxopneustidae. Comp Biochem Physiol 80B: 767–771

15 Matsuoka N (1987) Biochemical study on the taxonomic situation of the sea-urchin, *Pseudocentrotus depressus*. Zool Sci 4: 339–347

16 Matsuoka N (1989) Biochemical systematics of four sea-urchin species of the family Diadematidae from Japanese waters. Biochem Syst Ecol 17: 423–429

17 Matsuoka N (1990) Evolutionary relationships of sea-urchins at the molecular level. Comp Biochem Physiol 97B: 31–36

18 Matsuoka N (1991) Maintenance mechanism of enzyme polymorphism in echinoderms. Sci Rep Hirosaki Univ 38: 38–45

19 Matsuoka N, Hatanaka T (1991) Molecular evidence for the existence of four sibling species within the sea-urchin, *Echinometra mathaei* in Japanese waters and their evolutionary relationships. Zool Sci 8: 121–133

20 Matsuoka N, Suzuki H (1989) Electrophoretic study on the phylogenetic relationships among six species of sea-urchins of the family Echinometridae found in the Japanese waters. Zool Sci 6: 589–598

21 Matsuoka N, Yoshida K, Fukuda K, Shigei M (1991) Genetic variation in the starfish *Coscinasterias acutispina*. Comp Biochem Physiol 99B: 893–898

22 Mochizuki Y, Hori SH (1980) Immunological relationships of starfish hexokinases: Phylogenetic implication. Comp Biochem Physiol 65B: 119–125

23 Nei M (1972) Genetic distance between populations. Am Nat 106: 283–292

24 Nei M (1975) Molecular Population Genetics and Evolution. North-Holland, Amsterdam

25 Nei M (1983) Genetic polymorphism and the role of mutation in evolution. In "Evolution of Genes and Protein" Ed by M Nei, R Koehn, Sinauer,MA pp 165–190

26 Nei M, Graur D (1984) Extent of protein polymorphism and the neutral mutation theory. Evol Biol 17: 73–118

27 Sneath PHA, Sokal PR (1973) Numerical Taxonomy. Freeman, San Francisco, CA

28 Spencer WK, Wright CW (1966) Asterozoans. In "Treatise on Invertebrate Paleontology" Part U Ed by RC Moore, Geol Soc Am Univ Kansas Press, pp 4–107

29 Thorpe JP (1982) The molecular clock hypothesis: Biochemical evolution, genetic differentiation, and systematics. Ann Rev Ecol Syst 13: 139–168

30 Yamazaki T (1977) Enzyme polymorphism and functional difference: mean, variance, and distribution of heterozygosity. In "Molecular Evolution and Polymorphism" Ed by M Kimura, Mishima: National Institute of Genetics pp 127–147

Development
Growth & Differentiation

Published Bimonthly by the Japanese Society of Developmental Biologists
Distributed by Business Center for Academic Societies Japan, Academic Press, Inc.

Papers in Vol. 36, No. 2. (April 1994)

13. **REVIEW**: S. V. Cooke and B. D. Shur: Cell Surface β1,4-Galactosyltransferase: Expression and Function
14. C. C. Lambert, G. P. Gonzales and K. M. Miller: Independent Initiation of Calcium Dependent Glycosidase Release and Cortical Contractions during the Activation of Ascidian Eggs
15. Y. Hagiwara and E. Ozawa: A New Method for Fibroblast-less Primary Skeletal Muscle Cell Culture by the Use of Hydroxyurea
16. K. Yamazaki, R. Suzuki, E. Hojo, S. Kondo, Y. Kato, K. Kamioka, M. Hoshi and H. Sawada: Trypsin-like Hatching Enzyme of Mouse Blastocysts: Evidence for Its Participation in Hatching Process before Zona Shedding of Embryos
17. A. Iio, M. Mochii, K. Agata, R. Kodama and G. Eguchi: Expression of the Retinal Pigmented Epithelial Cell-Specific pP344 Gene during Development of the Chicken Eye and Identification of Its Product
18. S. Kuno, T. Nagura and I. Yasumasu: Insulin-Induced Outgrowth of Pseudopodial Cables from Cultured Micromere-Derived Cells Isolated from Sea Urchin Embryos at the 16 Cell Stage, with Special Reference to the Insulin-Receptor
19. T. Iwamatsu: Medaka Oocytes Rotate within the Ovarian Follicles during Oogenesis
20. L-N. Wei and Y-C. Hsu: Identification of a New Gene Expressed Specifically in Early Mouse Embryos
21. A. M. Fausto, M. Carcupino, M. Mazzini and F. Giorgi: An Ultrastructural Investigation on Vitellophage Invasion of the Yolk Mass during and after Germ Band Formation in Embryos of the Stick Insect *Carausius morosus Br.*
22. T. Shimizu, K. Yoshino and N. Suzuki: Identification and Characterization of Putative Receptors for Sperm-Activating Peptide I (SAP-I) in Spermatozoa of the Sea Urchin *Hemicentrotus pulcherrimus*
23. M. Kosaka, M. Takeda, K. Matsumoto and Y. Nishimune: F9 Cells Can be Differentiated toward Two Distinct, Mutually Exclusive Pathways by Retinoic Acid and Sodium Butyrate
24. T. Kaname, S. Matsubara, F. Murata, K. Yamamura, K. Miyata, and T. Muramatsu: The Upstream Sequence of a New Growth/Differentiation Factor, Midkine (MK), Mediates Developmentally Regulated *lac Z* Gene Expression in Transgenic Mice

Development, Growth and Differentiation (ISSN 0012–1592) is published bimonthly by The Japanese Society of Developmental Biologists. Annual subscription for Vol. 35 1993 U. S. $ 191,00, U. S. and Canada; U. S. $ 211,00, all other countries except Japan. All prices include postage, handling and air speed delivery except Japan. Second class postage paid at Jamaica, N.Y. 11431, U. S. A.

Outside Japan: Send subscription orders and notices of change of address to Academic Press, Inc., Journal Subscription Fulfillment Department, 6277, Sea Harbor Drive, Orlando, FL 32887–4900, U. S. A. Send notices of change of address at least 6–8 weeks in advance. Please include both old and new addresses. U. S. A. POSTMASTER: Send changes of address to *Development, Growth and Differentiation,* Academic Press. Inc., Journal Subscription Fulfillment Department, 6277, Sea Harbor Drive, Orlando, FL 32887–4900, U. S. A.

In Japan: Send nonmember subscription orders and notices of change of address to Business Center for Academic Societies Japan, 16–9, Honkomagome 5-chome, Bunkyo-ku, Tokyo 113, Japan. Send inquiries about membership to Business Center for Academic Societies Japan, 16–9, Honkomagome 5-chome, Bunkyo-ku, Tokyo 113, Japan.

Air freight and mailing in the U. S. A. by Publications Expediting, Inc., 200 Meacham Avenue, Elmont, NY 11003, U. S. A.

BRANCHES NOW OPEN IN USA AND EUROPE

Narishige.
The complete range for micromanipulation

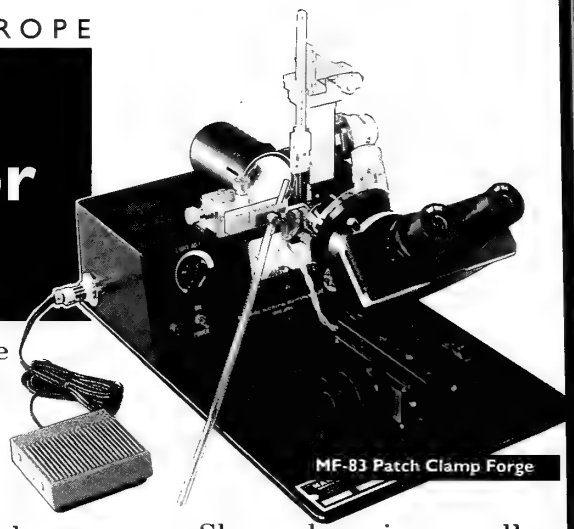
MF-83 Patch Clamp Forge

For over 30 years Narishige have been developing their extensive range of precision instruments for Physiology, Pharmacology, Zoology and Psychology research.

This large range includes micromanipulators, microelectrode pullers and microforges, microinjectors, microgrinders and stereotaxic instruments.

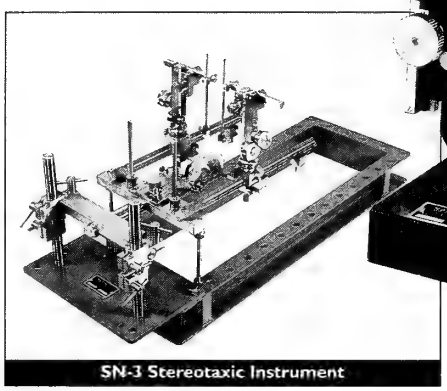
SN-3 Stereotaxic Instrument


MM-31 Miniature Micromanipulator

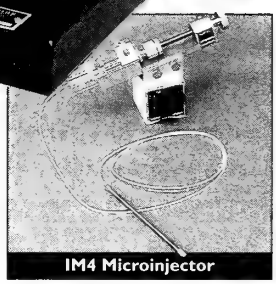
IM4 Microinjector


US-1 Miniature Stand

Shown here is a small selection of instruments from the extensive Narishige range.


Remote Control Hydraulic Micromanipulator

Narishige are pleased to announce that repair facilities have been opened in Europe and the USA.

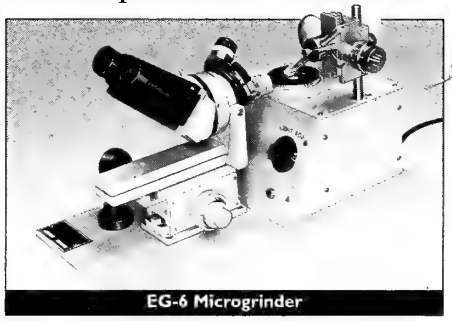
EG-6 Microgrinder

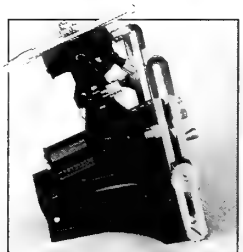
MP-1 Micromanipulator

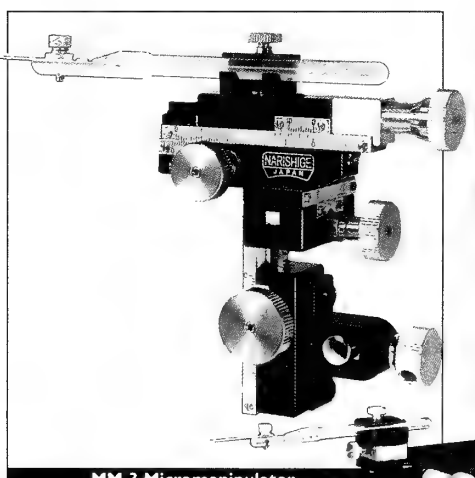
MM-3 Micromanipulator

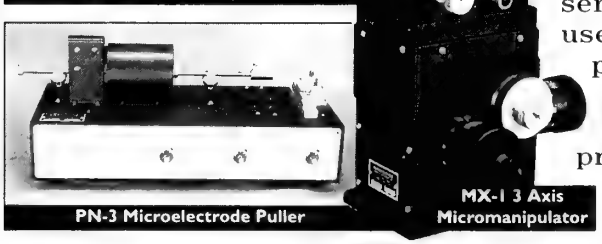
PN-3 Microelectrode Puller

MX-1 3 Axis Micromanipulator

This enables us to provide an improved service to the many users of our quality products throughout the world, including the upgrading of previous types of water filled hydraulic micromanipulators.

PE-2 Microelectrode Puller

Please contact us for more information.

REPAIRS, AFTER SALES SERVICE AND TECHNICAL SUPPORT

JAPAN **Narishige Scientific Instrument Laboratory**
9-28 Kasuya 4-Chrome, Setagaya-Ku, Tokyo 157, Japan. Tel: +81 (0) 3 3308 8233 Fax: +81 (0) 3 3308 2005

EUROPE **Narishige International London Branch**
Unit 7 Willow Business Park, Willow Way, London SE26 4QP U.K. Tel: +44 (0) 81 699 9696 Fax: +44 (0) 81 291 9678

U.S.A. **U.S. Narishige International Inc**
404 Glen Cove Avenue, Sea Cliff, New York 11579 U.S.A. Tel: +1 (516) 759 6167 Fax: +1 (516) 759 6138

NARISHIGE JAPAN

ZOOLOGICAL SCIENCE

VOLUME 11 NUMBER 2 APRIL 1994

CONTENTS

REVIEWS

Ward, A., P. Bierke, E. Pettersson and W. Engström: Insulin-like growth factors: Growth, transgenes and imprinting 167

Mizunami, M: Processing of contrast signals in the insect ocellar system 175

ORIGINAL PAPERS

Physiology

Aonuma, H., T. Nagayama, M. Hisada: Output effect of identified interneurons upon the abdominal postural system in the crayfish *Procambarus clarkii* (Gerard) 191

Immunology

Hirose, E., T. Ishii, Y. Saito, Y. Taneda: Phagocytic activity of tunic cells in the colonial ascidian *Aplidium yamazii* (Polyclinidae, Aplousobranchia) 303

Biochemistry

Harumi, T., K. Hoshino, N. Suzuki: *In vitro* autophosphorylation and cyclic nucleotide-dependent dephosphorylation of sea urchin sperm histone kinase 209

Mukai, M., T. Kondo, K. Yoshizato: Rapid and quantitative detection of aspartic proteinase in animal tissues by radio-labeled pepstatin A 221

Furukohri, T., S. Okamoto, T. Suzuki: Evolution of phosphagen kinase (III). Amino acid sequence of arginine kinase from the shrimp *Penaeus japonicus* 229

Developmental Biology

Furuya, H., K. Tsuneki, Y. Koshida: The development of the vermiform embryos of two mesozoans, *Dicyema acuticephalum* and *Dicyema japonicum* 235

Kimura, K., K. Usui, T. Tanimura: Female myoblasts can participate in the formation of a male-specific muscle in *Drosophila* 247

Yazaki, I., H. Harashima: Induction of metamorphosis in the sea urchin, *Pseudocentrotus depressus*, using L-glutamine 253

Ohya, Y., K. Watanabe: Control of growth and differentiation of chondrogenic fibroblasts in soft-agar culture: Role of basic fibroblast growth factor and transforming growth factor-β 261

Reproductive Biology

Okia, N. O.: Membrane-bound inclusions in the Leydig cell cytoplasm of the broad-headed skink, *Eumeces laticeps* (Lacertilia: Scincidae) 269

Yoshizaki, N.: Identification and localization of a ligand molecule of *Xenopus* cortical granule lectins 275

Nakamura, M., T. Yamanobe, M. Takase: Localization and purification of serum albumin in the testis of *Xenopus laevis* 285

Endocrinology

Ohta, N., T. Mori, S. Kawashima, S. Sakamoto, H. Kobayashi: Spatiotemporal pattern of DNA synthesis detected by bromodeoxyuridine labeling in the mouse endometrial stroma during decidualization 291

Tsai, P. I., S. S. Madsen, S. D. McCormick, H. A. Bern: Endocrine control of cartilage growth in coho salmon: GH influence *in vivo* on the response to IGF-I *in vitro* 299

Environmental Biology

Takaku, G., H. Katakura, N. Yoshida: Mesostigmatic mites (Acari) associated with ground, burying, roving carrion and dung beetles (Coleoptera) in Sapporo and Tomakomai, Hokkaido, northern Japan 305

Systematics and Taxonomy

Amemiya, S., Y. Mizuno, S. Ohta: First fossil record of the family Phormosomatidae (Echinothurioida: Echinoidea) from the Early Miocene Morozaki Group, central Japan 313

Grismer, L. L., H. Ota, S. Tanaka: Phylogeny, classification, and biogeography of *Goniurosaurus kuroiwae* (Squamata: Eublepharidae) from the Ryukyu Archipelago, Japan, with description of a new subspecies 319

Ohtani, H.: Polymorphism of lampbrush chromosomes in Japanese populations of *Rana nigromaculata* 337

Matsuoka, N., K. Fukuda, K. Yoshida, M. Sugawara, M. Inamori: Biochemical systematics of five asteroids of the family Asteriidae based on allozyme variation 343

INDEXED IN:
Current Contents/LS and AB & ES,
Science Citation Index,
ISI Online Database,
CABS Database, INFOBIB

Issued on April 15
Front cover designed by Saori Yasutomi
Printed by Daigaku Letterpress Co., Ltd., Hiroshima, Japan

ISSN 0289-0003

An International Journal

ZOOLOGICAL SCIENCE

Vol. 11 No.3

June 1994

PHYSIOLOGY
CELL and MOLECULAR BIOLOGY
GENETICS
IMMUNOLOGY
BIOCHEMISTRY
DEVELOPMENTAL BIOLOGY
REPRODUCTIVE BIOLOGY
ENDOCRINOLOGY
BEHAVIOR BIOLOGY
ENVIRONMENTAL BIOLOGY and ECOLOGY
SYSTEMATICS and TAXONOMY

published by Zoological Society of Japan
distributed by Business Center for Academic Societies Japan
VSP, Zeist, The Netherlands

ZOOLOGICAL SCIENCE

The Official Journal of the Zoological Society of Japan

The Zoological Society of Japan:
Toshin-building, Hongo 2–27–2, Bunkyo-ku,
Tokyo 113, Japan. Phone 03-3814–5461
Fax 03-3814-5352

ZOOLOGICAL SCIENCE is devoted to publication of original articles, reviews and rapid communications in the broad field of Zoology. The journal was founded in 1984 as a result of unification of Zoological Magazine (1888–1983) and Annotationes Zoologicae Jasponenses (1897–1983), the former official journals of the Zoological Soceity of Japan. An annual volume consists of six regular numbers and one supplement (abstracts of papers presented at the annual meeting of the Zoological Society of Japan) of more than 850 pages. The regular numbers appear bimonthly.

MANUSCRIPTS OFFERED FOR CONSIDERATION AND CORRESPONDENCE CONCERNING EDITORIAL MATTERS should be sent to:

Dr. Tsuneo Yamaguchi, Editor-in-Chief, Zoological Science, Department of Biology, Faculty of Science, Okayama University, Okayama 700, Japan, in accordance with the instructions to authors which appear in the first issue of each volume. Copies of instructions to authors will be sent upon request.

SUBSCRIPTIONS. ZOOLOGICAL SCIENCE is distributed free of charge to the members, both domestic and foreign, of the Zoological Society of Japan.To non-member subscribers within Japan, it is distributed by Business Center for Academic Societies Japan, 5–16–9 Honkomagome, Bunkyo-ku, Tokyo 113. Subscriptions outside Japan should be ordered from the sole agent, VSP, Godfried van Seystlaan 47, 3703 BR Zeist (postal address: P. O. Box 346, 3700 AH Zeist), The Netherlands. Subscription rates will be provided on request to these agents. New subscriptions and renewals begin with the first issue of the current volume.

[Publication of Zoological Science has been supported in part by a Grant-in-Aid for Publication of Scientific Research Results from the Ministry of Education, Science and Culture, Japan.]

ZOOLOGICAL SCIENCE 11: 351–361 (1994)

REVIEW

Regulation of Gonadotropin Receptors and Its Physiological Significance in Higher Vertebrates

KAZUYOSHI TSUTSUI[1] and SEIICHIRO KAWASHIMA[2]

[1]*Faculty of Integrated Arts and Science, Hiroshima University, Higashi-Hiroshima 724 and* [2]*Zoological Institute, School of Science, University of Tokyo, Tokyo 113, Japan*

INTRODUCTION

Gonadotropins, follicle-stimulating hormone (FSH) and luteinizing hormone (LH), are secreted by the anterior pituitary in response to gonadotropin releasing-hormone (GnRH) of the hypothalamus. It is well established that in mammals and birds both FSH and LH are indispensable for the biological function of the gonad. In the testis, FSH first acts on Sertoli cells [3, 27, 56, 74], and Sertoli cells are involved in the initiation and maintenance of spermatogenesis [39, 87]. LH acts on Leydig cells to stimulate the androgen production in the testis [78]. The male sex characters and spermatogenesis are under androgenic regulation. In the ovary, LH together with FSH interacts with the theca interna and membrana granulosa, and regulates the follicular maturation, ovulation and steroidogenesis (for review, see [23]).

Binding of gonadotropins to specific receptor sites on the plasma membrane is accepted as the first indispensable step for their action. Therefore, the activity of target cells is dependent not only on the circulating gonadotropin level but also on the number of gonadotropin receptor sites. Thus, to understand the cellular function of the gonad, the studies concerning receptor changes and the regulatory mechanism are essential. Over the past 20 years, radioimmunoassay has been the main tool for the determination of circulating gonadotropin levels. As for gonadotropin receptor assay, the pioneering studies by Means and Vaitukaitis [57] and Bhalla and Reichert [11] on the radioligand receptor assay in rats opened the door to a wide range of research application.

This paper summarizes the advances made in our understanding of physiological changes in gonadotropin receptors and the regulatory mechanism in higher vertebrates. Although both studies on the ovarian and testicular gonadotropin receptors will be dealt with, more emphasis is placed on the latter. For detailed reviews on the ovarian gonadotropin receptors the reader is referred to References [1, 15, 23, 40].

Received April 7, 1994

RECEPTORS FOR GONADOTROPINS

Radioligand receptor assay

For the identification of target cells for gonadotropins in the gonad, the development of techniques for radiolabeling protein hormones was essential. Precaution is needed in that radiolabeled FSH and LH retain biological activities. In several species of domestic and laboratory mammals, specific receptor sites in the testis for FSH and LH have been found exclusively in Sertoli cells and Leydig cells, as ascertained by autoradiography and radioligand binding assays [14, 55, 66, 82, 88]. Similar results have been obtained in a domestic avian species [47]. It is also well established in the ovary that FSH receptors are located in the granulosa cells and LH receptors are located in the cells of the theca interna, membrana granulosa and corpora lutea.

Binding of FSH or LH to target cell receptors shows common physicochemical properties, such as, hormone specificity, high affinity, *etc.* With these discoveries, several investigators developed specific and sensitive radioligand receptor assays based on the ability of radioiodinated FSH or LH to bind specific receptor sites in the gonadal homogenates of mammals [14, 18, 58, 69, 103] and birds [12, 29, 44, 45, 52, 95].

Specificity for hormones

Hormone specificity of the receptor can be examined by means of competitive inhibition of the binding of radioiodinated hormone by various unlabeled hormone preparations. For example, testicular FSH receptors of rodents bind specifically mammalian FSHs but not LHs or TSH (Fig. 1) [98, 99, 103]. Similarly, FSH receptors in the avian gonad specifically recognize mammalian and avian FSHs [12, 44, 45, 101]. Hormone specificity of LH receptors has also been demonstrated [22].

Affinity

To estimate the affinity of binding, equilibrium analysis of the binding should be performed. Scatchard plot analysis of the FSH binding data unanimously reveals that the equilib-

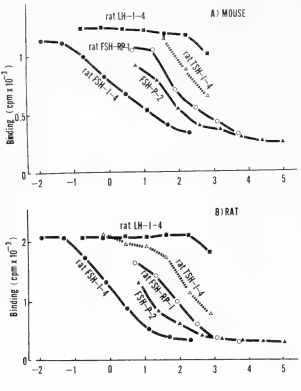

FIG. 1. Competition of specific binding of labeled rat FSH to the particulate fraction of testicular homogenates of mice (A) and rats (B) by various gonadotropin preparations. Incubation for 120 min at 37°C.

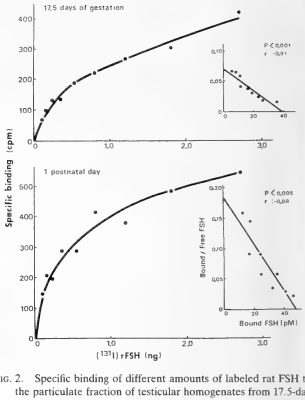

FIG. 2. Specific binding of different amounts of labeled rat FSH to the particulate fraction of testicular homogenates from 17.5-day fetuses and rats at 1 postnatal day of age. Labeled FSH (0.105–2.7 ng) and receptor preparations equivalent to 1.8 mg wet tissue were incubated with or without excess amounts of porcine FSH for 120 min at 37°C. Inset, Scatchard plots of the specific binding. See [97] for details.

rium dissociation constant (Kd) ranges between 10^{-9} to 10^{-10} M in the testis of mammals [11, 14, 18, 57, 98, 99, 103] and of birds [12, 29, 44, 45, 75]. A similar affinity value (Kd) for LH has been obtained with the mammalian [100] and avian testis [52].

CHANGES IN GONADOTROPIN RECEPTORS AND GONADOTROPIN RESPONSIVENESS

During 1970s and 1980s, several investigators asked the following questions. First, when during development do gonadotropin receptors appear in the gonad? Second, what are the changes of gonadotropin receptors in the maturing and matured gonad? Many studies have been carried out to determine the number of gonadotropin receptor sites and binding affinity during fetal and postnatal life.

Fetal life

The ontogeny of testicular FSH receptors during fetal life was first presented by Warren *et al.* [108]. In fetal rats, FSH binding was detectable at 17.5 days of gestation and the binding level significantly increased at 20.5 days [108]. The kinetics of basic properties of FSH binding were conducted by Tsutsui and Kawashima [96]. The FSH binding to the testis of rat fetuses at 17.5 days of gestation showed a saturable process with respect to the concentration of FSH (Fig. 2). Competition experiments revealed that the FSH binding was effectively displaced by rat FSH but not by rat LH. These results confirm that the appearance of specific FSH-binding sites is at 17.5 days of gestation.

Interestingly, the affinity for FSH calculated from the straight lines of the Scatchard plots in 17.5-day fetuses was significantly lower than that in 1-day postnatal rats (Fig. 2). Therefore, it is probable that the molecular form of rat FSH receptor at the beginning of receptor manifestation is different from that during postnatal life. Sprengel *et al.* [84] found that rat FSH receptor is a single straight polypeptide bearing carbohydrate moisty. Therefore, splicing of precursor RNA for mRNA production may be the cause for multiple forms of FSH receptor molecules. At any rate, capacity of receptor sites per gland gradually increased as a function of fetal age [97].

The differentiation of Sertoli cells took place in the seminiferous tubules prior to the appearance of FSH receptors, as shown by an electron microscopic study of Magre and Jost [54]. Recently, new findings that paracrine modulators, such as P-Mod-S secreted by peritubular myoid cells and β-endorphin secreted by Leydig cells, either positively or negatively act on Sertoli cells to coordinate their differentiation have been obtained in mammals [28, 30, 62, 83]. Although the role of FSH in the regulation of testicular

function during fetal life is feasible from the fact that certain levels of circulating FSH were detected in male rat fetuses [19], the role has not yet been established.

Similar to FSH receptors, the characterization of LH receptors during fetal life in mammals has been carried out in several laboratories [13, 32, 34, 42, 107, 108].

Postnatal development

The increase in FSH receptors during postnatal life has been documented by a number of investigators in several species of mammals (Table 1). Developmental changes in FSH receptors were also reported in photostimulated birds (Table 1). The pattern of changes in FSH receptors during testicular development has been characterized by an increase in the total number and the concentration of FSH-binding sites only before the attainment of puberty (Fig. 3) [4, 24, 45, 51, 53, 91, 97, 103]. Unlike during fetal life, no significant change in the binding affinity was detected during postnatal life. FSH binding was restricted to Sertoli cells, and Sertoli cells underwent rapid division around birth and ceased to divide after the first 2–3 weeks of postnatal life [47, 63, 64, 86, 87]. The increase in FSH-binding sites during prepubertal life is believed to be caused by an increase in the number of binding sites per Sertoli cell in addition to an increase in Sertoli cell number. Orth [65] reported that FSH is a major factor in controlling the expansion of the Sertoli cell population.

It was reported in several species of mammals and birds that developmental changes in FSH receptors were followed by a rise in the circulating level of FSH [51, 99, 103]. The parallel increase in the circulating FSH level and the number of FSH receptors suggests the possibility that an increase in FSH induces its own receptors.

A detailed profile of developmental changes in LH receptors has also been demonstrated in mammals [20, 51, 59, 67]. Both the concentration and total number of LH-binding sites increased during the initial phase of testicular development. According to Clausen *et al.* [20], a steady increase in LH-binding sites per Leydig cell was observed during testicular development in rats. In contrast, Pahnke *et al.* [67] reported in rats that the number of LH-binding sites per Leydig cell decreased after puberty. Although the cause of this discrepancy is not known, an increase in LH-binding sites per Leydig cell before puberty is a common phenomenon.

In addition to the age-related changes in the capacity of gonadotropin receptors, various biochemical responses of Sertoli and Leydig cells to gonadotropins change during testicular growth [3, 25–27, 56, 76]. These responses are mediated by cyclic adenosine 3′, 5′-monophosphate (cAMP) which is produced by the activation of adenylate cyclase associated with G-proteins which are coupled with the extracellular domain of gonadotropin receptors [70]. Van Sickle *et al.* [106] and Tsutsui *et al.* [104] have found that the accumulation of cAMP by FSH stimulation increases during prepubertal life in rats and mice.

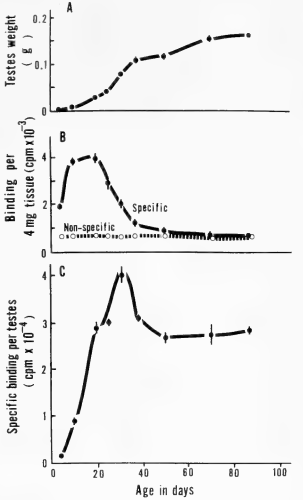

FIG. 3. Changes in mouse testes weight with age (A), specific and nonspecific bindings of labeled rat FSH per 4 mg testicular tissue (B), and specific binding of labeled rat FSH per two testes (C). Incubation for 120 min at 37°C. See [103] for details.

TABLE 1. Developmental changes in FSH receptors during testicular growth in mammals and birds

Animal		Investigators
Mammal	rat	Desjardins *et al.* (1974)
		Ketelslegers *et al.* (1978)
		Thanki and Steinberger (1978)
		Tsutsui and Kawashima (1987)
	mouse	Tsutsui *et al.* (1985)
	hamster	Klemck *et al.* (1987)
		Tsutsui *et al.* (1988)
	ram	Barenton *et al.* (1983)
	primate	Berman and Sairam (1984)
Bird	sparrow	Ishii and Farner (1976)
	quail	Tsutsui and Ishii (1978)
	fowl	Ishii *et al.* (1978)

Adult life

The number of FSH-binding sites in the testis increased progressively with age and the maximum level of binding sites was maintained at adulthood in rats [103] and domestic quails [96]. The plasma FSH level in rats reached a peak at onset of puberty, and then it gradually decreased when the FSH-binding sites still showed an increase. In contrast to these animals, Tsutsui *et al.* [103] found in mice that a decrease in the number of FSH-binding sites was noted when the testis still continued growing and the adult level of FSH binding was kept constantly lower than the maximum level of FSH binding observed immediately prior to puberty (Fig. 3). Thus, the adult level of FSH receptors shows variation among species.

Unlike testicular gonadotropin receptors, the number of ovarian gonadotropin receptors changed during estrous cycle in rats (for review, see [71]) and mice [49]. The number of LH-binding sites in the cells of the membrana granulosa and theca interna markedly increased on proestrus, whereas FSH-binding sites remained constant throughout the estrous cycle. Loss of FSH- and LH-binding sites occurred during luteinization. During pregnancy the change in gonadotropin receptors also occurred in rodents [71, 73, 93]. The number of FSH-binding sites in granulosa cells of developing follicles during early and mid pregnancy was constant but lower than that observed during estrous cycle. LH-binding sites in granulosa cells increased progressively during early pregnancy and decreased during mid pregnancy. Abrupt increases in FSH- and LH-binding sites occurred during late pregnancy.

Wild animals

In contrast to the laboratory and domestic animals which are maintained in constant environmental conditions, the reproductive activity of most species of wild animals inhabiting the temperate and subtropical zones shows a seasonal variation. The variation is the consequences of interaction between external environmental and internal hormonal factors. In wild animals, the reproductive activity is usually confined to a short breeding period. At the termination of breeding season, the reproductive system undergoes morphological and functional regression and remains quiescent until the approach of next breeding season. Puberty in young individuals generally coincides with the onset of breeding season.

Recently, Tsutsui *et al.* [98] provided the profiles of seasonal changes in FSH receptors in a wild rat (short-tailed bandicoot rat, *Nesokia indica*), found abundantly in burrows in fields and gardens of northwestern India. Unlike laboratory albino rats, *N. Indica* exhibits a seasonal change in reproductive activity in natural environment [33, 35]. The testicular content of FSH-binding sites during nonbreeding phase was lower than those during other phases [98]. Barenton and Pelletier [5] also reported that the contents of FSH and LH receptors in the ram testis increased before and decreased during breeding phase, and that the increase in the LH receptor number preceded that of intratesticular testosterone content. In addition to these wild mammals, a wild avian species (Indian weaver bird, *Ploceus philippinus*) markedly responded to natural environmental conditions by showing not only the changes in the testicular weight but also in the FSH receptor number (Table 2) [101]. In contrast, the number of ovarian FSH receptors was rather stable in *P. philippinus* [101].

REGULATION OF GONADOTROPIN RECEPTORS

As mentioned above, concurrently with the increase in gonadotropin receptors during maturation in the male, an increase occurs in the biochemical responsiveness of Sertoli and Leydig cells. The question which immediately follows these findings is what mechanism is operating for the regulation of gonadotropin receptors.

Up-regulation

To identify the hormonal factors inducing testicular FSH receptors, Tsutsui and Ishii [94–96] conducted *hypophysectomy and hormonal replacement therapy*, fundamental methods in the field of endocrinology. If pituitary hormones and/or sex steroids are required in the developmental acquisition of FSH receptors, the number of FSH receptors should change after hypophysectomy. In fact, hypophysectomy of adult domestic quails resulted in the reduction in the numbers of FSH-binding sites and germ cells, but the number of Sertoli cells was not affected [95]. In contrast, injections of FSH to immature [94] and hypophysectomized adult domestic quails [95] induced the hypertrophy of Sertoli cells and an increase in the number of FSH-binding sites per Sertoli cell (Table 3). In addition, injections of testosterone induced an increase in FSH-binding sites without inducing hypertrophy of Sertoli cells (Table 3)

TABLE 2. Affinity (Kd) and capacity of FSH binding to the testis in Indian weaver birds [101]

Phase	Kd (nM)	Number of binding sites (fmol)	
		per mg tissue	per testes
Breeding	0.36 (0.31–0.43)[a]	2.61 (2.40–2.97)	331
Regressive	0.37 (0.18–3.07)	0.64 (0.51–2.45)	5.76
Nonbreeding	0.41 (0.23–5.50)	4.03 (3.30–25.5)	7.25
Progressive	0.52 (0.30–2.03)	0.82 (0.66–1.86)	12.2

[a] 95% confidence interval.

TABLE 3. Effect of treatment with FSH and testosterone on FSH binding to the testis in hypophysectomized adult quails [95]

Treatment	Specific binding (cpm)		
	per 4 mg tissue ($\times 10^{-3}$)	per two testes ($\times 10^{-3}$)	per Sertoli cell ($\times 10^{4}$)
None	1.5±0.1	8.3±1.1	3.0±0.2
FSH	2.2±0.2*	21.9±5.3*	6.7±1.0**
Testosterone	2.8±0.3**	24.3±4.3**	6.8±1.0**
FSH+testosterone	3.0±0.2**	44.1±4.9**	13.1±1.2**

Differences from controls: *P<0.05; **P<0.01.

[94, 95]. Furthermore, FSH and testosterone showed a marked synergism in increasing the number of FSH-binding sites (Table 3) [94, 95]. Thus, the up-regulation of FSH receptors by FSH and testosterone is evident in the Japanese quail.

Until the recent studies by Closset and Hennen [21] and Tsutsui [92], the up-regulation of testicular FSH receptors had not been established in mammalian species. Tsutsui [92] used hypophysectomized immature (25 days of age) rats. The absence of pituitary and/or gonadal hormones was not followed by an increase in FSH-binding sites per two testes (Fig. 4), suggesting that the induction of receptors depends on these hormones. The results of replacement therapy supported this hypothesis. FSH administration to hypophysectomized immature rats induced a dose-dependent increase in the total number of FSH-binding sites in the testis and testicular weight. The stimulatory effect of FSH on the testicular FSH receptors has already been reported by Closset and Hennen [21]. The study of Tsutsui [92] further indicated that testosterone induced an increase in FSH-binding sites with no influence on the testicular weight. There is evidence indicating that Sertoli cells of rats possess a cytosol receptor-nuclear acceptor system for testosterone [60, 61, 76]. Thus, direct effect of testosterone on Sertoli cells is probable.

From the results in quails and rats, it may be generally stated that Sertoli cells require at least FSH and testosterone to induce FSH receptors in the developing testis (Fig. 5). As for the synergistic effects of FSH and testosterone on Sertoli cell function, secretion of androgen-binding protein (ABP) has been reported in immature rats [37]. Synergism of FSH and testosterone on FSH receptors may be present in immature male rats [92]. The up-regulation of FSH receptors by FSH and estradiol was also observed in the ovarian granulosa cells of female rodents [71, 72].

It has been shown in the rat that FSH activates membrane bound adenylate cyclase of Sertoli cells and stimulates various biological processes, such as production of ABP, transferrin and insulin-like growth factor (IGF), activation of protein kinase and RNA polymerase, steroid metabolism and morphological changes including hypertrophy [3, 27, 56, 74, 76]. On the other hand, testosterone enhances the action of FSH to increase ABP production [36] and potentiates the

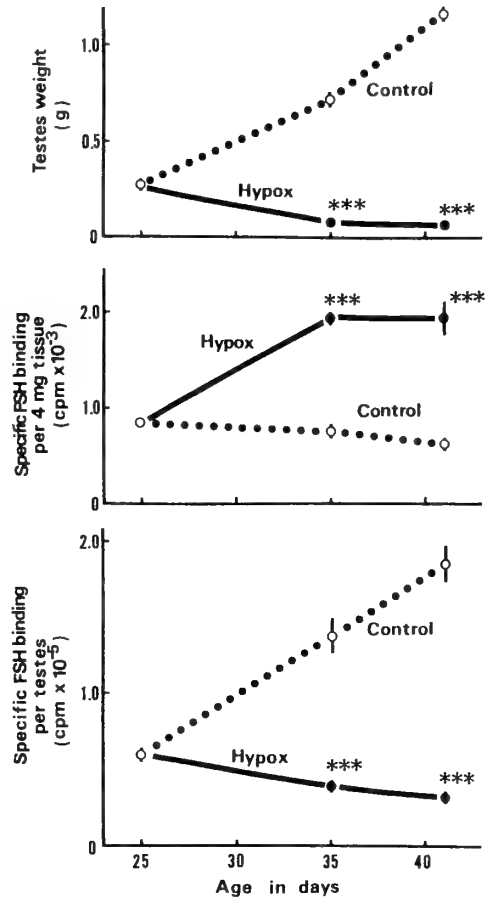

FIG. 4. Long term effects of hypophysectomy (Hypox) on specific FSH binding per 4 mg testicular tissue and per two testes in rats. Rats were hypophysectomized at 25 days of age, and binding was measured 10 and 16 days after surgery. Intact rats served as controls. Incubation was performed for 150 min at 35°C. Significant differences from matched controls: ***P<0.001. See [92] for details.

effect of FSH on Sertoli cells to increase incorporation of ^{32}P [46]. The increase in FSH receptors is the only reported FSH-independent effect of testosterone on Sertoli cells. Accordingly, it is highly probable that testosterone, acting on chromatin of Sertoli cells, specifically induces synthesis of FSH receptors (Fig. 5). In contrast, FSH may activate

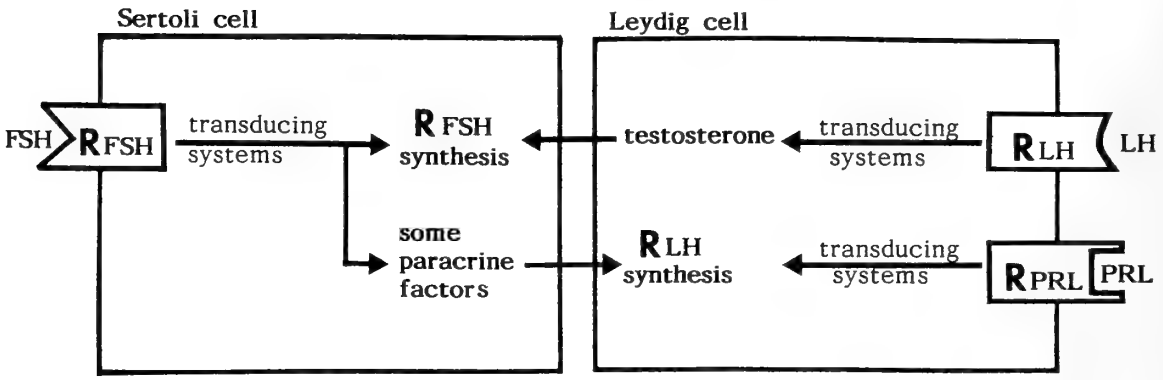

FIG. 5. A model for up-regulation of testicular gonadotropin receptors. FSH stimulates, by acting with testosterone secreted by Leydig cells, the synthesis of its receptors (R_{FSH}) in Sertoli cells. Sertoli cells possess specific receptor sites for not only FSH but also testosterone. LH receptor (R_{LH}) synthesis in Leydig cells is controlled by PRL and FSH (indirectly by some paracrine factors). There are no receptors for FSH on Leydig cells, although Leydig cells possess PRL receptors (R_{PRL}).

general protein synthesis nonspecifically acting at some level after transcription (Fig. 5).

Interestingly, other factors that are independent of pituitary and sex hormones may also contribute to the testicular FSH receptor induction. According to Tsutsui [92], hypophysectomy in neonatal (9 days of age) rats was followed by an increase of FSH-binding sites in the testis after the operation, although the rate of increase in receptors in hypophysectomized rats was less than that in intact control rats. Such an increase in FSH receptors after hypophysectomy suggests not only pituitary and gonadal hormones but also other factors contribute to the receptor induction. Recent studies with mammals have revealed that not only hormones but also paracrine factors modulate Sertoli cell function [3, 28, 62, 83]. According to Skinner [83], P-Mod-S was effective in stimulating Sertoli cell function. However, it is considered that the production of P-Mod-S in the peritubular myoid cell is androgen regulated [83]. Accordingly, some unknown paracrine modulators that are not under direct influence of pituitary and gonadal hormones may take part in the induction of FSH receptors during fetal and neonatal periods.

In contrast to FSH receptors, the induction of LH receptors is more closely linked with the pituitary hormones, since hypophysectomy was followed by a marked loss of LH-binding sites in both immature and adult rats [92]. In terms of the LH receptor induction, the most striking observation is the heterologous up-regulation by prolactin (PRL) and FSH (Fig. 5). It has been reported that PRL treatment enhances both LH-binding sites and LH-stimulated steroidogenesis in hamsters exposed to short day (SD) photoperiods [9], and in immature and adult hypophysectomized rats [68, 110] and mice [89, 90]. In addition, knowledge has been accumulated in rats and mice that FSH augments the number of LH receptors and Leydig cells [17, 21, 50, 89, 90]. Prepubertal rise in testicular LH receptors coincides with the increase in plasma level of FSH in rats [51] and mice [59]. However, the mechanism of action of FSH on LH receptor induction is not known. Although Leydig cells possess PRL receptors, there are no receptors for FSH on Leydig cells. Presumably FSH effect on Leydig cells is mediated by Sertoli cells. Some paracrine factors secreted by Sertoli cells may have a positive effect on LH receptor induction in Leydig cells (Fig. 5) [79]. Another possibility is that the described effect of FSH was due to the small amounts of LH contaminating the FSH preparations [68]. However, treatment with the estimated quantity of LH alone had no effect on the *in vitro* Leydig cell response [105].

Down-regulation

In addition to up-regulatory effect of FSH on FSH receptors, FSH reduces its own receptors in the testis. This phenomenon is called down-regulation. Tsutsui *et al.* [103] reported that in mice persistently high concentrations of plasma FSH levels since the onset of puberty act to reduce the number of FSH receptors in the testis and through this mechanism FSH receptors are maintained at a low level throughout the adult life (Fig. 6). To confirm this hypothesis, hypophysectomy and hormonal replacement therapy were conducted by Tsutsui *et al.* [103]. If down-regulation is crutial for the regulation of testicular FSH receptors in adult mice, the number of FSH receptors should increase after hypophysectomy. Hypophysectomy at adulthood (90 days of age) induced a decrease in the testicular weight, but the concentration and total number of FSH-binding sites were increased after the operation (Fig. 7). In contrast, the administration of FSH to hypophysectomized adult mice reduced the number of FSH-binding sites (Fig. 7). O'Shaughnessy and Brown [66] also reported in intact adult rats that direct injection of a high dose of FSH into the testis induced a decrease in the FSH binding to about 50% within 24 hr. Recently, down-regulation of testicular FSH receptors has been found in adult hamsters [53]. Thus, it appears that FSH contributes as an inhibitory factor to the maintenance of adult level of FSH receptors in these rodents. The higher relative plasma FSH concentrations in mice after puberty compared to rats seems to be the cause for the observed difference in the adult level of FSH receptors

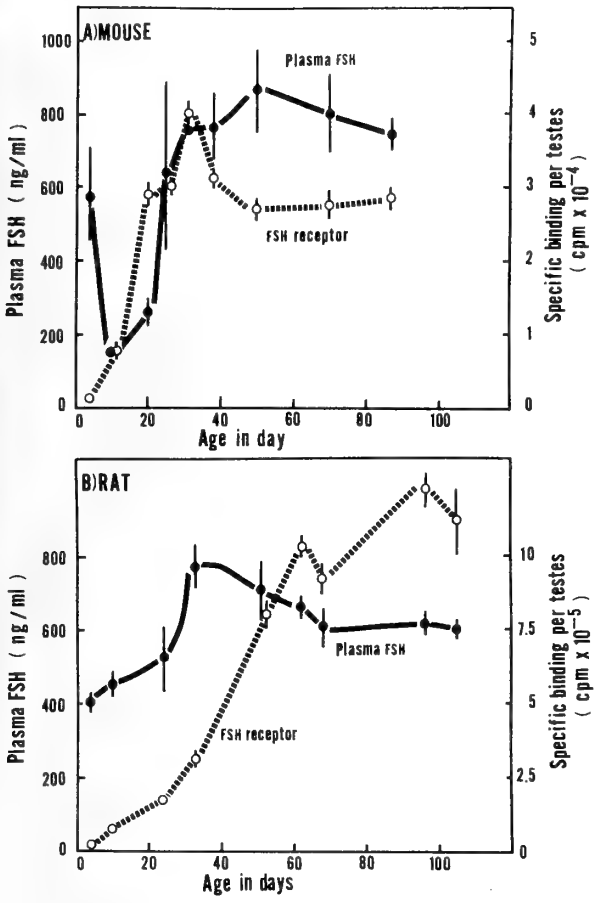

FIG. 6. Changes with age in plasma FSH level and specific binding of labeled rat FSH per two testes in mice (A) and rats (B). Concentrations of plasma FSH are expressed as nanograms of NIADDK-rat FSH-RP-1 per ml. See [103] for details.

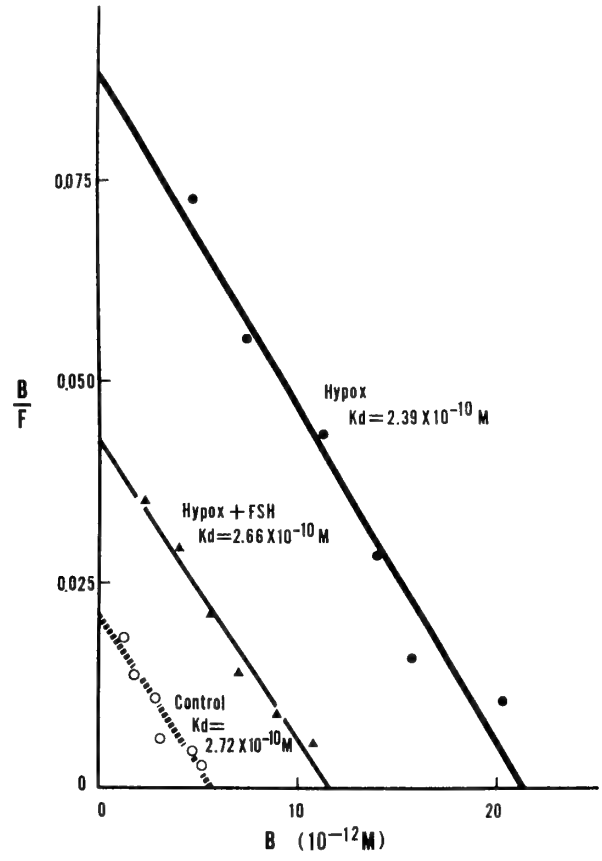

FIG. 7. Scatchard plots of the binding of rat FSH to the particulate fraction of testicular homogenates of intact control mice, hypophysectomized mice and FSH-treated hypophysectomized mice. Hypophysectomy was performed at 90 days of age. Hypophysectomized mice were given injections of 50μg NIH-FSH-P-2 twice daily for 10 days. B, Concentration of bound hormone at apparent equilibrium; F, concentration of free hormone at apparent equilibrium. See [103] for details.

between rats and mice (Fig. 6).

In rats and mice several biochemical responses to FSH decrease after puberty [3, 25–27, 56, 76]. Since these responses are mediated by cAMP, the decrease may be due to the decrease in the capacity of FSH receptors in Sertoli cells. Tsutsui *et al.* [104] found that the accumulation of cAMP by FSH treatment was lower in adult mice than prepubertal mice, and the low responsiveness of adult mice was modified by hypophysectomy. These changes in FSH responsiveness were in parallel with those in FSH-binding sites per Sertoli cell [103]. Therefore, it is considered that the down-regulation of FSH receptors brings forth a lowered responsiveness to FSH at adulthood. The desensitization of adenylate cyclase system associated with G-proteins may also account for the lowered responsiveness based on the studies with rats [106].

With the use of light and electron microscopic autoradiography, Shimizu *et al.* [82] found that ^{131}I-FSH after binding to the cell-surface receptors translocates into the intracellular organelles by receptor-mediated endocytosis. Shimizu and Kawashima [80] further investigated the behavior of ^{131}I-FSH after binding to cell-surface receptors in purified Sertoli cells of mice in culture, and proposed a kinetic model for the intracellular processes. The model clearly shows that the internalization of ligand-receptor complexes and the degradation of the complexes in lysosomes are important processes for down-regulation [80, 81]. In LH receptors, a number of investigators have also demonstrated that systemic injections of LH or human chorionic gonadotropin decrease the apparent number of LH-binding sites in the testis of rats [16, 22, 38, 41, 68, 77]. These findings altogether indicate that FSH or LH interacts with its receptor in Sertoli or Leydig cells and the hormone-receptor complexes are internalized and then degraded in lysosomes.

Species difference in receptor regulation

The effect of hypophysectomy on the capacity of FSH-binding sites was different among species of animals. A marked decrease in the capacity of FSH-binding sites in hypophysectomized quails suggests that up-regulation is actually manifested in the testis of quails [94, 95]. However, a reduction in the number of FSH-binding sites was less

obvious in hypophysectomized adult rats [92]. In contrast, both the concentration and content of FSH-binding sites increased after hypophysectomy in adult mice [103]. To sum up, down-regulation is effectively operative in mice especially after maturation and the function of up-regulation is apparent in quails. It is well known that photosensitive birds show a rapid testicular growth when exposed to long day (LD) photoperiods [31]. Tsutsui *et al.* [102] stated that the testicular growth during sexual maturation was much more rapid in quails and fowls than in mice and rats. The active up-regulation as a consequence of the elevation in gonadotropin level may induce rapid testicular growth in photostimulated birds [94–96].

ENVIRONMENTAL CUES AND RECEPTOR REGULATION

In the majority of animals, reproductive functions do not continue throughout the year. Although the timing of the onset and termination of reproductive function depends on a complex interaction of internal biological rhythms with a variety of environmental cues, including day length, ambient temperature, and the availability of food, seasonal changes in the time of sunrise and sunset (photoperiod) appear to be most important in many species. For investigations on the role of environmental cues in the regulation of gonadotropin receptors in mammals, the hamster has served as an excellent model.

Tsutsui *et al.* [99] observed that photoperiod is a more important environmental factor than ambient temperature for the regulation of FSH receptors in the Djungarian (Siberian) hamster, *Phodopus sungorus* (Fig. 8). They studied the effects of artificial photoperiod and ambient temperature on testicular FSH receptor numbers and plasma FSH levels in adult males. In their experiments, hamsters were transferred to LD photoperiods (16-hr light, 8-hr dark) after adaptation in SD photoperiods (8-hr light, 16-hr dark), but the ambient temperature was maintained at 25°C. An increase in the content of FSH-binding sites and testicular growth occurred after transfer to LD, concomitant with the increase in circulating FSH levels. When hamsters reared under LD were transferred to SD, the content of FSH-binding sites and the plasma FSH level decreased. In contrast to the photoperiodic influence, they could not detect any clear-cut influence of different ambient temperatures on the capacity of FSH binding in adult Djungarian hamsters (Fig. 8) [99]. An inhibitory effect of SD on the content of FSH-binding sites in the golden (Syrian) hamster, *Mesocricetus auratus* was also reported by Amador *et al.* [2]. Photoperiod-related changes in the testicular FSH receptor levels and circulating FSH levels suggest that up-regulatory mechanism of FSH on FSH receptors does exist in the hamster.

Information on the effect of artificial photoperiod on the number of testicular LH receptors in the hamster has also been accumulated. A number of studies demonstrated that testicular levels of LH-binding sites declined after transfer to

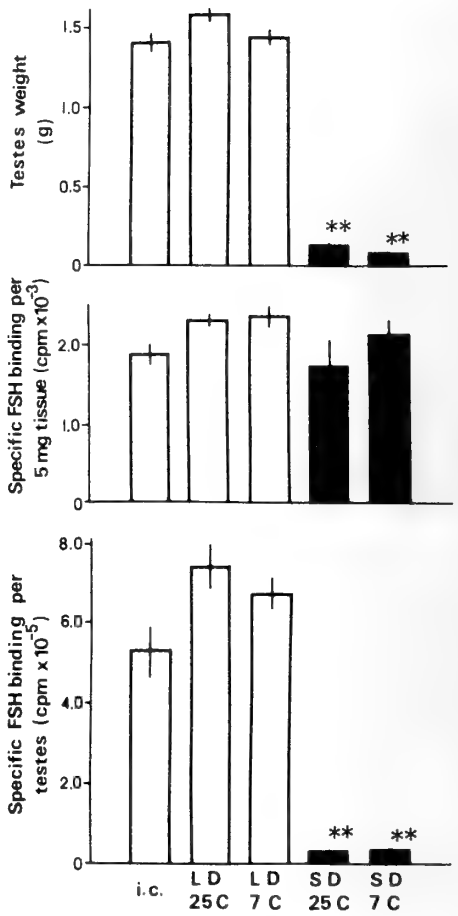

FIG. 8. Effects of photoperiod and ambient temperature on the testicular weight, specific binding of labeled rat FSH per 5 mg tissue, and specific binding of labeled rat FSH per two testes in hamsters. Incubation for 120 min at 35°C. Significant differences from matched LD groups: $^{**}P<0.01$. See [99] for details.

SD in the golden hamster [6, 7, 9, 10, 85] and Djungarian hamster [100]. Tsutsui *et al.* [100] further demonstrated in the Djungarian hamster that LD exposure after adaptation to SD induced an increase in the capacity of LH binding. Experimental evidence suggests that PRL is a major stimulator of the number of LH-binding sites in the hamster [7, 8]. Yellon and Goldman [109] reported in the hamster that circulating PRL concentration was higher after LD exposure than after SD exposure.

Similar photoinduced changes in the testicular gonadotropin receptor number have been extensively reported in several species of temperate zone birds (white-crowned sparrow [45]; domestic quail [94]; domestic fowls [47]). Recently, Kawashima *et al.* [48] have also demonstrated that photoperiod regulates the number of FSH receptors in the testis of a subtropical bird (Indian weaver bird, *Ploceus philippinus*). In addition, Ishii [43] reported that testicular responsiveness to gonadotropins was elevated in photostimulated white-crowned sparrows with growing testes. As indices of gonadotropin sensitivity of the testis, rates of changes in testosterone release and cAMP accumulation in excised testes incu-

bated with graded doses of FSH were employed in his study. Furthermore, the parallel increase in the circulating gonadotropin level and the number of FSH receptors in male Indian weaver birds subjected to LD [48] agrees well with the findings of Tsutsui and Ishii [94–96] that in the quail FSH and testosterone act synergistically on Sertoli cells to increase FSH receptor numbers and to elevate the testicular responsiveness to FSH.

CONCLUSIONS

Gonadotropins exert their action after binding to specific membrane receptors in target cells of the gonad. Testicular Sertoli and Leydig cells are target cells for FSH and LH, respectively. From the studies with laboratory or domestic animals, FSH receptors begin to appear in Sertoli cell during fetal life. Steady increase in the number of FSH receptors takes place during testicular growth of postnatal life. After the puberty the adult FSH receptor levels are maintained. Ontogenetic and developmental changes in LH receptors are almost similar to those in FSH receptors. Sertoli cell-to -Leydig cell cooperation contributes to the gonadotropin receptor induction. A homologous hormone, FSH, and a heterologous hormone, testosterone secreted by Leydig cells, act to Sertoli cells to induce FSH receptors in the developing testis (up-regulation). Testosterone acting on chromatin, may specifically synthesize or activate FSH receptors. FSH may activate general protein synthesis nonspecifically acting at some level after transcription. The LH receptor synthesis or activation can be controlled by several heterologous hormones including PRL and FSH. PRL can act directly on Leydig cells and FSH action on LH receptor induction may be mediated by Sertoli cells.

In addition to up-regulation of gonadotropin receptors by homologous and heterologous hormones, down-regulation of FSH and LH on their own receptors becomes apparent especially after maturation. The circulating gonadotropin level may be a main determinant of the adult level of gonadotropin receptors. The acceleration of internalization of hormone-receptor complexes seems to be an important cause for down-regulation.

Unlike laboratory or domestic animals, the reproductive function in the majority of wild animals does not continue throughout the year but is confined to a fixed short breeding period in the majority of animals. Seasonal changes in endocrine and gametogenic function of the testis in wild animals are associated with the changes in gonadotropin levels and the availability of gonadotropin receptors in the testis. Photoperiod is a more important environmental factor than temperature for the regulation of gonadotropin receptors.

To conclude, the testicular responsiveness to gonadotropins in both domestic and wild animals is generally correlated with the level of gonadotropin receptors. Thus, not only circulating levels of gonadotropins but also capacity of their receptors must be taken into account for the elucidation of testicular function.

ACKNOWLEDGMENTS

This study was supported in part by the Japan Society for the Promotion of Science as the International Joint Research Project, and Grants-in-Aid from the Ministry of Education, Science, and Culture, Japan. We are grateful to Prof. S. Ishii (Department of Biology, Waseda University) for his constant collaboration during this study and valuable advice in preparing the manuscript. Cordial thanks are also due to Dr. S. Raiti, National Institute of Arthritis, Diabetes, and Digestive and Kidney Diseases (NIADDK) and Dr. A. F. Parlow, Pituitary Hormones/Antisera Center, Harbor-UCLA Medical Center for the supply of pituitary hormones. We are grateful to Prof. R. N. Saxena (Department of Zoology, University of Delhi, India) and to Prof. T. Oishi (Department of Biology, Nara Women's University) for their collaborations.

REFERENCES

1 Adashi EY, Hsueh AJW (1984) In"The Receptors" Ed by PJ Conn, Academic Press, London, Vol 1, pp 587–636
2 Amador A, Bartke A, Klemcke HG, Siler-Khodr TM, Stallings MH (1985) J Reprod Fertil 74: 693–701
3 Armstrong DT, Moon YS, Fritz IB, Dorrington JH (1975) In"Current Topics in Molecular Endocrinology Vol 2" Ed by FS French, V Hansson, EM Ritzen, SN Nayfeh, Plenum Press, New York, pp 117–191
4 Barenton B, Hochereau-de Reviers MT, Perreau C, Saumande J (1983) Endocrinology 112: 1447–1453
5 Barenton B, Pelletier J (1983) Endocrinology 112: 1441–1446
6 Bartke A, Goldman BD, Bex FJ, Kelch RP, Smith MS, Delterio S, Doherty PC (1980a) Endocrinology 106: 167–172
7 Bartke A, Goldman BD, Klemcke HG, Bex FJ, Amador AG (1980b) In"Functional Correlates of Hormone Receptors in Reproduction" Ed by VB Mahesh, TG Muldoon, BB Saxena, WA Sadler, Elsevier North Holland, Inc., New York, pp 171–185
8 Bartke A, Klemcke HG, Amador A, van Sickle A (1982) Ann NY Acad Sci 383: 122–134
9 Bex FJ, Bartke A (1977) Endocrinology 100: 1223–1226
10 Bex FJ, Bartke A, Goldman BD, Dalterio S (1978) Endocrinology 103: 2069–2080
11 Bhalla VK, Reichert LE Jr. (1974) J Biol Chem 249: 43–51
12 Bona Gallo A, Licht P (1979) Gen Comp Endocrinol 37: 521–532
13 Catt KJ, Dufau ML, Neaves WB, Walsh PC, Wilson JD (1975) Endocrinology 97: 1157–1165
14 Catt KJ, Dufau ML, Tsuruhara T (1972) J Clin Endocrinol 34: 123–132
15 Catt KJ, Harwood JP, Clayton RN, Davies TF, Chan V, Katikineni M, Nozu K, Dufau ML (1980) Rec Progr Horm Res 36: 557–622
16 Chen Y-D, Payne AH (1977) Biochem Biophys Res Commun 74: 1589–1596
17 Chen Y-D, Payne AH, Kelch RP (1976) Proc Soc Exp Biol Med 153: 473–475
18 Cheng KW (1975) J Clin Endocrinol Metab 41: 481–491
19 Chowdhury M, Steinberger E (1976) J Endocrinol 69: 381–384
20 Clausen OPF, Purvis K, Hansson V (1981) Acta Endocrinol 96: 569–576
21 Closset J, Hennen G (1989) J Endocrinol 120: 89–96

22 Cooke BA, Rommerts FFG (1988) In "Hormones and Their Actions, Part II" Ed by BA Cooke, RJB King, HJ van der Molen, Elsevier, Amsterdam, pp 155–180

23 Dahl KD, Hsueh AJW (1988) In "Hormones and Their Actions, Part II" Ed by BA Cooke, RJB King, HJ van der Molen, Elsevier, Amsterdam, pp 181–192

24 Desjardins C, Zeleznik AJ, Midgley AR Jr. (1974) In"Current Topics in Molecular Endocrinology Vol 1" Ed by ML Dufau, AR Means, Plenum Press, New York, pp 221–235

25 Dorrington JH, Armstrong DT (1975) Proc Natl Acad Sci USA 72: 2677–2681

26 Dorrington JH, Fritz IB, Armstrong DT (1976) Mol Cell Endocrinol 6: 117–128

27 Dorrington JH, Roller NF, Fritz IB (1975) Mol Cell Endocrinol 3: 57–70

28 Eskeland NL, Lugo DI, Pintar JE, Schachter BS (1989) Endocrinology 124: 2914–2919

29 Etches RJ, Cheng KW (1981) J Endocrinol 91: 11–22

30 Fabbri A, Tsai-Morris CH, Luna S, Fraioli F, Dufau ML (1985) Endocrinology 117: 2544–2546

31 Follett BK, Farner DS (1966) Gen Comp Endocrinol 7: 111–124

32 Frowein J, Engel W (1974) Nature 249: 377–379

33 Gariyali V, Saxena RN (1975) Proc All India Rodent Semin 2: 133–139

34 George FW, Catt KJ, Neaves WB, Wilson JD (1978) Endocrinology 102: 665–673

35 Grover JL (1985) Ph D thesis, Univ of Delhi, India

36 Hansson V, French FS, Weddington SC, Nayfeh SN, Ritzen EM (1974) In"Current Topics in Molecular Endocrinology Vol 1" Ed by ML Dufau, AR Means, Plenum Press, New York, pp 287–290

37 Hansson V, Weddington SC, McLean WS, Smith AA, Nayfeh SN, French FS, Ritzen EM (1975) J Reprod Fertil 44: 363–375

38 Haour F, Saez JM (1977) Mol Cell Endocrinol 7: 17–24

39 Hodgson Y, Robertson DM, de Kretser DM (1983) Int Rev Physiol 27: 275–327

40 Hsueh AJW, Adashi EY, Jones PBC, Welsh TH (1984) Endocr Rev 5: 76–127

41 Hsueh AJW, Dufau ML, Catt KJ (1976) Biochem Biophys Res Commun 72: 1145–1153

42 Huhtaniemi IT, Korenbrot CC, Jaffe RB (1977) J Clin Endocrinol Metab 44: 963–967

43 Ishii S (1980) In"Avian Endocrinology Vol 4" Ed by DS Farner, JR King, KC Parkes, Academic Press, pp 1–15

44 Ishii S, Adachi T (1977) Gen Comp Endocrinol 31: 287–294

45 Ishii S, Farner DS (1976) Gen Comp Endocrinol 30: 443–450

46 Ishii S, Hirano S (1979) Gen Comp Endocrinol 37: 137–140

47 Ishii S, Tsutsui K, Adachi T (1978) In"Comparative Endocrinology" Ed by PJ Gaillard, HH Boer, Elsevier, Amsterdam, pp 73–76

48 Kawashima S, Tsutsui K, Saxena RN, Ishii S (1993) Gen Comp Endocrinol 92: 250–259

49 Kawashima S, Yamada Y, Tsutsui K (1986) J Sci Hiroshima Univ, Ser B Div 1, 32: 271–282

50 Kerr JB, Sharpe RM (1985) Endocrinology 116: 2592–2604

51 Ketelslegers J-M, Hetzel WD, Sherins RJ, Catt KJ (1978) Endocrinology 103: 212–222

52 Kikuchi M, Ishii S (1989) Biol Reprod 41: 1047–1054

53 Klemcke HG, van Sickle M, Bartke A, Amador A, Chandrashekar V (1987) Biol Reprod 37: 356–370

54 Magre S, Jost A (1980) Arch Anat Micros Morphol Exp 69: 297–318

55 Means AR, Dedman JR, Tash JS, Tindall DJ, van Sickle M, Welsh MJ (1980) Ann Rev Physiol 42: 59–70

56 Means AR, Tindal DJ (1975) In"Current Topics in Molecular Endocrinology Vol 2" Ed by FS French, V Hansson, EM Ritzen, SN Nayfeh, Plenum Press, New York, pp 383–398

57 Means AR, Vaitukaitis J (1972) Endocrinology 90: 39–46

58 Mendelson C, Dufau M, Catt K (1975) J Biol Chem 250: 8818–8823

59 Mori H, Tsutsui K, Kawashima S (1985) J Sci Hiroshima Univ, Ser B, Div 1 32: 143–156

60 Mulder E, Peters MJ, van der Molen HJ (1987) In "Current Topics in Molecular Endocrinology Vol 2" Ed by FS French, V Hansson, EM Ritzen, SN Nayfeh, Plenum Press, New York, pp 287–291

61 Nakhla AM, Mather JP, Janne OA, Bardin CW (1984) Endocrinology 115: 121–128

62 Norton JN, Skinner MK (1989) Endocrinology 124: 2711–2719

63 Orth J (1982) Anat Rec 203: 485–492

64 Orth J, Christensen AK (1977) Endocrinology 101: 262–278

65 Orth JM (1984) Endocrinology 115: 1248–1255

66 O'Shaughnessy PJ, Brown PS (1978) Mol Cell Endocrinology 12: 9–15

67 Pahnke VG, Leinberger FA, Kunzig HJ (1975) Acta Endocrinol 79: 610–618

68 Purvis K, Clausen OPF, Olsen A, Haug E, Hansson V (1979) Arch Androl 3: 219–230

69 Reichert LE Jr., Bhalla VK (1974) Endocrinology 94: 483–491

70 Reichet LE Jr., Dattatreyamurty B (1989) Biol Reprod 40:13–26

71 Richards JS (1980) Physiol Rev 60: 51–83

72 Richards JS, Irland JJ, Rao MC, Bernath GA, Midgley AR, Reichert LE Jr. (1976) Endocrinology 99: 1562–1570

73 Richards JS, Kersey KA (1979) Biol Reprod 21: 1185–1201

74 Risbridger GP, Hodgson YM, de Kretser DM (1981) In"The Testis" Ed by H Burger, DM de Kretser, Raven Press, New York, pp 195–212

75 Ritzhaupt LK, Bahr JM (1987) J Endocrinol 115: 303–310

76 Sanborn BM, Elkington JSH, Steinberger A, Steinberger E (1975) In"Current Topics in Molecular Endocrinology Vol 2" Ed by FS French, V Hansson, EM Ritzen, SN Nayfeh, Plenum Press, New York, pp 293–309

77 Sharpe RM (1976) Nature 264: 644–646

78 Sharpe RM (1982) In "Oxford Reviews in Reproductive Biology Vol 4" Ed by CA Finn, Oxford University Press, Oxford, pp 241–317

79 Sharpe RM (1986) Clin Endocrinol Metab 15: 185–207

80 Shimizu A, Kawashima S (1989) J Biol Chem 264: 13632–13639

81 Shimizu A, Kawashima S (1989) J Biol Chem 264: 13639–13641

82 Shimizu, A, Tsutsui K, Kawashima S (1987) Endocrinol Jpn 34: 431–442

83 Skinner MK (1988) Internat Congr of Endocrinol, Kyoto, Japan, pp 51 (Abstract)

84 Sprengel R, Braun T, Nikolics K, Segaloff DL, Seeburg PH (1990) Mol Endocrinology 4: 494–499

85 Stallings MH, Matt KS, Amador A, Bartke A, Soares MJ, Talamantes F (1985) J Reprod Fertil 75: 663–670

86 Steinberger A, Steinberger E (1971) Biol Reprod 4: 84–87

87 Steinberger A, Steinberger E (1972) In"Reproductive Biology" Ed by H Balin, S Glasser, Excerpta Medica, Amsterdam, pp 144–267

88 Steinberger A, Thanki KH, Siegal B (1974) In"Current Topics in Molecular Endocrinology Vol 1" Ed by ML Dufau, AR Means, Plenum Press, New York, pp 177–192

89 Takase M, Tsutsui K, Kawashima S (1990a) J Exp Zool 256: 200–209

90 Takase M, Tsutsui K, Kawashima S (1990b) Endocrinol Jpn 37: 193–203

91 Thanki KH, Steinberger A (1978) Andrologia 10: 195–202

92 Tsutsui K (1991) Endocrinology 128: 477–487

93 Tsutsui K (1992) J Exp Zool 264: 167–176

94 Tsutsui K, Ishii S (1978) Gen Comp Endocrinol 36: 297–305

95 Tsutsui K, Ishii S (1980) J Endocrinol 85: 511–518

96 Tsutsui K, Ishii S (1985) In"Current Trends in Comparative Endocrinology" Ed by B Lofts, WN Holmes, Hong Kong Univ Press, Hong Kong, pp 761–762

97 Tsutsui K, Kawashima S (1987) Endocrinol Jpn 34: 717–725

98 Tsutsui K, Kawashima S, Kumar V, Kapania R, Saxena RN (1989a) Gen Comp Endocrinol 73: 442–451

99 Tsutsui K, Kawashima S, Masuda A, Oishi T (1988) Endocrinology 122: 1094–1102

100 Tsutsui K, Kawashima S, Masuda A, Oishi T (1989b) J Exp Zool 251: 91–10

101 Tsutsui K, Kawashima S, Saxena RN, Ishii S (1992) Gen Comp Endocrinol 88: 444–453

102 Tsutsui K, Shimizu A, Kawamoto K, Kawashima S (1983) In"Recent Trends in Life Sciences" Ed by A Gopalakrishna, SB Singh, AK Saxena, Manu Publications, Kanpur, pp 93–102

103 Tsutsui K, Shimizu A, Kawamoto K, Kawashima S (1985) Endocrinology 117: 2534–2543

104 Tsutsui K, Shimizu A, Kawashima S, Ishii S (1986) Zool Sci 3: 497–501

105 van Beurden, Roodnat WMO, van der Molen HJ (1978) Int J Androl (Suppl) 2: 374–382

106 van Sickle M, Oberwetter JM, Birnbaumer L, Means AR (1981) Endocrinology 109: 1270–1280

107 Warren DW, Dufau ML, Catt KJ (1982) Science 218: 375–377

108 Warren DW, Huhtaniemi IT, Tapanainen J, Dufau ML, Catt KJ (1984) Endocrinology 114: 470–476

109 Yellon SM, Goldman BD (1984) Endocrinology 114: 664–670

110 Zipf WB, Payne AH, Kelch RP (1978) Endocrinology 103: 595–600

ZOOLOGICAL SCIENCE 11: 363–373 (1994)

REVIEW

Gonadotropin-Releasing Hormone: Present Concepts, Future Directions*

RAKESH K. RASTOGI and LUISA IELA

Department of Zoology, University of Naples "Federico II", via Mezzocannone 8, 80134 Napoli, Italy

ABSTRACT—There is an overwhelming amount of evidence to indicate that gonadotropin-releasing hormone (GnRH), a decapeptide, is found in multiple molecular forms, and is vital for the functional integration of brain-pituitary-gonadal axis in vertebrates. In simple terms, there is an overall agreement that GnRH acts as a neuroendocrine regulator of pituitary gonadotropin secretion, gonadal steroid secretion, sexual behavior, and reproduction. GnRHs are distributed widely within the vertebrate body, particularly in the brain. The brain GnRH neuronal system(s) varies in its morphology, ontogenesis and function across vertebrates. It is a highly dynamic structure which does not function at the same level throughout life. A large framework of studies completed to date attests to the emerging concept that GnRH neuronal system is regulated by a complex neural circuitry, comprised of diverse neurochemical signals, which may provide excitatory or inhibitory input to GnRH neurons. While general considerations on GnRH systems may be similar among vertebrates, it must not seduce us to generalize the more specific details. In fact, there may occur ontogenesis and reproductive status-related changes and a timetable of complex neuroendocrine events that are probably (certainly) species-specific.

INTRODUCTION

Gonadotropin-releasing hormone (GnRH=LHRH), a 10-amino acid bioregulatory neuropeptide, has a widespread occurrence within the living kingdom, and is not restricted just to vertebrates. In fact, from the evolutionary viewpoint one can go as far back as the yeast cells in which Loumaye *et al.* [55] demonstrated that a mating factor, called α-factor, necessary for sexual reproduction, has a strong similarity to GnRH, as evaluated by its ability to influence pituitary gonadotropin (GtH) secretion.

Brain is certainly the most complex organ of the vertebrate body. Within this highly specialized tissue there are cells characterized by their ability to synthesize GnRH. Originally isolated as a brain peptide, GnRH is well known for its regulatory role in the release of luteinizing hormone (LH) and follicle-stimulating hormone (FSH) from the anterior pituitary (pars distalis, adenohypophysis, ventral lobe). Since the isolation and structural elucidation of the hypothalamic GnRH in the early-1970s there have been numerous investigations to unveil the distribution pattern of GnRH-like peptide(s) in the brain of all vertebrate classes, from mammals down to cyclostomes [4, 6, 10, 22, 23, 44, 64, 77, 87]. During evolution this neuropeptide has undergone gene duplication with consequent structural diversification which is evident in the presence of multiple molecular forms across vertebrate species [see 45]. So far eight GnRH molecular forms have been described in the vertebrate brain, characterized and named for the vertebrate species in which they were first identified: mammalian (mGnRH), chicken I (cGnRH-I), chicken II (cGnRH-II), salmon (sGnRH), lamprey I and III (lGnRH), catfish (cfGnRH) and dogfish (dfGnRH) [10, 44–46, 64, 87, 86]. From a phylogenetic viewpoint cGnRH-II is considered to be the most conserved GnRH across vertebrates and residues 5, 7 and 8 vary among different forms. So far, only cGnRH-II has been described in all jawed vertebrates. Lamprey GnRH, however, varies from cGnRH-II in positions 3, 5, 6 and 8, and its presence has been demonstrated in cyclostomes only. An endogenous posttransational product of the GnRH precursor has been characterized in mammalian and frog hypothalamus: (Hydroxyproline^9)GnRH [29]. More recently, in *Xenopus laevis*, this form was shown to be distributed in the forebrain, midbrain and hypothalamus [46]. This peptide, as well as the C-terminal fragments of GnRH, are supposed to enhance sexual behavior as GnRH itself [30]. Novel GnRH forms described in oviparous mammals, reptiles, amphibians, bony and cartilaginous fishes and cyclostomes are yet to be characterized and still other GnRH forms are expected to be discovered [45–47, 64, 75]. Furthermore, over a couple of thousand analogs of GnRH ($GnRH_A$) have been synthesized whose availability becomes a powerful tool in understanding the regulatory roles and mechanisms of action of GnRH [42, 83]. The molecular heterogeneity is apparently the basis for a variety of regulatory functions of GnRH: as the stimulator of the reproductive system and sexual behavior, as a neuromodulator and/or neurotransmitter in the central and sympathetic nervous system, and as a paracrine/autocrine regulator in the pituitary, gonads, placenta, and in tumor cells.

This article is intended to give a "bird's eye view" of the morpho-functional features of GnRH neuronal systems

Received May 9, 1994

* This paper is dedicated to our mentor Professor Giovanni Chieffi.

across vertebrates, and to spotlight the new knowledge that has emerged from latest studies.

DISTRIBUTION

Evidences based upon radioimmunoassay (RIA), chromatography (HPLC), *in situ* hybridization histochemistry (ISHH) and immunohistochemistry (ICC) techniques indicate the presence of GnRH-like peptide(s) in several brain as well as outside brain areas of a variety of vertebrate species. Localization of GnRH-producing neurons and their projections has been studied in the brain of mammals, birds, reptiles, amphibians, bony and cartilaginous fishes and cyclostomes [4, 6, 10, 19, 21–23, 40, 50, 56, 57, 64, 68, 77, 78, 87]. In several vertebrates HPLC/RIA analyses have confirmed ICC data as far as the distribution of GnRH-like material in the brain is concerned. However, in some species of birds, reptiles and amphibians ICC and HPLC/RIA data have shown discrepancy regarding the presence and distribution of different molecular forms of GnRH [19, 24, 28, 57, 61, 67, 75, 78, 101, unpublished data].

Modern ICC techniques are considered highly efficient, and yet we can not exclude the possibility that there may be GnRH neurons which fall below the level of detectability of the ICC procedures. Taking into account this reservation, at the present time GnRH-containing neurons and their projections have been described in the rhinencephalon, telencephalon, diencephalon, mesencephalon, metencephalon and myelencephalon [6, 10, 19, 21, 23, 57, 64, 87]. Although there are remarkable interspecies differences, a large hypothalamic population constitutes the biggest group of GnRH neurons in the brain of most vertebrates. In the median eminence (ME) no GnRH cell bodies are found. Among mammals, only musk shrew brain contains a cluster of GnRH neurons in the mesencephalon [21], and it is not known whether this feature is common to other primitive mammals. No GnRH neurons have been described posterior to the midbrain in any mammalian species. GnRH neurons in the forebrain, however, send fiber projections to the midbrain in all mammals. In nonmammalian vertebrates, except urodele amphibians [19] and cyclostomes [48], a mesencephalic group of GnRH neurons has been described [50, 57, 61, 64, 65, 101, 106, unpublished data]. Projections of midbrain GnRH neurons in bony fishes may innervate the caudal neurosecretory system (urophysis) [23]. Conspicuous differences in the distribution pattern have been described within each vertebrate subgroup. For example, among anuran amphibians, *Rana esculenta* brain shows perhaps the most extensive network of GnRH neurons and fibers [24, 78], whereas *Pachymedusa dacnicolor* brain contains only a small number of GnRH neurons all located exclusively in the anterior preoptic area (POA) [40] from where axonal projections reach the ME. In cyclostomes, the POA-located GnRH neurons project to the neurohypophysis (PN; pars nervosa) [48]. In most vertebrates GnRH fiber endings in the ME are derived from the forebrain-located neurons, mainly in the hypothalamus and septum, and only in bony fishes do the POA-located GnRH neuron projections directly contact pituitary gonadotropes [23]. Several studies have established that the populations of GnRH cells in the forebrain that project to the pituitary, PN and/or ME are often completely separate from those GnRH neurons that give rise to brain stem and/or spinal cord projections [65]. In fact, a growing body of evidence indicates that there are subpopulations of anatomically distinct GnRH-neuronal systems in the vertebrate brain, and that GnRH neurons may be unipolar, bipolar or multipolar. At a subcellular level GnRH immunoreactivity is distributed around the outside of the nuclear envelope, associated particularly with the rough endoplasmic reticulum, secretory vesicles and Golgi apparatus, and in the neuronal projections [54, 59, 110]. Sex-related differences in subcellular organelles have been described in mares and stallions [59]. To the best of our knowledge, no ultrastructural study of GnRH neurons is available in nonmammalian vertebrates.

Numerous studies have demonstrated that more than one GnRH molecular form may be present in the brain, and there are several reports on a differential distribution of GnRH variants in distinct brain areas [10, 13, 44, 46, 61, 65, 96, 109]. Moreover, in the lizard, *Podarcis sicula*, more than one GnRH form were colocalized in the same neuron [57]. In the musk shrew, mGnRH is distributed all through the forebrain and diencephalon, whereas midbrain-located neurons contain only cGnRH-II [21]. In the midbrain of adult chicken only cGnRH-II is present, while cGnRH-I is present chiefly in the forebrain, diencephalon and ME [43]. However, in a later study, van Gils *et al.* [101] detected cGnRH-II in the ME of chicken as well as Japanese quail. Similarly, Millam *et al.* [61] did not find cGnRH-II in the ME of turkey by ICC, while in a later study RIA analysis showed the presence of cGnRH-II in the posterior pituitary [El Halawani, unpublished, see 60]. Further, in a turtle species, cGnRH-I and II are differentially distributed, the former being most concentrated in the ME in a ratio of 8:1 against the latter which is more abundant in the caudal regions [96]. Likewise, in *X. laevis* mGnRH is distributed throughout the brain, whereas cGnRH-II is more concentrated in the midbrain and hindbrain [46]. In the frog, *R. ridibunda*, cGnRH-II neurons, but not mGnRH neurons innervate the neurointermediate lobe of the pituitary; similarly, in *R. esculenta* mGnRH neurons project to ME and PN [78], and using a highly specific cGnRH-II antiserum GnRH neurons were revealed in the midbrain tegmentum and fiber endings in the pars intermedia [unpublished]. Differential distribution of GnRHs has been described in the brain of bony fishes as well [see 45, 47]. Recently, ring dove brain has been shown to contain GnRH-like material-containing nonneuronal cells [88]. Characterized as mast cells, component of the immune system, they are distributed mainly in the medial habenula. This interesting finding could be leading to investigate other vertebrate groups as well.

How does brain GnRH reach the target organs? In

tetrapods GnRH is conveyed to the pituitary via the hypothalamo-hypophyseal portal vessels; however, there are evidences to indicate that GnRH can also be secreted into the cerebral ventricles as well as in brain vessels. In bony fishes, which lack the ME, GnRH neurons are found to directly innervate pituitary gonadotropes. In elasmobranchs, the ventral lobe of the pituitary does not receive a portal supply, and GnRH is evidently released into the general circulation, where, in fact, GnRH and GnRH-binding protein molecules have been determined [83]. In cyclostomes, King *et al.* [48] have suggested that GnRH can be released into the third ventricle and transported by tanycytes to the pituitary; GnRH may also reach pituitary by simple diffusion from neuronal projections in the PN. In elasmobranchs, GnRH may reach pituitary and gonads via general circulation, and its presence has been ascertained in the cerebrospinal fluid [86, 107]. In tetrapods and bony fishes, GnRH can act on the gonads as a paracrine regulatory factor, and the idea is reinforced by the presence of GnRH-like molecules as well as of GnRH-binding sites in the gonads [27, 32, 35].

GnRH neurons have been described in the terminal nerve of mammals, birds, amphibians, and bony and cartilaginous fishes [19, 23, 64, 67, 103]. Fibre projections from these neurons may reach areas as far ahead as nasal capsule and as far behind as rhombencephalon, except the pituitary [69, 103]. In the dwarf gourami, a bony fish, using whole brain *in vitro*, it was shown that terminal nerve GnRH neurons may be the most extensively projecting GnRH cells in the brain [69]. Reptiles and cyclostomes remain the only vertebrate taxa in which GnRH neurons have not been described yet in the terminal nerve. In cyclostomes, however, the presence of a terminal nerve-like structure is still a question of debate.

Besides the brain and terminal nerve, GnRH-like material has been detected in a variety of other structures: gonads, mammary gland, tumor cells, human placenta and pancreas, follicular fluid, milk, olfactory epithelium, sympathetic ganglia, adrenal gland, liver, intestine and retina [10, 12, 35, 44]. GnRH-like material outside the brain and terminal nerve may be similar to or different than one of the GnRH variants characterized in the brain.

ONTOGENESIS

The embryonic origin(s) of GnRH neurons has received considerable interest in recent years. Several reports have described that these neurons, unique among brain cells, originate not in the brain but in the olfactory placode and migrate into the forebrain/diencephalon along the olfactory/terminal nerve. The extracranial origin, time course and route of GnRH neuronal migration has been clarified in some species of mammals, birds and amphibians [19, 64, 65, 84, 92]. In birds and urodele amphibians, this line of evidence has been confirmed by surgical removal of the olfactory placode which results in the elimination of GnRH neurons in the forebrain and diencephalon [1, 63, 64]. In anuran amphibians, however, the midbrain-located group of GnRH neurons is supposed to have an intracranial origin [18, 65, unpublished data]. Among tetrapods, the reptilian GnRH neuronal system is morphologically "atypical" in that GnRH neurons are mainly located in the midbrain and infundibulum [57], and they are not considered to have an extracranial origin [unpublished data]. Interestingly, the midbrain cluster of GnRH neurons is the first to appear during lizard ontogenesis, followed by their appearance in the infundibulum; we argue that these neurons may take origin in the nearby neuroepithelium [unpublished data]. However, the ontogenesis of GnRH neuronal system in reptiles need be investigated in more species to unequivocally clarify the intracranial origin of GnRH neurons in this group. In a bony fish, *Pterophyllus scalare*, the first ontogenetic appearance of GnRH-immunoreactive cells in the pituitary precedes that in the POA and this may be indicative of still another site of origin for GnRH-producing cells [16]. No information on the extracranial origin of GnRH neurons in the brain is available for cyclostomes; in this group Muske [64] suggests another line of origin of the POA-located GnRH neurons, and that is from the ventricular ependyma because of the periventricular localization of GnRH cell bodies. Needless to say, the phylogenetic picture of the embryonic origin of GnRH neuronal systems in the vertebrate brain is far from complete.

Biochemical and ultrastructural differentiation of GnRH neurons, during their olfactory placode-forebrain migration, has been analyzed in the mouse [54], in which GnRH gene is expressed early in ontogenesis [107] and the differentiation of GnRH neurons continues and is coordinated during migration. In this mammal, however, axonal projections are formed only upon entering the forebrain. In contrast, in the rhesus monkey axonal projections are elaborated while GnRH neurons are still in the nasal septum [82]. Similarly, in the chick [92] and newt [19] GnRH axons are seen in the terminal/olfactory nerve during early migratory stage. Prior to migration GnRH neurons are scattered as individual cell bodies in the placode, while during migration they come to lie in close apposition, as confirmed by electron microscopy [92, 110]. Cell-to-cell contact appears to be established when these neurons are located at the adult site. The nature of these contacts must be investigated at the ultrastructural level.

During ontogenesis, besides the morphological and biochemical changes, a remarkable change may also occur in the number of GnRH neurons. In the mouse, in fact, GnRH cell number decreases drastically in the last stages of migration [110], and it is suggested that programmed cell death may be one reason, or that after migration some neurons stop synthesizing GnRH and become undetectable by ICC. There is the need for further investigation as well as the necessity to draw more vertebrate groups in this repertoire.

CORRELATES OF BIOSYNTHETIC AND SECRETORY ACTIVITY, AND FUNCTIONS

Morphological and biochemical correlates

Indeed, the basic theme of investigations related to the morphological, histochemical and biochemical correlates of GnRH secretion and functions has almost always been around the age, sex and reproductive status-related changes in the hypothalamo-hypophyseal-gonadal system. The various steps are, in sequence, comprised of the identification of GnRH-like material in the brain, morphology, distribution and ontogenesis of the GnRH neuronal system, anatomical connections with the pituitary, and an analysis of the GnRH content in the brain, ME, portal blood and systemic circulation under different conditions. Among the central regulatory mechanisms involved in the control of the development of the hypothalamo-hypophyseal-gonadal axis until sexual maturity, the importance of GnRH has been emphasized in all vertebrates [see 31, 98, 104]. In the adult, besides the pulsatile pattern of GnRH secretion, abundantly referred to in mammals, insight into the functional relationships of the hypothalamo-hypophyseal-gonadal system is also gained through evaluating seasonal pattern of GnRH secretion [see 3, 26, 28, 80]. Among tetrapods GnRH content has been evaluated in tissue extract as well as in portal blood, and only in bony and cartilaginous fishes has the radioimmunoassayble GnRH been determined in general circulation [47, 73].

It has hitherto been demonstrated that GnRH neurons undergo morphological, distributional and numerical changes associated with the developmental stage and reproductive status of the animal. Prominent seasonal cycles in GnRH cell morphology are observed in a variety of vertebrates [see 78, 98, 108]. It is evident that a particular morphological feature of the GnRH neuron may be correlated with a particular aspect of reproduction. In hibernating mammals, degranulation of GnRH cells occurs during hibernation, and increased storage after arousal. In the male Djungarian hamster, there occurs an increase in the number of unipolar neurons correlated with the onset of puberty, whereas bipolar GnRH neurons increase only in postpubertal period [108]. An ultrastructural analysis of GnRH neurons in the pony brain has, furthermore, indicated that irregularly-contoured cells in the POA/organum vasculosum lamina terminalis may have higher synthetic activity as compared to most other neurons, and it is suggested that GnRH neurons may utilize ultrashort feedback [59]. In the Syrian hamster, it was ascertained that the inhibitory effects of short days on the reproductive axis are mediated through a suppression of GnRH neurons which, in turn, is reflected as an increase in the net content of GnRH within the brain [97]. In the cow, a quantitative light microscopical study describing morphological changes in GnRH neurons supports the hypothesis of reduced activity of GnRH neurons during early to middle stages of the puerperium [51] which is in line with the concept of postpartum infertility due to the suckling stimulus-mediated suppression of GnRH, and consequently of LH, secretion.

Functions

In all major vertebrate groups, the effects of exogenous GnRH/$GnRH_A$ have been investigated *in vivo* and *in vitro*. These comprise stimulation of pituitary GtH and, in some cases, growth hormone secretion, stimulation of pituitary-thyroid axis, gonadal steroidogenesis, gametogenesis, spermiation, ovulation, and sexual behavior. However, extremely varied experimental protocols, as well as different GnRH forms and/or $GnRH_A$ have been used, and thus it becomes rather arduous to unify these data in order to draw generalized considerations. Nevertheless, all native GnRH variants appear to have at least one characteristic in common, and that is the stimulation of GtH release from the pituitary. A series of studies have also provided evidences that naturally occurring GnRH variants may exhibit different biological potencies in different species in terms of their ability to enhance pituitary GtH secretion [see 10, 53, 73].

In a variety of mammals, including man, and in the domestic fowl, reproductive function can be inhibited by a prolonged treatment with GnRH/$GnRH_A$ [93, 94]. In the adult, initially, GnRH administration enhances pituitary GtH secretion but a continuous exposure to GnRH eventually leads to desensitization of the pituitary to GnRH with the consequent suppression of gonadal function [102]. It is also known that GnRH/$GnRH_A$ exert a differential control over FSH and LH. This may be credited to the fact that GnRH is released in pulses, inducing a pulsatile pattern of LH release, but not of FSH. Nonetheless, chronic GnRH treatment suppresses both LH and FSH. In contrast, in amphibians, it was demonstrated that pituitary is relatively resistant to desensitization due to chronic *in vivo* GnRH exposure which enhances GtH biosynthesis and secretion [53, 89]. However, in the goldfish GnRH desensitization has been reported [34]. Further, in some mammals and birds evidences are that, during ontogenesis, GnRH plays a role in the development of pituitary gonadotropes, and that GnRH, at least in the rat, is important for maintaining FSH synthesis [see 9, 104].

Differential distribution, distinct roles

Do naturally occurring GnRH variants play distinct roles? The answer is yet far from clear. However, it is becoming increasingly evident that native GnRHs are differentially distributed within the brain of jawed vertebrates [13, 21, 43, 46, 61, 96]. In the musk shrew, and some species of birds, reptiles, amphibians and bony fishes a quantitative predominance of cGnRH-II is found not in the forebrain, but in the midbrain and/or hindbrain, and this has led to the assertion that cGnRH-II may have an extrapituitary role. However, a specific role for this form has not yet been established. In birds, in which cGnRH-I seems to predominate in the forebrain/hypothalamus, it is argued that the potential function of cGnRH-I and II may diverge early in development [43, 60]. Among amphibians, based upon the

predominance of mGnRH in the hypothalamus in *X. laevis* it was suggested that this variant may be the prime regulator of GtH release, whereas cGnRH-II, abundant in the hindbrain, may have an extrapituitary role [45]. In *R. esculenta*, however, it was suggested that cGnRH-II may have a hypophysiotropic activity [28]. Further, in this species it was also seen that cGnRH-I and II and mGnRH all enhanced androgen production in intact males, whereas in hypophysectomized males only cGnRH-II enhanced testicular androgen production, suggesting that a cGnRH-II-like molecule, produced in the testis, may be the local paracrine regulator of testicular activity [20, 79]. None of the tetrapod species studied is responsive to lGnRH [see 53], in terms of pituitary GtH secretion. However, lGnRH enhances plasma androgen levels in intact male frog [20]. In the forebrain/hypothalamus of fishes the predominant form varies from mGnRH, sGnRH to catfish or dogfish GnRH, making it evident that any of these variants may have a hypophysiotropic role. However, cGnRH-II neuronal endings may terminate in the bony fish pituitary [see 45]. Perhaps, in lower vertebrates the specificity of GnRH variants is very low. Lovejoy *et al.* [56] have proposed the division of known native GnRHs in two groups: mGnRH, cGnRH-I and catfish GnRH with hydrophilic residues, and cGnRH-II, sGnRH and dogfish GnRH with hydrophobic residues. They suppose that this may lead to clarify, on a structural basis, their distinct functional roles. Naturally, lGnRH is not included in this classification, being this variant present exclusively in cyclostomes.

Interaction with sex steroids

Among vertebrates, the repertoire of GnRH functions appears to be remarkably complex and involves interactions with several hormonal and other factors. GnRH acts upon the pituitary gonadotropes through interaction with membrane-associated high affinity receptors [14]. GnRH-modulated pituitary GtH secretion regulates gonadal activity and reproduction. Sex steroids in turn influence GnRH-regulated GtH biosynthesis and secretion. For this the sex steroid signals from the gonads must be correctly interpreted within the brain. Further, it is necessary to mention that GnRH regulation of pituitary GtH secretion can be modulated by sex steroids at the level of the pituitary as well, positively or negatively [see 71]. Although GnRH neurons do not appear to have sex steroid receptors, their distribution pattern has a remarkable overlapping with that of sex steroid-concentrating neurons, and the latter may even project to other brain areas in order to transmit steroid-influenced signals [10, 22, 25, 62, 74]. Most likely, the GnRH neurons which send their axon terminal in the ME are affected by estrogen-sensitive afferent neuronal systems. Indeed, GnRH neurons in such areas may represent targets for the feedback of steroids, and this is substantiated by a recent study in the rat, in which the rostral medial POA contains estrogen receptors and the GnRH neurons situated in this area are sensitive to estrogen treatment. Changes in GnRH neuronal mRNA levels in this area of estrogen-supplemented ovariectomized rats are taken as the cellular correlates of the positive feedback effects of estrogen on GnRH neurons [74]. This experimental model may be used to examine temporal changes in GnRH gene transcription, GnRH mRNA stability and GnRH translation all contributing to the understanding as to how estrogen triggers the preovulatory hypersecretion of GnRH which leads to LH surge followed by ovulation. However, in the meanwhile pituitary sensitivity to GnRH is enhanced by preovulatory progesterone surge. Similarly, in *R. esculenta*, in which sex steroid-concentrating neurons abound in the anterior POA, gonadectomy in both sexes caused a severe quantitative depletion of GnRH neurons in this area, as evaluated by ICC [41]. Sex steroid-replacement therapy enhanced somal accumulation of immunoreactive material, indicative probably of an increased synthesis and storage. In *R. catesbeiana*, it is suggested that GnRH can enhance pituitary GtH secretion in juveniles, but biosynthesis of GtH is enhanced only at a later time, coincident with gonadal steroid production [90]. These authors suggest that androgens may augment GnRH receptor molecules in the pituitary as well as endogenous secretion of GnRH in the hypothalamus. It thus appears that GnRH-stimulated GtH release is influenced not only by age, sex, season or morpho-functional heterogeneity of pituitary gonadotropes, but also by sex steroids [see 89, 90, 96].

External factors

Of the behavioral cues, courtship enhances GnRH concentration in the terminal nerve in a urodele amphibian [76], whereas in the ring dove, it determines the appearance of nonneuronal GnRH-containing cells in the habenula [88], thus making it obvious that GnRH-producing brain areas may be differentially correlated with diverse reproductive aspects in different species.

An upsurge in interest in the implication of odours in animal reproduction dates long-long back, and it is widely contended that reproductive activity is dependent upon a fully functional olfactory system, and that pheromone signals can be transduced by terminal nerve GnRH system to influence reproductive activity through the modulation of GnRH secretion in the hypothalamus [22, 23, 91]. This concept is strengthened by the fact that limbic (hypothalamus, amygdala, hippocampus, POA) and olfactory systems indeed control reproductive behavior, and extensive GnRH projections between the terminal nerve and limbic systems are well placed to create a chain through the olfactory mucosa, brain, pituitary, and on to the gonad. In a recent study on the electrical activity and morphology of terminal nerve-GnRH neurons in the dwarf gourami, it was shown that these neurons display an endogenous rhythmic discharge pattern, a feature common to all peptidergic and monoaminergic modulator neurons, but are not projected to the pituitary, and thus it was assumed that they do not function as a hypophysiotropic GnRH system, but rather as neuromodulator [69].

Neural modulation of GnRH release and function

Besides the fact that GnRH neurons display neuroendocrine as well as neuromodulator function, their own secretory activity is influenced by multiple neurotransmitters and/or neuromodulators. Only recently is the pivotal importance of such relationhips becoming fully appreciated. Indeed, there are evidences to indicate that several neural circuits are involved in controlling the GnRH neuronal systems. Transmitters and modulators of importance include GABA (γ-amino butyric acid), neuropeptide-Y (NPY), neurotensin, catecholamines, FMRFamide, endogenous opioid peptides (EOP), and others. All these circuits may provide important inputs to the GnRH system and some of them might contain excitatory as well as inhibitory input to GnRH system. It is also conceivable that one or the other component may, in turn, be influenced pre-synaptically by other neural circuits or factors, like sex steroids, cytokines etc. In mammals, GnRH-induced LH release *in vivo* is potentiated by NPY, either probably as a paracrine regulator (NPY neurons may synapse on GnRH neurons in the POA), or through enhancing the binding of GnRH to pituitary GnRH receptors [8, 70]; NPY secretion is enhanced by the preovulatory surge of sex steroids, and in turn it stimulates GnRH secretion. GnRH enhances intracellular calcium levels through openining voltage-sensitive calcium channels and this post-receptor GnRH action is also potentiated by NPY [15]. A number of investigations has suggested that EOPs can act as powerful inhibitors of GtH release acting by primarily decreasing the amplitude of GnRH pulses, and are in turn influenced by gonadal steroids [5, 8]. EOP-containing neurons may communicate with GnRH neural circuitry by adjusting locally the influx of excitatory adrenergic signals along the hypothalamo-hypophyseal axis. There is evidence that corticotropin-releasing hormone (CRF) may deplete GnRH neuronal activity through central opioidergic pathways, although direct effects are also likely to occur [2]. In the rat, dopamine can inhibit calcium ionophore-induced GnRH release [49]. In the goldfish, GnRH release from the POA is inhibited by dopamine and enhnaced by noradrenaline [73]. Noradrenaline, however, may be excitatory to GnRH in the presence of estrogens and inhibitory in their absence [33]. GnRH release and GnRH gene expression can be markedly inhibited by cytokines and the effects may be direct or mediated by opioids and prostaglandins [81]. GABAergic fibers are reported to directly innervate GnRH neuronal cells and until recently this provided morphological basis for a role of the GABAergic system in the regulation of GnRH secretion. Recently, however, Li and Pelletier [52] have shown that the use of $GABA_A$ receptor agonists inhibit not only the release of GnRH but also GnRH gene expression evaluated by ISHH. Simultaneous localization of multiple neuropeptides in the same brain section may yield useful information in relation to the modulation of GnRH neuronal activity on part of the complex neuronal circuitry in vertebrates. Neurons and fiber projections containing GnRH, FMRFamide and EOPs are interspersed in same brain areas and this may be the morphological substrate of physiological interactions between these systems [17, 38, 99, 100]. The coexistence of FMRFamide-like peptide and GnRH within the same neuron in a fish has provided morphological basis to suggest that FMRFamide may have an autocrine action on GnRH secretion [7]. The neural mechanisms involved in the stimulation or inhibition of GnRH release need further study.

Secretory mechanism

One exciting line of investigations is related to the study of neurosecretory mechanisms of GnRH neurons. Based on the conservation of ultrastructural features of differentiated neuroendocrine cells, the pulsatile manner of GnRH secretion and the presence of functional gap junctions in the GnRH neuronal cell line GT1-7 it has recently been suggested that gap junctional coupling between GnRH neurons may be the signalling machinery underlying periodic (pulsatile/circadian/seasonal) secretion of hypothalamic GnRH neuronal system [57]. GnRH-GnRH cell contacts, like synaptic organizations, have been described in mammals [58, 105], and are supposed to be involved in the synchronous activity of an entire population of GnRH neurons. Consequently, innervation of only a few GnRH neurons on part of another category of neuron may account for a cascade excitatory or inhibitory paracrine role of a neurotransmitter/neuromodulator/neuropeptide. At the same time, GnRH-GnRH contact will suggest an autocrine regulation within a GnRH-neuronal population. Taken together, the current data would suggest that a full understanding of the anatomical substrates of GnRH/other neuropeptides interactions may provide the key to the correct interpretation of functional studies.

Binding sites, receptors and mechanism of action

High affinity binding sites for GnRH/$GnRH_A$ have been demonstrated in the pituitary and/or gonads of several vertebrate groups, as well as in the mammalian placenta, adrenal gland and mammary carcinoma [see 10, 11, 27, 44, 45]. GnRH receptor in the mammalian pituitary cells has been characterized and cloned [72]. It is composed of seven transmembrane segments, a feature of G-protein-coupled receptors. Studies are needed to understand the role of G-proteins in mediating the effects of GnRH as well as the amino acid sequence of the GnRH receptor of nonmammalian vertebrates.

In studying the mechanism of action of GnRH on its targets, extracellular and intracellular Ca^{2+}, protein kinase C, inositol phosphates, calmodulin, leukotrienes and arachidonic acid have been implicated in the mediation of GnRH-induced GtH secretion [see 66]. GnRH acts upon the pituitary gonadotropes through specific high affinity membrane-bound receptors [14], by modifying the frequency and amplitude of action potentials generated spontaneously in gonadotropes [37]. In mammals, chronic GnRH/$GnRH_A$ treatment causes desensitization of the pituitary by down-

regulating pituitary GnRH receptors and simultaneously by uncoupling GnRH signal transduction system and inactivating voltage-sensitive Ca^{2+} channels [11, 36, 37, 64]. Among bony fishes, there are two lines of evidences, one supporting the participation of protein kinase C pathway in the mediation of GnRH-stimulated GtH release, while the other supports the involvement of cAMP pathway [see 41].

FINAL COMMENTS

1. The most logical inference that can be drawn from the rather bulky and somewhat bizzare repertoire of data is that a uniform methodological approach should be used throughout vertebrates. However, because of the existence of amazingly diverse situations related to reproduction, the morpho-functional charatecristics of the GnRH neuronal system of a vertebrate group can not necessarily be generalized and extrapolated to other vertebrates. The discrepancies over the identification and distribution of GnRH-like material in the brain and other tissues may depend upon methodological variations, and despite the recognition of inherent difficulties, isolation and sequence analysis of GnRH-like material from more vertebrate species are needed.

2. A relevant amount of studies has provided the basis for additional investigations to fully resolve the questions of how GnRH regulates pituitary-gonadal activity, and reproduction as whole, involving direct GnRH effects on these organs as well as factors (hormonal and not) which in turn influence GnRH system. In relation to the last point it is imperative to clarify whether the stimulatory/inhibitory effects are exerted both on GnRH secretion and biosynthesis, and if there exists a direct relationship between alteration in GnRH release and biosynthesis. Moreover, in ICC analyses of reproductive status-related changes, corresponding ultrastructural studies are required to define whether diminished immunoreactivity is due to decreased biosynthesis or enhanced secretion and, *vice versa*, increased immunoreactivity is owing to an increased biosynthesis or a decline in release.

3. Although there have been some investigations, the potential importance of GnRH on the ontogenesis and postnatal development of pituitary gonadotropes is far from understood. Nevertheless, it is clear that an analysis of the number and distribution pattern of GnRH neuronal subtypes may turn out to be useful in understanding the ontogenetic mechanisms and the potential (differential) role of regional subpopulations of GnRH neurons in the process of sexual maturation. It is also conceivable that embryonic migration of GnRH neurons into the forebrain from the nasal area continues in the postnatal/posthatching/pro and postmetamorphosis period, and it is possible that precocious migration includes undifferentiated cells from the olfactory placode that are capable of division and differentiation at the time of sexual maturation/puberty. Future studies may involve more vertebrate species and, hopefully, be aimed to provide details not only about the extra- and intracranial migratory course of GnRH neurons and the developmental stage at which GnRH neurons reach their adult position, but also on the differential localization of GnRH neurons and processes showing immunoreactivity for different GnRH forms.

4. Morphological, distributional and molecular heterogeneity of GnRH render the variety of roles played by this neuropeptide plausible. There are GnRH receptor sybtypes in the pituitary which has made it possible to ascertain that C-terminal fragments of GnRH, or GAP, or $GnRH_A$ may have similar effects as GnRH itself. Much remains to be done before more concrete inferences may be drawn.

5. Besides electrophysiological methods to study the activity of individual neurons, it is argued that changes in mRNA levels reflect changes in neuronal activity. The availability of quantitative ISHH technique allows for measuring changes in mRNA levels in individual neurons. However, the current methods used to measure GnRH content and GnRH mRNA may not be sensitive enough to detect small changes in GnRH secretion. Hopefully, in the forthcoming years more sophisticated technologies will emerge which will allow us to reveal, record and interpret the electro-chemical and molecular signals released by individual GnRH neurons. There is a total dearth of information on the role of the genome in modulating GnRH neuronal activity. To date only one putative gene has been cloned in all species examined, and it is of comfort that ISHH unveils GnRH gene transcription and expression in neurons where GnRH itself is revealed by ICC.

6. It is hoped that latest studies will stimulate collaborative research among physiologists, biochemists, molecular biologists, genetists, neurobiologists and comparative endocrinologists to unveil the yet "secret" world of GnRH.

ACKNOWLEDGMENTS

The authors' personal research cited here has been supported by grants (40% and 60%) from M.U.R.S.T. and National Research Council (grant n. 93.00392.CT04) of Italy. A debt of gratitude is extended to Professor Joseph T. Bagnara for his ongoing support and advice. Thanks are also due to Dr Judy A. King, Professor V. Botte and Dr B. D'Aniello for useful suggestions.

REFERENCES

1 Akutsu S, Takada M, Ohki-Hamazaki H, Murakami S, Arai Y (1992) Origin of luteinizing hormone-releasing hormone neurons in the chick embryo: effect of the olfactory placode ablation. Neurosci Lett 142: 241–244

2 Almeida OFX, Nikolarakis KE, Sirinathsinghji DJS, Hertz A (1989) Opioid-mediated inhibition of sexual behavior and luteinizing hormone secretion by corticotropin-releasing hormone. In "Brain Opioid Systems in Reproduction" Ed by RG Dyer, RJ Bicknell, Oxford University Press, Oxford, pp 149–164

3 Amano M, Aida K, Okumoto N, Hasegawa Y (1992) Changes in salmon GnRH and chicken GnRH-II contents in the brain and pituitary, and GtH contents in the pituitary in female Masu salmon, *Oncorhynchus masou*, from hatching

through ovulation. Zool Sci 9: 375–386

4 Anderson AC, Tonon M-C, Pelletier G, Conlon JM, Fasolo A, Vaudry H (1992) Neuropeptides in the amphibian brain. Int Rev Cytol 138: 89–210

5 Angioni S, Nappi RE, Genazzani AD, Carunchio P, Criscuolo M, Guo A-L, Bidzinska B, Petraglia F (1993) Brain opioids and reproductive function. In "Cellular Communication in Reproduction" Ed by F Facchinetti, IW Henderson, R Pierantoni, A Polzonetti-Magni, J Endocrinol Ltd, Bristol, pp 33–40

6 Barry J, Hoffman GE, Wray S (1985) LHRH-containing systems. In "Handbook of Chemical Neuroanatomy Vol 4" Ed by A Bjorklund, T Hokfelt, Elsevier, Amsterdam, pp 166–215

7 Batten TFC, Cambre ML, Moons L, Vandesande F (1990) Comparative distribution of neuropeptide-immunoreactive systems in the brain of the green molly, *Poecilia latipinna*. J Comp Neurol 302: 893–919

8 Bauer-Dantoin AC, Knox KL, Schwartz NB, Levine JE (1993) Estrous cycle stage-dependent effects of neuropeptide Y on luteinizing hormone (LH)-releasing hormone-stimulated LH and follicle-stimulating hormone secretion from anterior pituitary fragments in vitro. Endocrinology 133: 2413–2417

9 Blake CA, Gary TC, Mascagni F, Culler MD, Negro-Vilar A (1993) Effects of injection of anti-luteinizing hormone (LH)-releasing hormone serum and anti-gonadotropin-releasing hormone-associated peptide serum into neonatal rats on LH and follicle-stimulating hormone cells. Biol Reprod 49: 965–971

10 Chieffi G, Pierantoni R, Fasano S (1991) Immunoreactive GnRH in hypothalamic and extrahypothalamic areas. Int Rev Cytol 127: 1–55

11 Clayton RN (1989) Gonadotropin-releasing hormone: its actions and receptors. J Endocrinol 120: 11–19

12 Clayton RN, Eccleston L, Gossard F, Thalbard J-C, Morel G (1992) Rat granulosa cell expression of the gonadotropin-releasing hormone gene: evidence from *in situ* hybridization histochemistry. J Mol Endocrinol 9: 189–195

13 Conlon JM, Collin F, Chiang YC, Sower SA, Vaudry H (1993) Two molecular forms of gonadotropin-releasing hormone from the brain of the frog, *Rana ridibunda*: purification, characterization, and distribution. Endocrinology 132: 2117–2123

14 Conn PM, Huckle WR, Andrews WV, McArdle GA (1987) The molecular mechanisms of action of gonadotropin-releasing hormone (GnRH) in the pituitary. Rec Prog Horm Res 43: 29–61

15 Crowley WR, Shah GV, Carroll BL, Kennedy D, Dokher ME, Kalra SP (1990) Neuropeptide Y enhances luteinizing hormone (LH)-releasing hormone-induced LH release and elevation in cytosolic Ca^{2+} in rat anterior pituitary cells: evidence for involvement of extracelular Ca^{2+} influx through voltage-sensitive channels. Endocrinology 127: 1487–1494

16 D'Aniello B (1994) Il GnRH nell'ontogenesi dei vertebrati: analisi immunoistochimica. Doctorate Thesis, University of Naples "Federico II"

17 D'Aniello B, Imperatore C, Fiorentino M, Vallarino M, Rastogi RK (1994) Immunocytochemical localization of POMC-derived peptides (adrenocorticotropic hormone, α-melanocyte stimulating hormone and β-endorphin) in the pituitary, brain and olfactory epithelium of the frog, *Rana esculenta*, during development. Cell Tissue Res, (in press)

18 D'Aniello B, Masucci M, di Meglio M, Ciarcia G, Rastogi RK (1991) Distribution of gonadotropin-releasing hormone-like peptides in the brain during development of juvenile male *Rana esculenta*. Cell Tissue Res 265: 51–55

19 D'Aniello B, Masucci M, di Meglio M, Iela L, Rastogi RK (1994) Immunohistochemical localization of GnRH in the crested newt (*Triturus carnifex*) brain and terminal nerve: a developmental study. J Neuroendocrinol 6: 167–172

20 D'Antonio M, Fasano S, de Leeuw R, Pierantoni R (1992) Effects of gonadotropin-releasing hormone variants on plasma and testicular androgen levels in intact and hypophysectomized male frogs, *Rana esculenta*. J Exp Zool 261: 34–39

21 Dellovade TL, King JA, Millar RP (1993) Presence and differential distribution of distinct forms of immunoreactive gonadotropin-releasing hormone in the musk shrew brain. Neuroendocrinology 58: 166–177

22 Demski LS (1984) The evolution of neuroanatomical substrates of reproductive behavior: sex steroid and LHRH-specific pathways including the terminal nerve. Am Zool 24: 809–830

23 Demski LS (1987) Phylogeny of luteinizing hormone-releasing hormone system in protochordates and vertebrates. In "The Terminal Nerve (Nervus Terminalis) Structure, Function, and Evolution Vol 519" Ed by LS Demski, M Schwanzel-Fukuda, Ann NY Acad Sci, pp 1–14.

24 di Meglio M, Masucci M, D'Anillo B, Iela L, Rastogi RK (1991) Immunohistochemical localization of multiple forms of gonadotropin-releasing hormone in the brain of the adult frog. J Neuroendocrinol 3: 363–368

25 di Meglio M, Morrell JI, Pfaff DW (1987) Localization of steroid-concentrating cells in the central nervous system of the frog, *Rana esculenta*. Gen Comp Endocrinol 67: 149–154

26 Fahien CM, Sower SA (1990) Relationship between brain gonadotropin-releasing hormone and final reproductive period of the adult male sea lamprey, *Petromyzon marinus*. Gen Comp Endocrinol 80: 427–437

27 Fasano S, de Leeuw R, Pierantoni R, Chieffi G, van Oordt PGWJ (1990) Characterization of gonadotropin-releasing hormone (GnRH) binding sites in the pituitary and testis of the frog, *Rana esculenta*. Biochem Biophys Res Commun 168: 923–932

28 Fasano S, Goos HJTh, Janssen C, Pierantoni R (1993) Two GnRHs fluctuate in correlation with androgen levels in the male frog *Rana esculenta*. J Exp Zool 266: 277–283

29 Gautron JP, Patton E, Bauer K, Kordon C (1991) (Hydroxyproline^9) luteinizing hormone-releasing hormone: a novel peptide in mammalian and frog hypothalamus. Neurochem Inter 18: 221–235

30 Gautron JP, Patton E, Leblanc P, L'HSitier A, Kordon C (1993) Preferential distribution of C-terminal fragments of (Hydroxyproline^9)LHRH in the rat hippocampus and olfactory bulb. Neuroendocrinology 58: 240–250

31 Goos HJTh (1993) Pubertal development: big questions, small answers. In "Cellular Communication in Reproduction" Ed by F Facchinetti, IW Henderson, R Pierantoni, A Polzonetti-Magni, J Endocrinol Ltd, Bristol, pp 11–20

32 Goubau S, Bond CT, Adelman JP, Misra V, Haynes MF, Murohy BD (1992) Partial characterization of the gonadotropin-releasing hormone (GnRH) gene transcript in the rat ovary. Endocrinology 130: 3098–4000

33 Grossmann R, Dyer RG (1989) Opioid inhibition of brainstem projections to the medial preoptic area in female rats. In "Brain Opioid Systems in Reproduction" Ed by RG Dyer, RJ Bicknell, Oxford University Press, Oxford, pp 112–124

34 Habibi HR (1991) Homologous desensitization of gonadotropin-releasing hormone (GnRH) receptors in the goldfish pituitary: effects of native GnRH peptides and a synthetic GnRH antagonist. Biol Reprod 44: 275–283

35 Habibi HR, Prati D (1993) Endocrine and paracrine control of ovarian function: role of compounds with GnRH-like activity in goldfish. In "Cellular Communication in Reproduction" Ed

by F Facchinetti, IW Hendersen, R Pierantoni, A Polzoneti-Magni, J Endocrinol Ltd, Bristol, pp 59–70

36 Hazum E, Conn PM (1988) Molecular mechanisms of gonadotropin-releasing hormone (GnRH) action. I. The GnRH receptor. Endoc Rev 9: 379–386

37 Heyward PM, Chen C, Clarke IJ (1993) Gonadotropin-releasing hormone modifies action potential generation in sheep pars distalis gonadotropes. Neuroendocrinology 58: 646–654

38 Hoffman GE, Fitzsimmons MD, Watson Jr RE (1989) Relationship of endogenous opioid peptide axons to GnRH neurones in the rat. In "Brain Opioid Systems in Reproduction" Ed by RG Dyer, RJ Bicknell, Oxford University Press, Oxford, pp 125–134

39 Iela L, D'Aniello B, di Meglio M, Rastogi RK (1994) Influence of gonadectomy and steroid hormone-replacement therapy on the gonadotropin-releasing hormone neuronal system in the anterior preoptic area of the frog (*Rana esculenta*) brain. Gen Comp Endocrinol (in press)

40 Iela L, Rastogi RK, Bagnara JT (1991) Reproduction in the Mexican leaf frog, *Pachymedusa dacnicolor*. V. Immunohistochemical localization of gonadotropin-releasing hormone in the brain. Gen Comp Endocrinol 84: 129–134

41 Jobin RM, Ginsberg J, Matowe WC, Chang JP (1993) Down-regulation of protein kinase C levels leads to inhibition of GnRH-stimulated gonadortopin secretion from dispersed pituitary cells of goldfish. Neuroendocrinology 58: 2–10

42 Karten MI, Rivier JE (1986) Gonadotropin-releasing hormone analog design. Structure function studies toward the development of agonists and antagonists. Rationale and perspective. Endoc Rev 7: 44–66

43 Katz IA, Millar RP, King JA (1990) Differential regional distribution and release of two forms of gonadotropin-releasing hormone in the chicken brain. Peptides 11: 443–450.

44 King JA, Millar RP (1991) Gonadotropin-releasing hormones. In "Vertebrate Endocrinology: Fundamentals and Biomedical Applications Vol IV" Ed by PKT Pang, MP Schreibman, Academic Press, New York, pp 1–31

45 King JA, Millar RP (1992) Evolution of gonadotropin-releasing hormones. Trends Endocrinol Metab 3: 339–346

46 King JA, Steneveld AA, Millar RP (1993) Differential distribution of gonadotropin-releasing hormones in amphibian (clawed toad, *Xenopus laevis*) brain. Regulatory Peptides 50: 277–289

47 King JA, Steneveld AA, Millar RP, Fasano S, Romano G, Spagnuolo A, Zanetti L, Pierantoni R (1992) Gonadotropin-releasing hormone in elasmobranch (electric ray, *Torpedo marmorata*) brain and plasma: chromatographic and immunological evidence for chicken GnRH II and novel molecular forms. Peptides 13: 27–35

48 King JC, Sower SA, Anthony ELP (1988) Neuronal systems immunoreactive with antiserum to lamprey gonadotropin-releasing hormone in the brain of *Petromyzon marinus*. Cell Tissue Res 253: 1–8

49 Koike K, Kadowaki K, Hirota K, Ohmichi M, Ikegami H, Sawada T, Miyake A, Tanizawa O (1993) Prolactin stimulates (^{3}H) dopamine release from dispersed rat tubero-infundibular dopaminergic neurons and dopamine decreases gonadotropin-releasing hormone release induced by calcium ionophore. Acta Endocrinol 129: 548–553

50 Kuenzel WJ, Blahser S (1991) The distribution of gonadotropin-releasing hormone neurons and fibers throughout the chick brain (*Gallus domesticus*). Cell Tissue Res 264: 481–495

51 Leshin LS, Rund LA, Kraeling RR, Crim JW, Kiser TE (1992) Morphological differences among luteinizing hormone-releasing hormone neurons from postpartum and estrous cyclic cows. Neuroendocrinology 55: 380–389

52 Li S, Pelletier G (1993) Chronic administration of muscimol and pentobarbital decreases gonadotropin-releasing hormone mRNA levels in the male rat hypothalamus determined by quantitative in situ hybridization. Neuroendocrinology 58: 136–139

53 Licht P, Porter DA (1987) Role of gonadotropin-releasing hormone in regulation of gonadotropin secretion from amphibian and reptilian pituitaries. In "Hormones and Reproduction in Fishes, Amphibians, and Reptiles", Ed by DO Norris, RE Jones, Plenum, New York, pp 61–85

54 Livne I, Gibson MJ, Silverman A-J (1993) Biochemical differentiation and intercellular interactions of migratory gonadotropin-releasing hormone (GnRH) cells in the mouse. Dev Biol 159: 43–656

55 Loumaye E, Thorner J, Catt KJ (1982) Yeast mating pheromone activates mammalian gonadotrophs: evoltionary conservation of a reproductive hormone? Science 218: 1323–1325

56 Lovejoy DA, Fischer WH, Ngamvongchon S, Craig AG, Nahorniak CS, Peter RE, Rivier JE, Sherwood NM (1992) Distinct sequence of gonadotropin-releasing hormone (GnRH) in dogfish brain provides insight into GnRH evolution. Proc Natl Acad Sci USA 89: 6373–6377

57 Masucci M, D'Aniello B, Iela L, Ciarcia G, Rastogi RK (1992) Immunohistochemical demonstration of the presence and localization of diverse molecular forms of gonadotropin-releasing hormone in the lizard (*Podarcis s. sicula*) brain. Gen Comp Endocrinol 86: 81–89

58 Matesic DF, Germak JA, Dupont E, Madhukar BV (1993) Immortalized hypothalamic luteinizing hormone-releasing hormone neurons express a connexin 26-like protein and display functional gap junction coupling assayed by fluorescence recovery after photobleaching. Neuroendocrinology 58: 485–492

59 Melrose PA, Littlefiedl-Chabaud MA, Pickel C, French DD (1993) Regional differences in the sunbcellular characteristics and synaptic connections with gonadotropin-releasing hormone (GnRH) neurons in the basal forebrain of adult ponies: sex-dependent differences found at the beginning of the anovulatory season. Proc 13th Int Symp Equine Physiol Nutrition, Gainsville, Fl, pp 344–345

60 Millam JR, Craig-Veit CB, Petitte JN (1993) Brain content of cGnRH I and II during embryonic development in chickens. Gen Comp Endocrinol 92: 311–317

61 Millam JR, Faris PL, Yougren OM, El Halawani ME, Hartman BK (1993) Immunohistochemical localization of chicken gonadotropin-releasing hormones I and II (cGnRH I and II) in turkey brain. J Comp Neurol 333: 63–82.

62 Morrell JI, Pfaff DW (1981) Characterization of estrogen-concentrating hypothalamic neurons by their axonal projections. Science 217: 1273–1276

63 Murakami S, Kikuyama S, Arai Y (1992) The origin of the luteinizing hormone-releasing hormone (LHRH) neurons in newt (*Cynops pyrrhogaster*): the effect of olfactory placode ablation. Cell Tissue Res 269: 21–27

64 Muske LE (1993) Evolution of gonadotropin-releasing hormone (GnRH) neuronal systems. Brain Behav Evol 42: 215–230

65 Muske LE, Moore FL (1990) Ontogeny of immunoreactive gonadotropin-releasing hormone neuronal system in amphibians. Brain Res 534: 177–187

66 Naor Z (1990) Signal transduction mechanisms of Ca^{2+} mobilizing hormones: the case of gonadotropin-releasing hormone. Endocr Rev 11: 326–353

67 Norgren RB, Lippert J, Lehman MN (1992) Luteinizing

hormone-releasing hormone in the pigeon terminal nerve and olfactory bulb. Neurosci Lett 135: 201–204

68 Nozaki M, Tsukahara T, Kobayashi H (1984) Neuronal systems producing LHRH in vertebrates. In "Endocrine Correlates of Reproduction" Ed by K Ochiai, Y Arai, T Ohioda, M Takahashi, Springer, Berlin, pp 3–27

69 Oka Y, Matsushima T (1993) Gonadotropin-releasing hormone (GnRH)-immunoreactive terminal nerve cells have intrinsic rhythmicity and project widely in the brain. J Neurosci 13: 2161–2176

70 Parker SL, Kalra SP, Crowley WR (1991) Neuropeptide Y modulates the binding of a gonadotropin-releasing hormone (GnRH) analog to anterior pituitary GnRH receptor sites. Endocrinology 128: 2309–2316

71 Pavgi S, Licht P (1993) Inhibition of in vitro pituitary gonadotropin secretion by 17β-estradiol in the frog *Rana pipiens*. Gen Comp Endocrinol 89: 132–137

72 Perrin MH, Bilezikjian LM, Hoeger C, Donaldson CJ, Rivier J, Haas Y, Vale WW (1993) Molecular and functional characterization of GnRH receptors cloned from rat pituitary and mouse pituitary tumor cell line. Biochem Biophys Res Commun 191: 1139–1144

73 Peter RE, Habibi HR, Chang JP, Nahorniak CS, Yu KL, Huang YP, Marchant TA (1990) Actions of gonadotropin-releasing hormmone (GnRH) in goldfish. In "Progress in Clinical and Biological Researc. Progress in Comparative Endocrinology" Ed by A Epple, CG Scanes, MH Stetson, Wiley-Liss, New York, pp 393–398

74 Petersen SL, McCrone S, Shores S (1993) Localized changes in LHRH mRNA levels as cellular correlates of the positive feedback effects of estrogen on LHRH neurons. Am Zool 33: 255–265

75 Powell RC, Ciarcia G, Lance V, Millar RP, King JA (1986) Identification of diverse molecular forms of GnRH in reptile brain. Peptides 7: 1101–1108

76 Propper CR, Moore FL (1991) Effects of courtship on brain gonadotropin hormone-releasing hormone and plasma steroid concentrations in a female amphibian (*Taricha granulosa*). Gen Comp Endocrinol 81: 304–312

77 Rance NE, Young WS, McMullen NT (1994) Topography of neurons expressing luteinizing hormone-releasing hormone gene transcripts in the human hypothalamus and basal forebrain. J Comp Neurol 339: 573–586

78 Rastogi RK, di Meglio M, Iela L (1990) Immunoreactive luteinizing hormone-releasing hormone in the frog (*Rana esculenta*) brain: distribution pattern in the adult, seasonal changes, castration effects, and developmental aspects. Gen Comp Endocrinol 78: 444–458

79 Rastogi RK, Iela L (1992) Spermatogenesis in amphibia: dynamics and regulation. In "Sex Origin and Evolution" Ed by R Dallai, Mucchi Editore, Modena, Italy, pp. 231–249

80 Rhim T-J, Kuehl D, Jackson GL (1993) Seasonal changes in the relationships between secretion of gonadotropin-releasing hormone, luteinizing hormone, and testosterone in the ram. Biol. Reprod. 48: 197–204

81 Rivest S, Rivier C (1993) Interleukin-1β inhibits the endogenous expression of the early gene c-fos located within the nucleus of LHRH neurons and interferes with hypothalamus LHRH release during proestrous in the rat. Brain Res 613: 132–142

82 Ronnekleiv OK, Resko JA (1990) Ontogeny of gonadotropin-releasing hormone-containing neurons in early fetal development of rhesus macaques. Endocrinology 126: 498–511

83 Schally AV, Bajusz S, Redding TW, Zalatnai A, Comaru-Schally AM (1989) Analogs of LHRH: the present and the future. In "GnRH Analogues in Cancer and in Human Reproduction: Basic Aspects Vol 1" Ed by BH Vickery, V Lunenfeld, Kluwer, Dordrecht, pp 5–31

84 Schwanzel-Fukuda M, Pfaff DW (1989) Origin of luteinizing hormone-releasing hormone neurons. Nature 338: 161–164

85 Sherwood NM (1986) Evolution of a neuropeptide family: gonadotropin-releasing hormone. Am Zool 26: 1041–1054

86 Sherwood NM, Lovejoy DA (1993) Gonadotropin-releasing hormone in cartilaginous fishes: structure, location, and transport. Env Biol Fish 38: 197–208

87 Silverman A-J (1988) The gonadotropin-releasing hormone (GnRH) neuronal systems: immunocytochemistry. In "The Physiology of Reproduction Vol 2" Ed by E Knobil, J Neil, Raven Press, New York, pp 1283–1304

88 Silverman A-J, Millar RP, King JA, Zhuang X, Silver R (1994) Mast cells with gonadotropin-releasing hormone-like immunoreactivity in the brain of doves. Proc Natl Acad Sci USA 91 (in press)

89 Stamper DL, Licht P (1993) Further studies on the influence of GnRH on the biosynthesis of gonadotropins in female frogs (*Rana pipiens*) Gen Comp Endocrinol 92: 104–112

90 Stamper DL, Licht P (1994) Influence of androgen on the GnRH-stimulated secretion and biosynthesis of gonadotropins in the pituitary of juvenile female bullfrog, *Rana catesbeiana*. Gen Comp Endocrinol 93: 93–102

91 Stoddart DM (1990) The Scented Ape: The Biology and Culture of Human Odour. Cambridge University Press, pp 79–119

92 Sullivan KA, Silverman A-J (1993) The ontogeny of gonadotropin-releasing hormone neurons in the chick. Neuroendocrinology 58: 597–608

93 Tilbrook AJ, Galloway DB, Williams AH, Clarke IJ (1993) Treatment of young rams with an agonist of GnRH delays reproductive development. Horm Behav 27: 5–28

94 Tilbrook AJ, Johnson RJ, Eason PJ, Walsh DJ, Trigg TE, Clarke IJ (1992) Short-term reduction in egg production in laying hens treated with an agonist of GnRH. Br Poult Sc 33: 611–628

95 Trudau VL, Murthy CK, Habibi HR, Sloley BD, Peter RE (1993) Effects of sex steroid treatments on gonadotropin-releasing hormone-stimulated gonadotropin secretion from the goldfish pituitary. Biol Reprod 48: 300–307

96 Tsai PS, Licht P (1993) Differential distribution of chicken-I and chicken-II in the turtle brain. Peptides 14: 221–226

97 Urbanski HF, Doan A, Pierce M (1991) Immunocytochemical investigation of luteinizing hormone-releasing hormone neurons in Syrian hamster maintained under long or short days. Biol Reprod 44: 687–692

98 Urbanski HF, Doan A, Pierce M, Fahrenbach H, Collins PM (1992) Maturation of the hypothalamo-pituitary-gonadal axis of the male Syrian hamster. Biol Reprod 46: 991–996

99 Vallarino M, Feuilloley M, D'Aniello B, Rastogi RK, Vaudry H (1994) Distribution of FMRFamide-like immunoreactivity in the brain of the lizard *Podarcis sicula*. Peptides (in press)

100 Vallarino M, Salsotto-Cattaneo M, Vaudry H (1993) Immunohistochemical localization of FMRFamide-like peptides in the brain of the frog, *Rana esculenta*. In "Cellular Communication in Reproduction" Ed by F Facchinetti, IW Henderson, R Pierantoni, A Polzonetti-Magni, J Endocrinol Ltd, Bristol, pp 45–48

101 Van Gils J, Absil P, Grauwels L, Moons L, Vandesande F, Balthazart J (1994) Distribution of luteinizing hormone-releasing hormone (LHRH) (LHRH-I and -II) in the quail and chicken brain as demosntrated with antibodies directed against synthetic peptides. J Comp Neurol (in press)

102 Vickery BH (1986) Comparisons of the potential for therapeutic utilies with gonadotropin-releasing hormone agonists and antagonists. Endoc Rev 7: 115–124

103 Wirsig-Wiechmann CR (1993) Pripheral projections of nervus terminalis LHRH-containing neurons in the tiger salamander, *Ambystoma tigrinum*. Cell Tissue Res 273: 31–40

104 Woods JG, Honan MP, Thomas RC (1989) Hypothalamic regulation of the adenohypophyseal-testicular axis in the male chick embryo. Gen Comp Endocrinol 74: 167–172

105 Wray S, Grant P, Gainer H (1989) Evidence that cells expresing luteinizing hormone-releasing hormone mRNA in the mouse are derived from progenitor cells in the olfactory placode. Proc Natl Acad Sci USA 86: 8132–8136

106 Wright DE, Demski LS (1991) Gonadotropin hormone-releasing hormone immunoreactivity in the mesencephalon of sharks and rays. J Comp Neurol 307: 49–56

107 Wright DE, Demski LS (1993) Gonadotropin-releasing hormone (GnRH) pathways and reproductive control in elasmobranchs. Env Biol Fish 38: 209–218

108 Yellon SM, Newman SW (1991) A developmental study of the gonadotropin-releasing hormone neuronal system during sexual maturation in the male Djungarian hamster. Biol Reprod 45: 440–446

109 Yu KL, Sherwood NM, Peter RE (1988) Differential distribution of two moelcular forms of gonadotropin-releasing hormone in discrete brain areas of goldfish (*Carassius auratus*). Peptides 9: 625–630

110 Zheng L-H, Pfaff DW, Scwanzek-Fukuda M (1992) Electron microscopic identification of luteinizing hormone-releasing hormone-immunoreactive neurons in the medial olfactory placode and basal forebrain of embryonic mice. Neuroscience 46: 407–418

Note added in proof

In a redent study, Licht *et al.* [111] identified only cGnRH-II and mGnRH in the brain of three species of *Rana* (*pipiens, ridibunda* and *esculenta*). While both GnRHs were distributed in the telencephalon and diencephalon, only cGnRH-II was found in the cerebellum and medulla. In the platyfish, lGnRH, together with mGnRH and sGnRH was revealed by ICC in some cells of the pituitary gland of animals of all ages [112].

111 Licht P, Tsai P-S, Sotowska-Brochocka J (1994) The nature and distribution of gonadotropin-releasing hormones in brains and plasma of ranid frogs. Gen Comp Endocrinol 94: 186–198

112 Magliulo-Cepriano L, Schreibman MP, Blum V (1994) Distribution of variant forms of immunoreactive gonadotropin-releasing hormone and β-gonadotropins I and II in the platyfish, *Xiphophorus maculatus*, from birth to sexual maturity. Gen Comp Endocrinol 94: 135–150.

ZOOLOGICAL SCIENCE 11: 375–379 (1994)

Effects of Rapid Cooling on Heart Rate of the Japanese Lobster *in vivo*

MOTONORI NAKAMURA, MASAKI TANI and TAKETERU KURAMOTO

Shimoda Marine Research Center, Laboratory of Physiology
University of Tsukuba, Shimoda, Shizuoka 415, Japan

ABSTRACT—Seasonal changes of the effects of rapid cooling on the *in vivo* heart rate of the lobster, *Panulirus japonicus*, were studied. Cardiac activity was monitored with chronically implanted electrodes. The mean heart rate was 45.5±6.0 bts/min during winter and 99.5±7.5 bts/min during the other seasons at the same acclimation temperature (20±1°C). When the ambient temperature was lowered (0.1–1.0°C/min, dT=5-6°C), the heart rate decreased along a linear line in spring, summer and fall. The correlation ratio of the heart rate and temperature was 0.98 with the minimum rate of 67.0 ±12.0 bts/min. The Q_{10} value was 2.2. In contrast, the heart rate in winter decreased only for the initial few minutes of cooling and little for the later phase with the minimum rate of 28.8±9.5 bts/min. Q_{10} was 2.6. The correlation plots for the heart rate and temperature appeared to regress on two linear lines. The ratio was 0.88 in the range of 19–21°C and 0.41 in the range of 15–19°C. These data may suggest that the lobsters in winter have some compensatory mechanisms for a heart rate drop by cooling as well as for the mean heart rate, which are different from those in the other seasons.

INTRODUCTION

The heart rate of crustaceans changes with variations in ambient temperature within the normal environmental range. Temperature coefficient (Q_{10}) for the range of 10–20°C of the crustacean heart rate is around 2, measured *in vivo* for slow temperature changes ([24] for review, [10]). Even though marine lobsters live under mild temperature environment, they meet daily with a warm or cold water brought about by tidal cycle. Moreover, they suffer seasonal changes. Our preliminary experiments show that temperature of the lobster pericardium will follow the change in ambient temperature within 30 sec. Electromechanical coupling of muscle fibers becomes less efficient with decreasing temperature [8]. A compensation mechanism has been described for leg muscle activity of crabs [9]. It may be that the lobsters are equipped with compensation mechanisms in the heart activity for a rapid drop in temperature. Few studies on the heart response to rapid temperature changes in crustaceans have been reported [28]. However, the presence of compensation in heart rate has been still unclear.

In the present study, the influence of rapid cooling on heart rate *in vivo* is examined over all seasons using Japanese spiny lobsters. The behavior of heart rate in winter was different from that in the other seasons.

MATERIALS AND METHODS

Japanese spiny lobsters (*Panulirus japonicus*, around 200g in body weight, both sexes, n=8) were used. They were captured around Nabeta Bay (Izu Peninsula, Japan) in April and October and were reared in an indoor aquarium ($1.5\times4\times1 m^3$) where the fresh natural sea water was continuously supplied. Natural light (around 20k lx at noon) was provided *via* windows. Electrocardiogram (ECG) was recorded from the unrestrained animals with chronically implanted electrodes. The recording methods were similar to those described previously [13, 14]. The electrodes consisted of silver wires, which were introduced through small holes drilled in the carapace of the dorsal thorax and fixed in position with epoxy resin. Then each lobster with the electrodes mounted was kept in a tank ($25\times40\times30 cm^3$) for a month before being subjected to cooling experiment. They were fed on a diet of live *Mytilus*. Coral sands were laid on the bottom of the tank as suggested by Florey and Kriebel [10]. The sea water in the tank was aerated and stirred with air and water pumps, respectively. The acclimation temperature was 20± 1°C because seasonal changes of the sea water temperature in the aquarium have ranged from 15 to 25°C. To cool the animal, the sea water cooled at 5°C was poured into the tank and mixed by stirring. Water temperature was monitored with an electronic thermometer. The cooling rates (0.1–1.3°C/min) and magnitudes (dT=5–6°C) were determined by pouring rate and volumes of the cold sea water. During experiment, major part of the tank was covered with black screen to minimize disturbance. Electrical signals amplified were recorded on a video tape (DC-2K Hz). These measurements were performed once a week. The electrical recordings were played back to a pen recorder (100 Hz). The heart rate was counted by hand and/or with an electronic counter using pulses of ECG. Statistical analysis of the data was performed with a personal computer software (StatView II: Abacus Concepts, Inc.).

RESULTS

Beating patterns of the heart became constant at 2 weeks after the lobster was transferred into the experimental tank. Thus the acclimation period of a month was long enough for the lobster to adapt to the experimental conditions. Large variations of heart rate accompanying with the body movement and spontaneous bradycardia often occurred. However, it was possible to measure the rate in a stable state since the animal often kept quiescent for 10 or more minutes in daytime. Complete recordings of ECG *in vivo* were obtained frequently during cooling. However, only few recordings were reliable for both cooling and rewarming processes because the unrestrained lobsters moved vigorously

Accepted April 22, 1994
Received February 15, 1994

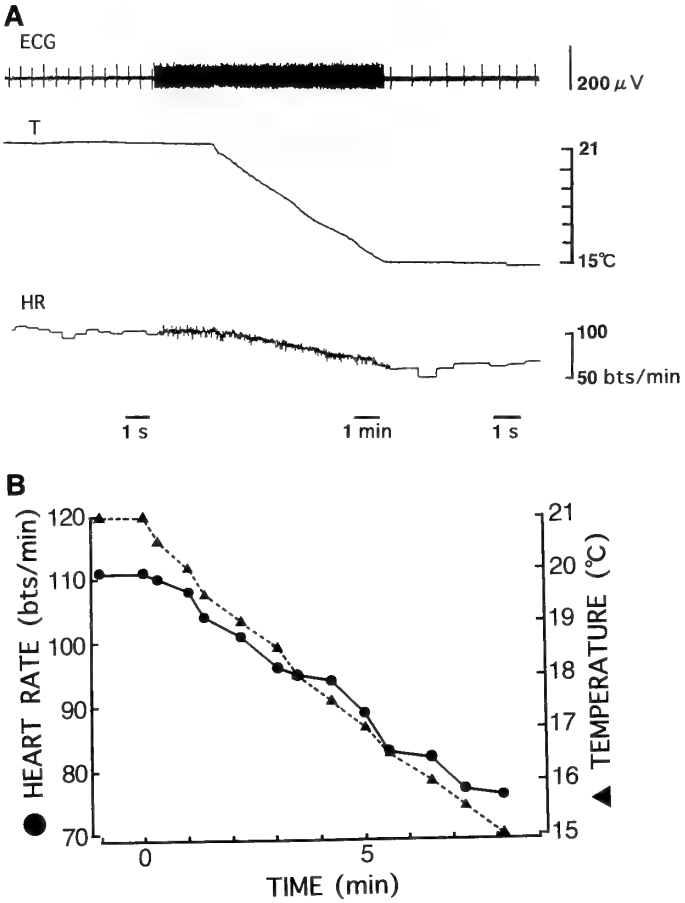

FIG. 1. Effects of cooling on the *in vivo* heart rate of the lobster in summer. A, a simultaneous recording of electrocardiogram (ECG, upper), ambient temperature (T, middle) and heart rate (HR, lower) displayed with fast and slow speeds. B, a graphic presentation of the heart rate change with decreasing temperature. Means of ten beats are successively plotted with the temperature. The data are from the same videotape recording shown in A.

during rewarming. Cooling rates ranged usually from 0.1 to 1.0°C/min and in few instances, to 1.3°C/min. Table 1 shows distributions of the heart rate measured from the 8 animals at 20±1°C and during cooling. At the acclimation temperature, the heart rate was 99.5±7.5 bts/min in the period from spring to fall while it was 45.5±6.0 bts/min in winter (December to February).

In spring, summer and fall, the heart rate decreased with the lowering of the ambient temperature (dT=5–6°C). Significant decreases in heart rate were observed by the lowering of temperature of more than 3°C and the minimum rate was 67.0±12.0 bts/min (Table 1). The heart rate recovered with rewarming. Moreover, a little higher heart rates (105–110 bts/min) than before cooling were often observed for a few minutes after the water temperature was resumed to 20±1°C (not shown in figure). Figure 1A shows an example of the ECG recordings obtained in June, where the ambient temperature was lowered from 21 to 15°C at the rate of 0.7°C/min. The mean values of ten heartbeats were plotted with the change in temperature in Figure 1B. The heart rate decreased with a rate of 4.5 bts/min, and a decrement of 6.4 bts/°C. Q_{10} for the range of 15–20°C of the heart rate was 2.2. These parameters did not change remarkably by the cooling rates within a range of 0.1–1.3°C/min (not shown in figure).

In winter, the heart rate decreased for the initial few minutes of cooling but did not for the later phase. Significant decreases in heart rate were observed by the lowering of temperature of more than 4°C and the minimum rate was 28.0±9.5 bts/min (Table 1). One of the ECG recordings obtained in February is shown in Figure 2A. The mean heart rate of each ten beats was plotted with the temperature in Figure 2B. In this case, the ambient temperature decreased from 21 to 16°C at the rate of 1.0°C/min but the decremental change of the heart rate against the temperature was small (3.2 bts/°C). Moreover, the heart rate did not

TABLE 1. Effects of cooling on heart rate of *P. japonicus*

Degree of cooling (dT °C)	Heart rate in seasons from spring to fall (Mean±SE bts/min)	Heart rate in winter (Mean±SE bts/min)
0.0	99.5± 7.5	45.5± 6.0
0.5	96.0±12.0	41.0± 5.0
1.0	97.0± 7.0	40.0± 5.0
1.5	92.0± 7.5	38.5± 9.0
2.0	89.0± 9.0	29.0± 5.0
2.5	84.0±11.5	31.0± 9.0
3.0	81.0±10.0	33.0±10.5
3.5	78.0± 9.0	29.0±10.0
4.0	76.0± 8.5	29.0± 8.5
4.5	73.0± 8.0	30.0±11.5
5.0	67.0±12.0	28.0± 9.5

Acclimation temperature was 20±1°C. Ambient temperature of the lobster was lowered to 16 or 15°C (dT=5°C). Spring: March to May. Summer: June to August. Fall: September to November. Winter: December to February. The cooling experiment was repeated four times per month from March, 1991 to February, 1993.

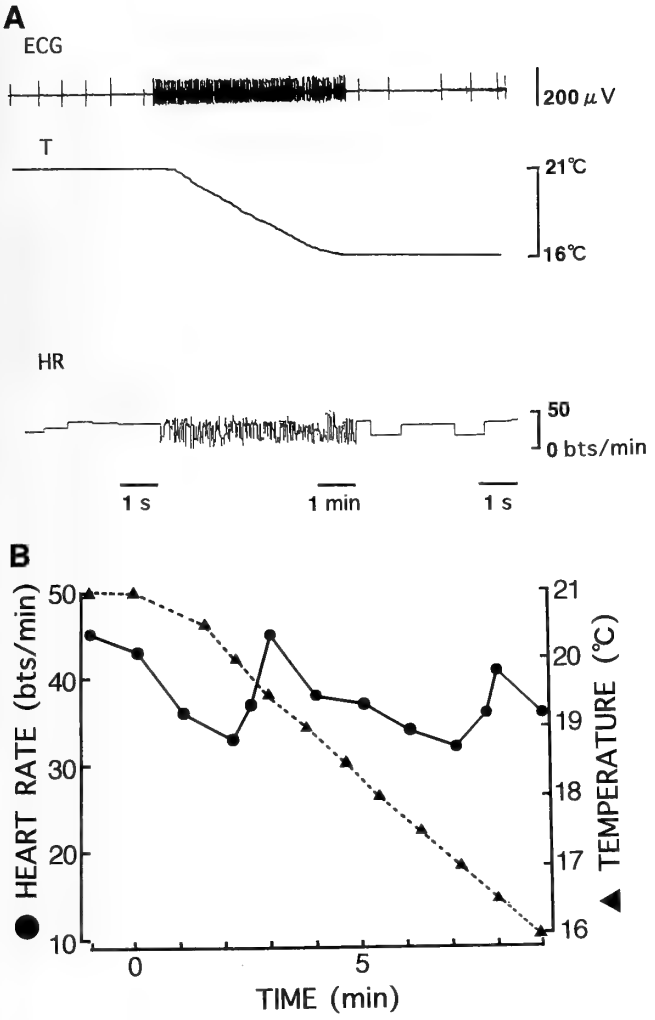

FIG. 2. Effects of cooling on the *in vivo* heart rate of the lobster in winter (14–2–1992). A, a simultaneous recording of ECG, ambient temperature (T) and heart rate (HR) displayed with fast and slow speeds. B, a graphic presentation of the heart rate change with decreasing temperature. Means of ten beats are successively plotted with the temperature. The data are from the same videotape recording shown in A.

always show a linear change with the decreasing temperature from 20 to 16°C. With rewarming, the heart rate returned and reached to a level of 5–10 bts/min higher than the initial rate before cooling (not shown in figure).

Correlation between the heart rate and temperature was analyzed statistically using the data shown in Table 1. In the period from spring to fall, the mean heart rates (68–99.5 bts/min) regressed on a positive linear line ($Y=6.43X-27.66$, $r=0.99$) within the temperature range of 15–20°C (Fig. 3a). In contrast, the mean heart rates in winter showed a lower value (28–45.5 bts/min) and regressed on another positive line ($Y=3.26X-26.38$, $r=0.88$) against the experimental temperature decrease (Fig. 3b). However, some plots digressed at around 19°C; the plots appeared to regress on two lines (Fig. 4A and B). The correlation ratio was 0.94 in the partial range of 19–21°C while it was 0.41 in the range of 15–19°C.

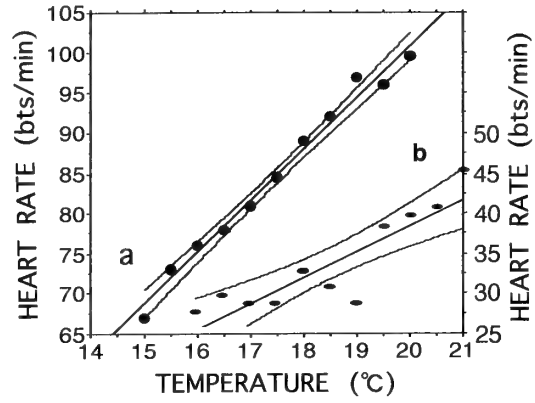

FIG. 3. Relationships between the heart rate and lowered temperature in the Japanese lobsters. The plots a, correlation between the mean heart rate and temperature measured during the period from spring to fall ($Y=6.43X-27.66$, $r=0.99$). The plots b, correlation between the mean heart rate and temperature measured during winter ($Y=3.26X-26.38$, $r=0.88$). A linear line and paired curves indicate the regression and 95% confidence bands for the true mean of the heart rate, respectively. The all data shown in Table 1 are used.

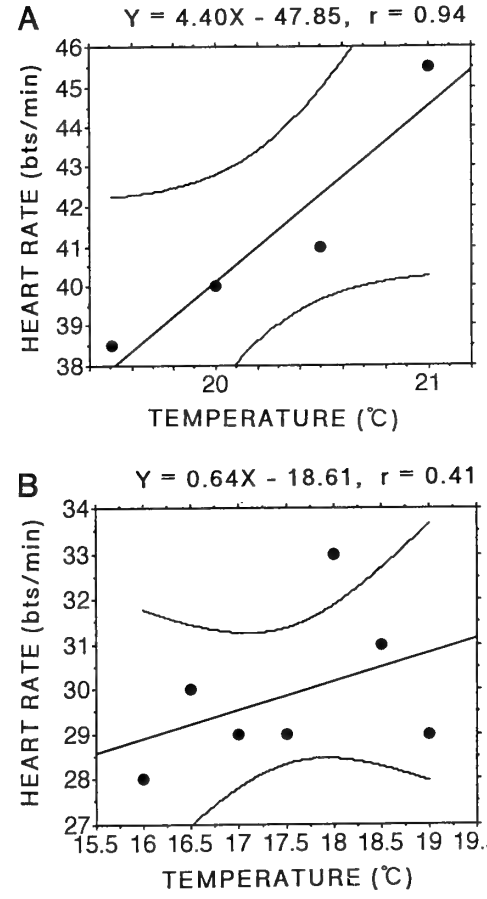

FIG. 4. The heart rate drop with cooling of the winter lobsters. A, the correlation between the mean heart rate and temperature in the range of 19.5–21°C. B, the correlation between the mean heart rate and temperature in the range of 15.5–19.5°C. A straight line and paired curves indicate the regression and 95% confidence bands for the true mean of the heart rate, respectively. The same data as shown in Fig. 3b are used.

DISCUSSION

The mean heart rate (45.5 bts/min) in winter was as low as half of that (99.5 bts/min) in the other seasons at the same acclimation temperature (Table 1). In *P. japonicus*, the heart rate around 60 bts/min is unstable both *in vivo* and *in vitro* [22]. In both the shrimp and the crayfish, the mean heart rate is lowered when reared under dark conditions [11, 23]. Since the lobsters used had been under natural light, they might perceive the decreases in both light dose and period toward winter. Therefore, the conditions of illumination may cause to lower the heart rate to 45.5 bts/min in winter lobsters. However, this idea is not acceptable at present because the experiments to prove it will be necessary.

The lobster heart in the pericardium is suspended by the ligaments and the arteries. The ligaments are associated with the pericardial alary muscles while the arteries with the pericardial septum, the circumference of which contains muscle fibers ([24] for review, [1]). These pericardial muscles are innervated by the segmental nerves coming from the thoracic ganglia [1]. Thus, the central nervous system (CNS) probably controls the heart rate *via* the suspensory elements mechanically. The importance of the suspensory elements for heart pumping activity has been noticed by several authors ([24, 25] for reviews, [13]). Meanwhile, we have observed that the beat rate of the isolated lobster heart is determined by pulling of the suspensory elements as well as filling pressure ([15], unpublished data). Therefore, the seasonal difference in heart rate levels *in vivo* might be determined by the degree of tension of the suspensory elements controlled by the pericardial muscles and the CNS.

The lobster heart *in vivo* is also controlled centrally *via* the dorsal nerves and the pericardial neurohemal organs [1–3, 26, 27]. The nervous control might contribute to the rapid change in heart rate observed frequently as fluctuations ([13, 14], Figs.1A and 2A). The pericardial organs of lobsters contain monoamines (serotonin, octopamine and dopamine) and peptides (proctolin and FMRFamide-related peptides) ([6] for review, [12, 29, 30]). The pericardial hormones slowly augment the beat of isolated lobster heart for minute-long periods [5, 17, 18]. By internal cooling of the body, the pericardial organs of *P. japonicus* are activated and probably release the pericardial hormones [21]. Even under the low temperature, octopamine markedly enhanced the beat rate and amplitude of the isolated heart [20]. Therefore, octopamine released from the pericardial organs could activate the *in vivo* heart under the low temperature. The pericardial peptides also may activate the *in vivo* heart [31, 32] but their actions under low temperature have not yet been proved.

The cooling rate of 1°C/min is faster than that applied to decapod crustaceans by others [7, 10, 28]. Despite of the rapid cooling, the Q_{10} value for the lobster heart rate was around 2, similar to that reported in the crab [10]. Thus we failed to find the effect of rapid cooling on the Q_{10} value. When the water temperature was resumed, however, the heart rate was often higher than that before cooling. This may suggest that the heart activation occurs during cooling and still continues during rewarming.

The Q_{10} between 10 and 25°C in the crustacean heart rate has been constant with an average value of about 2 while the Q_{10} of 3–5 has been often observed between 5 and 10°C ([24] for review). This indicates that the chemical pacemaking processes in the heart are enhanced under the cold conditions. The Q_{10} for the range of 15–20°C of the lobster heart rate was 2.6 in winter while it was 2.2 in summer. Moreover, the correlation between the heart rate and the lowered temperature was weaker in winter than in the other seasons (Fig. 3). Even if the starting heart rate was different, the decrease in heart rate against the same drop in temperature is much slow in winter (Fig. 4). It is therefore suggested that the heart activation for the cooling may occur markedly in winter.

The lobster cardiac muscle develops tension by excitatory junction potentials generated by motor neurons in the cardiac ganglion [4, 15, 19]. Tension produced in the myocardium is fed back to the cardiac ganglion since the cardiac neurons are sensitive for filling pressure ([24] for review, [15–18]). Thus, the responses of the heart to cooling should be explained by activities of the cardiac neurons and muscle fibers. The studies using the isolated hearts and their nerve-muscle preparations are in progress.

ACKNOWLEDGMENTS

The authors thank the staff of Shimoda Marine Research Center for supporting the present study. Contribution No. 569 from Shimoda Marine Research Center.

REFERENCES

1 Alexandrowicz JS (1932) The innervation of the heart of the crustacea. I. Decapoda. Q J Microsc Sci 75:181–249

2 Alexandrowicz JS (1953) Nervous organs in the pericardial cavity of the decapod Crustacea. J Mar Biol Ass UK 31: 563–580

3 Alexandrowicz JS, Carlisle DB (1953) Some experiments on the function of the pericardial organs in Crustacea. J Mar Biol Ass UK 32: 175–192

4 Anderson M, Cooke IM (1971) Neural activation of the heart of the lobster *Homarus americanus*. J Exp Biol 55: 449–468

5 Beltz BS, Kravitz EA (1986) Aminergic and peptidergic neuromodulation in crustacea. J Exp Biol 124: 115–141

6 Cooke IM, Sullivan RE (1982) Hormones and neurosecretion. In "THE BIOLOGY OF CRUSTACEA Vol. 3" Ed by HL Atwood, DC Sandeman, Academic Press, New York, pp 205–391

7 Dauscher H, Flindt R (1969) Vergleichende Untersuchungen zur Herztäigkeit bei freibeweglichen dekapoden Krebsen (*Astacus fluviatilis* Fab., *Astacus leptodactylus* Escholz und *Cambarus affinis* Say.). Z vergl 62: 291–300

8 Dudel J, Ruedel R (1968) Temperature dependency of electromechanical coupling in crayfish muscle fibres. Pflüer Arch 301: 16–30

9 Fisher L, Florey E (1981) Temperature effects on neuromuscular transmission (opener muscle of crayfish, *Astacus leptodactylus*). J Exp Biol 94: 251–268

10 Florey E, Kriebel ME (1974) The effects of temperature, anoxia and sensory stimulation on the heart rate of unrestrained crabs. Comp Biochem Physiol 48A: 285–300

11 Hara J (1952) On the hormones regulating the frequency of the heart beat in the shrimp, *Paratya compressa*. Annot Zool Jap 25: 162–171

12 Kobierski LA, Beltz BS, Trimmer BA, Kravitz EA (1987) FMRFamidelike peptides of *Homarus americanus*: distribution, immunocytochemical mapping, and ultrastructural localization in terminal varicosities. J Comp Neurol 266: 1–15

13 Kuramoto T (1990) Cardiac activity and pressure change in the lateral pericardium of the unrestrained lobster, *Panulirus japonicus*. Physiol Zool 63: 182–190

14 Kuramoto T (1993) Cardiac activation and inhibition involved in molting behavior of a spiny lobster. Experientia 49: 682–685

15 Kuramoto T, Ebara A (1984) Effects of perfusion pressure on the isolated heart of the lobster, *Panulirus japonicus*. J Exp Biol 109: 121–140

16 Kuramoto T, Ebara A (1985) Effects of perfusion pressure on the bursting neurones in the intact or segmented cardiac ganglion of the lobster, *Panulirus japonicus*. J Neurosci Res 13: 569–580

17 Kuramoto T, Ebara A (1988) Combined effects of 5-hydroxytryptamine and filling pressure on the isolated heart of the lobster, *Panulirus japonicus*. J Comp Physiol B 158: 403–412

18 Kuramoto T, Ebara A (1991) Combined effects of octopamine and filling pressure on the isolated heart of the lobster, *Panulirus japonicus*. J Comp Physiol B 161: 339–347

19 Kuramoto T, Kuwasawa K (1980) Ganglionic activation of the myocardium of the lobster, *Panulirus japonicus*. J Comp Physiol 139: 67–76

20 Kuramoto T, Nakamura M (1992) Effects of cooling on the heart beat of the Japanese lobster *in vitro*. Zool Sci 9: 1217

21 Kuramoto T, Tani M (1994) Cooling-induced activation of the pericardial organs of the spiny lobster, *Panulirus japonicus*. Biol Bull Mar Biol Lab Woods Hole 186: 319–327

22 Kuramoto T, Yamagishi H (1990) Physiological anatomy, burst formation, and burst frequency of the cardiac ganglion of crustaceans. Physiol. Zool, 63: 102–116

23 Larimer JL, Tindel JR (1966) Sensory modifications of heart rate in crayfish. Anim Behav 14: 239–245

24 Maynard DM (1960) Circulation and heart function. In "The Physiology of CRUSTACEA Vol. 1" Ed by TH Waterman, Academic Press, New York, pp 161–214

25 McMahon BR, Wilkens JL (1983) Ventilation, perfusion, and oxygen uptake. In "THE BIOLOGY OF CRUSTACEA Vol 5" Ed by LH Mantel, Academic Press, New York, pp 290–372

26 Shimahara T (1969a) The inhibitory synaptic potential in the cardiac ganglion cell of the lobster, *Panulirus japonicus*. Sci Rpt Tokyo Kyoiku Daigaku B14: 9–26

27 Shimahara T (1969a) The effect of the acceleratory nerve on the electrical activity of the lobster cardiac ganglion. Zool Mag 78: 351–355

28 Spaargaren DH, Achituv Y (1977) On the heart rate response to rapid temperature changes in various marine and brackish water crustaceans. Neth J Sea Res 11: 107–117

29 Sullivan RE, Friend BJ, Barker DL (1977) Structure and function of spiny lobster ligamental nerve plexuses: evidence for synthesis, storage and secretion of biogenic amines. J Neurobiol 8: 581–605

30 Timmer BA, Kobierski LA, Kravitz EA (1987) Purification and characterization of FMRFamidelike immunoreactive substances from the lobster nervous system: isolation and sequence analysis of two closely related peptides. J Comp Neurol 266: 16–26

31 Wilkens JL, McMahon BR (1992) Intrinsic properties and extrinsic neurohormonal control of crab cardiac hemodynamics. Experientia 48: 827–833

32 Yazawa T, Kuwasawa K (1992) Intrinsic and extrinsic neural and neurohumoral control of the decapod heart. Experientia 48: 834–840

ZOOLOGICAL SCIENCE 11: 381–384 (1994)

Effectiveness of Metoclopramide, Domperidone and Ondansetron as Anti-emetics in the Amphibian, *Xenopus laevis*

TOMIO NAITOH, MOTOKO MATUURA and RICHARD J. WASSERSUG*

Department of Biology, Shimane University, Matsue 690, Japan

ABSTRACT—We examined the effectiveness of three anti-emetic agents—metoclopramide, domperidone (both dopamine antagonists) and ondansetron (a $5HT_3$ receptor antagonist)—in the frog *Xenopus laevis*. Apomorphine and cisplatin were used to induce emesis. All three anti-emetics significantly retarded emesis when induced by apomorphine. The drugs, however, were not effective against cisplatin induced emesis in the limited dosage range that we examined. Paradoxically, both metoclopramide and domperidone themselves induced vomiting in some frog specimens at dosages where they retarded apomorphine-induced emesis in others.

Xenopus laevis appears to be particularly sensitive to a variety of emetic challenges. Our results suggest that neural mechanisms involved in the control of emesis in amphibians and mammals are similar, although there are differences in the sensitivity of frogs and mammals to emetic and anti-emetic agents. Since *Xenopus* is an easy frog to maintain and breed in captivity, it may be valuable as an alternative model to mammals in the pharmaceutical search for effective anti-emetic agents.

INTRODUCTION

We report here on the anti-emetic properties of three drugs in the African clawed frog, *Xenopus laevis*. Two are well established, anti-emetic, dopamine antagonists: metoclopramide and domperidone. The third, ondansetron, is a newer 5-HT_3 receptor antagonist, also an effective anti-emetic in man and other mammals (see "Proceedings of the Ondansetron Symposium" In European Journal of Cancer & Clinical Oncology 25 (Suppl. 1), 1989. Pergamon Press, Oxford).

There are two reasons for specifically exploring their effects in a lower vertebrate. The first is to understand the evolution and development of emesis in vertebrates in general. Some animals (e.g. dogs, cats, certain primates) have a well developed emetic response whereas others, such as rats, are incapable of vomiting [1], even when exposed to a strong emetic challenge. Similarly, in some organisms such as anurans (frogs and toads), the ability to vomit is linked to developmental stage [5]. The neural bases for these taxonomic and developmental differences are not known. We reasoned that similarity in the response to both emetic and anti-emetic agents among diverse vertebrates would provide indirect evidence of similar underlying neurochemical mechanisms.

There is a second, more applied reason for undertaking this study. If it can be shown that the neural mechanisms controlling emesis are conserved in vertebrate evolution, then lower vertebrates may serve as a convenient alternative to carnivorous mammals or primates in pharmaceutical research directed at improving anti-emetic therapies.

We have used the African clawed frog *Xenopus laevis* for our investigation because it is easy to breed and maintain in captivity. It is the most common amphibian used in research around the world.

MATERIALS AND METHODS

Xenopus laevis adults were initially purchased from a commercial dealer. They were maintained in the laboratory on fish food pellets, then bred. The animals used in our experiments were either from the parental stock or from subsequent generations. All of the frogs used were either adults or young that had fed freely and exhibited normal growth since metamorphosis. Both males and females were used. The frogs ranged in wet mass from 3.9–12.7 g as juveniles, 39.7–103.0 g as adult females, and 29.0–58.8 g as adult males (plus two sub-adult males of 18.9 and 25.1 g); however, only animals of similar size were used in any one experiment.

An hour or less before each experiment, the frogs were fed pieces of beef liver that weighed approximately 1.0–2.6% of the frog's wet mass. Ejection of this bolus of food was used to indicate emesis. No frogs were used more than once.

Nausea was promoted by either apomorphine hydrochloride (Sigma, St. Louis) or cisplatin (Bristol-Myers Squibb, Tokyo). Both are well known emetics. The former stimulates dopamine receptors and its effectiveness in mammals is inhibited by dopamine antagonists, like domperidone [7]. The latter is commonly used in chemotherapy for cancer patients.

The apomorphine was dissolved in 0.65% NaCl and injected into the dorsal lymph sac at a dose of 20μg per g wet body weight, following methods outlined in Naitoh *et al.* [4]. The cisplatin, made up for injection, was administered by similar injection at dosages of 0.5 to 100μg per g body weight. The absolute volume of any drug injection did not exceed 200μl/g. In all cases, where the frogs were subjected to these emetic agents, concurrent controls were injected with 0.65% NaCl, distilled water, or lactic acid solution (as appropri-

Accepted May 10, 1994
Received February 15, 1994
* Present address: Department of Anatomy and Neurobiology, Sir Charles Tupper Medical Building, Dalhousie University, Halifax, Nova Scotia, B3H 4H7, Canada

ate) and similarly observed (Fig. 1).

Metoclopramide monohydrochloride (Sigma, St. Louis), domperidone (Sigma, St. Louis) and ondansetron, in the form of ondansetron hydrochloride dihydrate (Glaxo Group Research Ltd., Greenford) were compared for their anti-emetic properties. Metoclopramide monohydrochloride dissolved in 0.65% NaCl, which had previously been shown to delay apomorphine-induced emesis in *X. laevis* [4], was administered at dosages of 10, 30, and 60μg per g body weight. The domperidone was administered at dosages of 1.0, 10 and 20μg per g body weight. Because domperidone solubility is pH sensitive, it was dissolved in 2.5% lactic acid solution. This was further diluted to equal 10μg/μl and the final dosages (as shown in Fig. 1) were made from that solution by additional dilution with distilled water. The ondansetron, which was also dissolved in 0.65% NaCl, was administered at dosages of 0.01, 0.1 and 1.0μg per g body weight. The specific dosages used in each experiment are noted in the figures and Results. Anti-emetic agents were administered by injection into the dorsal lymph sac anywhere from 3 hr to 30 min before or after the emetic administration. The order and times of all drug administrations are similarly noted in Figures 1–2 and the Results.

Some frogs were injected with ondansetron without apomorphine or cisplatin to determine whether this putative anti-emetic agent had any intrinsic emetic effects in and of itself.

For the first 4 hr after apomorphine administration and 10 hr after cisplatin administration, the frogs were observed continuously for ejected vomitus. After that they were observed at least once an hour for an additional two hours. If the frogs had not vomited by

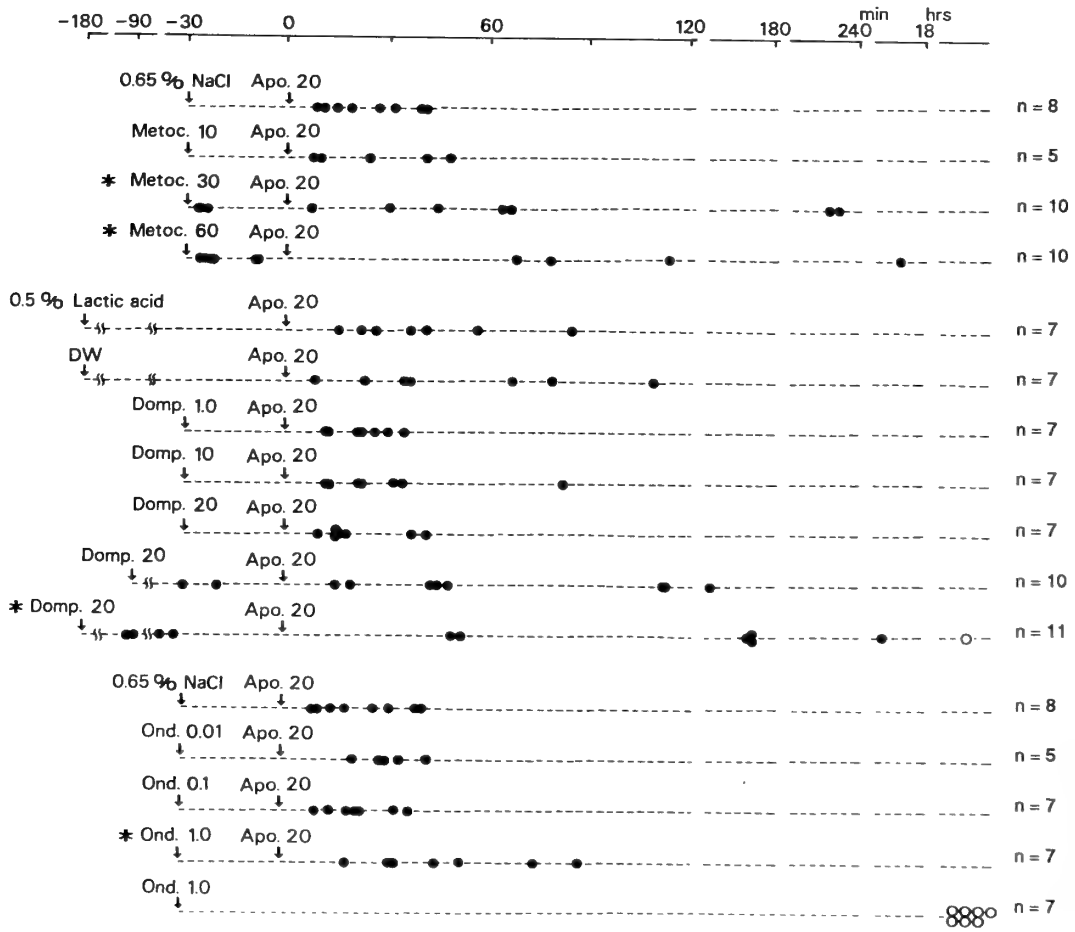

FIG. 1. Apomorphine-induced emesis in the frog *Xenopus laevis* and its inhibition by metoclopramide monohydrochloride (top), domperidone (middle) and ondansetron hydrochloride dihydrate (bottom). "Apo. 20" indicates administration of 20μg/g apomorphine hydrochloride. "DW" is distilled water. Each circle equals one frog; a solid circle indicates that an individual vomited at that time, open circles indicate individuals that did not vomit. Asterisks indicate statistically significant inhibition ($P<0.05$) of emesis in frogs which received both an anti-emetic and apomorphine compared to controls, shown at the top of each section. *Top*: "Metoc. 10", "Metoc. 30" etc. indicate times for the administration of 10, 30 and 60μg/g metoclopramide monohydrochloride, respectively. *Middle*: "Domp. 1.0", "Domp. 10" etc. indicate times for the administration of 1.0, 10 and 20μg/g domperidone, respectively. *Bottom*: "Ond. 0.01", " Ond. 0.1" etc. indicate times for the administration of 0.01, 0.1 and 1.0μg/g ondansetron hydrochloride dihydrate, respectively. The number of frogs used in each test is given to the right. The control tests in the *top* and *bottom* sections, labeled "0.65% NaCl Apo. 20", are one and the same. The data indicate that all three anti-emetics can significantly retard the onset of apomorphine-induced emesis at selected dosages, but metoclopramide and domperidone themselves induced emesis in some of the specimens. The time of vomiting for those particular specimens is indicated on the time lines to the left of the time when apomorphine was injected into the remaining specimens. Specimens that reacted to the anti-emetics alone were removed from the study once they vomited and were not further treated with apomorphine.

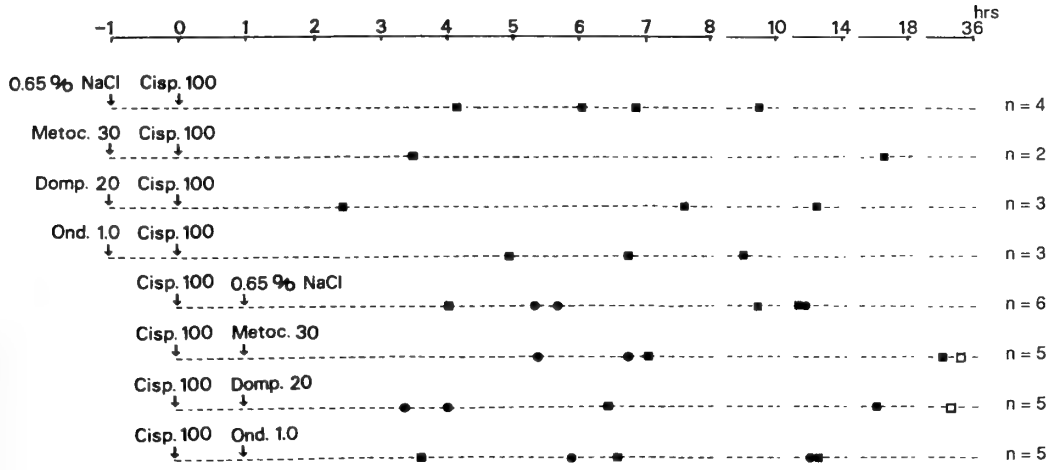

FIG. 2. Cisplatin-induced emesis in the frog *Xenopus laevis* and the effort to inhibit it with metoclopramide monohydrochloride, domperidone and ondansetron hydrochloride dihydrate. "Cisp. 100" indicates administration of 100μg/g cisplatin. The symbols are the same as in Fig. 1 except that squares indicate juvenile frogs and a solid square indicates that an individual vomited at that time, whereas an open square indicated no emesis. Again, the number of frogs used in each test is given to the right. "Metoc. 30", "Domp. 20" and "Ond. 1.0" indicate, respectively, the times when 30μg/g metoclopramide monohydrochloride, 20μg/g domperidone and 1.0μg/g of ondansetron hydrochloride dihydrate were administered. Although these dosages were most effective against apomorphine-induced emesis (Fig. 1), they were not effective against cisplatin.

then, they were intermittently checked for an additional day, at which point the experiment was terminated. All experiments were performed between 18–26.5°C. Statistical significance in the responses of the frogs was assessed with the non-parametric, Mann-Whitney U test.

Except for some preliminary tests, all experiments concerning apomorphine-induced vomiting were performed in December through March and the studies with cisplatin ran from November until March. A total of 148 frogs were used in these experiments. As indicated by the circles and squares in Figures 1 and 2, sample sizes for each individual anti-emetic test ranged from five to eleven for apomorphine-induced vomiting and from two to six for cisplatin-induced vomiting at any single dosage. Certain frogs, noted on the left side of Figure 1, vomited after injection with either metoclopramide or domperidone, but before exposure to apomorphine. These frogs were not treated with apomorphine. The time that they vomited was recorded in Figure 1 and then they were removed from the study.

RESULTS

Figure 1 (top) confirms that apomorphine is an effective emetic in *X. laevis*, as has been reported previously by Naitoh *et al.* [5]. Metoclopramide did not block this drug-induced emesis at the lowest dosages tested (=10μg/g), but it did significantly ($P<.05$) delay onset of apomorphine-induced emesis at the next two higher dosages (i.e. 30 and 60μg/g). A disturbing side effect of metoclopramide was that at all dosages for which it was effective against apomorphine-induced emesis, it was itself emetic in certain individual frogs. The mean latency period for metoclopramide-induced emesis, at dosages of 30μg/g or higher, was 9.1 min (see left side of Fig. 1, top section). This contrasts with a mean latency period of 28.8 min for apomorphine at 20μg/g, or more than three times as long as with metoclopramide.

A similar pattern is seen for domperidone (Fig. 1, middle section). This drug significantly ($P<.05$) delayed apomorphine-induced emesis, but, once again, only at dosages where it was itself an emetic (i.e. 20μg/g). Domperidone differed from metoclopramide in the speed with which it induced emesis in *Xenopus*. Although our sample of domperidone-induced emesis (n=2+4; left side of Fig. 1, lines 10 and 11, respectively) was smaller than for metoclopramide-induced emesis (n=3+6; left side of Fig. 1, lines 3 and 4, respectively) and the dosages were not exactly the same, the data suggest that domperidone takes from one half to two hours longer to induce emesis (Fig. 1).

Ondansetron, in contrast to the previous two anti-emetics, did not induce emesis itself at pharmacologically effective dosages. With dosages at or below 0.1μg/g ondansetron did not significantly inhibit or delay apomorphine induced emesis (Fig. 1, bottom section). At the next highest dosage tested, 1.0μg/g, ondansetron did significantly retard apomorphine-induced emesis ($P<.05$).

Cisplatin, at dosages of 30μg/g and higher, induced emesis in the frog as it does in mammals. Response times ranged from 3.5 hr up to 23 hr after the cisplatin administration. This anti-cancer agent did not provoke vomiting at dosages of 15μg/g or lower (in 15 frogs, not shown in Fig. 2). The response of *Xenopus* to cisplatin was more delayed and more variable than its response to apomorphine (cf. top of Fig. 1 with top of Fig. 2).

None of the three anti-emetic agents proved effective against emesis induced by 100μg/g dosages of cisplatin; i.e. the dosage that was most effective against apomorphine (Fig. 2). No differences in the sensitivity to or effectiveness of these drugs was noted depending on whether small (juvenile)

or large (adult) frogs were used. Two protocols were tried —one where the anti-emetic agent was presented one hour before the cisplatin and the other where the order of presentation was reversed. No differences between the two administrative regimes were observed.

DISCUSSION

Our data suggest that both the dopamine antagonists, metoclopramide and domperidone, and the 5-HT_3 antagonist, ondansetron, are anti-emetic agents in amphibians. This result is consistent with those of mammals where metoclopramide and domperidone [11] and the 5-HT_3 antagonist ICS 205–930 [2] are effective in inhibiting apomorphine-induced vomiting. As a 5-HT_3 receptor antagonist, ondansetron is a fundamentally different type of anti-emetic than either domperidone or metoclopramide [9]. The fact that it works as an anti-emetic in *Xenopus* suggests that the same or similar serotonin-based, as well as dopamine-based, neural pathways, associated with emesis in mammals, occur in frogs. Recently we have demonstrated that frogs, like mammals, are susceptible to motion-induced emesis [10]. Collectively these observations raise the prospect that frogs may serve as an alternative model to mammals in emesis and anti-emesis research, where financial or societal considerations restrain mammalian use.

The dosage ranges over which *Xenopus* responds to emetic and anti-emetic medications are not the same as for mammals, but it is difficult to directly compare dosages between homeothermic and poikilothermic vertebrates. The fact is that the *Xenopus* showed an emetic response to virtually all of the drugs that we experimented with, excluding the controls and the ondansetron. It is noteworthy that metoclopramide and domperidone, in particular, could themselves induce emesis in some frogs (although when they did not, they remained effective anti-emetics against apomorphine). This suggests that these frogs are particularly sensitive to certain emetic challenges, though the paradoxical emetic response induced by anti-emetics is not restricted to amphibians. Dogs may vomit in response to elevated dosages of domperidone [6] and ondansetron [8], and ferrets in response to the 5-HT_3 antagonist, zacopride [3].

The drug sensitivity of anurans may be viewed as a positive attribute in an animal being considered as a model species in emetic and anti-emetic research. In the same vein, it must be realized that cisplatin, as a cytotoxic agent, is a far more potent drug than apomorphine. The fact that none of the anti-emetics were effective in preventing or retarding emesis induced by cisplatin testifies to the toxicity of this agent in amphibians. Anti-emetics may still be effective against cisplatin-induced emesis in anurans, but more research would be necessary to establish the most effective time course for presenting the anti-emetics in relation to the emetic administration.

This work was conducted following the "Guiding Principles for the Care and Use of Animals in the Field of Physiological Sciences" set by the Physiological Society of Japan.

ACKNOWLEDGMENTS

This research was supported by funds from the Ministry of Education, Science and Culture (Japan), the Natural Science and Engineering Council (Canada) and the Japan Science and Technology Fund (Canada). We thank Glaxo Group Research Limited (Greenford) and Bristol-Myers Squibb KK (Tokyo) for supplying us with ondansetron and cisplatin, respectively. The draft manuscript profited from critical comments by B. M. Bain, L. Bourque, M. Fejtek and S. Pronych.

REFERENCES

1 Daunton NG (1990) Animal models in motion sickness research. In "Motion and Space Sickness" Ed by GH Crampton, CRC Press, Boca Raton, FL, pp 87–104

2 Costall B, Naylor RJ, Owera-Atepo JB, Tattersall FD (1989) The responsiveness of the ferret to apomorphine induced emesis. Brit J Pharmacol 96: Suppl 329P

3 King G L (1990) Emesis and defecations induced by the 5-hydroxytryptamine (5-HT_3) receptor antagonist zacopride in the ferret. J Pharmacol Exp Therap 253:1034–1041

4 Naitoh T, Imamura M, Wassersug RJ (1991) Interspecific variation in the emetic response of anurans. Comp Biochem Physiol 100C: 353–359

5 Naitoh T, Wassersug RJ, Leslie RA (1989) The physiology, morphology, and ontogeny of emetic behavior in anuran amphibians. Physiol Zool 62: 819–843

6 Niemegeers CJE, Schellekens KHL, Janssen PAJ (1980) The antiemetic effects of domperidone, a novel potent gastrokinetic. Archiv intern Pharmacodyn Thérap 244:130–140

7 Schwartz J-C, Agid Y, Bouthenet M-L, Javoy-Agid F, Llorens-Cortes C, Martres M-P, Pollard H, Sales N, Taquet H (1986) Neurochemical investigations into the human area postrema. In "Nausea and Vomiting: Mechanisms and Treatment" Ed by CJ Davis, GV Lake-Bakaar, DG Grahame-Smith. Advances in Applied Neurological Sciences 3, Springer-Verlag, Berlin, pp 18–30

8 Tucker ML, Jackson MR, Scales MDC, Spurling NW, Tweats DJ, Capel-Edwards K (1989) Ondansetron: Pre-clinical safety evaluation. Eur J Cancer Clin Oncol 25: Suppl 1, S79–S93

9 Tyers MB, Bunce KT, Humphrey PPA (1989) Pharmacological and anti-emetic properties of ondansetron. Eur J Cancer Clin Oncol 25: Suppl 1, S15–S19

10 Wassersug RJ, Izumi-Kurotani A, Yamashita M, Naitoh T (1993) Motion sickness in amphibians. Behav Neural Biol 60: 42–51

11 Wauquier A, Niemegeers CJE, Janssen PAJ (1981) Neuropharmacological comparison between domperidone and metoclopramide. Jpn J Pharmacol 31: 305–314

ZOOLOGICAL SCIENCE 11: 385–390 (1994)

Electrical Responses of Non-Taste Cells in Frog Tongue and Palate to Chemical Stimuli

OSAMU SATA* and TOSHIHIDE SATO**

Department of Physiology, Nagasaki University School of Dentistry, 1-7-1 Sakamoto, Nagasaki 852, Japan

ABSTRACT—The response characteristics of non-taste epithelial cells on the dorsal and ventral surface of the tongue and the palate of the bullfrogs were investigated with microelectrodes. The resting potential of the non-taste cells ranged from −11.7 to −20.1 mV, which was smaller than that in taste cells of the tongue. The mean amplitudes of depolarizing and hyperpolarizing responses of non-taste cells on the dorsal surface of the tongue for 0.5 mM acetic acid, 0.5 M NaCl, 10 mM quinine-HCl (Q-HCl) and water except for 1 M sucrose were mostly similar to those of the responses in taste cells. The time to peak of depolarizing responses in non-taste cells was the shortest (1–5 sec) with acetic acid, middle (7–21 sec) with sucrose and Q-HCl and the longest (26–34 sec) with NaCl. These values were almost the same as those in taste cells. It is probable that a depolarization of non-taste epithelial cells in response to taste stimuli is initiated by the generative mechanisms similar to those of a depolarization of taste cells.

INTRODUCTION

A taste cell responds to gustatory stimulation with a depolarizing or a hyperpolarizing response [20]. The response behaviors of taste cells have been reported in various species such as frog [1, 19, 20], mudpuppy [15, 24], tiger salamander [21], rat [5, 14], mouse [23] and hamster [5]. On the other hand, supporting non-taste cells in the taste bud or taste disk are known to respond to taste stimuli with a depolarization or a hyperpolarization [17, 18]. The response characteristics of supporting cells in the frog taske disk such as the dose-response curves, response profiles and changes in cell membrane resistance for four basic taste stimuli are comparable with those of taste cells [17].

Various types of non-taste cells, such as neuroblastoma cells [6], sciatic nerve fibers [3], *Tetrahymena* [2], free nerve endings [3] and *Nitella* cells [2] have been reported to respond to tastants.

Since it is supposed that non-gustatory epithelial cells in various areas of the mouth also respond to a variety of chemicals, the present study was undertaken to examine characteristics of non-taste cell responses in frog oral epithelia and to compare them with taste cell responses. An abstract of this study has appeared elsewhere [16].

MATERIALS AND METHODS

Preparation

The experiments were conducted with adult bullfrogs (*Rana catesbeiana*) weighing 250–520 g at a room temperature of 17–24°C. The animal was anesthetized by i.p. injection of a 50% urethane-Ringer solution (3 g/kg body wt.). To prevent the tongue from the spontaneous twitches the hyoglossal and geniohyoid muscles and the hypoglossal nerves were cut bilaterally.

Gustatory stimulation

The four basic taste stimuli (0.5 M NaCl, 0.5 mM acetic acid, 1 M sucrose and 10 mM quinine-HCl (Q-HCl) and deionized water were used for gustatory stimulation. Acetic acid, Q-HCl and sucrose were dissolved in 0.1 M NaCl to remove the hyperpolarizing shift of the membrane potential by solvent water of a stimulus solution. As shown in Fig. 1, non-gustatory epithelial cells on the dorsal and ventral tongue surface and the palate surface were used. These epithelial surfaces were adapted to a normal Ringer solution (mM) (115 NaCl, 2.5 KCl, 1.8 $CaCl_2$, 5 HEPES; pH 7.2), which was flowed at a rate of 0.08 ml/sec with a solution deliverer [10, 19]. The nozzle of deliverer was put on the tongue or palate about 2 mm away from the microelectrode inserted into a cell. After gustatory stimulation of the tongue and the palate, these surfaces were rinsed with Ringer. The time interval between each stimulation was more than 3 min.

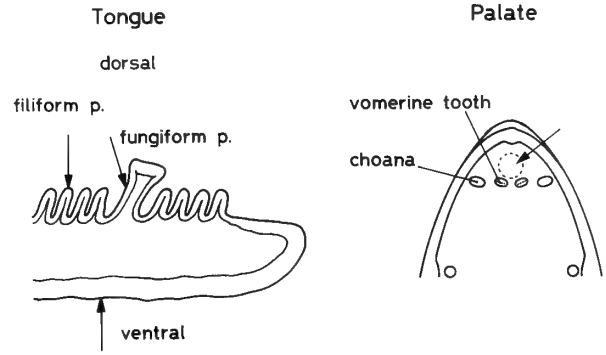

FIG. 1. Schematic illustration of the tongue and the palate in bullfrog. The intracellular responses of non-taste epithelial cells were recorded from the filiform papillae, the fungiform papillae, the ventral surface of the tongue and the palate near the vomerine teeth (arrows and dotted circle).

* Present address: Department of Endodontics and Operative Dentistry, Nagasaki University School of Dentistry, Nagasaki 852, Japan
Accepted June 10, 1994
Received May 25, 1994
** To whom all correspondence should be addressed.

Recording

The apical and middle area of the tongue was used for recordings. Intracellular recordings were made from non-gustatory epithelial cells of the filiform papillae, the side wall of the fungiform papillae, the ventral side of the tongue and the vomerine teeth area of the palate (Fig. 1). Intracellular responses were also recorded from taste cells within the taste disks of the fungiform papillae. Criteria for the taste cell identification have already been mentioned [1, 10, 17]. Glass capillary microelectrodes were filled with 3 M KCl and had a resistance of 20–50 MΩ. An indifferent electrode of glass capillary (tip outer diameter, 100μm) filled with 3% agar-3 M KCl was placed on the tongue or palate surface. The membrane potentials were amplified with a microelectrode amplifier (DPZ-16, Dia Medical System, Tokyo), monitored on an oscilloscope and recorded on a pen-recorder.

RESULTS

Resting potential

The resting potentials were recorded from taste cells of the taste disks in the fungiform papillae and from non-taste epithelial cells in the fungiform papillae, the filiform papillae, the ventral surface of the tongue and the palate. The amplitude of resting potentials in taste cells was -27.7 ± 1.0 mV (mean$\pm$SE, n=27). This value was significantly larger than the resting potentials of other non-taste cells in different portions, which ranged between -11.7 and -20.1 mV (Fig. 2).

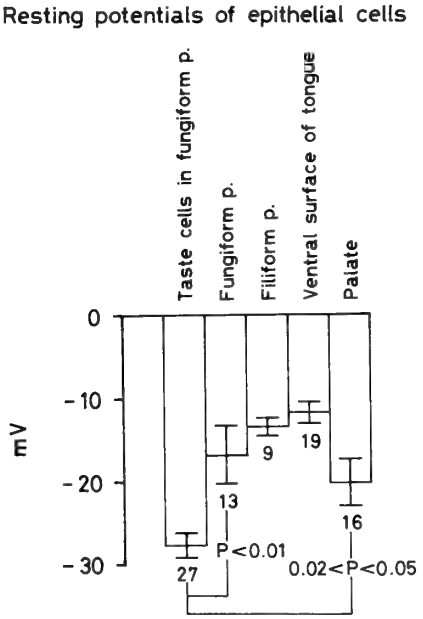

FIG. 2. Resting potentials. The taste cells were from the taste disk in the fungiform papillae and the non-taste epithelial cells were from the fungiform papillae, the filiform papillae, the ventral surface of the tongue and the palate. The vertical bars are SE. In this and the other figures, numerals under or over the columns are the number of sampled cells.

Electrical responses to four basic taste stimuli and water

Acid responses. Before taste stimulation the tongue and the palate were adapted to a normal Ringer solution. Intracellularly recorded acetic acid responses of one taste cell and five non-taste epithelial cells from various portions in the

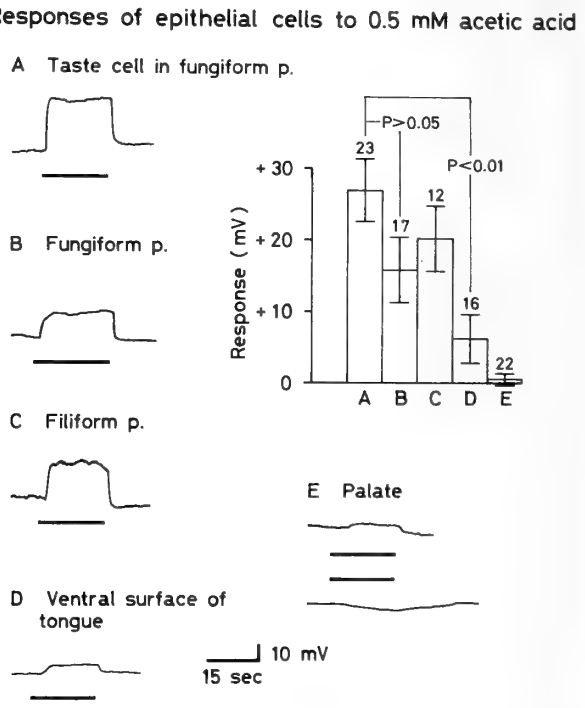

FIG. 3. Electrical responses of taste cells and non-taste cells to 0.5 mM acetic acid. Responses were recorded from a taste cell in the taste disk of the fungiform papilla (A) and from non-taste epithelial cells in the fungiform papilla (B), the filiform papilla (C), the ventral surface of the tongue (D) and the palate (E). The palate responses in (E) were obtained from two cells. The horizontal bars under or over the responses show the period of stimulus application. The vertical bars in the graph are SE. The inset graph shows the mean amplitudes of the acetic acid responses. In this and the other figures, A-E in the abscissa correspond to A-E marked over the electrical responses.

TABLE 1. Number of depolarized, hyperpolarized and no response cells for 4 basic stimuli and water in taste

Response type	0.5 mM acetic acid					1 M sucrose					0.5 M NaCl				
	A	B	C	D	E	A	B	C	D	E	A	B	C	D	E
Depolarization	23	17	12	12	9	19	4	10	8	6	24	15	12	14	21
Hyperpolarization	0	0	0	2	8	0	5	1	3	8	0	0	0	1	1
No response	0	0	0	2	5	1	1	0	0	0	0	0	0	0	1
Total	23	17	12	16	22	20	10	11	11	14	24	15	12	15	22

A; taste cells in the fungiform papillae. B-E; non-taste cells in the fungioform papillae, the filiform papillae, the

mouth are shown in Fig. 3. The responses were depolarizing or hyperpolarizing. The mean amplitudes of acid responses in taste cells, non-taste cells in the fungiform papillae and non-taste cells in the filiform papillae were 27.0, 15.9 and 20.3 mV, respectively, which did not show any statistical difference. These values were much larger than those in non-taste

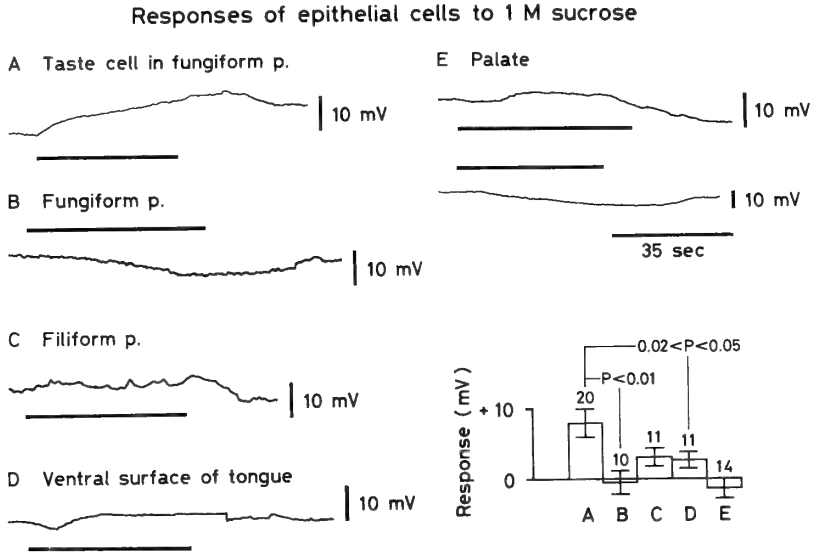

FIG. 4. Electrical responses of taste cells and non-taste cells to 1 M sucrose. (A) Taste cell response. (B)-(E) Non-taste epithelial cell responses at various portions described. The inset graph shows the mean amplitudes of the sucrose responses.

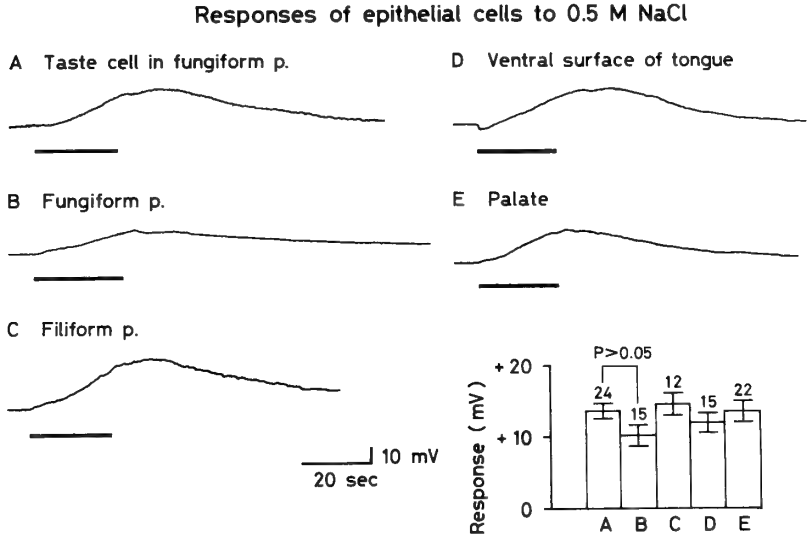

FIG. 5. Electrical responses of taste cells and non-taste cells to 0.5 M NaCl. (A) Taste cell response. (B)-(E) Non-taste epithelial cell responses at various portions described. The inset shows the mean amplitudes of the NaCl responses.

cells and non-taste cells in different epithelial areas

10 mM Q-HCl					water				
A	B	C	D	E	A	B	C	D	E
21	12	12	13	10	7	2	0	1	5
1	2	0	1	2	14	10	11	14	15
0	2	0	3	3	0	0	0	0	0
22	16	12	17	15	21	12	11	15	20

ventral surface of the tongue, and the palate, respectively.

cells of the ventral surface of the tongue and the palate. The time to peak of a depolarization induced by 0.5 mM acetic acid was 1–5 sec in taste cells as well as non-taste cells. These values were the smallest compared with the peak times of depolarizations induced by the other basic taste and water stimuli. Some non-taste cells in the ventral surface of the tongue and the palate were hyperpolarized or did not respond to acid (Table 1).

Sucrose responses. Electrical responses to 1 M sucrose of taste cells and non-taste cells are shown in Fig. 4. The

response magnitude in taste cells was 8.0±2.0 mV, which was significantly larger than those in non-taste cells in four different areas. As shown in Table 1, the hyperpolarized responses appeared in non-taste cells in a high percentage. The time to peak of a depolarization in response to the sucrose was a range of 11–21 sec in both types of cells.

NaCl responses. Figure 5 shows an example of responses to 0.5 M NaCl in taste cells and non-taste cells. Both types of cells investigated were mostly depolarized by 0.5 M NaCl (Table 1). The mean amplitudes of the responses were a range of 10.2–14.6 mV, where no significant difference was found. The peak time of a depolarization in both cells was from 26 to 34 sec, which was the longest of all taste stimuli used.

Q-HCl response. Figure 6 shows an example of Q-HCl responses in taste cells and non-taste cells. The amplitude of the Q-HCl responses in 22 taste cells was 3.2±0.5 mV, which was the smallest value of responses evoked by four basic taste stimuli. The Q-HCl responses in the other non-taste cells were almost the same values. Excepting non-taste cells in the filiform papillae, the hyperpolarized and no responses appeared in 20–30% of the non-taste cells in the other epithelia (Table 1). The peak time of a depolarization in both cells evoked by Q-HCl was a range of 7–21 sec.

Water responses. As shown in Table 1, many taste cells and non-taste cells responded to deionized water with hyperpolarizing responses. These responses are due to removal of the adapting Ringer solution covering each epithelium by deionized water. Some taste and non-taste cells were depolarized by water. As shown in the inset of Fig. 7, the mean magnitudes of responses in taste and non-taste cells for water were all negative (Fig. 7). A hyperpolarization range was from −2.7 to −14.7 mV. The hyperpolarizing response of the filiform papilla cells was generally larger than that of the other non-taste cells.

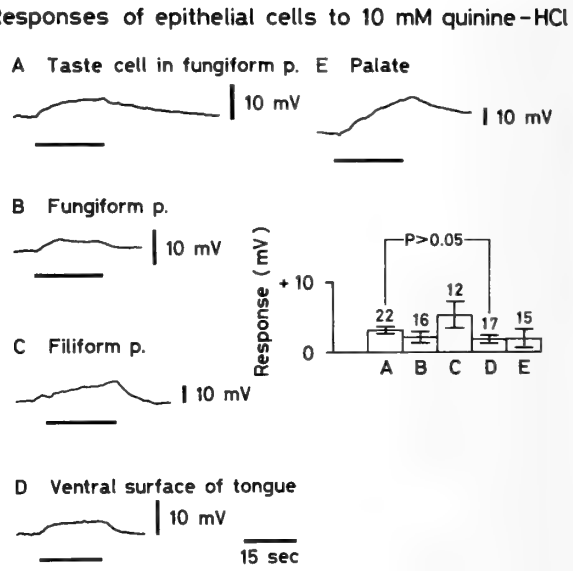

FIG. 6. Electrical responses of taste cells and non-taste cells to 10 mM Q-HCl. (A) Taste cell response. (B)-(E) Non-taste epithelial cell responses at various portions described. The inset shows the mean amplitudes of the Q-HCl responses.

DISCUSSION

It has been reported that supporting cells in the taste bud and the taste disk are depolarized by various chemical stimuli [17, 18, 24]. Depolarizing responses in non-taste cells besides the taste organ by various chemical stimuli are reported in mudpuppy epithelial cells [24], neuroblastoma cells [6], *Tetrahymena* and *Nittela* cells [2].

In the time course of electrical responses in taste and non-taste cells, the peak time of depolarization evoked by acid stimulus (Fig. 3) was much shorter than that by the other taste stimuli (Fig. 4–7). This result is consistent with the

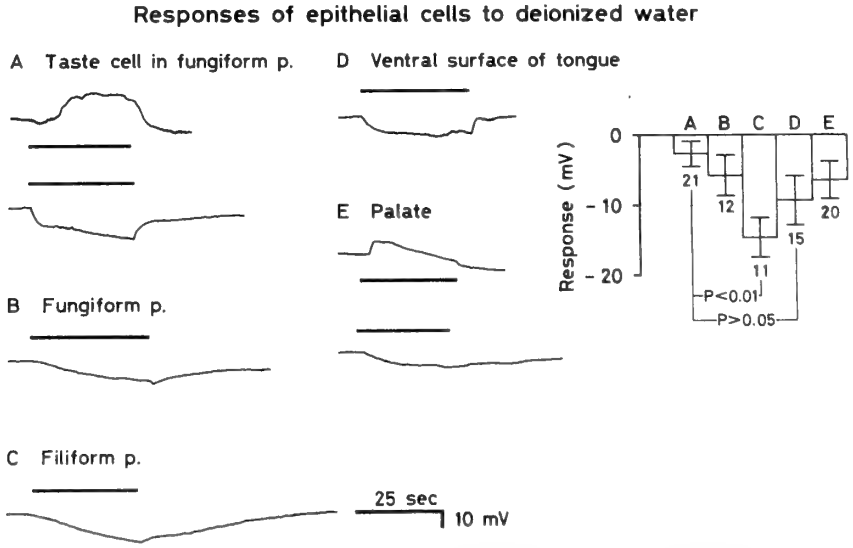

FIG. 7. Electrical responses of taste cells and non-taste cells to deionized water. (A) taste cell response. (B)-(E) non-taste epithelial cell responses at various portions described. The inset indicates the mean amplitudes of the water responses.

previous study with frog supporting cells in taste disk [17]. The amplitude of resting potentials of non-taste cells investigated in the present study was, on the average, 55% of that of the taste cells. The response amplitudes of taste cells and non-taste cells were almost the same when NaCl and Q-HCl were used. However, the response magnitude of taste cells for acetic acid was the same as those of non-taste cells in the dorsal surface of the tongue, but was much larger than those of non-taste cells in the ventral surface of the tongue and the palate. The sucrose responses in taste cells were much larger than those in non-taste cells at every region, suggesting that sugar-binding receptors are formed mostly in the taste cells, but hardly in non-taste cells (Fig. 4).

The response characteristics such as the amplitude of response and the peak time of response were, on the whole, very similar between taste cells and non-taste cells.

We have been studying ionic mechanisms of receptor potentials in frog taste cells induced by four taste stimuli and deionized water. We have proposed the following mechanisms: (1) In case of NaCl stimulation, the receptor potentials are generated by functions of cationic and anionic channels at the receptive membrane and second messenger-dependent cation channels at the basolateral membrane of the taste cells [8, 9]. (2) In case of acid stimulation, Ca^{2+} channels and H^+ transporters such as H^+ pump at the receptive membrane play an important role in generating acid-induced receptor potentials [7, 13]. (3) In case of bitter stimulation, the depolarization is produced by a secretion of intracellularly accumulated Cl^- through the apical receptive membrane [10]. (4) In case of sugar stimulation, the receptor potential is generated by an entry of extracellular H^+ through the apical receptive membrane [11]. (5) In case of water stimulation, the receptor potential is generated by a secretion of Cl^- through the apical membrane and by a blockage of K^+ outflow through the basolateral membrane [12].

It has been reported that a taste cell responds to odorants with a depolarization [4], while an olfactory cell responds to tastants with a depolarization [22]. However, the mechanisms underlying these responses have not yet been understood.

Although some non-taste cells in lingual epithelia and other tissues respond to chemical stimuli of very low concentrations [2, 17, 24], other non-taste cells slightly respond to chemical stimuli of very high concentrations alone (for example: frog striated muscle fibers, *Drosophila* salivary gland cells and frog stomach epithelial cells, unpublished data by Sato T).

Since the response characteristics of non-taste cells in the frog mouth examined in the present experiments are, on the whole, very similar to those of taste cells, it is probable that tastant-induced responses in both taste cells and non-taste cells are induced by some common chemo-electrical transduction mechanisms, which involve receptor sites and ionic channels of voltage-sensitive and ligand-sensitive types. Molecular transduction mechanisms in non-taste cells have to be clarified in the next step.

ACKNOWLEDGMENTS

This study was supported in part by Grants-in-Aid (Nos. 03304042, 05404063) for Scientific Research from the Ministry of Education, Science and Culture of Japan and by a Research Grant from Human Frontier Science Program Organization.

REFERENCES

1 Akaike N, Noma A, Sato M (1976) Electrical responses of frog taste cells to chemical stimuli. J Physiol 254: 87–107

2 Ataka M, Tsuchii A, Ueda T, Kurihara K, Kobatake Y (1978) Comparative studies on the perception of bitter stimuli in the frog, *Tetrahymena*, slime mold and *Nittela*.. Comp Biochem Physiol 61A: 109–115

3 Beidler L M (1965) Comparison of gustatory receptors, olfactory receptors, and free nerve endings. Cold Spring Harbor Symp Quant Biol 30: 191–200

4 Kashiwagura T, Kamo N, Kurihara K, Kobatake Y (1977) Responses of the frog gustatory receptors to various odorants. Comp Biochem Physiol 56C: 105–108

5 Kimura K, Beidler L M (1961) Microelectrode study of taste receptors of rat and hamster. J Cell Comp Physiol 58: 131–140

6 Kumazawa T, Kashiwayanagi M, Kurihara K (1985) Neuroblastoma cell as a model for a taste cell: mechanism of depolarization in response to various bitter substances. Brain Res 333: 27–33

7 Miyamoto T, Okada Y, Sato T (1988) Ionic basis of receptor potential of frog taste cells induced by acid stimuli. J Physiol 405: 699–711

8 Miyamoto T, Okada Y, Sato T (1989) Ionic basis of salt-induced receptor potential in frog taste cells. Comp Biochem Physiol 94A: 591–595

9 Miyamoto T, Okada Y, Sato T (1993) Cationic and anionic channels of apical receptive membrane in a taste cell contribute to generation of salt-induced receptor potential. Comp Biochem Physiol 106A: 489–493

10 Okada Y, Miyamoto T, Sato T (1988) Ionic mechanism of generation of receptor potential in response to quinine in frog taste cell. Brain Res 450: 295–302

11 Okada Y, Miyamoto T, Sato T (1992) The ionic basis of the receptor potential of frog taste cells induced by sugar stimuli. J Exp Biol 162: 23–36

12 Okada Y, Miyamoto T, Sato T (1993) The ionic basis of the receptor potential of frog taste cells induced by water stimuli. J Exp Biol 174: 1–17

13 Okada Y, Miyamoto T, Sato T (1993) Contribution of proton transporter to acid-induced receptor potential in frog taste cells. Comp Biochem Physiol 105A: 725–728

14 Ozeki M, Sato M (1972) Responses of gustatory cells in the tongue of rat to stimuli representing four taste qualities. Comp Biochem Physiol 41A: 391–407

15 Roper S D, McBride D W (1989) Distribution of ion channels on taste cells and its relationship to chemosensory transduction. J Membr Biol 109: 29–39

16 Sata O, Sato T (1988) Electrical responses of oral epithelial cells to taste stimuli in bullfrogs. J Physiol Soc Jpn 50: 507

17 Sata O, Sato T (1990) Electrical responses of supporting cells in the frog taste organ to chemical stimuli. Comp Biochem Physiol 95A: 115–120

18 Sata O, Okada Y, Miyamoto T, Sato T (1992) Dye-coupling among frog (*Rana catesbeiana*) taste disk cells. Comp Biochem

Physiol 103A: 99–103

19 Sato T, Beidler L M (1975) Membrane resistance change of the frog taste cells in response to water and NaCl. J Gen Physiol 66: 735–763

20 Sato T (1980) Recent advances in the physiology of taste cells. Prog Neurobiol 14: 25–67

21 Sugimoto K, Teeter J H (1991) Stimulus-induced currents in isolated taste receptor cells of the larval tiger salamander. Chem Senses 16: 109–122

22 Takagi S F, Iino M, Yarita H (1978) Effects of gustatory stimulants upon the olfactory epithelium of the bullfrog and the carp. Jpn J Physiol 28: 109–128

23 Tonosaki K, Funakoshi M (1984) The mouse taste cell response to five sugar stimuli. Comp Biochem Physiol 79A: 625–630

24 West C H K, Bernard R A (1978) Intracellular characteristics and responses of taste bud and lingual cells of the mudpuppy. J Gen Physiol 72: 305–326

ZOOLOGICAL SCIENCE 11: 391–398 (1994)

Immunogold Colocalization of Opsin and Actin in *Drosophila* Photoreceptors That Undergo Active Rhabdomere Morphogenesis

KENTARO ARIKAWA and ATSUKO MATSUSHITA

Department of Biology, Yokohama City University, 22-2 Seto, Kanazawa-ku, Yokohama 236, Japan

ABSTRACT—This paper describes the localization of visual pigment opsin and its association with actin in the photoreceptors of newly emerged (within 12 hr after emergence) *Drosophila melanogaster*. The photoreceptor of newly emerged flies was characterized by the rich content of rough-surfaced endoplasmic reticulum (rER) and the small rhabdomere: the photoreceptor is actively constructing rhabdomere, and therefore suitable to study the mechanism of rhabdomere morphogenesis. The photoreceptor specifically contained opsin-bearing structures some of which were enclosed by several layers of membranes. The structure became sparse in 10 d old flies. Opsins in the structure may be incorporated into the new rhabdomere. The antiopsin also labeled the plasma membrane facing to the intraommatidial space and the endomembranes in the cell body. Both regions were furnished by uniformly oriented actin filaments with the plus ends towards the rhabdomere. Such orientation makes the actin filaments possible to be involved in the vectorial transport of materials towards the rhabdomere by a presumptive interaction with the myosin-like *ninaC* proteins identified in *Drosophila* photoreceptors.

INTRODUCTION

Photoreceptor function is maintained throughout the life by continuous turnover of the photoreceptive membrane both in vertebrates [6, 9, 18] and invertebrates [7, 21]. In the arthropod compound eye, old membranes are removed from the phototransductive rhabdomere and digested by the lysosomal system in the photoreceptor itself [7, 25]. The removal of photoreceptive membranes is accompanied by the reciprocal addition of new membranes to the rhabdomeral microvilli. The new membranes should contain visual pigment opsin as an integral membrane protein, and should be transported from the cell body towards the base of the rhabdomeral microvilli where the membrane addition is taking place [8, 21–23].

The transport requires force. The force in this case must be able to transport materials towards the rhabdomere. A possible candidate of such a force-producing system is the actin-myosin interaction, because the photoreceptor cell body is furnished by actin filaments [2] and the myosin-like *ninaC* proteins (NINAC) [13, 17]. If the conventional actin-myosin interaction occurs between the actin and NINACs, the produced force could transport materials along the actin filaments towards their plus ends, which attach to the tip of the rhabdomeral microvilli in arthropod photoreceptors [2, 5, 12]. In fact, mutations in the myosin domain of a NINAC isoform disrupt the accumulation of calmodulin in the rhabdomere [19], suggesting that the actin-NINAC interaction is involved in the calmodulin transport into the rhabdomere. The interaction may also transport other rhabdomeral proteins such as opsin.

Accepted April 5, 1994
Received November 8, 1993

If the transport of opsin is mediated by actin, the moving opsins are expected to be found close to the actin filaments. Detection of the situation must be easier in the photoreceptors that are actively constructing the rhabdomere than in the mature photoreceptors. The first aim of this paper is to demonstrate that the newly emerged flies undergo active rhabdomere morphogenesis. Furthermore we present the distribution pattern of opsin and its association with actin filaments in the photoreceptors of the newly emerged flies revealed by the electron microscopic histochemistry.

MATERIALS AND METHODS

Animals

Newly emerged (within 12 hr after adult eclosion) and 10 d old flies of wild-type *Drosophila melanogaster* (Canton S strain) were obtained from a laboratory stock culture kept under a 12 hr light/12 hr dark cycle at 25°C.

Conventional electron microscopy

Light-adapted compound eyes were fixed with 2% glutaraldehyde plus 2% paraformaldehyde in 0.1 M sodium cacodylate buffer at pH 7.4 (CB) overnight at 4°C. After a brief wash with CB, the tissues were post fixed with 2% OsO_4 in CB for 2 hr at room temperature. The tissues were then dehydrated through a graded series of ethanol and embedded in Epon. Ultrathin sections, cut at the level of photoreceptor nuclei, were double stained with 4% uranyl acetate in 50% ethanol and Reynolds' lead citrate solution. The electron micrographs were taken with a JEOL 1200EX electron microscope. We measured the size of the rhabdomeres and other structures on electron micrographs using a digitizer tablet connected to a computer.

Electron-microscopic immunogold labeling

Light-adapted compound eyes were fixed with 2% glutaraldehyde plus 2% paraformaldehyde in 0.1 M sodium phosphate buffer

at pH 7.4 (PB) for 1 hr at room temperature. The tissues were then dehydrated through a graded series of methanol and embedded in L. R. White resin. Ultrathin sections were cut with a diamond knife and collected on nickel grids.

We used a monoclonal mouse IgG against *Drosophila* Rh1 (anti R1–6 opsin, provided by Dr. T. Tanimura) [10] and a monoclonal mouse IgM against chicken-gizzard actin (Amersham, code N.350). The antiactin detects a single band with apparent molecular weight of 42 kD on a Western blot of *Drosophila* head homogenate: the antibody labels both G- and F-actins [2]. The labeling was done by the following two methods.

Mixed-antibody method: Each step of the labeling was done by floating the grid on 5～50μl drop of solution. The sections were first etched with saturated sodium metaperiodate in distilled water for 1 hr, and then blocked with 4% bovine serum albumin (BSA) in PBSG (0.1 M sodium phosphate buffer at pH 7.4 plus 0.5 M NaCl, 0.25% gelatin) for 30 min. The blocking was followed by incubation with the mixture of antiopsin (final conc. 1:200～1:400 of the original) and antiactin (final conc. 10～25μg/ml) in 1% BSA in PBSG overnight at 4°C. After washing with PBSG the primary antibodies were detected by the mixture of goat-anti-mouse (GAM) IgG-conjugated 15nm-gold (Janssen, final conc. 1:50) and GAM IgM-conjugated 5 nm-gold (Janssen, final conc. 1:50) in PBSG . Thus the GAM IgG-15 nm gold detects antiopsin (mouse IgG) whereas the GAM IgM-5 nm gold detects antiactin (mouse IgM). Control labeling was done by removing either the antiactin or antiopsin from the primary antibody-mixture.

Two-surface method: Each step of the labeling was done by floating the grid with the appropriate side down on 10～50μl drop of solution. Etched and blocked surface was incubated with antiactin in PBSG plus 1% BSA (10～25μg/ml) overnight at 4°C. The antiactin was detected by GAM IgM-5 nm gold in PBSG (1:50). After washing with distilled water and air-drying, the other surface was etched, blocked, and incubated with antiopsin in PBSG plus 1% BSA (1:200 ～1:400 of the original) overnight at 4°C. The antiopsin was detected by GAM IgG-conjugated 15 nm-gold in PBSG (1:50). Control labeling was done by replacing either antiopsin or antiactin with 1% BSA in PBSG. The sections were then stained and observed as described above.

Decoration of actin filaments with myosin subfragment-1

This procedure follows that of Arikawa and Williams [4]. Briefly, isolated light-adapted compound eyes were first incubated with 1.0% Triton X-100 in a buffer solution (150 mM KCl, 2 mM DTT, 20 mM Tris-HCl, pH 7.4) at room temperature for 40 min with gentle agitation. After a wash with the buffer for 30–40 min, the eyes were incubated with myosin subfragment-1 (S1, 10～15 mg/ml in the buffer) for 2 hr at room temperature. The tissues were then similarly processed as for the conventional electron microscopy.

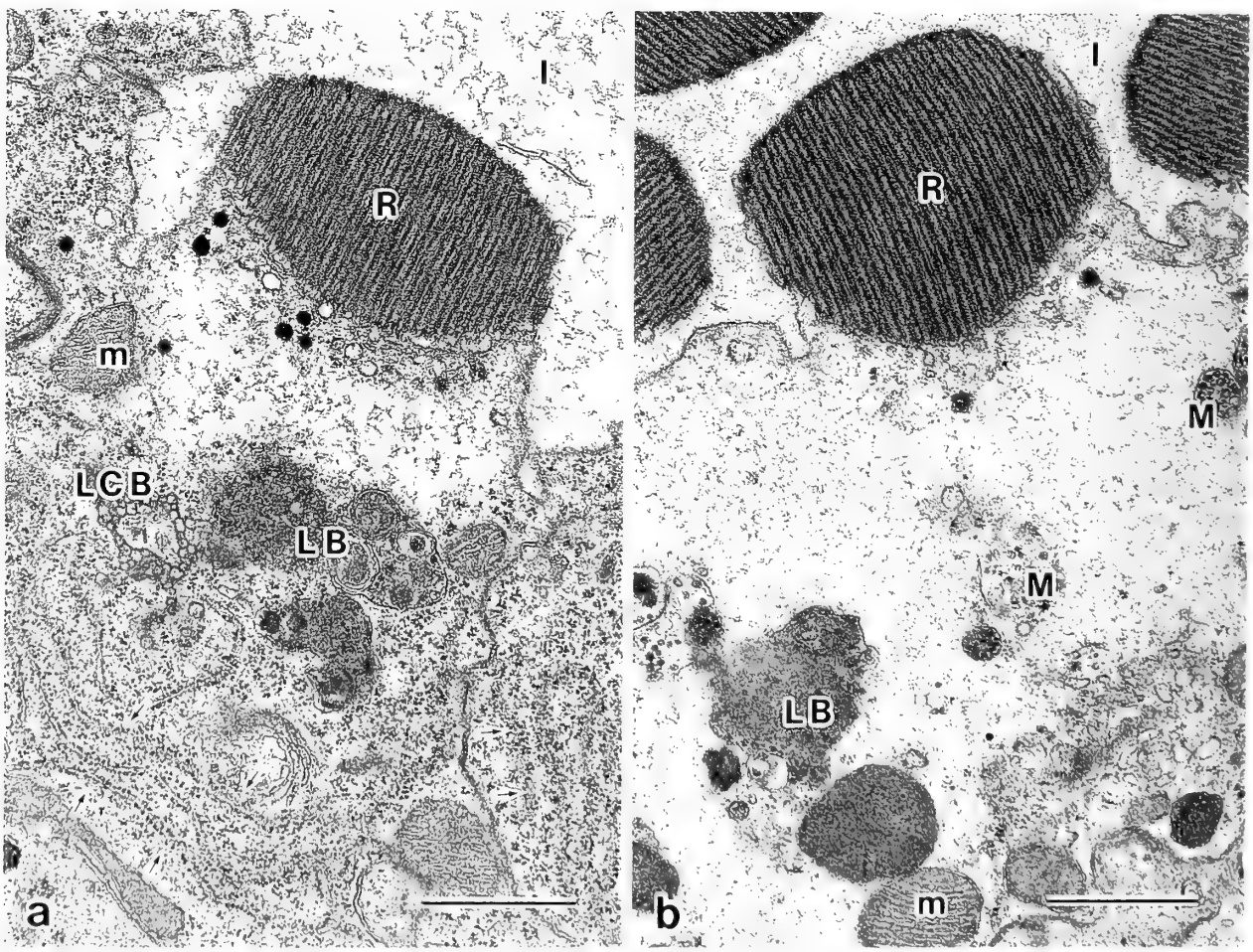

Fig. 1. Transverse section of *Drosophila* photoreceptor. (a) Newly emerged fly (within 12 h after emergence). Note the rich content of rER (arrows) in the cell body. (b) 10 d old fly. I; intraommatidial space, LB; lysosomal body, LCB; large complex body, M; multivesicular body, m; mitochondria, R; rhabdomere. Scale bar=1μm.

RESULTS

Anatomy of the photoreceptors of the newly emerged flies

A *Drosophila* ommatidium contains eight photoreceptor cells (R1–8) each bearing a rhabdomere. R1–6 provide the six peripheral rhabdomeres, and R7 and R8 form a tiered rhabdomere in the center of the ommatidium. Thus, only seven rhabdomeres are observed in any given transverse section of an ommatidium.

The photoreceptor of the newly emerged flies (within 12 hr after emergence) has a well-organized rhabdomere (Fig. 1). The rhabdomere is, however, significantly smaller than the fully developed rhabdomeres of 10 d old flies (Fig. 2): the rhabdomeres are still developing in this stage. The periphery of the photoreceptor cell body is characterized by the rich content of rER (Fig. 1). The amount of rER was quantified as the length appeared in transverse sections. The newly emerged flies contained significantly more rER compared to 10 d old flies (Fig. 2, $P<0.01$, Student's *t*-test).

Multivesicular bodies (MVBs, Figs. 1 and 3a) and lysosomal bodies (LBs, Figs. 1 and 3c) were commonly found. Also common was the large structure of irregular shape containing vesicles, ribosomes, and/or rER (Fig. 3e, g). The structures themselves were embedded in the rER mass. Several layers of membranes enclosed the structure in some cases (Fig. 3e). We hereafter refer the structure as the large complex body (LCB). We measured the areas occupied by the MVBs, LBs, and LCBs in R1–6 in transverse sections at the level of nuclei of the photoreceptors (Fig. 4). The LCB occupied about 1.6% ($4.77\pm1.61\mu m^2$) of the total area of R1–6 in newly emerged flies. The area significantly decreased in 10 d old flies to about 0.1% ($0.23\pm0.08\mu m^2$, $P<0.05$, Student's *t*-test), in which the LB reciprocally increased. The area occupied by the MVB remained constant (Fig. 4).

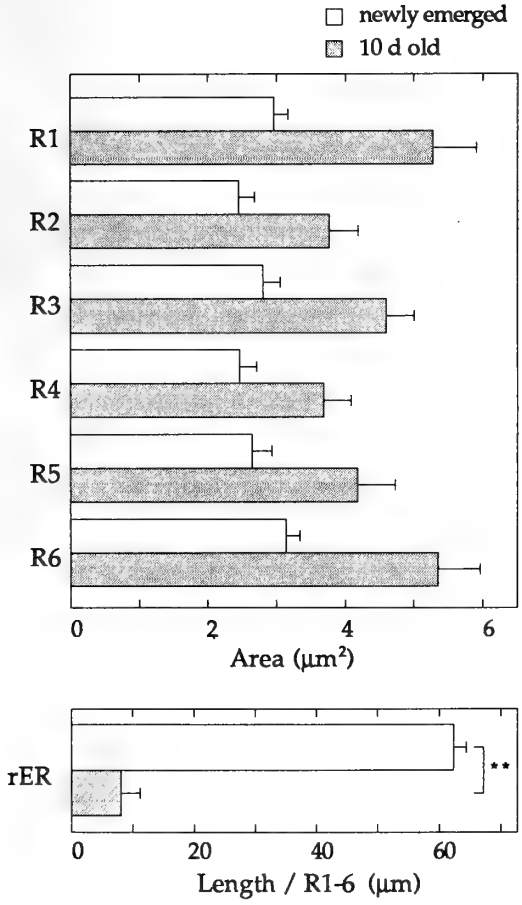

FIG. 2. Cross sectional area (mean ± se) of the rhabdomeres and the total length of the rER in R1–6 measured in transverse sections at the level of the photoreceptor nuclei. Any peripheral photoreceptor of the newly emerged flies has smaller rhabdomere ($P<0.05$, Student's *t*-test) and contains more rER (**; $P<0.01$, Student's *t*-test). Measurement was done on 20 ommatidia from 4 individuals for each age (n=4).

Distribution of opsin and actin

Figure 5 shows the results of control labeling for the mixed antibody method. Each section was first incubated with either antiactin (Fig. 5a) or antiopsin (Fig. 5b), and both were then reacted with the mixture of GAM IgG-15 nm gold and GAM IgM-5 nm gold. Since one of the primary antibodies was removed from the initial incubation, gold particles of only one size bound on each section, indicating that the detection system functioned properly. However, the density of antiactin labeling on the rhabdomeres was not consistent. Both in control and experimental double labeling, the density varied between rhabdomeres even in a single section (data not shown). The antiactin labeling in the cell body region and the antiopsin labeling are rather constant. Two surface method gave virtually the same result.

The antiactin recognizes actin in all photoreceptors [2], whereas the antiopsin specifically binds to Rh1, the opsin of R1–6 photoreceptors [10]. The following observations were therefore made on R1–6 photoreceptors.

Apparent colocalization of antiopsin and antiactin labeling was observed on the rhabdomere (e.g., Fig. 6). The antiopsin labeled the MVBs (Fig. 3b), LBs (Fig. 3d), and LCBs (Fig. 3f, h) in the cell body. The vesicles and the lamellated membranes contained in the LCBs were densely labeled with antiopsin, while the labeling was hardly detected on the associated ribosomes and rER. Other regions labeled with antiopsin were the plasma membrane facing to the intraommatidial space (Fig. 6a, b) and the endomembranes in the cell body (Fig. 6g, h). Opsin-bearing vesicles were found close to the plasma membrane (Fig. 6e). Although rarely, patchy labeling was detected on the rER (Fig. 6b, f). Table 1 summarizes the distribution of antiopsin labeling in a single photoreceptor. Nearly 45% of labeling was found outside the rhabdomere. Note the significant decrease in the labeling on the plasma membrane facing to the intraommatidial space in 10 d old flies (Table 1, $P<0.05$, Student's *t*-test). The difference in the particle numbers is directly attributed to the difference in the labeling density on the membrane, because unlike the LBs and LCBs, the length of the plasma membranes in the sections does not change between newly emerged and 10 d old flies.

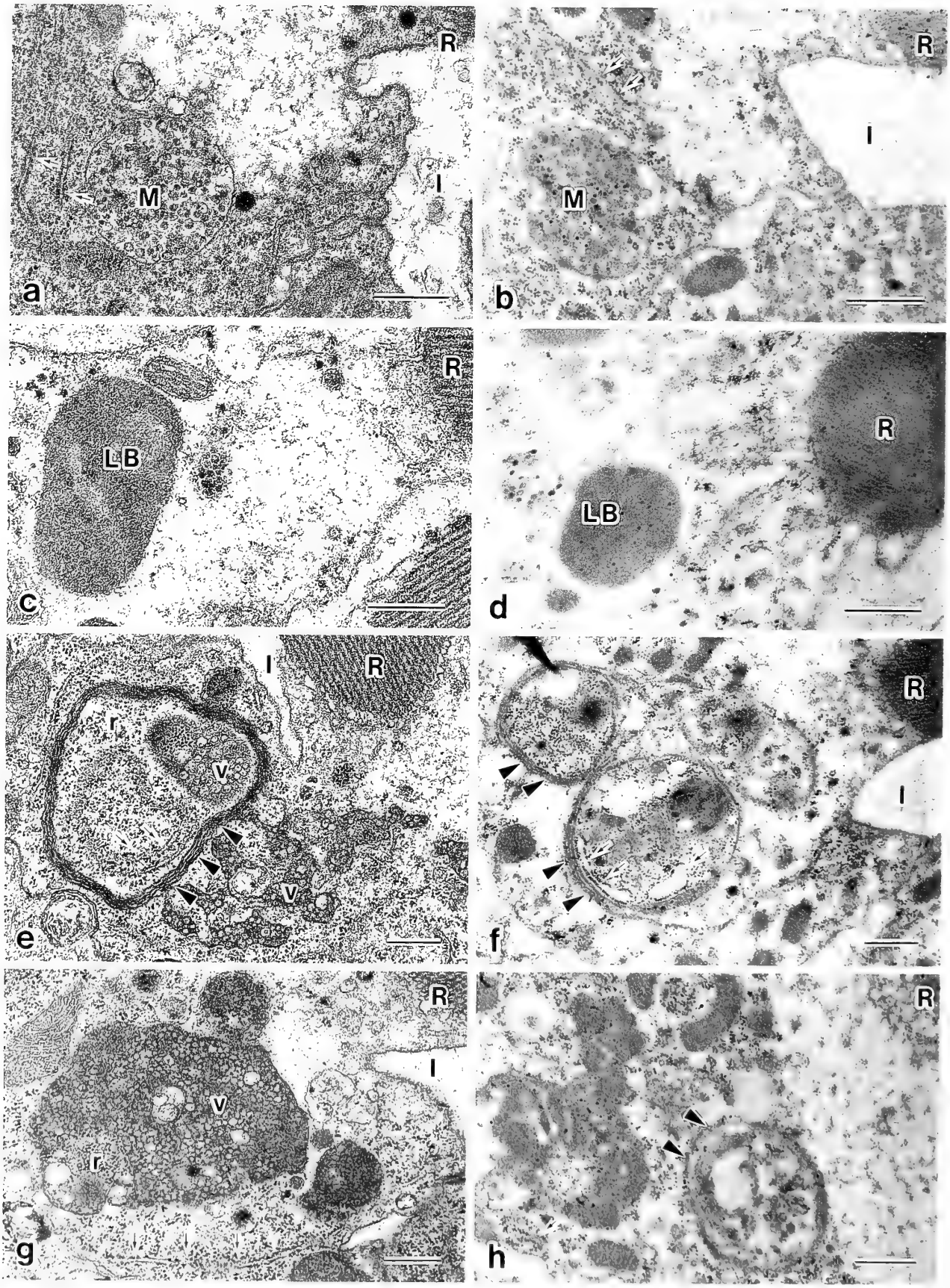
a
R
M
I
b
R
I
M
c
R
LB
d
R
LB
e
I
R
r
v
v
f
R
I
g
R
I
v
r
h
R

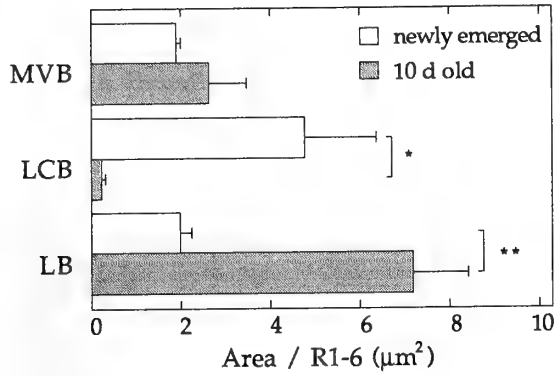

FIG. 4. Areas occupied by multivesicular body (MVB), large complex body (LCB), and lysosomal body (LB) in R1–6. Measurement was done on 23 ommatidia from 5 individuals for each age (n=5). **; $P<0.01$, *; $P<0.05$ (Student's t-test).

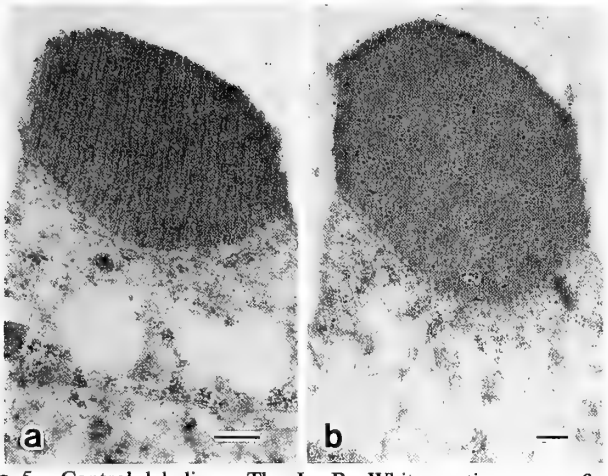

FIG. 5. Control labeling. The L. R. White sections were first labeled either with antiactin (a) or antiopsin (b), and were further treated with the mixture of 15 nm gold-conjugated GAM IgG and 5 nm gold-conjugated GAM IgM. Scale bar=0.2μm.

Figures 6c and d show S1-decorated actin filaments lining the plasma membrane. The actin filaments point away from the rhabdomere (arrowhead triplets): we could not detect any actin filaments with the opposite polarity in this region. The antiactin labeling around the plasma membrane most likely corresponds to these actin filaments (arrows in Fig. 6g). Antiactin also labeled the filaments in the space between the rhabdomere and the cell body (Fig. 6g, h, see also [2]).

DISCUSSION

The results reported here are the following. First, the rhabdomeres of newly emerged flies are developing. These flies are therefore suitable to study the cellular events associated with the rhabdomere morphogenesis. Second, we described opsin-containing large complex body (LCB) in the rER mass. The opsins in the LCB may be incorporated into the rhabdomeres. Finally, electron microscopic histochemistry of opsin and actin suggested that the actin filaments serve as a route for opsin transport towards the rhabdomere.

Double labeling

Two double labeling methods employed here both functioned properly, and gave similar results. The labeling density was consistent except for the antiactin labeling on the rhabdomere in both methods. The observed variation in the density of antiactin labeling is probably attributed to the arrangement of actin in the rhabdomere: actin contributes to the slender core of the microvilli [2, 20]. We cut the hexagonally packed microvilli, each of which is about 100 nm in diameter, roughly along their longitudinal axes. In the ultrathin sections, about 70 nm in thickness, the number of cores contained in a section would vary depending on the cutting angle and/or the degree of distortion of the microvilli arrangement. The number of cores in the section affects the frequency of epitopes exposed on the section surface, which is a determinant of the labeling density.

Opsin synthesis

The photoreceptors of newly emerged flies actively synthesize proteins, which is indicated by the rich content of rER in the cell body (Figs. 1 and 2). The proteins should include opsin, for the rER was occasionally labeled with antiopsin (Fig. 6b, f, Table 1).

The newly emerged flies appeared to have large opsin-bearing structures of irregular profile, which contain vesicles, ribosomes and/or rER, making the cross sectional appearance complex (Figs. 1 and 3). We therefore termed the structure as large complex body (LCB). Some LCBs were enclosed by several layers of membranes densely labeled with antiopsin (Fig. 3f, h). Although some of these resemble autophagic vacuoles, there is also a possibility that the opsins in the LCBs, in the lamellated membranes in particular, are newly synthesized rather than removed from the rhabdomere. Our preliminary observation indicates that the LCBs are abundant even in the late pupal stage and then mostly disappear within two days after emergence: the appearance of the LCBs coincides with the activity of the rhabdomere morphogenesis [15]. The functional significance of the LCBs is remained for further investigation.

MVBs and LBs are both involved in the membrane degradation [8, 11]. Although not frequent, the MVBs and LBs, both contain opsin, were also found in the newly

FIG. 3. Opsin-bearing structures embedded in the rER (arrows) in the photoreceptor cell body. The left column (a,c,e,g) represents the images of conventional EM, whereas the right column (b,d,f,h) represents the L. R. White sections double labeled with antiopsin and antiactin. (a) (b) Multivesicular body. (c) (d) Lysosomal body. (e) (f) Large complex body enclosed by the lamellated membranes (arrowheads). The membranes enclose some rER (arrows). (g) (h) Large complex body without the lamellated membranes. In (h), an LCB enclosed by the lamellated membranes (arrowheads) is also seen. I; intraommatidial space, LB; lysosomal body, M; multivesicular body, R; rhabdomere, r; ribosome, v; vesicles. Scale bar=0.5μm.

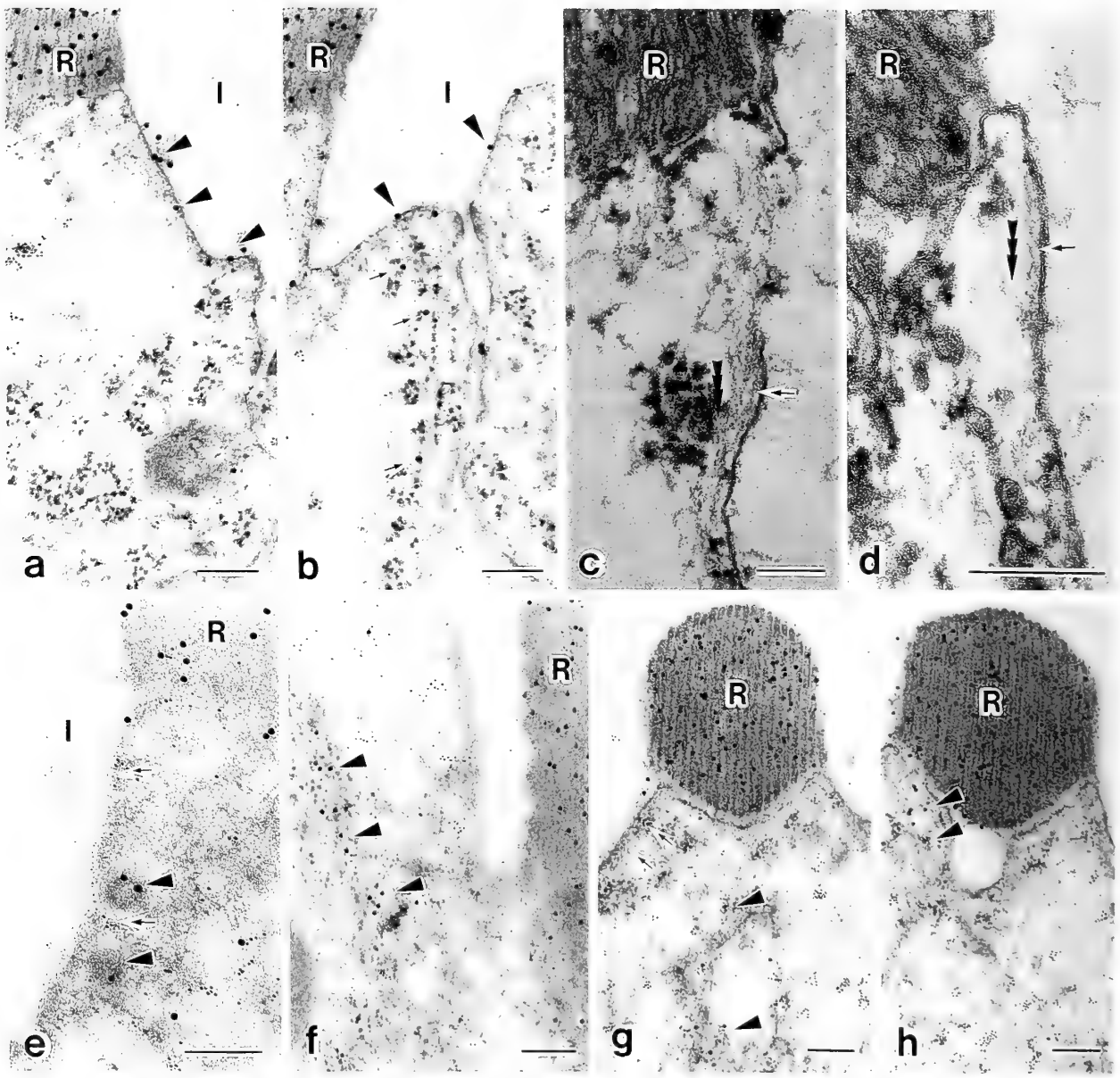

FIG. 6. Histochemistry of opsin and actin in the photoreceptors of newly emerged flies. (a) (b)Antiopsin labeling (arrowheads) on the plasma membrane facing to the intraommatidial space. Arrows in (b) indicate antiopsin labeling on the rER. (c) (d) S1-decorated actin filaments lining the plasma membrane (arrows). The polarity of the filaments was indicated on the left side of the filaments by arrowhead triplets. (e) Opsin-bearing vesicles (arrowheads) found close to the plasma membrane (arrowheads), which was partially lined with antiactin labeling (arrows). (f) Some portions of rER mass were labeled with antiopsin (arrowheads). (g) (h) Antiopsin labeling scattered in the cell body appeared to be associated with some endomembranes (arrowheads). arrows; antiactin labeling. I; intraommatidial space, R; rhabdomere. Scale bar=0.2μm.

emerged flies (Fig. 4), suggesting that the rhabdomere degradation was not inhibited during the stage where the rhabdomere morphogenesis is actively taking place.

Actin and transport of opsin

Transverse sections of the retina clearly show that the photoreceptors have two distinct domains: the rhabdomere and the cell body (Fig. 1). The opsins synthesized in the cell body should be transported to the site of function, the rhabdomere, through the gap between the domains.

There are two possible routes for new opsins to reach the rhabdomere: via the plasma membrane facing to the intraommatidial space [21], and through the subrhabdomeral cisternae (SRC) [14, 24].

Here the antiopsin clearly labeled the plasma membrane (Fig. 6a, b, Table 1). The opsins in the plasma membrane is probably being transported towards the rhabdomere rather than removed from there. One reason for this is that the rhabdomere volume is increasing in this stage (Fig. 2): the flies retain high activity of rhabdomere morphogenesis that

TABLE 1. Distribution of 15nm gold particles (antiopsin labeling) on the photoreceptors of newly emerged and 10d old flies

	mean particle number±se (%)			
	newly emerged, n=4		10 d old, n=4	
rhabdomere	116.7±18.1	(54.7)	90.1± 8.9	(61.3)
plasma membrane	4.9± 1.0	(2.5)	1.3± 0.1	(0.8)**
MVB	5.6± 2.5	(2.5)	12.1± 1.7	(7.8)
LB	8.4± 4.1	(3.6)	33.1± 2.3	(22.4)
LCB	65.9± 5.4	(33.1)	LCB not found	
other regions	6.4± 1.2	(3.5)	11.2± 1.3	(7.7)
Total	2.7.9±21.4	(100.0)	152.1±11.3	(100.0)

"Other regions" include endomembranes and rER. LCBs were not found in the measured micrographs of 10 d old flies. The particle numbers were compared with the corresponding regions in the different developmental stage. Particle counting was done on 57 photoreceptors (ranging 2–14 photoreceptors per individual) from 4 individuals for each age (n=4).
**; $P<0.05$, Student's *t*-test

should require opsin incorporation into the rhabdomere. Secondly, the labeling density on the plasma membrane is significantly higher in the newly emerged than in 10 d old flies (Table 1). Thirdly, the plasma membrane is lined with the uniformly oriented actin filaments with the plus ends towards the rhabdomere (Fig. 6c, d) and anti-NINAC labeling [13]. As suggested by Adams and Pollard [1] in *Acanthamaeba* myosin I, the myosin-like NINAC could move the membrane-embedded opsin towards the plus end of the actin filaments, i.e., towards the rhabdomere.

In fact, actin is probably involved in the rhabdomere morphogenesis. In a crab, *Hemigrapsus sanguineus*, the rhabdom volume increases at dusk and decreases around dawn [3]. The volume increase was inhibited by treating the isolated eye at dusk with cytochalasin D, which disrupts actin filaments. As the cytochalasin D treatment had no effect at night on the enlarged rhabdom, the inhibition of the volume increase should be attributed not to the disintegration of once established rhabdom but to the disruption of some proces-s(es) in the rhabdom morphogenesis [16]. The most plausible process mediated by the presumptive actin-myosin interaction is the transport of opsin. When applied also at dusk, colchicine, a microtubule inhibitor, failed to stop the volume increase, suggesting that the actin was more directly involved in the rhabdomere morphogenesis than the microtubules [16]. Further analyses using other inhibitory drugs are in progress.

The actin-NINAC interaction also explains another route of opsin transport through the SRC, which is an opsin-containing network that wraps the entire base of the rhabdomere [14, 24]. The SRC is connected to the rER with membrane tubules forming an extensive endomembrane system. The opsins in the SRC are probably originated from the rER, the site of opsin synthesis, through the membrane tubules, although no opsin had been so far localized in the tubules. Here we detected antiopsin labeling in the region between the rhabdomere and the cell body. The labeling appeared to be associated with the vesicles or pieces of membranes (Fig. 6g, h). These endomembranes are most likely parts of the tubules, for the tubules appear in transverse sections as elongated or swollen vesicles [14], or even as fragmented membranes if one side of the tubule was tangentially sectioned. The antiopsin labeling on the rER probably represents new opsins that will be transferred into the tubules (Fig. 6b, f).

The region between the rhabdomere and the cell body is furnished also with the NINAC [13]. By the presumptive interaction between actin and NINAC, the opsins embedded in the endomembranes can be transported towards the rhabdomere.

ACKNOWLEDGMENTS

We thank Dr. T. Tanimura for providing the monoclonal anti-*Drosophila* Rh1 opsin antibody. Drs. T. Tanimura, S. Stowe, and E. Eguchi provided helpful comments in the initial stages of the work. We also thank two anonymous referees for many valuable suggestions on the manuscript. The work was supported by the Grants to K. Arikawa from Whitehall Foundation (Florida, USA), Kihara Foundation for Life Sciences (Yokohama), and the Ministry of Education, Science, and Culture of Japan.

REFERENCES

1 Adams RJ, Pollard TD (1989) Binding of myosin I to membrane lipids. Nature 340: 565–568

2 Arikawa K, Hicks JL, Williams DS (1990) Identification of actin filaments in the rhabdomeral microvilli of *Drosophila* photoreceptors. J Cell Biol 110: 1993–1998

3 Arikawa K, Kawamata K, Suzuki T, Eguchi E (1987) Daily changes of structure, function and rhodopsin content in the compound eye of the crab *Hemigrapsus sanguineus*. J Comp Physiol A 161: 161–174

4 Arikawa K, Williams DS (1989) Organization of actin filaments and immunocolocalization of alpha-actinin in the connect-

ing cilium of rat photoreceptors. J Comp Neurol 288: 640–646

5 Baumann O (1992) Structural interactions of actin filaments and endoplasmic reticulum in honeybee photoreceptor cells. Cell Tissue Res 268: 71–79

6 Besharse JC, Horst CJ (1990) The photoreceptor connecting cilium. A model for the transition zone. In "Ciliary and flagellar membranes" Ed by R. A. Bloodgood, Plenum, New York, pp 389–416

7 Blest AD (1980) Photoreceptor membrane turnover in arthropods: Comparative studies of breakdown processes and their implications. In "The effects of constant light on visual processes" Ed by T. P. Williams and B. N. Baker, Plenum, New York London, pp 217–245

8 Blest AD (1988) The turnover of phototransductive membrane in compound eyes and ocelli. Adv Insect Physiol 20: 1–53

9 Bok D (1985) Retinal photoreceptor-pigment epithelium interactions. Invest Ophthalmol Vis Sci 26: 1659–1694

10 de Couet HG, Tanimura T (1987) Monoclonal antibodies provide evidence that rhodopsin in the outer rhabdomeres of *Drosophila melanogaster* is not glycosylated. Eur J Cell Biol 44: 50–56

11 Eguchi E, Waterman TH (1976) Freeze-etch and histochemical evidence for cycling in crayfish photoreceptor membranes. Cell Tissue Res 169: 419–434

12 Hafner GS, Tokarski TR, Kipp J (1992) Localization of actin in the retina of the crayfish *Procambarus clarkii*. J Neurocytol 21: 94–104

13 Hicks JL, Williams DS (1992) Distribution of myosin I-like *ninaC* proteins in the *Drosophila* retina and ultrastructural analysis of mutant phenotypes. J Cell Sci 101: 247–254

14 Matsumoto-Suzuki E, Hirosawa K, Hotta Y (1989) Structure of the subrhabdomeric cisternae in the photoreceptor cells of *Drosophila melanogaster*. J Neurocytol 18: 87–93

15 Matsushita A, Arikawa K, Eguchi E (1992) Distribution of opsin in the photoreceptors in the late pupal and newly emerged *Drosophila*. Zool Sci 9: 1232

16 Matsushita A, Arikawa K, Eguchi E (1993) Disruption of actin filament organization in the photoreceptors inhibits the rhabdom morphogenesis in a crab *Hemigrapsus*. Zool Sci 10: 86

17 Montell C, Rubin GM (1988) The *Drosophila ninaC* locus encodes two photoreceptor cell specific proteins with domains homologous to protein kinases and the myosin heavy chain head. Cell 52: 755–772

18 Papermaster DS, Schneider BG, Besharse JC (1985) Vesicular transport of newly synthesized opsin from the Golgi apparatus toward the rod outer segment: Ultrastructural immunocytochemical and autoradiographic evidence in *Xenopus* retinas. Invest Ophthalmol Vis Sci 26: 1386–1404

19 Porter JA, Yu MJ, Doberstein SK, Pollard TD, Montell C (1993) Dependence of calmodulin localization in the retina on the NINAC unconventional myosin. Science 262: 1038–1042

20 Saibil HR (1982) An ordered membrane-cytoskeleton network in squid photoreceptor microvilli. J Mol Biol 158: 435–456

21 Schwemer J (1986) Turnover of photoreceptor membrane and visual pigment in invertebrates. In "The molecular mechanism of photoreception" Ed by H Stieve, Springer-Verlag, Berlin Heidelberg New York Tokyo, pp 303–326

22 Stark WS, Sapp R, Schilly D (1988) Rhabdomere turnover and rhodopsin cycle: Maintenance of retinula cells in *Drosophila melanogaster*. J Neurocytol 17: 499–509

23 Stowe S (1980) Rapid synthesis of photoreceptor membrane and assembly of new microvilli in a crab at dusk. Cell Tissue Res 211: 419–440

24 Suzuki E, Hirosawa K (1991) Immunoelectron microscopic study of the opsin distribution in the photoreceptor cells of *Drosophila melanogaster*. J Electron Microsc 40: 187–192

25 Williams DS, Blest AD (1980) Extracellular shedding of photoreceptor membrane in the open rhabdom of a tipulid fly. Cell Tissue Res 205: 423–438

ZOOLOGICAL SCIENCE 11: 399–406 (1994)

Experimental Perturbations of the *Litonotus-Euplotes* Predator-Prey System

NICOLA RICCI and FRANCO VERNI

Dipartimento di Scienze dell'Ambiente e Territorio,
via A. Volta 6 56100 Pisa, Italy

ABSTRACT—A model previously proposed to demonstrate the interactions between *Litonotus* (predator) and *Euplotes* (prey), led to a new round of experiments. The different experimental approaches used to solve these questions (starved cells; killed cells; enzymes; lectins; ions; inhibitors) resulted in quite a new model of the cell interactions which accounts for the different steps of the phenomenon: the main point demonstrated by these experiments is that the cellular cortex of both predator and prey is involved in many of the successive steps of the cascade reactions enabling *Litonotus* to prey upon *Euplotes*

INTRODUCTION

Efforts spent in attempting to deepen our understanding of predation among protozoa are completely justified by the basic importance of the process. Protozoa, indeed, were not only the first primary consumers in the primeval Oceans, but the first predators as well [12]. Such a new trophic niche is quite an important one, due to the two consequences it leads to: (a) it creates new empty spaces for new organisms to settle in, (b) it triggers a sort of evolutionary competition between preys and predators (to escape and to strike each other, respectively) as to their morpho-functional acquisitions. Many examples have been already studied and the knowledge of the *Didinium-Paramecium* [1], *Dileptus-Colpidium* [34], *Enchelys-Tetrahymena* [5], *Chaenea-Uronema* [5]; *Homalozoon-Paramecium* [4] predator-prey systems, cannot but help us to complete our overall picture of this phenomenon considered from a more specific sinecological point of view: in this perspective, indeed, the study of predator-prey interactions also lends itself to be used in an attempt to penetrate the adaptive strategies, conditioning the reciprocal (co)evolution of predators and preys. Let us recall the example of the bat-moth relationships, as a truly paradigmatic one, to clarify our idea [28].

In this context we studied another predatory model, namely that of *Litonotus lamella-Euplotes crassus*, focusing our attention successively on (a) the ultrastructure of the toxicysts of the predators [11], (b) the ultrastructural analysis of the consequences to *Euplotes* of toxicyst discharge by *Litonotus* [32]; (c) the peculiar digestion process [33] and, finally, (d) the behavioural patterns following each other along a path characterised by the succession of several basic steps, namely casual encounter (CE); toxicyst discharge (TD); research (R); engulfment of the prey (PE)[8]. The predator-prey interaction model proposed in the previous paper focused our attention on several closely related problems, which represented the targets of the next round of experiments: (a) how is the toxicyst-discharging system triggered and controlled? (b) which are the spatio-temporal sequences of a toxicyst-discharge phenomenon?

The unique nature of our pet-organism protozoa (i.e. indeed perfect eukaryotic cells and complete organisms, at the same time) offers a double advantage: (a) it enables us to use all those techniques typical of experimental studies on cell interactions to investigate also the relationships between entire organisms and (b) it allows us to transfer any results obtained for these truly sophisticate organisms to the general field of cell biology.

MATERIALS AND METHODS

Both *L. lamella* and *E. crassus* were grown, collected and used as already described by Ricci and Verni [24]. The observations were made with a Wild M5 (20–60X) stereomicroscope, and a Leitz Orthoplan (400X) microscope (together with its Nomarsky interferential contrast), coupled to a Panasonic TVC camera and a VHS videorecorder. Unless otherwise indicated, the prey organism was *E. crassus*. The following specific procedures were followed for the different kinds of experiments:

Expt. 1 The effects of starvation on preys and on predators were studied using normal and starved *Litonotus*, exposed to both normal and starved *Euplotes*. Normal populations of predators were used 4 days after the last feeding, while the starved ones were tested after 11 days. Normal *Euplotes* were not fed for 24 hr, while the starved ones were used 7 days after the last feeding.

Expt. 2 To study the role played by the body itself, of both the predator and the prey, in the specific toxicyst discharge (TD) processes at the very moment when the two organisms come into direct contact with each other and the TD itself is triggered and actually occurs, both *Litonotus* and *E. crassus* were frozen, and then thawed at room temperature (the experimental populations were immersed in liquid nitrogen for 2 min): in this way the structurally and chemically preserved, but physically inert bodies of both *Litonotus* and *Euplotes* were tested with living prey or predator respectively. In some of these experiments homogenized *Euplotes* were also used.

Expt. 3 Whenever a predator contacts a prey TD occurs: does TD affect the microenviroment where it occurred? How far for TD area is such an effect perceived? How long does it persist? How is the behaviour of *Euplotes* affected? To solve these problems, many TD

Accepted May 31, 1994
Received December 16, 1993

events were videorecorded and the videotapes scored frame by frame according to the standard technique for behavioural studies reported elsewere by Ricci [20]. In this way we quantified: a) the subcircular area where the TD effects are perceived by *Euplotes*; b) their duration; c) the changes in behaviour of the prey.

Expt. 4 To assess the role possibly played by calcium concentration in the sea water, 3 different standard set ups (cf. Expt. 5) were prepared: the first contained standard marine water (control), the second 15 mM calcium chloride, the third the same concentration of $CaCl_2$ plus 0.1 mM EDTA, to inhibit the effects of the calcium. Previous experiments, carried out with 5, 10, 15, 20, and 25 mM Ca^{++} and with 0.01, 0.1 and 10 mM EDTA had shown that the best results were obtained with 15 mM Ca^{++} and with 0.1 mM EDTA. In other words these two concentrations were the lowest capable of inducing clearcut results. Five experiments were then carried out and microvideorecorded, to measure: (a) the time lag between the introduction of *Litonotus* and the first instance of TD (this period of time will be referred to as TD Δt throughout this paper, it somehow measures the efficiency to *Litonotus* in intercepting the prey); (b) the time lag between the introduction of *Litonotus* and the actual engulfment of the killed prey (this period of time will be referred to as I Δt in this paper, it somehow measures the efficiency of *Litonotus* feeding on the prey); (c) the length of the backward motion of *Litonotus* following TD; (d) the number of TD per *Litonotus*.

Expt. 5 The effects of trypsin (Sigma, T8253; concentration 2.5, 2, 1.5, 1 and 0.5%) were also studied. About 50 *Litonotus* were incubated in the different concentration for various time periods (15, 30, 60, 90, 120, 180, 210 and 240 min); they were washed 3 times and then used in a 50 μl droplet with concentrated *Euplotes*, to study the TD Δt, I Δt and the percentage of inhibited (namely not-toxicyst discharging) *Litonotus*. When 100% TD inhibition was induced, the *Litonotus* still incubated by trypsin were washed free of the enzyme fresh water and then used in *Euplotes* populations to monitor their recovery period.

Expt. 6-A The effects of concanavalin-A (Con-A, Sigma C2010; concentration 2, 1.5, 1, 0.5 and 0.25%; treatment time 15, 30, 60, 90, 120, 150, 180 and 210 min) on *Litonotus* were studied by washing the treated cells after different periods of time and measuring TD Δt, I Δt and the percentage of inhibited cells, when these experimental *Litonotus* were transferred into a 50 μl droplet of concentrated preys. The same treatments were also carried out on incubating *Litonotus* in the same dosages of Con-A and for the same times as before, in the presence of 40 mM of α-methyl-D-mannoside, well-known as a specific competitor of Con-A. The same parameters were measured.

Expt. 6-B Concentrations of 2 and 1% of Con-A were also used to incubate *Euplotes* for 15, 30, 60, 90, 120, 150, 180, 210, 270, 330, and 390 min: these populations were washed three times and then exposed to *Litonotus*, to measure the TD Δt, the I Δt, the percentage of non-discharging *Litonotus*.

Expt. 7 In a final experimental approach, *Litonotus* was treated with different concentrations (0.5, 0.25, 0.125, 0.06, 0.03 and 0.015%) of cycloheximide (Chx)(Sigma C-6255) for different times (1 to 9 hr); they were used singly with populations of *Euplotes* to measure TD Δt, IΔt and the percentage of TD inhibition. When 100% TD inhibition was obtained the still incubated cells were washed free of Chx and then used with *Euplotes* to study the kinetics of their recovery in terms of the percentage of TD inhibited cells.

RESULTS

Expt. 1 The effects of different starvation of *Litonotus* and *Euplotes*.

Previous microscope observations (Verni, unpublished results) had shown that the longer the starvation, the more caudal the distribution of toxicysts: the effects were statistically significant. On the basis of these findings, the consequences of starvation were studied more specifically.

The results obtained in this round of experiments demonstrated that (a) severe starvation affects the efficiency of predator's TD: Table 1, the III and the IV columns vs the I and the II; (b) the starvation of the preys affects, to a limited extent, the ingestion capability of *Litonotus* (Table 1, IΔt, the II vs the I column and the IV column vs the III), while it does not affect the corresponding TD Δt.

Expt. 2 The predatory interactions between *Litonotus* and frozen-thawed *Euplotes*.

Litonotus cannot be frozen and then thawed, without being disrupted: no result could be obtained, except that the area where a disrupted *Litonotus* lies is avoided by the preys. Normal *Litonotus* exposed to a population of frozen-thawed *Euplotes* demonstrated that: (a) *Litonotus* can ingest them without discharging any toxicysts (Fig. 1B); (b)IΔt is longer than twice as much as that of the control (Fig. 1: B vs A); (c) when freshly prepared homogenate of *Euplotes* is added to the system, ID Δt is strikingly reduced (Fig. 1C).

Expt. 3 The TD-affected area.

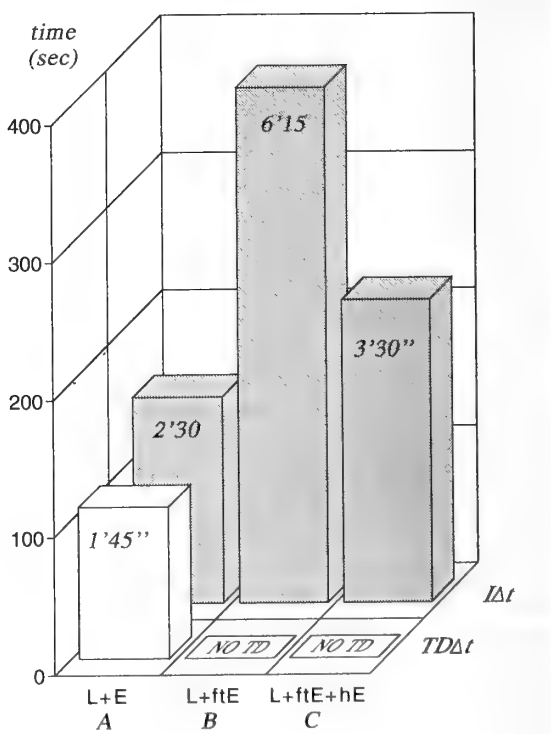

FIG. 1. The TDΔt (white bars) and the IΔt (shadowed bars) of *Litonotus* (L) in presence of [A] normal *Euplotes* (E), [B] frozen-thawed *Euplotes* (ftE) and [C] ftE and homogenated *Euplotes* (hE). On the ordinates the times in seconds are reported.

TABLE 1. The effects of starvation, on the predation of *Litonotus lamella* on *Euplotes crassus*, measured by the durations of the TDΔt and of the IΔt (described in Materials and Methods section).

		normal **Litonotus**		starved **Litonotus**	
		+ normal **Euplotes**	+ starved **Euplotes**	+ normal **Euplotes**	+ starved **Euplotes**
TDΔt	$\bar{x}$	**1'25"**	**1'20"**	**2'21"**	**2'15"**
	s	55"	50"	1'12	1'18"
	n	35	26	29	32
IΔt	$\bar{x}$	**2'30"**	**3'**	**3'42"**	**4'9"**
	s	1'	1'5"	1'15"	1'18"
	n	35	26	29	32

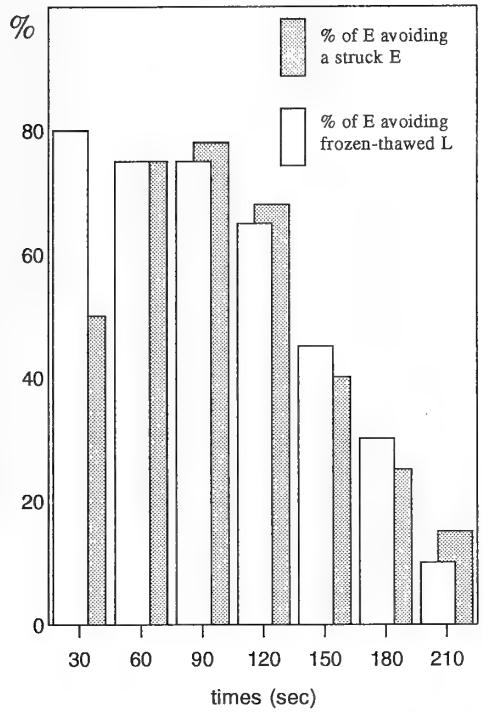

FIG. 2. The temporal trend of avoidance of the "toxic" area by *Euplotes*, expressed in terms of individuals (ordinate: %) creeping away from it, in the time (abscissa: sec). The shadowed bars show the same trend of *Euplotes* avoiding frozen-thawed *Litonotus*

The results we obtained are the following: (a) the effects of a TD event extend around the TD point over a sub-circular area of about 300μm in diameter, (b) the same effects increase up to their maximum for 90 sec after the TD event and last for about 3 min; (c) the behaviour of the preys is clearly affected by the TD event as demonstrated by the high frequency of avoidances induced in *Euplotes* by TD immediately afterwards (Fig. 2, shadowed areas); the avoidances correspond to the behavioural pattern called Side Stepping Reaction [19] and indicated as SSR; (d) these SSR occur according to a temporal pattern parallel to that of *Euplotes* avoiding the area where a frozen-thawed disrupted *Litonotus* is placed (Fig. 2, white areas).

TABLE 2. The effects of Ca^{++} (15 mM) on the 4 parameters indicated on the left; BM=the length of the backward motion of a *Litonotus lamella* after discharging its toxicysts: it is measured in Relative Units (RU): 1 RU=1 species-specific length of *Litonotus lamella* $\simeq$250μm. The number of observations for each parameter was of 50

populations / parameters studied	Control	15 mM Ca^{++}	15 mM Ca^{++} & 0.1 mM EDTA
TDΔt (sec)	43±17	41.5±18	42±26
BM (RU)	1.1±0.7	2.5±0.7	1.2±0.6
IΔt (sec)	132±30	186±80	139±33
n° of TD per *Litonotus*	1.2±0.4	2.4±0.5	1.2±0.5

Expt. 4 The role of Ca^{++} in the environment.

The results given in Table 2 clearly show that calcium ions affect the general physiology of the *Litonotus-Euplotes* system at least at three different levels: (a) TD Δt is not affected; (b) the length of the backward motion is doubled; (c) IΔt increases by about 50%; (d) the number of TD per *Litonotus* is doubled. EDTA inhibits calcium effects, as expected. As considered in the Materials and Methods section, the differential effects of calcium ions on TD Δt (no effect) and on IΔt (strong inhibition), actually demonstrate the importance of both parameters in interpreting correctly the effects of calcium ions on the *Litonotus-Euplotes* system.

Expt. 5 The effect of trypsin on *Litonotus*

The enzyme was already known to affect the physiology of *Litonotus*; progressively higher concentrations and longer treatments, indeed, induce (a) a progressive darkening of the cytoplasm, (b) a rounding of the body shape, (c) reduced locomotion, (d) immobilization and (e) lysis of the cell (Ricci and Verni, unpublished results). It was found (Fig. 3) that the different concentrations used for the different times indicated in Material and Methods, clearly affect TD Δt (the higher the concentration, the longer TD Δt) but not IΔt (the difference between TD Δt and IΔt is indeed rather constant). For a certain concentration a longer treatment affects the percentage of cells not discharging their toxicysts (Fig. 4), while TD Δt tends to be more or less constant, the different values depending solely upon trypsin concentration. Once

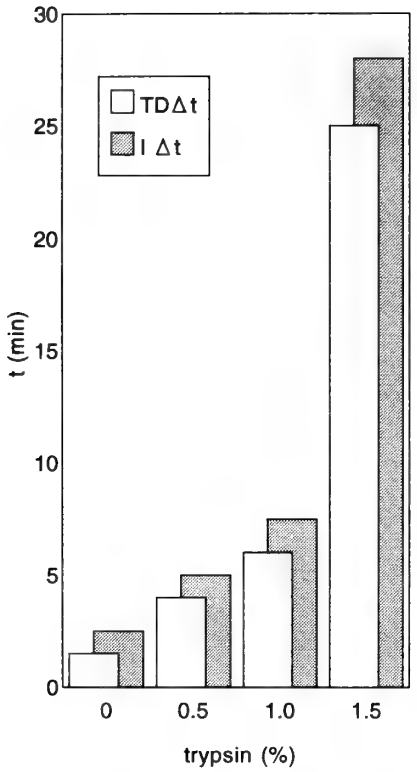

FIG. 3. The average TDΔt and IΔt induced by the concentrations of trypsin, given on the abscissa; 0% of trypsin=controls

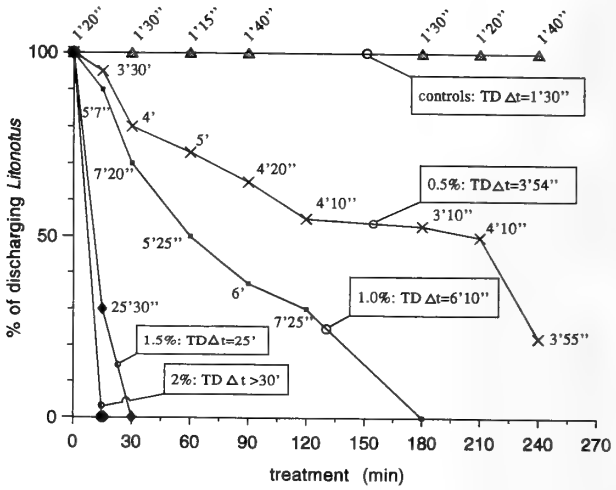

FIG. 4. The progressive action of the trypsin in the time: for a certain concentration the longer the treatment (abscissa) the smaller the percentage of discharging *Litonotus*. The figure close to each of the different points along the curves, represents the average TDΔt observed for that point; the figures in the small panels represent the trypsin concentration for the different curves and the relative mean values of the TDΔt.

100% inhibition is induced (namely, when no *Litonotus* can discharge its toxicysts) they still behave quite normally and their physiology seems to be unaffected: after washing, these completely inhibited populations recover 80% of their TD activity within 30–60 min, and 100% of their potentialities within 60–120 min.

Similar treatments with trypsin were also conducted on *Euplotes*; the enzyme either has no effect al all on both TD Δt or IΔt, and it kills the preys.

Expt. 6A The effects of Con-A on *Litonotus*.

The results of the experiments are the following: (a) the higher the Con-A concentration, the stronger the effect, on TD Δt, but not on IΔt (Table 3) (b) for the same concentration, the longer the treatment, the stronger the effect on TD Δt but not on IΔt (Table 3) (c) as the Con-A concentration

TABLE 3. The TDΔt and the IΔt of different populations of *Litonotus* treated by different concentrations of Con A (shown in the first line) for different times, given in the left column

t \ Con A		2%		1.5%		1%		0.5%		0.25%		control	
		TDΔt	IΔt	TDΔt	IΔt	TDΔt	IΔt	TDΔt	IΔt	TDΔt	IΔt	TDΔt	IΔt
	n	15	15	10	10	10	10	10	10			8	8
15'	$\bar{x}$	>30'	>35'	3'	4'	2'	3'20'	1'31"	2'20"	ND	ND	2'	3'
	s	—	—	1'20"	1'46"	50"	1'30"	1'	1'17"			1'05"	1'25"
	n	**14**	**14**	**14**	**14**	**12**	**12**	**11**	**11**	**12**	**12**	**8**	**8**
30'	$\bar{x}$	>30'	>35'	10'50"	15'30"	6'23"	7'30"	2'10"	3'30"	2'15"	3'24"	1'20"	2'30"
	s	—	—	2'19"	3'	3'55"	3'27"	1'	1'27"	1'	1'21"	1	1'50'
	n			**16**	**16**	**9**	**9**	**10**	**10**	**11**	**11**	**8**	**8**
60'	$\bar{x}$	†	†	>30	>35'	8'10"	11'50"	5'20"	7'	2'27"	3'40"	1'30"	2'55"
	s			—	—	5'15"	5'	2'20"	2'	1'12"	1'25"	1'15"	1'20"
	n					**10**	**10**	**7**	**7**			**8**	**8**
90'	$\bar{x}$			†	†	11'15"	13'30"	10'35"	12'15"	ND	ND	2'10"	3'15"
	s					5'18"	7'47"	2'20"	2'30"			050"	1'35"
	n					**18**	**18**	**13**	**13**			**8**	**8**
120'	$\bar{x}$					>30'	>35'	12'35"	13'43"	ND	ND	1'20"	2'20"
	s					—	—	1'24"	1'21"			1'05"	1'50"
	n							**6**	**6**	**10**	**10**	**8**	**8**
150'	$\bar{x}$					†	†	12'40"	13'26"	5'	6'42"	1'50"	3'
	s							1'25"	1'10"	1'36"	1'40"	1'10"	1'50"

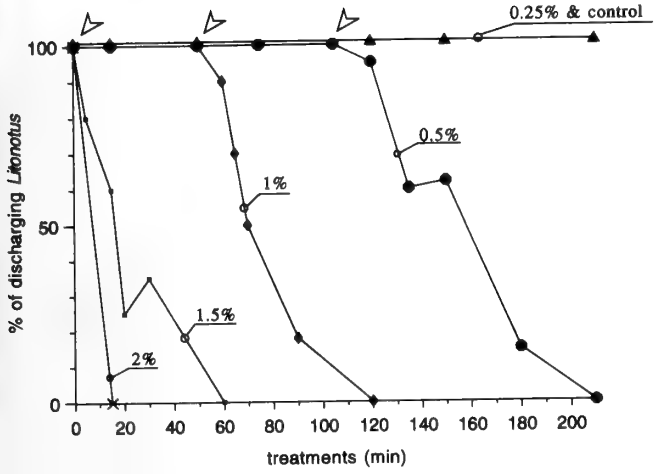

FIG. 5. The effects of Con-A (at the concentrations indicated for the different curves) are expressed as percentages of *Litonotus* discharging their toxicysts (ordinate), after being treated for different times (abscissa). The arrowheads indicate the onset of the inhibitory effects for the different concentrations.

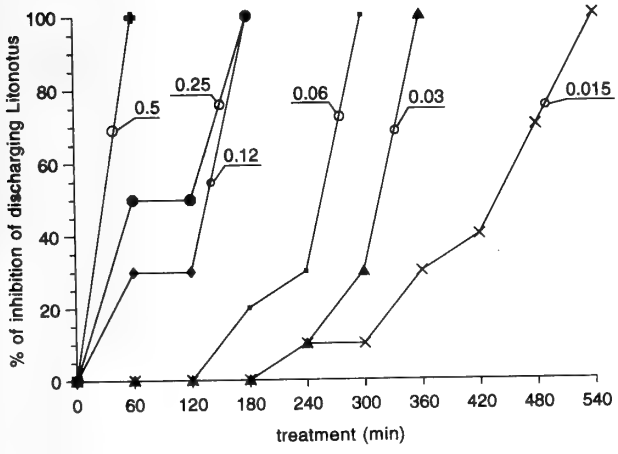

FIG. 6. The percentages of inhibited *Litonotus* (ordinate) given as a function of the different concentrations (indicated in the figure itself) and of the length of treatment (abscissa).

decreases (1.5; 1.0; 0.5%), the time which elapses between the onset of the treatment and the beginning of the inhibitory effects of the lectin itself increases (0; 50; 110 min respectively, as shown by the arrowheads in Fig. 5); (d) for the same concentration, the longer the treatment, the lower the percentage of *Litonotus* discharging their toxicysts (Fig. 5); (e) when *Litonotus* treated with Con-A are washed free from the lectin, the inhibitory effects are removed after a period whose length is roughly proportional to the Con-A concentration: while, for instance, 1% Con-A inhibits completely the TD after 90 min and the recovery period, after washing, is about 4 hr, 0.5% Con-A inhibits TD completely after 3.5 hr, but the populations start discharging their toxicysts again only 40 min after washing; (f) the effects of Con-A are specific, being completely inhibited by α -methyl-D-mannoside, the specific competitor of Con-A.

Expt. 6B The effects of Con-A on *Euplotes*.

The results showed that this lectin affects the prey in the same way as it proved to do with the predator: (a) Con-A treated *Euplotes* induce a reduction of TD Δt and the percentage of TD predators, according to a clearcut dose-dpendence; (b) the longer the treatment period of *Euplotes* with a certain concentration of Con-A, the longer the TD Δt of *Litonotus* and the higher the percentage of non TD predators; (c) when Con-A treated *Euplotes* do not induce any TD at all, they are washed: the recovery periods required for *Litonotus* to discharge its toxicysts again are proportional to the Con-A concentration used on *Euplotes*; (d) the effects of Con-A on *Euplotes* are specific, being completely inhibited by α -methyl-D-mannoside.

Expt. 7 The effects of cycloheximide on *Litonotus*.

When *Litonotus* is treated with cycloheximide TD is severely affected: (a) the higher the Chx concentrations, the longer TD Δt (Table 4) and the larger the amount of non TD *Litonotus* (Fig. 6). Also the interference effects of Chx are easily reversed upon washing and the recovery times are proportional to the concentrations used for a certain treatment.

DISCUSSION

The experiments reported here led to a widening and deepening of the general knowledge of the predator-prey relationships between *Litonotus* and *Euplotes* [24].

First of all, it was found that starvation acts on both elements of the system, although differentially: (a) in *Litonotus* it affects both the cortical areas where TD occurs (the more severe starvation, the more caudal the TD) and TD Δt, a parameter somehow measuring the "hunting efficiency" of *Litonotus*, (the longer the starvation, the more inefficient it becomes): (b) starved *Euplotes* are ingested in longer times.

TABLE 4. The inhibitory effects of Chx on TD of *Litonotus*: the TDΔt (min) on organisms treated by different concentrations (%, shown in the left column) for different hours (indicated in the first line)

%	1	2	3	4	5	6	7	8	9 hr
0.015	1'	1'30"	3'30"	5'00"	5'00"	5'00"	6'00"	8'00"	>30'
0.03	1'36"	1'54"	4'00"	6'00"	6'00"	>30'	>30'	>30'	>30'
0.06	2'	1'54"	5'00"	6'00"	>30'	>30'	>30'	>30'	>30'
0.125	3'50"	3'24"	>30'	>30'	>30'	>30'	>30'	>30'	>30'
0.25	4'24"	3'48"	>30'	>30'	>30'	>30'	>30'	>30'	>30'
0.5	>30'	>30'	>30'	>30'	>30'	>30'	>30'	>30'	>30'

In general it seems possible to conclude that a basic physiological "health" of both predator and prey represents a sort of prerequisite for predation to occur efficiently.

Freezing-thawing experiments provided several clues to a deeper understanding of our predation model. Frozen-thawed *Euplotes* (a) maintain their shape, (b) cannot induce TD in *Litonotus*, and (c) still suitable preys for *Litonotus* to eat. These results seem to suggest that some "activation energy" (related to the kinetic energy of a normally swimming *Euplotes*) might be required for TD. Similar results on the other hand, have also been found by Ricci *et al.* [26] regarding the mechanisms which trigger specific cell differentiation (giantic cell) in *Oxytricha bifaria*. Experiments carried out with paralyzed mutants of *Euplotes* [23] are expected to give more precise answers to the question: the fairly small amount of energy involved in this process, however, should not to be considered exceptional since the world of ciliates has already proved to be ruled by unexpectedly small forces, as demonstrated by Machemer [16] and by Ricci *et al.* [27]. According to these results, moreover, TD does not represent a step necessarily occurring before ingestion, although TD itself seems to facilitate somehow the actual ingestion, as demonstrated by IΔt of *Litonotus* engulfing frozen-thawed *Euplotes*: the values of these IΔt are, on average, more than twice than those of the controls. A further clue to the comprehension of the factors involved in the *Litonotus-Euplotes* interactions is given by the use of the homogenate of *Euplotes*, which strikingly reduces IΔt of *Litonotus* engulfing frozen-thawed *Euplotes*. These evidences seem to suggest that a cytoplasmatic factor (or complex of factors) of *Euplotes* (called ε) is capable of "activacting" *Litonotus*. The nature of this "activation" is at present being studied through a behavioural approach, namely investigation of the specific locomotory pattern of *Litonotus* exposed to the homogenate of *Euplotes*, and related to the normal searching activity of the predator already reported by Ricci and Verni [24].

The findings of experiment 3 show that a "toxic" (in its broadest sense) area persists, where a *Euplotes* has been killed by a *Litonotus*: its spatial extension and temporal duration recalls quite closely that of the area where a frozen-thawed *Litonotus* is placed. This finding strongly suggests that *Litonotus* releases a factor (or complex of factors), whenever it "breaks down" or discharges its toxicysts. According to our present understanding, a *Litonotus* must depolarize its membrane to discharge its toxicysts and this, in turn, cannot but lead it to creep backwards for a while. To "buffer", somehow, this unavoidable physiological handicap, *Litonotus* may be supposed to release a substance (called λ) at the TD point, capable of guiding it towards the prey: on the other hand the same λ might represent the "stay away" signal for *Euplotes*, thus producing what we called the "toxic area". Similar "repulsive" effects have been described also for *Colpidium* avoiding killed *Dileptus* [6]. The use of 15 mM Ca^{++} produced clearcut results, in terms of a larger number of TD per *Litonotus* and longer backward locomotion following the TD: these observations strengthened our hypothesis of electrically controlled TD for *Litonotus*, according to both what is already known for *Dileptus* [6] and to the more specific report of Hara *et al.* [13] for *Didinium*.

The dramatic effects of proteolytic enzymes on a wide range of biological phenomena of ciliates are already known: binary fission [36], conjugation [15, 22, 35] and feeding processes [6, 7, 30, 37]. The data reported here show that while no effect can be detected when trypsin acts on *Euplotes*, (Expt.5) the same enzyme affects (a) the physiology of *Litonotus* (cytoplasm, body shape, and locomotion) in much the same ways as in *Dileptus* [6], (b) the average TD Δt and (c) the recovery periods of washed populations, with a generally clearcut dose dependence. An exception is represented by the difference between IΔt and TD Δt, which is fairly constant at the different trypsin concentrations: this observation indicates that TD and ingestion differ from each other from a physiological point of view, as also suggested by the results of the experiments carried out with frozen-thawed *Euplotes*. The most surprising effect of trypsin, however, is the finding that induced TD Δt depends only on the concentration itself and not on the length of the treatment, which is on the contrary capable of inhibiting (completely and reversibly) the TD of the *Litonotus* population. Such a puzzling result (strong numerical inhibition of *Litonotus* vs constant TD Δt at a certain concentration of trypsin, upon longer treatment times) might be accounted for by a working hypothesis, based on some kind of accumulation of proteins, possibly involved in the TD processes (called TDP). Similar accumulations have already been hypothesized by Beisson and Rossignol [2] for the trichocyst discharging of *Paramecium*, by Heckmann and Siegel [14] for the preconjugant cell interactions of *Euplotes crassus*, and by Ricci *et al.* [25] for the differentiation of carnivorous giants in *Oxytricha bifaria*. According to our hypothesis, the higher the trypsin concentration (i.e. the larger the number of TDP molecules) the larger also the number of digested cortical TDP. If *Litonotus* can substitute them at a certain velocity, recruiting them from a cytoplasmic pool, the effect of trypsin can somehow be counterbalanced, at least for a certain time: the average number of newly-exposed and ready-to-work TDP can be expected to be inversely proportional to the number of trypsin molecules in the environment (and not related to the length of the treatment!). According to this way of thinking the reason why the trypsin concentration is directly proportional to the time required to reach the physiological threshold of TDP per surface unit requested for the TD itself can be easily explained. Only when the entire cytoplasmic pool of presynthetized TDP is exhausted is a *Litonotus* inhibited from discharging its toxicysts. The temporal trend of the progressive inhibition of the entire population, on the contrary, would depend upon the relative differences occurring among different *Litonotus* with regard to the pool of presynthetized TDP and to the TD threshold. This general working hypothesis seems to be supported and strengthened

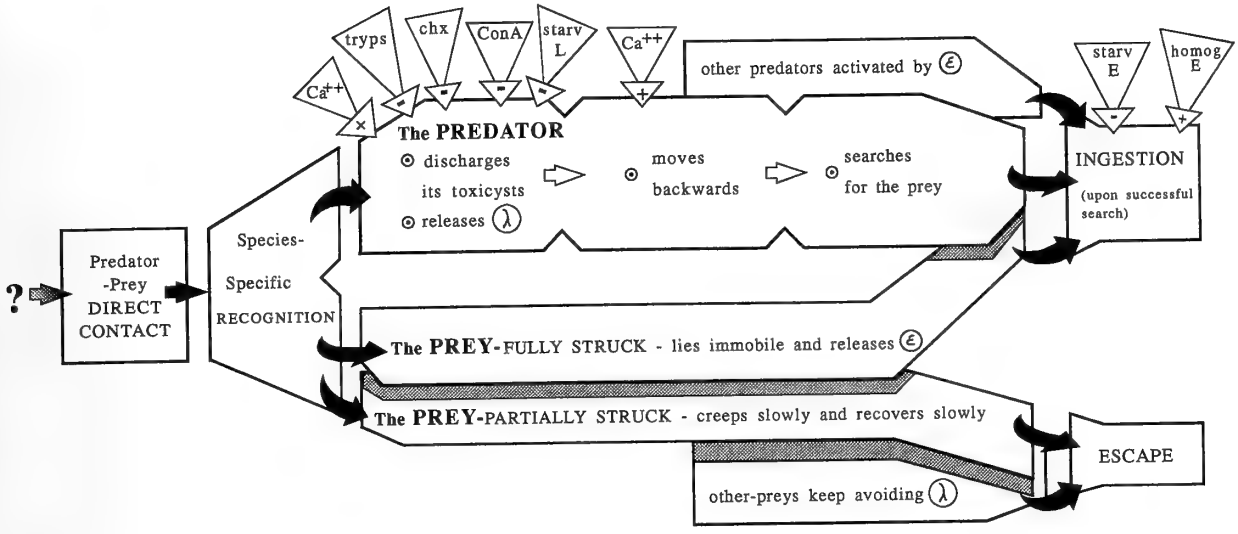

FIG. 7. The schematic drawing of the successive steps occuring when a *Litonotus* (predator) comes in direct contact with an *E. crassus* (prey): the upper, vertical arrows show the parameters affecting the different steps.

by the observed effects of cycloheximide, which induces increasingly long recovery periods for the synthesizing machinery, when increasingly strong treatments are used.

A final consideration must be made about the data obtained with Con-A, in the context of what is already known about its effects on different aspects of the biology of ciliates: feeding [10, 29], growth [3, 29, 35], conjugation [10, 17, 18, 21, 31], locomotion [9], cell differentiation [26]. The effects of Con-A show a clear dose dependence for both the inhibitory effect of TD and TD Δt itself. Con-A seems to affect the *Litonotus-Euplotes* system by reacting with cortical glycoproteins of both *Litonotus* and *Euplotes* and not through an aspecific toxicity, as demonstrated by the use of both the washing procedure and α-methyl-D-mannoside. What still remains to be ascertained is the degree of its specificity for TDP: does Con-A react specifically with TDP or, rather, with aspecific cortical glycoproteins, thus simply masking the TDP themselves? *Ad hoc* experiments presently being conducted are expected to solve the problem. Regardless of its way of acting on the *Litonotus-Euplotes* system, Con-A works differently from trypsin: (a) stronger dosages of this lectin, in fact, induce longer TD Δt; (b) Con-A inhibits TD in a population of *Litonotus* with a time delay roughly proportional to its dilution, while trypsin acts immediately.

The differentiated approches used to study the *Litonotus-Euplotes* biological system led us to draw a complex picture of the different steps following each other during the time elapsing between the initial contact between predator and prey and the actual ingestion (Fig. 7). Direct cell contacts are required for the phenomenon to occur, a species-specific recognition represents the first step of sort of double scale: the **Predator** (a) discharges its toxicysts and releases some chemical, λ; (b) it moves backwards, (c) it searches for the prey and if everything works out properly, (d) it ingests the prey. The **Prey**, on the other hand, may be either fully struck (it quits moving and releases a particular chemical, ε) or only partially struck (its locomotion is severely affected, but it slowly recovers its normal physiology). As indicated on the upper part of the figure itself, many factors, all contributing to the clarification of our understanding of the phenomenon, may interfere either positively or negatively with the physiology of the predator. Although quite complex, this synoptic scheme represents an interesting achievement, being not only an exhaustive summary of what is so far known, but rather a polyhedric working hypothesis, extremely useful for proceeding towards the next phases of investigation of the *Litonotus-Euplotes* story.

ACKNOWLEDGMENTS

The authors are truly indebted to Dr. Fabrizio Erra, for both the scientific discussions and the capable assistance in handling the graphic problems.

REFERENCES

1 Balbiani EG (1873) Observations sur le *Didinium nasutum*. Arch Zool Exp 2: 363–394

2 Beisson J, Rossignol M (1975) Movements and positioning of organelles in *Paramecium aurelia*. In "Molecular biology of nucleocytoplasmic relationships" Ed by S. Puiseux-Dao, Elsevier, Amsterdam, pp 291–294

3 Bessler WG, Lipps HJ (1976) Concanavalin A-induced nuclear division in *Stylonychia mytilus*. J Gen Microbiol 92: 221–223

4 Diller WF (1964) Observation on the morphology and life history of *Homalozoon vermiculare*. Arch Protistol 107: 351–362

5 Dragesco J (1962) Capture et ingestion des proies chez les infusories ciliès. Bull Biol Fr Belg 46: 123–167

6 Esteve JC (1981) Perturbation du comportement alimentaire par atteinte du revètement cellulaire chez le ciliè *Dileptus*. Protistologica 17: 479–488

7 Esteve JC (1984) Calcium, calmoduline, sites glucidiques et

ingestion chez le ciliè gymnostome *Dileptus* sp. Protistologica 20: 15–25

8 Fenchel T (1987) Ecology of Protozoa. Springer Verlag, Berlin

9 Frisch A, Bessler W, Lipps HJ, Ammermann D (1976) Immobilization of ciliates by concanavalin-A. J Protozool 23: 427–430

10 Frisch A, Loyter A (1977) Inhibition of conjugation in *Tetrahymena pyriformis* by Con A. Localization of Con A binding sites. Exp Cell Res 23: 337–346

11 Giambruni A, Verni F (1986) Studio ultrastrutturale delle toxicisti del ciliato predatore *Litonotus lamella* Boll Zool 53: 20

12 Gould SJ, Raup DM, Sepkoski JJ Jr, Schopf TJM, Simberloff DS (1977) The shape of evolution. A comparison of real and random clades. Paleobiology 3: 173–181

13 Hara R, Asai H, Naitoh Y (1985) Electrical responses of the carnivorous ciliate *Didinium nasutum* in relation to discharge of the extrusive organelles. J Exp Biol 119: 211–224

14 Heckmann K, Siegel RW (1964) Evidence for the induction of mating-type substances by cell to cell contacts. Exp Cell Biol 36: 688–691

15 Kitamura A, Hiwatashi K (1978) Are sugar residues involved in the specific cell recognition of mating in *Paramecium*? J Exp Biol 203: 99–108

16 Machemer H (1993) Ciliate gravireception and graviresponses. IX Inter Congress Protozool July 25–31 Berlin, Germany

17 Offer L, Levkovitz H, Loyter A (1976) Conjugation in *Tetrahymena pyriformis*. The effect of polylysine, concanavalin A and bivalent metals on the conjugation process. J Cell Biol 70: 287–293

18 Revoltella R, Ricci N, Esposito F, Nobili R (1976) Cell surface control in *Blepharisma intermedium* Bhandary (Protozoa Ciliata). I. Distinctive membrane receptors-sites in mating type 1 cells for various interacting ligands. Monitore Zool Ital (N.S.) 10: 279–292

19 Ricci N (1981) The ethogram of *Oxytricha bifaria* (Ciliata, Hypotrichida). II. The motile behaviour. Acta Protozool 20: 393–410

20 Ricci N (1992) Qualitative study and quantitative analysis of behavior of ciliated protozoa: principles, tecniques, tricks. In "Protocols in Protozoology" Ed by JJ Lee, AT Soldo, Soc Protozol, Allen Press, Lawrence, Kansas, pp B-14.1–14.16

21 Ricci N, Esposito F, Nobili R, Revoltella R (1976) Cell surface control in *Blepharisma intermedium* (Protozoa Ciliata). Blocking of gamone II-induced omotypic pairing by different membrane interacting ligands. J Cell Physiol 88: 363–370

22 Ricci N, Cetera R, Banchetti R (1980) Cell to cell contacts mediating mating type dependent recognition(s) during the preconjugant cell interactions of *Oxytricha bifaria* (Ciliata, Hypotrichida). J Exp Zool 211: 171–183

23 Ricci N, Miceli C, Giannetti R (1987) The ethogram of *Euplotes crassus* (Ciliata, Hypotrichida). II. The paralyzed mutant. Acta Protozool 26: 295–307

24 Ricci N, Verni F (1988) Motor and predatory behavior of *Litonotus lamella* (Protozoa, Ciliata). Can J Zool 66: 1973–1981

25 Ricci N, Grandini G, Bravi A, Banchetti R (1991) The giant of *Oxytricha bifaria*: a peculiar cell differentiation triggered and controlled by cell to cell contacts. Eur J Protistol 27: 127–133

26 Ricci N, Bravi A, Grandini G, Cifarelli D, Gualtieri P, Coltelli P, Banchetti R (1991) The formation of giants in *Oxytricha bifaria*: a peculiar multi-step cell differentiation. Eur J Protistol 27: 264–268

27 Ricci N, Erra F, Russo A, Banchetti R (1992) The interface between air and water: a perturbation source adaptive behaviour in Ciliates. J Protozool 39: 521–525

28 Roeder KD (1968) Interactions of bats and moths. Kybernetik 13: 75–87

29 Sharabi Y, Gilboa-Garber N (1980) Interactions of *Pseudomonas aeruginosa* hemagglutinins with *Euglena gracilis, Chlamydomonas reinhardi* and *Tetrahymena pyriformis*. J Protozool 27: 80–83

30 Tolloczko B (1975) Endocytosis in *Paramecium*. 1. Effects of trypsine and pronase. Acta Protozool 14: 313–320

31 Tsukii Y, Hiwatashi K (1978) Inhibition of early events of sexual process in *Paramecium* by concanavalin A. J Exp Zool 205: 439–446

32 Verni F (1985) *Litonotus-Euplotes* (predator-prey) interaction: ciliary structure modification of the prey caused by toxicysts of the predator (Protozoa, Ciliata). Zoomorphology 105: 333–335

33 Verni F, Rosati G (1992) A comparative study of digestion in a raptorial ciliate and in the facultative carnivorous form of a filter feeding ciliate. Tissue and Cell 24: 443–453

34 Visscher JP (1923) Feeding reactions in the Ciliate *Dileptus gigas* with special reference to the function of the trichocysts. Biol Bull 45: 113–143

35 Watanabe T (1977) Chemical properties of mating substances in *Paramecium caudatum*: effect of various agents on mating reactivity of detached cilia. Cell Struct Funct 2: 241–247

36 Wyroba E (1978) Cell multiplication following partial enzymatic removal of surface coat. Cytobiologie 17: 412–420

37 Wyroba E, Brutkowska M (1978) Restoration of phagocytic activity of *Paramecium tetraurelia* suppressed by previous digestion of surface coat. Acta Protozool 17: 515–524

ZOOLOGICAL SCIENCE 11: 407–412 (1994)

Immunochemical Studies of an Actin-binding Protein in Ascidian Body Wall Smooth Muscle

YUKIO OHTSUKA[1], HIROKI NAKAE[2], HIROSHI ABE and TAKASHI OBINATA[1,3]

[1]*Department of Biology, Faculty of Science, Chiba University, Yayoi-cho, Inage-ku, Chiba, Chiba 263, and* [2]*Advanced Research Laboratory, Research and Development Center, Toshiba Corporation 1, Komukai Toshiba-cho, Saiwai-ku, Kawasaki 210, Japan*

ABSTRACT—A monoclonal antibody (McAb, AS23) was prepared to the proteins extracted from ascidian body wall smooth muscle by a dilute alkaline salt solution. The McAb recognized a protein of about 80 kDa (termed 80K protein) and the protein was detected most abundantly in the body wall smooth muscle by both immunoblotting and immunocytochemical methods. The 80K protein was enriched in isolated thin actin filaments, and in addition, it was observed that AS23 binds to one end of thin filaments by immunoelectron microscopy. The results indicate that the 80K protein is an actin-binding protein which can associate with filamentous actin in ascidian body wall smooth muscle.

INTRODUCTION

The body wall, or mantle, of ascidian is constituted of two layers of smooth muscle which resembles smooth muscles of vertebrates morphologically, especially in the pattern of myofilament arrangement [17]. This muscle has attracted attention since it is unique multinucleated [16, 18] and troponin-containing smooth muscle [22]; it is the only known example of a troponin/tropomyosin-regulated muscle which contains no organized sarcomeric structures. Thus, the ascidian smooth muscle is not obviously homologous with either vertebrate smooth or striated muscle, but appears intermediate between smooth and striated muscles of vertebrates.

Contractile proteins, actin and myosin, of this muscle have been investigated [14]. In addition, three troponin components, troponin T, I and C, [5] and tropomyosin [11] have been isolated and characterized. However, nothing is known as to the actin-binding proteins which may be involved in the regulation of actin assembly and/or filament organization in this muscle. According to electron microscopic observations [17–19], the contractile apparatus consists of many irregularly arranged filament bundles which are separated from each other by a network of intermediate filaments. Actin-containing thin filaments appear considerably longer than those in vertebrate smooth or striated muscles [17]. During the contraction of the body wall muscle, the arrangement of myofilaments is significantly altered [20]. Therefore, it is of interest how the arrangement of myofilaments is controlled in the cytoplasm. In order to understand the ascidian muscle cells from functional and structural aspects, it seems to be indispensable to characterize actin-binding proteins which may be involved in assembly, organization and re-distribution of actin filaments.

In this investigation, as the first step to clarify actin-binding proteins in ascidians, we prepared monoclonal antibodies to ascidian muscle protein extracts which we assumed to contain actin-binding proteins as judged by the knowledge on vertebrate smooth muscle [7]. One of the antibodies recognized an 80 kDa protein which is enriched in ascidian body wall smooth muscle and is associated with its thin actin filaments.

MATERIALS AND METHODS

Muscle source

Ascidians, *Halocynthia roretzi*, were obtained from a local seafood market. The fresh body wall muscle was isolated, frozen immediately in liquid nitrogen, and stored at −80°C until use.

Antibodies

The proteins as an immunogen were prepared as described previously [12]; Briefly, the isolated body wall muscle was homogenized in ice-cold distilled water containing 0.5 mM phenylmethyl sulfonyl fluoride (PMSF) and washed extensively in the same solution. The final residue was extracted with 5 volumes of 4 mM Tris-HCl, pH 8.5, containing 1 mM EDTA and 0.5 mM PMSF for 30 min at room temperature. The pH of the extract was adjusted to 7.2, and then 1 M $MgCl_2$ was added gradually to give 10 mM at final concentration. The solution was stirred on ice for 15 min, and centrifuged at 7,000×g for 10 min. The supernatant was subjected to ammonium sulfate fractionations; The proteins salted out at 28–78% (0.15–0.55 g/ml) ammonium sulfate were collected and they were dialyzed against 20 mM Tris-HCl, pH 7.6, 20 mM NaCl, 0.1 mM EDTA, 15 mM 2-mercaptoethanol, and 0.5 mM PMSF. The proteins of about 70–150 kDa were then prepared by preparative SDS-PAGE and used for an immunogen.

The monoclonal antibody, AS23, was produced through hybri-

Accepted May 16, 1994
Received April 14, 1994
[3] To whom correspondence and reprint requests should be addressed.

doma formation between spleen cells of BALB/c mice immunized with the immunogen and nonsereting myeloma cell line P3x63.Ag8U1 cells using the technique of Galfre *et al.* [8] as modified by Gefter *et al.* [9]. Hybridoma cells producing antibody were subcloned twice by a limiting dilution method. Supernatants from subcloned cultures were used as the sources of antibodies.

The monoclonal antibody to troponin T (NT-302) was prepared as described previously [1]. Horseradish-peroxidase (HRP)-labeled goat anti-mouse IgG (GAM) was purchased from Bio-Rad (Richmond, California) and fluorescein (FITC)-labeled GAM was from Tago (Burlingame, California).

Gel electrophoresis and immunoblotting

Isoelectric focusing gel electrophoresis (IEF) was carried out according to O'Farrell [15]. SDS-PAGE was performed using 10% polyacrylamide gel in a discontinuous Tris-glycine buffer system as described by Laemmli [10]. Proteins were electrophoretically transferred from SDS-polyacrylamide gel to nitrocellulose filter by the method of Towbin *et al.* [21]. The filter was treated with 3% gelatin in TBS, 0.5 M NaCl containing 10 mM Tris-HCl (pH 7.5), and then incubated with AS23 for 1hr, followed by the treatment with HRP-GAM for 1 hr. After immunoreaction, the filter was washed with TBS. HRP-GAM bound to the filter was detected as the product of diaminobenzidine reaction with nickel and cobalt ions according to De Blas *et al.* [3].

Preparation of ascidian native thin filaments

Native thin filaments were isolated from ascidian body wall muscle as described by Toyota *et al.* [22]; briefly, the body wall muscle was homogenized in a KMP buffer (0.05 M KCl-1 mM $MgCl_2$-10 mM K-phosphate buffer, pH 7.0) and centrifuged at 15,000 $\times$g. Thin filaments in contractile structures were released from the precipitate by a relaxing buffer containing 5 mM ATP and 0.1 mM EGTA and collected by ultracentrifugation at 100,000$\times$g.

Indirect immunofluorescence microscopy

Pieces of freshly dissected ascidian tissues were immersed in liquid nitrogen-cooled isopentane and transverse cryosections were cut at 10 μm. The sections were fixed with 4% paraformaldehyde containing phosphate-buffered saline (PBS) and 10 mM glycine, washed with PBS containing 10 mM glycine without air-drying, and treated with PBS/2% bovine serum albumin (BSA). They were then exposed to AS23, followed by staining with FITC-labeled GAM. The antibody reaction was performed for 60 min at room temperature. The specimens were mounted in 10 mg/ml p-phenylenediamine-50% glycerol-50% PBS, pH 8.0, and their fluorescence was observed and photographed under a Zeiss fluorescence/phase contrast microscope.

Electron microscopy

Isolated thin filaments suspended in a KMP buffer were placed on carbon-coated Formbar grids, treated with 1% BSA in the KMP-buffer and then reacted with AS23, followed by the treatment with 10 nm-gold conjugated GAM in 1% BSA/KMP buffer. The antibody reaction was performed for 30 min at room temperature. The specimens were washed thoroughly with the KMP-buffer after each antibody reaction and stained negatively with 1.5 % uranylacetate. The specimens were observed under a JEOL JEM 100CX electron microscope at an accelerating voltage of 80 kV.

RESULTS

We extracted proteins from the smooth muscle of ascidian body wall by a dilute alkaline salt solution according to the procedure which was originally devised for extracting the proteins from adhesion plaques [6, 7]. Several proteins in the molecular weight range of 70–150 kDa were detected as major components in the extract [12]. In this study, we isolated the proteins around 70–150 kDa by preparative SDS-PAGE and used as immunogens to prepare monoclonal antibodies. The culture medium of a hybridoma clone named AS23 recognized a single protein band of about 80 kDa, when the whole lysate of the ascidian body wall muscle was examined by immunoblotting combined with SDS-PAGE (Fig. 1, lanes b&i). The lysates of the other ascidian tissues scarcely reacted with the antibody (Fig. 1, lanes j-n). These results indicate that the antigen recognized by AS23, tentatively we call 80K protein, is enriched in the body wall

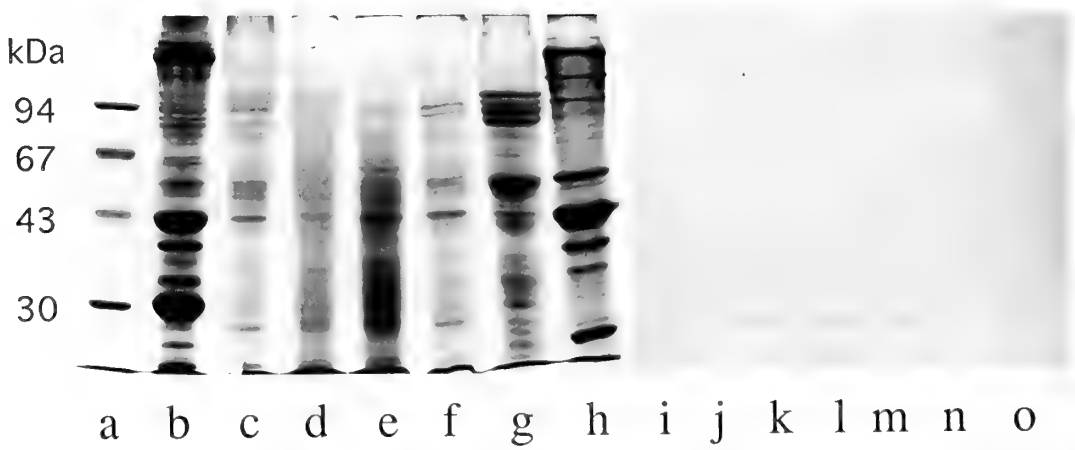

FIG. 1. Immunoblot analysis of the AS23 antigen. Proteins were extracted with 8 M guanidine-HCl from the tissue pieces of ascidian (b-g and i-n) or chicken (h, o), dialyzed against an SDS-buffer, and then applied to SDS-PAGE. Sample amount was adjusted so that the same wet weight of the tissue was in each lane. The left panel (a-h) denotes the electrophoresis patterns visualized by staining with Coomassie Brilliant Blue. The right panel (i-o) denotes the patterns of immunoblotting stained with AS23. a, molecular weight markers; b and i, body wall muscle; c and j, gut; d and k, stomach; e and l, liver; f and m, branchial sac; g and n, gonad; h and o, chicken gizzard.

muscle. We also examined the extracts of chicken gizzard (Fig. 1, h&o) and mouse smooth muscles with AS23, but none of the protein bands from these tissues were recognized by AS23.

To further clarify the protein recognized by AS23, the lysate of body wall muscle was displayed on a two-dimensional gel by a combination of isoelectric focusing and SDS-PAGE, and the protein blotted were reacted with AS23 by an immunoblotting method. AS23 recognized three major spots of about 80 kDa which differ slightly in pI (Fig. 2). Although it remains to be examined empirically, it seems likely that the spots recognized by AS23 were generated by post-translational modification of the protein, for example phosphorylation or acetylation etc.

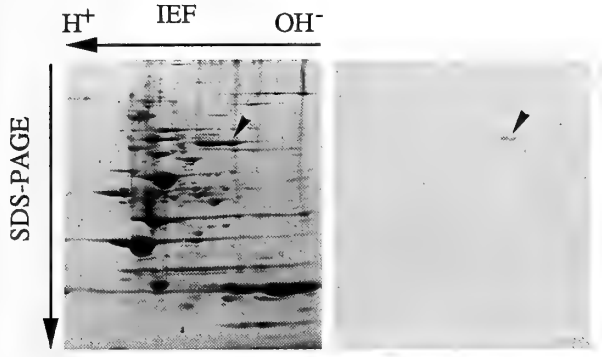

FIG. 2. Immunoblotting combined with two-dimensional PAGE. Proteins were extracted with a lysis buffer for IEF from ascidian body wall muscle and applied for two-dimensional PAGE (IEF/SDS-PAGE). Left, electrophoresis pattern stained by Coomassie Brilliant Blue; right, the result of immunostaining with AS23. The major spot of the 80K protein is marked by arrowheads.

Tissue distribution of the 80K protein was examined by immunocytochemical methods. Ascidian muscle and non-muscle tissues were cryosectioned, treated with AS23, and examined by indirect immunofluorescence methods. The cells in the body wall but not the extracellular matrix were positively stained with AS23 (Fig. 3, b). Almost all of the cells in the body wall were positively stained with AS23 as well as a monoclonal antibody (NT-302) to troponin T, a specific marker for muscle cells (Fig. 3, b&c). The AS23-positive cells were regarded as muscle cells. These cells were brightly stained by rhodamine-phalloidin (Fig. 3, d), indicating enrichment of actin filaments in the cytoplasm. In the immunoblot assay, the 80K protein was scarcely detected in non-muscle tissues, but by the immunocytochemical method, we detected AS23-positive cells among non-muscle tissues. As shown in Figure 3-f, we detected AS23-positive regions in the cryosection of hepatopancreas and associated tissues, although we have not yet been determined what type of tissues or cells they were. They were not stained by NT-302 (Fig. 3, f). Therefore, it is concluded that the 80K protein exists predominantly in muscle cells but its existence is not restricted to muscle cells. The amount in non-muscle tissues appears small.

In order to clarify intracellular localization of the 80K protein in ascidian body wall smooth muscle, the muscle was homogenized in a KMP buffer and the homogenate was subjected to subsequent fractionation, and the distribution of the 80K protein in various fractions was examined by immunoblotting. As shown in Figure 4, we found that the protein was concentrated in the fractions containing thin filaments during the procedure of thin filament isolation; the 80K protein appeared in the supernant at 15,000×g (Fig. 4, b&d), and it was detected more clearly in the isolated thin filaments not only with AS23 but also by staining with Coomassie Brilliant Blue (Fig. 4, c, e&f). These results suggest that the 80K protein may be an actin-binding protein, but its amount in thin filaments was much smaller than the amounts of actin, tropomyosin, and troponin. The 80K protein was detected in the solbule cytoplasmic fraction although small in amount, suggesting that the 80K protein can be free from actin filaments in the cells (data not shown).

Since the 80K protein was present in the thin filament fraction, it was matter of interest how the protein is associated with actin filaments. In order to visualize binding of the 80K protein to thin filaments, we applied an immunoelectron microscopic method: isolated thin filaments were treated with AS23 and subsequently with gold-labeled GAM. Gold particles certainly associated with one end of some thin filaments. The thin filaments without the particles were also observed (Fig. 5).

DISCUSSION

In this investigation, we succeeded in preparing a monoclonal antibody which recognizes a specific protein of about 80 kDa. The antigen, 80K protein, was detected predominantly in body wall smooth muscle cells. Therefore, it is likely that this protein plays some functional role in the ascidian body wall smooth muscle. For further characterization of the 80K protein, attempts to isolate this protein and its cDNA are now in progress. The monoclonal antibody, AS23, could be an excellent probe for such purpose.

Our present data suggest that the 80K protein is an actin-associated protein. Since nothing is known as to regulatory proteins for actin assembly in ascidian body wall smooth muscle, characterization of the 80K protein may provide to the clue to clarify regulation of actin dynamics in the ascidian body wall smooth muscle.

When we examined binding of AS23 to isolated thin filaments under an electron microscope, the antibody bound to the end of the filaments. However, many thin filaments without immuno-labeling were also observed. We assume the reasons as follow: 1) Affinity of the 80K protein to actin filaments would be rather weak and the protein might be released from the filaments during preparation of the specimen, 2) during the preparation of thin filaments, filaments were fragmented and then filament ends without the 80K protein were generated, and 3) procedure for immunostain-

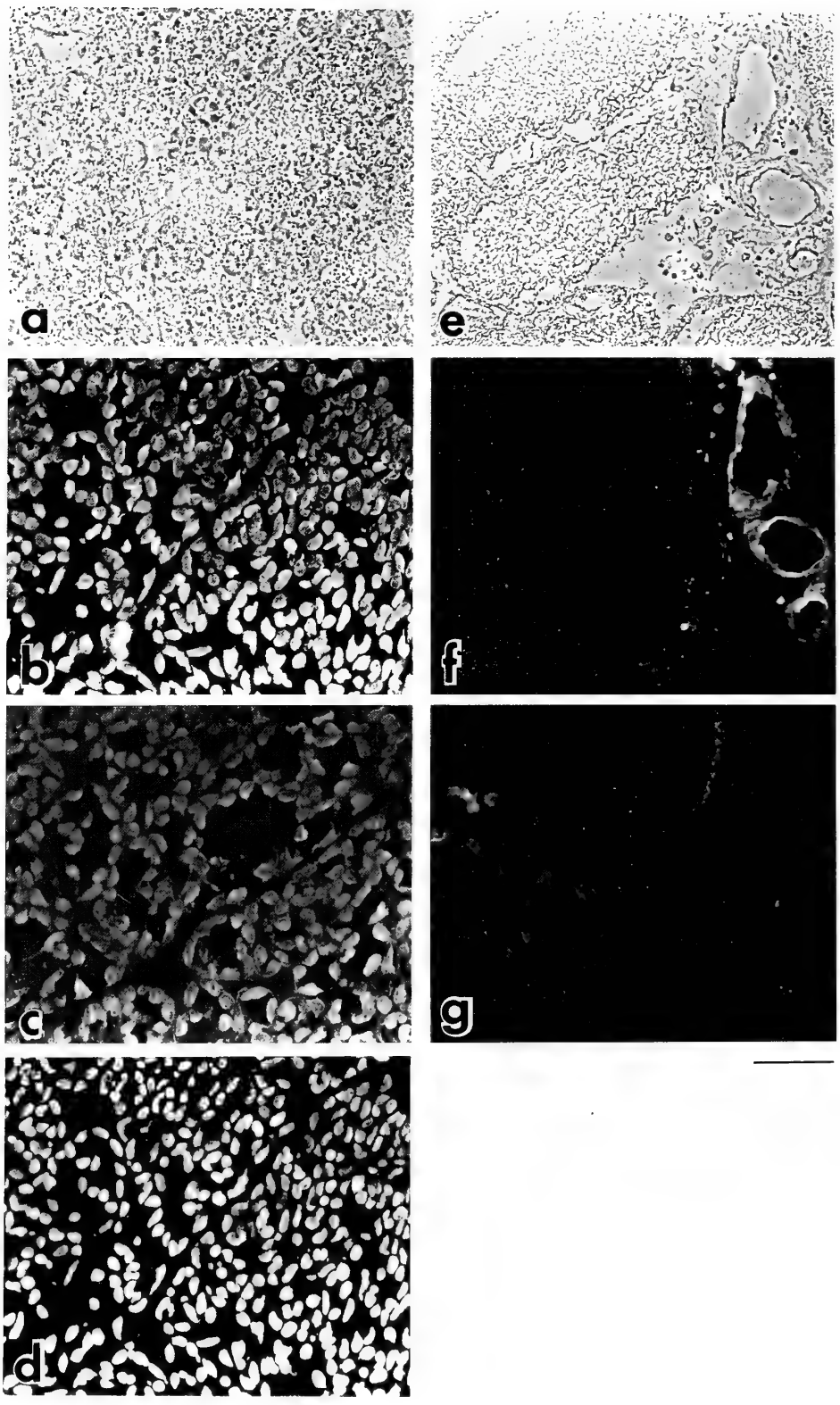

FIG. 3. Immunocytochemical localization of the AS23 antigen on sections of ascidian tissues. Cryosections (8 μm) of ascidian body wall muscle (a-d) and hepatopancreas and associated tissues (e-g) were examined. Phase-contrast micrographs (a, e) and corresponding immunofluorescence micrographs (b-d and f-g) are shown. The sections were stained with AS-23 (b, f), with anti-troponin T antibody (NT-302) (c, g) or with rhodamine-labeled phalloidin (d), respectively, Bar, 100 μm.

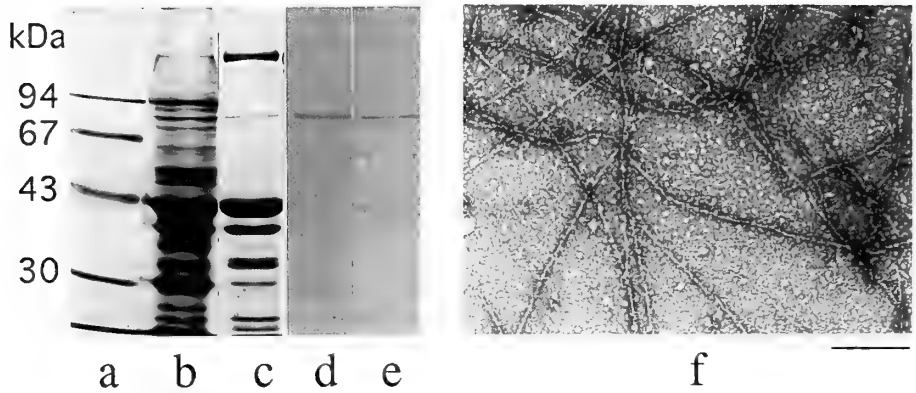

FIG. 4. Immunoblot analysis of the AS23 antigen in isolated thin filaments. Actin-containing fractions, the supernatant at 15,000×g (b&d) and the isolated thin filaments (c&e) (see Materials and Methods), were dissolved in an SDS-solution, and applied to SDS-PAGE. a, molecular weight markers; b and c, the electrophoresis patterns visualized by staining with Coomassie Brilliant Blue; d and e, the patterns of immunoblotting stained with AS23. f, an electron micrograph of the isolated thin filaments. Bar, 0.2 μm.

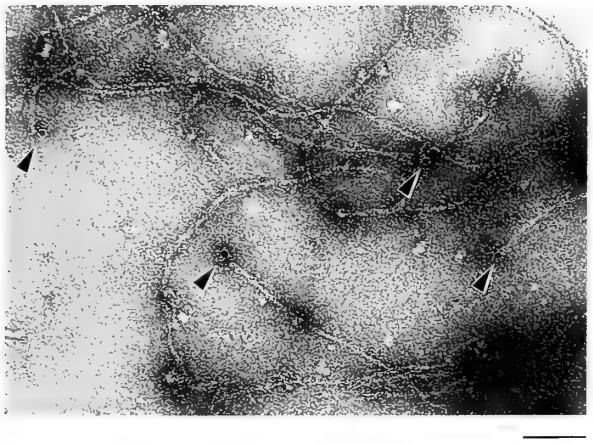

FIG. 5. Electron micrographs of ascidian thin filaments which were stained by AS23 and 10 nm-gold conjugated GAM. Location of gold particles were marked by arrowheads. Bar, 0.2 μm.

ing were not satisfactory. Nevertheless, the results suggest that the 80K protein can bind to the end of ascidian thin filaments, in other words, that the 80K protein might be a capping protein for actin filaments.

Although it is too early to discuss about the nature of the 80K protein, as judged by the size, binding to the filament end, and the tissue distribution, the 80K protein might be something like gelsolin in vertebrates. According to a previous report [2], vertebrate gelsolin gives several spots on two dimentional gels which focus in pH range 6.0–6.5, just as the 80 K protein. Gelsolin is known to exist in vertebrate smooth muscle [4, 13]. AS23, however, did not recognize any proteins in chicken and mammalian smooth muscles.

ACKNOWLEDGMENTS

This work was supported by research grants from Ministry of Education, Science and Culture, Yamada Science Foundation, and Futaba Denshi Memorial Foundation.

REFERENCES

1 Abe H, Komiya T, Obinata T (1986) Expression of multiple troponin T variants in neonatal chicken breast muscle. Dev Biol 118: 42–51

2 Bader M-F, Trifaro J-M, Langley OK, Thierse D, Aunis D (1986) Secretory cell actin-binding proteins: identification of a gelsolin-like protein in chromaffin cells. J Cell Biol 102: 636–646

3 De Blas AL, Chervinski HM (1983) Detection of antigens on nitrocellulose paper immunoblots with monoclonal antibodies. Anal Biochem 133: 214–219

4 Ebisawa K, Maruyama K, Nonomura Y (1984) Ca^{2+} regulation of vertebrate smooth muscle thin filaments mediated by an 84K Mr actin-binding protein: purification and characterization of the protein. Biomed Res 6: 161–173

5 Endo T, Obinata T (1981) Troponin and its components from ascidian smooth muscle. J Biochem. (Tokyo) 89: 1599–1608

6 Evans RR, Robson RM, Stromer MH (1984) Properties of smooth muscle vinculin. J Biol Chem 259: 3916–3924

7 Feramisco JR, Burridge K (1980) A rapid purification of α -actinin, filamin, and a 130,000-dalton protein from smooth muscle. J Biol Chem 255: 1194–1199

8 Galfre G, Howe SC, Milstein C, Butcher GW, Howard JC (1977) Antibodies to major histocompatibility antigens produced by hybrid cell lines. Nature 266: 550–552

9 Gefter ML, Margulies DH, Scharff MD (1977) A simple method for polyethylene glycol-promoted fusion of mouse myeloma cells. Somatic cell Genet 3: 231–236

10 Laemmli U (1970) Cleavage of structural proteins during the assembly of the head of bacteriophage T4. Nature 227: 680–685

11 Meedel TH, Hastings KEM (1993) Striated muscle-type tropomyosin in a chordate smooth muscle, ascidian body-wall muscle. J Biol Chem 268: 6755–6764

12 Nakae H, Sugano M, Ishimori Y, Endo T, Obinata T (1993) Ascidian entactin/nidogen. Implication of evolution by shuffling two kinds of cysteine-rich motifs. Eur J Biochem 213: 11–19

13 Nodes BR, Shackelford JE, Lebherz HG (1987) Synthesis and secretion of serum gelsolin by smooth muscle tissues. J Biol Chem 262: 5422–5427

14 Obinata T, Ooi A, Takano-Ohmuro H (1983) Myosin and actin from ascidian smooth muscle and their interaction. Comp Biochem Physiol 76B: 437–442

15 O'Farrell, PH (1975) High resolution two-dimensional electrophoresis of proteins. J Biol Chem 250: 4007–4021

16 Shinohara Y, Konishi K (1982) Ultrastructure of the body wall muscle of the ascidian, (*Halocynthia roretzi*): smooth muscle cell with multiple nuclei. J Exp Zool 221: 137–142

17 Terakado K (1987) Fine structure of ascidian smooth muscle. Zool Sci 4: 751–761

18 Terakado K, Obinata T (1987) Structure of multinucleated smooth muscle cells of the ascidian *Halocynthia roretzi*. Cell Tissue Res 247: 85–94

19 Terakado K (1988) The pattern of organization of intermediate filaments and their asymmetrical association with dense bodies in smooth muscle of an ascidian *Halocynthia roretzi*. Cell Tissue Res 252: 23–32

20 Terakado K (1989) Pattern of filament arrangement that produces easily their ball-like aggregates in smooth muscle fibers. Zool Sci 6: 1206

21 Towbin H, Stahlin T, Gordon J (1979) Electrophoretic transfer of proteins from polyacrylamide gels to nitro-cellulose sheets: Procedure and some applications. Proc Natl Acad Sci USA 76: 4350–4354

22 Toyota N, Obinata T, Terakado K (1979) Isolation of troponin-tropomyosin-containing thin filaments from ascidian smooth muscle. Comp Biochem Physiol 62B: 433–441

ZOOLOGICAL SCIENCE 11: 413–421 (1994)

Developmental Changes in Pteridine Biosynthesis in the Toad, *Bufo vulgaris*

SHIN-ICHIRO TAKIKAWA and MOTOKO NAKAGOSHI

Biological Laboratory, Kitasato University, Sagamihara City, Kanagawa 228, Japan

ABSTRACT—The presence of blue-violet fluorescent pteridines, neopterin, biopterin, pterin and isoxanthopterin, in a toad tadpole in the various development stages was determined by HPLC with fluorimetric detection. Changes in the activities of pteridine- synthesizing enzymes, GTP cyclohydrolase I, 6-pyruvoyl-tetrahydropterin synthase and sepiapterin reductase, were also investigated. In contrast to an older report by Hama, neopterin was already found in the tadpole larval stage, as well as in the young adult stage. Also, biopterin was found not only in the tadpole larval stage but also in the young adult stage. Neopterin constitutes the major portion of the pteridines of the animal and biopterin makes up the minor one throughout the whole development stage. In spite of the high content level of neopterin in the young adult stage, the activity of GTP cyclohydrolase I, which produces dihydroneopterin triphosphate, declined; and the activity of 6-pyruvoyl-tetrahydropterin synthase, which metabolizes dihydroneopterin triphosphate as a substrate, rose in the same stage.

INTRODUCTION

Tailless amphibians contain fairly large amounts of pteridines as fluorescent compounds in their skin, both in the larval and the adult stages. Hama proposed the name "Rana-chromes" for the fluorescent substances isolated from the skin of *Rana nigromaculata* as the collective name [15]. Afterwards, Rana-chrome 1 was identified as biopterin [12], Rana-chrome 2 as riboflavin [14], Rana-chrome 3 as 6-hydroxymethylpterin [1, 17], Rana-chrome 4 as isoxanthopterin [29] and Rana-chrome 5 as pterin-6-carboxylic acid [15], respectively. On the other hand, the other fluorescent substances of the pteridine type were isolated from the skin of the adult toad, *Bufo vulgaris*, and were named "Bufo-chromes" [18]. Bufo-chrome 2 was identified as pterin [18], and Bufo-chrome itself, which was generally considered specific for *Bufo*, was proved to be neopterin [8].

The kind and quantity of pteridines differ according to the kind of chromatophore, the age, and the species of the amphibians. At the time of metamorphosis in amphibians, a striking change in the pteridine patterns occurs in some species [1, 13, 16]. In the toad (*Bufo vulgaris*) neopterin appears at the end of metamorphosis (stage 46) and is very abundant in the adult stage, whereas biopterin is abundant in the larval stage and disappears at the end of metamorphosis [16]. The biosynthesis of pteridines in the skin of the tadpole, *Rana catesbeiana*, has also been investigated, and guanine [20], guanine nucleotide [32] and GTP [7] were proposed as precursors of pteridines.

In all of the above-mentioned investigations, however, pteridines were semi-quantitatively determined by fluorimetric estimation on paper chromatograms and the biosynthetic pathway of pteridines was not elucidated yet at that time. Nowadays, high performance liquid chromatography (HPLC) with fluorimetric detection allows for excellent separation and accurate quantitative determination of pteridines [31]. Furthermore, in the past few years, the biosynthetic pathway of tetrahydrobiopterin (BH_4) from GTP via dihydroneopterin triphosphate and 6-pyruvoyl-tetrahydropterin (PPH_4) has been revealed, as shown in Figure 1 [19, 24, 27, 28, 30, 33–35]. In this pathway, GTP cyclohydrolase I (EC 3.5.4.16), PPH_4 synthase and sepiapterin reductase (EC 1.1.1.153) are shown to be the indispensable enzymes for the biosynthesis of BH_4. The purposes of the present study are to demonstrate the developmental change in the activities of these three pteridine-synthesizing enzymes in relation to the change in the pteridine patterns in *Bufo vulgaris* and to measure the accurate content of various pteridines by HPLC with fluorimetric detection in several stages of the toad's development.

Accepted May 20, 1994
Received February 9, 1994

MATERIALS AND METHODS

Animals

Fertile eggs of *Bufo vulgaris*, deposited by a single female, were collected in the suburbs of Tokyo and hatched in our laboratory at 23°C. The tadpoles were fed on boiled spinach. The stages of the development from the fertilized egg through metamorphosis were classified according to Limbaugh and Volpe [21]. Whole bodies of embryos at the prefeeding stage (external gill completed; stage 21, each set of sample composed of 20 individuals) were collected and weighed without dissection. Tadpoles at stage 25 (operculum completed, each set 10 individuals), stage 30 (limb-bud bullet-shaped and about 1 mm in length, each set 5 individuals), stage 40 (hind legs completed, each set 2 individuals), stage 42 (both forelimbs protrude, each set 2 individuals) and stage 46 (metamorphosis complete and tail resorbed, each set 2 individuals) were collected and weighed after the removal of stomach and intestine by dissection. They were stored at −30°C until use.

Chemicals

Sepiapterin, biopterin, neopterin, pterin and isoxanthopterin were purchased from Dr. B. Schircks Laboratories (Jona, Switzer-

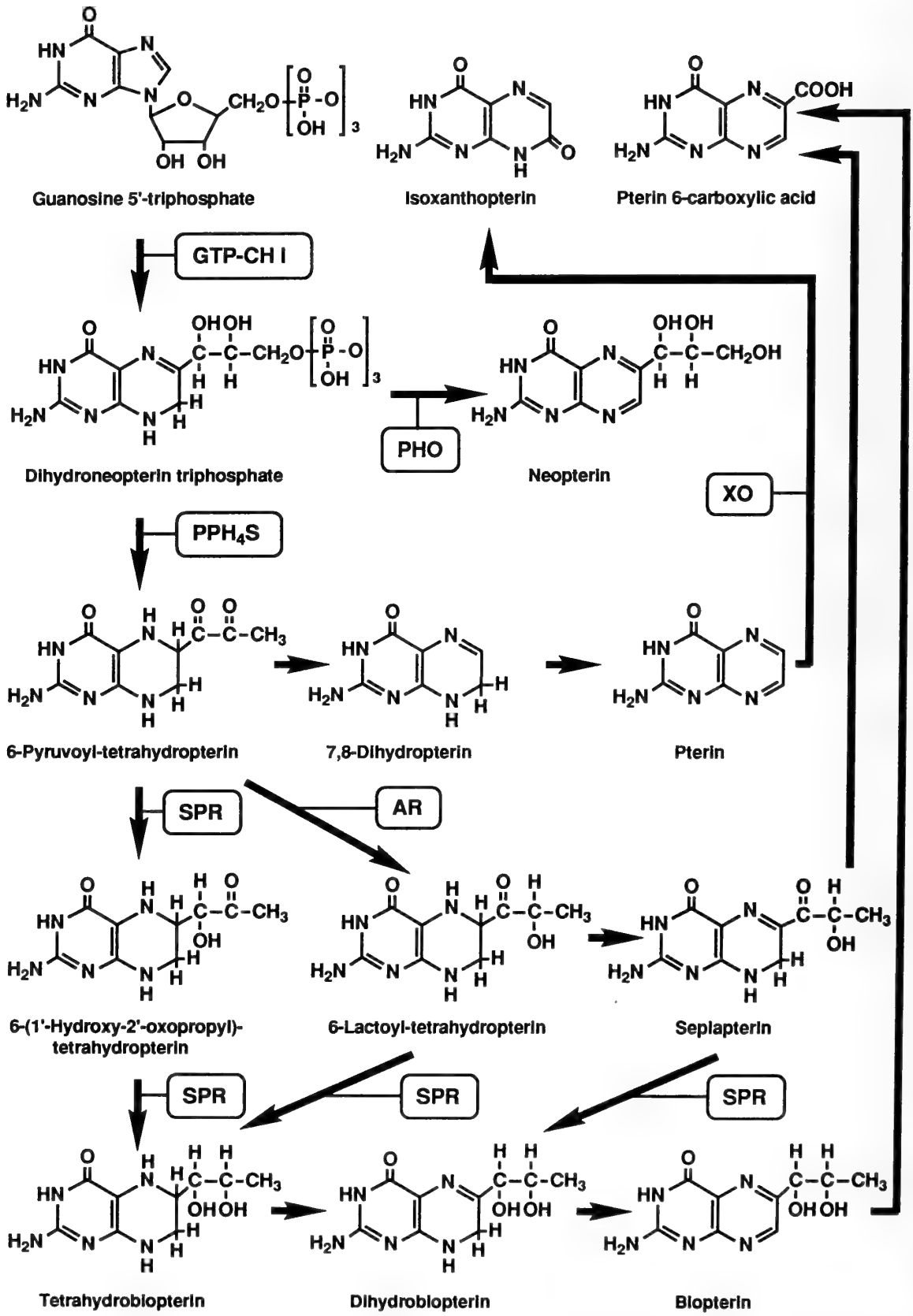

FIG. 1. The biosynthetic pathway of tetrahydrobiopterin and degradation process of the related pteridines. Neopterin also degraded to pterin-6-carboxylic acid. Enzymes are shown in round boxes: GTP-CH I, GTP cyclohydrolase I; PPH_4S, 6-pyruvoyl-tetrahydropterin synthase; SPR, sepiapterin reductase; AR, aldose reductase; PHO, phosphatase; XO, xanthine oxidase.

land). Sepiapterin, the substrate for sepiapterin reductase, was purified by column chromatography on phospho-Sephadex [11] and by recrystallization. The other pteridines were used without further purification. Dihydroneopterin triphosphate, the substrate for PPH_4 synthase, was prepared enzymatically from GTP by the method of Yoshioka *et al.* [37] using GTP cyclohydrolase I purified from chicken liver [6]. GTP lithium salt, alkaline phosphatase, Trizma base and bovine serum albumin were obtained from Sigma Chemical Co. Sephadex G-25 (fine) was purchased from Pharmacia Fine Chemicals. NADPH was bought from Oriental Yeast Co. Other reagents were of an analytical grade from commercial sources.

Sample preparation for pteridine analysis

Pteridines in tadpoles are present in their reduced and oxidized forms [9]. Acidic oxidation converts all forms of pteridines to the fully oxidized forms [10]; thus, the total amount of pteridines present is measured in this experiment. Preliminary experiments proved that pteridines were found mainly in the skin of tadpoles, but it was very difficult to separate the skin from other tissues; therefore, whole bodies of tadpoles were used through the experiment.

Tadpoles were thawed and homogenized with 4 volumes of 50% ethanol in a tapered tissue grinder with Teflon-pestle (Wheaton, NJ USA) for 2 min, and the homogenate was heated at 70°C for 10 min in a boiling water bath. After cooling, the homogenate was centrifuged at $10,000\times g$ for 10 min and the supernatant fluid was collected. Pteridines were extracted once more from the precipitate in the same way. The supernatant from the second extraction was combined with that from the first extraction, and the total volume was measured. A portion of the supernatant (200μl) was acidified by adding 40μl of 20% trichloroacetic acid (TCA) and oxidized with 40μl of iodine solution (1% I_2, 2% KI). After standing for 60 min in the dark, excess iodine was reduced by the addition of 40μl of 2% ascorbic acid. The mixture was then centrifuged at $10,000\times g$ for 7 min. The oxidized pteridines in the supernatant were determined by HPLC.

Sample preparation for enzyme activities

All subsequent procedures were carried out at 4°C. Tadpoles were thawed and homogenized with 4 volumes of 25 mM triethanolamine-HCl buffer (pH 7.4) in a tapered tissue grinder with Teflon-pestle for 2 min. The homogenate was centrifuged at $10,000\times g$ for 20 min. The resultant supernatant was applied to a Sephadex G-25 column (fine, 1 cm i.d. $\times$15 cm) equilibrated with the same buffer as extraction buffer, and then eluted with the same buffer. The elution pattern was monitored by mini UV monitor II (Atto Co.) at the wavelength of 280 nm, and the proteins in the main peak were used as the preparation of enzymes. Protein concentration was determined by the method of Lowry *et al.* [22] using bovine serum albumin as the standard.

Assay for GTP cyclohydrolase I

The enzyme activity was measured by a modification of the method reported by Duch *et al.* [2]. The reaction mixture was composed of 100 mM Tris-HCl buffer (pH 7.8), 2 mM GTP and 200μl of the Sephadex eluate, in a final volume of 250μl. The mixture was incubated for 60 min at 37°C in the dark. The reaction was terminated by the addition of 25μl of a 5 : 1 mixture of 1% I_2, 2% KI : 5N HCl. The mixture was allowed to stand for 20 min in the dark and then excess iodine was reduced by the addition of 25μl of 2% ascorbic acid. The reaction mixture was neutralized by the addition of 25μl of 1N NaOH. The neopterin triphosphate produced in the reaction mixture was dephosphorylated by incubation with 2 units of alkaline phosphatase for 60 min at 37°C in the dark. The reaction was terminated by the addition of 50μl of 20% TCA. Following centrifugation, the amount of neopterin in the supernatant was determined by HPLC. One unit of the enzyme activity was defined as the amount that catalyzes the production of 1 nmole of neopterin under the above conditions.

Assay for PPH_4 synthase

The assay of the enzyme activity is based on the fact that PPH_4 is decomposed to pterin and pyruvic acid under acidic condition [36]. The enzyme activity was measured by pterin production with a slight modification of the methods reported by Masada *et al.* [25] and Yoshioka *et al.* [37]. The reaction mixture was composed of 100 mM Tris-HCl buffer (pH 7.4), 8 mM $MgCl_2$, 30μM dihydroneopterin triphosphate and 117μl of the Sephadex eluate, in a final volume of 200μl. The mixture of the buffer and enzyme was heated at 80°C for 1 min before use to inactivate heat-labile phosphatases. The reaction was started by the addition of the substrate and the reaction mixture was flushed with N_2 gas and sealed. After incubation at 37°C for 60 min in the dark, the reaction was terminated by adding 40μl of 20% TCA and 40μl of iodine solution (1% I_2, 2% KI). After standing for 10 min in the dark, excess iodine was reduced by the addition of 40μl of 2% ascorbic acid. The mixture was then centrifuged and the supernatant was subjected to HPLC for estimation of pterin. One unit of the enzyme activity was defined as the amount that catalyzes the production of 1 nmole of pterin under the above conditions.

Assay for sepiapterin reductase

The enzyme activity was measured by a modification of the method reported by Ferre and Naylor [5]. The reaction mixture contained 100 mM potassium phosphate buffer (pH 6.4), 100μM NADPH, 50μM sepiapterin and 140μl of the Sephadex eluate, in a final volume of 200μl. The mixture was incubated at 37°C for 60 min in the dark. The reaction was stopped by adding 40μl of 20% TCA and 40μl of iodine solution (1% I_2, 2% KI). After standing for 20 min in the dark, excess iodine was reduced by the addition of 40μl of 2% ascorbic acid. The mixture was centrifuged and the fluorescence of the resulting biopterin in the supernatant was measured by HPLC. One unit of the enzyme activity was defined as the amount that catalyzes the production of 1 nmole of biopterin under the above conditions.

Analysis of pteridines by HPLC

The HPLC system consisted of an 887 PU pump (Japan Spectroscopic Co.), an FP-210 spectrofluorometer (Japan Spectroscopic Co.), a D-2500 chromato-integrator (Hitachi Co.) and a 655A-40 auto sampler (Hitachi Co.). An Asahipak GS-320H column (7.6$\times$250 mm, Asahikasei Co.) was used for the analyses of pteridines in the tadpoles, for the determination of GTP cyclohydrolase I activity with neopterin detection and for PPH_4 synthase activity with pterin detection, using 5 mM ammonium acetate as the mobile phase. For the assay of sepiapterin reductase activity with biopterin detection, HPLC was performed on a pre-column (4.6$\times$50 mm) of ODS-80T_M reverse phase (10μm, Tosoh Co.) in series with an analytical column (4.6$\times$150 mm) of ODS-80T_M (5μm) using 7% aqueous methanol as the elution solvent. Pteridines were detected by fluorimetry using an excitation wavelength of 360 nm and an emission wavelength of 445 nm at a flow rate of 1.0 ml/min.

RESULTS

Pteridines in the toad tadpoles

As shown in Figure 2, blue and violet fluorescent pteridines in the toad tadpoles were well separated by HPLC on Asahipak GS-320H column; therefore, the pteridines levels could be quantitatively determined using the known amount of the authentic samples of pteridines by fluorimetric detection.

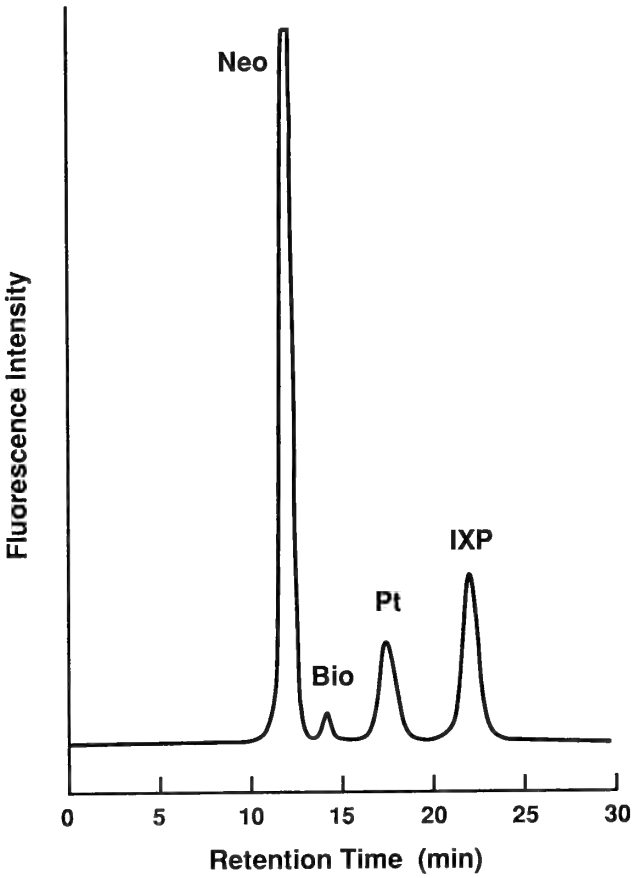

FIG. 2. An HPLC chromatogram of oxidized pteridines extracted from toad tadpoles at stage 40 with fluorimetric detection. The analysis was performed on an Asahipak GS-320H column (7.6× 250 mm) with 5 mM ammonium acetate as the mobile phase at a flow rate of 1.0 ml/min. Excitation at 360 nm, emission at 445 nm. Neo: neopterin, Bio: biopterin, Pt: pterin, IXP: isoxanthopterin.

Pteridine levels in individual tadpoles in the various development stages are shown in Figure 3. The results of the quantification of pteridines by HPLC indicate that neopterin constitutes the major portion of the pteridines of this animal and, in contrast with this finding, that the biopterin level is relatively low throughout metamorphosis. The levels of neopterin, pterin and isoxanthopterin continued to rise gradually in the development process (Fig. 3A, 3C, 3D). On the contrary, changes in the biopterin level during development displayed a particular pattern. The average value of biopterin reached a minimum at stage 25 and increased gradually during development, reaching a maximum at mid-climax and then declining slightly at the end of metamorphosis (stage 46) (Fig. 3B).

As for the content of pteridines per body weight, the changes in the levels of neopterin, pterin and isoxanthopterin showed the same pattern. They continued to rise gradually in the development process (Fig. 4A, 4C, 4D). In contrast, the biopterin content decreased gradually during development (Fig. 4B).

Activities of pteridine-synthesizing enzymes

The changes in the activities of the three pteridine-synthesizing enzymes, GTP cyclohydrolase I, PPH_4 synthase and sepiapterin reductase, during development are represented in three ways: the total activities contained in an individual tadpole (Fig. 5); the specific activities per mg protein (Fig. 6); and the activities per mg body weight (Fig. 7).

Concerning the changes in GTP cyclohydrolase I activity, the total activity increased gradually in the development process, reaching a maximum at stage 42, and then decreasing suddenly at the end of metamorphosis (stage 46) (Fig. 5A). The specific activity of the enzyme tends to decline gradually in the development process and reached a minimum at stage 46 (Fig. 6A). The activity of the enzyme per body weight also decreased gradually in the development process and reached a minimum at stage 46 (Fig. 7A).

As for changes in PPH_4 synthase activity, the activity levels were initially low, and then increased gradually in the development process, showing the highest values at the end of metamorphosis. This phenomena can be observed in all three changes in the total activity (Fig. 5B), the specific activity (Fig. 6B) and the activity per body weight (Fig. 7B).

The levels of the total activity of sepiapterin reductase were initially low and then increased gradually in the development process, reaching a maximum at stage 42 and declining at the end of metamorphosis (Fig. 5C). On the contrary, the specific activity of the enzyme and the activity per body weight were initially high and rapidly decreased in the development process, then they increased gradually, showing a small peak at stage 42 (Fig. 6C, 7C).

DISCUSSION

Hama [16] reported the changes in pteridine patterns during the metamorphosis of amphibians. According to his data, the toad, *Bufo vulgaris*, in the tadpole larval stage contains biopterin and no neopterin, whereas an adult toad at the end of metamorphosis contains neopterin and no biopterin. However, according to our present data, neopterin was already present in the tadpole larval stage, and the levels of total neopterin in individual tadpoles increased extremely in the development process (Fig. 3A). Also, the neopterin level per body weight increased in the development process (Fig. 4A). Furthermore, our data indicate that the total amount of biopterin in individual tadpoles increased gradual-

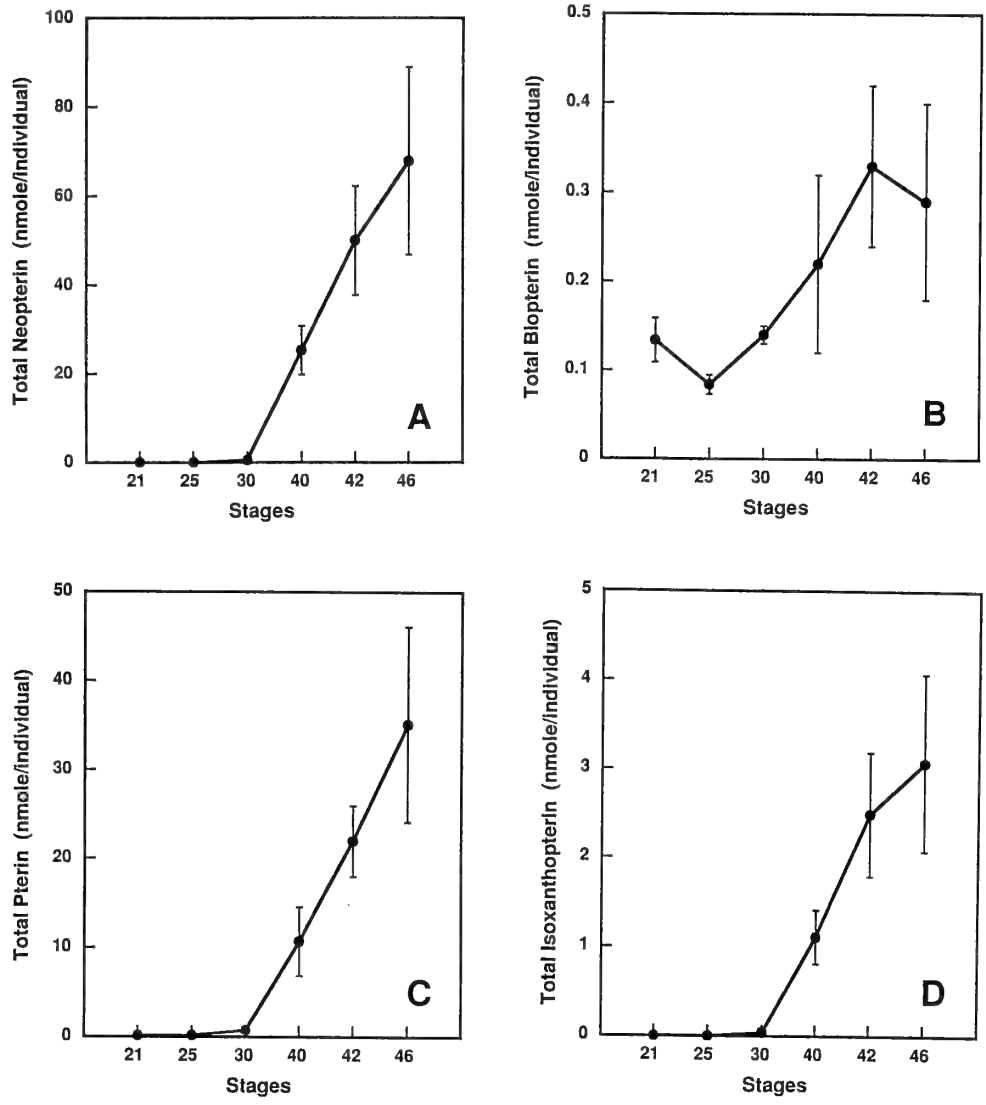

FIG. 3. The changes in levels of total pteridines contained in individual toad tadpoles in the various development stages. Each point and vertical line represent the mean of 5 determinations and standard error of the mean, respectively. A: Change in neopterin content. B: Change in biopterin content. C: Change in pterin content. D: Change in isoxanthopterin content.

ly in the development process, although the level decreased at the end of metamorphosis (stage 46) (Fig. 3B). On the contrary, the biopterin content per body weight decreased gradually in the development process (Fig. 4B). However, the level of biopterin did not fall to zero at the end of metamorphosis in our present experiment. Such a discrepancy between our present data and previously reported data by Hama [16] can be attributed to the difference in the respective analytical methods employed. Analysis by HPLC with fluorimetric detection is much more sensitive and accurate than that by paper chromatography. In any case, neopterin is a major pteridine and biopterin is a minor one in *Bufo vulgaris* throughout the whole development stage. The improved analytical method using HPLC revealed the complete absence of pterin-6-carboxylic acid in *Bufo vulgaris* throughout the whole development stage, while Hama found the compound on the paper chromatogram using the same experimental animal [16]. However, he already supposed that pterin-6-carboxylic acid might be an artifact product [17], the likelihood of which was proved by our present work.

The developmental change in the total GTP cyclohydrolase I activity indicates that the pteridine synthesizing activity decreased rapidly at the end of metamorphosis (Fig. 5A). The decrease in the enzyme activity seems to cause the decrease in the level of various pteridines, because the enzyme catalyzes the first step to synthesize pteridine from GTP (Fig. 1). However, the level of various pteridines, except biopterin, increased gradually in the development process and did not decrease at stage 46 in spite of the decrease in the enzyme activity. Also, in the case of *Drosophila melanogaster*, there is no relationship between the drastic change in GTP cyclohydrolase activity and levels of isoxanthopterin, sepiapterin and drosopterin during development [4]. The change in biopterin levels during the develop-

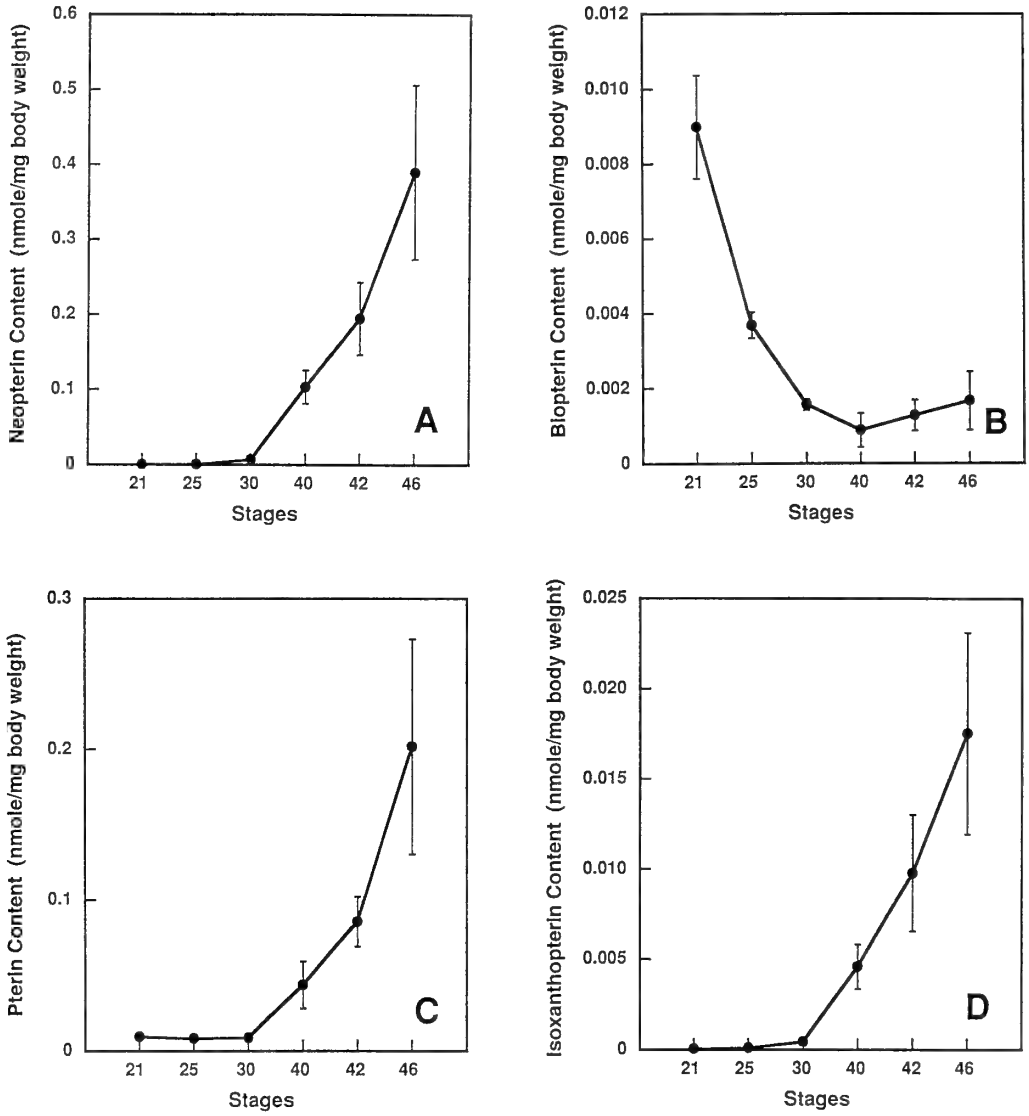

FIG. 4. The changes in pteridines content per body weight of toad tadpoles in the various development stages. Each point and vertical line represent the mean of 5 determinations and standard error of the mean, respectively. A: Change in neopterin content. B: Change in biopterin content. C: Change in pterin content. D: Change in isoxanthopterin content.

ment of *D. melanogaster* also was not affected by the change in biopterin synthase (it must be just the same as sepiapterin reductase) activity. That is, the level of biopterin increased gradually in the development process in spite of the decrease in the enzyme activity [3]. Such contradictions may be explained by the following. In lower vertebrates and invertebrates, pteridines are contained in pigment granules such as pterinosomes in chromatophores [26]. Therefore, pteridines may accumulate continuously in the granules during development, and they may not be lost from the granules when once they have been accumulated in the granules. However, the decrease in the total amount of biopterin at stage 46 (Fig. 3B) cannot be explained by this idea. This decrease may be attributed to the morphological change the tadpole undergoes as it loses its tail at the end of metamorphosis. The pteridines contained in the tail are lost [23]. Then the decrease in the total amount of biopterin is markedly affected because of its small amount, while the decrease in the levels of other pteridines are not so affected because of their relatively large amounts.

As for PPH_4 synthase, the total activity (Fig. 5B), the specific activity (Fig. 6B) and the activity per body weight (Fig. 7B) were initially low and increased gradually in the development process. The three profiles of these changes resemble one another. At the end of metamorphosis the enzyme activity still increased; therefore, much more of the enzymatic product, PPH_4, may be produced. Finally, the product will be changed into biopterin, which will accumulate, if the sepiapterin reductase activity is high. On the contrary, the sepiapterin reductase activity decreased at this stage; therefore, PPH_4 will decompose to pterin instead of being catalyzed by sepiapterin reductase (see Fig. 1). Then, the accumulation of pterin at stage 46 can be seen, as shown in Figure 3C. The increase in the enzyme activity at stage

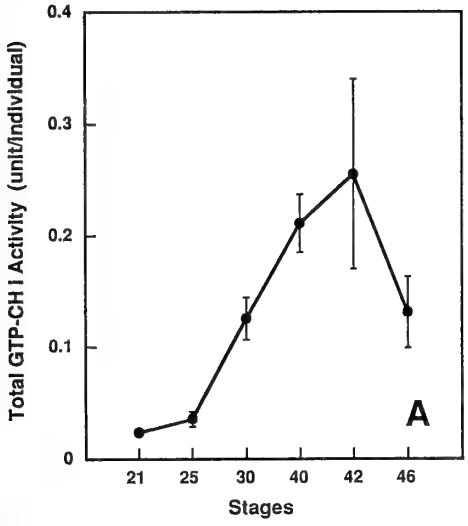

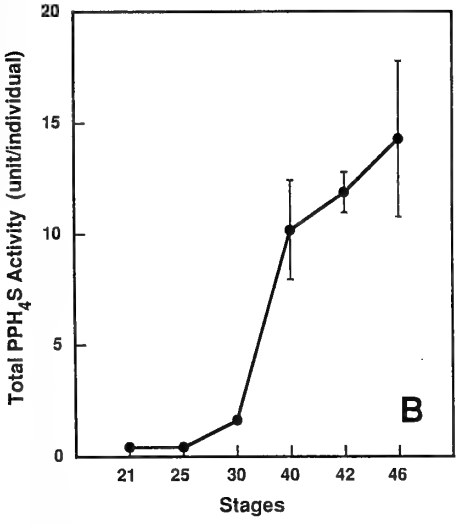

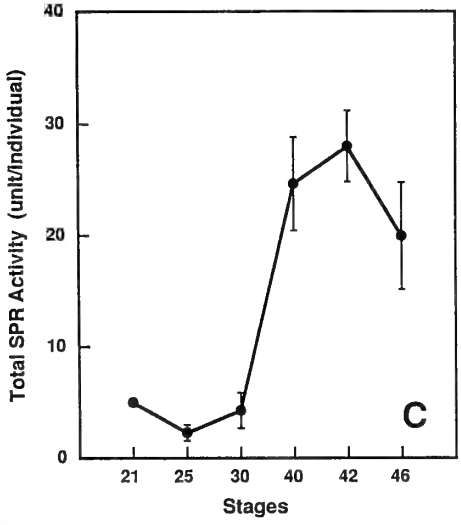

FIG. 5. The changes in levels of the total activity of pteridine-synthesizing enzymes contained in individual toad tadpoles in the various development stages. Each point and vertical line represent the mean of 5 determinations and standard error of the mean, respectively. A: Change in GTP cyclohydrolase I activity. B: Change in 6-pyruvoyl-tetrahydropterin synthase activity. C: Change in sepiapterin reductase activity.

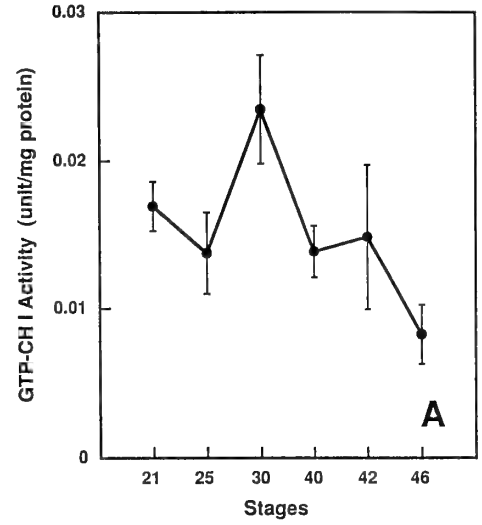

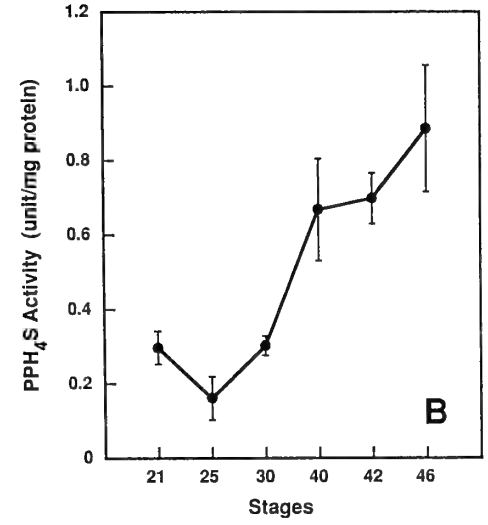

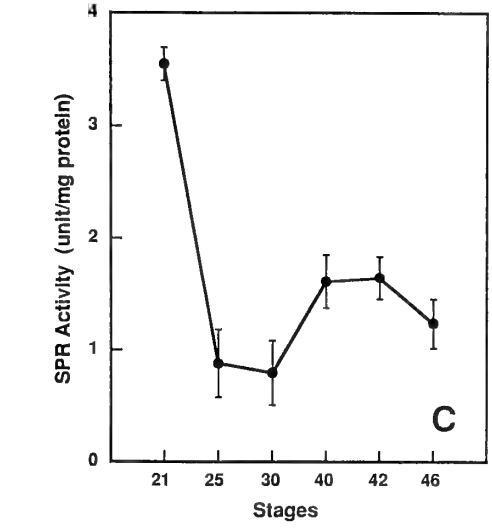

FIG. 6. The changes in levels of the specific activity of pteridine-synthesizing enzymes contained in toad tadpoles in the various development stages. Each point and vertical line represent the mean of 5 determinations and standard error of the mean, respectively. A: Change in GTP cyclohydrolase I activity. B: Change in 6-pyruvoyl-tetrahydropterin synthase activity. C: Change in sepiapterin reductase activity.

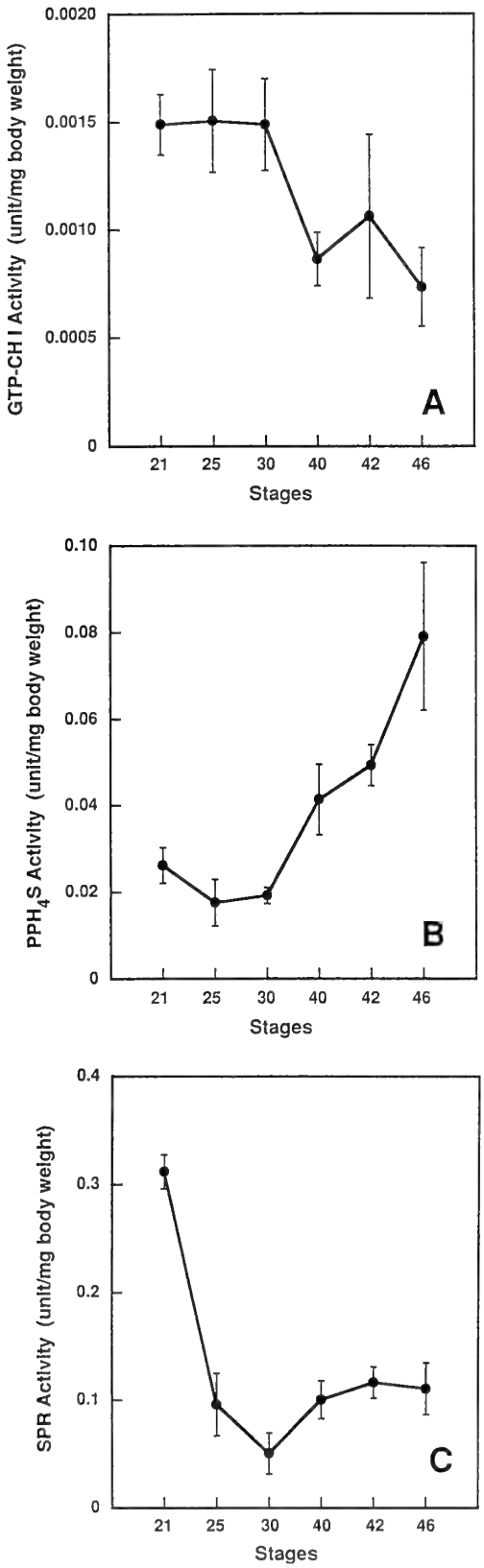

FIG. 7. The changes in levels of the activity of pteridine-synthesizing enzymes per body weight of toad tadpoles in the various development stages. Each point and vertical line represent the mean of 5 determinations and standard error of the mean, respectively. A: Change in GTP cyclohydrolase I activity. B: Change in 6-pyruvoyl-tetrahydropterin synthase activity. C: Change in sepiapterin reductase activity.

46 also seems to cause the decrease in the concentration of the substrate for the enzyme at this stage by being catalyzed with the enzyme. Thus, a decrease in the concentration of dihydroneopterin triphosphate at stage 46 can be expected; consequently, a decrease in neopterin content can be also expected (see Fig. 1). On the contrary, the neopterin content still increased at this stage (Fig. 3A, 4A). We cannot explain the reason for this interesting result at present.

The characteristic feature in the activity of sepiapterin reductase could be seen in an early stage. Although the total activity was very low in this stage (Fig. 5C), the specific activity and the activity per body weight were markedly high only in this stage (Fig. 6C, 7C). This may be a reason why biopterin content per body weight is very large in this stage (Fig. 4B).

In the present work we investigated the changes in activities of only pteridine-synthesizing enzymes and the correlation between these activities and levels of several pteridines during the development of the toad. However, it would be necessary to investigate also the changes in activities of pteridine-decomposing enzymes, phosphatase which produces neopterin via dihydroneopterin from dihydroneopterin triphosphate, xanthine oxidase which produces isoxanthopterin from pterin and dihydropterin oxidase reported by Fan and Brown [3]. The comparison of K_m values of every enzyme or investigations into mechanism of positive accumulation of pteridines in the pterinosomes would give more accurate information about our experimental results.

REFERENCES

1 Bagnara JT, Obika M (1965) Comparative aspects of integumental pteridine distribution among amphibians. Comp Biochem Physiol 15: 33–49

2 Duch DS, Bowers SW, Woolf JH, Nichol CA (1984) Biopterin cofactor biosynthesis: GTP cyclohydrolase, neopterin and biopterin in tissues and body fluids of mammalian species. Life Sci 35: 1895–1901

3 Fan CL, Brown GM (1979) Partial purification and some properties of biopterin synthase and dihydropterin oxidase from *Drosophila melanogaster*. Biochem Genet 17: 351–369

4 Fan CL, Hall LM, Skrinska AJ, Brown GM (1976) Correlation of guanosine triphosphate cyclohydrolase activity and the synthesis of pterins in *Drosophila melanogaster*. Biochem Genet 14: 271–280

5 Ferre J, Naylor EW (1988) Sepiapterin reductase in human amniotic and skin fibroblasts, chorionic villi, and various blood fractions. Clin Chim Acta 271: 271–282

6 Fukushima K, Richter WEJ_R, Shiota T (1977) Partial purification of 6-(D-*erythro*-1′,2′,3′-trihydroxypropyl)-7,8-dihydropterin triphosphate synthetase from chicken liver. J Biol Chem 252: 5750–5755

7 Fukushima T (1970) Biosynthesis of pteridines in the tadpole of the bullfrog, *Rana catesbeiana*. Arch Biochem Biophys 139: 361–369

8 Fukushima T, Akino M (1968) Nuclear magnetic resonance studies of some biologically active dihydropterins. Arch Biochem Biophys 128: 1–5

9 Fukushima T, Kobayashi K, Eto I, Shiota T (1979) A differential microdetermination for the various forms of biopterin.

Anal Biochem 89: 71–79

10 Fukushima T, Nixon JC (1980) Analysis of reduced forms of biopterin in biological tissues and fluids. Anal Biochem 102: 176–188

11 Fukushima T, Shiota T (1972) Pterins in human urine. J Biol Chem 247: 4549–4556

12 Goto T, Hama T (1958) Über die fluoreszierenden Stoffe aus der Haut eines Frosches *Rana nigromaculata*. I: Isolierung und Eigenschaften des "Rana-chrom 1". Proc Jap Acad 34: 724–729

13 Günder I (1955) Quantitative Untersuchung über die Entwicklung der Pterine und des Riboflavins in der Haut und im Auge von *Bufo bufo*. Z Naturf 10b: 173–177

14 Hama T (1952) Chemical properties of Rana-chromes. Zool Mag 61: 89 (Abstract, in Japanese)

15 Hama T (1953) Substances fluorescentes du type ptérinique dans la peau ou les yeux de la grenouille (*Rana nigromaculata*) et leurs transformations photochimiques. Experientia 9: 299–300

16 Hama T (1963) The relation between the chromatophores and pterin compounds. Ann N Y Acad Sci 100: 977–986

17 Hama T, Fukuda S (1964) The role of pteridines in pigmentation. In "Pteridine Chemistry" Ed by W Pfleiderer, EC Taylor, Pergamon Press, Oxford, pp 495–505

18 Hama T, Obika M (1958) On the nature of some fluorescent substances of pterin type in the adult skin of toad, *Bufo vulgaris formosus*. Experientia 14: 182–184

19 Heintel D, Ghisla S, Curtius H-Ch, Niederwieser A, Levine RA (1984) Biosynthesis of tetrahydrobiopterin: Possible involvement of tetrahydropterin intermediates. Neurochem Int 6: 141–155

20 Levy CC (1964) Pteridine metabolism in the skin of the tadpole, *Rana catesbeiana*. J Biol Chem 239: 560–566

21 Limbaugh BA, Volpe EP (1957) Early development of the gulf coast toad, *Bufo valliceps* Wiegmann. American Museum Novitates No. 1842, 1–32

22 Lowry OH, Rosebrough NJ, Farr AL, Randall RJ (1951) Protein measurement with the folin phenol reagent. J Biol Chem 193: 265–275

23 Manabe T, Kobayashi K, Horiuchi S (1989) Observation on release of pterins during metamorphosis of bullfrog, *Rana catesbeiana*. Zool Sci 6: 1139

24 Masada M, Akino M, Sueoka T, Katoh S (1985) Dyspropterin, an intermediate formed from dihydroneopterin triphosphate in the biosynthetic pathway of tetrahydrobiopterin. Biochim Biophys Acta 840: 235–244

25 Masada M, Matsumoto J, Akino M (1990) Biosynthetic pathways of pteridines and their association with phenotypic expression in vitro in normal and neoplastic pigment cells from goldfish. Pigment Cell Res 3: 61–70

26 Matsumoto J (1965) Studies on fine structure and cytochemical properties of erythrophores in swordtail, *Xiphophorus helleri*, with special reference to their pigment granules (pterinosomes). J Cell Biol 27: 493–504

27 Milstien S, Kaufman S (1983) Tetrahydro-sepiapterin is an intermediate in tetrahydrobiopterin biosynthesis. Biochem Biophys Res Commun 115: 888–893

28 Milstien S, Kaufman S (1985) Biosynthesis of tetrahydrobiopterin: Conversion of dihydroneopterin triphosphate to tetrahydropterin intermediates. Biochem Biophys Res Commun 128: 1099–1107

29 Nawa S, Goto M, Matsuura S, Kakizawa H, Hirata Y (1954) Studies on pteridines: VI. The pterin from *Bombyx mori* (silkworm) and *Rana nigromaculata* (frog). J Biochem (Tokyo) 41: 657–660

30 Smith GK, Nichol CA (1984) Two new tetrahydropterin intermediates in the adrenal medullary *de novo* biosynthesis of tetrahydrobiopterin. Biochem Biophys Res Commun 120: 761–766

31 Stea B, Halpern RM, Smith RA (1979) Separation of unconjugated pteridines by high-pressure cation-exchange liquid chromatography. J Chromatog 168: 385–393

32 Sugiura K, Goto M (1968) Biosynthesis of pteridines in the skin of the tadpole, *Rana catesbeiana*. J Biochem (Tokyo) 64: 657–666

33 Switchenko AC, Brown GM (1985) The enzymatic conversion of dihydroneopterin triphosphate to tripolyphosphate and 6-pyruvoyl-tetrahydropterin, an intermediate in the biosynthesis of other pterins in *Drosophila melanogaster*. J Biol Chem 260: 2945–2951

34 Switchenko AC, Primus JP, Brown GM (1984) Intermediates in the enzymic synthesis of tetrahydrobiopterin in *Drosophila melanogaster*. Biochem Biophys Res Commun 120: 754–760

35 Takikawa S, Curtius H-Ch, Redweik U, Leimbacher W, Ghisla S (1986) Biosynthesis of tetrahydrobiopterin: Purification and characterization of 6-pyruvoyl-tetrahydropterin synthase from human liver. Eur J Biochem 161: 295–302

36 Tanaka K, Akino M, Hagi Y, Doi M, Shiota T (1981) The enzymatic synthesis of sepiapterin by chicken kidney preparations. J Biol Chem 256: 2963–2972

37 Yoshioka S, Masada M, Yoshida T, Inoue K, Mizokami T, Akino M (1983) Synthesis of biopterin from dihydroneopterin triphosphate by rat tissues. Biochim Biophys Acta 756: 279–285

ZOOLOGICAL SCIENCE 11: 423–431 (1994)

Neural Crest Development in Reptilian Embryos, Studied with Monoclonal Antibody, HNK-1

LING HOU[1] and TAKUJI TAKEUCHI[2]*

Biological Institute, Faculty of Science, Tohoku University, Aoba-yama, Sendai 980, Japan

ABSTRACT—We report here early development of cranial and trunk neural crest, and migratory routes of HNK-1-immunoreactive cells in embryos of a primitive amniote, the softshell turtle. The cranial neural crest cells begin to emigrate shortly after the neural tube closure. It seems that the migratory timing of the cranial neural crest cells in the turtle is different from those of birds and mammals. Presence of two major migratory routes were found in the trunk: (1) a dorsolateral pathway between the epidermal ectoderm and somite; (2) a ventral pathway between the anterior portion of dermomyotome and the sclerotome of each somite. Our results suggest that the trunk neural crest cells have characteristic mode of migration in development of amniotes including the turtle unlike that of teleosts and *Xenopus*. It is likely that ventrally migrating neural crest cells are the source of pigment cells of some extracutaneous tissues in the turtle embryo.

INTRODUCTION

Cellular morphogenic movement in embryonic development of most organisms, particularly that of the vertebrates, is a significant process because it is related to the cytodifferentiation and the spatial patterning of the body. The neural crest is an extraordinary embryonic tissue that appeared during the evolution of vertebrates and contributes to a variety of neuronal and nonneuronal structures as a result of extensive migration during embryogenesis [14, 23]. In avian embryos, this transient tissue originates along the dorsal midline of the closing neural tube during neurulation and migrates along characteristic pathways throughout cephalic and trunk regions of the embryo to reach appropriate destination of the body, where they give rise to numerous cellular phenotypes and structures such as (1) most of the craniofacial cartilage, skeletal and connective tissues; (2) neurons and supporting cells of the peripheral nervous systems; (3) pigment cells; (4) adrenomedullary cells, *etc.* [23]. Their highly migratory, multipotent features have long attracted attention of many biologists [14, 23, 38]. Thus, neural crest has been widely used in the investigation of cell migration and differentiation [2, 3, 11, 19, 22, 29, 34, 39]. However, our knowledge concerning the migration and differentiation of neural crest cells is based on limited information from a few species, which mostly belong to three groups of vertebrates; amphibians, birds and mammals. Our understanding on the neural crest development in reptiles is poor [14] though reptiles have been recognized as materials that provide unique biological information such as temperature-dependent sex determination in embryonic development [7], migration mode of primordial germ cells [16], spatial pattern of neural crest-derived pigment cells [10]. It seems, therefore, significant to investigate the development and migration pattern of neural crest of reptiles as ancestors to both birds and mammals in animal phylogeny.

On the other hand, the neural crest-derived pigment cells in the turtle embryos are found in the skin as well as in the various extracutaneous tissues such as dorsal aorta, aorta of kidney, lung and skeletal muscle, *etc.* [17]. It was also found that the melanoblasts were located corresponding to the ventral route of neural crest cell migration in warm-blooded animals. This leads us to a question regarding the enigmatic migration routes of the melanogenic crest cells in the turtle.

In order to visualize migratory neural crest cells *in situ*, various methods including radioactive labeling, differential chromatin marking and vital dye labeling have been utilized in other species of vertebrates [amphibian: 30; birds: 22, 32, 37; mammals: 32]. However, the study on the neural crest cell migration in reptiles has been difficult because of the lack of specific label or marker that recognizes the nascent crest to follow the migratory route in embryos. In recent years, development of a monoclonal antibody, HNK-1 (NC-1) which recognizes an acidic sulfated glycosphingolipid with five sugars, made it possible to identify migrating neural crest cells in chick and rat, as well as teleost, embryos [2, 5, 11, 29, 31, 36]. We have previously studied the differentiation of neural crest cells *in vitro* in the turtle embryos and found that the antibody specifically recognizes migrating neural crest cells [18]. Judging from the results mentioned above, this antibody provides a useful tool for the study of neural crest cell migrating of reptiles.

In the present study, we investigate development of the turtle neural crest using the monoclonal antibody, HNK-1,

[1] Present Address: Department of Microbiology and Immunology, Indiana University School of Medicine, 635 Barnhill Dr., Indianapolis, IN 46202, USA
[2] Present Address: Nihon Gene Research Laboratories, Inc. 3–11–18 Tsubamesawa-higashi, Miyagino-ku, Sendai 983, Japan
Accepted April 14, 1994
Received Feburary 10, 1994
* To whom all correspondence should be addressed.

and examined the source of the neural crest-derived pigment cells in some extracutaneous tissues. These studies will be an important step towards understanding the developmental patterns of reptile neural crest. The information we obtain can also be compared with that of other species for further understanding the mechanism of cell migration and differentiation in relation to the evolutionary process of the developmental mechanisms.

MATERIALS AND METHODS

Incubation of eggs

The softshell turtle, *Trionyx sinensis japonicus* was used in our experiments. Fertilized eggs of the turtle were obtained from Hattori-Nakamura Nursery of Shizuoka, Japan. The method of incubation for this species was previously described [15]. Briefly, the eggs were incubated in laboratory incubator at 33°C, with about 90% relative humidity.

Isolation of embryos

The softshell turtle embryos were staged according to the criteria of authors [15]; its specific feature of the early development is presented in Table 1. The assignment of each embryo to developmental stages was made by isolating it from the eggs. Embryos of stages 6 to 14 were used in our experiment.

Histological methods

For light microscopic studies, embryos were fixed at the indicated stages in Bouin's fixative (75 parts saturated picric acid, 25 parts formalin, 5 parts glacial acetic acid) at room temperature for 24 hr, then transferred to 70% ethanol. The embryos were dedhydrated, embedded in paraffin (Merk, Germany) and sectioned serially at 7–8 μm thickness. Sections were stained with hematoxylin and eosin.

Immunohistochemical methods

The monoclonal antibody, HNK-1 (Beckton-Dickinson, CD57, IgMκ), which ha been shown to recognize the surface epitope of neural crest cells of some vertebrates [31, 36] was used for this immunostaining. The turtle embryos of various stages were fixed in 4% paraformaldehyde in phosphate-buffered saline (PBS, pH 7.4) either at 4°C for overnight or at room temperature for 3–6 hr, and then washed in several changes of PBS. The fixed embryos were dehydrated, embedded in paraffin and serially sectioned at 10 μm. The sections were placed on neoprene-coated microslide glasses. They were deparaffinized in xylene, then dehydrated through a graded series of ethanol, and rinsed in PBS. Before staining, specimens were treated with PBS-3% bovine serum albumin (BSA) and were then incubated with the monoclonal antibody at 1:50 dilution in PBS-0.5% BSA for overnight at 4°C. After several washes with PBS, they were incubated for 1 hr with rabbit anti-mouse IgM antibody (RAM), followed by several washes in PBS. They were then stained with FITC-conjugated goat anti-rabbit antibody (FITC-GAR, Cappel) for 1 hr. The sections were washed in PBS and mounted in PBS containing 2.5% diazobicyclooctane (DABCO). In control experiments, mouse IgM protein (Zymed) was used as the first antibody. No specific staining was found in the control series at any embryonic stage.

For whole mount staining, embryos of stages 11 and 12 were for the sections, except the time and concentration of antibody reaction. The embryos were incubated with the antibody HNK-1 at 1:25 dilution in PBS-0.5% BSA for 2–3 days at 4°C, then incubated for 2 days with RAM, and stained with FITC-GAR for 2 days. The specimens were examined and photographed with a Olympus epifluorescence microscope, BH2-RFL.

RESULTS

Early development of neural crest

In embryos of stage 6, the edges of the neural plate moved fo form the neural folds, while the neural groove appeared in the anterior region of embryo. At stage 7, the neural groove closed to form the neural tube in the head region; the enclosure progressed toward the anterior region of trunk. The presumptive neural crest was observed on the dorsal wall of the neural tube of head region (Fig. 1A); they are located at junction between the ectoderm and the neural tube in the anterior region of embryo (Fig. 1B). At stage 8, neural crest was clearly segregated from the neural tube and appeared at the cephalic region of embryos. A mass of crest cells covered the neural tube of presumptive mesencephalon and rhombencephalon region (Fig. 1C). At stage 9, neural crest cells detached from neural tube and located at the space

TABLE 1. Developmental features in the early stages of embryos of the turtle, *Trionyx sinensis japonicus*

Stage	Age	Number of somites	Specific features
5	15–16 hr	0	Notochord and neural plate appear.
6	24 hr	1	Neural groove formation; amnion and blood islands appear.
7	33–35 hr	4–5	Neural tube formation; primordium of heart appears.
8	42–43 hr	6–7	Formation of mesencephalon and rhombencephalon; primary optic vesicles appear.
9	48–56 hr	9–11	Otic pits appear.
10	64–65 hr	13–14	Otic vesicle formation; amnion extends to blastopore region.
11	72–74 hr	16–18	Lens formation; heart beat starts.
12	96 hr	20–21	Amnion closed; nasal placode appears.
13	5 day	27–28	Limb-buds appear.
14	6 day		Pigment cells of retina appear.

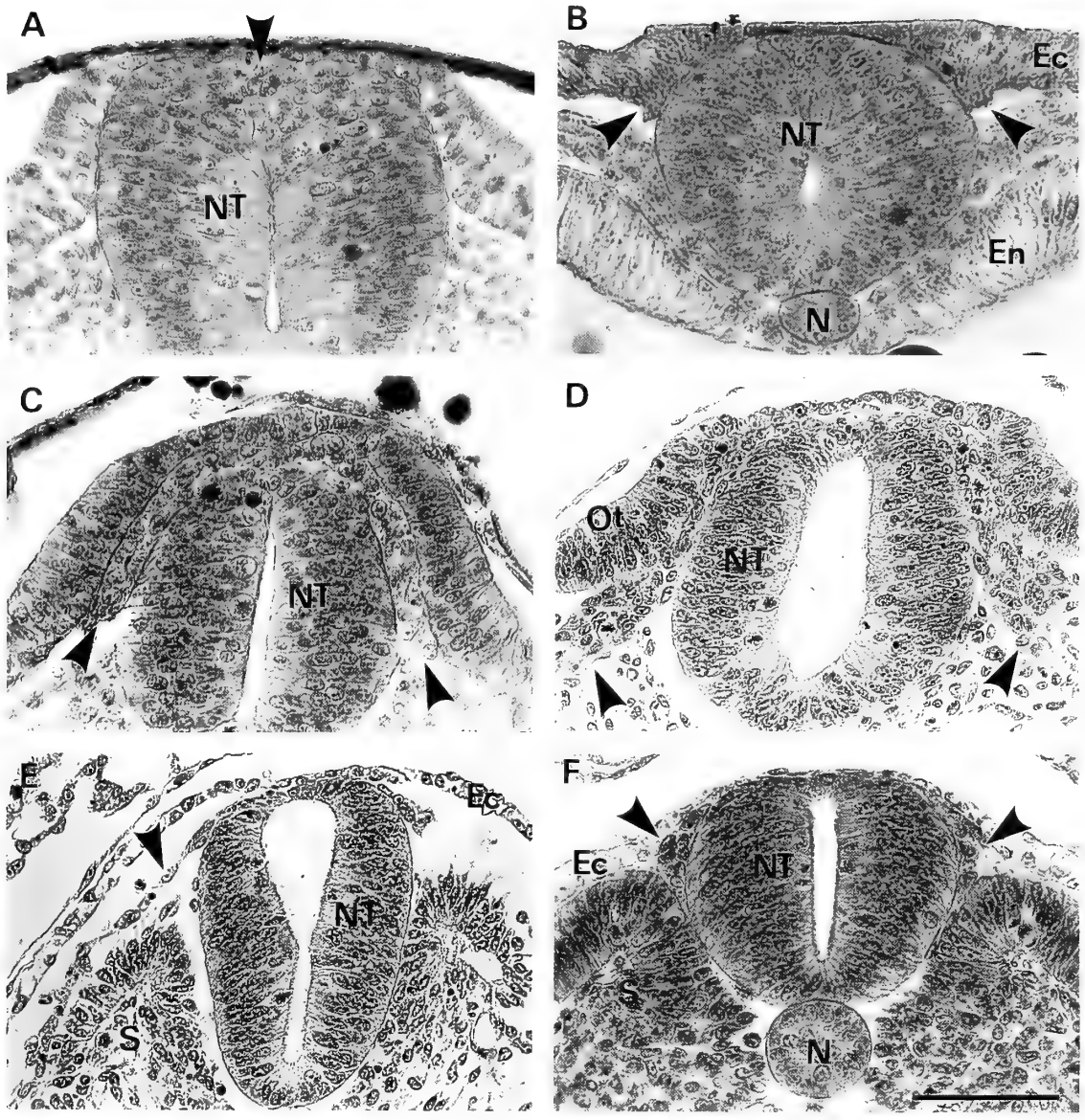

FIG. 1. Cross sections of the neural tube of the turtle embryos. A, stage 7. Neural crest population located at the dorsal border of the neural tube of head region. B, Stage 7. Presumptive neural crest appears at the junction between the ectoderm and the neural tube. C, Stage 8. A mass of crest cells cover the dorsum of the mesencephalon and rhombencephalon. D, Stage 9. The front line of crest cell population moves the area between the ectoderm and the mesoderm (arrow). E, Stage 9. A cross-section through first somite. Crest cells are found between the ectoderm and the somite. F, Stage 9. A cross section through the 7th somite. Crest cells are located laterally to the neural tube. Ec, ectoderm; En, endoderm; N, notochord; NT, neural tube; Ot, otic placode; S, somite. Arrowhead indicate neural crest cells. Scale bar = 100 μm.

between the ectoderm and mesoderm in the cephalic region (Fig. 1D, E), while individual neural crest cells were found on the neural tube of trunk region at this stage; most of them were located between the ectoderm and the neural tube prior to the beginning of their migration (Fig. 1F). The onset of migration of the neural crest follows an anterior-to-posterior order. At these stages, however, cells identified as individual neural crest cells by morphological observation did not react to the antibody, HNK-1, except a few positive cells.

Cephalic crest cell migration

The earliest cells to emigrate from the mesencephalon appeared at stage 8 towards stage 9. By advanced stage 10, HNK-1-immunoreactive crest cells have separated from the neural tube and dorsolaterally moved under the epidermis (Fig. 2A), being localized laterally to the optic vesicles. Numerous migrating crest cells were also found ventrally to the space between the optic vesicle and prosencephalon, and the area surrouding the developing eye (Fig. 2B). At more rostral level, some crest cells from the mesencephalon moved cranially over the optic vesicle to the cell free space between the epidermis and prosencephalon (Fig. 2C). The HNK-1-immunoreactive cells can be detected in the vicinity of the nasal placode at stage 12. At later stage, the mesencephalic

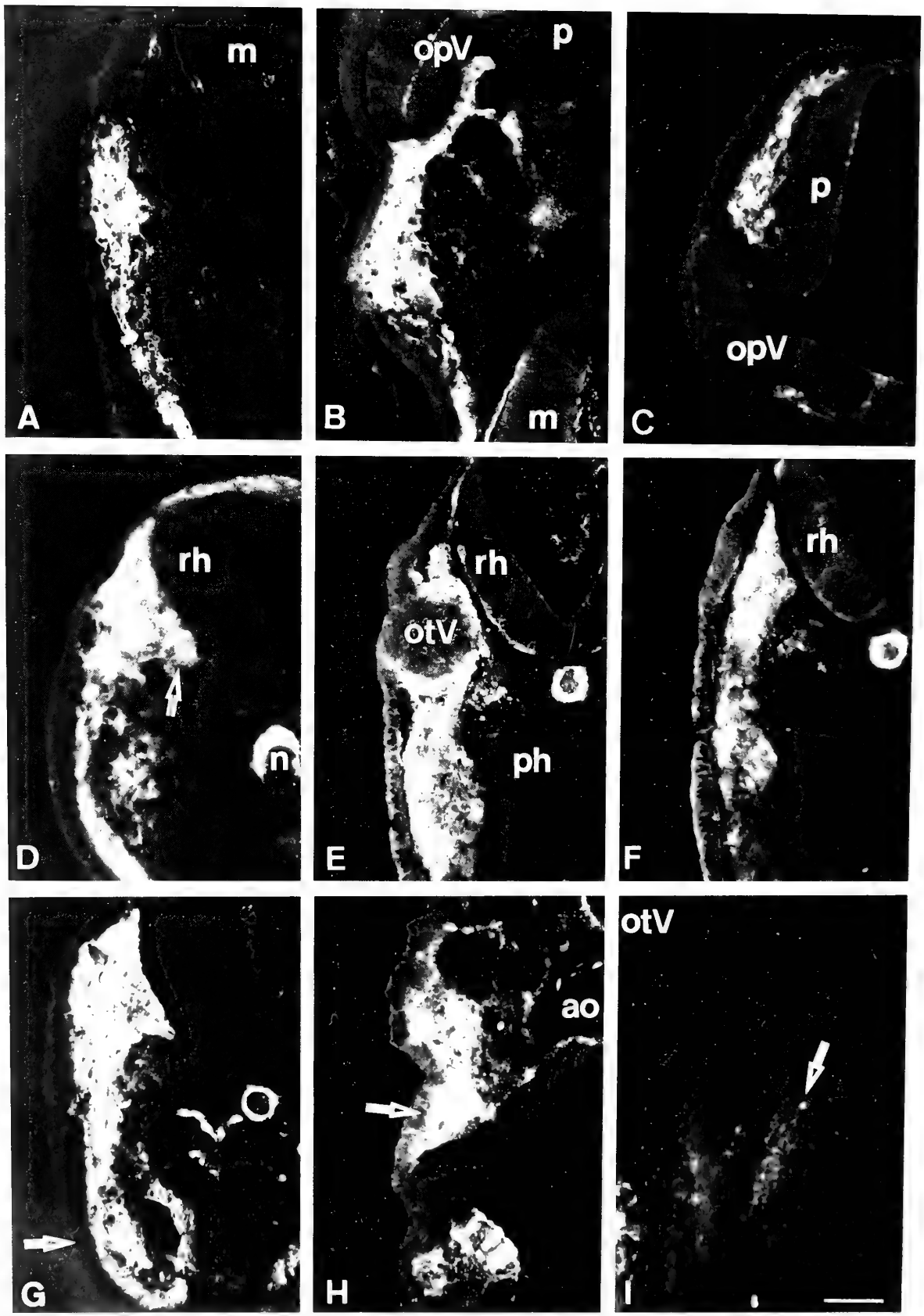

FIG. 2. Migration of HNK-1-immunoreactive crest cell in cephalic region. A, Stage 10. Crest cells are seen in the mesencephalon region dorsolaterally migrating along the epidermis. B, Stage 11. Crest cells are ventrally located at the space between optic vesicle and prosencephalon. C, Stage 11. Sole population of crest cells distributes between the epidermis and prosencephalon. D, Stage 10. Crest cells migrating dorsolaterally under the epidermis and ventrally toward the bottom of the anterior rhombencephalon (arrow). E, Crest cells

crest cells will give rise to mesenchymal components to contribute to the maxillary and nasal processes as previously described [13]; some of them also differentiate into melanocytes at the choroid and nasal connective tissue (Data not shown).

At stage 10, crest cells arose out of anterior rhombencephalon (anterior to the otic placode) and continued to migrate dorsolaterally along the ectoderm, while some of the cells ventrally along the tube of anterior rhombencephalon (Fig. 2D). Two distinct streams of migration of rhombencephalic neural crest were observed at this region. First, front line of the crest cell polulation moved under the epidermis and reached the pharynx; they intercede into second visceral (hyoid) arch. Second, other crest cells move toward the bottom region of rhombencephalon and contribute to the trigeminal ganglion formation at stage 11 of embryos. The crest cell migration was seen at the region of posterior rhombencephalon (hind brain after the optic placode) at this stage. The foremost cells of posterior rhombencephalic crest population moved along the area between the ectoderm and mesoderm, and already reached the pharynx (Fig. 2E, F). The crest cells in cephalic region were stained intensely probably reflecting the fact that the density of the crest cells was high.

At the level of the first visceral arch, a population of crest cells have migrated laterally between the ectoderm and mesoderm. They moved into the developing first visceral arch and into the area surrounding the first aortic arch in the embryo of stage 10 (Fig. 2G). They seem to provide the

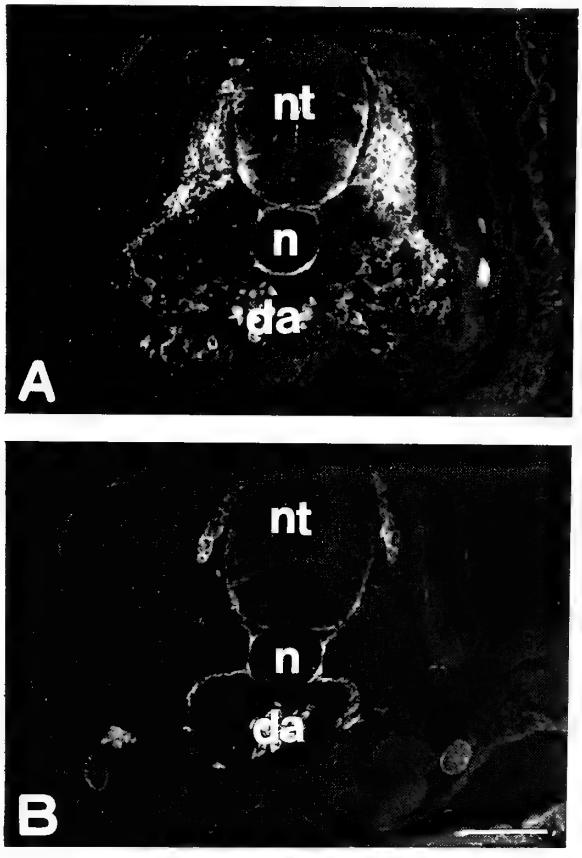

FIG. 3. Detection of HNK-1-immunoreactive cell in trunk. A, A cross section through the anterior half of the 8th somite at stage 12. Crest cells pass a space between the dermomyotome and the sclerotome and move toward the dorsal aorta. B, A cross section through the posterior half of the somite. Crest cells are located between the neural tube and the somite, but do not migrate into the posterior sclerotome. n, notochord; nt, neural tube; da, dorsal aorta. Scale bar=100 μm.

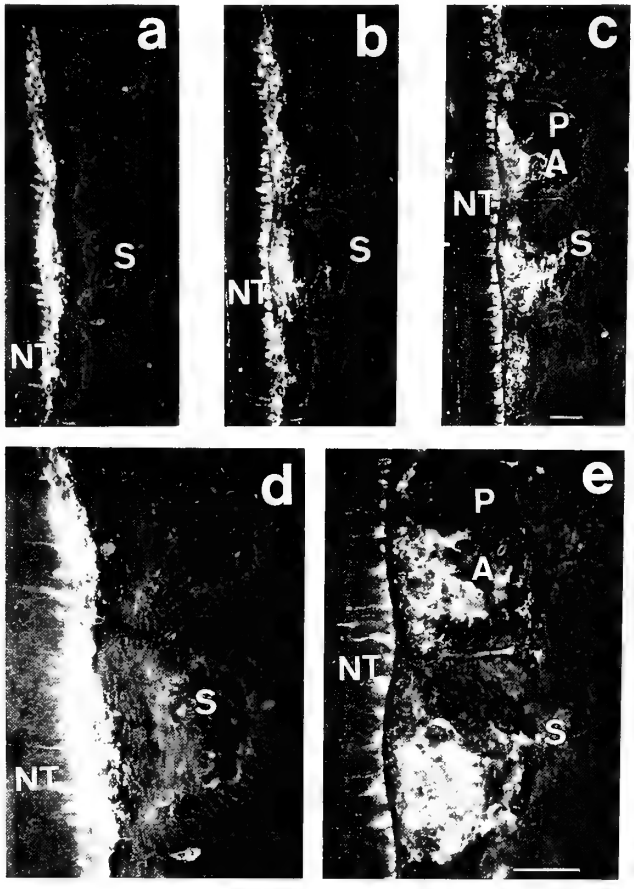

FIG. 4. HNK-1-immunoreactive cells migrating along somites (6th to 9th). Longitudinal sections of a stage 11 embryo are shown from top (a) to bottom (c). a, A section below the dorsal surface of the neural tube and the somite. Crest cells are uniformly distributed as a continuous longitudinal population at the space between the neural tube and the somite. b, A. section 10 μm ventral to (a). c, 20 μm ventarl to (b). Neural crest cells are only observed in the anterior half of each somite. (d) and (e) are enlarged from (a) and (c). A, anterior; NT, neural tube; P, posterior; S, somite. Scale bar=100 μm.

located under the epidermis at the level of posterior region of the anterior rhombencephalon. F, Crest cells at posterior rhombencephalon. G, A cross-section through 1st visceral arch. Crest cells move into the 1st visceral arch (arrow). H, Stage 12. A cross section through the 3rd and 4th visceral arches, crest cells are located in the 3rd and 45th visceral arch (arrow). I, Stage 12. Crest cells are mostly detected in the 4th visceral arch (arrow). ao, aorta; m, mesencephalon; n, notochord; OpV, optic vesicle; OtV, otic vesicle; p, prosencephalon; ph, pharynx; rh, rhombencephalon. Scale bar=100 μm.

mesenchymal components to contribute the mandibular pocesses and morphological differentiation of Meckel's cartilage in 12-day-old embryos (data not shown). By the stage 12, numerous crest cells from posterior rhombencephalon were found in third and fourth visceral arches (Fig. 2H, I). In cephalic region, the characteristics of neural crest cell are to migrate as a coherent sheet of cells in contrast with their migration in trunk region.

Trunk neural crest migration

The neural crest cell migration mostly occurred after morphological differentiation of the somite into the dermomyotome and sclerotome in the trunk of embryos. At stage 10, HNK-1-immunoreactive crest cells seem to migrate into the somite; numerous migrating crest cells were observed in the somite at stage 11 and 12. These cells are usually located at the anterior portion of each somite, where they seem to migrate between the anterior dermomyotome and sclerotome (Fig. 3A). Very few cells were found in the posterior part of the somites (Fig. 3B). Fig. 4 illustrates the distribution of neural crest cells in longitudinal section through the trunk. The migration of trunk neural crest cells in the somite was always restricted to the anterior half of each sclerotome (Fig. 4C, E) in spite of the fact that there is no morphological difference between the anterior and posterior half of each somite. It seems that their migration is suppressed in the posterior half of each sclerotome, but is stimulated in the anterior half.

At stage 11, neural crest cells were detected dorsolaterally between the ectoderm and the somite in the trunk (Fig. 5A). In general, they seem to migrate as individual cells. HNK-1-immunoreactive crest cells located in the area between the ectoderm and dermomyotome are illustated in Fig. 5B. It is interesting to note that the neural crest cells in the developing somite are often located in the medial space of the dermomyotome of the anterior half of somite and within the myotome (Fig. 5C, D). In some cases, we observed HNK-1-immunoreactive cells migrating into the dermomyotome.

Thus, our results indicate the presence of two major pathways of their migration in this region; (1) a dorsolateral pathway between the epidermal ectoderm and somite; (2) a ventral pathway between the anterior portion of the dermomyotome and sclerotome of each somite. No crest cell was observed migrating around the notochord area.

In addition, we found that numerous HNK-1-immunoreactive crest cells passing through the dorsal mesen-

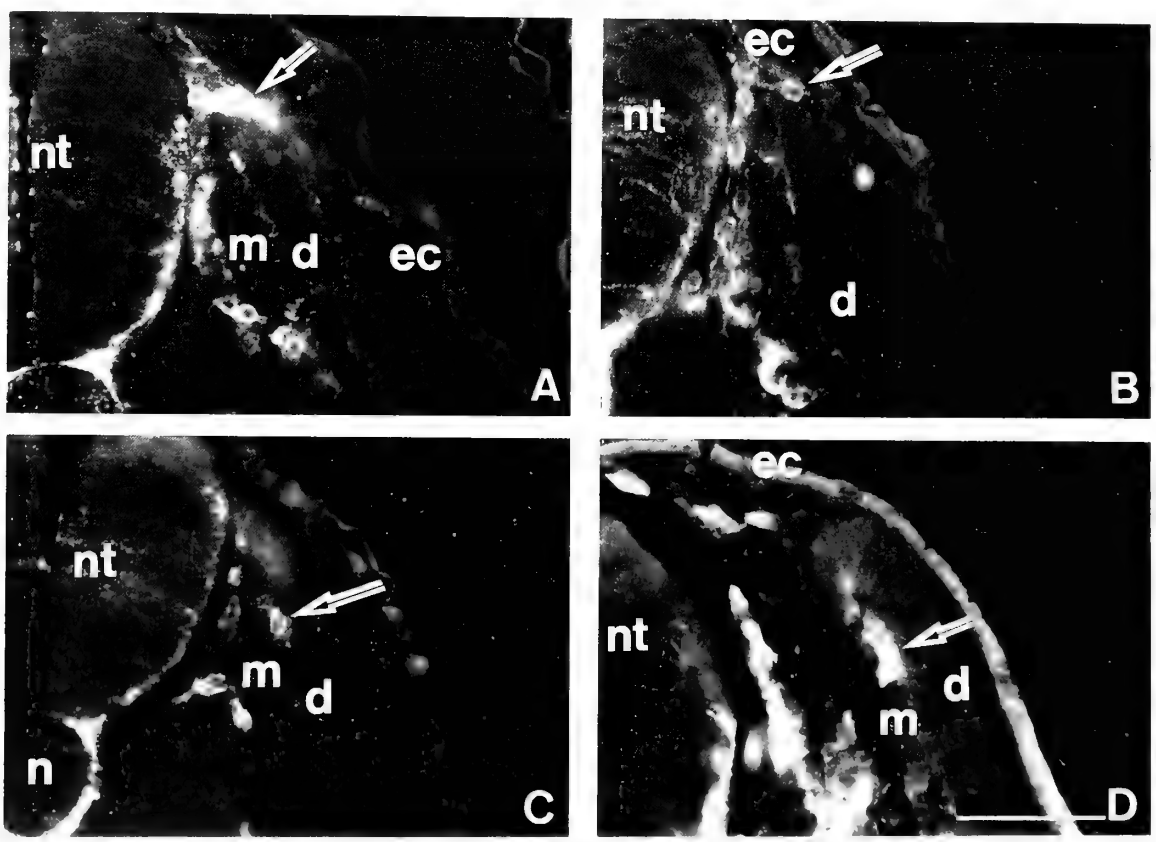

FIG. 5. Fluorescence micrographs of neural crest cell migrating in trunk region of a stage 11 embryo. A, A cross section through the 7th somite of trunk. Several crest cells migrate into the area between the ectoderm and the dermomyotome (arrow). Positive cells are also detected in the area between the dermomyotome and the sclerotome. b, A cross section through the 8th somite of trunk. Crest cell is located between the epidermis and the dermomyotome (arrow). Numerous crest cells migrate along ventral route at the same time. C, A cross section through the anterior somite of posterior region of trunk at stage 11. Crest cells intercalate into the medial space of the dermomyotome (arrow). D, Crest cells localized within the myotome at stage 14. d, dermomyotome; ec, ectoderm; m, myotome; n, notochord; nt, neural tube. Scale bar = 100 μm.

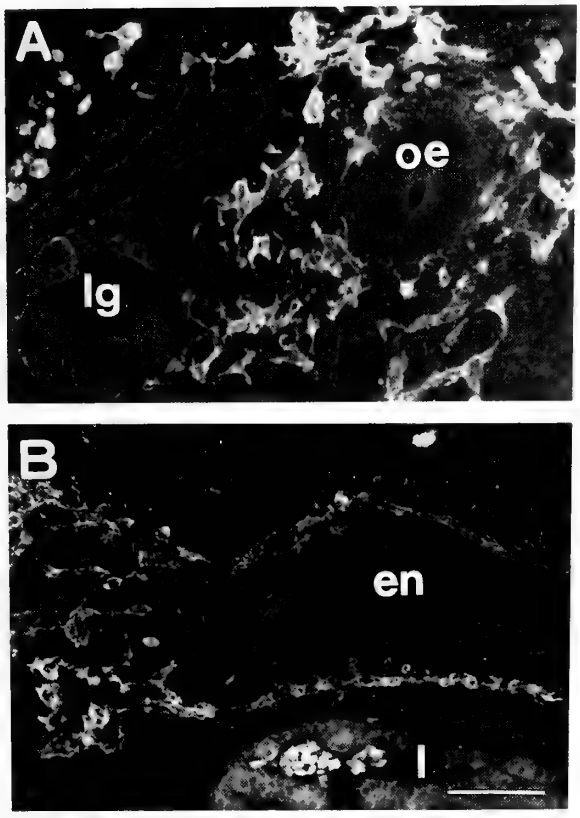

FIG. 6. HNK-1-immunoreactive creast cells distributed in the developing lung and foregut at stage 14 embryo. A, A cross section through the level of oesophagus (oe) and lung bud (lg). Crest cells are seen in the mesenchyme of the vicinity of lung bud. B, A longitudinal section through the level of foregut, the crest cells are observed between the endoderm and mesoderm of foregut. en, endoderm of the gut; 1, liver. Scale bar=100 μm.

tery at stage 12. They were found at stage 13 migrating into the lung buds. By stage 14, a number of crest cells were observed in the lung buds and foregut (Fig. 6A, B).

DISCUSSION

To our knowledge, there are only a few reports on the distribution of cranial neural crest cells in reptiles [12, 25]. The principal contribution of the present investigation was to demonstrate precise migratory routes of cranial and trunk neural crest cells in the reptilian embryo by using monoclonal antibody, HNK-1. We found that the mode of neural crest cell migration is different according to various cephalic regions and that the cranial neural crest cells seem to follow pathways similar to those of other vertebrate species studied previously [chick: 8, 26; *Xenopus*: 30; teleost: 31]. However, it has been noticed that the time of onset of cranial neural crest migration varies in non-reptile vertebrate groups [13, 14]. In mammals, Tan and Morriss-Kay [35] reported that the cranial neural crest migration already began when the neural tube is still open at neural fold stage. In birds, it has been shown that quail neural crest cells start their migration immediately before the complete closure of the neural tube [23]. On the other hand, the neural crest cell migration generally corresponds with the closure of the neural tube in amphibia [14]. In the turtle, no distinguishable neural crest cell was found when the neural tube is closed in the cephalic region. At advanced stage 8, individual neural crest cells segregated from the tube of mesencephalon and rhombencephalon, and begin their migration after aggregating once on the neural tube. Our results indicate that the cranial neural crest of the turtle has characteristic migration pattern and timing different from birds and mammals. We do not know the underlying mechanism responsible for the above-mentioned difference. Recently, however, it is increasingly accepted that the ECM (extracellular matrix) molecules may play an important role in determing the direction of neural crest cell migration and/or that ECMs provide permissive migratory substrates for their migration [28, 38]. The difference in the migratory timing of cranial neural crest cells among different vertebrate groups is likely due to the difference in environmental factors such as ECM and other unknown factors.

The migratory pathway of trunk neural crest cells has not been reported previously for reptiles. So far, the studies of the migration of trunk neural crest cells in non-reptile vertebrates have shown the following two major routes: (1) a dorsolateral pathway between the ectoderm and somite; (2) a ventral pathway between the neural tube and somite. It is noteworthy that a ventral pathway of migrating neural crest cells in somewhat different between anamniotes such as teleosts or *Xenopus* and aminotes such as birds or mammals. In birds and mammals, neural crest cell along the ventral pathway passes through the area between the anterior dermomyotome and the sclerotome [2, 11, 29]. The trunk neural crest cells in teleosts and *Xenopus* embryos migrate along the ventral pathway passing near the notochord and do not migrate into the somite [30, 31]. In our study, neural crest cells in the trunk were found to migrate along ventral pathway, which is similar to that of birds and mammals unlike that of teleosts and *Xenopus*. The difference in the anteroposterior pattern of ventral crest cell migration might be attributable to the somite tissue [4]. The ventral migrating pathway through the somite seems to be evolutionary conserved as principal character of neural crest development of amniotes. The pattern of neural crest migration along the somite is likely to be regulated by the similar nature of developmental and molecular mechanisms among reptiles and other aminotes [11].

It has been assumed that migratory pathways of neural crest cells are related to their differentiated cellular phenotypes, for example, a dorsolateral pathway is the migrating route of non-neuronal cell type including pigment cells in other vertebrate groups [fish: 31; amphibia: 27, 30; birds: 2, 20, 32; mammals: 33], whereas neural crest cells migrating along a ventral pathway will contribute to various neuronal phenotypes in the chick and mouse [20, 23, 24, 32]. We have found that, in the turtle embryos, pigment cells are

located in the skin as well as in the various extracutaneous tissues such as skeletal muscle, dorsal aorta, aorta of kidney and lung [17].

Question arises as to the migration route of these extracutaneous pigment cells. The neural crest cells have been found along ventral route migrating into the myotome, on the dorsal aorta and in the lung buds. In addition, presence of some melanogenic neural crest cells located at the sites corresponding to the ventral pathway seems to indicate that pigment cells of some extracutaneous tissues are derived from neural crest cells migrating along the ventral pathway [17]. This assumption was verified by another series of experiments involving the culture of isolated somite from stage 12 embryo; the results suggest that the melanogenic crest cells along the ventral route are associated with the somite (unpublished data).

For the migration of neural crest-derived pigment cells in the trunk of the turtle embryos three possible routes can be suggested: a) They migrate along a dorsolateral pathway and give rise to pigment cells of the skin; b) they migrate along ventral pathway, while some crest cells intercalate into the myotome during midway of migration and differentiate into pigment cells of skeletal muscle; c) other precursor cells continue to migrate along ventral pathway toward the dorsal aorta and the developing kidney, where they finally differentiate into pigment cells.

It has been known that the pigment cells are not normally localized in the above-mentioned sites in the white leghorn, the quail or the mouse and that the neural crest cell migrating along a ventral pathway contributes to the dorsal root ganglia (DRG) and sympathetic ganglia (SG) [1, 20, 21]. However, the cells of DRG and SG are shown to differentiate *in vitro* into several cell types including pigment cells [6, 9, 35]. The cells of DRG and SG seem to lose the potency of differentiation into pigment cells at later stages of development [6, 9]. It is conceivable that crest cells migrating along ventral pathway are basically pluripotent in amniotes and that the loss of differentiation potency toward melanogenesis is regulated under the tissue environment in the embryo. These observations lead us to an assumption that species-specific environmental factor(s) responsible for the final differentiation of neural crest cells is present in this region.

ACKNOWLEDGMENTS

The authors thank Hattori-Nakamura Nursery of Shizuoka for providing us with the turtle eggs used in our study. This research was supported by Grant-in-aid from the Ministry of Education, Science and Culture to T. T., and Japanese Government Research Scholorship from the Ministry of Education, Science and Culture to L. H.

REFERENCES

1 Bronner ME, Cohen AM (1979) Migratory patterns of cloned neural crest melanocytes injected into host chicken embryos. Proc Natl Acad Sci USA 76: 1843–1847

2 Bronner-Fraser M (1986) Analysis of the early stages of trunk neural crest migration in avian embryos using monoclonal antibody HNK-1. Devl Biol 115: 44–55

3 Bronner-Fraser M, Fraser S (1988) Cell lineage analysis reveals multipotency of some avian neural crest cells. Nature 335: 161–164

4 Bronner-Fraser M, Stern C (1991) Effects of mesodermal tissues on avian neural crest cell migration. Devl Biol 143: 213–217

5 Chou KH, Ilyas AA, Evans JE, Quarles RH, Jungalwala FB (1985) Structure of a glycolipid reacting with monoclonal IgM in neuropathy and with HNK-1. Biochem Biophys. Res Comm 128: 383–388

6 Ciment G, Glimelius B, Nelson D, Weston JA (1986) Reversal of a developmental restriction in neural crest-derived cells of avian embryos by phorbol ester drug. Devl Biol 118: 392–398

7 Deeming DC, Ferguson MWJ (1988) Environmental regulation of sex determination in reptiles. Phil Trans R Soc Lond B 322: 19–39

8 Duband JL, Thiery JP (1982) Distribution of fibronectin in the early phase of avian cephalic neural crest cell migration. Devl Biol 93: 308–323

9 Duff RS, Langtimm CJ, Richardson MK, Sieber-Blum M (1991) *In vitro* clonal analysis of progenitor cell patterns in dorsal root and sympathetic ganglia of the quail embryo. Devl Biol 147: 451–459

10 Buncker HR (1985) The neural crest. In "Pigment Cell, Vol 7" Ed by JT Bagnara, S. Klaus, E Paul, M Schartl, Univ Tokyo Pres, Tokyo, pp 255–269

11 Erickson CA, Loring JF, Lester SM (1989) Migratory pathways of HNK-1-immunoreactive neural crest cells in the rat embryo. Devl Biol 134: 112–118

12 Ferguson MWJ (1985) Reproductive biology and embryology of the crocodilians. In "Biology of the Reptiles, Vol. 14" Ed by C Gans, F Billett, PF Maderson, John Wiley & Sons, New York, pp 329–492

13 Hall BK (1987) Tissue interaction in the development and evolution of the vertebrate head. In "Development and Evolutionary Aspects of the Neural Crest" Ed by PFA Maderson, John Wiley & Sons, New York, pp 215–259

14 Hall BK (1988) THe Neural Crest, Oxford Univ Press, London

15 Hou L (1984) Studies on the embryonic development of the turtle, *Trionyx sinensis*. Nat Sci J Hunan Normal Univ 2: 59–70

16 Hou L (1987) Cytogenesis of the primordial germ cells in the turtle, *Trionyx sinensis*. Acta Herp Sin 6: 5–10

17 Hou L, Takeüchi T (1991) Differentiation of extracutaneous melanocytes in embryos of the turtle (*Trionyx sinensis japonicus*). Pigment Cell Res 4: 158–162

18 Hou L, Takeuchi T (1992) Differentiation of reptilian neural crest cells *in vitro*. In Vitro Cell Dev Biol 28A: 348–354

19 Ito K, Takeuchi T (1984) The differentiation in vitro of the neural crest of mouse embryo. J Embryol exp Morphol 84: 49–62

20 Kitamura K, Takiguchi-Hayashi K, Sezaki M, Yamamoto H, Takeuchi T (1992) Avian neural crest cells express a melanogenic trait during early migration from the neural tube: observation with the new monoclonal antibody, "MEBL-1". Development 114: 367–378

21 Klein-Szanto A, Bradl M. Porter S, Mintz B (1991) Melanosis and associated tumors in transgenic mice. Proc Natl Acad Sci USA 88: 169–173

22 Le Douarin NM (1973) A biological cell labeling technique and its use in experimental embryology. Devl Biol 30: 217–222

23 Le Douarin NM (1982) The neural crest. Cambridge Univ

Press, Cambridge

24 Le Douarin NM (1986) Cell line segregation during peripheral nervous system ontogeny. Science 231: 1515–1522

25 Meier S, Packard DS Jr (1984) Morphogenesis of the cranial segments and distribution of neural crest in the embryos of the snapping turtle, *Chelydra serpentina*. Devl Biol 102: 309–323

26 Noden DM (1975) An analysis of the migratory behavior of avian cephalic neural crest cells. Devl Biol 42: 106–130

27 Perris R, Von Boxberg Y, Lofberg J (1988) Local embryonic matrices determine region-specific phenotypes in neural crest cells. Science 241: 86–89

28 Perris R, Bronner-Fraser M (1989) Recent advences in defining the role of the extracellular matrix in neural crest development. Comm Develop Neurobiol 1: 61–83

29 Rickmann M, Fawcett JW, Keynes RJ (1985) The migration of neural crest cells and the growth of motor axons through the rostral half of the chick somite. J Embryol exp Morphol 90: 437–455

30 Sadaghiani B, Thiebaud CH (1987) Neural crest development in the *Xenopus laevis* embryos, studies by interspecific transplantation and scanning electron microscopy. Devl Biol 124: 91–110

31 Sadaghiani B, Vielkind JR (1990) Distribution and migration pathways of HNK-1-immunoreactive neural crest cells in teleost fish embryos. Development 110: 197–209

32 Serbedzija GN, Bronner-Fraser M, Fraser SE (1989) A Vital dye analysis of the timing and pathways of avian neural crest cell migration. Development 106: 809–819

33 Serbedzija GN, Fraser SE, Bronner-Fraser M (1990) Pathways of trunk neural crest cell migration in the mouse embryos as revealed by vital dye labeling. Development 108: 605–612

34 Sieber-Blum M (1989) Commitment of neural crest cells to the sensory neuron. Science 243: 1608–1611

35 Tan SS, Morriss-Kay GM (1985) The development and distribution of the cranial neural crest in the rat embryo. Cell Tissue Res 240: 403–416

36 Vincent M, Thiery JP (1984) A cell surface marker for neural crest and placodal cells: Further evolution in peripheral and central nervous system. Devl Biol 103: 468–481

37 Weston JA (1963) An radioautographic analysis of the migration and localization of trunk neural crest cells in the chick. Devl Biol 6: 279–310

38 Weston JA (1983) Regulation of neural crest cell migration and differentiation. In "Cell Interaction and Development" Ed by KM Yamada, John Wiley & Sons, New York, pp 153–184

ZOOLOGICAL SCIENCE 11: 433–439 (1994)

The Second Maturation Division and Fertilization in the Spider *Achaearanea japonica* (Bös. *et* Str.)

HIROHUMI SUZUKI[1] and AKIO KONDO

Department of Biology, Faculty of Science, Toho University, 2-1, Miyama 2 chome, Funabashi-shi, Chiba 274, Japan

ABSTRACT—Formation of the main layer of the vitelline membrane, the second maturation division and fertilization were examined in the spider *Achaearanea japonica* by light and electron microscopy. Newly laid eggs had already accepted a sperm nucleus near the periphery. The sperm nucleus was observed as a mass of condensed chromatin, which was not enclosed by a nuclear envelope. Bundles of microtubules, which separated the large yolk granules that surrounded the perinuclear cytoplasm into radial arrays immediately after oviposition, seem likely to play an important role in the migration of the sperm nucleus together with perinuclear cytoplasm to the center of the egg. The matrix that was released from the vesicles, by exocytosis, into the space between the cell membrane and the outer layer of the vitelline membrane appeared to form the main layer of the vitelline membrane. The second maturation division of the first polar body progressed to telophase, but daughter nuclei were not formed. The maturation division of the secondary oocyte was strictly synchronized with respect to that of first polar body, and it generated the female pronucleus and the nucleus of the second polar body. The female pronucleus moved toward the egg's center, in which the male pronucleus was now located, for conjugation. The larger pronucleus was probably the male pronucleus, and the other one was probably the female pronucleus.

INTRODUCTION

Embryos of many spiders have been examined in detail under the light microscope. However, very little information is available about the maturation and fertilization of the egg. We have previously examined the fine-structural changes at the egg's surface during the first maturation division in the spider *Achaearanea japonica* (unpublished data). The cell membrane begins to invaginate from the egg's surface, and then the lumen of each invagination becomes wider, forcing the large yolk granules into outer radial columns and an inner spherical mass (see Fig. 5). The matrix that is discharged at the egg's surface by secretion granules appears to form the outer layer of the vitelline membrane. In this report, we describe the formation of the main layer of the vitelline membrane, the second maturation division and fertilization in *A. japonica*.

MATERIALS AND METHODS

Mature females of *Achaearanea japonica* (Bös. *et* Str.) lay eggs 5–6 times in mid- and late summer, and about 100 eggs are released at each oviposition. The eggs are spherical and 0.5 mm in diameter. Eggs collected on the campus of Toho University were used for the present study. They were incubated at 25°C.

Routine light microscopy was carried out using paraffin-embedded serial sections. Eggs fixed in FAA (formalin, ethyl alcohol and acetic acid, 5:15:1, v/v) were dehydrated in a graded alcohol series, cleared in toluene and embedded in paraffin. The samples were cut off by 30 μm with a microtome, left in distilled water for 3 days and then sectioned at 6- to 8- μm thickness. For more detailed light-microscopic observations, eggs were fixed for the most part in a mixture of 2.5% glutaraldehyde and 2% paraformaldehyde in 0.1 M phosphate buffer, pH 7.4, that contained 0.2 M sucrose, and they were punctured during fixation with a tungsten needle. Dehydrated samples were embedded in methacrylate resin Technovit 7100 (Kulzer). The resin-embedded specimens were sectioned at 1- to 5- μm thickness with a glass knife on a LKB-4800 ultramicrotome. The sections were stained with Mayer's acid-haemalum and eosin.

For fine-structural observations, the eggs were prefixed, at room temperature, for 3 hr in a mixture of 2% paraformaldehyde and 2.5% glutaraldehyde in 0.1 M phosphate buffer, pH 7.4, that contained 0.2 M sucrose. During fixation, the eggs were cut in half with a tungsten needle. After rinsing for more than one hour with the same buffer plus 0.2 M sucrose, the samples were postfixed, at room temperature, for one hour in 2% osmic acid in 0.1 M phosphate buffer, pH 7.4, without sucrose. After rinsing with the same buffer without sucrose, samples were dehydrated in a graded alcohol series, transferred to propylene oxide, and embedded in epoxy resin Quetol 812 (Nisshin EM). Ultrathin sections were cut with a diamond knife on the ultramicrotome, stained with uranyl acetate and lead citrate, and examined under a JEOL JEM-1210 or a Hitachi HU-12A electron microscope. Thick sections were prepared simultaneously, and these sections were stained with toluidine blue for light microscopy. They were reembedded in the same epoxy resin for electron microscopy as needed.

RESULTS

Just at the time when oviposition occurred, the eggs had already accepted a sperm nucleus near the periphery, about 50 μm from the egg's surface (Fig. 1). No spermatozoa were observed at all. The cytoplasm was distributed at the egg's surface as periplasm, 10–20 μm in thickness, and in the

Accepted June 6, 1994
Received March 28, 1994
[1] To whom correspondence should be addressed.

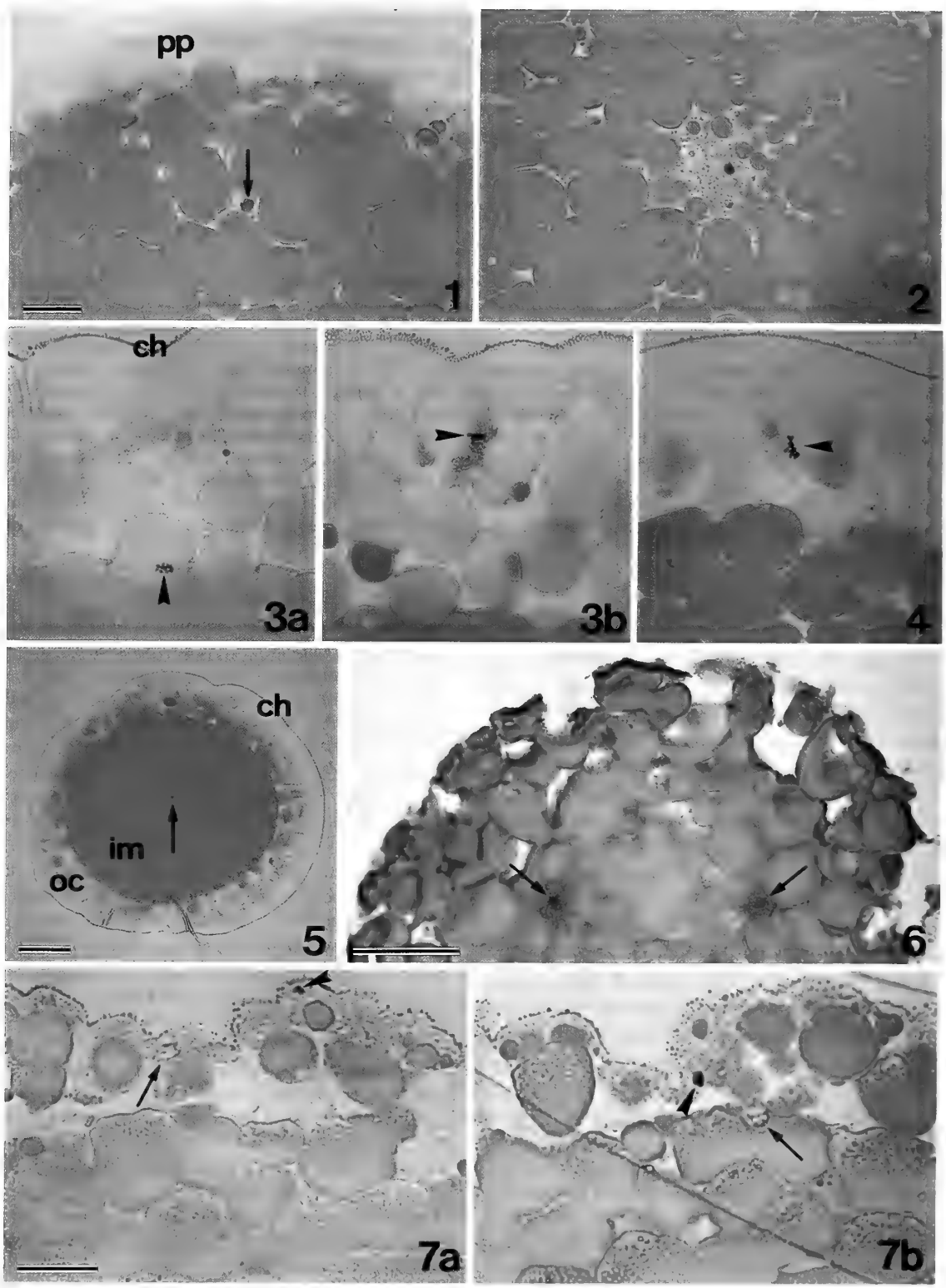

FIGS. 1–4. Technovit-embedded sections. Scale bar = 20 μm. Fig. 1. Just at the time of oviposition. The egg has already accepted a sperm nucleus (arrow). The cytoplasm is distributed at the egg's surface as periplasm (pp) and in the perinuclear zone. Fig. 2. Twenty minutes after oviposition. The large yolk granules surrounding the perinuclear cytoplasm of the sperm nucleus are organized in radial arrays. Fig. 3a. Forty-five minutes after oviposition. The large yolk granules are arranged in outer radial columns and an inner spherical mass (compare with Fig. 5). The maturation division of the secondary oocyte at metaphase (arrowhead) is seen at the surface of the inner spherical yolk mass. The equatorial plane is perpendicular to the egg's surface. ch, chorion. Fig. 3b. Same egg as in Fig. 3a. The second maturation division of the first polar body at metaphase (arrowhead) is seen in the cytoplasm located among the outer radial columns of yolk granules. The equatorial plane is parallel to the egg's surface. Fig. 4. A different egg, 45 min after oviposition. The first polar body at metaphase during the second maturation division (arrowhead) is seen in the periplasm. The equatorial plane is perpendicular to the egg's surface.

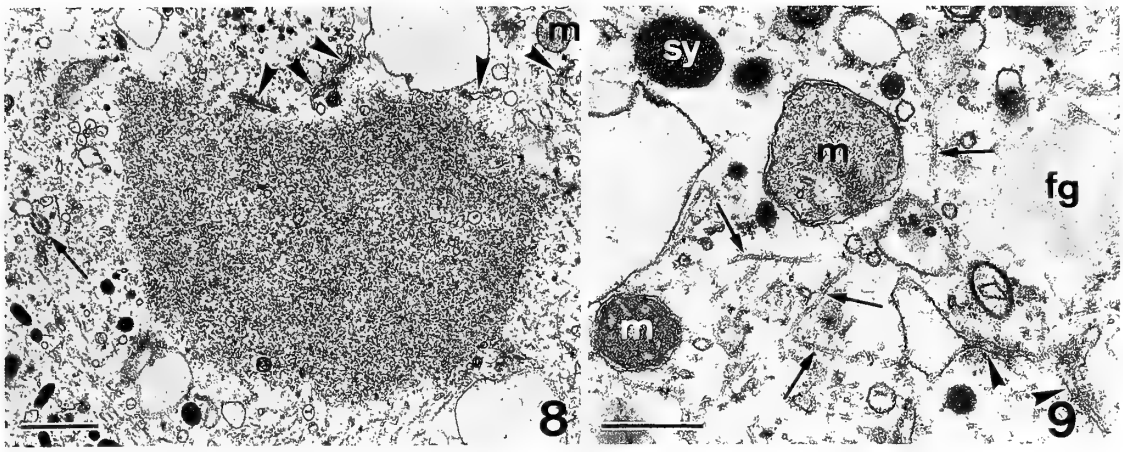

FIG. 8. Electron micrograph showing the sperm nucleus. The sperm nucleus is seen as a mass of electron-dense chromatin without a nuclear envelope. A cross section of axial filament of the spermatozoon (arrow) and fragments of the nuclear envelope (arrowheads) are visible in the perinuclear cytoplasm. Scale bar=1 μm. m, mitochondrion with a weakly electron-dense matrix.

FIG. 9. The perinuclear cytoplasm of the sperm nucleus. Microtubules are scattered around (arrows). Mitochondrion with a highly electron-dense matrix (m, white lettering) and that with a weakly electron-dense matrix (m, black lettering) are visible. Scale bar=0.5 μm. arrowheads, fragments of the nuclear envelope; fg, fatty granule; sy, small yolk granule.

perinuclear zone around the sperm nucleus. The first maturation division of the oocyte, which was in the telophase, was visible in the periplasm (data not shown). The sperm nucleus, about 5 μm in diameter, migrated toward the center of the egg as development proceeded. It was clear that this nucleus was not cleavage nucleus. Under the electron microscope, the sperm nucleus was observed as a mass of electron-dense chromatin (Fig. 8). A complete nuclear envelope was not observed but fragments of nuclear envelope were observed in the perinuclear cytoplasm (Fig. 8 and 9). Axial filament of the spermatozoon was observed near the nucleus (Fig. 8). Microtubules were scattered about (Fig. 9). Mitochondria were spherical or oval with faintly developed cristae. Some of them had a highly electron-dense matrix but others had a weakly electron-dense matrix (Fig. 9). The large yolk granules surrounding the perinuclear cytoplasm were organized in radial arrays from 20 min after oviposition (Fig. 2).

Thirty minutes after oviposition, the bursting of vesicles was observed at the surface of the egg, and the matrix of the vesicles was scattered in the space between the cell membrane and the outer layer of the vitelline membrane (Fig. 10). Mucous material and fibrils, which were of the same electron density as the matrix of the vesicles, began to accumulate under the outer layer of the vitelline membrane. Microvilli protruded from the cell membrane. The eggs were difficult to dechorion from this stage.

Forty-five minutes after oviposition, two chromosome plates at metaphase, one being that of the secondary oocyte and the other being that of the first polar body, were observed. The second maturation division of the secondary oocyte occurred at the surface of the inner spherical yolk mass, and its equatorial plane was perpendicular to the egg's surface (Fig. 3a). A total of 15 eggs was employed for examination of the second maturation division of the first polar body. The spindle was situated at the periplasm in 9 eggs, while in the other 6 eggs it was observed at the cytoplasm somewhere among the outer radial yolk columns. In the former case, the equatorial plane was located perpendicularly to the egg's surface (Fig. 4), by contrast, in the latter case it was parallel to the egg's surface (Fig. 3b). Electron micrographs of maturation divisions could not be obtained because of failure in the staining of thick, epoxy-resin-embedded sections.

One hour after oviposition, the sperm nucleus arrived at the center of the egg (Fig. 5). Until this stage, in a few eggs, several nuclei resembling the sperm nucleus were observed (Fig. 6). The number of such nuclei per egg was usually two or three, while the maximum number was seven, in the present investigation. They were considered to be the result of polyspermy.

Ninety minutes after oviposition, the vitelline membrane

FIG. 5. One hour after oviposition. Technovit-embedded section. The large yolk granules are arranged in outer radial columns (oc) and an inner spherical mass (im). The sperm nucleus, accompanied by perinuclear cytoplasm, is seen at the center of the egg (arrow). The large yolk granules surrounding the perinuclear cytoplasm are organized as radial arrays. Scale bar=100 μm. ch, chorion.

FIG. 6. One hour after oviposition. Paraffin-embedded section. Two sperm nuclei, a result of polyspermy, are visible in the egg (arrows). Scale bar=50 μm.

FIG. 7. One hour and thirty minutes after oviposition. Technovit-embedded sections of an egg. Scale bar=20 μm. Fig. 7a. The nucleus of the second polar body (arrow) and one chromosomal mass after the second maturation division of first polar body (arrowhead) are seen in the periplasm. Fig. 7b. Another chromosomal mass, generated by the division of the first polar body, (arrowhead) is seen in the periplasm, and the female pronucleus (arrow) is seen at the surface of the inner spherical yolk mass.

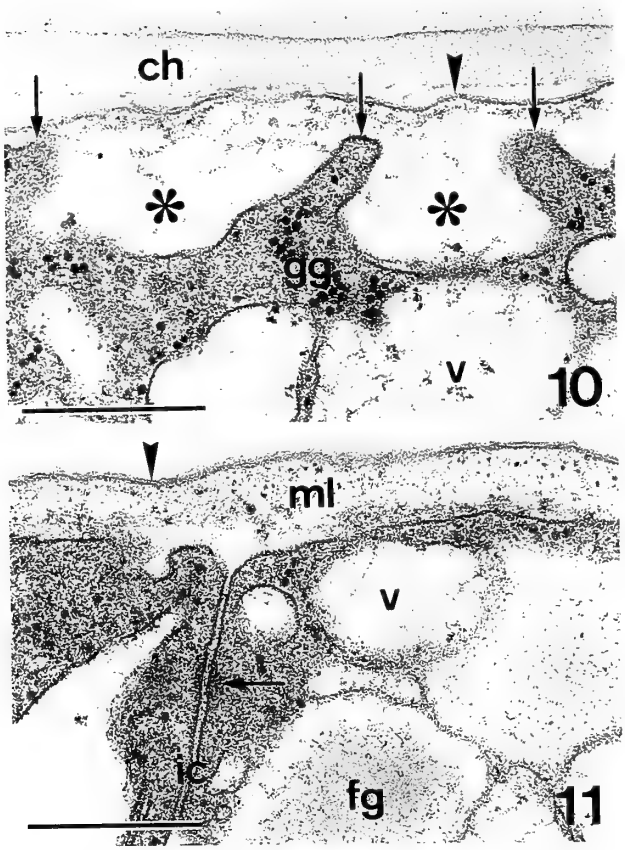

FIG. 10. The surface of the egg, thirty minutes after oviposition. The bursting of vesicles is seen at the egg's surface (asterisks). The matrix of vesicles is dispersed into the space between the cell membrane and the outer layer (arrowhead) of the vitelline membrane. It forms the mucous material and the fibrils under the outer layer, generating the main layer. Microvilli (arrows) protrude from the cell membrane. Scale bar=0.5 μm. ch, chorion; gg, glycogen granules; v, vesicle.

FIG. 11. The surface of the egg, one hour and thirty minutes after oviposition. The vitelline membrane consists of a highly electron-dense outer layer (arrowhead) and a weakly electron-dense main layer (ml). The inner surface of the main layer lacks any limiting structures. A desmosome-like structure (arrow) is faintly visible in the invagination of the cell membrane (ic). Scale bar=0.5 μm. fg, fatty granule; v, vesicle.

consisted of an electron-dense outer layer of about 30 nm in thickness and a weakly electron-dense main layer of 0.1–0.3 μm in thickness (Fig. 11). The main layer increased in thickness as development proceeded. The inner surface of the main layer lacked any limiting structures. Microvilli were faintly visible. Desmosome-like structures were faintly visible between invaginated cell membranes in the surface region (Fig. 11), and they became more apparent as development proceeded. In the periplasm, which decreased in thickness, two masses of chromatin and a nucleus of about 7 μm in diameter were observed. These structures were all situated close to each other (Fig. 7a, b). The two masses of chromatin were due to the condensation of chromosomes after the second maturation division of first polar body. The nucleus was considered to be the nucleus of the second polar body, generated during the second maturation division of the secondary oocyte. While these profiles of polar bodies were observed until 14 hr after oviposition, no protrusion of polar bodies from the egg was observed. Just under the masses of chromatin of the first polar body and the nucleus of the second polar body, a nucleus, which was the same size as the nucleus of the second polar body, was located at the surface of the inner spherical yolk mass (Fig. 7b). It was considered to be the female pronucleus.

At the center of the egg, the male pronucleus, which was about 15 μm in diameter, was observed. Decondensed chromatin was enclosed by a complete nuclear envelope (Fig. 12). Bundles of microtubules radiating from the perinuclear cytoplasm, were observed among the large yolk granules (Fig. 13).

Two hours after oviposition, at the center of the egg, two pronuclei lay closed to one another (Fig. 14). The nuclear envelopes of the two pronuclei ran alongside each other at a distance of about 0.2 μm (Fig. 15). There was always a size difference between the two pronuclei, but no other morphological differences were observed. The larger pronucleus, which was about 15 μm in diameter, was probably the male pronucleus and the other, which was about 12 μm in diameter, was probably the female one, as judged from the sizes at the previous stage. Much vesicular, smooth-surfaced endoplasmic reticulum appeared in the perinuclear cytoplasm, but no rough-surfaced endoplasmic reticulum was observed (Fig. 16). Mitochondria with a highly electron-dense matrix increased in number.

Three hours after oviposition, two pronuclei of about 22 μm and about 20 μm in diameter, respectively, or a single nucleus of about 25 μm in diameter were observed at the center of the egg. Figure 17 shows the single nucleus at this stage. This nucleus is probably the zygote nucleus formed by the conjugation of the male pronucleus and the female pronucleus. No mitochondria with a weakly electron-dense matrix were found at the stage at which the putative zygote nucleus was observed.

Three hours and thirty minutes after oviposition, the first nuclear division had occurred at the center of the egg. A chromosome plate at metaphase was observed (Fig. 18).

DISCUSSION

The vitelline membrane

It is generally accepted that the vitelline membrane is located internally with respect to the chorion in spider eggs. There are a few observations relevant to the details of its formation. Rempel [8] studied the embryonic development of *Latrodectus mactans* and reported that, during the first few hours after oviposition, the vitelline membrane adhered closely to the underlying periplasm and the overlying chorion. Hence, the removal of the chorion was difficult. Soon, however, the chorion and the vitelline membrane separated from each other, and the removal of the chorion became easy. Rempel suggested that the vitelline membrane con-

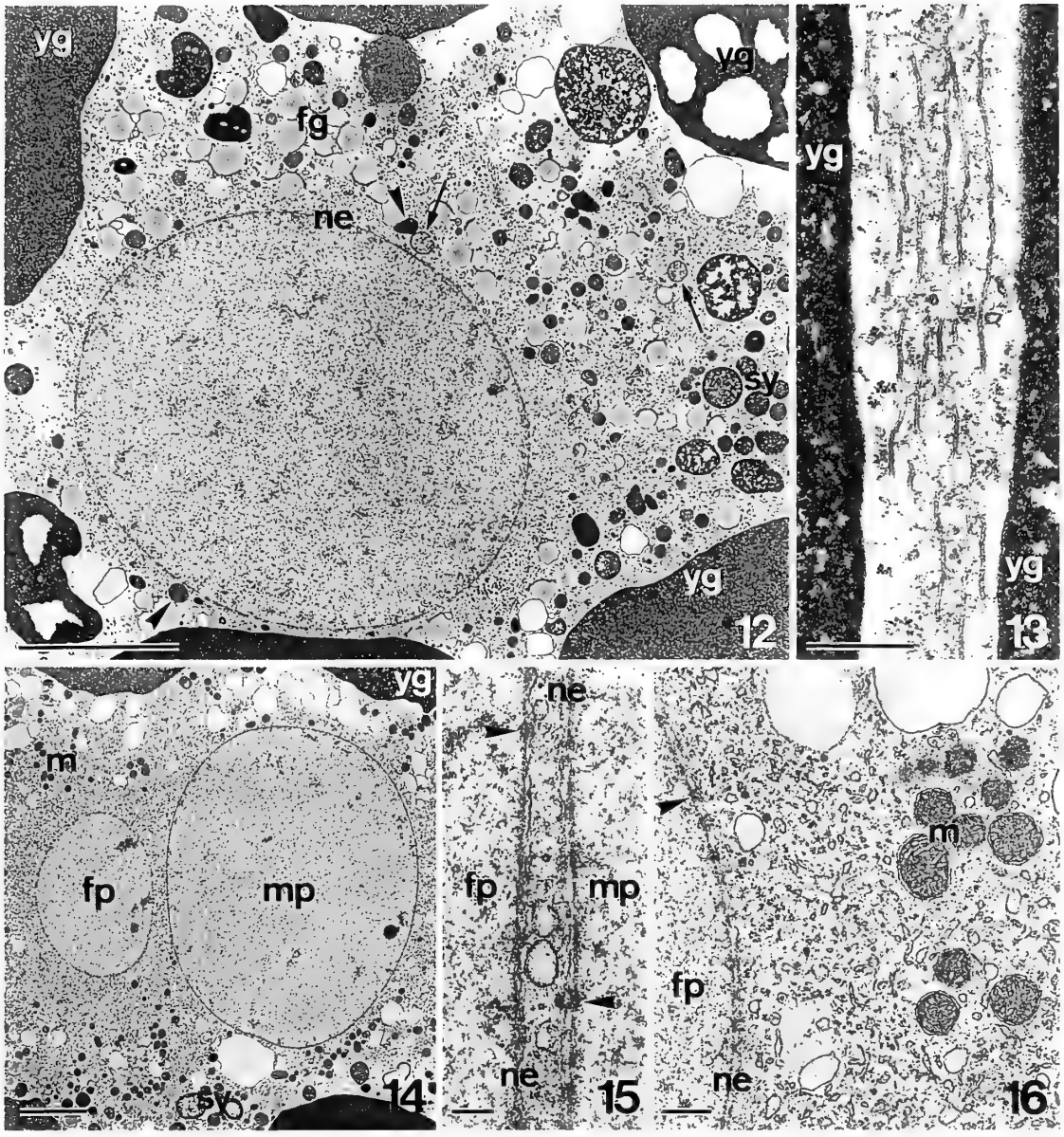

FIG. 12. Electron micrograph showing a male pronucleus and perinuclear cytoplasm. The male pronucleus is enclosed by a complete nuclear envelope (ne) and contains dispersed chromatin. The perinuclear cytoplasm is surrounded by large yolk granules (yg), which are arranged radially (see Fig. 2). Scale bar=5 μm. arrows, weakly electron-dense mitochondria; arrowheads, highly electron-dense mitochondria; fg, fatty granules; sy, small yolk granules.

FIG. 13. Bundles of microtubules between large yolk granules (yg), which are arranged radially around the male pronucleus. Scale bar=0.5 μm.

FIG. 14. Two pronuclei close to one another. The larger pronucleus is probably the male pronucleus (mp) and the other is probably the female pronucleus (fp). Scale bar=5 μm. m, mitochondria; sy, small yolk granules; yg, large yolk granule.

FIG. 15. The nuclear envelopes (ne) of two pronuclei run parallel to each other at a distance of 0.2 μm. The putative female pronucleus (fp) is on the left and the putative male pronucleus (mp) is on the right. Scale ar=0.2 μm. arrowheads, nuclear pores.

FIG. 16. Smooth-surfaced endoplasmic reticulum round the putative female pronucleus (fp). Scale bar=1 μm. arrowhead, nuclear pore; m, highly electron-dense mitochondria; ne, nuclear envelope.

trolled the entrance of sperm into the egg while sperm could pass freely through the chorion. According to Kondo [4], in lycosid spiders, only the thin outer layer of a vitelline membrane, which could not be recognized by light microscopy, was present 30 min after oviposition. The main layer of the vitelline membrane was formed as a very low electron dense layer, containing fibrils, under the outer layer. Kondo suggested that the vitelline membrane bore some resemblance, in terms of its formation, to the fertilization membrane. By contrast, Seitz [9] reported that "the funiculus cells" secreted a precursor component of the vitelline membrane during the first vitellogenic phase in *Cupiennius salei*.

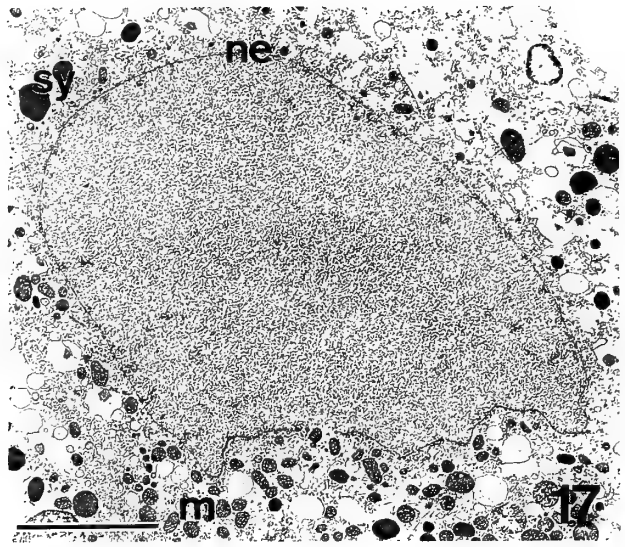

FIG. 17. The zygote nucleus after conjugation. Scale bar=5 μm. m, mitochondria; ne, nuclear envelope; sy, small yolk granules.

The observations of these authors appear to contradict one another in terms of the origin of the vitelline membrane.

The results of the present investigation strongly support the observations of Kondo [4]. The matrix scattered from the vesicles, by exocytosis, in the space between the cell membrane and the outer layer appeared to form the mucous material and fibrils under the outer layer, and it probably forms the main layer of the vitelline membrane. The formation of the outer layer and that of the main layer may be successive processes that require different materials.

Maturation of the egg

The second maturation division of the first polar body progressed until telophase, but no daughter nuclei were formed. Such division seems similar to that in eggs of *A. tepidariorum* [6]. According to Warren [11], division of the first polar body ceased at metaphase in *Palystes natalius*.

The maturation division of the secondary oocyte was strictly synchronized with respect to that of the first polar body. Montgomery [6] reported that the nucleus of the second polar body was located in the outer radial column of yolk granules. He may have observed the nucleus, as it migrated to the periplasm, immediately after division. Warren [11] described only anaphase in a discussion of the division of the secondary oocyte.

According to Montgomery [6], the chromosomes of the first polar body were not found more than 2 hr after oviposition, and the last time at which the nucleus of the second polar body was observed was 169 min after oviposition. In *A. japonica*, two masses of chromatin of the first polar body and the nucleus of the second polar body were found until 14 hr after oviposition. It is unclear from the present study whether or not polar bodies are eliminated from the egg via the invaginations of the cell membranes.

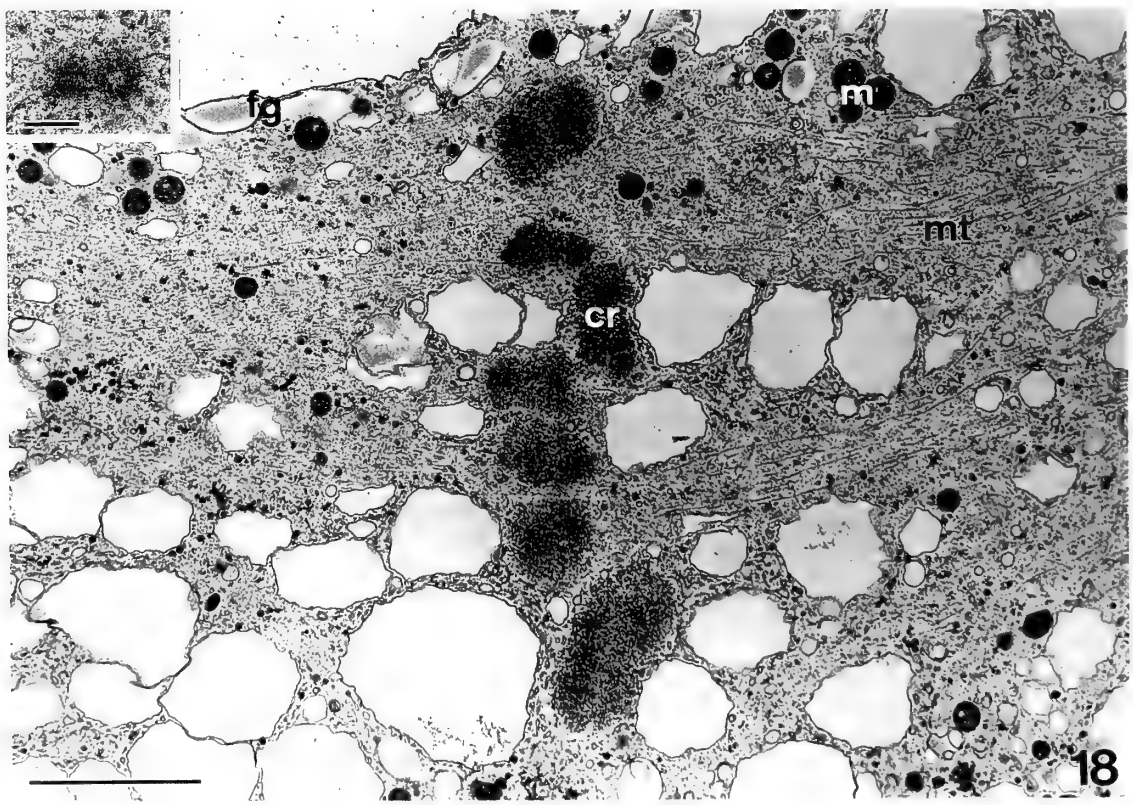

FIG. 18. The first nuclear division at metaphase. Chromosomes (cr) are aligning at the equatorial plane. Scale bar=5 μm. fg, fatty granules; m, mitochondria; mt, microtubules. Inset. Centrioles at a spindle pole. Scale bar=1 μm.

Fertilization

The time at which the sperm is incorporated into a spider's egg remains unknown. Montgomery [6] reported that eggs accepted a sperm nucleus that was located about halfway between the periphery and the center of the egg at oviposition, while Warren [11] and Rempel [8] suggested that fertilization occurs after oviposition. The present investigation supports the evidence reported by Montgomery. From the location of the sperm nucleus in the newly laid egg, the incorporation of sperm in the ovarian cavity can be postulated.

The sperm nucleus was observed as a mass of condensed chromatin, and it was not enclosed by a nuclear envelope. The nuclear envelope may be broken down at the time of incorporation of the sperm. Mitochondria that had a weakly electron-dense matrix may have been of paternal origin. The large yolk granules surrounding the perinuclear cytoplasm were arranged radially from immediately after oviposition. This arrangement of large yolk granules may be caused by the radially distributed cytoplasm that contains numerous bundles of microtubules that radiate from the perinuclear cytoplasm. Holm [2] called the cytoplasm that connects the perinuclear cytoplasm to the periplasm "plasm threads", and he suggested that they allow cleavage nuclei to migrate toward the periphery of the egg. By contrast, Kondo [4] suggested that the migration of the cleavage nuclei might be related to the decomposition of yolk granules and to motion of the cell membrane, and he also suggested that the plasm threads, which he described as a protoplasmic reticulum, only lay between the perinuclear cytoplasm and the periplasm. He would not have detected any bundles of microtubules because he prepared his samples by fixation at 0–4°C. Microtubules tend to be depolymerized at such low temperatures [10]. We suggest that the radial bundles of microtubules are equivalent to the plasm threads and that they play an important role in the migration of the sperm nucleus, accompanied by the perinuclear cytoplasm, to the center of the egg.

In previous studies of many spiders [1–3, 5, 7, 12], a nucleus has been noted at the center of the egg immediately after oviposition. This nucleus may have been the male pronucleus. The sperm nucleus arrives at the center of the egg and then develops into the male pronucleus. The chromatin ceases to be condensed, and fragments of the original nuclear envelope may be reconstructed as the complete nuclear envelope. The female pronucleus, generated by the second maturation division, should then move toward the center of the egg, in which the male pronucleus is now located. However, no migrating female pronucleus was observed in the present study.

In *A. japonica*, the male and female pronuclei lie close to one another for about one hour before conjugation, and each increases in size. Montgomery [6] stated that the larger nucleus was certainly the sperm nucleus because it was similar in volume to the supernumerary sperm nuclei.

Most of the mitochondria with a highly electron-dense matrix may have immigrated with the female pronucleus. While rod-shaped mitochondria were observed in the periplasm (Suzuki and Kondo, unpublished data), they were hardly ever observed in the perinuclear cytoplasm.

REFERENCES

1 Holm Å (1952) Experimentelle Untersuchungen über die Entwicklung und Entwicklungsphysiologie des Spinnenembryos. Zool Bidr Uppsala 29: 293–424

2 Holm Å (1954) Notes on the development of an orthognath spider, *Ischnothele karschi* Bös. & Lenz. Zool Bidr Uppsala 30: 109–221

3 Kishinouye K (1891) On the development of Araneina. J Coll Sci Imp Uni Tokyo 4: 55–88

4 Kondo A (1969) The fine structures of the early spider embryo. Sci Rep Tokyo kyoiku Daigaku Sec B 14: 47–67

5 Locy WA (1886) Observations on the development of *Agelena nævia*. Bull Mus Com Zool 12: 63–103

6 Montgomery TH (1908) On the maturation mitoses and fertilization of the egg of *Theridium*. Zool Jb Anat 25: 237–250

7 Morin I (1887) Zur Entwicklungsgeschichte der Spinnen. Biol Zentralbl 6: 658–663

8 Rempel JG (1957) The embryology of the black widow spider, *Latrodectus mactans* (Fabr.). Canad J Zool 35: 35–74

9 Seitz KA (1971) Licht- und elektronenmikroskopische Untersuchungen zur Ovarentwicklung und Oogenese bei *Cupiennius salei* Keys. (Araneae, Ctenidae). Z Morph Tiere 69: 283–317

10 Tilney LG, Porter KR (1967) Studies on the microtubules in Heliozoa, II. The effect of low temperature on the formation and maintenance of the axopodia. J Cell Biol 34: 327

11 Warren E (1926) On the habits, egg-sacs, oogenesis and early development of the spider *Palystes natalius* (Karsch). Ann Natal Mus 5: 303–349

12 Yoshikura M (1955) Embryological studies on the liphistiid spider, *Heptathela kimurai*. Part 2. Kumamoto J Sci Ser B 2: 1–86

ZOOLOGICAL SCIENCE 11: 441–444 (1994)

Neuron-like morphology expressed by perinatal rat C-cells *in vitro*

ICHIRO NISHIYAMA[1], TADACHIKA OOTA[2] and MANABU OGISO[3]

[1]*Biological Laboratory, Komazawa Women's College, Inagi, Tokyo 206,* [2]*Isotope Center, Tokyo University of Agriculture, Setagaya-ku, Tokyo 156, Japan,* [3]*Cell and Information, PRESTO, Research Development Corporation of Japan (J.R.D.C.), and Department of Physiology, Toho University School of Medicine, Ohta-ku, Tokyo 143, Japan*

ABSTRACT—Thyroid C-cells (calcitonin-producing cells) are endocrine derivatives of the neural crest. The morphological plasticity of rat C-cells was examined under cell culture. In a primary culture of perinatal rat thyroid glands, a small number of C-cells were found to extrude neurite-like processes, some of which reached 350μm in length. The processes frequently branched and had varicosity-like structures. The processes were intensely stained with anti-α-tubulin antibody, suggesting that microtubular cytoskeleton participated in their elongation and maintenance. In primary cultures of C-cells derived from postnatal rats at day 2 or later, no neurite-like processes were observed. These findings suggest that at least some C-cells in the perinatal rat thyroid retain the potential to extrude neurite-like processes, as do chromaffin cells in adrenal medulla, another type of crest-derived endocrine cell.

INTRODUCTION

Although calcitonin-producing cells (C-cells) in the thyroid gland are classified as endocrine cells, they have phylogenetic, embryological and biochemical relationships with enteric serotonergic neurons [1]. As befits their neuroectodermal origin, C-cells have several neuronal properties. They produce calcitonin gene-related peptide (CGRP), a putative neurotransmitter, as an alternative product of the calcitonin gene [12]. C-cells are capable of synthesizing serotonin from L-tryptophan and accumulate it in their secretory granules with neuron-specific serotonin binding protein [1]. Our recent study [9] revealed that C-cells express neural cell adhesion molecules on their surfaces. Neuronal characteristics of C-cells have also been confirmed by electrophysiological techniques [5, 13, 14]. Although C-cells share some neuronal properties, they do not display neuron-like morphological features in the thyroid gland [4].

In this communication, we report that a small number of C-cells derived from perinatal rats displayed neuronal morphology *in vitro*, suggesting their morphological plasticity.

MATERIALS AND METHODS

For immunohistochemical study, thyroid glands were excised from 20-day-old fetuses or 9-week-old male rats of Wistar strain. The day on which sperm were observed in vaginal smears was designated as day 0 of pregnancy. The glands were fixed in freshly prepared 4% paraformaldehyde in 0.1 M phosphate buffer (pH 7.4) at 4°C overnight. After being rinsed with phosphate-buffered saline (PBS), the specimens were immersed in 20% sucrose in PBS at 4°C for 24 hr, and subsequently frozen in an OCT compound (Miles). Transverse sections of 6μm in thickness were cut on a cryostat and mounted on glass slides coated with egg white.

Calcitonin immunoreactivity in the sections was detected using rabbit anti-human calcitonin antiserum (1:800, ICN ImmunoBiologicals) and rhodamin-labeled goat anti-rabbit IgG antiserum (1:100, Cappel). The specimens were observed under a NIKON DIAPHOT-TMD microscope equipped with fluorescence optics. The procedures were detailed in our previous paper [8].

For primary cultures, the thyroid glands were dissected out from perinatal rats ranging in age from embryonic day 16 (E16) to postnatal day 4 (P4), and dispersed with collagenase (Worthington, CLS II) and Dispase (Godo Shusei) [7]. The dispersed cells were cultured on glass coverslips (14 mm in diameter) in 24-well multidishes (Falcon) with Dulbecco's modified Eagle's medium (GIBCO) containing 5% fetal bovine serum (GIBCO). The cell density was controlled to obtain approximately 500 C-cells/well after 48 hr of incubation, as detailed in our previous paper [7]. The cultures were maintained at 37°C in a humidified atmosphere of 5% CO_2 in air. Primary cultures were also prepared from the thyroid glands of young (4- and 9-week-old) and aged (80-week-old) rats as described above.

After being incubated for 48hr, the cells were fixed with 4% paraformaldehyde in 0.1 M phosphate buffer (pH 7.4) for 1 hr, and permeabilized with 0.25% Triton X-100 for 10 min. Calcitonin was immunocytochemically detected as described above, and the number of neuron-like C-cells, which were defined as calcitonin-immunoreactive cells with at least one process longer than 150μm, were counted. In some experiments, CGRP was detected using rabbit anti-rat CGRP antiserum (1:400, Peninsula). For double-immunostaining of calcitonin and α-tubulin, mouse monoclonal anti-α-tubulin antibody (1:500, BioMakor) and fluorescein-labeled goat anti-mouse IgG antiserum (1:100, Kirkegaard and Perry Lab) were used in combination with the immunostaining of calcitonin described above. The specificity of the immunoreactions was determined by omitting the primary antibody, or by preincubation of the antibody with an excess of antigen. No specific immunoreactivity was found in these controls.

RESULTS AND DISCUSSION

In the sections of thyroid gland, C-cells were oval or

Accepted June 6, 1994
Received March 28, 1994

polygonal in shape, and were located close to the basal portion of the follicular epithelium (Fig. 1). In the E20 fetal thyroid, some of the C-cells were found to extrude short processes (Fig. 1A, *arrows*). The length of these processes was estimated to be 40μm at most. In contrast, no processes were observed in adult thyroid C-cells (Fig. 1B).

To determine whether these C-cells extend processes *in vitro*, the thyroid glands of both fetal and adult rats were dissociated into single cells and grown in culture. In the cultures of 9-week-old rat thyroid, C-cells displayed oval or triangular shapes. Although a few C-cells had short processes of up to 30μm, C-cells with long processes were not observed in the cultures of adult thyroid up to day 5 *in vitro* (data not shown). In the cultures of E20 fetal thyroid glands, most of the C-cells exhibited ovoid or triangular shapes, as in the cultures of adult thyroid (Fig. 2A). However, a small fraction of these C-cells displayed neuron-like features (Fig. 2 B-D). Most of the neuron-like C-cells were monopolar, and the processes frequently bifurcated. Varicosity-like structures were observed along some of these processes (*arrows* in Fig. 2 B and C). The cytoplasm, including the processes, of the C-cells was filled with calcitonin and CGRP immunoreactant. All the C-cells examined expressed CGRP immunoreactivity irrespective of whether the C-cells possessed the neurite-like processes. The longest process reached 350μm in length. Two to seven neuron-like C-cells (0.4–1.4%) were detected among approximately 500 C-cells in each culture well. Prolonged incubation of up to 5 days did not increase the proportion of neuron-like C-cells (data not shown).

The neurite-like processes of C-cells were intensely stained with anti-α-tubulin antibody (Fig. 2 E and F), suggesting that microtubular cytoskeleton participated in the formation and/or maintenance of these processes. Microtubules in neurites are stabilized by microtubule-associated proteins, such as MAP-2 and tau [15]. Our recent study revealed that both thyroid C-cells and a C-cell line produce tau-immunoreactive protein with an apparent molecular mass of 110,000 (Nishiyama *et al.*, in preparation), probably corresponding to the high molecular weight tau found in PC-12 cells [3] and neuroblastoma cells [2]. Therefore, it is plausible that microtubules in the processes of the neuron-like C-cells are associated with the high molecular weight tau protein.

The results of this study indicated that a small percentage of fetal rat C-cells, but none of adult origin, had the ability to extend long neurite-like processes. Next, we determined the ratio of neuron-like C-cells in thyroid cell cultures of perinatal rats of varying ages. As shown in Table 1, neuron-like C-cells were also observed at almost the same ratio in cultures of E19 fetal rat thyroid glands as in those of E20 fetuses, and at much lower ratios in cultures of E17, E18, P0 and P1 rat thyroid glands. No neuron-like C-cells were detected in the thyroid cell cultures of E16 fetuses, P2 and P3 pups (Table 1), or P28, P63 and P560 rats (data not shown). These results show that neuron-like C-cells appeared in thyroid cell cultures during only a limited perinatal period.

A question arises as to why only a subpopulation of C-cells extend processes in thyroid cultures of perinatal rats. This implies a heterogeneity in the microenvironment surrounding the C-cells or in the properties of C-cells themselves. To answer this question, it is important to know whether C-cells without process have the potential to extend processes in response to some factor(s). An attempt to induce neurite-like process outgrowth in the C-cells *in vitro* is now in progress using various growth factors and hormones.

Although the neural crest origin of C-cells has been confirmed by several investigators [6, 10, 11], the developmental process of restricting C-cell phenotypic traits in the neural crest lineage remains to be elucidated. Our findings suggested that a small number of C-cells from perinatal rats, especially those obtained one or two days before birth, had the potential to extrude *in vitro* long neurite-like processes, a hallmark of the neuronal phenotype. Future experiments using this culture system will shed light upon commitment and

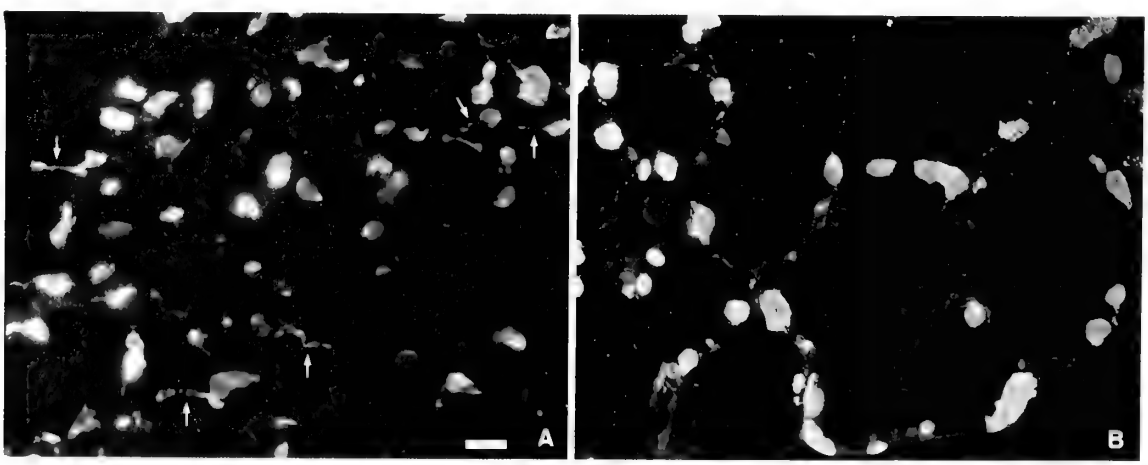

FIG. 1. Morphology of C-cells in the thyroid glands of fetal (A) and young adult (B) rats. Transverse sections of 20-day-old rat fetuses (A) and 9-week-old rats (B) were immunostained using an anti-calcitonin antiserum. Fetal C-cells appeared to extrude short processes (*arrows* in A). Scale bar=20μm.

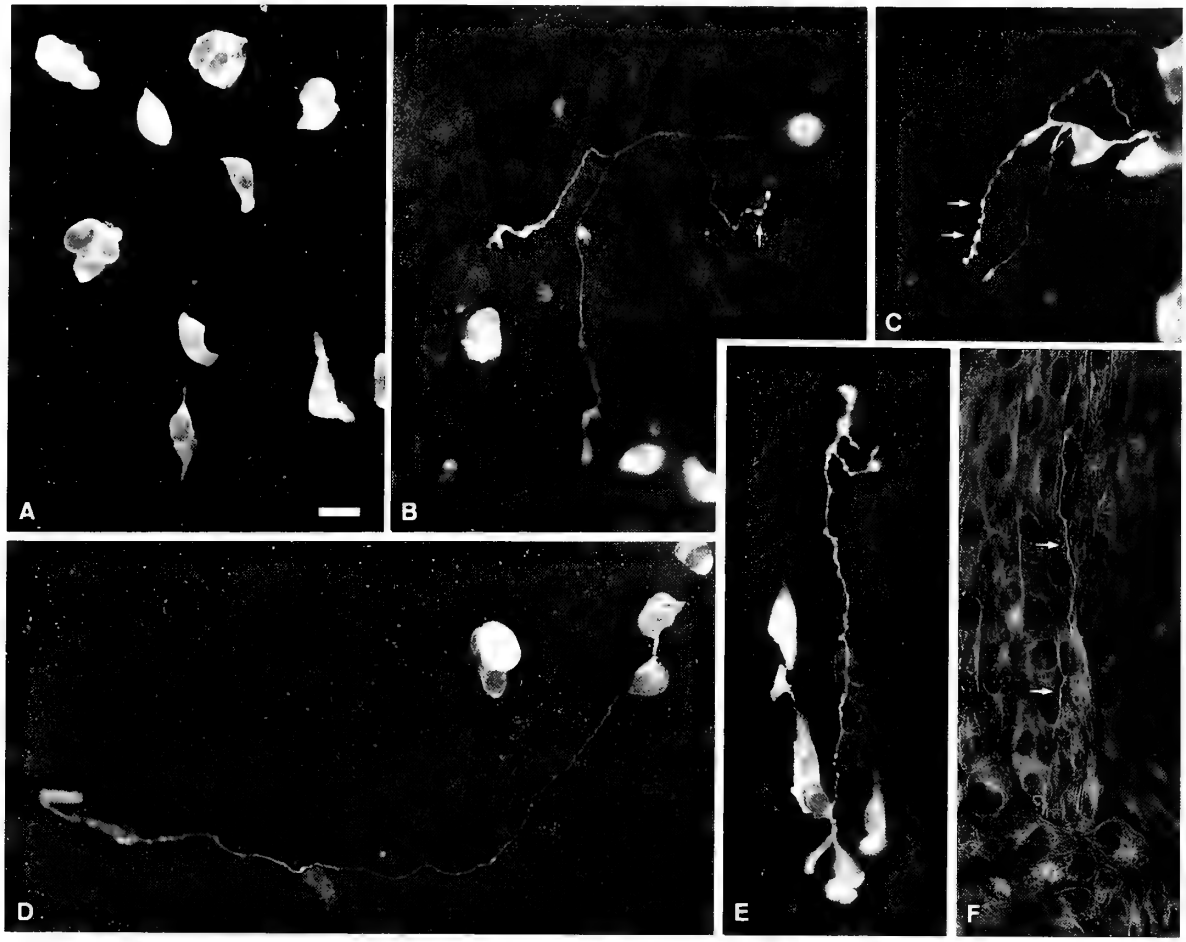

FIG. 2. C-cells in primary culture of dissociated thyroid glands of 20-day-old rat fetuses. The cells were cultured for 48 hr, and immunostained with antisera to calcitonin (A-C) and calcitonin gene-related peptide (D). C-cells with neurite-like processes were observed in the cultures at a low ratio (B-D). Their processes frequently branched and had varicosity-like structures (*arrows* in B and C). Calcitonin (E) and α-tubulin (F) immunoreactivities were detected in the same specimen. The neurite-like process of the C-cell was intensely reactive with anti-α-tubulin antibody (*arrows* in F). Scale bar=20μm.

TABLE 1. Frequency of neuron-like C-cells in primary cultures derived from rat thyroid glands of various ages

Age		Number of Neuron-like C-cells per 1,000 C-cells
Embryonic day	16	0
	17	0.1±0.07
	18	1.2±0.73
	19	7.3±1.54
	20	8.4±2.16
Postnatal day	0	2.2±1.35
	1	0.2±0.09
	2	0
	3	0

Thyroid glands of rat fetuses or pups at the ages indicated were enzymatically dissociated and cultured for 48 hr. The cells were immunostained using an anti-calcitonin antiserum, and the ratios of neuron-like C-cells, which were defined as calcitonin-immunoreactive cells bearing at least one process longer than 150μm, were determind. At least three samples, each of which contained approximately 500 C-cells, were counted for each experiment. The values are means±SEM of four independent experiments.

the plasticity of the phenotype in C-cells.

REFERENCES

1 Bernd P, Gershon MD, Nunez EA, Tamir H (1979) Localization of a highly specific neuronal protein, serotonin binding protein, in thyroid parafollicular cells. Anat Rec 193: 257–268

2 Couchie D, Mavilia C, Georgieff IS, Liem RKH, Shelanski ML, Nunez J (1992) Primary structure of high molecular weight tau present in the peripheral nervous system. Proc Natl Acad Sci USA 89: 4378–4381

3 Goedert M, Spillantini MG, Crowther RA (1992) Cloning of a

big tau microtubule-associated protein characteristic of the peripheral nervous system. Proc Natl Acad Sci USA 89: 1983–1987

4 Kameda Y (1987) Localization of immunoreactive calcitonin gene-related peptide in thyroid C cells from various mammalian species. Anat Rec 219: 204–212

5 Kawa K (1988) Voltage-gated sodium and potassium currents and their variation in calcitonin-secreting cells of the chick. J Physiol 399: 93–113

6 Le Douarin N, Fontaine J, Le Lièvre C (1974) New studies on the neural crest origin of the avian ultimobranchial glandular cells—Interspecific combinations and cytochemical characterization of C cells based on the uptake of biogenic amine precursors. Histochemistry 38: 297–305

7 Nishiyama I, Fujii T (1989) Somatostatin-immunoreactive C-cells in primary culture of fetal, neonatal and young rat thyroid glands. Biomed Res 10: 353–359

8 Nishiyama I, Fujii T (1992) Laminin-induced process outgrowth from isolated fetal rat C-cells. Exp Cell Res 198: 214–220

9 Nishiyama I, Seki T, Oota T, Ohta M, Ogiso M (1993) Expression of highly polysialylated neural cell adhesion molecule in calcitonin-producing cells. Neuroscience 56: 777–786

10 Pearse AGE, Polak JM (1971) Cytochemical evidence for the neural crest origin of mammalian ultimobranchial C cells. Histochemie 27: 96–102

11 Polak JM, Pearse AGE, Le Lièvre C, Fontaine J, Le Douarin NM (1974) Immunocytochemical confirmation of the neural crest origin of avian calcitonin-producing cells. Histochemistry 40: 209–214

12 Sabate MI, Stolarsky LS, Polak JM, Bloom SR, Varndell IM, Ghatei MA, Evans RM, Rosenfeld MG (1985) Regulation of neuroendocrine gene expression by alternative RNA processing. J Biol Chem 260: 2589–2592

13 Sand O, Jonsson L, Nielsen M, Holm R, Gautvik KM (1986) Electrophysiological properties of calcitonin-secreting cells derived from human medullary thyroid carcinoma. Acta Physiol Scand 126: 173–179

14 Sand O, Ozawa S, Gautvik KM (1981) Sodium and calcium action potentials in cells derived from a rat medullary thyroid carcinoma. Acta Physiol Scand 112: 287–291

15 Tucker RP (1990) The roles of microtubule-associated proteins in brain morphogenesis: a review. Brain Res Rev 15: 101–120

ZOOLOGICAL SCIENCE 11: 445–449 (1994)

Proliferation of Pituitary Cells in Streptozotocin-induced Diabetic Mice: Effect of Insulin and Estrogen

SUMIO TAKAHASHI, SOUICHI OOMIZU
and YASUO KOBAYASHI

Department of Biology, Faculty of Science, Okayama University, Tsushima, Okayama 700, Japan

ABSTRACT—Insulin has growth-stimulatory actions in various tissues. The present study is aimed to clarify whether insulin stimulates the proliferation of anterior pituitary cells. Estrogen is the mitogenic factor in pituitaries and female reproductive tracts. We studied the insulin-estrogen relationship in the pituitary cell proliferation. The proliferation of uterine epithelial cells was also studied, since the uterus was one of the most typical estrogen-responsive organs. Ovariectomized ICR mice were given streptozotocin (STZ, 100 mg/kg) intraperitoneally to make mice insulin-deficient. Estradiol-17β (50 μg, E_2) and insulin (0.2 or 0.4 IU per twice a day) were given in STZ-treated mice. Insulin significantly stimulated the mitosis of pituitary cells and PRL cells in both normal control mice and STZ-treated diabetic mice. E_2 stimulated the mitosis of pituitary cells (10.93 ± 0.73 cells/mm^2), compared with controls (3.59 ± 0.67 cells/mm^2) in control mice. In STZ-treated mice E_2 failed to increase the mitosis (4.91 ± 0.99 cells/mm^2), compared with controls (2.47 ± 0.43 cells/mm^2). Insulin recovered the diminished response to estrogen in pituitary cells of STZ-treated mice to the level comparable to control mice. In the uterus insulin at the high dose used stimulated the proliferation of luminal epithelial cells in normal control mice. However, insulin deficiency did not alter the responsiveness of uterine epithelial cells to estrogen. The present study suggests that insulin is involved in the proliferation of pituitary cells and probably uterine luminal epithelial cells, but the mechanism of insulin action on the cell proliferation may differ between pituitary cells and uterine cells.

INTRODUCTION

Estrogen stimulates proliferation of various cells including pituitary cells and uterine cells. Recent reports concerning the estrogen-induced cell proliferation suggest that estrogen action is not a direct action and is mediated by autocrine or paracrine growth factors [24, 27, 32]. Transforming growth factor α and epidermal growth factor are growth factors for pituitary cells, particularly for prolactin (PRL) cells [3]. It is highly probable that other growth factors are involved in pituitary cell proliferation. Insulin is known to have growth-promoting activity in various tissues [26]. Insulin is indispensable for estrogen-induced pituitary growth [6]. Pituitary tumor cells, GH_3 cells, require insulin for the optimal growth in serum-free medium [11]. The present study was undertaken to clarify effects of insulin on the estrogen-induced proliferation of pituitary cells in ovariectomized mice made diabetic by streptozotocin (STZ) administration. The proliferation of PRL cells was particularly examined, since insulin stimulates PRL secretion [13, 25]. Uterine growth is regulated by estrogens and progesterone. The proliferation of uterine luminal epithelial cells in STZ-treated diabetic mice was also studied in the present study.

MATERIALS AND METHODS

Adult female mice (2 month old) of the Jcl:ICR strain (Clea Japan) were used. They were kept under temperature-controlled conditions, and given food and water *ad libitum*. All mice were ovariectomized under ether anesthesia. Ten days after ovariectomy, STZ (Wako Pure Chemicals) was intraperitoneally given at a dose of 100 mg/kg BW. STZ was dissolved in 0.05 M citric acid (65 mg/ml). Control mice were given the vehicle. All mice had been in advance deprived of food for 16 hr before STZ treatment.

Estrogen treatment

Estradiol-17β (E_2, Sigma), dissolved in sesame oil (1 mg/ml), was subcutaneously given 7 days after STZ treatment at a dose of 50 μg. Control mice were given sesame oil.

Insulin treatment in STZ-treated mice

Seven days after STZ treatment insulin (0.2 or 0.4 IU for each mouse, Novo Actrapid MC, Novo Nordisk), diluted in saline (1 or 2 IU/ml), was intraperitoneally given twice a day (9.00 AM and 5.00 PM) for 3 days. Control mice were given the vehicle. On the last day insulin was given only in the morning, and 5 hr later pituitaries were collected for the study.

The mitotic activity of pituitary cells and uterine epithelial cells

Colchicine (Wako Pure Chemicals), dissolved in saline (1 mg/ml), was subcutaneously given at a dose of 5 mg/kg BW. The pituitary gland and uterine horns were removed 5 hr after the colchicine injection, that is, 48 hr after estrogen treatment, and then fixed in Bouin's solution. The pituitary glands and uteri were embedded in paraplast, and horizontal pituitary and cross uterine serial sections (5 μm thickness) were cut. The colchicine-arrested mitotic cells were observed. For the counting of mitotic pituitary cells, sections near the horizontal medial plane were selected. The number of mitotic pituitary cells was counted. In the sections used for the counting, the area of anterior pituitary glands was measured with a planimeter. The mitotic activity was expressed as the number of mitotic cells per mm^2. For the counting of mitotic uterine luminal epithelial cells, sections near the cross medial plane were selected.

Accepted May 25, 1994
Received March 14, 1994

The number of total luminal epithelial cells and the mitotic luminal epithelial cells was counted. The mitotic activity of uterine cells was expressed as the percentage of mitotic luminal epithelial cells in total luminal epithelial cells.

Immunocytochemical identification of PRL cells

PRL cells were identified in the ABC method using the rabbit anti-mouse PRL serum (Shikibo). The specificity of anti-mouse PRL serum was checked with the immunoblotting method. The antiserum detected a single band of mouse prolactin, and did not cross-react with mouse growth hormone.

Measurement of blood glucose level

Mice were lightly anesthetized with ether vapor, and the blood was obtained from the tail vein. The blood glucose level was determined by the glucose oxidase method using the kit (Glucoscan, Eiken), and expressed as mg/dl.

Statistics

Statistical analysis was carried out by Bonferroni's multiple t-test. Differences of $P<0.05$ were considered as statistically significant.

RESULTS

Mitotic activity of pituitary cells

STZ treatment lowered the basal mitotic activity of pituitary cells, although statistical difference was not detected between control mice and STZ-treated mice (Fig.1). Insulin alone (0.2 IU, 0.4 IU) increased the mitotic activity of pituitary cells in control and STZ-treated mice. Estrogen administration resulted in a three-fold increase in the mitotic activity of pituitary cells of control mice (control, 3.59 ± 0.67 cells/mm^2; E2, 10.93 ± 0.73 cells/mm^2; Fig. 1). However, in STZ-treated diabetic mice estrogen administration failed to increase the mitotic activity of pituitary cells (control, 2.47 ± 0.43 cells/mm^2; E_2, 4.91 ± 0.99 cells/mm^2). The number of mitotic pituitary cells in STZ-treated mice with estrogen treatment was significantly lower than that of corresponding control mice ($P<0.001$). Insulin administration in association with estrogen further increased the mitotic activity in control mice. In STZ-treated mice receiving insulin, estrogen was able to increase the mitotic activity of pituitary cells to the level comparable to control mice. Thus, insulin administration stimulated the proliferation of pituitary cells and recovered the diminished response of pituitary cells to estrogen in STZ-treated mice.

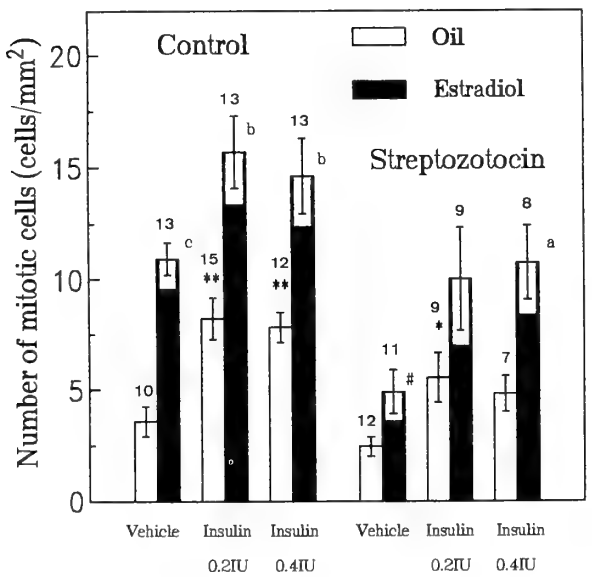

FIG. 1. Influence of estradiol-17β and insulin (0.2IU, 0.4IU) on the number of mitotic pituitary cells (mean$\pm$SE of the mean) in control ovariectomized mice and streptozotocin-treated ovariectomized mice. The number above each column depicts the number of mice. *, $P<0.05$; **, $P<0.01$ *vs.* respective vehicle group. #, $P<0.01$ vs. respective corresponding group of control mice. a, $P<0.05$; b, $P<0.01$; c, $P<0.001$ *vs.* respective oil group.

STZ treatment without estrogen injection did not lower the mitotic activity of PRL cells (Fig. 2). Estrogen administration resulted in an increase in mitotic activity of PRL cells, but the level in STZ-treated mice was lower than that in control mice ($P<0.01$). Insulin alone or in association with estrogen increased the mitotic activity of PRL cells in control and STZ-treated mice. However, high dose of insulin (0.4 IU) failed to increase the mitotic activity of PRL cells in control mice. Insulin administration at the high dose may have depleted the storage of PRL, resulting in the decrease in the number of immuno-positive PRL cells.

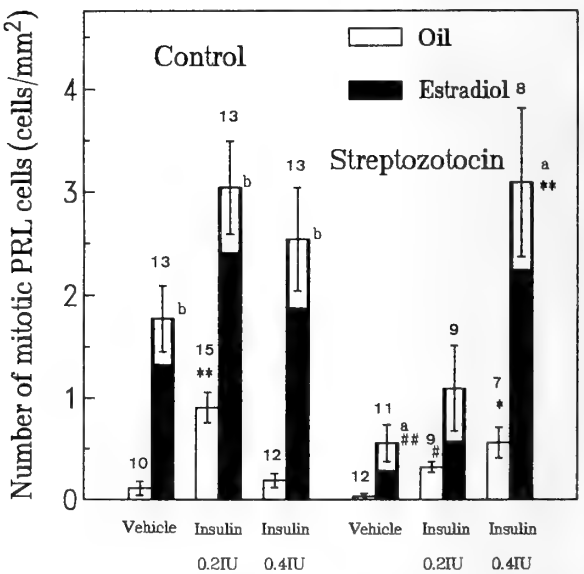

FIG. 2. Influence of estradiol-17β and insulin (0.2 IU, 0.4 IU) on the number of mitotic PRL cells (mean$\pm$SE of the mean) in control ovariectomized mice and streptozotocin-treated ovariectomized mice. The number above each column depicts the number of mice. *, $P<0.05$; **, $P<0.01$ *vs.* respective vehicle group. #, $P<0.05$; ##, $P<0.01$ *vs.* respective corresponding group of control mice. a, $P<0.05$; b, $P<0.001$ *vs.* respective oil group.

Mitotic activity of uterine luminal epithelial cells

Insulin administration at the high dose (0.4 IU) increased the mitotic activity of luminal epithelial cells in control mice. E_2 administration increased the mitotic activity of luminal epithelial cells in control mice and in STZ-

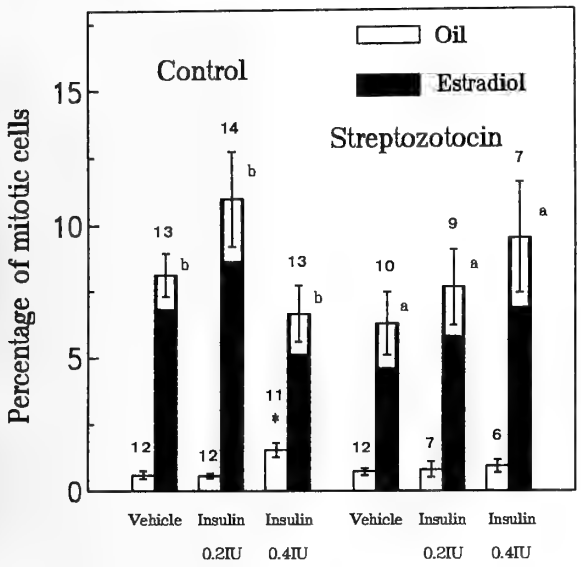

FIG. 3. Influence of estradiol-17β and insulin (0.2 IU, 0.4 IU) on the percentage of mitotic uterine luminal epithelial cells (mean $\pm$ SE of the mean) in control ovariectomized mice and streptozotocin-treated ovariectomized mice. The number above each column depicts the number of mice. *, $P<0.01$ *vs.* respective vehicle group. a, $P<0.01$; b, $P<0.001$ vs. respective oil group.

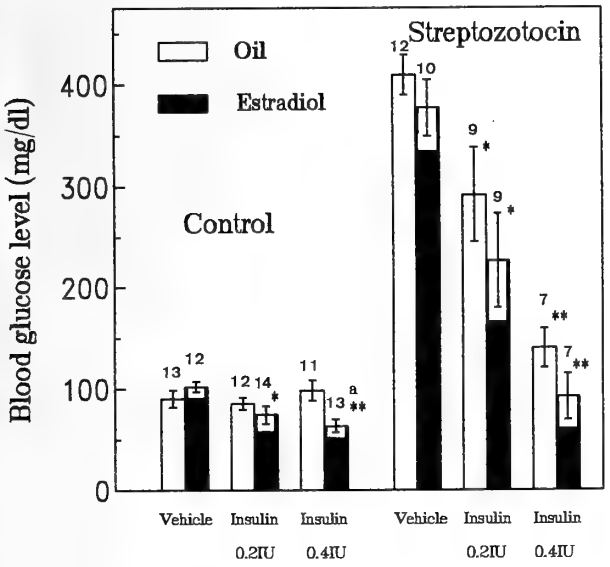

FIG. 4. Blood glucose levels in control ovariectomized mice and streptozotocin-treated ovariectomized mice receiving estradiol-17β or insulin. The number above each column depicts the number of mice. *, $P<0.05$; **, $P<0.01$ *vs.* respective vehicle group. a, $P<0.01$ *vs.* respective oil group.

treated mice (Fig. 3). Insulin administration in association with estrogen did not further increase the mitotic activity of luminal epithelial cells in both control and STZ-treated mice.

Blood glucose level

Normal blood glucose level was 90.1 ± 8.4 mg/dl (n= 13). Estrogen treatment did not change the blood glucose level, although in insulin-treated control mice estrogen decreased glucose level (Fig. 4). STZ treatment increased blood glucose levels (409.0 ± 19.6 mg/dl, n=12, at 20 days after STZ injection). Insulin decreased blood glucose levels in a dose-dependent manner in STZ-treated mice.

DISCUSSION

The present study revealed that insulin stimulated the proliferation of pituitary cells. Growth promoting action of insulin on uterine epithelial cells had been already demonstrated in rats and mice [9, 15]. Rat pituitary tumor cells, GH_3 cells, require insulin for the optimal growth *in vitro* system [11]. However, as far as we know, stimulatory effect of insulin on the proliferation of normal pituitary cells has never been reported.

STZ administration induces diabetes in mice and rats, which is ascertained by serum hyperglycemia and significant loss of body weights. Insulin administration was able to decrease the elevated serum glucose levels in STZ-induced diabetic mice. Our preliminary study showed that STZ (100 mg/kg) injection significantly decreased serum insulin levels (control male mice, 51.1 ± 8.9 μU/ml; STZ-treated males, 12.0 ± 5.1 μU/ml).

In STZ-treated mice, estrogen failed to increase the mitotic activity of pituitary cells. Repeated injection of insulin recovered the reduced responsiveness of pituitary cells to estrogen in STZ-treated diabetic mice to the level observed in normal mice. Insulin (0.4 IU) increased the mitotic activity of luminal uterine epithelial cells in control mice. Ineffectiveness of insulin in STZ-treated mice on the proliferation of luminal cells may be accounted for by the reduced responsiveness of uterine epithelial cells to insulin in insulin-deficient mice. Insulin was not able to enhance further the estrogen-induced proliferation of uterine cells. These results indicate that insulin stimulates the cell proliferation in pituitary cells and uterine epithelial cells, but the pathway of signal transduction leading to cell division may be different.

Several studies described the proliferation of pituitary cells in rats [4, 22, 23, 28]. Growth hormone-secreting cells (somatotrophs) and PRL cells are the most actively proliferating cells in pituitary secretory cells. PRL cells were particularly analyzed in the present study, since PRL secretion is known to be regulated by insulin [13, 25]. STZ-treated diabetes decreased PRL secretion in rats [6, 12]. In PRL cells of such diabetic rats the decrease in number of secretory granules and the atrophy of cell organelles were electron microscopically observed [34]. The present study showed that insulin stimulated the proliferation of PRL cells. The enhanced proliferation of PRL cells by insulin may be correlated with the enhanced PRL secretion [29]. Further analysis is needed for the understanding of the secretion and proliferation-coupling of PRL cells.

IGF receptors as well as insulin receptors are localized in pituitary glands [10], and in uterine tissues [7]. Our preliminary *in vitro* study indicated that IGF-I was more potent (about 100-fold) in stimulating the proliferation of cultured

pituitary cells than insulin (Oomizu and Takahashi, unpublished observation). Therefore, insulin action may be mediated by insulin-like growth factor-I (IGF-I) receptors in pituitary glands.

Several studies indicate that estrogen action on the cell proliferation is indirect and mediated by autocrine or paracrine growth factors [24, 27, 32]. Transforming growth factor α and epidermal growth factor are candidates of growth factors in the pituitary gland and the uterus [3, 16, 19, 20, 31]. Insulin or IGF-I may be another candidate of estrogen-associated growth factors. IGF-I and IGF-I mRNA are detected in pituitary glands [1, 18, 21]. Estrogen increased levels of IGF-I mRNA, IGF binding and IGF binding proteins [17]. As mitogenic action of estrogen is well known, the increase in pituitary IGF-I level by estrogen treatment may be closely associated with the estrogen-induced proliferation of pituitary cells. Estrogen administration may stimulate the secretion of IGF-I from pituitary cells, and in turn IGF-I secreted may stimulate the proliferation of pituitary cells in an autocrine or paracrine fashion. It is highly probable that insulin administered in the present study is able to accelerate the pituitary cell proliferation by the stimulation of intrinsic pituitary IGF-I system. In the uterus IGF-I is also detected [18], and its synthesis is stimulated by estrogen [2, 8]. IGF-I receptors are detected in uterine cells [7]. These results strongly suggest the autocrine or paracrine control of IGF-I on the proliferation of uterine cells. Therefore, it is also highly probable that insulin acts on IGF-I receptors, resulting in the stimulation of uterine epithelial cells.

Reduced responsiveness to estrogen on prolactin secretion had already reported in STZ-treated rats [6, 30, 33], and this reduction is partly due to the alteration in pituitary estrogen receptor system [30, 33]. Most of pituitary secretory cells including PRL cells had estrogen receptors [14]. Ineffectiveness of estrogen on the proliferation of pituitary cells in STZ-treated mice may result from altered mechanism of estrogen receptors.

In the previous study using STZ-treated or alloxan-treated diabetic rats, the response of uterine epithelial cells to estrogen on the proliferation was significantly reduced, and this was restored by insulin treatment [15]. Their result does not agree with our result. They had used the lower dose of estradiol-17β (4 μg/100 g body weight) compared with the dose of estrogen used in the present study. As we clearly found the diminished response in pituitary cells with this estrogen dose, one possible reason for this discrepancy is that the uterine epithelial cells in rats may be more responsive to estrogen than the pituitary cells. Estrogen receptor kinetics and estrogen activity for protein synthesis were altered in the uteri of STZ-induced diabetic rats, and restored by insulin treatment [5]. Thus, STZ treatment in the rat more severely may affect the estrogenic mechanism in the uterus. We preliminarily found that insulin and IGF-I stimulated the proliferation of mouse uterine epithelial cells *in vitro* (Takahashi and Miyake, unpublished observation). Further study on insulin or IGF-I action on the mouse uterine cells is needed.

Chronic estrogen administration increases pituitary weights, which mainly results from the hypertrophy and hyperplasia of PRL cells [29]. Gala and Jaques [6] demonstrated that STZ-induced insulin deficiency retarded estrogen-induced pituitary growth in the rat. The retarded growth of pituitary glands in STZ-treated rats is thought to be partly due to the diminished mitotic activity of pituitary cells, since the lower mitotic activity of pituitary cells including PRL cells in STZ-treated mice was shown in the present study.

In conclusion, the present *in vivo* study clearly showed that insulin administration increased the cell proliferation of pituitary cells. In pituitary cells insulin was required for estrogen-induced cell proliferation. Molecular basis of insulin-estrogen interaction must be studied using the *in vitro* system.

ACKNOWLEDGMENTS

This study was supported in part by the Ryoubiteien Foundation.

REFERENCES

1 Bach MA, Bondy CA (1992) Anatomy of the pituitary insulin-like growth factor system. Endocrinology 131: 2588–2594

2 Beck CA, Garner CW (1992) Stimulation of DNA synthesis in rat uterine cells by growth factors and uterine extracts. Mol Cell Endocrinol 84: 109–118

3 Borgundvaag B, Kudlow JE, Mueller SG, George SR (1992) Dopamine receptor activation inhibits estrogen-stimulated transforming growth factor-α gene expression and growth in anterior pituitary, but not in uterus. Endocrinology 130: 3453–3458

4 Carbajo-Peréz E, Watanabe YG (1990) Cellular proliferation in the anterior pituitary of the rat during the postnatal period. Cell Tissue Res 261: 333–338

5 Ekka E, Vanderheyden I, De Hertogh R (1984) Normalization of estradiol receptor kinetics and hormonal activity in uterus of streptozotocin-induced diabetic rats treated with insulin. Endocrinology 114: 2271–2275

6 Gala RR, Jaques S, Jr (1979) The influence of estrogen on pituitary growth and on prolactin production *in vitro* in the diabetic rat. Proc Soc Exp Biol Med 161: 583–588

7 Ghahary A, Murphy LJ (1989) Uterine insulin-like growth factor-I receptors: regulation by estrogen and variation throughout the estrous cycle. Endocrinology 125: 597–604

8 Ghahary A, Chakrabarti S, Murphy LJ (1990) Localization of the sites of synthesis and action of insulin-like growth factor-I in the rat uterus. Mol Endocrinol 4: 191–195

9 Ghosh D, Danielson KG, Alston JT, Heyner S (1991) Functional differentiation of mouse uterine epithelial cells grown on collagen gels or reconstituted basement membranes. In Vitro Cell Dev Biol 27A: 713–719

10 Goodyer CG, Lucie de Stéphano, Wei Hsien Lai, Guyda HJ, Posner BI (1984) Characterization of insulin-like growth factor receptors in rat anterior pituitary, hypothalamus, and brain. Endocrinology, 114: 1187–1195

11 Hayashi I (1984) Growth of GH_3, a rat pituitary cell line, in serum-free, hormone-supplemented medium, In "Methods for

Serum-Free Culture of Cells of the Endocrine System" Ed by DW Barnes, DA Sirbasku, GH Sato, Alan R. Liss, Inc, New York, pp 1–13

12 Ikawa H, Irahara M, Matsuzaki T, Saito S, Sano T, Aono T (1992) Impaired induction of prolactin secretion from the anterior pituitary by suckling in streptozotocin-induced diabetic rat. Acta Endocrinol 126: 167–172

13 Keech CA, Gutierrez-Hartmann A (1991) Insulin activation of rat prolactin promoter activity. Mol Cell Endocrinol 78: 55–60

14 Keefer DA (1980) In vivo estrogen uptake by individual cell types of the rat anterior pituitary after short-term castration-adrenalectomy. Cell Tissue Res 209: 167–175

15 Kirkland JL, Barrett GN, Stancel GM (1981) Decreased cell division of the uterine luminal epithelium of diabetic rats in response to 17 β-estradiol. Endocrinology 109: 316–318

16 Kudlow JE, Kobrin MS (1984) Secretion of epidermal growth factor-like mitogens by cultured cells from bovine anterior pituitary glands. Endocrinology 115: 911–917

17 Michels KM, Lee W-H, Seltzer A, Saavedra JM, Bondy CA (1993) Up-regulation of pituitary [^{125}I] insulin-like growth factor-I (IGF-I) binding and IGF binding protein-2 and IGF-I gene expression by estrogen. Endocrinology 132: 23–29

18 Murphy LJ, Bell GI, Friesen HG (1987) Tissue distribution of insulin-like growth factor I and II messenger ribonucleic acid in the adult rat. Endocrinology 120: 1279–1282

19 Nelson KG, Takahashi T, Bossert NL, Walmer DK, McLachlan JA (1991) Epidermal growth factor replaces estrogen in the stimulation of female genital-tract growth and differentiation. Proc Natl Acad Sci USA 88: 21–25

20 Nelson KG, Takahashi T, Lee DC, Luetteke NC, Bossert NL, Ross K, Eitzman BE, McLachlan JA (1992) Transforming growth factor-α is a potential mediator of estrogen action in the mouse uterus. Endocrinology 131: 1657–1664

21 Olchovsky D, Bruno JF, Gelato MC, Song J, Berelowitz M (1991) Pituitary insulin-like growth factor-I content and gene expression in the streptozotocin-diabetic rat: evidence for tissue-specific regulation. Endocrinology 128: 923–928

22 Sakuma S, Shirasawa N, Yoshimura F (1984) A histometrical study of immunohistochemically identified mitotic adenohypophysial cells in immature and mature castrated rats. J Endocrinol 100: 323–328

23 Shirasawa N, Yoshimura F (1982) Immunohistochemical and electron microscopical studies of mitotic adenohypophysial cells in different ages of rats. Anat Embryol 165: 51–61

24 Sirbasku DA (1978) Estrogen induction of growth factors specific for hormone-responsive mammary, pituitary, and kidney tumor cells. Proc Natl Acad Sci USA 75: 3786–3790

25 Stanley FM (1992) An element in the prolactin promoter mediates the stimulatory effect of insulin on transcription of the prolactin gene. J Biol Chem 267: 16719–16726

26 Starus DS (1984) Growth-stimulatory actions of insulin *in vitro* and *in vivo*. Endocr Rev 5: 356–369

27 Sutherland RL, Watts CKW, Clarke CL (1988) Oestrogen action. In "Hormones and their actions, Part I" Ed by BA Cooke, RJB P King, HJ van der Molen, Elsevier Science Publishers BV, Amsterdam pp 197–215

28 Takahashi S, Okazaki K, Kawashima S. (1984) Mitotic activity of prolactin cells in the pituitary glands of male and female rats of different ages. Cell Tissue Res 235: 497–502

29 Takahashi S, Kawashima S (1987) Proliferation of prolactin cells in the rat: effects of estrogen and bromocriptine. Zool Sci 4: 855–860

30 Tesone M, Ladenheim RG, Charreau EH (1985) Alterations in the prolactin secretion in streptozotocin-induced diabetic rats. Correlation with pituitary and hypothalamus estradiol receptors. Mol Cell Endocrinol 43: 135–140

31 Tomooka Y, DiAugustine RP, McLachlan JA (1986) Proliferation of mouse uterine epithelial cells *in vitro*. Endocrinology 118: 1011–1018

32 Webster J, Scanlon MF (1991) Growth factors and the anterior pituitary. Bailliere's Clin Endocrinol Metab 5: 699–726

33 Weisenberg L, Fridman O, Libertun C, De Nicola AF (1983) Changes in nuclear translocation of estradiol-receptor complex in anterior pituitary and uterus of rats with streptozotocin diabetes. J Steroid Biochem 19: 1737–1741

34 Yamauchi K, Shiino M (1986) Pituitary prolactin cells in diabetic rats induced by the injection of streptozotocin. Exp Clin Endocrinol 88: 81–88

ZOOLOGICAL SCIENCE 11: 451–454 (1994)

Molecular Evolution of Shark C-type Natriuretic Peptides

MASAYOSHI TAKANO[1], YUICHI SASAYAMA[2]
and YOSHIO TAKEI[3]

Ocean Research Institute, University of Tokyo, Minamidai, Nakano, Tokyo 164 and [2]Department of Biology, Faculty of Science, Toyama University, Gofuku, Toyama 930, Japan

ABSTRACT—C-type natriuretic peptides (CNP) of varying length were isolated from the atrium or ventricle of a shark, *Lamna ditropis* and their amino acid sequences were determined. Although the sequence of *Lamna* CNP was highly homologous to those of other CNPs sequenced to date, the *Lamna* CNP-41, the longest CNP identified in this study, has one amino acid replacement from those of *Triakis scyllia* and *Scyliorhinus canicula*, and three amino acid replacements from that of *Squalus acanthias*. The degree of similarity of CNP molecules coincides well with their systematic positions in the cladogram of elasmobranchs; *Lamna, Triakis* and *Scyliorhinus* belong to the same order, but *Lamna* and *Squalus* belong to different orders. The facts that *Lamna* and *Triakis* are in different suborders but *Triakis* and *Scyliorhinus* are in the same suborder and have identical CNP-41, also support this evolutionary implication.

INTRODUCTION

C-type natriuretic peptide (CNP) is a member of the natriuretic peptide family first identified in the brain of pig and teleost fishes [2, 4, 9]. In contrast to other members of the peptide family, namely atrial (A-type), B-type and ventricular natriuretic peptides (ANP, BNP and VNP) which are cardiac hormones circulating in the blood, CNP has been isolated from the brain in all species from teleost to mammals, and its plasma and cardiac concentrations are too low to be detected in mammals [8]. Thus CNP is regarded as a neuropeptide in mammals. However, we have isolated CNP from the heart of two species of dogfish shark, *Triakis scyllia* and *Scyliorhinus canicula* [5, 6]. In these fish, plasma and cardiac concentrations of CNP are extremely high, and other cardiac natriuretic peptides, ANP, BNP and VNP, are not identified in their hearts [7]. Furthermore, only CNP cDNA has been cloned from the cDNA library of the heart of spiny dogfish, *Squalus acanthias* [3]. Therefore it is likely that CNP is the only natriuretic peptide present in elasmobranchs. It is also noted that the amino acid sequence of CNP is more conserved than any other natriuretic peptides, namely ANP, BNP and VNP [8]. Thus, CNP might be an ancestral molecule of the natriuretic peptide family, and other members might be reproduced by gene duplication.

As a prototype of the natriuretic peptide family, it seems of interest to examine chemical evolution of the CNP molecule. In previous studies, we have found that amino acid sequences of CNP-22, a mature form stored in the brain, of *Triakis* and *Scyliorhinus* are identical, and even proCNP differs in only 3 out of 115 amino acid residues [5,6]. However, *Squalus* CNP-22 predicted from the cDNA sequence differs from that of *Triakis* in 2 amino acid residues, and the difference was much greater at the level of prohormone [3]. Systematically, *Triakis* and *Scyliorhinus* belong to the same suborder *Scyliorhinoidei*, but *Squalus* is different from the two species at the level of order [1]. We recently have obtained the heart of *Lamna ditropis*. This fish belongs to the order *Lamniformes* as do *Triakis* and *Scyliorhinus,* but to the suborder different from those sharks. Therefore, we attempted in the present study to isolate CNP from the *Lamna* heart and to compare its structure with those of other sharks.

MATERIALS AND METHODS

Isolation of CNP

The shark, *Lamna ditropis*, of approximately 3 m in body length was caught in Toyama Bay and was obtained from fishermen 5 h after capture. The heart was immediately dissected out, the atrium and ventricle separated, and frozen in a deep freezer at −50°C. The atrium (106.4 g) and ventricle (333.2 g) were treated separately. ANP-like peptides in the heart were isolated with protocols described previously [5]. The frozen tissues were crushed in a pulverizer, boiled in 5 volumes (atrium) or 3 volumes (ventricle) of water for 10 min, acidified with AcOH to a concentration of 1 M, and homogenized in a Polytron homogenizer (Kinematika, Germany) for 90 sec at maximum speed. The homogenate was centrifuged at 16,000×g for 30 min at 4°C. The supernatant was added to 2 volumes of cold acetone, and centrifuged at 16,000×g for 30 min at 4°C. The supernatant was evaporated, reconstituted in 30 ml of 1 M AcOH, and added to 2 liters of cold acetone. After centrifugation, the pellet was dissolved in 30 ml of 1 M AcOH, and applied onto a column (5×85 cm) of Sephadex G-25 fine (Pharmacia, Sweden) for desalting. The fractions which contain molecules with $Mr>$ca. 2,000 were applied onto a column of SP-Sephadex C-25 (1.6×20 cm), and adsorbed materials were eluted successively with 150 ml each of 1 M AcOH, 2 M pyridine, and 2 M pyridine-AcOH, pH 5.0. Each fraction was evaporated and assayed for relaxant activity in the

Accepted June 7, 1994
Received April 4, 1994
[1] Present address: Research Institute, Zenyaku Kogyo Co. Ltd., Ohizumimachi, Nerima, Tokyo 178, Japan
[3] To whom all correspondence should be addressed

chick rectum as described below. Bioactive fractions were subjected to cation-exchange high performance liquid chromatography (HPLC) in an IEC-CM column (7.5×75 mm, Jasco, Japan). Each bioactive fraction was then subjected to reverse-phase HPLC in an ODS-120T column (4.6×250 mm, Tosoh, Japan) with different gradients of CH_3CN concentrations. The detailed chromatographic conditions are described in the legend of each figure. The purified material was subjected to amino acid sequencing in a protein sequencer (477A, Applied Biosystems, USA). Validity of the amino acid sequence was examined by mass spectrometry (JMS-HX110, JEOL, Japan).

ANP-like activity was assayed at each step of purification using a relaxant activity in the chick rectum [10]. New-born male chicks were purchased from Kanagawa Poultry Cooperation (Yokohama) and reared under a infra-red lamp with free access to food and water. The chick was decapitated, rectum immediately isolated, and set up in a trough whose temperature was controlled at 37°C. The rectum was precontracted with 2×10^{-6} M carbachol (Sigma, USA), and the relaxation was quantified by a displacement transducer connected to a transducer amplifier (1829 and 45347, NEC-Sanei, Japan). ANP-like activity was expressed as equivalents to eel ANP which was used as standard.

RESULTS

Same molecules were isolated from atrial and ventricular extracts. After Sephadex G-25 chromatography, fractions of 1–70, which contain molecules larger than CNP-22 [5], were pooled and subjected to SP-Sephadex C-25 chromatography (Fig. 1a). Since only the fraction eluted with pyridine-AcOH exhibited rectum-relaxant activity, this fraction was subjected to cation-exchange HPLC. The bioactive

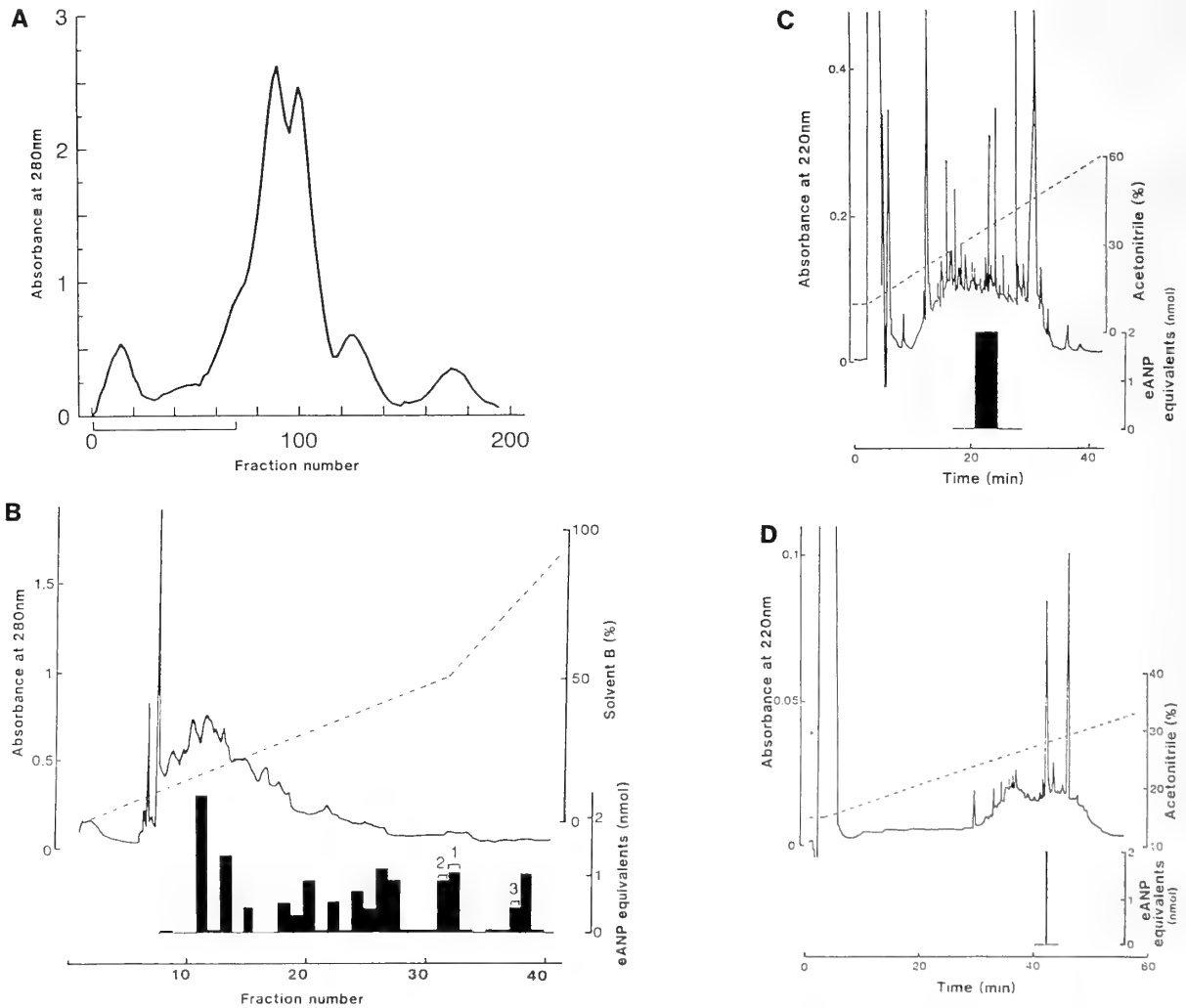

Fig. 1. Purification of C-type natriuretic peptide (CNP) from *Lamna* atrium. Solid columns represent relaxant activity in the chick rectum expressed as equivalents to eel atrial natriuretic peptide (eANP). A: Sephadex G-25 chromatography of crude atrial extract. Fractions marked by square bracket were subjected to SP-Sephadex C-25 chromatography. B: cation-exchange high-performance liquid chromatography (HPLC) of the fraction eluted with pyridine-AcOH in SP-Sephadex C-25 chromatography. Broken lines show gradient of solvent B (1 M NH_4OAc : CH_3CN=9:1) against solvent A (10 mM NH_4OAc : CH_3CN=9:1). CNP-29, CNP-38 and CNP-41 were recovered, respectively, from fractions marked with bracket 1, 2, and 3. C and D: reverse-phase HPLC of fraction 37 of panel B and a fraction with bioactivity in panel C, respectively. Sequence analysis of bioactive peak in panel D revealed that the peak is that of CNP-29. Broken lines show gradient of CH_3CN concentrations.

principle was purified only from fractions 31, 32 and 37 of cation-exchange HPLC, although bioactivity was also noted in other fractions (Fig. 1b). A rectum-relaxant principle was isolated from fraction 32 by two steps of reverse-phase HPLC (Figs. 1c, d). Final yield was 2 nmol equivalent to eel ANP as determined by the rectum-relaxant activity and 363 pmol equivalent to eel ANP as determined by absorbance at 220 nm. Sequence analysis of 3/4 of the purified peptide revealed that the sequence was H-Phe-Lys-Gly-Arg-Ser-Lys-Lys-Gly-Pro-Ser-Arg-Gly-(Cys)-Phe-Gly-Val-Lys-Leu-Asp-Arg-Ile-Gly-Ala-Met-Ser-Gly-Leu-Gly-(Cys)-OH (Fig. 2). The presence of two cysteine residues was deduced from the similarity to other CNPs thus far sequenced. Thus the peptide was named *Lamna* CNP-29. The sequence was confirmed by mass spectrometry using the remaining 1/4. A CNP with 12 amino acid residues (Arg-Leu-Leu-Lys-Asp-Leu-Ser-Asn-Asn-Pro-Leu-Arg-) elongated from the N-terminus of CNP-29 was isolated from fraction 37 and thus named *Lamna* CNP-41. The final yield was 260 pmol as judged by absorbance at 220 nm. Sequence analysis of 3/4 of the purified peptide could determine only 28 amino acid residues from the N-terminus. However, it was apparent that the peptide had longer sequence and terminated with the second-half cysteine at the C-terminus, because mass analysis calculated the MH^+ of 4433 which coincides well with the average mass of predicted sequence of CNP-41 (Mr=4432.3). CNP-38 was also isolated from fraction 31 with the final yield of 312 pmol. Although many other fractions showed bioactivity, no bioactive principle could be isolated from those fractions.

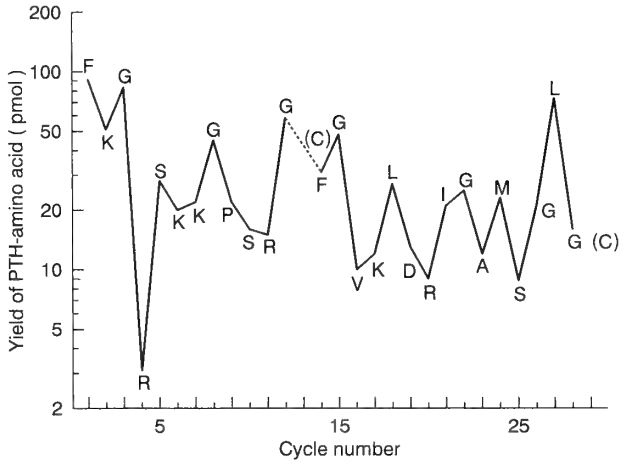

FIG. 2. The yield of phenylthiohydrantoin-derivatized (PTH) amino acid at each cycle of Edman degradation in the sequence analysis of CNP-29. No PTH amino acid was detected at 13th and 29th cycle. The presence of cysteine residues, denoted by (C), was estimated at these cycles from analogy to other CNPs and from the result of mass spectrometry.

DISCUSSION

We isolated three short forms of CNP from the heart of *Lamna ditropis* in the present study. In previous attempts to isolate ANP-like peptides from the heart of other sharks, *Triakis scyllia* and *Scyliorhinus canicula*, large amounts of proCNP and small amounts of CNP-38 and CNP-39 were isolated [5, 6]. CNP-38 was also isolated in this study, but

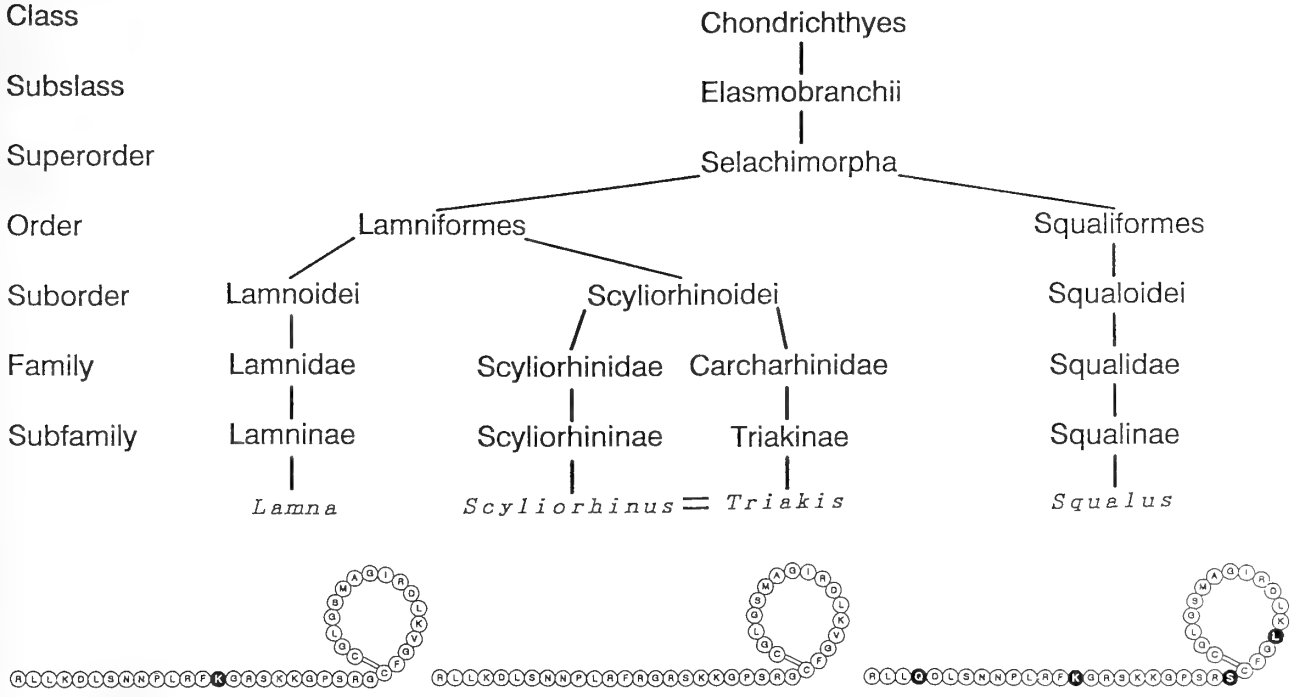

FIG. 3. Phylogenetic cladogram of 4 species of sharks and their amino acid sequences of CNP-41. The cladogram was depicted after Nelson [1]. Amino acid residues different from *Triakis* or *Scyliorhinus* CNP are shaded.

proCNP and CNP-39 were not identified. Instead, CNP-29 and CNP-41 were recovered from the *Lamna* heart. Several peaks with bioactivity, which may contain other fragments of CNP, were also identified after ion-exchange HPLC. This may indicate that a different processing system is operating in the *Lamna* heart, or the shorter forms are degradation products of proCNP. The latter is more likely because it took longer to freeze the *Lamna* heart after its death. In previous studies using *Triakis* and *Scyliorhinus*, hearts were frozen on dry ice immediately after isolation from anesthetized fish.

In addition to *Triakis* and *Scyliorhinus* CNP, CNP cDNA has been cloned from the heart of *Squalus acanthias* [3]. Comparison of the amino acid sequence of CNP-41 between *Triakis* and other sharks revealed that *Triakis* CNP-41 is identical to that of *Scyliorhinus*, is different by one amino acid residue from that of *Lamna*, and is different by four amino acid residues from that of *Squalus* (Fig. 3). As also shown in Figure 3, *Lamna, Triakis* and *Scyliorhinus* belong to the same order (*Lamniformes*) but *Squalus* is in a different order [1]. *Triakis* and *Scyliorhinus* are the same even at the level of suborder, whereas *Triakis* and *Lamna* are in different suborders. It is of interest to note, therefore, that the chemical evolution of CNP molecule is closely related to the cladogram of cartilaginous fishes which is drawn based on the morphological proximity (Fig. 3).

During the course of purification, we utilized relaxant activity in the chick rectum as an assay system. We found that the final yield of CNPs quantified by this assay was always much greater than that deduced from absorbance at 220 nm. It seems therefore that the shark CNP has much greater relaxant activity than eel ANP which was used as standard for the assay.

ACKNOWLEDGMENTS

The authors are grateful to Dr. Hideshi Kobayashi of Zenyaku Kogyo Co. Ltd. for critical reading of the manuscript, and to Dr. T. Takao and Professor Y. Shimonishi of the Institute for Protein Research, Osaka University for performing mass spectrometry. We also thank Dr. T. Sato of Misaki Marine Biological Station, University of Tokyo for his advice on the classification of elasmobranchs and Mr. H. Kaiya and K. Ukawa of Toyama University for their help in the initial part of purification. This investigation was supported in part by grants from the Ministry of Education, Science and Culture of Japan, from the Fisheries Agency of Japan and from Zenyaku Kogyo Co. Ltd.

REFERENCES

1 Nelson JS (1984) Fish of the World. John Willey & Sons, New York, 2nd ed, pp 49–59

2 Price DA, Doble KE, Lee TD, Galli SM, Dunn BM, Parten B, Evans DH (1990) The sequencing, synthesis, and biological actions of an ANP-like peptide isolated from the brain of the killifish, *Fundulus heteroclitus*. Biol Bull 178: 279–285

3 Schofield JP, Jones DSC, Forrest Jr JN (1991) Identification of C-type natriuretic peptide in heart of spiny dogfish shark (*Squalus acanthias*). Am J Physiol 261: F734–F739

4 Sudoh T, Minamino N, Kangawa K, Matsuo H (1990) C-type natriuretic peptide (CNP): A new member of natriuretic peptide family identified in porcine brain. Biochem Biophys Res Commun 168: 863–870

5 Suzuki R, Takahashi A, Hazon N, Takei Y (1991) Isolation of high-molecular-weight C-type natriuretic peptide from the heart of a cartilaginous fish (European dogfish, *Scyliorhinus canicula*). FEBS Lett 282: 321–325

6 Suzuki R, Takahashi A, Takei Y (1992) Different molecular forms of C-type natriuretic peptide isolated from the brain and heart of an elasmobranch, *Triakis scyllia*. J Endocrinol 135: 317–325

7 Suzuki R, Togashi K, Ando K, Takei Y (1994) Distribution and molecular forms of C-type natriuretic peptide in tissues and plasma of an elasmobranch, *Triakis scyllia*. Gen Comp Endocrinol (in press)

8 Takei Y, Balment RJ (1993) Natriuretic factors in non-mammalian vertebrates. In "New Insights in Vertebrate Kidney Function" Ed by JA Brown, RJ Balment, JC Rankin, Cambridge University Press, Cambridge, pp 351–385

9 Takei Y, Takahashi A, Watanabe TX, Nakajima K, Sakakibara S, Takao T, Shimonishi Y (1990) Amino acid sequence and relative biological activity of a natriuretic peptide isolated from eel brain. Biochem Biophys Res Commun 170: 883–891

10 Watanabe TX, Noda Y, Chino N, Nishiuchi Y, Kimura T, Sakakibara S, Imai M (1989) Structure-activity relationships of alpha-human atrial natriuretic peptide. Eur J Pharmacol 147: 49–58

ZOOLOGICAL SCIENCE 11: 455–465 (1994)

Systematic Study on the *Chaenogobius* Species (Family Gobiidae) by Analysis of Allozyme Polymorphisms

TAKESHI AIZAWA, MACHIKO HATSUMI* and KEN-ICHI WAKAHAMA

Department of Biology, Faculty of Science, Shimane University
1060 Nishikawatsu-cho, Matsue 690, Japan

ABSTRACT—Isozyme polymorphisms of eight *Chaenogobius* species (Family Gobiidae) were studied in order to understand the phylogenetic relationships between them. Fifteen loci from ten enzymes and sarcoplasmic protein were detected by horizontal starch gel electrophoresis. The phylogenetic tree obtained from genetic distances between species essentially agreed with morphological and ecological studies previously reported. In addition, two new features were revealed. First, Nei's genetic distance between *C. laevis* from Saitama and that from Akita suggested that they are differentiate from each other on the species level. Second, the undescribed taxon, *C.* sp., from Lake Shinji was closely related to *C. laevis* from Akita and the genetic distance between them was 0.114. The smallest genetic distance between distinct species of *Chaenogobius* was 0.103 between *C. urotaenia* and *C. isaza* obtained in this study. This shows the possibility that *C.* sp. is the different species of *C. laevis*, from Akita.

INTRODUCTION

The family Gobiidae accomplished distinctive adaptive radiation. Each species adapted to various environments and has various life histories. This makes Gobiidae an excellent material for studying the mechanisms of evolution and speciation in Pisces. *Chaenogobius*, one genus of Gobiidae, consists of several species members that have various life histories, namely, species adapted in brackish water or fresh water, marine species, amphidromous species and land-locked species. The ecological and evolutionary genetic studies of this genus may especially supply us useful information on evolutionary process of adaptation of fishes.

The phylogenetic study on the members of this species has been carried out, but not completed, yet [23]. Takagi [31] demonstrated that *C.urotaenia* (Hilgendorf) and *C. castaneus* (O'Shaughnessy) are different species. Morphological and ecological studies showed three types of *C. urotaenia*, one lives in freshwater, another lives in brackish water and the other lives in the middlereach type, and now these types are recognized as distinct species and called *C.urotaenia* (Japanese name, Ukigori), *C.*sp.2 (Japanese name, Shimaukigori) and *C.*sp.1 (Japanese name, Sumiukigori), respectively [1, 7, 15, 31, 32]. Takagi [33] discriminated *C. laevis* (Steindachner) from *C. castaneus* based on its morphology. *Chaenogobius castaneus* has three pairs of pit organs connected by sensory canals and lives in brackish water, whereas *C. laevis* has no canal system and lives in freshwater. His study was followed by the description of new morph of *Chaenogobius* species (Japanese tentative name; Shinjiko-haze by Koshikawa [12]) from Lake Shinji in Japan [13]. This morph lives in brackish water of lower salt condensation than *C. castaneus* lives. It is similar to *C. laevis* for its color pattern and nuptial color of female but different from *C. laevis* and *C.castaneus* since shinjiko-haze has two pairs of pit organs connected by sensory canals on its head. This opening pattern of sensory canals is quite similar to *C. taranetzi* Pinchuk distributing Ussuri Bay in Russia and North Korea [9,23]. From these facts there are three possibilities of phylogenetic position of the species from Lake Shinji; namely, this species is one geographic variation of *C. laevis* or *C. taranetzi*, this is different species of *C. laevis* or *C. taranetzi*, and this species and *C. taranetzi* are the geographic variation of *C. laevis*.

In two decades of population biology, it was turned out that molecular approach is powerful to study phylogenetic relationships of various organisms [6, 18, 22, 27, 35]. Isozyme polymorphisms detected by electrophoresis supply useful measurement of genetic differentiation between populations or species, in terms of, the genetic distance [16, 17]. Many groups of species were studied on isozyme polymorphisms [24]. Accumulated data revealed that there were levels of genetic differentiation between local populations, subspecies, species or genus [6, 16, 17, 22, 24]. Using these levels, a phylogenetic tree could be constructed by cluster analysis from genetic distances [17, 2, 3, 4, 5]. For the species under consideration, electrophoretic studies should supply useful information on the phylogenetic relationships of *Chaenogobius* species.

In this study we analyzed allozyme polymorphisms of eight members of *Chaenogobius* species, six taxa mentioned above, *C. isaza* Tanaka, endemic to Lake Biwa in Japan, and *C. heptacanthus* (Hilgendorf), marine species, in order to clarify the phylogenetic relationships of this group and to characterize the species from Lake Shinji genetically.

Accepted May 10, 1994
Received November 20, 1994
* To whom all correspondence should be addressed.

MATERIALS AND METHODS

Animal sampling

Materials used in this experiment were *C. castaneus, C. laevis, C. heptacanthus, C. urotaenia, C.* sp. 1, *C.* sp. 2, *C. isaza* and an undescribed taxon collected from Lake Shinji , Shimane Prefecture in Japan. Since we could not conclude the undescribed taxon from Lake Shinji as *C. laevis* or *C. taranetzi*, we called this as *C.* sp. here. Table 1 shows the collection data of materials and Figure 1 shows the sites of collection. Six populations were kindly supplied by others, or, *C.* sp. 1 from Daitobetsu river by Dr. A. Goto, Faculty of Fisheries, Hokkaido University, *C. laevis* from Lake Hachiro-gata by Mr. K. Shibuya, Akita Prefectural Fisheries Consulting Center, *C. laevis* from Koma river by Mr. A. Iwata, Akasaka Imperial Palace, C. castaneus from Tama river by Mr. I. Kimoto, Tokyo Metropolitan Fisheries Experiment Station, *C. isaza* from Lake Biwa by Dr. S. Takahashi and Mr. S. Matsuoka, Shiga Prefecture and C. heptacanthus from Lake Nakaumi, Mawatashi by Mr. T. Kawashima, Mitoya Inland Water Fisheries Branch, Shimane Prefectural Fisheries Experiment Station.

Sample preparation for electrophoresis

Samples of fishes were stored at −25°C before dissection. Liver and lateral muscle were dissected out from each individual melted on ice. Three times or same amount of distilled water was added to liver or muscle, respectively, and homogenized in a microcentrifuge tube by plastic homogenizer on ice. The sample was centrifuged at 10000×*g* for 15 min. at 4°C. The supernatant was absorbed by capilalies and stored at −25°C until electrophoresis.

Individuals from which the tissues were removed were fixed in 10% formaldehyde. Identification of three species, *C. castaneus, C. laevis* and *C.* sp. was made by their color patterns after fixation and patterns of sensory canals, according to the method by Takagi [34].

Electrophoresis

Ten different enzymes and sarcoplasmic protein prepared from the species were analyzed by horizontal starch gel electrophoresis (Table 2). Two buffer systems were used in this experiment. One is citrate-aminopropyl morphorine buffer [8] and the other is citrate-tris buffer [21]. The staining methods of enzymes used were described by Shaw and Prasad [29] or Selander *et al.* [28]. Gels were dried between serophan to form films [20] and the isozyme patterns were documented on the films. When one enzyme had two loci, each locus was numbered in order of lower mobility to the anode.

TABLE 1. Collection data of materials

Species	P*	Locality, prefecture	Date	N**
C. castaneus	1.	Lake Nakaumi (Shimo-itou), Shimane	Dec. 1989	55
	2.	Iinashi River, Shimane	Nov. 1990	20
	3.	Lake Shinji (Matsue-Onsen), Shimane	Jan. 1990	20
	4.	Lake Shinji (Hamasada), Shimane	Jan. 1990	14
	5.	Lake Shinji (Tamayu), Shimane	Jan.-Feb. 1990	5
	6.	Tama River, Tokyo	Oct. 1989	3
C. sp.	7.	Lake Shinji (Matsue-Onsen), Shimane	Jan.-Feb. 1990	20
	8.	Lake Shinji (Hamasada), Shimane	Jan. 1990	21
	9.	Lake Shinji (Tamayu), Shimane	Jan.-Feb. 1990	34
C. laevis	10.	Lake Hachirou-gata, Akita	Dec. 1989	75
	11.	Koma River, Saitama	Oct. 1990	20
C. heptacanthus	12.	Lake Nakaumi (Mawatashi), Shimane	Dec. 1989	34
C. urotaenia	13.	Shinshi River, Shimane	Feb.-Mar. 1990	5
	14.	Satoji River, Shimane	Apr. Dec. 1990	4
	15.	Fukaura River, Shimane	Dec. 1990	2
	16.	Motoya River, Shimane	Dec. 1990	3
C. sp. 1	17.	Daitobetsu River, Hokkaido	Nov. 1990	20
C. sp. 2	18.	Shinshi River, Shimane	Feb.-Mar. 1990	13
	19.	Satoji River, Shimane	Apr. 1990	10
	20.	Fukaura River, Shimane	Dec. 1990	8
	21.	Ujiki River, Shimane	Dec. 1990	10
	22.	Oku River, Shimane	Jan. 1991	10
C. isaza	23.	Lake Biwa, Shiga	Jan.-Feb. 1991	45

P*; Population number.
N**; No. of individuals used for analysis.

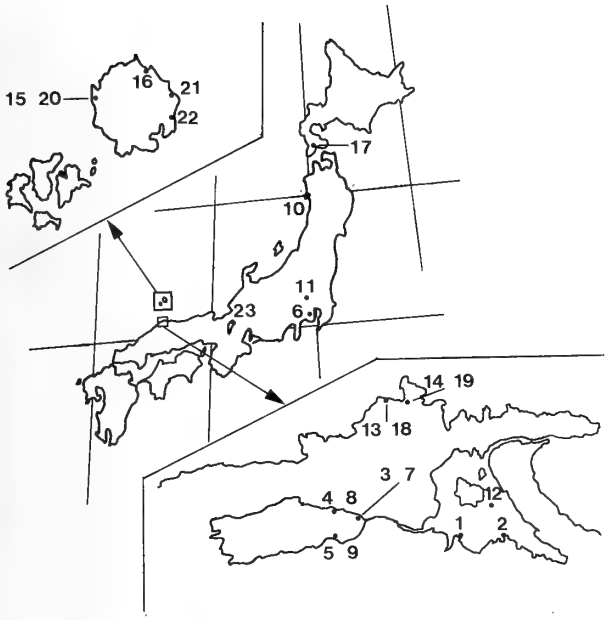

FIG. 1. The map of Japan showing sampling localities. Each number is corresponding to the population number in Table 1.

RESULTS

Fifteen loci were postulated in ten enzymes and sarcoplasmic protein from electrophoretic morph on starch gels among eight taxa of the genus *Chaenogobius*. Examples of zymograms were shown in Figure 2. Two types of bands were observed in one of the sarcoplasmic proteins. One type showed a single band and the other type showed double bands (Fig 2d, *sp-1*). Since each species had one of these types alternatively, double bands should not be heterozyotes and may be originated from gene duplication or post-translational modification. We named *b* to the allele of single band and *a* to the allele of double bands.

One locus, the *sarcoplasmic protein 2*, was monomorphic and the *Ldh* locus was also monomorphic with one exceptional individual from the Akita populations of *C. laevis* (Fig. 2b) but other loci had more than two alleles. Table 3 shows the allelic frequencies at thirteen loci on each population.

Each species had fixed allele at five loci, namely, *Aat, Ck, Me-1, Me-2* and *Sp-1*. In these loci *Ck, Me-1 Me-2* and *Sp-1* had only two variants. One type of variants was shared by *C. castaneus, C. sp., C. laevis, C. heptacanthus* and the other type was shared by *C. urotaenia, C.* sp. 1, *C.* sp.2 and *C. isaza*.

Other loci were polymorphic in some species. More than six alleles were observed at the *α-Gpd, Gpi-2, Mdh,* and *Pgm* loci. Twenty three populations were polymorphic for any of these four loci. Related species and populations were compared to each other for alleles of these four loci. At the *α-Gpd* locus, allele *f* was shared by *C.* sp. and the Akita population of *C.laevis* whereas the Saitama population of *C. laevis* had allele *d*. In *C. castaneus*, allele *e* of this locus was common. Two populations of *C. castaneus* had allele *b* at low frequencies while allele *b* was fixed in *C. heptacanthus* and *C.* sp. 1 and was at high frequency in *C. urotaenia*. *C.* sp.2 had allele *a* and *C. isaza* had allele *c* at the *α-Gpd* locus. At the *Gpi-2* locus, allele *c* was observed at high frequency in *C. castaneus*, *C.* sp. and *C. laevis* from Saitama while allele *b* was observed at high frequency in *C. laevis* from Akita and *C. heptacanthus*. *C. urotaenia, C.* sp.1 and *C.* sp. 2 had allele *d* at high frequency and allele *f* at low frequency. *C. isaza* had two alleles, *d* and *f*, at equal frequency at the *Gpi-2* locus. At the *Mdh* locus allele *e* and allele *f* were shared by *C. castaneus* and *C. laevis* but frequency was different in species. *C.* sp. had allele *e* and allele *a* but not allele *f*. *C. urotaenia, C.* sp. 1, *C.* sp. 2, *C. heptacanthus* and *C. Isaza* were monomorphic for the *Mdh* locus. At the *Pgm* locus allele *e* was common in *C. castaneus, C.* sp. and *C. laevis* from Akita whereas *C. laevis* from Saitama did not have allele *e* but had allele *c* and allele *b*. *C. urotaenia, C.* sp. 1, *C.* sp. 2 and *C. isaza* shared allele *c* at the *Pgm* locus at high frequency with other variants at low frequency. *C. heptacanthus* had allele *d* and allele *f* specifically.

The *Gpi-1* locus had two alleles, *a* and *b*. In almost all species, allele *b* was fixed. At the *Gpi-1* locus allele *a* was

TABLE 2. The list of Enzymes and proteins detected

Enzyme and protein (Abbreviation)	E.C.Number	Tissue*	Buffer**
Asparate aminotransferase (AAT)	2.6.1.1	M	CT
Creatine Kinase (CK)	2.7.3.2	M	CT
α-glycerophosphate dehydrogenase (α-GPD)	1.1.1.8	M	CT
Glucosephosphate isomerase (GPI)	5.3.1.9	M	CT
Isocitrate dehydrogenase (IDH)	1.1.1.42	M, L	APM
Lactate dehydrogenase (LDH)	1.1.1.27	M	APM
Malate dehydrogenase (MDH)	1.1.1.37	L	APM
Malic enzyme (ME)	1.1.1.40	M	CT
Phosphoglucomutase (PGM)	2.7.5.1	M	APM
Superoxide dismutase (SOD)	1.15.1.1	L	APM
Sarcoplasmic protein (SP)	—	M	APM

*; M means muscle and L means liver. **; AMP means citrate, aminopropyl mophorine buffer and CT means citrate-tris buffer.

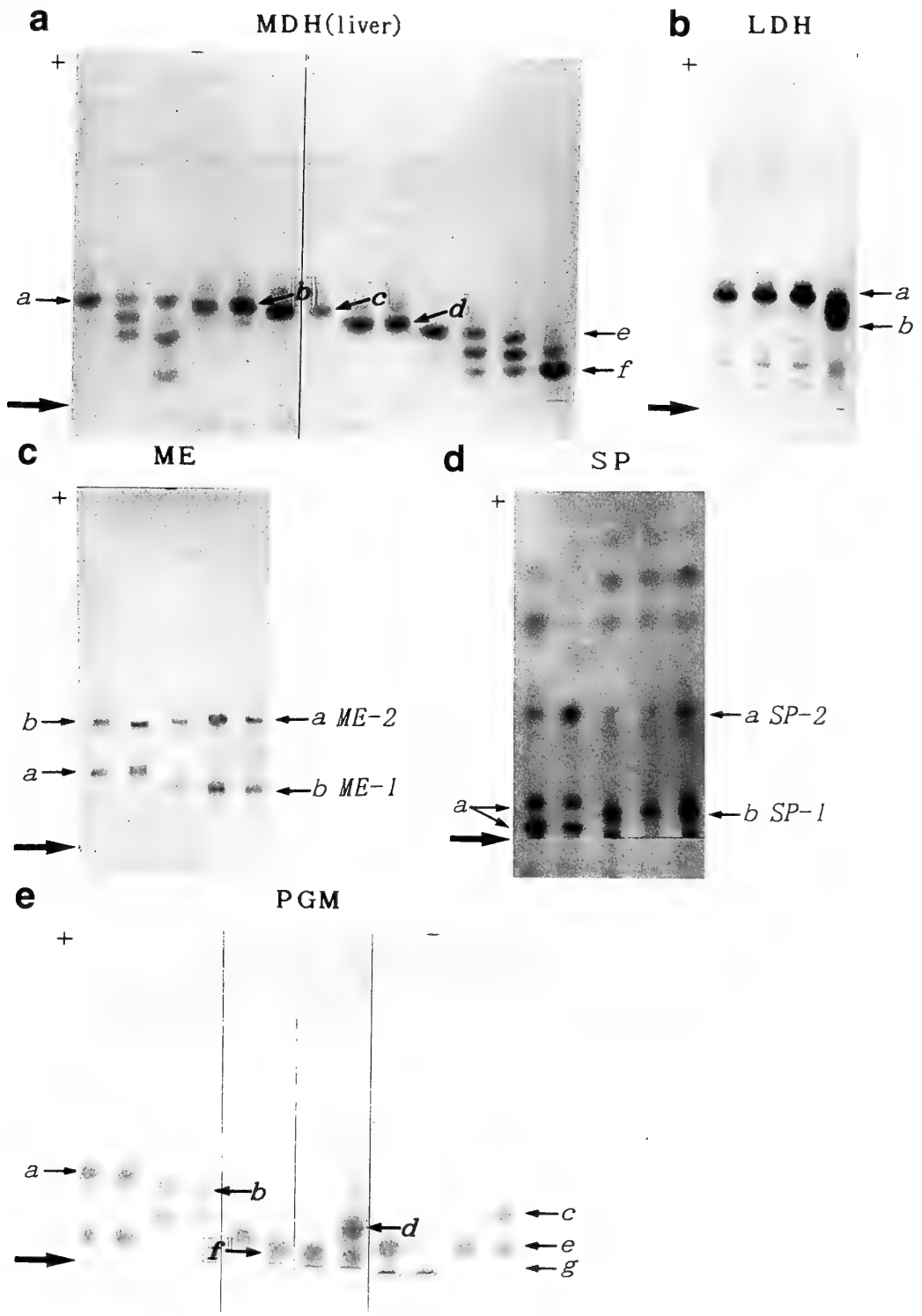

FIG. 2. Zymograms of four enzyme systems and a sacroplasmic protein. Thick arrows indicate origin.

only found in *C.* sp. and *C.* sp.1. The *Idh-1* locus had four alleles, the *Idh-2* had three alleles and the *Sod* had four alleles. These three loci, however, were not so polymorphic as other loci.

Nei's genetic distances [16] were calculated from the allele frequencies. Table 4 gives the matrix of average minimal and maximal genetic distances between each pair of species. The genetic distances between populations within species were 0 to 0.018 except 0.194 between the Akita and Saitama populations of *C. laevis*. This made us to list average genetic distances of each population of *C. laevis* separately. The genetic distances between species ranged from 0.092 between *C. urotaenia* and *C. isaza* to 1.595 between *C. heptacanthus* and *C.* sp. 2.

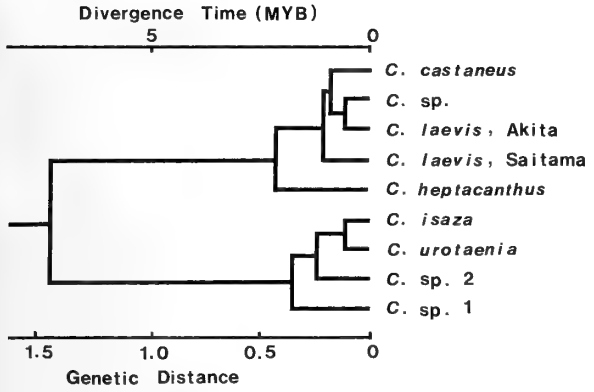

FIG. 3. Phylogenetic tree showing the relationships among eight species of genus *Chaenogobius* based on values of genetic distance.

A phylogenetic tree was constructed from genetic distances by average distance method (UPGMA) devised by Sneath and Sokal [30] and modified by Nei [17]. Figure 3 shows the phylogenetic tree of nine taxa of *Chaenogobius* constructed from average genetic distances in this study. The tree was not different topologically from the tree constructed from genetic distances between populations.

Eight species were divided into two groups. One was *C. castaneus* group including *C. castaneus, C.* sp. *C. laevis* and *C. heptacanthus* and the other was *C. urotaenia* group including *C. urotaenia, C.* sp. 1, *C.* sp. 2 and *C. isaza*. The genetic distances between two species from different groups were more than 1.2. In *C. castaneus* group *C. heptacanthus*, marine species, was separate from other three species, since the genetic distances between *C. heptacanthus* and other species in *C. castaneus* group were larger than 0.3. In *C. urotaenia* group, *C. urotaenia* and *C. isaza*, endemic to Lake Biwa, were closely related and the average genetic distance between them was 0.103.

Figure 3 shows the curious situation of *C. laevis*. The Akita population of *C. laevis* was differentiated from the Saitama population of *C. laevis* genetically. The Akita population was most closely related to *C.* sp. from Lake Shinji and closely related to *C. castaneus* more than the Saitama population of *C. laevis*.

DISCUSSION

In the above studies, it is seen that genetic variabilities in populations were low in *Chaenogobius* species. Expected average heterozygosity ranged from 0.006 in *C.* sp. 2. to 0.062 in *C.* isaza and polymorphic loci, from 0% in *C.* sp. 1 and *C.* sp. 2 to 26.7% in *C. castaneus* and *C. laevis* (Table 5). However these values are comparable to those in populations of Pisces species previously reported [19,24].

This study showed that the application of molecular taxonomy, based on isozyme polymorphisms, is useful to reveal the phylogenetic relationships among morphologically similar Gobiidae species as Masuda *et al.* [14] showed in their studies of *Rhinogobius* species.

The genus *Chaenogobius* was divided into two groups in this study (Fig. 3). One was *C. castaneus* group and the other was *C. urotaenia* group. One group shared the alleles different from the other group's at four loci, *Ck, Me-1, Me-2* and *Sp-1* (Table 3). The morphological studies have shown that *C. urotaenia, C.* sp.1, *C.* sp. 2 and *C. isaza* are similar to each other in its lateral line system and its large mouth when they were compared to other *Chaenogobius* species [1, 23]. Moreover the genetic distance between the two groups was more than 1.2 and this value was large enough to regard that they were genetically differentiated at genus level [18].

It was confirmed that three species of *C. castaneus* group, *C. castaneus, C.* sp. and *C. laevis*, morphologically similar each other, are closely related species. In addition, it was found that two *C. laevis* populations were highly differentiated. The Akita population of *C. laevis* was closely related to *C.* sp. and have more similar genetic population structure to *C. castaneus* than to the Saitama population of *C. laevis*. We could not find any difference in their sensory canals on their heads between individuals from Saitama and Akita of *C. laevis* although morphological differences between local populations of *C. laevis* were observed (Iwata, personal communication). In Lake Shinji, *C. castaneus* and *C.* sp. are sympatrically distributed and no hybrid individual was observed in this study. Because hybrid individuals should be easily detected, if they are, since different *α-Gpd* alleles were fixed in each species. This shows that there is no gene exchange between *C.castaneus* and *C.* sp. in Lake Shinji, which confirmed that *C. castaneus* and *C.* sp. are different species. This also suggests that *C. castaneus* and the Akita population of *C. laevis* are different species because the genetic distance between them was larger than that between *C. castaneus* and *C.* sp. And it is possible that the Akita population of *C. laevis* is different species of the Saitama population of *C. laevis* since the Saitama population situated on a different cluster from *C. castaneus, C.* sp. and *C. laevis* from Akita (Fig. 3). This is supported by the fact that Akita population was different from Saitama population in variants of *α-Gpd* and *Pgm* loci.

The genetic distance between *C.* sp. and the Akita population of *C. laevis* is 0.114. It is difficult to decide from this value whether *C.* sp. and the Akita population of *C. laevis* are different species or not. There are species whose genetic identity (I) between closely related species are about 0.9 [36] that corresponds to 0.105 of Nei's genetic distance. Furthermore *C.* sp. is different from *C. laevis* from Akita in patterns of sensory canals and pit organs on its head. These facts suggests the possibility that *C.* sp. and the Akita population of *C. laevis* are incipient species or subspecies.

The genetic distance between populations of *C. urotaenia* and *C. isaza*, sympatric species in Lake Biwa, was from 0.092 to 0.120. This is comparable to the genetic distance between *C.* sp. and the Akita population of *C. laevis* from 0.113 to 0.115. The studies on reproductive isolating mechanisms and/or ecological studies on these two species

TABLE 3. Allele frequencies at 14 loci in

Locus	Allele	*C. castaneus*						*C.* sp.			*C. laevis*		*C. heptacanthus*
		1	2	3	4	5	6	7	8	9	10	11	12
Aat	*a*	1.00	1.00	1.00	1.00	1.00	1.00	1.00	1.00	1.00	1.00	1.00	—
	b	—	—	—	—	—	—	—	—	—	—	—	1.00
	c	—	—	—	—	—	—	—	—	—	—	—	—
	d	—	—	—	—	—	—	—	—	—	—	—	—
Ck	*a*	1.00	1.00	1.00	1.00	1.00	1.00	1.00	1.00	1.00	1.00	1.00	1.00
	b	—	—	—	—	—	—	—	—	—	—	—	—
Gpi-1	*a*	—	—	—	—	—	—	.03	—	—	—	—	—
	b	1.00	1.00	1.00	1.00	1.00	1.00	.97	1.00	1.00	1.00	1.00	1.00
Gpi-2	*a*	—	—	—	—	—	—	—	—	—	—	—	.09
	b	.01	—	—	—	—	—	—	—	—	.93	—	.85
	c	.98	1.00	.97	1.00	1.00	1.00	.97	1.00	1.00	.07	1.00	.06
	d	—	—	—	—	—	—	—	—	—	—	—	—
	e	.01	—	.03	—	—	—	.03	—	—	—	—	—
	f	—	—	—	—	—	—	—	—	—	—	—	—
α -Gpd	*a*	—	—	—	—	—	—	—	—	—	—	—	—
	b	.01	.03	—	—	—	—	—	—	—	—	—	1.00
	c	—	—	—	—	—	—	—	—	—	—	—	—
	d	—	—	—	—	—	—	—	—	—	—	1.00	—
	e	.99	.97	1.00	1.00	1.00	1.00	—	—	—	—	—	—
	f	—	—	—	—	—	—	1.00	1.00	1.00	1.00	—	—
Idh-1	*a*	—	—	—	—	—	—	—	—	—	.03	—	—
	b	.16	.08	.08	—	.20	—	1.00	1.00	1.00	.88	1.00	1.00
	c	—	—	—	—	—	—	—	—	—	—	—	—
	d	.84	.92	.92	1.00	.80	1.00	—	—	—	.09	—	—
Idh-2	*a*	—	—	—	—	—	—	.03	.05	—	—	—	—
	b	1.00	1.00	1.00	1.00	1.00	1.00	.94	.95	1.00	1.00	1.00	—
	c	—	—	—	—	—	—	.03	—	—	—	—	—
Ldh	*a*	1.00	1.00	1.00	1.00	1.00	1.00	1.00	1.00	1.00	.99	1.00	1.00
	b	—	—	—	—	—	—	—	—	—	.01	—	—
Mdh	*a*	—	—	.03	—	—	—	.18	.29	.22	.01	—	—
	b	—	—	—	—	—	—	—	—	—	—	—	—
	c	—	—	—	—	—	—	—	—	—	—	—	—
	d	—	—	—	—	—	—	—	—	—	—	—	—
	e	.44	.45	.30	.36	.30	.50	.82	.71	.78	.10	—	—
	f	.56	.55	.67	.64	.70	.50	—	—	—	.89	1.00	1.00
Me-1	*a*	—	—	—	—	—	—	—	—	—	—	—	—
	b	1.00	1.00	1.00	1.00	1.00	1.00	1.00	1.00	1.00	1.00	1.00	1.00
Me-2	*a*	1.00	1.00	1.00	1.00	1.00	1.00	1.00	1.00	1.00	1.00	1.00	1.00
	b	—	—	—	—	—	—	—	—	—	—	—	—
Pgm	*a*	.01	—	—	—	.10	—	—	—	—	—	—	—
	b	—	—	—	—	—	—	—	—	—	—	.28	—
	c	.05	.05	—	—	—	—	—	.02	—	—	.72	—
	d	—	—	—	—	—	—	—	—	—	—	—	.03
	e	.94	.95	1.00	1.00	.90	.83	1.00	.98	1.00	.81	—	—
	f	—	—	—	—	—	—	—	—	—	—	—	.97
	g	—	—	—	—	—	.17	—	—	—	.19	—	—
Sod	*a*	—	—	—	—	—	—	—	—	—	—	—	—
	b	—	—	—	—	—	—	—	—	—	—	—	—
	c	—	—	—	—	—	—	—	—	—	—	—	—
	d	1.00	1.00	1.00	1.00	1.00	1.00	1.00	1.00	1.00	1.00	1.00	1.00
Sp-1	*a*	—	—	—	—	—	—	—	—	—	—	—	—
	b	1.00	1.00	1.00	1.00	1.00	1.00	1.00	1.00	1.00	1.00	1.00	1.00

population of *Caenngobius species*

C. urotaenia				*C.* sp. 1	*C.* sp. 2					C. isaza
13	14	15	16	17	18	19	20	21	22	23
—	—	—	—	—	—	—	—	—	—	—
—	—	—	—	—	—	—	—	—	—	—
—	—	—	—	1.00	—	—	—	—	—	—
1.00	1.00	1.00	1.00	—	1.00	1.00	1.00	1.00	1.00	1.00
—	—	—	—	—	—	—	—	—	—	—
1.00	1.00	1.00	1.00	1.00	1.00	1.00	1.00	1.00	1.00	1.00
—	—	—	—	.03	—	—	—	—	—	—
1.00	1.00	1.00	1.00	.97	1.00	1.00	1.00	1.00	1.00	1.00
—	—	—	—	—	—	—	—	—	—	—
—	—	—	—	—	—	—	—	—	—	—
—	—	—	—	—	—	—	—	—	—	—
1.00	1.00	1.00	1.00	.97	.92	.89	.87	1.00	.90	.44
—	—	—	—	—	—	—	—	—	—	—
—	—	—	—	.03	.08	.11	.13	—	.10	.56
—	.13	—	.17	—	1.00	1.00	1.00	1.00	1.00	—
1.00	.87	1.00	.83	1.00	—	—	—	—	—	—
—	—	—	—	—	—	—	—	—	—	1.00
—	—	—	—	—	—	—	—	—	—	—
—	—	—	—	—	—	—	—	—	—	—
—	—	—	—	—	—	—	—	—	—	—
—	—	—	—	—	—	—	—	—	—	—
—	—	—	—	—	—	—	—	—	—	—
1.00	1.00	1.00	1.00	1.00	1.00	1.00	1.00	1.00	1.00	1.00
—	—	—	—	—	—	—	—	—	—	—
1.00	1.00	1.00	1.00	—	1.00	1.00	1.00	1.00	1.00	1.00
—	—	—	—	1.00	—	—	—	—	—	—
—	—	—	—	—	—	—	—	—	—	—
1.00	1.00	1.00	1.00	1.00	1.00	1.00	1.00	1.00	1.00	1.00
—	—	—	—	—	—	—	—	—	—	—
—	—	—	—	—	—	—	—	—	—	—
—	—	—	—	—	1.00	1.00	1.00	1.00	1.00	—
1.00	1.00	1.00	1.00	1.00	—	—	—	—	—	1.00
—	—	—	—	—	—	—	—	—	—	—
—	—	—	—	—	—	—	—	—	—	—
—	—	—	—	—	—	—	—	—	—	—
1.00	1.00	1.00	1.00	1.00	1.00	1.00	1.00	1.00	1.00	1.00
—	—	—	—	—	—	—	—	—	—	—
—	—	—	—	—	—	—	—	—	—	—
1.00	1.00	1.00	1.00	1.00	1.00	1.00	1.00	1.00	1.00	1.00
—	—	—	—	—	—	—	—	—	—	—
.13	.00	.50	.33	—	—	—	—	—	—	—
.87	1.00	.50	.67	.97	1.00	1.00	1.00	.95	1.00	.98
—	—	—	—	—	—	—	—	—	—	—
—	—	—	—	.03	—	—	—	.05	—	—
—	—	—	—	—	—	—	—	—	—	—
—	—	—	—	—	—	—	—	—	—	.02
—	—	—	—	—	—	—	—	—	—	.27
1.00	1.00	1.00	1.00	1.00	—	—	—	—	—	.73
—	—	—	—	—	1.00	1.00	1.00	1.00	1.00	—
—	—	—	—	—	—	—	—	—	—	—
1.00	1.00	1.00	1.00	1.00	1.00	1.00	1.00	1.00	1.00	1.00
—	—	—	—	—	—	—	—	—	—	—

Table 4. Mean (Min.-Max.) genetic distance

Species	1. *C. castaneus*	2. *C.* sp.	3. *C. laevis*, 10*	4. *C. laevis*, 11**	5. *C. heptacanthus*	6. *C. urotaenia*
1.	0.003 (0.000–0.007)	0.160 (0.145–0.175)	0.204 (0.187–0.221)	0.210 (0.186–0.226)	0.502 (0.473–0.523)	1.565 (1.541–1.587)
2.		0.001 (0.000–0.001)	0.114 (0.113–0.115)	0.198 (0.194–0.201)	0.478 (0.474–0.482)	1.573 (1.546–1.591)
3.			—	0.194 —	0.311 —	1.568 (1.558–1.575)
4.				—	0.375 —	1.395 (1.372–1.425)
5.					—	1.315 (1.294–1.335)
6.						0.008 (0.002–0.018)
7.						

*; Lake Hatirou-gata. **; Koma River.

Table 5. Estimates of genetic variability in genus *Chaenogobius*

Species	Population No.	No. of alleles per locus	% polymorpic loci	Average heterozygosity (expected)
C. castaneus	1	1.467	26.7	0.061
	2	1.267	20.0	0.052
	3	1.267	13.3	0.043
	4	1.067	6.7	0.031
	5	1.200	20.0	0.061
	6	1.133	13.3	0.052
	Mean	1.234	16.7	0.050
C. sp.	7	1.133	13.3	0.033
	8	1.200	6.7	0.036
	9	1.067	6.7	0.023
	Mean	1.200	8.9	0.031
C. laevis	10	1.467	26.7	0.058
	11	1.067	6.7	0.027
C. heptacanthus	12	1.200	6.7	0.022
C. urotaenia	13	1.067	6.7	0.015
	14	1.067	6.7	0.015
	15	1.067	6.7	0.033
	16	1.133	13.3	0.048
	Mean	1.084	8.4	0.028
C. sp.1	17	1.200	0.0	0.010
C. sp.2	18	1.067	6.7	0.009
	19	1.067	6.7	0.013
	20	1.067	6.7	0.015
	21	1.067	6.7	0.006
	22	1.067	6.7	0.012
	Mean	1.067	6.7	0.011
C. isaza	23	1.200	13.3	0.062
Overall mean		1.157	10.7	0.032

between *Chaenogobius* species

7. *C.* sp. 1	8. *C.* sp. 2	9. *C. isaza*
1.286 (1.272–1.301)	1.570 (1.545–1.589)	1.529 (1.531–1.562)
1.310 (1.305–1.319)	1.577 (1.549–1.593)	1.554 (1.535–1.566)
1.290 —	1.574 (1.566–1.577)	1.549 —
1.146 —	1.376 (1.372–1.386)	1.352 —
1.301 (1.296–1.306)	1.593 (1.591–1.595)	1.567 —
0.237 (0.227–0.249)	0.225 (0.206–0.252)	0.103 (0.092–0.120)
—	0.414 (0.401–0.412)	0.358 —
8.	0.000 (0.000–0.001)	0.235 (0.232–0.242)
	9.	—

should supply significant information to establish the taxonomic relationship between them.

Three species of *C. urotaenia, C.* sp.1 and *C.* sp. 2 were confirmed that they were different species each other. Genetic distances between them ranged from 0.225 to 0.412 on average. These values are large, indicating that they are different species. *C. urotaenia* and *C.* sp. 2, distributing sympatrically at the four rivers in the Shimane Prefecture, had different alleles at the *Sod* locus and at the *Mdh* locus from each other and no heterozygote at these loci was observed through this study. Ecological study also showed that they are ethologically isolated [10].

This study revealed phylogenetic position of *C. isaza* which is specialized to land-locked freshwater and endemic to Lake Biwa. It was closely related to *C. urotaenia*, amphidromous species as previously suggested [11]. We used the estimation of divergence time from genetic distance proposed by Nei [18], $t=5\times10^6D$. It suggested that *C. isaza* was differentiated from *C. urotaenia* about 0.5 million years ago. This time agrees with the origin of other endemic species in Lake Biwa, which was suggested by fossil records [25, 26]

Isozyme polymorphisms supplied the information on population system in some species. The comparison between populations within three amphidromous species, *C. castaneus, C. urotaenia* and *C.* sp. 2, showed that the differentiation of populations did not reflect the geographic distance between populations from different rivers (data was not shown). This suggests that genetic mixture between populations occurs when larvae go down to the sea and they have no behavioral character to return to the river where they were born. This study indicates the effectiveness of application of isozyme polymorphism to ecological study of *Chaenogobius* species that have various life histories.

ACKNOWLEDGMENTS

We thank Dr. Akira Goto, Hokkaido University, Mr. Kazuharu Shibuya, Akita Prefectural Fisheries Consulting Center, Mr. Akihisa Iwata, Imperial Household, Mr. Makoto Itoh, Tokyo Metropolitan Bureau of Labor and Economy, Mr. Isao Kimoto, Tokyo Metropolitan Fisheries Experimental Station, Dr. Sachiko Takahashi and Mr. Shoichi Matsuoka, Shiga Prefecture, Mr. Takatoshi Kawashima, Shimane Prefectural Fisheries Experimental Station, Mr. Kouichi. Itoh, Mr. Mikio Kadowaki, Mr. Kazuo Fukuda, and Mr. Tomitada Nagashima, Shimane Prefecture for supplying materials. We also thank Dr. Ryozo Kakizawa, Yamashina Institute for Ornithology, and Mr. Ikuo Takabatake, Shimane University, for technical support and Dr. Nobuhiko Mizuno, Ehime University, Dr. Iwao Sakamoto, Shimane Medical Collage, Mr. Toshiki Koshikawa, Akae Junior School, Mr. Akihisa Iwata and Masayoshi Hayashi, Yokosuka City Museum for useful suggestion to complete this study. We thank especially Mr. Takatoshi Kawashima and Mr. Hitoshi Sato, Shimane Prefectural Office for useful discussion and encouragement through this study. We thank Dr. K. M. Yin, Kent State University for his critical reading this manuscript.

REFERENCES

1 Akihito, Prince (1984) Genus *Chaenogobius*. In "The Fishes of the Japanese Archipelago". Ed by H Masuda, H K Amaoka,K C Araga, T Ueno, T Yoshino, Tokai University Press, Tokyo, pp 264–266 (in Japanese)

2 Avise J C (1974) Systematic value of electrophoretic data. Syst Zool 23: 465–481

3 Avise J C (1976) Genetic differentiation during speciation. In "Molecular Evolution Vol. 7" Ed, by F J Ayala, Sinauer. Sunderland, Mass; pp 106–122

4 Ayala F J (1975) Genetic differentiation during the speciation process. Evol Biol 8: 1–78

5 Ayala F J, Tracy M L, Hedgecock D, Richmond R C (1974) Genetic differentiation during the speciation process in *Drosophila*. Evolution 28: 576–592

6 Buth D G (1984) The application of electrophoretic data in systematic studies. Ann Rev Ecol Syst 15: 501–522

7 Dotu Y (1955) The life history of a Goby, *Chaenogobius urotaenia* (Hilgendorf).Sci Bull Fac Agr Kyushu Univ 15: 367–374

8 Clayton J W, Tretiak D N (1972) Amine-citrate buffers for pH control in starch gel electrophoresis. J Fish Res Bd Canada 29: 1169–1172

9 Hayashi M, Sato H (1987) One species of genus Chaenogobius from Shinji Lake, Shimane prefecture. Proc Ann Meet Japan Ichthyol Soc 48 (abstract in Japanese)

10 Ishino K (1987) Freshwater fishes in Japan, their distribution, variation and speciation. Ed by M, Mizuno, A Goto, A Tokai Univ Press, pp 189–197 (in Japanese)

11 Kawanabe H (1978) Some biological problems. Verh Internal Verein Limmol 20: 2674–2677

12 Koshikawa T (1989) Shinjikohaze, *Chaenogobius* sp. In "Freshwater Fishes of Japan" Ed by H, Kawanabe, N Mizuno, Yama-Kei Publishers Co., Ltd., pp 614–615 (in Japanese)

13 Koshikawa T, Sato H (1986) Synopsis of new recorded goby, *Chaenogobius* sp. of Lake Shinji.The Freshwater Fishes, 12: 51–55 (in Japanese)

14 Masuda Y, Ozawa T, Enami S (1989) Genetic differentiation among eight color types of the fresh water goby, *Rhinogobius brunneus*, from Western Japan. Japan J Ichthyol 36: 30–41

15 Nakanishi T (1978) Comparison of color pattern and meristic

characters among the three types of *Chaenogobius annularis* Gill. Bull Fac Fish Hokkaido Univ 29: 223–232

16 Nei M (1972) Genetic distance between populations. Am Nat 106: 283–292

17 Nei M (1975) Molecular Population Genetics and Evolution. North-Holland Pub.Co., Amsterdam

18 Nei M (1987) Molecular Evolutionary Genetics. Columbia University Press, New York

19 Nevo E, Beliles A, Ben-Shlmo R (1984) The evolutionary significance of genetic diversity: Ecological, demographic and life history correlates. In "Evolutionary Dynamics of Genetic Diversity" Ed by G S Mani, Springer-Verlag, pp 13–213

20 Numachi K (1981) A simple method for preservation and scanning of starch gels. Biochem Genet 19: 233–236

21 Numachi K, Nagahora S, Iwata M (1979) Genetic demonstration of hybrids between chum and pink salmon in the northwest Pacific. Rep Otsuchi Mar Res Cent Univ Tokyo 5: 87–102

22 Pasteur N, Pasteur G, Bonhomme F, Catalau J, Britton-Davidian J (1988) Practical Isozyme Genetics. Ellis Horwood limited, England

23 Pinchuk V I (1978) Notes and supplements to the Family Gobiidae in the book by Lindberg and Krasyukova "Fish of the Sea of Japan and the neighboring part of the Sea Ohotsk and the Yellow Sea", Part 4, 1975 with a description of new species *Chaenogobius taranetzi*. J Ichtyol 18: 1–14

24 Powell J R (1975) Protein variation in natural populations of animals. Evol Biol 8: 79–119

25 Research Group of Natural History of Lake Biwa (1983) Fossil assemblages from the Pleistocene Katata formation of the Kobiwako group at Ogi-cho, Otsu City, Central Japan. Bull Mizunami Fossil Museum 10: 117–142

26 Research Group for Natural History of Lake Biwa (1986) Freshwater fossil assemblage from the Pleistocene Kobiwako group on the southwest side of Lake Biwa Bull. Mizunami Fossil Museum 13: 57–103

27 Richardson B J, Baverstock P R, Adams M (1986) Allozyme Electrophoresis. Academic Press, Australia

28 Selander R K, Smith M H, Yang S, Johnson W E, Gentry J B (1971) Biochemical polymorphism and systematics in the genus *Peromyscus*. I. Variation in the old-field mouse (*Peromyscus polionotus*). Stud Genet 6 Univ Texas Publ 7103; 49–90

29 Shaw C R, Prasad R (1970) Starch gel electrophoresis of enzymes-A compilation of recipes. Biochem Genet 4: 297–320

30 Sneath P H A, Sokal R R (1973) Numerical Taxonomy. Freeman, San Francisco, pp 188–308

31 Takagi K (1952) A critical note on classification of *Chaenogobius urotaenia* and its two allies. Japan J Ichthyol 2: 14–22

32 Takagi K (1966a) Taxonomic and nomenclatural status in chaos of the Gobiid fish, *Chaenogobius annularis* Gill I. Review of the original description, with special reference to estimation of the upper jaw relative length as a taxonomic character. J Tokyo Univ Fish 52: 17–27

33 Takagi K (1966b) Taxonomic and nomenclatural status in chaos of the Gobiid fish, *Chaenogobius annularis* Gill Tomiyama with description of the genus *Rhodoniichtys*, Gen Nov J Tokyo Univ Fish 52: 29–45

34 Takagi K (1967) Topologie du systeme sensoriel cephalique des Gobioidei. La Mer 5: 131–145

35 Thorpe J P (1982) The molecular clock hypothesis: Biochemical evolution, genetic differentiation and systematics. Ann Rev Ecol Syst 13: 139–168

36 Thorpe J P (1983) Enzyme variation, genetic distance and evolutionary divergence in relation to levels of taxonomic separation. In "Protein Polymorphism, Adaptive and Taxonomic Significance" Ed by G S Oxford, D Rollinson, Academic Press, London and New York, pp 131–152

ZOOLOGICAL SCIENCE 11: 465–471 (1994)

Speciation of Japanese Pond Frogs Deduced from Lampbrush Chromosomes of their Diploid and Triploid Hybrids

HIROMI OHTANI

Laboratory for Amphibian Biology, Faculty of Science, Hiroshima University, Higashi-hiroshima 724, Japan

ABSTRACT—To examine the hybrid origin hypothesis of *Rana porosa porosa* cytogenetically, the lampbrush chromosomes of triparental allotriploids comprising the genomes of *R. nigromaculata, R. p. brevipoda,* and *R. p. porosa* were investigated together with those of their intra- and interspecific hybrids. The behavior of their homologous lampbrush chromosomes provided little evidence that chromosomal material from *R. nigromaculata* is present in the genomic chromosomes of *R. p. porosa*. On the contrary, it is suggested that *R. p. porosa* and *R. nigromaculata* are phylogenetically more distant than are *R. p. brevipoda* and *R. nigromaculata*.

INTRODUCTION

With respect to the differentiation of *Rana porosa porosa* Cope, Moriya [13] and Kawamura and Nishioka [4–6] proposed the hypothesis of hybrid origin between *R. nigromaculata* Hallowell and *R. p. brevipoda* Ito. This hypothesis was supported by Kuramoto [7], but questioned by Matsui and Hikida [12]. Recently, Nishioka *et al.* [17] offered support for the hypothesis from electrophoretic analysis, though the support was not without a tinge of interested consideration. Although I was a collaborator of the latter paper, I now question the hybrid origin hypothesis in view of the fact that the lampbrush chromosomes of *R. p. porosa* closely resemble those of *R. p. brevipoda*, and yet there are no landmarks derived from *R. nigromaculata* throughout their axes (unpublished).

The hybrid origin should be demonstrated by comparing the behavior of lampbrush chromosomes in diploid hybrids between the above-mentioned three taxa, because the number of chiasmata that control the behavior of lampbrush chromosomes changes in accordance with the extent of similarity between the homologues of parental species [9, 14, 20]. Similarly, when the genomic chromosomes of these three taxa are placed together in an oocyte, provided that *R. p. porosa* receives many dominant and recessive genes from *R. nigromaculata* as suggested by Kawamura and Nishioka [4], some of the chromosomes of *R. p. porosa* should join inevitably to those of *R. nigromaculata* and act as a mediator in formation of trivalents.

The lampbrush chromosomes of *R. nigromaculata* are easily distinguished from those of *R. p. brevipoda* [16] and *R. p. porosa* (unpublished) by size, type, and position of the landmarks. Thus, the lampbrush chromosomes of triparental allotriploid females were examined to cytogenetically determine the relative degree of synaptic affinity among the chromosomes of these taxa together with those of their intra- and interspecific hybrid females. This paper describes these results and a new hypothesis of the differentiation of *R. p. porosa* is proposed.

Accepted May 16, 1994
Received Feburary 7, 1994

MATERIALS AND METHODS

The female frogs studied are described in Table 1. The parental frogs for crosses were from the lineages of *R. p. brevipoda* collected from Konko, Okayama Prefecture, *R. p. porosa* from Machida, a city of Tokyo, and *R. nigromaculata* from Hiroshima. The frogs were crossed by artificial fertilization. Autotriploid frogs were produced by cooling the fertilized eggs of *R. p. brevipoda* to $\fallingdotseq 1^{\circ}C$ for 2 hrs. Two kinds of allotriploid frogs were produced by inseminating a few diploid ova which *brevipoda* ♀ × *nigromaculata* ♂ hybrid females spawned with spermatozoa of the two subspecies. Tadpoles were fed on boiled spinach or chard, and frogs were fed on houseflies or tropical crickets.

Lampbrush chromosomes were removed from the ovarian eggs of two-year-old females just prior to hibernation (November) according to Gall's method with a slight modification [1, 20], and examined under a phase-contrast microscope. The abbreviations B, P, and N refer to *brevipoda, porosa*, and *nigromaculata* chromosomal sets, respectively. The letters in parentheses indicate the sources of cytoplasm. Chiasma frequencies per oocyte were compared using Student's or Aspin-Welch's *t*-test. Chi-square test also was used for the comparison of chiasma numbers in two kinds of allotriploids.

RESULTS

Autotriploid (B)BBB

Lampbrush chromosomes from 60 oocytes were analyzed in detail. All the oocytes contained 39 lampbrush chromosomes consisting of 13 triplets of homologues that belonged to five large chromosomes numbered 1 to 5 and eight small chromosomes numbered 6 to 13. These lampbrush chromosomes formed eight or more trivalents in all the oocytes; it was notable that those of six oocytes formed exclusively 13 trivalents (Table 2). All the chromosomes other than those

TABLE 1. Kind, origin, and number of female frogs used in the present study

Kind	Parental Origin		Number of females
	Female	Male	
Autotriploid (B)BBB (3n=39)	*R. p. brevipoda*	*R. p. brevipoda*	5
Allotriploid (B)BBN (3n=39)	*brevipoda* ♀ × *nigromaculata* ♂	*R. b. brevipoda*	5
Allotriploid (B)BPN (3n=39)	*brevipoda* ♀ × *nigromaculata* ♂	*R. b. porosa*	4
Diploid hybrid (P)PB (2n=26)	*R. p. porosa*	*R. p. brevipoda*	9
Diploid hybrid (P)PN (2n=26)	*R. p. porosa*	*R. nigromaculata*	9
Diploid hybrid (N)NP (2n=26)	*R. nigromaculata*	*R. p. porosa*	8
Non-hybrid (P)PP (2n=26)	*R. p. porosa*	*R. p. porosa*	11

TABLE 2. Number of oocytes having tri-, bi- and univalents in various combinations in the three kinds of triploids

No. of trivalents	No. of bivalents	No. of univalents	Kind (B)BBB	(B)BBN	(B)BPN
13 (39)	0	0	6		
12 (36)	1 (2)	1 (1)	16		
11 (33)	2 (4)	2 (2)	17		
10 (30)	3 (6)	3 (3)	13		
9 (27)	4 (8)	4 (4)	4		
8 (24)	5 (10)	5 (5)	4		
7 (21)	6 (12)	6 (6)			1
6 (18)	7 (14)	7 (7)			1
5 (15)	8 (16)	8 (8)		1	
4 (12)	9 (18)	9 (9)			2
3 (9)	10 (20)	10 (10)		8	2
2 (6)	11 (22)	11 (11)		12	1
1 (3)	12 (24)	12 (12)		12	4
0	13 (26)	13 (13)		11	6
0	0	39 (39)		2	8
	Total		60	46	25

Numbers in parentheses show numbers of lampbrush chromosomes forming tri-, bi-, or univalents.

of the trivalents formed bivalents and univalents of the same number.

The number of trivalents in chromosome Nos. 1 to 13 is presented in Table 3. Of the 655 trivalents, 189 joined three homologues in juxtaposition by four to 12 chiasmata and rarely by terminal fusions (Fig. 1A). In 359 other trivalents, two of the three homologues were joined by two to eight chiasmata and the rest was joined to one of them by one to three chiasmata, a terminal fusion, or both, in addition (Fig. 1B). In the remaining 107 trivalents, the three homologues were joined in tandem by one or two chiasmata or a terminal fusion (Fig. 1C).

In chromosome Nos. 1, 4, 6–9 and 12, the chiasma frequencies were about 1.5 times higher than those of diploid *R. p. brevipoda* (Table 4). Those of the remainder were slightly lower than 1.5 times. The number of chiasmata in each oocyte was between 35 and 76 (average, 55.0) in total.

Allotriploid (B)BBN

Lampbrush chromosomes from 57 oocytes were analyzed. Eleven of these oocytes, an aneuploid one (3n-2) lacking the *nigromaculata* chromosomes of Nos. 2 and 8, and 10 hexaploid ones, were omitted from the analysis. The remaining 46 oocytes contained 39 lampbrush chromosomes consisting of one *nigromaculata* and two *brevipoda* chromosomes in each of the 13 homologue triplets (Fig. 2). These chromosomes formed one to five trivalents in 33 oocytes (Table 2). The remaining 13 oocytes had no trivalents. All the chromosomes other than those of the trivalents formed bivalents and univalents of the same number, or simply univalents; two oocytes contained only 39 univalents.

In 64 of the 65 trivalents, a *nigromaculata* chromosome was always joined to one of the two *brevipoda* chromosomes by one or two chiasmata, a terminal fusion, or both, in addition (Table 3). The remaining one trivalent was seen in chromosome No. 6 and arranged three homologues of, in order, *brevipoda, nigromaculata* and *brevipoda*, which were each joined by one chiasma in tandem. On the other hand, in 507 triplets of homologues forming a bivalent and a univalent, the bivalent always consisted of two *brevipoda* chromosomes, and the univalent of a *nigromaculata* chromosome. In the remaining 26 triplets of homologues, they

TABLE 3. Behavior of homologous lampbrush chromosomes in each of the 13 triplets in the three kinds of triploids

Kinds	Chromosome behavior in a triplet	Chromosome no. 1	2	3	4	5	6	7	8	9	10	11	12	13	Total
(B)BBB	b-b-b	54	57	58	55	53	46	52	48	46	47	44	44	51	655
	b-b, b	6	3	2	5	7	14	8	12	14	13	16	16	9	125
	Total	60	60	60	60	60	60	60	60	60	60	60	60	60	780
(B)BBN	b-b-n	6	6	4	4	3	11	2	3	6	3	6	7	3	64
	b-n-b						1								1
	b-b, n	38	38	40	40	41	32	42	41	38	41	38	37	41	507
	b, b, n	2	2	2	2	2	2	2	2	2	2	2	2	2	26
	Total	46	46	46	46	46	46	46	46	46	46	46	46	46	598
(B)BPN	b-p-n or p-b-n	3	4	3	4		2	2	4	1	2	1	3	2	31
	b-n-p											1	1		2
	b-p, n	14	12	14	13	17	14	14	12	16	15	15	13	14	183
	b-n,p or p-n,b		1				1	1*	1					1*	5
	b, p, n	8	8	8	8	8	8	8	8	8	8	8	8	8	104
	Total	25	25	25	25	25	25	25	25	25	25	25	25	25	325

The abbreviations b, p, and n indicate *brevipoda, porosa,* and *nigromaculata* lampbrush chromosomes, respectively.
"-" indicates a connection between two homologues.
* Joining was effected between *brevipoda* and *nigromaculata* chromosomes.

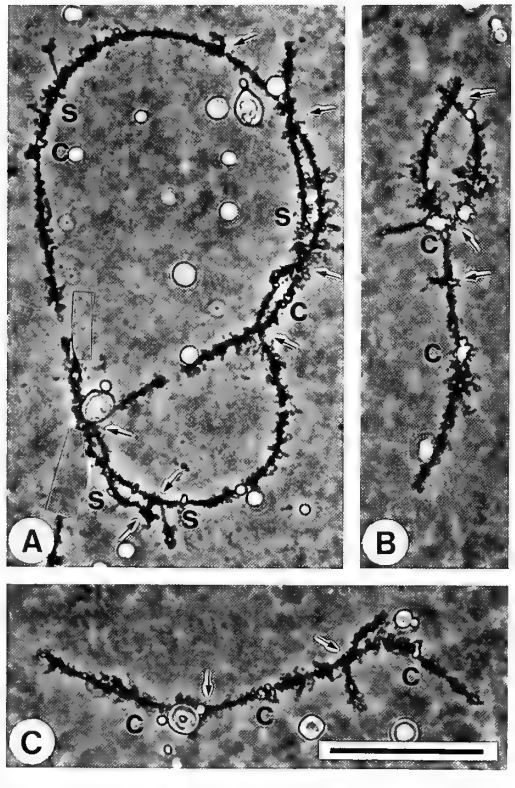

FIG. 1. Microphotographs of trivalents of chromosome Nos. 3 (A) and 10 (B and C) in an autotriploid, (B)BBB. Arrows indicate the positions of chiasmata. c and s represent compound- and simple-type giant loops, respectively. Bar=50 μm.

remained as univalents.

In all the trivalents, *nigromaculata* and *brevipoda* chromosomes were joined by 57 (3%) chiasmata in total except for the terminal fusions. By contrast, joining of two *brevipoda* chromosomes in the bivalents and trivalents was by 2033 (97%) chiasmata in total except for the terminal fusions.

The chiasma frequencies in chromosome Nos. 1 to 13 were about 1.2 times higher than those of diploid *R. p. brevipoda* except in chromosome Nos. 11 and 13, though the chiasmata for *nigromaculata* and *brevipoda* chromosomes accounted for no more than 3% of the total (Table 4). The number of chiasmata in each oocyte was between 0 and 60 (average, 45.4) in total. This average value was different from that of the diploid *R. p. brevipoda* (t=3.7, P<0.001) or the autotriploid (B)BBB (t=4.4, P<0.0001).

Allotriploid (B)BPN

Lampbrush chromosomes from 41 oocytes were analyzed. Sixteen of the 41 oocytes were seven aneuploid oocytes of 3n-1 (three), 3n-2 (two), and 3n-5 (two), and nine hexaploid oocytes; all of which were omitted from the analysis. In the remaining 25 normal triploid oocytes in which each triplet of homologues consisted of one *brevipoda*, one *porosa*, and one *nigromaculata* chromosomes, the lampbrush chromosomes were somewhat similar in behavior to those of the other allotriploid (B)BBN (Table 2). In 11 oocytes they formed one to seven trivalents, while all the chromosomes other than those of the trivalents formed bivalents and univalents of the same number (Fig. 3). In six other oocytes they formed 13 bivalents and 13 univalents. The remaining eight oocytes had only 39 univalents.

Of the 33 trivalents, 31 joined a *nigromaculata* chromosome to either of the *brevipoda* and *porosa* chromosomes by one or two chiasmata, a terminal fusion, or both, in addition (Table 3). The remaining two trivalents arranged three

TABLE 4. Frequency of chiasmata in chromosome Nos. 1 to 13

Type	Chromosome no. 1	2	3	4	5	6	7	8	9	10	11	12	13	Total
(P)PP	5.3	4.2	4.0	4.2	3.7	2.3	2.6	2.2	2.1	2.1	2.0	2.1	2.0	39.0
(B)BB*	4.8	4.7	4.1	4.1	3.6	2.4	2.3	2.3	2.0	2.2	2.1	1.9	2.0	38.7
(N)NN*	5.0	4.5	3.7	4.4	3.6	2.3	2.5	2.3	2.0	2.0	2.0	2.1	2.0	38.6
(B)BBB	7.2	6.4	5.7	6.1	5.1	3.6	3.5	3.3	3.1	2.8	2.7	2.8	2.8	55.0
(B)BBN	6.0	5.9	4.6	4.9	4.3	2.7	2.9	2.7	2.7	2.3	2.1	2.3	2.0	45.4
(B)BPN	5.0	4.3	3.6	4.0	3.7	2.3	2.0	1.8	2.1	1.6	1.9	1.6	1.6	35.7
(P)PB	5.0	3.6	3.2	4.0	3.4	2.5	2.4	2.2	1.6	2.1	1.9	2.1	1.9	35.8
(P)PN	2.6	2.6	1.9	2.5	2.1	1.7	1.7	1.9	1.4	1.9	1.7	1.6	1.6	25.2
(N)NP	2.9	2.8	2.3	2.1	2.1	1.9	1.7	2.0	1.5	2.0	1.6	1.6	1.3	26.0
(B)BN*	3.7	2.3	2.5	3.0	2.4	2.3	1.8	2.0	1.6	1.9	1.8	1.8	1.8	28.9
(N)NB*	3.4	2.3	2.6	3.0	2.7	2.0	1.7	1.9	1.5	1.8	1.6	1.6	1.6	27.6

* Data from [20]

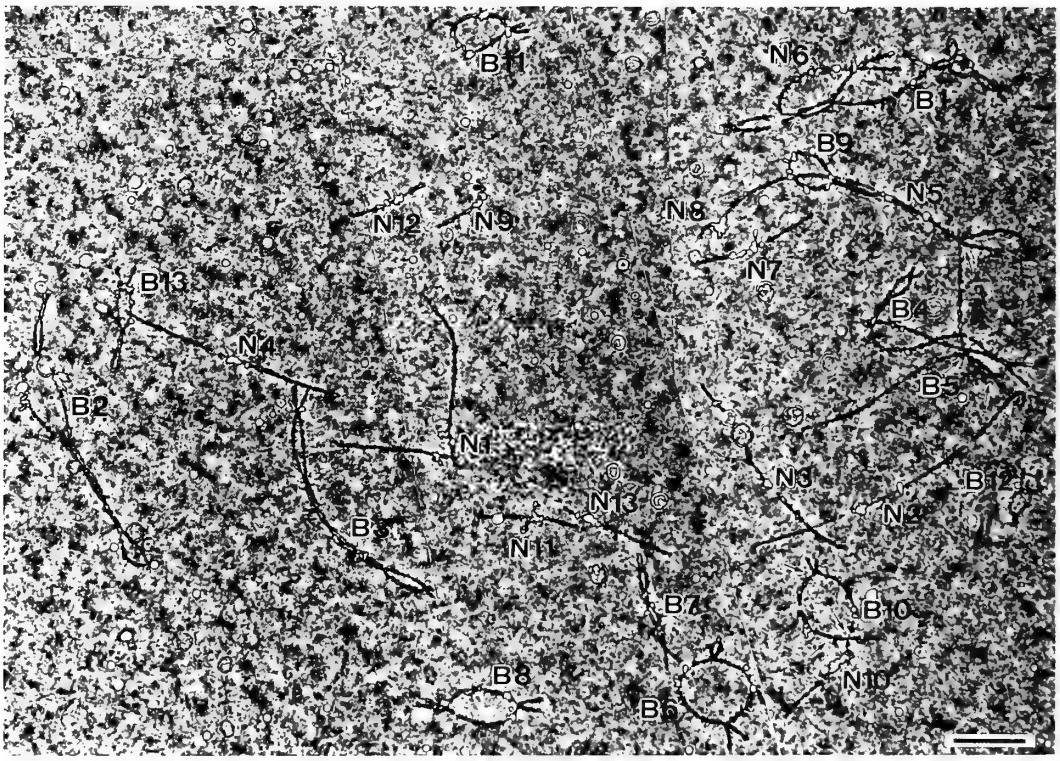

FIG. 2. Microphotographs of the lampbrush chromosomes in an oocyte of an allotriploid, (B)BBN. Number represents the chromosome number. B and N represent *brevipoda* and *nigromaculata* chromosomes, respectively. Two *brevipoda* chromosomes form a bivalent and one *nigromaculata* chromosome forms a univalent in chromosome Nos. 1 to 13 except for 5 and 10. The three homologues of chromosome Nos. 5 and 10 form a trivalent which joins a *nigromaculata* chromosome to one of the two *brevipoda* chromosomes by a single chiasma. Arrows indicate the positions of chiasmata. Bar=50 μm.

homologues of, in order, *brevipoda, nigromaculata* and *porosa*; the three homologues of chromosome No. 11 were each joined by one chiasma in tandem, and those of chromosome No. 12 also were joined by two chiasmata and by a terminal fusion. In 183 of the 188 triplets of homologues forming a bivalent and a univalent, the bivalents consisted of *brevipoda* and *porosa* chromosomes, and the univalents of *nigromaculata* chromosomes. In the remaining five triplets of homologues, bivalents included a *nigromaculata* chromosome.

In the bivalents and trivalents, joining of *nigromaculata* and *brevipoda* or *porosa* chromosomes was effected by 35 (4%) chiasmata in total except for terminal fusions. In contrast, *brevipoda* and *porosa* chromosomes were joined by 857 (96%) chiasmata in total except for the terminal fusions.

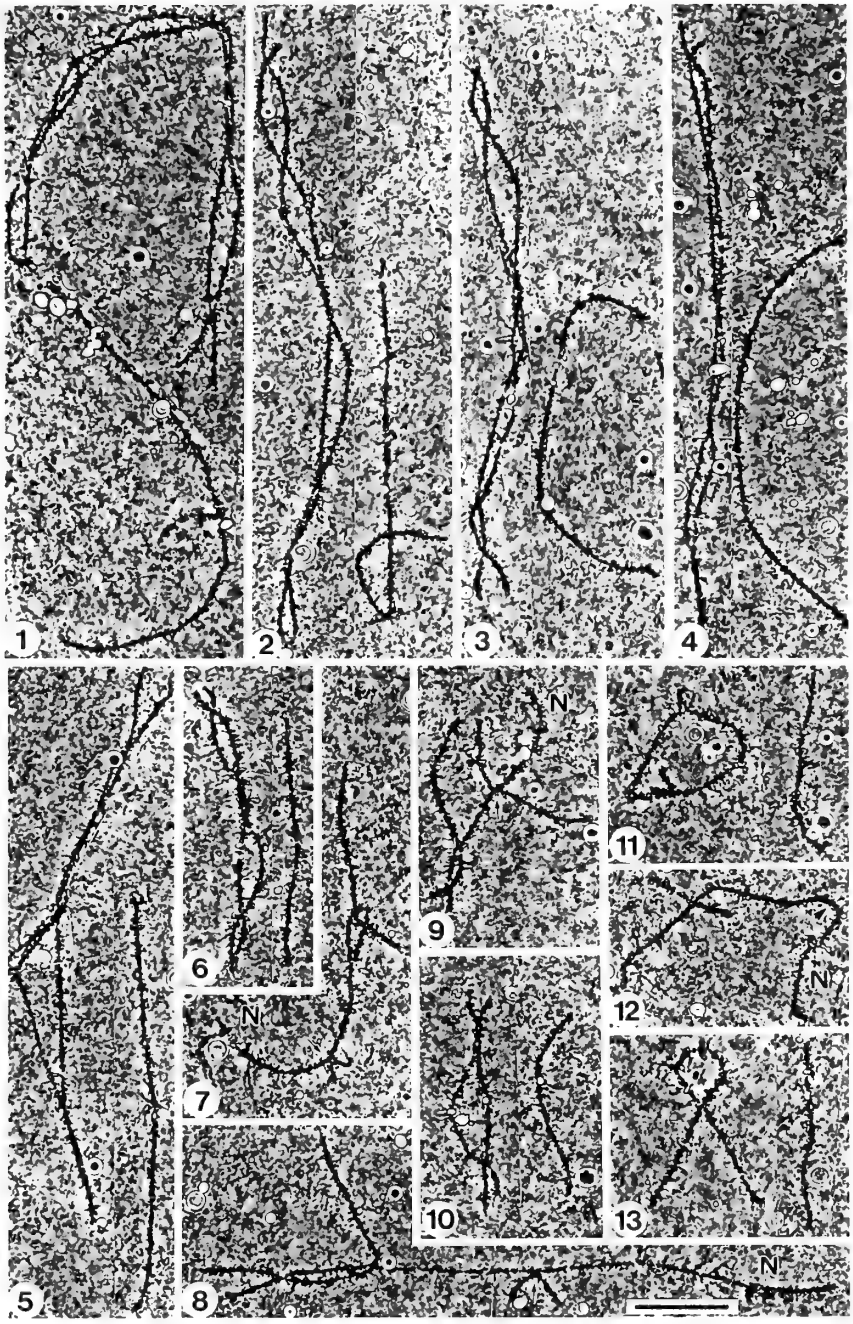

FIG. 3. Microphotographs of the lampbrush chromosomes in an oocyte of a triparental allotriploid, (B)BPN. The number in each photograph represents the chromosome number. The abbreviation N in photographs 7, 8, 9 and 12 represents a *nigromaculata* chromosome. Although landmarks did not develop very much in this preparation, *nigromaculata* chromosomes are infallibly distinguished from those of *brevipoda* and *porosa*. Two *brevipoda* and *porosa* chromosomes form a bivalent and one *nigromaculata* chromosome forms a univalent, in chromosome Nos. 1 to 13 except 7, 8, 9, and 12. The homologues of chromosome Nos. 7, 8, 9, and 12 form a trivalent which joins a *nigromaculata* chromosome by a single chiasma (arrow, in Nos. 7, 8, and 9), and by a terminal fusion (arrow head, in No. 12). Bar=50 μm.

These values were not different from those in the other allotriploid (B)BBN ($\chi^2=3.0$, $P=0.08$).

The chiasma frequencies in chromosome Nos. 1 to 13 were generally much lower than in another allotriploid (B)BBN (Table 4), but the total number of chiasmata in each oocyte (0–67, average=35.7) was not different from that of (B)BBN ($t=1.8$, $P=0.09$).

Intraspecific hybrid (P)PB

In the 30 oocytes examined, all the lampbrush chromosomes formed 13 bivalents like those of parental subspecies *R. p. brevipoda* and *R. p. porosa* (Table 5). The bivalents had one to eight chiasmata. When the chiasma frequency in chromosome Nos. 1 to 13 was compared with those of the two parental subspecies, those of chromosome Nos. 2, 3 and 9

TABLE 5. Number of oocytes having bi- and univalents in various combinations

No. of bivalents	No. of univalents	Kind (P)PP	(B)BB*	(P)PB	(P)PN	(N)NP
13 (26)	0	50	50	30	24	27
12 (24)	2 (2)				5	3
11 (22)	4 (4)				1	
Total		50	50	30	30	30

Numbers in parentheses show numbers of lampbrush chromosomes forming bi- or univalents.
* Data from [20]

were far lower, but those of the remaining chromosomes were similar (Table 4). The number of chiasmata in each oocyte was between 30 and 44 (average, 35.8) in total. This average value was different from that of *R. p. brevipoda* (t=3.3, P=0.001) or *R. p. porosa* (t=3.4, P=0.001).

Interspecific hybrid (P)PN and (N)NP

In 24 and 27 of the respective 30 oocytes examined, all the lampbrush chromosomes formed bivalents of which the homologues were connected by one to six chiasmata, terminal fusions, or both (Table 5). The remaining six and three oocytes had two or four univalents with 12 or 11 bivalents. The chiasma frequency in chromosome Nos. 1 to 13, except for No. 10, was far lower than those of the two parental species, *R. p. porosa* and *R. nigromaculata*, and the *porosa*♀ ×*brevipoda*♂ intraspecific hybrid (Table 4). The total number of chiasmata in each oocyte was between 15 and 32 (average, 25.2) in the *porosa*♀ *nigromaculata*♂ hybrid and between 16 and 33 (average, 26.0) in the reciprocal hybrid. Although the average values did not differ between these reciprocal interspecific hybrids (t=0.8, P=0.45), they were significantly lower than those of the *brevipoda*♀× *nigromaculata*♂ hybrid (t=4.8, P<0.0001) and the *nigromaculata*♀ ×*brevipoda*♂ hybrid (t=3.5, P<0.001).

DISCUSSION

Kawamura and Nishioka [4, 5] suggested that the inception of *R. p. porosa* was natural hybrids between *R. nigromaculata* and *R. p. brevipoda*. They also assumed that the newly divided population received subspecies rank as a result of accumulation of *nigromaculata* genes; such accumulation made it impossible to distinguish *R. p. porosa* from interspecific hybrids between *R. p. brevipoda* and *R. nigromaculata* by external appearance. However, as White [23] stressed, the presence of three related species, A, B, and C, forming a linear series with B as an intermediate form between the other two, does not necessarily imply that B is a species of hybrid origin.

In localized hybrid zones where two populations of closely related species come into contact, there are cases where many hybrid individuals and their descendants are produced [2, 8]. Nevertheless, the fact remains that there is often strong selection against hybrids within the hybrid zone, without the influence of introgression beyond the zone [3, 22]. In *R. p. porosa* also [17], the electrophoretic patterns caused by introgression of *R. nigromaculata* genes were found in some of the *R. p. porosa* collected from two stations where *R. p. porosa* coexists with *R. nigromaculata*, whereas they were not found in any of the *R. p. porosa* collected from eight other stations where *R. p. porosa* exists alone. Nishioka *et al.* [17] did not touch upon the latter case in supporting the hybrid origin hypothesis, though the former case was pointedly emphasized.

Results of the present study offer little support for the hypothesis of hybrid origin of *R. p. porosa*. While the autotriploid (B)BBB formed trivalents in 655 (84%) of the 780 triplets, both the allotriploids (B)BBN and (B)BPN only formed them in 65 (11%) of the 598 triplets and in 33 (10%) of the 325 triplets, respectively. If the chromosomes of *R. p. porosa* had received great numbers of dominant and recessive genes from *R. nigromaculata*, the homologues of the allotriploid (B)BPN should have formed far more trivalents through the intermediation of a *porosa* chromosome. However, those chiasmata for the allospecific chromosomes represented no more than 4% of the total, which was the same as the ratio of the other allotriploid (B)BBN.

The chiasma frequencies per oocyte of the reciprocal interspecific hybrids between *R. p. porosa* and *R. nigromaculata* were 25.2 ((P)PN) and 26.0 ((N)NP), both much lower than those for the two parental species (39.0 and 38.6) and the *porosa*♀ ×*brevipoda*♂ intraspecific hybrid (35.8). Moreover, these values were significantly lower than those of other reciprocal interspecific hybrids between *R. p. brevipoda* and *R. nigromaculata* (28.9 and 27.6). Therefore, *R. p. porosa* and *R. nigromaculata* must be phylogenetically more divergent than are *R. p. brevipoda* and *R. nigromaculata*.

I propose that the incipient population of *R. p. porosa* occurred simply as a result of geographical isolation. Populations of the pond frogs are susceptible to isolation in the area where a range of mountains reaches down to the coastline, since they are typical inhabitants of streams and marshes in the coastal plains. It seems probable that an ancestral distributional range of *R. porosa* which continuously existed along the Pacific coast of Honshu Island was divided into two geographical isolates, one eventually giving rise to *R. p. porosa* and the other to *R. p. brevipoda*, by the disappearance of the habitats in the mountainous Izu-Hakone areas. This isolation might be attributed to the upheaval caused by a collision between the central Honshu region and ancient Izu island (now a peninsula) about 0.5 million years ago [10]. In fact, if Nei's divergence time (1D=5 million years) [15] is available for a small genetic distance value, the divergence time of the two subspecies will be estimated from their genetic distance data (0.130~0.249, average=0.189) [17] at 0.95±0.2 million years (the average was limited using Chebyshev's theorem (k=2)). This divergence time seems

not to be so distant from the assumptive time of the collision. In addition, this upheaval has defended the Kanto plain from the invasion of *R. nigromaculata* [21]. Matsui [11] has reported that Japanese common toad, *Bufo japonicus* Schlegel, is divided into northeastern and southwestern types on the basis of morphometric variation analyses by the central Honshu region as a dividing line. Such geographic division seems to have affected the populations of *Rana japonica* Günther and *Rana rugosa* Temminck & Schlegel also. Their dendrograms based on genetic distance data [18, 19] suggest it, and the divergence times between the Tokai and Kanto populations are 0.50 ± 0.3 million years in *R. japonica* and 0.60 ± 0.2 million years in *R. rugosa*.

REFERENCES

1 Gall JG (1966) Techniques for the study of lampbrush chromosomes. In "Methods in Cell Physiology 2" Ed by DM Prescott, Academic Press, New York, pp 37–60

2 Gartside DF (1980) Analysis of a hybrid zone between chorus frogs of the *Pseudacris nigrita* complex in the southern United States. Copeia 1980: 56–66

3 Gollmann G (1991) Population structure of Australian frogs (*Geocrinia laevis* complex) in a hybrid zone. Copeia 1991: 593–602

4 Kawamura T, Nishioka M (1977) Aspects of the reproductive biology of Japanese anurans. In "The Reproductive Biology of Amphibians" Ed DH Taylor, SI Guttman, Plenum Press, New York and London, pp. 103–139

5 Kawamura T, Nishioka M (1978) Descendants of reciprocal hybrids between two Japanese pond-frog species, *Rana nigromaculata* and *Rana brevipoda*. Sci Rep Lab Amphibian Biol Hiroshima Univ 3: 399–419

6 Kawamura T, Nishioka M (1979) Isolating mechanisms among the water frog species distributed in the Palearctic region. Mitt Zool Mus Berlin 55: 171–185

7 Kuramoto M (1977) Mating call structures of the Japanese pond frogs, *Rana nigromaculata* and *Rana brevipoda* (Amphibia, Anura, Ranidae). J Herpetol 11: 249–254

8 Lamb T, Avise JC (1987) Morphological variability in genetically defined categories of anuran hybrids. Evolution 41: 157–163

9 Mancino G, Ragghianti M, Bucci-Innocenti S (1979) Experimental hybridization within the genus *Triturus* (Urodela: Salamandridae). II. The lampbrush chromosomes of F_1 species hybrids between *Triturus cristatus carnifex* and *T. vulgaris meridionalis*. Caryologia 32: 61–79

10 Matsuda T (1978) Collision of the Izu-Bonin Arc with central Honshu: Cenozoic Tectonics of the Fossa Magma, Japan. J Phys Earth 26 Suppl: S 409–421

11 Matsui M (1984) Morphometric variation analyses and revision of Japanese toads (Genus *Bufo*, Bufonidae). Contrib Biol Lab Kyoto Univ 26: 209–428

12 Matsui M, Hikida T (1985) *Tomopterna porosa* Cope, 1868, a senior synonym of *Rana brevipoda* Ito, 1941 (Ranidae). J Herpetol 19: 423–425

13 Moriya K (1954) Studies on the five races of the Japanese pond frog, *Rana nigromaculata* Hallowell. I. Differences in the morphological characters. Jour Sci Hiroshima Univ Ser B Div 1 15: 1–21

14 Müller WP (1977) Diplotene of chromosomes of *Xenopus* hybrid oocytes. Chromosoma 59: 273–282

15 Nei M (1987) Molecular Evolutionary Genetics. Columbia University Press, New York, pp 208–253

16 Nishioka M, Ohtani H, Sumida M (1980) Detection of chromosomes bearing the loci for seven kinds of proteins in Japanese pond frogs. Sci Rep Lab Amphibian Biol Hiroshima Univ 4: 127–184

17 Nishioka M, Sumida M, Ohtani H (1992) Differentiation of 70 populations in the *Rana nigromaculata* group by the method of electrophoretic analyses. Sci Rep Lab Amphibian Biol Hiroshima Univ 11: 1–70

18 Nishioka M, Sumida M, Borkin LJ, Wu Z (1992) Genetic differentiation of 30 populations of 12 brown frog species distributed in the Palearctic region elucidated by the electrophoretic method. Sci Rep Lab Amphibian Biol Hiroshima Univ 11: 109–160

19 Nishioka M, Kodama Y, Sumida M, Ryuzaki M (1993) Systematic evolution of 40 populations of *Rana rugosa* distributed in Japan elucidated by electrophoresis. Sci Rep Lab Amphibian Biol Hiroshima Univ 12: 83–131

20 Ohtani H (1990) Lampbrush chromosomes of *Rana nigromaculata, R. brevipoda, R. plancyi chosenica, R. p. fukienensis* and their reciprocal hybrids. Sci Rep Lab Amphibian Biol Hiroshima Univ 10: 165–221

21 Ohtani H (1994) Polymorphism of lampbrush chromosomes of Japanese pond frog, *Rana nigromaculata*. Zool Sci 11: 337–342

22 Szymura JM, Barton NH (1991) The genetic structure of the hybrid zone between the fire-bellied toads *Bombina bombina* and *B. variegata*: Comparisons between transects and between loci. Evolution 45: 237–261

23 White MJD (1978) Modes of Speciation. WH Freeman and Company, San Francisco, pp 323–349

ZOOLOGICAL SCIENCE 11: 473–484 (1994)

Karyotypes and Ag-NOR Variations in Japanese Vespertilionid Bats (Mammalia: Chiroptera)

TAKAO ONO[1] and YOSHITAKA OBARA[2]

Department of Biology, Faculty of Science, Hirosaki University, Bunkyo-cho, Hirosaki 036, Japan

ABSTRACT—The karyological relationships among 14 species of Japanese vespertilionid bats were investigated paying attention to the chromosomal location and frequency of Ag-NORs. The karyotypes of these bats could be classified into two groups: centromere-cap NOR (cmcNOR) and interstitial NOR (intNOR) lineages. The former contained *Myotis, Barbastella, Plecotus* and *Murina*, and the latter *Pipistrellus, Nyctalus, Vespertilio* and *Miniopterus*. In the former lineage Ag-NORs were all tiny in size and distributed to many acrocentrics. In contrast, those of the latter were comparatively massive in size and shared by only two pairs at the most. While cmcNORs showed in general intergeneric and inter specific variations as well as intraspecific variations in their distribution pattern, intNORs showed rather stable patterns of distribution even among genera. Detailed G- and NOR-banding analyses suggested that most of the NOR-carrying acrocentrics of the ancestral karyotype might have been involved in Robertsonian rearrangements in the course of karyotype evolution in the Vespertilionidae: cmcNORs may have been transferred to other acrocentrics through cytologic events such as NOR-associations and interchromosomal chromatid exchanges and/or have been deleted through a centric fusion process. The present findings on the type and distribution of Ag-NORs were essentially consistent, except for a certain extent of variations in the location of cmcNORs, with those in the European vespertilionid bats previously reported by Volleth in 1985, and reinforced the karyological dendrogram of Japanese vespertilionid bats proposed by Harada in 1988. Thus, Ag-NORs may also provide useful cytogenetic parameters, at least in the Vespertilionidae, for the determination of phylogenetic relationships.

INTRODUCTION

The bats of the family Vespertilionidae are among the largest taxa (38 genera, 319 species) in the order Chiroptera [20] and their karyotypes show a marked variation in chromosome constitution as well as in diploid number [7, 8, 17, 46]. It is well known that Robertsonian rearrangements, *i.e.*, centric fusions/fissions, may have played a major role in chromosomal evolution of the family Vespertilionidae, although other types of rearrangements such as translocations, inversions and additions or deletions of constitutive heterochromatin (C-heterochromatin) are also known in this family [10, 11, 13, 29–31]. Accordingly, most of the chromosome arms of vespertilionid bats have been conserved in the course of diversification of karyotypes [10, 27, 30, 45, 50]. Thus, vespertilionid bats may be especially desirable for elucidation of the relationship between Robertsonian rearrangements and evolutionary processes which pertain to phylogenetic diversification.

Recently it has been suggested that variations in the chromosomal location of nucleolus organizer regions (NORs) may provide useful information in reconstructing phylogeny irrespective of the presence or absence of karyotypic alteration [1, 21, 35, 54, 55, 57, 58]. The NOR-banding using silver nitrate visualizes the chromosomal sites of transcriptionally active ribosomal RNA gene clusters as Ag-NORs. The Ag-NORs correspond to satellite stalks and secondary constrictions of chromosomes in most animal species [32]. Although a large number of karyotype and G- and C-banding studies have been published on Chiroptera to date, NOR-banding has been done in only a few cases. Volleth [51] examined the chromosomal location of NORs in 21 species of European vespertilionid bats, using silver nitrate staining, and found marked interspecific and/or intergeneric variations in the location of NORs. In some genera, she also found multiple Ag-NORs located on the minute short arms close to the centromere of acrocentric chromosomes. In this paper, such Ag-NORs were tentatively termed centromere-cap NORs (cmcNORs). The relation of cmcNOR variation with Robertsonian rearrangements in this group of bats remains unresolved.

In order to shed light on this subject we examined, by means of G-, C- and NOR-banding techniques, the chromosomes of 14 species of Japanese vespertilionid bats inhabiting northern Honshu and Hokkaido, with special attention to chromosome homoeology and Ag-NORs.

MATERIALS AND METHODS

Ninety-seven live specimens of 14 species of Japanese vespertilionid bats were captured in northern Honshu and Hokkaido. Of these, 73 specimens contributed to the chromosomal findings based on the conventional and/or differential staining (Table 1).

Chromosome preparations were made using bone marrow cells

Accepted May 23, 1994
Received March 2, 1994

[1] Present address: Chromosome Research Unit, Faculty of Science, Hokkaido University, North 10, West 8, Kita-Ku, Sapporo 060, Japan

[2] To whom reprint requests should be addressed.

Table 1. Vespertilionid bat specimens examined in this study

Species	Abbreviation	Number of specimens examined ♂	♀	Collecting site
Subfamily Vespertilioninae				
Tribe Myotini				
Genus *Myotis*				
M. nattereri (Kuhl)	Myn	1	—	Ashiro, Iwate Pref.
M. hosonoi Imaizumi	Myh	2	—	Ichinohe, Iwate Pref.
		1	1	Ashiro, Iwate Pref.
M. frater kaguyae Imaizumi	Myf	—	4	Ichinohe, Iwate Pref.
		3	—	Ashiro, Iwate Pref.
M. pruinosus Yoshiyuki	Myp	—	1	Sawauchi, Iwate Pref.
		—	2	Ashiro, Iwate Pref.
		2	—	Takko, Aomori Pref.
M. macrodactylus (Temminck)	Mym	7	5	Ohwani, Aomori Pref.
Tribe Vespertilionini				
Genus *Pipistrellus*				
P. endoi Imaizumi	Pie	1	—	Ashiro, Iwate Pref.
		3	4	San-nohe, Aomori Pref.
P. abramus (Temminck)	Pia	2	—	Hirosaki, Aomori Pref.
		5	3	Urawa, Saitama Pref.
Genus *Nyctalus*				
N. furvus Imaizumi and Yoshiyuki	Nf	—	1	Iwaizumi, Iwate Pref.
N. aviator Thomas	Na	2	3	San-nohe, Aomori Pref.
Genus *Vespertilio*				
V. superans Thomas	Vs	3	5	Hirosaki, Aomori Pref.
Tribe Plecotini				
Genus *Barbastella*				
B. leucomelas darjelingensis (Hodgson)	Bl	1	—	Iwaizumi, Iwate Pref.
		1	1	Tamayama, Iwate Pref.
Genus *Plecotus*				
P. auritus sacrimontis G. Allen	Pla	—	2	Ohdate, Akita Pref.
		—	1	Shizunai, Hokkaido
		1	—	Ohwani, Aomori Pref.
Subfamily Miniopterinae				
Genus *Miniopterus*				
M. schreibersi fuliginosus (Hodgson)	Mis	1	1	Oga, Akiata Pref.
Subfamily Murinae				
Genus *Murina*				
M. silvatica Yoshiyuki	Mus	1	1	Fukaura, Aomori pref.
		1	—	Shizunai, Hokkaido

The scientific names of the bats examined were given according to the classification system of Yoshiyuki [56].

of radii and humeri according to Obara and Miyai [39] and Obara [38]. In *Myotis pruinosus*, chromosome preparations were obtained from the primary culture of tail tissue following the procedure of Obara and Saitoh [41].

G- and C-bandings were carried out according to the ASG method [49] and the BSG method [48], respectively. For NOR-banding the one step silver-staining method [23, 33] was adopted with a slight modification. Identification of the NOR-carrying chromosomes was done by means of sequential staining of G- and NOR-bandings: after photographing G-banded metaphases, the same metaphases were destained with Carnoy's fixative and then successively silver-stained and rephotographed.

Chromosomes were numbered according to the numbering system of Bickham [11], in which ordinal numbers were given to all of the autosomal arms based on G-banding pattern. Accordingly, a given biarmed chromosome has two arm numbers, e.g., 1/2, 3/4 and 5/6 chromosomes. Since almost half of the chromosomes of the Japanese pipistrelle *Pipistrellus abramus* have been structurally rearranged too much to be given arm numbers in this system, the author's numbering system [43] was adopted for the Ag-NOR analysis of this

TABLE 2. Cytologic findings of 14 species of bats examined

Species	2n	FN	Autosome pair			Sex chromosome		No. of cells karyotyped			
			M·SM	sSM·ST	A	X	Y	Conv.	G	C	N
Myn	44	50	3	1	17	M	A	8 (21)	5	2	12 (55)
Myh	44	52	3	2	16	M	A	3 (13)	5	—	7 (33)
Myf	44	52	3	2	16	M	ST	14 (77)	15	5	21 (125)
Mym	44	52	3	2	16	M	ST	17 (111)	25	—	25 (64)
Myp	44	52	3	2	16	SM	A	14 (44)	10	4	11 (43)
Pie	36	50	7	1	9	A	A	7 (45)	14	3	22 (163)
Pia	26	44	10	0	2	A	A	11 (37)	34	1	35 (165)
Nf	44	52	4	2	17	M	A	8 (45)	9	—	12 (76)
Na	42	50	5	1	15	M	A	11 (47)	20	—	26 (160)
Vs	38	50	6	1	11	M	A	8 (23)	11	—	25 (61)
Bl	32	50	9	1	5	M	A	6 (26)	10	—	17 (50)
Pla	32	50	9	1	5	M	A	11 (21)	14	2	19 (57)
Mis	46	50	2	1	19	M	A	8 (31)	17	—	15 (91)
Mus	44	56	3	4	14	M	A	6 (13)	3	—	9 (22)

2n, diploid number of chromosomes; FN, fundamental number; M, metacentric; SM, submetacentric; sSM, small submetacentric; ST, subtelocentric; A, acrocentric; Conv., conventional staining; G, G-band staining; C, C-band staining; N, NOR-band staining. Abbreviations for species name are the same as those in Table 1. Parentheses indicate the number of cells analyzed under microscope.

species.

The frequency of Ag-NORs (the mean number of Ag-NORs in each chromosome pair per cell) was calculated for 7–35 metaphases, mainly according to Volleth [51]: in a given chromosome a distinct Ag-NOR was calculated as 1.0 and indistinct one as 0.5, and therefore distinct homozygous Ag-NORs as 2.0, distinct heterozygous Ag-NOR as 1.0, indistinct homozygous Ag-NORs as 1.0, indistinct heterozygous Ag-NOR as 0.5 and a pair of distinct and indistinct Ag-NORs as 1.5.

RESULTS

G- and C-banding

Cytologic findings and analytic data of 14 species of vespertilionid bats examined were summarized in Table 2. The chromosomal findings were essentially consistent with those of the previous studies [2–4, 25, 27–31, 40–44]. A representative G-banded karyotype of *Myotis nattereri* is shown in Figure 1 as a standard of the karyotypes of these 14 bat species, since *Myotis* is regarded as the most "primitive" genus among these eight genera examined here [19, 56], and *M. nattereri* is considered, from a karyological viewpoint, an original form among the *Myotis* species of Japan [31]. The autosomes consisted of three pairs of large metacentrics [M] (Nos. 1/2, 3/4 and 5/6), one pair of small submetacentrics

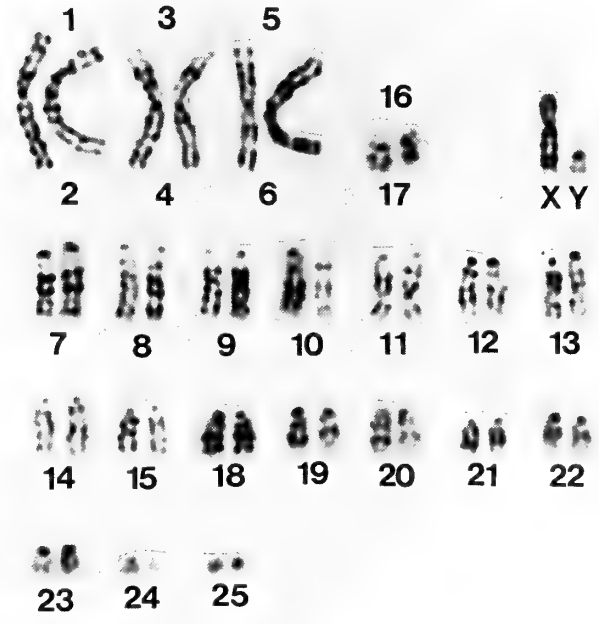

FIG. 1. G-banded karyotype of a male *Myotis nattereri*. Ordinal numbers indicate autosomal arm numbers.

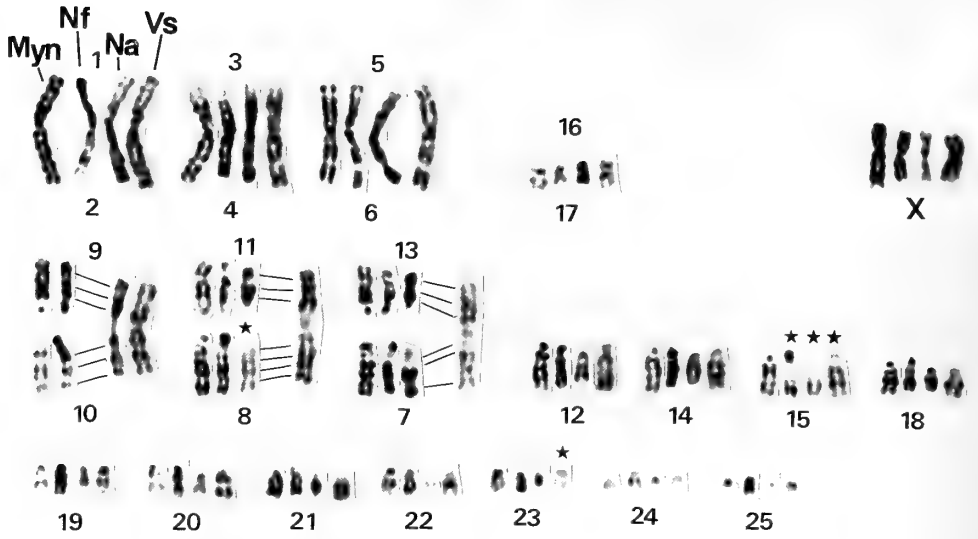

Fig. 2. Comparison of G-banded haploid karyotypes of *Myotis nattereri, Nyctalus furvus* (Nf), *N. aviator* (Na), and *Vespertilio superans* (Vs). Asterisks indicate NOR-bearing chromosomes: No. 8 of Na carries cmcNORs, and No. 15 of Nf, Na and Vs and No. 23 of Vs intNORs, which strictly correspond to the secondary constriction.

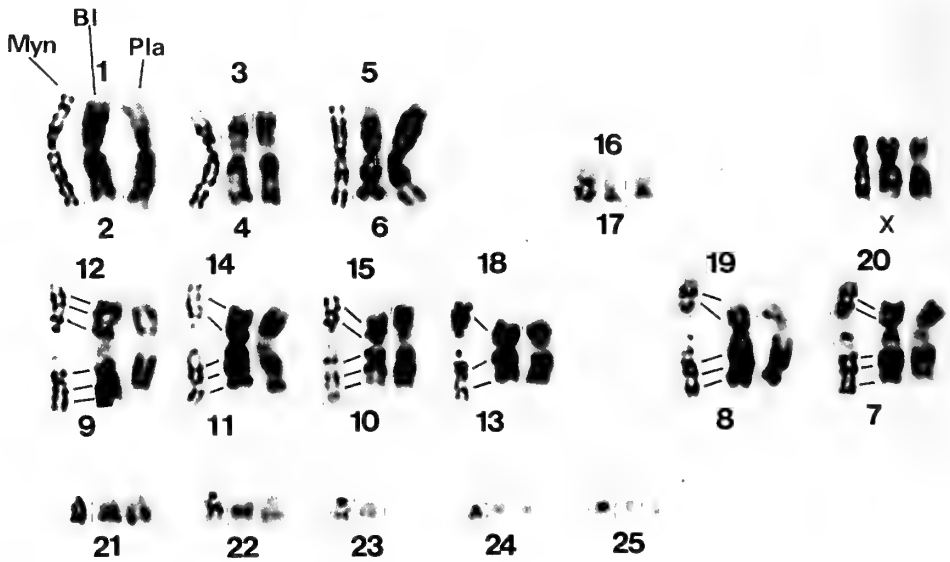

Fig. 3. Comparison of G-banded haploid karyotypes of *Myotis nattereri* (Myn), *Barbastella leucomelas darjelingensis* (Bl), and *Plecotus auritus sacrimontis* (Pla).

[SM] (No. 16/17) and 17 pairs of medium-to-small acrocentrics [A] (Nos. 7–15 and Nos. 18–25). The sex chromosomes X and Y were a medium-sized M and a small A, respectively. In the standard karyotype all the C-bands were centromeric except for the Y chromosome which was totally heterochromatic.

In each species, the chromosome arms were numbered on the basis of G-band homology to the *Myotis nattereri* chromosomes. Figure 2 shows a composite G-banded karyotype consisting of the haploid sets of four species of the Vespertilioninae (*Myotis nattereri, Nyctalus furvus, N. aviator,* and *Vespertilio superans*), in which all chromosome arms could be paired, like a tetraploid cell, in proper quantities among species. The karyotype of *Nyctalus furvus* (Nf) was almost the same as that of *Myotis nattereri* (Myn), except for the presence or absence of a distinct secondary constriction on the proximal region of the pair No. 15. So, the constitution of uni- and biarmed chromosomes was just the same as Myn and Nf, though some of the A's of Nf contained comparatively massive C-heterochromatin on their minute

short arms (data not shown). On the contrary, *Nyctalus aviator* (Na) had fewer A's than Myn by 2 pairs (Nos. 9 and 10), and the former had more large M's than the latter by 1 pair (No. 9/10). Similarly, *Vespertilio superans* (Vs) had fewer A's than Myn by six pairs (Nos. 7–11 and No. 13), and the former had more large M's than Myn by three pairs (Nos. 9/10, 11/8 and 13/7). Four biarmed chromosomes, Nos. 1/2, 3/4, 5/6 and 16/17, were common to these four bat species, the chromosomes with the same arm combination necessarily being regarded as homoeologous chromosomes in the same way as all other A's with the same arm numbers. Thus, the chromosomal relationship of these four bat species could be explained well by Robertsonian rearrangements.

Figures 3 and 4 are the composite karyotypes showing the chromosomal relationship of Myn with *Barbastella leucomelas darjelingensis* (Bl), *Plecotus auritus sacrimontis* (Pla), and *Pipistrellus endoi* (Pie). As clearly demonstrated by the pair-matching analysis, Robertsonian rearrangements were the main mechanism of karyotype evolution also in these vespertilionine species. On the other hand, four *Myotis* species (*M. nattereri, M. hosonoi, M. frater kaguyae,* and *M. macrodactylus*) showed quite similar karyotypes with closely resembling chromosome constitution, but differing from each other only in the size of the pair No. 25. The size variation of this pair could be attributed to the duplication of C-heterochromatin as suggested by Harada and Yosida [31]. The other *Myotis* species, *M. pruinosus* (Myp) was significantly different from Myn in the arm ratio of the pair No. 1/2 and the size of the X chromosome. The variation in the arm ratio could be explained by pericentric inversion, and the size variation of the X chromosomes by duplication of C-heterochromatin or translocation of an autosomal element of unknown origin to the X chromosome, as noted by Harada and Uchida [29].

The arm combination of biarmed autosomes of 13 bat species was summarized in Table 3. It is evident from the arm combination analysis that three large M pairs (Nos. 1/2, 3/4 and 5/6) and a small SM pair (No. 16/17) have been well conserved during the course of karyotypic diversification of these bat species except for *Miniopterus schreibersi* and *Pipistrellus abramus*. In the former species the pairs Nos. 3/4 and 16/17 were not detected at all. G-banding analysis proved three additional A's to have been formed from these biarmed pairs through centric fission and pericentric inversion in agreement with Bickham and Hafner [13]. Three large M pairs of *Pipistrellus abramus* had unusually large C-bands on either side of their centromeres, and the small SM chromosome corresponding to the pair No. 16/17 was not detected due probably to complicated rearrangements. Other than these three large M pairs (Nos. 1/2, 3/4 and 5/6), *Pipistrellus*

TABLE 3. Arm combination of the biarmed chromosomes in 13 species of bats examined

Genus Species	Combinations of chromosome arms									
Myotis										
Myn	1/2	3/4	5/6	16/17						
Myh, Myf, Mym	1/2	3/4	5/6	16/17	25[c]					
Myp	1/2[i]	3/4	5/6	16/17	25[c]					
Pipistrellus										
Pie	1/2	3/4	5/6	16/17[i]	13/9	11/8	12/10	18/14		
Pia	1/2[c]	3/4[c]	5/6[c]		13/9[c]	14/7*	? ?	? ?	?	
Nyctalus										
Nf	1/2	3/4	5/6	16/17	25[c]					
Na	1/2	3/4	5/6	16/17	9/10					
Vespertilio										
Vs	1/2	3/4	5/6	16/17	9/10	11/8	13/7			
Barbastella										
Bl	1/2	3/4	5/6	16/17	12/9	14/11	15/10	18/13	19/8	20/7
Plecotus										
Pla	1/2	3/4	5/6	16/17	12/9	14/11	15/10	18/13	19/8	20/7
Miniopterus										
Mis	1/2		5/6	10[i]						

i, pericentric inversion; c, duplicaiton of C-heterochromatin; *, NOR-bearing chromosome. ?, uncertain arm combination. See Table 1 for species abbreviations.

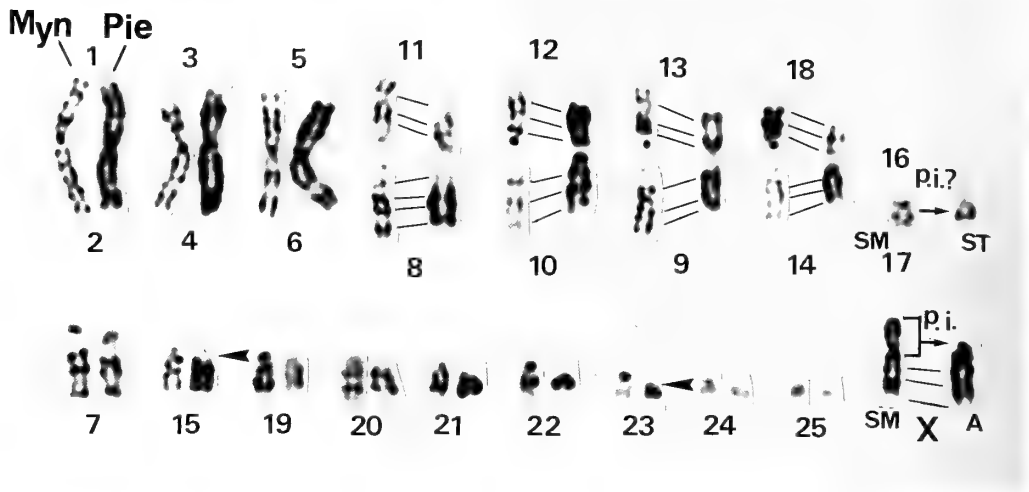

Fig. 4. Comparison of G-banded haploid karyotypes of *Myotis nattereri* (Myn) and *Pipistrellus endoi* (Pie). Arrowheads denote secondary constrictions which locate close to centromere. p.i., pericentric inversion; SM, submetacentric; ST, subtelocentric; A, acrocentric.

abramus contained 7 pairs of biarmed chromosomes (Nos. 13/9, 14/7 and 5 pairs of unknown combination) (Table 3). The G-banding pattern of *Murina silvatica* (Mus) was not obtained. These results are essentially consistent with the earlier study [26] except for discrepancy in the arm combination of *Pipistrellus endoi*.

NOR-banding

On the basis of their location on chromosomes, the Ag-NORs detected in this study were classified into two types: cmcNORs and intNORs. The former are located on the minute short arms of A's, appearing as a centromere cap, and the latter are located within chromosome arms as interstitial NORs which correspond to the secondary constrictions, irrespective of their size. Three examples of typical cmcNORs and intNORs are shown in Figure 5. In general, cmcNORs were quite small or fine in size and sometimes of variable occurrence. On the contrary, the one or two pairs of intNORs observed are massive in size and of consistent occurrence. Ag-NORs of the bat species examined here were located only on the A's irrespective of their types, i.e., "centromeric" or "interstitial", with the exception of *Pipistrellus abramus*.

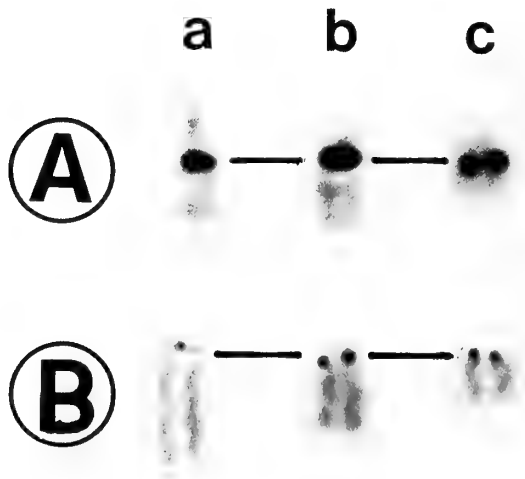

Fig. 5. Typical examples of silver-stained intNORs (A) and cmcNORs (B). The former are from No. 15 chromosomes of *Nyctalus furvus* (a) and *Pipistrellus endoi* (b) and No. 23 chromosome of P. *endoi* (c), respectively, and the latter from *Myotis pruinosus*, in which each chromosome could not be identified.

The distribution patterns of cmcNORs and intNORs of 12 bat species analyzed by successive sequential G- and NOR-bandings were summarized in Table 4 for an easy understanding of the interspecific relationship of NOR sites. All five *Myotis* species examined had multiple cmcNORs (No G-banding analysis was done in *Myotis pruinosus*). Representative metaphases of *Myotis hosonoi* sequentially stained are shown in Figure 6. The NOR patterns and their occurrence frequency were depicted in Figure 7 with histograms. These *Myotis* species showed marked variations in NOR distribution, despite their close similarity of karyotypes. The frequency of cmcNORs varied from individual to individual as well as from species to species, being below 1.0 in many chromosome pairs, while their distribution pattern seemed to be particular, even in consideration of some interindividual variation, to each species, as shown by 1) their steady occurrence in the pair No. 7 of *Myotis hosonoi* (Myh), 2) their distinct tendency to the small A's in *M. macrodactylus* (Mym) and 3) their wide distribution with different combination in *M. nattereri* (Myn) and *M. frater* (Myf). As a whole, Myn, Myh, Myf and Mym carried cmcNORs on 11, 5, 13 and 6 pairs of A's, respectively. Relatively high frequencies of cmcNORs were found in Nos. 8 and 9 of Myn, Nos. 7 and 23 of Myh, Nos. 8, 18 and 20 of Myf and Nos. 18, 20 and 23 of Mym.

Multiple types of cmcNOR were also found in *Barbastel-*

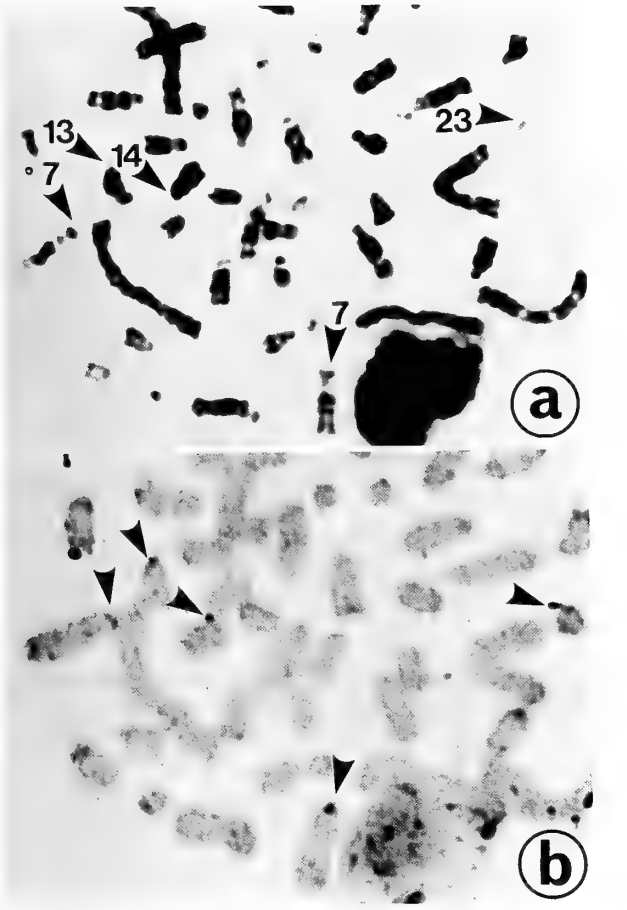

FIG. 6. Sequentially-stained metaphases of *Myotis hosonoi*. a, G-banded; b, NOR-banded. Arrowheads denote the NOR sites (a) and cmcNORs (b).

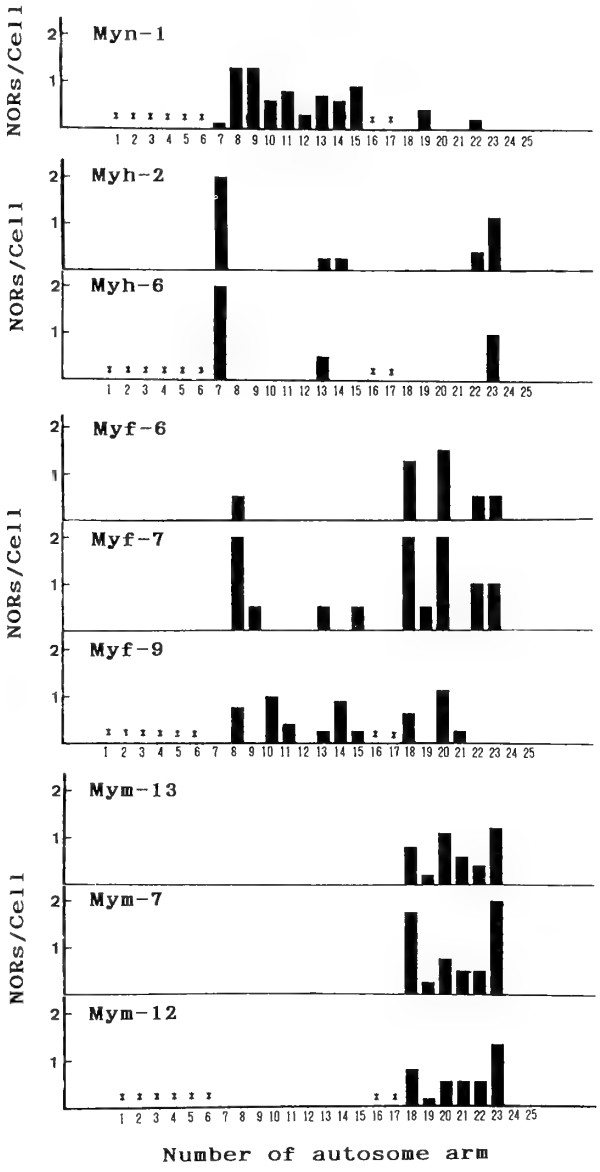

FIG. 7. Distribution pattern of cmcNORs in four *Myotis* species, *Myotis nattereri* (Myn), *M. hosonoi* (Myh), *M. frater kaguyae* (Myf) and *M. macrodactylus* (Mym). Asterisks indicate the arms of biarmed autosomes, and the numbers following species abbreviation individual numbers. See "materials and methods" for further details.

la leucomelas (Bl) and *Plecotus auritus* (Pla): the former had 5 pairs of A's (Nos. 21–25) in the chromosome complement, all of which carried cmcNORs, and the latter carried cmcNORs on only 4 A's (Nos. 21–24), in spite of the close similarity of karyotypes (Tables 3 and 4). The frequency of cmcNORs was relatively high in pair No. 24 of *B. leucomelas* and Nos. 21 and 22 of *P. auritus*, and the other A's showed highly variable frequencies of cmcNORs from individual to individual in both species (Fig. 8). *Murina silvatica* had multiple cmcNORs similar to those of *Myotis* species. Unfortunately, no sequential G- and NOR-band stainings were applied to this species.

Pipistrellus endoi and *Vespertilio superans* had intNORs on the pairs Nos. 15 and 23 in common (Table 4 and Figs. 5 and 9). As clearly demonstrated in Figs. 9 and 10, *Nyctalus furvus* possessed a single pair of intNORs on the pair No. 15, and *N. aviator* had cmcNORs on the pair No. 8 and intNORs on the pair No. 15. Similarly, *Miniopterus schreibersi* had cmcNOR on the pair No. 20 and intNOR on the pair No. 23 (Table 4), nevertheless this species carried more A's than those of *Myotis*. The intNOR of the pair No. 15 showed a frequency of almost 2.0 in *Nyctalus furvus, N. aviator* and *Vespertilio superans*, but under 1.5 in *Pipistrellus endoi* (Table 4), and that of the pair No. 23 of *P. endoi* showed distinct homozygous Ag-NORs calculated as 2.0. The cmcNOR of the pair No. 8 of *N. aviator* had a frequency under 1.5. The location of NORs of *Pipistrellus abramus* was quite exceptional in having intNORs on the proximal region of the long arm of the metacentric pair No. 5 which consists of Nos. 14 and 7 chromosomes of the standard karyotype (Table 4 and Fig. 11).

DISCUSSION

In general, vespertilionid species show a high degree of the intergeneric variation of karyotypes and a lower degree of

Table 4. Distribution pattern of Ag-NORs in 11 species of bats

species	Number of specimens analyzed	Number of autosomal arm																		
		7	8	9	10	11	12	13	14	15	16	17	18	19	20	21	22	23	24	25
Myn	1	+	+	+	+	+	+	+	+	+				+			+			
Myh	2	++						+	+								+	+		
Myf	4		+	+	+	+		+	+	+			+	+	+	+	+	+		
Mym	5												+	+	+	+	+	+		
Pie	6									✣								✣✣		
Nf	1									✣✣										
Na	5		+							✣✣										
Vs	6									✣✣								✣		
Bl	3															+	+	+	+	+
Pla	4															+	+	+	+	
Mis	2														+			✣		

species	Number of specimens analyzed	Number of autosome*											
		1	2	3	4	5	6	7	8	9	10	11	12
Pia	4					✣✣							

Abbreviations for species name are the same as those in Table 1. + and ✣, cmcNORs and intNORs. Single plus mark means under 1.5, and double plus mark more than 1.5. (See "materials and methods" for detail). *, according to the numbering system of Obara *et al.* [43].

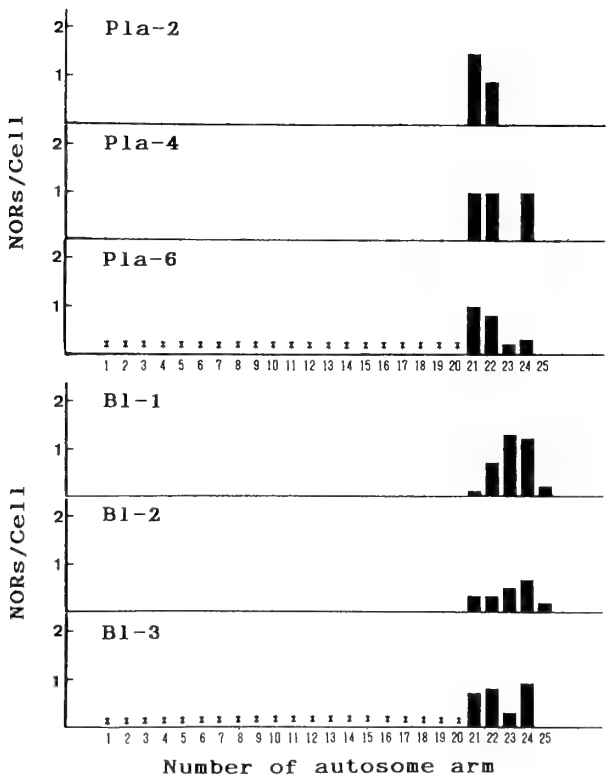

Fig. 8. Distribution pattern of cmcNORs in three specimens of *Plecotus auritus sacrimontis* (top) and in three specimens of *Barbastella leucomelas darjenlingensis* (bottom).

Fig. 9. NOR-banded karyotypes of three Vespertilionini species, *Nyctalus furvus* (A), *N. aviator* (B), and *Vespertilio superans* (C). Arrowheads indicate Ag-NORs. M, large metacentrics.

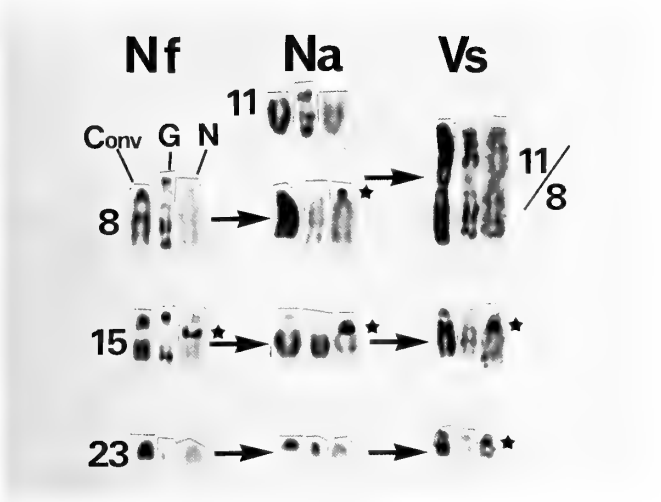

FIG. 10. Comparison of differentially stained NOR-bearing chromosomes of *Nyctalus furvus, N. aviator* and *Vespertilio superans*. Asterisks indicate Ag-NORs. Conv., conventionally stained; G, G-banded; N, NOR-banded.

intrageneric variation [6, 7, 10, 17, 46]. The vespertilionid bats of Japan are no exception to this view: the diploid numbers in eight genera of vespertilionid bats studied here varied widely from 2n=26 to 2n=46. On the other hand, each of five species of *Myotis* examined had similar karyotypes, showing the same chromosome number and only slightly variable chromosome constitution (Tables 2 and 3). In spite of such remarkable karyotypic uniformity, these *Myotis* species showed considerable variation in the location of NORs, and in addition their distribution patterns seemed to be species-specific, though a certain degree of intraspecific (inter- and intraindividual) variation in NOR distribution was observed (Table 4 and Figs. 6 and 7). A similar relationship has already been found in the European species of *Myotis* [51]. Taken together, it seems likely that variation in NOR location can be used to trace paths of taxonomic diversification of the *Myotis* group. Similar views have been presented for several other taxonomic groups of animals such as Pisces, Amphibia and Rodentia [1, 21, 24, 35, 54, 57, 58].

The distribution pattern of NORs of *Myotis nattereri* examined by Volleth [51] differs significantly from that of the same species collected from Japan in that the former carry only four pairs of cmcNORs and the latter eleven pairs of cmcNORs. This discordance in NOR pattern may be attributed to the subspecies distinctness; the former is the nominate subspecies *Myotis n. nattereri*, and the latter a Japanese subspecies *Myotis n. bombinus* [19, 20]. If this is true, the distribution analysis of NORs should be useful in detecting geographic differentiation of the karyotype within a single species or species complex.

As summarized in Table 4, intNORs showed a markedly low variation in their distribution, whereas in striking contrast cmcNORs were highly variable in their distribution among species. Further, intNORs were mostly massive in size with steady occurrence, and cmcNORs were distributed to many A's with various combinations and variable occurrence (Figs. 7 and 9 and Table 4). Since so-called NOR-association makes chromatid exchange physically possible irrespective of homologous or heterologous chromosomes, these findings suggest that cmcNORs of vespertilionid bats may be subject to transfer to another A's through NOR-association and interchromosomal chromatid exchange, while intNORs may be liable to include cmcNORs into themselves during the course of NOR-association, resulting in growing intNORs and diminishing cmcNORs. The NOR transferred to a given interstitial position of chromosomes may be stabilized in their gene activity as well as in their structural organization. The steady occurrence of intNORs plainly reflects this point of view. Our view on the marked stability of intNORs is well supported by the observation of Volleth [51] on the NORs of the European *Pipistrellus* species: the most "primitive" pipistrelle *P. pipistrellus* has no intNORs on any of the chromosomes, but multiple cmcNORs on several A's, and

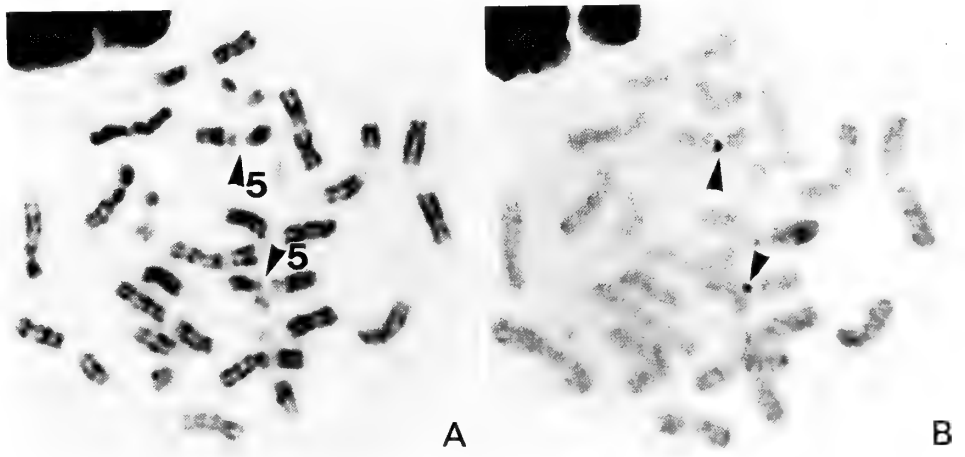

FIG. 11. A, G-banded metaphase of *Pipistrellus abramus*. Arrowheads indicate a No. 5 homologue which consists of Nos. 7 and 14 of the standard karyotype. B, same metaphase as in (A) after silver-staining, showing intNORs on the proximal site of the long arm (arrowheads).

"advanced" pipistrelles, *P. savii, P. kuhli* and *P. nathusii* have a typical secondary constriction on the proximal region of the long arm of the pair No. 15, which is the site of consistently-occurring intNOR. In this context, note that the little brown bats, *Myotis*, are among the most "primitive" taxa in the family Vespertilionidae [19] and all *Myotis* species so far examined showed cmcNORs regardless of their distribution in Europe or Japan. So, assuming that the cmcNORs have been conserved intact without altering in the genus *Myotis*, it follows, in contrast to Volleth's views, that the ancestral form of NORs of the family Vespertilionidae is not the interstitial type, but a cmc type.

The tube-nosed bats *Murina*, belonging to the subfamily Murinae, are characterized by a projecting tube-like nose. In spite of such a marked phenotypical specialization, *Murina aurata* closely resembled *Myotis nattereri* of Vespertilioninae in the NOR type (cmcNORs) as well as in the karyotypic profile. Therefore, *Murina* is considered to have been derived from the ancestral stock of *Myotis* without alteration in either NOR type nor chromosome morphology, unlike the general tendency of karyotype evolution in vespertilionid bats.

Karyotypes of six genera excluding *Myotis* and *Murina* have differentiated, more or less,through Robertsonian rearrangements, as revealed by the pair-matching analysis of G-banded chromosomes. As seen in Tables 3 and 4, these bats could be classified into the following three karyotypic lineages on the basis of the NOR type and arm combination of chromosomes: (1) *Pipistrellus-Nyctalus-Vespertilio*, (2) *Barbastella-Plecotus*, and (3) *Miniopterus*. The first lineage is characterized by the typical intNORs on the homoeologous chromosomes (Table 4, Figs. 5, 9 and 10), although their conventional karyotypes differ largely from each other because of chromosome rearrangements by centric fusion. The second lineage, Tribe Plecotini, carries multiple cmcNORs on the smaller A's (Fig. 8). Their karyotypes could also be regarded as the chromosome change-mediated products resulting from centric fusion as in the first lineage, but here the arm combination of the large M's was different from that of the first lineage (Table 3), suggesting that the *Barbastella-Plecotus* lineage has diverged from the ancestral *Myotis*-like form through its own process different from the first lineage. The third lineage is an offshoot derived from the ancestral stock of *Myotis* through centric fission, having two pairs of NORs: one pair of intNORs and the other, cmcNORs.

The pipistrelle species *P. endoi* and *P. abramus* of the first lineage were highly different from each other in their chromosome constitution as well as in their diploid number, although they are congeneric. *P. endoi* is fairly conservative in its arm constitution, following the general tendency of karyotype evolution in Vespertilionidae, whereas in striking contrast *P. abramus* attained a higher degree of non-Robertsonian rearrangements [26, 44]. With regard to Ag-NORs, the NOR-bearing chromosomes of *P. endoi* were identified as Nos. 15 and 23, while those of *P. abramus* were identified as No. 5, formed by the centric fusion between Nos. 14 and 7 chromosomes of the standard karyotype (Fig. 11). However, both species share at least 4 pairs of their large M's (Nos. 1/2, 3/4, 5/6 and 13/9) in their karyotypes (Table 3). Therefore, *P. endoi* and *P. abramus* may have derived from a common ancestor.

The vespertilionid bats carry few intNORs on biarmed chromosomes. The thick-thumbed pipistrelle *Glischropus tylopus* is an exceptional case with an intNOR on the proximal region of the long arm of one M pair [52], and this NOR-bearing chromosome seemed to correspond well with the pair No. 5 of *P. abramus* in G-banding pattern. Such coincidence in the type and location of NORs strongly suggests that *G. tylopus* is closely related to the lineage of *P. abramus*. Further, *P. abramus* (2n=26) remarkably resembles the American yellow bat *Lasiurus intermedius* (2n=26) in the chromomycin A_3 fluorescence pattern as well as in the chromosome constitution and G-banding pattern ([12], Obara, unpublshed data). This fact may also suggest a close relationship of *P. abramus* with *L. intermedius*.

The No. 15 chromosomes of *Nyctalus furvus, N. aviator*, and *Vespertilio superans*, all of which carry a typical secondary constrictions with a high activity of NORs, are probably homoeologous with each other, although the former two exhibit partial loss of the proximal region of the long arm (Figs. 2 and 10), and the pair-matching analysis revealed that the centric fusion rearrangements have occurred at first in the combination of Nos. 9 and 10, and then in the combination of Nos. 11 and 8, and Nos. 13 and 7. Further, *Pipistrellus endoi* also carries intNORs on the pair No. 15 like those three Vespertilionini species (Fig. 4). Therefore, it is possible that the noctule and particoloured bats *Nyctalus* and *Vespertilio* are the offshoots from a common ancestor of the "advanced" pipistrelles including *P. savii, P. kuhli, P. nathusii* and *P. endoi*: hence, both *Nyctalus* and *Vespertilio* belong to the *Pipistrellus* lineage. This type of secondary constriction and Ag-NORs of the pair No. 15 has been observed also in European species of *Nyctalus, Vespertilio* and *Pipistrellus* [15–18, 22, 50, 51].

The relationship between NOR variation and centric fusion in human D- and G-group chromosomes has been investigated by several researchers. They found that in most cases the M's resulting from centric fusion are lacking in NORs [5, 34, 36, 37, 59]. This pattern of NOR variation through centric fusion resembles that seen in the vespertilionid bats examined here. One exceptional case was found in *Pipistrellus abramus* which carried intNORs on the proximal region of one large M pair formed by centric fusion: the other centric fusion-mediated M's (11/8 in *Vespertilio superans* and 12/9, 14/11, 15/10, 18/13, 19/8 and 20/7 in *Barbastella leucomelas* and *Plecotus auritus*) were lacking in NORs. Nevertheless, cmcNORs have been present on most of the arms before fusion. According to Stahl *et al.* [47] who attempted to explain the relationship between centric fusion and cmcNORs from an electronmicroscopic viewpoint, whether or not cmcNORs remain on the proximal region of

the M's resulting from centric fusion depends on the point of the breakage/reunion at which centric fusions are induced. Therefore, in the case of vespertilionid bats breakage/reunion might have occurred in a point, making exclusion of cmcNORs possible. In the exceptional case of *Pipistrellus abramus*, breakage/reunion might have occurred in a point which made inclusion of cmcNORs possible.

Recently, Harada [26] presented a karyological dendrogram of Japanese vespertilionid bats based on the G- and C-banding patterns. The present chromosome findings support his classification system, and the findings from the silver staining reinforced this support. The Plecotini *Barbastella leucomelas* and *Plecotus auritus* and the Murinae *Murina silvatica* carried multiple cmcNORs as in *Myotis*, whereas the *Pipistrellus* lineage carried intNORs. Thus, the type and location of Ag-NORs are reflected, as the third cytogenetic parameter, by the phylogenetic lineage. So far as cytogenetic parameters are concerned, the former group has a closer relationship with *Myotis* than the latter group.

The relationship of NOR variation with karyotype evolution in vespertilionid bats could be clarified by the methods of molecular cytogenetic analysis such as *in situ* hybridization and by further investigation of the present and other bat species.

ACKNOWLEDGMENTS

The authors are grateful to Mr. Mitsuru Mukohyama of Aomori Prefectural San-nohe High School, for providing and identifying the bat specimens and to Mr. Yoshihiko Misumi of Ichinohe-cho, Iwate Pref., Mr. Azuma Abe of Aomori Prefectural Hirosaki High School and Mrs. Michiko Kiyomiya of Urawa, Saitama Pref., who cooperated in collecting the research materials. Our sincere thanks are also due to Emeritus Professor Kazuo Saitoh of Hirosaki University and Dr. Oscar G. Ward of the Department of Ecology and Evolutionary Biology, University of Arizona, for reading and refining the manuscript with expert criticism.

REFERENCES

1 Amemiya CT, Gold JR (1988) Chromosomal NORs as taxonomic and systematic characters in North American cyprinid fishes. Genetica 76: 81–90

2 Ando K, Tagawa T, Uchida TA (1977) Considerations of karyotypic evolution within Vespertilionidae. Experientia 33: 877–879

3 Ando K, Tagawa T, Uchida TA (1980) The C-banding pattern of 6 Japanese species of Vespertilioninae bats (Mammalia: Chiroptera). Experientia 36: 653–654

4 Ando K, Harada M, Uchida TA (1987) A karyological study on five species of *Myotis* and *Pipistrellus*, with special attention to comparison of their C-band materials. J Mammal Soc Japan 12: 25–29

5 Babu KA, Verma RS (1985) Structural and functional aspects of nucleolar organizer regions (NORs) of human chromosomes. Internat Rev Cytol 94: 151–176

6 Baker RJ (1970) Karyotypic trends in bats. In "Biology of Bats, Vol. 1" Ed by WA Wimsatt, Academic Press, New York and London, pp 65–96

7 Baker RJ, Bickham JW (1980) Karyotypic evolution in bats: extensive and conservative chromosomal evolution in closely related taxa. Syst Zool 29: 239–253

8 Baker RJ, Patton JL (1967) Karyotypes and karyotypic variation of North American vespertilionid bats. J Mammal 48: 270–286

9 Bengtsson BO (1980) Rates of karyotype evolution in placental mammals. Hereditas 92: 37–47.

10 Bickham JW (1979) Chromosomal variation and evolutionary relationships of vespertilionid bats. J Mammal 60: 350–363

11 Bickham JW (1979) Banded karyotypes of 11 species of American bats (Genus *Myotis*). Cytologia 44: 789–797

12 Bickham JW (1987) Chromosomal variation among seven species of *Lasiurus* bats (Chiroptera: Vespertilionidae). J Mammal 68: 837–842

13 Bickham JW, Hafner JC (1978) A chromosomal banding study of three species of vespertilionid bats from Yugoslavia. Genetica 48: 1–3

14 Bush GL, Case SM, Wilson AC, Patton JL (1977) Rapid speciation and chromosomal evolution in mammals. Proc Natl Acad Sci USA 74: 3942–3946

15 Capanna E (1968) Some considerations on the evolution of the karyotype of Microchiroptera. Experientia 24: 624–626

16 Capanna E, Civitelli MV (1967) I cromosomi di *Pipistrellus savii*. Caryologia 20: 265–272

17 Capanna E, Civitelli MV (1970) Chromosomal mechanisms in the evolution of chiropteran karyotype: Chromosomal tables of Chiroptera. Caryologia 23: 79–111

18 Capanna E, Romanini MGM (1971) Nuclear DNA content and morphology of the karyotypes in certain Palaearctic Microchiroptera. Caryologia 24: 471–482

19 Corbet GB (1978) The mammals of the Palaearctic region: A taxonomic review. Cornell Univ. Press, Ithaca, New York, 1st edition

20 Corbet GB, Hill JE (1980) A world list of mammalian species. British Museum (Natural History), London and Cornell Univ. Press, Ithaca, New York, 1st edition

21 Dev VG, Tantravahi R, Miller DA, Miller OJ (1977) Nucleolus organizers in *Mus musculus* subspecies and in the RGA mouse cell line. Genetics 86: 389–398

22 Dulic B, Soldatovic B, Rimsa D. (1967) La formule chromosomique de la noctule, *Nyctalus noctula* Schreber (Mammalia, Chiroptera). Experientia 23: 945–946

23 Gold JR, Ellison JR (1983) Silver staining for nucleolar organizing regions of vertebrate chromosomes. Stain Technol 58: 51–55

24 Gold JR, Amemiya CT (1986) Cytogenetic studies in North American minnows (Cyprinidae). XII. Patterns of chromosomal nucleolus organizer region variation among 14 species. Can J Zool 64: 1869–1877

25 Harada M (1973) Chromosomes of nine chiropteran species in Japan (Chiroptera). La Kromosomo 91: 2885–2895

26 Harada M (1988) Karyotypic evolution in the family Vespertilionidae. Honyurui Kagaku 28: 69–83 (in Japanese)

27 Harada M, Ando K, Uchida TA, Takada S (1987) Karyotypic evolution of two Japanese *Vespertilio* species and its taxonomic implications (Chiroptera: Mammalia). Caryologia 40: 175–184

28 Harada M, Ando K, Uchida TA, Takada S (1987) A karyological study on two Japanese species of *Murina* (Mammalia: Chiroptera). J Mammal Soc Japan 12: 15–23

29 Harada M, Uchida TA (1982) Karyotype of a rare species, *Myotis pruinosus*, involving pericentric inversion and duplicated translocation. Cytologia 47: 539–543

30 Harada M, Uchida TA, Yosida TA, Takada S (1982) Karyological studies of two Japanese noctule bats (Chiroptera). Caryologia 35: 1–9

31 Harada M, Yosida TH (1978) Karyological study of four Japanese *Myotis* bats (Chiroptera, Mammalia). Chromosoma 65: 283–291

32 Howell WM (1982) Selective staining of nucleolus organizer regions (NORs). Cell Nucleus 11: 89–142

33 Howell WM, Black DA (1980) Controlled silver-staining of nucleolus organizer regions with a protective colloidal developer: a 1-step method. Experientia 36: 1014–1015

34 Hurley JE, Pathak S (1977) Elimination of nucleolus organizers in a case of 13/14 Robertsonian translocation. Hum Genet 35: 169–173

35 Mahony MJ, Robinson ES (1986) Nucleolar organizer region (NOR) location in karyotypes of Australian ground frogs (Family Myobatrachidae). Genetica 68: 119–127

36 Mattei MG, Mattei JF, Ayme S, Giraud F (1979) Dicentric Robertsonian translocation in man. Hum Genet 50: 33–38

37 Mikkelsen M, Basli A, Poulsen H (1980) Nucleolus organizer regions in translocations involving acrocentric chromosomes. Cytogenet Cell Genet 26: 14–21

38 Obara Y (1982) Comparative analysis of karyotypes in the Japanese mustelids, *Mustela nivalis namiyei* and *M. erminea nippon*. J Mammal Soc Japan 9: 59–69

39 Obara Y, Miyai T (1981) A preliminary study on the sex chromosome variation in the Japanese house shrew, *Suncus murinus riukiuanus*. Jpn J Genet 56:365–371

40 Obara Y, Saitoh K (1977) Chromosome studies in the Japanese vespertilionid bats: IV. Karyotypes and C-banding pattern of *Vespertilio orientalis*. Jpn J Genet 52: 159–161

41 Obara Y, Saitoh K (1977) Some cytogenetic and cell physiologic aspects of a chiropteran cell line. Sci Rep Hirosaki Univ 24: 73–80

42 Obara Y, Tomiyasu T, Saitoh K (1976) Chromosome studies in the Japanese vespertilionid bats. I. Karyotypic variations in *Myotis macrodactylus* Temminck. Jpn J Genet 51: 201–206

43 Obara Y, Tomiyasu T, Saitoh K (1976) Chromosome studies in the Japanese vespertilionid bats. II. G-banding pattern of *Pipistrellus abramus* Temminck. Proc Japan Acad 52(B): 383–386

44 Obara Y, Tomiyasu T, Saitoh K (1976) Chromosome studies in the Japanese vespertilionid bats. III. Preliminary observation of C-bands in the chromosomes of *Pipistrellus abramus* Temminck. Sci Rep Hirosaki Univ 23: 39–42

45 Patton JC, Baker RJ (1978) Chromosomal homology and evolution of phyllostomatoid bats. Syst Zool 27: 449–462

46 Rushton AR (1970) Cytotaxonomy and chromosomal evolution of the bats. Ann Genet Sel Anim 2: 457–479

47 Stahl A, Luciani M, Hartung M, Devictor M, Berge-Lefrang JL, Guichaous M (1983) Structural basis for Robertsonian translocations in man: Association of ribosomal genes in the nucleolar fibrilar center in meiotic spermatocytes and oocytes. Proc Natl Acad Sci USA 80: 5946–5950

48 Sumner AT (1972) A simple technique for demonstrating centromeric heterochromatin. Exp Cell Res 75: 304–306

49 Sumner AT, Evans HJ, Buckland RA (1971) New technique for distinguishing between human chromosomes. Nature New Biol 232: 31–32

50 Volleth M (1985) Chromosomal homologies of the genera *Vespertilio, Plecotus* and *Barbastella* (Chiroptera: Vespertilionidae). Genetica 66: 231–236

51 Volleth M (1987) Differences in the location of nucleolus organizer regions in European vespertilionid bats. Cytogenet Cell Genet 44: 186–197

52 Volleth M, Yong HS (1987) *Glischropus tylopus*, the first known old-world bat with an X-autosome translocation. Experientia 43: 922–924

53 White MJD (1978) Modes of speciation. WH Freeman and Co, San Francisco, 455pp

54 Yamakage K, Nakayashiki N, Hasegawa J, Obara Y (1985) G-, C- and NOR-banding patterns on the chromosomes of the Japanese grass vole, *Microtus montebelli montebelli*, with special attention to the karyotypic comparison with the root vole, *M. oeconomus*. J Mammal Soc Japan 10: 209–220

55 Yoshida MA, Takagi N, Sasaki M (1983) Karyotypic kinship between the blue fox (*Alopex lagopus* Linn.) and silver fox (*Vulpes vulpes* Desm.). Cytogenet Cell Genet 35: 190–194

56 Yoshiyuki M (1989) A systematic study of the Japanese Chiroptera. Nat Sci Mus Tokyo, vi+242 pp

57 Yosida TH (1978) A preliminary note on silver-stained nucleolar organizer regions in the black and Norway rats. Proc Japan Acad 54(B): 353–358

58 Yosida TH (1979) A comparative study on nucleolus organizer regions (NORs) in 7 *Rattus* species with special emphasis on the organizer differentiation and species evolution. Proc Japan Acad 55 (B): 481–486

59 Zankl H, Hahmann S (1978) Cytogenetic examination of the NOR activity in a proband with 13/13 translocation and in her relatives. Hum Genet 43: 275–279

ZOOLOGICAL SCIENCE 11: 485–490 (1994)

Acoustic Characteristics of Treefrogs from Sichuan, China, with Comments on Systematic Relationship of *Polypedates* and *Rhacophorus* (Anura, Rhacophoridae)

MASAFUMI MATSUI[1] and GAN-FU WU[2]

[1]*Graduate School of Human and Environmental Studies, Kyoto University, Sakyo-ku, Kyoto 606, Japan, and* [2]*Chengdu Institute of Biology, Academia Sinica, P. O. Box 416, Chengdu, Sichuan, People's Republic of China*

ABSTRACT—Advertisement call characteristics of *Polypedates chenfui*, *P. dugritei*, and *P. omeimontis*, all from Sichuan, China, are described. Calls of the three species differ considerably from each other both in temporal and frequency patterns. Acoustically, these three species cannot be differentiated from some *Rhacophorus* species from Japan and Taiwan, and the systematic relationship of *Polypedates* and *Rhacophorus* needs reassessment.

INTRODUCTION

Rhacophorus Kuhl et van Hasselt, 1822 and *Polypedates* Tschudi, 1838 represent two major genera among the treefrog subfamily Rhacophorinae [4]. There are, however, conflicting opinions about the taxonomic relationship of these two genera. *Polypedates* has long been synonymized with *Rhacophorus* [13,18], but Liem [12], in revising the family Rhacophoridae, split the two genera on the basis of adult morphology. Later, Dubois [3] placed *Polypedates* as a synonym of *Rhacophorus* after reinterpreting Liem's data on adults [12] and utilizing Inger's data on tadpoles [6]. On the other hand, Jiang et al. [7] considered that *Polypedates* and *Rhacophorus* are separate lineages in China. Similarly, Channing [1] reanalyzed Liem's data [12] and showed that the two genera were not sister groups. Thus there is at present disagreement about the taxonomic relationship of *Polypedates* and *Rhacophorus*.

On the other hand, non-morphological characteristics including acoustic ones have been studied on some members of these two genera, and their bearing on systematics has been discussed [5, 9, 10, 11, 15]. The data hitherto accumulated, however, are still insufficient to utilize for outlining phylogenetic relationship of *Polypedates* and *Rhacophorus*. Regarding acoustic data of east Asian species, the knowledge of members from Japan and Taiwan is considerable, but nothing is known about Chinese members. Although China is famous for its rich amphibian fauna [21], very few studies have been made on the call characteristics of frog species [16, 17], and members of *Polypedates* and *Rhacophorus* are not exceptions. In order to better understand systematic relationship of these two genera, acoustic data on Chinese members are badly needed. In this communication, we will report acoustic characteristics of three rhacophorine species from China, i. e., *Polypedates omeimontis* Stejneger, 1924, *P. chenfui* (Liu, 1945), and *P. dugritei* David, 1871, and discuss phylogenetic relationship of the two genera.

MATERIALS AND METHODS

Recordings of calls were made in the field by the junior author using a cassette tape recorder (Sony WM-D3) with an external microphone (Sony ECM-909A). Ambient temperature was measured at the time of recording.

Calls of *P. chenfui* were recorded on Mt. Emei-shan at the altitude of 1400 m, Sichuan, China, on 13 May 1993. Air temperature at the time of recording was 13.0°C. Males were observed to call simultaneously with *P. omeimontis*. For the latter species, calls were recorded on Mt. Emei-shan at the altitude of 1400 m, on 13 and 15 May 1993. Air temperatures at the time of recording were 13.0°C and 11.0°C, respectively. Calls of *P. dugritei* were recorded on Mt. Wa-shan, Sichuan, China, at the altitude of 1600 m on 1 June 1993, and at the altitude of 2600 m on 2 June 1993. Air temperature at the time of each recording was 8.0°C and 4.0°C, respectively. For comparisons, data of the following species of Japanese and Taiwanese *Rhacophorus* are used: *R. arboreus* (Honshu, Japan); *R. schlegelii* (Honshu, Japan); *R. v. viridis* (Okinawajima and Kumejima, eastern Ryukyus); *R. owstoni* (Ishigakijima and Iriomotejima, western Ryukyus); *R. prasinatus* (northern Taiwan).

The recorded calls were analyzed using computer programs, SoundEdit Vers. 2 or SoundEdit Pro (MacroMind-Paracomp, Inc.) by a Macintosh computer. Advertisement calls as defined by Wells [19] were compared among the three species. In the following description, note means a pulse group, note duration the time from the beginning of the first pulse to the end of the last pulse in a note, and pulse repetition rate number of pulses per second. In order to examine relationships among call parameters, analysis-of-covariance (ANCOVA) was performed. Kruskal-Wallis tests with nonparametric multiple comparisons (=Dunn test [20]) or Mann-Whitney *U* tests were performed to detect the presence or absence of differences in the frequency distributions. The significance level was set at 0.05.

Accepted May 16, 1994
Received Feburary 7, 1994

TABLE 1. Call characteristics of three Chinese rhacophorid species (Mean±1SD, followed by sample size)

Species	Note duration (sec)	Pulse rate (N of pulse/sec)	Initial frequency (Hz)	Climax frequency (Hz)
Polypedates dugritei	4.0°C			
10 pulsed note	0.700	14.29	1500	1600
	1	1	1	1
11 pulsed note	0.895	12.30	1275	1525
	2	2	2	2
12 pulsed note	0.970±0.046	12.39±0.60	1391.7±159.4	1675.0± 41.8
	6	6	6	6
13 pulsed note	0.965±0.025	13.48±0.34	1445.0±170.3	1657.5± 39.2
	10	10	10	10
14 pulsed note	1.015	13.80	1350	1625
	2	2	2	2
Polypedates dugritei	8.0°C			
2 pulsed note	0.075	26.67	1450	2500
	1	1	1	1
3 pulsed note	0.190	15.79	1150	1450
	1	1	1	1
6 pulsed note	0.310	19.54	1412.5	1875
	2	2	2	2
7 pulsed note	0.445	15.83	1075	1750
	2	2	2	2
8 pulsed note	0.517	15.50	1191.7	1766.7
	3	3	3	3
9 pulsed note	0.510±0.029	17.69±0.97	1192.8±196.7	1764.3± 69.0
	7	7	7	7
10 pulsed note	0.637±0.023	15.72±0.58	1133.3± 57.7	1900.0±132.3
	3	3	3	3
11 pulsed note	0.700	15.71	1050	1900
	1	1	1	1
Polypedates omeimontis	11.0°C			
3 pulsed note	0.318±0.011	9.45±0.32	865.8± 30.1	936.7± 21.6
	6	6	6	6
4 pulsed note	0.460±0.022	8.71±0.41	865.5± 21.2	977.1± 49.8
	42	42	42	42
Polypedates omeimontis	13.0°C			
2 pulsed note	0.166±0.015	12.12±1.16	817.5± 53.8	827.5± 38.6
	4	4	4	4
3 pulsed note	0.325±0.018	9.25±0.52	804.6± 35.5	884.6± 68.1
	13	13	13	13
4 pulsed note	0.439±0.007	9.11±0.14	845.4± 32.3	913.1± 48.9
	13	13	13	13
5 pulsed note	0.584	8.56	770	850
	1	1	1	1
Polypedates chenfui	13.0°C			
2 pulsed note	0.158	12.64	2000	2100
	1	1	1	1
4 pulsed note	0.385±0.027	10.44±0.70	2120.0±102.1	2348.8± 53.6
	8	8	8	8
5 pulsed note	0.514±0.018	9.74±0.33	2082.1±133.5	2334.4±132.7
	34	34	34	34
6 pulsed note	0.645±0.042	9.35±0.61	2033.3±111.8	2318.9±125.8
	9	9	9	9

RESULTS

Polypedates chenfui

The call recorded at 13.0°C was a well pulsed note (Fig. 1B) and included two to six pulses. The note duration increased with increasing number of pulses, and the mean duration varied from 0.158 sec in the note with two pulses to 0.645 sec in the note with six pulses (Table 1). The duration differed significantly among the notes with different number of pulse (Dunn's multiple comparison test, $P<0.05$). The relationship of the number of pulse (X) and the note duration (Y) was expressed as $Y=0.126X-0.116$ ($N=52$, $r=0.965$, $P<0.01$). The pulse repetition rate tended to decrease with the increment of the pulse number, means varying from 12.64 in the note with two pulses to 9.35 in the note with six pulses. The rate was significantly greater in the note with four pulses than in the notes with five or six pulses (Dunn's multiple comparison test, $P<0.05$), but the latter two did not differ from each other. The relationship between the number of pulse (X) and the pulse repetition rate (Y) was $Y=-0.682X+13.221$ ($N=52$, $r=-0.718$, $P<0.01$). Each pulse had harmonics, and a slight frequency modulation was seen within a note (Fig. 1A). The mean dominant frequency in the initial pulse was about 2000–2120 Hz, but it slightly increased to 2100–2349 Hz in the climax pulse. In the climax pulse, the second dominant frequency was about 6000–6500 Hz, and six harmonic bands in total were apparent between 0–7500 Hz. Average harmonic interval, therefore, was about 1250 Hz, and this value corresponded to the fundamental frequency. The first dominant frequency, therefore, was the second harmonic and the second corresponded to the fifth harmonic of the spectrogram. The dominant frequency of either the initial or the climax pulses did not differ significantly among the notes with different number of pulse (Kruskal-Wallis test, $P>0.05$). Thus, there were insignificant correlations between the number of pulse (X) and dominant frequencies (Y) of either the initial ($r=-0.111$, $P>0.05$) or the climax pulse ($r=0.097$, $P>0.05$).

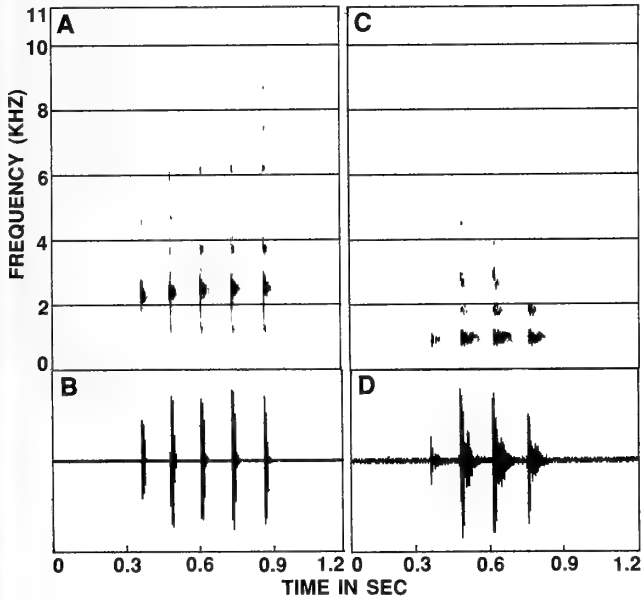

FIG. 1. Sonagrams (A, C) and sound wave forms (B, D) of advertisement calls of *Polypedates chenfui* (A, B, recorded at 13.0°C) and *P. omeimontis* (C, D, recorded at 11.0°C).

Polypedates omeimontis

Calls of *P. omeimontis* included several call types, but only the advertisement call [8, 19] is considered here. The advertisement call was a well pulsed note (Fig. 1C, D) and at 11.0°C, it included three or four pulses. The mean note duration of 0.318 sec in the note with three pulses was significantly shorter than 0.460 sec in the four pulsed note (Mann-Whitney U test, $P<0.05$). The mean pulse repetition rate in the three pulsed note (9.45) was significantly larger than that in the four-pulsed note (8.71; Mann-Whitney U test, $P<0.05$). Each pulse had harmonics, but they are usually not clear in the initial pulse. A weak frequency modulation was seen within a note. Parameters of frequencies did not differ between notes with three and four pulses (Mann-Whitney U test, $P>0.05$). The dominant frequency in the initial pulse was about 866 Hz, but it increased to 936–977 Hz in the climax pulse. In the climax pulse, the second dominant frequency was about 2300 or 2900 Hz. Seven harmonic bands in total could be traced between 0–7350 Hz. Average harmonic interval was about 1050 Hz and corresponded to the fundamental frequency. The first dominant frequency was judged to be the fundamental and the second corresponded to the second or third harmonic of the spectrogram. The dominant frequency in either the initial or the climax pulse did not differ between the notes with three and four pulses (Mann-Whitney U test, $P>0.05$).

The calls recorded at 13.0°C had basically similar traits, but the number of pulses included in a note tended to be smaller than in 11.0°C (median=three pulses in 13.0°C, compared with four in 11.0°C). The mean note durations varied from 0.166 sec in the note with two pulses to 0.584 sec in the note with five pulses (Table 1), but they were statistically not different (Kruskal-Wallis test, $P>0.05$). Similarly, the note durations did not differ significantly between the notes with the same number of pulses, and recorded at 13°C and 11.0°C (Mann-Whitney U test, $P>0.05$). The pulse repetition rates varied from 12.12 in the note with two pulses to 8.56 in the note with five pulses, but their difference was insignificant (Kruskal-Wallis test, $P>0.05$). In the four-pulsed notes, repetition rate in 13.0°C (9.11) was larger than that in 11.0°C (8.71; Mann-Whitney U test, $P<0.05$). The dominant frequency slightly increased from 777–845 Hz in the initial pulse to 828–913 Hz in the climax pulse. Dominant frequencies in the initial and climax pulses were significantly lower in some calls recorded at 13.0°C than in 11.0°C (initial pulse in the three-pulsed note, and climax pulse in the four-pulsed note: Mann-Whitney U test, $P<0.05$).

Comparisons with calls of syntopic *P. chenfui* simultaneously recorded at 13.0°C, using the four-pulsed note resulted in the followings. The note duration of *P.*

omeimontis was significantly longer than that of *P. chenfui* (Mann-Whitney *U* test, $P<0.05$), and in the pulse repetition rate *P. omeimontis* was slightly smaller than in *P. chenfui* (Mann-Whitney *U* test, $P<0.05$). Much greater interspecific differences were found in frequency characteristics. The dominant frequency in the climax pulse was significantly lower in calls of *P. omeimontis* than in *P. chenfui* (Mann-Whitney *U* test, $P<0.01$), so was the dominant frequency in the initial pulse (Mann-Whitney *U* test, $P<0.01$).

The relationship of the number of pulse (X) and the note duration (Y) was expressed as $Y=0.166X-0.201$ ($N=48$, $r=0.762$, $P<0.01$) and $Y=0.131X-0.079$ ($N=31$, $r=0.986$, $P<0.01$) in the calls recorded at 11°C and 13°C, respectively. The slope of the former equation was significantly steeper than the latter (ANCOVA, $P<0.05$). The latter slope was not significantly different from syntopic *R. chenfui*. The number of pulse (X) and the pulse repetition rate (Y) had the relationships of $Y=-5.951X+32.773$ ($N=48$, $r=-0.660$, $P<0.01$) and $Y=-1.043X+13.038$ ($N=31$, $r=-0.694$, $P<0.01$) in the calls recorded at 11°C and 13°C, respectively. The slope of the former regression line was significantly steeper than that of the latter (ANCOVA, $P<0.05$), which in turn was insignificantly different from the slope in syntopic *R. chenfui* (ANCOVA, $P>0.05$). In the calls recorded at 11.0°C, there were significant correlations between the number of pulse (X) and dominant frequencies (Y) of both the initial ($Y=-86.167X+1226.72$, $N=48$, $r=-0.495$, $P<0.01$) and the climax pulse ($Y=-53.048X+1197.25$, $N=48$, $r=-0.353$, $P<0.01$), but correlations were insignificant in the calls recorded at 13.0°C ($P>0.05$).

Polypedates dugritei

The call was again a well pulsed note (Fig. 2B, D) and at 4.0°C, it included ten to 14 pulses. The note duration tended to increase with increasing number of pulses, and the mean duration varied from 0.700 sec in the note with ten pulses to 1.015 sec in the note with 14 pulses. However, the duration did not differ significantly (Kruskal-Wallis test, $P>0.05$) among the notes with different number of pulses, probably because of small sample size. The mean pulse repetition rate varied from 12.30 to 14.29 but showed no correlation with the number of pulses ($r=0.378$, $P>0.05$). Each pulse had clear harmonics, and a frequency modulation was seen within a note. The dominant frequency in the initial pulse was about 1275–1500 Hz, but it increased to 1525–1675 Hz in the climax pulse, and slightly decreased to about 1500 Hz in the final pulse. In the climax pulse, the second dominant frequency was about 4500–4800 Hz. A total of seven harmonic bands could be traced between 0–11000 Hz, and average harmonic interval was about 1570 Hz. Thus, the first dominant frequency was the fundamental and the second corresponded to the third harmonic.

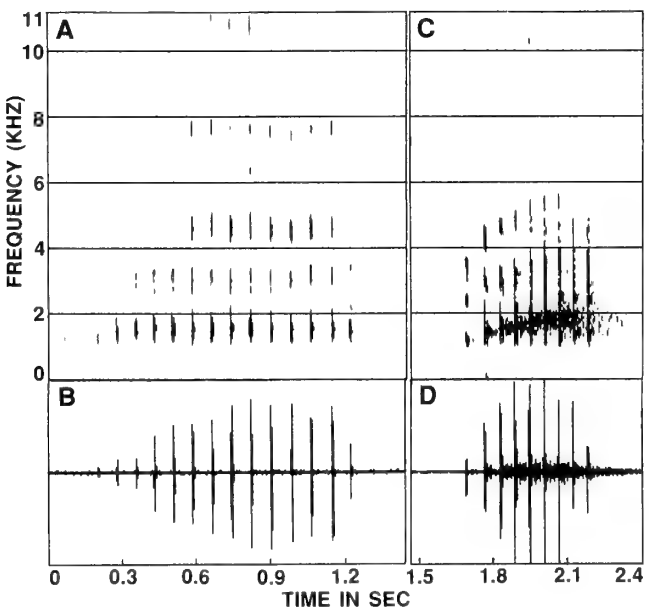

FIG. 2. Sonagrams (A, C) and sound wave forms (B, D) of advertisement calls of *Polypedates dugritei* (A, B, recorded at 4.0°C; C, D recorded at 8.0°C).

The calls recorded at 8.0°C (Fig. 2C, D) had basically similar traits, but a note tended to have smaller number of pulses (median=nine in 8.0°C and 13 in 4.0°C). Note durations seemed to be shorter than in 4.0°C, but the limited number of corresponding samples prohibited statistical comparisons. The mean note durations varied from 0.075 sec in the note with two pulses to 0.700 sec in the note with 11 pulses (Table 1), but they did not differ significantly in duration (Dunn's multiple comparison test, $P>0.05$), again probably due to small sample size. The pulse repetition rates varied from 15.50 to 26.67, but the mean was insignificantly different from that in 4.0°C (Dunn's multiple comparison test, $P>0.05$). The dominant frequency slightly increased from 1050–1450 Hz in the initial pulse to 1450–2500 Hz in the climax pulse. In the climax pulse, three harmonic bands were apparent at about 1850, 5600, and 9300 Hz. The harmonic interval was thus judged to be about 1850 Hz, and this corresponded to the fundamental and the first dominant frequency. The second and the third dominant frequencies corresponded to the third and fifth harmonic, respectively. The dominant frequency in either the initial or the climax pulse did not differ among the notes with different number of pulses regardless of the temperature difference (Dunn's multiple comparison test, $P>0.05$).

The relationship of the number of pulse (X) and the note duration (Y) was expressed as $Y=0.052X+0.303$ ($N=21$, $r=0.726$, $P<0.01$) and $Y=0.065X-0.042$ ($N=20$, $r=0.963$, $P<0.01$) in the calls recorded at 4.0°C and 8.0°C, respectively. Similarly, the relationship between the number of pulse (X) and the pulse repetition rate (Y) was expressed as $Y=-0.669X+22.637$ ($N=20$, $r=-0.557$, $P<0.01$) in the calls recorded at 8.0°C, but, as noted above, the relationship was statistically insignificant in the calls recorded at 4.0°C. In the calls recorded at either 4.0°C or 8.0°C, there were insignificant correlations between the number of pulse (X) and dominant frequencies (Y) of either the initial ($r=0.076$, $P>0.05$ and $r=-0.336$, $P>0.05$) or the climax pulse ($r=0.326$, $P>0.05$ and $r=-0.220$, $P>0.05$).

Interspecific comparisons

Although some parameters, such as the dominant frequency, did not vary with variant temperatures, others, such as the pulse repetition rate, varied in relation to temperatures. Interspecific comparisons of acoustic parameters, therefore, should be made by adjusting parameters at a standard temperature. Because calls of *P. chenfui* and *P. omeimontis* were recorded at 13°C, values of parameters at this temperature were calculated from the regression lines for *P. dugritei*. Figure 3 shows the relationships of the pulse rate and dominant frequency of the climax pulse among the above three Chinese species and some Japanese and Taiwanese species (Table 2). As clearly seen, the three Chinese species differ from each other completely. *Polypedates dugritei* had a high repetition rate and moderately high frequency. *Polypedates omeimontis*, on the other hand, had low repetition rates and low frequencies, which are in contrast to *P. chenfui* that was characterized by low repetition rates and high frequencies. *Polypedates chenfui* was placed near *R. schlegelii* and *R. viridis*, while *P. omeimontis* lay near *R. owstoni* and *R. arboreus*. *Rhacophorus prasinatus* was closest to *P. dugritei* on this graph.

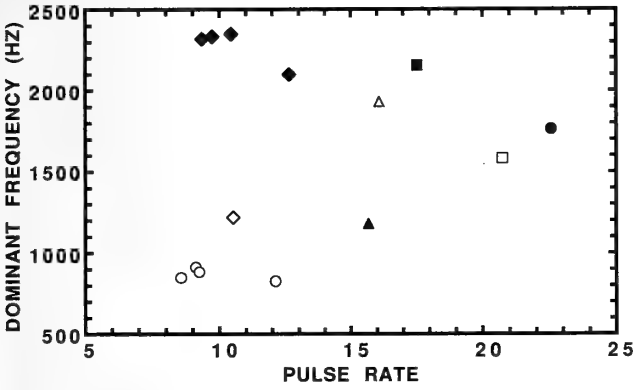

FIG. 3. Relationships of pulse repetition rate and dominant frequency of the climax pulse in the calls of *Polypedates chenfui* (closed diamond), *P. dugritei* (closed circle), *P. omeimontis* (open circle), *Rhacophorus schlegelii* (open triangle), *R. arboreus* (closed triangle), *R. viridis* (closed rectangle), *R. owstoni* (open diamond), and *R. prasinatus* (open rectangle). Values are adjusted to the ambient temperature of 13.0°C in all the species, except for *P. chenfui* and *P. omeimontis*, both of which represent the raw data.

TABLE 2. Parameters for regression lines Y=aX+B, where X =air temperature (in °C) and Y=pulse repetition rate, in *Polypedates dugritei* and some Japanese and Taiwanese species of *Rhacophorus* (data from Matsui, unpublished)

	a	B	r
P. dugritei	1.049	8.930	0.735
R. schlegelii	1.584	−4.554	0.944
R. viridis	1.570	−2.859	0.927
R. arboreus	1.460	−3.302	0.850
R. owstoni	0.452	4.645	0.804
R. prasinatus	1.583	0.156	0.994

DISCUSSION

From a cladistic analysis of adult morphology, Jiang et al. [7] classified 14 Chinese rhacophorid species into five genera, which classification is essentially the same as that proposed by Liem [12]. In their classification, all the three species treated in the present paper were classified as *Polypedates*, together with *P. dennysi*, *P. hungfuensis*, *P. nigropunctatus*, *P. leucomystax* (type species of the genus), and *P. mutus*. On the other hand, *R. rhodopus* and *R. reinwardtii* (type species of the genus) were placed in *Rhacophorus*. According to Jiang et al. [7], these two genera commonly possess Y-shaped terminal phalange, unopposable hand, and lack anterior process of hyale, but are distinguished from each other by heart-shaped intercalary cartilage, no skin fold, slightly or half webbed hand, and low vegetation habitat of *Polypedates*, in contrast to a wing-shaped intercalary cartilage, a broad skin fold, full hand webbing, and inhabiting on tall trees of *Rhacophorus*.

These differences, however, are not necessarily reliable, because all the Japanese and Taiwanese species currently assigned to *Rhacophorus* lack broad skin fold and full hand webbing [14]. Also, the habitat of an anuran species is very difficult to specify, and the above Chinese species are not sharply differentiated in this character. As to the shape of the intercalary cartilage, available information is too meager to assess whether or not it could be appropriately used for splitting the two genera.

Calls of the three species here reported completely differed from the call of *Polypedates leucomystax* [15] or from those of several *Rhacophorus* species from Southeast Asia [2]. Rather, the calls of the three species fairly resembled calls of some Japanese and Taiwanese species of *Rhacophorus* (see Fig. 3). Of the three Chinese species treated here, *P. omeimontis* and *P. chenfui* are syntopic on Mt. Emei-shan. The two species differ greatly in morphology and ecology; *P. omeimontis* is larger and lays an egg nest on the tree or grass [13], while *P. chenfui* is small and breeds on land. As shown above, these species differ greatly in acoustic characteristics, *P. omeimontis* with much lower frequency and slightly longer note duration. Interestingly, similar morphological, ecological, and acoustic relationships are found in the Japanese rhacophorids, *R. arboreus* and *R. schlegelii* from the Japan mainland [14]. The oviposition site of the larger species, *R. arboreus* is on the tree or on the grass, whereas the syntopic, smaller *R. schlegelii* lays an egg mass under the ground and never on the tree [14]. As shown in Fig. 3, calls of *R. arboreus* and *P. omeimontis* have similar temporal and frequency characteristics, so do calls of *R. schlegelii* and *P. chenfui*. Although another species, *R. owstoni* also lay close to *P. omeimontis* in Fig. 3, their calls are actually quite dissimilar. *Rhacophorus owstoni* occurs in the western Ryukyus, and has characteristically long calls that are composed of slow and fast units [9]. The two unit calls have variant pulse rates, and only the initial, slow unit resembles the call of *P. omeimontis*.

The relationships of the above allopatric species pairs, i. e., *P. chenfui* vs. *R. schlegelii* and *P. omeimontis* vs. *R. arboreus*, may be regarded as reflecting results of ecological convergence, but actual close phylogenetic relationships of these pairs are also plausible. This is inferred from the fact that there are some species pairs of *Rhacophorus* that are allopatric in distribution, similar in call characteristics, and deemed closely related phylogenetically. *Rhacophorus moltrechti* from Taiwan and *R. owstoni* from the western Ryukyus, or *R. schlegelii* from Japan mainland and *R. viridis* from the eastern Ryukyus are examples of such pairs [11].

Anyhow, the available evidence indicates that at least three Chinese species of *Polypedates* reported here cannot be differentiated acoustically from some *Rhacophorus* species from Japan and Taiwan. Acoustic studies of species from wider regions will surely contribute to better understanding the relationship of *Polypedates* and *Rhacophorus*.

ACKNOWLEDGMENTS

T. Hikida helped laboratory work and critically read the manuscript. This study was partly supported by National Geographic Society (No. 4505–91) to MM.

REFERENCES

1 Channing A (1989) A re-evaluation of the phylogeny of Old World treefrogs. S Afr Tydskr Dierk 24: 116–131

2 Dring JCM (1979) Amphibians and reptiles from northern Trengganu, Malaysia, with descriptions of two new geckos: *Cnemaspis* and *Cyrtodactylus*. Bull Br Mus Nat Hist (Zool) 34: 181–241

3 Dubois A (1986) Miscellanea taxinomica batrachologica (I). Alytes 5: 7–95

4 Frost DR (1985) Amphibian Species of the World: A Taxonomic and Geographical Reference. Allen Press, Lawrence

5 Heyer WR (1971) Mating call of some frogs from Thailand. Fieldiana: Zool 58: 61–82

6 Inger RF (1985) Tadpoles of the forested regions of Borneo. Fieldiana: Zool (New Ser) 26: 1–89

7 Jiang S-P, Hu S-Q, Zhao E-M (1987) The approach of the phylogenetic relationship and the supraspecific classification of 14 Chinese species of treefrogs (Rhacophoridae). Acta Herpetol Sinica 6: 27–42 (in Chinese, with English abstract)

8 Kasuya E, Kumaki T, Saito T (1992) Vocal repertoire of the Japanese treefrog, *Rhacophorus arboreus* (Anura: Rhacophoridae). Zool Sci 9: 469–473

9 Kuramoto M (1975) Mating calls of Japanese tree frogs (Rhacophoridae). Bull Fukuoka Univ Educ III 24: 67–77

10 Kuramoto M (1986) Call structures of the rhacophorid frogs from Taiwan. Sci Rep Lab Amphibian Biol Hiroshima Univ 8: 45–68

11 Kuramoto M, Utsunomiya T (1981) Call structures in two frogs of the genus *Rhacophorus* from Taiwan, with special reference to the relationships of rhacophorids in Taiwan and the Ryukyu Islands. Jpn J Herpetol 9: 1–6 (in Japanese, with English abstract)

12 Liem SS (1970) The morphology, systematics and evolution of the Old World treefrogs (Rhacophoridae and Hyperoliidae). Fieldiana: Zool 57: 1–145

13 Liu C-C, Hu S-C (1961) Chinese Tailless Batrachians. Kexue-chubanshe, Beijing (in Chinese)

14 Maeda N, Matsui M (1989) Frogs and Toads of Japan. Bunichi Sogo Shuppan, Tokyo (in Japanese, with English abstract)

15 Matsui M, Seto T, Utsunomiya T (1986) Acoustic and karyotypic evidence for specific separation of *Polypedates megacephalus* Hallowell from *P. leucomystax* (Boie). J Herpetol 20: 483–489

16 Matsui M, Wu G-F, Yong H-S (1993) Acoustic characteristics of three species of the genus *Amolops* (Amphibia, Anura, Ranidae). Zool Sci 10: 691–695

17 Mou Y, Zhao E-M (1992) A study of vocalization on thirteen species of four genera, Anura. In "Collected Papers on Herpetology" Ed by Y-M Jiang, Sichuan Publishing House of Science and Technology, Chengdu, pp 15–26 (in Chinese, with English abstract)

18 Nakamura K, Ueno S-I (1963) Japanese Reptiles and Amphibians in Colour. Hoikusha, Osaka (in Japanese)

19 Wells KD (1977) The courtship of frogs. In "The reproductive Biology of Amphibians" Ed by DH Taylor, SI Guttman, Plenum Press, New York, pp 233–262

20 Zar JH (1984) Biostatistical Analysis, 2nd edition. Prentice-Hall, New Jersey

21 Zhao, E-M, Adler K (1993) Herpetology of China. Contr Herpetol 10: 1–522

ZOOLOGICAL SCIENCE 11: 491–494 (1994)

[RAPID COMMUNICATION]

Glutamate Substitution for Glutamine at Position 5 or 6 Reduces Somatostatin Action in the Eel Intestine

TOSHIHIRO UESAKA[1], KEIICHI YANO[2], MOTOO YAMASAKI[2] and MASAAKI ANDO[1]*

[1]*Laboratory of Physiology, Faculty of Integrated Arts and Sciences, Hiroshima University, Higashi-Hiroshima, Hiroshima 724, and*
[2]*Tokyo Research Laboratories, Kyowa Hakko Kogyo Co. Ltd, 3-6-6 Asahimachi, Machidashi, Tokyo 194, Japan*

ABSTRACT—Isolating a new somatostatin-like peptide from eel gut, the active residues to potentiate somatostatin action in the eel intestine were determined. In the newly-isolated peptide, the 5th or 6th Gln of the eel somatostatin (eSS-25II) was replaced with Glu. Although this peptide also enhanced the short-circuit current (I_{sc}) across the intestine of the seawater eel, higher concentrations (approximately 30 fold) were required to obtain the same effects as eSS-25II. Since the I_{sc} is due to active Cl^- transport, this indicates that a structure formed by Gln-Gln residues at position 5 and 6 potentiates the somatostatin action to enhance ion and water transport across the intestine of the eel.

INTRODUCTION

Various somatostatin-related peptides have been isolated from diverse vertebrates. They have similar sequences containing 14 amino acids with a disulphide linkage between two Cys residues. In addition, in many vertebrates including eel, N-terminally extended somatostatins were also found [4, 5, 8, 14]. However, the physiological significance of these large somatostatins is controversial. In gastric secretion, the inhibitory effect of somatostatin was greater in short somatostatin (SS-14) than in large form (SS-28) [6, 7, 9]. In contrast, growth hormone secretion from pituitary cells was inhibited more efficiently by SS-28 rather than by SS-14 [11].

Recently, we demonstrated that a large somatostatin (eSS-25II) isolated from the eel gut enhanced NaCl and water absorption across the intestine at lower concentrations than the short somatostatin (eSS-14II) [13], indicating that the 11 N-terminal amino acid residues potentiate somatostatin action in the eel intestine. However, it is not determined which residue(s) among the 11 amino acids contribute(s) to the potentiation. If a single amino acid substitution alters potency of a polypeptide, that residue must contribute to the activity. Fortunately, such a single-substituted somatostatin was isolated from the eel gut. A primary structure of the newly-isolated peptide was characterized at first, and the potency was compared between this peptide and the eSS-25II.

Accepted April 28, 1994
Received March 8, 1994

* To whom correspondence should be addressed.

MATERIALS AND METHODS

Purification

Bioactive peptides were extracted with 0.1% trifluoroacetic acid (TFA) after boiling the guts (593 g) of 300 eels, *Anguilla japonica*, as described previously [13]. The extract was evaporated to dryness. The dried material was dissolved in 0.1% TFA (50 ml) and forced through disposable Sep-Pak C_{18} cartridges (Millipore). The retained material was eluted with 50% acetonitrile containing 10% 2-propanol and 0.1% TFA, applied to a column of Toyopearl HW-40F (2.6 cm×100 cm; Tosoh) and eluted with 1 M acetic acid and 10% 2-propanol at a rate of 1.5 ml/min. An aliquot of each fraction (18 ml) was assayed for its ability to enhance the transepithelial potential difference (PD) across the eel intestine. Bioactive fractions were pooled and subjected to HPLC separation (LC-6AD system, Shimadzu) with a C_8 reverse-phase column (Asahipak C8P-50, Asahi Chemical Industry). The retained material was eluted with a 60-min linear gradient of 0% to 60% acetonitrile containing 10% 2-propanol and 0.1% TFA, and each fraction was bioassayed. Bioactive fractions were further applied to a C_{18} reverse-phase column (TSKgel ODS-80T_M, Tosoh) and eluted with a 100-min linear gradient of 0% to 20% acetonitrile containing 5% 2-propanol and 0.1% TFA. The active fractions were applied to a cation-exchange column (TSKgel CM-5PW, Tosoh) and eluted with a 35-min linear gradient of 0–0.35 M NaCl in 20 mM phosphate buffer (pH 6.7) containing 10% 2-propanol (see Fig. 1A). Bioactive peak was rechromatographed on a C_{18} reverse-phase column (TSKgel ODS-80T_M) with a 50-min linear gradient of 5% to 15% acetonitrile in 5% 2-propanol and 0.1% TFA. Final purification was performed using the same column under isocratic condition (see Fig. 1B).

Amino acid compositions were determined with a PICO-TAG amino acid analysis system (Millipore). Amino acid sequence analysis of the peptide was carried out by automated Edman degradation with a gas protein sequencer (PPSQ-10, Shimadzu). To determine molecular mass, fast bombardment mass spectrometry (FAB-MS) was performed with JMS-HX110A (Jeol).

Bioassay

An aliquot of each fraction was assayed for its ability to enhance the transepithelial potential difference (PD) across the seawater eel intestine. Details are described elsewhere [2, 13]. Before bioassay, the cultured Japanese eels, weighing about 220 g, were kept in sea water (20°C) for more than 1 week. After decapitation, the intestine was excised and the outer muscle layers were stripped off according to previous methods (1). The mucosal segment (posterior section) was opened and mounted as a flat sheet between two Ussing-type half-chambers with an exposed area of 0.5 cm^2. The tissue was bathed in Krebs bicarbonate Ringer's solution consisting of (mM) 118.5 NaCl, 4.7 KCl, 3.0 $CaCl_2$, 1.2 $MgSO_4$, 1.2 KH_2PO_4 and 24.9 $NaHCO_3$ and containing 5 mM glucose and alanine. The bathing solutions (2.5 ml each) were kept at 20°C and circulated continuously by bubbling with a 95% O_2 : 5% CO_2 gas mixture (pH 7.4). The PD was recorded through a pair of calomel electrodes with a polyrecorder (EPR-151A, Toa Electronics) as the potential of the serosa with respect to the mucosa. To determine the tissue resistance (R_t), rectangular pulses, 30 μA for 500 msec, were applied across the intestinal sheet every 5 min through an isolator (SS-201J, Nihon Kohden) connected to a stimulator (SEN-3301, Nihon Kohden). The I_{sc} was obtained from the ratio of PD to R_t.

RESULTS AND DISCUSSION

Figure 1A shows the elution profile on cation-exchange HPLC for bioactive fractions after partial purification on C_8 and C_{18} reverse-phase HPLC. Two fractions (peaks 1 and 2 eluted at 35 and 26 min, respectively) resulted in enhancement of serosa-negative PD. Previous study (13) has already revealed that peak 1 contains 2 kinds of eel somatostatin (eSS-25I and eSS-25II). Since the peak 2 is apparently far from the peak 1 on the chromatogram, a new substance distinct from eSS-25I and eSS-25II must be contained in the peak 2. Thus we tentatively named it EI-2. The final purification profile of EI-2 is shown in Figure 1B.

Amino acid composition of EI-2 is shown in Table 1. Apparently, the composition profile was similar between EI-2 and eSS-25II, indicating that EI-2 also consists of similar amino acid residues as eSS-25II. As shown in Table 2, the amino acid sequence analysis revealed that the amino acid sequence of EI-2 was almost the same as that of eSS-25II, except for appearance of both Glu and Gln at 5th and 6th cycles. The contents of Glu and Gln were almost identical (1 : 1) at both 5th and 6th cycle. Although the amino acid residues at 14th and 25th cycle were not determined, these residues may be Cys, since Cys was not detected in this sequence analysis. In FAB-MS, a molecular ion peak was obtained at 2859 m/z $(M+H)^+$ in the native EI-2. After reducing the EI-2, the molecular ion peak shifted to 2861 m/z $(M+H)^+$. The two mass increase after reduction seems to indicate an existence of disulphide bond between these two Cys residues in EI-2. Since the molecular ion peak of eSS-25II is 2858 m/z $(M+H)^+$ (13), the one mass increase in EI-2 can be explained by a substitution of Glu for Gln at position 5 or 6 in the eSS-25II. In fact, Glu was detected at position 5 and 6 in the sequence analysis (Table 2), and EI-2 was eluted earlier than the eSS-25II in cation-exchange HPLC (Fig. 1A). The latter phenomenon indicates that EI-2 is more negatively charged than eSS-25II at pH 6.7. The reason why both Glu and Gln are detected at 5th and 6th cycle is not clear yet. A most plausible explanation is that

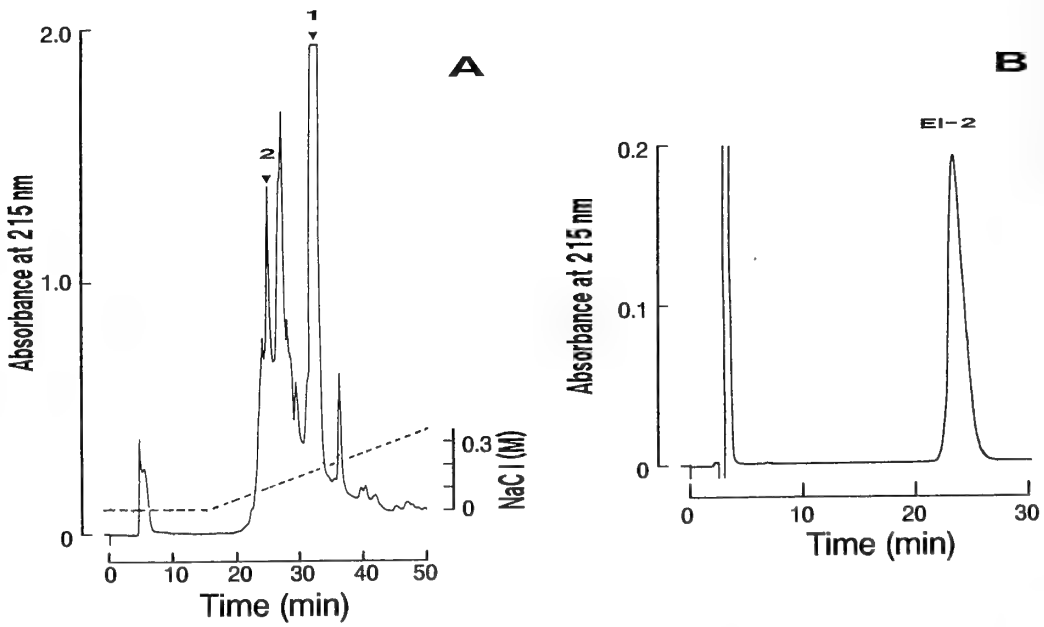

FIG. 1. HPLC purification of EI-2 from the eel guts. A. Cation-exchange chromatogram of the bioactive fractions (peaks 1 and 2) after partial purification by reverse-phase HPLC. The respective fractions were eluted with a 35-min linear gradient of 0–0.35 M NaCl in 10% 2-propanol and 20 mM phosphate buffer (pH 6.7). Flow rate was 0.5 ml/min. EI-2 was isolated from peak 2. From peak 1, two eel somatostatins (eSS-25I and eSS-25II) had been isolated previously [13]. B. The final purification of EI-2 by the reverse-phase HPLC. EI-2 was eluted isocratically with 12% acetonitrile containing 5% 2-propanol and 0.1% TFA (pH 2.2). Flow rate was 0.5 ml/min.

TABLE 1. Amino acid composition of EI-2

	Ser	Val	Asx	Glx	Arg	Lys	Ala	Gly	Cys	Phe	Tyr	Trp	Pro	Thr
EI-2	2.1 (2)	0.9 (1)	2.5 (3)	2.4 (2)	1.7 (2)	2.1 (2)	1.0 (1)	3.1 (3)	ND	0.9 (1)	0.9 (1)	ND	1.0 (1)	1.2 (1)
eSS-25II[a]	2	1	3	3	2	3	1	3	2	1	1	1	1	1

Values indicate the amount of an amino acid relative to Ala, where Ala=1. Parentheses indicate the nearest integer. ND, not determined.

[a]Amino acid composition of eSS-25II was obtained from the primary structure characterized previously [5, 13]

TABLE 2. Automated Edman degradation of EI-2

Cycle NO.	1	2	3	4	5	6	7	8	9	10	11	12	13	14	15	16
Residue	Ser	Val	Asp	Asn	Gln	Glu	Gly	Arg	Glu	Arg	Lys	Ala	Gly		Lys	Asn
Yield (pmol)	30.1	130.4	42.6	84.6	48.3	41.7	65.7	20.2	51.2	24.5	55.2	63.7	46.6	ND	39.8	42.1
					Glu	Gln										
					43.3	59.1										

Cycle NO.	17	18	19	20	21	22	23	24	25
Residue	Phe	Tyr	Trp	Lys	Gly	Pro	Thr	Ser	
Yield (pmol)	45.9	36.7	17.1	24.9	23.3	18.1	6.9	2.8	ND

ND, not determined.

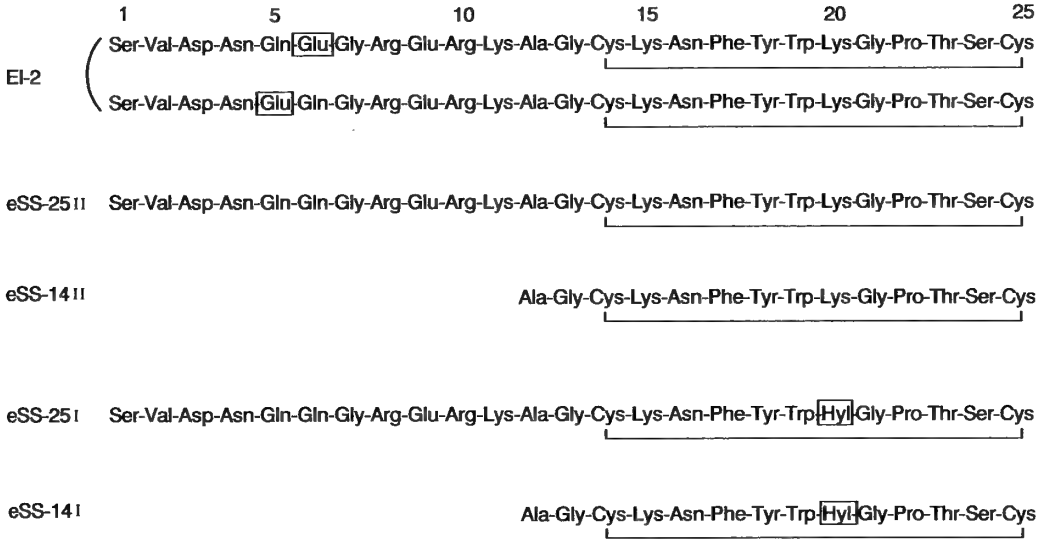

FIG. 2. Primary structures of somatostatin-like peptides isolated from the eel gut. eSS-25II, eSS-14II, eSS-25I and eSS-14I are already characterized in the previous study [13]. The intramolecular disulphide linkage between Cys residues is represented by a line. Amino acid residues that differ from eSS-25II are boxed.

the fraction EI-2 is a mixture of the following structures:

Glu^5eSS-25II: SVDNE QGRER KAGCK NFYWK GPTSC

Glu^6eSS-25II: SVDNQ EGRER KAGCK NFYWK GPTSC

At the present time, we have no technique to separate these two peptides further. Even if EI-2 is a mixture of Glu^5eSS-25II and Glu^6eSS-25II, the molecular weight should be the same in these peptides. Thus, isolation yield can be estimated as 5.6 μg (2 nmol) from 593 g guts. For comparison, primary structures of all somatostatin-like peptides isolated from the eel gut are shown in Figure 2.

Similarly as eSS-25II, EI-2 also enhanced the serosa-negative PD, I_{sc} and R_t (data not shown). Figure 3 shows dose-response curve for the effect of EI-2 on I_{sc}, with a threshold concentration of 10^{-9} M and a maximal effect at 3×10^{-8} M. Since the I_{sc} is due to active Cl^- transport (3), the enhancement in I_{sc} means stimulation of active Cl^- transport. Although not measured in the case of EI-2, the previous study (13) has demonstrated that eSS-25II directly

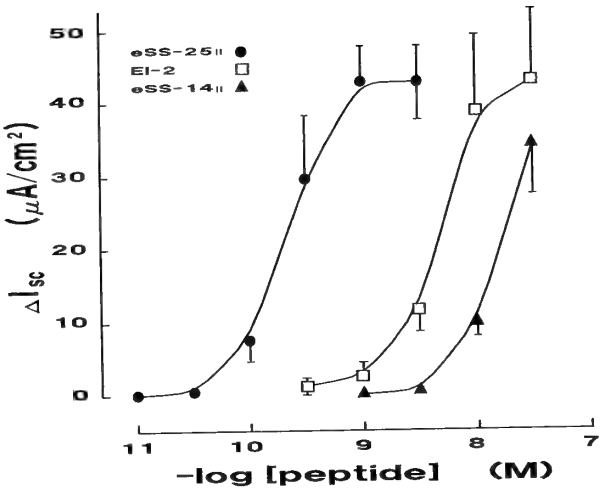

FIG. 3. Dose-response curve of EI-2 (□). The change in I_{sc} after addition of the peptide was plotted against its concentration (on a logarithmic scale). To compare the potency, dose-response curves of eSS-25II (●) and eSS-14II (▲) were also presented. Each point and vertical bar indicate the mean value and S.E.M. (N=5).

enhances Na^+, Cl^- and water absorption across the intestine of the seawater eel. The dose-response curve of EI-2 was shifted to the right from that of eSS-25II, indicating that Glu substitution for Gln at position 5 or 6 lowers the potency of the eel somatostatin. On the other hand, eSS-14II was less potent than EI-2 (Fig. 3). Since the C-terminal sequence of EI-2 is identical to eSS-14II (Fig. 2), this indicates that the N-terminal truncation is more effective to reduce the potency than Glu substitution. Probably Glu at position 5 or 6 modulates a structure formed by the N-terminal 11 amino acid residues.

Although it is not clear yet whether EI-2 really regulates intestinal absorption under physiological condition, eSS-25II may be an important regulator for intestinal ion and water absorption, because this form is effective at the lowest concentrations among various somatostatin-like peptides shown in Figure 2.

Since substantial amount of EI-2 was isolated from the gut , EI-2 must be synthesized in the intestinal tissue. EI-2 might be originated from deamidation of eSS-25II, since various cells contain glutaminases [12]. In this case, eSS-25II and EI-2 may coexist in the same cell. Such coexistence may be favorable to protect eSS-25II, a most effective peptide at least in the eel intestine, from further deamidation by the enzyme(s), since metabolic product usually acts as a feedback inhibitor. On the other hand, extracellular ammoniagenesis by another glutaminase has also been reported in the renal tubules [10, 15]. If such a glutaminase exists in the eel intestine, it may inactivate eSS-25II by converting into EI-2 extracellularly. This process may generally contribute to an inactivation of regulatory peptides which contain Gln residues.

ACKNOWLEDGMENTS

The authors wish to express their sincere thanks to Professors Yojiro Muneoka and Makoto Kobayashi, Faculty of Integrated Arts and Sciences, Hiroshima University, for their helpful advice. This research was supported in part by Grants-in-Aid no. 02804062 from the Ministry of Education, Sciences and Culture, Japan, and no. 9233 from Salt Science Research Foundation, Japan.

REFERENCES

1 Ando M, Kobayashi M (1978) Comp Biochem Physiol 61A: 497–501
2 Ando M, Omura E (1993) J Comp Physiol B163: 64–69
3 Ando M, Utida S, Nagahama H (1975) Comp Biochem Physiol 51A: 27–32
4 Conlon JM (1989) In "The Comparative Physiology of Regulatory Peptides" Ed by S Holmgren, Chapman and Hall, London and New York, pp. 344–369
5 Conlon JM, Deacon CF, Hazon N, Henderson IW, Thim L (1988) Gen Comp Endocr 72: 181–189
6 Hirst B, Conlon J, Coy D, Holland J, Shaw B (1982) Reg Peptides 4: 227–237
7 Konturek S, Kwiecien N, Obtulowicz W, Bielanski W, Oleksy J, Schally A (1985) Scand J Gastroenterol 20: 31–38
8 Plisetskaya EM (1989) In "The Comparative Physiology of Regulatory Peptides" Ed by S Holmgren, Chapman and Hall, London and New York, pp. 174–202
9 Seal A, Yamada T, Debas H, Hollinshead J, Osadchey B, Aponte G, Walsh J (1982) Am J Physiol 243: G97–G102
10 Simon EE, Merli Ch, Herdon J, Hamm LL (1990) Am J Physiol 259: F402–F407
11 Srikant C, Heisler S (1985) Endocrinology 117: 271–278
12 Swierczynski J, Bereznowski Z, Makarewicz W (1993) Biochim Biophys Acta 1157: 55–62
13 Uesaka T, Yano K, Yamasaki M, Nagashima K, Ando M (1994) J Exp Biol 188: 205–216
14 Vaudry H, Chartrel N, Conlon JM (1992) Biochem Biophys Res Commun 188: 477–482
15 Welbourne TC, Dass PD (1988) Pfluger Arch 411: 573–578

Development
Growth & Differentiation

Published Bimonthly by the Japanese Society of Developmental Biologists
Distributed by Business Center for Academic Societies Japan, Academic Press, Inc.

Papers in Vol. 36, No. 3. (June 1994)

M. Ishikawa: Masao Sugiyama (1908–1993)

25. **REVIEW**: S. Yasumasu, I. Iuchi and K. Yamagami: cDNAs and the Genes of HCE and LCE, Two Constituents of the Medaka Hatching Enzyme

26. K. Mikami and R. Ohtsu: Effects of K^+ and the K^+ Ionophore Valinomycin on the Post-Conjugational Nuclear Differentiation of *Paramecium caudatum*

27. T.-I. Chen, J. D. Green and W. H. Clark, Jr.: Sperm Penetration of the Vitelline Envelope of *Sicyonia ingentis* Eggs is Mediated by a Trypsin-like Lysin of Acrosomal Vesicle Origin

28. Y. Fujita, K. Yamasu, T. Suyemitsu and K. Ishihara: A Protein That Binds an Exogastrula-Inducing Peptide, EGIP-D, in the Hyaline Layer of Sea Urchin Embryos

29. J. Motoyama, K. Taki, N. Osumi-Yamashita and K. Eto: Retinoic Acid Treatment Induces Cell Death and the Protein Expression of Retinoic Acid Receptor β in the Mesenchymal Cells of Mouse Facial Primordia *in Vitro*

30. S. Kuno, K. Mitsunaga-Nakatsubo, T. Nagura and I. Yasumasu: Changes in Insulin-Binding Capacity of the Plasma Membrane Fraction during Culture *in vitro* of Cells Derived from Micromeres of 16-Cell-Stage Sea Urchin Embryos

31. N. Yoshizaki and S. Yonezawa: Cathepsin D Activity in the Vitellogenesis of *Xenopus laevis*

32. P. K. Mahapatra and P. Mohanty-Hejmadi: Vitamin A-Mediated Homeotic Transformation of Tail to Limbs, Limb Suppression and Abnormal Tail Regeneration in the Indian Jumping Frog *Polypedates maculatus*

33. T. Miyata and M. Ogawa: Developmental Potentials of Early Telencephalic Neuroepithelial Cells: A Study with Microexplant Culture

34. P. M. Tomy, N. P. Anilkumar and P. R. Sudhakaran: Multiple Laminin Binding Proteins in Human Fetal Heart

Development, Growth and Differentiation (ISSN 0012–1592) is published bimonthly by The Japanese Society of Developmental Biologists. Annual subscription for Vol. 35 1993 U. S. $ 191,00, U. S. and Canada; U. S. $ 211,00, all other countries except Japan. All prices include postage, handling and air speed delivery except Japan. Second class postage paid at Jamaica, N.Y. 11431, U. S. A.

Outside Japan: Send subscription orders and notices of change of address to Academic Press, Inc., Journal Subscription Fulfillment Department, 6277, Sea Harbor Drive, Orlando, FL 32887–4900, U. S. A. Send notices of change of address at least 6–8 weeks in advance. Please include both old and new addresses. U. S. A. POSTMASTER: Send changes of address to *Development, Growth and Differentiation,* Academic Press. Inc., Journal Subscription Fulfillment Department, 6277, Sea Harbor Drive, Orlando, FL 32887–4900, U. S. A.

In Japan: Send nonmember subscription orders and notices of change of address to Business Center for Academic Societies Japan, 16–9, Honkomagome 5-chome, Bunkyo-ku, Tokyo 113, Japan. Send inquiries about membership to Business Center for Academic Societies Japan, 16–9, Honkomagome 5-chome, Bunkyo-ku, Tokyo 113, Japan.

Air freight and mailing in the U. S. A. by Publications Expediting, Inc., 200 Meacham Avenue, Elmont, NY 11003, U. S. A.

POWERFUL PARTNERS FOR LONG-TERM PATCH CLAMPING

The MHW-3 water hydraulic micromanipulator features a refined slide mechanism and a 5:1 hydro/mechanical ratio to keep drift to an absolute minimum — just 1/17.5th of earlier, oil-based hydraulic units. Consequently, patch recording is accurate and reliable over extended periods. The MHW-3 has a full, pipette movement range of 2mm in ultra-fine 0.2μm graduations to allow fine remote control movement in all three axes, thereby providing exceptionally precise specimen pinpointing.

The MHW-30 features a movement range of 10mm, minimum graduations down to 1μm, and a 1:1 hydraulic system.

Three-Dimensional Water Hydraulic Micromanipulators

with coarse and fine manipulation

MHW-3 and MHW-30

For further information and maintenance service:

NARISHIGE JAPAN

NARISHIGE SCIENTIFIC INSTRUMENT LAB.

9-28, Kasuya 4-chome, Setagaya-ku, Tokyo 157, Japan
Phone: (INT-L) 81-3-3308-8233 Fax: (INT-L) 81-3-3308-2005 Telex: NARISHIGE J27781

U.S. NARISHIGE INTERNATIONAL INC.
404 Glen Cove Avenue, Sea Cliff, New York 11579, U.S.A.
Telephone: +1 (516) 759-6167 Telefax. +1 (516) 759-6138

NARISHIGE INTERNATIONAL LTD.
Unit 7, Willow Business Park, Willow Way, London SE26 4QP, UK
Telephone: +44 (0) 81-699-9696 Telefax: +44 (0) 81-291-9678

ZOOLOGICAL SCIENCE

VOLUME 11 NUMBER 3 JUNE 1994

CONTENTS

REVIEWS

Tsutsui, K., S. Kawashima: Regulation of gonadotropin receptors and its physiological significance in higher vertebrates 351

Rastogi, R. K., L. Iela: Gonadotropin-releasing hormone: present concepts, future directions 363

ORIGINAL PAPERS

Physiology

Nakamura, M., M. Tani, T. Kuramoto: Effects of rapid cooling on heart rate of the Japanese lobster *in vivo* 375

Naitoh, T., M. Matuura, R. J. Wassersug: Effectiveness of metoclopramide, domperidone and ondansetron as antiemetics in the amphibian, *Xenopus laevis* 381

Sata, O., T. Sato: Electrical responses of non-taste cells in frog tongue and palate to chemical stimuli 385

Cell Biology

Arikawa K., A. Matsushita: Immunogold colocalization of opsin and actin in *Drosophila* photoreceptors that undergo active rhabdomere morphogenesis 391

Ricci, N., F. Verni: Experimental perturbations of the *Litonotus-Euplotes* predator-prey system 399

Biochemistry

Ohtsuka, Y., H. Nakae, H. Abe, T. Obinata: Immunochemical studies of an actin-binding protein in ascidian body wall smooth muscle 407

Takikawa, S., M. Nakagoshi: Developmental changes in pteridine biosynthesis in the toad, *Bufo vulgaris* ... 413

Developmental Biology

Hou, L., T. Takeuchi: Neural crest development in reptilian embryos, studied with monoclonal antibody, HNK-1 423

Suzuki, H., A. Kondo: The second maturation division and fertilization in the spider *Achaearanea japonica* (Bös. *et* Str.) 433

Nishiyama, I., T. Oota, M. Ogiso: Neuron-like morphology expressed by perinatal rat C-cells *in vitro* 441

Endocrinology

Uesaka, T., K. Yano, M. Yamasaki, M. Ando: Glutamate substitution for glutamine at position 5 or 6 reduces somatostatin action in the eel intestine (RAPID COMMUNICATION) 491

Takahashi, S., S. Oomizu, Y. Kobayashi: Proliferation of pituitary cells in streptozotocin-induced diabetic mice: effect of insulin and estrogen 445

Takano, M., Y. Sasayama, Y. Takei: Molecular evolution of shark C-type natriuretic peptides 451

Systematics and Taxonomy

Aizawa, T., M. Hatsumi, K. Wakahama: Systematic study on the *Chaenogobius* species (family Gobiidae) by analysis of allozyme polymorphisms 455

Ohtani, H.: Speciation of Japanese pond frogs deduced from lampbrush chromosomes of their diploid and triploid hybrids 465

Ono, T., Y. Obara: Karyotypes and Ag-NOR variations in Japanese Vespertilionid bats (Mammalia: Chiroptera) 473

Matsui, M., G. Wu: Acoustic characteristics of treefrogs from Sichuan, China, with comments on systematic relationship of *Polypedates* and *Rhacophorus* (Anura, Rhacophoridae) 485

INDEXED IN:
Current Contents/LS and AB & ES,
Science Citation Index,
ISI Online Database,
CABS Database, INFOBIB

Issued on June 15
Front cover designed by Saori Yasutomi
Printed by Daigaku Letterpress Co., Ltd., Hiroshima, Japan